



# 72<sup>nd</sup> Highway Geology Symposium

## 2023 PROCEEDINGS

---

August 14-17, 2023 • Hotel Murano • Tacoma, Washington



## Grateful Acknowledgments

We would like to thank the following people who helped make made this Symposium possible.

Samantha Denham

John Pilipchuk

Gabe Taylor

Sam Johnston

Kerri Woehler

Jon Major

Eric Smith

HGS Steering Committee

Washington Geological Survey

Pat Pringle

Delaney Event Management

Todd Hansen

Krystle Pelham



# 72nd Highway Geology Symposium

August 14-17, 2023

Hotel Murano  
Tacoma, Washington

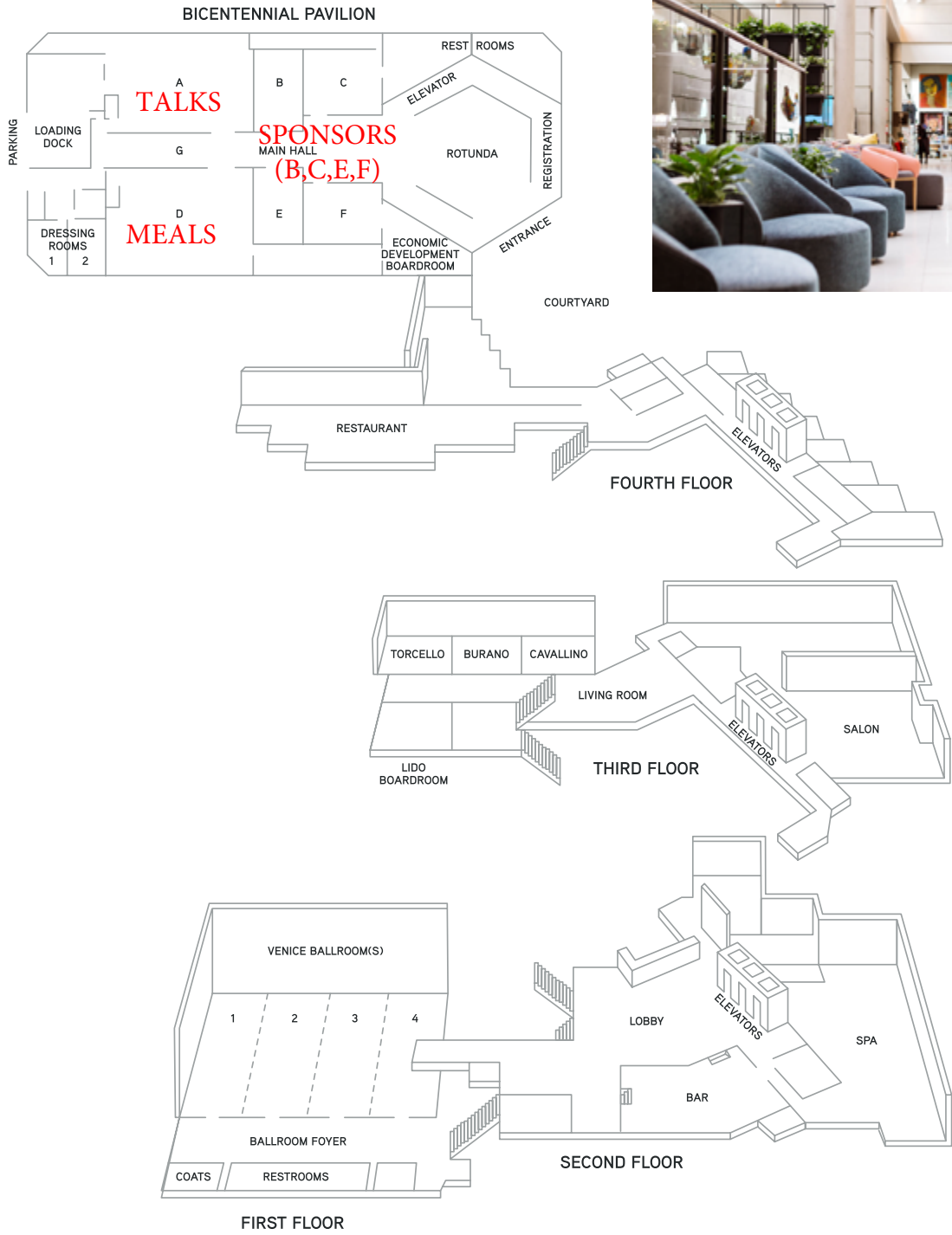


# TABLE OF CONTENTS

SCHEDULE OF EVENTS .....	3
WORKSHOPS AND TRB MID-YEAR MEETING .....	8
Rockfall Fragmentation Demo .....	8
FHWA Workshop .....	8
Transportation Research Board Session .....	8
BANQUET KEYNOTE SPEAKER .....	9
FIELD TRIP SCHEDULE .....	10
HIGHWAY GEOLOGY SYMPOSIUM HISTORY, ORGANIZATION, AND FUNCTION .....	11
YOUNG AUTHOR AWARD .....	16
HGS MEDALLION AWARD RECIPIENTS .....	17
EMERITUS MEMBERS OF THE STEERING COMMITTEE .....	17
HGS NATIONAL STEERING COMMITTEE OFFICERS .....	18
HGS NATIONAL STEERING COMMITTEE MEMBERS .....	18
HIGHWAY GEOLOGY SYMPOSIUM: PAST, PRESENT, AND FUTURE SYMPOSIUM CONTACT LIST .....	21
SPONSORS AND EXHIBITORS .....	22
PAPERS .....	45

# SCHEDULE OF EVENTS

## MONDAY, AUGUST 14, 2023

Time	Event	Location
8:00 AM – 12:00 PM	Rockfall Fragmentation Demo (Pre-Registration Required)	Offsite: UW Tacoma Milgard Hall Room 311
8:30 AM – 5:00 PM	Registration Open	Rotunda
9:00 AM – 4:00 PM	Sponsor and Exhibitor Setup	Pavilion BCEF
9:00 AM – 11:30 AM	FHWA Workshop: “What you Need to Know About Seismic Geophysics for Engineering Applications” (Pre-Registration Required)	Pavilion AG
1:00 PM – 5:00 PM	Transportation Research Board Session: “Geotechnical Data Sourcing and the Quality and Use of Models for Geotechnical Design” (Pre-Registration Required)	Pavilion AG
5:00 PM – 6:30 PM	National Steering Committee Meeting	Torcello/Burano
6:00 PM – 8:00 PM	Icebreaker Reception Sponsored by Landslide Technology	Pavilion BCEF

## TUESDAY, AUGUST 15, 2023

Time	Event	Location
7:00 AM – 8:00 AM	Breakfast Sponsored by Shannon & Wilson	Pavilion D
7:00 AM – 5:00 PM	Registration	Rotunda
8:00 AM – 8:50 AM	HGS Welcome & Opening Remarks	Pavilion AG
8:00 AM – 8:30 AM	Marc Fish WSDOT State Eng. Geologist & Kerri Woehler WSDOT Deputy Asst. Secretary	
8:30 AM – 8:50 AM	Washington Geology, Trevor Contreras, WA Geological Survey	
8:50 AM – 9:30 AM	<b>Technical Talks – Session 1</b> (Moderator Chris Ruppen, Geostabilization International)	Pavilion AG
8:50 AM – 9:10 AM	Innovative Geophysical Application for Bridge Foundation Design and Construction <i>Young Author: Ronan Jones</i>	
9:10 AM – 9:30 AM	Design and Construction of a Bottom-up Retaining Wall in Slickensided Red Bed Material <i>Young Author: Kirsten Grant</i>	

**TUESDAY, AUGUST 15, 2023 (CONTINUED)**

<b>Time</b>	<b>Event</b>	<b>Location</b>
9:30 AM – 10:00 AM	Mid-Morning Break	Pavilion BCEF
10:00 AM – 12:00 PM	<b>Technical Talks – Session 2</b> (Moderator Sarah McInnes, PADOT)	Pavilion AG
10:00 AM – 10:20 AM	Impacts of Weak Rock Units on Cut Slope Construction <i>Young Author: Justin Manning</i>	
10:20 AM – 10:40 AM	Comparative Analysis of Rock Slope Scaling Quantities and Crew Hours: A Strategic Approach for Standardizing the Practice <i>Young Author: Katelyn Card</i>	
10:40 AM – 11:00 AM	Seward Highway Rockfall Mitigation, Anchorage, Alaska <i>Young Author: Sebastian Dirringer</i>	
11:00 AM – 11:20 AM	A Multi-Phased Approach to Rockfall Mitigation at Don Pedro Dam: Lessons Learned for Critical Facilities and Roadways <i>Young Author: Joey Renner</i>	
11:20 AM – 11:40 AM	Bolt Creek Fire: Post-Wildfire Debris Flow Risk Assessment and Barrier Design on US 2, Near Grotto, WA <i>Young Author: Cody Chaussee</i>	
11:40 AM – 12:00 PM	Emergency planning and mitigation for post-fire debris flows in Glenwood Canyon, Colorado <i>Young Author: Aliena Debelak</i>	
12:00 PM – 1:00 PM	Lunch Sponsored by GeoStabilization International & Access Limited	Pavilion D
1:00 PM – 3:00 PM	<b>Technical Talks – Session 3</b> (Moderator Simon Boone, Access Limited Construction)	Pavilion AG
1:00 PM – 1:20 PM	Freemont Hall Landslide <i>Young Author: Jamie Cravens</i>	
1:20 PM – 1:40 PM	Landslide Study and Final Repair Design Route 3 Randolph County, Missouri <i>Author: John Szturo</i>	
1:40 PM – 2:00 PM	The SR112 / Clallam Bay Landslide(s) – Characterization and Mitigation <i>Author: Gabriel Taylor</i>	
2:00 PM – 2:20 PM	State Route 112: Landslide Alley – Striving for Resiliency <i>Author: Tom Badger</i>	
2:20 PM – 2:40 PM	Raised Draperies – Defining Hybrid Barriers and Attenuators by Application <i>Author: John Duffy</i>	
2:40 PM – 3:00 PM	How To Develop Rockslope Mitigation For Very Large Roadway-Dipping Blocks Along an Interstate Highway <i>Author: Stephen Newman</i>	

## TUESDAY, AUGUST 15, 2023 (CONTINUED)

Time	Event	Location
3:00 PM – 3:30 PM	Afternoon Break Sponsored by Rock Supremacy LLC	Pavilion BCEF
3:30 PM – 4:40 PM	<b>Technical Talks – Session 4</b> (Moderator Tom Badger, Landslide Technology)	Pavilion AG
3:30 PM – 3:50 PM	“What If the Rock Only Threatens to Fall?” Emergency Response to a Decoupled Cliff Face in Washington State <i>Author: Eric Smith</i>	
3:50 PM – 4:30 PM	I-90 Rock Slopes: A Retrospective of the Snoqualmie Pass Project <i>Author: Norm Norrish</i>	
4:40 PM – 5:00 PM	Mt. Rainier Field Trip Preview (Gabe Taylor, WSDOT)	Pavilion AG
6:00 PM – 8:00 PM	Sailing Cruise on Lady Washington (Pre-Registration Required)	Offsite

## WEDNESDAY, AUGUST 16, 2023

Time	Event	Location
7:30 AM – 8:00 AM	Grab N' Go Breakfast	Hotel Lobby
8:00 AM	Board Buses for HGS Field Tour	
8:00 AM – 6:00 PM	HGS Field Tour to Mount Rainier National Park Sponsored by Geobrugg & Maccaferri Inc.	
	Spider Demonstration Geostabilization International	

## THURSDAY, AUGUST 17, 2023

Time	Event	Location
7:00 AM – 8:00 AM	Breakfast Sponsored by Haley & Aldrich	Pavilion D
7:00 AM – 5:00 PM	Registration	Rotunda
8:00 AM – 5:00 PM	Exhibits Open	Pavilion BCEF
11:00 AM – 5:00 PM	Companion Activities	Offsite: 7 Seas Brewery & Museum of Glass
8:00 AM – 10:00 AM	<b>Technical Talks – Session 5</b> (Moderator Bill Gates, Delve Underground)	Pavilion AG
8:00 AM – 8:20 AM	Climate Resilience and Infrastructure Adaptation on California's National Forests <i>Author: Gordon Keller</i>	
8:20 AM – 8:40 AM	Geohazard Management on Colorado SH 133 From Planning to Mitigation <i>Author: Randy Post</i>	

**THURSDAY, AUGUST 17, 2023 (CONTINUED)**

Time	Event	Location
<b>Technical Talks – Session 5 (continued)</b>		
8:40 AM – 9:00 AM	The State of Measurement While Drilling for the Washington State Department of Transportation <i>Author: Mike Mulhern</i>	
9:00 AM – 9:20 AM	Advancing Subsurface Investigations Beyond the Borehole with Passive Seismic Horizontal-to-Vertical Spectral Ratio and Electromagnetic Geophysical Methods at Transportation Infrastructure Sites in New Hampshire <i>Author: J.R. Degnan</i>	
9:20 AM – 9:40 AM	Non-destructive Surface Wave Geophysics Characterizes Salt Dissolution 140m Under US Highway 50 at Brandy Lake, Reno County, Kansas <i>Author: Johari Pannalal</i>	
9:40 AM – 10:00 AM	Mitigation Alternatives for Salt Dissolution Subsidence Impacting US Highway 50 at Brandy Lake, Reno County, Kansas <i>Author: Jeff Keaton</i>	
10:00 AM – 10:30 AM	Mid-Morning Break Sponsored by Global Rope Access	Pavilion BCEF
10:30 AM – 11:50 AM	<b>Technical Talks – Session 6</b> (Moderator Ken Ashton WV Geological Survey)	Pavilion AG
10:30 AM – 10:50 AM	Using State-of-the-Art Technologies and Tools for Geotechnical Investigation and Design <i>Author: Brian Collins</i>	
10:50 AM – 11:10 AM	The Development and Utilization of a Cloud-Based Database and Visualization App for Pile Results and Design: PileTrac <i>Author: Kyle Halverson</i>	
11:10 AM – 11:30 AM	Pavement Bump at the Bridge End Elimination <i>Author: Jeremiah Kokes</i>	
11:30 AM – 11:50 AM	US 460 Bridges over Marrowbone Creek, Pond Creek and Russell Fork River <i>Author: Tony Beckham</i>	
11:50 AM – 1:00 PM	Lunch	Pavilion D
1:00 PM – 3:00 PM	<b>Technical Talks – Session 7</b> (Moderator Sebastian Dirringer, Landslide Technology)	Pavilion AG
1:00 PM – 1:20 PM	Taking into Account the Fragmentation and Variability of Rockfall and the Third Dimension in Rockfall Barrier Design <i>Author: Tim Shevlin</i>	
1:20 PM – 1:40 PM	Introducing A New Impact Alert System for Rockfall Barriers <i>Author: Sage Evans</i>	
1:40 PM – 2:00 PM	The Geohazard Pro must know “Section 262 Slope Scaling” <i>Author: Todd Hansen</i>	

**THURSDAY, AUGUST 17, 2023 (CONTINUED)**

Time	Event	Location
<b>Technical Talks – Session 7 (continued)</b>		
2:00 PM – 2:20 PM	Rock Stabilization at Pompeys Pillar National Monument: The Use of Numerical Modeling to Analyze Risk of Toppling Failure <i>Author: Anya Brose</i>	
2:20 PM – 2:40 PM	Padden Creek I-5 Stream Crossing <i>Author: Mark Rose</i>	
2:40 PM – 3:00 PM	The Erodibility Index in Washington State’s Intermediate Geomaterials: The Need for a Practical Tool <i>Author: Robert Humphries</i>	
3:00 PM – 3:30 PM	Afternoon Break	Pavilion BCEF
3:30 PM – 5:30 PM	<b>Technical Talks – Session 8</b> (Moderator Todd Hansen FHWA WFL)	Pavilion AG
3:30 PM – 3:50 PM	Accelerating the Transition to Digital Deliverables <i>Author: Katie Aguilar</i>	
3:50 PM – 4:10 PM	GIS Enterprise-based Prototype Erosion and Slope Stability Screening Tool for Transportation Infrastructure Management <i>Author: Bin Wang</i>	
4:10 PM – 4:30 PM	Integrating Field Data with Physics Engine Simulations of Fragmental Rockfalls <i>Author: R. MacPhail</i>	
4:30 PM – 4:50 PM	Emergency Response and Cures for Karst on Chemical Road <i>Author: Sarah McInnes</i>	
4:50 PM – 5:10 PM	A Comprehensive Approach to Rock Slope Design Solutions along NC-88 in Ashe County, North Carolina <i>Author: Bret Watkins</i>	
5:10 PM – 5:30 PM	Hybrid Design Approach for Anchored Wire Mesh: Towards A Displacement Based Design <i>Author: Lucas Martins</i>	
5:30 PM – 6:30 PM	Student Poster Social Sponsored by Ameritech Slope Constructors, Inc.	Rotunda
6:30 PM – 9:00 PM	HGS Closing Banquet Keynote Sponsored by WSP Jon Major, Cascades Volcano Observatory, Volcanic Hazards of the Cascades	Pavilion D
	Young Author Awards – Chris Ruppen Next Year’s Highway Geology Symposium – Kyle Halverson Closing Remarks and Adjournment of the Symposium	

# WORKSHOPS AND TRB MID-YEAR MEETING

## Rockfall Fragmentation Demo

### DATE

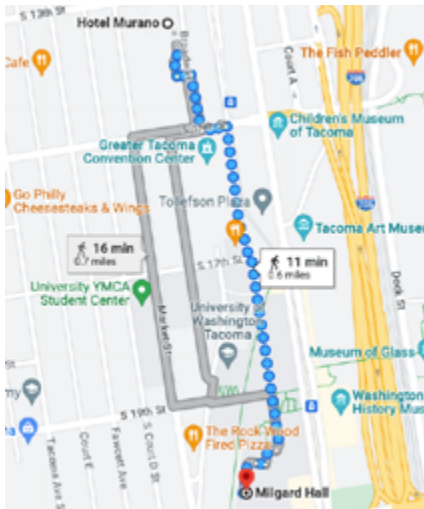
Monday, August 14

### TIME

8:00 AM – 12:00 PM

### LOCATION

UW Tacoma Milgard Hall  
Room 311



As a part of the pool-funded study that aims to develop and calibrate fragmental rockfall models using physics engines, the research team from Oregon State University, University of Washington, and Queen's University (Canada) are hosting a workshop. The first part of the workshop will provide some hands-on training on the field procedures to track 3D trajectories followed by a demonstration of the output of the data processing work to understand the movement parameters (limited spots). The second part of the workshop will focus on selecting input data for rockfall analysis. We will consult with attendees to understand how rockfall data is collected in the field, and which parameters are most useful. This collection of the current state of practice will support our work to develop field data collection methodologies and to understand user preferences for rockfall fragmentation modeling (open to all).

### Directions from Hotel Murano to UW

1. Head south toward Broadway
  2. Turn left toward Broadway
  3. Turn right onto Broadway
  4. Turn left onto S 15th St
  5. Turn right onto Commerce St
  6. Turn right onto S C St
  7. Turn right
  8. Slight left
- Destination will be on the left.**

## FHWA Workshop

### DATE

Monday, August 14

### TIME

9:00 AM – 11:30 AM

### LOCATION

Bicentennial Pavilion AG

### *“What you Need to Know About Seismic Geophysics for Engineering Applications”*

The session is intended to be practical; reviewing and discussing each of the surface and borehole methodologies, working through where and when each should be applied, and what can be expected from each: Best practices, limitations/pitfalls, benefits and the similarities and differences among the methods. Session partners include Geophysics Users Group (GPUG), TRB AKG 20 and AKG 60, DFI SCC, and GI EG&SC.

## Transportation Research Board Session

### DATE

Monday, August 14

### TIME

1:00 PM – 5:00 PM

### LOCATION

Bicentennial Pavilion AG

### *“Geotechnical Data Sourcing and the Quality and Use of Models for Geotechnical Design”*

This session at HGS will highlight how though the application and use of new innovative sources of geotechnical data, engineers can increase reliability and certainty of various geotechnical design models. The use of these new data sources more readily available coupled with innovative technology such as measurement while drilling, CPT, and geophysical techniques can enhance our geotechnical site characterization.

# BANQUET KEYNOTE SPEAKER

## LAVAS AND MUDFLOWS AND ASH—OH MY!

### **Jon Major**

Scientist-in-Charge  
U.S. Geological Survey  
Cascades Volcano Observatory  
Vancouver, Washington

The Cascades Range is home to many volcanoes, but how active and dangerous are they? What are the greatest hazards from volcanoes in the Pacific Northwest, who monitors them, and how? In this presentation, Jon Major explores volcanic processes associated with volcanic eruptions and their aftermath, provides insights on the greatest threats posed by the Cascades volcanoes, and reveals how our regional volcanoes are monitored and why. The great 1980 eruption of Mount St. Helens fundamentally changed how scientists viewed volcanic eruptions. The four decades since have seen significant advancements in our understanding of volcanic histories, processes, hazards, monitoring capabilities, and the role that scientists have in communicating with governmental agencies and the public.

Jon received his B.S. from University of Dayton, M.S. from Penn State, and Ph.D. from the Department of Geological Sciences at the University of Washington. His research focuses on physical responses to landscape disturbances, particularly in volcanic river systems. He has worked at volcanoes in Washington, Oregon, Alaska, El Salvador, Chile, and the Philippines. He has been working at Mount St. Helens since 1981 and has been with the USGS Cascades Volcano Observatory since 1983.



# FIELD TRIP SCHEDULE

August 16, 2023

Time	Bus 1	Bus 2	Bus 3	Bus 4
7:30 AM	Gather at Hotel Murano			
8:00 AM	8:00 AM – All Buses Depart Tacoma			
9:00 AM	Bus discussions: lahars, debris flows, Alder dam, rockfall			
9:00 AM	Arrive at Mt. Rainier National Park			
10:00 AM	Bus 1	Bus 2	Bus 3	Bus 4
10:00 AM	Arrive at Paradise		<b>Ricksecker Point</b>	
11:00 AM	LUNCH	LUNCH	Arrive at Paradise	
12:00 PM	Hiking and visiting Paradise	Hiking and visiting Paradise	LUNCH	LUNCH
1:00 PM			Hiking and visiting Paradise	Hiking and visiting Paradise
2:00 PM	2:00 PM – Buses depart!		Hiking and visiting Paradise	Hiking and visiting Paradise
3:00 PM	<b>Ricksecker Point</b>			
4:00 PM	Travel to SR 7 Demonstration			
5:00 PM	SR 7 Demonstration			
6:00 PM	Travel back to Tacoma (Hotel Murano)			
7:00 PM				

# HIGHWAY GEOLOGY SYMPOSIUM HISTORY, ORGANIZATION, AND FUNCTION

## Inaugural Meeting

Established to foster a better understanding and closer cooperation between geologists and civil engineers in the highway industry, the Highway Geology Symposium (HGS) was organized and held its first meeting on March 14, 1950, in Richmond Virginia. Attending the inaugural meeting were representatives from state highway departments (as referred to at that time) from Georgia, South Carolina, North Carolina, Virginia, Kentucky, West Virginia, Maryland, and Pennsylvania. In addition, a number of federal agencies and universities were represented. A total of nine technical papers were presented.

W.T. Parrott, an engineering geologist with the Virginia Department of Highways, chaired the first meeting. It was Mr. Parrott who originated the Highway Geology Symposium.

It was at the 1956 meeting that future HGS leader, A.C. Dodson, began his active role in participating in the Symposium. Mr. Dodson was the Chief Geologist for the North Carolina State Highway and Public Works Commission, which sponsored the 7th HGS meeting.

## Symposium Locations

Since the initial meeting, 69 consecutive annual meetings have been held in 33 different states. Between 1950 and 1962, the meetings were east of the Mississippi River, with Virginia, West Virginia, Ohio, Maryland, North Carolina, Pennsylvania, Georgia, Florida, and Tennessee serving as host state.

In 1962, the symposium moved west for the first time to Phoenix, Arizona where the 13th annual HGS meeting was held. Since then it has alternated, for the most part, back and forth from the east to the west. The Annual Symposium has moved to different location as shown on the next page.

## Organization

Unlike most groups and organizations that meet on a regular basis, the Highway Geology Symposium has no central headquarters, no annual dues and no formal membership requirements. The governing body of the Symposium is a steering committee composed of approximately 20 – 25 engineering geologist and geotechnical engineers from state and federal agencies, colleges and universities, as well as private service companies and consulting firms throughout the country. Steering committee members are elected for three-year terms, with their elections and re-elections being determined principally by their interests and participation in and contribution to the Symposium. The officers include a chairman, vice chairman, secretary, and treasurer. all of whom are elected for a two-year term. Officers, except for the treasurer, may only succeed themselves for one additional term.

A number of three-member standing committees conduct the affairs of the organization. The lack of rigid requirements, routing and relatively relaxed overall functioning of the organization is what attracts many participants.

The symposia are generally scheduled for two and one-half days, with a day-and-a-half for technical papers plus a full day for the field trip. The Symposium usually begins with a TRB session and an evening Ice-Breaker the first day, a full day of technical presentations the second day, a field trip on the third day followed by the annual banquet that evening, and a half day of technical presentations on the final day.

## The Field Trip

The field trip is the focus of the meeting. In most cases, the trips cover approximately 150 to 200 miles, provide for six to eight scheduled stops, and require about eight hours. Occasionally,

cultural stops are scheduled around geological and geotechnical points of interests. To cite a few examples: in Wyoming (1973), the group viewed landslides in the Big Horn Mountains; Florida's trip (1976) included a tour of Cape Canaveral and the NASA space installation; the Idaho and South Dakota trips dealt principally with mining activities; North Carolina provided stops at a quarry site, a dam construction site, and a nuclear generation site; in Maryland, the group visited the Chesapeake Bay hydraulic model and the Goddard Space Center. The Oregon trip included visits to the Columbia River Gorge and Mount Hood; the Central mine region was visited in Texas; and the Tennessee meeting in 1981 provided stops at several repaired landslide in Appalachia regions of East Tennessee.

In Utah (1988) the field trip visited sites in Provo Canyon and stopped at the famous Thistle Landslide, while in New Mexico, in 1990, the emphasis was on rockfall treatments in the Rio Grande River canyon and included a stop at the Brugg Wire Rope headquarters in Santa Fe.

Mount St. Helens was visited by the field trip in 1994 when the meeting was in Portland, Oregon, while in 1995 the West Virginia meeting took us to the New River Gorge Bridge that has a deck elevation of 876 feet above the water.

In Cody, Wyoming the 1996 field trip visited the Chief Joseph Scenic Highway and the Beartooth Uplift in northwest Wyoming. In 1997 the meeting in Tennessee visited the newly constructed future I-26 highway in the Blue Ridge of East Tennessee. The Arizona meeting in 1998 visited the Oak Creek Canyon near Sedona and a mining ghost town at Jerome, Arizona. The Virginia meeting in 1999 visited the "Smart Road" Project that was under construction. This was a joint research project of the Virginia Department of Transportation and Virginia Tech University. The Seattle Washington meeting in 2000 visited an ancient lahar in the Mount Rainier area. A stop during the Maryland meeting in 2001 was the Sideling Hill road cut for I-68 which displayed a tightly folded syncline in the Allegheny Mountains.

The California field trip in 2002 provided a field demonstration of the effectiveness of rock netting against rock falls along the Pacific Coast Highway. The Kansas City meeting in 2004 visited the Hunt Subtropolis which is said to be the "world's largest underground business complex". It was created through the mining of limestone by way of the room and pillar method. The Rocky Point Quarry provided an opportunity to search for fossils at the North Carolina meeting in 2005. The group also visited the US-17 Wilmington Bypass Bridge which was under construction. Among the stops at the Pennsylvania meeting were the Hickory Run Boulder Field, the No.9 Mine and Wash Shanty Museum, and the Lehigh Tunnel.

The New Mexico field trip in 2008 included stops at a soil nailed wall along US-285/84 north of Santa Fe and a road cut through the Bandelier Tuff on highway 502 near Los Alamos where rockfall mesh was used to protect against rockfalls. The New York field trip in 2009 included the Niagara Falls Gorge and the Devil's Hole Trail. The Oklahoma field trip in 2010 toured the complex geology of the Arbuckle Mountains in the southern part of the state along with stops at Tucker's Tower and Turner Falls.

In the bluegrass state of Kentucky, the 2011 HGS field trip included stops at Camp Nelson which is the site of the oldest exposed rocks in Kentucky near the Lexington and Kentucky River Fault Zones. Additional stops at the Darby Dan Farm and the Woodford Reserve Distillery illustrated how the local geology has played such a large part in the success of breeding prized Thoroughbred horses and made Kentucky the "Birthplace of Bourbon".

In Redding, California, the 2012 field trip included stops at the Whiskeytown Lake, which is one in a series of lakes that provide water and power to northern California. Additional stops included Rocky Point, a roadway construction site containing Naturally Occurring Asbestos (NOA), and Oregon Mountain where the geology and high rainfall amounts have caused Hwy 299 to experience local and global instabilities since first constructed in 1920.

The 2013 field trip of New Hampshire highlighted the topography and geologic remnants left by the Pleistocene glaciation that fully retreated approximately 12,000 years ago. The field trip included stops at various overlooks of glacially-carved valleys and ranges; the Old Man of the Mountain Memorial Plaza, which is a tribute to the famous cantilevered rock mass in the Franconia Notch that collapsed on May 3, 2003; the lacustrine deposits and features of the Glacial Lake Ammonoosuc; views of the Presidential Range; bridges damaged during Tropical Storm Irene in August 2011; and the Willey Slide, located in the Crawford Notch where all members of the Willey family were buried by a landslide in 1826.

The 2014 field trip presented a breathtaking tour of the geology and history of southeast Wyoming, ascending from the high plains surrounding Laramie at 7000 feet to the Medicine Bow Mountains along the Snowy Range Scenic Byway. Visible along the way were a Precambrian shear zone, and glacial deposits and features. From the glacially carved Mirror Lake and the Snowy Range Ski Area, the path wound east to the Laramie Mountains and the Vedauwoo Recreational Area, a popular rock climbing and hiking area before returning to Laramie.

In Sturbridge, MA, the 2015 field trip focused on the Connecticut Valley, a Mesozoic rift basin that signaled the breakup of Pangea, and the Berkshires, which represents the collision and amalgamation of an island arc system with the North American Laurentian margin.

The field trip in 2016 was an urban setting along the western edge of Colorado Springs and around Manitou Springs. Stops included the Pikeview Quarry, Garden of the Gods Visitor Center, and several other locations where rockfall and debris flow mitigation, post-flooding highway embankment repair, and a nonconformity in the rock records that spans 1.3 billion years were observed.

The 2017 field trip provided an opportunity to view the geology of northern Georgia. Stops included the Bellwood Quarry, which, at one time was run by

the City of Atlanta and also served as a prison labor camp. It will eventually serve as a 2.4 billion-gallon water storage facility for the City of Atlanta upon completion of a tunnel to connect the quarry to two water treatment plants and three pump stations. Additional stops included the Buzzi Unicem Cement Plant to get a close up view of the Clairmont Melange, The Cooper Furnace near the Allatoona Dam, and the New Riverside Ochre-Emerson Barite mine.

The 2018 field trip in Portland Maine provided a good overview of the geology of coastal Maine. Field trip stops included a stop at the Sherman Salt Marsh near Newcastle which was recently restored to its natural state after the dam that carried US Highway 1 washed out during a 2005 storm. Additional stops included the site of the 1996 landslide near Rockland Harbor that consumed several homes and the rock slope remediation project at the Penobscot Narrows Bridge near Prospect Maine. A lobster lunch along the shore of Penobscot Bay was one of several highlights of the field trip.

The 2019 field trip in Portland Oregon travelled the Columbia River Gorge west. Starting at the Crown Point Vista House and Portland Women's Forum State Scenic Viewpoint above the gorge to learn about the river highway. Descending into the gorge, we stopped at scenic Multnomah Falls and Benson Bridge, and saw flexible rockfall fence installed to protect the lodge and historic Columbia River Highway. Other stops included lunch at Cascade Locks, Bonneville Landslide and rockfall areas along the highway.

The 2022 field trip in the Ashville area took us through Ordovician (500 my) to Precambrian (1.2 by) migmatized ortho and paragneisses, metamorphosed intrusives, thrust faults and contacts representing three orogenies and complex sequences of basement and terranes. We crossed the Brevard Fault zone several times, which is a structure that has been studied and interpreted for 100 years. Various attempts to define the structure have been made, especially in the pre-plate tectonic

era. It has been theorized that these structures were as high, or higher than the Rockies at formation. 200 million years of rifted erosion leave us with an exposed look at deep orogenic roots of multiple thrust events. Precipitation in the areas is between 60-100" per year. There are deep ancient colluvial deposits, complex mineralization and weathering profiles, and non-linear/planar discontinuities. These deposits and precipitation make for distinct issues within the state. Deep foundations rarely present problems. We traveled over I-26 and the Blue Ridge Escarpment where they highway is being widened. Stops included the I-26 Old Howard Gap Slide Area, the US 74 Gerton Slide, a shallow landslide barrier on I-40 W, and the Buckner Gap Cut.

## Technical Sessions

At the technical sessions, case histories and applied state-of-the-art papers are most common; with highly theoretical papers the exception. The papers presented at the technical sessions are published in the annual proceedings. All proceedings are available to download from [www.HighwayGeologySymposium.org](http://www.HighwayGeologySymposium.org).

Banquet speakers are also a highlight and have been varied through the years.

Member Recognition: A Medallion Award was initiated in 1970 to honor those persons who have made significant contributions to the Highway Geology Symposium. The selection was- and is currently made from the members of the national steering committee of the HGS.

## Emeritus Member

A number of past members of the national steering committee have been granted Emeritus status. These individuals, usually retired, resigned from the HGS Steering Committee, or are deceased, have made significant contributions to the Highway Geology Symposium. A total of 42 persons have been granted Emeritus status.

## Dedications

Several Proceedings volumes have been dedicated to past HGS Steering Committee members who have passed away. The 36th HGS Proceedings were dedicated to David L. Royster (1931 – 1985, Tennessee) at the Clarksville, Indiana Meeting in 1985. In 1991 the Proceedings of the 42nd HGS held in Albany, New York were dedicated to Burrell S. Whitlow (1929 – 1990, Virginia). The 64th HGS Proceedings were dedicated to Earl Wright (1931 – 2012) at the North Conway, New Hampshire meeting. The 65th proceedings were dedicated to Nicholas Priznar (1952 – 2014) at the Laramie, Wyoming meeting. The 76th HGS held at Colorado Springs, Colorado dedicated the proceedings to Vern McGuffy (1934 – 2016). The proceedings for the 68th HGS held in Marietta, Georgia were dedicated to Richard (Dick) Cross (1944 – 2016). The proceedings for the 69th HGS are dedicated to Dave Bingham (1932 – 2018) and Joe Gutierrez (1926 –2018). The Proceedings of the 71st HGS are dedicated to Vernon (Vern) Bump.

## List of Highway Geology Symposium Meetings

Meeting sites are chosen two to four years in advance and are selected by the Steering Committee following presentations made by representatives of potential host states. These presentations are usually

made at the steering committee meeting, which is held during the Annual Symposium. Upon selection, the state representative becomes the state chairman and a member of the Steering Committee.

No.	Year	HGS Location
1st	1950	Richmond, VA
2nd	1951	Richmond, VA
3rd	1952	Lexington, VA
4th	1953	Charleston, WV
5th	1954	Columbus, OH
6th	1955	Baltimore, MD
7th	1956	Raleigh, NC
8th	1957	State College, PA
9th	1958	Charlottesville, VA
10th	1959	Atlanta, GA
11th	1960	Tallahassee, FL
12th	1961	Knoxville, TN
13th	1962	Phoenix, AZ
14th	1963	College Station, TX
15th	1964	Rolla, MO
16th	1965	Lexington, KY
17th	1966	Ames, IA
18th	1967	Lafayette, IN
19th	1968	Morgantown, WV
20th	1969	Urbana, IL
21st	1970	Lawrence, KS
22nd	1971	Norman, OK
23rd	1972	Old Point Comfort, VA
24th	1973	Sheridan, WY
25th	1974	Raleigh, NC
26th	1975	Coeur d'Alene, ID
27th	1976	Orlando, FL
28th	1977	Rapid City, SD
29th	1978	Annapolis, MD
30th	1979	Portland, OR
31st	1980	Austin, TX
32nd	1981	Gatlinburg, TN
33rd	1982	Vail, CO
34th	1983	Stone Mountain, GA
35th	1984	San Jose, CA
36th	1985	Clarksville, TN

No.	Year	HGS Location
37th	1986	Helena, MT
38th	1987	Pittsburg, PA
39th	1988	Park City, UT
40th	1989	Birmingham, AL
41st	1990	Albuquerque, NM
41st	1991	Albany, NY
43rd	1992	Fayetteville AR
44rd	1993	Tampa, FL
45th	1994	Portland, OR
46th	1995	Charleston, WV
47th	1996	Cody, WY
48th	1997	Knoxville, TN
49th	1998	Prescott, AZ
50th	1999	Roanoke, VA
51st	2000	Seattle, WA
52nd	2001	Cumberland, MD
53rd	2002	San Luis Obispo, CA
54th	2003	Burlington, VT
55th	2004	Kansas City, MO
56th	2005	Wilmington, NC
57th	2006	Breckinridge, CO
58th	2007	Pocono Manor, PA
59th	2008	Santa Fe, NM
60th	2009	Buffalo, NY
61st	2010	Oklahoma City, OK
62nd	2011	Lexington, KY
63rd	2012	Redding, CA
64th	2013	North Conway, NH
65th	2014	Laramie, WY
66th	2015	Sturbridge, MA
67th	2016	Colorado Springs, CO
68th	2017	Marietta, GA
69th	2018	Portland, ME
70th	2019	Portland, OR
71st	2022	Asheville, NC
72nd	2023	Tacoma, WA

# YOUNG AUTHOR AWARD

The Highway Geology Symposium has always encouraged participation of Young Professionals, realizing that Young Professionals are the future of the Organization. This participation was taken formal in 2014, with the formation of an annual National Young Author Competition, where Young Authors have the opportunity to prepare papers and present their work. To participate, Young Author's must be up to 35 years old or younger, the principal

author of the paper and the sole presenter of the paper at the Symposium. Papers are reviewed and judged based on Technical Presentation of the Paper (including Geology), Originality of the Work, Applicability of the Work to Others and Paper Layout. One Young Author is selected each year to receive the coveted Young Author Award, with presentation of the award conducted at the annual Symposium banquet

## Young Author Award Winners

**2014 Simon Boone,**

*"Performance of Flexible Debris Flow Barriers in a Narrow Canyon"*

**2015 Cory Rinehart,**

*"High Quality H20: Utilizing Horizontal Drains for Landslide Stabilization"*

**2016 Todd Hansen,**

*"Geologic Exploration for Ground Classification: Widening of the I-70 Veterans Memorial Tunnels"*

**2017 James Arthurs,**

*"Construction of Transportation Infrastructure in Weathered Volcanic Ash Soils"*

**2018 Brian Felber,**

*"Geotechnical Challenges for Bridge Foundations & Roadway Embankment Design in Peats and Deep Glacial Lake Deposits"*

**2019 Anya Brose,**

*"The Assessment and Remediation of Wabasha St. Rock Fall"*

**2022 Christopher Mayer**

*"Using Geophysics to Evaluate the Results of a Grouting Program in Karstic Geology"*

## HGS MEDALLION AWARD RECIPIENTS

Hugh Chase	1970	Vernon Bump	1986	Ken Ashton	2008
Tom Parrott	1970	C.W. "Bill" Lovell	1989	A. David Martin	2008
Paul Price	1970	Joseph A. Gutierrez	1990	Michael Vierling	2009
K.B. Woods	1971	Willard McCasland	1990	Dick Cross	2009
R.J. Edmondson	1972	W.A. "Bill" Wisner	1991	John F. Szturo	2009
C.S. Mullin	1974	David Mitchell	1993	Christopher Ruppen	2012
A.C. Dodson	1975	Harry Moore	1996	Jeff Dean	2012
Burrell Whitlow	1978	Earl Wright	1997	Eric Rorem	2012
Bill Sherman	1980	Russell Glass	1998	John Pilipchuk	2015
Virgil Burgat	1981	Harry Ludowise	2000	Peter Ingraham	2016
Henry Mathis	1982	Sam Thornton	2000	Richard Lane	2017
David Royster	1982	Bob Henthorne	2004	Steve Sweeny	2018
Terry West	1983	Mike Hager	2005	John Duffy	2018
Dave Bingham	1984	Joseph A. Fischer	2007	Krystle Pelham	2018

## EMERITUS MEMBERS OF THE STEERING COMMITTEE

Emeritus Status is granted by the Steering Committee

R.F. Baker	Mike Hager	David L. Royster
John Baldwin	Rich Humphries	Bill Sherman
David Bingham	Charles T. Janik	Willard L. Sitz
Vernon Bump	John Lemish	Mitchell Smith
Virgil E. Burgat	Richard Lane	Jim Stroud
Robert G. Charboneau	Bill Lovell	Steve Sweeney
Hugh Chase	A. David Martin	Sam Thornton
Jim Coffin	Henry Mathis	Berke Thompson
Dick Cross	William McCasland	Mike Vierling
A.C. Dodson	George S. Meadors, Jr.	Burrell Whitlow
Walter F. Fredricksen	David Mitchell	W.A. "Bill" Wisner
Brandy Gilmore	Harry Moore	Earl Wright
Russell Glass	W.T. Parrot	Ed J. Zeigler
Robert Goddard	Paul H. Price	
Joseph Gutierrez	Nicholas Priznar	

# HGS NATIONAL STEERING COMMITTEE OFFICERS

---

## **Krystle Pelham – Chairman**

NEW HAMPSHIRE DEPT. OF TRANSPORTATION  
BUREAU OF MATERIALS AND RESEARCH

PO Box 483  
5 Hazen Drive  
Concord, NH 03302-0483

**Phone:** (603) 271-1657

**Email:** Krystle.Pelham@dot.nh.gov

---

## **Kyle Halverson – Secretary**

KANSAS DEPARTMENT OF TRANSPORTATION  
BUREAU OF STRUCTURES AND GEOTECHNICAL  
SERVICES

700 SW Harrison St.  
Topeka, KS 66603

**Office:** 785-291-3860

**Cell:** 785-845-4332

**Email:** kyle.halverson@ks.gov

---

## **Bill Webster – Vice-chairman**

CALTRANS

5900 Folsom Blvd.  
Sacramento, CA 95819

**Phone:** (916) 662-1183

**Email:** bill\_webster@dot.ca.gov

---

## **John Pilipchuk – Treasurer**

NCDOT GEOTECHNICAL ENGINEERING UNIT

1020 Birch Ridge Drive  
Raleigh, NC 27699-1589

**Phone:** (919) 707-6851

**Email:** jpilipchuk@ncdot.gov

---

# HGS NATIONAL STEERING COMMITTEE MEMBERS

## **Ken Ashton – (Membership)**

WEST VIRGINIA GEOLOGICAL SURVEY

1 Mont Chateau Road  
Morgantown, WV 26508

**Phone:** (304) 594-2331

**Fax:** (304) 594-2575

**Email:** ashton@wvgs.wvnet.edu

---

## **Vanessa Bateman**

ENGINEERING & CONSTRUCTION HEADQUARTERS  
U.S. ARMY CORPS OF ENGINEERS

441 G Street NW  
Washington, DC 20314-1000

**Phone:** (202) 761-7423

**Email:** vanessa.c.bateman@usace.army.mil

---

## **Jeff Dean**

TERRACON

4701 North Stiles Avenue  
Oklahoma City, OK 73015

**Phone:** (405) 445-3280

**Email:** jeff.dean@terracon.com

---

## **John D. Duffy**

CALTRANS (RETIRED)

128 Baker Ave.  
Shell Beach, CA 93449

**Phone:** (805) 440-9062

**Email:** JohnDuffy@charter.net

## HGS NATIONAL STEERING COMMITTEE MEMBERS (CONTINUED)

---

### Mark Falk

WYOMING DOT

5300 Bishop Blvd.  
Cheyenne, WY 82009

**Phone:** (307) 777-4205

**Email:** mark.falk@wyo.gov

---

### Marc Fish

WSDOT STATE GEOTECHNICAL OFFICE

1655 S. 2nd Ave  
Tumwater, WA 98512

**Phone:** (360) 709-5498

**Email:** FishM@wsdot.wa.gov

---

### Kyle Halverson (Secretary)

KANSAS DEPARTMENT OF TRANSPORTATION  
BUREAU OF STRUCTURES AND GEOTECHNICAL  
SERVICES

700 SW Harrison St.  
Topeka, KS 66603

**Office:** (785) 291-3860

**Cell:** (785) 845-4332

**Email:** kyle.halverson@ks.gov

---

### Bob Henthorne

KANSAS DEPARTMENT OF TRANSPORTATION  
BUREAU OF STRUCTURES AND GEOTECHNICAL  
SERVICES

700 SW Harrison Street  
Topeka, KS 66603-3754

**Phone:** (785) 296-3531

**Email:** bob.henthorne@ks.gov

---

### Peter Ingraham

SCARPTEC INC.

19 Lord Jeffrey Drive  
Amherst, NH 03031

**Phone:** (603) 785-0262

**Email:** peter@scarptec.com

---

### Jody Kuhne

APPALACHIAN LANDSLIDE CONSULTANTS

78 Flint Street  
Asheville NC 28801

**Phone:** 828-779-9482

**Email:** jody@appalachianlandslide.com

---

### Richard Lane

NHDOT (RETIRED)

213 Pembroke Hill Rd.  
Pembroke, NH 03275

**Phone:** (603) 485-3202

**Email:** lanetrisbr@hotmail.com

---

### Sarah McInnes

PA DOT

District 6-0  
7000 Geerdes Blvd.  
King of Prussia, PA 19406

**Phone:** (610) 205-6544

**Email:** smcinnes@pa.gov

---

### Krystle Pelham (Chairman)

NEW HAMPSHIRE DEPT. OF TRANSPORTATION  
BUREAU OF MATERIALS AND RESEARCH

PO Box 483  
5 Hazen Drive  
Concord, NH 03302-0483

**Phone:** (603) 271-1657

**Email:** Krystle.Pelham@dot.nh.gov

---

### John Pilipchuk (Treasurer)

NCDOT GEOTECHNICAL ENGINEERING UNIT

1020 Birch Ridge Drive  
Raleigh, NC 27699-1589

**Phone:** (919) 707-6851

**Email:** jpilipchuk@ncdot.gov

---

## HGS NATIONAL STEERING COMMITTEE MEMBERS (CONTINUED)

---

### **Victoria Porto**

PA DOT (RETIRED)

10 Pine Lake Drive  
Carlisle, PA 17015

**Phone:** (717) 805-5941

**Email:** vamporto@aol.com

---

### **Erik Rorem**

GEOBRUGG NORTH AMERICA, LLC

20483 Whistle Punk Rd. 97702  
Bend, OR 97702

**Phone:** 1 505 690 7144

**Email:** erik.rorem@geobrugg.com

---

### **Christopher A. Ruppen (Young Author Committee)**

GEOSTABILIZATION INTERNATIONAL

3808 Sunflower Road  
New Brighton, PA 15066

**Phone:** (724) 272-7532

**Email:** chris.ruppen@gsi.us

---

### **Stephen Senior**

ONTARIO MIN OF TRANS. (RETIRED)

11 Dewbourne Ave.  
Richmond Hill, ON L4B 3G7 Canada

**Phone:** (416) 235-3734

**Email:** sa.senior@rogers.com

---

### **Tim Shevlin, R.G.**

GEOBRUGG NORTH AMERICA LLC

Salem, OR 97302

**Phone:** (503) 423-7258

**Email:** tim.shevlin@geobrugg.com

---

### **Deana Sneyd**

PETROLOGIC SOLUTIONS, INC.

3997 Oak Hill Road  
Douglasville, GA 30135

**Phone:** (678) 313-4147

**Email:** dsneyd@gmail.com

---

### **Steven Sweeney**

NY THRUWAY (RETIRED)

105 Albert Rd.  
Delanson, NY 12053

**Email:** 2ssweeney@gmail.com

---

### **John F. Szturo**

HNTB CORPORATION

715 Kirk Drive  
Kansas City, MO 64105

**Phone:** (816) 527-2275 (Direct Line)

**Cell:** (913) 530-2579

**Email:** jszturo@hntb.com

---

### **Bill Webster (Vice-chairman)**

CALTRANS

5900 Folsom Blvd.  
Sacramento, CA 95819

**Phone:** (916) 662-1183

**Email:** bill\_webster@dot.ca.gov

---

### **Terry West (Medallion, Emeritus)**

EARTH AND ATMOSPHERIC SCIENCE DEPT.  
PURDUE UNIVERSITY

West Lafayette, IN 47907-1297

**Phone:** (765) 494-3296

**Email:** trwest@purdue.edu

---

# HIGHWAY GEOLOGY SYMPOSIUM: PAST, PRESENT, AND FUTURE SYMPOSIUM CONTACT LIST

2013	New Hampshire	Krystle Pelham	603-271-1657	Krystle.Pelham@dot.state.nh.us
2014	Wyoming	Jim Coffin	307-777-4205	Jim.coffin@wyo.gov
2015	Massachusetts	Peter Ingraham	603-688-0880	peter_ingraham@golder.com
2016	Colorado	Ty Ortiz	303-921-2634	Ty.ortiz@state.co.us
2017	Georgia	Deana Sneyd	678-313-4147	Dsneyd61@gmail.com
2018	Maine	Krystle Pelham	603-271-1657	Krystle.Pelham@dot.state.nh.us
2019	Oregon	Scott Burns	503-725-3389	BurnsS@pdx.edu
2022	North Carolina	John Pilipchuk	919-707-6851	jpilipchuk@ncdot.gov
		Jody Kuhne	828-250-3285	jkuhne@ncdot.gov
2023	Washington	Marc Fish	360-485-5825	fishm@wsdot.wa.gov
2024	Kansas	Kyle Halverson	785-845-4332	kyle.halverson@ks.gov

# SPONSORS

The following companies have graciously contributed toward the sponsorship of the Symposium. The HGS relies on sponsor contributions for refreshment breaks, field trip lunches and other activities. We gratefully appreciate the contributions made by these sponsors.

## Platinum Level Sponsors

---



### Geobrugg

Kathryn Byrnes  
Email: [kathryn.byrnes@geobrugg.com](mailto:kathryn.byrnes@geobrugg.com)  
Phone: 505-771-4080  
<https://www.geobrugg.com/>

Wednesday  
Field Trip Lunch  
& Transportation

Geobrugg is the global leader in the supply of high-tensile steel wire, safety nets and meshes. 65 years of experience have made Geobrugg the answer to reliable solutions against natural hazards.

---



### GeoStabilization International & Access Limited

Paige Barnett  
Email: [paige.barnett@gsi.us](mailto:paige.barnett@gsi.us)  
Phone: 425-758-4757  
<https://www.geostabilization.com/>

Tuesday  
Lunch

GeoStabilization International® is the leading geohazard mitigation firm operating throughout the United States and Canada. We specialize in emergency landslide repairs, rockfall mitigation, and grouting using design/build and design/build/warranty contracting. GeoStabilization's team includes some of the brightest and most dedicated professionals in the geohazard mitigation industry. Our expertise, specialized tools, and worldwide partnerships allow us to repair virtually any slope stability or foundation problem in any geologic setting.

Our patented tools include the Soil Nail Launcher™, the Biowall® System, ScourMicropiles™, and SuperNails™, all of which we install using a combined fleet of over 50 purpose-built Soil Nail Launchers™ and purpose-built limited access drill rigs.

---

## Platinum Level Sponsors

---



### Maccaferri Inc.

Mike Koutsourais

Email: [m.koutsourais@maccaferri.com](mailto:m.koutsourais@maccaferri.com)

Phone: 301-223-6910

[www.maccaferri.com/us](http://www.maccaferri.com/us)

Wednesday

Field Trip Lunch  
& Transportation

With over 60 years' experience in rockfall and geohazard mitigation, Maccaferri offers both active systems to stabilize rock faces, soil slopes and snow masses and passive systems to overcome hydro-geological problems such as detachment of rock boulders, debris flows and shallow landslides. Maccaferri offers a wide range of engineered systems, certified and tested by leading institutes, in accordance with the latest standards. Our solutions are designed using state-of-the-art modeling software and techniques. 'Engineering a Better Solution': Maccaferri doesn't merely supply products; we work in partnership with our clients, offering technical expertise to deliver versatile, cost-effective and environmentally sound solutions. We aim to build mutually beneficial relationships through the quality of our service and solutions. Please visit us @ [maccaferri.com/us](http://maccaferri.com/us)

---

# Gold Level Sponsors

---



## **Ameritech Slope Constructors, Inc.**

Roger Moore  
Email: [rmoore@ameritech.pro](mailto:rmoore@ameritech.pro)  
Phone: 828-782-0522  
[ameritech.pro](http://ameritech.pro)

Thursday  
Closing Banquet  
Social Hour

Ameritech Slope Constructors, Inc. is geohazard mitigation company working in the U.S., Caribbean and Hawai'i. Ameritech constructs rockfall mitigation systems including rockfall barriers, rockfall drapes, rock bolting, rock scaling and rock drains. Ameritech constructs slope stabilization systems consisting of soil nails, steel mesh and spike plates. Ameritech also installs dry mix shotcrete as the surface material for stabilizing soil or rock slopes with soil nails or rock bolts. We also break larger rock blocks using a mechanical rock splitter or expansive grout.

---



## **Landslide Technology**

Darren Beckstrand  
Email: [darren.beckstrand@ccilt.com](mailto:darren.beckstrand@ccilt.com)  
Phone: 503-452-1200  
[www.landslidetechnology.com](http://www.landslidetechnology.com)

Monday  
Ice Breaker  
Reception

Landslide Technology, a division of Cornforth Consultants, Inc., provides planning, design, and construction services to owners of transportation infrastructure impacted by slope stability and geologic hazards (i.e., landslides and rockfall). Our experienced technical staff are available to assist design teams develop projects from initial concept through successful completion. Our focused expertise and nimble size allow us to respond quickly to projects across the nation and develop cost-effective strategies to mitigate complex geotechnical issues.

---

## Gold Level Sponsors

---



### Shannon & Wilson

Christina Steinburg  
Email: [christina.steinburg@shanwil.com](mailto:christina.steinburg@shanwil.com)  
Phone: 206-695-6743  
<https://www.shannonwilson.com/>

Tuesday  
Breakfast

Shannon & Wilson is an employee-owned geotechnical and environmental consulting firm headquartered in Seattle, Washington. Committed to technical excellence and high-quality service, we provide integrated geotechnical engineering, engineering geology, environmental, and natural resource services for clients worldwide. Since 1954, we have delivered comprehensive engineering and environmental solutions for the most challenging infrastructure planning, design, permitting, and construction conditions. We are dedicated to improving our communities, preserving the environment, and utilizing the most innovative science practices in all our work.

---



### WSP

Cody Stopka  
Email: [cody.stopka@wsp.com](mailto:cody.stopka@wsp.com)  
Phone: 307-461-1431  
<https://www.wsp.com/en-us>

Thursday  
Closing Banquet  
Keynote Speaker

WSP is a world leading engineering and professional services firm with representation in all 50 states. Passionate about solving geotechnical problems within the transportation and linear infrastructure industries, WSP is united by the common purpose of creating positive, long-lasting impacts on the communities and organizations we serve through innovation, integrity, and inclusion.

---

# Silver Level Sponsors

---



## Gannett Fleming

Deanna Cope  
Email: [dcope@GFNET.com](mailto:dcope@GFNET.com)  
Phone: 904-490-3103  
<https://www.gannettfleming.com/>

Symposium WiFi

Gannett Fleming is an international planning, design, technology, and construction management firm. For more than a century, we have pioneered important components of our nation's infrastructure. A cornerstone of our long history is the experience of our geotechnical and geological service in dams and earth structures, groundwater resources, building sites, and transportation corridors – including ports and harbors. Our professionals perform exploration, analysis, and design related to soil, rock, and groundwater.

---



## Global Rope Access

Josh Wagner  
Email: [josh.wagner@globalropeaccess.com](mailto:josh.wagner@globalropeaccess.com)  
Phone: 925-951-3956  
<https://www.globalropeaccess.com/slope-stabilization/>

Thursday  
AM Break

Global Rope Access is a niche geohazard mitigation contractor with expertise in high angle and remote access projects. Our crews are comprised entirely of SPRAT certified rope access technicians with experience working in varied environments ranging from highwall mines in the arctic circle to steep river canyons in mountainous terrain to unstable slopes along highways throughout western North America.

---

# Silver Level Sponsors

---



## Haley & Aldrich

Rachel Gamelin  
Email: [rgamelin@haleyaldrich.com](mailto:rgamelin@haleyaldrich.com)  
Phone: 617-862-6783  
<https://www.haleyaldrich.com/>

Thursday  
Breakfast

Haley & Aldrich, Inc. is committed to delivering the value our clients need from their capital, operations, and environmental projects. Our one-team approach allows us to draw from our 900 engineers, scientists, and constructors in more than 35 offices for creative collaboration and expert perspectives. Since our founding in 1957, we have had one goal in all we do: deliver long-term value efficiently, no matter how straightforward or complex the challenge.

---



## Rock Supremacy LLC

Rowan Anderegg  
Email: [rocksupremacyllc@gmail.com](mailto:rocksupremacyllc@gmail.com)  
Phone: 541-383-7625  
<https://rocksupremacy.com/>

Tuesday  
PM Break

Rock Supremacy, LLC is a civil construction company specializing in rockfall mitigation, slope stabilization, and tunnel rehabilitation with over 30 years of experience.

---

## Bronze Level Sponsors

---



### Apex Rockfall

Sarah Walton  
Email: [swalton@apexrfm.com](mailto:swalton@apexrfm.com)  
Phone: 925-503-7078  
[www.apexrockfall.com](http://www.apexrockfall.com)

Apex Rockfall Mitigation is a leader in the rockfall and geo-hazard stabilization industry. Our experience in restricted and limited access locations is unsurpassed. Apex continues to create and deploy some of the most hi tech equipment, materials, techniques and tools available to the industry. Apex Rockfall Mitigation has wide ranging ability allowing us to provide rock solid services throughout the country.

---



### BGC Engineering

Julia Frazier  
Email: [jfrazier@bgcengineering.ca](mailto:jfrazier@bgcengineering.ca)  
Phone: 720-598-5982  
<https://www.bgcengineering.ca/>

BGC Engineering is an international company of over 750 professional engineers, geoscientists, technicians, and software professionals with specialists in the areas of geotechnical engineering, engineering geology, risk assessment, asset management, geohazard identification and mitigation, and software development. We invest significantly in research and development programs and partner with university researchers and others around the world to advance the state of practice for our clients. BGC Engineering focuses on measurably reducing disruptions to linear infrastructure from geohazards using onsite inspections and incorporating remote sensing technology such as lidar change detection, InSAR and other earth observation data analysis into asset management and informed decision making. We have developed GIS and web-based software services and have used machine learning for calibration of predictive algorithms that inform operational risk management decisions for over 200,000 miles of pipeline and transportation assets throughout North America. BGC Engineering pioneers responsible solutions to complex earth science challenges.

---



### Delve Underground

Allison Halvorson  
Email: [halvorson@delveunderground.com](mailto:halvorson@delveunderground.com)  
Phone: 925-705-4133  
[www.delveunderground.com](http://www.delveunderground.com)

Delve Underground is a leader in heavy civil engineering, serving the transportation, water, wastewater, and energy industries. Specializing in tunnel design, we provide innovative solutions to the most challenging underground problems. We offer comprehensive design, construction management, and dispute resolution capabilities. Founded in 1954, as Jacobs Associates, Delve Underground is an employee-owned firm with 21 offices and 350 team members throughout the United States, Canada, Australia, and New Zealand.

---

## Bronze Level Sponsors

---



### Hager-Richter Geoscience, Inc.

Jeffrey Reid

Email: [jeff.reid@hager-richter.com](mailto:jeff.reid@hager-richter.com)

Phone: 603-370-7518

<http://hager-richter.net/>

HAGER-RICHTER GEOSCIENCE, INC. (HRGS) is an established small business that specializes in surface and borehole geophysics services for engineering and environmental applications (NAICS 541360). The firm has been in business since 1984, has grown to be one of the largest full service geophysical specialty firms in the eastern United States, and has earned a national reputation for quality geophysical services. HRGS has fully staffed and equipped offices in New Hampshire and New Jersey, allowing rapid response to projects anywhere in the eastern United States. HRGS specializes in surface and borehole geophysical services for environmental and engineering projects, geotechnical support services, subsurface utility engineering services (designation and mapping), and non-destructive testing services.

---



### Jean Lutz North America LLC

Michel Lariau

Email: [contact@jeanlutzna.com](mailto:contact@jeanlutzna.com)

Phone: 330-702-1476

<https://www.jeanlutzamerica.com/>

Manufacturer of advanced quality assurance monitoring instrumentation applied to Deep Foundations, MWD and Geotechnical Construction.

---



### Voss Signs

Tom Tenerovicz

Email: [tom@vosssigns.com](mailto:tom@vosssigns.com)

Phone: 315-682-6418

<https://vosssigns.com/>

Signage Sponsor

Since 1965, Voss Signs, LLC has produced custom and stock signs for various customers that include: Forestry Professionals, Land Owners, State and Federal Government Agencies.

---

# ADVERTISEMENTS



## OUR SERVICES

- Rock Scaling
- Soil Nailing
- Slope Stabilization
- Rock Bolting
- Rockfall Drapes
- Rockfall Barriers
- Slope Drains
- Shotcrete

## CONTACT INFORMATION

Office Address:

21 Overland Industrial Blvd,  
Asheville , NC 28806

Mailing Address:

PO BOX 2702  
Asheville, NC 28802

Phone: 828-633-6352

Fax: 828-633-6353

Website: [www.ameritech.pro](http://www.ameritech.pro)

**SHANNON & WILSON**

Geotechnical Engineering	Seismic Engineering
Geologic Hazard Evaluations	Hydrogeology
Construction Dewatering	Surface Water
Environmental Remediation	Tunneling
Natural Resources	Instrumentation

**INTEGRATED SERVICES FOR TRANSPORTATION PROJECTS**

LOCAL EXPERTISE | OFFICES NATIONWIDE

[WWW.SHANNONWILSON.COM](http://WWW.SHANNONWILSON.COM)



**Landslide  
Remediation**

**Bridge  
Rehabilitation**

**Sinkhole  
Repair**

**Rockfall  
Mitigation**



**Why Partner With Us:**

- Design/Build cost effective solutions
- Reopen critical infrastructure in days, not months
- No-obligation, fixed-cost proposals within 24 hours
- 24/7 emergency response across the United States and Canada

**Spider Excavator  
Demonstration!**

See us at our booth for details.



**855.647.6150**  
**GeoStabilization.com**



# Creating Better Geotechnical and Geological Solutions, Together.

[gannettfleming.com](http://gannettfleming.com)



## ROCK SOLID PROFESSIONALS.

100% SPRAT CERTIFIED  
GEOHAZARD MITIGATION  
SERVICES

- ▲ SCALING
- ▲ DRILLING
- ▲ MESH SYSTEM INSTALLATION
- ▲ BARRIER INSTALLATION

[www.globalropeaccess.com](http://www.globalropeaccess.com)

1-866-762-5439



# Rock Supremacy



### Slope Stabilization

We are a one-stop-shop for your next retaining wall project from a basic cantilevered concrete, battered micropile foundation or a heavy duty anchored soldier pile wall.



### Rockfall Mitigation

We are highly skilled in stabilizing rock slopes using pinned faco® systems, cable/ting netting, and double twist wire mesh. We also perform rock scaling, rock bolting/bowling and many other rockfall mitigation measures.



### Drilling

We have extensive experience in drilling multiple variations of rock bolts/rock dowels, cable anchors, micropiles, rock sockets, tie-backs or horizontal drains in all types of subsurface environments.



### Tunnel Rehabilitation

We specialize in rehabilitating or providing new tunnel construction with steel set erection, road heading, tunnel notching, liner removal, and applying shotcrete.



### Shotcrete

We use a proprietary formula to effectively seal canals, soil nail walls or rock/soil surfaces. Our mix design is extremely durable and can be colored to match existing native landscapes. We also perform sculpting & staining services.



### Landslide Remediation

We have years of experience solving landslide problems with a wide range of solutions to reach the perfect solution.



541.383.ROCK (7628) | [info@RockSupremacy.com](mailto:info@RockSupremacy.com) | [RockSupremacy.com](http://RockSupremacy.com)

66147 N Hwy 87, Bend, OR 97701



# STABILIZATION AND EROSION PROTECTION IN ONE

## TECCO® GREEN Slope Stabilization

**Geobrugg North America, LLC**

22 Centro Algodones  
Algodones, NM 87001 USA



[www.geobrugg.com/tecco](http://www.geobrugg.com/tecco)



Question  
today/  
*Imagine*  
*tomorrow*/  
Create for  
the future

---



Find out what we  
can do for you.  
[wsp.com](http://wsp.com)



## Novel approaches for a better result

**That's the Haley & Aldrich way.**

### **Our services**

- Construction
- Contaminated site management
- EHS compliance
- Geotechnical engineering
- Lean consulting
- Resilience
- ESG and sustainability
- Water resources

[haleyaldrich.com](http://haleyaldrich.com)

A graphic element on the right side of the slide, featuring a dark grey background with a light grey geometric pattern of interconnected lines forming various shapes. The Haley & Aldrich logo is positioned at the bottom right of this graphic.

**HALEY  
ALDRICH**



**MACCAFERRI**

*Wash DOT I-90 Snoqualmie Pass*

## Safeguard Highways with *MACCAFERRI ROCKFALL PROTECTION*

### Why Choose Maccaferri?

**Superior Performance:**

Engineered systems, certified and tested by leading institutes offering state of the art solutions for geohazard mitigations.

**Superior Reliability:**

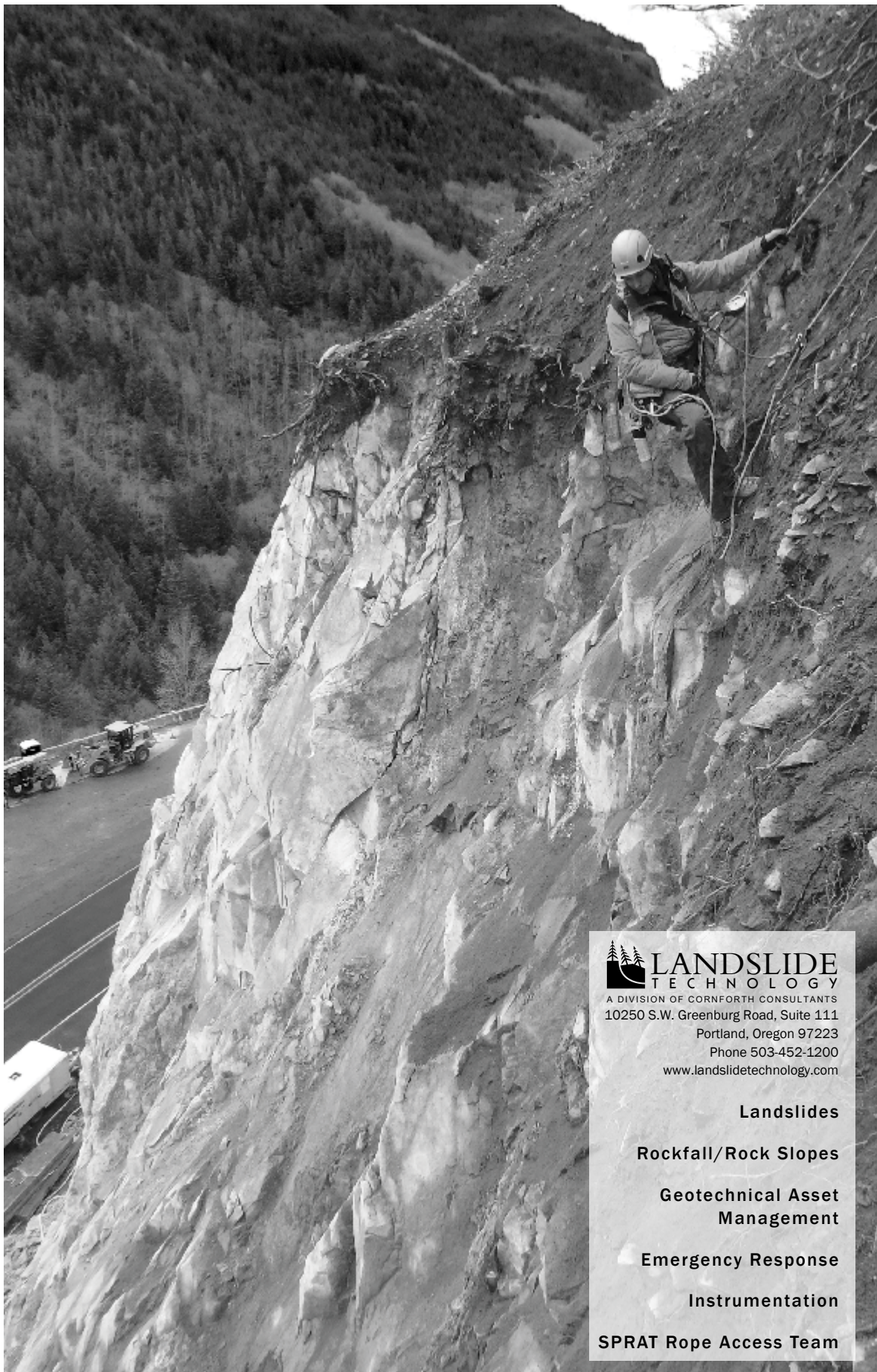
Over 60 years of experience stabilizing rockfaces, soil slopes, shallow landslides, debris flow, and avalanche hazards.

**Superior Integration:**

Polymeric coatings seamlessly blend with the environment while providing increased service life and protection.

<https://www.maccaferri.com/us/>





 **LANDSLIDE  
TECHNOLOGY**  
A DIVISION OF CORNFORTH CONSULTANTS  
10250 S.W. Greenburg Road, Suite 111  
Portland, Oregon 97223  
Phone 503-452-1200  
[www.landslidetechnology.com](http://www.landslidetechnology.com)

**Landslides**

**Rockfall/Rock Slopes**

**Geotechnical Asset  
Management**

**Emergency Response**

**Instrumentation**

**SPRAT Rope Access Team**

## Exhibitors

---



### **Acker Drill Co., Inc.**

John Lang

Email: [jlang@ackerdrill.com](mailto:jlang@ackerdrill.com)

Phone: 570-586-2061

<https://www.ackerdrill.com/>

Celebrating over 100 Years! Acker Drill Company was founded in 1916 and has been exporting its products worldwide since 1960. Today, we are recognized as a world leader in the manufacture of drill rigs and tooling for the geotechnical, environmental, mineral exploration, mining, and civil engineering industries.

---



### **BoreDM LLC**

Louis Aaron

Email: [louis@boredmlogs.com](mailto:louis@boredmlogs.com)

Phone: 602-492-3076

<https://www.boredmlogs.com/landing>

BoreDM is web-based software for logging, reporting, analyzing, and sharing geotechnical and environmental data. At its core, BoreDM is a data management program; it is designed to provide DOTs and consultants with unconstrained access to their borehole and laboratory data in a well-structured format. BoreDM also includes critical reporting exports (like stick diagrams and gradation plots) and powerful analysis tools which were previously infeasible due to uncontrolled customization and variation across DOT and consultant data. Though BoreDM is principally a data management tool, it also provides an intuitive user interface, eliminating common barriers to entry and enabling effortless adoption for firms and public entities of all sizes. It integrates the critical features provided by gINT (including Excel-like data tables) with a modern user interface which is accessible to engineers of all backgrounds. BoreDM provides a single platform for your entire geotechnical workflow, from data entry and calculations to internal review and report generation:- Fast and familiar data entry- GIS mapping- 2D cross sections- Exports to Excel, KML, DXF +- Rock solid data security- DOT + DIGGS compatibility- Lab data and calculations- Minimal-typing tablet app for field- Zero downloads, everOur approach is rooted in the experience of gINT users and executed with the urgency of a tech company. Since our software is web-based, we can implement your feature requests within a day. Contact us at [hello@boredmlogs.com](mailto:hello@boredmlogs.com) to learn more.

---

## Exhibitors

---



### Central Mine Equipment Company

Bill White

Email: [BWhite-CME@prodigy.net](mailto:BWhite-CME@prodigy.net)

Phone: 800-325-8827

<https://cmeco.com>

CME manufactures auger, core and rotary drilling rigs mounted on trucks, skids, tracks, and rubber-tire all-terrain carriers. We also manufacture hollow stem augers, conventional flight augers, sampling and drilling tools to support our machines.

---



### DOWL

Keri Nutter

Email: [knutter@dowl.com](mailto:knutter@dowl.com)

Phone: 503-620-6103

<https://www.dowl.com/>

DOWL provides a wide range of civil and structural engineering and related services, including the design of roadways, highways, airfields, and trail systems; bridges and structures; geotechnical engineering and materials testing; water, sewer and storm drain systems; environmental documentation and permitting; water rights planning and design. Our staff of dedicated professionals consistently exceeds our client's expectations and has enabled us to develop into one of the West's leading planning, surveying, civil/transportation, and environmental services firms. Today, we offer a wide range of engineering services to public and private clients, with offices in Alaska, Arizona, Colorado, Montana, Nevada, Oregon, Washington, and Wyoming. DOWL's geoscience professionals use soil & rock mechanics, geophysical surveys, and soils engineering to solve practical problems related to infrastructure development comprised of or supported by soil and rock. Drawing on the expertise of our geotechnical engineering and geoscience professionals, and using current and innovative tools, we specialize in evaluating subsurface conditions and their impacts for any project; from the planning and permitting stages, into fieldwork and data collection, and through design and construction.

---

# Exhibitors

---



## **Foothills Drilling Equipment, Inc.**

Paul Hale

Email: [paul@foothillsequipment.com](mailto:paul@foothillsequipment.com)

Phone: 828-802-1015

<https://foothillsequipment.com/>

Foothills Drilling Equipment serves the construction drilling industry with the highest quality products and equipment on the market. We pride ourselves on our excellent customer service and responsiveness. Our product line of TEI Drills, Intric Grout Plants, and now TesCar limited access shaft drilling rigs means Foothills has the solution you need to get the job done.

---



## **Foundation Testing & Consulting, LLC (FTC)**

William Jones

Email: [cj@ftandc.com](mailto:cj@ftandc.com)

Phone: 913-626-8499

<https://www.ftandc.com/>

Foundation Testing and Consulting, LLC provides the full range of deep foundation testing services to support the construction of pile and drilled shaft supported bridge foundations. Our services include cross-hole sonic logging and thermal integrity profiling of drilled shafts and dynamic pile testing.

FTC has expanded its service line to include compilation of historical pile installation data for departments for transportation into our PileTrac application. PileTrac is a relational database with cloud-based interactive dashboards that permits a full range of data analytics to understand past design and installation challenges and to identify trends and root causes. The PileTrac application is an online, subscription based service. FTC also provides seismic refraction survey services to better characterize subsurface soil and rock conditions at bridge sites and to provide better predictions for likely pile tip elevations.

---

## Exhibitors

---



### GeoEngineers, Inc.

Andy Caneday

Email: [acaneday@geoengineers.com](mailto:acaneday@geoengineers.com)

Phone: 425-861-6000

<https://www.geoengineers.com/>

GeoEngineers is an earth science and engineering consulting firm headquartered in the Pacific Northwest. With nearly 400 employees in 21 nationwide offices, we provide local, state and Federal agencies with geotechnical, engineering geology, and seismic engineering services for transportation projects across the U.S.

---



### GEOKON

Beth Culver

Email: [bculver@geokon.com](mailto:bculver@geokon.com)

Phone: 603-448-1562

<https://www.geokon.com>

GEOKON is a recognized world leader in the manufacture of structural and geotechnical instrumentation. Founded in 1979, GEOKON has grown to more than 130 associates and offers a full complement of instrumentation for a wide range of industries including tunnels, dams, mines, piles, bridges, pipelines, landfills, embankments, transportation and wind turbines. Over 45 GEOKON agents distribute products globally to North and South America, Europe, Middle East, China, Russia, Asia Pacific, Australia and New Zealand. GEOKON incorporates state-of-the-art manufacturing processes and equipment to produce the highest quality and performing products on the market. Mechanical, electrical and software engineering teams collaborate to develop the most innovative, accurate and reliable instrumentation in the industry. As a result, GEOKON has been awarded ISO 9001:2015 registration from both ANSI•ANAB, USA and UKAS of Great Britain. GEOKON's calibration program complies with ANSI/NCSL Z540-1 and all primary calibration standards are traceable to the US Department of Commerce, National Institutes of Standards and Technology (NIST), in Washington, DC, and are calibrated by laboratories with ISO/IEC 17025 accreditation. In addition, GEOKON is a qualified supplier for US Nuclear Facilities in accordance with the American Society of Mechanical Engineers (ASME)/Nuclear Quality Assurance (NQA)-1, Quality Assurance Program Requirements. GEOKON products are supported by an experienced team of factory-trained associates ready to assist with instrument design, selection and installation. All products include a full, 13-month warranty. For more information, please visit [www.geokon.com](http://www.geokon.com), email us at [info@geokon.com](mailto:info@geokon.com) or call +1-603-448-1562.

---

# Exhibitors

---



## Geoprevent

Severin Staehly

Email: [severin.staehly@geoprevent.com](mailto:severin.staehly@geoprevent.com)

Phone: 4-177-222-5525

<https://www.geopraevent.ch/?lang=en>

Geoprevent develops, installs and operates premium alarm and monitoring systems for natural hazards. We focus on customer-specific and highly reliable solutions. Thanks to our multidisciplinary team we are able to develop, build and install hardware as well as software in-house. This allows us to act fast and implement projects straightforwardly.

---



## Geovert LLC

Steve Farrand

Email: [steve.farrand@geovert.com](mailto:steve.farrand@geovert.com)

Phone: 303-547-2027

<https://www.geovert.com/>

Geovert is a specialist construction contractor specializing in difficult-access slope stabilization and rockfall solutions. As a global leader, Geovert offers a wide range of services that address complex geotechnical challenges in various industries.

---

# Exhibitors

---



## **Gilson Company Inc**

Jen Hanley

Email: [jhanley@gilsonco.com](mailto:jhanley@gilsonco.com)

Phone: 800-444-1508

[www.globalgilson.com](http://www.globalgilson.com)

Gilson Company, Inc. is a 3rd generation family-owned company that has provided over 80 years of service to our industry. Throughout all these years our core values have never changed, we continue to treat our customers with the best care possible, even if it means pointing them in a different direction. Helping them find the best solutions to their problems is the most important thing to us. As the company has grown, so has our reputation for superior expertise, innovation, and development. While we constantly seek and develop new and better products, our values stay the same; we offer high-quality products at a competitive price, and backup our great customer service with dedicated technical support.

---



## **Multi-Power Products**

Joel Savard

Email: [jsavard@multipowerproducts.com](mailto:jsavard@multipowerproducts.com)

Phone: 250-860-6969

<https://multipowerproducts.com/english/>

Multi-Power Products is a Canadian manufacturer of Geotechnical, Environmental and Exploration drills and drilling equipment located in Kelowna, British Columbia.

---



## **Pacific Blasting**

Chris Fahr

Email: [chris.fahr@norlandlimited.com](mailto:chris.fahr@norlandlimited.com)

Phone: 604-809-8852

<https://www.pacificblasting.com/blasting/>

Pacific Blasting have provided a wide range of mining, rock slope stabilization and precision blasting services locally and internationally since 1954. During the last 60 years, our team of specialists have successfully completed hundreds of projects in the most challenging of conditions. This experience enables us to develop innovative and cost effective solutions for safely and efficiently completing any project.

---

# Exhibitors

---



## **Rocscience**

Robert Bradford

Email: [sofia.melnychenko@rocscience.com](mailto:sofia.melnychenko@rocscience.com)

Phone: 416-698-8217

<https://www.rocscience.com/>

Since 1996, Rocscience has been a company focused on bridging the gaps in analysis, design, and visualization tools for the mining and civil engineering industries. Born as a spin-off company from the University of Toronto, our software development combines innovation and research, allowing us to develop world-class software solutions that work for you today and will evolve to meet your needs tomorrow. Our motto “Geotechnical tools, inspired by you” means we are continuously listening to your specific geotechnical challenges so that we can build tools to help you overcome them. Whether you’re focused on slope stability, excavation design, or foundation analysis, our comprehensive suite of 18 programs means that no matter what your needs are, we have a software solution for your projects.

---



## **SIMCO Drilling Equipment Inc.**

Ryan Gross

Email: [RGROSS@SIMCODRILL.COM](mailto:RGROSS@SIMCODRILL.COM)

Phone: 515-490-3868

<https://SIMCODRILL.COM>

SIMCO® Drilling Equipment, Inc. began designing and building all-hydraulic, tophead drive drilling rigs in 1971 at our manufacturing facility located in Osceola, Iowa. SIMCO rigs are used for water well and geothermal well drilling, geotechnical and environmental drilling, mineral exploration, geothermal wells, construction and utility work, and a wide range of other diverse applications.

---

# Exhibitors

---



## **Trumer Schutzbauten**

Ahren Bichler

Email: [a.bichler@trumer.cc](mailto:a.bichler@trumer.cc)

Phone: 604-732-0325

[www.trumerschutzbauten.com](http://www.trumerschutzbauten.com)

TRUMER SCHUTZBAUTEN is a world leader in the design and manufacturing of geohazard mitigation structures that protect against rockfall, debris flow, avalanche and unstable slopes. From slope mesh to massive barriers, we protect life, buildings and infrastructure where failure is not an option. With TRUMER's recent acquisition of Pfeifer Isofer (now TRUMER ISOFER), they offer product lines tested following Austrian, Swiss and European approvals to make sure their clients receive the solution that best suits their needs.

---



## **Williams Form Engineering Corp.**

Ryan Williams

Email: [ryan@williamsform.com](mailto:ryan@williamsform.com)

Phone: 616-785-6168

[www.williamsform.com](http://www.williamsform.com)

Williams Form Engineering Corporation has been providing threaded steel bars and accessories for rock, soil and concrete anchors, post-tensioning systems, and concrete forming hardware systems in the construction industry for over 100 years. Our rock and soil anchor product line includes our Spin-Lock mechanical rock anchors, polyester resin anchors, multiple corrosion protection anchors, soil nails, strand anchors, Manta Ray soil anchors, Geo-Drill Hollow-Bar anchors, and micropiles. For concrete anchoring we offer Spin-Lock anchors, undercut anchors, reusable anchors and cast-in-place anchors. We also have a full line of All-Thread Rebar for tiebacks, micropiles and post-tensioning.

---

# PAPERS

**Tuesday, August 15, 2023**

No.	Time	Title	Primary Author	Page
1	8:50 AM – 9:10 AM	Young Author Presentation: Innovative Geophysical Application for Bridge Foundation Design and Construction	Ronan Jones	51
2	9:10 AM – 9:30 AM	Young Author Presentation: Design and Construction of a Bottom-up Retaining Wall in Slickensided Red Bed Material	Kirsten Grant	62
3	10:00 AM – 10:20 AM	Young Author Presentation: Impacts of Weak Rock Units on Cut Slope Construction	Justin Manning	82
4	10:20 AM – 10:40 AM	Young Author Presentation: Comparative Analysis of Rock Slope Scaling Quantities and Crew Hours: A Strategic Approach for Standardizing the Practice	Katlyn Card	102
5	10:40 AM – 11:00 AM	Young Author Presentation: Seward Highway Rockfall Mitigation, Anchorage, Alaska	Sebastian Dirringer	123
6	11:00 AM – 11:20 AM	Young Author Presentation: A Multi-Phased Approach to Rockfall Mitigation at Don Pedro Dam: Lessons Learned for Critical Facilities and Roadways	Joey Renner	142
7	11:20 AM – 11:40 AM	Young Author Presentation Bolt Creek Fire: Post-Wildfire Debris Flow Risk Assessment and Barrier Design on US 2, Near Grotto, WA	Cody Chaussee	161
8	11:40 AM – 12:00 PM	Young Author Presentation: Emergency planning and mitigation for post-fire debris flows in Glenwood Canyon, Colorado	Aliena Debelak	187

## PAPERS (CONTINUED)

Tuesday, August 15, 2023 (continued)				
No.	Time	Title	Primary Author	Page
9	1:00 PM – 1:20 PM	Young Author Presentation: Freemont Hall Landslide	Jamie Cravens	207
10	1:20 PM – 1:40 PM	Landslide Study and Final Repair Design Route 3 Randolph County, Missouri	John Szturo	227
11	1:40 PM – 2:00 PM	The SR112 / Clallam Bay Landslide(s) - Characterization and Mitigation	Gabe Taylor	248
12	2:00 PM – 2:20 PM	State Route 112: Landslide Alley – Striving for Resiliency	Tom Badger	266
13	2:20 PM – 2:40 PM	Raised Draperies - Defining Hybrid Barriers and Attenuators by Application	John Duffy	283
14	2:40 PM – 3:00 PM	How To Develop Rockslope Mitigation for Very Large Roadway-Dipping Blocks Along an Interstate Highway	Stephen Newman	300
15	3:30 PM – 3:50 PM	“What If the Rock Only Threatens to Fall?” Emergency Response to a Decoupled Cliff Face in Washington State	Eric Smith	316
16	3:50 PM – 4:30 PM	I-90 Rock Slopes: A Retrospective of the Snoqualmie Pass Project	Norm Norrish	336

## PAPERS (CONTINUED)

### Thursday, August 17, 2023

No.	Time	Title	Primary Author	Page
17	8:00 AM – 8:20 AM	Climate Resilience and Infrastructure Adaptation on California’s National Forests	Gordon Keller	338
18	8:20 AM – 8:40 AM	Geohazard Management on Colorado SH 133 From Planning to Mitigation	Randy Post	355
19	8:40 AM – 9:00 AM	The State of Measurement While Drilling for the Washington State Department of Transportation	Mike Mulhern	372
20	9:00 AM – 9:20 AM	Advancing Subsurface Investigations Beyond the Borehole with Passive Seismic Horizontal-to-Vertical Spectral Ratio and Electromagnetic Geophysical Methods at Transportation Infrastructure Sites in New Hampshire	J.R. Degnan	387
21	9:20 AM – 9:40 AM	Non-destructive Surface Wave Geophysics Characterizes Salt Dissolution 140m Under US Highway 50 at Brandy Lake, Reno County, Kansas	Johari Pannalal	411
22	9:40 AM – 10:00 AM	Mitigation Alternatives for Salt Dissolution Subsidence Impacting US Highway 50 at Brandy Lake, Reno County, Kansas	Jeff Keaton	428
23	10:30 AM – 10:50 AM	Using State-of-the-Art Technologies and Tools for Geotechnical Investigation and Design	Brian Collins	443
24	10:50 AM – 11:10 AM	The Development and Utilization of a Cloud-Based Database and Visualization App for Pile Results and Design: PileTrac	Kyle Halverson	461
25	11:10 AM – 11:30 AM	Pavement Bump at the Bridge End Elimination	Jeremiah Kokes	473
26	11:30 AM – 11:50 AM	US 460 Bridges over Marrowbone Creek, Pond Creek and Russell Fork River	Tony Beckham	493

## PAPERS (CONTINUED)

Thursday, August 17, 2023 (continued)				
No.	Time	Title	Primary Author	Page
27	1:00 PM – 1:20 PM	Taking into Account the Fragmentation and Variability of Rockfall and the Third Dimension in Rockfall Barrier Design	Tim Shevlin	513
28	1:20 PM – 1:40 PM	Introducing A New Impact Alert System for Rockfall Barriers	Sage Evans	526
29	1:40 PM – 2:00 PM	The Geohazard Pro must know “Section 262 Slope Scaling”	Todd Hansen	537
30	2:00 PM – 2:20 PM	Rock Stabilization at Pompeys Pillar National Monument: The Use of Numerical Modeling to Analyze Risk of Toppling Failure	Anya Brose	554
31	2:20 PM – 2:40 PM	Padden Creek I-5 Stream Crossing	Mark Rose	573
32	2:40 PM – 3:00 PM	The Erodibility Index in Washington State's Intermediate Geomaterials: The Need for a Practical Tool	Robert Humphries	593
33	3:30 PM – 3:50 PM	Accelerating the Transition to Digital Deliverables	Katie Aguilar	629
34	3:50 PM – 4:10 PM	GIS Enterprise-based Prototype Erosion and Slope Stability Screening Tool for Transportation Infrastructure Management	Bin Wang	643
35	4:10 PM – 4:30 PM	Integrating Field Data with Physics Engine Simulations of Fragmental Rockfalls	R. MacPhail	665
36	4:30 PM – 4:50 PM	Emergency Response and Cures for Karst on Chemical Road	Sarah McInnes	685
37	4:50 PM – 5:10 PM	A Comprehensive Approach to Rock Slope Design Solutions along NC-88 in Ashe County, North Carolina	Bret Watkins	711
38	5:10 PM – 5:30 PM	Hybrid Design Approach for Anchored Wire Mesh: Towards A Displacement Based Design	Lucas Martins	735

# **Seismic Refraction Case Studies: Correlation with PDA Plan Tip Elevation**

**Ronan Jones**

Foundation Testing & Consulting LLC

16500 Lucille St.

Overland Park, KS 66062

(913)-263-2336

RJones@FTandC.com

### **Acknowledgements**

The author is deeply appreciative of the individuals and entities that have contributed to the insights and findings regarding seismic refraction presented in this study:

Casey Jones, P.E., P.G. - Foundation Testing and Consulting LLC  
Jordan Toogood – President & CEO at King Construction Company, Inc.  
Gretchen Schmauder Ph.D., MBA, P.G. – Geometrics

### **Disclaimer**

Statements and views presented in this paper are strictly those of the author(s), and do not necessarily reflect positions held by their affiliations, the Highway Geology Symposium (HGS), or others acknowledged above. The mention of trade names for commercial products does not imply the approval or endorsement by HGS.

### **Copyright Notice**

Copyright © 2023 Highway Geology Symposium (HGS)

All Rights Reserved. Printed in the United States of America. No part of this publication may be reproduced or copied in any form or by any means – graphic, electronic, or mechanical, including photocopying, taping, or information storage and retrieval systems – without prior written permission of the HGS. This excludes the original author(s).

## ABSTRACT

Geophysics, particularly seismic refraction and multi-channel analysis of surface waves (MASW), has emerged as a reliable method for sub-surface investigations in the design of deep foundations for bridges. Our company, Foundation Testing and Consulting, has developed and brought to market an innovative geophysical application for bridge foundation design over the past year. In this research, we have developed a strong correlation between compression wave velocities and historical PDA-tested capacity and penetration depths for piling.

This paper provides a detailed discussion on the use of seismic refraction and MASW in bridge foundation design and highlights the advantages it offers over traditional methods.

This paper presents the first instance in which our geophysical application was utilized to save a contractor over \$60,000 on shortened pile lengths in Wichita, Kansas. The study area included a well-known weathered Wellington shale profile that presented challenges for pile foundation design. By using our geophysical application, we were able to identify the depth of the bedrock and assess the soil properties and likely pile penetration depths within weathered shale bedrock to optimize pile order lengths and reduce project delays.

Our geophysical application offers a non-destructive, fast, and cost-effective alternative and supplement to traditional site investigation methods, making it an attractive option for pile supported projects of all sizes.

## INTRODUCTION

### Overview of Seismic Refraction

Seismic refraction, a geophysical principle employed in diverse geological and engineering contexts, exploits the refractive properties of seismic waves to elucidate subsurface structures. It is frequently utilized to outline variations in ground hardness, detect subterranean cavities or profile site stratigraphy, but is seldom used for bridge site characterization. Furthermore, due to its efficient deployment by a small crew, it offers a cost-effective solution for subsurface investigations.

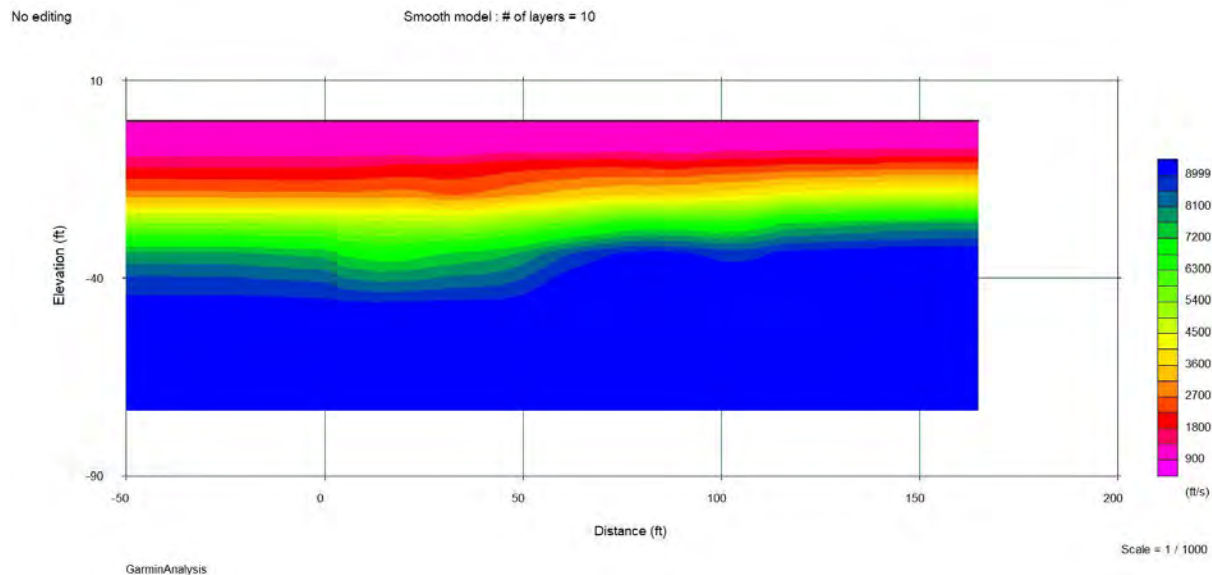


**Figure 1 – Seismic Refraction Plot Example**

### Purpose of the Study and Research Questions

Emerging trends from the compilation of the PileTrac database, a relational PDA piling database, produced by Foundation Testing and Consulting, LLC of Overland Park, Kansas, indicated significant pile plan length discrepancies were often linked to inadequate subsurface investigation or data misinterpretation. This study seeks to examine the efficacy of seismic refraction as a method of subsurface investigation to predict pile tip penetrations. The study utilized a 3-week geode seismograph rental from Geometrics, and through this, seismic refraction was performed on 18 bridge sites in Kansas. However, this paper focuses on the 8 sets with high-quality seismic refraction data and robust historical PDA site data. This study seeks to answer:

- Can a correlation between compression wave velocity profiles and PDA results be established?

- How effectively can seismic refraction predict pile tip penetrations in diverse geological contexts?
- What insights and improvements can be drawn from our novel case studies?
- What implications might these findings have for future geophysical survey applications and bridge site characterizations?

## **Prior Methods for the Accurate Prediction of Pile Tip Elevation**

Predicting pile tip elevation before pile installation is a critical component of construction projects' planning and design phase. Established subsurface investigation methods, such as soil sampling and in-situ tests like Standard Penetration Tests (SPT), and Cone Penetration Tests (CPT), assist in predicting the depth to which a pile needs to be driven to achieve the required capacity. However, due to significant variability in results based on factors such as the drilling crew's experience, distance from the substructure, and interpretation of results, the integration of these validated approaches with additional geophysical survey methods could potentially improve pile tip elevation prediction accuracy and reliability. This gap in the existing engineering literature represents a potential area this study seeks to address.

## **Research Design**

### *1. Selection and Description of Case Studies*

This investigation included bridge construction sites across Kansas with a spectrum of geological conditions. All tests were performed on pre-existing bridge structures with steel piling, with PDA data performed and sourced from FTC. Selected sites had safe access to perform a 160-240 feet long array either along the shoulder of the road or parallel to an abutment. Given there are only 8 sites represented in the study, all bridge sites have either steel HP12X53 or HP10X42 and are end-bearing.

### *2. Data Collection Method*

We selected seismic refraction due to its cost-effectiveness, ease of deployment with a two-man crew, and ability to provide adequate compression wave velocity resolution to a depth of about 100 feet. For the survey, we used a Geode Seismograph 24-channel array provided by Geometrics and their software suite for analysis.

### *C. Correlation Methodology*

A comprehensive field log was maintained to optimize data collection procedures. A database was created to record the seismic refraction data and subsequently create data visualizations. Sites not included in the data set could then be compared to sites in the dataset with similar foundations and subsurface conditions.

## Case Studies

Across the span of this research, seismic refraction surveys were conducted at a total of 18 distinct sites, 8 of which were used in the data visualization in Figure 2. For brevity and focus, this paper will concentrate on examining three specific sites. These sites were chosen due to their varied geophysical properties and the unique characteristics they presented.

In the interest of providing a clear summary of the collected data, a graphical representation of the compression wave velocities will be included. This comprehensive data visualization will distill the gathered information across all surveyed sites into an easily digestible format. It allows for the comprehension of the correlation between the compression wave velocities of the soil and the pile-driving characteristics, thereby communicating the reliability and accuracy of seismic refraction for subsurface investigation.

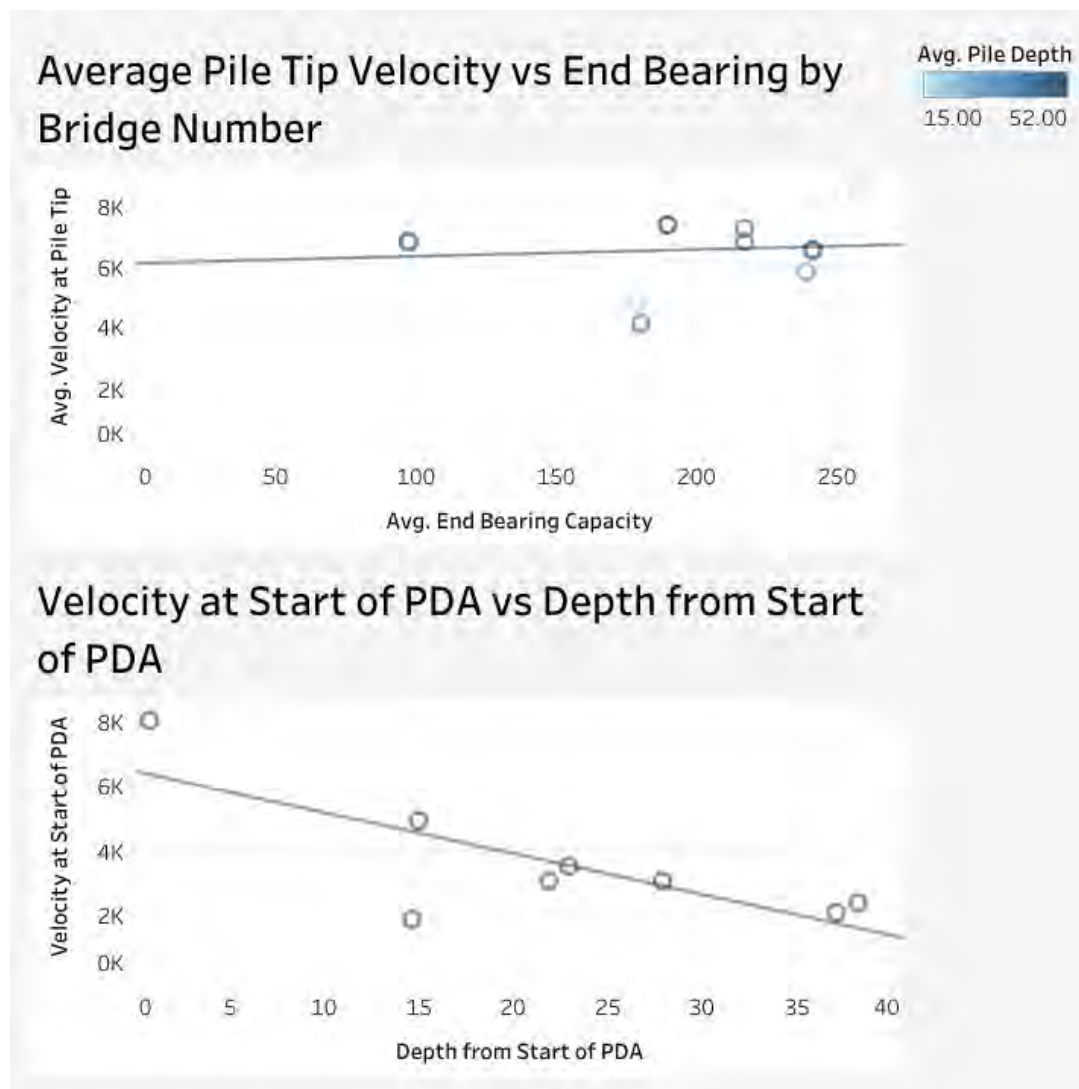


**Figure 2 – Compression Wave Velocities Visualization**

The selected sites to be highlighted in the case studies include Kansas bridge sites in Johnson County, Atchison County, and the Amidon Avenue Bridge in Wichita.

#### *Case Study 1: Johnson County*

The soil consists mainly of silty clays situated over shale bedrock and limestone. Soil borings have shown that the top of the shale is at an elevation of approximately 1,050 feet at Abutment 2. PDA test results corroborate this and indicate that the top of the limestone is at an elevation of approximately 1,037 feet.

The processed profile data extends to a maximum depth of 42 feet below grade, with compression wave velocities ranging from 900 to 7,300 feet per second (fps). The PDA test data from Abutment 2 overlaps with the seismic refraction profile, and this has allowed for a reliable correlation between the two sets of data.

The PDA data suggests that there is considerable resistance to driving through the stiff clays overlying the weathered shale bedrock, with an estimated between 100 kips to 200 kips driving resistance. The zone of 7,000 to 7,300 fps at the bottom of the refraction profile corresponds to the limestone layer in the bedrock beneath the shale contact.

#### *Case Study 2: Atchison County*

This site consists primarily of glacial till. Soil borings extended to a maximum depth corresponding to an elevation of approximately 935 feet. Pile Driving Analyzer (PDA) tests were carried out at Abutment 1, and Piers 1 and 2, with starting pile tip elevations ranging from 957 to 975 feet. The piles were tested per the PDA to depths between 26.5 and 42 feet below grade.

The processed profile reached a maximum depth of 55 feet below grade, with the bottom of the compression wave velocity profile at an elevation of 933 feet. Compression wave velocities within this depth ranged from 1,500 to 4,100 feet per second (fps).

Close examination of the PDA test location closest to the survey line (Pier 2) reveals an average pile capacity of approximately 140 kips from an elevation of 969 feet to 948 feet, within which the compression wave velocities ranged from 3,300 to 4,100 fps. From elevation 948 feet to 936 feet, the pile capacity increased from 140 kips to 230 kips. The final 12 feet of pile section represents a capacity increase comparable to a similar length section in the highly weathered Wellington shale regions of Kansas.

#### *Case Study 3: Amidon Avenue Bridge project in the City of Wichita.*

This survey, which was performed before bridge construction for client King Construction, was FTC's first paid project for seismic refraction surveying and was performed following completion of our research program. The purpose was to assess potential pile penetration depths and to supplement existing soil borings data with seismic refraction results, to see whether planned pile order lengths could be reduced.

The project involved more than two lineal miles of planned piling on the bridge, with a suspicion that the planned pile lengths were probably at least 10 to 18 feet longer than necessary or could effectively be driven into the Wellington Shale. FTC planned the refraction lines in advance using Google Earth, providing a comparison between velocity profiles and scaled soil boring logs. FTC also used the PileTrac database to draw upon PDA work from 2009 that was conducted close to the current project. Those results showed pile penetration was about 6 to 10 feet into the Wellington Shale.

After gathering and analyzing all the information, FTC recommended that the contractor order approximately 1,340 lineal feet less piling than originally planned. This recommendation was based on seismic refraction data and comparisons with nearby jobs. This reduced pile order length accounted for an extra 5 feet of piling that was also added for each of the piles over our predicted pile lengths for an additional margin of safety in proving the new methodology for pile length prediction. By implementing these recommendations, the contractor was able to save over \$60,000 in material costs compared to the original plan. Notably, the City of Wichita does not pay for pile cut-offs for piles driven shorter than the plan length. The results on this project were successful in demonstrating the effectiveness and commercial viability of seismic refraction surveys for subsurface investigation on pile-supported structures.

Moreover, this reduction in the piling length had significant environmental implications. By reducing the requirement of the HP12x53 steel pile by 1,340 lineal feet, approximately 35.5 metric tons of steel were saved. Considering the high carbon emissions associated with steel production - approximately 1.85 tons of CO<sub>2</sub> per ton of steel, a figure from the World Steel Association (1), this equates to a reduction in CO<sub>2</sub> emissions by roughly 65.7 metric tons. Hence, FTC's recommendation led not just to significant cost savings but also played a part in mitigating the environmental impact of the construction project.

### **Correlation between Seismic Refraction and PDA Plan Tip Elevation across Case Studies**

Looking at the data visualization on page 3, a distinct relationship is apparent. It suggests that the end-bearing pile is likely to reach its desired capacity when the compression wave velocity at the pile tip reaches approximately 7000ft/s. The successful outcomes of the Amidon Avenue Bridge project served as a solid affirmation of the findings from our correlation study.

### **Interpretation of Findings**

The analysis of our study's results highlights several key points that answer our core research inquiries and offers insights into the broader applications of seismic refraction in civil engineering projects, particularly for pile-supported bridge projects.

One clear insight is the observable correlation between compression wave velocity profiles and PDA results. End-bearing piles were found to often reach their desired capacity at a compression wave velocity of around 7000ft/s at the pile tip. This relationship implies that seismic refraction can be a reliable predictor of a pile's performance and can be integrated into the planning and execution of pile installations.

Our case studies demonstrated that seismic refraction has proven effective at predicting pile tip penetrations across a range of geological contexts. It functioned well in different geologic conditions, including silty clays over shale bedrock, glacial till, and the Wellington Shale. The effectiveness of seismic refraction under varying geologies underscores its versatility, reinforcing its value as a tool for geotechnical investigations.

Looking at the potential implications of these findings, it's clear that the incorporation of seismic refraction in pile tip penetration prediction for bridge constructions could lead to significant improvements in subsurface investigation and planning accuracy. The practical implications of this can extend to cost savings, reduced carbon footprint, and more effective construction project management.

On a broader level, our results underscore the potential value of integrating geophysical survey methods, such as seismic refraction, into standard construction planning practices. The insights gained through this research contribute significantly to the understanding of subsurface conditions, which, in turn, can positively impact the accuracy and efficiency of construction planning and execution. While our study focused on bridge construction, these findings could also influence a wide range of civil engineering projects where accurate prediction of pile penetration depths is crucial.

### **Implications for Seismic Refraction and PDA Plan Tip Elevation**

These findings propose an intriguing opportunity: to integrate seismic refraction into conventional construction planning practices for better prediction of pile penetration depths, hence improving the accuracy and efficiency of subsurface investigation. This shift could not only yield substantial financial savings but could also reduce the environmental footprint of construction projects.

Overall, this study extends the academic and practical discourse around seismic refraction and its role in geotechnical investigations. While focusing on bridge construction, the implications of these findings could permeate a broad spectrum of civil engineering projects where precise prediction of pile penetration depths is of crucial importance.

### **Suggestions for Future Research**

This study has proven seismic refraction to be a valuable asset in enhancing the prediction of pile penetration depths and a better understanding of subsurface conditions. With this, there still exist numerous opportunities for future research.

For instance, the utilization of seismic refraction and other geophysical methods such as downhole seismic to predict installed depths for friction piling. While our current data concerning end-bearing H-pile could be extrapolated easily to other end-bearing piling sections this topic may warrant a more quantitative study for friction piles within compression wave velocity profiles.

Additional investigations could also be performed at existing bridge sites to develop correlations based on a greater variety of pile types, sizes and end conditions.

Lastly, time-dependent capacity changes may be correlated with the compression wave velocity profile. A better understanding of these effects could help prescribe various PDA restrike intervals to reach the required capacity based on the subsurface compression wave velocities.

**REFERENCES:**

1. World Steel Association AISBL. *Sustainability Indicators*. World Steel Association. <https://worldsteel.org/steel-topics/sustainability/sustainability-indicators/>. Accessed July 13, 2023.

**Title: Design and Construction of a Bottom-up Retaining Wall in Slickensided Red Bed Material**

**Kirsten Grant, PE**  
Schnabel Engineering  
3 Dickinson Drive, Ste. 200  
Chadds Ford, PA 19317  
(610)696-6066  
KGrant@schnabel-eng.com

**George Aristorenas, Ph. D., PE**  
Schnabel Engineering  
46020 Manekin Plaza, Ste. 150  
Sterling, VA 20166  
(703) 779-0773  
GAristorenas@schnabel-eng.com

**Philip Shull, PE**  
Schnabel Engineering  
3 Dickinson Drive, Ste. 200  
Chadds Ford, PA 19317  
(610)696-6066  
PShull@schnabel-eng.com

**Chad Mayers, PE**  
Schnabel Engineering  
9800 Jeb Stuart Parkway  
Glen Allen, VA 23059  
CMayers@schnabel-eng.com

**Allen Cadden, PE, D. GE**  
Schnabel Engineering  
3 Dickinson Drive, Ste. 200  
Chadds Ford, PA 19317  
(610)696-6066  
ACadden@schnabel-eng.com

### **Acknowledgements**

The authors would like to thank the individuals/entities for their contributions in the work described:

Michael Senior – Schnabel Engineering  
Majid Khabbazian – Schnabel Engineering  
Kayla Nelson – Schnabel Engineering  
Daniel Le – Schnabel Engineering

### **Disclaimer**

Statements and views presented in this paper are strictly those of the author(s), and do not necessarily reflect positions held by their affiliations, the Highway Geology Symposium (HGS), or others acknowledged above. The mention of trade names for commercial products does not imply the approval or endorsement by HGS.

### **Copyright Notice**

Copyright © 2023 Highway Geology Symposium (HGS)

All Rights Reserved. Printed in the United States of America. No part of this publication may be reproduced or copied in any form or by any means – graphic, electronic, or mechanical, including photocopying, taping, or information storage and retrieval systems – without prior written permission of the HGS. This excludes the original author(s).

## ABSTRACT

This paper describes the design considerations and challenges of a 4,000 ft long, 40 ft high permanent bottom-up retaining wall constructed on a slope with historic instabilities due to geologic conditions. A portion of West Virginia Route 2 (WV2) required expansion to support a new bridge crossing the Ohio River into Brilliant, Ohio just south of Wellsburg, West Virginia. The proposed location of this bridge, and therefore the area requiring expansion, is located along a mountainside sloping towards the river on the West Virginia side. Historical, deep-seated instabilities are present along the proposed roadway alignment due to a thin creep zone of low residual strength material, known as the Pittsburgh red beds, located at the soil-rock interface. A fill wall was identified as the most economical option due to the existing topography and geology of the site. The presence of the slickensided material limited the applicable wall types as global stability of the entire slope needed to be addressed. An in-depth understanding of the Pittsburgh Red Bed material and the subsurface stratigraphy were required to properly address these challenging site conditions. A three-dimensional model was created to understand the subsurface stratigraphy and identify areas of concern. Advanced numerical analyses were utilized to better identify the material properties of this complex subsurface stratigraphy and understand the impact on the design through construction staging. This paper will also address the observed subsurface conditions and challenges encountered during construction in a variable geology.

## INTRODUCTION

A new bridge over the Ohio River was designed and constructed to connect the towns of Wellsburg, West Virginia and Brilliant, Ohio. To support this new bridge, the existing two-lane roadway, West Virginia Route 2 (WV2), required widening and realignment to allow bridge access. The existing two-lane roadway was redesigned to include two 12 ft wide lanes with a 12 ft wide turn lane adjacent to the bridge on-ramp. An 18 ft wide median is present at the turn lane locations with 22 ft wide shoulders on either side of the roadway to allow for incorporation of additional lanes in the future.

A bottom-up retaining wall was constructed to provide the footprint needed to expand the roadway. However, the subsurface conditions at the wall location required careful consideration of applicable retaining walls. A proper understanding of the subsurface conditions, including the type, strength, and stratigraphy of the materials present at this site were critical to design.

## Project Overview

The site is located within the panhandle of West Virginia, approximately 35 miles southwest of Pittsburgh and adjacent to the Ohio River, as shown in Figures 1 and 2. The site is located just south of the town of Wellsburg. A coal plant is located 2 miles south of the site on the other side of the Ohio River. An 11-mile-long historic trail along the river, the Brook Pioneer Trail, runs parallel to the roadway and is located at the bottom of the proposed wall.

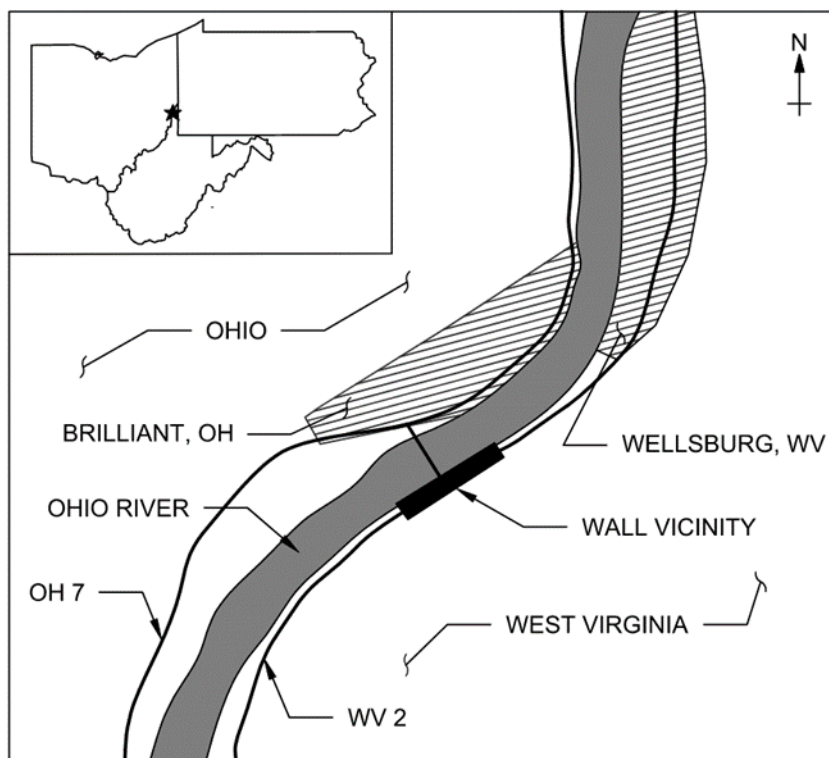


**Figure 1 - Site Vicinity Map**

The existing steep topography at the site had historically constrained the narrow two-lane road to the pre-construction footprint. To widen the roadway without excavating the

mountainside, a bottom-up wall needed to be constructed along the south-bound side of the road towards the river. Expansion on the north-bound side into the mountain utilizing standard top-down construction was not presented as an option by the owner, the West Virginia Department of Highways (WVDOH); presumably because of the steep mountainside, right of way limitations, extensive rock excavation, and/or potential to intercept soil layers that could lead to future instabilities. Deep-seated existing landslides are prevalent in the site vicinity, especially on steep hillsides. The proposed retaining wall needed to limit the potential of landslides from the existing slope while providing stability for the new backfill and traffic loading. The retaining wall required a 100-year design life. The proposed retaining wall alignment consisted of two retaining wall structures, with a total alignment length of 4,000 ft and a maximum exposed height of about 40 ft. The two retaining wall structures, one in front of the other, allow for pedestrian access from the trail to the roadway through a supplemental pathway, providing access to the bridge for vehicular traffic via the new roadway and pedestrian traffic via the pathway.



**Figure 2 - Photograph of Wall During Construction**

The initial bid documents allowed for utilization of a Mechanically Stabilized Earth (MSE) retaining wall system. MSE retaining walls are often utilized in highway design as a cost-effective system to allow for fill placement and meet a bottom-up wall construction requirement. However, this type of system relies on a stable subgrade to meet global stability requirements. This type of wall can be utilized with deep foundations or ground improvement elements to stabilize the existing ground. However, due to the extent and depth of the slope instabilities present on this site, including the historic landslides, this proposed retaining wall was not considered as a viable option. The extent of the global instabilities due to the deep creep zone were the main challenge for this retaining wall design, which was required to not only support

the proposed backfill but to support the entire slope below the exposed wall to the top of bedrock. Therefore, anchoring to the competent bedrock below the creep zone was required.

### *Project Criteria*

The owner of the project, WVDOH, set the design criteria. The design was to be in compliance with WVDOH Standard Specifications (2017 Edition), AASHTO LRFD 2016 Bridge Design Specification, and project specific criteria provided in the bid documents for the project. Notable design criteria for the permanent retaining wall include a minimum design life of 100 years, maximum deflection of 2 in, a global stability factor of safety of 1.5 for slippage through the retaining wall, a global stability factor of safety of 1.3 for slippage downslope of the retaining wall, and a rapid drawdown global stability factor of safety of 1.1.

## SUBSURFACE CONDITIONS

The subsurface conditions on this site consist of existing fill and colluvial soil underlain by bedrock from the Pennsylvanian-aged Conemaugh Group. The Conemaugh group is 300 million years old and was deposited at the bottom of the inland sea during a time where shorelines were shifting considerable distances (Wu 1987). The shifting of the shoreline resulted in multiple depositions of varying sediments that formed the interbedded sandstone, siltstone, claystone, and shale with coal and limestone rocks found in this formation. These rocks are generally horizontally bedded but can also slightly slope down towards the river in some locations. Figure 3 below represents a typical subsurface profile at the project site.

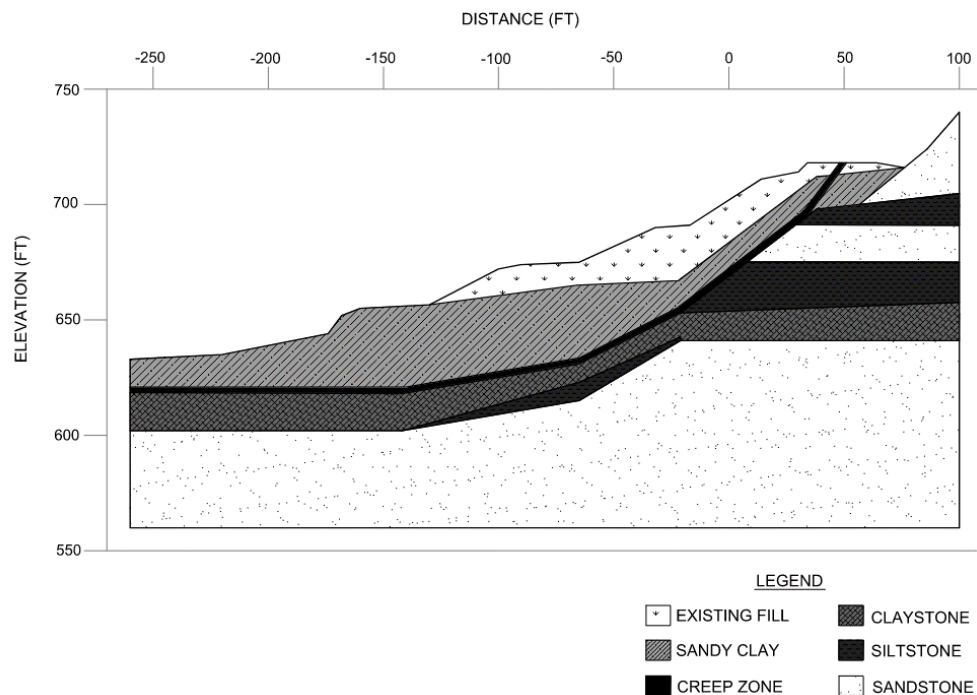


**Figure 3 - Existing Stratigraphy**

The claystone material is a soft rock that deteriorates into clay that is sticky and slippery when wet. Rapid deterioration occurs when this rock is exposed to water, and water may be

unable to drain from the rock due to the strong, fresh rock below the weathering, causing instability and further deterioration (Licastro 2016). This residual soil is typically found at the soil to rock interface and is a low-strength material. It is known for a deep red color, from which they receive the local term “Pittsburgh Red Beds”. The red color is produced due to oxidation of sediments (Wu 1987). The weathered soils are typically 5 to 15 feet in thickness and stiff, however their residual strength make them prone to downhill movement (Landsliding in Western Pennsylvania). Due to the chemical weathering process and quality of the original deposition, the Pittsburgh Red Beds have randomly oriented, closely spaced fractures (Kutschke 2007). At the project site, the layered rock has eroded and colluvial soil has been deposited over the red beds resulting in a steep hillside with deep-seated, low strength creep zones below colluvial and fill and within the residual material. A weathering profile may be observed with depth, transitioning from soil to decomposed rock, then solid bedrock.

The Greater Pittsburgh area, specifically Western Pennsylvania and Northern West Virginia, are notorious for landslides. One of the main contributing factors is the existence of these low-strength clays coupled with the presence of steep slopes, both naturally occurring and manmade. The topography in this region is susceptible to the gravity-induced earth movements (Licastro 2016), so much so that the Monongahela (of which the river was named) is interpreted as ‘river with the sliding banks’ (Landsliding in Western Pennsylvania). It is understood that recent landslides are reactivated prehistoric landslides, typically due to disturbances such as construction and loading (Shultz 2002). Previous landslides reoriented the clay particles in such a way as to create a “polished” surface and reduce the shear strength of the soils, therefore they have less frictional resistance and are more susceptible to instabilities due to changes in the slope; this is referred to as slickensided clay.

Inclinometers were installed along the proposed retaining wall alignment and monitored for five months prior to the wall design. During that timeframe, some movement was observed in the inclinometers, as shown in Figure 4. The movement was observed at the top of the bedrock surface, within the low-strength creep zone material previously mentioned. Rigid body type movement occurred in the soil mass above the creep zone.

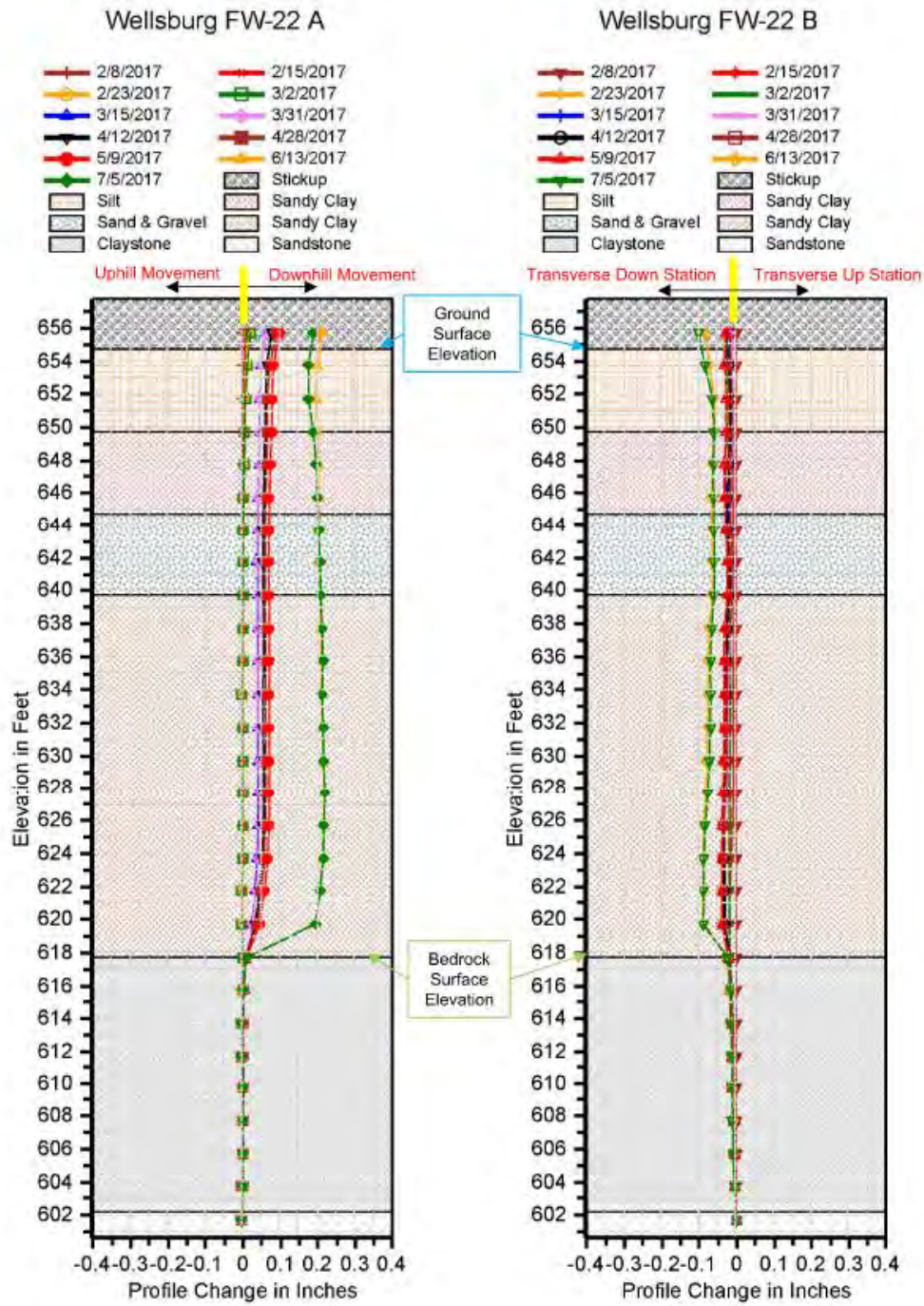


**Figure 4 - Project Inclinometer Readings**

In addition, several historic landslides were noted based on accumulation of soil along the riverbank, also referred to as slide debris, visually observed from the topographic survey of the site and from aerial photographs. An example of this soil accumulation is shown in Figure 5 below. This area of accumulated soil was utilized as a staging area of construction activities.

Landslides are common along riverbanks, especially where rivers have extensive flood plain deposits due to erosion (Delano 2001). Movement of the stream removes mass from the bottom of the slope, resulting in continued landslides.



**Figure 5 - Previous Landslide Location Indicated by Toe Material**

Actions that can trigger landslides include excavations in unstable materials, overuse of fill materials, disruption of drainage, removal of material at bases of slope, and vibrations due to traffic or construction surcharge (Licastro 2016). Considering constructing on a previous landslide, “In many cases, a landslide that has moved once will start to move again with greater ease, because the clay and other materials along the surface of rupture have been smoothed and smeared, and original friction is reduced” (Delano 2001). This construction activity in combination with the introduction of water due to exposure at the top of the slope can lead to future instabilities.

## **DESIGN BACKGROUND**

The primary calculations for this retaining wall design were performed using Plaxis 2D, a two-dimensional finite element software. This program is a widely utilized commercial finite element analysis software that can model soil-structure interaction design sections with complicated geometries, loading conditions, and construction staging. Non-linear stress-strain-strength soil behavior is inherently defined and is dependent on the effective stress. The effective stress formulation is built in the soils, allowing for fully coupled pore pressure and deformation-induced stresses to evolve. Additionally, various types of structural elements are available, including beams (plates) to model walls and node-to-node anchors to model tiebacks. The variation of structural elements allows for a model that closely represents the actual elements that

will be utilized in the field. The model is also capable of calculating the stability factors of safety.

The retaining wall design focused on the development of the subsurface profile and soil parameters, geotechnical and structural strength of the retaining wall, and constructability of the system. All three major design components were equally important and contingent on each other to develop an efficient retaining wall for the client. Considering the site history and the challenging subsurface conditions, the retaining wall design was more robust than originally anticipated by the owner and construction team. Following discussions on the failure mechanisms and implications of the geologic history of the site, the team was educated enough to understand the importance of the robust retaining wall system and how critical assuring the subsurface condition requirements were met.

## Design Sections

The retaining wall was designed using a total of nine design sections throughout the wall alignment. These design sections were selected primarily at locations where previous instabilities were observed, featuring characteristic subsurface conditions, maximum design heights and specific loading sections, and intermediate sections throughout the wall to allow for optimization of the design at less demanding areas. A summary of the design sections is shown in Table 1 below.

**Table 1 - Summary of Design Sections**

Design Station	Station Extents of Applicability	Design Retained Height ft	Depth to Rock ft	Comments
198+50	195+70 - 200+00	34	25	Signs of past movement <sup>b</sup>
203+50	200+00 - 205+00	26	39	Active moment <sup>c</sup>
205+50	205+00 - 212+00, 215+00 - 218+00, 219+00 - 220+00	40	32	Signs of past movement <sup>b</sup>
213+50	212+00 - 215+00	38	43	Active moment <sup>c</sup>
218+50	218+00 - 219+00	31	17	Signs of past movement <sup>a,b</sup>
220+50	220+00 - 224+50	28	20	Signs of past movement <sup>b</sup> , overlap of retaining walls
224+50	224+50 - 225+50	12	20	overlap of retaining walls
227+50	225+50 - 228+00	27	12	Signs of past movement <sup>b</sup>
230+00	228+00 - 235+50	21	26	Signs of past movement <sup>b</sup>

a. This section includes a bridge abutment, which makes total retained soil for earth pressure calculations equal to 40ft.

b. Signs of past movement inferred from visual observations

c. Active movement confirmed from inclinometer readings from subsurface investigation

STA 203+50 and STA 213+50 were priorities in the analyses as they provided critical information for our designs because they were located at areas of observed inclinometer

movement. A preliminary design was performed at both of these stations to understand the extent of strength requirements, both geotechnically and structurally, that would be needed for the retaining wall.

### **Subsurface Design Parameters**

Gathering an in-depth understanding of the subsurface stratigraphy of the site, including geologic history of the general area, was the first step in the design process. Another geotechnical firm performed the geotechnical subsurface investigation prior to Schnabel's involvement in the project and the draft geotechnical report was provided for review. Schnabel was not provided the opportunity to perform our own geotechnical investigation. The previous firm had retained their soil and rock samples, allowing us to request a limited amount of laboratory tests to better understand the soil and rock. However, the majority of our data was gathered from the available information and general knowledge of the Conemaugh group and Pittsburgh Red Beds.

A desktop study was performed by the design team to understand the site background and the Conemaugh group. Understanding the background of the red bed material in the vicinity of the site was critical to relating the previous slope instabilities observed both by inclinometer data and topographic features. A three-dimensional model of the site was created using an in-house program engine to assist in visualization of the subsurface stratigraphy. The existing borings and topography were inserted into the program. The software was used to interpolate between the borings to generalize the limits of the soil and rock stratum. The location of the retaining wall was inserted into the model to assist with visualization. Figure 6 below represents sections of this model. The model was used to better understand the likely subsurface conditions between borings and help identify which borings should be considered to develop the design sections. Including a three-dimensional visualization tool provided a level of confidence to the design team that our design considerations were close to, or conservative compared to, the existing conditions.

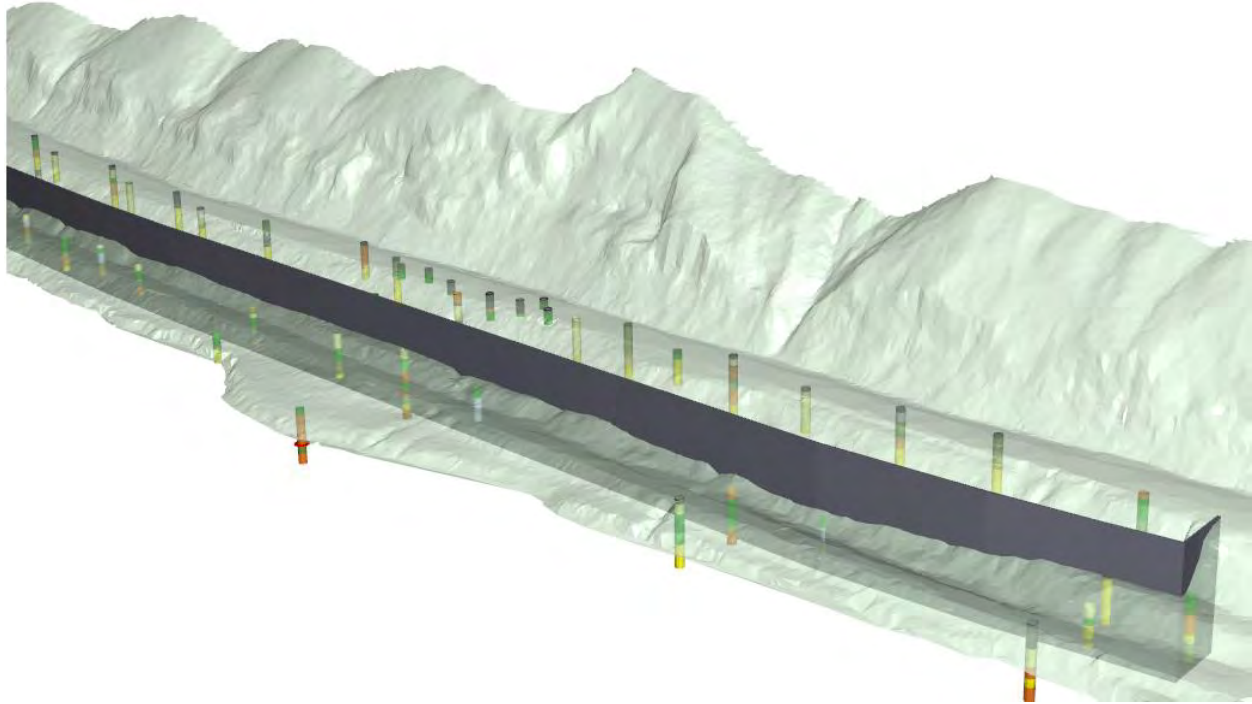


**Figure 6 - 3D model showing the wall and boring locations**

Soil parameters were back calculated using a Plaxis 2D analysis, considering the existing slope is at or close to failure (slow creep) in its current state. Limit equilibrium stability analysis in Plaxis 2D was used to interactively extend the creep zone along the high shear strain locations to develop the most likely failure condition. This was done using a combination of friction angle and cohesion for the strength of the soil. The limit equilibrium stability analysis allowed for input soil and rock strength and structural element strength to incrementally decrease until global yielding occurred, with the factor of safety equivalent to the ratio of the input and decreased strength. Visually, Plaxis 2D highlights the extent and shape of the unstable mass due to the global yielding, therefore the creep zone could be defined. The defined creep zone allowed for optimization of the design while having a prediction of the instability area due to the location of the red bed materials. The final creep zone for one of the design sections is shown in Figure 7 below. It should be noted that two likely creep zones were investigated in some design sections for steady state flow and rapid drawdown conditions.

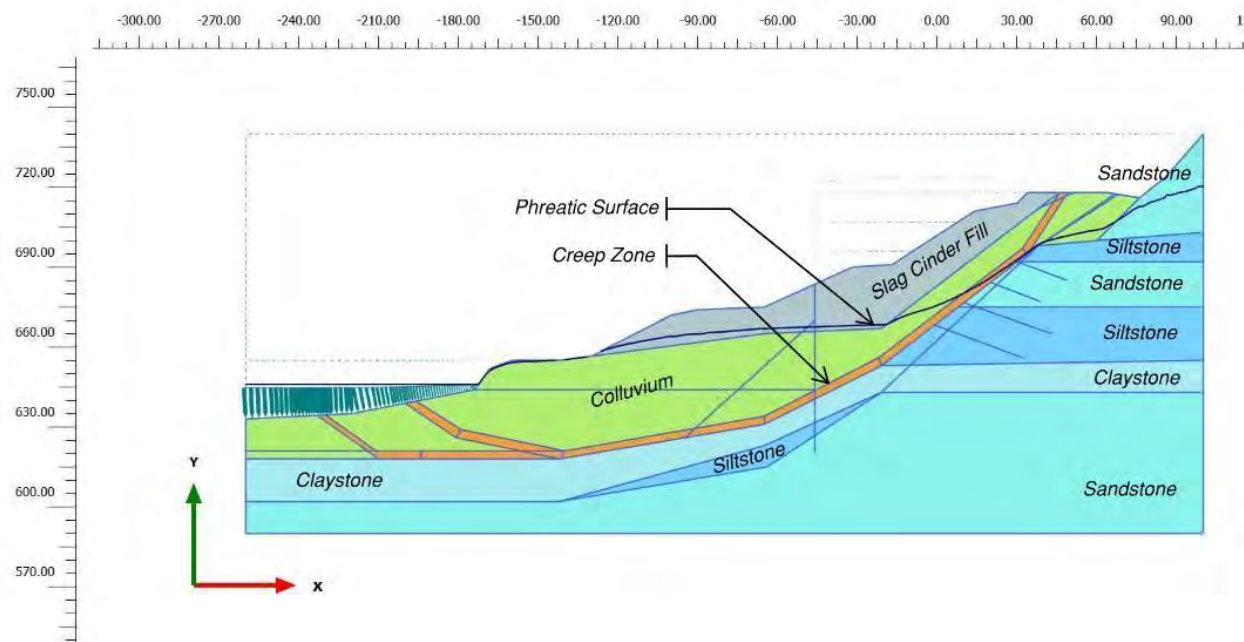


**Figure 7 - Plaxis Analysis to Develop Creep Zone Extent**

The soil parameters used for the wall design are summarized in Table 2. In addition to the back-calculated soil parameters mentioned above, the soil and rock strengths and unit weights were developed using data from the geotechnical investigation, including SPT values and laboratory testing, and standard WVDOT Presumptive Soil Parameters.

**Table 2 - Long-term Soil Parameters for Retaining Wall Analysis**

Material	Unit Weight pcf	Friction Angle degrees	Cohesion psf
Compacted Fill	140	32	0
Existing Fill	120	26	50 <sup>a</sup>
Sandy Clay Colluvium	125	28	210
Creep Zone	125	24 <sup>a</sup>	0 <sup>a</sup>
Claystone	145	21	467
Siltstone	145	27	704
Sandstone (STA 196+50 - 216+50)	155	44	1480
Sandstone (STA 216+50 - 235+50)	155	52	3397

a. Parameter determined using back-calculation

### Wall Design

The retaining wall system chosen for this site consisted of drilled soldier piles and prestressed tieback anchors with precast concrete lagging spanning between piles. Deflection at the top of the high sections of wall was controlled using tierods connected to a deadman system. This allowed for adjustment of the soldier pile verticality throughout the backfilling process of

the retaining wall. Precast concrete lagging was utilized to retain the earth backfill between the steel piles. The tiebacks penetrated through the soldier piles utilizing a built-up system to allow for a flush face and easier wall construction. Both the soldier piles and tiebacks penetrated beyond the creep zone into competent rock to increase stability of the existing slope.

Plaxis 2D was again used to design the retaining wall system. Staged construction was modeled in the numerical model program to evaluate the impact of construction loading, backfill placement, tieback prestressing, and traffic load application on the wall system (see Figure 8). Soldier piles and tiebacks were designed for fixity and bond, respectively, below the creep zone and into the competent rock material.

Our design considered tiebacks to be installed when 1 foot of backfill was placed above the tieback elevation. Our design considered tieback installation with the drill rig behind the wall, requiring the drill to extend between the placed soldier piles and drill through the front of the wall. A load test and tieback prestressing were to be performed at this time, as was required for stability of the retaining wall structure. Plaxis 2D analysis was able to evaluate the impact of the prestressing and compaction of material following the prestressing event on the final tieback condition. By understanding the impact of this initial load, avoidance of overloading the tiebacks due to the construction activities after lock-off was achieved. Additionally, the impact of construction activities, such as the tieback lock-off and stress from backfilling, was understood to meet the soldier pile deflection criteria provided.

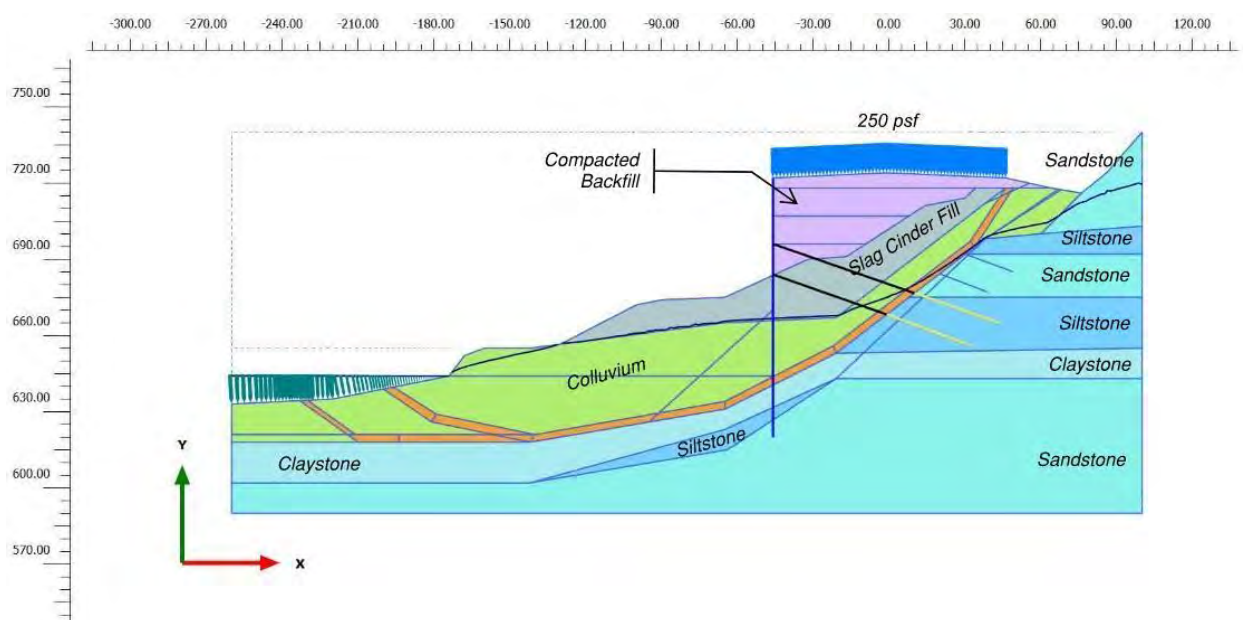


**Figure 8 - Plaxis Analysis Considering Staging**

Rock embedment of the soldier piles was a critical consideration in our design. The embedment of the soldier piles needed to be beyond the creep zone for assurance of fixity of the piles. This is a critical definition in the design as insufficient embedment of the soldier piles could result in slope instability or failure of the wall. The subsurface profiles at each section considered three rock types (Claystone, Siltstone, and Sandstone) below the creep zone material

based on the available data. These rocks were considered as rock, not weathered rock, as the creep zone may be present in the relic rock structure. The strength parameters are shown in Table 2 above. As shown in this table, the sandstone has a much higher strength and stiffness than the claystone and siltstone; therefore embedment specifically in sandstone was also important as the sandstone provided more lateral resistance. A minimum embedment in both rock (including all three types) and a minimum embedment in competent sandstone were included in the drawings.

A note was included in the drawings that the competent sandstone was to be the same quality as encountered during the subsurface investigation, and as defined by a Schnabel on-site representative at the start of production soldier pile drilling. It is well-known throughout the industry that competent sandstone can be defined differently based on location; a hard sandstone in one region may be stronger than a hard sandstone found in another region. Therefore, designs must consider the regional definition of the material. This is the reasoning behind the on-site definition of the material based on actual borings installed at the site.

Global stability analyses were performed to determine the critical slip surface of the final design. There are limitations to the global stability analyses that can perform in Plaxis as only the most critical slip surface in the analysis is presented in the model output. Due to the existing slope conditions, this critical slip surface was often found downslope of the retaining wall since the retaining wall was more stable. The stability of the toe of the slope between the retaining wall and the river was outside of the project scope of work and was not a concern to the WVDOH if a global factor of safety considering a slip surface extending beneath the retaining wall system equal to or exceeding 1.3 was achieved. To demonstrate that the retaining wall system provided an internal factor of safety greater than 1.5, a second analysis using GeoStudio Slope/W, a limit equilibrium analysis software, was performed to force a slip surface through the retaining wall.

The structural design was performed using the controlling axial compression, shear, and bending moment load combination on the soldier piles, in accordance with the Load Resistance Factor Design method (LRFD). Tiebacks at each level were designed for the maximum tension using Allowable Stress Design method (ASD). Soldier piles and tiebacks were designed for each design section to maximize design efficiency. A fabricated double wide flange pile, consisting of (2) W24x68 or (2) W24x76, with a full penetration weld along the two flanges. The use of the fabricated pile required a 36 in diameter drill hole for placement of the soldier piles, a smaller pile diameter considering strength requirements, while meeting the strength requirements, theoretically reducing the drill time for the piles and concrete volume. The soldier piles were designed for tieback penetration through the connected flanges in place of a waler system; the removed steel was made up utilizing cover plates. Penetrating the tiebacks through the soldier piles rather than utilizing walers allowed for precast panel placement uninterrupted by waler penetration, providing flexibility of panel design, tolerances in the field, and a flush face. Tiebacks were designed according to PTI (2014) using 150 ksi bar, ranging in diameter from 1-3/8 in to 2-1/4 in with estimated bond lengths ranging from 15 to 38 ft and inclinations of 20 to 30 degrees. The final tieback bond length design was the responsibility of the contractor based on the achievable bond values of the rock and their drilling methods. The tiebacks were installed through a 7-5/8 in diam. steel casing extending 10 to 15 ft behind the front soldier pile flange to mitigate settlement effects on the structural integrity of the tieback anchor. This steel sleeve was designed to move independent of the soldier pile as no fixed connections were installed,

therefore allowing the steel casing to rotate with movement. All production tiebacks were either performance or proof tested to confirm design bond values.

The design included distances from the top tieback to the top of the soldier pile wall of up to 26 ft, which exceeds the general industry standard of 15 ft to limit deflection. A 1 in diameter, 150 ksi tierod was installed 10 ft below top of wall where the distance between the top tieback and top of soldier pile wall exceeded 15 ft. The tierods were designed to connect to concrete deadman structure 45 ft behind the back of soldier pile. This distance was calculated considering the active earth pressure failure wedge of the wall and the passive earth pressure wedge of the deadman for the tallest section of wall for simplicity of installation. Although the tierods were essentially provided to control wall deflections, their presence added stability to the retaining wall. A typical design section is found in Figure 9 below.

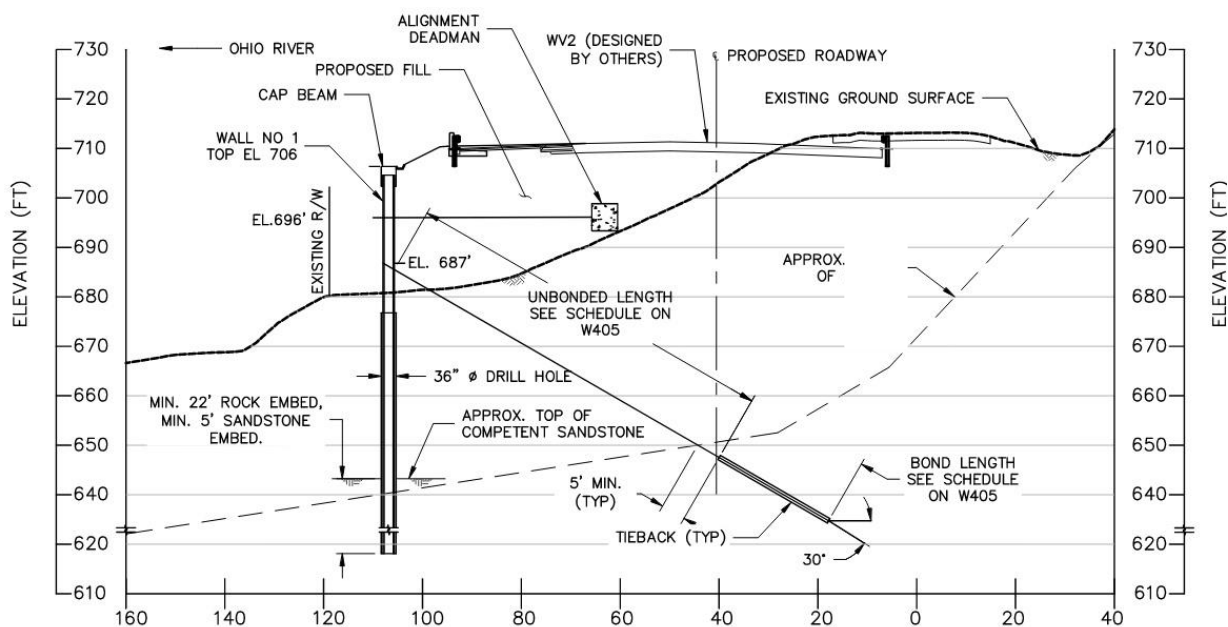


**Figure 9 - Example Section View (STA 203+50)**

It was strongly advised by Schnabel that full-time construction observation by the design engineer (Schnabel) be performed. Construction observation by the design engineer provides an additional level of quality control to the construction process, while providing confirmation that the design intent of the retaining wall is being met during construction. The observation of an engineer familiar with the design is especially important when design criteria is reliant on classification of subsurface material.

## CONSTRUCTION

### General

Schnabel was retained by the contractor for part-time construction observation for the retaining wall construction. A Schnabel representative performed site visits at critical points in construction, as defined by Schnabel and agreed upon by the Contractor. These site visits were performed to attempt to confirm that the design intent of the wall was being met during

construction activities, while providing an opportunity for hands-on assistance in answering questions and working through problems. General construction activity was observed during each of these visits. The contractor provided drill logs for the drilled shafts and tiebacks as well as test logs for the tiebacks.

### **Soldier Pile Installation**

The soldier piles were fabricated in a shop to adhere to the design requirements. Soldier piles were installed in 36-inch diameter drill holes to start, however due to availability of drilling equipment soldier piles were also installed in 42-inch diameter drill holes as well. The holes were excavated using a hydraulic fixed mast rotary drill rig, using both a soil auger and core barrel for soil and rock penetration, respectively. The soil auger and core barrel were used interchangeably in weathered rock, depending on the consistency of the material and location of the water. The total drill depths were determined generally by the contractor based on the minimum embedment requirements set forth in the drawings. It was observed that holes were cleaned, and water was removed, if encountered, prior to placement of the soldier piles. Water was typically only present in some instances where holes were left open overnight. Soldier piles were hoisted utilizing a crane and placed using a contractor-created template to control alignment and location. The soldier pile annulus was backfilled with end-dumped Portland cement concrete with a minimum strength of 3,500 psi.

As previously mentioned, the proper identification of the rock utilized for embedment is critical for implementation of the design. Schnabel was asked to visit the site towards the end of drilling due to concerns regarding rock classification by WVDOH's quality assurance engineers. Schnabel observed that the driller's definition of rock and competent rock varied from that of Schnabel at the beginning of the project. Schnabel observed drilling of adjacent soldier piles and compared the classifications, as can be seen in Figure 10 below. As some soldier piles were already installed without Schnabel's presence, evaluation of the as-built conditions was required to determine if additional steps were required to stabilize these soldier piles as removal would be an expensive alternative. The design section for this area was re-analyzed with the actual embedment and wall heights, which resulted in an increase in tieback loading that was handled through the existing tiebacks with no changes in design. Schnabel was retained to observe rock embedment for the remaining soldier pile structures (approximately 20% of the soldier piles installed).

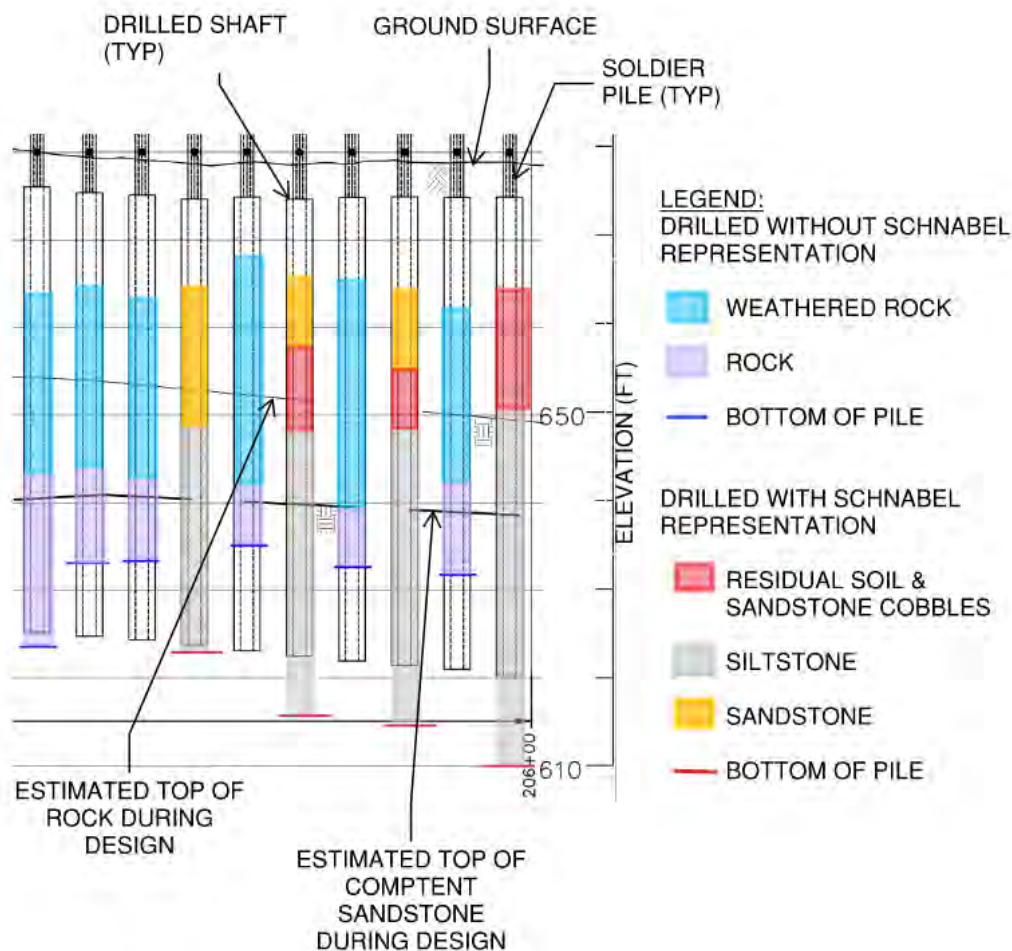


**Figure 10 - Comparison of Contractor vs. Design Engineer Material Classification**

### **Tieback Installation**

Most of the tiebacks required for stability of the retaining wall were not installed from the face of the wall using the temporary working platform provided by the contractor. The contractor elected to install tiebacks in the existing soil bank at surveyed locations, then extend the tieback to the face of the wall during backfill placement. Tiebacks were drilled with a 15-25 Ton Hydraulic Tieback drill rig. Tiebacks drilled in the bank were installed with excess tieback extending beyond the face of the soil to allow for coupling the extension; the bond length of each of the tiebacks was installed in the soil and rock, with the extension portion of the tieback always occurring within the unbonded zone. Extension was performed using couplers and corrosion protection was overlapped according to manufacturer requirements. Utilizing this methodology required additional casing over the length of the extension to confirm grout cover requirements according to PTI were met. Additionally, compaction of the soil around the casing was required to limit settlement. This proved to be a difficult task, requiring No. 57 stone at the soldier pile to tieback interface due to the angle of the tieback. The tiebacks that were reachable from ground surface were drilled from the front of the wall. Grouting was performed using an on-site high shear 500 E bulk grout plant.

Load test schedules were developed by Schnabel in accordance with PTI (2014). Four pre-production verification tests were performed, one every 1,000 ft along the alignment at locations selected by the Contractor and approved by Schnabel prior to the initiation of construction to confirm assumed bond strengths based on drilling methods. Performance tests were performed on 5% of the production tiebacks, and the remaining production tiebacks were proof tested. The contractor performed and recorded the load test results and submitted them to the design team for review. Tiebacks installed in the bank were load tested using cribbing against the bank material prior to extending them to the face of the wall. Following extension of the tiebacks, the tiebacks were load tested to 50% of the design load to verify the unbonded zone of the tiebacks met requirements. Tiebacks that failed to meet the load test criteria were redrilled at a 5 degree increase in inclination and installed. The soldier piles for these locations were still in fabrication at the time of the load tests, so fabrication at these locations was altered to accommodate this inclination. These tiebacks were derated to a load with a factor of safety of 2, considering the maximum sustained load on the tieback, and additional tieback anchors were installed below the bottom of the panels using external walers.

## **SUMMARY**

A comprehensive review of the subsurface conditions present at the project location allowed for an effective and optimized design for a new infilled roadway above a landslide-prone area. General understanding of the regional geology, including the Pittsburgh Red Bed creep material, was critical in the design. Identification of the creep zone was done using available subsurface information, instrumentation, and interactive limit equilibrium analyses. A tiedback soldier pile and lagging wall was determined to be an appropriate retaining wall system for this purpose.

The retaining wall was analyzed using Plaxis 2D so construction staging could be accounted for in the design. Additionally, the use of the numerical modeling software allowed for a detailed soil strata geometry to be input into the design software for consideration, especially considering the creep zone definition. The soldier piles and tiebacks were embedded into rock for fixity.

Bottom-up wall construction with anchored soldier pile and lagging can be challenging. Understanding the design intent and implementing it correctly is critical, therefore the contractor and Engineer need to be on the same page.

**REFERENCES**

1. West Virginia Department of Transportation Division of Highways. *Standard Specifications Roads and Bridges. 2017 Edition*. Charleston, WV.
2. Wu, T., Williams, R., Lynch, J., and Kulatilake, P. Stability of Slopes in Red Conemaugh Shale of Ohio. *Journal of Geotechnical Engineering* vol. 113 (3), March 1987, pp. 248-264.
3. Licastro, P. *What Are the Pittsburgh 'Red Beds'*. LinkedIn, September 16, 2016. <https://www.linkedin.com/pulse/what-pittsburgh-red-beds-peter-licastro/>. Accessed February 20, 2018.
4. Landsliding in Western Pennsylvania. *The Pittsburgh Geological Society*.
5. Kutschke, W., Petersen, W., and Meyers, J. Rock Slope Protection System for Differential Weathering Materials. *Geo-Denver 2008, ASCE Geotechnical Special Publications*, 1-10. 2008.
6. Delano, H., Wilshusen, J. Landslides in Pennsylvania. *Department of Conservation and Natural Resources, vol. 9*.
7. Post Tensioning Institute. *Recommendations for Prestressed Rock and Soil Anchors. Fifth Edition*. PTI DC35.1-14. Farmington Hills, MI., 2014.

**Impacts of Weak Rock Units on Cut Slope Construction  
Case Study: Interstate 78, Section 12M Reconstruction Project  
Berks County, Pennsylvania**

**Justin Manning, GIT**  
Gannett Fleming, Inc.  
1010 Adams Avenue  
Audubon, PA 19403  
610-783-3908  
[jmanning@gfnet.com](mailto:jmanning@gfnet.com)

**Joseph Krupansky, P.G.**  
Gannett Fleming, Inc.  
1010 Adams Avenue  
Audubon, PA 19403  
610-783-3799  
[jkrupansky@gfnet.com](mailto:jkrupansky@gfnet.com)

**Scott M. Cressman, P.E.**  
Pennsylvania Department of Transportation, Engineering District 5-0  
1002 Hamilton Street  
Allentown, PA 18101  
610-871-4520  
[sccressman@pa.gov](mailto:sccressman@pa.gov)

Prepared for the 72<sup>nd</sup> Highway Geology Symposium, August 2023

### **Acknowledgements**

The authors would like to thank PennDOT Engineering District 5-0; H&K Group, Inc.; Michael Baker International; Pickering, Corts & Summerson; American Engineers Group; and Gannett Fleming's Valley Forge, Camp Hill, and Pittsburgh offices, for their work on the various aspects of this project.

### **Disclaimer**

Statements and views presented in this paper are strictly those of the author(s), and do not necessarily reflect positions held by their affiliations, the Highway Geology Symposium (HGS), or others acknowledged above. The mention of trade names for commercial products does not imply the approval or endorsement by HGS.

### **Copyright Notice**

Copyright © 2023 Highway Geology Symposium (HGS)

All Rights Reserved. Printed in the United States of America. No part of this publication may be reproduced or copied in any form or by any means – graphic, electronic, or mechanical, including photocopying, taping, or information storage and retrieval systems – without prior written permission of the HGS. This excludes the original author(s).

## **ABSTRACT**

Sections of the recently excavated 1.5H to 2H:1V rock cut slopes along the 10-mile long I-78 Section 12M Reconstruction Project Corridor in Berks County, Pennsylvania experienced a series of planar-type rockslide failures following periods of persistent rain beginning in late January of 2022. The existing cut slopes prior to the reconstruction project generally ranged from 2H:1V to 1H:1V, were almost entirely vegetated (minimal rock exposures), and had no reported history of stability issues.

Gannett Fleming engineers and geologists worked closely with PennDOT's construction and geotechnical units, the project geotechnical engineer, and the construction manager to turn around an emergency anchored mesh design to stabilize two primary areas of stability concern within the project limits. In addition, a combination of excavation and mechanical scaling methods were used to mitigate localized areas of sliding by removing pervasive weak rock units that were observed to be daylighting the cut slope.

This case study presents the results of the stability analyses that show how the geologic structural discontinuity orientations and properties of the underlying weak rock exposed during construction aligned in such a way to intersect a very small potential failure envelope.

Unless adverse subsurface conditions are identified during design, or site history dictates, detailed stability analyses are not typically performed for shallow cut slopes (generally 2H:1V or less). The objective of this paper is to emphasize the importance of characterizing subsurface conditions during design and provide a real-world example on the impacts of encountering weak rock materials during cut slope construction.

## **INTRODUCTION**

Planar-type rockslide failures along recently widened 2H to 1.5H:1V cut slopes were observed at various locations within the I-78 Reconstruction Corridor following periods of persistent rain between late January and early March of 2022. No prior evidence of rockfall or rockslide activity was documented along the existing cut slopes. Back analysis showed that these failures occurred as a result of the adverse geometric orientation of bedrock discontinuities with respect to the cut surface. Specifically, bedding surfaces striking parallel to the slope face were exposed during excavation and were dipping at an angle greater than the interface friction of the surface. In this case, the interface friction between the thinly interbedded rock units was found to be exceptionally low (around 22°). Based on the persistence of these exposed weak geologic units and the need to protect the work zone from similar events, PennDOT District 5 engaged Gannett Fleming to evaluate the cut slope conditions and develop quick turn-around mitigation designs unique to each area of observed failure.

The existing cut slopes along the reconstruction corridor were approximately 20 to 50 feet in height and ranged from 1H:1V in the eastern zone to 1.5H:1V in the western zone, with slopes of 2H:1V in some areas. Parts of the western cut slope surfaces were covered with weathered shale and decomposed rock material, while the eastern cut slopes contained localized layers of interbedded sandstone with the weathered/decomposed shale. During the design phase investigations, the existing slopes were heavily vegetated with a variety of young to mature trees and brush, which made the observation and characterization of surficial geologic conditions exceedingly difficult.

According to Santi and Doyle (8), weak materials are defined as “intact, unweathered to slightly weathered materials that have low compressive strength or are highly fractured”, whereas weathered materials are described as “materials that show significant deterioration, particularly near the ground surface or along fractures.” Weak and weathered rock can be characterized based on several engineering characteristics, including low compressive strengths, high reactivity to water, high clay content, poor induration, a significant amount of matrix between hard blocks, or measurable loss of strength over time. For the purposes of this paper, we characterize the rock units observed within the cut slopes along the reconstruction corridor as weak. This characterization is based on factors such as fissility (ease of splitting along planes of weakness), resulting in a low interface friction angle and lack of cohesion; ease of excavation; apparent loss of strength since original cut slope construction; and the degree of differential weathering between the interbedded rock units.

## **PROJECT BACKGROUND**

The PennDOT SR 0078 (Interstate 78) Section 12M Reconstruction Project spans a total of 8.9 roadway miles, stretching from the SR 143 interchange in Lenhartsville, Berks County to just beyond the county line in New Smithville, Lehigh County. A combined Site Location and Bedrock Geology Map is included as Figure 1 below. The primary objective of this reconstruction project is to implement improvements that adhere to current design criteria and to improve and maintain mobility through the project area. As per the PennDOT Berks County

Traffic Volume Map (5), this section of I-78 carries more than 45,000 vehicles per day and serves as a vital arterial route connecting Harrisburg and Allentown, Pennsylvania.

The overall project entails the reconstruction and widening of the existing roadway to facilitate expanded shoulder widths and the inclusion of multiple truck climbing lanes. To accommodate the widening, the existing cut slopes within the hilly topography had to be expanded and, in certain instances, steepened to mitigate overall project impacts.

### **Site Geology**

The site is situated within the Great Valley Section of the Ridge and Valley Physiographic Province in Pennsylvania (9). The topography of the Great Valley Section is characterized by overly broad valleys, with dissected uplands in the northwest and low karst terrain in the southeast, featuring dendritic and karst drainage patterns. The predominant underlying rock types in this region are shale and sandstone in the northwest, while limestone and dolomite dominate the southeast. The geological structure of this area exhibits thrust sheets, nappes, overturned folds, and steep faults. The formation of this area can be attributed to fluvial erosion, carbonate rock dissolution, and some periglacial mass wasting.

The entire study area is underlain by the Hamburg Sequence Rocks, which are of Ordovician age and specifically referred to as the Windsor Township Formation – Dreibelbis Member. This formation primarily consists of thin- to very thickly bedded, calcareous graywacke sandstone interbedded with fissile to poorly cleaved mudstone, siltstone, and shale (3,4). These rocks exhibit a range of colors, from dark greenish-gray to light olive-gray and maroon. In the western zone of the site, the predominant rock type is greenish-gray and maroon phyllitic shale (Oh), often silty and siliceous. In contrast, the eastern zone is characterized by shale with distinctive zones of graywacke sandstone (Ohsg).

The project area exhibits a notable geological structure marked by extensive folding and faulting. The primary orientation of the fold and fault systems in the project area aligns approximately east-west, with the roadway alignment generally parallel to this axis. The area encompasses numerous overturned anticlines and synclines, along with several thrust faults that originated during the compression of the bedrock in the region (10). The strike of the bedding planes along and adjacent to the roadway generally follows an east-west direction, consistent with the fold pattern, and the predominant dip is towards the south.

According to Geyer and Wilshusen (2), the sandstone units are characterized as having moderate resistance to weathering and moderate weathering to a shallow depth, while the shale units are described as moderately resistant to weathering but exhibit moderate to high weathering to a greater depth. Excavation is moderately easy in shale, while it becomes more challenging in sandstone. Cut-slope stability is considered fair, primarily due to the disintegration of the rock when exposed to moisture for a relatively brief period of time.

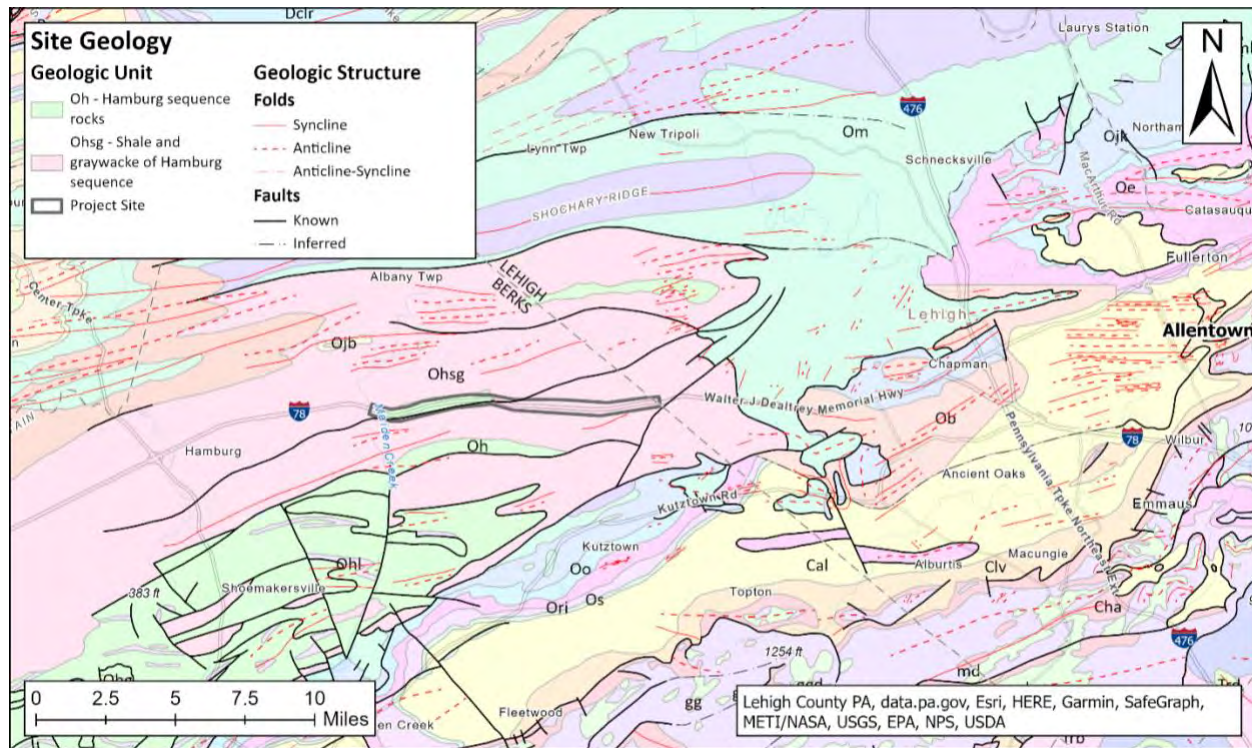


**Figure 1 – Combined Site Location and Bedrock Geology Map (modified from PA DCNR, PAGEODE, Web-Mapping Application) (11).**

## Design Phase

The project design team for Section 12M was led by Pickering, Corts & Summerson (PCS) of Newtown, Pennsylvania, with geotechnical support provided by American Engineers Group, LLC (AEG), of Harrisburg, Pennsylvania. For the purpose of this paper, we will focus on the investigation and design elements related to cut slope construction.

### *Existing Conditions*

This section of rural interstate is characterized by long, steep roadway profiles that traverse rolling terrain. According to historical information provided at pahighways.com (6), construction of the 78<sup>th</sup> Division Highway (I-78) between Lebanon and Lehigh counties took place between 1950 and 1970, originally as an upgraded alignment of US 22. The Section 12M project area was constructed in 1957.

The roadway within the project area comprises two 12-foot-wide travel lanes in each direction, with 9-foot-wide inside shoulders and 8-foot-wide outside shoulders. Eastbound and westbound traffic is separated by a 4-foot-high double-faced center concrete median barrier. The existing cut slopes in the area vary in slope ratio, ranging approximately from 1H:1V to 2H:1V, with heights typically between 20 and 50 feet. In general, the existing slopes were covered with a soil mantle containing isolated sandstone and shale bedrock outcrops and were heavily vegetated

with a variety of young to mature trees and brush. An example existing cut slope condition is provided in Figure 2, below.

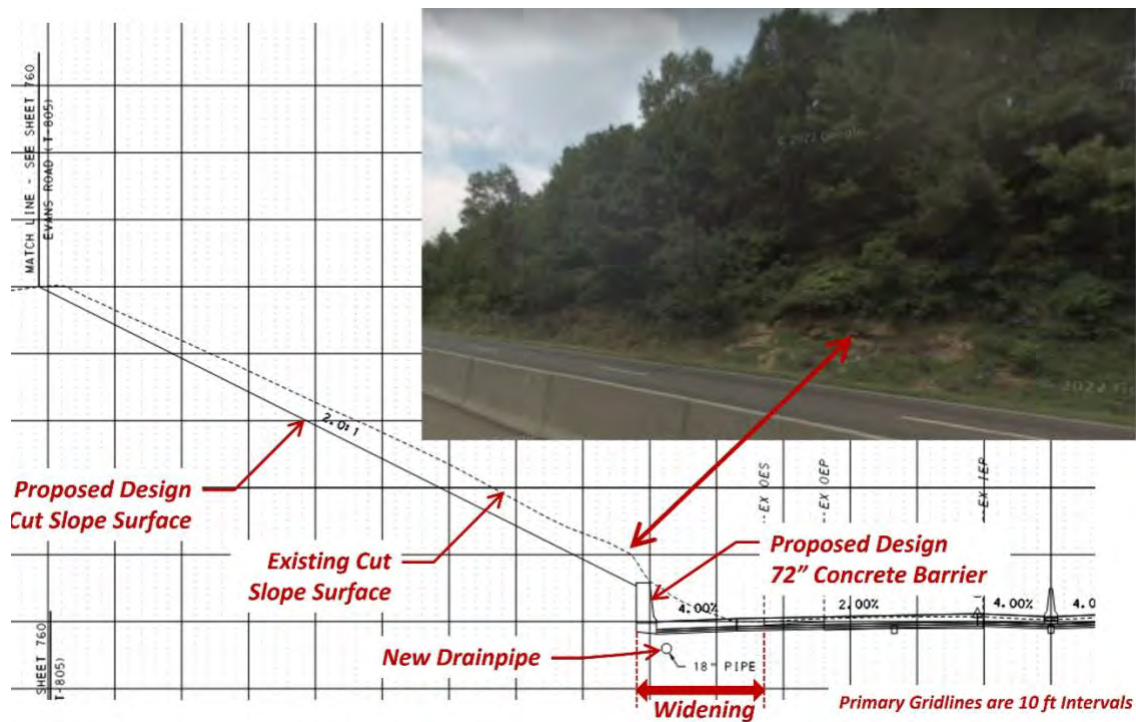


**Figure 2 – Existing and Proposed WB Cut Slope Conditions at Approx. Sta. 666+00. Modified from (7). Inset photo from 2018 Google Maps Street View.**

### *Geotechnical Investigation*

The geotechnical investigation consisted of field reconnaissance activities and test borings in support of roadway, structures, pavement, stormwater facility, and cut slope designs. The final Geotechnical Engineering Report (GER) was prepared by AEG and approved PennDOT in April 2018.

Field reconnaissance observations were limited to the portions of the cut slopes that were not obstructed by vegetation and exposed bedrock outcrops. According to the GER (1), widespread intact bedrock was not visibly evident within the existing cut slopes. The observed isolated outcrops were described as weathered shale material, with certain areas containing sections of sandstone. Some localized zones were noted where small rock fragments had accumulated on and at the base of the slopes. According to the field observations, there were no apparent indications of significant movement or historical failures and appeared to be stable at the time of the investigation.

The subsurface investigation included a total of 201 test borings, including 85 in support of cut slope design. Borings in support of cut slope design targeted a depth of 5-feet below the bottom of the cut elevation. In general, the borings in support of cut slope design encountered a

subsurface profile characterized by residual soils composed of well-graded angular gravel and sand, along with appreciable amounts of silt and clay. These soils were found to overlie interbedded shale and sandstone bedrock, consistent with the description of the Hamburg Sequence rock units.

As reported in the GER, a significant aspect of the encountered residuum is the gradual transition from the overburden soil material to the underlying bedrock. According to the GER and evident from the boring logs and profiles, the transition included the presence of very dense saprolitic material (weak rock) that maintained the fabric of the parent rock. As the residuum becomes more dense with increasing depth, the recoveries of SPT (Standard Penetration Test) samples significantly diminish, posing challenges for accurate material characterization. Attempts to sample this material using rock coring methods also yielded poor recoveries due to its inability to maintain cohesion under equipment and fluid pressures.

The distinction between the residuum soils and weathered bedrock stratum was not immediately evident in the subsurface, as the transition to coreable rock material with good recovery is gradual. Figure 3 below presents a cross-sectional view of the cut slope, including graphical representation of the test boring data at Station (Sta.) 666+003.

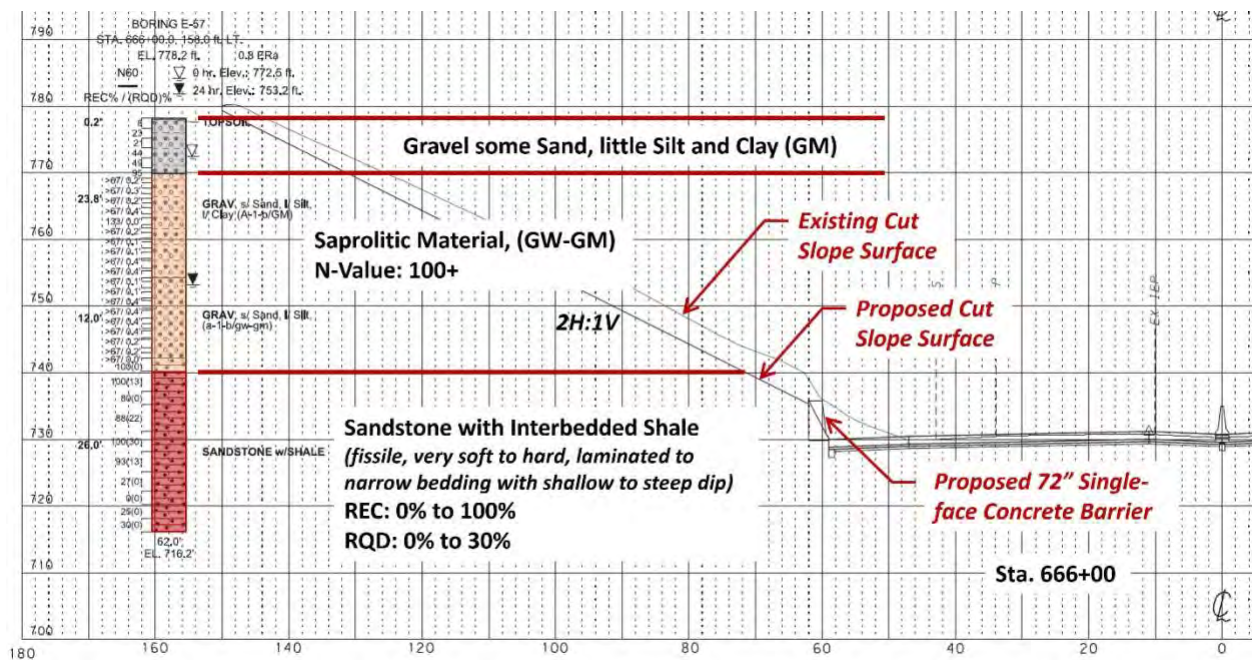


**Figure 3 – Westbound Cut Slope at Sta. 666+00 with Graphical Test Boring Data. Modified from (7).**

### *Cut Slope Widening Design*

The cut slope widening design was based on test boring data and stability analyses using GSTABL7 software developed by Gregory Geotechnical Software for soil cut slopes of 2H:1V; as well as observations of rock type and condition of the limited bedrock exposures, stereonet

(kinematic) analyses using available discontinuity measurements, and an estimation of the rock's relative resistance to erosion for rock cut slopes ranging from 1.5H to 2H:1V.

The modeled subsurface conditions and parameters used in the cut slope stability analysis (soil cut slopes) were derived from the test boring data as shown in Figure 3, above. The model was based on a two-layer subsurface profile consisting of a silty gravel (GM) decomposed rock material with a friction angle of  $38^\circ$  and zero cohesion, horizontally overlaying bedrock with a friction angle of  $42^\circ$  and a cohesion of 1,000 pounds per square foot (psf). The results of the stability analyses indicated that the factor of safety values ranged from 1.4 to 1.7 for potential near-surface/shallow depth failures and 1.5 to 2.2 for potential deep-seated failures for the widened 2H:1V cut slopes.

Stability analyses of rock cuts were based on stereonet and kinematic analyses using the discontinuity features that were observed and recorded along the exposed bedrock outcrops during design phase field reconnaissance activities. The purpose of geologic discontinuity stereonet analyses is to understand the underlying structural patterns and behaviors of rock masses. Stereonet plots provide a method of identifying the mean orientation of geological structures, such as bedding planes, faults, joints, or any other planar or linear features within a rock mass. The results obtained from stereonet plots, specifically the mean orientation of discontinuity sets, serve as a fundamental component for conducting a kinematic analysis. This analysis aims to identify potential modes of failure (e.g., planar, wedge, or toppling) by considering the geometric relationships between the orientations of the discontinuities and the cut slope surface.

In order for failure (sliding) to occur along planar discontinuities or along the intersection of discontinuities (wedge failure), the following geometrical conditions must be satisfied (13):

1. The plane or intersection on which sliding occurs must strike parallel or nearly parallel (generally  $\pm 20^\circ$ ) to the slope face.
2. The sliding plane or intersection must "daylight" in the slope face, which means that the dip of the plane or intersection must be less than the dip of the slope face.
3. The dip of the sliding plane or intersection must be greater than the angle of friction of the rock discontinuity surface.
4. The upper end of the sliding surface intersects the upper slope or terminate in a tension crack (or release joint).
5. Release surfaces that provide negligible resistance to sliding must be present in the rock mass to define the lateral boundaries of the slide.

Based on the rock type and visual discontinuity characteristics observed along the limited rock outcrop exposures, an estimated rock mass discontinuity interface friction angle of  $28^\circ$  was selected for the analyses. This angle represents the assumed resistance to sliding along the rock mass discontinuities. A kinematic analysis plot for the proposed 1.5H:1V cut slope in the vicinity of Sta. 665+75 based on estimated design phase parameters is presented in Figure 4, below.

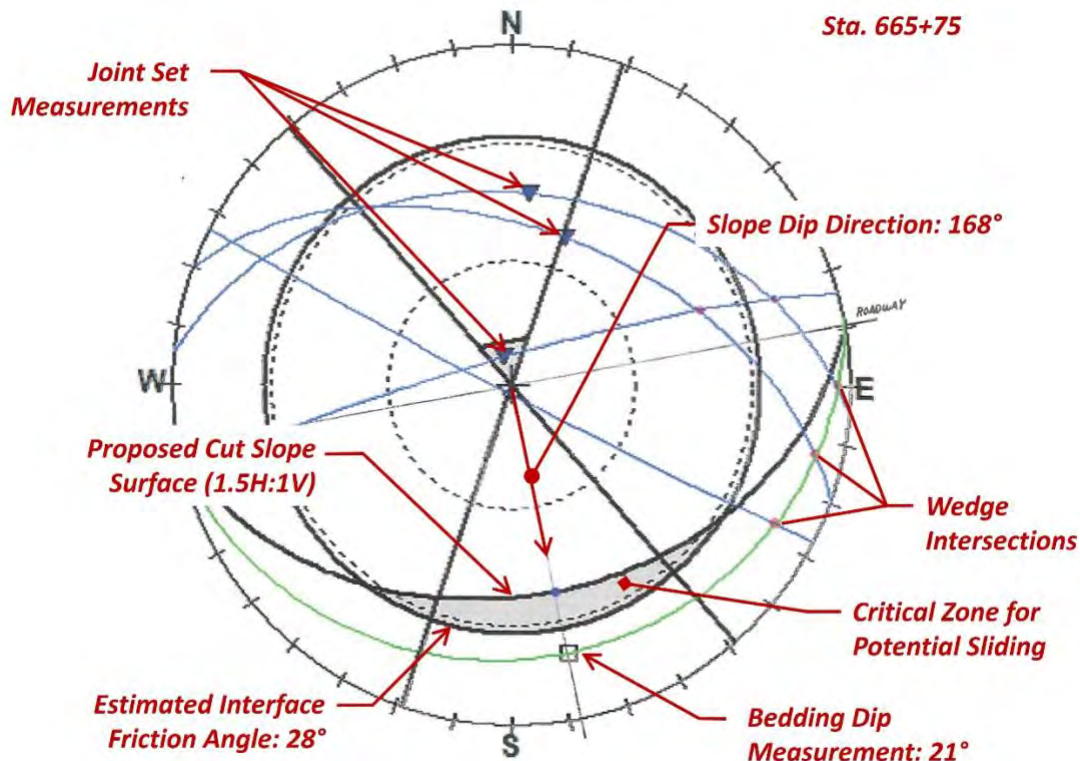


**Figure 4 – Annotated Kinematic Analysis based on Parameters Estimated During Design. Modified from project Geotechnical Engineering Report (I).**

The results of the stereonet and kinematic analyses indicated that cut slopes ranging from 1H:1V to 1.25H:1V were feasible in some locations evaluated. However, to ensure consistency in the design throughout the project, a maximum slope gradient of 1.5H:1V was selected. This choice helps maintain a more consistent cut slope design throughout the project. An annotated cut slope design cross-section at Sta. 666+00 is presented in Figure 2, above.

## CONSTRUCTION PHASE

The bid package for the project was advertised through PennDOT's Electronic Construction Management System (ECMS) system. The successful bidder, awarded in November 2018, was general contractor H&K Group, Inc. (H&K), based in Skippack, Pennsylvania. Specialty slope stabilization work, including drilling and installation of rock anchors and wire mesh facing, was performed by H&K Structures Division. Michael Baker International (Baker) of Pittsburgh, Pennsylvania, was selected to provide construction management services.

## Timeline of Events

As mentioned earlier, this section of I-78 initially had few rock exposures along existing cut slopes and had no history of slope failures. However, after the commencement of cut slope

construction utilizing mechanical excavation methods in late 2021, a series of slope failures and areas of ongoing movement concern were identified between January and March 2022. These failures occurred within the newly constructed cut slopes, which had gradients of 1.5H:1V and 2H:1V and were located adjacent to the westbound lanes on the north side of the roadway. The observed conditions included the following:

- Planar sliding along bedding planes
- Localized wedge failures known as “Rock block pop-outs”
- Surficial slumps of overburden soils and weathered rock material

At the time these failures were observed, initial cut slope construction had already been completed and adjacent trench excavation for the 18-inch stormwater drainpipe at the toe of the slope was in progress. Several of the initial failure locations that occurred between January and February 2022, were addressed using mechanical scaling methods under the guidance of AEG field geologists.

Following periods of heavy rain in late March 2022, two (2) separate locations experienced significant planar sliding, referred to as the primary failures herein. At each location, the slide debris impacted steel trench boxes supporting the drainpipe excavation. Cut slope grading and trenching operations were immediately postponed following these events until remedial measures could be implemented.

Based on the observed site conditions, projected failure modes (which involved planar sliding along daylighting bedding joints), and considering the remaining cut slope and trenching work yet to be completed, the design team recommended mitigation via mechanical scaling and regrading to improve stability in the areas where the proposed drainpipe had already been installed or not planned. For areas where additional toe cuts and pipe installation were still pending, the design team proposed rock anchor or similar stabilization. Due to the time-sensitive nature of the project and limited resources available to the design team, PennDOT engaged Gannett Fleming, Inc. in late March 2022 to prepare the design for the slope sections identified for stabilization.

Between March and May 2022, mechanical scaling operations and removal of slide debris were conducted to address the stability issues along the cut slopes. The majority of scaling operations were conducted over a 600-foot section of 2H:1V cut slope (Sta. 653+00 to Sta. 659+00), where retrogressive slide activity was impacting the work zone. Scaling operations were closely scrutinized in the field to follow the recommendations of the design team to clear only loose material above the exposed bedrock slip surface and **avoid any potential over excavation, specifically at the toe of slope**. Overall, the scaling operations resulted in the removal of more than 3,500 cubic yards of rock debris in this particular section.

Stabilization construction was performed between June and November 2022 (both slope sections). The details of the stabilization investigation, analysis, design, and construction of these primary failure areas is summarized below.

In late December 2022, the 600-foot section of cut slope (Sta. 653+00 to Sta. 659+00), that was scaled 7 months prior, experienced another large volume planar rockslide failure, see Figure 5. This failure occurred while the contractor was performing final toe cuts (< 1-foot) in support of final roadway grading. This very small cut caused a new failure surface to daylight the slope face. This section was mechanically scaled a second time, following the same recommendations as the previous effort. The exposed slide surface was found to be only a few inches thick where it was disturbed at the toe of slope but projected as much as 5-feet under the overburden materials at higher reaches of the slope. As a result of this failure and additional scaling, approximately 3,000 cubic yards of rock debris was removed from this section. Despite the small size of the toe cut, the failure had significant consequences, highlighting the complexities of designing and constructing cut slopes through weak geologic units.



**Figure 5 – Failure resulting from contractor grading activities (< 1-foot toe cut) at previously scaled slope section (Sta. 653+00 to Sta. 659+00).**

### **Stabilization of Primary Failure Areas**

Based on communication with PennDOT and construction personnel, rockfall related hazards and near surface rockslides had been an ongoing issue along the I-78 westbound cut slopes since slope clearing and grading operations commenced in late 2021. Specifically, two rockslide type events of significant volume occurred following a period of persistent heavy rainfall at the locations noted below.

- Slope Section 1 – Sta. 663+10 to Sta. 668+50, 2H:1V, 35- to 46-feet in height
- Slope Section 2 – Sta. 613+20 to Sta. 620+25, 1.5H to 2H:1V, 24- to 36-feet in height

Cut slope grading, including the near-vertical excavation for the proposed concrete barrier had been completed for approximately one month prior to failure, while excavation for the new 18-inch drainpipe adjacent to the toe of the cut was ongoing. Photos of the slope in the vicinity of Sta. 665+00 to 666+50 shortly after failure are provided in Figure 6, below.

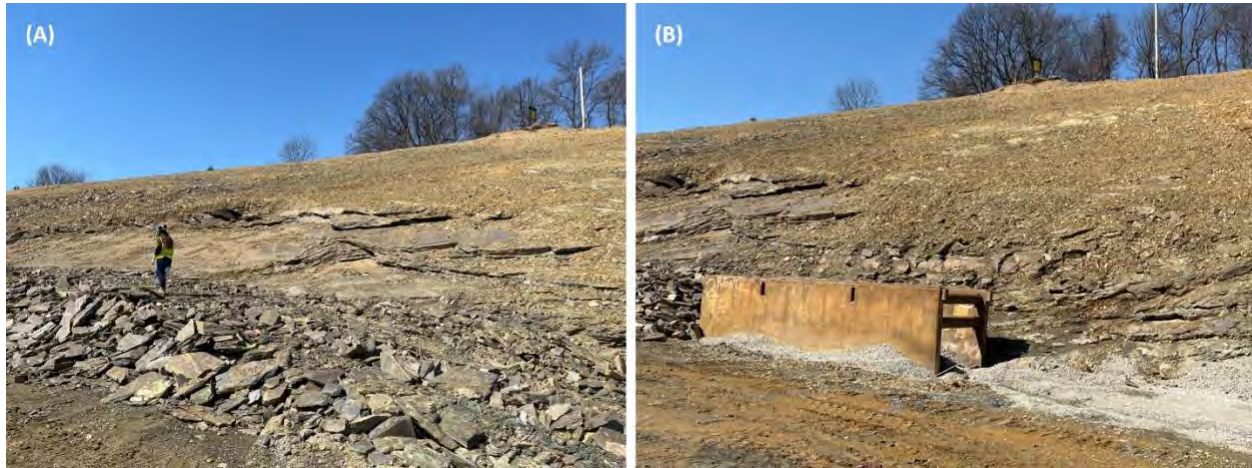


**Figure 6 – Planar Rockslide Failures, March 18, 2022. (A) Approx. Sta 665+00 to 666+00. (B) Eastern Flank of Failure at Drainpipe Trench Box, Approx Sta. 666+50.**

The project team recognized that these cut slope sections posed safety concerns for ongoing construction activities. PennDOT acted quickly in engaging Gannett Fleming to expedite the development of stabilization designs for these two sections. The objective was to ensure the safety of the work crews for the remainder of the construction period and establish long-term slope stability. The stabilization design, which involved the use of anchored mesh reinforcement, was completed within a four-week timeframe.

#### *Field Reconnaissance*

Upon receiving the notice to proceed, Gannett Fleming engineering geologists conducted thorough field reconnaissance activities. The objective was to visually assess the existing site conditions, obtain geologic discontinuity measurements from accessible bedrock exposures, and evaluate the nature of recent rockfall incidents at the site and the potential impact on the proposed construction operations. Unlike the original field investigation during the design phase, the Gannett Fleming team had the advantage of examining the freshly exposed rock units along the length of the cut slopes.

In general, the geologic conditions and discontinuity orientations exposed at both primary failure areas were consistent. The rock units observed were comprised of reddish and reddish gray interbedded shale and graywacke (sandstone), consistent with the description of the Hamburg Sequence – Dreibelbis Member.

The exposed rock units exhibited typical depositional and tectonic joint patterns. The strike of the bedding planes was found to be trending east-west (nearly parallel with the alignment of

the roadway) and dip to the south (toward the roadway). The observed bedding planes exhibited flexural folding (localized undulation), resulting in a wide range of dip angles. Measured bedding dip angles ranged from nearly flat ( $4^\circ$ ) to steep ( $42^\circ$ ). Several of the exposed bedding surfaces contained slickenside striations indicative of past movements along these surfaces. These slickenside surfaces were primarily observed between shale beds and were considerably smooth. Additionally, thin seams of clay infilling between bedding joints were observed at discrete locations. Apart from the bedding joints, steeply dipping to near-vertical stress-release orthogonal joints and secondary fractures were observed throughout the exposed rock slopes. During the field reconnaissance, the cut slope was dry; however, others reported groundwater seepage following precipitation events.

In order to obtain a general representation of the interface friction angle along the smooth bedding surface containing slickensides (failure surface), a series of “Field Tilt Tests” were performed. These tests involved placing representative blocks of rock (shale and sandstone) on surfaces with varying degrees of inclination to estimate the minimum angle at which sliding will occur along the tested surface (smooth bedding joint). The field tilt tests revealed that the minimum interface friction angle between a shale block and the smooth shale bedding surface was approximately  $22^\circ$ , while the interface friction angle between a sandstone block and the coarser sandstone bedding surface was observed to be up to  $36^\circ$ .

In addition to observing the geologic structure conditions exposed in the cut slopes, the Gannett Fleming team had the opportunity to view and characterize the transition zone material between the residual overburden soils and the intact rock strata, where good sample recoveries during the original investigation were unable to be retrieved. As indicated in the geotechnical report, a transition zone of decomposed rock was observed in the cut slope; however, it was considerably less thick than estimated. Approximately 22-feet of the transition zone characterized as a well-graded gravel with silt (GW-GM) based on recovered SPT samples, was discovered to be very thin to thinly bedded weak shale and sandstone units that still maintained the structure of a coherent rock mass.

The typical geologic conditions, in cross-section along the failure area in the vicinity of Sta. 666+00 interpreted from the available boring data and observed cut slope conditions, is included in Figure 7, below (see Figure 3, above, for a comparison to original interpreted subsurface conditions). The inset image is a panoramic photo of the cut slope conditions just prior to the installation of stabilization measures.

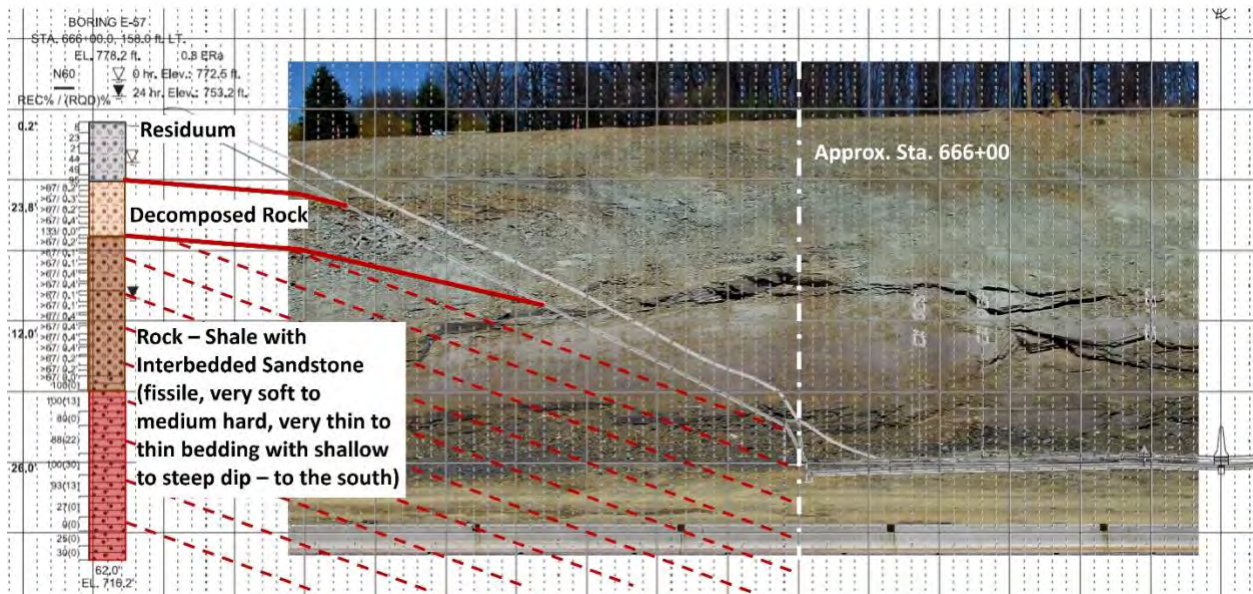


**Figure 7 – Geologic conditions in the vicinity of Sta. 666+00 interpreted from boring data and observed cut slope conditions after failure. Inset – panoramic photo of the cut slope conditions just prior to the installation of stabilization measures.**

Discontinuity measurements were collected during the field reconnaissance using a geologic compass iPhone Application – GeoID, developed by Seoul National University of South Korea. The application corrects for magnetic declination based on location and provides Dip and Dip Direction measurements of planar surfaces that the device is resting on. In total, 184 discontinuity orientation measurements (dip and dip direction) were obtained in the area of Slope Section 1 (Sta. 662+00 to Sta. 669+00) and 127 measurements in the area of Slope Section 2 (Sta. 611+50 to Sta. 621+00).

### *Stability Analysis and Stabilization Design*

Similar to the slope evaluation performed during the design phase, Gannett Fleming performed stereographic kinematic analyses to identify potential modes of slope failure based on the collected discontinuity measurement data. The data was imported into RocScience’s DIPS software, which generated contoured pole plots on a Schmidt equal area stereonet and provided statistical analyses. The contoured pole-vector plot allowed for the identification of primary discontinuity sets and the determination of mean orientation values for each set.

According to the FHWA Rock Slopes Reference Manual Table 3.1 (12), the interface friction angle of “low-friction” sedimentary and meta-sedimentary rock varies considerably, typically ranging from 20° to 27°, depending on roughness of discontinuity surfaces and mineral content. Based on the smooth texture of the exposed rock units, localized clay infilling seams observed, and the results of the field tilt testing, a friction angle of 20° was estimated and used in the analyses. The kinematic analysis dip vector plot for the area of Slope Section 1 (662+00 to Sta. 669+00), is depicted in Figure 8, below. As demonstrated by the observed failure, the kinematic

analysis indicated that planar-type failures would occur for bedding surfaces with dip angles greater than interface friction angle ( $20^\circ$ ) but less than the cut slope surface angle.

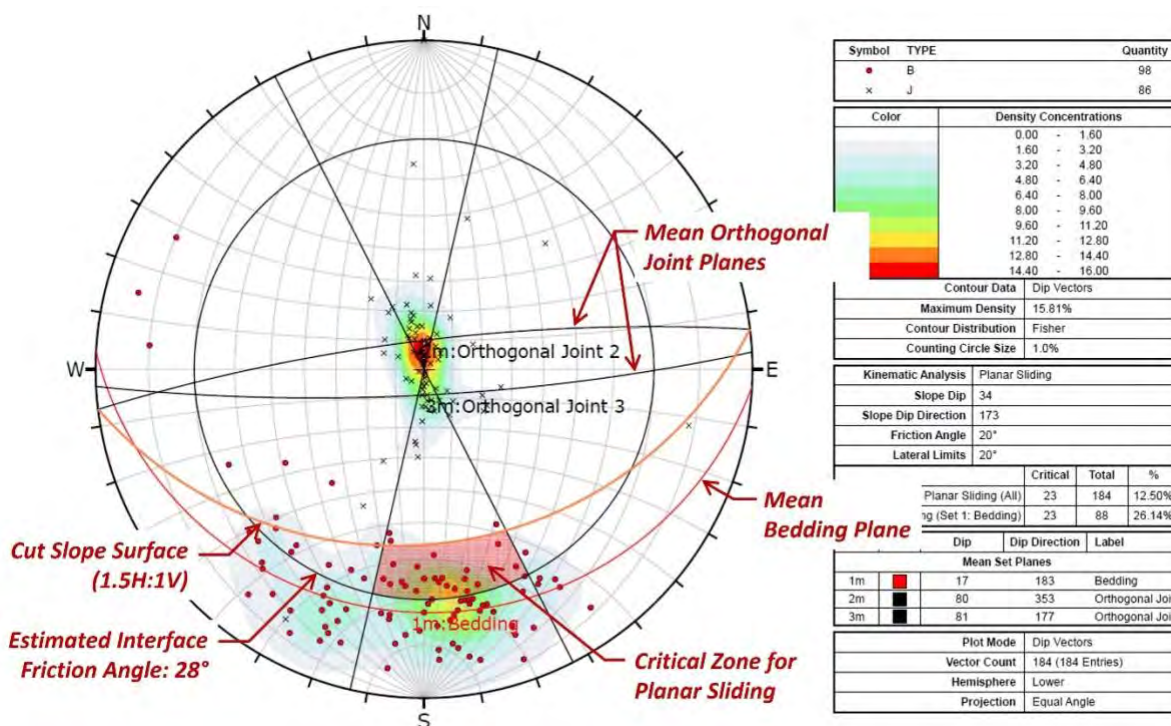


**Figure 8 – Kinematic Analysis Dip Vector Plot based on Discontinuity Measurements across Slope Section 1 (Sta. 662+00 to Sta. 669+00).**

This figure shows how the geologic structural discontinuity orientations and properties of the underlying weak rock exposed during construction aligned in such a way to intersect an exceedingly small envelope of potential failure.

Detailed limit equilibrium analyses were performed using RocPlane software by RocScience to assess the factor of safety against planar sliding failures. These analyses considered several factors, including rock slope geometry, measured discontinuity orientations, estimated groundwater conditions, and estimated properties of the rock mass. The analyses were performed for both the existing condition (post-failure) and the proposed anchored condition (passive rock dowels), as described below.

In the analysis, RocPlane software calculated the factor of safety for planar slide geometry as a function of driving and resisting forces. Based on the observations in the field, the existing cut slope condition (post failure) was anticipated to be very near the equilibrium state (F.S. = 1.0) under normal conditions. The rockslide-type failures in March 2022 occurred following a period of significant rain. The limit state equilibrium analysis input parameters (interface friction, inclination of failure surface, and percent of discontinuity saturation) were slightly adjusted to achieve a realistic back analysis model of the observed failure condition (F.S. slightly less than 1.0) to verify parameter assumptions.

Based on the results of the existing condition results, mitigation measures in the form of passive rock dowels were added to the limit equilibrium model until the selected design factor of safety (1.3) was achieved. In order to protect the work zone from potential rockfall hazards and provide additional resistance to surficial movements, the project team decided to attach a high-tensile strength steel wire mesh system to the rock dowels. A rock dowel analysis was performed to determine the appropriate rock dowel properties and design load. The analysis involved dimensioning the steel wire mesh system using RUVOLUM® online tool by GeoBrugg and calculating the size and length of the rock dowels following FHWA guidelines. To determine the minimum required dowel bond length beyond the projected failure surface, an estimated ultimate bond stress of 120 psi was used for the interbedded shale and sandstone. A design section, showing the typical stabilization treatment layout at Slope Section 1, is depicted in Figure 9, below.

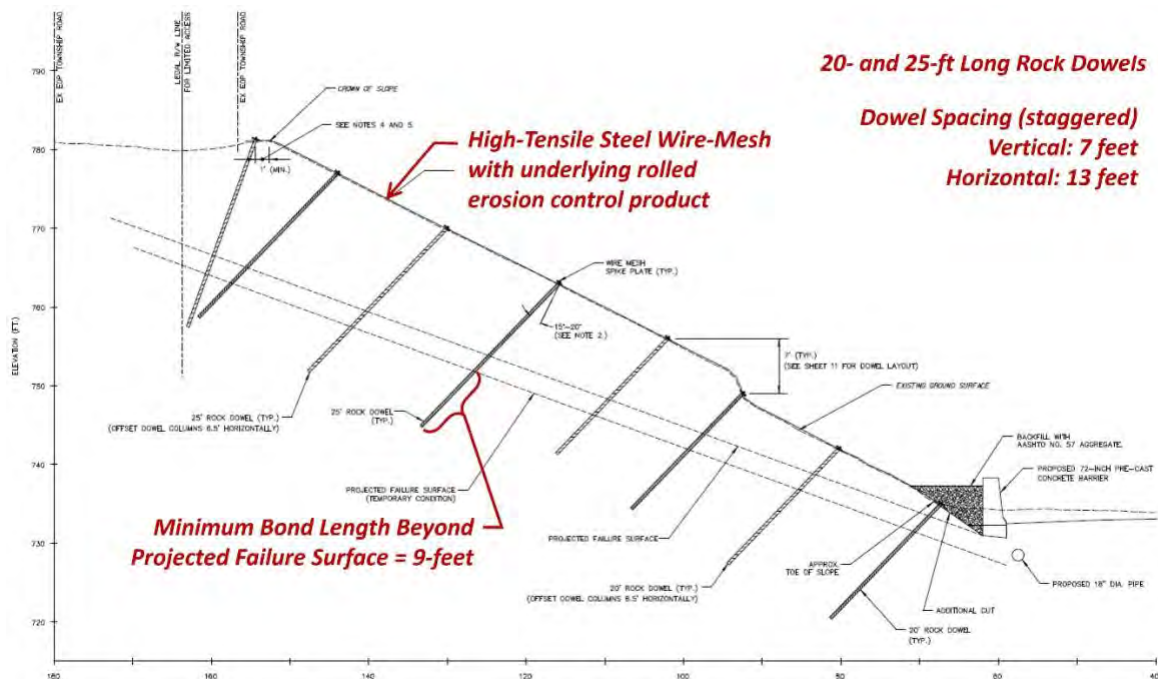


**Figure 9 – Typical Stabilization Design Section at Slope Section 1  
(Sta. 662+00 to Sta. 669+00).**

### *Stabilization Construction*

The rock slope stabilization design for the combined primary slope sections consisted of 599 fully grouted 20- and 25-ft long pattern rock dowels; 11,800 square yards of GeoBrugg TECCO® G65/3 steel wire mesh with underlying permanent rolled erosion control product; and as-directed spot rock dowels. All rock dowels consisted of 1.25-inch diameter, epoxy-coated, continuous thread, 75-ksi steel bars. The inclination angle of the drill holes was within 15° to 20° of normal to the slope face, optimizing the applied normal force with respect to the bedding joints exposed

along the cut slope. The inclination angle of the top row of rock dowels was steepened in the field, as needed, to avoid conflicts with the adjacent township right-of-way.

Baker personnel provided full time construction inspection, with regular on-site support from Gannett Fleming geologists. Gannett Fleming's primary role during construction was to provide quality assurance and quality control guidance for the dowel and mesh installation operations. This included support during layout of the dowel pattern, oversight of verification and proof testing activities, and identifying the need and locations for spot rock dowels.

The drilling work was performed by H&K Structures Division, utilizing a combination of excavator-, telehandler-, and crane-mounted rock drills. To maintain the project schedule and optimize working hours, multiple operations were conducted concurrently for both stabilization sections, including drilling, rock dowel preparation and installation, grouting, and mesh installation. In total, the stabilization work was completed within a six-month period from June to November 2022. Final paving operations and construction of the barrier walls along the toe of the cut slopes are expected to be completed by the end of June 2023. An oblique photo of Slope Section 1, six-months after completion of stabilization activities, is include in Figure 10, below.



**Figure 10 – Slope at Section 1 Six-Months following Stabilization Construction.**

## **CONCLUSIONS AND LESSONS LEARNED**

To date, more than seven months since the completion of the stabilization work, the mitigated cut slopes appear to be performing well with no obvious visual indicators of active movement, even after the region experienced heavy levels of precipitation during the early part of 2023. This indicates that stabilization measures have been effective. This dynamic project has provided a number of valuable lessons and suggested best practices for future cut slope construction projects where weak rock may be encountered.

When evaluating the proposed geometry of cut slopes, it is crucial to thoroughly review the available geologic structure data. In sedimentary rock units, linear excavations that align with the

axis of a fold, whether regional or localized, are at a higher risk of encountering adversely oriented discontinuities. These discontinuities can pose a significant threat to the slope's stability and overall condition.

Characterizing subsurface conditions, particularly when core sample recoveries are limited or surficial outcrops are obstructed or extensively deteriorated, can be challenging, particularly when dealing with weak rock and weathered material. To enhance the exploration program and obtain accurate discontinuity data, additional investigative techniques, such as downhole imaging with optical and/or acoustical televiwer geophysical methods or using a larger diameter core barrel may be beneficial. These measures will help overcome the inherent limitations and enable a more comprehensive understanding of the subsurface conditions, facilitating the development of a more accurate subsurface model.

In some cases, conclusions about subsurface geologic conditions can be inferred from slopes with limited bedrock exposures. The accumulation of rock fragments and debris at the slope's base, the extent of vegetative cover, and differential weathering features can indicate the level of weathering and deterioration the slope has undergone since its initial construction. Analyzing the shape, surface texture, and the degree of fragmentation of small, detached rock blocks along the slope can also provide valuable information for estimating interface friction angles along discontinuities and characterizing the strength properties of the underlying rock unit.

Excavations and scaling operations on cut slopes that involve unfavorably oriented rock units or slopes with a history of previous failures require diligent monitoring by an experienced engineering geologist or geotechnical engineer. Effective communication of the objectives and limitations of the scaling/excavation activities to the contractor is crucial to avoid counterproductive outcomes. This project serves as a clear example of the costly consequences that can arise from even a minor toe-cut, measuring less than one foot.

**REFERENCES**

1. American Engineers Group, LLC. *S.R. 0078, Section 12M, Berks and Lehigh Counties Pennsylvania*. MPSM No. 10466. Final Geotech Engineering Report, April 2018.
2. Geyer, A.R. and Wilshusen, J.P. *Engineering Characteristics of the Rocks of Pennsylvania*. 2<sup>nd</sup> Edition. Pennsylvania Geological Survey, Harrisburg, PA, 1982.
3. Lash, G.G. *Geologic Map of the Kutztown Quadrangle, Berks and Lehigh Counties, Pennsylvania*. Map. U.S. Geological Survey, Reston, VA, 1985.
4. Lash, G.G. *Geologic Map of the Hamburg Quadrangle, Schuylkill and Berks Counties, Pennsylvania*. Map. U.S. Geological Survey, Reston, VA, 1987.
5. Pennsylvania Department of Transportation, *2021 Annual Average Daily Traffic Volume Map, Berks County, Pennsylvania*. Map. Pennsylvania Department of Transportation, 2022.
6. Pennsylvania Highways website. *78th Division Highway (I-78)*. <https://www.pahighways.com/interstates/I78.html>. Accessed May 2023.
7. Pickering, Corts and Summerson, Inc., American Engineers Group, LLC, and AECOM. *Drawings for Construction, State Route 0078, Section 12M, Berks and Lehigh Counties Pennsylvania*. PennDOT ECMS No. 10466. 2018.
8. Santi, P.M., & Doyle, B.C. The locations and engineering characteristics of weak rock in the U.S. *Characterization of Weak and Weathered Rock Masses, Association of Engineering Geologists Special Publication #9*: Association of Engineering Geologists, Denver, CO, 1997.
9. Sevon, W.D. *Physiographic Provinces of Pennsylvania*. Pennsylvania Department of Conservation and Natural Resources, Bureau of Topographic and Geologic Survey, 2000.
10. Shultz, C.H. *The Geology of Pennsylvania*. Pennsylvania Geological Survey, Special Publication 1, 1999.
11. Pennsylvania Department of Conservation and Natural Resources (PA DCNR). *PaGEODE Web-mapping Application*. United States Department of the Interior, U.S. Geological Survey (USGS). <http://www.gis.dcnr.state.pa.us/maps>. Accessed May 2023.
12. Wyllie, D.C. and Mah, C.W. *Rock Slopes: Reference Manual*. FHWA-HI-99-007. Federal Highway Administration, U.S. Department of Transportation, 1998.
13. Wyllie, D.C. and Mah, C.W. *Rock Slope Engineering: Civil and Mining*. 4<sup>th</sup> Edition. Spon Press, 2004.

## **Comparative Analysis of Rock Slope Scaling Quantities and Crew Hours**

**Katelyn Card**

Washington State Department of Transportation  
310 Maple Park, Transportation Building  
Olympia, Washington 98504  
(360) 789-8334  
CardKat@wsdot.wa.gov

Prepared for the 72<sup>st</sup> Highway Geology Symposium, August, 2023

## **Acknowledgements**

The author would like to thank the individuals/entities for their contributions in the work described:

Samuel Johnston – Washington State Department of Transportation  
Marc Fish – Washington State Department of Transportation  
Mike Mulhern – Washington State Department of Transportation  
Cody Chaussee – Washington State Department of Transportation

## **Disclaimer**

Statements and views presented in this paper are strictly those of the author(s), and do not necessarily reflect positions held by their affiliations, the Highway Geology Symposium (HGS), or others acknowledged above. The mention of trade names for commercial products does not imply the approval or endorsement by HGS.

## **Copyright Notice**

Copyright © 2023 Highway Geology Symposium (HGS)

All Rights Reserved. Printed in the United States of America. No part of this publication may be reproduced or copied in any form or by any means – graphic, electronic, or mechanical, including photocopying, taping, or information storage and retrieval systems – without prior written permission of the HGS. This excludes the original author(s).

### ABSTRACT

Rock slope scaling is a common method used to reduce the risk of rockfall and debris impacting the highway. Currently, there are no set standards at the Washington State Department of Transportation (WSDOT) or industry-wide regarding design or quantity estimates for rock slope scaling. Presumably, this is because it is difficult to measure and estimate these quantities and scaling hours. Various rock types, weathering agents, and discontinuities are some of the factors that make estimating scaling quantities and crew hours very difficult. By investigating how these projects have been quantified in the past, we will be able to identify opportunities for improvement and progress toward a common standardized practice. The purpose of this paper will be to analyze past rock slope scaling projects throughout Washington state (WA) and identify potential impacts of site conditions to calculated estimates versus actual quantities of debris removal and scaling crew hours. Prior investigations into quantity estimates for rock slope scaling projects are limited. A previous study conducted by California Department of Transportation (CalTrans) in 2016 presented a method that geo-professionals may use to assess and quantify rock slope scaling operations. Based on previous WSDOT project information, we compare the estimated quantities of rock slope scaling debris and scaling crew hours with actual values after the project was completed. We compared various factors that may influence estimates determined by the Project Engineer or designer including climate and groundwater, dominant weathering agents, rock strength, discontinuity characteristics, and rock type. This paper presents the findings of this research and offers an guide to standardizing quantity estimates for rock slope scaling projects at WSDOT.

## **INTRODUCTION**

Rock slope scaling is a crucial process in the field of geotechnical engineering that focuses on assessing and quantifying the stability of rock slopes. It involves the systematic evaluation and measurement of discontinuities within rock masses, such as joints, faults, and bedding planes, to determine their potential for failure. Rock slope scaling plays a vital role in various industries, including mining, construction, and transportation, as it enables engineers and geologists to identify potential hazards and develop appropriate mitigation strategies. By analyzing the characteristics of different rock masses, we can formulate more accurate estimates for rock slope scaling to the safety and stability of slopes, minimizing the risk of rockfall and slope instability incidents. Currently, there are no set standards at the Washington State Department of Transportation (WSDOT) or industry-wide regarding design or quantity estimates for rock slopes scaling. The purpose of this paper is correlate rock characteristics and rock slope dimensions with the accuracy of project estimations compared to actual values recorded.

## **BACKGROUND**

Rock slope scaling is an essential technique used in geotechnical engineering and engineering geology to assess the stability of rock slopes. When dealing with steep slopes, such as those encountered in mining operations, road construction, or natural rock formations, understanding the behavior of the rock mass is crucial to ensure the safety of both workers and the public. One of the key factors in evaluating slope stability is the quantification of debris quantities.

Debris quantities refer to the amount of loose or detached rock material that may pose a risk of falling from a slope (Figure 1). These debris materials can range in size from small rock fragments to large boulders, and their presence on a slope can significantly increase the potential for rockfall incidents. Debris quantities are influenced by various factors, including the geological characteristics of the weathering rating, rock strength, discontinuity characteristics, and overall rock type.



**Figure 1 – Rock Slope Scaling Crew at US 12 MP 145.75**

Accurate assessment of debris quantities is vital for effective slope management and risk mitigation. It helps engineers and geologists understand the potential hazards associated with a slope and develop appropriate strategies to minimize the risk of rockfall incidents. By quantifying the volume, size distribution, and spatial distribution of debris, engineers can identify areas of high risk and implement appropriate measures, such as rockfall protection barriers or slope stabilization techniques, to ensure the safety of nearby infrastructure, human populations, and the environment.

The process of quantifying debris quantities typically involves field surveys and measurements, including detailed mapping of the slope, collection of rock samples, and the use of remote sensing techniques. The collected data is then analyzed to determine the potential sources of debris, evaluate the stability of the slope, and estimate the likelihood of future rockfall events.

In recent years, advances in technology and data analysis techniques have enhanced the accuracy and efficiency of debris quantity assessments. Remote sensing technologies, such as LiDAR (Light Detection and Ranging) and photogrammetry, allow for the rapid collection of high-resolution data, enabling precise mapping and measurement of slopes. Furthermore,

computer-based modeling and simulation tools have been developed to simulate the behavior of rock masses and assess the potential impact of debris movements.

Overall, understanding the background and quantification of debris quantities is critical for effective slope management and ensuring the safety of infrastructure and people in areas prone to rockfall incidents. Ongoing research and technological advancements continue to improve our ability to assess and mitigate the risks associated with unstable rock slopes, leading to safer and more sustainable engineering practices.

## **METHODS**

For the purpose of this paper, we analyzed 15 projects across Washington state with varying geologic conditions and rock masses. We used these projects to identify any possible connections with scaling crew hours and debris quantity estimates compared to actual values reported. For each project site, we identified the rock type, rock strength, weathering rating, regional climate, and rock slope dimensions. We compared the Engineer or designer's estimates for crew hours required for scaling and debris quantities by the actual hours and quantities that were billed.

## **FINDINGS**

We analyzed 15 projects across Washington state using available geotechnical report documents available. Below is a summary of the conditions for each site with a summary table of the engineering estimate, actual quantities, and the difference between them.

### **SR 2 – ½ Mile East of Climbing Lane Rock Slope Mitigation Geotechnical Report**

According to the associated WSDOT geotechnical report (1), the site is located west of the Cascade crest in the Northern Cascade physiographic province, which is primarily influenced by a moist, maritime climate with cold, wet winters and over 90 inches of annual rainfall at nearby weather stations. The site falls within the mapped area of the Grotto Batholith, covering approximately 50 square miles and composed mainly of granite and granodiorite. Within the project area, the rock is a grey, strong (R4) granodiorite, ranging from slightly weathered to fresh, with moderate weathering observed along some discontinuities. The slope exhibits both persistent and local discontinuities, with variable conditions along its length and slightly rough surfaces and typical apertures between 1/32nd and 1/8th inch. Discontinuities were generally not infilled. Site observations indicate a significant groundwater flow throughout the year, increasing during the winter and spring months. The slope measures approximately 250 feet in length with an overall height ranging from 60 to 90 feet, resulting in an estimated area of 18,750 square feet.

<b>Table 1. SR 2 – ½ Mile East of Climbing Lane Rock Slope Mitigation Estimates vs Actual Rock Slope Scaling Quantities</b>					
Engineers Estimate		Actual Quantities		Actual is greater or less than estimate	
Crew Hours	Debris Removal (CY)	Crew Hours	Debris Removal (CY)	Crew Hours	Debris Removal
100	500	295	2884.5	3x greater	6x greater

### **SR 20 Deception Pass State Park Unstable Slopes**

According to the WSDOT geotechnical report (2), the site is located in the Puget Lowland physiographic province on the northern tip of Whidbey Island. The province experiences a moist, maritime climate characterized by cold and wet winters. The annual average precipitation at the project site, measured in Anacortes, WA, is approximately 26 inches per year. Rainfall is the dominant form of precipitation, with over 80% occurring between October and April.

The bedrock at the site is mapped as an ophiolite sequence within the Fidalgo Complex, as described by Brown (1). Ophiolites are remnants of ancient oceanic crust formed at spreading centers and subsequently thrust onto land. The moderately weathered ophiolite sequence at the project site consists of fine-grained ocean sediments (cherts, limestone, etc.) at the top, followed by slightly weathered, weak pillow basalt and intrusive mafic and ultramafic rocks.

The rock mass at the site exhibits blocky zones with block sizes reaching up to 6 feet in diameter. Numerous persistent discontinuities, including joints and bedding planes, dissect other areas of the slope. These discontinuities are partially filled and define potential failure modes such as wedging, planar sliding, and toppling. Trees have rooted themselves in many of these discontinuities, causing "root jacking" and displacement of loose rock blocks. Seepage was observed in the slope during late fall and early winter.

The slope measures approximately 250 feet in length and 40 feet in height. The estimated area of the exposed rock face is approximately 10,000 square feet.

<b>Table 2. SR 20 Deception Pass State Park Unstable Slopes Estimates vs Actual Rock Slope Scaling Quantities</b>					
Engineers Estimate		Actual Quantities		Actual is greater or less than estimate	
Crew Hours	Debris Removal (CY)	Crew Hours	Debris Removal (CY)	Crew Hours	Debris Removal

280	500	144	807.3	2x less	2x greater
-----	-----	-----	-------	---------	------------

#### SR 4, East of County Line Park Rockfall Work

According to the WSDOT geotechnical report (3), the project area is situated along the north shoreline of the Columbia River in Cowlitz County. It falls within the Willapa Hills physiographic province, which is characterized by a moist maritime climate. Winters tend to be cool and wet, while summers are typically dry and warm.

The Willapa Hills physiographic province is located in the southwestern quadrant of Washington state. It is distinguished by its rounded topography and deeply weathered soils. The unstable slope section consists of two Columbia River Basalt flows, specifically the Saddle Mountains - Pomona Member and the Wanapum - Frenchman Springs Member, with an interbed of siltstone (Astoria Formation) between them. The lower excavated basalt slope (Saddle Mountains - Pomona Member) is approximately 45 feet high and exhibits a near-vertical orientation. The bedrock is moderately to slightly weathered but remains strong. Discontinuities are moderately to closely spaced with low persistence. The bedrock surface is irregular, rough, and undulating, featuring small to medium-sized blocks. Surface water was observed within the landslide area, flowing downslope towards the west side of the slope through a ditch.

The dimensions of this slope measure approximately 175 feet in length and 225 feet in height. Based on these measurements, the estimated area of the slope is 39,375 square feet.

<b>Table 3. SR 4, East of County Line Park Rockfall Work Estimates vs Actual Rock Slope Scaling Quantities</b>					
Engineers Estimate		Actual Quantities		Actual is greater or less than estimate	
Crew Hours	Debris Removal (CY)	Crew Hours	Debris Removal (CY)	Crew Hours	Debris Removal
80	200	127.5	392	2x greater	2x greater

#### US 2 – West of Leavenworth Slope Stabilization

According to the WSDOT report (4), in the town of Leavenworth, situated approximately 8 miles south of the project site, average daily temperatures hover slightly above freezing, with nighttime temperatures dropping well below freezing. During the summer, average daytime temperatures reach around 85 degrees Fahrenheit, while nighttime temperatures drop to around 50 degrees Fahrenheit. Winter snow depths typically range between 10 to 20 inches, and the total annual precipitation is estimated to be approximately 26 inches.

The project site lies within the North Cascades physiographic province. The rock mass at the site consists of slightly to moderately weathered, blocky, and strong ultrabasic rocks, specifically the gabbro/serpentine peridotite of the Ingalls Tectonic Complex. The stability of the rock slope is influenced by the existing geologic structure. Some of the rock mass discontinuities contain calcite and serpentine minerals, likely formed due to thermal metamorphic processes. The rock mass exhibits pervasive fracturing, likely influenced by the proximity of the Leavenworth Fault. Rockfall debris and colluvium mantle the bedrock along discontinuities. Certain rock structures within the slope experience seasonal wetting from surface water and groundwater that seeps into discontinuities, particularly during spring runoff. Alternating freeze/thaw cycles contribute to the widening of discontinuities, leading to rockfall.

The slope measures approximately 1,120 feet in length and has a height ranging from 50 to 150 feet. Based on these measurements, the estimated overall area of the slope is approximately 112,000 square feet.

<b>Table 4. US 2 – West of Leavenworth Slope Stabilization Estimates vs Actual Rock Slope Scaling Quantities</b>					
Engineers Estimate		Actual Quantities		Actual is greater or less than estimate	
Crew Hours	Debris Removal (CY)	Crew Hours	Debris Removal (CY)	Crew Hours	Debris Removal
128	810	527.12	2688.5	4x greater	3x greater

### **US 2 Pine Canyon Emergency Repair**

According to the WSDOT geotechnical report (5), the climate in this location closely resembles that of the US 2 - West of Leavenworth Slope Stabilization project. The rock mass at the site is slightly to moderately weathered, characterized as medium strong to strong. Discontinuities exhibit a range from very closely to moderately spaced, with persistence ranging from low to very high, and varying from tight to partly open. The presence of adverse-oriented foliation and fractures creates potential failure modes such as planar sliding, wedging, and toppling. The bedrock in this area is mapped as Swakane Gneiss intruded by rhyolite dikes. The geotechnical report associated with this rock slope did not report the presence of groundwater.

The slope measures approximately 525 feet in length and 115 feet in height, resulting in an estimated overall area of approximately 60,375 square feet.

<b>Table 5. US 2 – US 2 Pine Canyon Emergency Repair Estimates vs Actual Rock Slope Scaling Quantities</b>					
Engineers Estimate		Actual Quantities		Actual is greater or less than estimate	
Crew Hours	Debris Removal (CY)	Crew Hours	Debris Removal (CY)	Crew Hours	Debris Removal
40	200	30	630.8	1.3x less	3.15x greater

### US 12 – West of White Pass – Stabilize Slopes

Based off the information from the WSDOT geotechnical report (6), the project area experiences a temperate climate in the summer and cold, wet conditions during the winter. Around 7% of the annual precipitation occurs between June and August, while approximately 50% occurs between November and January. The total annual snowfall reaches approximately 150 inches, with the majority falling between December and February. Snow accumulation often exceeds two feet in depth.

The project area is situated near Lava Creek Falls on the north slope of Ayance Canyon, within the southern Cascade Range physiographic province. It is located approximately six miles west of White Pass and twenty miles southeast of Mt Rainier. Ayance Canyon contains the Clear Fork of the Cowlitz River, which flows westward from the Cascade Range to the Pacific Ocean. The Cascade Range in Washington State is a complex assemblage of terranes, representing foreign rock bodies that accreted onto the western coast of North America during the Late Mesozoic Era. These terranes have undergone extensive volcanic activity, plutonic intrusions, uplift, metamorphism, erosion, and glaciation. The rock slope consists of slightly to highly weathered, weak to very strong basalt and associated volcanoclastic rock and soil. The slightly weathered basalt exhibits low to moderate persistence of discontinuities, some infilling, and closely spaced fractures. Although no groundwater was observed during the summer months, weathering patterns on the slope face suggest that water may seep from fractures and discontinuities near the base of the slope in the highly weathered volcanoclastic rock during the wet season.

The slope measures approximately 200 feet in length and varies in height from 25 to 100 feet. Based on these measurements, the estimated overall area of the exposed slope is approximately 16,120 square feet.

<b>Table 6. US 12 – West Side White Pass – Stabilize Slopes Estimates vs Actual Rock Slope Scaling Quantities</b>		
Engineers Estimate	Actual Quantities	Actual is greater or less than estimate

Crew Hours	Debris Removal (CY)	Crew Hours	Debris Removal (CY)	Crew Hours	Debris Removal
60	100	310	4602.4	5.16x greater	46x greater

### SR 14 / 0.8 & 1.1 Miles West of Wind River Road – Slope Stabilization

The following summary is based on the information provided in the WSDOT geotechnical report (7). The project area experiences a temperate climate during the summer and cold, wet conditions in the winter. It is located within the South Cascade physiographic province of Washington State. The South Cascades have a complex geological history spanning over 200 million years, characterized by tectonic accretion, folding, faulting, uplift, erosion, magmatic intrusion, and sedimentary deposition. This has resulted in a diverse assemblage of terranes overlain by Tertiary volcanic and sedimentary rocks. The Columbia River has carved the Columbia River Gorge, which was further shaped by ice-aged floods (Missoula Floods) originating in western Montana. The project location in the Columbia River Gorge exposes Tertiary volcanic and sedimentary sequences, along with portions of the uplifted mountain range core.

The slope primarily consists of moderately fractured, slightly to highly weathered, moderately strong to very strong basaltic andesite and andesitic flow breccia. The slope exhibits limited structural features, but there are some roadway dipping joints that contribute to planar failures. Block sizes typically range from 6 inches to 10 feet. The joints have low to medium persistence, open aperture, some infilling, and rough surfaces, with a Joint Roughness Coefficient (JRC) ranging between 10 and 18. Instability issues in this rock mass generally arise from poor rock quality rather than adverse orientation of structurally controlled features. No groundwater was observed at the location; however, surface water has been observed on the slope face.

The slope is approximately 1600 feet in length and varies in height from 50 to 150 feet, resulting in an estimated overall area of approximately 160,000 square feet.

<b>Table 7. SR 14 / 0.8 &amp; 1.1 Miles West of Wind River Road – Slope Stabilization Estimates vs Actual Rock Slope Scaling Quantities</b>					
Engineers Estimate		Actual Quantities		Actual is greater or less than estimate	
Crew Hours	Debris Removal (CY)	Crew Hours	Debris Removal (CY)	Crew Hours	Debris Removal
140	500	84	708	1.6x less	1.4x greater

### SR 410/Chinook Pass Vicinity – Stabilize Slopes – MP 69.68 to 70.73

According to the WSDOT geotechnical report (8), the project area experiences a temperate climate during the summer and cold, wet conditions in the winter. The primary geology of the site consists of volcanic and volcanoclastic rocks belonging to the Oligocene-age Ohanapecosh Formation. These rocks are predominantly andesite, with lesser amounts of dacite, basalt, and rhyolite. The Ohanapecosh Formation underwent folding, uplift, and deep erosion before the deposition of the overlying Stevens Ridge Formation. The Stevens Ridge Formation consists of thin layers of pumice and ash. Multiple episodes of alpine glaciation during the Pleistocene period resulted in significant erosion, shaping deep U-shaped valleys, exposing older underlying rocks, and transporting sediment downstream. The slopes are covered by remnants of glacial deposits and coarse colluvial materials formed by weathering and gravity-driven transport downslope. The slopes primarily consist of highly fractured, fresh to slightly weathered, and strong andesite. Discontinuities within the rock mass are closely spaced and partially open. Groundwater was observed seeping from these discontinuity structures and flowing down the rock face.

The slope measures approximately 4174 feet in length and varies in height from 40 to 200 feet. Based on these measurements, the estimated area of the slope is approximately 521,875 square feet.

<b>Table 8. SR 410/Chinook Pass Vicinity – Stabilize Slopes – MP 69.68 to 70.73_Estimates vs Actual Rock Slope Scaling Quantities</b>					
Engineers Estimate		Actual Quantities		Actual is greater or less than estimate	
Crew Hours	Debris Removal (CY)	Crew Hours	Debris Removal (CY)	Crew Hours	Debris Removal
1240	7400	1019.42	9250	1.2x less	1.3x greater

### SR 165/S of Carbonado. USMS Slope #3005

This summary is based off information from the WSDOT geotechnical report (9). The project area experiences a temperate climate during the summer and cold, wet conditions in the winter. The rock slope is situated in the Cascade Mountains and is primarily composed of blocky intrusive andesite and dacite from the Miocene to Oligocene age. According to Schuster (1), the unit is described as a massive porphyry surrounded by columnar-jointed porphyry, suggesting shallow emplacement. In some areas, the rock slope is deeply weathered, forming clay grus with common irregular-shaped cavities. The rock slope consists of highly fractured, strong andesite, identified as the intrusive andesite mapped in this location. Discontinuities within the rock mass play a crucial role in rock failures, with closely to moderately spaced and partly open discontinuities observed, some of which are infilled. A few discontinuities with adverse

orientations contribute to wedge, planar, and toppling-type failures. No surface water or groundwater was observed at this site.

The slope measures approximately 400 feet in length and ranges in height from 30 to 75 feet. Based on these measurements, the estimated area of the exposed rock slope is approximately 20,200 square feet.

<b>Table 9. SR 165/S of Carbonado. USMS Slope #3005 Estimates vs Actual Rock Slope Scaling Quantities</b>					
Engineers Estimate		Actual Quantities		Actual is greater or less than estimate	
Crew Hours	Debris Removal (CY)	Crew Hours	Debris Removal (CY)	Crew Hours	Debris Removal
40	240	37	168	1.1x less	1.4x less

### **I-90/Denny Creek Viaduct Vicinity – Stabilize Slope Project**

According to the WSDOT geotechnical report (10), The climate at this location typically exhibits a mild and dry summer, along with a cold and wet winter. The project site is situated in the central Cascade Range, which forms a western rampart of the North American Cordillera. Geologically, the region consists of an older basement comprising accreted terranes overlain by Tertiary sedimentary and volcanic rocks. The site is located just north of the transition zone between the "Western and Eastern Mélange belt" and the region to the south, where basement rocks are extensively covered by tertiary sedimentary and volcanic rocks. The bedrock at the site is mapped as a Miocene-age granitoid batholith, predominantly composed of medium-grained, mostly equigranular hornblende-biotite granodiorite and tonalite. Although an unnamed normal fault is mapped to traverse Denny Creek, north of the site, it is not mapped as crossing the section of the highway under consideration. Generally, the rock mass is slightly to moderately weathered and classified as moderately strong to strong granodiorite and tonalite. The discontinuities exhibit high persistence and wide spacing, with smooth planar surfaces. Certain rock structures within the rock slope are affected by surface water and groundwater, which seep into the discontinuities during spring runoff.

The slope measures approximately 1162 feet in length and has a height of 70 feet. Based on these measurements, the estimated area of the slope is approximately 81,340 square feet.

<b>Table 10. I-90/Denny Creek Viaduct Vicinity – Stabilize Slope Project Estimates vs Actual Rock Slope Scaling Quantities</b>					
Engineers Estimate		Actual Quantities		Actual is greater or less than estimate	
Crew Hours	Debris Removal (CY)	Crew Hours	Debris Removal (CY)	Crew Hours	Debris Removal
400	3000	430.2	1189.5	1.07x less	2.5x less

**SR 7 MP 24.41 to 24.44 and MP 24.61 to 24.64 – State-Wide Risk Reduction Scaling Program**

According to the WSDOT geotechnical report (11), the climate at this site is typically characterized by mild and warm conditions in the summer, while winters tend to be wet and cold. The slope primarily consists of highly fractured, slightly weathered, and strong intrusive andesite. Rockfall events have been observed, mainly occurring as planar and wedge-type failures. The discontinuities within the rock mass generally exhibit high persistence and wide spacing. During observations at the project location, no groundwater was detected.

The slope measures approximately 275 feet in length and has a height of 55 feet. Based on these measurements, the estimated area of the rock slope face is approximately 15,125 square feet.

<b>Table 11. SR 7 MP 24.41 to 24.44 and MP 24.61 to 24.64 – State-Wide Risk Reduction Scaling Program Estimates vs Actual Rock Slope Scaling Quantities</b>					
Engineers Estimate		Actual Quantities		Actual is greater or less than estimate	
Crew Hours	Debris Removal (CY)	Crew Hours	Debris Removal (CY)	Crew Hours	Debris Removal
80	200	55.5	268	1.44x less	1.34x more

**SR 20 MP 319.36 to 319.57**

According to the WSDOT geotechnical report (12), the site experiences a generally mild and warm climate during the summer months, while the winter season is characterized by wet and cold conditions. The rock mass at this location primarily consists of slightly weathered schist, exhibiting variations from locally fractured to massive and characterized by strong

properties. Discontinuities within the rock mass range from closely to widely spaced. Rockfall events typically occur as a result of adversely oriented joint sets, giving rise to planar, wedge, and topple-type failures. No significant seepage or groundwater was observed at this site.

The slope measures approximately 1000 feet in length and has a height of 75 feet, resulting in an estimated overall area of the slope face of approximately 82,500 square feet.

<b>Table 12. SR 20 MP 319.36 to 319.57 Estimates vs Actual Rock Slope Scaling Quantities</b>					
Engineers Estimate		Actual Quantities		Actual is greater or less than estimate	
Crew Hours	Debris Removal (CY)	Crew Hours	Debris Removal (CY)	Crew Hours	Debris Removal
200	1000	432.04	3762	2.2x greater	3.8x greater

### **SR 3 – 1.1 Miles South of SR 304 – Unstable Slope**

According to the WSDOT geotechnical report (13), The project site experiences a warm and dry climate during the summer, while the winter brings wet and cold conditions. It is located within the Puget Lowland, a broad topographic basin extending north to south between the Olympic Mountains and the Willapa Hills to the west and the Cascade Range to the east. The formation of the Puget Lowland basin is a result of both tectonic processes, which created the lowland as an extensional fore arc basin west of the Cascade volcanic arc, and isostatic depression caused by Pleistocene glaciation. The Puget Lowland is predominantly composed of Eocene volcanic rock, overlain unconformably by Eocene to Oligocene sedimentary rocks, which, in turn, are unconformably overlain by glacial sediments.

The project site is located on the easternmost outcrop of the Crescent Formation, an Eocene volcanic deposit that forms the eastern periphery of the Olympic Peninsula. The Crescent Formation consists of basalt flows, pillow basalts, basaltic breccias, and interbedded pyroclastic and sedimentary rocks. The dominant bedrock in the project area consists of massive, jointed, and locally vesicular basalt flows, which are characteristic of the upper member of the Crescent Formation. The project slope primarily consists of generally massive, highly to moderately weathered, and strong basalt. Discontinuities exhibit low persistence and are generally closely to moderately spaced. Although groundwater seeps have been reported at this location, they do not appear to be a significant contributing factor to slope instability.

The slope measures approximately 540 feet in length and has a height of 35 feet, resulting in an estimated overall area of approximately 18,900 square feet.

<b>Table 13. SR 3 – 1.1 Miles South of SR 304 – Unstable Slope Estimates vs Actual Rock Slope Scaling Quantities</b>					
Engineers Estimate		Actual Quantities		Actual is greater or less than estimate	
Crew Hours	Debris Removal (CY)	Crew Hours	Debris Removal (CY)	Crew Hours	Debris Removal
60	150	160	1405	2.6x greater	9.4x greater

### **SR 25 MP 62.10 to 62.18 – State-Wide Risk Reduction Scaling Program**

According to the WSDOT geotechnical report (14), the project area is characterized by a dry-summer continental climate, with hot summers and cold winters. The slope primarily comprises highly to moderately fractured, slightly weathered, and strong meta-volcanic rock. Discontinuities within the rock mass are closely to moderately spaced, exhibiting low persistence. Rockfall events are observed to occur from various joint sets, resulting in toppling features as well as localized wedge and planar type features. No significant seepage or groundwater has been reported at this location.

The slope measures approximately 400 feet in length and has a height of 40 feet. The estimated surface area of the slope is approximately 16,000 square feet.

<b>Table 14. SR 25 MP 62.10 to 62.18 – State-Wide Risk Reduction Scaling Program Estimates vs Actual Rock Slope Scaling Quantities</b>					
Engineers Estimate		Actual Quantities		Actual is greater or less than estimate	
Crew Hours	Debris Removal (CY)	Crew Hours	Debris Removal (CY)	Crew Hours	Debris Removal
80	300	432.04	3762	5.4x greater	12.54x greater

### **SR 21, Vicinity MP 112.80 to 113.01 Emergency Rockfall**

According to the WSDOT geotechnical report (15), the project area is characterized by a dry-summer continental climate, characterized by hot summers and cold winters. The slope primarily consists of highly to moderately fractured, slightly weathered, and strong meta-volcanic rock. However, it should be noted that the rock mass typically consists of highly to moderately fractured, slightly to moderately weathered, and strong granodiorite. Discontinuities within the rock mass exhibit a range from closely to widely spaced, with some being partly open

to open. Rockfall events are typically generated from adversely oriented joints, leading to planar, wedge, and toppling-type failures. However, in areas where the rock mass is moderately weathered, raveling-type failures can also occur. Seepage was consistently observed on the slope during each site visit for this project.

The slope measures approximately 1100 feet in length and varies in height from 20 to 60 feet. Based on these measurements, the estimated overall area of the slope is approximately 44,000 square feet.

<b>Table 15. SR 21, Vicinity MP 112.80 to 113.01 Emergency Rockfall Estimates vs Actual Rock Slope Scaling Quantities</b>					
Engineers Estimate		Actual Quantities		Actual is greater or less than estimate	
Crew Hours	Debris Removal (CY)	Crew Hours	Debris Removal (CY)	Crew Hours	Debris Removal
160	700	162.44	1815	1.01x greater	2.6x greater

## **DISCUSSION**

For the purpose of this paper and the scope of work for rock slope scaling estimates, we assume that anything less than 200% of the initial estimate and or less than the estimated about is within an acceptable range. We found that 4 out of 15 sites were estimated within that acceptable range, 2 out of 15 sites are an accurate value for crew hours and an underestimate for debris quantities, 1 site had an accurate estimate for crew hours and an overestimate for debris quantities, 1 site had an overestimate for crew hours and an underestimate for debris quantity, with the remaining 7 having underestimates for each. We evaluated each of the variables that may impact these estimates including climate, weathering rating, rock strength, discontinuity characteristics, and rock type.

### **Climate and Groundwater**

While evaluating the climatic differences between project sites, we noticed that many unstable slopes within our study area experience mild and warm summers followed by wet and cold winters. Most rockfall throughout the state is associated with periods of heavy rainfall and snow melt following the winter months. We were unable to delineate any climatic control differences between each project site. However, according to geotechnical documents, project sites that appear to be controlled by seepage within discontinuity structures have more accurate estimates for rock slope scaling debris quantities and crew hours. For locations without observed groundwater seepage, we observed that half of the estimates were acceptable, while the other half was underestimated.

## **Weathering Rating**

We anticipate that a potential impact for estimating rock slope scaling debris quantities may be attributed to weathering. The extent of weathering can vary, and rocks with higher weathering ratings are more susceptible to erosion and instability. Weakened and altered rocks may experience higher deformations and exhibit reduced load-bearing capacity, increasing the risk of slope failure. Additionally, highly weathered rocks with high permeability are more susceptible to water-related instabilities such as pore pressure buildup and erosion. We may expect more highly weathered slopes to produce more debris during scaling activities and possibly require less time to scale per crew hour.

We did not find a significant correlation between rock masses that were more slightly weathered compared to highly weather with the regard to the scaling hour and debris quantity estimates. However, there is a trend in which estimates are more accurate for highly weathered rock and less accurate with slightly weathered rock. In general, we are underestimating less weathered rock. This could be attributed to these less weathered rocks being structurally controlled by discontinuities and the dominant weathering processes occurring as localized weakening, resulting in failure, especially during rock slope scaling activities.

## **Rock Strength**

We considered how rock strength may influence the rock slope scaling estimates. WSDOT typically uses the standard rock strength descriptors including very weak, weak, moderately weak, medium, moderately strong, strong, very strong, and extremely strong. While these are generally qualitative assessments, they can provide insight into how the Engineer estimates scaling quantities, and their rock strength classification may influence the accuracy of their estimates.

In general, estimates for rock slope scaling for rock masses that were described as strong are typically underestimated. Projects where the rock was described as “strong” yielded inaccurate scaling debris quantity estimates. This could mean we need to conduct additional field exploration during our design phases.

## **Discontinuity Characteristics**

Discontinuity characteristics play a crucial role in rock slope scaling and stability assessments. Discontinuities encompass natural planes, fractures, joints, and bedding within a rock mass that create separations and planes of weaknesses. These characteristics can significantly influence the behavior and stability of rock slopes and may influence how the Engineer estimates the potential crew hours required for scaling and the volume of debris that may accumulate after scaling activities are performed. The main characteristics we recorded for these projects include persistence, spacing, infill, and orientation.

Based on our observations, it does not appear that persistence and orientation of discontinuities have a significant impact on the estimate for rock slope scaling crew hours and debris quantities. The most noteworthy characteristics we observed were correlations between spacing and infill. We found that discontinuities that are closely spaced are generally

underestimated, and moderately spaced discontinuities are usually more accurate. Closer spacing of discontinuities can reduce the intact rock bridges between them, leading to decreased slope stability. This may attribute to why rock masses with closely spaced discontinuities are often underestimated. We also found that were reported, discontinuities that were open and without infilling often had more accurate estimates. Discontinuities where infilling was present were often underestimated. It is possible that the infill materials are weaker than they appeared to be resulting in a reduction of shear strength along the discontinuities and a decrease in slope stability.

## **Rock Type**

Different rock types exhibit distinct mechanical and geologic properties, which influence the behavior and stability of rock slopes. We evaluated specific characteristics of rock types including weathering rating, rock strength, and discontinuity characteristics previously, but we wanted to compare those results with the rock type and how that may have impacted our estimates on past projects. We identified 8 major rock types across the 15 studied project areas. These rock types include granodiorite, ophiolite, basalt, ultrabasic rocks, gneiss, andesite, schist, and volcanic rocks. There was variable accuracy over the estimates for ophiolite, ultrabasic rocks, gneiss, and schist. We found that we often underestimate scaling activities for granodiorite and basalt and are often accurate with our estimates for andesite. These observations are likely attributed to weathering susceptibility and rock strength. Where rocks like granodiorite are generally less susceptible to weathering and stronger, we are underestimating the scaling hours. Whereas andesite can be more variable in Washington and more susceptible to weathering, but generally still strong, we are more accurate with our scaling quantity estimates.

## **Rock Slope Dimensions**

We recorded the rock slope dimensions of each project location. The dimensions of a rock slope play a significant role estimating rock slope scaling crew hours and debris quantities. The dimensions, including the slope length, slope height, and extent of the scaling area, influence the complexity and scale of debris generated. Based on our evaluation, we often overestimate crew hours and debris quantities on shorter and taller slopes compared to longer and higher slopes. It is possible that we are adjusting for specialized equipment that may be required or adjusting estimates based on ease access the slope, while we use conservative values for larger slopes and are generally more accurate with our estimates. Similarly, based on the scaling areas calculated for each project, we generally overestimate smaller areas and have more accurate estimates for larger areas. Larger scaling areas require more scaling crew members and equipment, resulting in increased crew hours. Scaling crew productivity may also vary depending on the size of the scaling area. We are underestimating for the smaller areas, which suggests we should use more conservative values when we make these estimations.

## **CONCLUSION AND FUTURE WORK**

The assessment of rock slope scaling crew hours and debris quantity estimates is crucial for understanding the scope and resources required for slope stabilization projects. The determination of crew hours provides insights into the manpower and equipment needed for

scaling activities, while debris quantity estimates help evaluate the volume and disposal requirements of removed material. By accurately estimating crew hours, project managers and engineers can allocate resources efficiently and ensure timely completion of the scaling operations. Additionally, reliable estimates of debris quantity enable effective planning for debris removal; and disposal, minimizing environmental impacts and promoting safety. These assessments should be based on careful site investigations, considering factors such as climate and groundwater, weathering rating, rock strength, discontinuity characteristics, and rock type. Ultimately, accurate scaling crew hours and debris quantity estimates contribute to the overall success and cost-effectiveness of rock slope stabilization projects. The information compiled in this report can be used as a guide for future projects and uses fluctuations of estimates to estimate the proper crew hours and debris quantities more precisely.

## REFERENCES:

- Geotechnical reports:
  1. Washington State Department of Transportation, *SR 2 – ½ Mile East of Climbing Lane Rock Slope Mitigation*, Geotechnical Report, 2003.
  2. Washington State Department of Transportation, *SR 20 Deception Pass State Park Unstable Slopes*, Geotechnical Report, 2004.
  3. Washington State Department of Transportation, *SR 4, East of County Line Park Rockfall Work*, Geotechnical Report, 2006.
  4. Washington State Department of Transportation, *US 2 – West of Leavenworth Slope Stabilization*, Geotechnical Report, 2010.
  5. Washington State Department of Transportation, *US 2 Pine Canyon Emergency Repair*, Geotechnical Report, 2016.
  6. Washington State Department of Transportation, *US 12 – West of White Pass – Stabilize Slopes*, Geotechnical Report, 2008.
  7. Washington State Department of Transportation, *SR 14 / 0.8 & 1.1 Miles West of Wind River Road – Slope Stabilization*, Geotechnical Report, 2020.
  8. Washington State Department of Transportation, *SR 410/Chinook Pass Vicinity – Stabilize Slopes – MP 69.68 to 70.73*, Geotechnical Report, 2013.
  9. Washington State Department of Transportation, *SR 165/S of Carbonado. USMS Slope #3005*, Geotechnical Report, 2018.
  10. Washington State Department of Transportation, *I-90/Denny Creek Viaduct Vicinity – Stabilize Slope Project*, Geotechnical Report, 2007.
  11. Washington State Department of Transportation, *SR 7 MP 24.41 to 24.44 and MP 24.61 to 24.64 – State-Wide Risk Reduction Scaling Program*, Geotechnical Report, 2008.
  12. Washington State Department of Transportation, *SR 20 MP 319.36 to 319.57*, Geotechnical Report, 2010.
  13. Washington State Department of Transportation, *SR 3 – 1.1 Miles South of SR 304 – Unstable Slope*, Geotechnical Report, 2010.
  14. Washington State Department of Transportation, *SR 25 MP 62.10 to 62.18 – State-Wide Risk Reduction Scaling Program*, Geotechnical Report, 2010.
  15. Washington State Department of Transportation, *SR 21, Vicinity MP 112.80 to 113.01 Emergency Rockfall*, Geotechnical Report, 2009.
- Journals:
  1. Brown, E. H., *Ophiolite of Fidalgo Island, Washington*, Oregon Department of Geology and Mineral Industries Bulletin, 1977, p.67-73.
- Maps
  1. Schuster, J.E., Cabibbo, A A., Schilter, J.H., Hubert, I.J., *Geologic Map of Tacoma 1:100,000-Scale Quadrangle, Washington*, Washington Department of Natural Resources, Map Series 2015-03.

**Seward Highway Rockfall Mitigation, Anchorage, Alaska**

**Sebastian Dirringer**  
Landslide Technology  
10250 SW Greenburg Rd., Suite 111  
Portland, Oregon 97223  
sebastian.dirringer@ccilt.com

**Ben George**  
Landslide Technology  
10250 SW Greenburg Rd., Suite 111  
Portland, Oregon 97223  
ben.george@ccilt.com

**Rachel Hunt**  
Landslide Technology  
5725 W Randolph Dr.  
Boise, Idaho 83705  
rachel.hunt@ccilt.com

Prepared for the 72<sup>st</sup> Highway Geology Symposium, August 2023

### **Acknowledgements**

The author would like to thank the individuals for their contributions to this project:

Jon Knowles, P.E. – Alaska Department of Transportation & Public Facilities

Jonathan Tymick, P.E. – Alaska Department of Transportation & Public Facilities

Jonathan Tague, P.E. – Alaska Department of Transportation & Public Facilities

Brent Black, P.G., C.E.G. – Landslide Technology

Darren Beckstrand, P.G., C.E.G. – Landslide Technology

Noah Kimmes, P.E., P.G. – Emprise Concepts

Anna Cassady, P.E. – Schnabel Engineering

### **Disclaimer**

Statements and views presented in this paper are strictly those of the author(s), and do not necessarily reflect positions held by their affiliations, the Highway Geology Symposium (HGS), or others acknowledged above. The mention of trade names for commercial products does not imply the approval or endorsement by HGS.

### **Copyright**

Copyright © 2023 Highway Geology Symposium (HGS)

All Rights Reserved. Printed in the United States of America. No part of this publication may be reproduced or copied in any form or by any means – graphic, electronic, or mechanical, including photocopying, taping, or information storage and retrieval systems – without prior written permission of the HGS. This excludes the original author(s).

## ABSTRACT

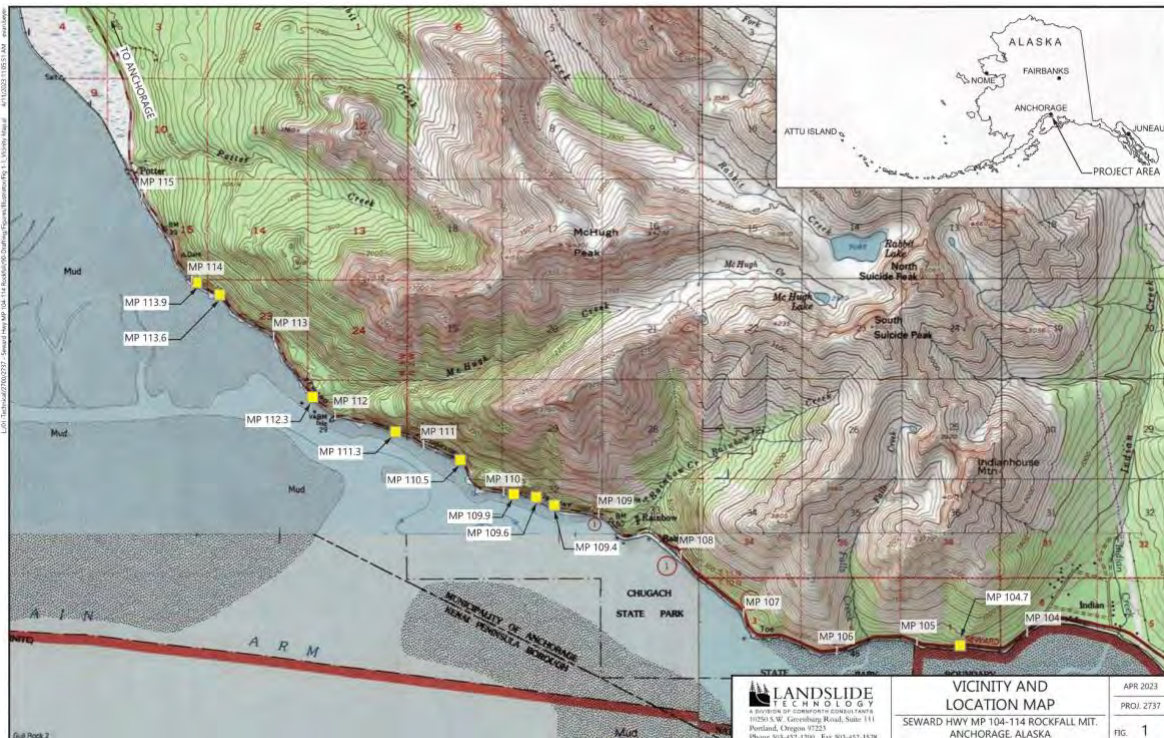
The Alaska Department of Transportation & Public Facilities (DOT&PF) retained Landslide Technology (LT) to develop rockfall mitigation for ten rock slopes adjacent to the Seward Highway (Hwy) between mile posts (MP) 104 and 114. The project area lies along the north bank of the Turnagain Arm of the Cook Inlet and runs approximately 13 to 23 miles southeast of Anchorage, Alaska. The project skirts the western foothills of the Chugach Mountains near Rainbow Peak, South Suicide Peak, and Indian House Mountain.

The Hwy has experienced rockfall safety concerns since its construction, resulting in an increased risk to roadway users and increased maintenance efforts. Rockfall mitigation was installed in 1992 to address safety concerns at several slopes adjacent to the highway. Since construction, rockfall activity has either permanently damaged or destroyed some of the mitigation. DOT&PF Maintenance & Operations (M&O) personnel has also observed increased activity and potential rockfall sources at sites in addition to those mitigated in 1992. During the 2018 magnitude 7.1 earthquake several of the slopes along the Seward Highway produced rockfall. This was especially true for sites at MP 111.3 and MP 113.9.

This paper will describe the process DOT&PF and LT utilized to select sites based on safety considerations and hazards observed during site investigations; details of the mitigation measures that were designed on a fast paced schedule; and construction observations, unique modifications, and lessons learned. Construction of the rockfall mitigation measures was completed in June 2023.

## INTRODUCTION

The Alaska Department of Transportation & Public Facilities (DOT&PF) retained Landslide Technology (LT), a division of Cornforth Consultants, Inc., to develop rockfall mitigation measures for ten rock slopes adjacent to the Seward Highway (Hwy) between mile posts (MP) 104 and 114 south of Anchorage. The process the DOT&PF utilized to select sites was based on safety considerations, documented rockfall events, and hazards observed during site investigations as described below. Details of the rockfall mitigation measures that were designed by LT in cooperation with the DOT&PF Materials personnel on a fast-paced schedule, and construction observations, unique modifications, and lessons learned are also discussed below. The ten rock slope sites are shown in Figure 1.



**Figures 1: Location and vicinity map of Seward Hwy Rockfall project**

## BACKGROUND

The Seward Highway is a two-lane highway, with one northbound lane and one southbound lane through the project area. The highway is owned by DOT&PF and is classified as a Rural Principal Arterial - Interstate. It is located on easements with the Chugach State Park and Alaska Railroad. The project corridor has a posted speed of 55 miles per hour. Annual Average Daily Traffic (AADT) at the Potter Valley Road permanent traffic recorder was 9,550 vehicles per day in 2022; however, traffic volumes increase significantly during summer months due to recreation and tourism.

The Seward Hwy has experienced safety concerns related to rockfall since its construction. Rockfall is of particular concern between MP 104 and 114. These safety concerns increase risk to

roadway users and increase maintenance efforts along the highway. Rockfall mitigation measures were installed in 1992 as part of a rockfall mitigation project to address safety concerns at several rock slopes adjacent to this section of the highway. Since construction, rockfall activity has either permanently damaged or destroyed some of the mitigation. DOT&PF Maintenance & Operations (M&O) personnel have also observed increased activity and potential rockfall sources at sites in addition to those mitigated in 1992.

During the November 30, 2018 magnitude 7.1 earthquake, several of the slopes along the Seward Highway produced rockfall. This was especially true for sites at MP 111.3 and MP 113.9. Details of earthquake related failures and observed slope features estimated to be related to earthquake damage at each of the sites was taken into consideration for site selection.

## **GEOGRAPHIC PROVINCE**

The Seward Highway project area lies along the north bank of the Turnagain Arm of the Cook Inlet and runs approximately 13 to 23 miles southeast of Anchorage, Alaska. It skirts the western foothills of the Chugach Mountains province on the flanks of Rainbow Peak, South Suicide Peak, and Indian House Mountain.

The Cook Inlet is comprised of the Knik and Turnagain Arms and bound by the Alaska-Aleutian, Chugach and Kenai Mountain Ranges and Kenai Peninsula. The elevation of the western Alaska-Aleutian Range is significantly higher than the eastern flats and ranges of the Kenai and western foothills of the Chugach.

Highway elevations are generally 40 to 50 feet above sea level while cut slopes rise up to 200 feet in elevation. Natural rock slopes adjacent to the highway rise to 450 feet above sea level while the mountains rise to 3,000 feet within two miles of the Seward Highway.

## **REGIONAL AND SITE GEOLOGY**

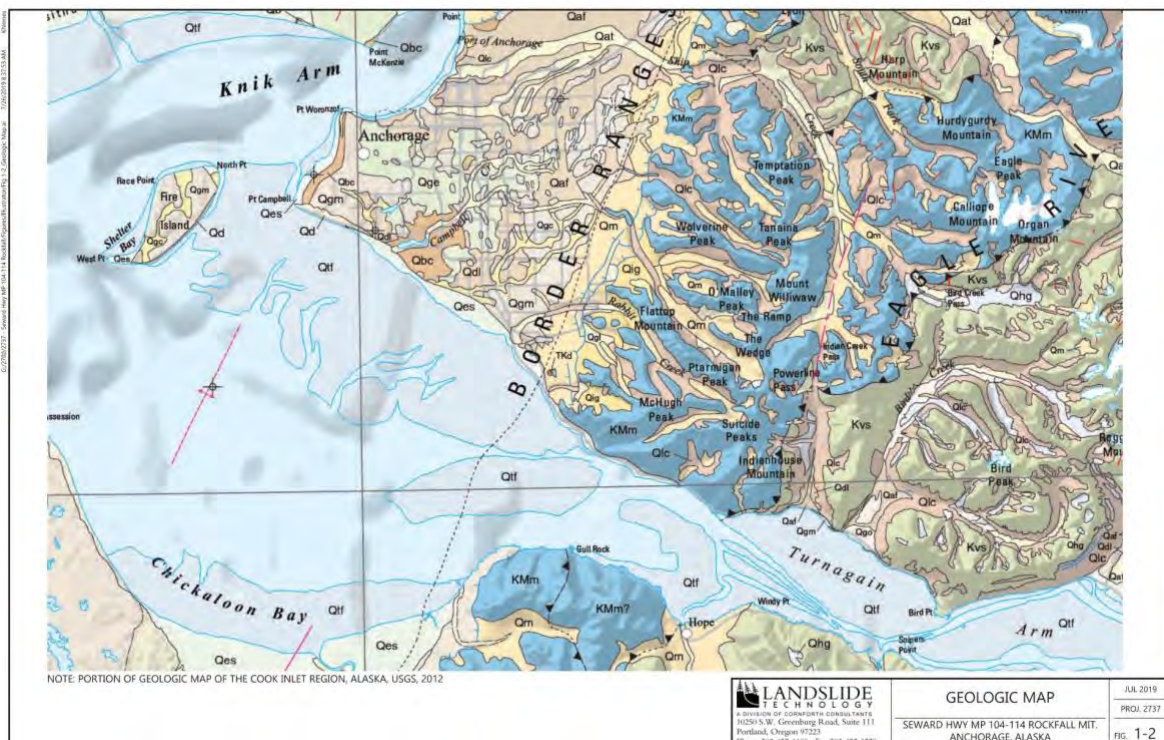
The regional geology of the area is dominated by accreted terrain of Mesozoic and younger belts of sedimentary rocks bounding the Cook Inlet. The accreted terrain forms the Alaska-Aleutian Mountain Range on the west side of the Inlet, the Talkeetna Mountains to the north and east, and the Chugach and Kenai Mountains to the south and east. Triassic and Jurassic batholiths and volcanics, as well as Tertiary sills and dikes are present throughout the region. Numerous faults transect the region. Active volcanoes such as Mount Saint Augustine are also present.

The project site is approximately bound by two distinct NE-SW trending faults along the Turnagain Arm of the Cook Inlet. The Border Ranges Fault lies at the western edge of the project area, while the Eagle River Fault cuts across the eastern constraint. The majority of the project area is mapped as the McHugh and Uyak Complex and Undivided Metasedimentary rocks, symbolled as KMm and Kvs, respectively (Wilson, et al., 2012).

The McHugh and Uyak Complexes (KMm) are described as a tectonic mélange consisting largely of Mississippian through mid-Cretaceous protoliths of oceanic deposits composed of gray, gray-green, and dark-green weakly metamorphosed siltstone, graywacke, arkose, and

conglomerate sandstone; metavolcanic sequences mostly of basaltic composition that are commonly cherty argillite and argillite; and small amounts of ultramafic rocks and marble that occur locally as isolated, discontinuous outcrops or lenticular masses. Large lenses of schist, amphibolite, marble, sandstone, conglomerate, diorite, gabbro, serpentinized ultramafic rocks, and mafic volcanic rocks are also present throughout these complexes.

The Undivided Metasedimentary rocks (Kvs) are described as dark-gray, thin- to thick-bedded, laumontite- to mid-greenschist facies composed of a thick sequence of rhythmically alternating, deformed metamorphosed sandstone-siltstone turbidites with beds generally ranging from a few centimeters to a few meters thick and locally, massive beds up to tens of meters thick. The metamorphosed beds are composed of moderately sorted to poorly sorted sandstone, siltstone, and mudstone flysch. The sandstone is fine- to coarse-grained and is mainly composed of plagioclase, quartz, and igneous rock fragments. A portion of the Geologic Map of the Cook Inlet Region, Alaska in relation to the project site is provided as Figure 2.



Figures 2: Geologic Map of the Cook Inlet Region, Alaska

## PROJECT DESCRIPTION

Highway users along Seward Highway are risk of rockfall due to high rockfall occurrence potential combined with the high AADT. This project was developed under the DOT&PF's Highway Safety Improvement Program (HSIP) to upgrade existing mitigation and install new systems at ten sites. The DOT&PF segmented the corridor into primary and secondary mitigation areas based on relative rockfall activity and potential rockfall occurrence at each site. A summary of the details,

site length, and maximum slope height for each rockfall site selected as part of the Seward Highway Rockfall Mitigation project reach are provided in **Error! Reference source not found.**

<b>Table 1 – Rockfall Site Information</b>				
<b>Rockfall Site</b>	<b>Approx. Station Range</b>	<b>Area Priority</b>	<b>Site Length (feet)</b>	<b>Max Slope Height (feet)</b>
Site 1 (MP 104.7)	1631+20 to 1635+65	Primary	445	160
Site 2 (MP 109.4)	1874+00 to 1878+35	Primary	435	120
	1878+35 to 1883+10	Secondary	575	240
Site 3 (MP 109.6)	1888+70 to 1895+00	Primary	630	110
	1895+00 to 1897+70	Secondary	270	110
Site 4 (MP 110.5)	1936+70 to 1938+15	Secondary	245	40
	1938+15 to 1942+60	Primary	445	70
	1942+60 to 1946+60	Secondary	400	60
Site 5 (MP 111.3)	1970+40 to 1973+00	Secondary	260	80
	1973+00 to 1989+35	Primary	1,535	260
Site 6 (MP 113.6)	2096+75 to 2098+20	Secondary	145	60
	2098+20 to 2103+15	Primary	495	120
	2103+15 to 2105+30	Secondary	215	100
Site 7 (MP 113.9)	2109+20 to 2113+65	Primary	435	180
	2113+65 to 2115+95	Secondary	230	70
State Site (MP 109.9)	1904+15 to 1905+10	Primary	95	110
State Site (MP 110.5)	1934+65 to 1935+20	Primary	55	105
State Site (MP 112.3)	2023+15 to 2024+60	Primary	145	125

## **SITE SELECTION**

Given the geology and extreme terrain, the DOT&PF recognized that it is impossible to eliminate all rockfall in the area with the limited available funding. After careful evaluation of various alternatives, DOT&PF selected an approach that focused on areas of greatest perceived risk and utilized work methods that do not require extended lead time for approvals by federal environmental and wildlife management agencies. The proposed scope of work for this project did not protect against major slope failures, rockfall originating from areas upslope of the project limits, and rockfall caused by earthquakes or hidden cracks or faults.

The DOT&PF assesses and manages infrastructure assets using an Unstable Slope Management Program (USMP), as developed by LT. This program helps monitor unstable slopes and guides the agency in responding to slope failures. The USMP ranks rock or soil slopes using both hazard and risk-based scores based on quantifiable measures at a given site. In order to identify locations of concern, slopes were ranked statewide using sub-score criteria from the USMP that focused on risk to drivers.

Rock slopes were ranked using block size or event volume, slope height, AADT, average vehicle risk, and percent decision sight decision (Beckstrand et al., 2017). In 2019, the DOT&PF

published a Federal Fiscal Year (FFY) HSIP Candidate Description and Cost Estimate. In this document, a table outlines risk-to-driver rankings of the top twenty worst performing rock slopes across the state. The Seward Highway occupied fifteen of the top twenty positions, all within the MP 104 to MP 114 range.

Of these fifteen sites, seven were chosen by the DOT&PF and were granted federal funding. Three additional sites were added by the DOT&PF and were funded by the state. Selected sites benefited from cost effective rockfall mitigation to reduce the risk of injuries and/or closures of the Seward Highway. Methods of rockfall mitigation included scaling, installing rockfall attenuators, rock bolts, rock dowels, draped wire mesh, reestablishing roadside ditch catchments, replacing affected signs and culverts, and repairing the road surface (including restriping and reinstalling rumble strips).

### **ROCKFALL DESIGN GOALS**

This project focused on rockfall mitigation and as such the standard preconstruction design criteria did not apply. The DOT&PF had no design criteria policy when it comes to rockfall mitigation.

In working with the DOT&PF, the following design goals were developed:

1. No increase in maintenance needs and a decrease in rockfall ditch maintenance.
2. Rockfall retention goal of 95% from rockfall originating on the cut face.
3. Improve safety from rockfall originating beyond the rock cut.

Retention of rock is measured as the percentage of simulated rocks that do not pass the highway edge-of-pavement.

### **ROCKFALL EVALUATION AND PRELIMINARY DESIGN DEVELOPMENT**

Development of preliminary rockfall reduction measures for Seward Hwy included researching historical information, site characterization, kinematic and rockfall analyses, and an alternative evaluation. During the reconnaissance efforts, LT met with the DOT&PF M&O personnel to discuss historical rockfall events and maintenance efforts for the project rock slopes. Data was collected at each site to characterize rock mass conditions, rockfall potential, and calibrate rockfall models.

Joint set and kinematic analyses were performed to assess potential failure modes at each site. Rockfall models were developed to evaluate existing rockfall containment and effectiveness of rockfall mitigation alternatives.

Rockfall mitigation alternatives and cost estimates were developed for each site. Group meetings were held to discuss proposed rockfall mitigation alternatives with emphasis on effectiveness, durability, constructability, cost, and aesthetics.

### **Photogrammetry**

Several unmanned aerial vehicle (UAV) photo sets were used to conduct the site specific analyses. One set of data was gathered at various sites in mid- to late-2018 and early 2019 by DOT&PF geotechnical staff. LT's subconsultant HDL conducted two UAV surveys, one on March 4, 2019 and a second on March 29, 2019. Georeferenced point clouds were developed to analyze geologic structure of exposed rock outcrops and measure rock slope features. Using these datasets, rockfall cross sections were generated to evaluate rockfall trajectories and characteristics. An example of cross section locations generated from point cloud data used for modeling is shown in Figure 3.

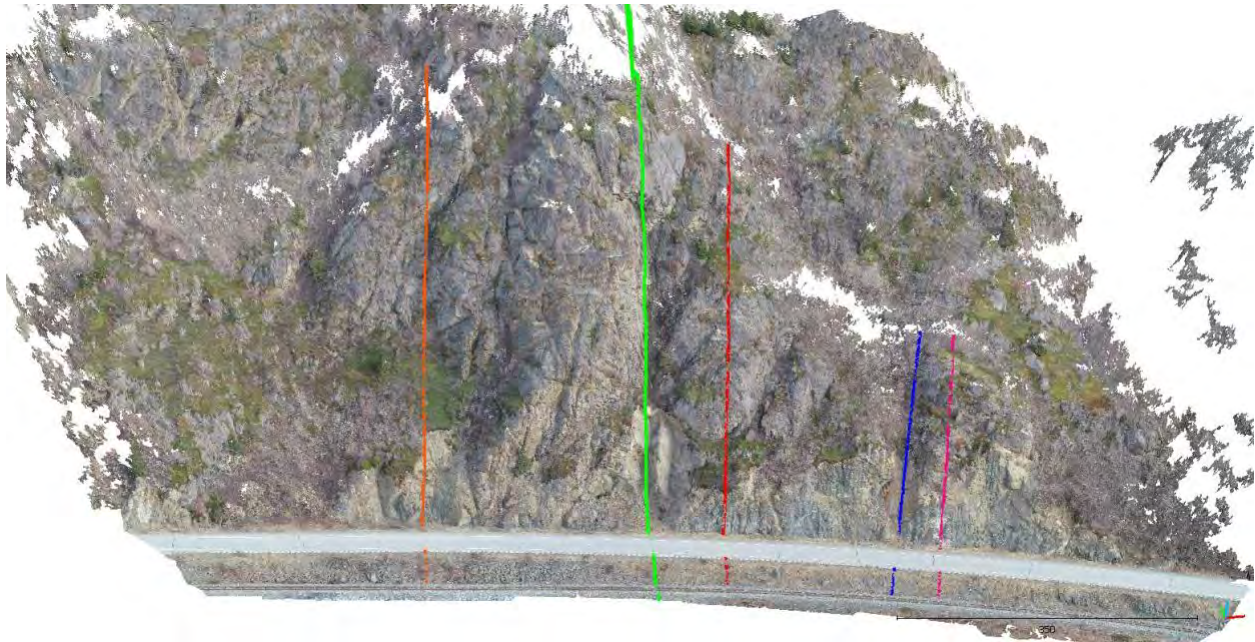


**Figure 3: Example cross-section locations identified in estimated rockfall trajectory paths.**

### Site Reconnaissance

An engineering geologist and geotechnical engineer from LT visited the sites in the Spring of 2019 to develop a field investigation plan for approval by DOT&PF. A team engineering geologists and geotechnical engineers from LT then conducted a week-long field investigation. Reconnaissance was completed using boom-lifts, rope access techniques, and on foot. Rock slopes adjacent to the highway were observed to document geology, evaluate rock mass and discontinuity characteristics, and assess existing rockfall conditions. Existing fallout areas (i.e. roadside ditches) and rockfall protection measures were evaluated. To aid in the development of rockfall models, the size and dimensions of rockfall debris and in-place rock blocks and slope properties were recorded. Potential rockfall sources upslope of the rock cuts were located and measured to characterize potential failure mechanisms.

While on site, the LT team met with DOT&PF maintenance personnel to obtain a better understanding of the rockfall within the limits of each project site. The frequency, size, extent, and occurrences of rockfall events were discussed and documented. In addition, maintenance efforts regarding ditch cleaning (frequency and volumes) and repairs to existing mitigation measures (pre-cast concrete barriers, rockfall (post and brace) attenuators) were discussed.

## **ROCKFALL MITIGATION DESIGN SELECTION**

Rockfall mitigation measures generally fall into three major categories: 1) Protection measures used to limit rockfall energy and restrict falling rocks from reaching the roadway (i.e. berms, rigid and flexible rockfall barriers, draped meshes, and rockfall attenuators, and rock excavation to increase the fallout area); 2) Stabilization measures used to prevent rockfall from occurring (i.e. removal such as scaling and reinforcement such as rock bolting); or 3) Avoidance of the potential rockfall by shifting the alignment horizontally and/or vertically to move the highway away from the base of a rock slope (where feasible) or raise the roadway grade to create a more effective rockfall catchment area. In all instances, avoidance was not an alternative available to the DOT&PF.

Rockfall mitigation alternatives developed by LT considered scaling, rock dowels, rock bolts, draped wire mesh, and rockfall attenuators. Alternatives explored multiple options at each site for both primary and secondary priority areas. DOT&PF selected preferred mitigation alternatives based on rockfall mitigation effectiveness, durability, constructability, cost, and aesthetics. LT developed final designs of the preferred alternatives on a fast-paced schedule and submitted Final Plans, Specifications, and Engineer's Estimate for the first seven sites in May of 2020. HI-TECH Rockfall Construction, Inc., of Forest Grove, Oregon was awarded the contract on June 30, 2020 and construction began in September 2020.

In early 2020, DOT&PF requested LT develop rockfall mitigation measures for four additional rock slopes between MP 107 and 113. Rockfall mitigation alternatives were developed and DOT&PF selected preferred mitigation options. DOT&PF selected the "do nothing" alternative for one of these sites. The three remaining rock slopes were amended to HTR's contract in 2020 for additional rockfall mitigation construction.

## **CONSTRUCTION PROGRESS**

Construction of the rockfall mitigation measures began in September 2020 and finished in June 2023. Rockfall mitigation components included: temporary rockfall protection, scaling and hand clearing of vegetation, rock bolting, rock doweling, rockfall attenuators, draped wire mesh, and cable lashings.

### **Temporary Rockfall Protection (TRP)**

TRP for the project consisted of a concrete barrier mounted fence extension. Fencing was constructed with 6-foot-tall steel posts and high-tensile strength 4-millimeter steel wire mesh supported by ¾-inch wire ropes on the top, bottom and sides of the mesh. The posts were mounted to the top of 2.5-foot-tall standard concrete barriers, as shown in Figure 4.



**Figure 4: TRP placed along centerline on the Seward Highway.**

This system required two to three days for set up and break down depending on the length being installed. It was selected to reduce risks to highway users as a result of construction activities and limit the protection measure footprint. TRP was placed along the centerline of the roadway prior to beginning on-slope mitigation efforts and was left in place until all on-slope work at a site was completed. Debris accumulated in the work zone was removed at the end of each shift. During non-working hours, traffic was active on both sides of the barrier. Crash cushions were placed at each terminal end of concrete barrier.

### **Scaling and Hand Clearing**

Hand scaling techniques included the use of scaling bars to remove small, loose rock and debris from the rock slopes. For heavier hand scaling efforts, pneumatic air pillows were utilized at locations where marginally stable rock blocks were identified with an adjacent fracture available for placement of the air pillow. When necessary, rock breaking techniques, such as boulder busters, were utilized to break up large rocks into smaller pieces prior to removal from the slope. Mechanical scaling was used occasionally to remove loose boulders from the slope by running a steel cable from the bucket of a loader to an identified boulder and pulling the boulder off the slope. Hand scaling techniques are shown in Figure 5.



**Figure 5: Contractor using scaling bars and air pillows to remove loose rock blocks.**

During active slope scaling, traffic holds were employed for up to 20 minutes or as traffic queues allowed. Over 2,100 scaling hours were used throughout the project.

Hand Clearing was completed at select locations along the crest of slopes where trees or larger vegetation interfered with rockfall attenuator or draped wire mesh installation. Hand saws or gas-powered chainsaws were used to cut vegetation as close to the ground surface as possible.

### **Rock Bolting and Rock Doweling**

Rock bolts and rock dowels were installed at all HSIP sites and one state funded site. Rock bolts were either 40-kip or 80-kip post tensioned elements. Several drilling methods were used to install rock bolts and rock dowels including a crane-suspended pneumatic drill (“dangle drill”), a crane boom-mounted hydraulic drill, and a wagon drill. Wagon drill operation is shown in Figure 6. A total of 11,115 linear feet of rock bolts and a total of 4,800 linear feet of rock dowels were installed across the project area.



**Figure 6: Wagon drill mobilization for rock bolt installation.**

## **Blasting**

Blasting was performed at Site 5 – MP 111.3 in March of 2021. This was conducted to remove a launch feature located below a highly active debris shoot. Forty-five production blast holes were drilled approximately 71 to 77 feet from the highway centerline, in a 7-foot by 7-foot pattern. The production blast holes were spaced 7 feet apart and drilled to depths ranging between 30 to 55 feet deep with a hole diameter of 3.5 inches. Each production hole was stemmed with drill cuttings to 7 feet. Thirty-six pre-split holes, spaced 30 inches apart, were drilled to depths ranging between 30 and 55 feet deep with inclinations ranging between 1 and 4 degrees. Each pre-split hole was stemmed with drill cuttings to 3 feet.

## **Rock Buttress**

A large trough 20 feet wide by 54.5 feet deep by 53.4 feet tall was excavated to facilitate blasting workers safety. This trough was later stabilized with construction of a geogrid reinforced rock buttress. Construction of the buttress was completed by stacking 3- to 6-foot boulders on the outboard side of the trough and 12-inch minus with up to 20 percent sand to silt sized material behind or upslope of the boulders. Mirafi 5XT Geogrid was placed on approximate 2-foot lifts in

the 12-inch minus material. The boulders and 12-inch minus materials were salvaged from shot rock produced from the blasting efforts. A view of the completed buttress and expanded ditch is provided in Figure 7.



**Figure 7: Completed shot rock buttress.**

### **Rockfall Attenuator**

Rockfall attenuators were installed at Sites 1 through 3, Site 5, and Site 7. Rockfall attenuators consist of cable net panels attached to top support cables that are suspended off of the slope by steel posts. The cable net panels consist of GeoBrugg® Rolled Cable Nets with DELTAX G80-2mm high-tensile strength wire mesh backing. All rockfall attenuators were constructed with 1-inch diameter top support rope. Top support rope lengths were limited to 160 feet with maximum 40-foot spans between posts at most locations. Top rope diameter was increased to 1-inch to accommodate spans of up to 70 feet across active debris shoots. Attenuators were constructed using either 12-foot-tall or 18-foot-tall steel posts. Attenuator net panels were hung with the assistance of a crane or by helicopter and rope access crews, as shown in Figure 8. The total area of attenuator installed across the project area exceeds 41,000 square yards.



**Figure 8: Attenuator net panel installation with the assistance of a crane and rope access crews.**

### **Draped Wire Mesh**

Draped wire mesh was installed at Sites 2 and 4. Draped wire mesh consist of Geobrugg® Tecco G65/3mm high-tensile-strength steel wire mesh panels attached to a top support rope. The top support rope was fixed to wire rope anchors upslope of the top support rope (“tagline” anchors) and wire rope anchors to the sides of the ends of the top support rope (“lateral” anchors). Wire mesh panels measuring 12.8 feet wide were picked and placed by either helicopter or crane. Wire mesh panels were temporarily attached to the top support cable by threading a ¼-inch diameter wire rope through each mesh opening and around the top support cable. Total draped wire mesh area across the project area exceeds 2000 square yards.

### **Cable Lashings**

Five cable lashings were installed at Site 2 to stabilize a large rock block above the crest of the slope at the south end of the site. Cable lashings consist of two wire rope anchors connected by a section of wire rope and turnbuckle to tighten the system. Holes for the wire rope anchors were drilled by hand to depths of 6 feet in competent rock. Turnbuckles were tightened to remove slack from the system and provide tension to each cable lashing against the rock block. Completed cable lashing at Site 2 is shown in Figure 9.



**Figure 9: Cable lashings for a large rock block at Site 2, MP 109.4.**

## **PROJECT OUTCOMES AND LESSONS LEARNED**

The Seward Highway Rockfall Mitigation project offered several challenges that were overcome with unique solutions. Stakeholders collaborated over the course of four construction seasons to address design complexities and safety concerns. Below are a few examples of lessons learned.

### **Traffic Maintenance and Temporary Traffic Control**

Throughout the project, traffic passage was maintained along the roadway. Traffic restrictions were employed at select times of day depending on the time of year, around holidays, and for the entire month of July. Lane restrictions, when required, were conducted so that traffic was not held more than 20 minutes, no more than 40 vehicles were held, and that traffic queue length did not exceed  $\frac{1}{4}$  mile. When any of these limitations were exceeded, the contractor paused construction activity, cleared the work zone, and reopened both travel lanes.

Coordination with local school bus organizations was also a unique consideration during this project. School bus schedules were acknowledged, and traffic restrictions were developed around their schedules. Similarly, any scaling or blasting efforts were halted when the Alaska Railroad trains passed through the work zone. Even with TRP in place, rockfall potential reaching the railroad alignment during activities such as blasting and scaling was elevated. The Alaska Railroad representative was present at all times during construction in case the railway was impeded with debris.

### **Temporary Rockfall Protection**

Designing TRP for a limited width corridor like the Seward Highway came with unique challenges. The DOT&PF required both lanes of traffic to be open during non-working hours. These restrictions reduced the number of TRP options available. By placing the concrete barrier

mounted fence extension system on centerline a work zone could be established during working hours, while providing full two-way traffic during non-working hours. Cleaning of the work zone was required after each shift.

It should be noted, numerous occasions arose where rockfall landed outside of the work zone, depositing into the only travel lane or even further towards the railroad alignment. During those types of situations, all traffic was held until the potential for rockfall was reduced. To address this potential a loader was available to quickly clean the one-way, flagger controlled lane during work hours.

Another TRP element that arose during construction was the amount of time it took to set up and break down TRP. Depending on the length requirements at each site, constructing TRP could take between two to five days depending on construction crew size. Breaking TRP down was often a more efficient effort.

Additionally, issues arose when installing the fence extension post brackets to the concrete barriers. Some reinforcement bars within the concrete barriers were unfortunately in the same location as the structural pin that fastened the post bracket to the concrete barrier. This was overcome by placing a spacer between the post saddle and the top of the concrete barrier. Crews created a new template for drilling holes for pin placement to avoid intersecting the reinforcing steel.

### **Site 7 Rock Block Reinforcement**

A large rock block found at Site 7 (MP 113.9) was about 25 feet by 15 feet by 16 feet in size and is shown in Figure 10. The bottom of the rock block had a prominent overhang of about 20 feet in length and up to 7 feet in depth. The rock block was bounded on the climber's right side by a continuous fracture with an aperture of up to 1-foot and climber's left side by hairline fractures. Several prominent discontinuous fractures were present within the rock block as well. This rock block was originally designated for removal (i.e., heavy scaling); however, the contractor proposed the block be considered for reinforcement.



**Figure 10: Large Rock Block at Site 7.**

LT developed a reinforcement approach based on 3D-modelling of the rock block and surrounding slopes, and multiple stability models. Designs considered static stabilization as well as during an approximate 975-year (5% in 50 years) seismic event. A sequencing work plan was developed to limit exposure of personnel to potential failure of the rock block during construction. Sequencing initially included scaling of the slopes above and surrounding the rock block. Next reinforcement three, 40-kip rock bolts were installed from the backside (i.e., climber's left) of the rock block towards the front (i.e., climber's right). Care was taken to ensure that the reinforcement holes did not daylight through the front of the block. Long-term stability of the rock block was addressed by installing eight 40-kip foundation rock bolts at the base of the block to support the weight of the rock block. Lastly, six 80-kip stabilization rock bolts were installed from the front of the rock block back into the slope. Care was taken to ensure that the reinforcement rock bolts were not impacted during drilling activities for the stabilization bolts, as based on 3D models.

### **Rockfall Attenuator Site Specific Modifications**

During site reconnaissance several debris chutes were identified at Sites 2 (MP 109.4), 3 (MP109.6), and Site 5 (MP 111.3). To avoid placement of a post in the chutes, which would likely have poor foundation conditions and would be in jeopardy of being compromised by debris chute activity, longer spans were designed for the top support rope and connection posts were required at either side of the chute. At these post locations, top rope termination anchors were installed and a single span top rope was extended across the chute. The diameter of the top support rope was increased from  $\frac{3}{4}$  inch to 1 inch to provide higher ultimate strength for the larger spans and associated mesh weight.

**REFERENCES:**

1. Wilson, F.H., Hulst, C.P., Schmoll, H.R., Heussler, P.J., Schmidt, J. M., Yehle, L.A., and Labay, K.A. *Geologic Map of the Cook Inlet Region, Alaska. United States*. Scientific Investigations Map 3153. Geological Survey (USGS), 2012.
2. Beckstrand, Darren, Barry A Benko, Aine E Mines, Lawrence A Pierson, Paul D Thompson, Robert E Kimmerling, Landslide Technology, et al. *Statewide Geotechnical Asset Management Program Development: Final Report for Rock Slopes, Unstable Soil Slopes and Embankments, Retaining Walls, Material Sites*, September 5, 2017. 01660107. <http://www.dot.state.ak.us/stwddes/research/assets/pdf/stp4000-126a.pdf>.

**A Multi-Phased Approach to Rockfall Mitigation at Don Pedro Dam:  
Lessons Learned for Critical Facilities and Roadways**

**Joey Renner, PG**

Gannett Fleming, Inc.  
2251 Douglas Blvd., Suite 200  
Roseville, California 95661  
916-846-3558  
[jrenner@gfnet.com](mailto:jrenner@gfnet.com)

**Syed Ul Haque, PE**

Gannett Fleming, Inc.  
2251 Douglas Blvd., Suite 200  
Roseville, California 95661  
916-521-1103  
[sulhaque@gfnet.com](mailto:sulhaque@gfnet.com)

**Evan Lucas, PE**

Turlock Irrigation District  
333 East Canal Drive  
P.O. Box 949  
Turlock, California 95381  
209-883-8608  
[emlucas@tid.org](mailto:emlucas@tid.org)

**Simon Boone, PG**

Access Limited Construction  
1102 Pike Lane  
Oceano, California 94335  
540-420-2678  
[simon@alcinc.com](mailto:simon@alcinc.com)

**Drew Kennedy, PG, CEG**

Gannett Fleming, Inc.  
2251 Douglas Blvd., Suite 200  
Roseville, California 95661  
916-521-1105  
[dkennedy@gfnet.com](mailto:dkennedy@gfnet.com)

*Prepared for the 72<sup>nd</sup> Highway Geology Symposium, August 2023*

### **Acknowledgements**

The authors would like to extend their thanks to all the personnel from Turlock Irrigation District, Gannett Fleming, and Access Limited Construction who worked to make this project a success.

### **Disclaimer**

Statements and views presented in this paper are strictly those of the author(s), and do not necessarily reflect positions held by their affiliations, the Highway Geology Symposium (HGS), or others acknowledged above. The mention of trade names for commercial products does not imply the approval or endorsement by HGS.

### **Copyright**

Copyright © 2023 Highway Geology Symposium (HGS)

All Rights Reserved. Printed in the United States of America. No part of this publication may be reproduced or copied in any form or by any means – graphic, electronic, or mechanical, including photocopying, taping, or information storage and retrieval systems – without prior written permission of the HGS. This excludes the original author(s).

## ABSTRACT

Turlock Irrigation District (TID) initiated a rockfall hazard evaluation and mitigation program in 2018 to reduce risk to its personnel and the Don Pedro hydropower facility, which is located in Tuolumne County, California. Gannett Fleming geologists performed an initial “screening level” visual assessment of the existing slopes surrounding the facility and identified five potential rockfall hazard areas requiring mitigation. Each area was evaluated based on the likelihood versus consequences of rockfall events, and a prioritized list was developed for TID to consider further investigation and rockfall mitigation measures. The highest hazard area was on the west canyon slope, where numerous large rock blocks appeared at risk of dislodging and potentially impacting the powerhouse and/or its only vehicle access road below. Gannett Fleming performed rockfall analyses and simulation, assessed alternatives, and designed TID’s preferred rockfall mitigation measures of what became known as Areas 3 & 4, which comprised scaling and installation of rockfall drapery, rock anchors, and wire-rope restraints. The rockfall mitigation measures were constructed in 2020 by Access Limited Construction. The project challenges included limited slope access during the assessment and design phases, a difficult slope configuration given its proximity to the powerhouse, and a requirement to keep the access road largely open during construction. During the construction phase, close cooperation between the owner, engineer, and contractor allowed all parties to respond quickly to design/construction changes based on the actual slope conditions encountered. This paper will detail the development and implementation of a rockfall mitigation program for critical facilities and roadways, including initial reconnaissance, detailed assessment, alternatives analysis, design, procurement, and construction.

## INTRODUCTION

Don Pedro Dam is located on the Tuolumne River in central California. Don Pedro Dam is an approximately 580-foot-tall zoned embankment dam that was completed in 1971. The dam is part of the Don Pedro Project, which is jointly owned by TID and Modesto Irrigation District (MID). A 203 MW hydroelectric facility is situated at the downstream toe of the dam and is operated by TID. The powerhouse facilities, which include a switchyard, warehouse, tunnel portal and access road, are located at the bottom of steep natural and excavated rocky slopes capable of producing significant rockfall (Exhibit 1).



**Exhibit 1 - West Slope Above Don Pedro Powerhouse And Access Road**

In 2018, as part of planning for the life extension program for the Don Pedro Powerhouse, TID initiated a rockfall hazard evaluation and mitigation program to evaluate and reduce risk to its facilities and personnel. The multi-phased program included: (1) rockfall hazard screening; (2) rockfall analysis and simulation; (3) analysis of alternatives; (4) design of rockfall mitigation measures; and (5) procurement and construction of rockfall mitigation measures.

This paper details the development and implementation of a rockfall mitigation program for critical facilities and roadways. The project challenges included limited slope access during the assessment and design phases, a difficult slope configuration and high voltage overhead lines given its proximity to the powerhouse which had to remain fully operational for the duration of

the project, and a requirement to keep the access road continuously open for foot traffic and returned to service quickly should a personnel or equipment issue arise during construction. During the construction phase, close cooperation between the owner (TID), engineer (Gannett Fleming), and contractor (Access Limited Construction) allowed all parties to respond quickly to design/construction changes based on the actual slope conditions encountered. The lessons learned from this project may be valuable to others working above critical facilities and roadways with similar challenges.

## **SITE DESCRIPTION AND HISTORY**

The dam is in a north-south-oriented canyon on the Tuolumne River. Natural rock outcrops and excavated rock cut slopes are present in the steepest portions of the canyon walls on either side of the powerhouse facility. The up to 100-foot-tall near vertical cut slopes above the powerhouse facility were scaled during original construction, and chain-link rockfall mesh combined with rock bolts were installed over the lower portions of the slope. However, the deterioration of these original rockfall mitigation measures, ongoing weathering of the cut slopes, identification of potential rockfall source areas in the natural rock outcrops above the cut slopes, and improvements in rockfall mitigation standards made improving the rockfall mitigation at the site a high priority.

The site vicinity was mapped by Clark (*I*) as underlain by metavolcanic rock of the Gopher Ridge Volcanics, which is composed largely of pyroclastic rocks (fine-grained siliceous tuff to coarse-grained volcanic breccia) with a schistose texture, and some lava rocks. The schistosity is often poorly-developed, particularly in the more massive and blocky lava rocks.

Since the facility was placed into service in 1971, periodic rockfall events have occurred from the surrounding rock slopes adjacent to the powerhouse facility. For example, in 2017, dislodged rock blocks traveled down the slope above the Outlet Works Access Tunnel portal and landed in a paved area periodically accessed by TID personnel. In addition, there have also been periodic small rockfall events that have impacted the access road, including an event in early 2018 that deposited rock and soil debris on the roadway. Localized rockfall along the access road typically occurred when the Flood Control Valve (Hollow Jet Valve) (Exhibit 2, item 5) is running, as it creates a misty and damp condition along the canyon wall. It should be noted that there have been no documented rockfall events that have damaged the powerhouse or switchyard.

## **ROCKFALL HAZARD SCREENING**

As part of the initial phase, Gannett Fleming (SAGE Engineers at the time) performed a “screening level” visual assessment of the slopes surrounding the facility to assess slope conditions for potential rockfall hazards, and prepared a summary report with a prioritized list of recommendations regarding the need for additional investigation and/or mitigation considerations.

Five areas of concern were identified based on the visual assessment, which are shown in Exhibit 2 below. For each area, we qualitatively assessed the source of rockfall hazards, probability of rockfall initiation, consequences of rockfall, and potential mitigation actions and their costs.



**Exhibit 2 - Google Earth Satellite View Of The Don Pedro Powerhouse And Five Slope Areas Of Concern. Slope Breaks Are Indicated With Dashed White Lines. Imagery: Google Earth 7.0, (2018) *Don Pedro Powerhouse 37.7°N, 120.4°W, Elevation 250 Feet.* [Online] Available At [Earth.Google.Com](http://Earth.Google.Com) [Accessed 2023].**

The highest hazard area was designated as Area 3 and is located on the west canyon slope above the powerhouse and extended from the powerhouse about 500 feet downstream. Area 3 is comprised of natural slopes above the steeper, mesh-covered cut slope face, which is referred to as Area 4. The sole access road to the facility runs directly below Area 3. Numerous large blocks within Area 3 appeared at risk of destabilizing and potentially impacting the powerhouse and/or the access road.

TID used the ranking developed during the Rockfall Hazard Screening phase to respond to each hazard area based on the relative risk level, operational needs, and resources available to implement rockfall mitigation measures. Following the screening phase, TID initiated construction of rockfall barriers at Area 1 and Area 2, comprising rockfall and concrete barriers, respectively, while Areas 3, 4, and 5 warranted further study. This paper focuses on the detailed rockfall hazard assessment and mitigation design performed at Area 3, as it was the most complex in its design and implementation.

### **AREA 3 RECONNAISSANCE AND ROCKFALL ANALYSIS**

Following the screening assessment, Gannett Fleming performed a detailed slope reconnaissance and geologic analysis of Area 3 as a basis for evaluating alternatives and design of rockfall mitigation measures. While Area 3 was the primary subject of the reconnaissance and analysis, Area 4 (the slope immediately below Area 3) was also included because of its position in the runout zone for rockfall originating in Area 3. Because directly accessing the slope using rope-

access techniques and equipment had the potential to dislodge rocks and potentially damage the road/facility below, TID and Gannett Fleming agreed to a visual reconnaissance, aided by aerial lifts (Exhibit 3), terrestrial LiDAR, and drone-collected aerial imagery/video. Due to the height of the slope, only the bottom margin of Area 3 was accessible via the aerial lifts. The primary objectives of the slope reconnaissance were to: (1) identify adverse rock slope conditions and potential failure mechanisms; (2) collect geologic information suitable for performing rock stability/rockfall analyses and engineering design; and (3) perform a preliminary layout of potential mitigation measures based on the observed conditions.

### **Slope Description**

Area 3 encompasses the portion of the slope that begins directly above the powerhouse and extends approximately 500 feet downstream (Exhibit 4). This area is comprised of natural slopes and is vertically bounded by the prominent construction road bench above it (approximately 280 feet above the powerhouse access road) and the steeper, mesh-covered cut slope face below it (Area 4; approximately 100 feet above the powerhouse access road). There is a 75-foot-long cast-in-place concrete retaining wall near the center of Area 3 that supports the construction road bench (visible in the top left of Exhibit 3). Area 3 includes a talus-covered mid-slope bench that is approximately 30- to 40-feet wide at the upstream end (near the dam face) and narrows to 15- to 20-feet wide as it progresses downstream.

The overall slope inclination of Area 3 is approximately 1V:1H. The slope surface is irregular, featuring numerous prominent rock outcrops and areas of colluvium and sporadic vegetation where the slope gradient is less steep. The rock outcrops are moderately (0.5 to 1.0-foot fracture spacing) to occasionally fractured (1 to 4-foot fracture spacing). Vegetation includes grasses, shrubs, and small trees. Many of the obstructions along the slope (trees, outcrops, lagging) have acted as catchments, accumulating rockfall debris (up to 6 feet in the longest dimension, although typically less than 1 foot) behind them.



**Exhibit 3 - Area 3 Slope Reconnaissance Using Aerial Lifts**

It is useful for the discussion of hazard, consequence, and mitigation alternatives to consider Area 3 as comprising an upstream zone and a downstream zone, divided by a prominent topographic swale. The Area 3 Upstream (U/S) Zone had rockfall runout paths that may have impacted the access road and powerhouse, while rockfall from the Area 3 Downstream (D/S) Zone would likely impact only the access road (as indicated on Exhibit 4).



**Exhibit 4 - Area 3 Aerial Photo With Rockfall Cross-Sections Indicated And Upstream Zone (Outlined In Red), And Downstream Zone (Outlined In Yellow)**

## **Photogrammetry Assessment**

Gannett Fleming used Agisoft Photoscan (now Metashape) to create a 3D model and point cloud from the drone imagery, and used Maptek I-Site (now Point Studio) to identify and visualize joint surfaces along the slope. Using this process, Gannett Fleming was able to collect dozens of joint surface orientations, which were validated by comparing to hand-measurements made in the field along the margins of Area 3 where the slope could be accessed via the aerial lift. The geologic structure of Area 3 includes four primary, near-orthogonal joint sets.

Rockfall sources within Area 3 included fractured rock outcrops, precariously balanced rock blocks on the outcrops or within the talus materials, and potentially unstable rock blocks, up to 6 feet long in the greatest dimension, formed by the primary joint sets. It is important to note that the natural slopes in Area 3 have been subject to weathering processes for much longer than the cut slopes below, and the Area 3 slopes were likely not scaled during construction of the powerhouse. Rockfall initiation or re-mobilization events included erosion, animal disturbances, locally increased water pressure during intense precipitation events, root or ice wedging, other upslope rockfalls, or seismic forces. There were several noticeable rock-casts (recently exposed rock faces, sometimes covered in soil or other non-durable joint-infill material) up to 3 feet in maximum dimension, which indicated ongoing rockfall initiation along the slope that had likely stopped on the slope due to other rock outcrops, talus piles, or vegetation.

Based on the data gathered during the field reconnaissance and photogrammetry analysis, Gannett Fleming performed quantitative assessments of rockfall on the slope, consisting of kinematic analyses and rockfall simulation as described below.

## **Kinematic Analyses**

Kinematic analyses were performed to determine the susceptibility of the slope to various rockfall failure modes given the slope geometry and joint orientations. Kinematic analyses considered planar sliding with a 20° lateral limit, wedge sliding, direct toppling, and flexural toppling. Based on field observations, a friction angle of 34° was selected for evaluating planar and wedge sliding failures. The analyses indicated that the most likely rockfall failure mode was wedge sliding, which was consistent with the numerous wedge-shaped rock casts visually observed within the slope. The stereonet below (Exhibit 5) indicates that the observed joints on the slope may have interactions conducive to wedge failures.

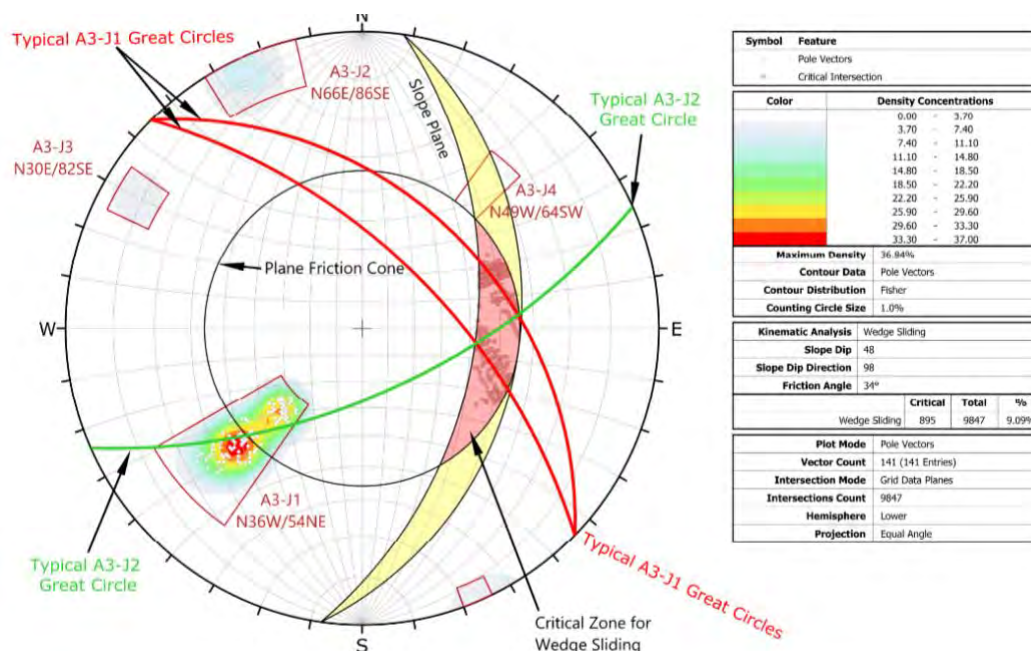


**Exhibit 5 - Stereonet Representation Of The Kinematic Assessment For Wedge Sliding. Interactions Between Joint Sets J1 And J2 Are Capable Of Producing Wedge Failures.**

## Rockfall Simulation

We performed computer-based rockfall simulations to estimate the energy and bounce heights within Area 3. Simulations were conducted using the rockfall simulation program RocFall 5.0 (RocFall), which uses probabilistic analysis and two dimensional (2-D) slope modeling to estimate rock block fall trajectories, energies, and bounce heights. Representative, idealized slope profiles were developed for the Area 3 Upstream Zone and Downstream Zone using the photogrammetry point cloud model.

Two profiles, Profile A-A' and B-B', were within the Upstream Zone, and three profiles, Profile C-C', D-D', and E-E', were located within the Downstream Zone (Exhibit 4). Vertical collection (or analysis) points, which are line segments used to generate summary statics and information about the rock trajectories that pass through the collection point, were added to all profiles for the purpose of evaluating the rockfall hazard to the powerhouse and access road.

Simulations were performed using two different rock block sizes: Metavolcanic Small (1,168 pounds) and Metavolcanic Large (7,785 pounds), based on recent rockfall blocks and fragments observed during the slope reconnaissance. Each model included an upper source area "seeder," where simulated rock blocks initiate their fall.

For the Area 3 U/S Zone, profiles (A-A' and B-B'), collection points were added at the downslope end of the existing talus covered, mid-slope bench (Collection Point 1), the inboard edge of the powerhouse access road (Collection Point 2), and the unit generator cover (Collection Point 3). At the Area 3 D/S Zone profiles, two collection points were added to the simulation models. Collection Point 1 is located at the downslope end of the existing mid-slope bench, and Collection Point 2 is located at the inboard edge of the powerhouse access road.

Each profile model included over 10,000 simulated rock block trajectories. The results of the rockfall simulations are presented in Table 2 below.

Hazard Area	Profile	Collection Point								
		1 (Mid-Slope Bench)			2 (Access Road)			3 (Powerhouse)		
		%Pass <sup>1</sup>	E <sub>MAX</sub> <sup>2</sup>	H <sub>95</sub> <sup>3</sup>	%Pass	E <sub>MAX</sub>	H <sub>95</sub>	%Pass	E <sub>MAX</sub>	H <sub>95</sub>
Area 3 U/S	A-A'	73	598	4.5	72	1,640	64	35	1,809	6
	B-B'	100	209	4	88	1,600	40	60	201	2.5
Area 3 D/S	C-C'	98	690	7.5	98	1,500	55	N/A		
	D-D'	98	774	11.5	98	1,932	80	N/A		
	E-E'	89	93	5.5	89	859	56	N/A		

1. %Pass = Percentage of rock block trajectories passing the Collection Point;
2. E<sub>MAX</sub> = The maximum energy rock block trajectory in kilojoules (kJ) impacting the Collection Point;
3. H<sub>95</sub> = The 95th percentile bounce height in Feet impacting the Collection Point.

The preliminary rockfall simulations for the Area 3 U/S Zone profiles indicated that a protective barrier constructed along the mid-slope bench would provide a significant degree of protection from individual rockfall blocks/boulders. Because the mid-slope bench narrowed in the downstream direction, a protective barrier along the bench at the Area 3 D/S Zone would provide less catchment and be less effective.

Based on the kinematic analyses and rockfall simulation, we rated the relative risk of Area 3 U/S and D/S using a system that defines risk as the combined qualitative measures of hazard probability and consequence (2). Hazard probability and consequence measures for Area 3 U/S and D/S are shown in Tables 3 and 4.

Rating	Description	Area
Almost certain [VH]	The event is expected to occur.	
Likely [H]	The event will probably occur under adverse conditions.	A3-U/S A3-D/S
Possible [M]	The event could occur under adverse conditions.	
Unlikely [L]	The event could occur under very adverse circumstances.	

Rating	Description	Area
Catastrophic [VH]	Complete destruction or severe damage to a facility that will require major repair and stabilization. Injuries or fatalities are likely.	
Major [H]	Extensive damage to a facility and significant maintenance effort and/or stabilization work. Injuries or fatalities are possible.	A3-U/S
Medium [M]	Moderate damage to a facility requiring routine and unscheduled maintenance. Injuries are possible.	
Minor [L]	Limited damage to a facility. Activity is primarily related to	A3-D/S

Rare [L]	The event is conceivable but only under exceptional circumstances.		Insignificant [L]	Little damage. Injuries would be rare or inconceivable.	
Not credible [L]	The event is inconceivable.				

The combination of probability and consequence of rockfall are the basis for risk rating for each site and are presented in Table 5 below.

<b>Table 5 - Hazard Area Relative Risk Rating</b>					
Very High (VH) Risk = Red High (H) Risk = Orange Moderate (M) Risk = Yellow Low (L) Risk = Gold		Probability			
		<i>VH</i>	<i>H</i>	<i>M</i>	<i>L</i>
Consequence	<i>VH</i>				
	<i>H</i>		A3-U/S		
	<i>M</i>				
	<i>L</i>		A3-D/S		

## ALTERNATIVES ANALYSIS

Based on conditions observed during our reconnaissance and the results of our assessment, Gannett Fleming developed alternatives for rockfall mitigation measures for the Area 3 Upstream and Downstream zones (which ultimately extended to significantly overlap with Area 4 below).

In the interim, Gannett Fleming recommended avoidance of the rockfall hazards at Area 3 by minimizing the amount of time that personnel or equipment were present on the powerhouse access road immediately beneath the slope. Methods of communicating hazard avoidance included education of personnel, updating ingress/egress policies, and signage.

### Area 3 Upstream Zone Alternatives

Gannett Fleming recommended two alternatives for rockfall mitigation in this zone. Slope scaling was not considered as a viable mitigation measure because of the likelihood for scaled material to impact the powerhouse and the limited to space to install temporary facility protection adjacent to an active hydroelectric facility with energized components.

Alternative 1 consisted of a rockfall barrier along the mid-slope bench whereas Alternative 2 consisted of an unsecured rockfall drapery (netting) system above and below the mid-slope bench. Because of the size of potential rockfall blocks, the drapery was anticipated to be a combination of cable-net panels underlain by double-twisted wire mesh. Both alternatives included local stabilization measures consisting of spot anchors (post-tensioned bolts or dowels) or cable lashing retention systems. The local stabilization measures would be designed and

installed as needed based on construction field observations of rock blocks or zones of rock blocks that exceed the design capacity of the rockfall barrier or drapery systems.

### **Area 3 Downstream Zone Alternatives**

Gannett Fleming recommended two alternatives for rockfall mitigation in this zone. Because the powerhouse is located well upstream and was not considered at risk from scaling operations in this area, scaling was considered a viable option.

Alternative 1 consisted of performing scaling to remove potentially unstable rock blocks, loose boulders, debris, and talus that has locally accumulated on the slope. Some surficial damage to the powerhouse access road was expected and would require maintenance/repair after scaling was completed. Temporary rockfall protection could be setup in front of existing guard rails and light poles to protect them from scaled debris. Local stabilization measures would be installed as needed based on field observations during construction (similar local stabilization measures as described above for the Upstream Zone alternatives).

Alternative 2 involved initial scaling of potentially unstable rock blocks and loose debris accumulated on the slope (as described under Alternative 1), followed by installation of an unsecured rockfall drapery. Because of the similar conditions with the Upstream Zone, the drapery system would consist of cable-net underlain by double-twisted wire mesh. Local stabilization measures would be installed as needed based on field observations during construction.

### **Preferred Rockfall Mitigation Alternative Selection**

TID opted to proceed with Alternative 2 (rockfall drapery) for the Upstream Zone, and Alternative 1 (rock scaling) for the Downstream Zone with local block stabilization where necessary in both zones. During construction, based on the field conditions encountered, TID opted to increase the extent of the rockfall drapery to include much of the Downstream Zone, essentially constructing Alternative 2 for the Area 3 Downstream Zone.

## **ROCKFALL MITIGATION DESIGN**

The design of rockfall mitigation measures consisted of three main elements: (1) rockfall drapery; (2) rock anchors (bolts); and (3) wire rope restraint systems for blocks too large or precarious to secure with rock anchors. The final locations and quantities of rock anchors and wire rope restraints were to be determined in the field once safe access (including temporary facility protection while access the slope) had been established.

The rockfall drapery design generally followed the procedure described in *Design Guidelines for Wire Mesh/Cable Net Slope Protection* published by the FHWA and WSDOT (3). The drapery comprised galvanized double-twist wire mesh attached to cable net suspended from a 3/4" galvanized top wire rope, attached to double-legged 3/4" wire rope anchors. The wire rope anchors were to be spaced up to 20 feet on center, and drilled and grouted a minimum of 10 feet below grade.

The rock anchors comprised galvanized #8 all-thread bars drilled and grouted a minimum of 15 feet below grade. The number and orientation of rock anchors to be installed would be determined by Gannett Fleming field geologists based on on-site observations of rock blocks that may overwhelm the drapery system. Generally rock blocks greater than 6 feet in the longest dimension, or rock masses greater than 10 cubic yards were considered for local stabilization measures.

The wire rope restraints were designed to restrain destabilized blocks from falling down the slope during anticipated static and seismic loading conditions, and comprised three 1-inch-diameter support wire ropes fitted across the downhill face of each unstable rock block. Each wire rope was anchored at both ends to double-legged 3/4" wire rope anchors located above the rock blocks on both sides. Galvanized cable net attached to the support ropes with lacing wire would be utilized to create a panel over the face of the rock to increase the contact area of the restraint system on the block. Two additional wire rope anchors were included adjacent to the hazard rock to maintain the position of the support ropes and cable net crossing the face of the rock.

## **CONSTRUCTION**

Access Limited Construction (ALC) was awarded the construction contract and performed the construction between June and September of 2020. Materials for the rockfall drapery, wire rope restraint systems, and rock anchors were provided by Geobruigg, Inc.

### **Engineering Support During Construction**

Gannett Fleming provided construction support services and as-needed technical support to TID during construction. Prior to construction, Gannett Fleming reviewed construction and materials submittals prepared by ALC. During construction, Gannett Fleming geologists and engineers performed periodic site visits to observe slope scaling, evaluate geologic conditions for consistency with design assumptions, observe layout and construction of the mitigation measures, evaluate conformance with the intent of the construction drawings and specifications, and to observe proof testing of anchors.

The presence of a Gannett Fleming geologist on-site allowed for improved quality control and quick responses to changed conditions encountered during construction. The field geologists were able to access the steep portions of the slope using rope access techniques to review conditions firsthand and to discuss potential options with ALC personnel. When ALC encountered rock blocks that were not well suited for any of the three mitigation measures included in the design, the on-site geologist was able to collaborate with the Gannett Fleming engineer to quickly produce a modified design of the wire rope restraints.

### **Temporary Facility Protection**

To protect the powerhouse, access road, and personnel during construction, ALC implemented temporary rockfall protection measures on the access road comprising a "Moveable Rockfall Barrier" (MRB) and crane-suspended rockfall netting. The MRB comprised a 180-foot-long by 12-foot-tall steel wire mesh rockfall netting that spanned between vertical steel posts which were bolted to steel trench plates at the bottom. The crane-suspended netting consisted of a 48-foot-

wide panel of steel wire rope netting and double-twist wire mesh, suspended from a spreader bar positioned by a crane. ALC staged the MRB and crane-suspended netting on the access road and shifted their locations throughout construction to be positioned downslope of construction activities on the Area 3 slope.

ALC also constructed a temporary 6-foot-tall chain-link fence immediately downslope of the upstream zone RFD top rope anchors to prevent slope materials and equipment from traveling downslope during anchor installation at the top of the slope.

During construction, TID had outage preparation work at the powerhouse, which could only be reached by the access road that passed below the rockfall area. ALC cleared the road of debris daily to allow for vehicle access to the powerhouse, and also maintained regular radio communication with TID personnel to coordinate passage of vehicles and personnel below the work zone.

The construction sequencing was performed in a way that maximized facility protection. ALC first partially installed the drapery over the slope, and then installed the rock anchors and wire rope restraint systems as needed. By working through or underneath the drapery, ALC was able to decrease the risk of rockfall initiation during drilling of the local stabilization measures.

### **Slope Scaling**

ALC performed slope scaling within part of the Area 3 Downstream Zone. Scaling activities included identifying and removing loose and potentially unstable rock blocks and debris from the slope that could adversely impact worker safety and/or downslope facilities during and after construction. Scaling was performed by hand using scaling bars and began at the downstream terminus of Area 3 and continued in the upstream direction. Gannett Fleming performed full-time construction observation during scaling activities to provide geologic input and identify rock blocks that may require wire rope restraints or rock anchors for long-term stability.

As the scaling work progressed upstream towards the powerhouse, the slope was found to contain more unstable rocks, and of a larger size, than anticipated. In addition, field personnel observed highly erratic trajectories of scaled rock blocks due to the irregular slope geometry, which raised concerns that scaled rock blocks could potentially impact the powerhouse facility.

Based on discussions with TID and ALC, Gannett Fleming proposed to reduce the extents of slope scaling in the downstream zone to approximately 200 feet downstream of the powerhouse, effectively creating a buffer zone, and to increase the quantity of rockfall drapery to cover the unscaled portion of the downstream slope. This approach removed the potential risks to the facilities that additional scaling likely presented, while still providing long-term mitigation of the rockfall risk posed to personnel on the access road below. ALC coordinated with Geobrugg to provide additional rockfall drapery with minimal impact to the schedule.

### **Rockfall Drapery**

ALC performed layout of the rockfall drapery top wire rope anchors, and Gannett Fleming reviewed and accepted the layout prior to installation. The wire rope anchors were drilled using a 4-inch-diameter rock drill mounted to either an articulated “Spider” excavator or a suspended

wagon-mounted drill. Competent bedrock was generally observed at the ground surface or within 1 to 2 feet below ground surface. Grout was batched onsite and tremied into the bottom of the drill holes. The drapery panels were primarily installed by helicopter on the upper portions of the slope, and by crane at the bottom of the slope (Exhibit 6).

As mentioned above, TID authorized installation of additional rockfall drapery in the Area 3 Downstream Zone in order to reduce the rockfall hazard to the powerhouse from rock blocks originating from the slope downstream of the powerhouse. Gannett Fleming issued exhibits to TID and ALC depicting the layout of the downstream rockfall drapery, which continued from the terminus of the upstream drapery to approximately 200 feet downstream of the powerhouse, and vertically from the slope break below the upper access bench down to the powerhouse access road (Exhibit 6).



**Exhibit 6 - Area 3 Slope After Installation Of Rockfall Drapery**

ALC procured additional materials for installation of the downstream drapery and performed layout of the downstream top wire rope anchors based on Gannett Fleming's exhibits.

ALC performed proof testing of three (3) top wire rope anchors in the upstream zone and two (2) top wire rope anchors in the downstream zone, respectively. The testing was performed in accordance with the plans and specifications and all anchors performed satisfactorily, as observed by Gannett Fleming.

## Rock Anchors

Gannett Fleming worked closely with ALC during construction in order to identify potentially unstable rock blocks that required in-place stabilization using rock anchors. Based on our observations, we identified four (4) rock blocks requiring rock anchors. We performed engineering analyses to determine the number of rock anchors required to stabilize each rock block and presented exhibits depicting the number and layout of anchors for review and approval by TID. Typical rock anchors are shown in Exhibit 8 below.



**Exhibit 8 - Rockfall Drapery Consisting Of Rolled Cable Net With Double-Twist Mesh Backing. Select Rock Blocks Were Stabilized With Rock Anchors**

Based on TID's approval, ALC performed layout of the anchors in the field, which was reviewed and accepted by Gannett Fleming. The drilling and installation of the rockfall anchors was performed after the rockfall drapery was installed, so that the drapery could capture any rock blocks that may be dislodged during drilling. A total of twenty-one (21) permanent rock anchors were installed to stabilize the potentially unstable rock blocks. The rock anchors were drilled using a 3-inch or 4-inch diameter wagon-mounted drill.

One sacrificial rock anchor was installed for proof testing at the top of the slope. ALC performed proof testing of the sacrificial rock anchor in accordance with the plans and specifications, and the anchor performed satisfactorily.

### **Wire Rope Restraint Systems**

Gannett Fleming and ALC identified two large rock blocks in the Area 3 upstream zone that required in-place stabilization utilizing wire rope restraint systems. Based on their size and orientation rock anchors could not be safely installed to stabilize the rock blocks. ALC and Gannett Fleming performed layout of the six upslope wire rope anchors and two downslope anchors for each rock block, which were drilled using a 3-inch or 4-inch diameter wagon-mounted drill. Additionally, a third rock block was stabilized using a modified wire rope restraint system comprising a rockfall drapery panel supported by two upslope wire rope anchors (Exhibit 9). ALC performed proof testing of two support wire rope anchors, which performed satisfactorily.



**Exhibit 9 – A Modified Wire Rope Restraint System, Consisting Of A Rockfall Drapery Panel And Wire Rope Anchors**

In total, approximately 122,000 square feet of drapery, 47 wire rope and rock anchors, and three wire rope restraint systems were installed. The construction work was completed in approximately 4 months, and the contractor was able to de-mobilize in time to avoid interference with outage-related work that TID had planned for the powerhouse.

## **CLOSURE**

A phased approach was utilized to evaluate and reduce rockfall hazards at the Don Pedro Powerhouse facility. By starting from a broad overview of the rockfall hazards on the slopes surrounding the powerhouse, TID was able to implement a multi-year plan to pursue rockfall hazard mitigation in balance with site access considerations, scheduling, and budget limitations. This approach allowed the project team to overcome challenges that included: (1) limited accessibility to the slope during the design, (2) a difficult slope configuration for facility protection; and (3) a requirement to keep the access road largely open during construction. Such an approach should be considered for rockfall hazard mitigation at other critical facilities.

The close cooperation between the owner, contractor, and engineer during construction allowed for timely responses to changed conditions that warranted modifications to the design. It also encouraged proactive solutions to facility protection, such as modifying the construction sequence to allow the rock anchors and rock restraints to be installed after the drapery, rather than before. This coordination, and continuity of personnel from initial reconnaissance through construction, contributed to the overall success of the rockfall mitigation project, and should also be considered for rockfall hazard mitigation projects at critical facilities.

## **References**

1. Clark, D.L. Stratigraphy and Structure of Part of the Western Sierra Nevada Metamorphic Belt, California, Geological Survey Professional Paper 410, prepared by the United States Department of the Interior in cooperation with the State of California, Department of Conservation Division of Mines and Geology, 1964.
2. Rockfall Characterization and Control, Chapter 3, pp 57-58, prepared by the Transportation Research Board of the National Academies, published 2012.
3. Design Guidelines for Wire Mesh/Cable Net Slope Protection, Report No. WA-RD 612.2, prepared by the Federal Highway Administration (FHWA)/Washington State Department of Transportation, dated April 2005.

**Bolt Creek Fire: Post-Wildfire Debris Flow Risk Assessment and Barrier  
Design on US 2, Near Grotto, WA**

**Author: Cody Chaussee**

WSDOT State Geotechnical Office

1655 S 2<sup>nd</sup> Ave SW, Tumwater, WA 98512

(564)-200-2455

[chaussc@wsdot.wa.gov](mailto:chaussc@wsdot.wa.gov)

Prepared for the 72<sup>nd</sup> Highway Geology Symposium, August 2023

### **Acknowledgements**

The author would like to thank the individuals/entities for their contributions in the work described:

Samuel Johnston – WSDOT State Geotechnical Office

Katelyn Card – WSDOT State Geotechnical Office

Tracy Trople – WSDOT State Geotechnical Office

Marc Fish – WSDOT State Geotechnical Office

### **Disclaimer**

Statements and views presented in this paper are strictly those of the author(s), and do not necessarily reflect positions held by their affiliations, the Highway Geology Symposium (HGS), or others acknowledged above. The mention of trade names for commercial products does not imply the approval or endorsement by HGS.

### **Copyright**

Copyright © 2023 Highway Geology Symposium (HGS)

All Rights Reserved. Printed in the United States of America. No part of this publication may be reproduced or copied in any form or by any means – graphic, electronic, or mechanical, including photocopying, taping, or information storage and retrieval systems – without prior written permission of the HGS. This excludes the original author(s).

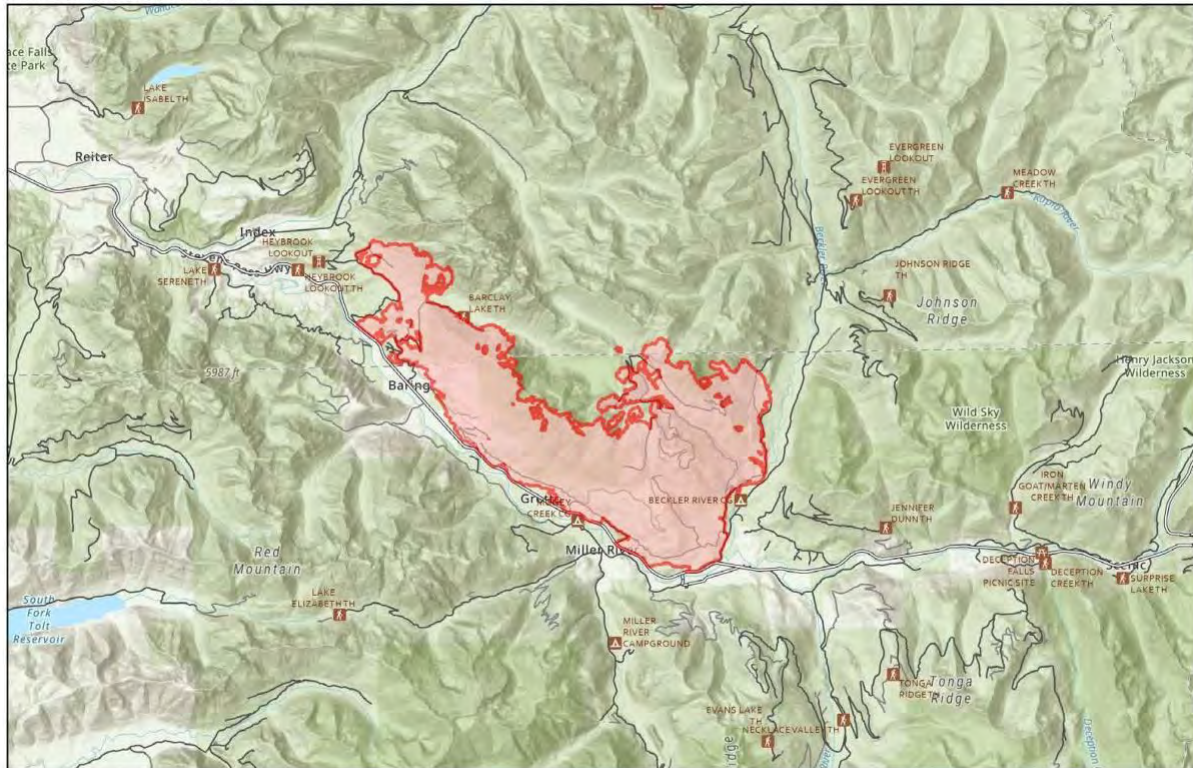
### ABSTRACT

Post-wildfire debris flow hazards created by the Bolt Creek Fire warranted rapid response from the USDA Forest Service, Washington Geologic Survey, and Washington State Department of Transportation (WSDOT), to analyze and mitigate the risk of debris flows reaching US Route 2 (US 2). The 2022 Bolt Creek Fire burned over 14,000 acres of forest along US 2 between approximate mileposts 40 and 50, creating debris flow hazards within the preexisting drainage network upslope. The Bolt Creek Fire burned area along US 2 is on the western slopes of the North Cascades, where the surface geology is composed of alluvial soils, Mesozoic metasedimentary, and Tertiary intrusive rock. The incised drainage network extends from US 2 approximately 4,000 feet upslope to the crests of Baring Mountain and Grotto Mountain. Post-wildfire assessments by the USDA Forest Service, USGS, and WGS provided specific points of concern for WSDOT with elevated debris flow risk, based on burn severity, and mapped alluvial fans intersecting US 2 and the town of Grotto, WA. WSDOT provided rapid response, by completing site specific evaluations of each point of concern. Evaluating available catchment and sediment delivery potential, WSDOT identified two locations with the highest risk of debris reaching US 2. To reduce the risk of debris flow impacts to the highway, WSDOT used hand calculations along with GeoBrugg Inc.'s dimensioning tools DEBFLOW and SHALLSLIDE to calculate estimated static and dynamic loads that would be generated in the event of a debris flow in these two locations. Using the results of the analysis, WSDOT recommended construction of post-supported debris flow (or shallow landslide) barriers (western and eastern) that will withstand impacts of up to 1570 psf ( $75 \frac{kN}{m^2}$ ). Rapid response, design, and construction times are required to construct the debris flow barriers in a timely manner, considering the estimated 1-to-5-year timeline in which the post-fire debris flow risks are the greatest.

## INTRODUCTION

The Bolt Creek Fire began on September 10, 2022, was determined to have been caused by humans, and burned approximately 14,900 acres before it was contained in October 2022. The burned area is north of US 2 on the border of King and Snohomish Counties and burned from the highway upslope to the crest of Klinger Ridge, Baring Mountain, and Grotto Mountain (Figure 1).

### Fire Information



#### Bolt Creek WA-NWS-000150

14,820 acres at 10/19/2022 @1837



**Figure 1. Map of Bolt Creek Fire burned area north of US 2 as of October 19, 2022 (1).**

According to the USDA Forest Service Burned Area Emergency Response Program (BAER) (1), over 1,800 acres of the burned area had a “High” soil burn severity, over 5,900 acres had a “Moderate” burn severity, over 3,900 acres had a “Low” burn severity, and over 3,300 acres were unburned. Land ownership within the limits of the burned area is approximately 25.8 percent Privately owned, 0.5 percent State owned, and 73.8 percent owned by the Forest Service (1). 29 percent of the fire area is designated as “Wilderness” while the remaining 71 percent is designated as “Non-wilderness”. Vegetation types in the area in ascending elevation are Douglas-fir, Western Hemlock, Pacific Silver Fir, and Mountain Hemlock (1). Dominant

soils within the area were identified as “volcanic colluvium, generally ashy sandy loam and ashy loamy sand from volcanic eruptions” (1). The USDA Forest Service BAER Report states that “The soils on the steeper slopes tend to be shallow and less productive, whereas the valley bottoms to mid slopes tend to be deeper and very productive” (1).

The Bolt Creek Fire burned area spans along US 2 from approximate milepost (MP) 40 to MP 50, where the route generally trends northwest southeast. Many areas within WSDOT right of way were burned, which burned vegetation as well as some of WSDOT’s assets. The fire not only caused immediate damage to WSDOT assets, but also put additional infrastructure at risk due to the increased risk of debris flows in the coming years within the burned area. In this case history, we present a summary of our response to the Bolt Creek Fire, our subsequent geotechnical investigation, debris flow risk assessment, analysis, and design processes that guided our recommendations to ultimately reduce the risk of post-wildfire debris flows reaching the roadway along US 2.

## **DEBRIS FLOWS**

According to the United States Geological Survey (USGS), “debris flows are fast-moving landslides that are particularly dangerous to life and property because they move quickly, destroy objects in their paths, and often strike without warning.” (2) “Debris flows generally occur during periods of intense rainfall or rapid snowmelt and usually start on hillsides or mountains.” (2) The USGS states that debris flows can travel up to speeds exceeding 35 mph and carry large objects such as boulders, trees or even cars. (2). Debris flows can travel several miles along existing stream channels and impact areas that may be unaware of the hazard (2). USGS also states that areas recently burned by a forest fire are especially susceptible to debris flows, including the areas downslope and outside of the burned area (2).

WSDOT has observed historic debris flows in several areas throughout Washington State. According to historical records in our Unstable Slopes Management System (USMS), there are over 150 unstable slopes that have been classified with a “Debris Flow” deficiency description. These debris flow sites are often located in the regions of the state with high topographic relief. For example, Washington State Route 20 (also known as the North Cascades Highway) accounts for over 20% of debris flow sites in the USMS, with 32 debris flow sites listed as “active” in the database. Debris flows in Washington State have historically stranded travelers, destroyed bridges, blocked culverts causing drainage problems, eroded stream channels and ditches, and have buried the roadway in up to tens of feet of debris. Debris flows can cause short- and long-term closures of the roadway, and often occur in remote areas where there are limited or no alternate routes available for detours, causing significant disruptions to the local and regional communities and traveling public.

## SITE CONDITIONS

### Regional Geology

The regional geology of the central Cascades is a mix of core bedrock composed of sedimentary, metamorphic, and igneous rock, with Quaternary deposits and alluvial soils deposited over the underlying core bedrock (Figure 2).

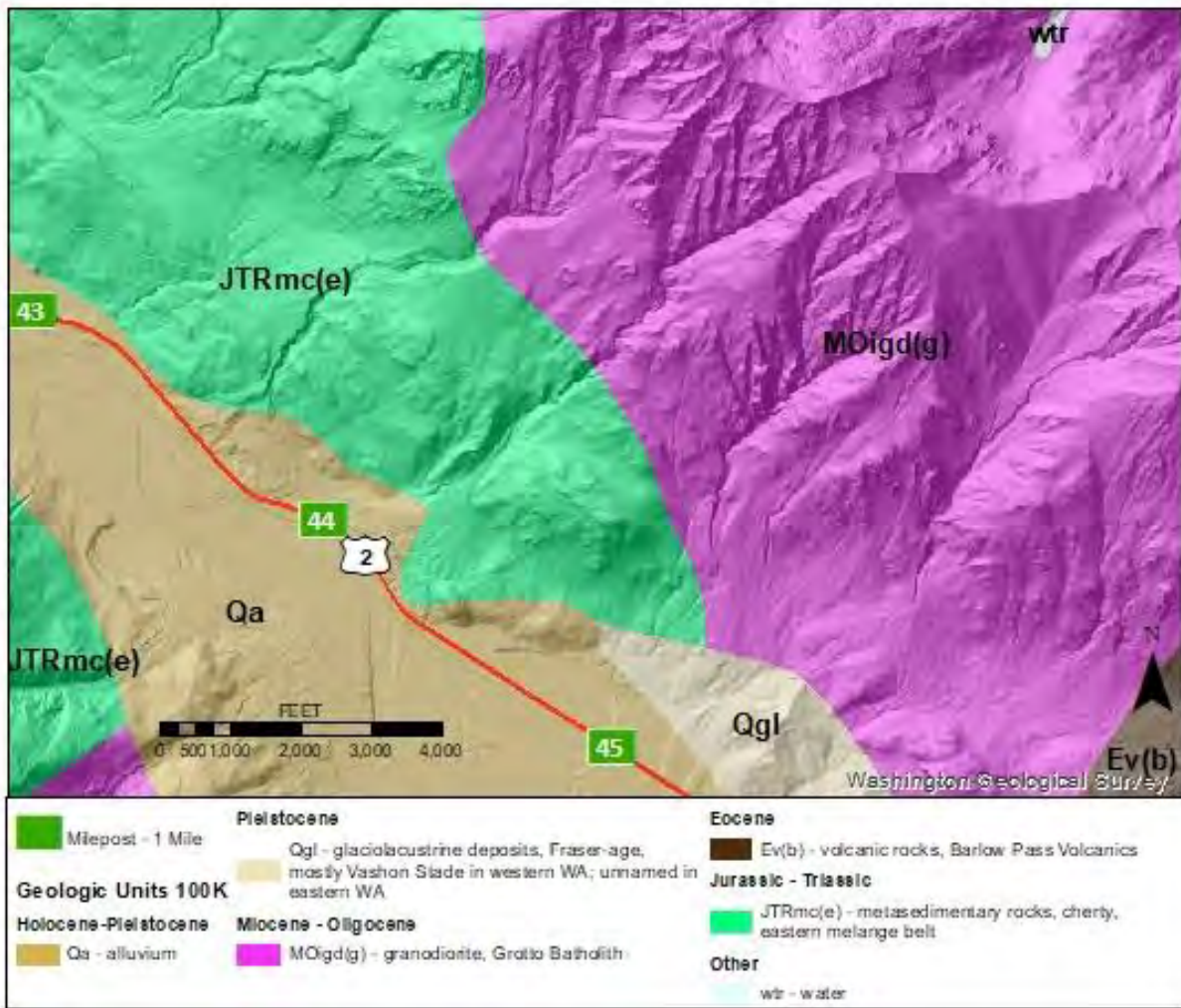


**Figure 2. Surface geology (1) near the site vicinity of the Bolt Creek Fire on US 2 MP 43 to 45. Lidar derived from WGS (2).**

The sites of interest are along a valley that is west of the Cascade Crest that divides Eastern and Western Washington and west of the Straight Creek Fault Zone which generally

trends north south. Regional Quaternary deposits in the vicinity are results of scores of late Pleistocene local cirque and valley glaciers and their outwash streams, Holocene streams and mass-wasting hillslopes, and scattered small volcanoes (1).

### **Local Geology and Geomorphology**

Within the Bolt Creek Fire burned area between MP 40 and 50 along US 2, the South Fork Skykomish River meanders down the valley floor and flows westward toward the Puget Lowland. The valley, along with US 2 and the adjacent railroad tracks, trend northwest-southeast at this location. US 2 and the adjacent railroad tracks trend parallel to the SF Skykomish River and are located between the SF Skykomish River and the burned area from the Bolt Creek Fire. The SF Skykomish River Valley has steep slopes on the valley walls that vary from 45 degrees to near vertical. The burned area from the Bolt Creek Fire is isolated to the northern side of the valley. Local geology is primarily composed of alluvial soils in the lower sections of the valley, and exposed bedrock, with generally thinner soil layers in the upper sections of the valley between Baring Mountain and Grotto Mountain.

In the lower flanks of the SF Skykomish River valley, there are several series of active and apparently relict channel networks incised into alluvial soils. The incised channel networks connect to rills and gullies that appear to extend to the crest of the slopes between Baring Mountain and Grotto Mountain (Figure 3). Primary sources of water appear to be from seasonal snowmelt, and springs of groundwater that appear to produce flow both seasonally and (in some locations) throughout the year. The Bolt Creek Fire drainage network leads either directly into tributaries to the SF Skykomish River, wetlands adjacent to US 2, or directly under US 2 in culverts, eventually discharging into the SF Skykomish River. Directly adjacent and below the highway are a series of flood plains and wetlands of the SF Skykomish River that appear to provide proximal basins connecting to the channel networks. US 2 appears to be approximately 20 to 30 feet above the SF Skykomish River on average.

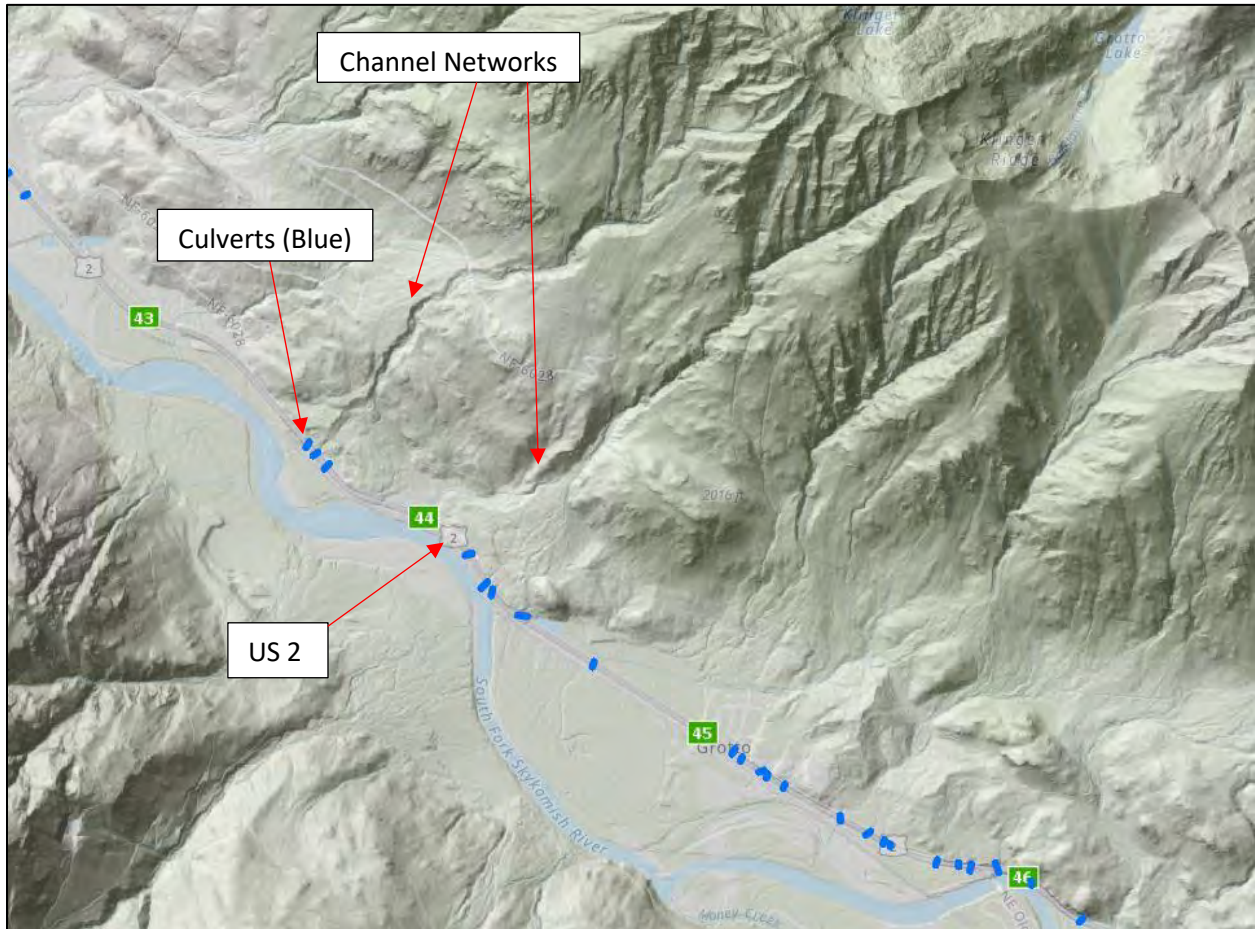


**Figure 3. Lidar image showing terrain, geomorphic features, and culverts in the vicinity of the site location. Lidar derived from WGS (2).**

In our USMS, we found an active landslide within a primary point of interest in the Bolt Creek Fire burned area. The landslide spans from US 2 MP 44.20 to 44.31 and has been previously characterized as active, large, deep seated, and slow moving, with monitored movements up to 0.5 inches per year according to readings from our installed instrumentation. The landslide headscarp is located upslope of US 2 and the landslide has caused roadway deformation several times over the years and as recently as January of 2016 (Figure 4).



**Figure 4. Roadway deformation caused by the landslide on US 2 MP 44.2. Image on the left is from January 2007, image on the right is from January of 2016.**

## **GEOTECHNICAL INVESTIGATION**

### **Risk Assessment**

As the Bolt Creek Fire burned through fall of 2022, several government agencies including WSDOT, USDA Forest Service, and the Washington Geologic Survey (WGS) prepared to mobilize for a geotechnical response effort. As the fire became contained, the WGS mobilized and evaluated the Bolt Creek Fire burned area for potential risk of flash floods and debris flows (2). According to the WGS (2), “wildfires can significantly change the hydrologic response of a watershed so that even modest rainstorms can produce dangerous flash floods and debris flows.” In order to complete their evaluation and response, the WGS coordinated with the USDA Forest Service and their BAER report (1) and assessed areas downstream of slopes for potential impacts of flash flooding and debris flows on infrastructure and public safety. WGS (2) mapped out alluvial fans in the area using lidar, orthoimagery, and field reconnaissance (Figure 5).



burned area without the precipitation threshold being reached, should a rain-on-snow event occur. Historically, we have observed rain-on-snow events cause hydrologic surges as a result of rain landing directly on snow, causing it to melt and contribute to runoff caused by the precipitation.

During the WGS study (2), they compiled a plate of points along the Bolt Creek Fire burned area in which they had mapped alluvial fans and provided the corresponding modeled hazard rating in the area. The WGS plate of points highlighted 9 areas within the Bolt Creek Fire burned area in which there was an elevated risk for flash flooding and debris flows. Among the 9 areas that WGS identified with an elevated risk for flash flooding, 5 of the points and mapped alluvial fans were adjacent to or directly intersected US 2 between mileposts 40 and 50 (Figure 4). After receiving the WALERT report from WGS (2), we mobilized to conduct field reconnaissance of the 5 sites along US 2 identified by the WGS. The 5 sites along US 2 that we visited coincided with points 3 through 6 from Plate 1 in the WALERT report produced by the WGS (2) (Figure 6).

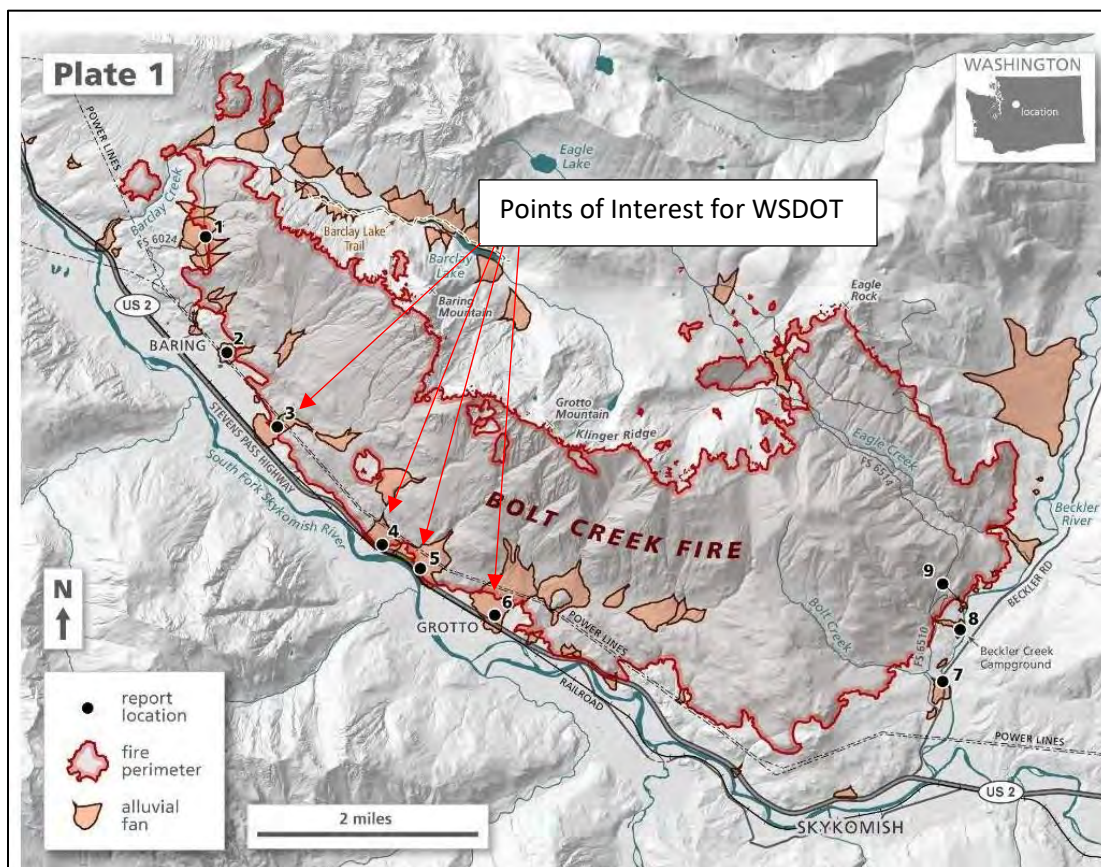


**Figure 6. Points of interest for WSDOT based on WALERT report produced by the WGS (2). Imaged modified from WGS (2).**

During our field reconnaissance, we walked each site, took photographs, mapped relevant geologic features using a handheld GPS unit, and took measurements of stream channels and drainage basins to characterize the catchment at each site (Figure 7).



**Figure 7. Field photo of catchment area taken during initial site reconnaissance and catchment assessment.**

We also characterized the local geology and geomorphic features we observed at each location. In addition to our field reconnaissance, we also conducted a detailed review of topographic maps, lidar, site history of debris flows and landslides, and an evaluation of technical reports as they related to the Bolt Creek Fire, including reports from our Unstable Slopes Management System (USMS), WGS, and USFS.

Using estimated area calculations of each potential debris flow source area, along with the potential for an estimated 25 tons per acre of sediment delivery potential derived from the USFS BAER report (1), we determined a tonnage estimate of potential sediment delivery as well as a tonnage estimate of potential catchment areas in the event of a debris flow at each location. The sediment delivery potential and catchment at each location are summarized in Table 1.

<b>Table 1. Mass of potential sediment delivery and catchment available at each point.</b>		
<b>Point of Concern</b>	<b>Estimated Available Catchment (tons)<sup>1</sup></b>	<b>Estimated mass of debris generated from source area (tons)<sup>2</sup></b>
Point 3	32,000	600
Point 4 (west end)	7,002	1,050
Points 4 & 5 (between)	25,000	1,850
Points 5 & 6	1,800,000	550

## Notes:

1 These are the catchment areas located directly adjacent to the roadway and do not include the other potential catchment areas in the channel networks upslope.

2 These quantities are based on the estimated value of 25 tons per acre of debris which is within the range of 22 to 31 tons per acre identified in BAER report (1).

Our risk assessment determined that out of all the points identified by WGS (2) with a high debris flow risk, there was one area in which there was insufficient catchment to accommodate potential debris flows. The area with the lowest amount of catchment was identified at a location within point 5 of Plate 1 from the WGS report (2) at milepost 44.25 along US 2 (Figure 8).

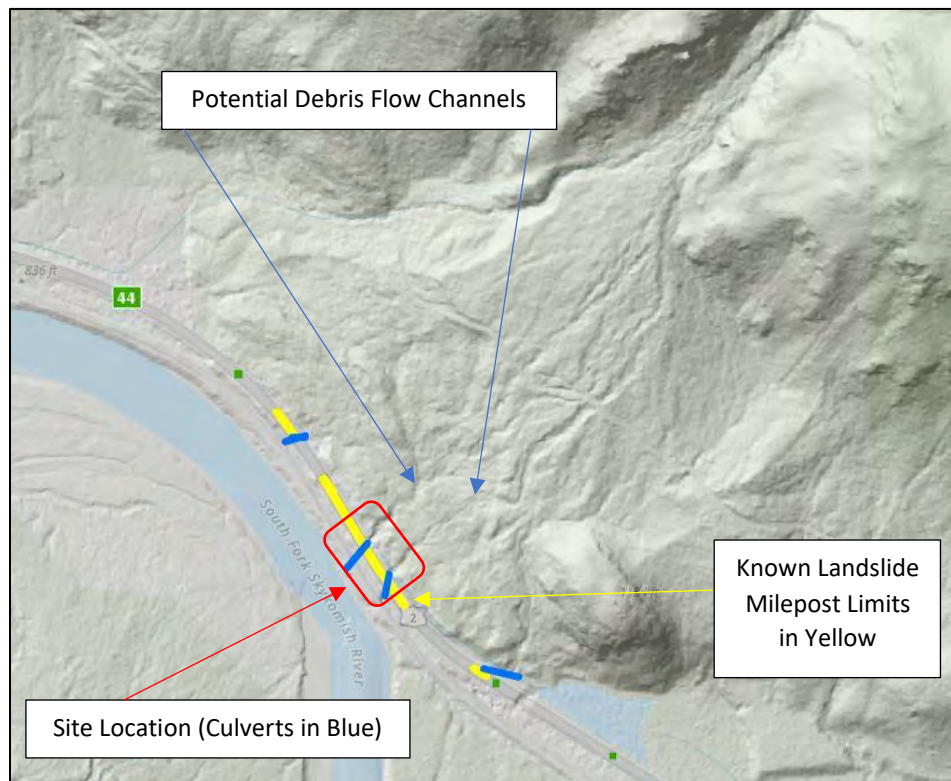


**Figure 8. Location along US 2 with highest risk of debris flows reaching the roadway.**

**Lidar derived from WGS (2).**

While we had not historically observed debris flows at this location, the mapped alluvial fan from WGS (2) is indicative that past debris flows at this location have occurred. We observed that should a debris flow occur at this location and follow the existing stream channel; it would likely reach a set of two culverts (Western and Eastern) that were installed underneath US 2 near milepost 44.25 (Figure 9).

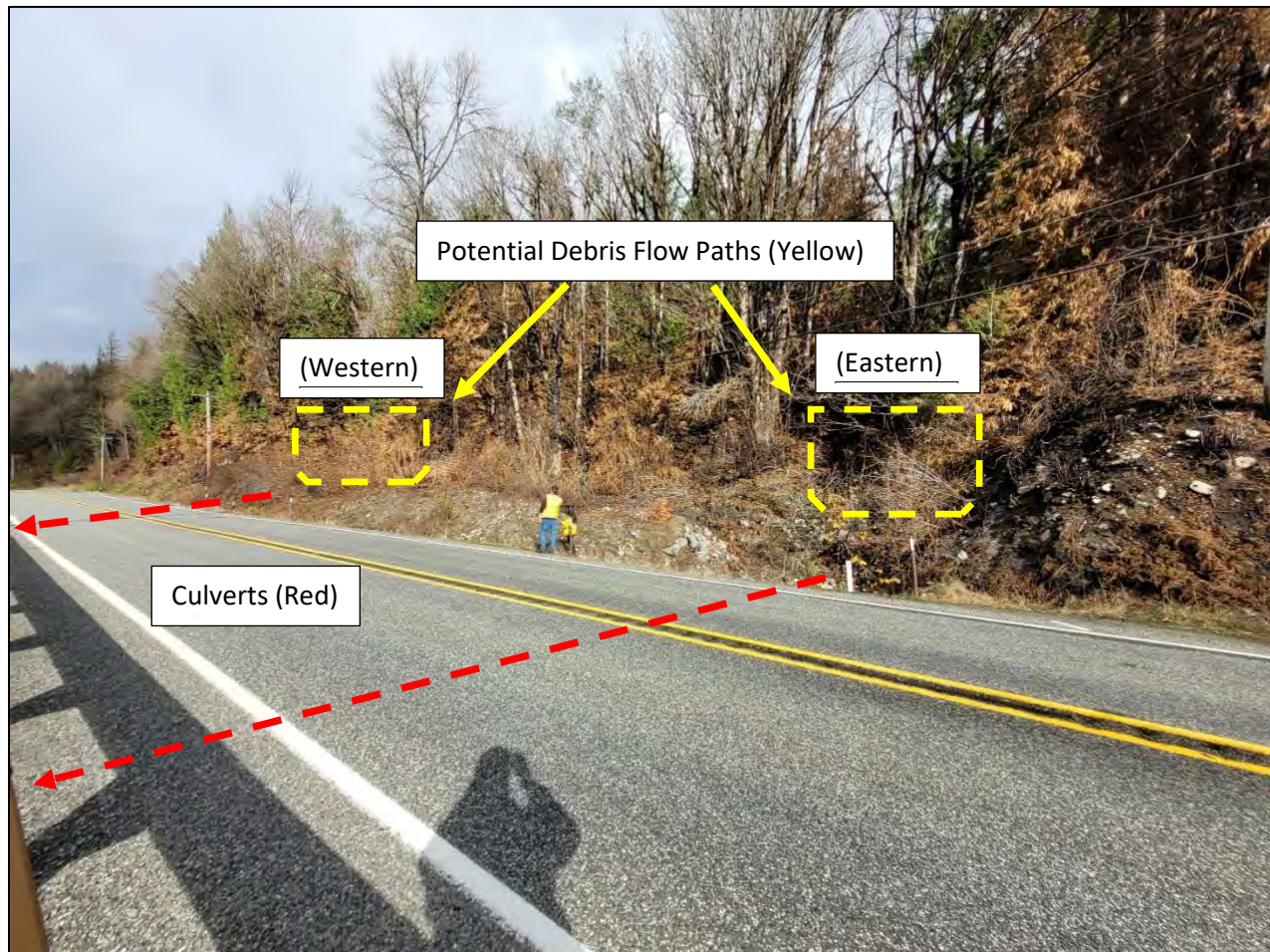


**Figure 9. US 2 MP 44.25 culverts and potential debris flow path locations with the highest risk identified during our initial site reconnaissance and catchment evaluation. Red dashed arrows indicate culverts and their flow direction.**

Any significant volume of debris traveling down either the western or eastern channel at this location would likely overwhelm the culverts, and directly impact the highway. Additionally, the culverts at this location are within the limits of the landslide that has historically caused roadway deformation at MP 44.2. With the highest risk area for debris flows

within the limits of an active landslide, we had to proceed carefully when considering the most appropriate mitigation options to pursue for a potential debris flow at this location.

### **Mitigation Options and Initial Geotechnical Recommendations**

After identifying our area of greatest concern for a potential debris flow, we offered short term and long-term mitigation options for the debris flow hazard at point 5 identified by WGS (2), which included:

- Installing concrete barrier along the shoulder of U.S. Route 2 that may act as a guide to direct debris to nearby catchment areas.
- Installing culvert inlet risers or manholes with debris cages to help prevent the culverts becoming clogged by debris.
- Developing and implementing a proactive monitoring plan of existing ditches and drainage channels that may provide catchment to prevent them from being overwhelmed with debris.
- Constructing flexible debris flow barriers, flexible shallow landslide barriers, or soldier pile debris flow deflector walls upslope of U.S. 2 to prevent debris from reaching the culverts and potentially impacting the roadway in the event of a debris flow or debris flows.

Additionally, we considered digging a series of trenches to increase the available catchment in the area. We also considered excavating and expanding the existing ditches, and constructing earthen berms with excavated material. However, considering the site is within the limits of a known landslide, we decided against any recommendations that would involve extensive excavation or grading that could potentially activate the landslide on site.

After our initial response and internal discussions regarding design time, construction time, right of way constraints, maintenance, and site conditions, we decided the best option to reduce the risk of debris flow reaching US 2 at this location was to install post-supported, flexible debris flow or shallow landslide barriers above the stream channels upstream of the two culvert inlets (western and eastern) at MP 44.25 (Figure 9). Initially, we had considered soldier pile debris flow deflector walls as well. However, considering the risk for debris flows is assumed to be highest within the first few years of the fire, we decided on flexible debris flow or shallow landslide barriers instead, because soldier pile walls would have taken longer to construct due to a more involved design process at our Geotechnical Office.

### December 2022 Debris Flow

After our initial site reconnaissance and geotechnical recommendations provided in November 2022, a single event occurred at the location of the previously identified eastern culvert (Figures 9, 10). According to Maintenance, on the afternoon of December 24, 2022, a debris flow occurred that blocked the culvert inlet with debris, snow, and ice, causing water to flow overtop US 2 and close the highway from MP 44 to 99, including Stevens Pass. According to WSDOT Maintenance, cleanup efforts removed approximately 70 cubic yards of material from the westbound ditch and area around the culvert inlet. WSDOT Maintenance stated that after they began removing material from the ditch, water eventually made its way back through the culvert, flushing the remaining material out before they finished cleanup operations. Considering WSDOT Maintenance did not reach out to our Geotechnical Office about the event, we received limited information, aside from anecdotes from WSDOT Maintenance and a single photo (Figure 10).



**Figure 10. December 24, 2022, debris flow along US 2 at approximate MP 44.2 that clogged the culvert inlet, causing water to flow over US 2.**

## Subsurface Conditions

Rather than take the time for an exploration phase and drilling, we decided to use nearby test boring data to characterize the subsurface conditions at the site of the potential debris flow channels at US 2 MP 44.25. During an assessment of the previously identified MP 44.2 landslide on site, 8 test borings were drilled, with piezometers and slope inclinometers installed in multiple locations throughout the assumed limits of the landslide. In Table 2 below, we have included information from the closest test borings to the proposed barrier locations, as well as their corresponding depths and the instrumentation types installed in each boring.

Boring Number	Total Depth	Instrumentation	Surface Elevation
H-5si-16	100 feet bgs	Slope Inclinometer	847 feet
H-6p-16	99 feet bgs	Piezometer	847 feet
H-7si-16	151 feet bgs	Slope Inclinometer	885 feet
H-8p-16	117 feet bgs	Piezometer	886 feet

Borings H-7si-16 and H-8p-16 were drilled approximately 230 feet from US 2 centerline, while borings H-5si-16 and H-6p-16 were drilled just beyond the shoulder of the eastbound travel lane of US 2. H-5si-16 and H-6p-16 are approximately 100 feet southwest of the debris flow site location. Considering these borings are closest to the site location, and have the highest frequency of samples taken, test borings H-5si-16 and H-8p-16 were used to interpret the site geological conditions. Three Engineering Stratigraphic Units (ESUs) have been identified; they are as follows:

**ESU 1 - Fill:** This unit is composed of fill that is described as medium dense, brown, moist, homogeneous, well graded SAND with sub-angular gravel. Only one sample was taken of ESU 1, which provided a field SPT “N” value of 18 blows/ft. No laboratory testing of samples was performed within this ESU.

ESU 1 was observed to be approximately 4 feet thick in test boring H-5si-16. ESU 1 was not observed in test boring H-8p-16.

**ESU 2 – Silty Sand with Gravel:** This unit is composed of cohesionless alluvial soils that are described as loose to very dense, gray to grayish brown, moist to wet, homogeneous, silty SAND with sub-angular gravel to well-graded sub-angular GRAVEL with cobbles. In test boring H-5si-16, deposits of ESU 2 consisted of silty SAND with gravel with field SPT “N” values ranging from 3 to 7 blows/ft. from four samples. In test boring H-8p-16, deposits of ESU 2 consisted of

GRAVEL with cobbles that were too coarse for SPT sampling. No laboratory testing of samples was performed within this ESU.

ESU 2 was approximately 5 feet thick between 5 to 9 feet below ground surface (bgs) in test boring H-5si-16. ESU 2 was also approximately 12 to 30 feet thick between 1 to 12 feet bgs and 15 to 45 feet bgs in test boring H-8p-16.

**ESU 3 - Silt:** This unit is composed of cohesive alluvial soils that are described as loose to very loose, grayish brown, homogeneous, sandy SILT to SILT with sub angular gravel or trace sand.

ESU 3 was approximately 15 feet thick between 9 to 24 feet bgs in test boring H-5si-16 and approximately 3 feet thick between 12 to 15 feet bgs in test boring H-8p-16. In test boring H-5si-16, field SPT “N” values ranged between 4 to 7 blows/ft. to a depth of 20 feet and no field SPT “N” values were collected in test boring H-8p-16. No laboratory testing of samples was performed within this ESU.

Based on our visual observations of the material on the sidewalls of the stream channels within the debris flow risk areas, we anticipated the subsurface soils at the debris flow barrier locations to be similar to ESUs 1 and 2 described above.

### Slope Conditions

At MP 44.25, the two shallow gradient incised channels exit the slope adjacent to the westbound lane and will potentially serve as debris flow channels. These incised channels create a drainage network that connects to rills and gullies that extend up to the top of the mountain ridge to the north. The west debris flow channel is approximately 45 feet in width, approximately 10 feet in depth, and extends thousands of feet upslope. The east debris flow channel is approximately 25 feet in width, approximately 5 feet in depth, and extends thousands of feet upslope.



**Figure 11. Western and Eastern debris flow channels. Image on left is facing upstream, image on right is facing downstream.**

We surmised that debris flow origination points may include eroded areas along the outer limits of the existing channel network that extends upslope, or any burned area that contributes to the immediate limits of the drainage basin that flows into the west and east channels at this location. The channel gradient in both channels is approximately 15 degrees. Approximately 65 feet west of the western limit of the west channel is a slope oriented approximately 45 degrees, that dips to the east. Immediately east of the eastern limit of the east channel is a slope oriented at approximately 45 degrees that dips to the west. Slopes in the area appear to be composed primarily of alluvial deposits of soil and rock.

## GEOTECHNICAL ANALYSIS

Using the British Columbia Ministry of Forests Manual (1996), along with field and remote-based measurements taken in both potential debris flow channels (western and eastern), we calculated the potential impact forces that would be generated in the event of a debris flow at each channel. We used the Poiseuille Equation, and the Momentum Equation to calculate impact forces, and then compared with GroBrugg's DEBFLOW (3) and SHALLSLIDE (4) dimensioning tool outputs for forces generated in the event of a debris flow in each channel. The Poiseuille Equation and Momentum Equation from the British Columbia Ministry of Forests Manual are described below.

The British Columbia Ministry of Forests Manual (1) provides estimates for debris flow velocity and impact loads based on the channel dimensions, gradient, and geometry. DEBFLOW (3) software developed by GeoBrugg uses input parameters based on the barrier geometry, torrent geometry, and flow parameters to test the proof of different debris flow barrier designs against the expected dynamic and static loads generated from a debris flow with the measured parameters selected by the user. In the event that there is limited data available to use DEBFLOW (3) parameter inputs, the user can use published values recommended by literature used to create the DEBFLOW dimensioning tool (3). DEBFLOW (3) then checks the proofs of static and dynamic loading against the debris flow barrier system load capacities that correspond to each debris flow barrier that is selected by the user. The SHALLSLIDE (4) dimensioning tool uses input parameters similar to DEBFLOW (3), and also checks the proofs of static and dynamic loading against the shallow landslide system load capacities that correspond to the shallow landslide barrier selected by the user.

Comparing hand calculations with GeoBrugg's DEBFLOW (3) and SHALLSLIDE (4) dimensioning tools using a conservative approach, we checked impact forces with a velocity slightly faster than what we calculated using the Poiseuille Equation (1). In both DEBFLOW and SHALLSLIDE, (3,4) we assumed a total debris flow volume of 4,103 cubic yards (3,137 cubic meters) and 3 surges at both channel locations (3 surges of 1,368 cubic yards (1,046 cubic

meters)). We calculated the volume based on a surface area estimate of the upstream drainage basin. The upstream drainage basin measures approximately 265 acres in surface area, measured using lidar derived from WGS (2) (Figure 12).

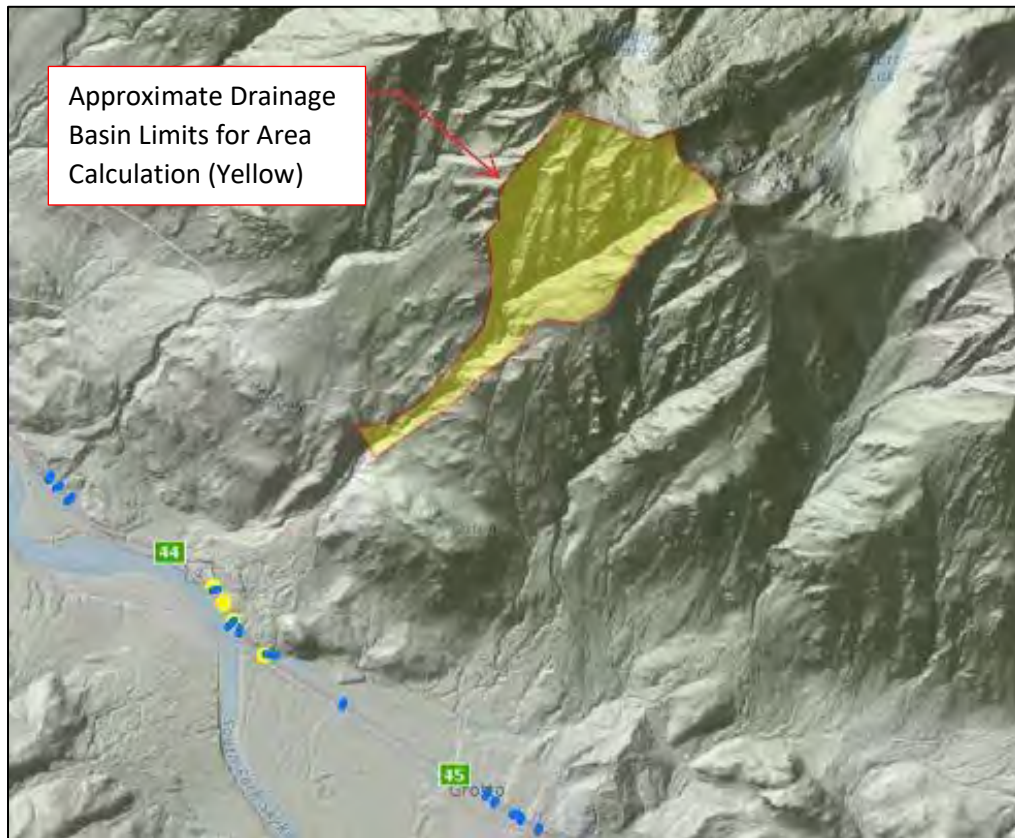


**Figure 12. Image of approximate drainage basin limits used in calculating potential sediment yield in the event of a debris flow. Lidar derived from WGS (2).**

Considering the estimate from the BAER report of 25 tons of sediment available per acre of surface area. This yielded a collective total of 6,625 tons of sediment available for transport through the debris flow channels at this location. Using a density of 120 pcf, we estimate that there are approximately 4,104 cubic yards (3,137 cubic meters) of potential debris flow mass available for entrainment in the upslope drainage basin. If a debris flow occurs in either of the channels at these locations, we estimate that there is less than 100 cubic yards of combined catchment from both channels where the channel meets the culverts under US 2.

### **Hand Calculations Compared with DEBFLOW & SHALLSLIDE (3,4)**

For the hand calculations, we used the Poiseuille Equation and the Momentum Equation as described in the British Columbia Ministry of Forests Manual (1) and defined below.

**Poiseuille Equation:**  $V = \frac{\gamma \sin \theta h^2}{lv}$

Where:

$V = \text{velocity}$

$\gamma = \text{unit weight of debris flow material}$

$\theta = \text{channel gradient (degrees)}$

$h = \text{flow depth}$

$l = \text{constant based on cross sectional shape of channel}$

$v = \text{dynamic viscosity of debris mass}$

**Momentum Equation:**  $F = \rho A v^2 \sin \beta$

Where:

$F = \text{dynamic thrust}$

$\rho = \text{density of debris}$

$A = \text{cross – sectional area of flow}$

$\beta = \text{the angle between the flow direction and the face of the structure}$

We first used the Poiseuille Equation (1) to calculate a potential velocity, based on published values and measurements that we took during our site reconnaissance. Then we input the velocity result from the Poiseuille Equation (1) into the Momentum equation (1) to calculate the dynamic thrust that may be generated at each culvert location in the event of a debris flow. Our front velocity from the hand calculations was approximately 8.2 ft/s. The flow depth is considered to be a critical value in this estimate, and we used a conservative value of 10 feet based on our measured depth of the western channel. In DEBFLOW (3) the recommended front velocity values were 24.6 ft/s and 22.6 ft/s according to the dimensioning tool's default options.

In addition to calculating the velocity and dynamic thrust, we had to calculate the potential discharge rates for a potential debris flow at each channel location. For hand calculations, we used our calculated velocity from the Poiseuille Equation (1) and the cross-sectional area of the channel. Our calculated discharge rates along with the values generated from GeoBrugg's dimensioning tools (3,4) calculated are summarized below in Table 3.

<b>Table 3. Discharge calculations by hand, and by using the GeoBrugg DEBFLOW (3) and SHALLSLIDE (4) dimensioning tools.</b>		
Discharge Values	Western Channel	Eastern Channel
Hand Calculated $ft^3/s$	2,260	2,260
DEBFLOW Value $ft^3/s$	1,060	1,090
SHALLSLIDE Value $ft^3/s$	1,170	2,750

We used the same channel geometries in the hand calculations as in DEBFLOW (3) and SHALLSLIDE (4). Using the measured channel dimensions and geometries from our field reconnaissance along with our calculated velocity and discharge values, we input values into DEBFLOW (3) and SHALLSLIDE (4) dimensioning tools and calculated out the potential impact loads generated in the event of a debris flow at each location. The results of the impact loads are in Table 4.

<b>Table 4. Potential impact loads in each channel along with barrier capacities calculated by hand, using the DEBFLOW dimensioning tool (3), and the SHALLSLIDE dimensioning tool (4).</b>			
Impact Loads	Western Channel	Eastern Channel	Capacity of Barrier
Hand Calculated (psf)	522	376	N/A
DEBFLOW value (psf)	731	1,210	2,880 (west) 9,150 (east)
SHALLSLIDE value (psf)	532	702	1,541 (west) 2,490 (east)

According to DEBFLOW and SHALLSLIDE (3,4) dimensioning tool outputs, some of the larger systems are capable of withstanding the potential static and dynamic loads generated by a debris flow at either channel, with load resistances in excess of 1,500 psf. As a result, we anticipated that it is feasible to construct a debris flow barrier at each location that will withstand the forces generated in the event of a debris flow at these locations.

## GEOTECHNICAL DESIGN

Using the outputs from our analysis, we recommended that post-supported debris flow or shallow landslide barrier systems be installed at the previously identified western and eastern channels at US 2 MP 44.25. We recommended the barriers be installed approximately 50 feet upslope from the US 2 centerline in order to keep the barriers and components within WSDOT right of way. We recommended that each barrier system be able to withstand repeated impact loads of 522 psf ( $25\frac{kN}{m^2}$ ), and static loads up to 1,570 psf ( $75\frac{kN}{m^2}$ ). We recommended a minimum barrier height of 10 feet, a minimum total length of 110 feet for the western barrier system, and a minimum total length of 60 feet for the eastern barrier system. We chose a 10-foot minimum height based on the 10-foot depth of the deeper (western) channel. Based on the potential for debris to spill out of the sides of the channels, we chose barrier lengths that extend well beyond the limits of each channel. Rather than having a single system span the length of both channels, we chose to recommend leaving a space between the barrier systems. We considered having space between the systems essential so that machinery would have access to reach behind the barrier systems for debris removal and maintenance. Approximate layout and dimensions of each barrier system are shown in Figure 13.

We recommended each barrier be constructed of typical flexible debris flow barrier components such as, posts, post foundations, wire rope, ring net or cable, wire mesh, braking elements, and ground anchors. Additionally, we recommended the bottom of the system be within 2 feet of the ordinary high-water mark of the streams at both channels. Due to environmental constraints, no components of the system would be able to be installed within the limits of the ordinary high-water mark of the stream. This included ground anchors and post foundations. In order to accommodate the western channel, we recommended an extension of the barrier system further down into the western channel to within 2 feet of the ordinary high-water mark. Due to the channel depth and geometry, a system spanning overtop of the stream channel would likely miss debris in the event of a debris flow, because the gap below the fence would be too large, allowing debris to pass beneath the barrier. We anticipated not having the same issue in the eastern channel because it is only 5 feet deep.

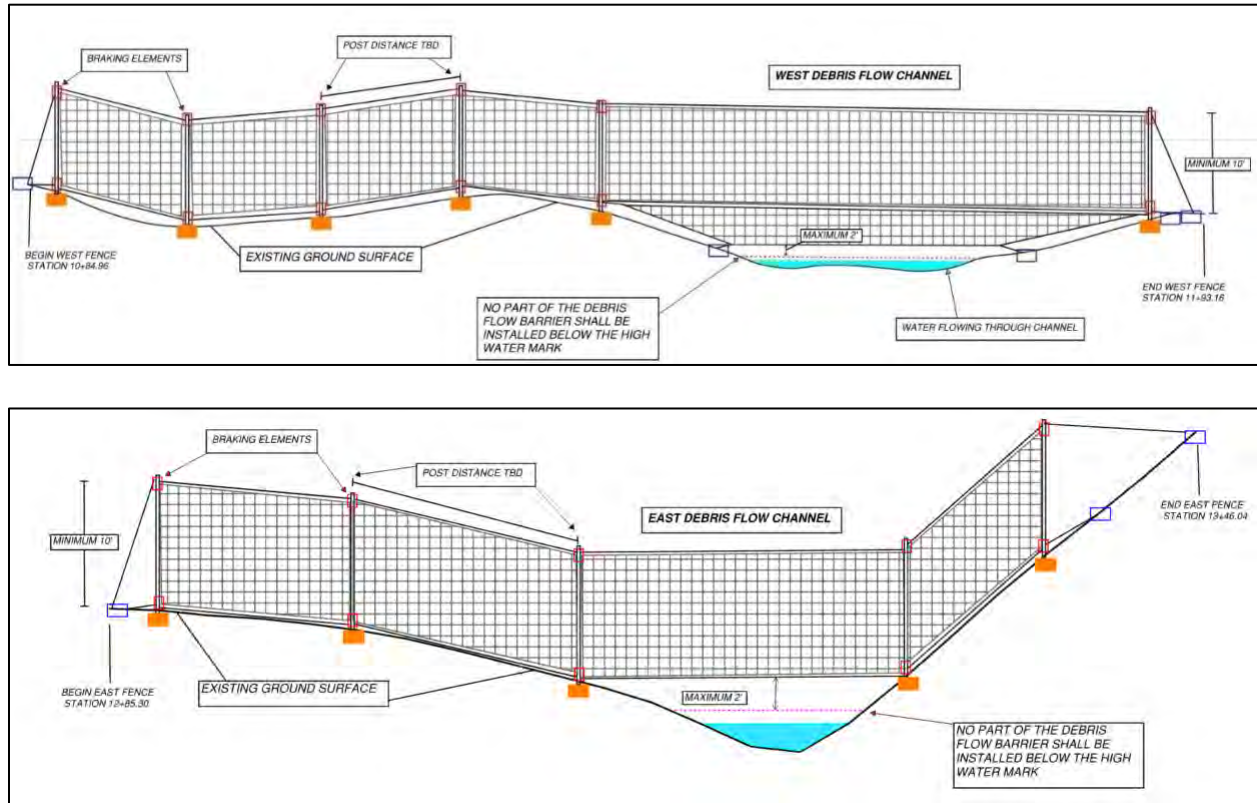


**Figure 13. West and east debris flow barrier layout as recommended. Note these are recommended as proprietary systems and were designed to be installed according to manufacturer’s specifications.**

We recommended that proprietary systems be installed at each location and chose only to specify the minimum barrier system height, lengths, and impact loads that the systems would need to be capable of withstanding. Recommendations for proprietary systems opened the project to multiple different debris flow barrier manufacturers, which we believed would ultimately yield competitive pricing when the project is advertised. Additionally, recommendations for a proprietary system shortened our internal design time required to provide geotechnical recommendations.

Currently, the project is scheduled to advertise in the summer of 2023, with construction to begin in the fall of 2023. With the rainy season to begin in late fall to winter, it is essential that construction is completed in early fall to avoid debris flows occurring at this location and impacting the highway before the barriers can be constructed.

## DISCUSSION & LIMITATIONS

Additional debris flow data more specific to the site would have aided in refining the design process. Having a model that incorporates the climate, vegetation, and geology of Washington State, and considers rain-on-snow events would aid in better quantifying the risk for post-wildfire debris flows throughout the State. In some cases, post-wildfire debris flows may occur in an area that has not previously experienced a debris flow. In these cases, it is difficult to constrain appropriate design parameters for potential impact forces that may be generated in the event of a debris flow. While impact load data is available from debris flow barrier testing, it is often not appropriate for use in design due to differences in site geology, debris flow channel characteristics, and local topography used in the testing environment compared to local site conditions. A better understanding of the risk of post-wildfire debris flows in Washington State would likely yield more confidence in design and likely reduce the over-engineering of barriers, ultimately improving benefit cost relationships for mitigation or risk reduction of debris flow hazards.

Debris flow behavior is difficult to impossible to predict. The debris flow barriers designed for this project are dependent on the subject debris flow(s) following the existing channel network. Having observed the areas upslope of the culverts at the barrier installation locations, we believe it is reasonable to consider that a debris flow may occur at either of these locations. However, it is also reasonable to consider that a debris flow may occur beyond the limits of the suggested project area and flow into one of the other catchment areas on the distal limits of the alluvial fan. Debris can easily clog a channel and quickly avulse to the next nearby channel, and with a relatively extensive drainage network at this location, there are many possible routes a debris flow at this location may take. While debris flows are not entirely possible to predict, we have identified possible triggers and catalysts, and identified potential routes that a debris flow at this location may take. Taking this into consideration, we believe that installing debris flow barriers at US 2 MP 44.25 was the best available option to reduce the risk of debris reaching US 2 and impact the community and traveling public.

## REFERENCES

### Reports

1. United States Department of Agriculture (USDA) Forest Service, Burned Area Emergency Response Program, *Burned-Area Report for the Bolt Creek Fire*, FS-2500-8 (2/20), 2022. pp 2-6.
2. Mickelson, K. and M. Allen. Wildfire-Associated Landslide Emergency Response Team (WALERT) Report – Bolt Creek, Suiattle River, Boulder Lake, and Lake Toketie Fires, King and Snohomish Counties, Washington State Department of Natural Resources, Washington Geological Survey, 2022. pp 1-4, 5, 9

### Websites

1. Incident Information System (Inciweb), *Fire Information, Bolt Creek WA-NWS-000150*, 10/19/2022, <https://inciweb.nwcg.gov/incident-maps-gallery/wanws-bolt-creek-fire> Accessed May 2023.
2. United States Geological Survey (USGS), Frequently Asked Questions, Natural Hazards, What is a debris flow? <https://www.usgs.gov/faqs/what-debris-flow> Accessed May 2023.
3. GeoBrugg Inc., DEBFLOW Online Dimensioning Tool & Software Manual, Revision from March 25, 2021. Accessed February 2023.
4. GeoBrugg Inc., SHALLSLIDE Online Dimensioning Tool & Software Manual, Revision from March 25, 2021. Accessed February 2023.

### Maps

1. Tabor, R. W., Frizzell, V. A., Booth, D. B., Waitt, R. B., Whetten, J. T., Zartman, R. E., 1993, Geologic Map of the Skykomish River 30- by 60-Minute Quadrangle, Washington, U.S. Department of the Interior, U.S. Geological Survey, 1:100,000 scale.
2. Washington State Department of Natural Resources, Washington Geologic Survey, Division of Geology and Earth Resources, Washington Lidar Portal, Public\_Geology/Lidar\_Hillshade (MapServer), 2010.

### Manual

1. British Columbia Ministry of Forests Research Program & Debris Flow Control Structures for Forest Engineering, 1996, pp. 13, 16.

**Emergency Planning and Mitigation for Post-Fire Debris Flows in Glenwood  
Canyon, Colorado**

**Aliena Debelak, PE**

WSP USA Inc.

7245 W. Alaska Drive, Suite 200

Lakewood, CO 80226

Aliena.Debelak@wsp.com

**Elizabeth Kidner, PE**

WSP USA Inc.

7245 W Alaska Drive, Suite 200

Lakewood, CO 80226

Elizabeth.Kidner@wsp.com

**Robert Group, PE**

Colorado Department of Transportation

4670 Holly St., Unit A

Denver, CO 80216

Robert.Group@state.co.us

### **Acknowledgements**

The authors would like to thank the individuals/entities for their contributions in the work described:

Kevin Carpenter – WSP USA, Inc.

Roger Pihl, PG – WSP USA, Inc.

Randy Post, PE – WSP USA, Inc.

Nicole Oester Mapes, PG – Colorado Department of Transportation

### **Disclaimer**

Statements and views presented in this paper are strictly those of the author(s), and do not necessarily reflect positions held by their affiliations, the Highway Geology Symposium (HGS), or others acknowledged above. The mention of trade names for commercial products does not imply the approval or endorsement by HGS.

### **Copyright Notice**

Copyright © 2023 Highway Geology Symposium (HGS)

All Rights Reserved. Printed in the United States of America. No part of this publication may be reproduced or copied in any form or by any means – graphic, electronic, or mechanical, including photocopying, taping, or information storage and retrieval systems – without prior written permission of the HGS. This excludes the original author(s).

## ABSTRACT

The Grizzly Creek fire started on August 10, 2020 near Glenwood Springs, Colorado. Over the next week, the fire covered most of the area surrounding Glenwood Canyon, including many of the tributary watersheds to the Colorado River. Interstate-70 (I-70), a major highway connecting the eastern and western slopes of Colorado, is in the bottom of Glenwood Canyon. Watersheds that have had recent wildfires have a higher likelihood of a debris event occurring and producing larger debris volumes. This was proven true in the summer of 2021 when approximately 30 debris flow events occurred within the canyon, damaging both decks of I-70 and depositing over 300,000 cubic yards of sediment on the road and in the Colorado River.

After the 2020 fires, the authors completed an emergency assessment of several burned watersheds to help understand the potential consequence of debris flow events using FLO-2D software and debris flow predictions from the USGS Emergency Assessment of Post-Fire Debris-Flow Hazards program. Characteristics and results from the predictive models were compared with the 2021 debris flow events and showed reasonably strong correlation.

The models and analyses were useful tools to understand the risk of debris flows to I-70, mitigation planning, and predicting emergency clean-up efforts.

## INTRODUCTION

A wildfire known as the Grizzly Creek Fire, started on August 10, 2020 in the median of Interstate 70 (I-70) several miles east of Glenwood Springs, Colorado. Over the next week, the Grizzly Creek Fire burned east and north eventually covering nearly all of the tributary watersheds to the Colorado River within the Glenwood Canyon. The wildfire covered around 33,000 acres in Glenwood Canyon (1). Figure 1 shows the severity of the fire, and burn extents are shown in Figure 2. The fire is adjacent to I-70 in a narrow canyon with steep slopes and a history of rockfall and occasional debris flows.

Watersheds that have had recent wildfires will have a higher likelihood of debris events occurring as well as the potential to produce larger debris flow volumes due to the consumption of the rainfall-intercepting canopy and soil-mantling litter and duff, intensive drying of the soil, generation of vegetative ash, the enhancement or formation of water-repellent soils and/or surface sealing of soil pores by wood ash. These outcomes result in decreased rainfall infiltration and significantly increased runoff and movement of soil (2). As such, the recent fire increases the risk of floods and potential debris flows.



**Figure 1: Photos taken during (a) and after (b) the Grizzly Creek Fire. Photos taken from [www.wildfiretoday.com](http://www.wildfiretoday.com) and [www.cpr.com/news](http://www.cpr.com/news)**

To help the Colorado Department of Transportation (CDOT) plan for the increased hazards resulting from the recent wildfire, Golder Associates Inc. (Golder, now part of WSP USA, Inc.) completed a preliminary study of several of the burned watersheds to help understand the potential consequence of a debris flow event, particularly the impacts to I-70. The watersheds were initially screened using the preliminary hazard assessment completed by the United States Geological Survey (USGS) post-fire debris flow hazards program (1), which provides a likelihood of a debris flow occurring and predicted volume in response to a specific rainfall event. The preliminary likelihood and volume predictions are based on the physical characteristics of the watershed and the area with moderate to high burn severity. Golder prioritized eight basins that had a higher likelihood to impact the highway. The eight basins were

prioritized because of the potential debris flow volumes exceeding 13,079.5 cubic yards (yd<sup>3</sup>) (10,000 cubic meters ([m<sup>3</sup>]) coupled with high probabilities of occurrence.

Golder prepared preliminary debris flow models for the eight priority basins to estimate the runout extents, volumes, and depths that may impact I-70. The objective was to simulate a debris flow triggered from a hypothetical precipitation event occurring in the burned watershed contributing to I-70 to better understand risks to the road, maintenance requirements, and potential mitigation options.

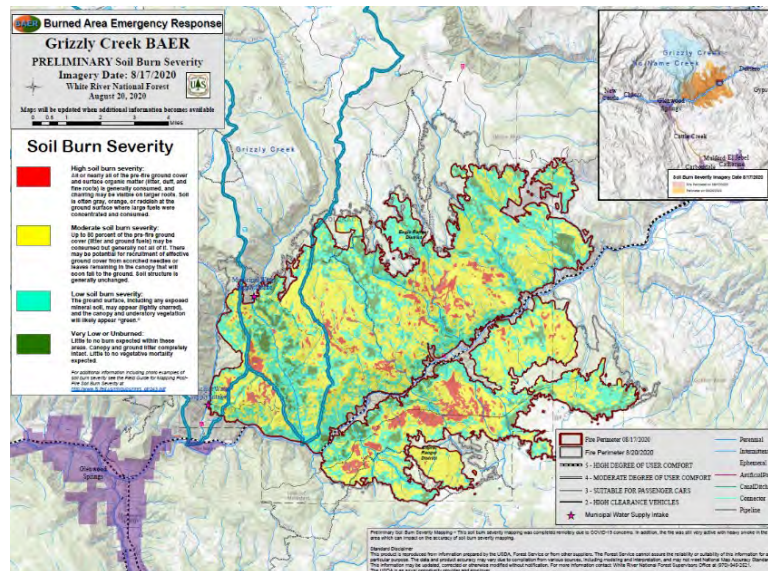


**Figure 2: Burn Severity and Extents of the Grizzley Creek Fire (3)**

Throughout the summer of 2021, moderately high-intensity rainfall events triggered multiple debris flow events within the canyon, depositing material on I-70 and in the Colorado River, and damaging surrounding infrastructure. After the 2021 debris flow events, Golder performed a variety of geohazard studies and preliminary mitigation designs to help CDOT plan for the potential hazards resulting from the recent wildfire. Additionally, Golder compared the predicted debris flow events and the actual debris flow events for two sites to refine estimates and improve confidence in mitigation design.

General design philosophy for the mitigation was to retain the solid fraction with debris fences, take advantage of and protect existing culverts to transport the water portion of flows beneath I-70, and to utilize or develop flatter topography in the channel or near the road to create additional storage. Using this design basis, Golder developed mitigation for nine sites throughout Glenwood Canyon. Mitigation was installed during the summer of 2022.

## POST-FIRE DEBRIS FLOW MODELING

Dozens of burned watersheds intersect I-70 within the 13-mile-long canyon. Using the USGS post-fire debris hazard models (1) (Figure 3) and estimates of event probability, debris/water volumes, and other factors, Golder conducted a corridor level debris flow study to prioritize CDOT mitigation efforts. Approximately 82 basins outlet directly to the I-70 corridor. Watersheds were sorted to prioritize highest risk areas that may impact I-70.

Approximately 32 basins met one of the below criteria from the USGS Hazard Model (1):

- Probability of flow greater than 50%
- Flow volume greater than 6539.8 yd<sup>3</sup> (5,000 m<sup>3</sup>)
- At least a moderate Hazard Classification (combination between likelihood and volume)

A summary of the hazard ranking is shown in Table 1.

**Table 1: Hazard Ranking of priority watersheds**

Name or MP	USGS Basin ID	Volume (m <sup>3</sup> )	Probability	Combined basin hazard (probability + volume rank)
<b>119.6</b>	<b>6383</b>	<b>7,443</b>	<b>44%</b>	<b>Moderate (5)</b>
119.8	6506	1,976	46%	Moderate (5)
119.9	6489	7,386	63%	Moderate (6)
<b>120.0</b>	<b>6472</b>	<b>18,175</b>	<b>59%</b>	<b>Moderate (6)</b>
<b>120b</b>	<b>6468</b>	<b>6,601</b>	<b>64%</b>	<b>Moderate (6)</b>
120.1	6567	1,720	83%	High (7)
<b>120.22</b>	<b>6678</b>	<b>10,347</b>	<b>67%</b>	<b>High (7)</b>
120.6	6656	3,611	67%	Moderate (6)
120.6	6655	1,082	43%	Moderate (5)
120.73	6975	2,130	61%	Moderate (6)
<b>122.4</b>	<b>6555</b>	<b>12,789</b>	<b>59%</b>	<b>Moderate (6)</b>
122.78	6261	4,264	48%	Moderate (5)
123.1	5900	1,242	68%	Moderate (6)
123.2	5681	9,275	57%	Moderate (5)
123.24	5652	11,409	47%	Moderate (6)
<b>123.4</b>	<b>5567</b>	<b>57,896</b>	<b>63%</b>	<b>High (7)</b>
<b>123.55</b>	<b>5479</b>	<b>10,895</b>	<b>75%</b>	<b>High (7)</b>
123.7	5564	2,777	51%	Moderate (5)
123.79	5590	1,714	43%	Moderate (5)
123.8	5595	3,114	63%	Moderate (6)
124.05	5622	1,603	83%	High (7)
124.18	5494	2,402	56%	Moderate (5)
<b>124.4</b>	<b>4990</b>	<b>46,502</b>	<b>43%</b>	<b>Moderate (6)</b>
124.5	4808	5,906	56%	Moderate (5)

126.3	3194	1,881	41%	Moderate (5)
126.42	3061	1,873	49%	Moderate (5)
<b>126.5</b>	<b>2923</b>	<b>16,201</b>	<b>52%</b>	<b>Moderate (6)</b>
<b>126.96</b>	<b>2494</b>	<b>3,344</b>	<b>50%</b>	<b>Moderate (5)</b>
127.9	1708	2,606	50%	Moderate (5)
128.2	1593	5,007	45%	Moderate (5)
<b>129.06</b>	<b>953, 528, 529</b>	<b>36,595</b>	<b>19%, 18%, 23%</b>	<b>Combined Basins</b>
129.7	1174	0	900%	Moderate (4)

From the 32 identified basins, Golder prioritized debris flow modeling in eight basins with the potential to impact the highway and having potential to produce large debris flow volumes coupled with high probabilities of occurrence. Selected basins are denoted by bold in Table 1. Golder prepared preliminary debris flow models to estimate the runout extents, volumes, and depths that may impact I-70.

The routing model was developed using FLO-2D modeling software (4) utilizing the mudflow calculation. FLO-2D is an unsteady, two-dimensional hydraulic model capable of analyzing hyperconcentrated sediment flows. As such, it is well suited to simulate debris flows incorporating characteristics of sediment-laden floods.

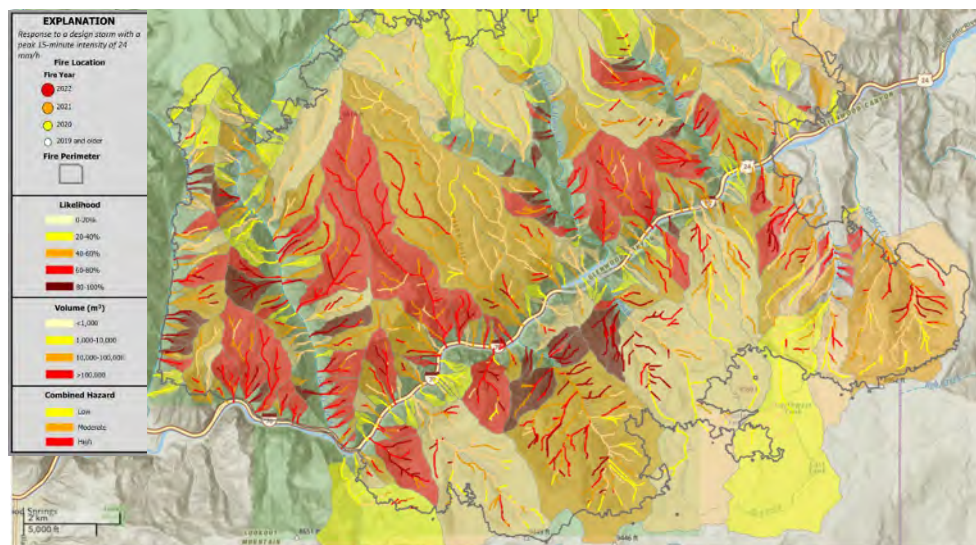


**Figure 3: USGS Post Wildfire Debris Flow Hazard Assessment Model (1)**

## Model Input Parameters and Assumptions

The precipitation volume and intensity for the watersheds evaluated (5) were obtained from NOAA Atlas 14, Volume 8, Version 2. The 15-min duration storm was used in this analysis, equaling 24 mm/hr, equivalent to about ¼ of an inch of rain in 15 minutes. This short-duration rainfall event has a recurrence interval in Glenwood Canyon of between a 1- to 2- year range. Cannon et. al. (2) found that in the intermountain west, the great majority of debris-flow events occur in response to high-recurrence (1-10 year events), low duration (<1 hour) convective thunderstorms. Furthermore, the 24 mm/hr rain burst is known to trigger debris flows at USGS monitoring sites in burn areas (1). Topography was developed from available 3-foot (ft) Lidar survey. The debris flow model was developed using the input parameters Table 2.

It is extremely difficult to predict debris flow volume as every watershed has unique geology and topography. Burned landscape recovery occurs at different rates when evaluating long-term model predictions (greater than about 2-years from the burn event). The USGS uses the Emergency Assessment Model (EAM) from Gartner et al. (7) to predict volumes in their post-fire debris flow hazard assessment. The EAM predicts volumes of sediment deposited by debris flows within two years of a fire.

**Table 2: Model Input Parameters**

Parameter	Value	Source
Hydrologic triggering event	15-min, 0.94 in/hr (24 mm/hr)	USGS (1)
Solids concentration of debris flow event	Ranged 30% to 45% by volume	Assumed
Duration of mudflow event	~1 hour	Assumed, hydrograph approximated from the water hydrograph during the 1-hour, 1-year event with the bulked debris flow distributed in the water hydrograph
Runoff curve number (CN)	90	Conservative estimate for moderate to severe post-fire hydrophobic soils (8)
Duration of simulation	48 hours	Assumed
Sediment specific gravity	2.65	Assumed
Resistance parameter for Laminar Flow	1,000	Bare clay-loam soil, eroded 100-500 Sparse vegetation 1,000-4,000 (9)
Manning's n of burned areas	0.04 – 0.06	Burned condition, minimal vegetation, rocks present. Higher manning's n used for rockier watersheds based on post-fire pictures.
Manning's n of road surfaces	0.012	Paved surface
Mudflow properties	Glenwood 4 (10)	High viscosity and moderate yield stress with high sediment concentrations
Debris flow volume	Varies per basin	Emergency Assessment Model (used by USGS) (1,7)

Note: min = minutes; in/hr = inches per hour; mm/hr = millimeters per hour

## Solids Concentration

The solids concentration was not calculated based on runoff volumes, but as a function of the available water from the precipitation event and the volume of solids that become mobilized. Golder used a simplified approach of estimating the water hydrograph (11) and then distributed the debris flow volumes using a similar shape and duration.

The behavior of the debris flow is dependent on the rheology of the fluid matrix and the specified solids concentration throughout the hydrograph. The rheology of the soils in the Grizzly Creek Fire burn area are unknown but were approximated using viscosity and yield stress parameters measured by O'Brien and Julien (12). Golder selected the "Glenwood 4" parameters which yield a high viscosity and moderate yield stress fluid with high sediment concentrations. This parameter is recommended by FLO-2D in the absence of site-specific data (10). The solids concentration was initially assumed to be between mudflow and mud flood, based on the definitions provided by FLO-2D (10). A sensitivity analysis on the assumed solids concentration was conducted for the watershed at mile post (MP) 120.0 to determine sensitivity of the solids concentration on the runout behavior.

### *Sensitivity Analysis*

The USGS model estimated a debris flow volume for the watershed contributing to MP 120.0 equal to 23,772 yd<sup>3</sup> (18,175 m<sup>3</sup>).

Golder initially assessed a constant sediment concentration of 55% solids by volume (Cv) over the hydrograph. 55% Cv is the limit between mudflow and landslides, and is characterized by dry, viscous flow that will not spread out on level surfaces (10). This scenario represents an upper limit of reasonable solids concentrations carried in a mudflow and is likely unrealistic for the Glenwood Canyon watersheds.

A second model was developed that used the USGS debris flow volume (23,772 yd<sup>3</sup>) but with a variable sediment concentration. Golder used the following guidelines from FLO-2D for modeling post-fire debris flows in developing the hydrograph (10):

- Average sediment concentration of ~30-35% by volume
- Bulk the frontal wave of the hydrograph with sediment concentrations ~45-53% by volume
- Bulk the hydrograph peak discharge ~ 40-45% by volume

A third model was developed that shows an intermediate between the base case model (55% sediment concentration by volume) and the variable sediment concentration model (24-48% sediment concentration by volume). The model used a similar technique to the base case model but specified a constant 45% sediment concentration over the hydrograph. The results are shown in Figure 4 below. The 45% sediment concentration by volume case was determined to be reasonable for predicting the potential impacts from the post-fire debris flows in the Glenwood Canyon.

The three hydrographs produce the same total volume of debris flow while changing the water and sediment volumes. In the variable sediment concentration case, when concentrations of sediment by volume are low, most of the fluid flows over I-70 and into the Colorado River. In contrast, the base case model (constant 55% sediment concentration by volume) results in most of the fluid cessation occurring around the shallow and moderate slopes on the road or near the basin outlet.

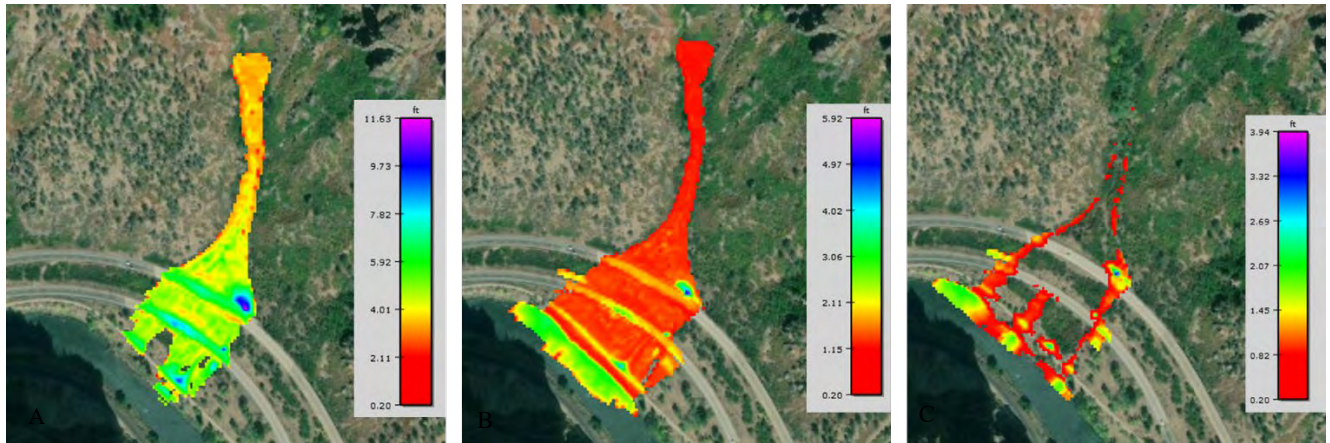


**Figure 4: Final Floodplain Depths After 48 Hours for Three Hydrographs Used in the Sensitivity Study. (A) Shows 55% Solids by Volume (B) Shows 45% Solids by Volume, and (C) Shows a Varying Sediment Concentration**

The results of the sensitivity analysis (Figure 4) show that the model is sensitive to the sediment concentrations assumed and distribution of sediment within the hydrograph. Based on the results of the analysis, the 45% sediment concentration by volume case was selected for predicting the potential impacts from the post-fire debris flows in the Glenwood Canyon.

### Preliminary Debris Flow Modeling Results

The USGS hazard model delineated 281 watersheds in the area of study and assigned a volume, probability, and hazard rating to each. Approximately 82 basins outlet directly to the I-70 corridor (1). Golder identified eight of the basins as Tier-One based on potential debris flow volumes exceeding 13,079.5 yd<sup>3</sup> (10,000 m<sup>3</sup>) coupled with high probability of occurrence. Three Tier-One basins were identified as High-Priority based on the basin size, the estimated flow volume, and the potential to impact I-70. Figure 5 shows the delineation of MP 123.4, which was identified as a High-Priority basin. Results of the modeling effort are shown in Table 3. An example of the final deposition results, shown for MP 120.0, is depicted in Figure 6. Results of the preliminary models were used to better understand debris flow risks to I-70, required clean-up efforts, potential maintenance requirements, and to guide development of potential mitigation options.

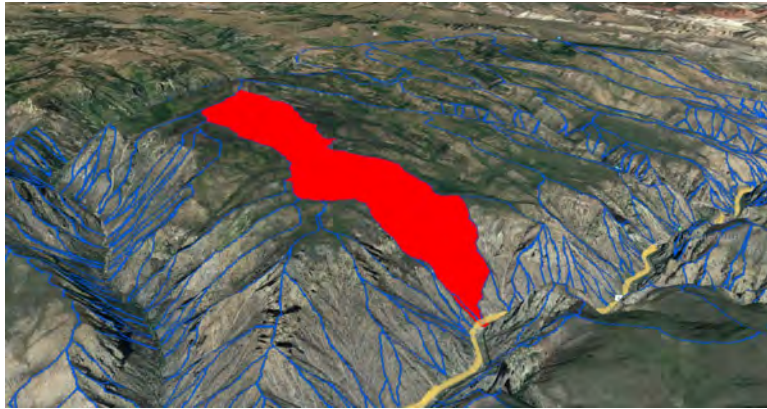


**Figure 5: Extents of MP 123.4, identified as a high-priority basin. Taken from Google Earth**

**Table 3: Summary of Preliminary Debris Flow Models**

Mile Post	USGS Basin No.	Basin Size (mi <sup>2</sup> )	USGS Probability Estimate (%)	USGS Flow Volume Estimate (yd <sup>3</sup> )	Max Flow Depth on Road (ft)	Deposition Depth on Road (ft)	Deposition Extents on road (ft)	Deposition Volume on Road (yd <sup>3</sup> )
120	6472	0.44	59	23,773	3-7	1-2	350-475	1,220
	6468		64	8,633	4	1-2	350-475	1,200
120.23	6678	0.24	67	13,534	6	1-2.5	235-350	1,100
122.4	6555	0.20	59	16,728	3.5-4	0.5-1.5	300	900
123.4 <sup>2</sup>	5567	1.76	63	75,728	8	0.5-2	320-550	1,540
123.55	5479	0.16	75	14,251	5-6	1.5-2.5	330	1,700
124.42 <sup>2</sup>	4990	2.55	43	60,825	8-10 <sup>1</sup>	1.5-3.3 <sup>1</sup>	300 <sup>1</sup>	1,070 <sup>1</sup>
126.5	2923	0.69	52	21,190	3-7 <sup>1</sup>	2-3.5 <sup>1</sup>	380 <sup>1</sup>	1,400 <sup>1</sup>
129.07 <sup>2,3</sup>	528	1.61	18	27,197	8 <sup>1</sup>	0.5-4 <sup>1</sup>	230 <sup>1</sup>	1,360 <sup>1</sup>
	529		23	20,669				

<sup>1</sup>WB lane is located on bridge and flow will pass under. Values are for EB only.

<sup>2</sup>Identified as High-Priority basin

<sup>3</sup>Debris flow assumed to occur at both basins simultaneously. Values reported for combined event.

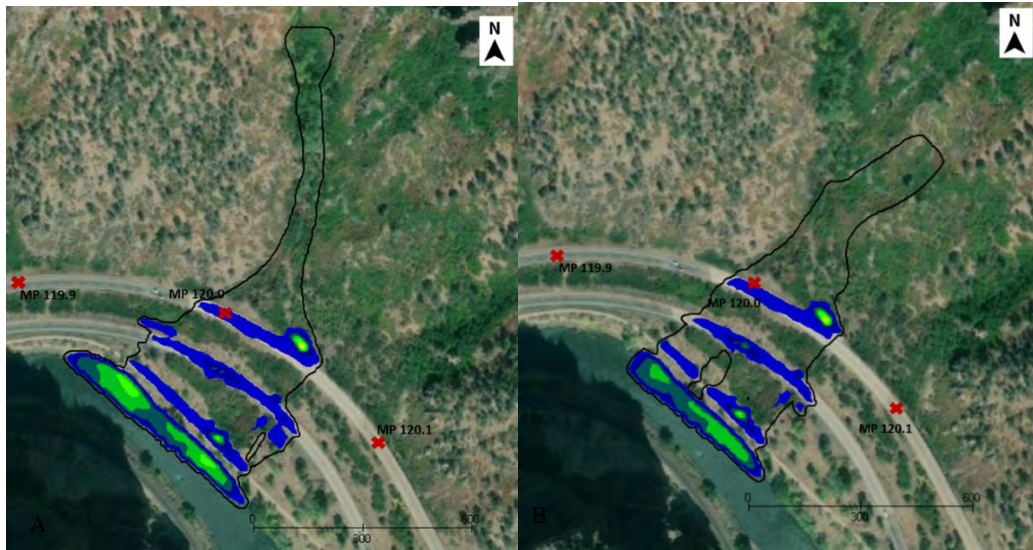


**Figure 6: Final Flow Depth After 48 Hours for Watershed 6472 (A) And 6468 (B).**

## 2021 DEBRIS FLOW EVENTS

Throughout the summer of 2021, moderately high intensity rainfall events triggered approximately 30 debris flows occurring over the span of nine different days. These events damaged both decks of I-70 in numerous areas, caused several road closures, deposited significant material in the adjacent Colorado River, and damaged the Union Pacific Rail line and Excel power line. Figure 7 shows an example of the debris flow material that was deposited on the highway and Figure 8 depicts the severity of scouring in the channels as a result of the debris flow events. As a result of CDOT understanding the potential consequences of the debris flows and pre-emptively closing the road in advance of predicted thunderstorms, there were no fatalities in any of the debris events that occurred in 2021.



**Figure 7: Example of debris flow material at MP 123.4 deposited on I-70**



**Figure 8: Example of the extent of scouring from a debris flow event**

Seven of the Tier-One basins experienced at least one debris flow, with five experiencing multiple flows. Two of the three basins identified as High-Priority experienced at least one debris flow during the 2021 events.

Due to the number of debris flow events during summer 2021, it was difficult to track the exact storm event that triggered each flow. However, the identified storms were around a 2-year annual return period. The precipitation depths are consistent with our understanding of typical thresholds that trigger debris flow event after fires.

### DEBRIS FLOW COMPARISON

Golder compared the predicted debris flow events (13) and two observed events for MP 120.23 and MP 120.0 to refine estimates and to calibrate future models. Table 4 presents a comparison between the predicted versus actual debris flow events. A comparison of the model results from MP 120.0 and a photo from the actual flow event is shown in Figure 9 and Figure 10.

**Table 4: Comparison of predicted debris flow events and observed events**

Mile Post	USGS Basin No.	Max Flow Depth on Road (ft)		Deposition Depth on Road (ft)		Deposition Extents on road (ft)		Deposition Volume on Road (yd <sup>3</sup> )		Estimated Solids Concentration (%)	
		<i>Predicted</i>	<i>Actual</i>	<i>Predicted</i>	<i>Actual</i>	<i>Predicted</i>	<i>Actual</i>	<i>Predicted</i>	<i>Actual</i>	<i>Predicted</i>	<i>Actual</i>
120.0	6472/ 6468	3-7	5-7	1-2	2-3.5	350-475	600-800	1,220	1,700	45	35
120.23	6678	6	4	1-2.5	0.5-1	235-350	1000	1,100	850	45	20-25



**Figure 9: Predicted (A) and Actual (B) Final Debris Flow Deposition Area**

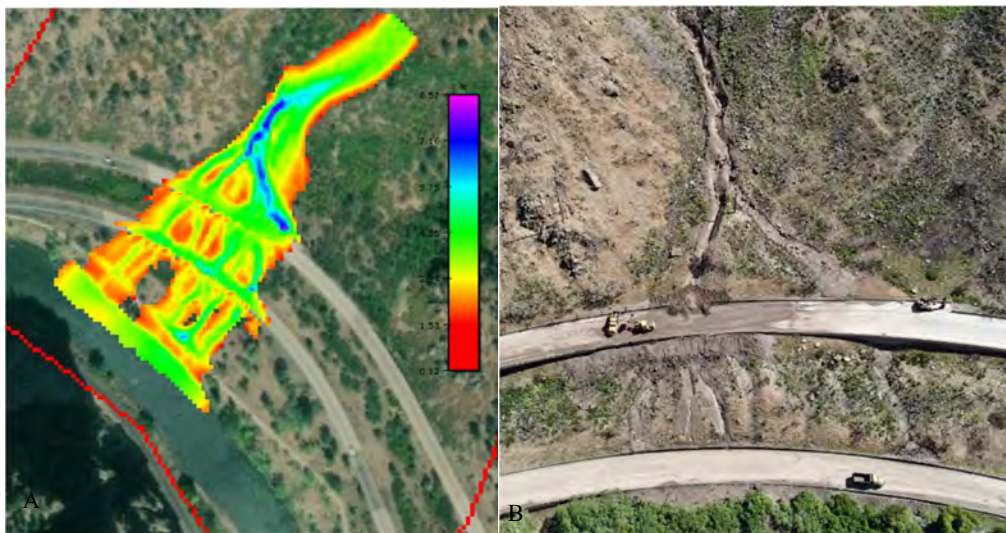


**Figure 10: Predicted (A) and Actual (B) Debris Flow Paths**

In general, there is good agreement between the model results and the actual debris flow event. Total flow volume is omitted from the comparison due to the uncertainty of the actual flow volume. Debris that is deposited up channel or into the Colorado River would not be accounted for during estimate of the flow event. The following observations were made during the comparison:

- The triggering event was short-duration, high-intensity with a return period around a 2-year storm event.
- Total volumes remaining on the road were reasonably close to estimated clean up volumes.
- Average solids concentration was less than what was used in the preliminary debris flow models. The average concentration used in the 2020 modeling was 45% by volume and the

estimated solids concentration based on the behavior of the fluid and visual observations is around 35% for MP 120.0 and 25% at MP 120.23.

- The length of road impacted was underpredicted. Reducing the solids concentration in the debris flow model would likely result in the fluid spreading out along the road, closer to the observations.

## DEBRIS FLOW MITIGATION

After the summer 2021 debris flow events, Golder used the results of the corridor level debris flow study conducted in 2020 to prioritize CDOT mitigation efforts. The basins selected in 2020 were compared to 2021 debris flow event data and screened to determine which watersheds would be feasible to mitigate (i.e. shallower terrain, clear channel, storage area at outlet, existing culvert, etc.). This was done using available topography, aerial imagery, site inspections, and Google Earth. Twenty-five basins were identified where mitigation may be feasible. Sites were prioritized based on frequency of debris flows in the basin, the debris flow deposition volumes seen during the 2021 events, and maintenance impacts seen during the 2021 events. Conceptual level debris flow mitigation was designed for eleven sites as shown in Figure 11 (14).

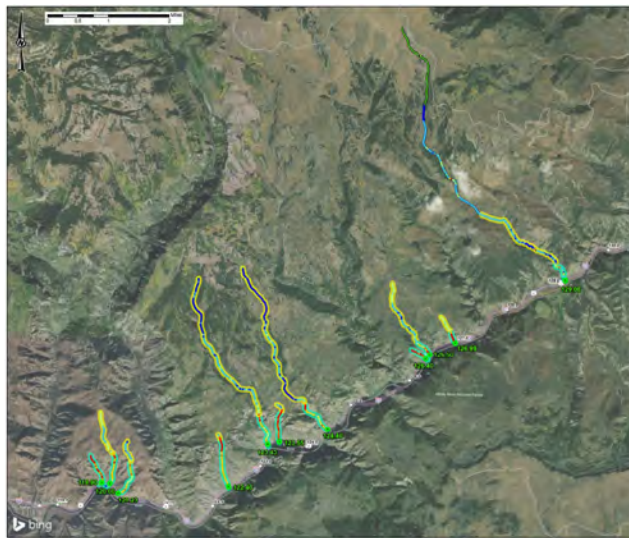


**Figure 11: Location of Priority Channels for Debris Flow Mitigation Design (14)**

### Debris Flow Mitigation Design Volume

Gartner et al. (7) developed the Long-Term Model (LTM) for predicting volumes of sediment deposited by a combination of debris flows and sediment-laden floods with no time limit since the most recent fire. Golder compared the Long-term Model (LTM) (7) to the Emergency Assessment Model (EAM) (1) used by the USGS Post-Fire Debris Flow Hazards Program. The EAM consistently provides higher volumes compared to the LTM. Volumes calculated from the

LTM, in combination with estimated volumes from the summer 2021 debris flow events were used as design volumes for mitigation efforts.

Golder used the LTM with a 2-year frequency storm event to design mitigation and to estimate the effectiveness of proposed mitigation measures. Design volumes were compared with a visual estimate from the 2021 storm events. The debris flow volumes for the selected watersheds are provided in Table 5.

**Table 5: Debris flow design volumes for mitigation design**

MP	Design Volume <sup>1</sup> : 2-yr LTM (total volume) yd <sup>3</sup>	Visual Estimate
119.9	3,000	5,200
120	7,700	5,800
120.23	5,680	6,000
122.4	4,900	N/A
123.4	26,300	146,000
123.55	4,000	6,500
124.4	33,700	43,500
126.4	700	1,200
126.5	11,000	2,700
126.95	1,600	6,200
129.06	33,500	2,500

<sup>1</sup>Volume from the 2-year return period long term model. We have assumed this is the total volume, including both solids and water.

## MITIGATION DESIGN

The nature of the debris flow mitigation design was an emergency response, and mitigation options were selected to be implemented quickly, with minimal procurement needs, engineering design, or construction logistics. Golder developed the design basis provided in Table 6 to aid in the development of conceptual mitigation options (15).

**Table 6: Debris Flow Mitigation Design Basis**

Emergency Response	The emergency response nature of the project required a quick response and, accordingly, designs are based on visuals, drone photos, CDOT input, and general experience in the Glenwood Canyon. It is expected that the designs and recommendations will be modified in the field, as needed.
Temporary	The mitigation is intended to serve a temporary purpose because higher risks of geohazards from fires usually last 2 to 5 years beyond the fire, after which they are generally expected to decrease. The temporary nature of the project means that some or all of the mitigation structures may be removed within a 2 to 5 year period.
CDOT Guidance	Geohazard mitigation design and siting locations were selected and/or approved by CDOT and are not intended to provide complete mitigation of future geohazards.

Constraint Driven	The cost/benefit of various mitigation options in conjunction with constraints such as existing road alignment, property ownership, and predicted efficacy were used to determine whether or not to implement mitigation. In some instances, no mitigation efforts were attempted because the cost of implementing the mitigation was likely higher than the cost savings of maintenance and infrastructure repair if damaged.
Future Mitigation	Future geohazard mitigation in addition to this current scope may be desired once this emergency response effort is complete.

Golder utilized four mitigation concepts for the designs, summarized in Table 7. Keeping mitigation consistent throughout the corridor allowed for a simplified engineering design process and minimized construction logistics. Golder designed conceptual level mitigation for the basins listed in Table 5.

**Table 7: Summary of Mitigation Concepts and Recommendations**

<i>Concept</i>	<i>Recommendation</i>	<i>Applicable Mileposts</i>
Repair and protect existing infrastructure	Remove previously deposited material and recover available storage upstream of the road.  Improve conveyance by cleaning out and repairing all existing culverts. Protect existing culverts from future damage or clogging such that the fluid fraction of the flows can continue to be transported beneath I-70.  Clean any material deposited behind previously existing rockfall fences. Repair damaged components of existing fence.  Protect bridge piers that are exposed to debris flow impact.	MP119.9, MP120, MP122.4, MP129.25
Strain out large material from debris flows	Reduce flow volume and energy by straining out the larger material from of the debris flow with debris flow fences or a series of vertical posts	MP120.23, MP123.4, MP123.55, MP126.4, MP126.5,
Store material within channel or debris fan	Utilize storage space provided by flatter topography existing higher in the channels.  Utilize or develop flatter topography near the road to create additional storage.  Create additional storage upstream of I-70 by installing new berms/walls and excavate additional storage.	M119.9, MP120, MP122.4, MP124.4, MP126.95, MP129.06
Do nothing	No mitigation is recommended based on the predicted flow volumes, topography of the basin, and other design constraints.	Considered for Final Design only

Golder provided preliminary mitigation designs CDOT (13). Based on the benefit/cost analysis, CDOT selected nine debris flow sites to move forward with construction level mitigation, summarized in Table 8 (16). Figure 12 shows the finished construction of one of the barriers at MP 122.4. Construction of mitigation was completed in the summer of 2022.

**Table 8: Summary of Selected Mitigation Options**

MP	Mitigation Recommendation(s)	Approx. % of Design Vol. Mitigated
119.9	Increase debris flow storage with mass excavation and gabion structure Clean out and protect existing culvert	49%
120.0	Increase debris flow storage with mass excavation and gabion structure Regrade channel at outlet to direct flow to excavated basin and existing culvert	13%

120.23	One flexible debris flow barrier	53%
122.4	No mitigation selected due to steep topography and costs-benefit analysis	
123.4	Two flexible debris flow barriers installed in series	6%
123.55	No mitigation selected due to ROW constrictions	
124.4	Increase debris flow storage with mass excavation and gabion structure	8%
126.4	No mitigation selected due to ROW constrictions and steep topography	
126.5	No mitigation selected due to ROW constrictions and steep topography	
126.95	Increase debris flow storage and gabion structure	69%
127.86 <sup>1</sup>	Increase debris flow storage with mass excavation and gabion structure	-
129.06	Increase debris flow storage with mass excavation	100%
129.25 <sup>1</sup>	Increase debris flow storage gabion structure Protect existing culvert	-

<sup>1</sup>Sites added by CDOT after the conceptual designs were submitted



**Figure 12: Finished construction of the barrier installed at MP 120.23**

## CONCLUSION

Watersheds that have had recent wildfires will have a higher likelihood of a debris event occurring as well as the potential to produce larger debris flow volumes. Typically, the increased risk of debris flows and increased flooding last from 2 to 5 years after the fire. Post-fire debris flows can occur after relatively routine, short-duration, high-intensity rainfall events.

It is important to understand the increased risk of debris flows after wildfires for emergency planning such as road closures and clean-up efforts. A risk-based corridor level hazard study

prioritizing basins based on probability of future debris flows and anticipated flow volume proved to be an effective tool for focusing modeling efforts. FLO-2D modeling software (4) was an effective tool to model previous flow events and to evaluate potential consequences of a future debris flow event.

The emergency response nature of the project required a design with limited information and utilization of visual observation, drone photos, CDOT input, quick response, and general experience in the Glenwood Canyon. The mitigation is intended to serve a temporary purpose because higher risks of geohazards from fires usually last 2 to 5 years beyond the fire, after which they are generally expected to decrease. Debris flow mitigation is watershed specific. Site topography, such as steep slopes, right-of-way limitations, and construction constraints provide design challenges and limit viable mitigation design options.

**REFERENCES**

- (1) United States Geological Survey USGS. Grizzly Creek Fire Post-Fire Debris Flow Hazards. Preliminary results from Aug. 18 Model. Emergency Assessment of Post-Fire Debris-Flow Hazards (usgs.gov).
- (2) Cannon et al. 2010. Predicting the probability and volume of post-wildfire debris flows in the intermountain western United States. Geological Society of America Bulletin. GSA Bulletin. January/February. v. 122. No.1/2. p. 127-144. doi: 10.1130/B26459.1.
- (3) United States Geological Survey USGS. Burned Area Emergency Response Portal. Grizzly Creek Fire. BAER | Burn Severity Portal (usgs.gov).
- (4) FLO-2D Software, Inc. (FLO-2D). 2014a. FLOW-2D Pro Software Program. Nutrioso, AZ.
- (5) National Weather Service, National Oceanic and Atmospheric Association Atlas 14, Volume 8, Version 2. Point Precipitation Frequency Estimates. Available online at the following link: [https://hdsc.nws.noaa.gov/hdsc/pfds/pfds\\_map\\_cont.html?bkmrk=co](https://hdsc.nws.noaa.gov/hdsc/pfds/pfds_map_cont.html?bkmrk=co). Accessed April 1, 2020.
- (6) Gartner, Joseph E., Susan H. Cannon, Paul M. Santi. 2014. Empirical models for predicting volumes of sediment deposited by debris flow and sediment-laden floods in the transverse ranges of southern California. Engineering Geology 176 (2014)45-56.
- (7) United States Soil Conservation Service (USSCS). 1986. Urban hydrology for small watersheds. Washington DC: US Department of Agriculture.
- (8) Woolhiser, David A. 1975, Simulation of Unsteady Overland Flow, Chapter 12, Unsteady Flow in Open Channels, Edited by K. Mahmood and V. Yevjevich, Water Resources Publication.
- (9) FLO-2D. 2014. <https://documentation.flo-2d.com/>
- (10) United States Army Corps of Engineers (USACE). Hydrologic Engineering Center (HEC). 2017. Hydrologic Modeling System (HEC HMS). (4.5). Davis, California, USA: US Army Corps of Engineers. March 1.
- (11) O'Brien, J.S. and P.Y. Julien. 1988. Laboratory Analysis of Mudflow Properties. American Society of Civil Engineers. Journal of Hydraulic Engineering.
- (12) Golder Associates Inc. (Golder). 2020. Grizzly Creek Fire – Preliminary Debris Flow Modeling Results – Phase 1. 1788442. September 21.
- (13) WSP Golder. 2022. Mitigation Options for Debris Flows along I-70. Glenwood Canyon – Grizzly Creek Fire Recovery. Draft. January 28.
- (14) Golder Associates Inc. (Golder). 2021. PR I-70 Glenwood Canyon Grizzly Creek Fire Design Report. CDOT Geohazards Task Order No. 1. 1788442-5-R. February 26.
- (15) WSP Golder. 2022. Glenwood Canyon Debris Flow Mitigation Final Drawings. April 20.

## **Stabilization of the Fremont Hall Landslide**

**Jamie L. Ross (Cravens), P.E.**

Yeh and Associates, Inc.  
391 Front Street, Suite D  
Grover Beach, CA 93433  
(805) 481-9590  
jcravens@yeh-eng.com

Prepared for the 72<sup>nd</sup> Highway Geology Symposium, August 2023

### **Acknowledgements**

The author would like to thank the individuals/entities for their contribution in the work described:

Judd King, P.E. – Yeh and Associates, Inc.  
Gresh Eckrich, P.E., C.E.G. – Yeh and Associates, Inc.  
Reed Hooke, E.I.T. – Yeh and Associates, Inc.  
Doug Jenevein, P.E. – Schnabel Geosturctural Design and Construction  
Pete Maskal, P.E. – Cannon  
Robb Moss, Ph.D., P.E. – California Polytechnic State University – San Luis Obispo

### **Disclaimer**

Statements and views presented in this paper are strictly those of the author(s), and do not necessarily reflect positions held by their affiliations, the Highway Geology Symposium (HGS), or others acknowledged above. The mention of trade names for commercial products does not imply the approval or endorsement by HGS.

### **Copyright**

Copyright © 2023 Highway Geology Symposium (HGS)

All Rights Reserved. Printed in the United States of America. No part of this publication may be reproduced or copied in any form or by any means – graphic, electronic, or mechanical, including photocopying, taping, or information storage and retrieval systems – without prior written permission of the HGS. This excludes the original author(s).

### ABSTRACT

A landslide occurred at California Polytechnic State University – San Luis Obispo during a period of heavy precipitation. It originated upslope of the Fremont Hall Dormitory and deposited saturated soil against the building, leading to evacuation and closure of the dormitory.

Published geologic maps show a Quaternary age landslide at the site. It was characterized as an earthflow composed of predominantly fine-grained soil prone to creeping and periodic relatively large-scale movement associated with heavy precipitation. The active portion of this landslide, termed the “2017 Landslide,” was identified based on review of historical aerial imagery, previous subsurface data, and data from the 2019 investigation. The 2019 investigation included drilling, test pits, large-diameter bucket auger borings, slope inclinometers, vibrating wire piezometers, and laboratory testing. Site geology was interpreted as interbedded colluvium/landslide deposits overlying a massive block of graywacke within the Franciscan Mélange. Concrete debris was encountered in a bucket auger boring at approximately 46 feet below the ground surface. It was concluded, based on the debris and historical aerial photograph review, that excess soil generated from the construction of the dormitories in the 1950’s was placed on the body of the Quaternary age landslide.

The stabilization consisted of a series of ground anchor galleries within the landslide mass and an anchored soldier pile wall at the toe of the stabilized slope. Horizontal drains and subdrains were installed within the landslide mass to collect and maintain design groundwater elevations.

The project was successfully completed in July 2022 and students have since reoccupied the dormitory.

## INTRODUCTION

Intense precipitation events impacted the coast of California during the winter of 2017. These events resulted in a deluge of landslides affecting multiple areas of the state. One such landslide occurred on the California Polytechnic State University campus in San Luis Obispo, California (see project location map in Figure 1). For a period of two to three days following the date of February 13, 2017, above-average rainfall saturated the slope directly above the Fremont Hall Dormitory resulting in an earthflow-type landslide. The landslide deposited approximately 8 feet of saturated soil and water against the one-story lounge area which extends towards the slope from the east side of the three-story dormitory (see Figure 2). The accumulation against the back of the lounge caused the brick masonry to crack, water and soil to enter the building, and led to the eventual closure and evacuation of the dorm on February 18, 2017.

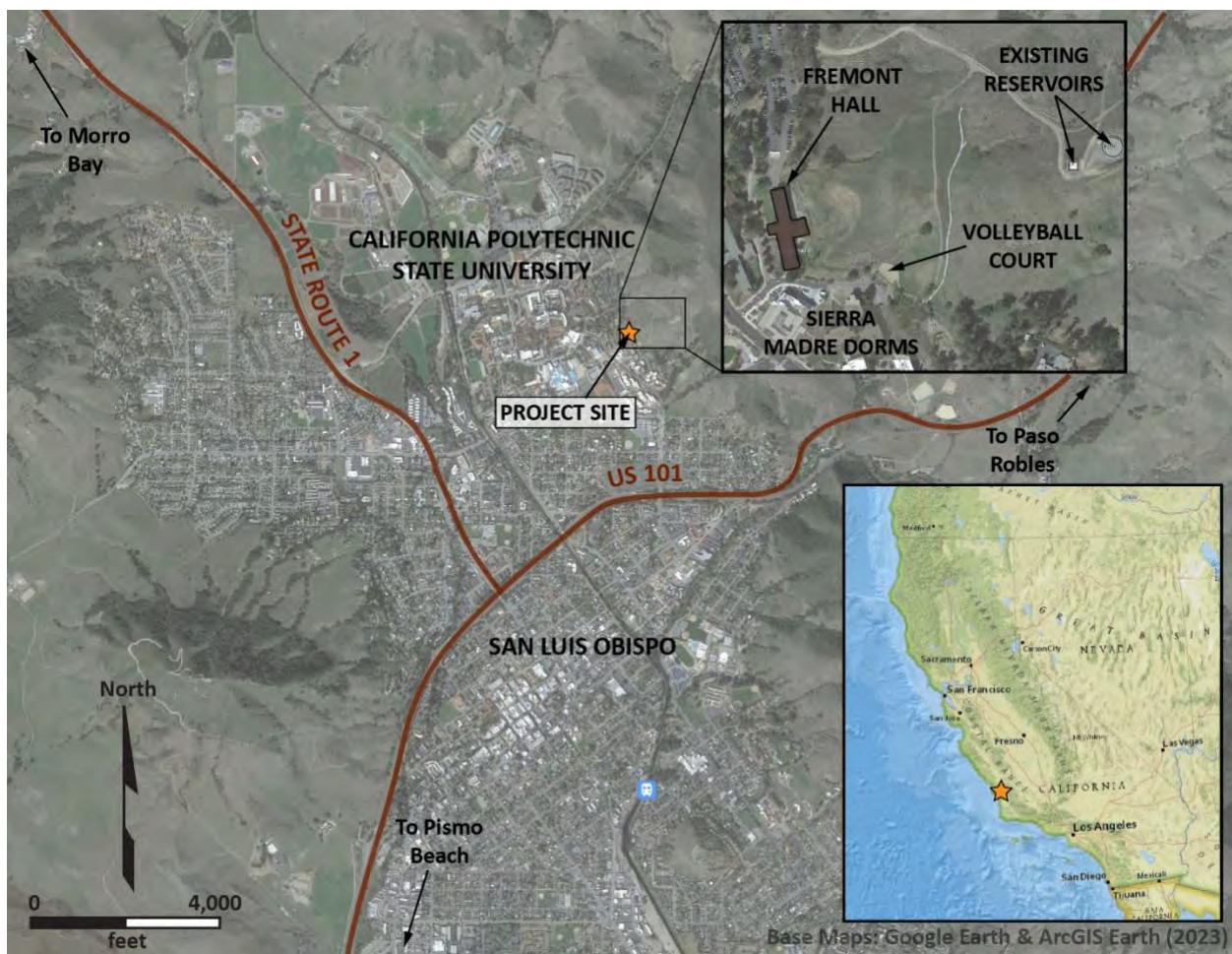


**Figure 1: Project Location Map**

Initial geotechnical studies of the landslide were performed by a local engineering firm following the 2017 event which included subsurface exploration, analyses, and a geotechnical report for an earth buttress solution. The earth buttress solution was not constructed due to constructability concerns. However, upslope surface and subsurface drainage improvements and a winterization project immediately behind the dorm were completed in 2017 to temporarily manage the

drainage and surficial erosion of the slope. This included a 20- to 25-foot-tall cut slope within the landslide toe that was regraded to 1.5:1 (horizontal to vertical).



**Figure 2: 2017 Fremont Hillside Landslide**

Another season of intense rainfall occurred in the winter of 2019, causing the existing landslide to mobilize towards Fremont Hall Dormitory once again (see Figure 3). Additional debris was deposited against the dormitory. A collaborative design-build approach was selected as the preferred delivery method for the project, with oversight by the University and peer reviewing geotechnical engineers and geologists. Schnabel Geotechnical Design and Construction was awarded the design-build contract in 2019 with Yeh and Associates and Cannon as the geotechnical and civil design subconsultants.

### **Site Description**

Fremont Hall dormitory was constructed in the late 1950s on a hillside located on the east side of the California Polytechnic State University – San Luis Obispo (Cal Poly) campus. Elevations vary from about elevation 420 feet at the dormitory and extend up to about 1,100 feet at the ridgeline above the dormitory. Slope grades range from 10 to over 40 percent with an average slope of 25 percent within the landslide limits. Two water storage reservoirs are located upslope and northeast of the dormitory, with a gravel access road to the reservoirs that traverses the hillside north of the slide limits (see Figure 1). Piping for the reservoirs runs along the access road and also within the landslide limits.

## **Project Goals and Challenges**

The scope of the project consisted of stabilization of the hillside above Fremont Hall for the 2017 landslide. Goals of the design-build project included performing a comprehensive geotechnical exploration and analyses to assess the 2017 landslide, design of a stabilization solution for the 2017 landslide, assessing the potential for debris flows to impact Fremont Hall, assessing the presence and potential extents of a possible deep-seated landslide below Fremont Hall, as well as performing a qualitative risk assessment as a tool for the University to use in planning and design of the project and future projects in the vicinity of the hillside.

Closure of the dormitory following mobilization of the landslide in 2017 caused strain to the University both with lack of availability of housing for students as well as lack of revenue generated from the dormitory when unoccupied. The University implemented an expedited schedule for design and construction of the project in hopes of reopening the dormitory as soon as possible. The design and construction of the project also coincided with the Covid-19 pandemic. Field work for the project was performed during the State of California Shelter-in-Place Order, and the entire design of the project was performed with staff working from home over remote and virtual platforms. Communication and technological challenges associated with the Covid-19 pandemic were experienced through design and early construction.

## **DATA REVIEW AND GEOTECHNICAL EXPLORATION**

Yeh reviewed previous studies at the project site, published and historical data, and performed a field exploration program for the project. Data obtained from these sources were used as input to the design of the stabilization solutions as well as input for the assessment of debris flow and deep-seated landslide potential.

### **Review of Previous Studies and Published Geologic Maps**

Twenty-four consultant reports for projects performed in the project vicinity were provided to Yeh by the University. These projects included the construction of the existing reservoirs upslope of the dormitory, construction of the dormitories and parking lots adjacent to Fremont Hall, as well as construction of the water lines and drainage improvements on the hillside. Yeh also reviewed published geologic maps by Hall and Prior (1), Dibblee and Minch (2) and Wieggers (3).

#### *Existing Data*

Twenty-one borings (including the installation of nineteen inclinometers) were previously performed on the hillside above the Fremont Hall dormitory by the geotechnical firm that performed the initial exploration following the 2017 landslide. Out of the existing nineteen inclinometers that were installed, only two were operational following the 2019 re-mobilization of the landslide. Four cone penetration tests (CPTs) and five large diameter bucket auger borings were also performed on the hillside above Fremont Hall as part of the 2017 study. Other available data from previous studies included additional borings and test pits. The previous data primarily focused on either the 2017 landslide or their respective studies. Data obtained from these studies were useful as input to the geotechnical characterization of the 2017 landslide,

however, were not deep enough and/or did not focus on the potential for a deep-seated landslide or debris flows.

### *Published Landslides*

The published geologic maps reviewed by Yeh noted an existing Holocene to Pleistocene-age landslide at the project site (see Figure 3). These mapped landslides led the University's concern of the potential for a deep-seated landslide at the site. Previous reports and documents for the existing reservoirs also noted landslide activity and the presence of landslide debris at the reservoir location upslope of Fremont Hall and within the mapped limits shown on the published maps. Landslide debris or the presence of landslides were not noted in the explorations downslope and adjacent to Fremont Hall.

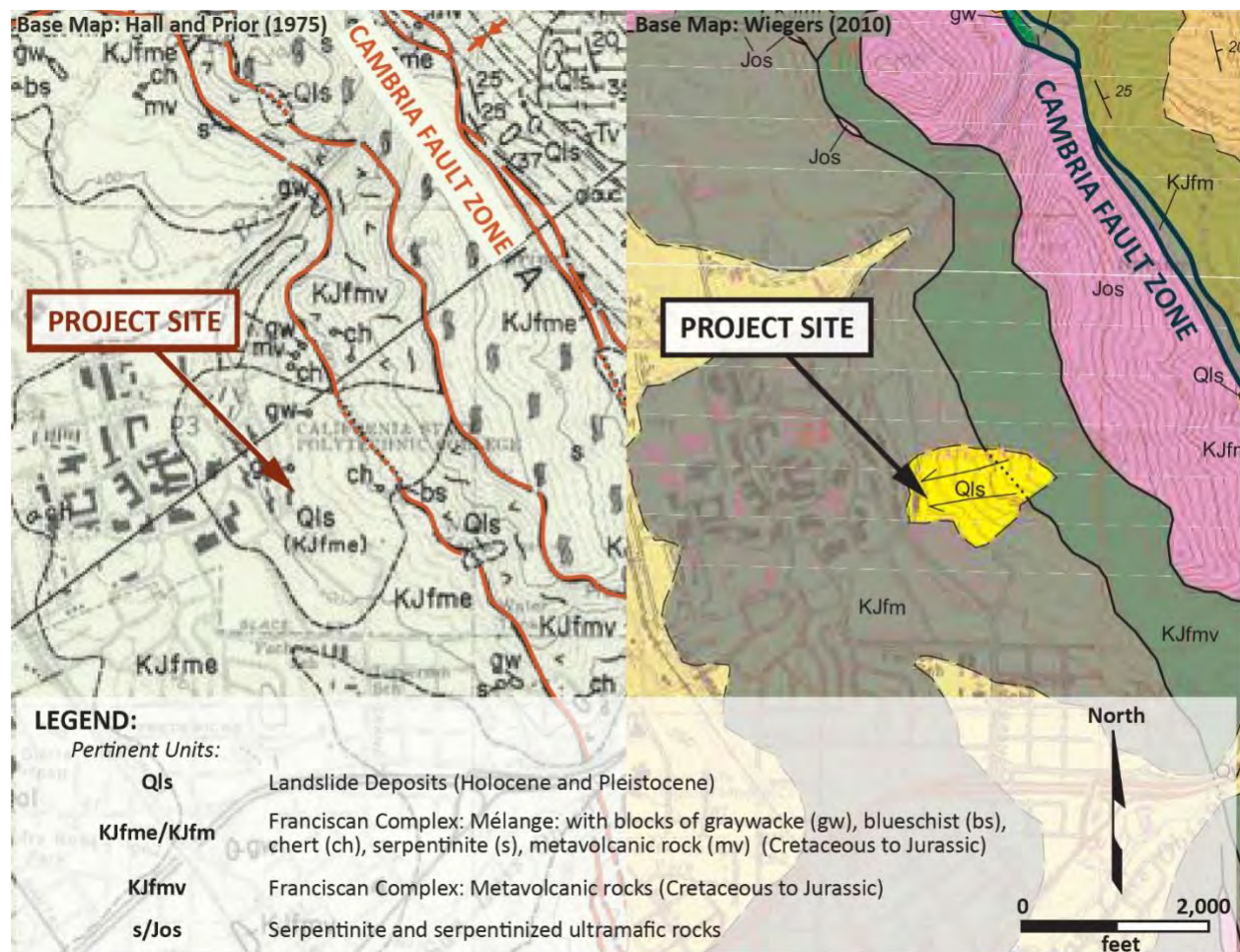


**Figure 3: Geologic Maps by Hall and Prior (1) and Wieggers (3) Showing Published Landslides**

### **Review of Historical Photographs, Historical Aerial Photographs, and As-Built Plans**

Yeh reviewed historical land-based photographs, historical aerial photographs, and as-built plans from the University archives and local sources. Yeh interpreted that the photographs taken prior to and after the construction of the Red-Brick Dorms (that include Fremont Hall) showed geomorphic features consistent with a landslide mass in the vicinity of Fremont Hall (see Figure 4).

Grading for the Red-Brick Dorms constructed in the late 1950s cut into and removed the lower portion of the landslide mass. The cut slope behind Fremont Hall was initially designed as an approximately 40-foot-high cut slope with inclination at 1h:1v (horizontal to vertical). “Slippage” of the new cut slope was noted on the as-built plans. The “slippage” area was mapped in the north portion of the cut slope on the as-built plans. Additional slippage and slope movement can be seen in historic photographs in the 1960s. Evidence of fill placement over the southern half of the landslide is seen in the aerial photographs from the late 1950s during construction of the Red-Brick Dorms. Fill was placed in the south-flowing and west-flowing drainages and on the slope above the present-day volleyball court east of Sierra Madre Hall. The thicknesses and slope inclinations of the fill appear to have been variable.

Yeh also reviewed selected photographic records, newspaper articles and did not find other records regarding slope movement after the 1960s documentation up until the movement that occurred in 2017. While not documented in photographic records or articles, slope instability was reported by University staff and documented in the project vicinity. In 1997, the waterlines within the access road to the Reservoir upslope from Fremont Hall were investigated due to landslide distress. In 2011, a small landslide also impacted the volleyball court east of Sierra Madre Hall, located adjacent to Fremont Hall.

### **Field Investigation, Instrumentation, and Laboratory Testing**

Yeh performed additional exploration to obtain data necessary for the assessment of deep-seated landslide and debris flow potential, as well as to install inclinometers to monitor the slope above Fremont Hall.

#### *Site Reconnaissance and Mapping*

Site reconnaissance and geologic mapping was performed by Yeh for the project. Yeh mapped the hillside behind Fremont Hall, noting any bedrock outcrops, tension cracking, drainages, and other prominent features. Yeh also performed a visual assessment and floor level survey of the dormitory for any structural distress or movement of the building that could potentially be attributed to deep-seated landsliding.

#### *Field Exploration*

Subsurface exploration by Yeh included drilling five rotary core exploratory borings, four large diameter bucket auger borings, and excavating five test pits. The rotary core borings were drilled to depths of 101 to 154 feet below the ground surface using mud rotary drilling and HQ rock coring methods. Sampling within the rotary borings included standard penetration test (SPT) split spoon and modified California samples as well as continuous HQ rock core samples.

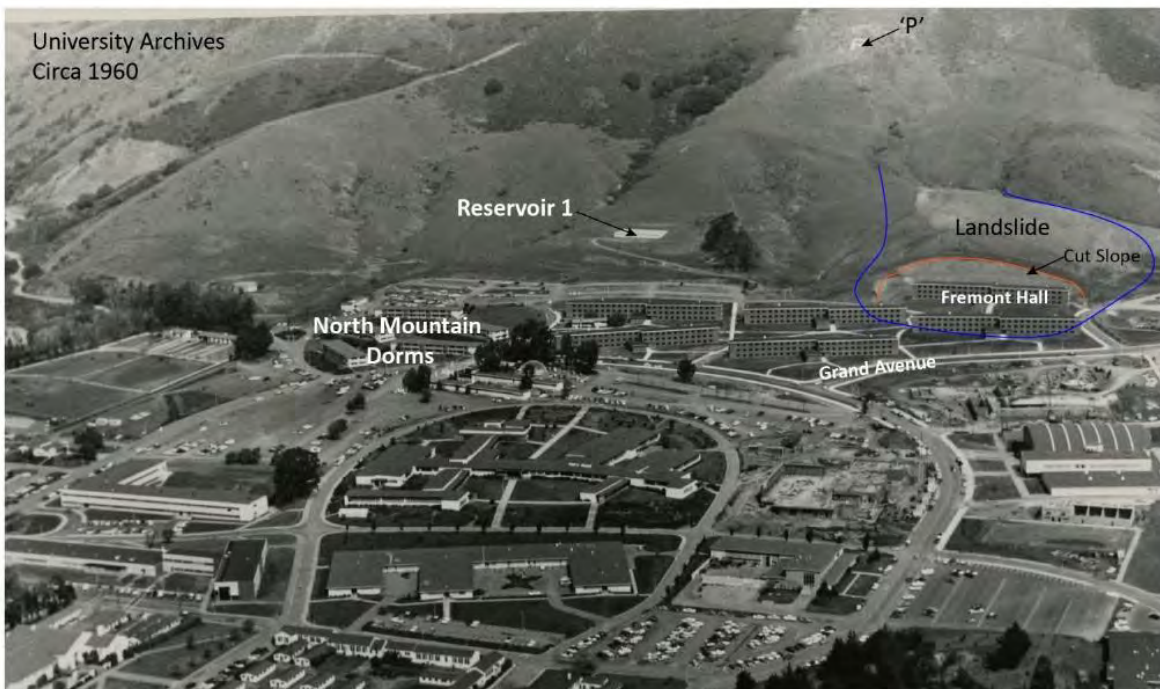
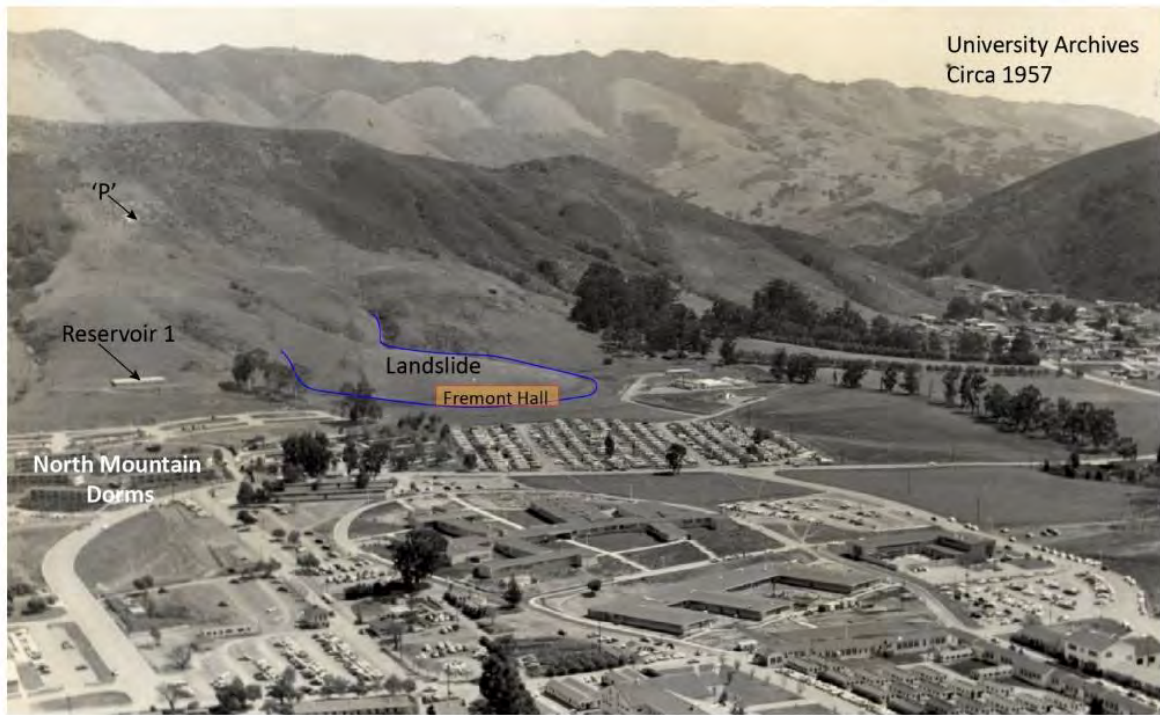


**Figure 4: Oblique Historical Photos – Fremont Hall Area**

The bucket auger borings were 24-inches in diameter and drilled to depths of 50 to 112 feet below the ground surface. Yeh personnel down-hole logged soil and rock type, consistency,

moisture, geology, and discontinuities. Changes in stratigraphy, geologic contacts, material type and bedding were all noted. Strike and dip angles of selected discontinuities, shear planes, and contacts were also measured. Yeh personnel also measured water levels and corresponding times where groundwater was encountered.

The test pits were excavated with a mini excavator and 18-inch-wide bucket to depths ranging from approximately 5 to 11.5 feet below the ground surface. Yeh staff logged the test pits identifying soil types, bedrock types, geologic contacts, and other data. Bulk samples of soil and rock were obtained from excavation spoils for visual classification.

Existing and current study data at and adjacent to Fremont Hall (for the 2017 landslide stabilization geotechnical characterization), as well as existing data for the east side of the University campus (for the assessment of deep-seated landslide potential) were reviewed and compiled. A reduced version of the exploration location map including both current study and previous study explorations near Fremont Hall are shown in Figure 5.

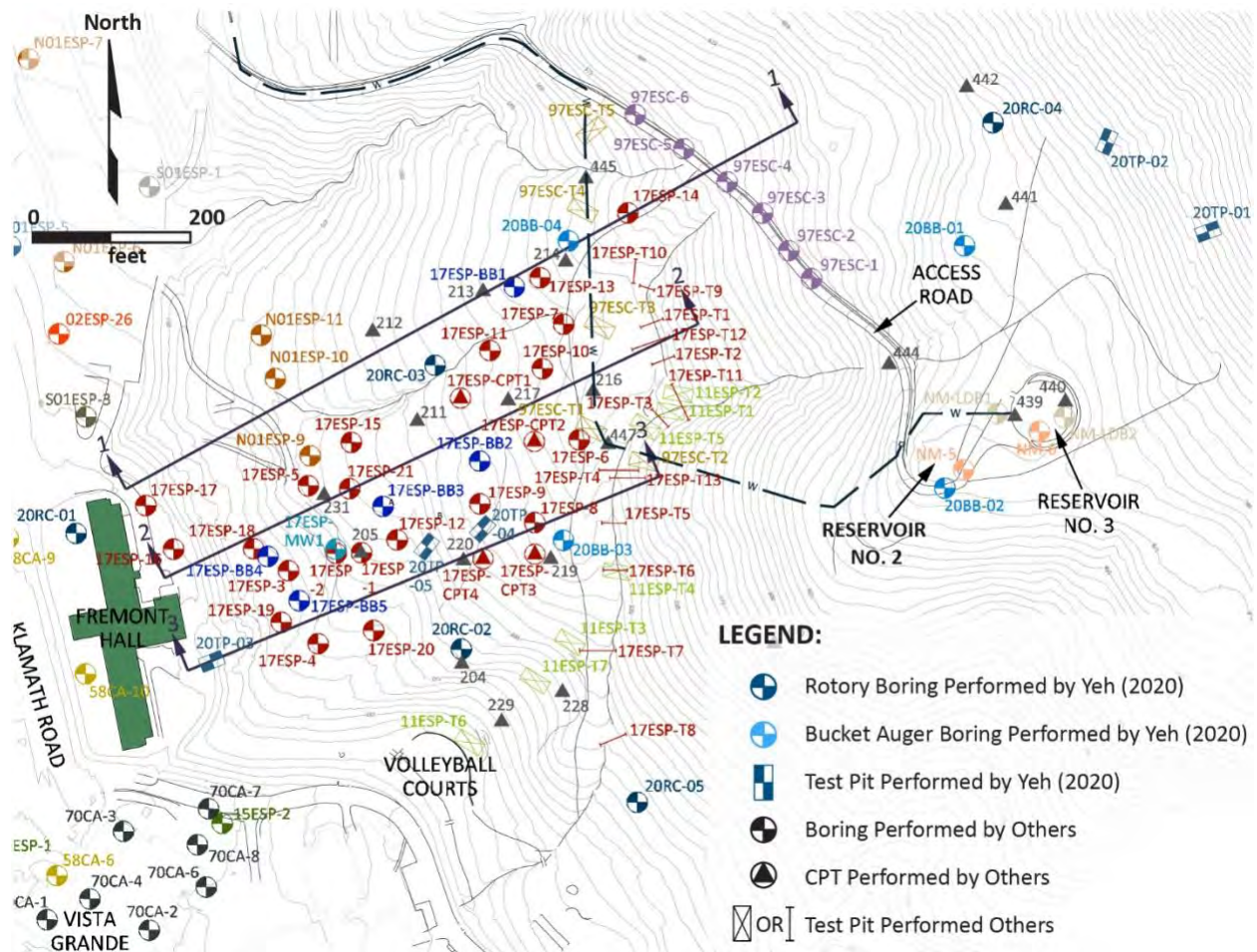


**Figure 5: Previous Study and Current Study Explorations Near Fremont Hall**

### *Instrumentation and Monitoring*

Two (2) vibrating wire piezometers (VWP), one (1) time domain reflectometer (TDR) cable and a 2.75-inch diameter slope inclinometer (SI) casing were installed in each of the five rotary core borings. Yeh also installed an on-site barometer in one of the rotary borings. The instrumentation was monitored on a monthly to bi-monthly basis during the duration of the project and through construction. Yeh used data obtained from the inclinometers as well as surface monitoring data surveyed by Cannon to monitor the activity of the hillside and direction of movement.

### *Laboratory Testing*

Laboratory testing was performed on selected soil and rock samples recovered from the field exploration program. Tests for classification and corrosivity were performed by Yeh as well as an outside laboratory consultant. Tests for soil triaxial compressive strength using consolidated undrained (CU) loading, torsional ring shear tests, residual direct shear, and unconfined compressive strength tests on rock cores were also performed by an outside laboratory consultant. Laboratory data was used as input for geotechnical characterization of the hillside and landslide shear plane, slope stability analyses, and seismic analyses.

## **ENGINEERING GEOLOGY AND SITE CONDITIONS**

### **Regional and Geology**

The regional geology in the site vicinity as mapped by Hall and Prior (1) and Wieggers (3) is shown on Figure 3. The project is located within the Coast Ranges geologic and geomorphic province, which extends from the Transverse Ranges in southern California to the Klamath Mountains in northern California and into Oregon. The province is characterized by north-northwest trending mountain ranges composed of sedimentary, volcanic, and metamorphic formations comprising predominantly Jurassic and Cretaceous age rocks with Tertiary to Quaternary age rocks and soil commonly overlying the older formations along the flanks and foothills of those ranges. Quaternary-age alluvium and colluvium are commonly mapped above the rock within intervening drainages, valleys, and coastal areas.

### **Site Geology**

Hall and Prior (1) mapped four different bedrock units at the project site: Jurassic age serpentinite (s), Cretaceous to Jurassic age metavolcanics (KJfmv), mélangé (KJfm) of the Franciscan Complex, and a large landslide (Qls). Dibblee and Minch (2) and Wieggers (3) mapped similar geology with modified contacts and descriptions. Yeh's interpretation of the site geology based on previous data as well as mapping and exploration performed for the project and previous studies is shown in Figure 6 and described below.

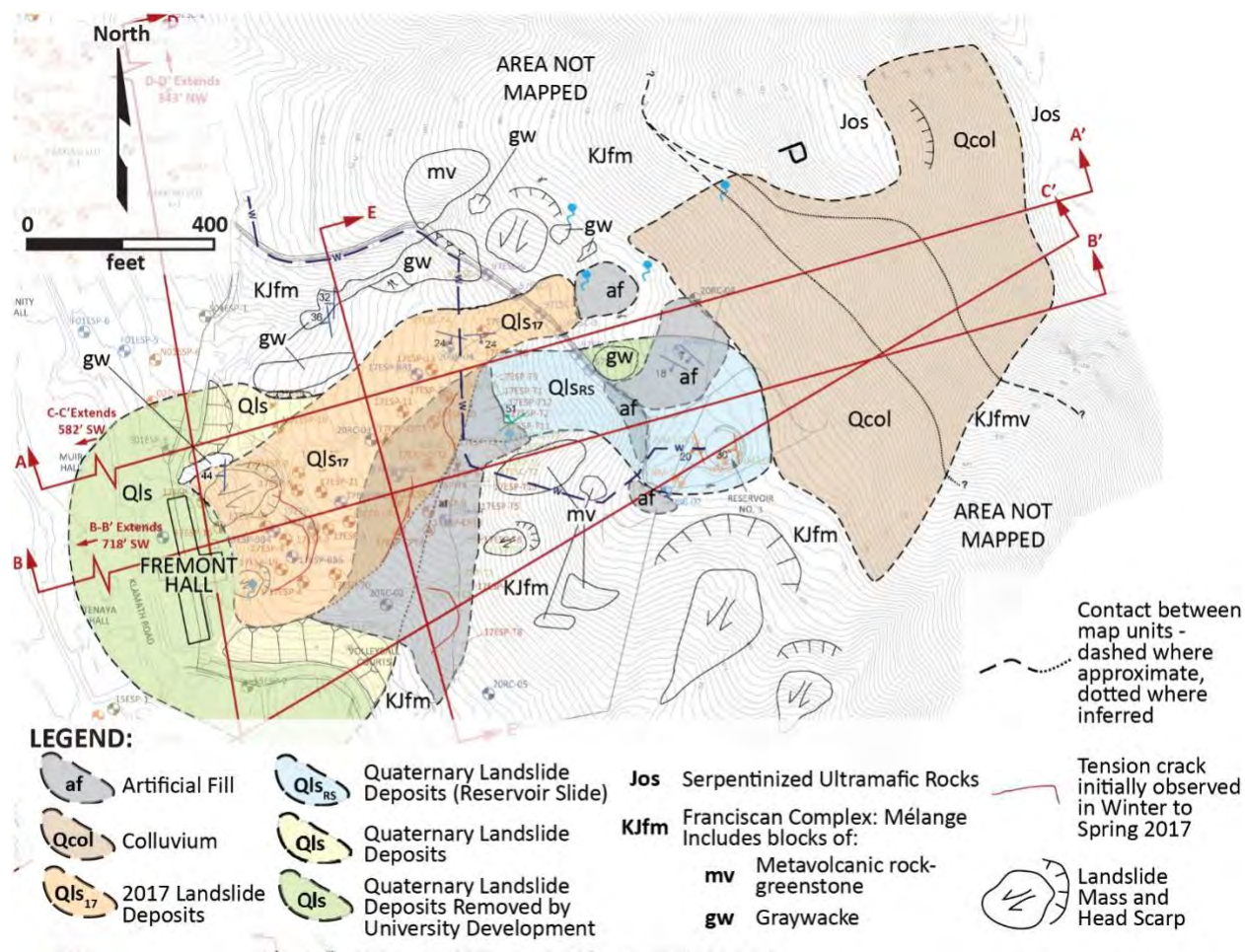


**Figure 6: Site Geology**

### *Artificial Fill (Af)*

The artificial fill mapped and encountered by Yeh's study was interpreted to be a relatively large fill associated with construction of Reservoir Nos. 2 and 3, the reservoir access road, the subdrainage and surface drainage system constructed after the 2017 Landslide, and general stockpiling of materials excavated during the grading for the dormitories in the late 1950s. The source of the 1950s stockpile was likely associated with University development, including the area shown on Figure 6 as removed landslide deposits (green Qls). The depth of fill varied from approximately 3.5 to 50 feet below the ground surface. Artificial fill encountered at various depths in Yeh's bucket auger borings included debris consisting of concrete, brick, clay pipe, and wood fragments, with the deepest concrete debris encountered at a depth of approximately 46 feet below the ground surface.

### *Colluvium (Qcol)*

Colluvium was present upslope of the landslide deposits and was interpreted to consist of soil derived from the underlying serpentinite and metavolcanic (KJfmv) rock of the Franciscan

Complex. The colluvium's thickness likely varies over the site but is interpreted to be generally thickest at the downslope limits and thinnest at the upslope limits where shown on the map.

### *Landslide Deposits (Qls)*

The large Quaternary-age landslide mapped by Hall and Prior (1) and Dibblee and Minch (2) is shown comprising most of the slope east of Fremont Hall and extending slightly west of other University buildings (see Figure 3). Hall and Prior (1) described the landslide deposits as predominantly debris from the underlying Franciscan *mélange*. The landslide mapped by Wiegiers (2010) extends eastward upslope but notably does not extend west of Fremont Hall. Yeh characterized the Quaternary-age landslide as an earthflow, which typically have a characteristic "hourglass" shape, elongated, and usually occur in fine-grained materials or clay-bearing rocks on moderate slopes and under saturated conditions (4). Earthflow-type landslides are typically characterized by relatively slow failure rates and creeping behavior (5) and can flow around or over large intact rock blocks, such as the blocks shown on Figure 6.

Yeh mapped the limits of the Quaternary landslide deposits as shown in Figure 6. The landslide mapped upslope of the 2017 Landslide (termed the "Reservoir Slide") was mapped based on the basal rupture surface encountered in a bucket boring performed by Yeh and the rupture surfaces reported previous studies. The orientations of the rupture surfaces were interpreted to be associated with landslide movement towards the downslope west-flowing drainage. The landslide was mapped as underlying Reservoir Nos. 2 and 3, and portions of the roadway and pipelines within the roadway that connect those facilities to campus. Evidence of active movement of the landslide was not reported by previous studies and surficial distress to the reservoir structures typically associated with slope movement was not observed. Therefore, the Reservoir Landslide was interpreted to be inactive and separate from the active 2017 landslide.

Yeh also mapped the 2017 Landslide that occurred within the limits of the Quaternary landslide based on inclinometer data collected from explorations performed for Yeh's 2020 study and previous studies, and tension cracks initially observed in Winter-Spring 2017 (see Figure 6). Inclinometers indicated movement trends at 10 to 56 feet below the surface with cumulative deflections up to 1.5 inches. Slickensided planes and rupture surfaces were observed within the bucket auger borings performed by Yeh. The depth of the 2017 Landslide was interpreted to vary from approximately 26 to 60 feet below the ground surface as encountered in the explorations performed by Yeh and by previous studies as well as the instrumentation monitored by Yeh.

### *Serpentinite (sp)*

Wiegiers (3) described the serpentinite as locally serpentinitized ultramafic rocks. Yeh did not encounter serpentinite within the Franciscan *Mélange* bedrock in the explorations performed for the project. Serpentinite was observed up slope and east of Reservoir No. 3 and exposed by cut slopes within hiking trails that traverse the ridgeline above the site.

### *Franciscan Mélange (KJfm)*

The *mélange* was described by Hall and Prior (1) and Dibblee and Minch (2) as pervasively sheared, greenish-black to dark gray claystone matrix with exotic blocks that typically consist of

graywacke, blueschist, metavolcanic rocks, chert, and serpentinite. Wiegers (3) described the *mélange* as a chaotic mixture of fragmented rock masses embedded in a penetratively sheared matrix of argillite and crushed metasandstone. Hall and Prior (1) noted the original structure of the *mélange* has been destroyed by shearing and mixing.

Hall and Prior (1) mapped blocks of graywacke, chert and blueschist upslope of Fremont Hall, within the limits of the Quaternary landslide. Individual rock masses contained in the matrix range from less than a meter to kilometers in scale (3) and are relatively resistant to weathering. Medley and Zekkos (6) noted that “the early summer browning of grass in *mélange* landscapes in northern California occurs first above blocks because the generally sandier soils dry faster than the clayey soils above matrix. The result is a mottling that is characteristic in *mélange* terrains and which is well exhibited in air photos taken in Spring and early Summer.” Yeh mapped the blocks shown on Plate 6 based on field mapping and review of historical aerial photography.

Two predominant units of the Franciscan *Mélange* were encountered below the artificial fill, colluvium, and landslide deposits in the explorations performed by Yeh; graywacke (gw) sandstone and *mélange* (KJfm). The *mélange* predominantly consisted of intensely weathered to decomposed sheared and slickensided claystone with subangular to angular blocks of graywacke sandstone. The blocks were chaotically distributed and ranged in size from sand to boulder. The graywacke blocks were fresh to slightly weathered, moderately soft to hard, and predominantly bounded by a moderately thin to thin veneer of dark gray fat clay (CH) with discontinuous, randomly oriented shear planes. Graywacke encountered by Yeh and also by previous studies performed in 2017 was intensely weathered and fractured at the bedrock surface and became less weathered and fractured with depth. Caliche deposits were commonly found in fractures within the graywacke sandstone. Yeh interpreted the graywacke sandstone found in borings drilled by Yeh and previous studies as a large block of graywacke within the Franciscan *Mélange*.

#### *Franciscan Metavolcanics (KJfmv)*

Hall and Prior (1) described the metavolcanic rocks as primarily metamorphosed basalt (greenstone) and diabase commonly associated with red chert. Dibblee and Minch (2) described the metavolcanic rocks as greenish-black, massive, aphanitic greenstone that weathers to a brown color and is veined with calcite-dolomite. Franciscan Metavolcanic Rocks were not encountered in explorations performed by Yeh. Metavolcanic outcrops were observed at the surface on slopes and clasts were found in explorations performed.

### **COLLABORATIVE STABILIZATION ALTERNATIVE SELECTION AND DESIGN PROCESS**

The design team and the University collaborated over multiple meetings to discuss the preliminary findings pertaining to risk assessment, geotechnical characterization, and alternatives analyses. Yeh also met with peer reviewing engineers and geologists on several occasions to perform field mapping and reconnaissance at the site.

Five alternatives for stabilization of the 2017 landslide were discussed between the design team and University. The five alternatives presented included an earthen buttress with imported fill, a deep soil mixed earthen buttress, a cantilevered pile wall, a tieback pile wall, and a soldier pile tieback wall with uphill anchor galleries. Alternatives were compared based on reliability,

constructability, weather impact (in relation to construction and constructability), carbon footprint and campus impact (such as traffic and greenhouse gas emissions due to trucking of the export and import of soil), and relative cost. The soldier pile tieback wall with uphill anchor galleries was recommended by the design team and selected by the University as the preferred option to restore and stabilize the hillside behind Fremont Hall.

## **GEOTECHNICAL ANALYSES AND DESIGN**

### **Data Compilation for Design**

Data from Yeh's explorations as well as data from previous study explorations on or near the hillside were compiled to create interpreted subsurface cross sections (see a portion of one of the cross sections in Figure 7). These cross sections were used as input to Yeh's models for slope stability analysis and as input to the design of the proposed soldier pile tieback wall and anchor galleries. The data was also compiled into software to create a 3-dimensional subsurface model of the interpreted geologic units and bedrock elevations. A contour map showing the top of bedrock elevation in relation to existing and proposed topography was created from the 3-dimensional subsurface model for Schnabel to use in estimating the unbonded lengths for the tiebacks.

### **Assessment for the Potential of a Deep-Seated Landslide**

Yeh evaluated the potential for the landslide mapped by published geologic maps to impact Fremont Hall, and to be potentially deeper than the depth of the 2017 Landslide rupture surface shown on the subsurface profiles. The basis for the University's concern was a review of aerial photography and the basal rupture surface reported by a previous study done at the reservoir site upslope of Fremont Hall. Yeh's evaluation included drilling the bucket auger and rotary core borings to help evaluate the potential for the deep-seated landslide along with a review of the historical slope performance.

The landslide was mapped on the published maps from a regional perspective, and the depth of the landslide deposits shown on published maps was not assessed without site-specific exploration. Borings were drilled to depths of approximately 109 to 112 feet below the interpreted rupture surface of the 2017 Landslide to help evaluate whether rupture surfaces were present that could be associated with a deep-seated landslide. Evidence of a deep-seated landslide rupture surface was not observed. Fremont Hall, Reservoir Nos.2 and 3, and other structures are located within the landslide limits shown on published geologic maps. The University had not reported historical distress to those structures that could be attributed to landslides, with the exception of the 2017 Landslide that impacted Fremont Hall. The results of Yeh's Fremont Hall floor level survey and condition assessment did not find evidence of movement, cracking or distress that would be associated with landslide movement other than the previously mentioned cracked exterior east wall resulting from the 2017 Landslide.

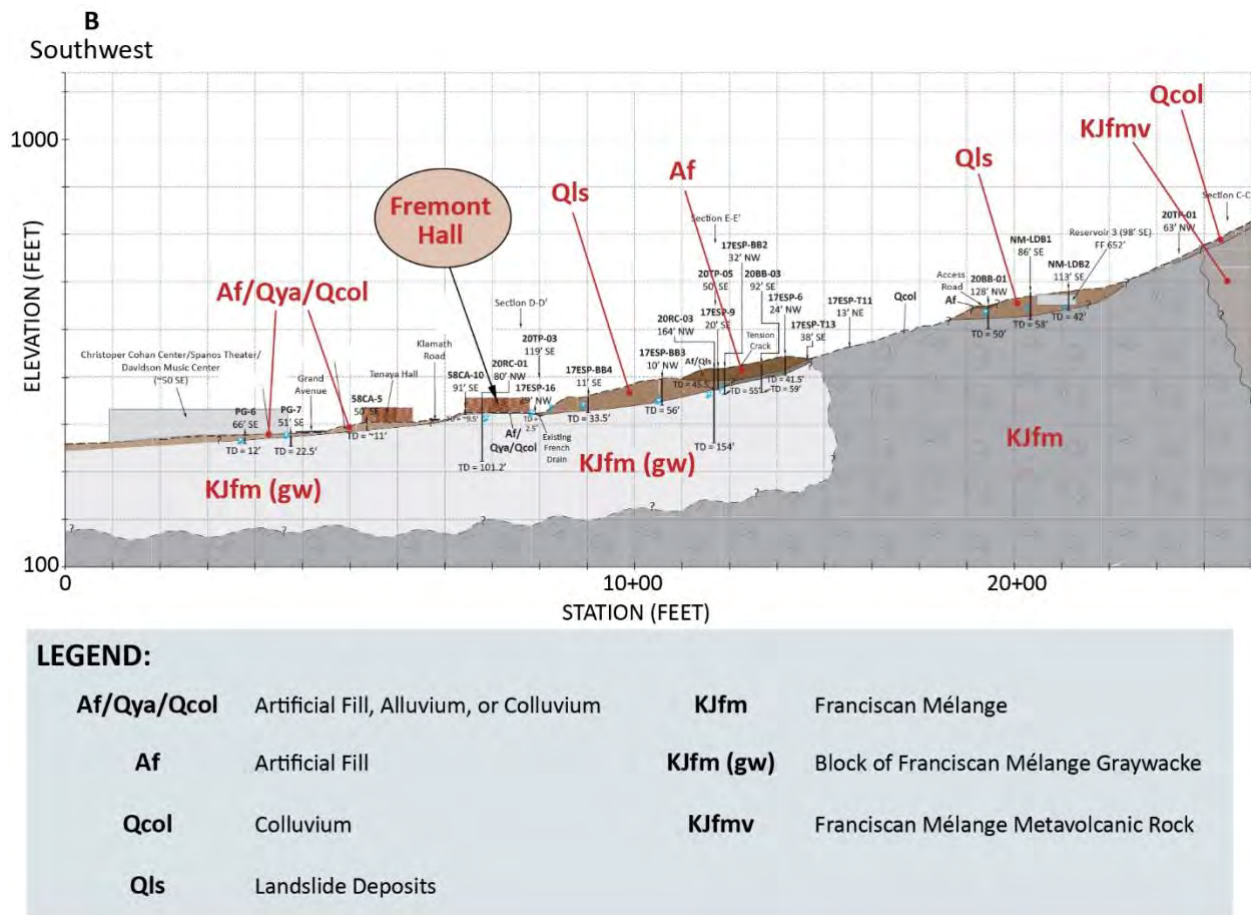


**Figure 7: Portion of Cross Section B-B'**

The potential for a deep-seated landslide below the 2017 Landslide plane depth or below Fremont Hall was considered low. Stabilization of a deep-seated landslide was not considered in the design of the slope improvements, and the potential for a deep-seated landslide to impact Fremont Hall was not considered in the study's risk assessment.

### Assessment of Debris Flow Potential

The University's peer reviewer initially interpreted the mapped Quaternary-age landslide deposits as prehistoric debris flow deposits and recommended an evaluation of the potential for debris flow events to impact Fremont Hall. They identified the colluvium mapped upslope of the access road and reservoir slope as the likely debris flow source. Subsurface conditions encountered by the previous 2017 study were interpreted to potentially represent multiple debris flow events, and bucket auger drilling was recommended by the peer reviewer to evaluate the thickness of individual prehistoric debris flow events as input to the design of debris flow mitigation, if necessary. Yeh's evaluation included review of geomorphic evidence, the subsurface conditions encountered in the explorations, and historical slope performance to assess the potential for debris flows to impact the project.

Geomorphic features shown on Yeh's hillside shade map upslope of the landslide deposits did not include remnant debris flow features such as shallow arcuate scarps or runout channels smoothed by erosion. The slopes were generally planar and were not anticipated to concentrate surface infiltration. Yeh observed two minor depressions that could potentially concentrate infiltration which were evaluated for runout distances. Yeh did not observe buried soil horizons or subsurface features indicative of rapid, episodic depositional events that would be considered evidence of multiple prehistoric debris flows in the bucket auger borings. Additionally, gravel and cobbles encountered in the rock core and bucket auger borings consisted of serpentinite, metavolcanics, chert, and graywacke typical of Franciscan Mélange. Therefore, it was interpreted that the landslide deposits were likely derived from the Franciscan Mélange. Evidence of prehistoric debris flow deposits in the borings would have consisted of predominantly serpentinite and metavolcanic clasts derived from those geologic units mapped underlying the colluvium.

The University reported no historical records of debris flows at the site. The average cumulative rainfall recorded at the Cal Poly weather station between 1870 and 2018 was approximately 22 inches. The average cumulative rainfall was exceeded 63 times during that period, with a maximum of approximately 54.5 inches in rainfall year 1968-1969 (7). Yeh did not observe or find evidence of debris flows occurring on the site as a result of higher-than-average rainfall events since 1870.

Yeh performed runout analyses to estimate potential consequences of debris flows for risk assessment. The runout analyses considered the area of the two depressions to estimate potential consequences of debris flows where there was a potential for surface water to infiltrate the colluvium and weathered bedrock. Yeh estimated that the thickness of the colluvium and weathered bedrock was 4 feet based on the subsurface conditions encountered in the test pits near the location. The 4-foot thickness was an input to the Rickenmann (8) correlation to estimate the runout paths. The estimated runout distances were approximately 600 and 660 feet which were approximately 850 feet upslope of Fremont Hall. It should be noted the Rickenmann (8) correlation does not provide an estimate of the thickness of debris at the runout end point, but it is anticipated the debris will disperse during runout and the debris thickness at the end point would be less than 1 foot. The potential for debris flows to impact Fremont Hall was considered low based on Yeh's evaluation of existing conditions and runout analysis. Yeh concluded there was a low potential for debris flows, considering existing and post-fire conditions, to impact Fremont Hall based on the results of the runout analyses, and therefore debris flow mitigation for the stabilization project was not needed.

### **Slope Stability Analyses**

Yeh performed two-dimensional limit equilibrium slope stability analyses for the interpreted subsurface cross-sections compiled by Yeh as well as the geostructural sections selected by Schnabel. The analyses were performed to provide a basis for the design, proposed stabilization of the landslide, and recommendations provided by Yeh. Material properties for the slope stability analyses were selected based on an analysis of laboratory test results from Yeh's exploration program as well as data from previous studies. Franciscan Mélange strength parameters were estimated based on laboratory test results and the methods described by Medley

(7) and Medley and Zekkos (6) for volumetric block proportion for block-in-matrix rocks (bimrocks).

The analyses were performed to calculate slope stability factors of safety under static and seismic loading conditions, estimate structural loads per foot for the anchors, and estimate slope displacement under the design seismic loading. The location of ground anchor galleries along the design sections was varied to optimize the support resistance and provide stability to the overall slope. Support locations were based upon design and analyses iterations and collaboration with Schnabel. The final design layout is shown in Figure 8.

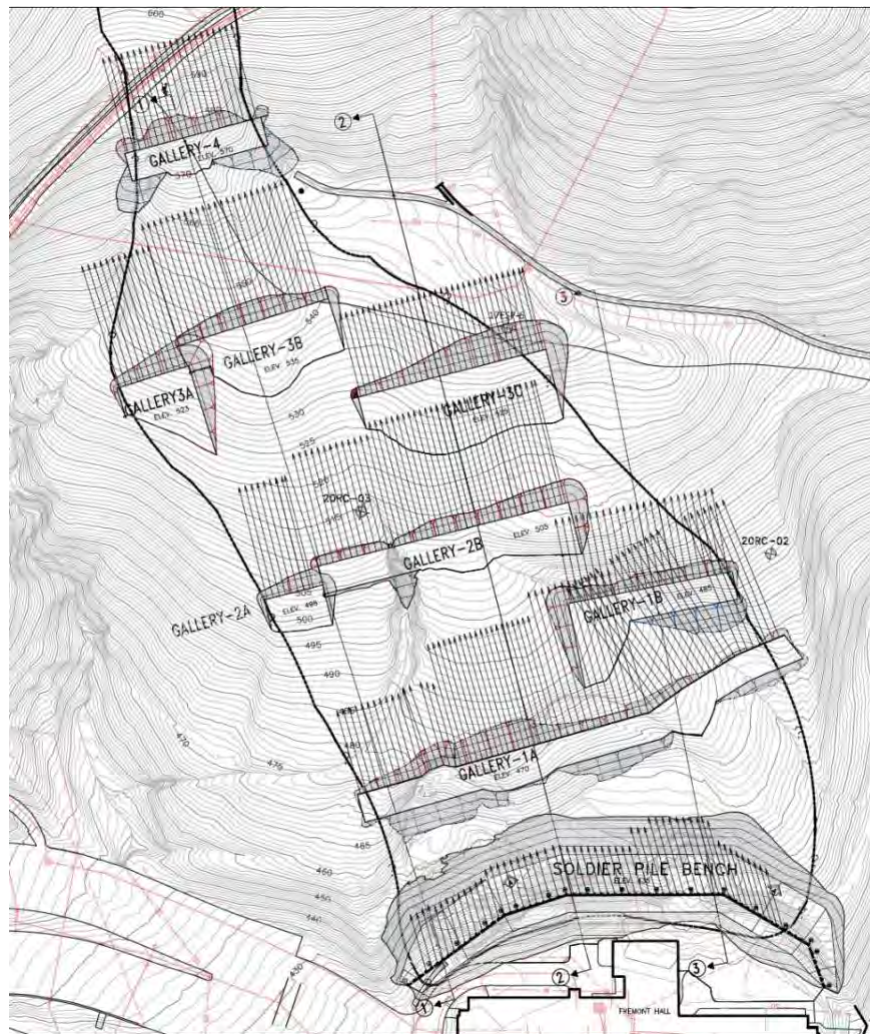


**Figure 8: Stabilization Design Layout**

## CONSTRUCTION AND MONITORING

Construction began in August 2021. Eight anchor galleries (1A, 1B, 2A, 2B, 3A, 3B, 3C, and 4) and one soldier pile tie-back wall were constructed for the project. The soldier pile wall had heights of 2 to 20 feet with one to two rows of tie-back anchors. A total of 353 tie-back anchors

with 3 to 9 strands with lengths of 35 to 124 feet were drilled, installed, and grouted for the wall and galleries. Tie-back anchors were tensioned to lock-off loads of approximately 103 to 264 kips. Long term monitoring of the slide was established during construction using a series of piezometers, inclinometers, and instrumented tieback anchors on each gallery and the soldier pile wall. Readings were collected on a regular basis to monitor movements during the construction process.

## CONCLUSION

The stabilization consisted of a series of ground anchor galleries within the landslide mass and an anchored soldier pile wall at the toe of the stabilized slope (see Figure 9). Horizontal drains and subdrains were installed within the landslide mass to collect and maintain design groundwater elevations. The project was successfully completed in July 2022 and students have since reoccupied the dormitory. A photo of the completed project is shown in Figure 9. Yeh is contracted to continue to monitor the existing twelve inclinometers, fifteen vibrating wire piezometers (VWPs), and fourteen instrumented anchors on a monthly basis. An “atmospheric river” event impacted the region in January 2023 which caused bridge failures, levee failures, and multiple landslides in the surrounding area. A rise in groundwater elevation of approximately 16 feet was recorded in the VWPs at the site and water was observed actively flowing from the horizontal drains. However, the data recorded from the inclinometers and anchors did not show evidence of slide mobilization. Besides surficial erosion of the newly-hydroseeded slopes, the slope stabilization performed well during the “atmospheric river” event and for the remainder of the above average precipitation that occurred in in the region during the Winter of 2023.



**Figure 9: Completed Project - September 2022**

## REFERENCES

1. Hall, C.A. and Prior, S.W.. *Geologic Map of the Cayucos-San Luis Obispo Region, San Luis Obispo County, California*, Miscellaneous Field Studies Map MF-686, Department of the Interior – United States Geological Survey, 1975, sheet 2 of 2.
2. Dibblee, T.W. and Minch, J.A.. *Geologic Map of the San Luis Obispo Quadrangle, San Luis Obispo County, California*. Dibblee Foundation Map DF-129, Dibblee Geological Foundation, 2004.
3. Wieggers, M.O.. *Geologic Map of the San Luis Obispo 7.5' Quadrangle, San Luis Obispo County, California: a digital database*. Preliminary Geologic Maps PGM-10-04, California Geological Survey, 2010.
4. Highland, L.M. and Bobrowsky, P.. *The Landslide Handbook – A Guide to Understanding Landslides*. Circular 1325, United States Department of the Interior - Geological Survey, 2008.
5. Keefer, D.K. and Johnson, A.M., *Earth Flows: Morphology, Mobilization, and Movement*, Geological Survey professional paper 1264, United States Department of the Interior – Geological Survey, 1983.
6. Medley, E.W. and Zekkos, D.. *Geopractitioner Approaches to Working with Antisocial Melanges*, Special Paper 480, The Geological Society of America, 2011.
7. California Polytechnic State University. *Irrigation Training & Research Center*, accessed April 2020, <http://www.itrc.org/databases/precip/>
8. Rickenmann, D.. *Empirical relationships for debris flows*, Natural Hazards, Vol. 19, No. 1, 1999, pp. 47-77.
9. Medley, E.W.. *Characterization of Franciscan melanges and other heterogeneous rock/soil mixtures*, California Geological Survey Bulletin 210, Engineering Geology Practice in Northern California: Association of Engineering Geologists Special Publication 12.

**Route 3, Randolph County, Missouri  
Landslide Remediation Study. Design and Construction**

**John F. Szturo R.G. P.G**

HNTB Corporation  
715 Kirk Drive  
Kansas City, MO 64105  
816 472-1201  
[jszturo@hntb.com](mailto:jszturo@hntb.com)

**Norman Norrish P.E.**

Wyllie & Norrish Rock Engineers Inc.  
909 Marine Drive Unit 110  
Bellingham, WA 98225  
206 790-3476  
[nnorrish@msn.com](mailto:nnorrish@msn.com)

**Wayne A. Duryee P.E.**

HNTB Corporation  
715 Kirk Drive  
Kansas City, MO 64105  
816 472-1201  
[wduryee@hntb.com](mailto:wduryee@hntb.com)

### **Acknowledgements**

The authors would like to thank the following individuals for their contribution in the work described:

Lydia Brownell P.E. Missouri Department of Transportation  
Zachary Troesser P.E. Missouri Department of Transportation

### **Disclaimer**

Statements and views presented in this paper are strictly those of the authors and do not necessarily reflect positions held by their affiliations, The Highway Geology Symposium (HGS), or others acknowledged above. The mention of trade names for commercial products does not imply the approval or endorsement by HGS.

### **Copyright Notice**

Copyright © 2023 Highway Geology Symposium (HGS)

All Rights Reserved. Printed in the United States of America. No part of this publication may be reproduced or copied in any form by any means – graphic, electronic, or mechanical, including photocopying, taping, or information storage and retrieval systems – without prior written permission of the HGS. This excludes the original authors.

## ABSTRACT

A landslide occurred at MoDOT Route 3 after an intense rain event in April of 2021. At the landslide location, 200+ feet deep, open pit quarries are located at the limits of the thirty foot right of way on both sides of the highway. Much of the landslide mass, comprised of overburden soils, slid down the highwall to the quarry floor. The initial study was to determine the extent and cause of the slide, stability of the 200-foot vertical high wall and shallow tunnels under the roadway connecting the two open pits. The final phase would develop feasible, economic alternatives for reopening the roadway.

The site is located in a complex geologic environment at the very border of glaciation. Bedrock geology is further complicated by the location of a Pennsylvanian Age channel fill sandstone cut through the underlying Mississippian limestone. Several piezometers were installed and indicated a very erratic groundwater pattern in the glacial.

The study involved performing borings, laboratory testing, soil slope stability analysis, rock slope stability analysis of the quarry wall, and rock stability analysis of the abandoned tunnels traversing the roadway.

Several remedial alternatives were considered in the study and the favorite was relocating the roadway to one side away from the slide as well as lowering the grade to near the failure surface of the landslide. Also, the slide mass had to be removed and replaced with shot rock to provide long term stability and promote long-term internal drainage. Both were necessary to keep further movement of the ground into the deep open pit quarry.

The consensus of the study led to final design which included relocating the roadway both horizontally and vertically. Included in the final design was removal and replacement of the slide mass.



## Existing Conditions

Limestone has been mined up to the existing right-of-way on both sides of Route 3 through the project area. Overburden stripping's were piled into berms along and adjacent to the roadway right-of-way. Past underground mining also occurred under Route 3. The open pit and the underground mines to the west of Route 3 are no longer active and have been abandoned. The open pit on the west side of Route 3 is partially filled with water and vegetation has overtaken much of the surrounding area. The berm construction and quarry are very near the existing right-of-way on both sides.

The east open pit quarry is active with the lowest level some 200-feet below the existing Route 3 grade. The open pit of the east side has been excavated below the previously underground mine level, exposing two parallel “tunnels” that traverse under Route 3. The underground mining ceased in approximately 2006. According to mine personnel, the underground mining was completed by room and pillar methods and was always dry and stable. The underground mine is no longer in operation and entry is prohibited.

Presently, the east quarry is expanding eastward, away from the roadway. According to conversations with quarry personnel, the east pit is expanding outwardly rather than down, although there is remaining rock that can be mined deeper. Over 100 years of mineral reserves remain on the property without deepening the pit.

When the soil overburden and shale were stripped to get to the limestone of the quarry, some of it was placed parallel to Route 3 in berms as both a visual and safety barrier to the traveling public. According to anecdotal information, the material was not placed as controlled engineered fill.

The slope failure occurred in the non-engineered berm and underlying glacial till – lean clay overburden. In its existing position, the scarp of the failure is at the east edge of the pavement with the slump extending to the top of the quarry highwall. Slumped material has also fallen over the highwall and down to the quarry floor (Figures 3 and 4). Small tension cracks have been noted in the roadway parallel to the landslide scarp.



**SLOPE FAILURE FROM EAST PIT – FIGURE 3**



**EAST PIT AND TUNNELS – SLIDE DEBRIS IN PIT FLOOR FIGURE 4**

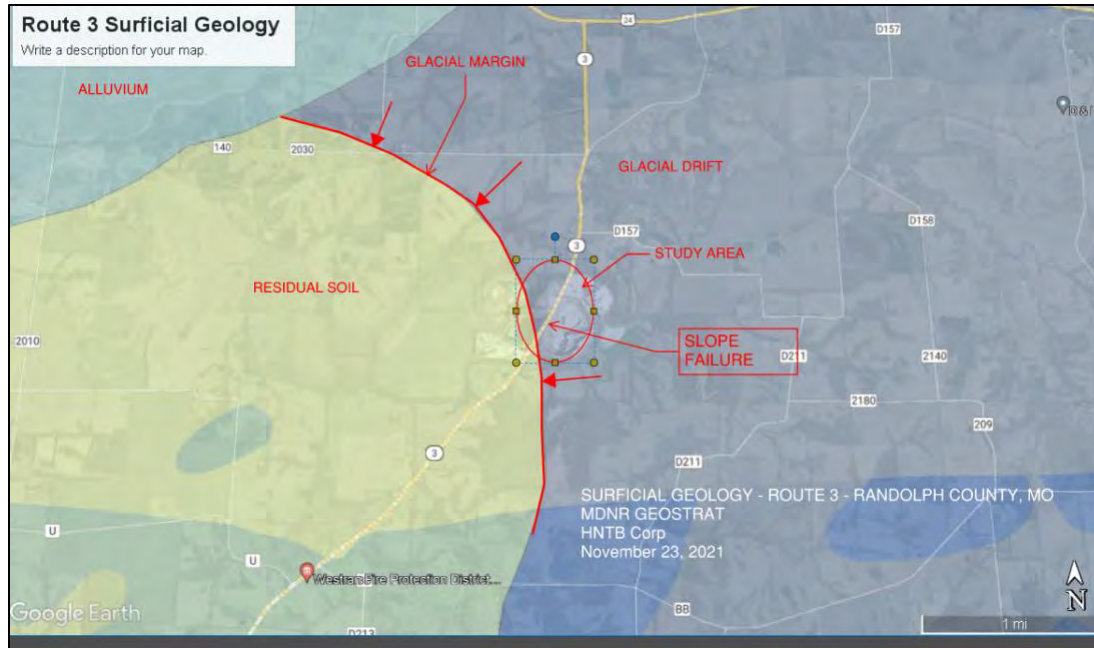


**EAST PIT AND TUNNELS FIGURE 5**



**SLIDE CLOSEUP – LOOKING SOUTH FIGURE 6**





**MAP OF SURFICIAL GEOLOGY FIGURE 8**

### **Regional Bedrock Geology**

The regional bedrock geology (Figure 9) is dominated by an atypical feature of Missouri geology, the Weldon River, Warrensburg, Moberly Sandstone. The sandstone lies unconformably on the underlying Lower Pennsylvanian and Mississippian formations. The sand was deposited in the channel of a large river that flowed across the landscape at the beginning of middle Pennsylvanian time, eroding its channel into the Marmaton and Cherokee Group sediments. The river may have joined another large river in west-central Missouri before emptying into a shallow sea. The Moberly channel sandstone has been traced for a continuous distance of over 55 miles. It ranges in width from less than 1 mile at its eastern end to more than 5 miles and is about 2 miles wide in the study area.

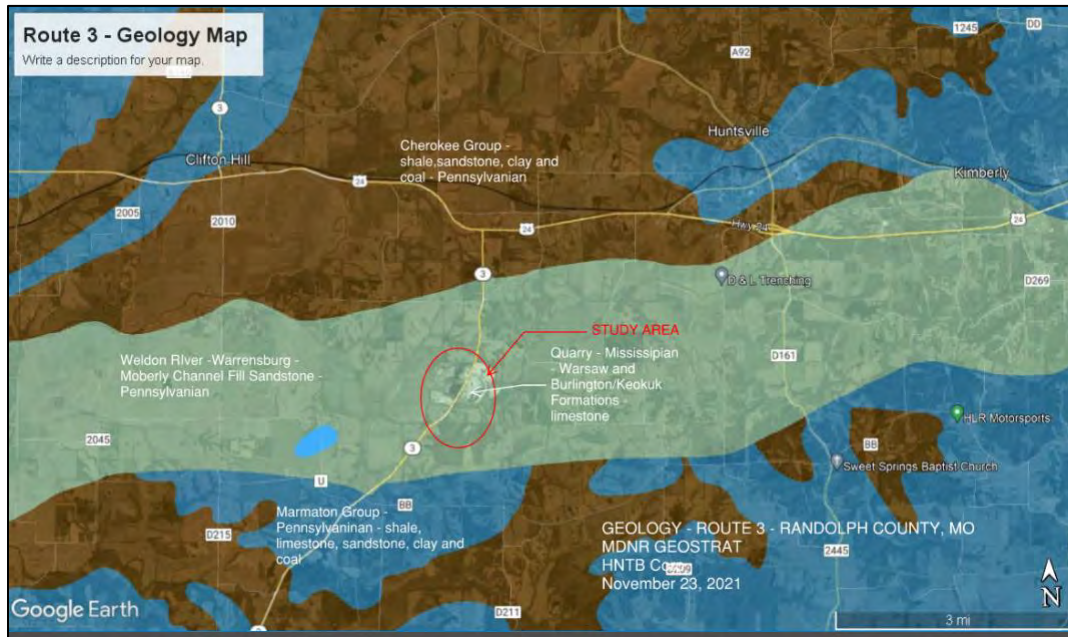
The channel fill sandstone runs east and west through the area and its geometry would be typical of an eroded, incised, river channel backfilled with cross-bedded sand, covered by additional sediments and later indurated into sandstone. Literature states the Formation may be up to 150 feet thick, however in the study area it may be thicker. The landslide location seems to be centered in this channel fill sandstone.

The adjacent Cherokee and Marmaton Group consists mostly of beds of shale and sandstone with minor beds of limestone. The group also contains significant coal beds that were commercially mined in the past.

The Mississippian Age limestone mined in the quarry consists of the Warsaw Formation overlying the Burlington-Keokuk Formation. Structurally, the limestones of the Warsaw, Burlington, and Keokuk are essentially flat lying, and thin to thick bedded. Anecdotal information from quarry personnel indicates a fault was encountered in the west underground through the limestone formations a few hundred feet northwest of the study area. The fault is thought to be normal with an offset of approximately 9-feet.

No known karstic features have been identified in the exposed rock or quarry. The limestone formations are known to be dry as no water was encountered in the underground quarry

nor is groundwater filling the open pit quarry requiring dewatering. It is assumed the abandoned quarry to the west is filled with surface water.



**Regional Geology Map FIGURE 9**

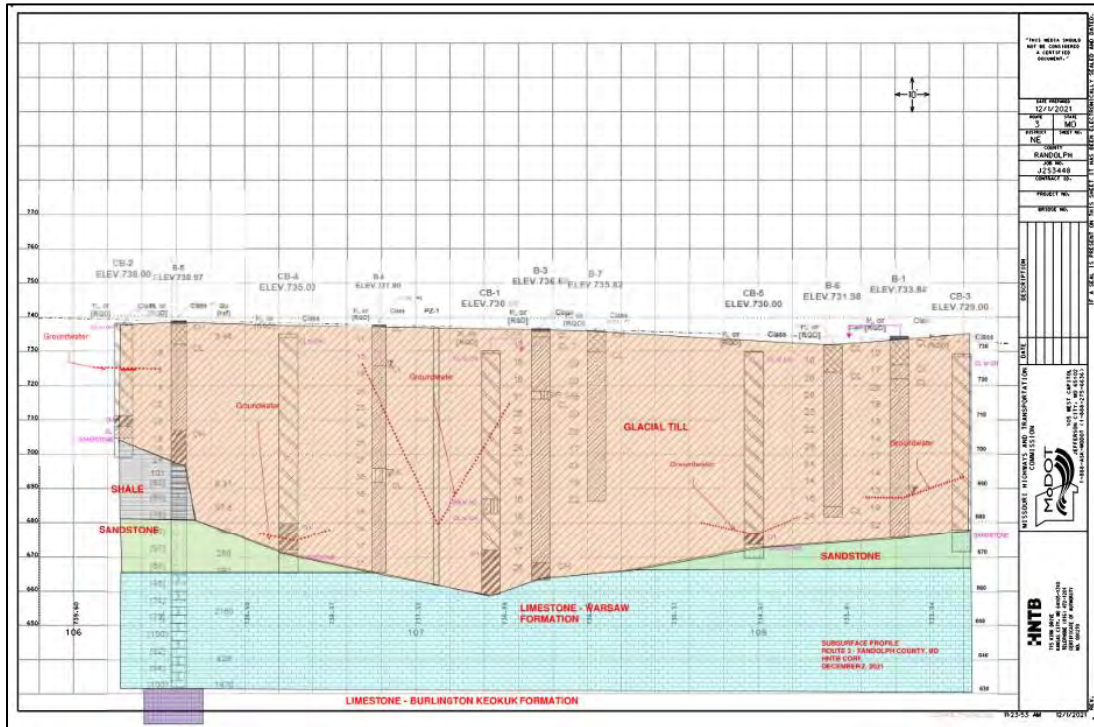


**GEOLOGY OF THE EAST PIT FIGURE 10**

### 3.0 Site Characterization

The subsurface can be generally characterized as glacial till over lower Pennsylvanian Channel sandstone (Weldon River, Warrensburg, Moberly) cut into and flanked by other Pennsylvanian shale and sandstone (Cherokee and Marmaton), all underlain by the Mississippian limestones (quarried material) of the Warsaw and Burlington – Keokuk Formations (Figure 10). The glacial till is described as mostly lean over-consolidated clay. Sand and gravel particles are interspersed within the clay matrix, characteristic of Northern Missouri glacial till. The glacial till

contains irregular lenses, layers and pockets of silt, sand, and gravel. Fat clay occurs above the top of rock, most likely derived from very weathered shale (Figure 11).



**SUBSURFACE PROFILE – FIGURE 11**

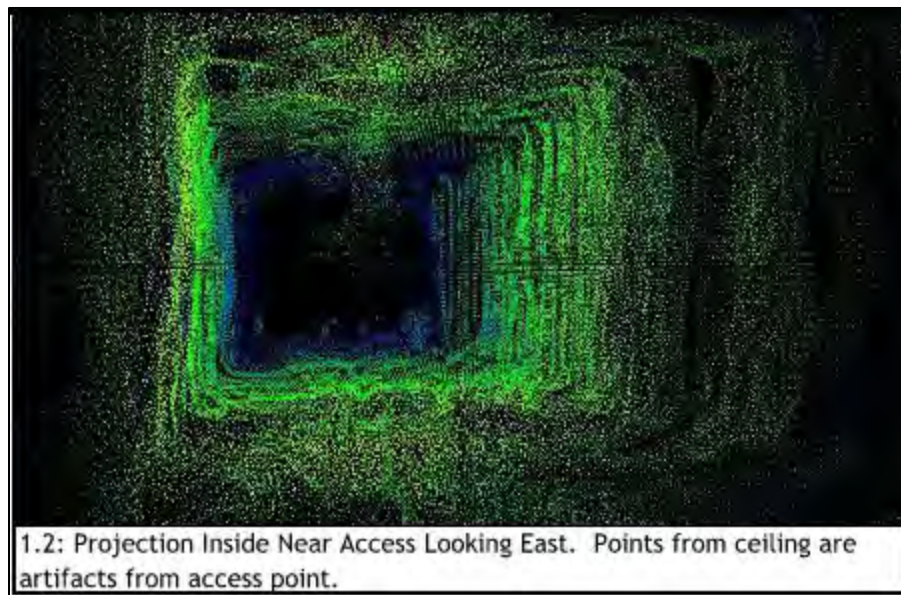
**Groundwater**

Groundwater levels varied from the 2021 study borings and the 2022 final design borings. The initial study borings indicated a highly variable and disconnected water level within the borings. The 2021 borings ranged from dry to 12-feet below top of ground. The perched and erratic water table appears to have stabilized to a piezometric surface that runs just above the impervious shale layer. Part of the cause of the slide may have been the presence of the highly perched water in the overburden till in the time after the significant rainfall event in April of 2021.

**4.0 Underground Survey**

HNTB subcontracted with COLOG, of Lakewood, CO, to perform a downhole laser survey of the mine tunnel directly beneath Route 3. A boring (B-5) was drilled from the roadway surface and penetrated the roof of the mine at a depth of 107 feet. The 3.25” ID hollow stem augers were left in the boring after drilling to keep it open and provide access for the geophysical laser scanning tool and camera (Figure 12).

The purpose of the laser scan was to view the general condition of the mine walls, floor, and ceiling, identify debris, as well as determine the size of the opening. In summary, the COLOG survey did not identify rock debris on the mine floor, and it appears the mine ceiling, floors and columns are intact. The logging operator reported water flowing down hole during the scanning procedure.



**DOWNHOLE LIDAR IMAGE OF THE TUNNEL - FIGURE 12**

## 5.0 Mine Stability

Subconsultant Wyllie & Norrish was retained to perform stability analyses of the highwall adjacent to Route 3 and of the underground tunnels that pass beneath Route 3. The analyses included borehole investigations, downhole LiDAR imagery of the south mine tunnel accessed via HNTB borehole B-5, laboratory testing, imagery from an Unmanned Aerial Vehicle (UAV), observations from ground reconnaissance, anecdotal recollections from long term mine personnel, published information, and engineering judgment.

### Rock Mass Characterization

Geologic study of the Warsaw and Burlington Limestones indicated a lack of post-lithification tectonic activity with the consequence that the units are essentially unjointed. This is consistent with anecdotal recollections of mine personnel who indicated the limestones exhibited “no vertical jointing”. They did indicate that a single fault was encountered in the west pit with 9-ft. offset, striking northwest and dipping approximately 45° to the west. The roof of the underground mines followed the Warsaw – Burlington contact and was flat lying. Contrary to the geologic evidence, observations of the current quarry walls suggested that the rock mass has a structural fabric that controls block size and shape (see previous oblique photographs). These discontinuities lack persistence, are probably syn-depositional and represent bona fide weakness planes within the limestone. Thus, for purposes of down-rating the intact limestone strength, the bedding planes and “joint-like” discontinuities were incorporated to develop conservative rock mass strength values.

The initial part of the analyses involved assignment of rock mass geomechanical parameters that would subsequently be input to slope stability and underground stability methods. Intact rock strength (from core samples), Rock Quality Designation (RQD from rock core logging) and spacing and surface properties of discontinuities were used to assign rock quality ratings in accordance with Bieniawski (1989). For the Warsaw and Burlington limestone formations this methodology yielded a conservatively estimated  $RMR_{89} = 77$ , consistent with a good to very good quality rock mass. The following parameters were used for the limestone Hoek-Brown Failure Criterion to assess the rock mass shear strength in circumstances where structural fabric does not control slope stability:

- $GSI = RMR_{89} - 5 = 77 - 5 = 72$  (as recommended by Marinos et al., 2005)
- $m_i$  constant based on rock type = **12** for limestone (Hoek et. al., 2002)
- **UCS = 8,000 psi** (conservatively downrated from UCS test average, Table 1)
- **D** (Disturbance Factor) = **0.7** (conservatively applied uniformly to entire rock mass)

The Hoek-Brown criterion defines a non-linear shear strength envelope. This was approximated by the commonly utilized Mohr-Coulomb criterion in which a linear shear strength envelope is defined by the friction angle,  $\phi$ , and cohesion, C, derived from the tangent to the Hoek-Brown non-linear envelope at the stress range applicable to the quarry walls. Thus, for input to wall stability analyses the following rock mass shear strength parameters were used:

$$\phi' = 55^\circ, C = 150 \text{ psi (for } D=0.7)$$

### Mine Highwall Stability

For stability analyses two cross sections for the west wall of the east pit adjacent to Route 3 were selected:

#### Section 7+00:

- nominal limestone slope height of 164 ft at 84° slope angle
- typical stratigraphy with 50-ft (nominal) of glacial till over limestone.

#### Section 8+70:

- nominal limestone slope height of 151 ft at 85° slope angle
- atypical stratigraphy with 70-ft (nominal) of glacial till over limestone. (corresponds to HNTB borehole B-3).

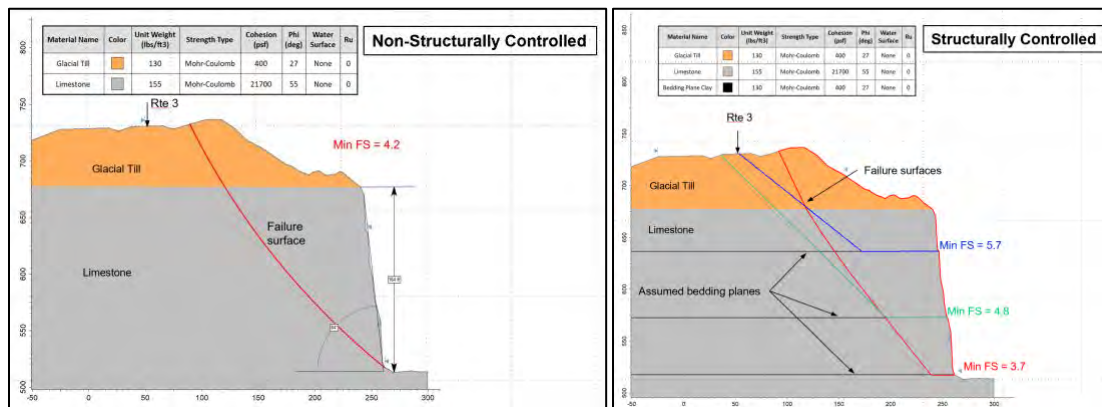
Note that sections to the north with shale and sandstone channel fill were not modelled as it was assumed the glacial till has lower strength than both rock units.

For each selected section, two models were developed: the first assuming no structural control of the failure surface (i.e. analogous to a circular material failure in soil slopes), and the second assuming partial structural control along horizontal bedding planes. The latter model conservatively assumed that clay-filled bedding planes as identified in borehole B-5 could occur anywhere within the limestone sequence (see margin photo). These planes were further assumed to be sufficiently thick to prevent rock-on-rock contact during shearing and to have shear strength parameters nominally equivalent to the glacial till. It was acknowledged that the collective assumptions relative to this model with partial structural control are improbable and represent a worst-case scenario, albeit instructive with respect to the evaluation of Route 3 longevity.



Figure 13

Limit equilibrium stability analyses employing Rocscience software Slide (ver, 6.039) with Spencer’s method (1967), yielded stability margins expressed as the Factor of Safety, FS. For permanent slopes adjacent to this public highway corridor, a minimum FS value of 2.0 is suggested for the quarry walls. For context, the typical acceptance criterion for a critical overall mine slope would be FS = 1.5 (Read and Stacey, 2009, Wyllie, 2018). The figures below summarize Spencer’s Method for the analyses and report minimum FS values for non-structurally controlled failures and structurally controlled failures of 4.0 and 3.7, respectively, assuming fully drained conditions. Given the conservatism incorporated in the geotechnical models coupled with the very favorable condition of the walls evident in the UAV video footage, these stability results are consistent with the expectation that long term overall stability of the nominal 160-foot high limestone quarry walls should not pose a risk to Route 3.



**Examples of Quarry Wall Stability Analyses – FIGURE 14**

### Progressive Rockfall Considerations

Rockfall talus aprons have developed along the base of the quarry walls and are more prevalent in the inactive west pit than in the active east pit. This long term, progressive slope degradation will continue in response to freeze-thaw processes and heavy precipitation events. To some extent, the rockfall progression will be self-stabilizing as an increasing proportion of the lower slope becomes covered with talus. Large volume events are not anticipated due to the relatively small size of blocks being shed. Mitigation at this stage is not warranted and the recommended course of action is periodic observation. In the very unlikely event that progressive rockfall begins to encroach near the MoDOT right-of-way, the quarry owner should be compelled to implement active mitigation measures.

### Underground Mine Stability

Empirical methods are typically used for characterizing rock mass parameters and designing underground openings. For this study, the Q-system has been employed. (Barton,1973,1974 and NGI, 2015):

$$Q = RQD/J_n \times J_r/J_a \times J_w/SRF$$

Applicable to the limestone, the following were assigned as tabulated below:

**“Q” Value Attribute Ratings**

<b>PARAMETER</b>	<b>RATIONALE</b> (see NGI,2015 for detail)
$RQD = 84\%$	As logged in borehole B-5
$J_n$ (joint set number) = 9	Excavated rock and rockfall talus aprons have blocks that are cubical to rhombohedral in shape (see photos from drone flights). Therefore, assume two joint sets & bedding,
$J_r$ (joint roughness number) = 3	Based on observations, joint surfaces are rough and irregular.
$J_a$ (joint alteration number) = 1	From observation, dominant surface characteristic is clean with only minor staining. Note this statement assumes that the clay partings noted in borehole B-5 at nominal depths 75 to 85 ft are anomalous and not representative of the entire limestone section.
$J_w$ (joint water reduction factor) = 1	It is assumed that the limestone sequence is fully drained based on 1) lack of seepage of rock faces from drone footage 2) lack of viable surface recharge or underground inflow to the narrow rib of rock between the east and west pits 3) quarry personnel recollection of “dusty” UG conditions
$SRF$ (stress reduction factor) = 1	Calculate ratio unconfined compressive strength (UCS) to maximum vertical stress ( $\sigma_v$ ). $UCS = 8000 \text{ psi}$ $\sigma_v = \text{avg unit weight} \times \text{depth of cover} = 150 \text{ pcf} \times 107 \text{ ft} = 111.5 \text{ psi}$ $UCS/\sigma_v = 8000/111.5 = 72$

The first quotient, comprised of RQD and  $J_n$ , is a rough measure of block size.  $J_r/J_a$  is a measure of the ease at which blocks of rock may rotate or slide as this incorporates the joint roughness and alteration which is an indication of inter-block shear strength. The  $J_w/SRF$  term simulates active stress. For the limestone formations, the following summation results:

$$Q = RQD/J_n \times J_r/J_a \times J_w/SRF$$

$$Q = (84/9) \times (3/1) \times (1/1)$$

$$Q = 28$$

Parallel tunnels connecting the Randolph Quarry’s east and west pits pass beneath Route 3. The tunnels have a nominal 40-ft wide by 25-ft high cross section and are transverse to the highway alignment with a right skew of 61° as measured from the centerline of the highway to the alignment of the tunnels. The distance between tunnel centerlines is 90-ft providing for a 50-ft wide rib pillar between the tunnels. Issues for Route 3 are the stability of the rib pillar and the stability of the tunnel roof.

Pillar stability was evaluated by comparing the ratio of the pillar strength to the vertical stress acting on the pillar. The assigned Hoek-Brown limestone rock mass parameters were:

- **GSI = 72**
- **$m_i = 12$**
- **UCS = 8,000 psi**
- **D (Disturbance Factor) = 0.7**

From these values, Rocscience software RocLab predicted a “global strength” of **1864 psi** appropriate to the pillar. In all likelihood, this is a conservatively low estimate due to the downrated UCS test value and to probable superior perimeter blasting employed in the underground workings, thereby resulting in less blast damage and a lower “D” factor.

The trailing figure 15, summarizes the estimated vertical stress acting in the pillar with the assumption that the entire rock and soil volume above the tunnels is supported by the rib pillar. As shown, this yields an estimated vertical stress in the rib pillar,  $\sigma_p$ , between 200 and 300 psi, depending on the assumption for rock volume carried by the pillar (i.e. degree of load arching onto the abutting rock).



**Rib Pillar Vertical Stress- FIGURE 15**

The ratio of pillar strength (1864 psi) to vertical stress,  $\sigma_p$ , indicates a **Factor of Safety > 6** consistent with the shallow cover over the tunnels and the strength of the limestone. It is concluded that the rib pillar has adequate long-term stability. As collateral evidence to the foregoing analysis, two pillar configurations in the historic underground mine with differing extraction ratios (ER) were analyzed:

1. Rectangular pillar (150 ft x 30ft), ER = 68.8%      Calculated  $\sigma_p = 359 \text{ psi}$     FS=5
2. Rectangular pillar (50 ft x 30 ft), ER = 76.6%      Calculated  $\sigma_p = 478 \text{ psi}$     FS~4

It was recalled by mine personnel that the earliest pillars were 40 ft x 40ft on a checkerboard pattern (ER unknown) and began to spall (“hourglass”) leading to a redesign with rectangular pillars. These rectangular pillars proved superior to the square pillars consistent with the above analysis.

Two approaches were employed to assess roof stability of the tunnels. The first was the empirical method using the Q system as described in NGI(2015). This is a well-tested design

methodology dating from the early 1970's. The second was the closed-form theoretical formula to calculate the stability of a bedrock roof beam with horizontal strata. The margin figure below shows the relationship between rock mass quality (i.e. expressed as "Q" value) and roof span (metric presentation) after NGI (2015). For the limestone penetrated by the tunnels beneath Route 3, the estimated Q value is 28. If one were designing the span for an unsupported roof, Figure A-8 shows the corresponding ratio of Span/ESR = 8. The Excavation Support Ratio (ESR) is a factor that takes account of the performance risk for a given type of underground facility. For permanent mine openings, water supply tunnels, hydro power tunnels, the recommended value for ESR is 1.6. This is judged equivalent to the project case with a public highway passing over a tunnel. Using this value, the computed unsupported span is:

The second was the closed-form theoretical formula

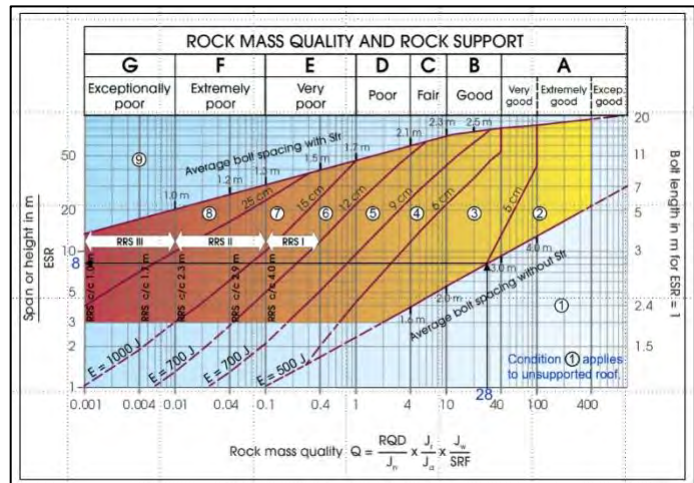


Figure 16

$$\text{Allowable Span} = \text{ESR} \times 8 = 1.6 \times 8\text{m} \times 3.28 = 42 \text{ ft.}$$

The twin tunnels have nominal spans of 40-ft. and are therefore deemed acceptable for long term stability based on empirical design methodology.

The second evaluation calculated the ratio of the roof beam tensile strength to the maximum tensile stress induced to the beam from the overlying strata. This stress was estimated from the formula for a simply supported beam with fixed ends:

$$\sigma_t = \gamma L^2 / 2T + PL^2 / 2t^2 \quad (\text{after Goodman, 1989})$$

$\sigma_t$  = maximum tensile stress

$\gamma$  = unit weight of roof beam = 155 pcf for limestone

L = span = 40 ft.

t = beam thickness (variable in the analysis)

P = pressure due to overlying strata (varies with beam thickness)

The maximum possible limestone beam thickness is 31-ft. if it acts as a monolithic unit. Bedding plane partings (shale, clay etc.) within the Warsaw Formation could reduce this beam thickness. For demonstration purposes, it was assumed the beam thickness could vary from 2-ft to 31-ft and for each value would have to support the limestone, sandstone, shale and glacial till above. The vertical stress at the tunnel crown was calculated at 100 psi (14,475 psf). Utilizing the intact tensile strength of the limestone at 667 psi, the relationship between beam thickness and maximum roof stress was

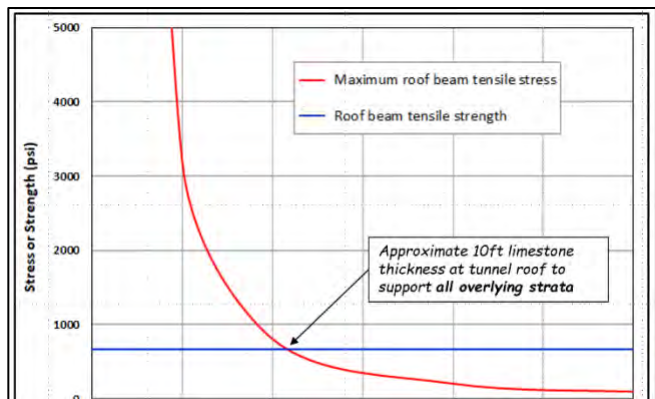


Figure 17

plotted (Figure 17). This demonstrates that for the worst-case assumption in which **all overlying strata** must be supported by the roof beam, a minimum thickness of slightly more than 10-ft is required. In actuality, the limestone above such a beam would also be self-supporting and only the glacial till and possibly channel deposits (shale/sandstone if present) would require support. Furthermore, there is no evidence in borehole B-5 of a persistent bedding plane parting that could potentially define a roof beam within 10-feet of the tunnel crown (see photo below).

On the bases of the empirical and numerical analyses, it was concluded that tunnel roof spans should be stable.

## 6.0 Remediation Alternatives

### Approaches to Slope Stability

There are four basic ways to approach slope stability in this case.

- A. Avoid
  - a. Relocate the roadway
  - b. Complete removal of the unstable materials
  
- B. Reduce Driving Forces
  - a. Change roadway line or grade
  - b. Reduce the driving weight
  
- C. Increase Resisting Forces
  - a. Use a buttress or a toe berm
  - b. Structural systems, retaining walls
  - c. Anchors
  
- D. Increase Internal Strength
  - a. Drain water from the subsurface
  - b. Use reinforced backfill
  - c. Install in-situ reinforcement

The following options were carried forward from the basic approaches:

#### Option 1 – Lower the Grade on the Existing Alignment

Lower the grade on the existing alignment. Remove and replace slide mass with rock fill.

##### Pros:

- Less additional right of way required.
- Provides adequate road and site drainage
- Creates visual and safety block of quarry and operations
- Less construction complexity
- Proven MoDOT methodology
- Multiple contractors qualified to bid and construct.

##### Cons:

- Does not provide an adequate distance from the existing landslide and potential future instability

- Requires relocation of waterline
- Requires lowering the existing entrance on the west side

### **Option 2 – Move Roadway to the West with same general vertical geometry**

Move the roadway centerline 15 to 25 feet west, retain similar vertical geometry. Remove and replace slide mass with rock fill.

#### **Pros:**

- Less construction complexity
- Proven MoDOT methodology
- Multiple contractors qualified to bid and construct

#### **Cons:**

- Creates complexity in roadway design with reverse curves and superelevation considerations.
- Does not provide an adequate distance from the existing landslide and potential future instability
- Requires relocation of waterline
- Does not create visual safety block to the quarry
- Requires additional right of way

### **Option 3 - Move Roadway to the West and Lower the Grade – Preferred**

Move the roadway centerline approximately 15-feet west and lower grade approximately 8 feet at location of present landslide. Remove and replace slide mass with rock fill.

#### **Pros:**

- Provides adequate road and site drainage
- Creates visual and safety block of quarry and operations
- Less construction complexity
- Proven MoDOT methodology
- Multiple contractors qualified to bid and construct

#### **Cons:**

- Creates complexity in roadway design with reverse curves and superelevation considerations.
- Requires relocation of waterline
- Requires additional right of way
- Requires lowering the existing entrance on the west side

### **Option 4 – Do Nothing**

Do nothing and leave Route 3 closed. Create a permanent detour or reconfigure state route system. Some maintenance will be required as the slope may continue to fail and foul the adjacent quarry.

A big picture detour would relocate the entire roadway to the west of the abandoned west pit. The roadway right of way could be swapped with the existing roadway location and the quarry could then mine the rock between the two pits.

#### **Pros:**

- Minimal costs

**Cons:**

- Continued impact to quarry
- Inconvenience to travelling public
- Increased emergency response times

**Option 5 – Retaining Walls or Mechanical Slope Stabilization**

Retaining walls and or mechanical stabilization were eliminated early on due to cost, construction complexity, and access to working areas. For Option 5 a soldier pile wall and lagging wall with tiebacks was studied. One or two levels of anchors may be required.

**7.0 Landslide Repair Stability Analyses and Recommendations**

The previous study phase included back-analyses of the original slope failure and preliminary analyses of a proposed solution for the landslide repair.

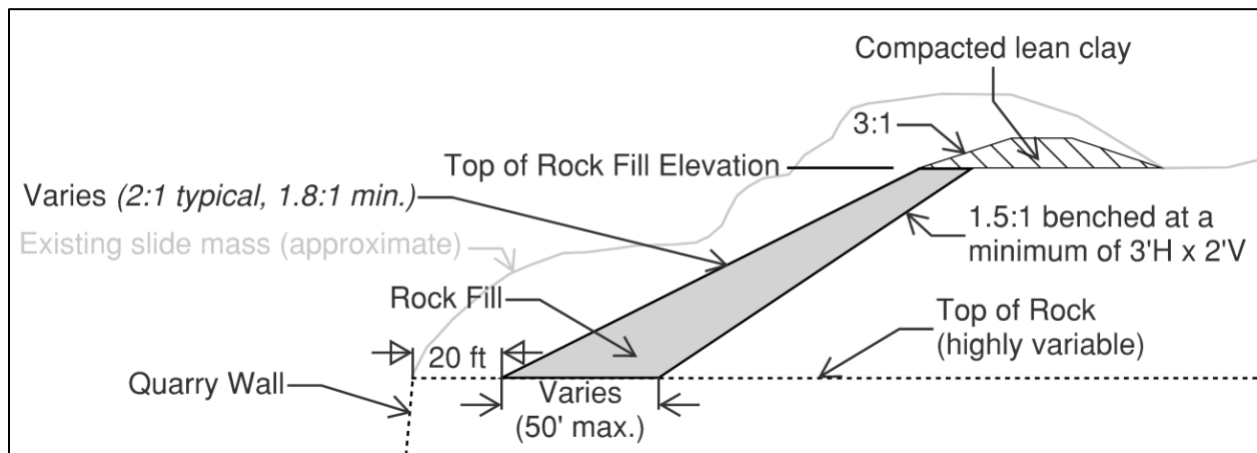
In the final design phase, the roadway has been relocated away from the slide location approximately 30-feet west of the existing alignment and approximately 14-feet lower than the existing grade. The landslide repair solution evaluated in final design further develops the idea considered during preliminary design, which included: (1) Excavate and remove slide mass to top of rock, (2) Construct a substantial rock fill slope, from the bottom up, capped by a compacted soil embankment, and (3) Regrade as necessary to transition from rock fill to stable existing slopes.

Final design of the Rock Fill landslide repair was subject to the following geometric constraints:

- For safety, toe of Rock Fill must be offset 20-feet from the quarry wall
- Base width of Rock Fill varies based on global stability analyses, with a maximum base width of 50-feet.
- Rock Fill slope must be no steeper than 1.8H:1V.
- The back of the Rock Fill zone is placed against the native soil slope at a 1.5H:1V slope stepped with excavation steps of at least three feet horizontal and two feet vertical.
- Compacted soil embankment slopes above Rock Fill must be no steeper than 3H:1V.
- Top of compacted soil embankment must be at least 4 feet above the roadway crown.

Global stability was analyzed using GeoStudio 2021.4 (SlopeW) and Spencer's method. As the project is in cut, drained conditions are anticipated to be critical. At locations where rock fill is needed to repair the slide and provide long term stabilization of the roadway, a minimum Factor of Safety (FS) of 1.5 required. Beyond the slide repair limits, the typical minimum FS of 1.3 for roadway embankments and backslopes is considered adequate.

The top of rock surface is highly variable throughout the site. Based on available borings and other geologic information, an interpreted top of rock surface was developed, and the rock fill landslide repair applied that met the required factors of safety. A schematic of the final landslide repair is shown below. Figure ???



**Schematic of Final Landslide Repair – FIGURE 18**

The overall three-dimensional shape of the rock fill repair is estimated to be concave relative to the new roadway alignment, similar to an amphitheater, due to the variable bedrock surface. This concavity is most nearly tangent to the roadway alignment where bedrock is deepest, at approximately Sta. 107+50, which is also the estimated center of the original slide mass. Both upstation and downstation of Sta. 107+50, the rock fill sections gradually taper out to match existing grading. The rock fill repair was applied until the existing grading achieved a satisfactory FS with respect to overall slope stability. Based on the stability analyses, the transitions from rock fill to existing grading are at Sta. 105+50 to the north and Sta. 109+50 to the south.

The rock fill repair provides a drainage path for controlling and lowering the variable groundwater surface within the landslide repair area, which is important to the long-term stability of the slope. Groundwater and surface infiltration will be directed along the base of the rock fill section and drain by gravity out of the rock fill at the low point at Station 107+50 to exit beyond the toe towards the quarry cut face. To limit surface infiltration into the rock fill, the embankment above the rock fill should be cohesive, lean clay soil. For long term stability of the roadway and adjacent slopes, roadway ditches should be undercut to a depth of 2 feet and replaced with cohesive lean clay soil.

At station 107+50, which has 1.8H:1V slope angle, the factor of safety was slightly lower than 1.5 but it is our judgement that this value is conservative as the two-dimensional global stability model does not account for beneficial three-dimensional effects, such as arching between adjacent sections. A typical rock fill slope angle of 2H:1V has been maintained at most sections while the rock fill base width (and thus the overall rock fill thickness) has been optimized in proportion to the total height of the slope above top of rock.

North of Sta. 105+50, slope stability is not a concern as the slope adjacent to the quarry face is primarily composed of shale and sandstone. While shale and sandstone are susceptible to long-term raveling and weathering, the existing slopes are anticipated to remain stable at the present steep slope angle.

From approximately Sta. 108+75 to Sta. 111+50, a bench is present along the existing slope, which is likely a haul road from a previous configuration of the quarry. From Sta. 109+50 to the south, soil slope stability of the east slope is not a concern due to the presence of the bench in combination with an overall decrease in the roadway elevation from north to south.

Stability of the soil slopes adjacent to the West quarry pit were evaluated at Sta. 109+25, Sta. 110+00, and Sta. 114+00. By observation, the west soil slopes are densely covered with trees and other vegetation. The analyses indicate that the existing west soil slopes are stable without modification.

**Construction** – We hoped to have photographs and a write up of the construction, however the bids were delayed, and the project is not underway as of this writing.

## REFERENCES

- Barton, N. (1973). Review of a new shear strength criterion for rock joints. *Engineering Geology*. Vol. 7, pp 287-332.
- Barton, N., Lien, R. and Lunde, J. (1974). Engineering Classification of Rock Masses for the Design of Tunnel Support. *Rock Mechanics and Rock Engineering* 6(4), 189-236.
- Bieniawski, Z.T. (1989). “Engineering Rock Mass Classifications.” Wiley and Sons, New York. 251pp.
- Goodman, R.E. (1989). *Introduction to Rock Mechanics*, Second Ed., John Wiley & Sons, 562 pp.
- Hoek, E., C. Carranza-Torres, and B. Corkum (2002). Hoek-Brown criterion - 2002 edition. NARMS-TAC Conference. Toronto, pp 267-273.
- Marinos, V., Marinos, P. and Hoek, E. (2005). The geological strength index; applications and limitations. *Bull Eng Geol Environ*, 64: pp. 55 – 65.
- NGI, 2015, *Using the Q-system – Rock mass classification and support design*, Allkopi AS, Norway. 54pp.
- Read, J and Stacey, P (2009). *Guidelines for Open Pit Slope Design*, CSIRO Publishing, 496 pp.
- Spencer, E. (1967). A method of analysis of the stability of embankments assuming parallel inter-slice forces. *Geotechnique*, Vol. 17, pp 11-26.
- Wyllie, D.C. (2018). *Rock Slope Engineering Civil Applications*. CRC Press. Fifth Edition. 568 pgs.

## **SR 112 / Clallam Bay Landslides – Characterization and Mitigation**

**Gabriel Taylor, LEG**

WSDOT State Geotechnical Office

PO Box 47365

Olympia, Washington, 98504-7365

(360) 480-6821

[taylorg@wsdot.wa.gov](mailto:taylorg@wsdot.wa.gov)

Prepared for the 72<sup>nd</sup> Highway Geology Symposium

### **Acknowledgements**

The author would like to thank the individuals/entities for their contributions in the work described:

Rebecca Garriss, LEG – WSDOT Geotechnical Office  
Jennifer DiGiulio, LG – WSDOT Geotechnical Office  
Katelyn Card – WSDOT Geotechnical Office  
Kerry Cooper – WSDOT Geotechnical Office  
Jesse Alton, WSDOT Environmental Services Office  
Gerald Page, WSDOT Area 3 Maintenance  
Dan McKernan, WSDOT Port Angeles Project Engineering Office

### **Disclaimer**

Statements and views presented in this paper are strictly those of the author(s), and do not necessarily reflect positions held by their affiliations, the Highway Geology Symposium (HGS), or others acknowledged above. The mention of trade names for commercial products does not imply the approval or endorsement by HGS.

### **Copyright Notice**

Copyright © 2022 Highway Geology Symposium (HGS)

All Rights Reserved. Printed in the United States of America. No part of this publication may be reproduced or copied in any form or by any means – graphic, electronic, or mechanical, including photocopying, taping, or information storage and retrieval systems – without prior written permission of the HGS. This excludes the original author(s).

### **ABSTRACT**

In November 2021, during a period of intense rainfall, an unstable hillslope collapsed above a coastal highway on the north coast of the Olympic Peninsula on Washington State Route 112. The debris slide buried approximately 200 feet of the highway with 15- to 20-feet of debris and extended hundreds of feet into the Strait of Juan de Fuca. This large debris slide blocked the sole access to coastal communities west of Clallam Bay, WA, including the Makah Reservation. By comparing pre-debris slide lidar to a post-debris slide UAV-generated ground surface, WSDOT developed a strategy to regrade and stabilize the landslide. Stabilization was complicated by the discovery of an older landslide that had been buried by the November 2021 event. The pre-existing landslide was uncovered and further destabilized during the project's grading operations. Emergency stabilization measures were not adequate to mitigate the reactivated landslide and a subsequent phase of geotechnical work was conducted to develop permanent stabilization measures. Both landslides were found to have resulted, at least partially, from poor land use activities. This case-history summarizes the mechanisms that caused the failure and the methods employed to characterize and stabilize this complex landslide.

## **BACKGROUND**

Landslides affecting Washington State Route 112 (SR 112) present an ongoing maintenance and engineering challenge to the Washington State Department of Transportation (WSDOT). Factors contributing to landslides affecting SR 112 include weak subsurface materials, coastal geography, a wet climate (annual precipitation over 80 inches), and land use. Slope failures that block the highway, impede drainage, or erode embankments below the highway are common maintenance concerns throughout the year, especially during the winter. Large-scale landslides that destroy hundreds of feet of highway have resulted in months-long full closures, most recently in 2021, 2009, and 1990.

The subject landslides are located approximately one mile west of Clallam Bay, WA, on SR 112 at milepost 15.85, on the coast of the Strait of Juan de Fuca. The highway consists of two approximately 12-foot-wide travel lanes with narrow paved shoulders. The embankment is approximately 20 feet tall on the north side, where it slopes down to the beach. The south side of the highway consists of a ditch at the base of an approximately 300-foot-tall slope oriented between 30° and 35°. A single cross-culvert conveys water from a drainage upslope to the beach below the highway.

The first of the subject landslides was activated in approximately 2006 and remains active. The second landslide became active in November 2021 and was stabilized in 2022.

## **LAND USE ACTIVITIES CONTRIBUTING TO LANDSLIDES**

The first observations of ground deformation at this location were reported in January 2006, by Maintenance, as a seasonal uplift or 'heave' of the eastbound lane at milepost 15.85. Based on the regional geology and frequency of landslides in this area, the ground deformation was presumed to be related to a previously unknown upslope landslide.

The emergent 'heave' issue was contemporary with development of an RV Park (Coho Estates) on the adjacent property to the west, a mapped landslide<sup>1</sup>. The RV Park development involved constructing roads and drainage, mining of an upslope aggregate source, wasting unsuitable materials, placing fill, and building pads for RVs and trailers. The development resulted in a 2005 fill failure that caused erosion and flooding on the highway immediately west of the subject site. Outreach to regulatory agencies indicated that the development was likely occurring without adequate oversight, however no enforcement action was taken, and the development was completed. As daily traffic counts for the highway and the cost to maintain the 'heave' were low, no geotechnical investigation was conducted.

---

<sup>1</sup> Washington State Department of Natural Resources Geologic Hazard Maps

## 2021 DEBRIS SLIDE

On November 14-15, 2021, an atmospheric river brought heavy rain into northwest Washington. Total rainfall for this two-day event was measured in Forks, WA (approximately 20 miles SW) as 10.5 inches, with 7 inches of rain occurring on November 15<sup>2</sup>. On November 15, 2021, a large debris slide initiated upslope of the highway, below a private gravel road that connects Coho Estates to its aggregate source.

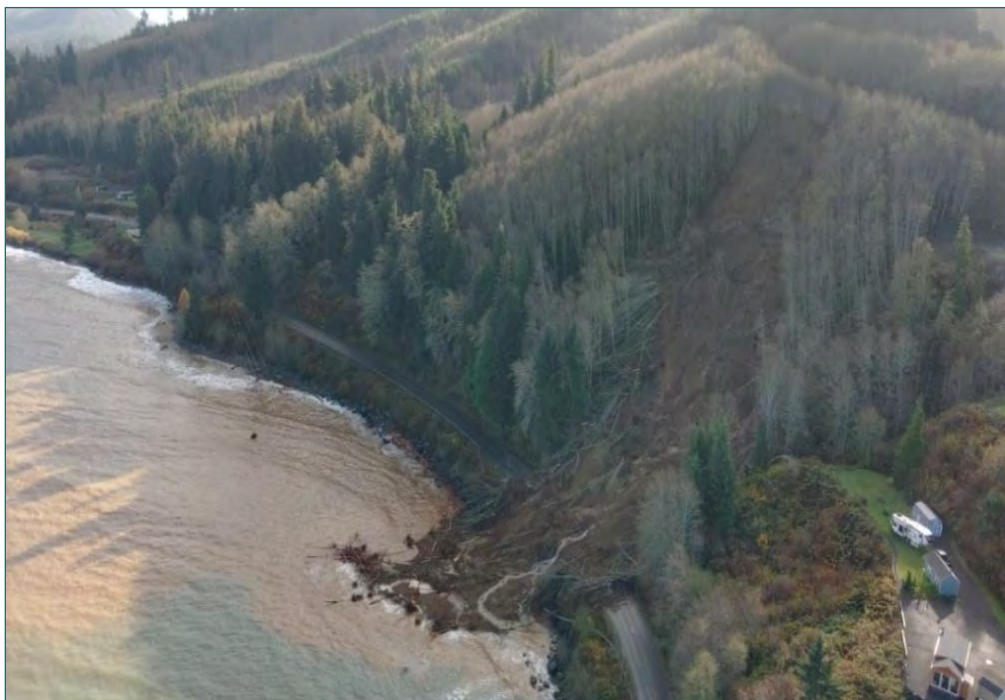


**Figure 1: Photograph of the debris slide taken from a helicopter on November 16, 2021**

We estimate that the debris slide mobilized tens of thousands of cubic yards of side cast material that had been dumped below the gravel road, as well as weak native soils present along the lateral margins and toe of the landslide. We estimate that approximately one hundred thousand cubic yards of debris mobilized in the event. The landslide buried SR 112 in nearly 20 feet of debris and extended several hundred feet north into the Strait of Juan de Fuca (Figure 2). The debris slide was approximately 340 feet high, 800 feet long and up to 400 feet wide.

The mobilized debris bifurcated around a resistant knob of rock and trees mid-slope, forming two lobes. The larger lobe (west debris lobe) buried and destroyed approximately 200 feet of SR 112, broke the Clallam County PUD water line that was buried under the ditch, and entered the Strait of Juan de Fuca. The smaller lobe (east debris lobe) accumulated on a forested bluff

---

<sup>2</sup> NOAA National Weather Service website, accessed December 1, 2021

72<sup>nd</sup> HGS 2023: Taylor

above SR 112 (Exhibit 3). Debris also accumulated at the base of the headscarp, where it impounded water and formed a sag pond.

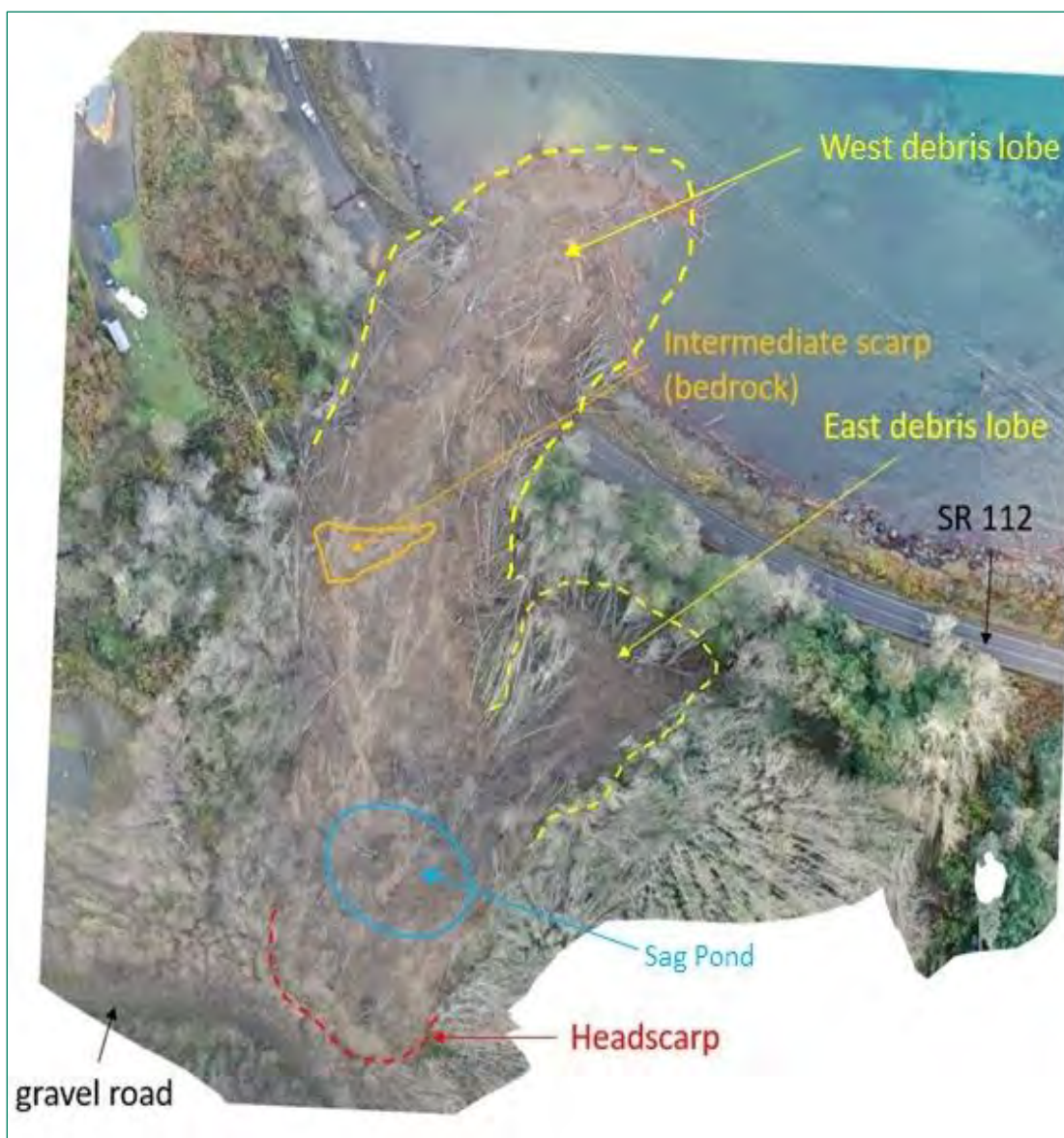


**Figure 2: Orthomosaic photo from 11/21/2021 UAV flight, annotated with major debris slide features**

Surface water was observed flowing from a drainage ditch on the adjacent property, through the lower portion of the debris slide area. Prior to the debris slide, this discharged water flowed through a steeply incised gully at the base of the slope and then under SR 112 through a cross-culvert. The gully and culvert were both destroyed by the debris slide. This surface water was later found to be a contributing factor to the 2006 heave issue, which is later referred to as the 'secondary landslide'.

72<sup>nd</sup> HGS 2023: Taylor

On November 25-28, a subsequent storm brought approximately 8 inches of rain into the area over a four-day period, with approximately 3.5 inches falling on the last day of the storm<sup>3</sup>. During this event, the headscarp collapsed, retrogressing the landslide upslope, into the gravel road. Debris from the headscarp collapse, consisting of fill (soil, boulders, stumps), impacted the sag pond and remobilized much of the downslope debris. Most of the debris from this event flowed into the smaller east lobe, overtopped the debris that had accumulated on November 15, and flowed over the bluff onto SR 112. This event further damaged the upslope gravel road and laterally expanded the debris on the highway to the east by approximately 200 feet. Remobilized debris on the west lobe accumulated on the slope above the highway. Deformation of a temporary flexible water line that Clallam County had installed over the debris suggests that this event resulted in approximately 40 feet of additional movement of the west debris lobe.

### **GEOTECHNICAL INVESTIGATION (PHASE 1)**

Geotechnical investigation of the debris slide consisted of a review of geologic mapping and literature, geologic reconnaissance, and unmanned aerial vehicle (UAV) flights. These methods were employed to develop an initial characterization of the landslide geometry and to monitor ongoing ground movement. The geometric information was later used for development of geotechnical recommendations for landslide stabilization, quantity estimates, and contract plans.

The site is mapped<sup>4</sup> as being underlain by landslide deposits and bedrock associated with the sedimentary rocks of the Pysht Formation. The site is flanked by mapped landslide deposits, nearby to the east and immediately adjacent to the west. Sedimentary rock bedding is mapped as dipping approximately 35° to the northeast.

Geologic reconnaissance and UAV imagery were used to monitor movement of the debris slide over the initial two-week period. Geologic reconnaissance also provided initial site characterization and informed our understanding of the landslide mechanisms and geometry. Geologic reconnaissance identified areas where there was poorly placed fill exposed in the headscarp, thick slide debris accumulation, seeps, and ponded surface water. Discontinuity measurements were collected from bedrock outcrops and were found to conform to published geologic mapping. Based on recurring site visits and UAV flights, we determined that debris slide activity effectively ceased after November 28, 2021.

---

<sup>3</sup> NOAA National Weather Service website, access December 1, 2021

<sup>4</sup> Snavely, P.D., Macleod, N.S., Niem, A.R., Minasian, D.L., Pearl, J.E., and Rau, W.W., 1993, Geologic map of the Cape Flattery, Clallam Bay, Ozette Lake, and Lake Pleasant quadrangles, northwestern Olympic Peninsula, Washington, U.S. Geological Survey, Miscellaneous Investigations Series Map I-1946, 1:48,000

72<sup>nd</sup> HGS 2023: Taylor

UAV flights were conducted on November 17, 2021, November 21, 2021, and December 2, 2021. The November 17, 2021, UAV flight provided initial aerial reconnaissance of the debris slide. Imagery from subsequent UAV flights were used with Structure from Motion software to develop a Digital Terrain Model (DTM) of the debris slide area. The DTM surface was used in conjunction with pre-landslide lidar<sup>5</sup> to conduct change analysis and to develop project geometry design cross-sections, stabilization plans, and estimations of material quantities.

### **STABILIZATION WORK (PHASE 1)**

Due to the observed instability of the debris remaining on the slope and the shallow depth to intact materials (including bedrock), we pursued a removal strategy for stabilization of the debris slide area. The intent was to remove slide debris and hazard trees, and to grade the ground surface to a more uniform and stable slope. Drainage channels would also be constructed to control surface water. Our recommendations were provided in a geotechnical memorandum<sup>6</sup> and used to develop a construction contract (009766). The contract was awarded to a contractor for \$1.2 million on February 1, 2022.

During the stabilization work, the headscarp was graded to an approximately 2H:1V slope before any other work downslope was conducted. This required realignment and repair of the private gravel road. To prevent destabilized trees from potentially falling into the grading area during construction, falling onto the highway, or interfering with future drainage, we removed approximately 200 small trees (mostly poplar and alder) that were situated along the lateral scarps of the debris slide and the trees that were still upright in the debris slide area.

Although we recommended that the approximately 40,000 cubic yards of landslide debris be removed from the top-down, the contractor elected to clear the highway first, to allow haul trucks and equipment access to both sides of the work zone. Debris removal then resumed at the top of the landslide area and proceeded downward. Slide debris varied in thickness and was considered to include all material that was above the elevation of the planned final graded surface. Some “field-fitting” and adjustments to grading plans were expected. Undulations following natural bedrock outcrops and natural slope breaks were acceptable deviations from the planned final ground surface. Debris ranged from zero thickness (where bedrock was exposed) to approximately 15-20 feet in the “upper sag pond area” and the vicinity of the buried highway. Debris included soft saturated soils, logs, stumps, and boulders. Debris was removed and wasted off-site. Boulders were stockpiled nearby at the community harbor and jetty.

---

<sup>5</sup> Olympics North Opsw 2018

<sup>6</sup> May 16, 2022, WSDOT Geotechnical Memorandum, MP 15.85 Clallam Bay Debris Slide

72<sup>nd</sup> HGS 2023: Taylor

Following debris removal, drainage channels were constructed to ensure positive drainage of water to the new highway cross-culvert. Drainage channels were constructed to be approximately 12-feet-wide and 3-feet-deep, with 6-foot-wide side slopes oriented at approximately 2H:1V. To stabilize the drainage channels and prevent them from eventually filling in with fine-grained material, they were lined with a geosynthetic and covered with a minimum of 12 inches of quarry spalls. The drainage channels drained to a new culvert installed under SR 112.

Once the debris removal and drainage worked was completed, erosion control, roadway resurfacing, and new guardrail were installed.

### **Remobilization of the 'Heave' (Secondary Landslide)**

On March 18, 2022, during execution of Contract 9766 and on the day the highway was scheduled to reopen to public traffic, the Geotechnical Office received a report of the eastbound lane of SR 112 heaving upward, approximately 16 inches at MP 15.85. This heave occurred in the same location that it had been observed since January 2006. The heave was larger in magnitude and more rapid than had been observed previously and delayed the reopening of SR 112.

We determined that the heave area, which we refer to as the 'secondary landslide' was a reactivation of the 2006 landslide. This 'secondary landslide' had been periodically uplifting the eastbound lane since 2006 and was buried by the November 2021 debris slide. The 'secondary landslide' was reactivated following grading activity, which removed material from the base of the slope and unloaded the toe.

During our March 18 site visit, we excavated a test pit (TP-1-22) in the heave area of the highway to a depth of approximately 6 feet below the highway elevation. The landslide failure plane was exhibited in the test pit as a fracture seeping water that deformed visibly over the period of approximately 30 minutes that the test pit was left open. The floor of the test pit was found to consist of a very dense deposit of granular material that we interpreted at the time as weathered bedrock.



**Figure 3: Test pit excavated into the ‘heave’ area with paint marks denoting the failure plane**

Following these observations, the test pit was expanded approximately 5 feet upslope and 50 feet laterally to the west and then backfilled with boulders that had been previously removed from the slide debris and stockpiled at the community jetty. The expanded and backfilled test pit served as an ‘emergency shear key’, a short-term landslide mitigation measure. Following these emergency stabilization measures, the highway was repaired and opened to traffic.

Our office conducted limit-equilibrium analysis to evaluate the efficacy of the emergency shear key that was implemented during construction to mitigate the reactivated landslide. We found that the emergency shear key provided a minor increase in Factor of Safety (FS) and was insufficient as a permanent stabilization measure. We also found that stability of the ‘secondary landslide’ was sensitive to groundwater elevation. Based on these results, we produced a second geotechnical memorandum<sup>7</sup> which recommended that a ‘tightline’ be installed to capture and control the water being discharged from the adjacent property and to convey it under the roadway to the beach. The tightline (a 30-inch-diameter pipe) was installed in July of 2022.

---

<sup>7</sup> May 16, 2022, WSDOT Geotechnical Memorandum, MP 15.85 Clallam Bay Landslide Repair – Secondary Landslide



**Figure 3: July 2022 installation of tightline to capture water draining from adjacent property**

Based on our findings, and our expectation that the emergency shear key and tightline were not adequate to permanently stabilize the landslide, we initiated a second phase of investigation and mitigation design.

### **GEOTECHNICAL INVESTIGATION (PHASE 2)**

Phase 2 of the geotechnical investigation expanded upon previous work and consisted of additional geologic reconnaissance, collection of terrestrial lidar data, geotechnical borings, laboratory testing, monitoring of instrumentation installed in the boreholes, review of a boring log provided by Clallam County PUD, a seismic refraction survey, and additional geotechnical analysis.

#### **Terrestrial Lidar**

WSDOT collected terrestrial lidar data of the area on March 23, 2022, following the stabilization work for the debris slide. This lidar-generated surface was used for additional change analysis and for design of the permanent stabilization of the 'secondary landslide'.

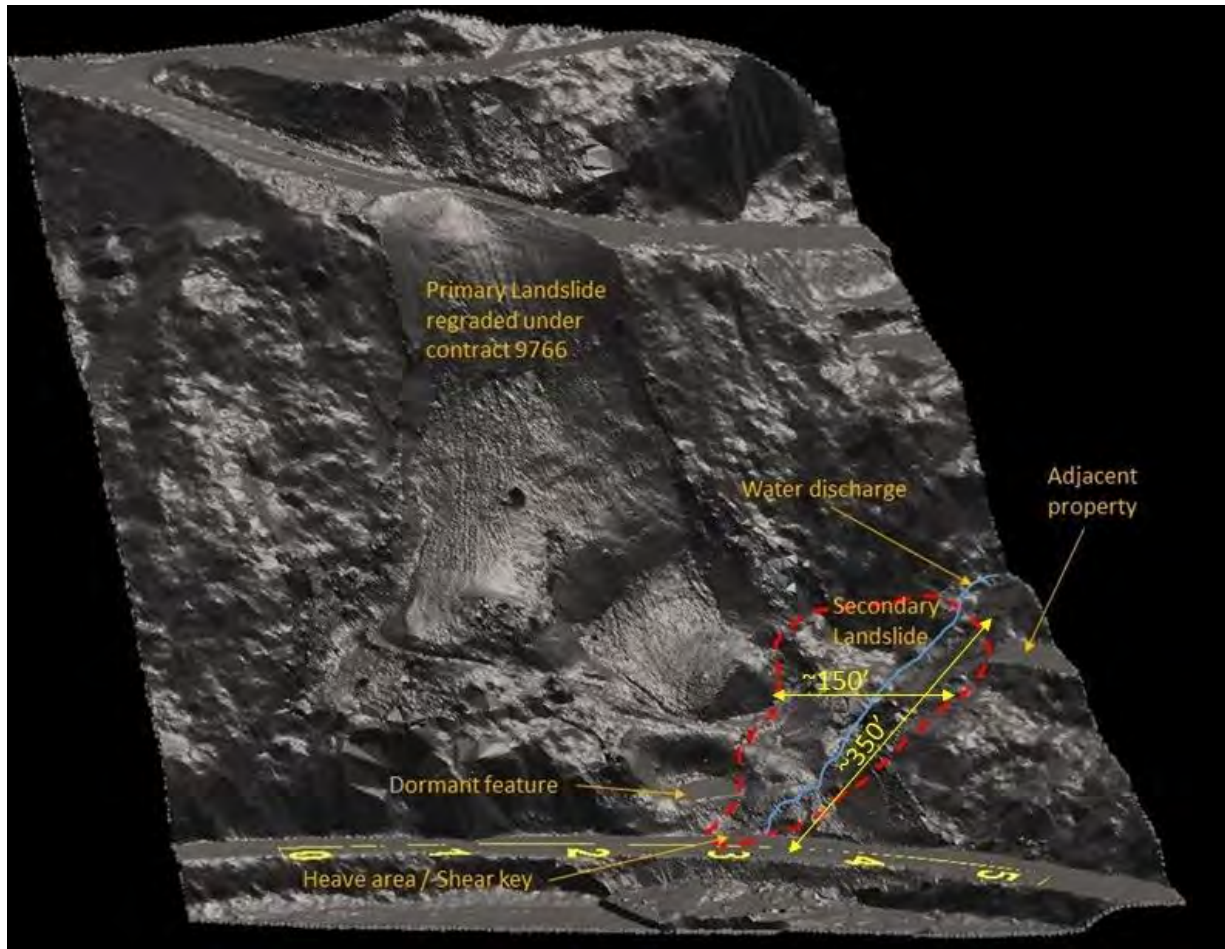


**Figure 4: Annotated terrestrial lidar hillshade showing the approximate limits of the 2006 'secondary landslide' with a red dashed line.**

### Geotechnical Borings

Three test borings were drilled in the body of the landslide, upslope of the heave area in 2022. The upslope test borings were advanced to depths of approximately 60 to 70 feet below ground surface. Two test borings were drilled in the ditch along the south side of SR 112 in 2023. The test borings in the ditch were advanced to depths of approximately 30 to 40 feet below ground surface. All borings were advanced using wet rotary drilling methods and a casing advancer system.

Disturbed samples were generally obtained in conjunction with the Standard Penetration Test (SPT) at a frequency of two per 5-foot interval. A triple-tube core barrel system was used to advance and collect samples through boulders and bedrock. Boring CB-2p-22 was drilled adjacent to CB-1si-22 for the purposes of installing a piezometer and no samples were taken or SPT test conducted. Measurement while drilling (MWD) technology was employed in the 2023 borings in the SR 112 ditch. A WSDOT drill crew inspector observed the drilling and sampling

72<sup>nd</sup> HGS 2023: Taylor

activities, collected soil samples, and completed a visual classification of the recovered samples. The samples were returned to our laboratory for further review by our staff and selection of samples for laboratory testing.

### **Laboratory Testing**

The WSDOT Materials Laboratory performed laboratory tests on selected soil and rock samples for the purposes of classification and evaluation of soil properties. Laboratory testing included natural moisture content, Atterberg Limits (plasticity), grain size distribution (including hydrometer), remolded ring shear testing, and unconfined compressive strength (UCS) testing of retained rock core. Laboratory testing was performed in general accordance with appropriate American Society for Testing and Materials (ASTM) and American Association of State Highway and Transportation Officials (AASHTO) test methods.

### **Slope Inclinometers**

Slope inclinometer casing was installed in geotechnical borings CB-1si-22 and CB-3si-22, upslope of the heave area and within the body of the 'secondary landslide'. Installation of slope inclinometer casing allows an inclinometer probe to be deployed into a borehole to measure borehole vertical orientation (tilt), on two axes (longitudinal and transverse to the landslide), at 2-foot intervals. The first measurement provides a baseline for subsequent measurements. Measurements are typically repeated, over a period of several days or weeks, to allow for an analysis of change along the borehole profile and a determination of depth to the shear zone.

Due to observed landslide movement during drilling of the slope inclinometer borings, we deployed a 'poor man's inclinometer' in each slope inclinometer borehole. A poor man's inclinometer consists of a steel pipe (or similar) connected to a rope of known length. The steel pipe is lowered to near the bottom of the borehole and secured to the top of the monument with the rope. If the borehole casing deforms or shears before the initial inclinometer reading, the steel pipe is unable to be withdrawn past the shear zone and a measurement of rope can provide an approximate height from the bottom of the borehole to the landslide shear zone.

Both inclinometer casings deformed before the inclinometer probe could be deployed to take baseline measurements. Fortunately, the poor man's inclinometers allowed for approximate measurements to the depth of the shear zone. An inclinometer probe was later lowered in the boreholes, to the allowable depth, and measurements of the casing were taken on three occasions over a period of approximately four weeks. These inclinometer probe measurements supported the approximate depth to the shear zone provided by the poor man's inclinometers and indicated that the deformation was most pronounced in the first week after installation, and then slowed significantly.

## Groundwater Monitoring

A piezometer was installed in test boring CB-2p-22 to obtain groundwater measurements. A pressure transducer was installed in the piezometer and connected to a datalogger to collect and store measurements at 6-hour intervals. The piezometer indicated that groundwater is present at a depth of approximately seven to eight feet below ground surface at the location of CB-2p-22.

Monitoring of piezometer CB-2p-22 is ongoing. The piezometer indicates that groundwater elevation was lowered by approximately 2 feet, shortly after the tightline was installed in July 2022 (Figure 5). Based on groundwater monitoring data through the following year, the tightline does not appear to adequately lower groundwater during the winter, and the reduction in groundwater we observed after the installation of the tightline may be a function of the dry season, rather than our efforts to eliminate water from infiltrating into the landslide with the tightline.

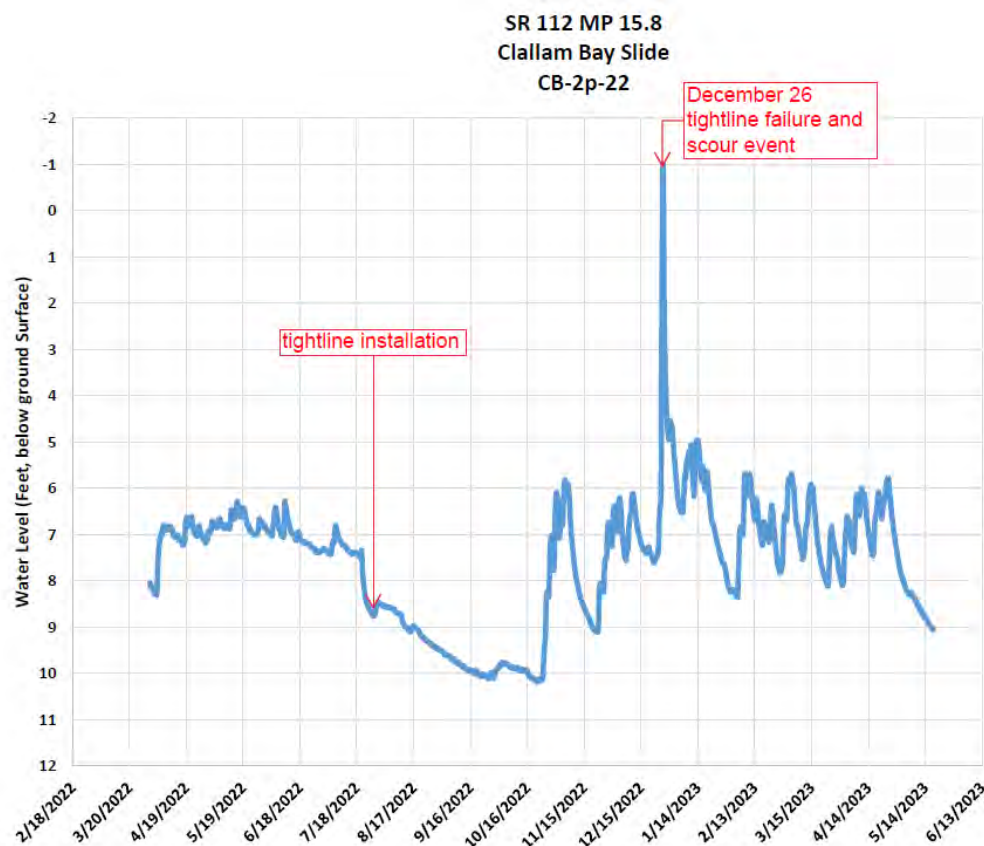


Figure 5: CB-2p-22 groundwater monitoring data

### **December 2022 Storm Event**

On December 26, 2022, a heavy precipitation event caused a pulse of debris to flow down the drainage channel above the tightline and plugged the inlet of the tightline. Water flowed around the tightline and scoured a channel (up to approximately 6 feet deep) through the ground surface to the highway. Bedrock was exposed in two locations in the scour channel. Material eroded from the slope during this event was deposited on the highway and in the ditch, causing flooding and a temporary closure of SR 112. The 'secondary landslide' also reactivated during the event and resulted in several inches of heave on the highway, in the same location where heave had been observed since 2006.

Groundwater monitoring was ongoing during this event (Figure 5) and the data indicate that water flowed directly into the top of the piezometer, presumably because there was sheet flow across the local ground surface. This is supported by reports from WSDOT Maintenance who observed the event and were responding to the debris and flooding on the highway.

WSDOT Maintenance was able to manually clear the inlet of the tightline. Maintenance also took some measures to improve the sump at the tightline inlet and made some repairs to the drainage channel that had been damaged during the event. This event indicated that the tightline, in its current condition, is not a resilient structure and will require ongoing maintenance and repairs as it is subject to being plugged by upslope debris.

### **Seismic Refraction Survey**

A seismic refraction survey was conducted on the 2006 'secondary landslide' on February 23-24, 2023. Seismic refraction was conducted with a 24-channel seismograph using a 'Betsy gun' as an energy source. Data was collected on three transects, one longitudinal to the landslide, and two transverse to the landslide axis, including one along the ditch of SR 112. The geophysical work was conducted under challenging conditions, during a snowstorm and with frozen ground. The seismic refraction survey was successful in detecting a near-surface unit of relatively higher density than the surficial soils. However, the depth to this unit, and the p-wave velocity, corresponded to groundwater, rather than bedrock. As a result, the seismic refraction did not produce useful information for characterizing the geometry of the subsurface bedrock surface. The seismic refraction did indicate that groundwater was present within approximately 3-7 feet of the ground surface.

### **Geotechnical Analysis**

Using the pre-landslide aerial lidar (2018) and post-stabilization terrestrial lidar (2022), we developed and compared cross-sections longitudinal to the secondary landslide. We confirmed that the stabilization work had removed material from the toe of the 2006 secondary landslide.

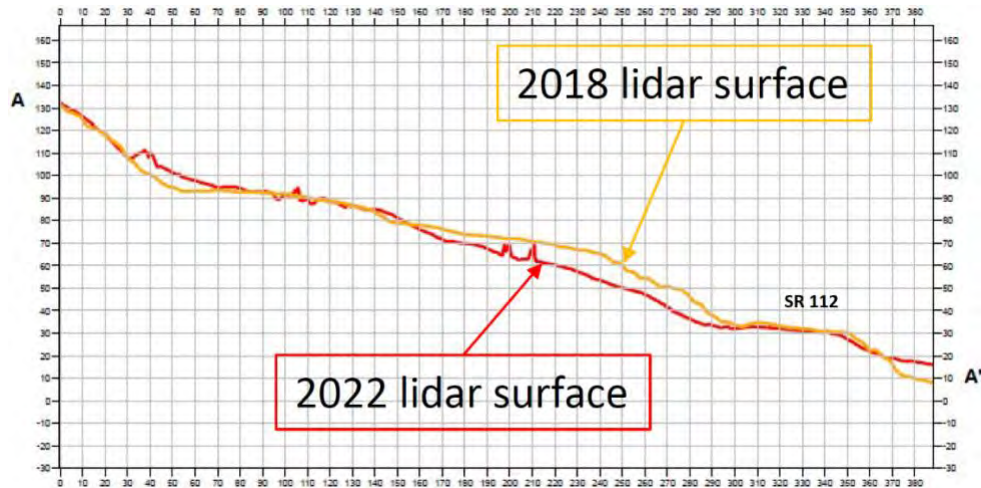


**Figure 6: A comparison of the ground surface along a longitudinal cross-section of the secondary landslide showing that material had been removed from the landslide toe during grading work.**

Based on the information collected from the geotechnical investigation, we developed a subsurface interpretation along the longitudinal cross-section of the landslide developed from the 2022 terrestrial lidar data (Figure 5).

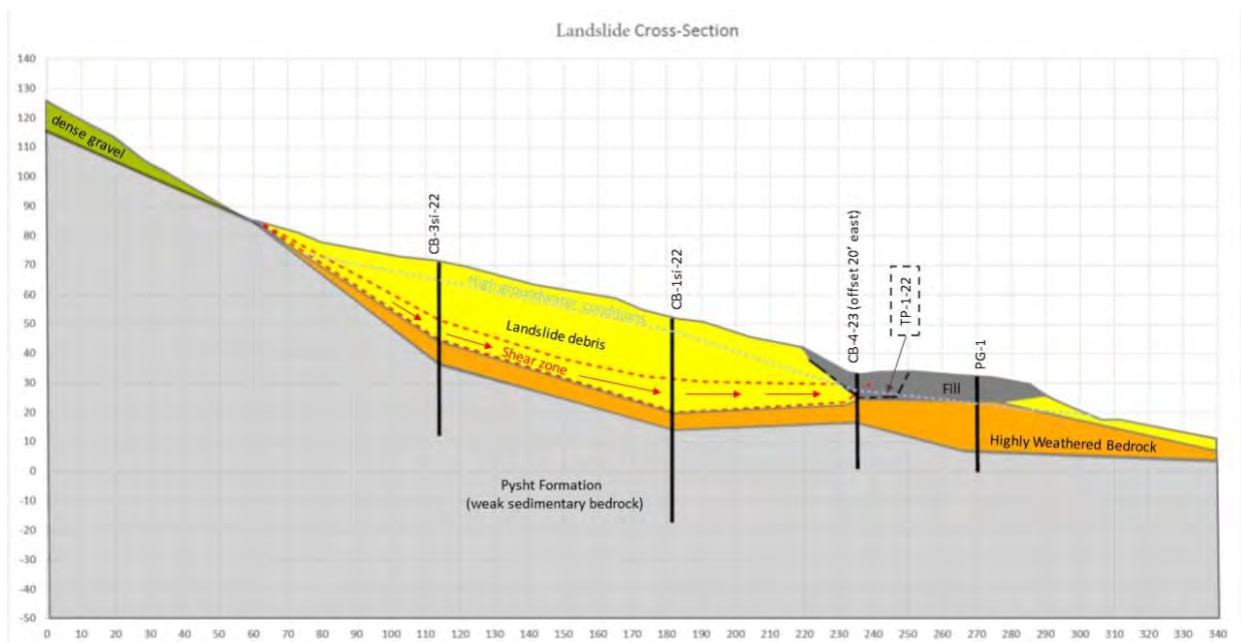


**Figure 5: Landslide subsurface interpretation**

This subsurface interpretation was input into Rocscience SLIDE2, a limit-equilibrium slope stability analysis program. Engineering properties for subsurface materials were selected with guidance from laboratory index testing of samples retained from drilling in conjunction with

72<sup>nd</sup> HGS 2023: Taylor

published correlations. These engineering parameters were then refined through back-analysis of the landslide to a FS of 1.0.

Slope stability analysis (employing Bishop simplified and GLE/Morgenstern-Price methods) allowed us to better understand that the emergency shear key only marginally increased slope stability. We also determined that the stability of the landslide is highly sensitive to groundwater elevation.

Limit-equilibrium analysis was then conducted to design a permanent stabilization of the 'secondary landslide'. A shear key rock buttress was selected to mitigate the landslide. A shear key rock buttress provides a low-risk permanent restraint to the base of the landslide and has been successfully employed across Washington state to stabilize many other landslides. Drainage solutions, such as horizontal drains, were considered, but in our experience, these measures alone present more risk than a rock buttress and have a shorter service life.

## STABILIZATION WORK (PHASE 2)

The shear key rock buttress was designed to meet or exceed a minimum Factor of Safety (FS) of 1.25 during high groundwater conditions (Figure 7). Our analysis indicates that the rock buttress requires a wide shear key to resist the landslide failure plane at the highway elevation and must extend upslope approximately 140 feet to prevent overtopping failures from above the buttress. The rock buttress will be 150 feet wide, along SR 112, to mitigate the entire landslide area.

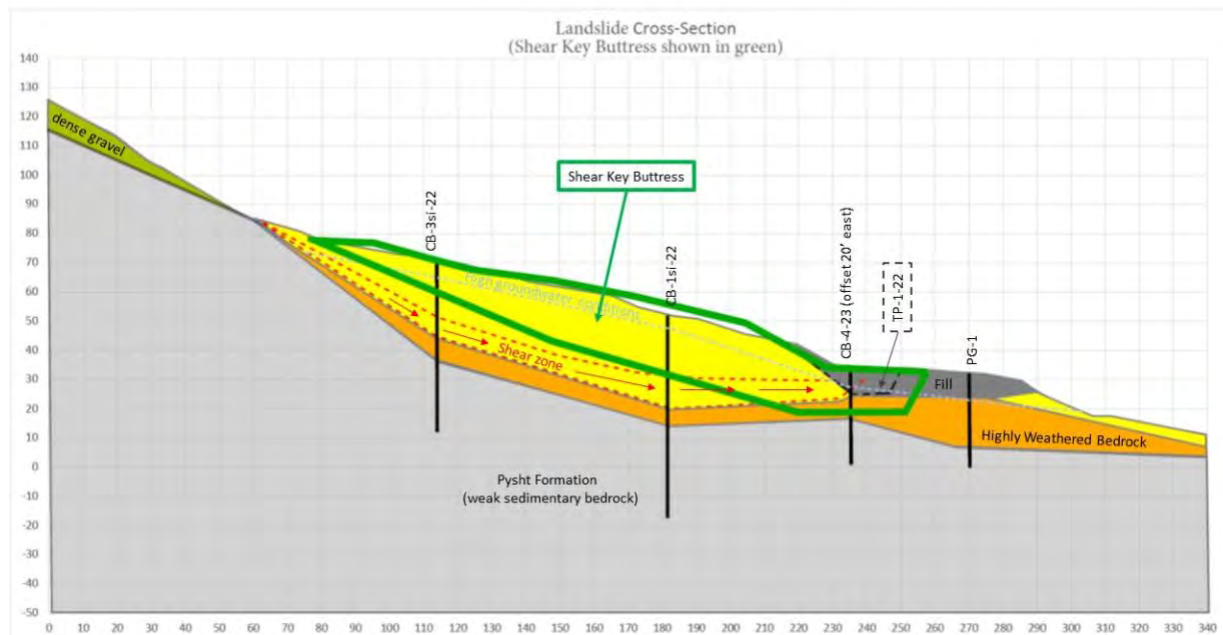


**Figure 7: Landslide subsurface interpretation with the approximate limits of the proposed shear key rock buttress overlain with a bold green line.**

In addition to reinforcing the toe of the landslide, the buttress will have the added benefit of being constructed from well drained rock material and will lower the groundwater elevation within the landslide mass.

The existing inlet of the tightline installed during 2022 is vulnerable to blockage by debris from upstream. To correct this problem, the inlet of the tightline will be improved to capture surface flow and more efficiently prevent debris from blocking the inlet. This inlet improvement will likely require a grated and flared pipe opening to be attached to the inlet, as well as upstream clearing and minor grading.

Phase 2 of the stabilization work consisting of constructing a shear key rock buttress and improving drainage will be constructed in the summer of 2024.

## **CONCLUSIONS**

SR 112 is the sole access to several coastal communities on the north coast of the Olympic Peninsula, including the Makah Reservation at Neah Bay. Long-term closures of the highway due to landslides present an ongoing challenge to WSDOT for operating and maintaining the highway and have negative implications for public safety and local economies.

The Clallam Bay landslides are an example of how the combination of wet climactic conditions, weak subsurface materials, and land use practices result in landslides that present these challenges to WSDOT and local communities. The Clallam Bay landslides damaged and eventually closed SR 112 for several months. This isolated local communities and required costly mitigation efforts. Stabilization efforts were complicated by the presence of two landslides at the same location, with a large debris slide overtopping a pre-existing landslide.

A wide variety of geotechnical tools and analysis methods were employed to address the Clallam Bay landslides. Several methods of characterizing ground surface geometry, including aerial lidar, UAV-developed DTMs, and terrestrial lidar were employed. These methods were used to monitor and identify areas of ground deformation and to design mitigation measures. Several subsurface exploration methods were employed to characterize subsurface conditions and to understand the mechanics of the failures, including a test pit, geotechnical borings, and a seismic refraction survey. Laboratory testing and geotechnical instrumentation were critical elements of the subsurface characterization and geotechnical stabilization design.

An iterative approach to stabilization was ultimately required, as the various complexities of the landslide became apparent over the course of the design and construction of the project. The combination of poor land use practices, difficult access, soft and unstable ground, complex subsurface conditions, varying landslide movement rates, and varying failure mechanisms highlight the need for a broad suite of geotechnical tools for characterization and analysis.

## **State Route 112: Landslide Alley – Striving for Resiliency**

**Thomas C. Badger**  
Landslide Technology  
10250 SW Greenburg Rd Ste 111  
Portland, OR 97223  
360-628-6143  
[tbadger@ccilt.com](mailto:tbadger@ccilt.com)

**Tracy Trople, Cody Chaussee, Sam Johnston, and Marc Fish**  
WSDOT Geotechnical Office  
State Materials Laboratory  
1655 S. 2nd Ave.  
Tumwater, WA 98512

Prepared for the 72<sup>nd</sup> Highway Geology Symposium, August, 2023

### **Disclaimer**

Statements and views presented in this paper are strictly those of the author(s), and do not necessarily reflect positions held by their affiliations, the Highway Geology Symposium (HGS), or others acknowledged above. The mention of trade names for commercial products does not imply the approval or endorsement by HGS.

### **Copyright Notice**

Copyright © 2023 Highway Geology Symposium (HGS)

All Rights Reserved. Printed in the United States of America. No part of this publication may be reproduced or copied in any form or by any means – graphic, electronic, or mechanical, including photocopying, taping, or information storage and retrieval systems – without prior written permission of the HGS. This excludes the original author(s).

## ABSTRACT

State Route (SR) 112 serves as the primary access for the northwestern Olympic Peninsula of Washington State and the remote communities situated along the Strait of Juan de Fuca west of Port Angeles. Particularly unfavorable geology underlies the western half of SR 112, which combined with steep topography and an exceptionally wet winter climate, result in one of the most landslide-afflicted highway corridors in the State. Landslides and flooding of low-lying areas routinely impact highway travel most winters. Traffic interruptions are commonly limited to a single lane or closure of both lanes for short duration through persistent maintenance efforts. On a longer cycle of a few years to a decade or two, major landslide events severely damage or destroy the highway in one or more locations resulting in long-duration closures of three to six months, or more. Detour options are limited to nonexistent (for some hazard conditions), and communities and local businesses are significantly impacted during these long-duration closures until highway repairs can be made or floodwaters recede.

The WSDOT Geotechnical Office commissioned a planning-level study to assess geologic and hydrologic hazards that impact the highway and provide recommendations to improve its resiliency. The study focuses on two segments of the highway that are most frequently and severely impacted by landslides: 1) MP 0 at the Makah Reservation Boundary to MP 17 at Clallam Bay; and 2) MP 29 near the terminus of the Pysht River to MP 38 at West Twin River.

The two highway segments were subdivided into ten subsegments of two to four miles in length for detailed evaluation. Subsegments were selected based on access constraints, geographic boundaries, and geologic/topographic conditions. Seven hazard types (shallow and deep-seated landslides, lowland flooding, coastal erosion, sea-level rise, earthquakes, and tsunamis) were evaluated for each subsegment. The likelihood of occurrence and potential consequences were assessed with input from stakeholders. Consequences included service disruptions, direct and indirect costs, and public safety. Over the past decade, direct costs for repair of emergent events have totaled around \$11 million, equating to an annualized cost of about \$1.1 million for repairs and direct impacts. A risk matrix was then generated for each hazard type and a risk register was built for each subsegment.

Repairing damages from emergent events has been the primary management approach employed by WSDOT for this highway to address the more consequential hazard events. Given the extent of hazards throughout the corridor and anticipated limitations in available funding, it was judged infeasible to proactively stabilize or fully protect the highway for a sufficiently large population of high-risk slopes to significantly reduce impacts within a reasonable timeframe of several decades. Mitigation strategies to build resiliency of the highway focused on reducing service disruptions and damages and improving safety. Recommendations to proactively reduce risk and impacts and build resiliency included: 1) various alternative routes, permanent or temporary, to address the subsegments most impacted by service interruptions; 2) site-specific geotechnical investigations for potentially imminent damage; and 3) management actions entailing increased regional and site-specific deformation monitoring, review of adjacent land-use practices, updating the Unstable Slopes database, and assessing Region Maintenance capabilities and resources.

## INTRODUCTION

State Route (SR) 112 serves as the primary access for the northwestern Olympic Peninsula of Washington State and the remote communities situated along the Strait of Juan de Fuca west of Port Angeles (Figure 1). Particularly unfavorable geology underlies the western half of SR 112, which combined with steep topography and an exceptionally wet winter climate, result in one of the most landslide-afflicted highway corridors in the State. Landslides and flooding of low-lying areas routinely impact highway travel most winters. Traffic interruptions are commonly limited to a single lane or closure of both lanes for short duration through persistent maintenance efforts. On a longer cycle of a few years to a decade or two, major landslide events severely damage or destroy the highway in one or more locations resulting in long-duration closures of three to six months, or more. Detour options are limited to nonexistent (for some hazard conditions), and communities and local businesses are significantly impacted during these long-duration closures until highway repairs can be made or floodwaters recede.

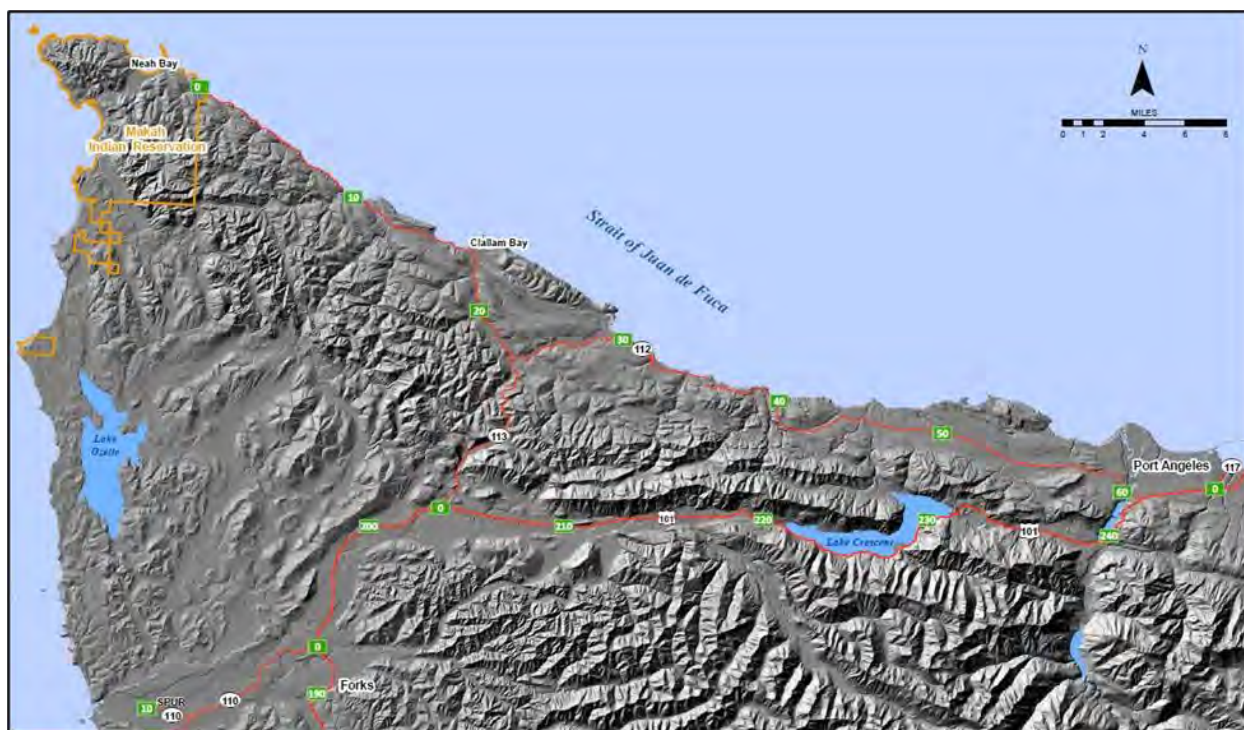


**Figure 1 – Location Map**

With growing evidence of climate-change impacts, building the resiliency of existing facilities has become a strategic priority for public and private infrastructure entities. The WSDOT Geotechnical Office commissioned a planning-level study as an initial effort to examine the highway's vulnerabilities to geologic and hydrologic hazards. This study focuses on two segments of the highway that are most frequently and severely impacted by landslides. These include:

- MP 0 at the Makah Reservation Boundary to MP 17 at Clallam Bay; and
- MP 29 near the terminus of the Pysht River to MP 38 at West Twin River.

It concludes with conceptual recommendations on where and how actions and funding can better target areas of highest vulnerability and reduce consequences associated with recurrent geologic and hydrologic hazards.

## **Route Description**

After decades of evolution from trails to wagon roads, an automobile route along the Strait from Joyce to Neah Bay was completed in 1931. The route was added to the state highway system in 1955 (SSH 9A) and fully paved and renumbered around 1964 to State Route (SR) 112 and the Burnt Mountain section, linking Clallam Bay and Sappho, to SR 113. In 2000, SR 112 was designated as a National Scenic Byway. The highway serves many dispersed rural residences and the larger communities of Joyce, Clallam Bay, Sekiu, and Neah Bay (tribal center of the Makah Reservation), linking them to US 101 and the municipalities of Port Angeles and Forks. The highway also provides the sole access to the Olympic National Seashore at Ozette and Shi Shi Beach.

Mile Post (MP) 0 is located just west of Neah Bay at the Makah Reservation boundary. The highway is sited within a few hundred feet of the Strait of Juan de Fuca to MP 11, before diverting inland to Sekiu around MP 15. Here, the highway runs along the shoreline of Clallam Bay (MP 17), where the highway again diverts south, connecting to SR 113 at MP 23. At the junction, SR 112 then follows the low-lying Pysht River valley before climbing onto a plateau around MP 29 several hundred feet in elevation above the Strait. The highway drops off the plateau and crosses the West Fork Twin River near MP 39, where the river empties into the Strait. The highway again diverts inland, passes through the community of Joyce around MP 50, and then terminates at US 101 at MP 61 a few miles west of Port Angeles. SR 112 has a functional classification as a major collector. It is a two-lane facility with 11 to 12-ft-wide lanes and typically 1 to 4-ft-wide shoulders. Traffic counts for various segments range from around 900 to 1800 vehicles per day, with up to about a quarter being trucks.

## **Resiliency**

National attention has been drawn to system vulnerabilities (weak links) due to increases in service disruptions resulting from aging infrastructure, more frequent and severe natural disasters, changing climate, etc. Legislation passed in 2021 explicitly incorporates resiliency improvements in Federal funding of transportation projects from weather events and natural disasters. Resiliency improvement objectives focus on the ability to better withstand and/or reduce the magnitude or duration of impacts, and to improve recovery times from these events. Resiliency improvements can harden, relocate, and/or incorporate redundancy to achieve these objectives.

Prior to the Federal legislation, the Governor's 2016-19 Directive addressing preparedness and response to seismic hazards and the State's Resilient Washington Plan direct review of prioritization criteria for post-disaster response and to strengthen the transportation system.

WSDOT's internal policy to enhance resiliency is outlined in the Secretary's 2020 Executive Order #: E 1113.00 directing employees to manage risk and strengthen the transportation system, considering, for example, impacts associated with natural hazards. WSDOT's Strategic Plan incorporates planning and invests in resources to improve its ability to mitigate, prepare for, and respond to emergencies; combat climate change; and build a transportation system that provides equitable services, improves multimodal access, and supports Washington's long-term resilience.

Because of the frequent and often long-duration closures due primarily to landslides, WSDOT has identified SR 112 as a particularly vulnerable, high-priority corridor and seeks to reduce service disruptions and improve resiliency. The strategy to accomplish this objective is to identify vulnerabilities and prioritize actions to reduce impacts that will improve the overall resiliency of the facility.

## **STUDY METHODS**

Initial efforts involved a review of geologic references, climate and sea-level data, bare-earth lidar, and Washington Department of Ecology shoreline photography. Geotechnical Office files were queried for historical information on landslide activity and responses to these events, as were Maintenance records for emergency callouts and closures related to landslides and flooding, as well as impact costs for repairs. Internal and external stakeholders were also interviewed to better understand the associated indirect impacts.

GIS analyses were performed by the Geotechnical Office utilizing a wide range of public domain and internal data sources. Because no comprehensive landslide mapping was available along the full length of the corridor, landslides were remotely and cursorily delineated within a roughly one-mile-wide corridor along the highway following Washington Geological Survey's streamlined landslide identification (mapping) protocol (*I*).

A multi-day field review was also conducted with Area Maintenance and Geotechnical Office personnel to gain further insight into problematic sites, impacts, detour alternatives and function.

## **SITE CONDITIONS**

### **Physiography**

The Olympic Peninsula is bound by the Pacific Ocean to the west, the Strait of Juan de Fuca on the north, and the Puget Lowlands and Puget Sound to the east. On the northern flank, terrain transitions from sea level to small hills/mountains up to around 1500 feet in elevation between Neah Bay and Clallam Bay to a several-mile-wide shelf around 1000 feet in elevation eastward toward Joyce and beyond. Steeper E-W trending mountainous ridges lie to the south and form the northern flank of the Olympic Mountains. Numerous watersheds drain northward into the Strait. The shoreline is composed of long linear segments extensively exposing sedimentary rock with intermittent bays and smaller depositional features windward and leeward of rocky headlands. Longshore drift is dominantly eastward.

The mean annual precipitation along the north coast of the Peninsula ranges from about 100 inches at Neah Bay, 80 inches at Clallam Bay, dropping to around 25 inches in Port Angeles. The wettest months are October through March. Multi-day storms off the Pacific are common occurrences that one or more times per winter may yield 10 or more inches of precipitation. Southwest to west winds dominate during winter months and low-pressure systems. Strong northerlies can occur during winter high-pressure fronts, which can result in lowland flooding and more severe coastal erosion, especially if they coincide with higher tides.

The wet climate supports dense forests of mixed conifer (Sitka spruce, Western hemlock, Western red cedar) and deciduous species (red alder and bigleaf maple). Red alder is a colonising species and is a common source of treefall from slopes adjacent to the highway.

### **Geologic Setting**

The formation of the Olympic Peninsula began around 50 Ma with the collision of a thickened slab of oceanic volcanic rocks, namely the Crescent Basalts, onto the North American tectonic plate. Development of an active subduction zone to the west and accretion of primarily marine sediments onto this Crescent Terrane followed. This assemblage of Crescent Basalt and deformed marine sedimentary rocks form the core of the Peninsula and Olympic Mountains. Post-collisional basins formed around the perimeter of this accreted terrane, which filled with sediment shed from the eroding continental margin (2). Continued convergence of the oceanic Pacific Plate with the North American continental plate along the Cascadia Subduction Zone has led to uplift of the Peninsula and tilting and folding of these peripheral sediments. These sedimentary rocks are referred to as the peripheral assemblage, and they form a horseshoe configuration (open to the west) around the core rocks (3) (Figure 2). Along the north side of the Peninsula in the vicinity of the highway, this peripheral assemblage of sedimentary rocks is tilted steeply (30° to 50°) toward the Straits. The lower northern flank of the Peninsula was extensively modified by Pleistocene-age continental glaciers that advanced into the Puget Lowlands and westward out the Strait.

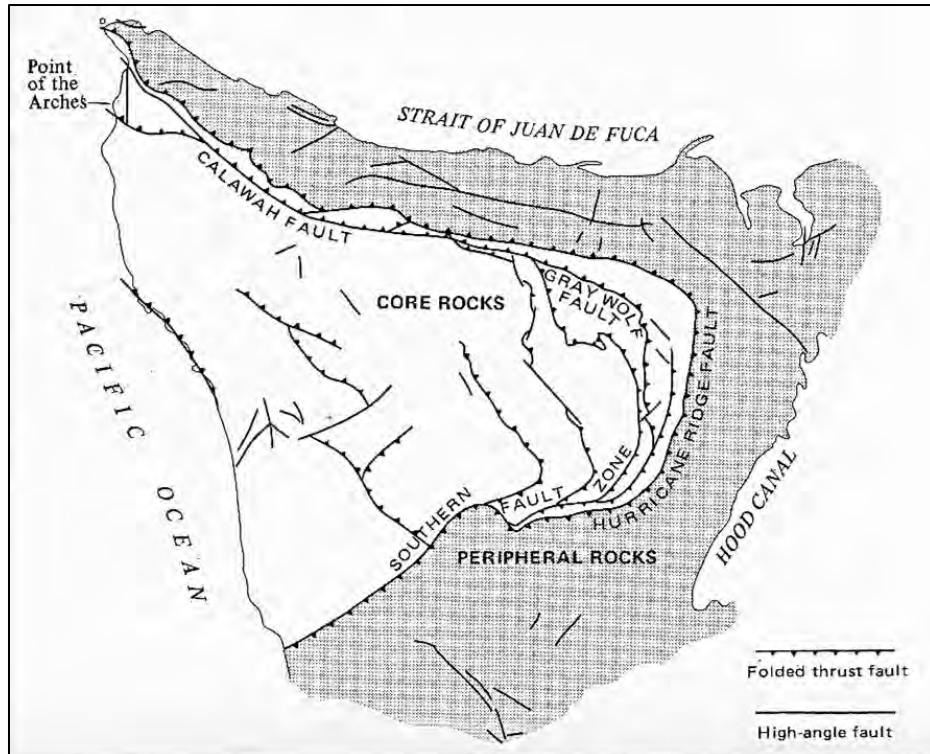


**FIGURE 1: GEOLOGIC ASSEMBLAGES OF THE PENINSULA (FROM 3)**

Relevant to the abundance of landslides along the highway corridor between Neah Bay and Joyce are two of the younger sedimentary units of the peripheral assemblage, the Makah and Pysht Formations. These appear as E-W-trending bands of rock on the geologic map, with the Makah present from the reservation boundary to Clallam Bay, and the Pysht rocks present for the segment between the Pysht and West Twin Rivers (Figure 3) (modified from 4). The Makah Formation consists of interbedded sandstone and mudstone, and the Pysht Formation consists of primarily siltstone and mudstone. The weak nature of these fine-grained bedded rocks, weathering susceptibility, and adverse inclination are the primary geologic contributors to the contiguity of deep-seated landslides for tens of miles along the Strait (5).

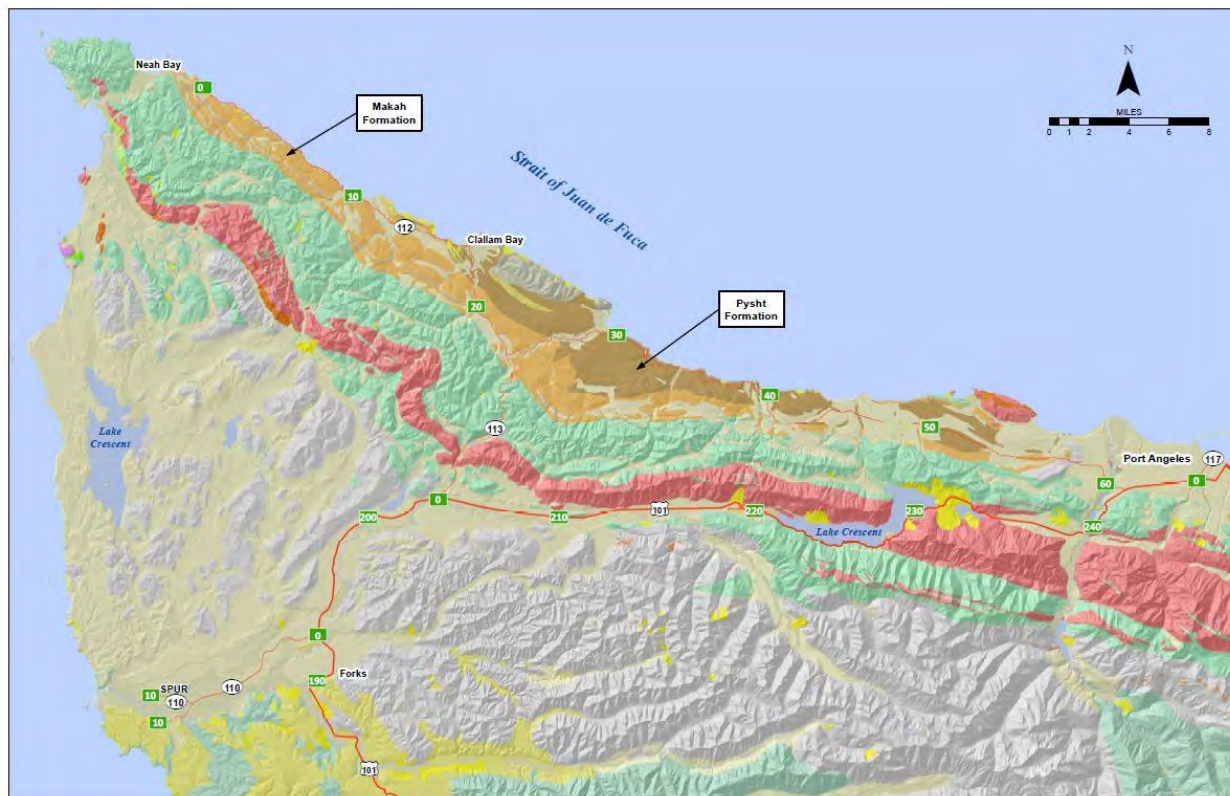


**FIGURE 2: GEOLOGIC MAP (MODIFIED FROM 4)**

The northwest flank of the Olympic Peninsula is replete with recurrent geologic and hydrologic hazards that impact the function of the highway at various time scales.

### Geologic Hazards

Significant contributions to the abundance of landsliding within the corridor include adverse geology; the considerable topographic relief, in particular the often-steep slopes above and below the highway; and the exceptionally wet winter climate. The speed at which a landslide moves and the coherence of its mass during transport are important factors in characterizing its hazard and consequence potential. A simplistic classification scheme of shallow and deep-seated landslides was used for providing context of the hazard, consequence, and considered mitigation.

Shoreline erosion occurs through longshore drift and direct wave attack, the effects of which can be significantly amplified during high tides with concurrent adverse barometric pressure. Shoreline erosion undermines slopes and seasonally removes counterbalancing beach sediment, resulting in shallow or deep-seated landsliding that damage the highway.

Of the three sources of earthquakes in Western Washington, two are relevant to the outer coast – the Cascadia Subduction Zone and active tectonic faults in the upper crust. Very large magnitude earthquakes of 8 to 9  $M_w$  are associated with partial or full rupture along the subduction zone, resulting in minutes of severe shaking and likely catastrophic damage to infrastructure and steep slopes. Additionally, up to several meters of rapid subsidence along the

outer coast are anticipated. For the portion along the Washington coast, reliability analysis of the earthquake record indicates a 360-year recurrence interval with more than a quarter exceeding this interval. Several gaps in recurrence of more than 1000 years are also evident in the 10,000-year record, suggesting clusters of shorter recurrence earthquakes (6). The last major rupture of Cascadia is thought to have occurred on January 26, 1700 (7), the last of five events in the last 1500 years. It is unknown whether the next Cascadia event will occur as part of the latest cluster, say within the next 50 years, or we are in the early half of a 1000-year gap. Numerous faults with surface manifestation and activity within the last 15,000 years have been mapped in the vicinity of Lake Crescent and offshore in the Strait (8) and are the second potential source of strong earthquakes in the study area.

## **Hydrologic Hazards**

The Hoko and Pysht River valleys are recurrent areas of lowland flooding from storms. The elevational proximity of the highway in these valleys translates to highway closures during times of river flooding. Streambank erosion has also caused damage where the highway is proximal to meander bends. Concurrent high tides and low-pressure systems exacerbate flooding in these valleys and other low areas along the coast toward Neah Bay. Flood-related closures are typically short duration events of a few days.

Predicted rise in global sea levels is relative to the elevational stability of the adjacent land mass. Historic data show a relative drop in sea level of between 1.5 to 2 mm/year at Neah Bay and virtually no change at Port Angeles (9). Projections for Neah Bay and Port Angeles show up to about 5 feet of sea-level rise by 2100. Relative lowering of sea level at Neah Bay is likely related to tectonic uplift along the outer coast. Rapid subsidence on the order of several meters is anticipated with future rupture of the subduction zone.

Recent tsunami modeling of a magnitude 9.0 Cascadia event along the coastline from the Makah Reservation boundary (MP 0) to West Twin River (MP 38) show extensive zones of significant inundation potential that would impact the highway (10). The vulnerability of low-lying bridges along SR 112 that may be inundated by tsunamis has not been assessed by the WSDOT Bridge and Structures Office, and existing bridges have not been designed for the potential loading.

## **CONSEQUENCE**

Service disruptions, impact costs, and public safety are the primary consequences with respect to functionality of the facility.

### **Service Disruptions**

In addition to the communities and residences that are served by SR 112, the timber, sport and commercial fisheries, and tourism industries, as well as many small businesses, are similarly reliant on the highway. In addition, the State operates a maximum-security correctional

facility in Clallam Bay. Employees, contractors, and suppliers that support its operation rely on the highway, as well.

Highway closures that occur west of Clallam Bay are especially impactful to residents and communities in this segment, as no paved highway detour routes exist. For Neah Bay, the community typically can sustain itself for several days before food and fuel supplies become limited (11). Supplies then need to be barged in, and emergency medical evacuation requires helicopter support. An unpaved 14-mile-long network of private logging provides access to smaller vehicles, but only for one-way-controlled traffic flow with pilot-car assist and an additional 25 minutes of travel time to the 90-minute trip to Port Angeles. Recurrent flooding of the lower Hoko River around MP 12 and coastal flooding between the Hoko and Sekiu Rivers pose another hinderance to residents west of these locations and for those who live in the Hoko valley. No detour route exists for this portion of SR 112. Another preexisting network of private and public roads was utilized as a detour route between Sekiu and Clallam Bay (MP 15 to 17) during the winter of 2021-22, when a large landslide interrupted service for about five months (Figures 4 and 5). SR 113 offers a detour alternative to US 101 for service disruptions that occur east of Clallam Bay.



**FIGURE 4 AND 5: CLALLAM BAY LANDSLIDE AND RELATED TRAFFIC CONGESTION ON DETOUR**

Storms and other triggering events commonly result in multiple sites of disruption to the highway and multiple external entities being concurrently affected by a different suite of problems. Utilities and the proximal network of private and public roads are also often damaged. For the area west of Clallam Bay, a single direction of access from the east can severely constrain emergency response for sites further to the west. Constrained highway access for external entities needing to respond to their issues creates a cascading effect of delays and impacts.

To better characterize the locations and nature of service disruptions, several WSDOT data sources were queried. An example frequency plot of callouts for Maintenance callouts by subsegment is depicted in Figure 6.

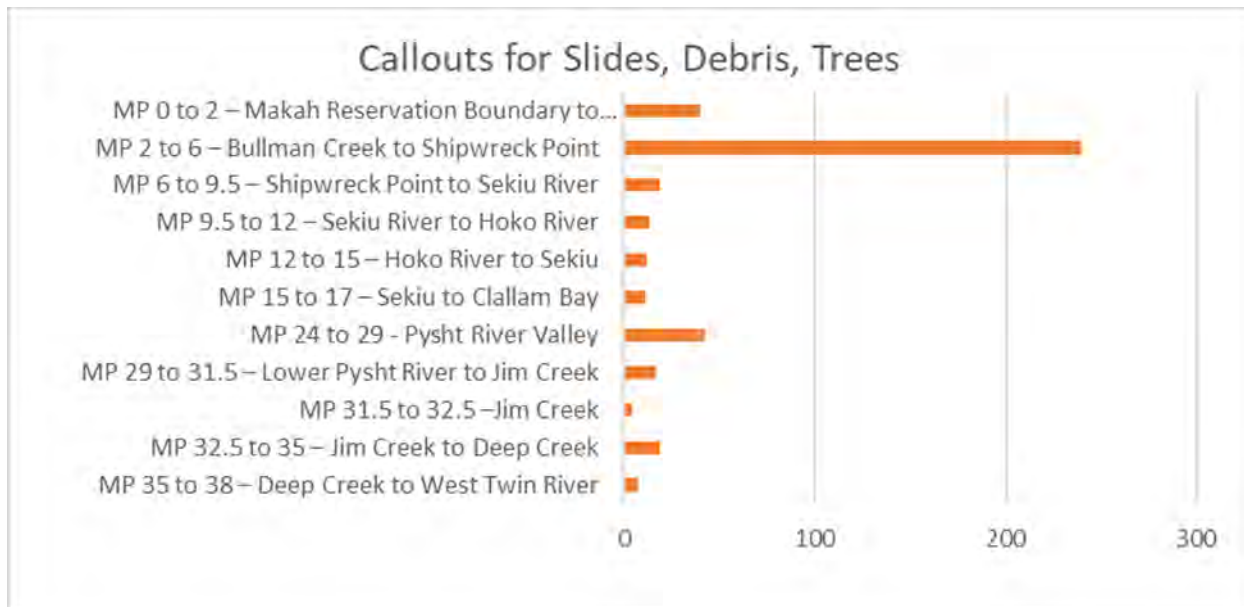


**FIGURE 6 – MAINTENANCE CALLOUTS FOR SLIDES, DEBRIS, TREES ON ROADWAY 2008-2022**

### Cost Impacts

Direct costs from landslide and flooding impacts involving emergency response and repair of the highway are spread across various offices for different functions. Commonly, multiple sites arise from a single storm event, and response and repair costs may be combined. Both State and Federal funds may also be involved. As a result, direct cost impacts for a specific event are often difficult to accurately establish. Indirect costs are yet more difficult to assess as multiple external groups are impacted often in less tangible and potentially more impactful ways than cost.

The past decade was the most eventful period of significant landslides in the six decades of available records. For the past decade, there were nine emergency WSDOT projects for a total accrued cost of about \$7.35 million in emergency repairs and \$3.48 million in Maintenance expenditure, for a total of around \$10.84 million related to emergency repairs due to landslides and flooding, or an annualized direct cost of about \$1.1 million.

WSDOT estimates indirect costs to motorists by considering vehicle delay. Delay cost assigns a per vehicle cost for the average daily traffic counts for both passenger vehicles and trucks, and the portion of the travel lanes impacted. For a 24-hour closure of both east and west travel lanes, the estimated delay costs are:

- MP 0 to 8 Delay Cost = \$568,934 per day
- MP 8 to 14 Delay Cost = \$666,010 per day
- MP 14 to 17 Delay Cost = \$1,433,894 per day
- MP 33 to 37 Delay Cost = \$639,360 per day

These daily costs assume no detour is available to diminish impacts. As an example, a 3-day closure of the highway at the Hoko River (MP 11) due to flooding is estimated to result in nearly \$2 million in indirect costs to users. Had no detour route had been available for the 2021 MP 16 landslide, the estimated delay costs for the five-month closure would have exceeded \$200 million.

## **Public Safety**

A query of Washington State Patrol logs identified three vehicular accidents related to fallen debris on the highway in the last decade, two around MP 5 and one at MP 16. No accidents were reported for the easterly segment between MP 29 and 38.

Despite the low number of recorded accidents on SR 112, there is an inherent elevation for likelihood of accidents, injuries, and fatalities related particularly to landslides when compared with other rural routes in the state. This elevated likelihood is largely due to the frequency and intensity of storms along the Strait, the widespread extent of unstable slopes, and the often-poor highway geometrics. The primary factor for ameliorating the number of recorded landslide-related incidents is the relatively low traffic volume during the winter when these events most often occur.

## **RISK ASSESSMENT**

Risk is the product of a particular hazard, the likelihood of its occurrence, and the consequences of the event.

### **Likelihood**

Evaluation of likelihood relies upon records of historic occurrence (about the last 30 years), judgments on existing site conditions, and references of work performed by others. Determination of likelihood further involves assumptions or decisions about the timeframe to consider. The varied hazards considered in this study occur at different time intervals. Climate-driven events commonly occur every few years, whereas Cascadia earthquakes and tsunamis associated with them occur on multi-century to millennial time intervals.

For the purposes of this study, we have relied on a qualitative rather than a quantitative assessment of likelihood of occurrence (Table 1). Hazards that are actively occurring or are expected to recur every few years would be assigned a very high to high level of likelihood. Because of the scientific uncertainty for when the next Cascadia earthquake will occur, we have selected the likelihood of a Cascadia earthquake and associated coastal inundation by a tsunami as being low. Events unlikely to inconceivable occurrence would receive a very low ranking. Different determinations of likelihood may be made, influenced by Agency priorities and/or more in-depth evaluation of historical occurrence and site conditions.

<b>Table 1 – Likelihood of hazard occurrence</b>	
Ranking	Description
Very Low	inconceivable or only under exceptional circumstances
Low	could occur under very adverse conditions
Medium	could occur under adverse conditions
High	will probably occur under adverse conditions
Very High	expected to occur

## Consequence

Evaluation of consequence requires historical records of past events, either from within or outside the region; knowledge of site conditions and existing or potential hazards; and judgment about performance (resiliency). Consequence is heavily influenced by the proximity of the highway to the hazard as well as various site-specific conditions that may worsen/lessen the impacts.

For the purposes of this study, we have relied on a qualitative rather than a quantitative assessment of consequence (Table 2). Hazards that have the potential to destroy hundreds of feet of highway and require months to design mitigation and construct repairs would be assigned a high to very high ranking. Debris cleanup of small landslides or shoulder/embankment repairs from shoreline/river erosion that would require a few days to reopen the highway would be assigned a medium ranking. Those expected to cause no or minimal damage and result in only routine maintenance would be ranked low to very low consequence.

<b>Table 2 – Consequence of hazard occurrence</b>	
Ranking	Description
Very Low	little damage; injuries rare to inconceivable
Low	minor damage requiring routine maintenance; injuries unlikely
Medium	moderate damage requiring unscheduled maintenance; injuries possible
High	extensive damage requiring significant mitigation; injuries possible
Very High	catastrophic damage requiring major mitigation; injuries likely

## Highway Subsegment Risk Assessments

A qualitative risk assessment was completed for each of the ten subsegments that included a description of site conditions and hazards, a reference map, and a risk register. The map uses a lidar-derived, shaded-relief base image (viewed looking south) overlain with the highway and mile posts at roughly a 1:24,000 scale. Turquoise-colored linework on the map delineates apparent landslides based solely on a remote geomorphic interpretation of the lidar and other GIS data and photography. The risk register is a modification of a Federal Highway Administration register (12) and considers each of the seven hazards, their likelihood of occurrence, and the anticipated consequences. A matrix plots the risk associated with each hazard. A subsegment example is included (Figures 7 and 8).



or recurrent highway damage and closures may arguably attract more focus of mitigation planning than other areas judged to be at high to very high risk that have not been historically active. This approach has the benefit of addressing areas of known need but has the potential of depleting attention and resources that if applied more strategically may build greater resiliency for a broader range of hazards and for more stakeholders.

Low likelihood-high consequence hazards (earthquakes and tsunamis) challenge mitigation planning, because 1) the area and magnitude of impacts may be far more extensive than other more recurrent hazards (flooding and landslides); 2) meaningful mitigation is often far more costly than other hazards; and 3) there is the possibility that the return on investment is not realized within a reasonable life cycle of the highway.

Indirect costs associated with these emergent events have not been estimated, but based on WSDOT's method, delay (indirect) costs would likely total an order of magnitude or greater than accrued direct costs. While indirect costs need to be considered in strategic planning, they are typically not equally valued primarily because they are generally not an incurred expenditure or realized savings for the entities funding the mitigation. Indirect costs are broadly distributed amongst all stakeholders.

Repairing damages from emergent events has been the primary management approach employed by WSDOT for this highway to address the more consequential hazard events. Given the extent of hazards throughout the corridor and anticipated limitations in available funding, it was judged infeasible to proactively stabilize or fully protect the highway for a sufficiently large population of high-risk slopes to significantly reduce impacts within a reasonable timeframe of several decades. Mitigation strategies to build resiliency of the highway focused on reducing service disruptions and damages and improving safety. Recommendations to proactively reduce risk and impacts and build resiliency included: 1) various alternative routes, permanent or temporary, to address the subsegments most impacted by service interruptions; 2) site-specific geotechnical investigations for potentially imminent damage; and 3) management actions entailing increased regional and site-specific deformation monitoring, review of adjacent land-use practices, updating the Unstable Slopes database, and assessing Region Maintenance capabilities and resources.

## REFERENCES:

1. Slaughter, S.L., W.J. Burns, K.A. Mickelson, K.E. Jacobacci, A. Biel, and T.A. Contreras, 2017, Protocol for Landslide Inventory Mapping from Lidar Data in Washington State, Washington Geological Survey Bulletin 82, 35 p.
2. Donaghy, E., 2022, Stratigraphy of the Olympic Peninsula, Quimper Geological Society 10/15/2022 presentation; [https://www.youtube.com/watch?v=4QKp8FjxT\\_Y](https://www.youtube.com/watch?v=4QKp8FjxT_Y) ; accessed 01-08-2023.
3. Tabor, R.W. and W.M. Cady, 1978, Geologic Map of the Olympic Peninsula, Washington, USGS Miscellaneous Investigation Series MP I-994.
4. Schasse, H.W., 2003a, Geologic Map of the Washington Portion of the Cape Flattery 1:100,000 Quadrangle, Washington Division of Geology and Earth Resources Open File Report 2003-5.

5. Schasse, H.W., 2003b, Geologic Map of the Washington Portion of the Port Angeles 1:100,000 Quadrangle, Washington Division of Geology and Earth Resources Open File Report 2003-6.
6. Badger, T.C., 1993, Structurally-controlled landslides northwestern Olympic Peninsula, USA, in Anagnostopoulous et al. (eds), proceedings for Geotechnical Engineering of Hard Soils-Soft Rocks, pp. 1051-1056.
7. Goldfinger, C., 2023, The next Cascadia earthquake – how did we get here?, Quimper Geological Society 2/18/2023 presentation; <https://quimpergeology.org/2022/02-18-2023-goldfinger-cascadia/>
8. Atwater, B.F., Musumi-Rokkaku, S., Satake, K., Tsuji, Y., Ueda, K., and Yamaguchi, D.K., 2005, The orphan tsunami of 1700—Japanese clues to a parent earthquake in North America, 2nd ed.: Seattle, University of Washington Press, U.S. Geological Survey Professional Paper 1707, 135 p.
9. USGS Quaternary Fault and Fold Database of the United States, <https://www.usgs.gov/programs/earthquake-hazards/faults>, accessed 3/5/2023.
10. NOAA Sea Level Rise Portal, <https://oceanservice.noaa.gov/hazards/sealevelrise/>, accessed 3/5/2023.
11. Dolcimascolo, A; Eungard, D. W.; Allen, C.; LeVeque, R. J.; Adams, L. M.; Arcas, D.; Titov, V. V.; González, F. I.; Moore, C.; Garrison-Laney, C. E.; Walsh, T. J., 2022, Tsunami hazard maps of the Olympic Peninsula—Model results from an extended L1 Mw 9.0 Cascadia subduction zone megathrust earthquake scenario: Washington Geological Survey Map Series 2022-01, 14 sheets
12. Denney, L., Community Planning Manager, Makah Tribe; 10/24/2022 telephone interview.
13. Federal Highway Administration (FHWA), Risk Management Register, <https://highways.dot.gov/federal-lands/pm/cfl/risk-management-register>, accessed 4/23/2023.

**Raised Draperies: Defining Hybrid Barriers and Attenuators by  
Application**

**John D. Duffy P.G., C.E.G.**

Yeh and Associates

391 Front Street, Suite D, Grover Beach, CA 93433

(805) 440-9062

[jduffy@yeh-eng.com](mailto:jduffy@yeh-eng.com)

Prepared for the 72<sup>nd</sup> Highway Geology Symposium, August 14-17, 2023.

### **Acknowledgements**

The author would like to thank these individuals for their contributions in the work described:

Jon Blanchard, Yeh and Associates  
Loree Berry, Yeh and Associates  
Thomas Whitman, Yeh and Associates

### **Disclaimer**

Statements and views presented in this paper are strictly those of the author, and do not necessarily reflect positions held by their affiliations, the Highway Geology Symposium (HGS), or others acknowledged above. The mention of trade names for commercial products does not imply the approval or endorsement by HGS.

### **Copyright Notice**

Copyright © 2023 Highway Geology Symposium (HGS)

All Rights Reserved. Printed in the United States of America. No part of this publication may be reproduced or copied in any form or by any means – graphic, electronic, or mechanical, including photocopying, taping, or information storage and retrieval systems – without prior written permission of the HGS. This excludes the original author.

## ABSTRACT

Beginning in the 1980s, research and development of flexible rockfall fence systems resulted in a wide variety of systems developed to protect facilities from falling rocks. These systems were basically a fence with a wire mesh supported by an infrastructure of cables and posts that were specifically designed to be flexible. Specialty manufacturers offered up a suite of designs and systems for a broad range of rock impact energies and rockfall bounce heights. Soon practitioners were applying these systems to a wide variety of terrain that included the standard fence at the base of the slope, placing modified versions of flexible rockfall barriers and unsecured draperies in incised drainages, draping long steep slopes, and placing barriers and drapery over rock slopes in narrow corridors with limited catchment. The systems designed for these slope conditions were being developed not to stop the falling rock but to attenuate the rocks energy and control the rocks trajectory so that it would be deposited at a safe location. Soon the industry ended up with two common names for these systems: Hybrids and Attenuators. Most practitioners acknowledge these two titles, but the definition of which term applies to which system often gets blurry between agencies, manufacturers, academics, and consultants. There is an important distinction. While the two systems are very similar construction, as both systems provide a standard unsecured drapery with the added benefit of elevating the upslope end of the drapery off the ground surface to catch rocks rolling down slope above. In one design, rockfall is channeled directly into a suitable containment area at the bottom of the installation, and in the other design the rockfall exits the bottom of the mesh to continue down the slope into a series of similar systems that dampen motion and control the rocks trajectory that is eventually guided into the containment area at the base of the slope. To obtain some standardization in product development, proper usage, and testing methods terms that allow distinction between these different types of systems needs to be formalized throughout the industry. This paper reviews the history and defines the terms for attenuator and hybrid systems, current design methodology, results from full scale tests and discusses nomenclature and performance characteristics that can guide the development of industry standards.

## INTRODUCTION

Beginning in the 1980s, research and development of flexible rockfall fence systems began and continues today resulting in a wide variety of systems developed to protect facilities from falling rocks. These systems were basically a fence with a wire mesh supported by an infrastructure of cables and posts and specifically designed to be flexible. The flexibility of these systems increased the time for the impacting rock to stop and thus reduced the forces on the system (Figure 1) with versatile and economical materials that have proven to be reliable for mitigating rockfall.

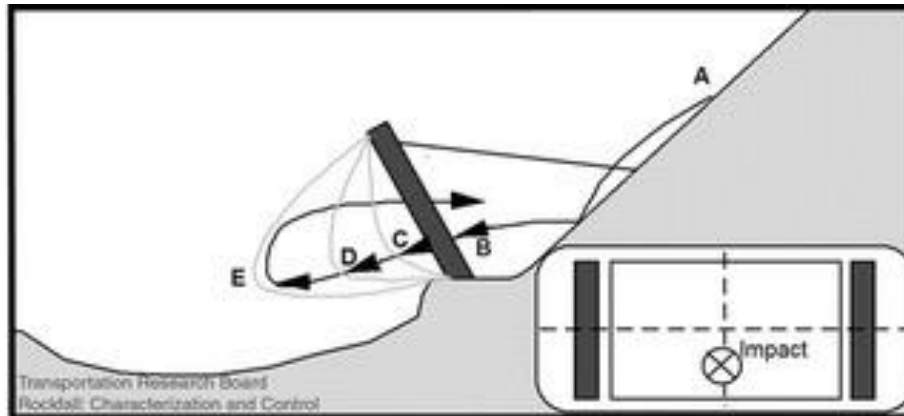


**Figure 1: Fully flexing fence (Duffy, Badger 2012).**

The initial rockfall systems were developed to place a flexible wire fence near the base of a slope and above the facility to be protected. Upon impact the rock remained entrapped behind the fence. The entrapped rock eventually had to be removed to keep the catchment area clear and allow the system to continue to perform properly, but typically at a time that could be scheduled versus as an emergency response if the rocks had impacted the facility being protected. Therefore, the system was positioned, typically at the base of a slope, where access was available to maintain the fence. This of course limits where one can construct a system and continue to be able to maintain the system within reasonable maintenance costs and may only provide limited protection for longer slopes that may produce high energy rockfall with relatively high bounce heights.

Long before the development of these new flexible rockfall fences, unsecured wire mesh draperies were commonly being hung on slopes for rockfall protection. The early unsecured drapery design was a single or double twist wire mesh laid on the slope and supported at the top of a slope with simple ground anchor system (Figure 2). The unsecured drapery covered the slope to mitigate only rockfall covered by that system and did not address rockfall generated from the slopes above. The drapery allowed rocks beneath it to move downslope in a slow and controlled trajectory and be deposited into a catchment area at the base of the slope where the rocks could be more easily removed by maintenance forces. This design approach remained relatively unchanged for years.

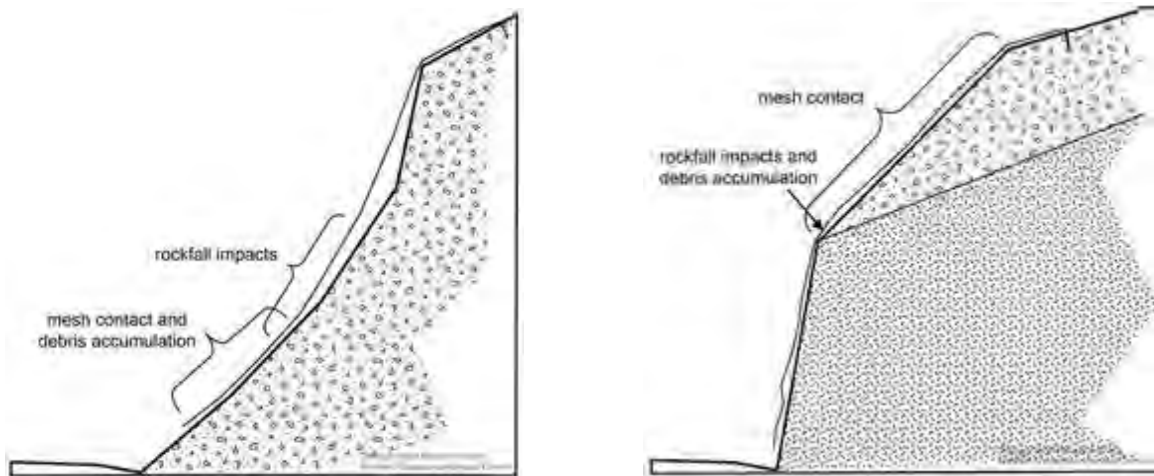


**Figure 2: Typical schematic of unsecured drapery (Badger, Duffy 2012).**

While both flexible barrier and drapery systems were rapidly advancing in design and capabilities, they both had limiting features that could not always address the wide variety of terrains where mitigation for rockfall was needed. For example, fences were mostly restricted to following the same elevation contours and draperies, from a practical perspective, could not cover an entire mountain side that was generating rockfall. The need to protect infrastructure beyond the simple slope geometry emerged and with it came the need to change the standard fence and drapery designs to address more complex slope geometry and terrain. As demand for these systems increased, practitioners were modifying the designs even as new testing and research to understand the properties and limitations of those systems were still being developed. These modifications were made to accommodate varying and irregular slope geometries, reduce construction costs, and reduce maintenance efforts along incised drainages, long steep slopes, and narrow corridors with limited catchment where rockfall mitigation may have previously been unfeasible or cost prohibitive. More applications to address aging rock slopes, both natural and anthropogenic, were being installed, and to address increasing environmental constraints that often limited the scope of rockfall mitigation systems. These needs fueled the development of modifying these relatively lightweight, durable, and compact systems to fit in almost any location and rockfall condition.

An initial modification was to raise the top of an unsecured drapery to help capture rock fall generated from the slope above. A series of draperies installed in combination with flexible rockfall fences could be installed on long slopes whereby the rock is stopped by a fence and the rock can migrate under the draperies to the base of the slope. These modifications were initially referred to as Hybrid systems. A hybrid being made by combining the two different elements to achieve the benefits of both. In this case a flexible rockfall fence was combined with unsecured drapery (Figure 3).

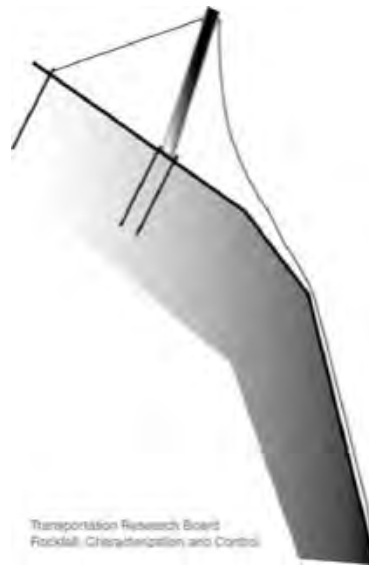


**Figure 3. Schematic of a typical flexible rockfall fence and an unsecured drapery combined (Badger, Duffy, 2012).**

Practitioners also understood that these systems were dampening the rockfall energy and controlling, to various degrees, where the rockfall would eventually stop. In other words, these systems were attenuating the falling rocks' energy, velocity, and trajectory without stopping the rocks on the slope. Confidence in such systems was developed by understanding the essential elements of flexible rockfall fences and unsecured draperies systems- flexibility. By increasing the time it took for an object to stop there was a decrease on the total force on the systems. The combined designs were much more flexible than the standard fence and draped systems implying they have at least equal to if not greater capacity, and allowed for a series of lighter weight flexible components to be installed even when higher energy or more frequent rock falls were anticipated. Soon the term “attenuator” was being used interchangeably with “hybrid” to describe these various systems.

## DEFINITIONS

The Transportation Research Board (Badger, Duffy, 2012) describes hybrid drapery, also referred to as an attenuator, a hybrid barrier, or hanging nets: as a standard unsecured drapery with the added benefit of intercepting rockfalls sourced upslope of the installation by elevating the upper part of the drapery off the surface. This modification exposes the upper portion of the drapery to impacts orthogonal to the plane of the mesh. Rockfall is then channeled under the drapery and its trajectory confined within the plane of the mesh. Since the mesh is not restrained, it has the ability to deform and attenuate the impact energy and then control the trajectory into a suitable containment area at the bottom of the installation (Badger, Duffy, 2012).

The California Department of Transportation recognizes suspended wire and cable mesh barriers as a hybrid of drapery systems and flexible rockfall fences. Also referred to as attenuators, these systems catch rolling and bouncing rocks, attenuate the energy, suppress the trajectory, and guide the rock to the base of the slope into a catchment area (California Department of Transportation, 2023).

In the state of Washington practitioners describe Hybrid drapery (also called attenuator) as a passive rockfall protection system consisting of a flexible, woven wire or cable fabric suspended from a horizontal top support cable that is raised off the ground by posts or by anchoring across a chute (Badger et.al. 2011). No internal, side, or bottom anchoring of the fabric is generally included, allowing for controlled deformation of the fabric and providing either full containment or attenuation of the rockfall trajectory at the base of the installation. Hybrid drapery addresses rockfall source areas both underneath and upslope of the installation, and control the rock's descent under the mesh, combining the performance of standard unsecured draperies and flexible rockfall barriers (Badger et.al. 2011).

The Colorado Department of Transportation identifies a type of protection measure, termed an attenuator system. Rather than trying to arrest the rocks on the slope, attenuator systems are designed to intercept and dissipate the velocities and energies of the rockfall blocks as they pass through the system, and, as a result, the blocks can be retained in a designated collection area, such as a roadside ditch, along the base of the slope. As these systems combine the attributes of standard drapery with a flexible rockfall fence/barrier, they are in some instances also referred to as "hybrid drapery" or "hybrid barrier" (Arndt et. al., 2009).

Practitioners in Canada describe the principle of attenuators is that the rock is deflected by the net into the ground such that the net structure only absorbs a portion of the impact energy, with a major portion of the energy being absorbed by the ground (Wyllie et al 2015). This is in contrast to conventional nets where all the impact energy is absorbed by the net. Significant advantages of attenuators are that they can be constructed with lighter structures compared with conventional fences, in addition they are self-cleaning which minimizes maintenance costs (Wyllie et. al., 2015).

Geobrugg (USA) manufactures Attenuator Barriers that are a system that will dissipate the energy of rockfalls and direct rocks into the catchment zone. The system allows removal of boulders from the slope above without incurring additional costs or time. (Geobrugg 2023).

Maccaferri (USA) manufactures Attenuator Systems which are used on slopes where there is available "run-out" space beneath the barrier in which the rocks can ultimately stop or be safely collected. Their rockfall Attenuator Barriers combine the interception structure of a dynamic rockfall barrier with the reduced maintenance advantages of drapery mesh; they are used in passive rockfall hazard mitigation. Rather than being secured to a lower support cable, the fence mesh is made longer and to drape down the slope to slow down the descent of falling rocks. (Maccaferri 2023).

Trumer (Canada) manufactures Rockfall Attenuators and identifies that their primary function is to reduce the energy of falling debris and control the bounce heights. The systems normally have no lower bearing ropes and so the material is free to exit the system, though normally with reduced velocity and an altered trajectory. In the case of a hybrid system, the function lies somewhere between the two preceding cases. The debris may still be contained between the upper and lower bearing ropes but differs since the lower bearing rope has been removed from the base of the post to a strategic position further down slope where the accumulation of debris is more easily removed. (Trumer 2023).

### ATTENUATOR/HYBRID SYSTEMS TODAY

To date nearly countless numbers of these hybrid/attenuator systems have been effectively installed where natural topography channels rockfall trajectories or along abrupt slope convexities. All shapes, sizes, and configurations imaginable have been installed with fixed posts, hinged posts or hung from cables and incorporate all available version of wire and cable meshes. These systems can range from wide suspension spans to versions closer to the original flexible rockfall fence, versions with a lot of height and versions with very little, and versions with suspended drape sections within a longer stretch of barrier. All these possible configurations are described with terms used interchangeably.

Combining key elements of a flexible rockfall fence and an unsecured drapery create a hybrid design whose purpose is to attenuate rockfall energy and trajectory. Is it a hybrid: yes. Is it an attenuator: yes. In either case there seems to be two general designs evolving. Both designs intercept rockfalls by elevating the upper part of the design off the surface exposing the upper portion of the design to impacts orthogonal to the plane of the mesh where rockfall is then channeled under the design and its trajectory confined within the plane of the mesh. But in one design, the rock immediately falls into a suitable containment area at the bottom of the mesh and stops (Figure 4).

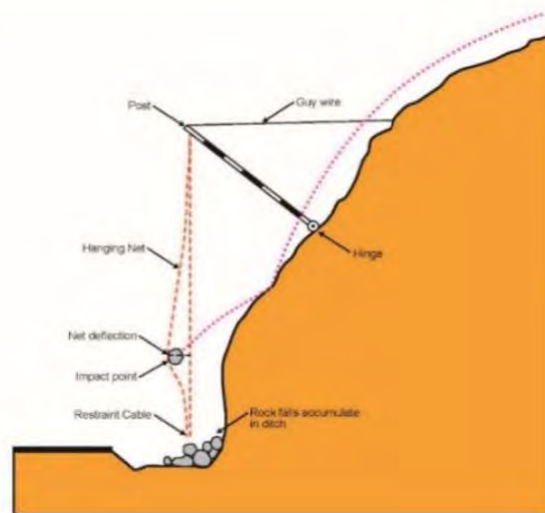


**Figure 4. Schematic of a typical design where the rock immediately falls into a suitable containment area at the bottom of the mesh and stops (Wyllie et. al., 2017).**

The other design allows the rocks to continue down the slope essentially restarting the descent from a very low velocity. The rock blocks can then continue downslope at a much-reduced speed and trajectory into a suitable containment at the base of the slope or into a series

of similar systems to control the rock blocks trajectory down a long slope eventually guided into a suitable containment area at the base of the slope (Figure 5).

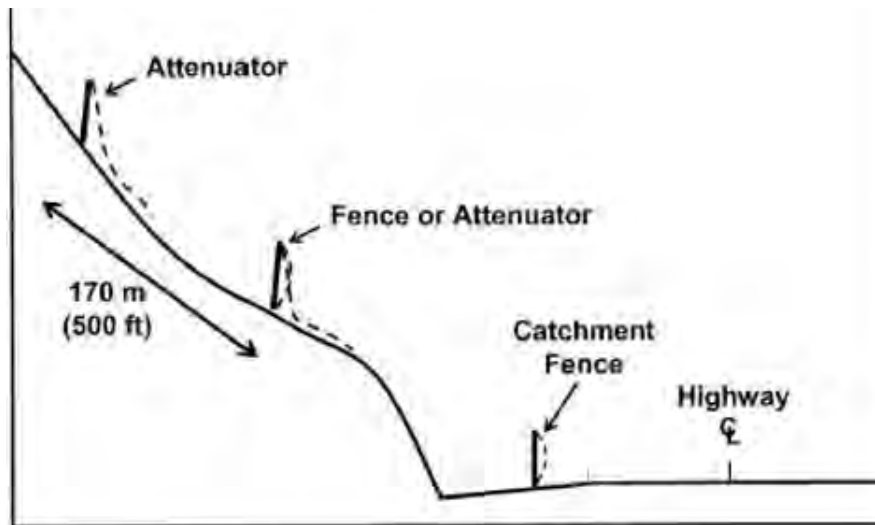


**Figure 5. Schematic of a typical design allows the rock blocks to continue down the slope essentially restarting the descent from a very low velocity (Arndt et. al. 2009).**

But what do we really know about their performance and capacity? There is risk associated with expanding systems that are installed based only on past experience if a practitioner wants to apply the same type of system to a case with larger or heavier rockfall and does not know the actual capacity of wire mesh and attenuator system. Reviewing what performance testing has been done should help direct the industry to develop a standardized test method to better quantify hybrid and attenuator type systems used to control rockfall.

### FULL SCALE TESTS

In the late 1950s, and early 1960s Arthur M Ritche conducted a landmark research project where over 300 rocks were rolled off natural slopes to develop the Ritche catchment ditch criteria including some rocks rolled into hanging chain link fences (Ritche, 1963). In the 1980s the California Department of Transportation published their Rockfall Mitigation Manual. Part of that work entailed rolling rocks off various slopes of different geometries and material types and measuring the rocks' trajectories. The researchers also rolled rocks into various chain link fences, some of which were hanging fences (McCauley, et. al., 1983). In both cases the rocks were small and fence performance was visually evaluated and described as reducing the bounce height and speed, but no comprehensive analytical work was performed.

In 1989 the Colorado Department of Transportation tested what they called attenuators at their Rifle Colorado test site (Barrett et. al., 1989). These designs used tires and timbers hanging from a cable infrastructure. Energies were measured and performance was evaluated. Possibly for the first time this attenuating concept was considered for higher energy rockfalls. The feeling

at the time was that the only way to control high impact rockfall energies was to stop the rock with a robust structure like an earthen berm or perhaps slowing the rock down (attenuating) using a lighter, smaller, less robust designs.

Seventeen years later the use of hybrid/attenuators was in full swing. In 2007 the first flexible hybrid attenuator system full scale test was performed in Italy by the company IGOR Parimmissi (Badger et. al., 2008). Four manufactured concrete rocks were rolled on a natural slope, and impact energies and rock trajectories were measured. The test design was 20 meters (65 feet) wide with three ring mesh panels supported by 4-meter (13 feet) high posts. The drapery section below the fence was 12 meters (39 feet) long ending at the at-grade bench. The mesh was a ring net. The system, referred to as a hybrid system, was placed at the edge of a break in a slope above a small cut slope with an open natural slope above (Figure 6). There were three flexible rockfall fence panels supported by four posts. The bottom was not fixed. At the base of the posts the drapery was connected to the bottom of the fence panels extending downslope in contact with the ground to a bench. This single design and wire mesh were tested. The design intent was to catch the rock, attenuate the energy, and guide the rock into a flat catchment area at the base of the slope. The maximum kinetic energy measured during the tests was 500 kJ (185 foot-tons). The system performed as intended with no maintenance required between tests.



**Figure 6. 2007 IGOR Parimmissi Italy First Hybrid/Attenuator tests (Badger et. al., 2008)**

Two years later in 2009 the Colorado Department of Transportation published the results of their comprehensive study for what they referred to as an attenuator (Arndt, et. al., 2009). In these full-scale tests two infrastructure designs were used one was a single panel width of 6 meters (20 feet) and the other was a three-panel width of 18 meters (69 feet) (Figure 7). Eleven different mesh panel materials and two different post configurations were evaluated. Like the Italian tests this testing used a near vertical flexible rockfall fence that were 3 and 6 meters high (10 and 20 feet), not connected at the base but instead a drapery was attached below the fence varying in length from 1.5 to 9 meters (5 to 30 feet). One hundred and twenty-five rock-rolling tests were performed by dropping concrete and rocks onto a ramp (unnatural slope) and into the

system. Six sizes of concrete test rocks were used weighing up to 3,800 kg (8,360 pounds). The maximum total kinetic energy measured during the testing was 500 kJ (185 foot-tons). The design approach was to test each design to failure and evaluate their ability to attenuate (reduce) rockfall energy, the amount of deformation, the maintenance required, the amount of tail (drape length) required to adequately attenuate the rockfall energies, the durability of the post-to-foundation connections, and the amount of fly-up of the drapery tail that occurred upon rock impact (Arndt et. al., 2008).



**Figure 7. Hidden Valley attenuator full scale test site (Arndt et. al., 2008).**

In 2010 the Swiss Federal Institute for Forest, Snow, and Landscape Research (WSL) in collaboration with Geobruugg performed full scale field testing examining the attenuation properties of a hybrid system (Figure 8) (Glover et. al., 2010). The tests were performed for a single system that consisted of a near vertical flexible rockfall fence that was 3 meters tall and 8 meters wide creating a 6-meter-long impact zone. A drapery was attached to the base of the fence that extended 40 meters along the slope below the fence. The mesh was a high tensile spiral wire rope net. At the base of the slope was a ditch created and a 3-meter (10 feet) high flexible rockfall fence. Seven rocks were rolled by dropping natural rocks onto a ramp, onto a natural slope, and down into the system. The natural rock weights ranged between 300 to 1,200 kg (660 to 2600 pounds). This test focused on reduction in kinetic energy, bounce height, impact energy, and exit velocity. The system performed as intended with no maintenance required between tests.



**Figure 8. Saint Leonard Attenuator and Hybrid Design full scale test site (Glover et. al., 2010) (Badger, Duffy, 2012)**

In 2015, full scale testing of a rockfall attenuator began at the Nicolum Quarry near Hope BC, Canada (Wyllie, Shevlin 2015). This design was different from the Italian, Swiss, and Colorado tests. The attenuator design was 9 meters wide (30 feet) and 11 meters tall (36 feet). The two post supports were installed 10 meters (34.5 feet) apart at an angle of 45 degrees away from the slope allowing the mesh to hang vertically from the top of the posts to the ground within the catchment area. There was no mesh contact with the slope (Figure 7). A total of 26 rocks, both natural and concrete, were rolled on a natural slope to test the system. The maximum test rock size was one cubic meter. The maximum impact energy measured during the testing was 400 kJ (150 foot -tons). This test program focused on measuring impact energy, and the effect of impact energy as transferred from the moving block into the net. The attenuator was able to stop these blocks with no significant damage. Overall, the attenuator functioned as intended by redirecting the trajectory of the falling block into the ground where a significant portion of the impact energy was absorbed when the block landed on the ground (Wyllie, Shevlin 2015).

In 2016 full scale testing continued at the Nicolum Site. An attenuator similar to the 2015 design underwent full scale testing, with the mesh hanging vertically from the top of the posts to the ground within the catchment area (Figure 9). The principle of this attenuator design is that rocks were deflected by the net into the ground such that the net structure only absorbed a portion of the impact energy, and the major portion of the energy was absorbed by the ground (Wyllie et. al., 2017). Rocks, natural and concrete, as large as 950 kg (2200 lbs.) were used in the tests.

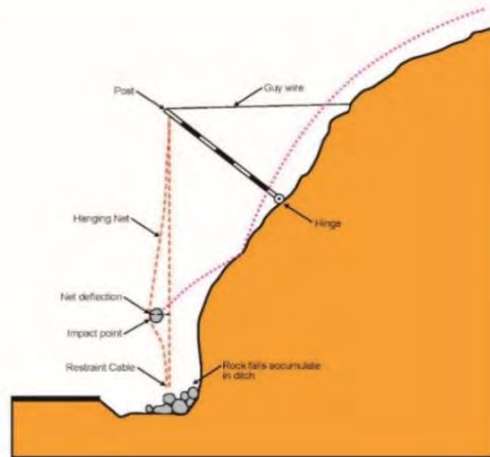


**Figure 9. Nicolum Test site and schematic of attenuator configuration tested (Wyllie, et. al., 2017).**

In 2015 and 2016, a total of 46 tests were performed at the Nicolum test site. Rocks were rolled on natural ground and analysis provided dynamic measurements of rockfalls and attenuator interaction. Translational velocity, and where necessary the rotational speed of the blocks, were measured from the time just before impact with the net, to time of impact with the ground. In these tests, the impact of rockfalls with the attenuator net system were analyzed using the conservation of momentum principle. During the time the block is in contact with the net the loss of momentum of the test blocks was equal to the gain in momentum in the net. This full-scale testing for attenuators was carried out to evaluate the detailed mechanics of their behavior during impact with respect to such factors as net impact, load transfer into the support cables, and net deflection (Wyllie et. al., 2017).

These five full-scale tests on attenuator/hybrid systems have provided a great deal of knowledge regarding their complex performance that are generally positive and encouraging. But since the designs were often not stressed to a point of structural failure, what the designs are fully capable of is still uncertain. Are the system designs as efficient as they could be, withstand higher forces or impacts, or be made lighter and easier to handle and maintain? What quality assurance is there that the designs are reasonable for the impact forces they may be exposed to? These considerations are reminiscent of the evolution of flexible rockfall fences prior to European Union Testing Guidelines. With evolving designs, the need for standardization and quality assurance became essential for the future of flexible rockfall fences and is needed now for attenuator/hybrid systems. The time has come to develop nomenclature, guidelines, and

parameters for specifying and testing attenuator/hybrid systems so that these systems can be installed and relied upon based on sound engineering principles and standards.

## **SUMMARY**

Raised draperies, hanging nets, attenuators, and hybrid designs for rockfall mitigation come in many configurations and designs to fit in a wide variety of terrain. However, whatever the name, two fundamental design applications stand out: one having a flexible barrier where the mesh on the lower portion of the system is in contact with the ground, and another where the mesh hangs free with no ground contact. Both types of systems have been installed around the world.

Each site has different design requirements regarding site geometry and how the impacting rocks exit the system. Where there is a mesh that has ground contact the intent is the rock will exit with a low velocity and zero bounce height into another system or into a catchment basin. With no mesh ground contact the rock is directed into the ground where significant energy is absorbed and the rock stops at that location. The design also needs to address the components of each design. Common to both designs are the mesh strength, weight, flexibility, and surface area all of which are in direct contact with the impacting rock. These impact forces are transmitted into the infrastructure cables, posts, ground anchors and hardware connecting the infrastructure. Each design's success is dependent on all these components. Both systems share the invisible vertical plane through which the rock passes with some amount of kinetic energy (KE) before impact. Rock mass, translational and rotational velocity are measured along this plane. In a standard flexible rockfall fence the design is to stop the rock. Impact energy must be diminished to zero within the fence for success. Not so for attenuator/hybrid systems that reduce the impact energy but allow the rocks to pass. The various full-scale tests have been focused on evaluating impacting velocities, both translational and rotational, and estimating exiting velocities from the systems. Of course, the bounce height dampening was also a very important factor, but probably the most insightful outcome of these full-scale field tests of elevated flexible barriers is the concept of conservation of momentum as a measure of system performance. During the time the rock is in contact with the system, the loss of momentum of the impacting rock is equal to the gain in momentum in the system. These values and the system performance are best evaluated from full-scale field tests. As has been learned many years ago, computer modeling and correlations to empirical data have value and limitations, but only full-scale testing provides the answers that allow for reliable standards and design methods to be developed.

## **DISCUSSION**

What separates flexible rockfall fences and unsecured draperies from hybrid/attenuator systems is its many titles, the way in which the rock is stopped, and the analysis of performance.

These systems have been referred to as hanging nets, hybrid draperies, hybrid barriers, suspended cable, and wire mesh barriers, raised draperies and attenuators. The most common title seems to be "attenuator", and there are two types, one where the lower portion of the mesh

has direct ground contact and another where the lower portion of the mesh is free hanging with no ground contact.

Attenuators with ground contact systems tend to cause impacting rocks to exit at low velocities and transition into another system. Attenuators with non-ground contact systems tend to cause impacting rocks to exit at higher velocities and abruptly end in contact with the ground. Both systems attempt to slow rock velocity and direct the rock to stop into suitable catchment areas. Catchment area location and geometry are an integral part of both designs.

When analyzing the capabilities of these systems, performance is more accurately described when evaluated in terms of conservation of momentum - velocity in and velocity out and the relationship of the rock mass and the system mass.

**References:**

Arndt, B., Ortiz, T., Turner, K. Colorado's Full-Scale Field Testing of Rockfall Attenuator Systems. Transportation Research Circular E-C141, Transportation Research Board, Washington, D.C., October 2009.

Badger, T. C., J. D. Duffy, F. Sassudelli, P.C. Ingraham, P. Perreault, B. Muhunthan, H. Radhakrishnan, O. S. Bursi, M. Molinari, and E. Castelli. Hybrid Barrier Systems for Rockfall Protection. Proceedings; Interdisciplinary Workshop on Rockfall Protection, Morschach, Switzerland, 2008, pp. 10–12.

Badger T.C. and J.D. Duffy. Drapery Systems. Rockfall: Characterization and Control Transportation Research Board, National Academy Press, Washington, D.C. 2012, pp 554-576.

Barrett, R. K., T. Bowen, T. Pfeiffer, and J. D. Higgins. Rockfall Modeling and Attenuator Testing. Colorado Department of Transportation Report CDOH-DTD-ED3/CSM-89-2. Denver, Colo., 1989.

Duffy.J.D. and Badger T.C. Flexible Rockfall Fences in Rockfall: Characterization and Control Transportation Research Board, National Academy Press, Washington, D.C. 2012, pp 526-533.

ETAG27. Guideline for European Technical Approval of Falling Rock Kits, (February, 2008), European Organisation for Technical Approvals, Brussels, Belgium, 2008.

Geobrugg web site, [https://www.geobrugg.com/en/Rockfall-Protection-77472,7858.html?branche\\_id=59494](https://www.geobrugg.com/en/Rockfall-Protection-77472,7858.html?branche_id=59494), Accessed June 5, 2023.

Glover, J.; Volkwein, A.; Dufour, F.; Denk, M.; Roth, A. Rockfall attenuator and hybrid drape systems - design and testing considerations. Third Euro-Mediterranean Symposium on Advances in Geomaterials and Structures. Third Edition, Djerba, 2010, pp. 379-384.

Maccaferri website, <https://www.maccaferri.com/solutions/attenuator-barriers/>. Accessed June 5, 2023.

Trumer website, <https://trumerschutzbauten.com/rockfall-fences/>. Accessed June 5, 2023.

McCauley, M., et. al. Rockfall Mitigation. California Department of Transportation, Sacramento, California. 1983.

Muhuthan, B., S. Shu. Sasiharan, O.A. Hattamleh, T.C. Badger, S.L. Lowell, J.D. Duffy. Analysis and Design of Wire Mesh/Cable Net Slope Protection. Washington State Transportation Center, Seattle, Washington, WA-RD 612.1, 2005, 267p.

Ritchie, A. M. Evaluation of Rockfall and Its Control. *Highway Research Record 17*, Highway Research Board, National Research Council, Washington, D.C., 1963, pp. 13–28.

Duncan Wyllie, Duncan, Shevlin, Tim. Attenuators for controlling rock fall: Do we know how they work? Can we specify what they should do? Prepared for the 66th Highway Geology Symposium, Sturbridge, Massachusetts, September 2015.

Wyllie, Duncan, Shevlin, Tim, Glover, James, Wendeler, Corinna. Development of design method for rockfall Attenuators. Prepared for the 68th Highway Geology Symposium, Marietta, Georgia, May, 2017.

# **How To Develop Rockslope Mitigation For Very Large Roadway-Dipping Blocks Along an Interstate Highway**

**Stephen Newman, L.E.G.**  
Washington State Department of Transportation  
1655 S 2<sup>nd</sup> Ave. SW  
Tumwater, WA 98512  
(360)-705-7000  
NewmanS@wsdot.wa.gov

Prepared for the 72<sup>nd</sup> Highway Geology Symposium, August, 2023

### **Acknowledgements**

The author would like to thank the following individuals for their contributions in the work described:

Tom Badger, L.E.G., L.H.G, P.E. – Landslide Technology  
Marc Faucher – Washington State Department of Transportation  
Marc Fish, L.E.G. – Washington State Department of Transportation  
Eric Smith, L.E.G. – Washington State Department of Transportation

### **Disclaimer**

Statements and views presented in this paper are strictly those of the author(s), and do not necessarily reflect positions held by their affiliations, the Highway Geology Symposium (HGS), or others acknowledged above. The mention of trade names for commercial products does not imply the approval or endorsement by HGS.

### **Copyright Notice**

Copyright © 2023 Highway Geology Symposium (HGS)

All Rights Reserved. Printed in the United States of America. No part of this publication may be reproduced or copied in any form or by any means – graphic, electronic, or mechanical, including photocopying, taping, or information storage and retrieval systems – without prior written permission of the HGS. This excludes the original author(s).

## ABSTRACT

Several large rock slabs sit perched above westbound Interstate 90 at milepost 40 in Washington State. A highly persistent adversely dipping joint set comprises the basal surfaces of these blocks, granting them kinematic freedom to slide towards the interstate. Two additional joint sets, oriented sub-orthogonally to the highway-dipping joint set, provide lateral/rear release. The Washington State Department of Transportation (WSDOT) recently completed engineering geologic design to mitigate the slope, with construction slated for spring 2024.

In support of design, WSDOT conducted rope-access reconnaissance to characterize the engineering geology of the 200-ft.-high slope. Safety constraints prevented rope access to the entire slope, so WSDOT supplemented the field reconnaissance with terrestrial and unmanned aerial vehicle (UAV) laser scanning, and UAV Structure-from-Motion photogrammetry. WSDOT used these datasets to construct 2D numerical models of the blocks to calculate the reinforcements required to mitigate the slope.

Mitigation will include installation of approximately 3700 linear feet of untensioned rock dowels. Mitigation will also include targeted vegetation removal, significant slope scaling to remove loose rocks and debris from the slope face, and installation of approximately 900 linear feet of uncased horizontal drains in rock.

To protect the travelling public during slope work, the rightmost westbound lane of traffic will be closed. The entire work zone will be separated from live traffic by concrete barrier and by weighted conex rockfall barrier. Crane-supported rockfall containment nets will be suspended between the conex barrier and the slope during scaling. Rolling slowdowns may also be employed during scaling of larger blocks.



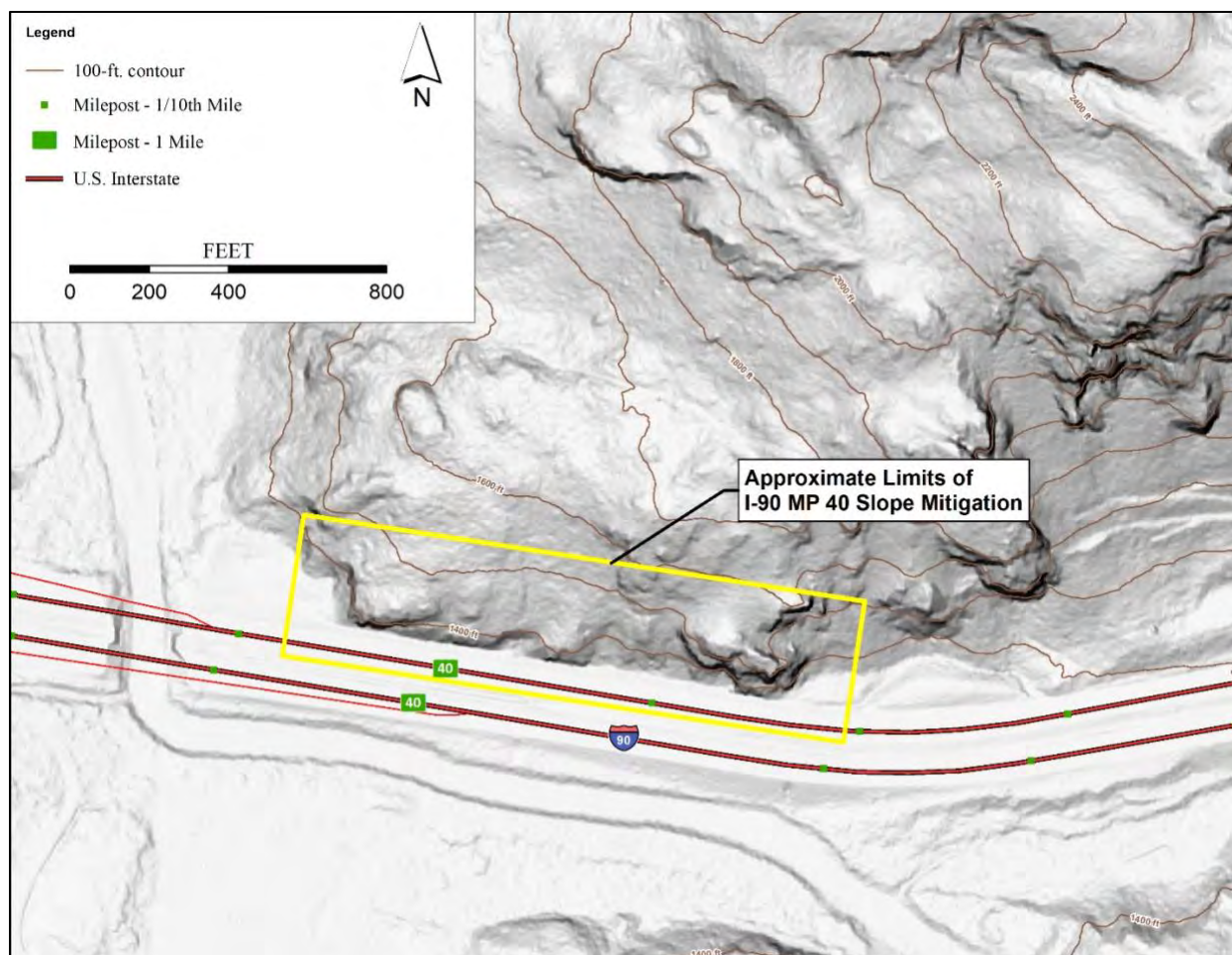


**Figure 2 – Lidar Hillshade Map of the I-90, MP 40 Site Vicinity.**

#### SITE DESCRIPTION

The rock slope is located immediately north of westbound (WB) I-90, in the vicinity of MP 40. At this location, I-90 is oriented east-west, and both eastbound (EB) and WB I-90 consist of three 12-foot-wide travel lanes, separated by an approximately 45- to 50-foot-wide median. The right WB shoulder and ditch have a combined width that varies between approximately 35 and 48 feet, with no guardrail or barrier separating the WB shoulder from the ditch.

The portion of the slope slated for mitigation ranges from approximately 75 feet to over 200 feet in height, and measures approximately 1200 feet in width (E-W dimension). The slope topography exhibits planar and locally highly irregular (convergent and divergent) terrain features (see Figure 2). The inclination of the slope ranges from sub-horizontal (i.e., platform- or bench-like) to subvertical (i.e., bluff-like) to vertical and overhanging (i.e., cliff-like).

WSDOT's Unstable Slope Management System (USMS) database retains records of the slope dating back to 2000. Based on the available USMS records and conversations with WSDOT maintenance crews, no historic slope failures (e.g., rockslides, rockfall) have been reported at this site that have impacted the travel lanes. The infrequency of rockfall has also not necessitated regular ditch cleanout to maintain catchment effectiveness.

Despite the lack of documented historical instability on the slope, the large rock slabs resting on highway-dipping fractures present hazards to I-90 that necessitate geotechnical slope mitigation measures (Figure 3).



**Figure 3 – Oblique Aerial Photograph Showing Some of the Highway-Dipping Rock Slabs Perched Above WB I-90 at MP 40 in Washington State.**

## **GEOTECHNICAL INVESTIGATION**

### **Office data review**

During the desktop phase of its geotechnical investigation, WSDOT reviewed selected available published geologic maps, literature and WSDOT records. Several key remote-sensing datasets were also reviewed, including:

- Public-domain lidar data.
- Unmanned aerial vehicle (UAV) photographs, UAV lidar point clouds, and Structure-from-Motion (SfM) point clouds.
- UAV photographs and video.
- Terrestrial lidar point clouds.

### Field Data Collection

Engineering Geologists (EGs) from the WSDOT Geotechnical Office performed geologic reconnaissance at the site, both on foot and via rope access. They collected limited measurements of discontinuity orientations from selected locations on the slope and made observations of their conditions (persistence, smoothness, infilling, etc.) following ISRM methods (1). The field-derived orientation measurements were also used as a check on subsequent systematic measurements of discontinuity orientations and analyses performed by the WSDOT GeoMetrix Office on the available point clouds.

While in the field, WSDOT EGs used the Joint Roughness Coefficient (JRC) to record small-scale (i.e., 1/20-inch to 1/2-inch scale) joint roughness observations along selected rock structures in the field. The standard JRC chart, printed to scale, was used in the field to accurately measure JRC (2). JRC measurements were primarily targeted along selected apparent potential sliding surfaces that were safely reachable via rope access. Evidence of medium-scale roughness (i.e., roughness on the order of inches to feet) was locally observed along some rock structures, but due to rope-access limitations medium-scale roughness could only be measured in the field on a handful of exposures.

Additionally, a total of 10 rock samples were collected from various locations on the subject rock slope and from the WB I-90 ditch. The rock samples ranged from cobble- to boulder-sized.

### Laboratory Testing

Laboratory testing, for purposes of classification and development of rock engineering properties, was performed on a single hand sample and on three rock core samples. A representative unit weight for the intact rock was derived from the unweathered hand sample. Three uniaxial compressive strength (UCS) tests were performed on rock core samples that were extracted from the above-mentioned field samples using a drill press and a diamond coring bit. UCS tests were performed in general accordance with appropriate American Society of Testing and Materials (ASTM) test methods.

Prior to UCS testing, an attempt was made to measure the basic friction angle ( $\phi_r$ ) of the polished sidewalls of the rock core samples, using a non-standard tilt-test method modified after published ISRM methods (3). Per the ISRM methods, the rock core sidewalls are assumed to be polished by the core bit during drilling. Unfortunately, due to minor drift in the drill press during extraction of the rock core, the core sidewalls exhibited enough small-scale waviness to preclude them from being used for measuring  $\phi_r$ .

### Site Geology

During site reconnaissance visits, WSDOT observed bedrock composed primarily of fine- to medium-grained metagabbro, which is consistent with published geologic mapping that indicates the site is underlain by massive to foliated, locally sheared, fine- to medium-grained metagabbro rock comprising a large tectonic block transported within what is known as the *western mélangé belt* (4) (Figure 4). No widespread small-scale (i.e., hand-sample scale or smaller) ductile or brittle sheared textures were observed during field reconnaissance visits or during subsequent review of hand samples retrieved from the site. Several brittle structures of

apparent tectonic origin were observed at the outcrop and slope scales, but these structures lacked evidence of significant shear displacement. Fresh to slightly weathered, weak to very strong basalt is also present at the project site as sills and dikes within the metagabbro. The volume of basalt observed in surface outcrops is one to two orders of magnitude smaller than the volume of metagabbro observed.

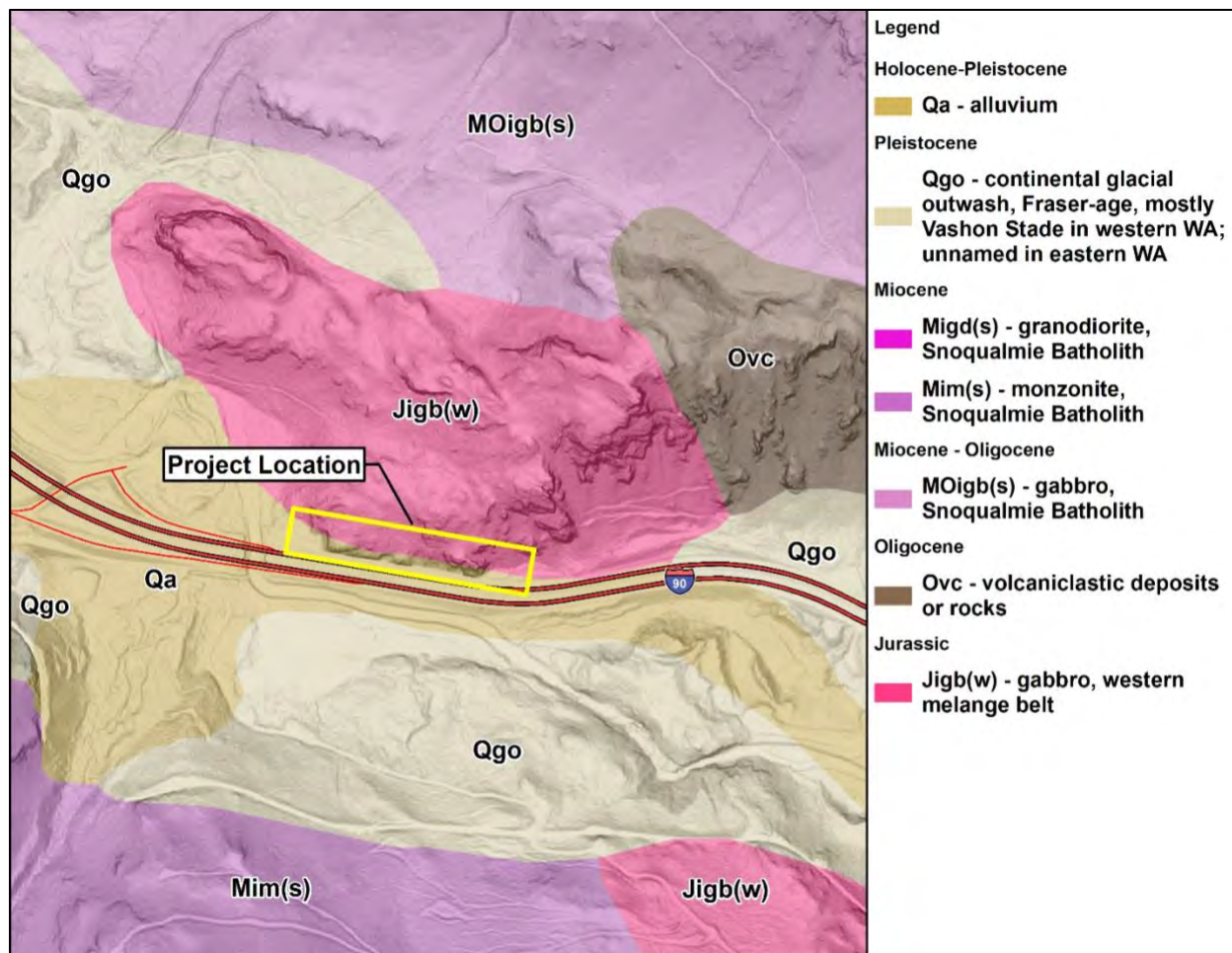


Figure 4 – Excerpt of 1:100,000-Scale Geologic Map in the Vicinity of I-90, MP 40 (4).

Bedrock is exposed at ground surface in significant portions of the slope, especially within the bluff- and cliff-like portions. Elsewhere within the subject slope, where bedrock is not exposed at the ground surface, a variably thick layer of soil and forest duff mantles bedrock. Soil deposits, where present, consist primarily of subangular to subrounded non-cohesive granular deposits, with clasts ranging in size from sand to cobbles and boulders. Isolated, loose, detached cobbles and boulders are also present on some bedrock portions of the slope and are locally obscured by a veneer of moss. Scattered dead snags and sparse to dense, juvenile to mature conifers and hardwood trees are locally present on exposed bedrock and on soil-mantled portions of the slope.

### Site Engineering Geology

During field reconnaissance, significant amounts of loose rock were locally observed on the slope. A handful of isolated boulders were also observed resting in the WB ditch at the base of the slope, indicating that some amount of historic rockfall has occurred, which may not have been observed or reported by WSDOT maintenance crews.

The rock mass on the slope is moderately to highly fractured (jointed) and exhibits at least one prominent discontinuity set that dips toward the I-90 travel lanes, with dip directions ranging between 170° and 220°, and dip angles ranging between approximately 40° and 75° from horizontal (Figure 5). In at least three locations, basalt sills were observed that were coplanar with the highway-dipping discontinuity set (Figure 6). This set commonly exhibits high to very high persistence and very wide to extremely wide spacing, in some cases defining very large, adversely dipping slabs 10s of feet thick and 100 or more feet in extent.

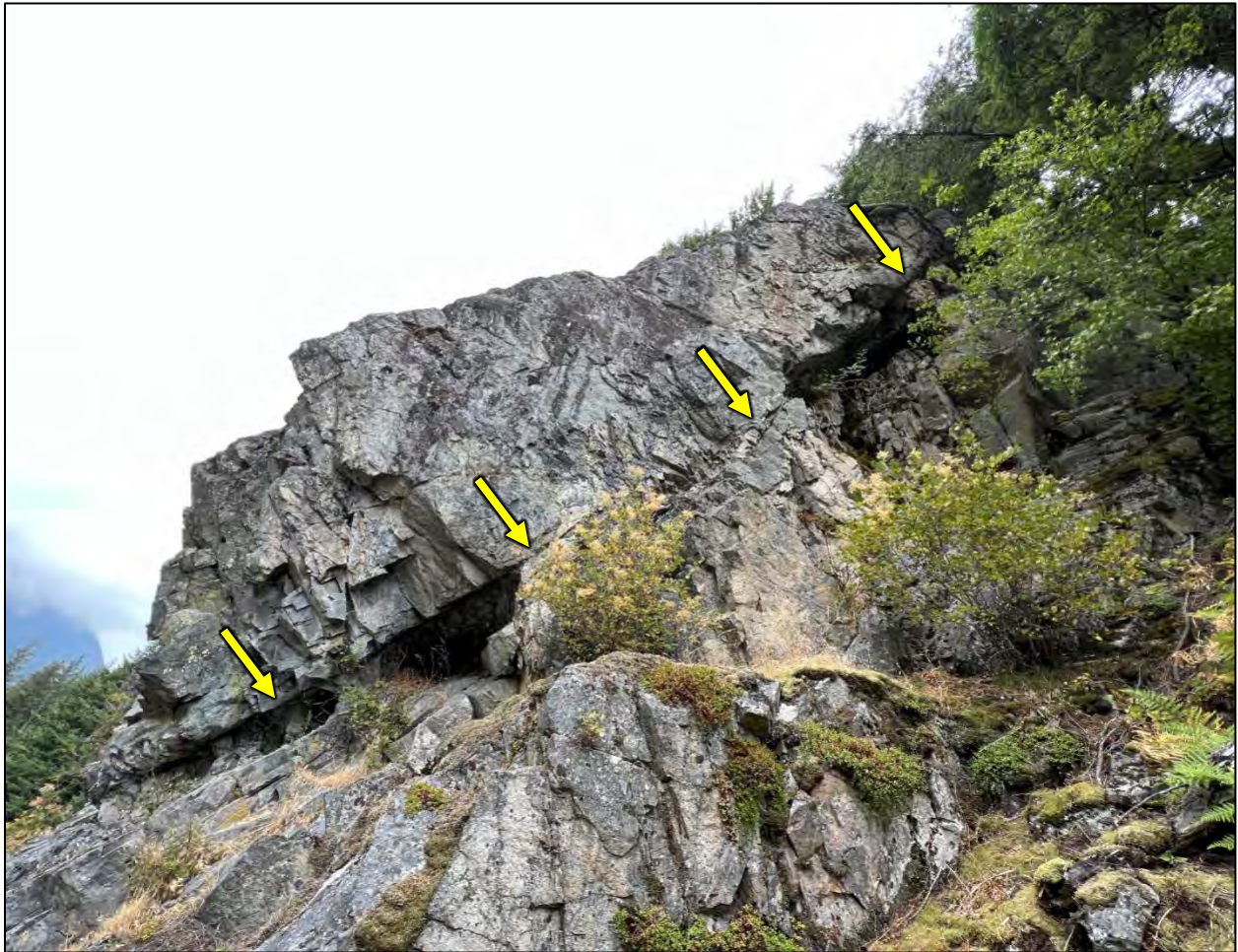


**Figure 5 – 2022 Field Photograph of the Primary Highway-Dipping, High-Persistence Joint Set (Yellow Arrows). The I-90 Travel Lanes are Out of Frame, Downslope to the Left.**



**Figure 6 – 2022 Field Photograph of a Basalt Sill (Yellow Arrows) Parallel to the Highway-Dipping, High-Persistence Joint Set. The Sill Shown Here is Approximately 0.5 Feet Thick.**

The rock mass also exhibits at least two additional prominent discontinuity sets, both of which are oriented roughly sub-orthogonal to the highway-dipping discontinuity set and to each other, and which exhibit low to very high persistence and close to very wide spacing. These rock structures locally delimit rock blocks of variable size, some of which have kinematic freedom to slide and/or topple out of the slope. Half-casts, apparently from drilled blast holes, are visible along the base of the slope at multiple locations, indicating that some or all of the lower slope was blasted, presumably during initial construction of the highway.

Bedrock at the site consists primarily of fresh to slightly weathered, moderately strong to very strong fractured metagabbro bedrock. Relatively minor amounts of fresh to slightly weathered, weak to very strong fractured basalt crop out within the metagabbro at many locations across the slope. UCS testing on three selected core samples, which we extracted from metagabbro boulders exposed at ground surface, resulted in UCS values of 33,636 pounds per square inch (psi), 30,561 psi and 32,392 psi. A non-standard unit-weight test for a single gabbro hand sample yielded a unit weight of 181.2 pounds per cubic foot. Neither the UCS test samples nor the single unit-weight test sample contained basalt.

Several large, conspicuous voids are present along the bases of two of the largest highway-dipping rock blocks on the slope (Figure 7). These voids are apparently the result of preferential weathering of hackly-fractured basalt sills that are present along the base of these two blocks.



**Figure 7 – 2022 Field Photograph of a Large Void Caused by Preferential Weathering of a Basalt Sill Along the Base of a Highway-Dipping Rock Slab. I-90 is Visible at Lower Left.**

#### **Surface Water and Groundwater**

Water streaking and other indications of intermittent seepage and surface water flow were observed on some of the bedrock bluffs and cliffs at the site. Some seepage was observed draining from the primary highway-dipping discontinuity set. The presence of local pockets of perched water within bedrock fractures is possible, but does not appear widespread.

#### **STABILITY ANALYSES**

Due to the cliff-like nature of the bedrock outcroppings and their associated rope-access limitations, WSDOT EGs could not systematically record orientations and conditions of rock structures while in the field. They instead recorded targeted measurements along selected rock structures that were safely accessible via ropes, and recorded visual observations from the highway shoulder. More systematic rock structural orientation measurements were extracted remotely using the 3D terrestrial lidar, UAV lidar, and UAV SfM point clouds.

Based on field and remote observations, WSDOT identified several large adversely oriented planar structures on the slope that underlie large rock blocks, and which may act as

basal shear surfaces. These surfaces were then analyzed for kinematic feasibility using Dips software (5). Where Dips suggested that planar sliding along one of these significant planar features was kinematically feasible, a more detailed sliding-block analysis was then performed using the two-dimensional (2D) limit-equilibrium software RocPlane (6). The 2D block geometries modeled in RocPlane were constructed using the 3D lidar and SfM point cloud data.

As described above, large voids were observed along the bases of two of the largest rock blocks on the slope, both of which were selected for RocPlane modeling. Based on analyses of the available lidar point clouds, which successfully illuminated these voids, both of the potentially unstable rock blocks appear to be in contact with only about 95 percent of the surface area of their respective potential failure planes. Consequently, the 2D model geometries for the two partially undermined blocks were manually adjusted to better reflect the driving and resisting forces of each block.

Each RocPlane model was first back-analyzed to a FOS of 1.05, assuming dry conditions. A FOS of 1.05 was selected for back calculation because the slope has been repeatedly subjected to strong pre-historic seismic shaking with no observed evidence of shear displacement along the potential slide planes. Only joint strength parameters were adjusted during back analysis to achieve the desired FOS; the model geometries and joint orientations remained static. Following back calculation to FOS=1.05, sufficient passive reinforcement was then added to achieve a FOS of between 1.20 and 1.25. The modeled passive reinforcement was then used to determine the appropriate size and number of untensioned rock dowels needed to reinforce the slope.

The joint strength model applied in RocPlane was the Barton-Bandis joint strength model, which assumes that structures that delimit potential slide blocks are fully persistent (i.e., no intact rock is bridging across the two sides of the planar structure that might impart cohesion). This assumption is likely conservative, as intact rock bridges were locally present along a few of the highway-dipping structures observed in the field. Small-scale surface roughness (i.e., on the order of 1/20-inch to 1/4-inch) was incorporated into the joint strength model via the JRC. Medium-scale roughness (i.e., on the order of inches to feet), however, was not incorporated (i.e., no waviness angle applied). Because no reported  $\phi_r$  values for gabbro/metagabbro were available, the values of  $\phi_r$  applied in the joint strength model fell within the typical range reported for granite, which was assumed to have  $\phi_r$  values similar to gabbro (2).

Sensitivity analyses conducted in each of the RocPlane models indicated that the factor of safety (FOS) was most sensitive to changes in JRC. As a result, conservatively low (i.e., smooth) values of JRC were applied in all of the RocPlane models. These conservative values were based on relatively low JRC values measured along the basal surface of one of the more prominent highway-dipping rock slabs on the slope. For most of the modeled rock blocks, JRC could not be directly measured because only a few of the basal surfaces could be safely accessed on ropes.

Table 1 presents the ranges of parameters applied in the RocPlane models.

**Table 1 – RocPlane Model Parameters**

Rock Unit	Unit weight (pcf)	Slide plane inclination (°)	Waviness angle (°)	Barton-Bandis Joint Strength Model		
				JRC	JCS* (psf)	$\phi_r^\ddagger$ (°)
Metagabbro	181	39 - 60	0	6 - 7	4.6x10 <sup>6</sup>	29 - 34

Notes:

\* JCS model parameter derived from UCS test results.

<sup>‡</sup> Residual angle of friction (i.e., the angle of friction for a smoothly cut and polished rock surface), derived from look-up tables (2).**DESIGN RECOMMENDATIONS**

The WSDOT Geotechnical Office recommended that slope scaling be utilized to systematically remove loose rock blocks from the slope to improve safety for workers, and to remove loose blocks situated on the slope that would not be contained in the ditch should they fall. Intensive slope scaling should be concentrated on the brow areas of the slope, as needed, and in areas where significant loose rock is present on the slope face. In these areas, aggressive removal of loose and strained rock material should be performed. Additional areas requiring scaling may be revealed during vegetation removal.

WSDOT originally recommended that an energy absorption blanket, consisting of overlapping steel plates overlain by a blanket of aggregate, be placed along the WB ditch to protect the high-capacity fiber optic lines buried in the ditch from rockfall during scaling operations. Per an existing easement with the utility company that operates the buried fiber optic lines, the utility is responsible for the cost of protecting the lines during any highway construction. The utility, however, has declined to pay for the cost of the energy absorption blanket, and has accepted the risk that falling rocks might damage the fiber optic lines. Consequently, no energy absorption blanket is planned during construction.

WSDOT also recommended that a crane-supported Rockfall Containment Net (RCN) be deployed during scaling operations. An RCN consists of rolled cable-net panels backed with double-twist wire mesh, which are seamed together for a total length of approximately 100 feet, and a total width of approximately 50 feet. A spreader bar and crane are then used to hoist the RCN in front of the slope, where it functions as a makeshift rockfall attenuator during scaling.

In addition to the RCN, WSDOT recommended that 1200 linear feet of Conex Rockfall Barrier be deployed in the rightmost WB I-90 lane for the duration of the project. The Conex Rockfall Barrier will be placed immediately inboard (i.e., north of) a continuous row of concrete barrier that will separate the active travel lanes from the work area. A minimum of 6 tons of concrete barrier should be installed inside each of the deployed conex boxes that comprise the Conex Rockfall Barrier.

Based on the reinforcement quantities modeled in RocPlane, WSDOT recommended installing approximately 3700 linear feet of untensioned rock dowels in the slope, with capacities ranging from 25,000 lbs (25 kips) to 100 kips (Figure 8). Post-tensioned rock bolts were not considered for this project, due to the increased time required during installation and testing of

rock bolts, and due to significant recent increases in bid prices received for post-tensioned rock bolt installation projects.

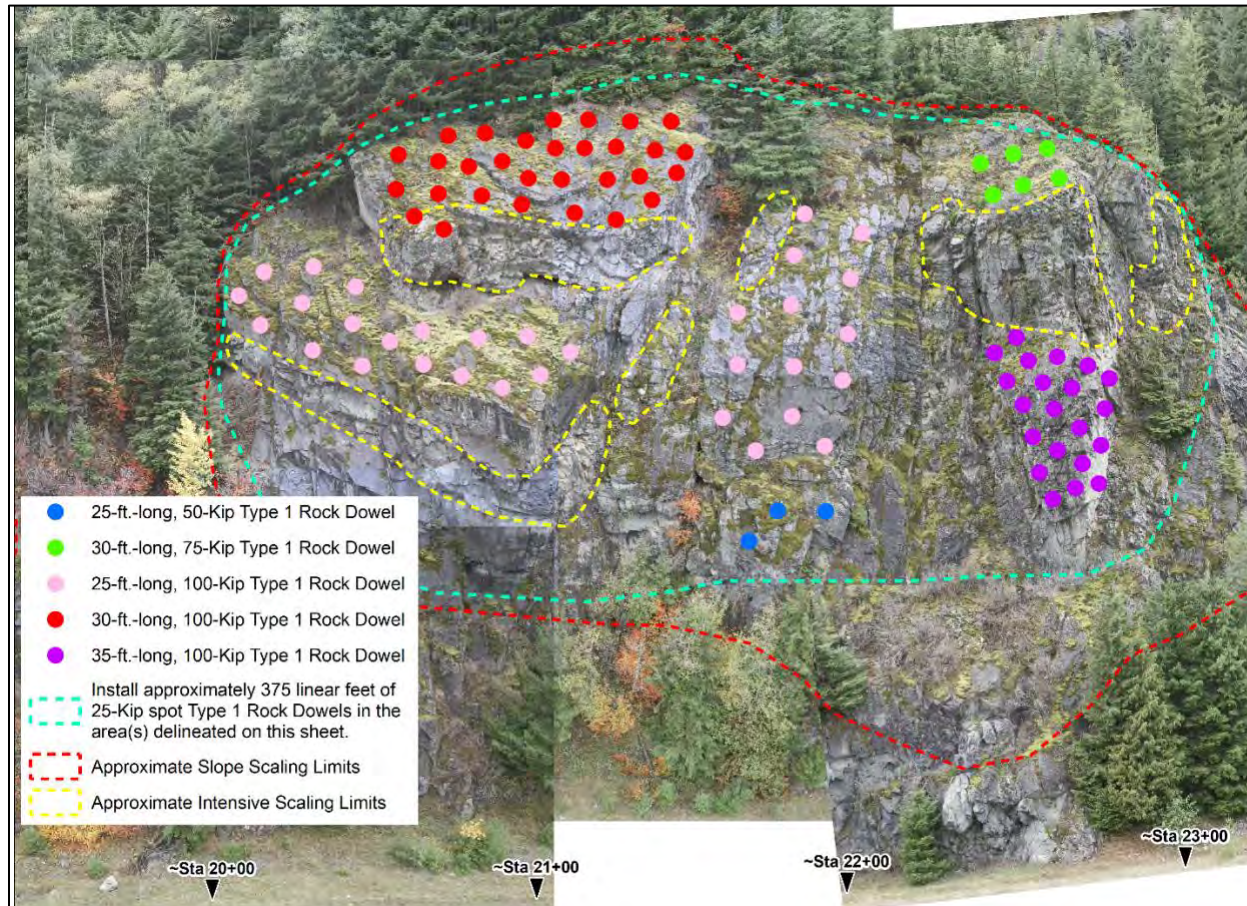


**Figure 8 – Selected Excerpt of Proposed Slope Mitigation Plans, Showing Preliminary Layout of Slope Scaling and Rock Dowel Installations.**

In addition to untensioned rock dowels, WSDOT also recommend that approximately 900 linear feet of uncased horizontal drains be installed at selected locations in the rock slope.

#### Estimated Quantities

Estimated construction quantities are as follows:

- Tree Removal: 112 trees
- Slope Scaling: 322 crew hours
- Debris Removal: 1000 cubic yards
- Conex Rockfall Barrier: 1360 linear feet
- 25-Kip Untensioned Rock Dowels: 1000 linear feet
- 50-Kip Untensioned Rock Dowels: 125 linear feet
- 75-Kip Untensioned Rock Dowels: 180 linear feet
- 100-Kip Untensioned Rock Dowels: 2435 linear feet
- Horizontal Drains – Uncased in Rock: 865 linear feet

## **CONSTRUCTION CONSIDERATIONS**

Due to the presence of the Conex Rockfall Barrier, the crane-supported RCN, and other construction equipment, it will be necessary to close the rightmost (northernmost) WB lane of I-90 for the duration of the project. Rolling slowdowns may also be necessary during scaling of especially large rock blocks from the slope.

Although most of the safety scaling and slope scaling will occur on portions of the slope where bedrock crops out at the ground surface, the contractor will need to be prepared to scale selected lesser portions of the slope where soil is present at the ground surface. Similarly, although all of the rock dowels are likely to be installed at locations where bedrock crops out at the ground surface, the contractor will need to be prepared to drill and install rock dowels at locations where bedrock is mantled by soil deposits measuring up to approximately 1 foot thick. The contractor may also need to employ techniques that can ameliorate difficult drilling conditions, which could be encountered due to variable rock-mass conditions. The contractor may need to use grout socks or other grout-retention techniques if grout loss occurs.

Because slope scaling operations are often successful at removing rock blocks that were designated for reinforcement, representatives from the WSDOT Geotechnical Office will need to reassess the slope following slope scaling operations, to make necessary modifications to the rock dowel plans, and to assist in laying out final rock dowel locations.

## **CLOSURE**

WSDOT expects this project to go to bid in summer 2023, with a single season of construction scheduled to occur in spring and summer 2024.

## REFERENCES

- (1) Barton, N., 1978, Suggested methods for the quantitative description of discontinuities in rock masses: International Society for Rock Mechanics, International Journal of Rock Mechanics and Mining Science & Geomechanics Abstracts, v. 15, p 319-368. Available online: [https://www.researchgate.net/publication/313659691\\_Suggested\\_methods\\_for\\_the\\_quantitative\\_description\\_of\\_discontinuities\\_in\\_rock\\_masses\\_International\\_Society\\_for\\_Rock\\_Mechanics](https://www.researchgate.net/publication/313659691_Suggested_methods_for_the_quantitative_description_of_discontinuities_in_rock_masses_International_Society_for_Rock_Mechanics).
- (2) Barton, N., and Choubey, V., 1977, The shear strength of rock joints in theory and practice: Rock Mechanics v. 10., p 1-54. Available online: [https://www.researchgate.net/publication/227011689\\_The\\_shear\\_strength\\_of\\_rock\\_joints\\_in\\_theory\\_and\\_practice](https://www.researchgate.net/publication/227011689_The_shear_strength_of_rock_joints_in_theory_and_practice).
- (3) Alejano, L., Muralha, J., Ulusay, R., Li, C., Pérez-Rey, I., Karakul, H., Chryssanthakis, P., and Aydan, Ö., 2018, ISRM Suggested Method for Determining the Basic Friction Angle of Planar Rock Surfaces by Means of Tilt Tests: Rock Mechanics and Rock Engineering, v. 51., no. 12, p. 3853 – 3859. Available online: [https://www.researchgate.net/publication/328595765\\_ISRM\\_Suggested\\_Method\\_for\\_Determining\\_the\\_Basic\\_Friction\\_Angle\\_of\\_Planar\\_Rock\\_Surfaces\\_by\\_Means\\_of\\_Tilt\\_Tests](https://www.researchgate.net/publication/328595765_ISRM_Suggested_Method_for_Determining_the_Basic_Friction_Angle_of_Planar_Rock_Surfaces_by_Means_of_Tilt_Tests).
- (4) Tabor, R. W., Frizzell, V. A., Booth, D. B., and Waitt, R. B., 2000, Geologic Map of the Snoqualmie Pass 30- by 60-Minute Quadrangle, Washington: U.S. Geological Survey Geologic Investigations Series I-2538, scale 1:100,000. Available online: <http://geopubs.wr.usgs.gov/i-map/i2538>.
- (5) Rocscience Inc. 2022, Dips Version 8.020 – Graphical and Statistical Analysis of Orientation Data. [www.rocscience.com](http://www.rocscience.com), Toronto, Ontario, Canada.
- (6) Rocscience Inc. 2022, RocPlane Version 4.010 – Planar Wedge Analysis for Slopes. [www.rocscience.com](http://www.rocscience.com), Toronto, Ontario, Canada.

## **What if the Rock Only Threatens to Fall?**

### **Emergency Response to a Decoupled Cliff Face in Washington State**

**Eric L. Smith, L.E.G.**

Washington State Department of Transportation

1655 S 2<sup>nd</sup> Ave. SW

Tumwater, WA 98512

(360)-280-5041

[smithe@wsdot.wa.gov](mailto:smithe@wsdot.wa.gov)

Prepared for the 72<sup>nd</sup> Highway Geology Symposium, August, 2023

### **Acknowledgements**

The author would like to thank Marc Faucher, remote sensing specialist with the WSDOT GeoMetrix Office, who analyzed the terrestrial LiDAR data and provided timely and innovative results that greatly supported the design and construction efforts. The author also wishes to thank Gabriel Taylor for procuring valuable petrographic analyses and to Marc Fish for reviewing the blasting submittals. Thanks also to the WSDOT drill crews, instrumentation team, GIS support personnel, and laboratory staff for their timely support of this emergency project.

### **Disclaimer**

Statements and views presented in this paper are strictly those of the author(s), and do not necessarily reflect positions held by their affiliations, the Highway Geology Symposium (HGS), or others acknowledged above. The mention of trade names for commercial products does not imply the approval or endorsement by HGS.

### **Copyright Notice**

Copyright © 2023 Highway Geology Symposium (HGS)

All Rights Reserved. Printed in the United States of America. No part of this publication may be reproduced or copied in any form or by any means – graphic, electronic, or mechanical, including photocopying, taping, or information storage and retrieval systems – without prior written permission of the HGS. This excludes the original author(s).

## ABSTRACT

Many engineering geologists are familiar with the following scenario: hundreds of cubic yards of rock debris have blocked a roadway with resultant disruption to traffic and commerce. Assessment is necessary to evaluate whether additional unstable rock material remains on the slope and whether the debris on the roadway can be safely cleared to reopen (or partially reopen) the road. What if, however, instead of hundreds of cubic yards, the event included several thousand cubic yards of material, all within a single rock slab, which suddenly decoupled from the rock face, and essentially teetered above the roadway? Such an event occurred on Washington State Route 503 during the spring of 2017. A single slab of volcanic rock (measuring approximately 65 to 70 feet tall, 100 to 105 feet wide and 15 to 20 feet thick) suddenly detached from a vertical cliff face upslope of the highway, dropped approximately 15 feet, and came to rest in a precarious sub-vertical position on a highway-sloping bench. This paper will discuss the subsequent WSDOT emergency response; the follow-on design and bid contract to remove (trim-blast) the slab and mitigate (reinforce) unstable areas behind and adjacent to the failure site; the combination of geologic, topographic and hydrogeologic factors that led to this failure; and how these site conditions are informative to geohazard specialists working in volcanic terrain.

## INTRODUCTION

At the request of the Southwest Region of the WSDOT, the Geotechnical Office responded on March 13, 2017 to a reported rockfall event on SR 503 (vicinity MP 34.34) that had occurred earlier that morning, resulting in the closure of SR 503, approximately 20 miles east of Woodland, Washington (Figure 1). Site observations revealed that, in addition to the

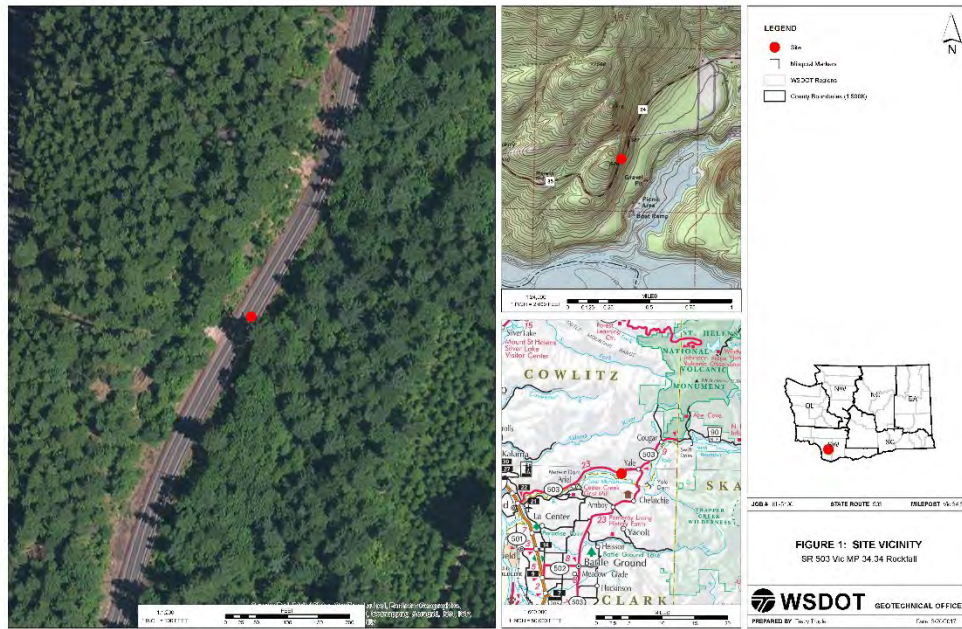


**Figure 1. Site vicinity map**

rockfall, trees and debris on the highway, a large subvertical rock slab had decoupled from the cliff face north of the highway and had come to rest in a precarious subvertical orientation on a highway-sloping bench (Figure 2). Further investigation revealed that adjacent rock slabs were also at risk of decoupling and falling in a similar manner. A fast-tracked response, development of partial mitigation recommendations, safety monitoring of the slope, initial partial mitigation (discussed in more detail below), and partial reopening of the highway followed. Concurrent with the above activities, a follow-on bid contract was developed to address a longer-term mitigation. The bulk of the Phase 2 mitigation was completed in January 2018. The repaving portion of the mitigation was completed in late March 2018. This paper outlines the Geotechnical Office's response, investigation, and recommendations, as well as the completion of the recommended mitigation under the emergency and Phase 2 contracts.

## GEOTECHNICAL INVESTIGATION

The scope of the geotechnical investigation included emergency site geologic reconnaissance; research and review of selected available published geologic maps/literature and WSDOT records, public-domain LiDAR data, and Region-procured unmanned aerial vehicle (UAV) data; geologic mapping; terrestrial LiDAR scans and safety monitoring (change analysis)



**Figure 2. Oblique aerial view of debris on highway at vicinity MP 34.34 and exposed western edge of subvertical decoupled rock slab (red arrow) above the highway (image taken 3/16/17).**

through the GeoMetrix office; drilling of 3 exploratory test borings; laboratory testing; petrographic analysis; development of emergency response recommendations (conveyed via various e-mails and conference calls); development of a long-term mitigation design for use in the Phase 2 contract plans; and preparation of a Summary of Geotechnical Conditions for use in the Phase 2 Contract Provisions.

### **Subsurface Exploration and Instrumentation Program**

A total of 3 test borings were advanced within the project limits for purposes of characterizing subsurface materials, installing instrumentation, retaining samples for laboratory testing, and obtaining three-dimensional distribution data for a suspected weak geologic rock unit underlying the area. The locations of the test borings and instrumentation are shown in Figure 3.

In general, the test borings were advanced using wet rotary methods with an HW casing advancer/HQ triple tube system. HQ-sized core was retained from the bedrock.

Test hole core samples were collected and logged by WSDOT drill inspectors. Descriptions of the subsurface materials, groundwater conditions, and borehole completion were noted during drilling operations. Following drilling, samples were reviewed for consistency with the field descriptions, and samples were selected for laboratory testing.

As an aid to kinematic and slope stability analysis of the bedrock in the failure area, two of the test borings (H-1si-17 and H-2vw-17) were selected for down-hole instrumented logging,

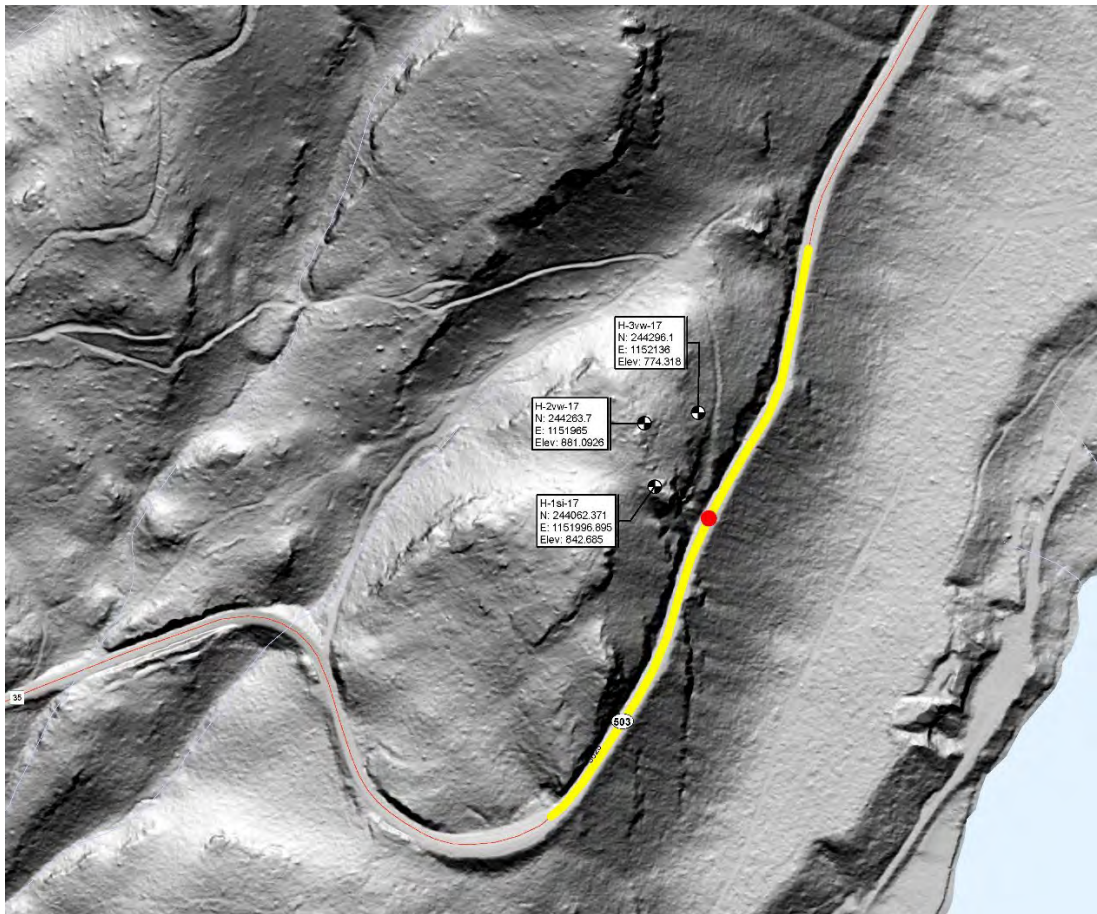


**Figure 3. LiDAR map showing test boring locations (red dot is centered on the subject failure area).**

using optical and acoustic viewers.

Vibrating wire piezometers were installed in two of the test borings (H-2vw-17 and H-3vw-17) advanced for this study. Inclinator casing was installed in one of the test borings (H-1si-17), located atop a relatively flat-topped spur ridge, upslope and behind the work area, as an early warning system of slope movement or creep during construction. The piezometers were fitted for automated groundwater measurements, utilizing a datalogger system (reading at 2-hour intervals), with the data downloaded in the field at selected intervals. Manual measurements were collected from the slope inclinometer at selected intervals. No slope movement was detected in the inclinometer during this study period (April 2017 through March 2018).

### Laboratory Testing

Laboratory testing was performed on selected core samples and grab samples for purposes of classification and development of rock engineering properties. The laboratory testing for the proposed mitigation included grain size distribution (of two grab samples), ring shear tests, direct shear tests, uniaxial compression tests, point load tests, jar slake tests, and slake durability tests.

All laboratory testing was performed in general accordance with appropriate American Society of Testing and Materials (ASTM) and American Association of State Highway and Transportation Officials (AASHTO) test methods.

In order to better understand the provenance and alteration products of the rock units involved in the subject failure event, we sent selected core samples and grab samples to a university laboratory for petrographic analysis.

## **SITE CONDITIONS**

### **Site Description**

The subject portion of SR 503 trends northeast/southwest, along the southeastern flank of an approximately 700-foot-tall rocky ridge that overlooks Lake Merwin in Cowlitz County, Washington. For purposes of further description in this paper, it is assumed that the highway trends east-west and that the subject slope failure is on the north side of the highway. At this location, the north side of the highway is dominated by near-vertical cut slopes that were notched (blasted) from the rock, presumably during original construction. A steep (apparently natural) slope descends below the highway to an inlet (“Speelyai Bay”) of Lake Merwin. A picnic area and boat launch, with associated access roads, are located along the lakeshore, south and west of the failure.

To the east and west of the failure site, bedrock cut slopes ascend to intersect steeply south-sloping natural terrain below the crest of the ridge. At the failure site, there is a reentrant in the cut slope, where a mid-slope bench is present, which in turn is backed by nearly vertical bedrock cliffs. An abandoned access road descends westerly from the ridge top down to the mid-slope bench in the failure area, suggesting that past grading and/or blasting may have occurred within this reentrant and bench area. It is unclear whether this road serviced logging operation(s), original construction or other purpose(s). The existing right-of-way (ROW) plans show a northward extension (widening) of the ROW line that surrounds much of this failure site. We were unable to obtain the Final Record Notes for the original construction to indicate whether previous slope stability issues were encountered at this location. At the time of the subject failure, both sides of the highway were heavily timbered, largely obscuring the cliffs to the north.

### **Regional Geology**

The site is located within the South Cascades physiographic province. Published regional geologic mapping indicates the site is underlain by basaltic andesite and volcanoclastic rocks (Evarts, 2005). The following excerpt from Evarts (2005) describes the mapped rock units underlying the site:

*Tba: Flows and flow breccia of dark-gray to brown, porphyritic to seriate to aphyric basaltic andesite; unit locally includes minor andesite and basalt flows and volcanoclastic rocks too small or poorly exposed to map.*

Field observations and data from test borings were found to be consistent with this description. Regional tectonism has resulted in southwestward tilting of the once subhorizontal layers (Figure 4).

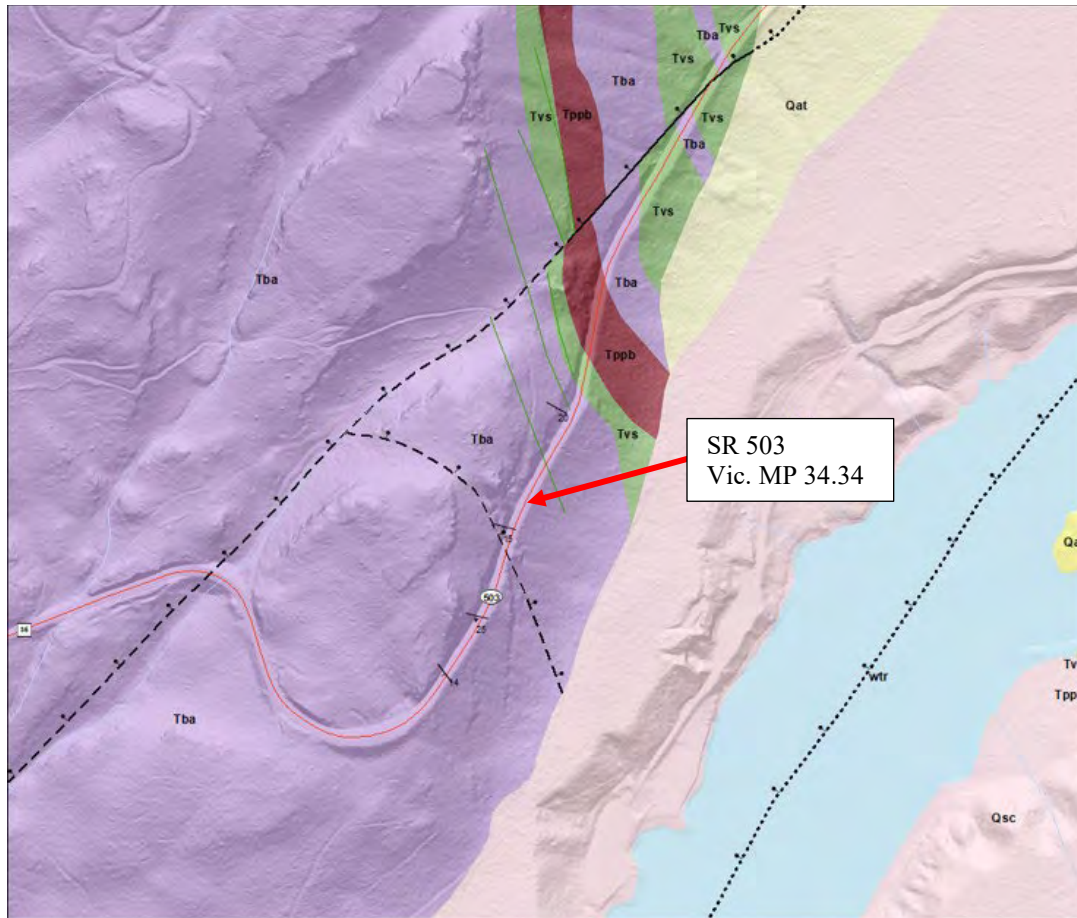


**Figure 4. Site geologic map (adapted from Evarts, 2005)**

### Site Engineering Geology

Based on a preliminary point cloud derived from the UAV data (via structure from motion software), the original failed rock slab measured approximately 60 to 65 feet tall, 100 to 105 feet wide and 10 to 20 feet thick (Figure 5). Using the average measured unit weight of the in-situ rock (174 lbs./ft.<sup>3</sup>) and the dimensions shown in Figure 5 (excluding any embedment in the duff or vegetation cover), the slab constituted approximately 4,360 cubic yards of material and weighed approximately 20.5 million pounds or approximately 10,250 tons.

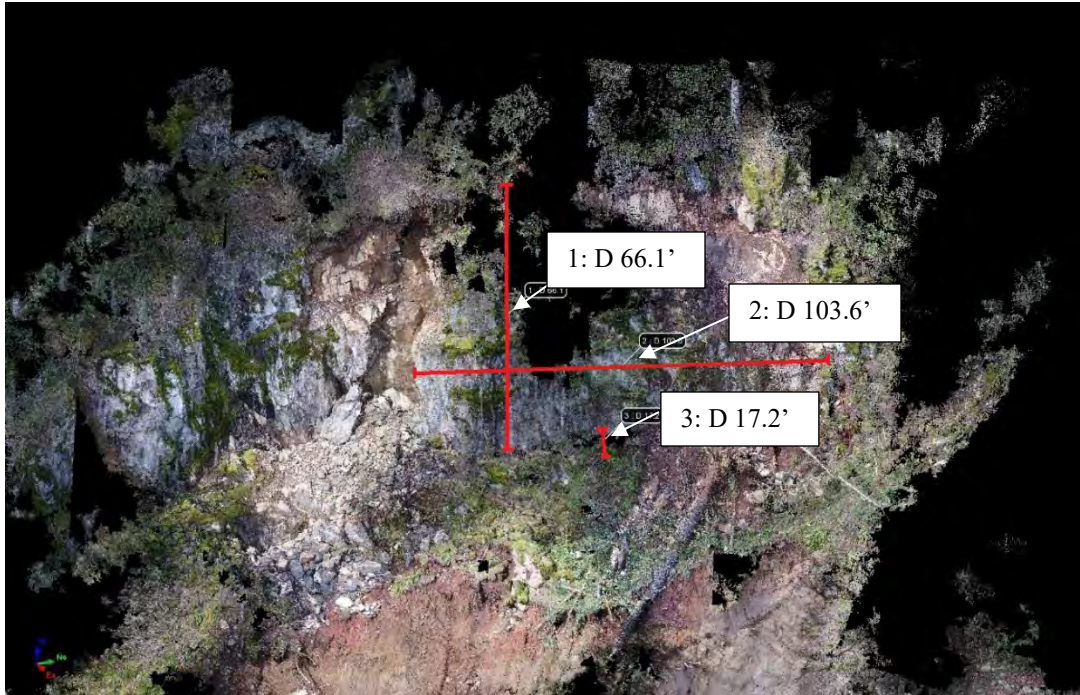


**Figure 5. Oblique view, north, toward failed rock slab, in point cloud derived from UAV data and pulled into point cloud processing software by the GeoMetrix Office. Approximate exposed dimensions of the failed rock slab are shown (in feet).**

The site engineering geologic conditions that were found to be conducive to the initial failure (and found to persist in areas immediately adjacent to the initial failure) included the following.

- A generally northeast-southwest striking (highway parallel) subvertical, highly persistent discontinuity (fracture) set that tends to act as both release surfaces for slab-like rock failures and as infiltration paths for groundwater.
- A generally southwesterly-dipping basal weak rock layer composed of differentially weathered (and locally thermally metamorphosed/oxidized) volcanoclastic rock that tends to provide basal slip surfaces for failing rock blocks/slabs.
- The presence of locally significant perched groundwater (see Surface Water and Groundwater section).

While the volcanic rock types are variable at the site, for purposes of reinforcement design, they were grouped into generalized rock units (Engineering Stratigraphic Units, or ESUs) based on their relative strengths and engineering properties/behaviors. These units are briefly described below.

#### *ESU 1*

ESU 1 is a variable mix of crystalline igneous rock (basaltic andesite) that includes flows of both basaltic and andesitic composition as well as moderately strong to strong and relatively unweathered volcanoclastic rock. The basaltic andesite rocks make up the bulk of the exposures

in the cut slopes and cliffs at and above the highway in this area. Where exposed on steep slopes, it tends to form steep cliffs, subparallel to its dominant southwesterly-striking discontinuity set (Figure 6). Uniaxial compression tests of samples within this rock sequence (sampled primarily from the relatively unweathered volcanoclastic rock) yielded strengths ranging between 1,125 psi and 4,989 psi.



**Figure 6. View west, toward top of subject detached rock slab (red arrow). Also visible is an end-on view of the dominant subvertical discontinuity set (highlighted by red dashed lines) that tends to act as release surfaces for failures and to allow infiltration of rainwater. A scaler standing in the photo (yellow circle) provides scale. SR 503 is visible at lower left corner. (Region photo, dated 4-1-17).**

### *ESU 2*

ESU 2 is a persistent southwesterly-dipping volcanoclastic rock unit that underlies the subject failure area. In exposures, it is generally olive brown in color and capped by an approximately 1-to-3-foot-thick reddish brown layer (Figure 7), interpreted to be a “baked zone” (thermally oxidized portion of the top of the volcanoclastic rock). This unit was initially encountered in “float” (disaggregated surface rocks) below the failure site, in an outcrop immediately west of the failure site, in two of the three test borings, and in later exposures during construction. Uniaxial compression tests of grab samples (from the failure area) of this highly weathered form of the volcanoclastic unit yielded strengths ranging between 86.1 psi and 231 psi. These low strengths are in stark contrast with the in-situ strengths of this unit, as encountered in

the test borings, deep in the slope. It is differentially weathered and significantly weaker in exposures within the failure area (likely due to the presence of perched groundwater and



**Figure 7. Photos showing locations where ESU 2 was encountered: lower left, in float; upper left, in outcrop west of the failure; and at right, in the drill core. The center photo illustrates weathering in ESU2 at an existing discontinuity.**

differential weathering lower in the slope) and for this reason is herein defined as its own ESU. The in-situ, relatively unweathered form of the rock (as encountered in the borings) is generally gray in color. However, the characteristic olive brown color of the weathered portion was observed locally in the rock cores as well, generally parallel to natural fractures (groundwater paths), indicating its susceptibility to weathering by water. The petrographic analyses indicated that, among the constituents of the volcanoclastic unit, those that are vulnerable to weathering included abundant feldspar minerals (mainly of the plagioclase group) and volcanic glass, which tend to alter to various clay minerals in-situ during weathering. The petrographic analysis also reported the presence of hematite (an oxide of iron) within the interpreted baked zone, a mineral often reported within rock units that have undergone thermal metamorphism.

The subject decoupled rock slab consisted of a single very large block or slab of ESU 1 that failed within the upper few feet of ESU 2, while one of several subparallel highly persistent subvertical discontinuities served as a release surface. Through the GeoMetrix Office, we conducted safety monitoring of this decoupled slab (via baseline and follow-on terrestrial LiDAR scans) in the days and weeks following the initial failure, and during the emergency contract period. These scans confirmed the precarious nature of the rock slab's configuration, as the lower edge of the slab was found to be creeping slowly in the downhill direction (Figure 8).

Site observations and the UAV data indicated that nearly identical failure scenarios were already progressing within rock masses immediately behind and adjacent to the subject failure, as evidenced by large rock blocks that were bounded by highly persistent subvertical discontinuities that were dilated (with separations up to 2 to 4 feet in some cases), soil-and-tree root-filled, and

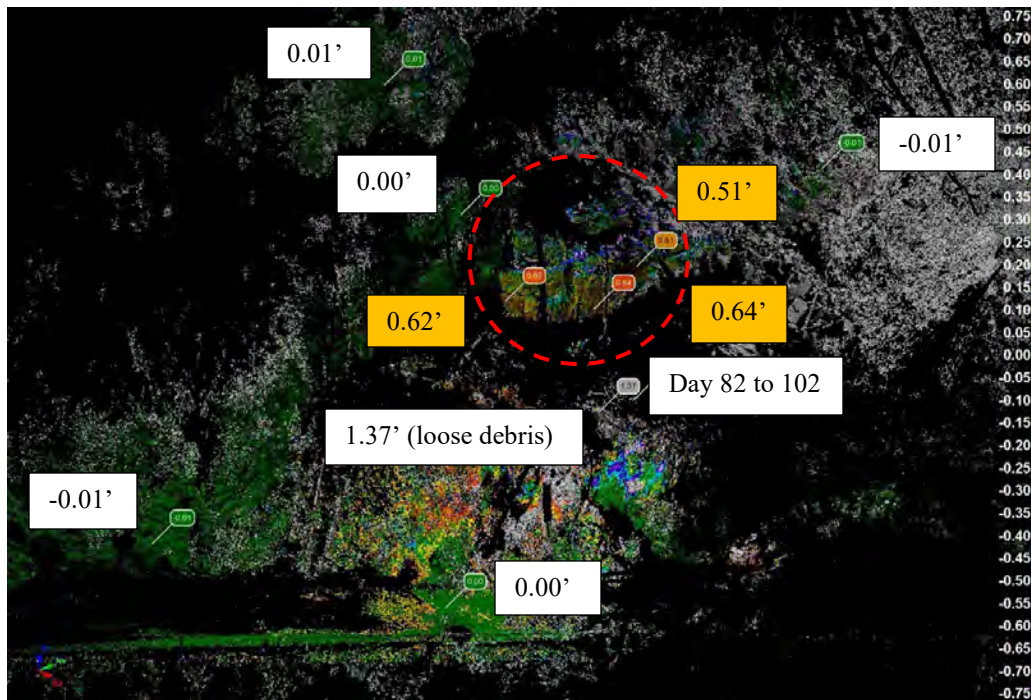


**Figure 8. Terrestrial LiDAR change analysis, in feet (day 82 to 102, 2017), showing that the detached rock slab (circled area) had moved outboard approximately 7-½ inches in 20 days. The above movement predates the first trim blast of the top of the rock slab that occurred on 4-13-2017.**

underlain by ESU 2. Using the terrestrial LiDAR data, we determined the dimensions of these high-risk areas for analysis. The following is a brief description of the areas (rock masses) identified (Figure 9).

#### *Area 1*

Area 1 essentially represents the remnant back wall of the initial rock slab failure, as well as the remnant portion of the failed rock slab that had yet to be completely trim-blasted (or mechanically disaggregated with a hoe-ram) and removed from the mid-slope bench.

#### *Area 2*

Area 2 is essentially a westward continuation of the rock structure of the original slab failure into an area that, although dilated and unstable, did not fail during the subject rockfall event.

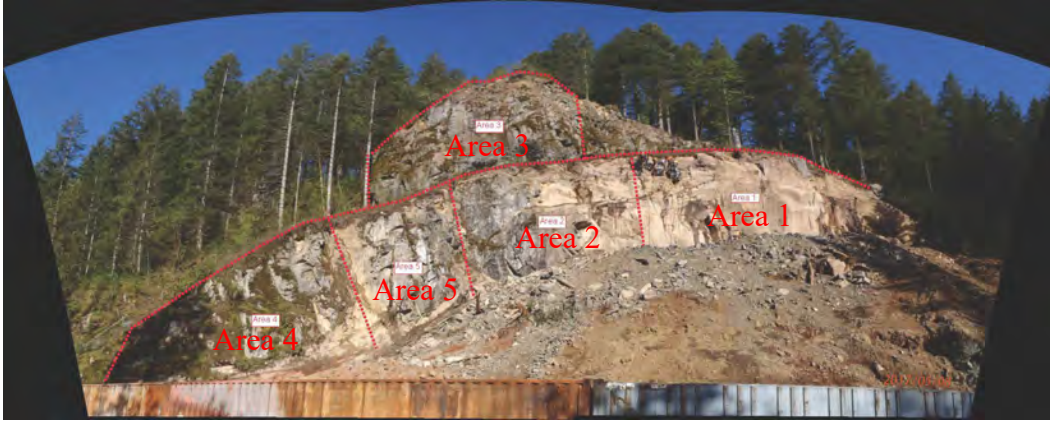


**Figure 9. View, north, toward the site from the vantage of the highway, following the majority of the emergency contract work, and showing the selected areas for Phase 2 mitigation design. Most of the original failed rock slab had been trim-blasted (in front of Area 1), and the remainder of the slab is at this point largely surrounded by blasted and scaled rock debris. A conex rockfall barrier is visible in the foreground.**

### *Area 3*

Area 3 represents the outboard (highway-facing) rock face of the high bluff above and west of the failed rock slab area, the outboard face of which is bounded by a dilated subvertical discontinuity. The crest of this bluff is approximately 200 to 210 feet above the elevation of the highway. Using the terrestrial LiDAR data and the point-cloud processing software Polyworks (by InnovMetric), it was determined that this highly persistent and dilated discontinuity projected behind Areas 1 and 2 as well and, based on corroborating field observations, became the design target plane behind which to anchor proposed reinforcement in Areas 1, 2 and 3 (Figure 10).

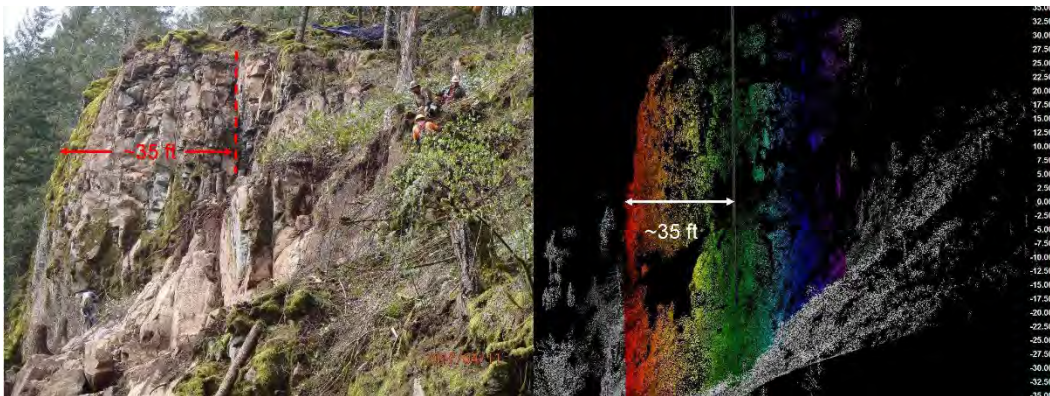


**Figure 10. Photo (left) and LiDAR isopach (right), both facing west, showing the thickness of the Area 3 reinforcement area and the targeted highly persistent and dilated subvertical discontinuity and potential release surface, beyond which reinforcement would be embedded.**

Although Area 3 is not directly underlain by ESU 2, a similar flow boundary and baked zone was encountered in test boring H-1si-17 at the approximate elevation of an apparently differentially weathered highway sloping ledge, and, coupled with the dilated and soil-and-root-filled discontinuity, also indicated marginal stability.

#### *Area 4*

Area 4 is located in the lower west portion of the project area and consists of a rock mass that is bounded on its upslope side by a subvertical and dilated (2-to-4-ft.-wide) highly persistent discontinuity, and also underlain by ESU 2.

#### *Area 5*

Area 5 is essentially the rock mass located between Areas 3 and 4, bounded on its upslope and downslopes sides by highly persistent subvertical and dilated discontinuities. It was analyzed as its own discreet block due to the stability implications of potentially removing all or a portion of Area 4.

### **Surface Water and Groundwater**

Surface runoff within the project area is generally directed southward toward the highway via sheet flow on the steep rocky slopes. Portions of the runoff from the abandoned access road drain southwesterly toward the mid-slope bench below the failure area. Groundwater appears to be locally perched within the slope, with the partially clay-altered ESU 2 likely acting as an aquitard. A few of the drilled holes for the initial reinforcement/mitigation effort (Type I rock dowels and horizontal drains) during the emergency response contract produced significant water volumes. Several areas of seepage were also noted in the rock face during March through May 2017. Reports of perched water in the drilled holes for the Type I dowels were up to about 45 feet above the existing mid-slope bench. Initial output of the first horizontal drains was approximately 5 to 6 gallons per minute, tapering to approximately 1.5 gallons per minute two days after installation. During the latter stages of the Phase 2 contract, nearly all the drilled holes for horizontal drains reportedly initially produced water.

### **STABILITY ANALYSES**

Using the field data gathered and the terrestrial LiDAR data provided (including cross sections, discontinuity orientations and block sizes) by the GeoMetrix Office (Figure 11), we performed limit-equilibrium slope stability analyses using the analysis program RocPlane (v. 2.045) by Rocscience for the above-described domains or areas.

We first back analyzed the original block failure as a planar block with an approximately 60% full, water-filled tension crack to  $FS = 0.99$  (failure). Sensitivity analyses regarding the orientation of the basal slip surface, tension crack filling (hydrostatic pressure), and block dimensions were performed to closely match the observed and inferred field conditions at failure. We then applied the derived strengths to the individual rock mass/block dimensions in Areas 1

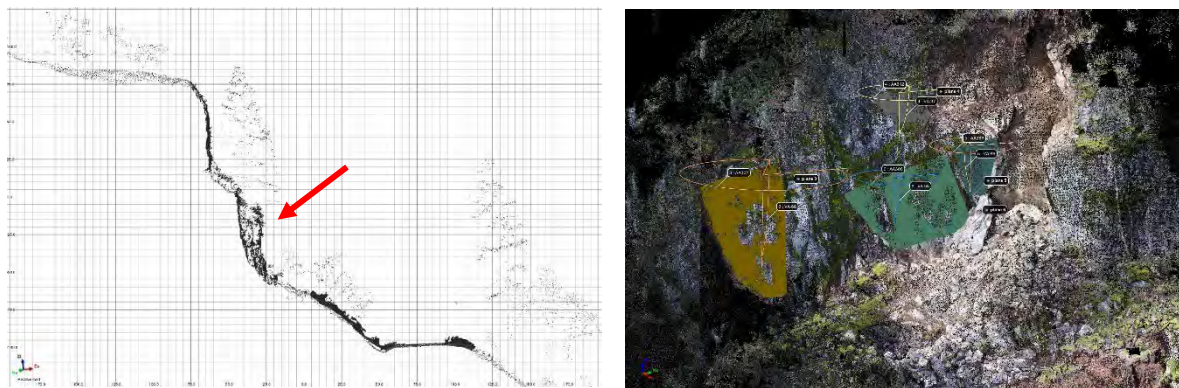


**Figure 11. A) An example of a cross section cut directly from a terrestrial LiDAR point cloud. The arrow points to the western edge of the failed rock slab. B) A screen capture of some of the discontinuity orientations mapped on the terrestrial LiDAR.**

through 5 (that were measured via the terrestrial LiDAR data in Polyworks) to estimate the required reinforcement capacities (Figure 12).

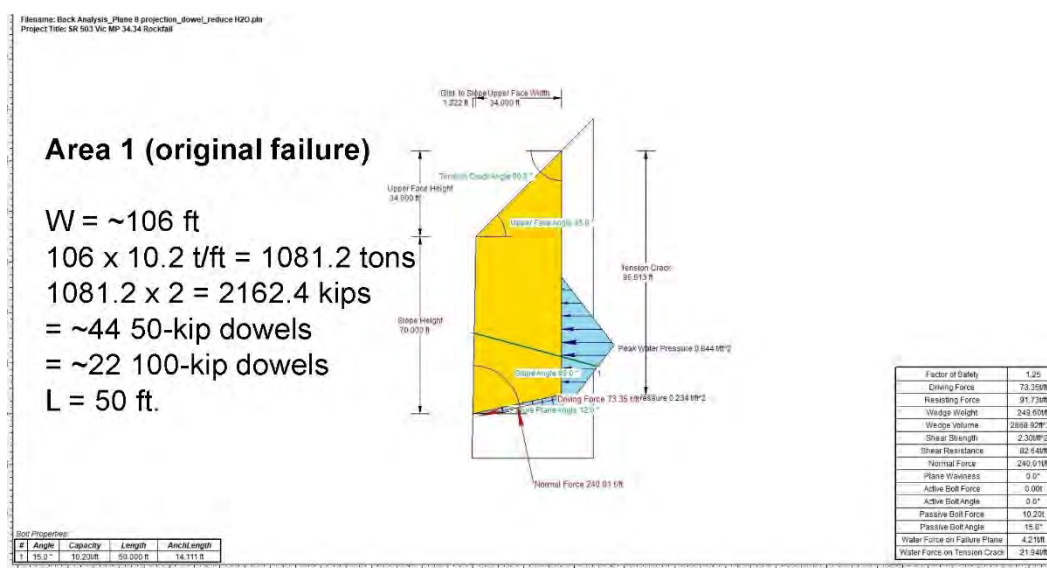


**Figure 12. Typical limit-equilibrium analysis using RocPlane by Rocscience.**

## RECOMMENDATIONS PRESENTED TO THE REGION PROJECT OFFICE

### Initial Emergency Recommendations & Region Emergency Contract

Due to the precarious nature of the decoupled slab, the Geotechnical Office made the following initial recommendations to the WSDOT Southwest Region during various e-mails and conference calls.

- The highway should remain closed in the near-term (intermittent rockfall occurred for several days following the initial event).

- Field personnel should not traverse the slope below the failed and precarious rock slab (and ancillary intermittent rockfall source area) or clear the debris on the highway in the near-term.
- Warnings should be issued regarding the potential for rockfall below the highway, extending to the lake.
- The Region should consider entering into an emergency contract with a qualified rockfall mitigation contractor to provide initial clearing (tree falling) of the brow and work area; rock scaling (safety scaling) of the work area; and to help in developing an approach to safely trim-blast the decoupled rock slab to the point where partial reopening of traffic could occur.
- The GeoMetrix Office should be tasked to provide initial and follow-on scans for both safety monitoring (change analyses) and to provide point-cloud topographic and rock structure data for design.
- Approximately three test borings should be drilled above the failure area to determine whether the apparent weak rock layer (visible in the float below the failure and in outcrop west of the failure) extended beneath and behind the original failure site (and beneath adjacent visibly dilated rock masses), and to obtain rock core samples, rock layer distribution, rock discontinuity orientation data, and groundwater information for analysis.
- The loose material on the mid-slope bench and slope should be left in place for the time being as it likely provided a small measure of toe buttressing for marginally stable rock slabs behind and adjacent to the initial failure.
- Once the failed slab had been reduced in size and relegated to a more stable temporary equilibrium on the bench, the felled trees had been cleared, the existing rock bluffs had been safety-scaled, and most of the largest loose rocks, fallen trees, and other debris had been cleared from the slope immediately above the highway, the roadway itself could be cleared, a conex rockfall barrier established in the inboard lane, and the highway reopened to one lane of signaled traffic, pending the Phase 2 mitigation contract.

In general, the above recommendations were implemented. The Region contracted with a rockfall mitigation specialty company for the emergency response work and the Geotechnical Office conducted a drilling program toward a long-term mitigation design. The specialty contractor performed initial clearing and developed a general blast plan and shot-specific blast plans for trim-blasting of the failed rock slab (submitted to and reviewed by the Geotechnical Office). Trim blasts began on April 13, 2017 and were generally done in 8-ft. vertical lifts.

During this time, the Geotechnical Office was also developing long-term mitigation recommendations for the unstable rock masses behind and adjacent to the original failure. Once the maximum design embedment depths for reinforcement were determined, we consulted with the Region and their specialty contractor to arrive at an optimum reinforcement bar size and length that could be used, given the equipment and techniques available and employed by the contractor. It was determined that no. 9 bars at 50-ft. lengths would be a useful “work horse” size. We recommended the Region consider the following initial order:

*Typically no. 9 nominal 1.125” diameter Grade 75 steel bar, continuously threaded, deformed bar conforming to AASHTO M 31.*

*Minimum ultimate tensile strength : 100 kips*

*Minimum Yield Strength: 75 kips*

*Hot-tip galvanized or epoxy-coated*

*Bearing Plates: 8 in x 8 in x ¾ in conforming to ASTM A36, Grade 36*

*Lengths: Delivered to the site in mill lengths of a minimum 50 feet*

*Anchorage devices (plates, nuts, washers, couplers) shall be galvanized. The contractor shall supply a manufacturer's certification that the coupler has an ultimate strength equal or greater than that of the bar stock. Centralizers shall be placed on the bar on 10-foot centers prior to grouting within a minimum of three centralizers per bar. The lower centralizer shall be located within one foot of the end of the bar.*

*We suggest the initial order be approximately 2500 lineal feet (50 x 50-ft. bars).*

On Monday May 1, 2017, we discovered that one of the subcontractors had excavated a significant amount of the rock material from the top and sides of the mid-slope bench, partially exposing the top of ESU 2 (and thereby undermining portions of Areas 1, 4 and 5). Due to the then-confirmed through-going persistent nature of this weak rock unit, the continued seepage high on the rock face, and the recently experienced rock slab failure, we recommended that further excavation be suspended until such time as some reinforcement is installed in Area 1. By this time, the Region had informed the contractor and the Geotechnical Office that the emergency contract would soon be suspended and that a follow-on bid contract would be developed. The contractor suspended grading operations and concentrated on beginning to install reinforcement (per a preliminary layout provided to the Region on 5/5/2017) prior to the end of the emergency contract. During drilling of these dowels, abundant perched groundwater was encountered up to about 45 feet above the mid-slope bench. We therefore recommended that two horizontal drains be drilled in the lower portion of the exposed rock face near the Area 1/Area 2 transition (but above ESU 2) to relieve some of this hydrostatic pressure before the end of the emergency contract (layout provided to the Region on 5/12/2017).

The two horizontal drains and a few of the dowels were drilled prior to suspension of the emergency contract. At that point, the failed slab had been significantly reduced in size and follow-on scans (change analyses) showed no additional movement of the rock slab. It was therefore deemed feasible to set up a conex rockfall barrier in the inboard lane and to open the outboard lane to signaled traffic, pending issuance of the Phase 2 contract.

## **Recommendations for Phase 2 Contract**

Based on slope stability analyses and the site observations and experience gained during the emergency response contract phase, we recommended the following mitigation elements in Phase 2.

- The conex rockfall barrier should be maintained throughout the Phase 2 mitigation.
- Additional rock scaling: Only preliminary safety scaling was accomplished during the emergency contract. Additional scaling would be needed to remove additional marginally stable material and to render the work area safe for drilling activities.
- Areas 1 through 5 should be reinforced with Type 1 rock dowels (50-kip or 100-kip capacities) per area allotments sent to the Region on 5/25/2017, with final positions to be

determined in the field following additional safety scaling activities for the drilling effort. (Since the contract would go out to bid, the Region had requested some flexibility in the bar size that could be used. We therefore provided capacities based on both 50- and 100-kip dowels).

- Horizontal drains should be installed in each of the 5 areas according to an allotment forwarded to the Region on 5/31/2017, with final positions to be determined in the field following additional scaling activities for the drilling effort and the final configuration of Area 4.
- Trim blasting should be used to further reduce and eliminate the originally failed rock slab and to remove unstable material in Area 4 that cannot be successfully reinforced.
- The unstable rock material in Area 4 should be removed by trim blasting or reinforced in-situ - or some combination to be determined during construction. (Based on input from the emergency response contractor that the dilated discontinuity visible at the back of Area 4 was too wide to bridge with grout, the Region opted to present only trim blasting of Area 4 and reinforcing Area 5 in the contract).
- We recommended the construction staging generally proceed in the following order: install reinforcement and drainage provisions in Areas 1 and 2 before trim blasting the remainder of the failed slab; install reinforcement and drainage provisions in Area 3 before attempting mitigation in Areas 4 and 5; sequence mitigation efforts in Areas 4 and 5 per the supplement in the Trim Blasting Special Provision.

## **CONSTRUCTION AND POST-CONSTRUCTION MAINTENANCE**

The Phase 2 contract was awarded to a different specialty contractor than the emergency response phase. The Phase 2 scope of work was accomplished largely per the recommendations outlined herein. One item of interest noted during the later stages of the Phase 2 project was that, when the bottom of the original failed slab was exhumed and removed from the mid-slope bench, several feet of olive brown ESU 2 material below the reddish baked zone horizon was observed adhering to the bottom of the slab (Figure 13). This suggests that, while it is unclear whether it had been primarily a sliding failure or a bearing failure (or a combination), it did not occur specifically on or within the baked zone. Figure 14 shows the site conditions nearing the end of the Phase 2 contract.



**Figure 13. View, west, toward exhumed bottom remnant of the original failed rock slab, showing the overlying basaltic andesite still in contact with a remnant of the reddish “baked zone” (red arrow) and a remnant of the olive brown weathered volcaniclastic unit (orange arrow). Note the in-situ contact above and to the right, indicating the failed slab had dropped about 15 feet.**



**Figure 14. View, north, toward the project site, nearing conclusion of the Phase 2 contract work. The conex rockfall barrier has been removed and both lanes of traffic would soon be opened.**

## CLOSURE

This unusual rockfall event resulted from a combination of factors, which, acting together, produced a relatively unique and dangerous geohazard risk condition. These factors included:

- very strong rock overlying very weak rock;
- a highly persistent slope-parallel vertical discontinuity set that formed release surfaces for large slabs of rock and also provided avenues for direct groundwater infiltration;
- an aquitard at the weak basal gently west-sloping volcanoclastic rock contact, resulting in significant buildup of hydrostatic pressure in the slope; and
- steep upland topography that promoted slope creep and dilation of discontinuities.

While such an event is relatively rare in the WSDOT Geotechnical Office's experience, the conditions leading to this failure appear to be less than rare in nature, especially in volcanic terrain.

## REFERENCES:

- Federal Government Reports
  1. Evarts, R.C. *Geologic Map of the Amboy Quadrangle, Clark and Cowlitz Counties, Washington*. Scientific Investigations Map 2885, U.S. Geological Survey, 2005.
- State Government Reports
  1. Phillips, W.M., compiler. *Geologic Map of the Vancouver Quadrangle, Washington*. Open-File Report 87-10, Washington Division of Geology and Earth Resources, 1987.

# **I-90 Rock Slopes: A Retrospective of the Snoqualmie Pass Project**

Norm Norrish

Wyllie & Norrish Rock Engineers

110-909 Marine Drive

Bellingham, WA 98225

## **ABSTRACT**

In the early 2000's, the Washington State Department of Transportation (WSDOT) sought to improve the capacity of Interstate 90 (I-90) through that portion of highway that traversed Snoqualmie Pass in the Cascade Mountains. The project included widening to increase travel lanes from four to six, replacement of an aging snowshed, reduction of snow avalanche vulnerability, inclusion of wildlife passageways across the corridor, riparian upgrades and permanent stabilization of required rock and soil cut slopes. Two early phases of the project, designated 1B and 1C (collectively herein the "Project"), created two continuous miles of steep cut slopes with heights achieving 150 feet. The design and construction were complicated by the narrow corridor, Federal no-fill stipulations for the adjacent Lake Keechelus reservoir, and the current high ADT. Project concept studies were performed between 2000 and 2006, design studies from 2006 to 2010 and construction from 2010 to 2019.

The topic of specific interest to this paper is the investigation, design and construction monitoring of the required rock slopes. Concern for this component was heightened by the occurrence of an unforeseen major rock slope failure during construction of the prior alignment in 1957. Research, coupled with forensic analysis of that event, was undertaken to minimize the probability of a similar occurrence some 50 years later, especially one with the potential to be undetected prior to failure.

The rock slope program for the Project was cognizant of the site construction history, the marginal quality of the volcanic regime, the limitations imposed by the narrow traffic corridor and the intermittent excavation progress in which slope integrity had to be ensured between construction seasons. For a rock slope project of this magnitude, multiple unique (and perhaps unprecedented) design and construction strategies were implemented:

### **Pre-Construction:**

- Structure mapping using analyses of point cloud images and terrestrial photographs.
- Borehole televiewer logging.
- Telemetry of piezometric data for multiple years prior to construction.
- Selection of reinforcement methodology.

### **Construction:**

- Near exclusive utilization of passive reinforcement installed prior to, or contemporaneous with, slope excavation.
- Real time, remote monitoring of slope response to blasting, including input to decisions on post blast traffic control.

- Three complementary slope displacement and load detection systems; robotic total station with prisms, strain gage application to surrogate reinforcement bars, and differential terrestrial LiDAR scanning.
- Correlation of slope behavior to transient hydrologic and environmental influences.
- Modification to slope designs during construction in response to slope displacement behavior.

Post Construction:

- Long term loading behavior of passive reinforcement elements utilizing internet deployment.
- Integration of installed rock slope components with long term asset management and the requirements for future slope maintenance.

Lessons that were learned throughout the Project will hopefully add to the professional record for the benefit of future investigators on similar corridor expansions in mountainous terrain.

# CLIMATE RESILIENCE AND INFRASTRUCTURE ADAPTATION ON CALIFORNIA'S NATIONAL FORESTS

G. R. Keller, PE, GE  
Genesee Geotechnical, Quincy, California  
[gordonrkeller@gmail.com](mailto:gordonrkeller@gmail.com)

D. N. Lindsay, PG, CEG, PE, GE  
California Geological Survey, Redding, California  
[Don.lindsay@conservation.ca.gov](mailto:Don.lindsay@conservation.ca.gov)

## ABSTRACT

California's Sierra Nevada mountain range and Southern California's forests contain a huge amount of infrastructure, including 70,000 kilometers of roads and trails, over 800 bridges, numerous culverts, and other infrastructure on land managed by the US Forest Service. Over the last 40 years these mountain regions have been hit by numerous climate change-related events including droughts, major forest fires, and major storms. Billions of dollars in damage have been sustained and numerous lives lost as a result of these events.

To address these issues and help develop climate resilient strategies, state and federal agencies, including California Department of Transportation, California Geological Survey, and the Forest Service have been involved in infrastructure assessment, risk evaluation, and the identification and implementation of climate resilient strategies and adaptation measures. Efforts have ranged from greenhouse gas reduction from agency vehicles, evaluating alternative and redundant transportation routes, and implementing "stormproofing" road design measures.

Recent projects by the Forest Service have involved climate model studies of future anticipated weather conditions and storm events, community outreach for public understanding of climate impacts, assessment efforts, identification of road adaptation and resiliency measures, and publication of these findings.

Identified adaptation measures include the following:

- Timely road maintenance;
- Positive road surface drainage systems;
- Adequate culvert and bridge scour protection;
- Trash racks on culverts;
- Stream diversion prevention measures;
- Conservative drainage designs using stream simulation concepts;
- Roadway stabilization methods;
- Cost-effective slope stabilization measures such as deep patch, bioengineering, and geosynthetic reinforced soil slopes; and
- Thorough erosion control measures including drainage control, ground cover, and use of deep-rooted vegetation.

## 1. INTRODUCTION

The Sierra Nevada and other mountains throughout California contain a huge amount of infrastructure, including 70,000 kilometers of roads and trails, over 800 bridges, and

numerous culverts and low-water crossings, on the National Forests managed by the USDA Forest Service. Most roads are relatively low standard unpaved or gravel low-volume roads, but paved Forest Highways also exist. This infrastructure represents over 16 billion dollars (US) of investment. Over the last 40 years this region has been hit by numerous climate change-related events including droughts, major forest fires, and major storms and flooding. Billions of dollars in damage have been sustained and numerous lives lost as a result of these events.

Key road adaptation, or “stormproofing” measures discussed in this paper include:

- Timely road maintenance;
- Road relocation out of stream channel migration zones;
- Positive road surface drainage systems such as rolling dips, inslope or outslope roads, frequent cross drains, etc.;
- Adequate culvert protection, including trash racks on culverts to minimize plugging failures, stream diversion prevention measures such as relief dips in case a pipe plugs, and adoption of stream simulation designs;
- Roadway stabilization methods such as aggregates, soil stabilization, and pavements;
- Cost-effective slope stabilization measures such as deep patch, bioengineering, and geosynthetic reinforced soil slopes and walls;
- Debris flow mitigations and adaptation using ring net and other debris retention structures, and debris flow diversion measures;
- Thorough erosion control measures, ground cover, and use of deep-rooted vegetation.

Other infrastructure impacts and adaptation strategies used to minimize the impacts of climate change or reduce the vulnerability of infrastructure include keeping a historical record of storm damage locations and vulnerable sites; having local road crews that can work during periods of storm activity; keeping low-volume roads to a minimum (but safe) design standard; implementing “self-maintaining” road measures where possible; increasing pipe capacity; adding culvert mitered inlet structures; installing bridges that span the entire active stream channel width; and developing a redundant transportation system that offers route alternatives during times of disaster. These and other adaptation strategies are discussed in the publication “Storm Damage Risk Reduction Guide for Low-Volume Roads” [1].

## **2. BACKGROUND**

The U. S. Department of Agriculture, Forest Service (USFS), has recently been involved in climate model studies to help forecast future anticipated weather conditions and storm events, given several greenhouse gas emission scenarios. To help the public and agency personnel understand the project and consequences of a changing climate, community outreach efforts have been made, including local workshops, website information, newsletters, and publication of the project findings. Different agency vulnerability assessment methods have been evaluated. Finally, a major effort has involved identification of road adaptation and resiliency measures, particularly measures that are practical and implementable with a minimum of cost.

To address these issues and help develop climate resilient strategies, most state and federal agencies have been involved in infrastructure assessment, risk evaluation, and the identification and implementation of climate resilient strategies and adaptation measures to

minimize the impacts of climate-related events. Efforts to reduce the impacts of climate change have ranged from greenhouse gas reduction from agency vehicles, evaluating alternative and redundant transportation routes, energy-saving measures, and implementing “stormproofing” road design measures to reduce the vulnerability of infrastructure to extreme climate-related events.

A significant amount of infrastructure is at risk in California’s mountainous regions from climate-induced events, including the 70,000 kilometers of roads, 800 bridges, as well as other infrastructure. Roads and facilities are subject to a wide variety of climate-induced events including landslides, floods, washouts, erosion, freeze-thaw, and fires, all of which can damage or destroy infrastructure (Figure 1). Roads, bridges, and culverts are susceptible to increased runoff during storm events and failures due to washouts, plugging, overtopping, stream diversion, and scour. Storm-induced landslides, debris slides, and rockfalls occur due to saturated soils during major storms, particularly if storms include high-intensity rainfall. The combination of fires followed by heavy rains has led to plugged culverts, severe erosion, and debris flows from deep canyons in steep terrain (Figure 2). Debris flows often damage or destroy most types of infrastructure in their path. Damage from fires, floods, and instability have cost taxpayers billions of dollars in recent years.

Significant impacts to infrastructure also result from more subtle climate change phenomena, including: (1) less snowpack and earlier snowmelt that allow early access to and use of roads, trails, campgrounds, and facilities, (2) more dust on roads during prolonged drought periods, (3) drying of traditional water sources in late summer, and (4) limited funding for maintenance due to increased allocation of funds to fire management.



Figure 1 - Road and culvert damage caused by major mountain storms in California.



Figure 2 - Culverts plugged and damaged by the sequence of forest fires and then floods.

### 3. CLIMATE STUDIES AND PROJECTIONS

Climate change in the Sierra Nevada is expected to cause the temperature to increase by 6 to 10 °F by the end of the 21<sup>st</sup> century. Total precipitation is expected to increase slightly in winter, and precipitation extremes and rainfall intensities are expected to increase [2]. Warmer temperatures will result in a higher proportion of rainfall rather than snowfall, particularly at 1,500 to 2,500 meter elevations. With less snowfall and warmer temperatures, the snowpack is expected to disappear sooner than historically, opening up the high country earlier.

Extreme events such as “atmospheric rivers” or a “pineapple express,” with large quantities of warm Pacific moisture, are projected to increase precipitation [3]. Although individual storms may be larger, the time between storm events is expected to be longer. Warmer temperatures combined with variable weather may lead to more periods of drought [2].

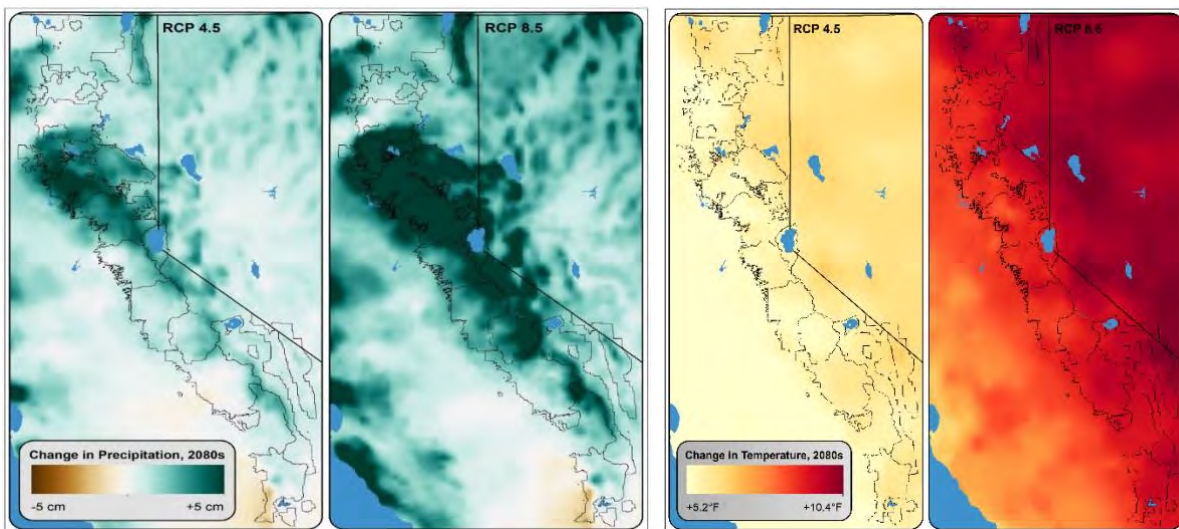


Figure 3 - Projected future changes in precipitation and temperature by 1980 in the Sierra Nevada, depending on either an RCP (Representative Concentration Pathway) 4.5 or RCP 8.5 emissions scenario for greenhouse gases.

Impacts on infrastructure are projected to be more severe than in the past, both from floods and drought-related forest fires. The northern Sierra Nevada is expected to see the biggest increase in precipitation. Southern California mountains may not see major increases in total precipitation, but an increase in storm intensity. In addition, microbursts (similar to small localized tornados) have periodically been observed in mountains, a result of extreme weather conditions that are expected to increase in frequency and intensity.

Examples of the climatic variability impacts facing California were observed in northern California in 2017 and 2018. In 2017, record flooding created a crisis at the Oroville Dam where the primary spillway was extensively damaged (repair costs exceeded \$1.1 billion), and possible use of the untested emergency spillway triggered the evacuation of almost a quarter million people in the Central Valley. In 2018, in the same watershed and only 24 kilometers away, the town of Paradise was destroyed by a wildfire, resulting in the worst wildfire in California history. Eighty-five residents died, 19,000 structures were destroyed, and insurance repair estimates are \$7.5–10 billion. A second glimpse of potential climate

impacts is provided by looking at recent weather patterns in California where prolonged droughts with record-high average annual temperatures in 2022 were followed by a series of nine atmospheric rivers in early 2023 with record rain and snow fall. The onslaught of atmospheric rivers caused significant flooding and landslides that impacted the environment, damaged infrastructure, and contributed to 21 deaths.

#### **4. RISK ASSESSMENT PROCESSES**

Since funds are always limited to harden infrastructure, an assessment of the risks and consequences of damage must be made. The vulnerability assessment process includes a synthesis of best available science to: (1) identify infrastructure at risk, (2) quantify the level of risk relative to value, age, condition, and a combination of climatic exposure and sensitivity to exposure, and (3) summarize appropriate actions needed to minimize the risk. These actions help prioritize where funds are best invested and include adaptation measures needed to increase the resilience of infrastructure.

Various agencies have vulnerability assessment processes, but most follow similar steps. The Federal Highway Administration (FHWA) uses the following comprehensive process [4]:

1. Define the objectives and scope, including climate information, actions and products needed, and assets at risk;
2. Compile available data on the assets, hydrology, and climate;
3. Assess the vulnerability of assets, considering asset history and engineering information;
4. Develop and prioritize adaptation options; and
5. Incorporate results into decision making. Process and results should be periodically monitored and evaluated.

The USFS has a similar process, including: (1) define objectives and establish an interdisciplinary team, (2) define the scope of work relative to assets and climate stressors, (3) collect asset information, climate data, and indicators, and (4) identify and prioritize asset vulnerabilities. These steps are followed by guidance and scoring tools for adaptation strategies of assets at risk [5]. Developing a clear approach minimizes data collection and analyses, streamlines the evaluation process for complex climate change issues, and saves money.

The Canadian forestry industry follows a similar process, developed by the Public Infrastructure Engineering Vulnerability Committee (PIEVC) [6], which has been used in assessing vulnerability of their forest roads. The California Department of Transportation has developed climate change vulnerability assessments for each of their districts. Their reports address highway vulnerabilities, extreme weather impacts, risk management, and adaptation designs that incorporate climate change into decision making.

Fundamental to all processes that evaluate infrastructure vulnerability is the initial need to have good inventories of assets, including roads, bridges, dams, and buildings. Needed expertise is provided by an assessment or interdisciplinary team, consisting of personnel familiar with infrastructure and site history, local terrain stability, climate information, and other relevant information.

Relevant historical observations and future climate projections throughout California's mountains are needed. This helps establish exposure of infrastructure to potential climate

stressors. Using asset data and history, in conjunction with projected climate and hydrologic data, a risk can be assessed for general or specific infrastructure assets. Ranking assets in the context of risk will then help identify asset vulnerabilities and will help prioritize planning, funding, replacement, and maintenance activities. Assessing and prioritizing are critical because funding and resources are always limited. Potentially problematic areas or sites must be identified and the consequences of damage considered in advance of actual impacts.

## **5. GENERAL ADAPTATION STRATEGIES**

Agencies have been involved in a number of measures to help reduce greenhouse gas emissions and minimize the threat of climate change. Mitigation and adaptation measures to minimize climate change can be addressed at the global, national, regional, and local scales. The publication “Climate-resilient infrastructure: adaptive design and risk management” [7] provides a comprehensive overview of adaptation and risk, and climate issues involving infrastructure. Local and federal governments and agencies such as the USFS are implementing programs to reduce carbon emissions, as well as many other efforts worldwide documented by the Intergovernmental Panel on Climate Change (IPCC)

[8]. Specific actions for reducing emissions include carpooling, using efficient and alternative-energy vehicles, building bike paths, and using efficient LED lighting. Sustainable forest management is important for sequestering carbon and includes good logging practices (e.g., reduced impact logging), minimizing conversion of forests to other uses, promoting rapid reforestation in timber harvest areas and burned areas, and supporting fuel reduction programs to reduce wildfire intensity. In addition, agencies can use public education to increase awareness of climate change impacts and the need for action.

Local forest adaptation measures to climate change include: planning for earlier access on forest roads due to less snowpack but when subgrade soils are still saturated; ensuring that maintenance is current and road surface drainage measures are functioning properly and minimizing concentration of water; modifying bridge and culvert designs to accommodate larger design flows; addressing potential scour problems at bridges; installing trash racks and culvert diversion prevention measures to deal with increased debris in channels; designing culverts to match channel bankfull width; repairing old retaining structures and fill slopes in poor condition; applying additional dust palliatives on project roads during droughts; moving some facilities away from streams or in areas of potential landslides and debris flows; and ensuring that critical slopes are well covered with vegetation.

## **6. SPECIFIC ADAPTATION MEASURES**

Several road related adaptation measures have been shown to be relatively inexpensive, very cost-effective, and particularly useful to reduce or prevent a great deal of road damage. These include preventing road-stream encroachment; having effective road surface drainage measures in place that prevent the concentration of water and remove water rapidly off the roadway surface; measures to reduce the likelihood of culverts plugging or washing out the road through increasing the size of culverts, mitering inlets to conform to the fill slope, installing drop inlet structures, and use of trash racks and overflow dips; implementing stream simulation designs; and debris slide prevention, deflection or catchment areas. Each of these issues are described briefly below. A more detailed description of these hazards and their

adaptation measures is found in the publication “Climate Change Vulnerability and Adaptation for Infrastructure and Recreation in the Sierra Nevada” [9].

## 6.1. Timely Road Maintenance

Routine and periodic maintenance is important for roads to function properly any time of year, and particularly when large storms occur. When a large storm is forecast, maintenance becomes critical, yet at that time there may be limited opportunity to do needed maintenance. Properly functioning road surface drainage and stream crossing structures are critical. This applies to roads of all maintenance levels. Unfortunately, a common comment heard from road managers today is the inability to do all needed maintenance because of lack of funds.

Important items of road maintenance include the following:

- Grade and shape the roadway surface to maintain a distinct inslope, outslope, or crown shape to move water rapidly off the road surface, prevent water from pooling, remove ruts, and avoid concentrated discharge points;
- In areas damaged by fire, remove slope ravel material and rocks that end up on the road;
- Remove logs and debris from around the inlet area of culverts and cross-drains;
- Repair collapsed or damaged culverts or ditch relief cross-drain pipes;
- Remove debris from trash racks upstream of culverts;
- Clean ditches to avoid blockage and ponding of water;
- Remove unwanted berms that have formed along the outside edge of the road that concentrate water on the road; and
- Patch potholes and seal cracks in asphalt surfaces to prevent water intrusion and accelerated road damage.

## 6.2. Channel Migration and Preventing Road-Stream Encroachment

Roads have frequently been located where construction required the least amount of work, so many early roads were located on gentle-sloping river terraces adjacent to a river or on channel floodplains. The normal stream meander process frequently undermines or removes road sections, causing high repair costs and travel disruptions. Areas where there are significant changes in stream gradient, or alluvial fan areas, are particularly problematic, because the stream channel may fill with sediment over time and shift its channel. At times, the road may capture the entire river, resulting in complete relocation of the channel to the road alignment.

Roads located along streams, in floodplains, and in channel migration zones are high-risk sites that should be avoided. An ideal management response to road damage is to move the road. High-risk roads can be closed or relocated away from the channel or upslope on a hillside. Although major relocation may be costly and administratively and physically difficult, relocating local sections of roads away from streams or floodplains can eliminate future costly channel encroachment repairs and loss of road function for extended periods. Alternatively, vulnerable areas can be armored with rock riprap to restrain the river and prevent scour or erosion of the streambank. Also, a variety of stream measures such as log and vegetation armoring can be used, or flow can be directed away from the streambank with spur dikes, J-

hooks, rock vanes, rock drop structures, or other methods [10]. Many treatments use a combination of soil bioengineering treatments with rock riprap. Figure 4 (upper photos) shows road damage and a road washout caused by constriction of the natural stream channel or road construction on a historic floodplain. The lower photos show nature-based solutions for streambank stabilization or protection using a combination of rock riprap, tree trunk logs, native vegetation, or spur dikes.



Figure 4 - Examples of roads damaged or washed out because of a location adjacent to streams or built on a floodplain (upper photos), and some streambank stabilization measures with logs, riprap, and spur dikes (lower photos from J. McCullah).

### 6.3. Road Surface Drainage Measures

With traffic and time, ruts will form in most roads, necessitating periodic maintenance. Keeping road maintenance current and drainage measures functional is key to preventing storm damage. A variety of measures are used to prevent the concentration of water, move water rapidly off the road, and facilitate control of water. The best road surface drainage measures to prevent ruts and water concentration are rolling grades, rolling dips, or an inslope, outslope, or crown road section, as seen in Figure 5. Roll grades or undulating the road profile frequently disperses water off the road and prevents water concentration. Cross-drain structures such as either rolling dips or ditch relief cross-drain pipes periodically moves water off the road surface or drains the ditch (Figure 5, lower photo). Road surface drainage measures are relatively inexpensive and can prevent a lot of damage!

Construction of an outslope, inslope, or crown roadway section prevents water from standing on the road. Cross-slopes are typically around 5 percent of unsurfaced roads and 2 percent for paved surfaces. Use of frequently spaced leadoff ditches prevents the accumulation of excessive water in the roadway ditches. Protect the cross-drain outlets with rock (riprap),

brush, or logging slash to dissipate energy and prevent erosion, or locate the outlet of cross-drains on stable, non-erodible soils or bedrock.

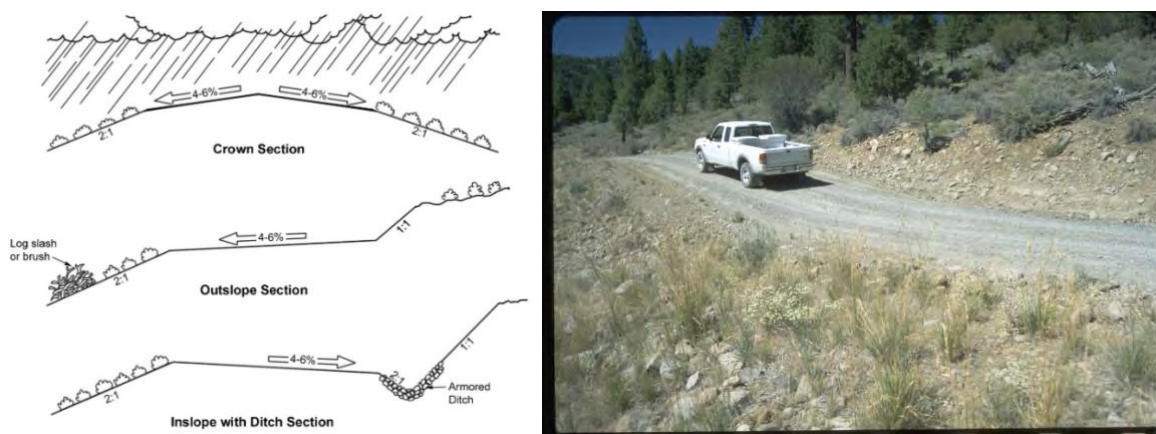


Figure 5 - Road surface drainage measures including an inslope or outslope road (left) or a rolling dip (right photo) used to prevent water concentration.

#### 6.4. Culvert Protection and Improvements

Culverts often plug because of being under-designed (undersized for current storm events), damaged over time, lack of maintenance, and plugging from sediment and debris. Also, undersized culverts or pipes with a waterfall at the outlet often form a barrier to aquatic organism and fish passage. In a mountain environment, plugging is the most common form of culvert failure [11], but plugging can be mitigated [12]. A subsequent problem is stream diversion where the plugged culvert causes the streamflow to be diverted down the road, often damaging a large section of road. Use of trash racks, oversized culverts with mitered inlets, and drop inlet structures with vented risers can aid in the prevention of culvert plugging, and if a culvert does plug, a well-placed overflow dip can at least keep the “overflow” in the same drainage. To prevent a culvert plugging failure, a properly sized large pipe or a ford rather than a culvert may be ideal.

##### 6.4.1 Plugging Protection with Trash Racks

Many existing culverts are undersized and susceptible to plugging, particularly in a woodland or mountain environment. Thus, to prevent plugging, a wide variety of trash racks or debris racks have been used, including steel, rebar, railroad iron, and wood or logs. Flared inlets also help pass debris through culverts. If used, trash racks must periodically be maintained and debris cleaned out. Figure 6 shows examples of metal trash racks used to prevent culvert plugging.



Figure 6 - Photos showing a variety of trash racks used to prevent a culvert from plugging.

#### 6.4.2 Stream Diversion Prevention

Stream diversion occurs when a culvert plugs, the water overtops the roadway embankment, and the road grade allows the water to flow down the road rather than back into the natural drainage. Major road damage has occurred when this happens. To prevent this, an overflow dip can be constructed into the road to ensure that the water remains or returns rapidly in its natural drainage [13]. The dip serves as a “controlled failure” point. Figure 7 shows the road damage from a plugged culvert and flow diversion down the road, and concept of an armored overflow dip in the case of culvert plugging to prevent stream diversion.

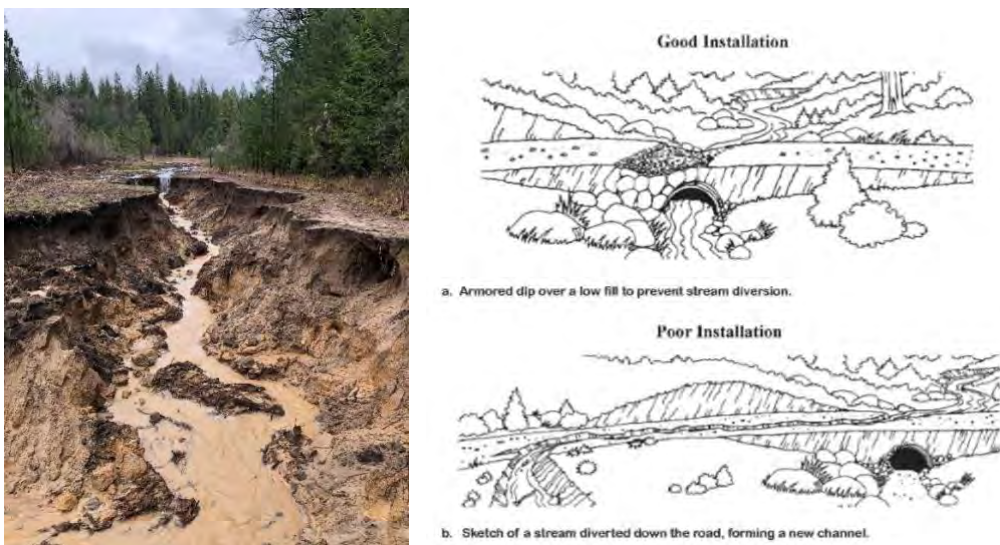


Figure 7 - Photo of a stream that has been diverted down a road and figure showing the concept of a stream diversion prevention dip (right drawing) used to minimize roadway damage from a plugged culvert.

#### 6.4.3 Stream Simulation Culvert Design

Many culverts have been replaced in recent years to improve aquatic organism passage (AOP), fish habitat, and improve stream function. Typically, open-bottomed arch structures or bridges are used to accommodate fish passage at a range of flows. Natural channel-design techniques that mimic natural stream-channel condition upstream and downstream of the crossing and a natural channel bottom material through the structure are being used at these crossings. They promote both AOP and wildlife movement. Additionally, this design concept

often has a culvert design capacity for a 100-year flood event, appropriate for climate change conditions. Key elements are a width equal to or greater than the natural stream bankfull width, and a natural stream substrate through the culvert. For a comprehensive discussion on stream simulation and aquatic organism passage, see “Stream simulation: an ecological approach to providing passage for aquatic organisms at road-stream crossings” [14].

Examples of stream simulation projects are found throughout California’s mountains, as seen in Figure 8. Many of the streams are ephemeral on the mountains of Southern California, but headwater reaches are perennial so resident fish populations benefit from AOP projects. Several stream simulation culvert projects were evaluated on the Green Mountain National Forest, Vermont, following Hurricane Irene in 2011, with flows exceeding the 100-year design flood. The structures survived with minimal problems, while many other conventional culverts and bridges in the region were damaged or destroyed. Only some movement of the bed material was observed [15].

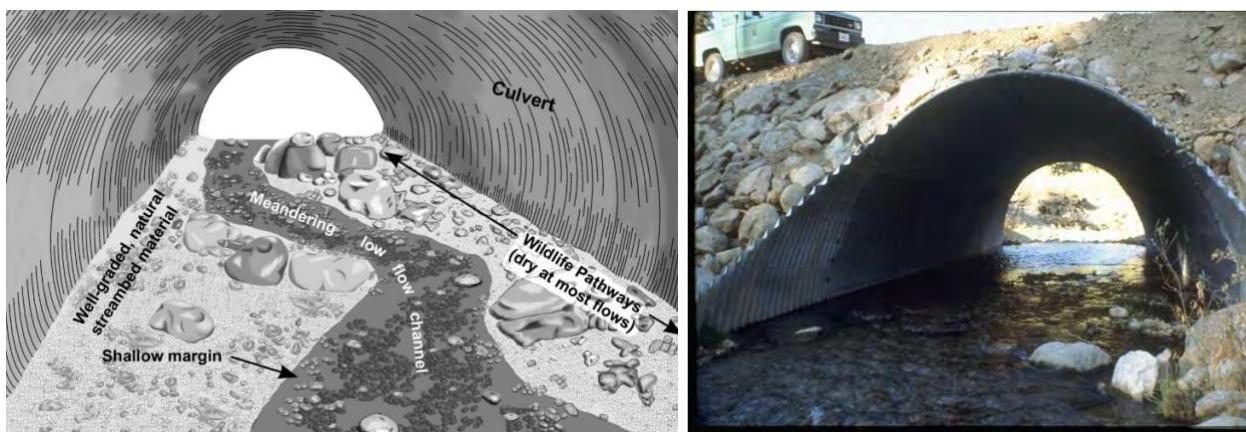


Figure 8 - Drawing and an example photo of stream simulation designs through culverts, replicating a natural stream channel bottom substrate.

### 6.5. Road Surface Stabilization

Most forms of a hardened road surface will perform relatively well during storm events, especially if the road surface is well drained. A surfacing such as gravel or cobblestone, a seal coat, or an asphalt or concrete surface all improve resistance to or eliminate surface erosion. However, the road must be well drained to prevent ditch undercutting of the road.

In areas where the road grade is difficult to drain or where there is higher water table that results in unstable, yielding subgrades, surface stabilization measures are often needed and generally consist of two common methods. The first method consists of building the road prism up using imported aggregate, often pit-run material, that is placed in lifts and worked into the subgrade until sufficient strength and load carrying capacity is obtained in the road prism. The second approach consists of first placing a layer of geosynthetic (either geotextile fabric or geogrid, depending on site variables) down over the yielding subgrade and then covering it with a reduced section of select import. In many cases, the use of geosynthetics can be more economical because it requires far less import [16].

### 6.6. Slope Stabilization Improvements

A wide variety of slope stabilization measures exist than can prevent slope failures, ranging from drainage, use of deep-rooted vegetation and soil bioengineering, flattening or terracing the slope, buttresses, reinforced fills, anchors, and retaining structures. Cost and

effectiveness depend on the situation. Most cost-effective retaining structures include mechanically stabilized earth (MSE) or geosynthetic reinforced soil (GRS) structures, and simple geotextile wrapped walls appear to be the least expensive wall that can be built. Vegetated reinforced soil slopes, using either geotextiles or geogrids, also offer a desirable nature-based but structurally designed slope stabilization treatment. However, most retaining structures are built as a repair after storm damage rather than an adaptation treatment to prevent failure.

Techniques such as vegetation establishment, drainage management, fill compaction, and road surface maintenance are simple and inexpensive, and can prevent slope failures. Removing loose, settling, fill material is also a common approach for reducing storm damage. Implementation of slope stabilization treatments, either for slide prevention or slide repair, should be based on local experience, occasional subsurface investigation and analysis, and preferably site investigation by geotechnical or engineering geology personnel.

### 6.6.1 Deep Patch Shoulder Repairs

Uncompacted fills on steep slopes often progressively settle, are a maintenance problem, and are at risk of failure. Grading does not stop the settlement but starts a long-term commitment to continual roadway repair, and can lead to a slope failure during a storm. Deep patch reduces or stops the continual settlement, and decreases road maintenance costs. It can improve the site from a marginally unstable site to a stable site.

The “deep patch” design is a shallow road-fill slope repair where the upper 1-2 meters of the subsiding section of roadway is excavated, the fill material is replaced with compacted select backfill or gravel, and several layers of geogrid or geotextile are installed for reinforcement (Figure 9). A drain may or may not be included. Deep patches have slowed or stopped slope surface movement on sections of roads crossing areas of large-scale slope settlement and the technique has been used successfully on numerous sites on forest roads and highways [17].

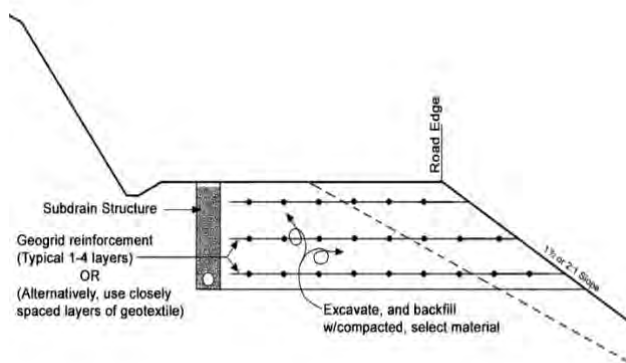


Figure 9 - Drawing of the basic deep patch design and photo of a deep patch repair under construction (right photo).

### 6.7. Debris Flow Forecasting, Mitigation, and Adaptation

Debris flows are a common problem in steep mountain watersheds where a fire has removed the vegetation off the slope, and then the area receives a high-intensity rainstorm. Debris flows have been common in the mountains of Southern California, but have also occurred in the Sierra Nevada and other mountains of the Western United States, as well as the mountains of Europe, Asia, and South America. Debris flows can cause a large amount of

damage, depending on the location and infrastructure in their path. Agencies such as the US Geological Survey has often been involved in mapping and forecasting debris flow hazards in steep mountain terrain after a fire [18] [19].

Post-fire debris flows are a mass movement involving rapid flow of debris of various kinds, including mud, rocks, and logs down a channel. They begin as sheet flow on a slope, particularly accelerated by hydrophobic soils that increase runoff, eventually concentrating the flow, and then causing erosion and rilling which begins to transport sediment. The transported soil and water eventually concentrate in the main channels. The sediment laden flow increases shear at the interface with channel bed, causing downcutting and transport of large diameter material along with finer slope deposition material and woody fire debris.

A variety of management and physical adaptation measures can be used to protect areas of high debris-flow risk, including:

- Moving recreation vehicle trailers or closing vulnerable facilities, roads, and campgrounds when heavy rains are forecast;
- Rapidly replanting burnt upper watershed areas with grasses and deep-rooted shrubs so they will hopefully mature prior to heavy rainfall;
- Building debris retention structures. This can include gabion walls, “porous” open check dams and slotted concrete dams, bollard debris racks, debris flow netting, and ring-nets to trap sediment or large, coarse boulders and logs. Large debris or sediment retention basins have been used at the mouth of major canyons. Smaller structures such as gabions or ring-net structures are more commonly used upstream in drainages;
- Building debris-flow deflection structures to change the direction of debris flows away from infrastructure or bridge abutments; and
- Placing local K-rails and concrete barriers to either stop or deflect small debris flows.

The U.S. Geological Survey has often assisted the Forest Service in landslide hazard mapping and identifying areas of high debris flow risk after forest fires [20]. The “Sediment/Debris Bulking Factors and Post-fire Hydrology for Ventura County” manual [21] provides engineering designs for flood and sediment retention systems under different bulking and watershed conditions. Bulking factors can more than double the flood flow volume beyond clear water flow [22]. Application of a bulking factor (increase in flow volume due to sediment) can help determine flood risk and provide information to determine an adequate size for debris retention structures.

Figure 10 (upper left photo) shows the source area of debris flows on steep, fire-scarred slopes, while the right photo shows typical damage to roads, culverts, and structures, as well as the types of material moving in debris flows. Note the quantity of large boulders being moved in each debris flow. The lower photos show a variety of methods to mitigate damage from debris flows, including bollards, trash racks, debris retention basins, and ring nets.





Figure 10. Upper photos show a debris flow from a fire-scarred areas that has blocked the road and plugged a culvert (left photo), and damage caused by debris flows. The lower photos showing debris retention basins, trash racks with bollards, and ring nets used to trap sediment and debris from a debris flow (lower right photo from Jonathon Schwartz).

## 6.8. Erosion Control and Prevention

The two key prevention measures for erosion control are 1) control of surface water flow and 2) providing ground cover over the soil. Erosion prevention on roads, the entire road prism, and on disturbed areas is fundamental for the conservation of topsoil, protection of water quality, and prevention of damage during storms. Also, erosion control measures are typically inexpensive and very cost-effective. Road and trail surfaces, roadway cut and fill slopes, and disturbed developed areas all contribute to accelerated erosion and can be damaged by intense rainfall, particularly after a fire. Sediment in drainages that is mobilized during intense storm events lead to debris torrents and debris flows.

From a climate resilience standpoint, drainage control measures, already discussed, are needed and maintaining a good vegetative groundcover is important. After a fire, quickly re-establishing a vegetative groundcover is again one of the best treatments to minimize erosion and instability problems. Hillslope treatments should also be aimed at increasing infiltration, using a combination of seeding, mulching, and log or wattle erosion barriers.

### 6.8.1 Soil Bioengineering

Soil bioengineering and biotechnical treatments use integrated ecological principles to assess, design, construct, and maintain living vegetative systems to prevent or repair damage caused by erosion and slope failures [23]. These treatments are labor intensive, useful to prevent shallow slope failures, are aesthetic or natural looking, and are typically under-utilized. Common soil bioengineering and biotechnical treatments include live stakes (with willows, etc., that will re-sprout) embedded in the face of the slope to re-sprout; fascines, wattles, or bundles of branches that are laid in a trench along contour lines that sprout and grow; brush layering placed into terraces in the slope, covered with moist soil and compacted; vegetated gabions or other walls interplanted with live vegetation cuttings; and vegetated reinforced soil slopes, such as geosynthetic reinforced soil slopes with brush placed on each lift along with the reinforcement (Figure 11).



Figure 11 - Common soil bioengineering treatments of brush layering (left photo) and live stakes through riprap (right photo) (photos courtesy of Robbin Sotir).

## 7. CONCLUSIONS

The mountains of California provide a significant amount of water for the state, major recreation opportunities, and a wide range of other resources. The major road systems, including thousands of bridges, culverts and fords, a major trail system, and numerous dams, all part of the infrastructure needed for sustainable management of the forests. These facilities represent a major investment in infrastructure that will be increasingly vulnerable to current and future stressors associated with climate change. Key climate stressors include warmer temperatures, larger storms, more intense precipitation, reduced snowpack, altered timing of peak streamflows, periods of drought, and large wildfires.

This paper describes the infrastructure (roads, bridges, culverts, etc.) found in the mountains of California and their vulnerabilities. Specific measures can be taken to adapt to projected climate change effects, thus minimizing damage from storms and fires, as discussed above. These include timely road maintenance, properly located roads, well designed culverts, stabilized road surfaces, practical slope stabilization measures, and thorough erosion control.

The Forest Service has an extensive and expensive inventory of infrastructure in the region, yet funds are very limited such that even routine maintenance is often beyond the capacity of current personnel and funding. The additional challenges posed by climatic variability and change will make it more difficult to ensure long-term functionality of infrastructure, so assessing vulnerabilities, ranking resources at risk, and prioritizing adaptation actions are critical. Implementing “climate change thinking” and “stormproofing” in day-to-day resource management and agency operations, will improve the likelihood of sustaining critical infrastructure for future generations.

## ACKNOWLEDGMENTS

The basic information of this paper was originally written for the Transportation Research Board, 13<sup>th</sup> International Conference on Low-Volume Roads and also adapted for PIARC, the World Road Association Congress in Prague, 2023.

## REFERENCES

1. Keller, G.; Ketcheson, G. (2015). Storm damage risk reduction guide for low-volume roads. Tech. Rep. 1277-1814. San Dimas, CA: U.S. Department of Agriculture, Forest Service, San Dimas Technology and Development Center.
2. Dettinger, M.; Alpert, H.; Battles, J. [et al.]. (2018). Sierra Nevada summary report. California's Fourth Climate Change Assessment. Pub. SUM-CCCA4-2018-004. Sacramento, CA: State of California.
3. Warner, M.D.; Mass, C.F. (2017). Changes in the climatology, structure, and seasonality of Northeast Pacific atmospheric rivers in CMIP5 climate simulations. *Journal of Hydrometeorology*. 18: 2131–2141.
4. U.S. Department of Transportation, Federal Highway Administration [USDOT FHWA]. (2017). Vulnerability assessment and adaptation framework. 3rd edition. FHWA-HEP-18-020. Washington, DC. 86 p.
5. U.S. Department of Agriculture, Forest Service [USDA FS]. (2018). U.S. Forest Service transportation resiliency guidebook: addressing climate change impacts on U.S. Forest Service transportation assets. Washington, DC.
6. Engineering Canada. (2016). PIEVC engineering protocol for infrastructure vulnerability assessment and adaptation to a changing climate—principles and guidelines. Version PG-10.1. Ottawa, Ontario, Canada.
7. ASCE Committee on Adaptation to a Changing Climate. (2018). Climate-resilient infrastructure: adaptive design and risk mgmt. ASCE Manuals and Reps. on Engin. Prac. 140. Reston, VA: American Society of Civil Engineers. 294 p.
8. Intergovernmental Panel on Climate Change. (2022). Climate Change 2022: Impacts, Adaptation, and Vulnerability-Summary for Policymakers, In: Portner, H; Roberts, D.; Adams, H. [et al.], eds. Contribution of Working Group II to the sixth assessment report of the Intergovernmental Panel on Climate Change. Cambridge, United Kingdom. 2022. 3675 p.
9. Halofsky, J. E., Peterson, D. L., Buluç, L. Y., and J. M. Ko, eds. (2021). Climate change vulnerability and adaptation for infrastructure and recreation in the Sierra Nevada. Gen. Tech. Rep. PSW-GTR-272. Albany, CA: U.S. Department of Agriculture, Forest Service, 275 p.
10. McCullah, J., and D. Gray, D. (2005). NCHRP Report 544: Environmentally sensitive channel and bank protection measures. Transportation Research Board, National Cooperative Highway Research Program. Washington, DC: 2005. 50 p.
11. Furniss, M.; Ledwith, T.; Love, M. [et al.]. (1998). Response of road- stream crossings to large flood events in Washington, Oregon, and Northern California. 9877-1806-SDTDC, San Dimas, CA: U.S. Department of Agriculture, Forest Service, San Dimas Technology and Development Center. 14 p.
12. Cafferata, P., Lindsay, D., Spittler, T., Wopat, M., Bundros, G., Flanagan, S., Coe, D., Short, B. (2017). Designing Watercourse Crossings for Passage of 100-Year Flood Flows, Wood, and Sediment (Updated 2017). 10.13140/RG.2.2.32656.71682.
13. Furniss, M.; Love, M.; Flanagan, S. (1997). Diversion potential at road-stream crossings. Water-Road Interaction Tech. Ser. 9777 1814-SDTDC. San Dimas, CA: U.S. Department of Agriculture, Forest Service, San Dimas Technology and Development Center. 12 p.
14. Stream Simulation Working Group. (2008). Stream simulation: an ecological approach to providing passage for aquatic organisms at road-stream crossings. 7700—Transportation Mgmt. 0877 1801—SDTDC. San Dimas, CA: U.S. Department of Agriculture, Forest Service, National Technology and Development Program. 2008.
15. Gillespie, N.; Unthank, A.; Campbell, L.; Anderson, P.; Gubernick, R.; Weinhold, M.; Cenderelli, D.; Austin, B.; McKinley D.; Wells, S.; Rowan, J.; Orvis, C.; Hudy, M.; Bowden. A.; Singler, A.; Fretzl, E.; Levine, J., and R. Kirn. (2014). Flood effects on road–stream crossing infrastructure: Economic and ecological benefits of stream simulation designs. *Fisheries*, 2014.39:2, 62-76,
16. Holtz, R.D, Barry, C.R., and Berg, R.R. (2008). Geosynthetic Design and Construction Guidelines: FHWA-NHI-07-092, p. 592
17. Cuelho, E., Perkins, S., and M. Akin, M. (2012). Deep patch repair, Phase 1: Analysis and Design. FHWA-WFL/TD-12-003. Western Transportation Institute and Federal Highway Administration, Bozeman, MT and Vancouver, WA. 254 p.

18. Tillery, A.; Matherne, A.M. (2013). Post-wildfire debris flow hazard assessment of the area burned by the 2012 Little Bear Fire, south-central New Mexico. Open-File Rep. 2013-1108. Reston, VA: U.S. Department of the Interior, Geological Survey.
19. Staley, D.M., Negri, J.A., Kean, J.W., Laber, J.M., Tillery, A.C., and Youberg, A.M. (2016). Updated logistic regression equations for the calculation of post-fire debris-flow likelihood in the western United States: U.S. Geological Survey Open-File Report 2016–1106, 13 p., <http://dx.doi.org/ofr20161106>.
20. Cannon, S. H., and DeGraff, J. (2009). The increasing wildfire and post-fire debris-flow threat in western USA, and implications for consequences of climate change. In *Landslides—disaster risk reduction*. (K. Sassa & P. Canuti, eds.), Springer. 2009, pp. 177–190.
21. WEST Consultants, Inc. (2011). Sedimentation/Debris bulking factors and post-fire hydrology for Ventura County. Task Order No. PW09-171. Ventura County Watershed Protection District, Ventura, Ca. 2011.184 p.
22. Lindsay, D.N. McCoy, S.W., Cavagnaro, D.N., Thomas, M. A., Swanson, B.J., Delgado, N. (2022). Post-fire runoff response across multiple hydrogeomorphic provinces in California: A look at using peak bulk-flow multipliers to estimate flow type, Geological Society of America: DOI: [10.1130/abs/2022AM-382969](https://doi.org/10.1130/abs/2022AM-382969),
23. Gray, D., and Sotir, R. (1996). *Biotechnical and soil bioengineering slope stabilization: a practical guide for erosion control*, New York: John Wiley and Sons. 1996. 378 p.

## **Geohazard Management on Colorado SH 133 From Planning to Mitigation**

### **Randy Post, PE**

WSP USA Inc.  
177 N. Church Ave., Ste. 1105  
Tucson, AZ 85701  
520-888-8818  
randy.post@wsp.com

### **Roger Pihl, PG**

WSP USA Inc.  
7245 W Alaska Drive, Suite 200  
Lakewood, CO, 80226  
970-379-5341  
roger.pihl@wsp.com

### **Nicole Oester Mapes**

Colorado Department of Transportation  
4670 Holly Street, Unit A  
Denver, CO 80216  
303-398-6603  
nicole.oester@state.co.us

### **Bob Group, PE**

Colorado Department of Transportation  
4670 Holly Street, Unit A  
Denver, CO 80216  
303-398-6589  
robert.group@state.co.us

### **Acknowledgements**

This paper describes the outcomes of a major highway corridor study report, and over 5 design and construction projects spanning a period of 7 plus years. Many people have contributed their time and talents to aspects of the projects. The authors would like to thank the following individuals (listed in alphabetical order) for their contributions in the work described:

Ben Arndt, PE – RJ Engineering  
Alex Brown, PE – BGC Engineering  
Kevin Carpenter – WSP USA Inc.  
Makenzie Carroll, EIT – WSP USA Inc.  
Aliena Debelak, PE – WSP USA Inc.  
Regan French – CDOT Geohazards Program  
Richard Johnson, PE – RJ Engineering  
Numa LoCascio – WSP USA Inc.  
Curtis Jeffries, PE – US Environmental Protection Agency  
Ty Ortiz, PE – Rocksol Engineering  
Matt Tello – CDOT Geohazards Program  
Ty Trulove – Aerial Altitude, LLC  
Tina Trulove – Aerial Altitude, LLC  
Kimberly Vander Vis, PE – WSP USA Inc.

### **Disclaimer**

Statements and views presented in this paper are strictly those of the author(s), and do not necessarily reflect positions held by their affiliations, the Highway Geology Symposium (HGS), or others acknowledged above. The mention of trade names for commercial products does not imply the approval or endorsement by HGS.

### **Copyright Notice**

Copyright © 2023 Highway Geology Symposium (HGS)

All Rights Reserved. Printed in the United States of America. No part of this publication may be reproduced or copied in any form or by any means – graphic, electronic, or mechanical, including photocopying, taping, or information storage and retrieval systems – without prior written permission of the HGS. This excludes the original author(s).

## ABSTRACT

Highway safety, mobility, and maintenance effort on Colorado State Highway (SH) 133 between Carbondale and Paonia, Colorado is severely impacted by rockfall, debris flows, landslides, avalanches, and the occasional sinkhole. This paper presents a case study on the implementation of a risk-based geohazard management approach commissioned by the Colorado Department of Transportation (CDOT) for SH 133. The goal of the study was to evaluate the geohazard sites from an asset management perspective, considering quantitative risk, life-cycle costs, and benefit/cost ratio for proactive mitigation measures. A total of 300 geohazard sites were inventoried, and 125 sites were subjected to quantitative risk assessment. The assessment considered event likelihood, consequence analysis, and annual risk exposure in terms of safety, mobility, and maintenance impacts. Conceptual mitigation options with preliminary cost estimates were prepared for 50 of the highest risk sites, allowing for benefit-cost ratios to be computed. Based on the findings, five mitigation projects were undertaken, representing 21 sites that have been mitigated, are under construction, or are under design. When these projects are completed, they will ultimately result in an approximate \$18.5 million reduction in risk exposure compared to \$16.8 million in construction costs. Along the way, the authors found that financial realities required that some sites were dropped out of the projects. Some of these sites became shovel ready projects for construction using other contractual mechanisms or simply ready for when future funding becomes available. The paper discusses the challenges of geohazard assessment and emphasizes the importance of expert judgment in the absence of comprehensive data. The example of the SH 133 risk-based geohazard management shows how effective these methods can be, despite the challenges of these types of programs. But it is important to remember that there is no perfect system for geohazard management, but an imperfect one is better than nothing.

## INTRODUCTION

Highway facilities and those that use and maintain them are affected by geohazards such as rockfall, landslides, debris flows, and sinkholes. The traditional way of addressing these hazards was a reactionary approach, responding to emergency events when and where they occurred. With the implementation of MAP-21 legislation in 2012, agencies are now required to implement performance-based metrics and asset management principles for their inventory of highway assets. Although geohazard assets are not yet mandated to be managed the same way as bridges and pavements, many agencies, including the Colorado Department of Transportation (CDOT), have begun to move in that direction. Asset management enables a more proactive approach to geohazard management, quantifying risk for sites in a geohazard inventory, and considering benefit/cost ratios for mitigation projects. The approach also provides a basis for measurement of performance increases related to mitigation spending.

This paper describes the implementation of such an approach to reducing geohazard risk for the State Highway (SH) 133 corridor. The process began with a corridor study, inventorying and quantifying geohazard risk, and has culminated in 5 mitigation design and construction projects. These projects are expected to result in a present worth total reduction in risk exposure of approximately \$18.5 million.

## MANAGING GEOHAZARD RISK

### Overview of CDOT Geohazards Management Approach

The CDOT Geohazards Management Plan (GMP) (1), last revised in 2017, documents the general management approach for approximately 800 sites, approximately 38 corridors with over 50 high hazards rockfall sites. Colorado has approximately 200 documented natural landslides that affect the state's roads. In addition, hundreds of embankment failures are managed through the GMP. Debris flows, anticipated to increase in frequency and severity due to climate change, have been added to the list of hazards more recently.



**Figure 1 – An example of typical maintenance response to rockfall events (left), and a large boulder that just missed causing significant damage as it bounced over the highway**

CDOT has moved away from a top-down approach based on the Colorado Rockfall Hazard Rating System, which was developed and populated in the 1980's and 1990's. Mobility is severely impacted by geohazard related road closures in the mountainous parts of the state because detours and alternate routes are long and sometimes not available in a practical sense. The top-down approach encourages focus on mitigating singular sites, but it only takes one site to close an entire corridor. That realization moved CDOT toward a corridor system that focuses on improving resiliency on a more regional basis.

Inventory, maintenance, and repair of existing mitigation systems is part of the Plan. Budget is allocated to cleaning and repairing fences, maintaining monitoring, removing fallen rock from ditches and other similar activities prevent reduction in efficiency of mitigation systems.

Measurable risk reduction and related performance measures are facilitated by site selection based on estimated annual risk exposure compared to estimated cost to mitigate. The present worth life cycle costs to mitigate and maintain a site are compared to the “do nothing” present worth value of annual risk exposures over the practical life of the asset. The present worth of a series of reduced risk exposures for a corridor is one measure of improved performance and resilience of that corridor and, by extension, the roadway system in that entire region.

### **Challenges with Risk-Based Geohazard Assessment**

Many agencies rely heavily on geohazard assessments based on the Rockfall Hazard Rating System (RHRS) or other similar slope inventories. The authors consider the RHRS and similar rating systems (2) to be a qualitative risk assessment. Although the RHRS contains the parameters “Average Vehicle Risk”, and “Rockfall History”, these are bins that do not truly assess the likelihood of impactful rockfall events in the future, or the consequence in terms of dollars. It is typical for the future risk at a site to be temporarily reduced after a rockfall or debris flow event since the assumption is that the most hazardous rock falls first or that sediment in a basin must recharge after an event to be available for the next event. However, since there are often large existing datasets, there may be use in considering some consensus of minimum acceptable RHRS score (3), or bins of scores that help identify slopes that should be subjected to more rigorous quantitative risk assessment.

It may be tempting to assume that technological or procedural means alone can assess the frequency of geohazard events. Examples of technological methods include rockfall events noted using change detection of 3D lidar or photogrammetry models to fill out a magnitude/frequency plot such as those described by C. Dussauge-Peisser et al. (4), or InSAR measurements of landslide movement. Sometimes landslide occurrence is tied to precipitation intensity and duration and the likelihood of those storm events is used as a proxy for landslide likelihood (5). Procedural means could include a system for having road maintenance forces report rockfall events to a central database. However, all these methods have potential issues that can prevent them from being useful in corridor or system-level geohazard risk management.

Many technological methods focused on detecting rockfall can only be deployed in a localized area. However, risk-based geohazard assessments are commonly applied on a corridor or network level, meaning several sites may have good event frequency data, but the majority will have little to no data. Collecting data long enough at a site to capture the recurrence interval of

geohazard events is another problem. Although sites like the White River in British Columbia have a long time series of event data with impressive results (6), these are special cases and applying similar monitoring across multiple sites would be logistically challenging and very expensive. Rainfall data may not be available in some of the remote areas where geohazards occur which could make meteorological likelihood models less useful.

There are two problems with relying on procedural methods for logging historic events. First, they are subject to underreporting. Consider a rockfall that occurs but bounces over the road and is not reported, or the “Good Samaritan” that pushes a rock off the road when they pass by. The second and perhaps more common issue is that different parts of an organization implement logging procedures differently. The authors have observed that some CDOT maintenance patrols routinely report rockfall events and others do not or do so with less regularity, even when events are known to occur. On a single “rock run” a plow driver may remove rocks from a dozen locations making reporting an unachievable burden.

So, what is the solution to the challenges posed by technological and procedural means of geohazard frequency estimates? Like many aspects of geoen지니어ing, the solution relies heavily on the experience of subject matter experts to supplement the data collected and arrive at a subjective estimate of geohazard event frequency. Although this “fuzzy” method of risk calculation may be at odds with other types of quantitative risk assessment in asset management, geoen지니어ing practitioners must be realistic about the complex, infrequent nature of geohazard events, and the lack of better methods at the present time.

### **GEOHAZARD RISK ON THE SH 133 CORRIDOR**

The study area extends along both sides of State Highway 133 (SH 133) from Mile Post (MP) 0.0 at the south end to MP 62.35 on the north end, but very few hazardous areas exist between MP 0.0 and MP 14.95. The study area is shown on Figure 2. The corridor is located within CDOT Region 3 and stretches through three counties: Delta, Gunnison, and Pitkin.

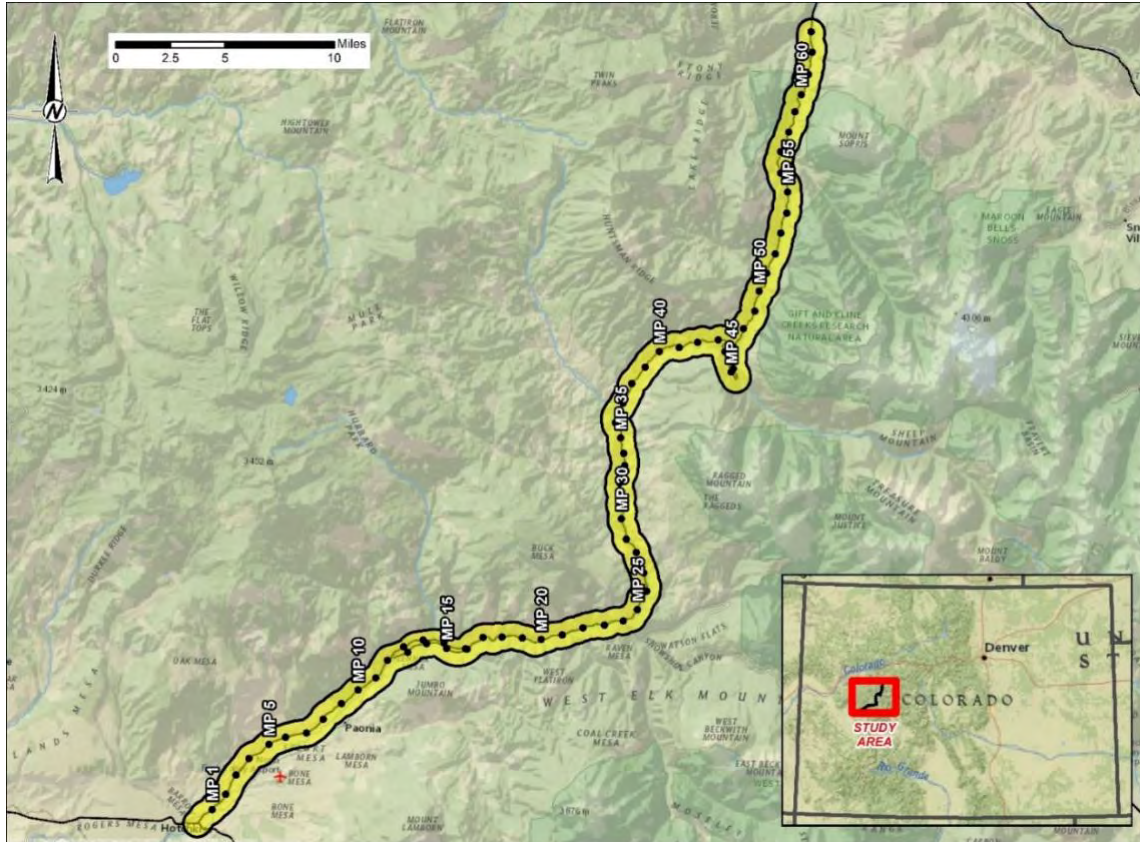


**Figure 2 – SH 133 Corridor Overview**

The SH 133 corridor has a long history of being impacted by geological hazards. South of McClure Pass, the highway is aligned within the North Fork of the Gunnison River Valley through layers of the Mancos and Mesa Verde Formations that are predisposed to landslide activity. Realignment of the highway during construction of the Paonia Dam and Reservoir resulted in numerous unstable cut slopes above the road and unstable fill slopes below the road. To the north of the Pass, the highway is aligned within the Crystal River Valley with steep cliffs of Maroon Formation red sandstone interrupted by short sections of unconsolidated alluvial soils, glacial soils and intruded igneous rock in the Avalanche Creek area. The section within the Maroon Formation has numerous, unstable soil and rock cuts above the road and areas where surface water flowing over the steep, rugged basins of the Maroon Formation result in frequent mud flood, mud flow and debris flow events.

The authors conducted a preliminary “desktop” study, field reconnaissance, and interviews with CDOT maintenance staff to identify geological hazards. These natural hazards include rockfall, debris flow, avalanche, and unstable natural and man-made slopes. When combined with severe horizontal space limitations, these issues present continuous challenges for reliable transportation within the corridor and result in significant safety, mobility and maintenance risk. Approximately 300 sites were included in the SH 133 assessment. Approximately 125 were selected for quantitative risk assessment. These sites were selected using a preliminary screening process that involved expert-based selection of a preliminary risk rating to sort the sites into severity classes.

## **Why Focus on SH 133**

The I70 mountain corridor is vital to the economic wellbeing and safety of the State so significant resources have been expended to reduce the impact of geohazards and improve performance of that highway. SH 133 represents a much lower volume road that has historically been notoriously impacted by rockfall, debris flows, landslides and embankment failures. Agricultural goods and commuters from economically challenged parts of the state are connected to markets and jobs by this segment of road making it regional important with respect to social justice. The density and severity of hazards severely impacts traveler safety and mobility along with requiring an outsized portion of the region's maintenance budget. Long detours that are seasonal or unsuitable for truck traffic increase the mobility impact of long closures.

## **Event Likelihood**

Clearly, there is no one-size-fits-all approach to geohazard risk management. The authors opinion of best practice is to consider several sizes of geohazard events and to work with available frequency data and institutional knowledge to estimate the annual probability of occurrence and corresponding consequences for each size event. For example, a minor event might be a rock on the road that needs to be pushed off, or a debris flow or slope failure that has a minor impact on the system with short or partial road closure and no other damage. A major event may close part of a lane for a few hours, needs a larger maintenance response, and may include property damage or minor injuries. A catastrophic event may close the road for days or even weeks, have hundreds of thousands or millions of dollars in maintenance and repair costs, and result in serious injuries or fatalities. Obviously, more severe events are less frequent.

As noted, the likelihood component of geohazard risk assessment is not a simple matter. With incomplete reporting data, or in many cases, little to no data at all, owners may be wondering where to start. The author's approach is to begin by interviewing maintenance staff and those with institutional knowledge. Often, interviews can produce invaluable likelihood/frequency estimates with some simple questions such as "about how many times a month/year do you push rocks off the road?", "about what percentage land on the road?", "have you seen any major or catastrophic events and when?". For major events such as large rockslides and debris flows, the recurrence interval can simply be estimated as the number of events divided a time interval and then converted into an annual probability. Barring this level of data, it may be up to an expert to make an assessment to estimate likelihood.

In the case of the SH 133 corridor, CDOT had data in their event tracker database that helped estimated geohazard frequency. However, there was almost certainly underreporting of events for the reasons described above. Accordingly, the authors placed equal weighting on frequencies estimated from the database and observational data collected by interviews with maintenance and Region personnel. The event tracker frequencies and the observational frequencies were computed separately and averaged to come up with the estimated annual probability of occurrence.

## **Event Consequence**

Several magnitudes of events were considered that ranged from minor to catastrophic. Impacts to safety, mobility, and maintenance were considered for each magnitude. All consequence values were expressed in dollars to allow risk comparisons with other CDOT asset classes. For example, a property damage only event may have a safety consequence of a few thousand dollars, while an injury event may be in the 10's to 100's of thousands of dollars, and a fatal event would likely be in the millions of dollars. A mobility impact was computed by estimating the number of hours of partial or full road closure multiplied by some hourly user delay cost per person. Detour costs were factored in for longer closures. Maintenance impacts were perhaps the simplest to calculate as the costs for maintenance forces to respond to different size events were generally known.

## **Annual Risk Exposure**

The three components of risk exposure (safety, mobility, and maintenance) were computed as the product of the consequences and the annual probability of occurrence for minor, major and catastrophic events. The concept of risk exposure is based on the fact that the department may incur the consequences of an event with a positive annual probability in any year, whether or not the event occurs in that specific year. For example, for planning purposes, an agency might establish an annual budget of \$10,000,000 to cover the recovery costs from a 100-year flood event with an annual probability of occurrence equal to 1.0%. In other words, the annual risk exposure is \$100,000.

## **Development of Probable Cost Estimates**

Most agencies, including CDOT, already know where they have a geohazard problem and often have an intuitive sense of where the worse areas are. The quantitative risk assessment is a good first step to establish numbers for things they already know, but it is only by advancing preliminary cost estimates for mitigation that agencies can begin the process of reducing their total risk exposure and meeting other organizational goals.

The authors computed multiple conceptual options for over 50 of the highest risk geohazard sites. Options were developed that factored in effectiveness, retention, constructability, and long-term benefit on highway operations and maintenance. Quantities were estimated using a combination of field and office measurements, including extensive use of 3D models collected using drone-based photogrammetry. The 3D models were an excellent tool for the conceptual mitigation design by providing preliminary topography and cross-sections and allowing quick evaluation of multiple mitigation options.

The authors managed a data set of over 370, 3D models (meshes) that were hosted on ArcGIS Online (AGOL) and accessible to the consultant team, CDOT Geohazards Program members, other CDOT staff, and even other consultant teams. A thinned-out collection of over 5,000 of the photos used to produce the models was uploaded to AGOL to allow evaluation of areas in high resolution. No special software was needed to access the data, everything was done in a web browser interface. Other features of the AGOL portal included over 20 custom-built web apps, and over five custom mobile field apps to assist with field data collection.

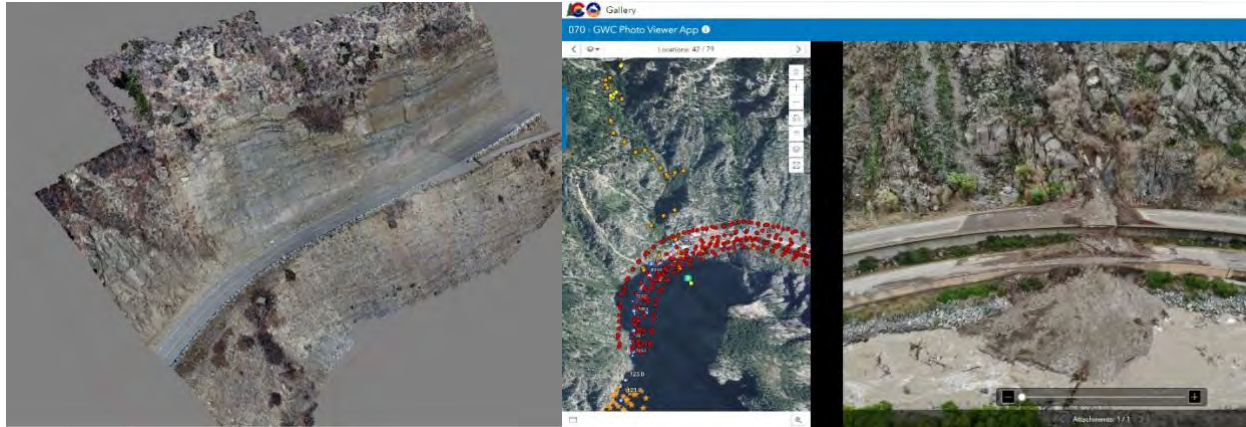


**Figure 3 – Example of AGOL Meshes and other tools used for virtual site visits and to estimate quantities and refine mitigation options**

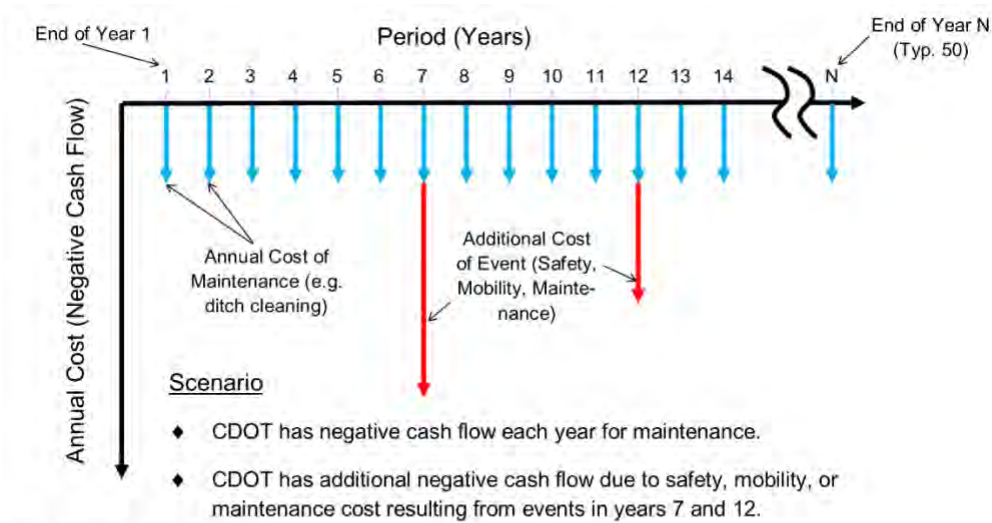
Only minimal engineering design was done for these conceptual mitigation options, a necessity when so many sites needed to be evaluated with finite time and budget. Preliminary mitigation options and estimates of their effectiveness relied heavily on the experience and judgement of the authors and others involved in the project. To simplify cost estimating, “system level” cost estimating was favored over “item level” cost estimates typical for bid-ready projects. For example, soil nail walls to increase rockfall ditch width would be estimated by the linear foot of wall (assuming a certain height) instead of by estimating all the individual bid items.

Only geohazard costs were computed using this method, no roadway, traffic control, pavement, seeding, or storm water management items were included. These items and others needed for a complete project cost were accounted for using a multiplier on the geohazard costs based on past mitigation projects.

### **Life Cycle and Benefit/Cost Evaluation**

The calculation of benefit/cost ratios for mitigation of geohazard sites is essentially a comparison between two or more “negative” hypothetical cash flows reduced to a present worth value based on time-value-of-money principles. The cost side is simply the present worth of the cost of mitigation and its maintenance calculated using an interest or discount rate equal to the estimated construction inflation cost over some period of time. The benefit is the present worth of a series of hypothetical cash flows that represent annual risk exposure.

In the case of the do-nothing option, or existing conditions, there is a series of hypothetical negative cash flows (away from CDOT) representing the annual risk exposure (Figure 4). The cash flow diagram for each mitigation option represents an initial outlay of cash for the construction of the mitigation, and a corresponding reduction in the annual risk exposure based on the estimated efficiency of the mitigation (Figure 5).



Present Worth (Pw) Calculations

$$Pw = \text{Annual Cost of Maintenance} \left[ \frac{(1+i)^N - 1}{i(1+i)^N} \right] + \text{Cost for Year 7 Event} \left[ \frac{1}{(1+i)^7} \right] + \text{Cost for Year 12 Event} \left[ \frac{1}{(1+i)^{12}} \right]$$

*i* = Interest rate which is annual general and construction inflation (taken as 4% for this study)

Pw50 = Present worth of cash flows over a 50 year period (N = 50 years).

**Figure 4 – Example of present worth analysis for existing conditions or unmitigated site**

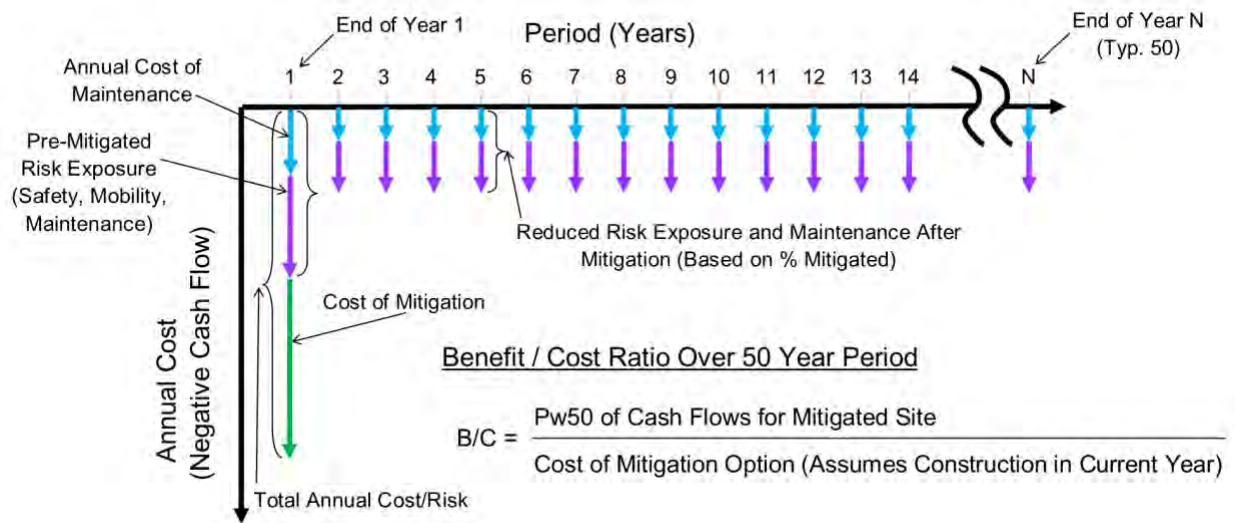


**Figure 5 – Example of present worth analysis for a mitigated site**

Solutions are rarely 100% effective at mitigating risk. So, a percent mitigated was estimated by experience and professional judgement for each mitigation option considered. This percent mitigated was applied to the present worth value of the initial risk exposure to estimate the risk reduction and is taken as the “benefit” in the benefit/cost evaluation. The computed benefit is the

numerator, and the estimated construction cost for the option is the denominator providing the benefit/cost ratio for each site and mitigation option.

### **MITIGATION PROJECTS ON SH 133**

A total of five design and construction projects have been undertaken as a result of the corridor study work. A brief description of the projects is provided below. References to “South” and “North” refer to the side of McClure Pass on which the project is located.

#### **MP 21.7 Landslide Ground Anchor Repair**

This landslide had been a continual maintenance problem for years before a significant period of movement in spring 2017 resulted in several feet of vertical offset with pavement crack offsets up to 8 inches. The length of the failure area was approximately 300 feet, encompassing both lanes of SH 133. After considering a variety of options, the authors selected and designed a ground anchor stabilization system for the slide. The construction of the mitigation was successfully completed in fall 2022 and no additional cracking or pavement distress has been observed in the repaired section.



**Figure 6 – The MP 21.7 site required frequent maintenance prior to mitigation**

#### **North Rockfall Mitigation, Phase I**

This project included the repair of five rockfall hazard sites on the north side of McClure Pass. This included rock cuts from 50 to 150 feet in height in Dakota Sandstone, and in Maroon Formation sandstone. One talus slope across from a popular hot springs parking area had a concrete barrier that required maintenance several times per year and produced frequent rocks that entered the road.

Mitigation for the rock cuts included a combination of blasting/rock excavation, scaling, and draped mesh or cable nets. The talus slope at Penny Hot Springs was mitigated using a double-sided MSE wall with large pre-cast concrete blocks as facing to satisfy aesthetic requirements. This solution essentially requires zero maintenance.

The Nettles Cut had adversely dipping bedding planes and had a history of producing large sandstone blocks up to 20 feet in diameter that blocked the roadway (Figure 7). The cut was stabilized by scaling and installing a pattern of rock dowels to stabilize the sliding blocks with the shear capacity of the dowels. A roughly 15' boulder at the top of the slope was stabilized using shotcrete buttressing with additional dowels, and a draped mesh with a “hybrid” stickup of

3 to 4 feet to direct rocks falling from higher up the slope under the mesh. This project was constructed in the Summer of 2021.



**Figure 7 – The Nettles Cut had a history of major rockfall events prior to stabilization**

### North Rockfall Mitigation, Phase II

Although referred to as a rockfall mitigation project, this project included only one rockfall area consisting of two adjacent cuts, and a total of three debris flow sites, some with multiple channels. The rock cut, referred to as the Headgate Cut, had a smaller cut approximately 60 feet high, and a larger cut up to 120 feet high with a portion of that overhanging, albeit farther from the road at that location. The rockfall mitigation design includes scaling, some excavation to improve ditch configuration, spot bolting, and installation of draped mesh for the smaller cut and the lower hazard portions of the large cut, and heavier mesh / cable net for the worst portions of the large cut.



**Figure 8 – The Headgate Cut (left) will be mitigated with scaling, rock bolting, and light and heavy-weight draped mesh. Debris flows that occurred during the summer of 2021 (right) closed the highway for several days until they could be cleaned up.**

The north side of the SH 133 corridor experienced approximately forty debris flows in the summer of 2021, including several that closed the highway for multiple days and involved

significant cleanup efforts. The authors determined that it wasn't practical from a cost or right-of-way (ROW) perspective to completely mitigate the debris flows, but if storage for debris flow material could be provided within the ROW, then it greatly reduces the mobility risk and turns an emergency maintenance operation into a planned one since the flow material can be cleaned from the enhanced ditch instead of from the roadway. Storage options included flexible debris flow barriers, ditch excavation, ditch excavation in combination with concrete barrier, and various retaining walls. The final project includes a short flexible debris flow barrier at one site, and ditch excavation with temporary concrete barrier at two other sites. This project is under construction at the time of writing this paper.

### South Embankments Stabilization

The portion of SH 133 near the Paonia Reservoir was constructed using conventional side-cast construction methods, cutting into the slope on the uphill side, and using the material from the cut to construct the embankment on the downhill side. Many of these embankment slopes are over steepened, were not properly compacted or benched into the existing slope, or have activated failure surfaces at the contact between native colluvium and bedrock. These failures are expressed in the form of cracks in the pavement, sagging, undermined guardrails, or combination of all three.

A total of 32 embankment failures were identified in the Paonia Reservoir segment during the corridor study. The sites were prioritized based on progression and likely consequence of failure. A total of six locations were selected for geotechnical investigations and potential mitigation. Those six sites were further reduced to four sites for this mitigation project to fit within the budget. A variety of mitigation options were considered, including deep patch, ground anchors, road realignment, lightweight fill, and coupled shear piles. The most economical method to repair these locations was soil nails retaining walls to stabilize the roadway prism and allow removal of some of the driving forces by removing the embankment in front of the wall line. Keeping the same mitigation method for all four sites offered benefits in terms of simplifying construction and the economies of scale.



**Figure 9 – Embankment failures are common along the Paonia Reservoir (left). Six locations were selected for geotechnical investigations (right).**

This project includes a total of approximately 8,000 square feet of soil nail wall at four locations. At the time of writing this paper, an apparent low bidder has been announced, but the project has not started construction yet.

### **South Rockfall Mitigation**

SH 133 has several high risk rockfall risk segments south of McClure Pass, including some of the highest ranked (in terms of risk exposure) sites on the corridor. However, some of these areas are so challenging to mitigate that one site would require the entire annual budget of the CDOT Geohazards program, or more. Accordingly, CDOT and the authors selected six sites along the Paonia Reservoir area to design rockfall mitigation; an attempt to fix as many sites as possible with the available funds.

The geology at these sites is primarily interbedded marine and deltaic sandstone and shale beds of the Mesaverde Group. The sandstone layers form blocks from approximately one-foot diameter to as large as six-feet in diameter. The shale and mudstone beds are much more erodible and often contribute to the rockfall by undermining the sandstone beds. There are often colluvium layers at the top of the cuts with cobbles and small boulders that erode out of the matrix, particularly at the vegetated “brow” that can become essentially vertical over a height of 5 to 10 feet and is readily erodible.



**Figure 10 – Rockfall consisting of medium to large blocks are common in this segment of SH 133.**

Mitigation options considered for these areas included scaling, rock bolts, draped mesh or cable net, attenuators, and soil nail walls (with or without drape/attenuator) to create additional ditch for storage. The proposed mitigation currently consists of scaling and draped mesh for 5 of the 6 cuts, and scaling only for the 6<sup>th</sup> cut, with spot bolting where appropriate. While the soil nail wall option was attractive, particularly at one location with bad sight distance, it added project cost and ultimately was eliminated. The elimination of draped mesh at the 6<sup>th</sup> site is also an example of fine-tuning project elements to mitigate as many sites as possible within the existing budget.

This project is currently under design with advertisement scheduled for winter of 2024 and construction in the summer of 2024.

## CONCLUSIONS

This paper has shown an example of the entire process of risk-based geohazard mitigation at the highway corridor level. The first step is an inventory of geohazards, and a qualitative risk assessment to narrow down the number of sites on which to perform a quantitative risk assessment. The quantitative risk assessment must consider events of several different magnitudes and be expressed in terms of annual probability of occurrence, and the consequence and risk exposure in terms of dollars. CDOT considers safety, mobility, and maintenance impacts, but other agencies may utilize different criteria.

Once the quantitative risk has been computed for the selected sites, the true work begins of figuring out how best to fix the problem. Conceptual cost estimating can be a difficult and time-consuming process. But it is important to remember that these are high-level, planning costs, that will be used to help select sites for mitigation. Since sites are compared against each other, relative consistency is more important than estimating accuracy. Short cuts in the form of system-level cost estimates and using multipliers on geohazard costs to get total project costs can help make these more manageable. But the authors have found that proficiency and speed of making these estimates has improved with practice.

The selection of sites for mitigation is always subject to fiscal and logistical constraints. Some of the highest risk sites, e.g. the largest rockfall sites or major landslides, would consume CDOT's entire annual budget for geohazard mitigation, or even exceed it. Instead, the approach taken by the authors and CDOT Geohazards Program in general has been to attempt to fix as many medium to high-risk sites as possible with the budget available.

### **Additional conclusions and lessons learned are summarized below:**

- Begin a geohazard mitigation project with more sites than you have budget for. As the design progresses, ROW, environmental constraints or cost may require eliminating sites. They can be added to later projects or put on the shelf.
- It's difficult to stick with highest benefit/cost ratio only for selecting sites for mitigation. The purpose of asset management isn't to make hard decisions for agencies. Site selection should be made using other sources of information, including common sense. Consideration of total available funds, maintenance staff preferences, similar construction techniques on the project, proximity of sites, and packaging of sites into a reasonable sized project must also be considered.
- Projects that might be bid by specialty geohazard contractors should be kept below a value of construction cost that ensures multiple local bidder because of limitations of bonding by these generally small contractors.

The combined mitigation projects on SH 133 that were a direct result of the corridor study and the conscious efforts of CDOT to reduce overall geohazard risk on the corridor have been a success. A total of 21 sites have been mitigated or are in the process of being mitigated. The present worth of the total reduction in risk exposure for those projects is approximately \$18.5 million compared to approximately \$16.8 million in anticipated construction costs.

The process of quantitative risk assessment for geohazards is not an exact science. It relies heavily on experience and professional judgement, as well as input from maintenance staff and others with institutional knowledge of the sites to fill in the gaps of data from systems designed to catalog geohazard event occurrence. However, this is to be expected given the complex, infrequent nature of geohazards and inherent variability in natural and man-made slopes. It is important to remember that there is no perfect system for geohazard management, but an imperfect one is better than nothing.

## REFERENCES

1. Colorado Department of Transportation (CDOT). FY2018 *Geohazards Management Plan*. Working Draft. 2017.
2. Ferrari, F., Giacomini, A. and Thoeni, K. (2016) ‘Qualitative Rockfall Hazard Assessment: A Comprehensive Review of Current Practices’, *Rock Mechanics and Rock Engineering*, 49(7), pp. 2865–2922. <https://doi.org/10.1007/s00603-016-0918-z>.
3. Anderson, S., Dodson, M.D. and Greer, M. (2017) ‘Application of a Risk-Based Rock Slope Standard’, in *Landslides: Putting Experience, Knowledge and Emerging Technologies into Practice. 3rd North American Symposium on Landslides*, Roanoke, Virginia, USA (AEG Special Publication 27), pp. 730–739.
4. Dussauge-Peisser, C., Helmstetter, A., Grasso, J.-R., Hantz, D., Desvarreux, P., Jeannin, M., and Giraud, A. (2002) ‘Probabilistic approach to rock fall hazard assessment: potential of historical data analysis’, *Natural Hazards and Earth System Science*, 2(1/2), pp. 15–26.
5. Brunetti, M.T., Peruccacci, S., Rossi, M., Luciani, S., Valigi, D., and Guzzetti, F. (2010) ‘Rainfall thresholds for the possible occurrence of landslides in Italy’, *Natural Hazards and Earth System Sciences*, 10(3), pp. 447–458.
6. Kromer, R.A. *et al.* (2015) ‘Identifying rock slope failure precursors using LiDAR for transportation corridor hazard management’, *Engineering Geology*, 195, pp. 93–103. Available at: <https://doi.org/10.1016/j.enggeo.2015.05.012>.



## **The State of Measurement While Drilling (MWD) for the Washington State Department of Transportation**

**Michael Mulhern**

Washington State Department of Transportation  
1655 S. Second Ave, Tumwater, WA, 98504  
360-239-8882  
[mulhern@wsdot.wa.gov](mailto:mulhern@wsdot.wa.gov)

**Jennifer DiGiulio**

Washington State Department of Transportation  
1655 S. Second Ave, Tumwater, WA, 98504  
360-480-0488  
[digiulj@wsdot.wa.gov](mailto:digiulj@wsdot.wa.gov)

Prepared for the 72<sup>nd</sup> Highway Geology Symposium, August 13-19, 2023

### **Acknowledgments**

The authors would like to thank the following individuals for their contributions in the work presented in this paper:

Marc Fish – Washington State Department of Transportation  
Eric Smith – Washington State Department of Transportation

### **Disclaimer**

Statements and views presented in this paper are strictly those of the author(s), and do not necessarily reflect positions held by their affiliations, the Highway Geology Symposium (HGS), or others acknowledged above. The mention of trade names for commercial products does not imply the approval or endorsement by HGS.

### **Copyright**

Copyright © 2023 Highway Geology Symposium (HGS)

All Rights Reserved. Printed in the United States of America. No part of this publication may be reproduced or copied in any form or by any means – graphic, electronic, or mechanical, including photocopying, taping, or information storage and retrieval systems – without prior written permission of the HGS. This excludes the original author(s).

## ABSTRACT

In 2022, the Washington State Department of Transportation (WSDOT) Geotechnical Office became involved with measurement while drilling (MWD) through the A-Game initiative, headed by the Federal Highway Administration (FHWA), and joined the national MWD Users Group to learn more about this technology. In mid-2022, WSDOT purchased Jean Lutz B2 ML1 MWD technology to install on an already-ordered CME LC 55 track-mounted drill rig that was expected to arrive in the Fall of 2022. Following the A-Game initiative, WSDOT's goal was to use this MWD technology to improve its drilling efficiency and interpretation of subsurface materials for geotechnical applications. Although MWD has been in use for decades (mainly for directional drilling in the oil and gas industry), it is a relatively new application in the geotechnical field.

The new drill rig and MWD technology became functional in early January 2023, and WSDOT soon realized that equipment modifications, standard operating procedures, data interpretation, data analysis, data storage, and data presentation would all be needed. Also in January 2023, WSDOT attended a MWD workshop at the annual Transportation Research Board meeting (TRB) and in March 2023, joined a FHWA sponsored peer exchange between several DOTs to discuss the efficacy of MWD in geotechnical applications.

This paper will describe WSDOT's experiences with these workshops, user groups, and peer exchanges, as well as our implementation of MWD technology into our standard operating procedures. A discussion will be presented that includes the installation of the sensors on the drill rig, training on the use of the sensors, data collection while drilling, and data management. We will also summarize our preliminary interpretation/correlation of the data, and what WSDOT's future steps may be regarding the use of MWD technology.

## **BACKGROUND**

Measurement While Drilling (MWD) is the remote collection of borehole data, typically in real time. Bottomhole data are acquired incrementally from sensors located near the bit in a drill hole. The sensors continuously collect data for each monitored parameter without interfering with the drilling process and are displayed in real time. Measurements may include directional information (hole inclination, azimuth, tool facing), drilling parameters (penetration rate, thrust pressure, torque, rotation, vibration), etc. (SEG Wiki, 2018). MWD applications began in the 1960s when the oil and gas industry began using the technology to assist with directional drilling and became mainstream in that industry by the late 1970s to early 1980s. Offshore oil and gas drilling companies soon began utilizing MWD in the 1980s to 1990s, followed by the mining industry in the late 1990s, and tunneling and grouting operations in the early 2000s. The geotechnical field began using MWD in the early 2010s and is still in its incipient stages for optimizing drilling efficiency and design work (FHWA, 2016).

Although MWD is an emerging practice in the geotechnical industry, several state transportation departments are currently using the equipment/software or are on the verge of purchasing it. The list includes but is not limited to: Washington, Montana, New Hampshire, Nebraska, Wyoming, Florida, Kansas, Ohio, Illinois, Georgia, Idaho, Michigan, Pennsylvania, Minnesota, Arkansas, Virginia, North Carolina, South Carolina, Tennessee, Maryland, Indiana, Alabama, Colorado, Hawaii, Iowa, Maine, Mississippi, New Mexico, New Jersey, New York, Oklahoma, Utah, Vermont and Wisconsin. Along with the state transportation departments, the Federal Highway Administration (FHWA) is a leader in the implementation of MWD in the geotechnical field.

The Washington State Department of Transportation (WSDOT) became involved in researching the geotechnical applications of MWD in 2022. This paper describes our experiences implementing MWD technology, our preliminary opinions on the strengths and weaknesses of the technology, and what WSDOT's future steps may be regarding the use of MWD technology.

### **WSDOT'S INTRODUCTION TO MWD TECHNOLOGY AND TRAINING**

WSDOT began researching the geotechnical applications of MWD in 2022 with the purchase of the Jean Lutz B2 ML1 MWD Technology and a CME LC 55 track-mounted drill rig. Through collaboration between WSDOT, Jean Lutz, and CME, the MWD equipment was installed directly onto the new drill rig and delivered to WSDOT in October, 2022 (Figure 1). Hands-on training was conducted on October 10 and 11, 2022. Representatives from Jean Lutz and CME were both present for the training, as well as engineering geologists from the WSDOT Geotechnical Office, and the entire WSDOT Headquarters drill crew (Figure 2).

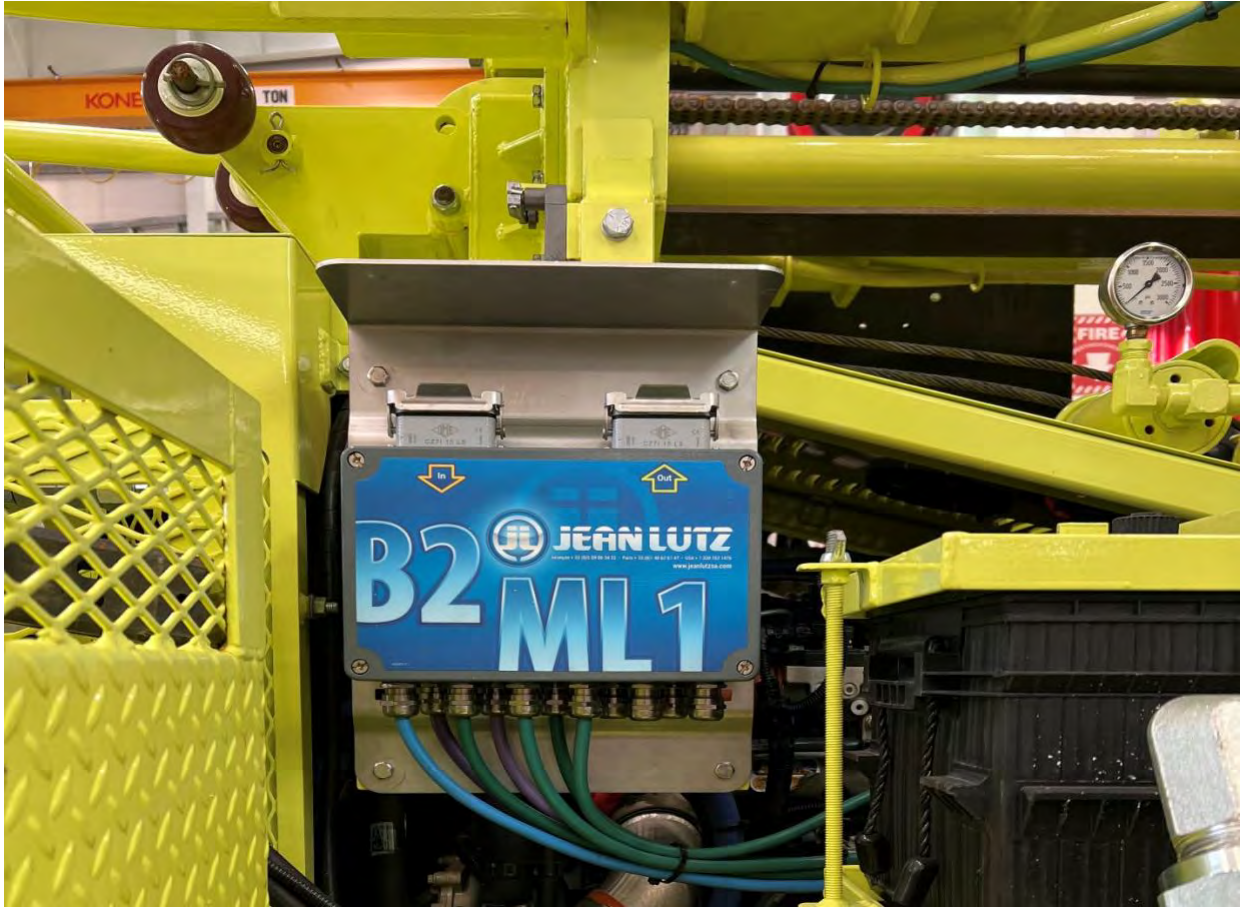


**FIGURE 1: THE B2 ML1 JEAN LUTZ COMPUTER ON THE CME LC 55 TRACK-MOUNTED DRILL RIG, FOLLOWING INSTALLATION.**



**FIGURE 2: THE ON-SITE DEMONSTRATION OF THE MWD EQUIPMENT, FOLLOWING INSTALLATION.**

The Jean Lutz/CME MWD drill rig contained numerous modifications and custom sensors including: a depth sensor, flow meter, hydraulic pressure sensor, and a water flow sensor. The sensors were placed per Jean Lutz's and CME's recommendations, as they have jointly installed MWD equipment onto drill rigs several times before. A torque sensor was not a part of WSDOT's initial MWD equipment. WSDOT is currently working on configuring the drill rig to install a torque sensor, per recommendations from the Montana Department of Transportation (MTDOT). The MWD sensors are attached to the downhole drill bit through a number of sensitive cables and wires, and record data in real time as drilling advances. Drilling parameters collected through WSDOT's MWD system include drilled depth, drilling time, drilling (penetration) rate, rotation speed, down pressure (thrust, crowd force), mud circulation, injection (water) pressure, injection flow, tool frequency, and vibration.

Once all the MWD equipment was installed, a display monitor was plugged into the computer mounted on the drill rig, and the equipment was then ready to begin recording data (Figure 3). The driller manually presses the "measure" button to begin recording and the "wait" button to stop recording between samples. Ideally, the drill clamps would start/stop the recording of data; however, we learned it is best to manually override the clamps (discussed further in the "Limitations" section, below). Real-time downhole data is displayed on the monitor's screen (Figure 4). Data collection continues for the duration of drilling, until the driller ends the recording. The MWD data is stored in the monitor and is extractable using a removable USB device (e.g., flash drive). From there, the flash drive is inserted into a computer, containing the Jean Lutz software (EXEPF, DRDPR), and the downhole MWD data for the boring can be viewed and used for geotechnical applications.



**FIGURE 3. THE DRILL RIG IN THE FIELD WITH THE MWD EQUIPMENT. NOTE THE LOCATION OF THE MONITOR AND COMPUTER.**



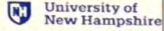
**FIGURE 4. THE MONITOR DURING DRILLING OPERATIONS. NOTE THE DRILL IS CURRENTLY IN THE “WAIT” MODE. THE DRILLER WILL PRESS THE “MEASURE” BUTTON TO RESUME RECORDING MWD DATA.**

## WSDOT’S EXPERIENCE AND DEVELOPING PRACTICES

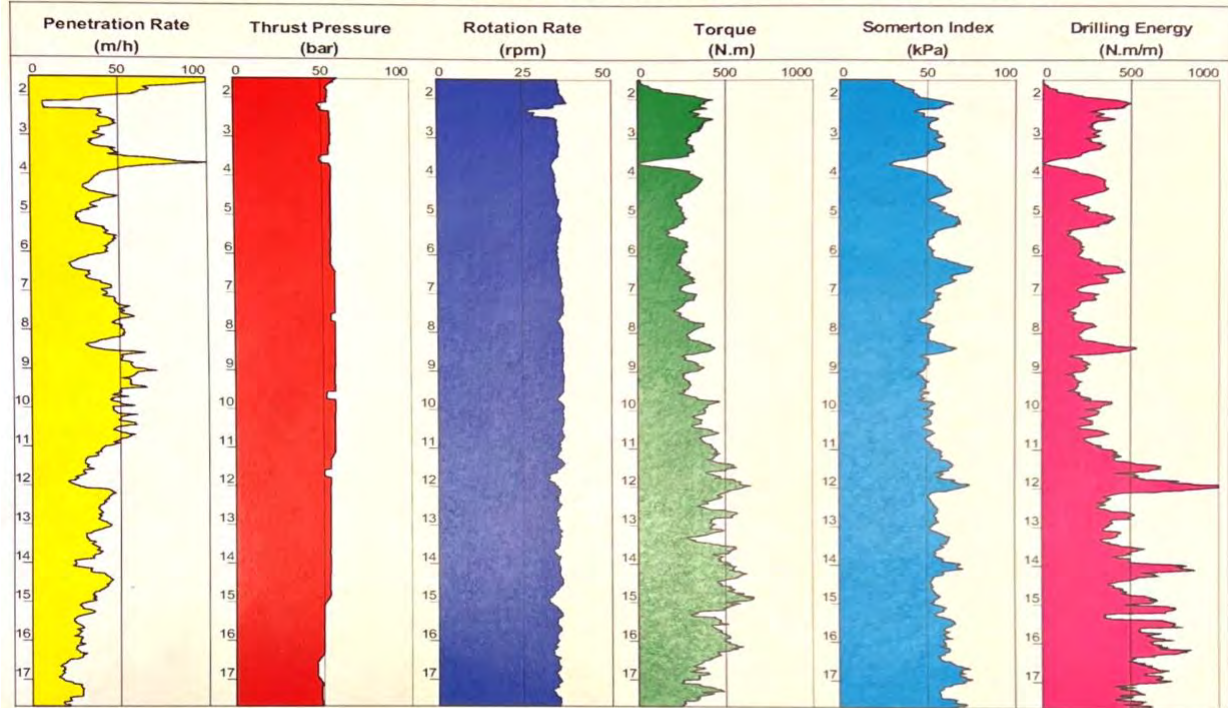
Along with our initial on-site training, WSDOT continues to develop its understanding of MWD and its capabilities. We currently attend peer-to-peer meetings (which are held virtually), every couple of months. These peer-to-peer meetings typically include WSDOT, MTDOT (at times attended by Nebraska DOT and Wyoming DOT) and FHWA. MTDOT is in the forefront of using MWD, in the western US, for geotechnical work and they often lead the discussion; however, it is an open forum. A typical meeting consists of any updates a specific group might have regarding their MWD system, discussions on new advances in the equipment/software, successes and failures we might have come across since our last meeting, etc.

WSDOT is also a part of an MWD User Group, which includes WSDOT, other DOTs (all listed above in the Background section) and FHWA. These meetings are also open forum, where we all share our experiences using MWD and the capabilities we see for the future. The MWD User Group meetings are typically held every 2 to 3 months.

The WSDOT Geotechnical Office attended the Transportation Research Board (TRB) annual meeting in January 2023 and participated in a workshop that was specifically about MWD (Figure 5). FHWA’s workshop, *Exploring Measurement While Drilling (MWD) for Transportation Projects*, discussed the MWD equipment, drilling parameters, MWD standards, MWD applications and concluded with a group exercise describing MWD data recovered from certain projects.

  	<b>102 TRB ANNUAL MEETING - MWD WORKSHOP</b> Drilling Parameters
Date : 12/01/2023 Begin : 09:00:00 End : 12:00:00	Drill Depth : 1.50-17.69 m Data provided by Fondasol

**EXERCISE 3(b): Calculating compound parameters for a single soil layer (20-cm average)**



$$\text{Somerton index: } S_d \approx P_E \cdot \left( \frac{V_R}{V_A} \right)^{1/2} \approx \frac{P_E}{\sqrt{V_A}}$$

$$\text{Drilling energy: } E_S = \frac{C_R \cdot V_R}{V_A}$$

Where:

Penetration rate,  $V_A$

Thrust pressure,  $P_E$

Rotation rate,  $V_R$

Torque,  $C_R$

**FIGURE 5: AN FHWA PRESENTATION SLIDE FROM TRB 2023 ON MWD.**

WSDOT attended the Shallow Exploration Drillers Clinic (SEDC) in Butte, MT on May 1-3, 2023. Among several different presentations, MWD was a highlighted topic of the conference, led by MTDOT, with an on-site demonstration on May 2<sup>nd</sup> (Figure 6).



**FIGURE 6. THE ON-SITE FIELD DEMONSTRATION DURING THE RECENT SHALLOW EXPLORATION DRILLERS CLINIC IN BUTTE, MT (MTDOT).**

Since January 2023, WSDOT has successfully utilized the MWD equipment for several projects in Washington State. To date, we have completed drilling, with simultaneous MWD data collection, on 10 projects (99% soil drilling / <1% rock drilling) including over 2,000 lineal feet of drilled depth. We are gathering the collected information and comparing it to the boring logs which also contain lab results (Figures 7a through 7c). Comparing the draft boring log to the MWD plots, the geotechnical designer is often able to more accurately interpret/select the depths of soil change contacts (see Figures 7a through 7c).

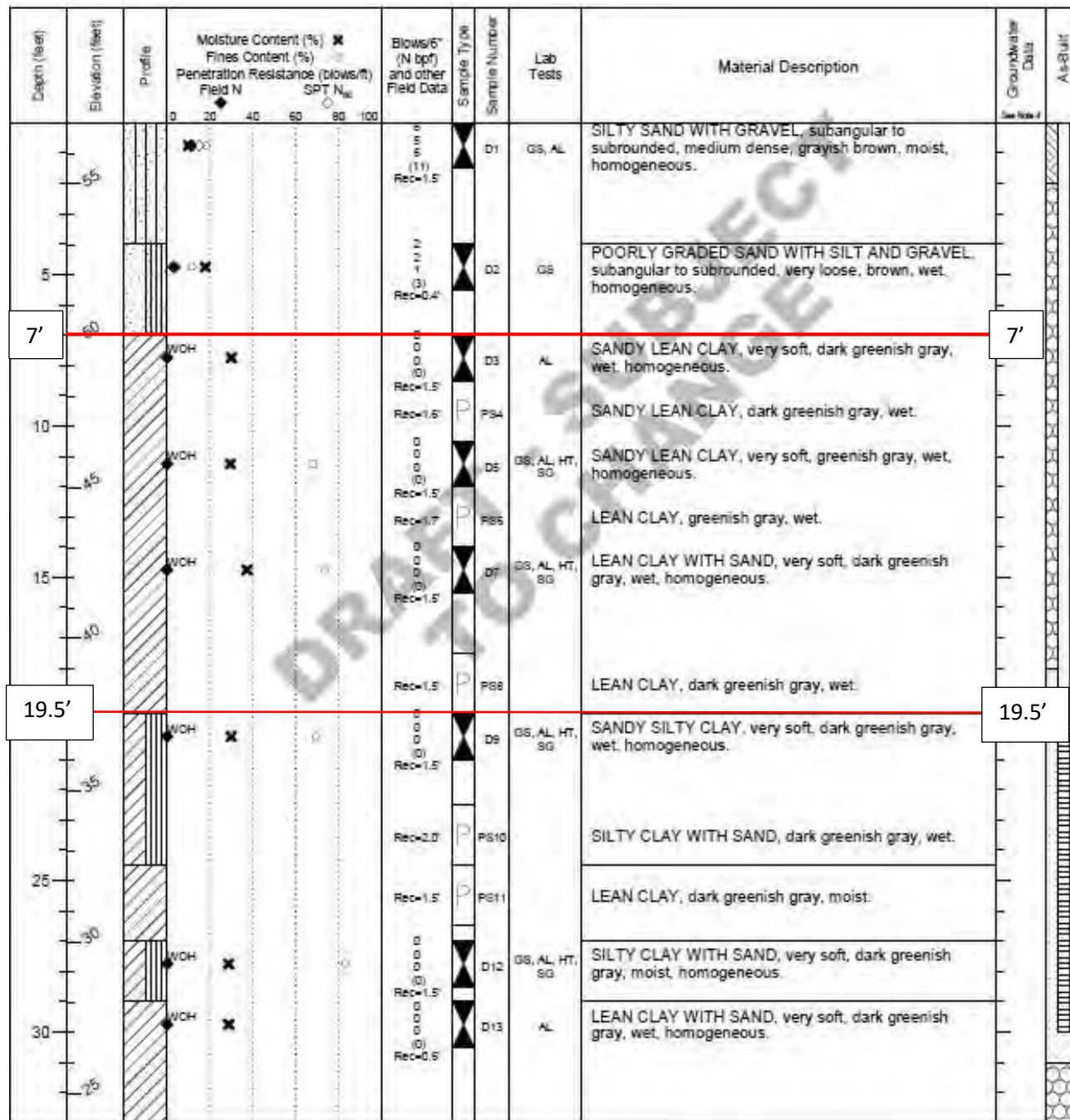
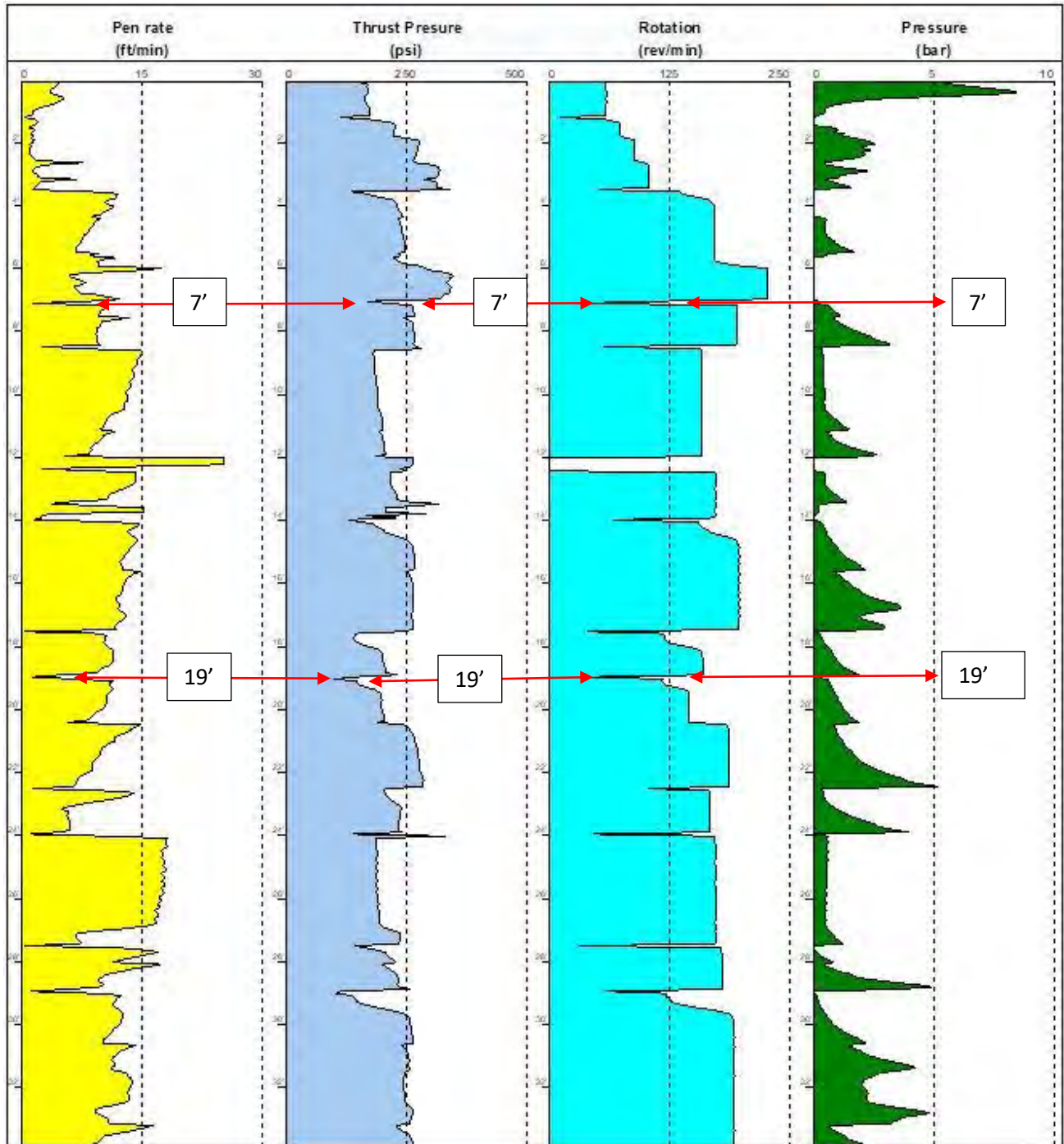


FIGURE 7A. AN EXAMPLE DRAFT BORING LOG DRILLED WITH THE MWD EQUIPMENT (SEE FIGURE 7B).



**FIGURE 7B. AN EXAMPLE MWD OUTPUT PLOT FOR THE SAME BORING AS IN FIGURE 7A. NOTE THE SOIL CHANGE CONTACT ON THE BORING LOG IS SLIGHTLY DIFFERENT THAN THE MWD PLOT (~19'). THE MWD PLOT CAN OFTEN HELP THE GEOTECHNICAL DESIGNER MAKE MORE ACCURATE CONTACT DEPTH INTERPRETATIONS.**

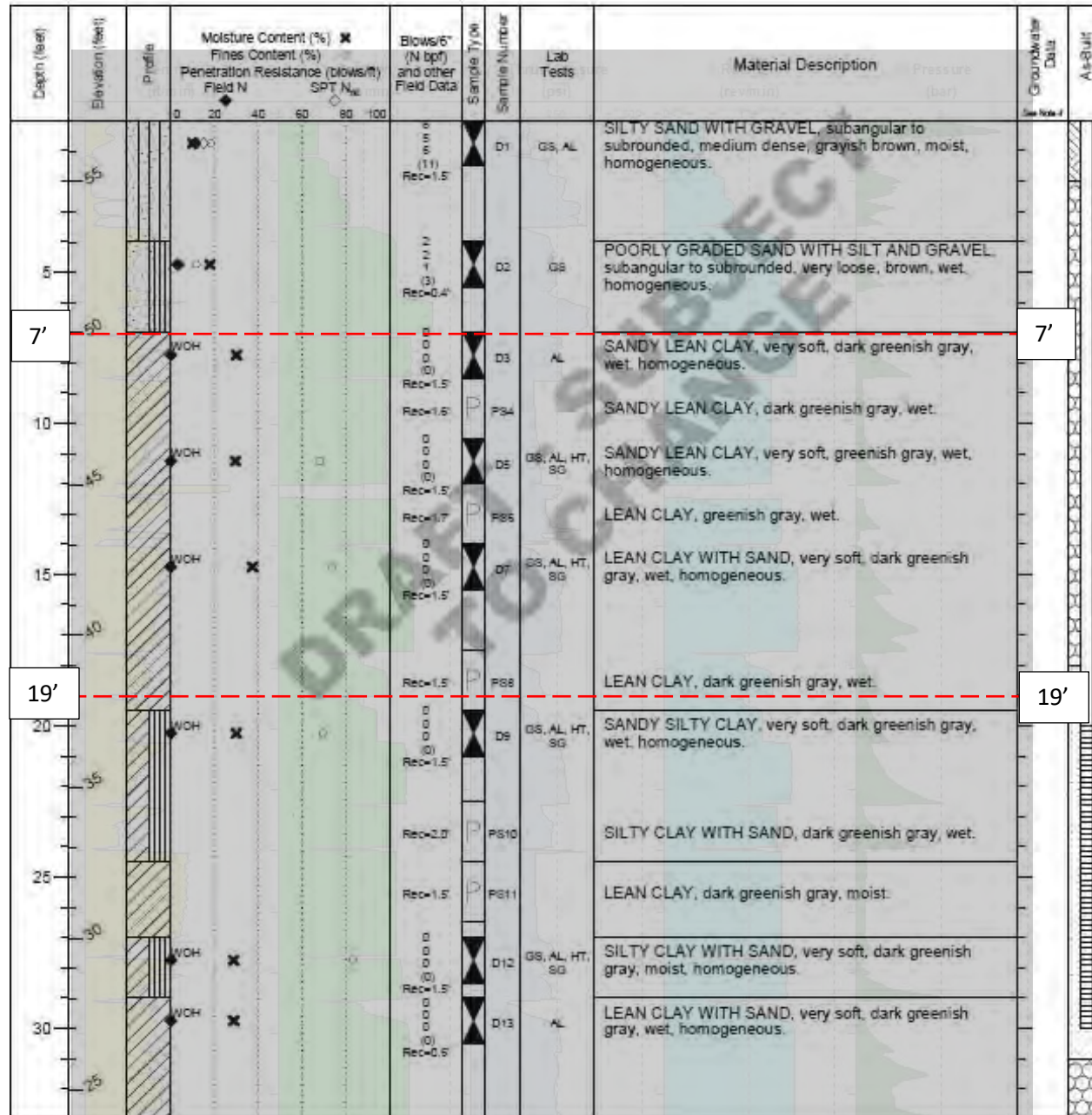


FIGURE 7C. AN EXAMPLE MWD OUTPUT PLOT OVERLYING THE SAME DRAFT BORING LOG (SEE FIGURES 7A AND 7B).

In addition to assisting the geotechnical designer with more accurate subsurface contact depths, WSDOT will soon begin collecting strength data from selected lab samples and begin assigning them to known soil units. This will give the geotechnical designer a preliminary range of anticipated strengths, when looking at the MWD plot only, before submitting samples to the lab. Armed with such data, the geotechnical designer can begin preliminary analyses without waiting for the lab results. MTDOT has been collecting strength data over the past few years and is beginning to use the general strength data for preliminary design/analysis.

## **MWD STRENGTHS AND LIMITATIONS**

### **Strengths:**

Once the Jean Lutz MWD technology is installed on the CME drill rig, the process of setting up the MWD data collection is relatively simple. The computer, as described above, is mounted on the drill rig (see Figures 1 and 3). The monitor is stored in a carrying case when not in use and is simply plugged into the computer and mounted above the driller's area when needed (see Figure 3). When drilling begins, the MWD sensors begin reading, with downhole results transmitted to the computer and instantly shown on the monitor in real time. The driller and/or geotechnical designer (if on site during drilling) can then observe the monitor and possibly reduce the number of subsurface samples needed in the same unit. For example, if the monitor is reading the same subsurface conditions for several 10s of feet (or more), then the geotechnical designer might change the sample frequency from every 2.5 feet to every 5 feet or possibly every 10 feet or more. Once the MWD equipment indicates differences in subsurface conditions, a sample can be taken at that depth to record the difference in subsurface units.

The Jean Lutz software packages (EXEPF and DRDPR) are relatively user friendly. Both software packages show downhole plots of MWD parameters. The parameters and display options are customizable, the user interfaces are clean, and Jean Lutz provides reliable manufacturer support.

### **Limitations:**

As with any new technology, WSDOT has found that MWD has a learning curve. For example, the housing for the monitor broke during our first drilling operation with the MWD equipment installed. The monitor was placed on a table beside the drill and was able to record data; however, the driller was unable to read the monitor while operating the drill. Another setback that was observed in the field while drilling is that the clamps on the drill that are intended to “stop measuring” are too sensitive and “start/stop reading” every time the driller taps the clamps (Figure 8). We quickly realized that our subsurface elevation readings were inaccurate, since the MWD equipment continued to measure even though it should have been in “stop measuring” mode. Currently, we bypass the sensor on the clamps and manually press the “measure/wait” button while drilling (see Figure 4).

There are some limitations to the Jean Lutz software, which the manufacturer hopes to resolve in the future. Chief among these is the inability to import or export gINT files into or out of the Jean Lutz software packages. The limitation is true for CSV and ASCII files as well. The result is an inability to view stratigraphy/lithology logs side-by-side with the downhole MWD plots. As such, boring logs and downhole MWD plots must be manually superimposed to make accurate correlations between them (see Figure 7c). Other, minor limitations exist within the software packages, which can be easily resolved with the manufacturer (e.g., occasional errors with metric to imperial unit conversions, certain units that don't display, etc.).



**FIGURE 8. A CLOSE-UP PHOTOGRAPH SHOWING THE CLAMPS ON THE DRILL. CURRENTLY, THE DRILLER PASSES THE “MEASURE/WAIT” BUTTON ON THE MONITOR INSTEAD OF RELYING ON THE CLAMPS (SEE FIGURE 4).**

Additionally, our drillers are skeptical to the benefits of utilizing the real-time MWD output when it comes to more efficient drilling. It is our understanding that the driller can set one of the MWD parameters (down pressure, torque, penetration rate, etc.) at a “normalized” setting (to remain constant) and the results will assist both the driller for efficiency and quality of drilling and the geotechnical designers to more accurately read the MWD output plot. We primarily use mud rotary drilling techniques and to achieve the best drilling results through different subsurface conditions, our drillers constantly need to change the normalized setting (i.e., down pressure, water pressure, etc.). WSDOT drillers rely on “feel” and how the drill rig “sounds” during drilling and adjust the settings accordingly.

It is our understanding that MWD is a very effective tool, while drilling in rock. As mentioned above, WSDOT has very limited experience drilling in rock with the MWD equipment, to date. The “normalized” setting of certain parameters might assist in rock but that has yet to be determined.

In addition to the drillers having difficulty seeing the benefits of the MWD system assisting them while drilling, the geotechnical designers are also having difficulty seeing the benefits of the system when it comes to design/analysis. While there is a major benefit of possibly reducing the sample frequency during drilling, we have not seen the benefit for use during design/analysis. The range of collected material strengths mentioned above will assist with the preliminary design/analysis; however, most geotechnical designers have been submitting samples to derive specific strengths that represent the actual subsurface unit(s) they are working in, not a range of strengths that come from different areas of Washington State. The geotechnical designers find the MWD plot has many parameters available for consideration

during design, but they have been unsure of the benefits this data presents and how to use it in their analyses.

### **WSDOT'S MWD CONSIDERATIONS**

- Need to develop a Standard Operating Procedures (SOP) manual – For both drillers and geotechnical designers to assist with setting up the MWD equipment and maximizing drilling efficiency and to aid in design/analysis.
- Proper data management – The SOP should have a section that covers the proper way to store and manage data. Currently, WSDOT retains all the information on the MWD computer, downloads the recent information to a thumb drive, and then uploads it to the WSDOT server. Can the information from the MWD computer be deleted, once it is transferred to the WSDOT server, and what's the proper procedure to do this?
- Simpler techniques to compare the MWD data to SPT samples and geophysical data – WSDOT is still finding it difficult to interpret the MWD data when compared to SPT data and possible geophysical data. Do we gain an advantage by using the MWD equipment?
- Proper data usage – What is the best way for us to use the massive amounts of MWD data we collect in the design/analysis of our projects?
- Data display – What's the best way to standardize figures for use in reports?

### **CONCLUSION AND RECOMMENDATIONS**

MWD is an emerging technology for geotechnical applications that is both exciting and challenging. MWD for geotechnical use is still in its infancy and much more experience is required to realize the benefits that might be available for design/analysis in the future. Drillers need experience and assistance on how real-time data can be used to assist them with drilling efficiency and drilling quality. More drilling experience is needed in both soil and rock to help the driller become more confident and capable while drilling with MWD equipment. Geotechnical designers need experience in interpreting the MWD data and applying it to project outcomes. As with newer technology, much more time and effort are needed to fully understand MWD's capabilities for use in the geotechnical field.

### **REFERENCES:**

- Website
  1. SEG Wiki. *Measurement-while-drilling*. [Measurement-while-drilling - SEG Wiki](#). Accessed June 5, 2023.
- Conference Proceedings
  1. Rivers, B. S., *Measurement While Drilling (MWD)*. Geohazards Forum, 2016. US Department of Transportation, Federal Highway Administration. FHWA – Resource Center.

**Advancing Subsurface Investigations Beyond The Borehole With Passive  
Seismic Horizontal-To-Vertical Spectral Ratio And Electromagnetic  
Geophysical Methods At Transportation Infrastructure Sites In  
New Hampshire**

**James Degnan**

U.S. Geological Survey  
New England Water Science Center  
331 Commerce Way  
Pembroke, NH 03275-3718  
603-226-7826  
jrdegan@usgs.gov

**Krystle Pelham**

New Hampshire Dept. of Transportation  
Bureau of Materials and Research  
PO Box 483, 5 Hazen Drive,  
Concord, NH 03302-0483  
603-271-1657  
Krystle.Pelham@dot.nh.gov

**Neil Terry**

U.S. Geological Survey  
New York Water Science Center  
425 Jordan Road  
Troy, NY 12180  
860-487-7402 Ext. 18  
nterry@usgs.gov

**Sydney Welch**

U.S. Geological Survey  
New England Water Science Center  
331 Commerce Way  
Pembroke, NH 03275-3718  
603-226-7800  
smwelch@usgs.gov

**Carole Johnson**

U.S. Geological Survey  
Water Resources Mission Area  
11 Sherman Place, Unit 5015  
University of Connecticut  
Storrs Mansfield, CT 06269  
860-487-7402  
cjohnson@usgs.gov

### **Acknowledgments**

Appreciation is expressed for site access coordination and preliminary geotechnical information sharing by Chuck Corliss, NHDOT Railroad Operations Engineer and Kurt Yuengling and Adam Carr, NHDOT Geologists. Michael Howley, New Hampshire Geological Survey Geophysicist, provided data, data collection assistance, and site information. Deirdre Nash of the NHDOT Research Advisory Council provided help coordinating the project and project meetings with the technical advisory group. Jeffrey Reid of Hager Richter Geoscience offered project advice through participation in the technical advisory group and led data collection in the field with his equipment and a new method to help verify results.

Eric White of the U.S. Geological Survey Hydrologic Remote Sensing Branch, provided training to project staff in the use and interpretation of the geophysical data and assisted in the collection of field data. Tom Mack, U.S. Geological Survey Office of International Programs, provided training to project staff in the collection and processing of the geophysical data and completed a technical review of a draft of this manuscript. Colton Medler, U.S. Geological Survey Dakota Water Science Center, completed a technical review of a draft of this manuscript. Adam Benthem, U.S. Geological Survey New England Water Science Center, provided geomorphology expertise and assisted with data collection and management. Jeremy Foote, U.S. Geological Survey New England Water Science Center, provided GIS and remote sensing support. Any use of trade, firm, or product names is for descriptive purposes only and does not imply endorsement by the U.S. Government.

### **Disclaimer**

Statements and views presented in this paper are strictly those of the author(s), and do not necessarily reflect positions held by their affiliations, the Highway Geology Symposium (HGS), or others acknowledged above. The mention of trade names for commercial products does not imply the approval or endorsement by HGS.

### **Copyright © 2023 Highway Geology Symposium (HGS)**

All Rights Reserved. Printed in the United States of America. No part of this publication may be reproduced or copied in any form or by any means – graphic, electronic, or mechanical, including photocopying, taping, or information storage and retrieval systems – without prior written permission of the HGS. This excludes the original author(s).

## ABSTRACT

The U.S. Geological Survey (USGS), in cooperation with the New Hampshire Department of Transportation (NHDOT), surveyed transportation infrastructure sites using rapidly deployable geophysical methods to assess benefits added to a comprehensive site characterization with traditional geotechnical techniques. Horizontal-to-vertical spectral-ratio (HVSr) passive-seismic and electromagnetic-induction (EMI) methods were applied at four sites including a roadway-stream crossing, roadway-bridge rail-trail crossing, commuter-parking expansion, and a railroad-adjacent river-cutbank slope-failure site. Additionally, ground-penetrating radar (GPR) was used at the slope-failure site. Typically, at transportation projects, subsurface geotechnical properties are determined from boring data; however, borings are often spaced hundreds of feet apart, potentially missing important spatial variability between boreholes. Geotechnical site characterization including geophysical surveys helped provide a more accurate characterization by using continuous or near continuous profiling.

Three-component ambient noise measured with the HVSr method was used to determine site resonance frequency for estimating sediment thickness. The method works best when there is a strong shear-wave acoustic impedance contrast ( $> 2:1$ ) between sediment and bedrock. Sediment thickness estimates from HVSr measurements were combined with boring data to make detailed maps of the bedrock surface elevation. The bulk electrical conductivity of the subsurface was indirectly measured with EMI methods and was used to identify lithologic variations, shallow bedrock, and conductive groundwater. Ground penetrating radar, which transmits pulses of electromagnetic energy into the subsurface and records the amplitude and timing of reflected signals, was used to identify bedding and changes in lithology or water content. By combining geophysical and boring data analyses, transportation projects produced more spatially comprehensive representations of geotechnical subsurface conditions than would be determined using conventional borings alone.

## INTRODUCTION

Geotechnical site characterization guided by direct information from conventional borings, which is often used at the initiation of roadway projects by departments of transportation, sometimes cannot fully characterize the subsurface (overburden stratigraphy, hydrologic conditions, and the bedrock topography). Incompletely characterized field sites with unknown subsurface complexity between borings can disrupt work plans, force revision of designs, and lead to cost increases from schedule delays or change orders (Boeckmann and Loehr, 2016). Typically, sediment samples and water levels are obtained from the subsurface during drilling to characterize geotechnical properties, but often, due to the prohibitive expense of drilling, borings are spaced hundreds of feet apart. Additional detail from geophysical surveys could help provide a more thorough characterization of the subsurface, such as a locally shallow water table, by enabling more accurate interpolation between borings. By combining analysis of geophysical and boring data, transportation projects can produce a more comprehensive representation of geotechnical subsurface conditions than can be determined using conventionally spaced borings alone.

Incorporation of more geophysical measurements into transportation projects is recognized by goals established in the Federal Highway Administrations EDC-5: Advanced

Geotechnical Methods in Exploration (A-GaME) initiative (U.S. Department of Transportation, Federal Highway Administration, 2020). Data collection in support of these goals could help assess the utility of such methods in improving geotechnical characterization at New Hampshire Department of Transportation (NHDOT) roadway project sites. Results can be used to evaluate the potential to improve timing of project completion and cost savings. Geophysical data collected using methods such as HVSr and EMI at sites in New Hampshire (fig. 1) could help identify geologic and hydrologic conditions that can affect transportation infrastructure planning, design, construction, and maintenance. A variety of NHDOT infrastructure sites requiring geotechnical investigations planned in 2022 were selected by this project for HVSr and EMI geophysical data collection and analysis. Geotechnical properties of the subsurface from boring data from previous and ongoing investigations, as well as other information from geologic maps, landfill feasibility hydrogeological investigations, and remote sensing can be considered to constrain geophysical investigation interpretations.

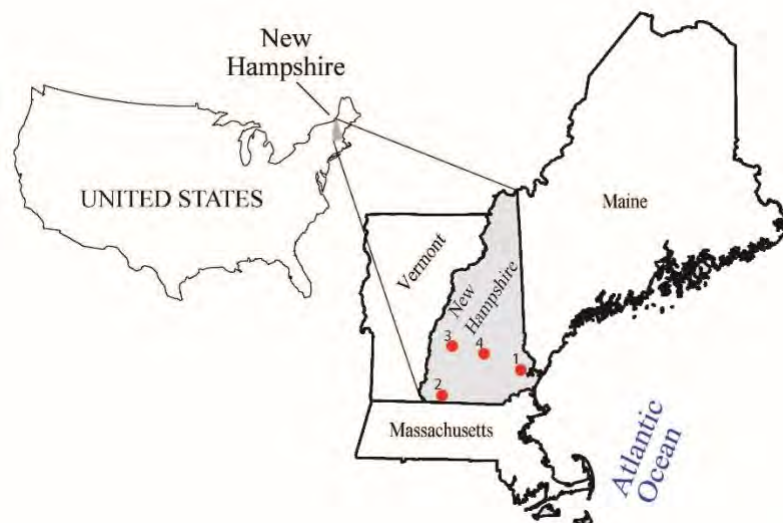


Figure 1. Map showing site numbers and locations (red circles): site 1: roadway crossing stream, Lee, New Hampshire; site 2: roadway crossing rail trail, Troy, New Hampshire; site 3: carpool and bus stop parking, New London, New Hampshire; and site 4: railroad adjacent to slope failure, Canterbury, New Hampshire.

The purpose of this study is to assess the utility of integrating geophysical techniques with routine geotechnical assessments to provide additional information to ongoing NHDOT projects in varied transportation infrastructure, geotechnical, and hydrogeologic settings. Results from this study can also be used to guide future survey designs and to further refine geophysical results at future NHDOT and USGS investigation sites.

### Methods of data collection and analysis

Two primary geophysical methods were used in the study: (1) passive horizontal-to-vertical spectral ratio (HVSr) seismic (Cox and others, 2020; Johnson and Lane, 2016; Mack, 2020) and (2) frequency domain electromagnetic induction (EMI) (Huang and Won, 2000). Ground penetrating radar (GPR) was also used at one site where additional characterization was needed. These methods were chosen because they can be rapidly deployed and are well suited for

improving cross sections of the subsurface compared to those generated with conventionally spaced borings alone.

Analysis focused on improvement in bedrock-surface, stratigraphic, and saturated-zone mapping for geotechnical site characterization. Regional and local surface-water and groundwater quality, geologic, and hydrologic data were reviewed to help site characterization and to categorize method efficacy in a variety of typical NHDOT settings. Enhanced cross sections of subsurface conditions can then be generated with integrated results of borings (Yuengling, K. R., 2022, Carr, A. R., 2022a and b, and Jacques Whitford Company, Inc., 2004) and geophysical surveys to improve site characterization.

HVSR is not widely used but the effectiveness of the methods of data processing and associated regression models have been documented regionally and by specific site. The method requires developing accurate regression models with coefficients that are representative of the region or site where the data are collected. For example, the development of a data base of regression coefficients determined for specific materials at sites or within regions could help NHDOT and others streamline future HVSR seismic processing. Electromagnetic induction and GPR methods provide independent information based on unique responses to electrical properties of the subsurface; EMI measures electrical apparent conductivity (average of a given half space), whereas GPR measures distinct boundaries of materials with different properties with patterns that often give an indication of general sediment grain size (Beres and Haeni, 1991; Haeni, 1996). However, sites where the subsurface and groundwater electrical conductivity might be altered by road salt may limit the utility of some geophysical methods such as EMI and GPR due to attenuation of the signal; alternatively at some sites, such conditions might enhance the utility of geophysical methods. It is important to consider geologic information and hydrologic data to understand how seasonal or hydrologic event-based conditions (drought or flooding) might affect data interpretation.

### **Horizontal-to-vertical spectral ratio**

The HVSR method is used to determine the peak resonance frequency ( $f_0$ ) induced by ambient seismic noise in unconsolidated sediments overlying bedrock when there is an adequate contrast in shear-wave acoustic impedance between the two layers ( $> 2:1$ ). Spectral ratio analysis of the combined horizontal and vertical components of the seismic data was used to determine  $f_0$ . A regression model (equation) to solve for sediment thickness using a power law function fit to the HVSR-determined  $f_0$  versus depth to rock was developed to use in HVSR seismic data processing equations (Bignardi, 2017, Johnson and Lane, 2016, Mack, 2020, and Medler, 2021). Plots of the horizontal to vertical spectral ratio versus resonance frequency were examined to determine a qualitative peak frequency quality. The peak frequency quality is a qualitative classification, on a scale from 1 to 5, and is based on how clear and sharp the peak is with 5 being the best and 1 being the worst. The quality of the HVSR result peak and the maximum horizontal to vertical spectral ratio standard deviation generated by the processing software (MOHO, 2020, SESAME WP04, 2004) were compared to data collection conditions. Three HVSR seismometers were deployed simultaneously at different measurement locations at each site to maximize data collection time efficiency. A variety of coupling techniques were tested in different settings, as seismometer coupling to the ground affects data quality. Additional information about the surveys and data are available in a data release (Degnan and others, 2022).

Shear wave velocities ( $v_s$ ) were computed for each HVSR measurement with an adjacent boring with a known depth to bedrock using equation 1. Mean shear wave velocities for each site were used to calculate bedrock depth from HVSR measurements that were not near borings for bedrock surface profiling and mapping using equation 2 (Johnson and Lane, 2016).

$$v_s = z (f_0 * 4); \quad (1)$$

$$z = v_s / (f_0 * 4) \text{ and} \quad (2)$$

where

$z$  is the depth to bedrock in feet;  
 $v_s$  is the overburden shear wave velocity in feet per second; and  
 $f_0$  maximum (peak) horizontal to vertical spectral ratio in Hertz.

### Electromagnetic induction

Bulk electrical conductivity of the subsurface was indirectly measured with EMI methods using induced electromagnetic fields (Zohdy and others, 1974) at several frequencies and coil spacings. Frequencies with sufficient signal to noise ratio for a given survey were selected for inverse modeling to better understand conductivity variations with depth (Abraham and others, 2006). Variations in electrical conductivity, both laterally and vertically, were measured with one of two frequency-domain EMI instruments used in this study: (1) multiple frequency GEM-2 and (2) the larger, multiple spacing and dual orientation, DUALEM-421. The GEM-2 has a fixed transmitter-receiver (Tx-Rx) coil spacing and sweeps through several logarithmically-separated transmitter frequencies. Measurements made with lower frequencies are generally capable of sensing deeper apparent conductivity values at the cost of a lower signal to noise ratio, while measurements made with higher-frequencies provide shallower but increased signal to noise ratio. The DUALEM-421 uses a single 9-kHz frequency with multiple Tx-Rx coil spacings and orientations, where measurements made with larger coil spacings sense a larger volume and hence deeper conductivity values, while shorter coil spacings provide increased resolution of the shallow subsurface. Additional information about the surveys, data, and processing are available in a data release (Welch and others, 2023).

Raw data from the GEM-2 consist of measurements of the real and imaginary normalized magnitude of the magnetic field quadrature at each of the transmitter frequencies (in units of parts per million). A further processing step can be applied to convert these values to apparent electrical conductivity and apparent magnetic susceptibility using the Invertor software (Geophex). This analytic conversion assumes an electromagnetically homogeneous earth below the sensor. The DUALEM-421 automatically performs the conversion from normalized magnetic field components to apparent electrical conductivity and magnetic susceptibility.

Data were processed to remove erroneous data points that were characterized by extreme high or low values (noise) following the methods described by Johnson and others (2019) and resampled to 1-meter spacing using a moving averaging window. The apparent conductivity data were inverted with a Laterally Constrained Inversion to produce depth versus electrical resistivity (1/conductivity) along 2D profiles. This type of inversion encourages a smoothed out but stable solution when fitting data to models. As part of the inversion process, a depth of investigation (DOI) was computed to estimate the depth to which the measurement is reliable (Christiansen and Auken, 2012). Results were output as text files that included positions, DOI, inversion metrics (data and model residual), and inverted resistivity models (Welch and others, 2023);

these outputs were used to generate profiles of electrical conductivity to compare to other data using plotting tools in R (R Core Team, 2023; Wickham, 2016).

### **Ground-penetrating radar**

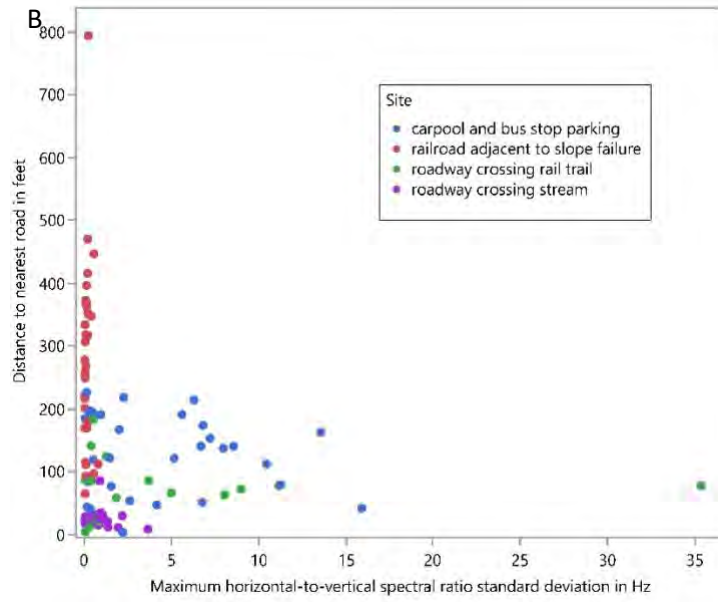
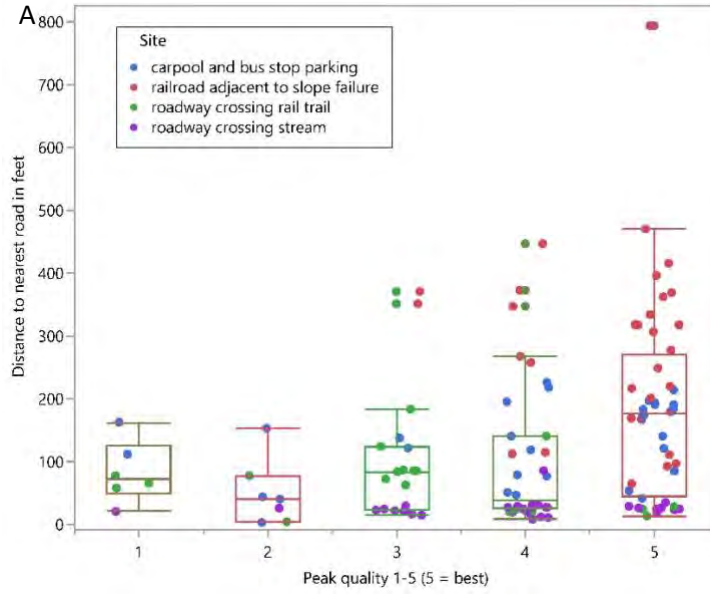
Ground-penetrating radar (GPR) profiles were generated with an antenna with a fixed Tx-Rx offset contained within a tow-body. GPR transmits pulses of electromagnetic energy into the subsurface and records the amplitude and timing for the return of reflected signals to image the subsurface (Keary and Brooks, 1991). The radar-wave propagation is affected by electromagnetic properties of the subsurface materials including dielectric permittivity, electrical conductivity, and magnetic susceptibility caused by differences in lithology, water content and specific conductance, and sediment type (Milsom, J. and Eriksen, A. 2011). The penetration of GPR signals is limited where bulk electrical conductivity of the subsurface is high or where the radar-wave reflection is scattered from discrete objects too small to generate a coherent geometric reflection, such as large cobbles. Here, GPR data were collected using an 80-MHz shielded antenna. Depth to reflectors is not inherently known from GPR data, given that the speed at which radar waves travel depends on study area subsurface properties. Therefore, estimates of GPR velocity are required to present GPR data with a depth axis to estimate depths to observed reflectors. Published velocity estimates (Beres and Haeni, 1991) and velocity measurements from diffraction hyperbola fitting in the ReflexW software (MALA, 2022) were used to calculate depth from reflected radar-wave travel time. GPR velocities used ( $n = 37$ ) ranged from 0.057 meters per nanosecond to 0.22 meters per nanosecond, with a median value of 0.12 meters per nanosecond. These two end-member velocities likely represent fully saturated soils with high water content (low velocity) versus loose dry soil with significant air space (high velocity).

## **RESULTS**

Results of HVSR, EMI, and GPR field data collection and analysis at four selected transportation infrastructure sites are presented in this section. Before discussing results from each site individually, general observations from HVSR and EMI surveys are discussed to provide background information necessary for interpretation of geophysical datasets. All data from geophysical surveys are publicly available in published data releases. Data from HVSR measurements are available in Degnan and others (2022) and EMI and GPR survey data are available in Welch and others (2023).

### **General geophysical surveys**

One important observation from HVSR measurements was that data quality varied with distance from roadways. Frequency peaks in the best quality category (category 5) from HVSR analysis were obtained at various distances from roadways; however, the best quality category had the highest median distance from roadways (fig. 2A). Therefore, although it is possible to get good quality data near a road, most of the best-quality category data were obtained farther from roadways. Additionally, standard deviations were much smaller for measurements made 200 ft (feet) or farther from a roadway (fig. 2B). Also, the best quality data (with the lowest standard deviation) were acquired when the seismometers were well coupled in compact sands, and the highest median standard deviations were associated with loose soil, which generally has poor coupling (fig. 2C).



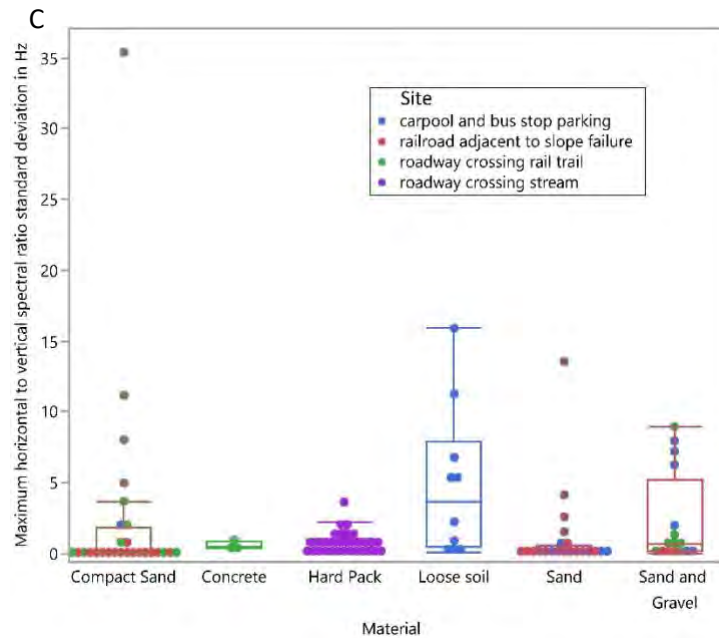


Figure 2. Charts showing passive seismic horizontal-to-vertical spectral ratio (HVSr) data quality indicators, (A) resonance frequency peak quality using a categorical rating system from 1 (worst) to 5 (best), and (B) standard deviation from horizontal-to-vertical spectral ratio measurement versus distance from nearest roadway and (C) coupling material versus horizontal-to-vertical spectral ratio measurement standard deviation.

Shear wave velocities were computed for each HVSr measurement with an adjacent boring with a known depth to bedrock (**Table 1**) using equation 1 above. Velocities were similar to those reported in other locations with similar overburden stratigraphy in the region (Marvinney and Glover, 2015). A mean site shear wave velocity was used to calculate depth to bedrock at sites with more than one boring available.

A regression equation (3) was developed using  $f_0$  measurements and depths to bedrock from borings (Table 1) so bedrock depth can be calculated at similar sites without boring information (Lane and others, 2008).

$$z = af_0^b \text{ and} \quad (3)$$

where

- $z$  is the depth to bedrock in feet;
- $a$  computed regression parameter is 423.51;
- $b$  computed regression parameter is -1.167;
- $f_0$  and is the resonance frequency.

The resulting regression equation, based on the 17 depths to bedrock and corresponding  $f_0$ , was similar to those generated by studies in similar nearby settings (Johnson and Lane, 2016, Fairchild and others, 2013, and Panthi and others, 2023).

Table 1. Depth to bedrock from borings and shear-wave velocities computed from maximum horizontal-to-vertical spectral ratio by site and material. [ft, feet;  $v_s$ , shear wave velocity; ft/s, feet per second;  $f_0$ , resonance frequency peak; hertz, Hz]

Site	Boring	Bedrock depth from boring, in ft	Shear-wave velocity ( $v_s$ ) (ft/s)	Maximum $f_0$ Hz	$F_0$ standard deviation in Hz	Mean site $v_s$ (ft/s)	Overburden lithologic summary
roadway crossing stream	B01	50.9	1198	5.91	1.3	1148	fill, alluvium, marine, and till
	B02	45.6	1027	5.63	0.3		fill, alluvium, marine, and till
	B03	25.3	1096	8.06	0.1		fill, alluvium, and till
	B04	36.5	1263	8.66	0.29		fill, alluvium, and till
roadway crossing rail trail	B03	92.0	1611	4.38	0.73	1628	glacial outwash and lacustrine
	B02	99.5	1656	4.16	0.37		glacial outwash and some lacustrine
	B01	102	1530	3.75	0.46		glacial outwash and some lacustrine
	B04	94.0	1715	4.56	0.82		glacial outwash, lacustrine, and some till
carpool and bus stop parking	B-08	15.1	879	14.6	1.54	984	fill and till
	B-04	14.8	1322	22.3	2.21		till
	B-06	14.4	722	12.4	0.04		fill and till
	B-02	8.86	912	25.3	0.61		glacial outwash and till
	B07	20.8	1014	12.2	0.10		fill and till
	B11	5.50	767	34.9	6.80		silt and till
	B13	5.00	399*	19.9	0.48		silt and till
	B10	7.50	1219	40.6	11.3		silt and till
B03	7.70	1034	33.6	0.35	glacial outwash and till		
railroad adjacent to slope failure	TW-103	179	1211	1.77	0.03	1211	stream terrace, glacial lake, some till

\*outlier not used in mean calculation

Median apparent electrical conductivity values were similar at the four sites surveyed. The roadway crossing stream site was selected to be surveyed with both the multiple-coil spacing and multiple-frequency instruments to provide a comparison of results between the two methods. This was done because the site had several forms of interference described in the section below and had a range of overburden materials and depths. Three sites were surveyed using the multiple coil spacing instrument and two were surveyed using the multiple-frequency instrument (Table 2). The carpool and bus stop parking site had the thinnest overburden, which was mostly till that would be expected to produce a less conductive response than thick marine and lacustrine sedimentary lithologies found at the other three sites. However, the maximum values were highest at sites directly adjacent to roadways and were likely related to metal infrastructure or legacy de-icing chemicals (road salt) in groundwater (Table 2).

Table 2. Apparent conductivity summary statistics in millisiemens per meter (mS/m) from the electromagnetic induction surveys by site.

Site	N Rows	Mean depth of Investigation (DOI, feet)	Apparent Conductivity in mS/m				
			Mean	Median	Max	Interquartile Range	25 <sup>th</sup> Percentile
roadway crossing rail trail*	2877	12.59	13.50	7.6	424.8	10.4	3.6
roadway crossing stream*	2230	18.39	8.35	7.1	215.3	7.4	3.7
roadway crossing stream**	13413	14.92	18.02	7.50	8608	7.28	3.96
railroad adjacent to slope failure*	2786	19.53	5.99	3.8	102.5	3.7	2.2
carpool and bus stop parking expansion site**	32609	10.91	28.31	7.14	31065	11.75	3.18

\*Data collected with multiple-coil-spacing instrument

\*\*Data collected with multiple-frequency instrument

## SITE-SPECIFIC SURVEYS

### Roadway crossing stream, site 1, Lee, New Hampshire

The roadway crossing stream site (site 1) is in Lee, NH, where the Little River flows under State Route 125 through a large metal culvert. Geotechnical investigations to support a culvert replacement design and work plan were scoped to determine the overburden stratigraphy, the depth to bedrock, existing fill materials, and the location of former bridge abutments buried on each side of the culvert beneath the roadway.

Twenty-five HVSr measurements were made at 20 measurement locations along the roadway shoulder behind the guard rail at the roadway crossing stream site. Three of the HVSr locations were selected to correspond with boring locations with documented overburden stratigraphy and depth to bedrock. The other 17 measurements were used to delineate the bedrock surface profile line within and beyond the boring investigation locations. Measurements were repeated at four locations to compare results from different traffic patterns at about 5, 10, and 15 ft from the general path of traffic. The first round of measurements was completed when the drill rig and traffic diverting package (traffic control flags, cones, and impact absorbing vehicle) were on site. Traffic diversion caused measurements on the same side of the roadway (east) as the drill rig to be about 5 ft farther from the path of vehicle travel and measurements on the opposite side of the roadway (west) were about 5 ft closer to the path of vehicle travel. In general, HVSr peak quality was better with increasing distance from the path of traffic.

The apparent conductivity results show anomalies (patterned variation) interpreted to represent the surface of the bedrock (fig. 3 A-D). Some anthropogenic effects from power lines and buried metal structures are likely present. Above-ground powerlines are located along State Route 125 and may have impacted the multiple-frequency EMI instrument dataset. Data were collected on the side of road away from the powerlines to attempt to reduce those effects.

The Little River culvert appears in multiple-frequency EMI instrument results as a broad conductive anomaly and a large in-phase anomaly. Both instruments detected a highly resistive anomaly in the middle of the surveyed area along the northwest edge adjacent to bedrock outcrop. The area of this resistive anomaly represents the expression of shallow bedrock subcropping (fig. 3A and B).

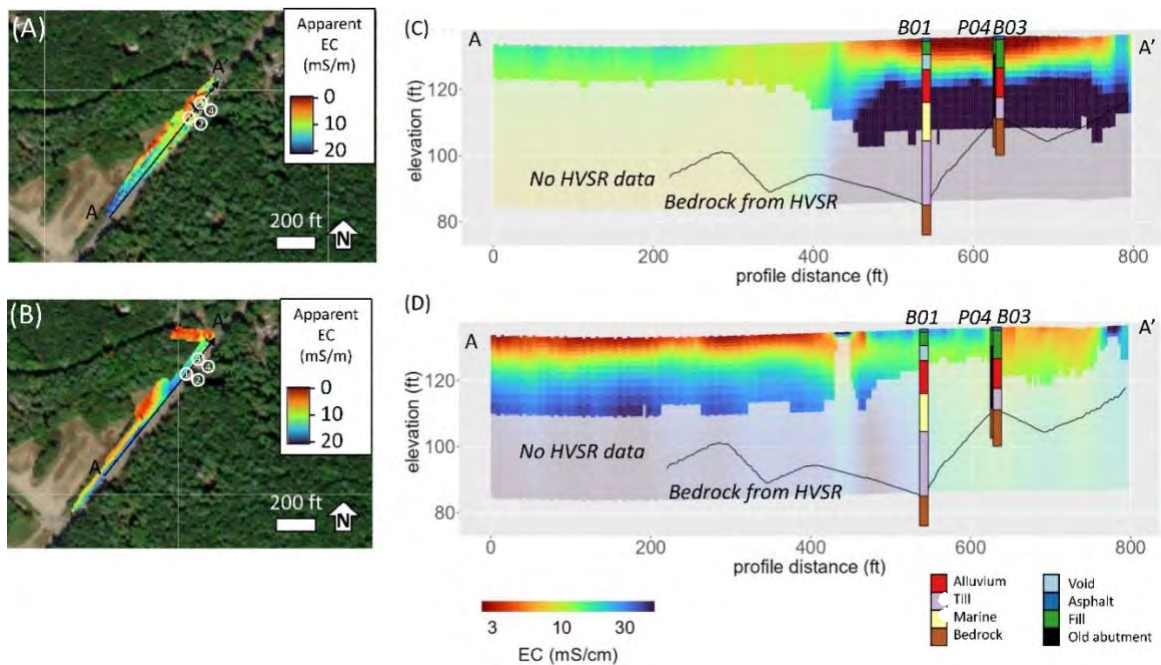


Figure 3. Electromagnetic induction survey results from the A-A' cross section at site 1, roadway crossing stream, in Lee, New Hampshire, showing (A) a map of apparent electrical conductivity (EC) from the multiple-frequency instrument 47,970 Hz band; (B) a map of apparent conductivity from the multiple-coil-spacing instrument (4-m-spaced horizontal coplanar coils); (C) profiles of inverted electrical conductivity from the multiple-frequency instrument with borings and the bedrock surface from passive seismic horizontal-to-vertical spectral ratio results; and (D) profiles of inverted electrical conductivity from the multiple-coil-spacing instrument with borings and the bedrock surface from passive seismic horizontal-to-vertical spectral ratio results. White circles with labels on panels (A) and (B) correspond to borings on panels (C) and (D).

### Roadway crossing rail trail, site 2, Troy, New Hampshire

The roadway crossing rail trail site (site 2) is located in Troy, NH, where State Route 12 crosses the Cheshire Rail Trail. The rail trail is a recreational and commuter trail along a former railroad with tracks removed or buried to facilitate travel by foot or bicycle. Bedrock outcrop and blasted railroad rockcut features are aligned with the direction of the trail south of the bridge on the northwest side of the trail. Geotechnical investigations support a bridge replacement design and were scoped to characterize overburden stratigraphy, depth to bedrock, the top 10 ft

of bedrock with core, existing fill materials, and identify the extent of the existing bridge abutment footings. Despite the interference, the data shown is useful and provides information about the subsurface as described below.

Twenty-one HVSR measurements were made at 21 selected locations at the roadway crossing rail trail site; three correspond with boring locations with a documented overburden stratigraphy and depth to bedrock; and 16 measurements along the rail trail were of good quality and used to delineate the bedrock surface profile line within and beyond the boring investigation locations (fig. 4). One measurement was not used due to the lack of a clearly define peak. Measurement locations had a 65.6 ft spacing along the rail trail starting in the southwest adjacent to the railroad rockcut and extending northeast 730 ft to the bridge and 285 ft to the northeast beyond the bridge. The five measurements made adjacent to the railroad rockcut have directional H/V maximum intensities between 100- and 125-degree azimuths with a 113-degree median; whereas the deeper bedrock surface identified at the other end of the survey line north of the bridge had between 158- and 180-degree azimuth with a 170-degree median.

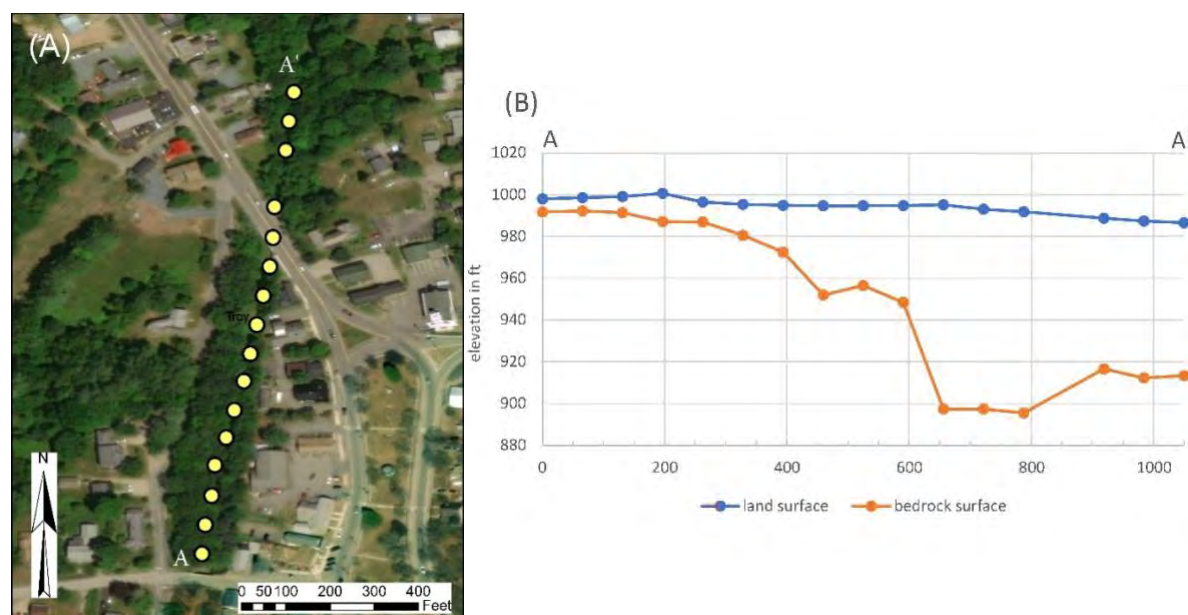


Figure 4. Passive seismic horizontal-to-vertical spectral ratio measurement results from the A-A' cross section at site 2, roadway crossing rail trail, Troy, New Hampshire, showing (A) a map of measurement locations and (B) a cross section of bedrock surface and land surface.

The EMI results from the roadway crossing rail trail site had the highest residuals and the least successful inversion of all the sites (fig. 5). This may be a result of (1) noise and (or) coupling effects which were strong and likely affected the data near shallow buried metal from the former railroad throughout the survey area and (2) metal from the State Route 12 bridge in the center of the survey area. It is possible that the old rails or other metal hardware were not removed and instead buried on site. Comparison to borings was difficult because electrical noise was higher in this area than at other sites. Inversions were successful but had higher data residuals compared to other sites. The geophysical inversion process used to analyze EMI data assumes a smoothly varying or layered bulk electrical conductivity distribution of the subsurface and has difficulty fitting features that violate these assumptions, such as discrete human-made objects.

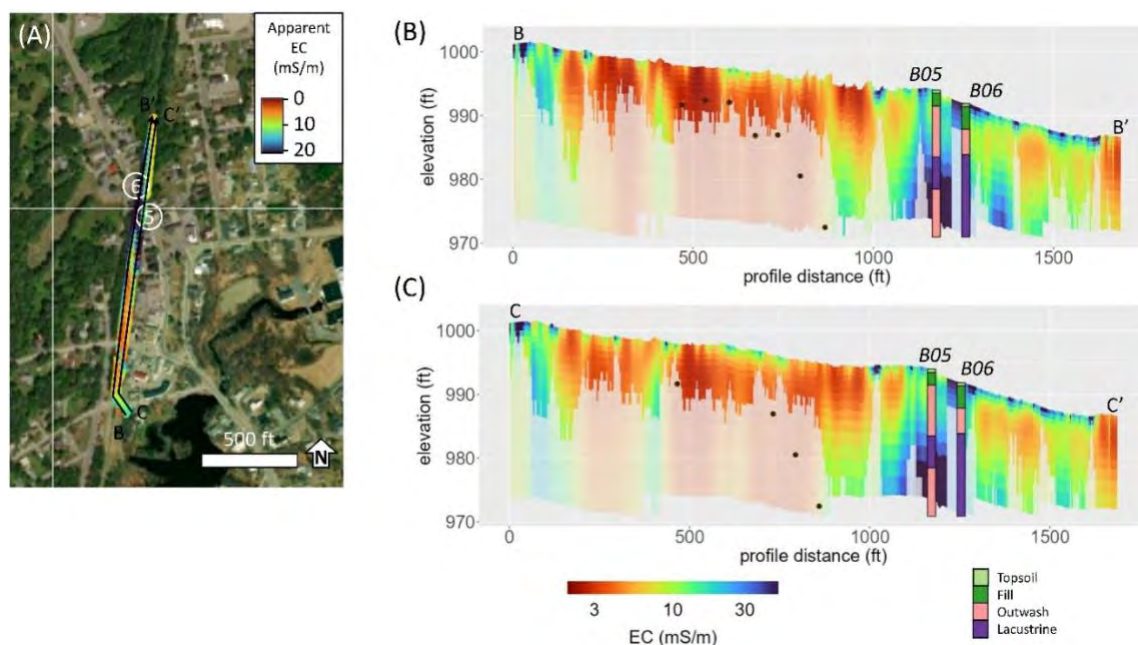


Figure 5. Electromagnetic induction survey results from the multiple-coil spacing instrument from the B-B' and C-C' cross sections at site 2, roadway crossing rail trail in Troy, NH, showing (A) a map of apparent electrical conductivity from the 4-m-spaced horizontal coplanar coils with cross section and boring locations shown with white circles and (B) and (C) profiles of electrical conductivity from inverted frequency domain electromagnetic induction data demarcated in (A). Black dots on profiles show estimated depth to bedrock from passive seismic horizontal-to-vertical spectral ratio measurements.

The bedrock surface generated with HVSr results and borings indicates shallow bedrock to the south and deep bedrock to the north (fig. 4). This is consistent with outcrops and railroad rockcuts observed at the site and with the resistive EMI results.

In general, the site results suggest a thin conductive layer overlying resistive materials. Potentially, the conductive upper layer is related to the old railroad, and the resistive materials are outwash with moisture in the vadose zone and groundwater at depth. In the area around the State Route 12 bridge and other roadways, the results indicate higher conductivity, likely due to increased porewater conductivity due to residual road salt used for deicing. Many of the shallow conductive “anomalies” visible in this profile may be related to infrastructure as opposed to soils or geology.

### **Carpool and bus stop parking, site 3, New London, New Hampshire**

The carpool and bus stop parking site (site 3) is accessed from State Route 103A and is located between State Route 103A to the west and State Route 11 to the north and Interstate Highway 89 to the east in New London, NH. Seeps with iron fouling at the southern toe of the existing parking lot embankment drain to an unnamed stream that flows south along the west edge of the site. Geotechnical site characterization described fill materials, overburden stratigraphy, depth to bedrock, and core from the top 10 ft of bedrock in order to aid in the design of a construction plan for the extension of the parking lot.

Thirty-one HVSr measurements were made at 29 measurement locations along the parking lot shoulder, embankment, slope toe, and in the adjacent woods at the carpool and bus stop parking expansion site. Nine of the HVSr locations were selected to correspond with boring

locations with a documented overburden stratigraphy and depth to bedrock. The other 21 measurements were used to delineate the bedrock surface within and beyond boring locations. Measurements were repeated at two locations to compare results with different ground coupling methods. Two repeat measurements were completed using a gravimeter plate and had higher quality peaks and coupling signals than those collected with direct coupling. The gravimeter plate also was used at 14 other measurement locations because cobbles and tree roots prohibited direct ground coupling.

Electromagnetic induction data were collected with the multiple-frequency instrument at this site and exhibited lateral variation in apparent conductivity, but the method had limited ability to achieve the depth of investigation produced at other sites. Shallow electrically resistive bedrock may have limited the propagation of the EMI signal at this site.

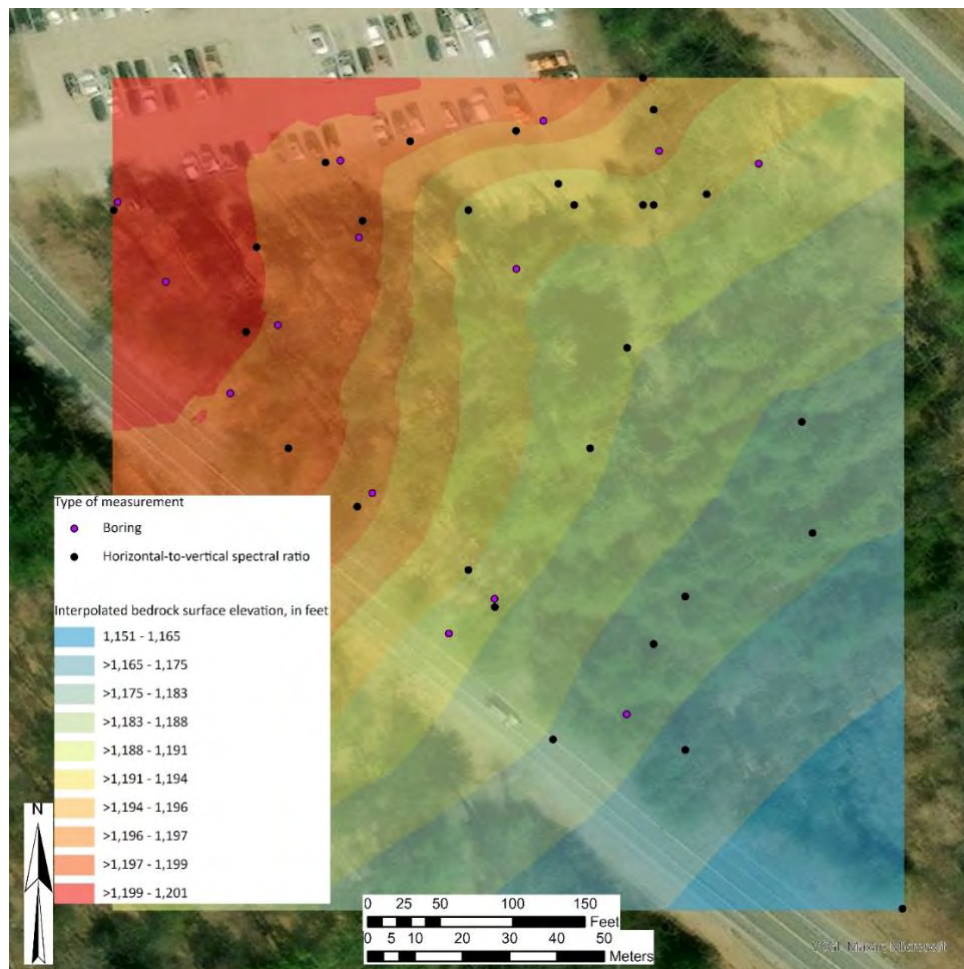


Figure 6. Map of the bedrock surface elevation calculated from passive seismic horizontal-to-vertical spectral ratio measurements at the carpool and bus stop parking site.

Bedrock outcropping was not observed at the site; therefore, shallow bedrock was not expected. However, this site had the most shallow bedrock of all the sites—as shallow as 5 ft in some locations (Table 1). The interpolated bedrock surface elevation map from HVSR results (fig. 6) indicates a higher elevation bedrock surface to the northwest that deepens to the southeast. Further, there is a northwest-southeast trending shallow trough in the bedrock surface at the northern edge of the map just to the south of the existing carpool and bus stop parking site

(fig. 6). The bedrock surface is deeper in the location of the trough that also corresponds with the location of seeps with iron fouling and with thicker variably saturated overburden, interpreted from the EMI results (fig. 7).

The multiple-frequency EMI instrument results are high quality (consistently positive and showing smooth, non-noisy variation in space) and suggest sensitivity to the upper layer of materials and the bedrock surface because the various depths of the inverted electrical conductivity values are above and below the contact. However, results do not indicate a strong ability to distinguish soil layers or bedrock in the areas most affected by roadway runoff, likely because of legacy deicing chemical contamination (fig. 7, high EC values). Comparison of electrical conductivity data to boring information indicated topsoil and outwash generally had low bulk electrical conductivity values, alluvium had moderate electrical conductivity values, and fill (from existing parking lot) had the highest electrical conductivity values. Inverted electrical conductivity values with depth do not consistently show ability to discern between different soil layers in the borings.

The multiple frequency EMI instrument data was likely influenced by vehicles and other infrastructure in the parking lot. Evidence of this influence was apparent based on large positive returns of in-phase components observed when surveying near the parking lot. Interference from metal items near the parking lot rendered EMI data uninterpretable and therefore could not be used to delineate the subsurface electrical conductivity in this area. The remainder of the site (forested area in fig. 7) exhibited low interference and yielded data free of noise contamination.

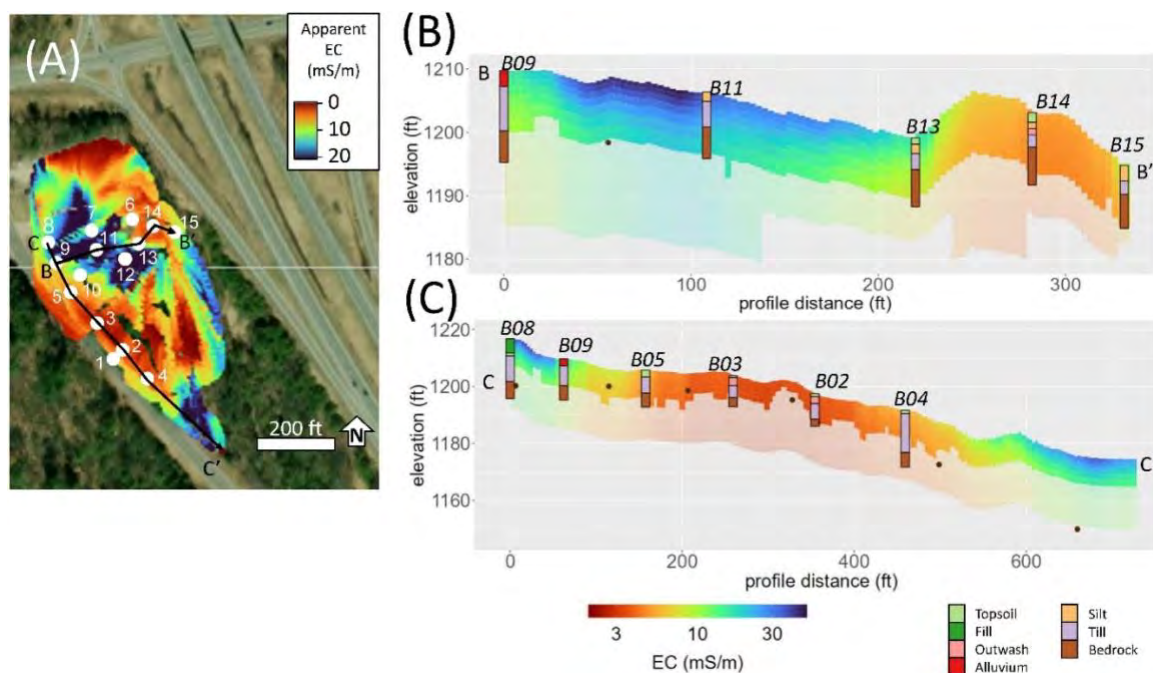


Figure 7. Electrical conductivity (EC) from electromagnetic induction survey results from the multiple-frequency instrument from the B-B' and C-C' cross sections at site 3, carpool and bus stop parking, New London, New Hampshire, showing (A) map of apparent electrical conductivity from the 47,970 Hz band and cross section locations. The white circles show boring locations. (B) and (C) show cross sections demarcated in (A) of inverted electrical conductivity with the bedrock surface from passive seismic horizontal-to-vertical spectral ratio results shown with black dots and borings identified.

### **Railroad adjacent to slope failure, site 4, Canterbury, New Hampshire**

The railroad adjacent to slope failure site (site 4) is located in Canterbury, NH, on the east (left) bank of the Merrimack River to the west of Interstate Highway 93 (fig. 8b). The river reach has an oxbow meander bend with a cutbank that causes erosion and sediment transport, which also has caused failure in the slope above. The top of the slope failure scarp is approximately 20 ft from the railroad and 100 vertical feet above the riverbed. This site does not have an active geotechnical drilling investigation, but driller's logs are available from a previous hydrogeologic investigation associated with a formerly proposed landfill (Aries Engineering, Inc., 2005). The geophysical surveys at the site were scoped to determine the bedrock surface elevation and overburden stratigraphy at and adjacent to the slope failure.

Thirty-two HVSR measurements were made at locations along the top of the slope failure scarp, on the failed slope, and in a grid pattern in the adjacent wooded area between the railroad and Interstate 93. One of the HVSR locations was adjacent to a boring location with documented overburden stratigraphy and depth to bedrock, and the other 31 measurements were used to delineate the bedrock surface (fig. 8).

The multiple-coil-spacing EMI instrument was used to collect data along three survey lines at the railroad adjacent to the slope failure site. Apparent conductivity values were inverted and provided stratigraphic information to depths of 40 ft below land surface. Survey line 1 was parallel to the river and the closest survey line to the river. Electromagnetic induction results from survey line 1 showed an approximately 6 ft thick resistive layer overlying a conductive layer (fig. 9). Survey line 2 was upslope and parallel to the river (and line 1) and had an approximately 3-6 ft thick resistive layer overlying a conductive layer. At some locations along survey line 2 the conductive material was observed near the surface, which was corroborated by varved clay and silt seen in outcrop adjacent to the line. Survey line 3 was perpendicular to and south of survey lines 1 and 2. Low conductivity sand with minimal variation in EC values was indicated in results from survey line 3 (not shown), and inversion results had a very shallow depth of investigation, likely due to a low signal overall from resistive ground. In general, conductivity increased with distance from the river in lines 1 and 2.

Ground penetrating radar (GPR) was used only at this site, to improve the interpretation of the subsurface stratigraphy. Results provided information as deep as 100 ft in many locations. Penetration of the GPR signal was enhanced in electrically resistive materials and was best along lines 1 and 3 on the slope failure and above the scarp where the stratigraphy was relatively undisturbed by the failure.

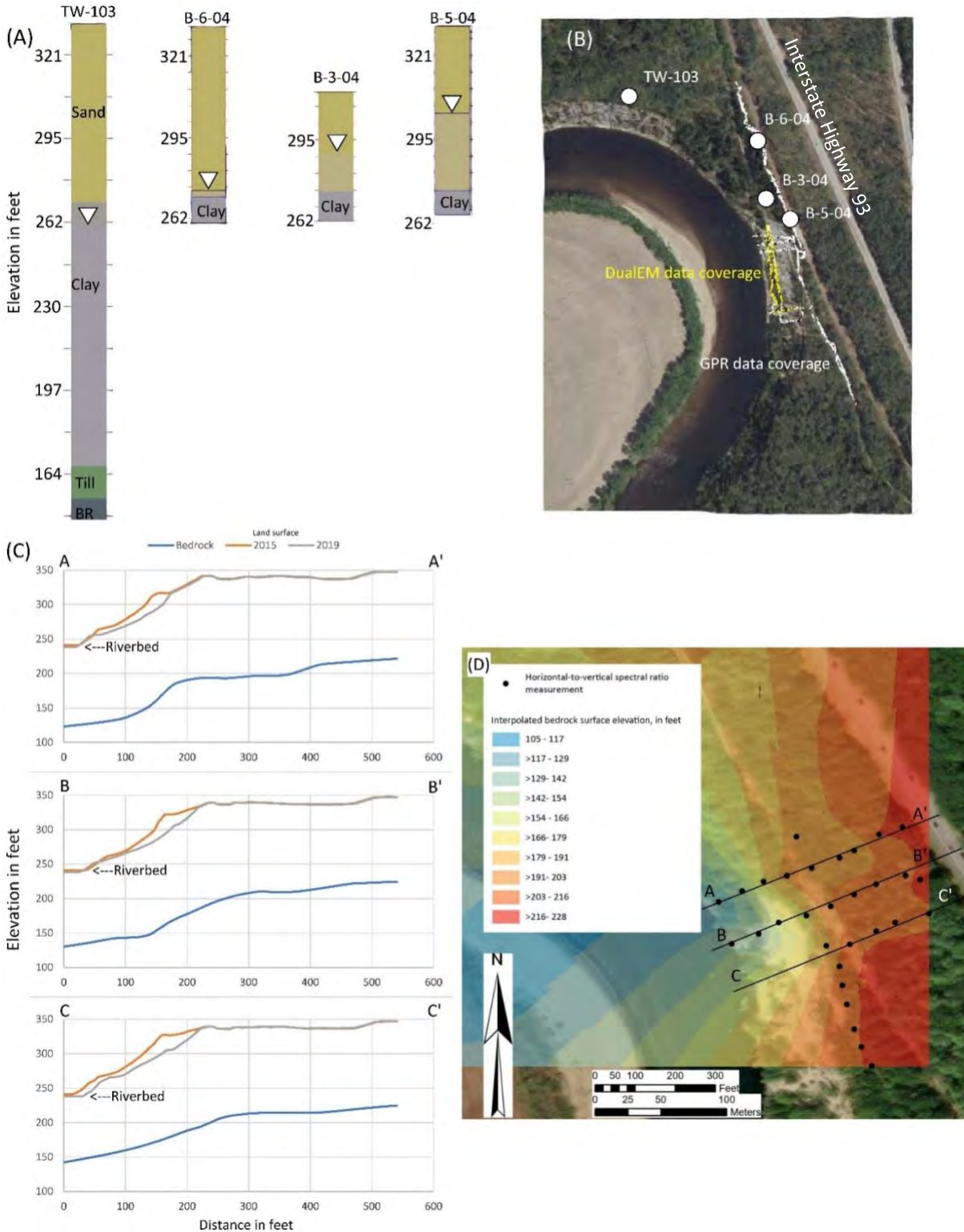


Figure 8. Boring logs and passive seismic horizontal-to-vertical spectral ratio measurement results from the A-A', B-B', and C-C' cross sections at site 4, railroad adjacent to slope failure, Canterbury, New Hampshire, showing (A) lithologic logs, (B) boring location map, (C) cross sections of the bedrock surface and land surface, and (D) map of interpolated bedrock surface elevation from passive seismic horizontal-to-vertical spectral ratio measurements.

The bedrock surface elevation delineated by HVSR is higher towards the northeast. The location of the bedrock surface does not provide any protection from additional riverbank erosion as it is well below (approximately 100 ft) the bed of the river (fig. 8B and C) and would not limit channel migration.

The B-B' EMI profile suggests conductive materials (fine sands or clays) below resistive materials (sands) (fig. 9B). The C-C' EMI profile suggests conductive materials (fine sands or clays) below resistive materials (sands), which are deeper compared to the B-B' line (fig. 10).

Ground penetrating radar data identified many anomalies that could not be interpreted because of limited information from wells and (or) test pits. Some layered GPR reflectors are indicated by the different colored arrows in fig. 11; these are likely soil layers or in the slope, possibly features related to the slope failure, such as fissures or shear planes (fig. 11B and C). The red arrows may indicate the water table in the C-C' GPR cross section (fig 11C) because the reflector is near the previously identified water-table depth (Aries Engineering, Inc., 2005).

The multiple-coil-spacing EMI instrument and GPR data are of high quality. Near-river profiles show a high resistivity layer over a high conductivity layer. A reasonably strong GPR reflector, that gets deeper closer to river, is also present.

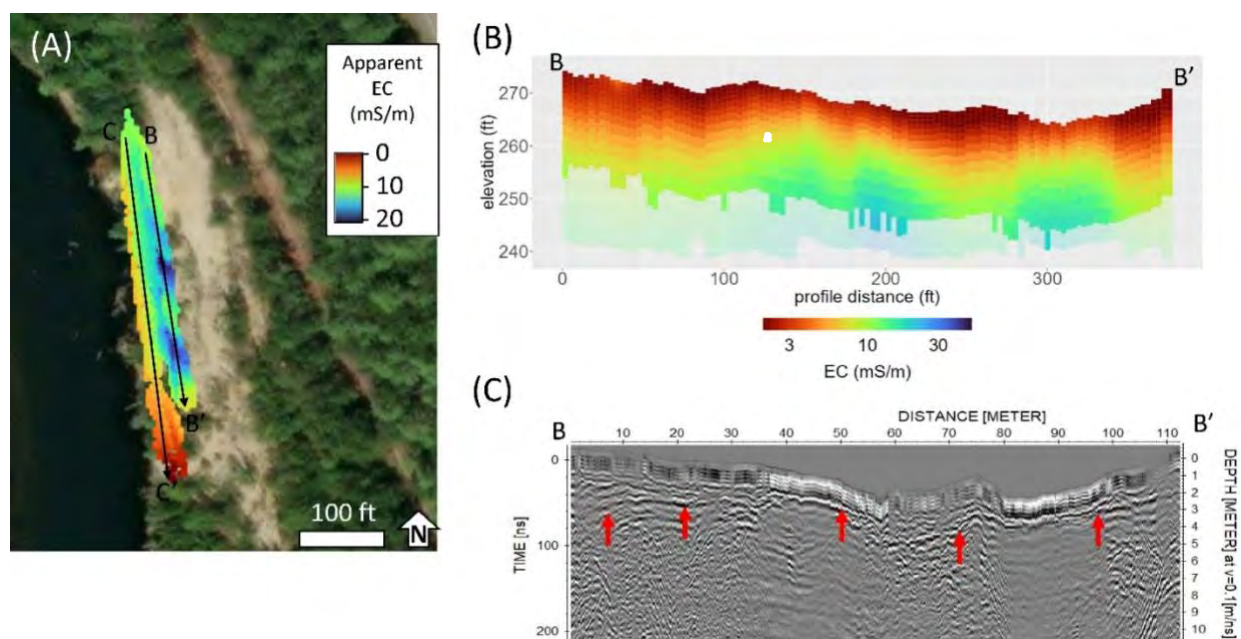


Figure 9. Multiple-frequency electromagnetic induction instrument and ground-penetrating radar survey results from the B-B' cross section at site 4, railroad adjacent to slope failure Canterbury, New Hampshire, showing (A) map of apparent electrical conductivity (EC) from the 4-m-spaced horizontal coplanar coils and cross section locations, (B) cross section of inverted electrical conductivity, and (C) ground-penetrating radar survey results.

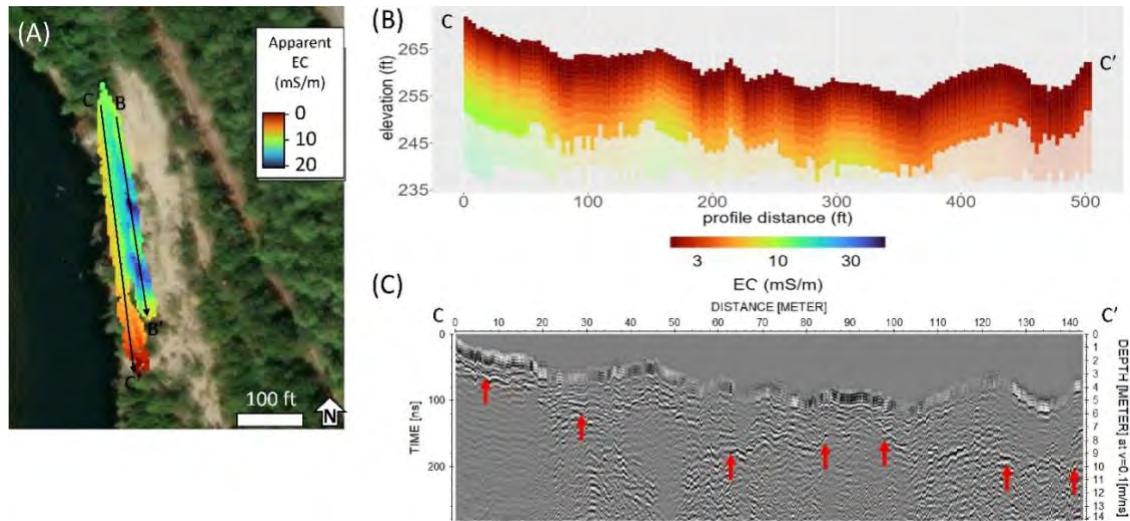


Figure 10. Multiple-frequency electromagnetic induction instrument and ground-penetrating radar survey results from the C-C' cross section at site 4, railroad adjacent to slope failure Canterbury, New Hampshire, showing (A) map of apparent electrical conductivity (EC) from the 4-m-spaced horizontal coplanar coils and cross section locations, (B) cross section of inverted electrical conductivity, and (C) ground-penetrating radar survey results.

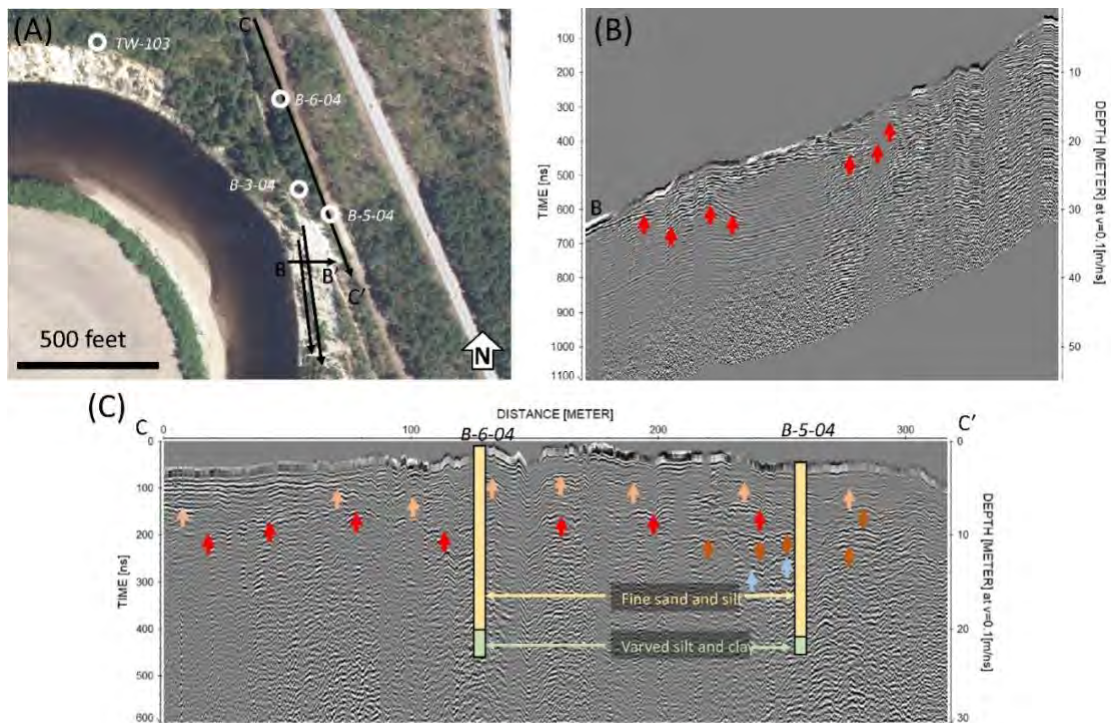


Figure 2. Ground penetrating radar results at site 4, railroad adjacent to slope failure Canterbury, New Hampshire, showing (A) map of survey and boring locations, (B) B-B' cross section, and (C) C-C' cross section. Different colored arrows indicate multiple reflectors that were observed. Materials described by boring logs and their depths are indicated along this profile.

## SUMMARY AND CONCLUSIONS

The utility of geophysical techniques to supplement geotechnical investigations was evaluated during this study. Application of geophysical surveys using horizontal-to-vertical spectral-ratio (HVSr) passive-seismic and electromagnetic-induction (EMI) surveys near geotechnical borings at New Hampshire Department of Transportation (NHDOT) project sites showed that additional information on the bedrock surface could be provided beyond what was identified by borings alone. Results from HVSr and EMI surveys enhanced the information from existing borings and successfully delineated topographic highs and lows in the bedrock surface. At some sites, troughs in the bedrock surface were delineated, whereas at other sites bedrock highs, in the form of buried ridges or knobs, were detected. For example, at the roadway crossing rail trail site (site 1), higher elevation bedrock was discovered just south of the bridge. At this site, boreholes had a horizontal resolution of about 200 ft in the vicinity of the bridge and geophysical surveys expanded the extent by an order of magnitude with the same or better resolution along a 2,000-ft long survey line.

Information from geophysical surveys, when combined with geotechnical data from borings, can lead to more detailed interpretations by filling in data gaps between borings. Additionally, geophysical surveying is a cost-effective way to enhance drilling operations and can provide greater resolution or a larger extent at geotechnical investigation sites given the right conditions are met for each method. The instruments used were quick and easy to deploy, do not require permanent installation of equipment or excavation of material, and can be used in areas that are inaccessible to drill rigs. For example, borehole drilling was difficult in wooded areas at the carpool and bus stop parking site (site 3); however, it was possible to collect geophysical data in wooded areas. In addition, HVSr is passive, requiring no artificial sound source, as is required with traditional seismic refraction bedrock detection techniques. These additional data points helped identify a southeast sloping bedrock surface and trough beneath the forest that was only partially apparent from the borings.

Sediment EC variability was detected with EMI and when interpreted with HVSr, drillers' logs, or GPR can indicate general sediment grain size. For example, the fine grained varved sediment at the railroad adjacent to slope failure site (site 4) were further defined with GPR. This site also had the lowest mean electrical conductivity measured with the multiple-coil-spacing EMI instrument despite having the most conductive fine-grained material indicated in the lithologic logs. Electrical conductivity at the other sites may have been elevated due to buried metal, their proximity to areas affected by runoff with road salt applied for deicing, which likely increases the overall conductivity of sites near roadways. When dissolved in runoff, road salt can increase the specific conductance of water, which can contribute to increases in the apparent conductivity of vadose-zone infiltration and groundwater recharge that are detectible with EMI instruments.

Horizontal-to-vertical spectral ratio measurement results appeared to provide more definitive subsurface information than EMI methods at most sites because HVSr data were not sensitive to buried metal objects or too much of the above-ground infrastructure; however, the added value that EMI provides for identifying and delineating stratigraphy and characterizing different zones of groundwater quality make the combination of HVSr and EM useful. Additionally, the HVSr and EMI methods were able to successfully characterize the subsurface in most areas despite being near roadways with sources of interference such as vehicle traffic, electromagnetic noise (powerlines), and buried debris (bridge and railroad sites). Data collection

and analyses presented here have also furthered the understanding of how geophysical methods can help delineate features important to water availability, such as the bedrock surface, and to help identify zones with different groundwater quality. Future use of geophysical methods at NHDOT project sites have the potential to enhance the Department's site assessments in design and construction phases (Boeckmann and Loehr, 2016).

## REFERENCES CITED

- Abraham, Jared, Deszcz-Pan, Maria, Fitterman, David, and Burton, Bethany, 2006, Use of a handheld broadband FDEM induction system for deriving resistivity depth images, in Symposium on the Application of Geophysics to Engineering and Environmental Problems, 19, Las Vegas, Nevada, February 10–14, 2002, Proceedings: Denver, Colo., Environmental and Engineering Geophysical Society CD-ROM, p. 1782–1799.
- Aries Engineering, Inc., 2005, Proposed Concord Regional Solid Waste/Resource Recovery Landfill Evaluation, Canterbury, New Hampshire, 42 pages
- Beres, Milan, Jr., and Haeni, F.P., 1991, Application of ground-penetrating-radar methods in hydrogeologic studies: *Ground Water*, v. 29, no. 3, p. 375–386.
- Bignardi, S., 2017, The uncertainty of estimating the thickness of soft sediments with the HVSR method: A computational point of view on weak lateral variations: *Journal of Applied Geophysics*, v. 145, p. 28-38.,  
<http://www.sciencedirect.com/science/article/pii/S0926985117302422>
- Boeckmann, Andrew Z. and Loehr, J. Erik, 2016, Influence of Geotechnical Investigation and Subsurface Conditions on Claims, Change Orders, and Overruns A Synthesis of Highway Practice, Transportation Research Board, National Academy of Sciences, 76 p., ISBN 978-0-309-27204-9, <https://doi.org/10.17226/21926>
- Carr, A. R., 2022a, Test Boring Report, Troy, 40371, State of New Hampshire Department of Transportation Materials & Research Bureau - Geotechnical Section, 23 pages
- Carr, A. R., 2022b, Test Boring Report, New London 42877, State of New Hampshire Department of Transportation Materials & Research Bureau - Geotechnical Section, 15 pages
- Christiansen, A. V. and Auken, E., 2012, A global measure of depth of investigation: *Geophysics*, v. 77, p. WB171-WB177.
- Cox, B.R., Cheng, T., Vantassel, J.P., and Manuel, L., 2020, A statistical representation and frequency-domain window-rejection algorithm for single-station HVSR measurements: *Geophysical Journal International*, v. 221, no. 3, p. 2170-2183.,  
<https://doi.org/10.1093/gji/ggaa119>
- Degnan, J.R., Welch, S.M., White, E.A., Johnson, C.D., and Benthem, A.J., 2022, Passive seismic horizontal-to-vertical spectral ratio measurements at transportation infrastructure sites in New Hampshire, 2022: U.S. Geological Survey data release,  
<https://doi.org/10.5066/P943EEFQ>.
- DUALEM-Manual, DUALEM website, accessed December 2022 at DUALEM.COM
- Evenson, E.J., Orndorff, R.C., Blome, C.D., Bohlke, J.K., Herschberger, P.K., Langenheim, V.E., McCabe, G.J., Morlock, S.E., Reeves, H.W., Verdin, J.P., Weyers, H.S., and Wood, T.M., 2012, Strategic directions for U.S. Geological Survey water science, 2012–2022—Observing, understanding, predicting, and delivering water science to the Nation: U.S. Geological Survey Open-File Report 2012–1066, 42 p.
- Fairchild, G.M., Lane, J.W., Jr., Voytek, E.B., and LeBlanc, D.R., 2013, Bedrock topography of western Cape Cod, Massachusetts, based on bedrock altitudes from geologic borings and

- analysis of ambient seismic noise by the horizontal-to-vertical spectral-ratio method: U.S. Geological Survey Scientific Investigations Map 3233, 1 sheet, maps variously scaled, 17-p. pamphlet, on one CD-ROM. (Also available at <http://pubs.usgs.gov/sim/3233>.)
- Geophex, Ltd. 2009, GEM-2 Broadband EMI sensor: accessed January, 2009 at <http://www.geophex.com/GEM-2/GEM-2%20home.htm>
- Haeni, F.P., 1996, Use of ground-penetrating radar and continuous seismic-reflection profiling on surface-water bodies in environmental and engineering studies in Carpenter, Phil, ed., Groundwater Geophysics Special Issue: Journal of Environmental and Engineering Geophysics, v. 1, no. 1, p. 27–35.
- Huang, Haoping, and Won, I.J., 2000, Conductivity and susceptibility mapping using broadband electromagnetic sensors: Journal of Environmental and Engineering Geophysics, v. 5, no. 4, p. 31–41.
- Ibs-von Seht, M., Wohlenberg, J., 1999. Microtremor measurements used to map thickness of soft sediments. Bull. Seismol. Soc. Am. 89 (1), 250–259. [http://refhub.elsevier.com/S0926-9851\(17\)30242-2/rf0090](http://refhub.elsevier.com/S0926-9851(17)30242-2/rf0090)
- Jacques Whitford Company, Inc., 2004, Construction Details of Wells and Piezometers Proposed Concord Cooperative Landfill Access Road, 17 pages
- Johnson, C.D. and Lane, J.W., Jr., 2016, Statistical comparison of methods for estimating sediment thickness from horizontal-to-vertical spectral ratio (HVSr) seismic methods: An example from Tylerville, Connecticut, USA, in Symposium on the Application of Geophysics to Engineering and Environmental Problems, March 20-24, 2016, Denver, Colorado, 7 p., <https://water.usgs.gov/ogw/bgas/publications/SAGEEP2016-Johnson/SAGEEP2016-Johnson.pdf>
- Johnson, C.D., White, E.A., Werkema, D., Terry, N., Phillips, S.N., Ford, R., and Lane, J.W., 2019, GEOPHYSICAL ASSESSMENT OF A PROPOSED LANDFILL SITE IN FREDERICKTOWN, MISSOURI: Symposium on the Application of Geophysics to Engineering and Environmental Problems 2019, <https://doi.org/10.4133/sageep.32-031>.
- Kearey, P., and Brooks, M., 1991, An introduction to geophysical exploration second edition: Blackwell Scientific Publications, Cambridge, Mass., 254p
- Lane J. W. Jr, White, E. A., Steele, G. V., & Cannia, J. C. (2008). Estimation of bedrock depth using the horizontal-to-vertical (H/V) ambient-noise seismic method. In: Symposium on the Application of Geophysics to Engineering and Environmental Problems, Philadelphia, Pennsylvania, Proceedings: Denver, Colorado, Environmental and Engineering Geophysical Society, p. 13, 6–10 Apr 2008.
- Mack T.J. (2020) Passive Seismic Survey of Sediment Thickness, Dasht-e-Nawar Basin, Eastern Afghanistan. In: Guth P. (eds) Military Geoscience. Advances in Military Geosciences. Springer, Cham., [https://doi.org/10.1007/978-3-030-32173-4\\_12](https://doi.org/10.1007/978-3-030-32173-4_12)
- Marvinney, R.G. and Glover, H., 2015, The influence of the Presumpscot Formation on seismic hazard in southern coastal Maine, 2015 Symposium on the Presumpscot Formation, Portland, ME, 20 p.
- Medler, C.J., 2022, Delineating the Pierre Shale from geophysical surveys east and southeast of Ellsworth Air Force Base, South Dakota, 2021: U.S. Geological Survey Scientific Investigations Map 3497, 3 sheets, 15-p. pamphlet, <https://doi.org/10.3133/sim3497>.
- Milsom, J. and Eriksen, A. (2011). Ground Penetrating Radar. In Field Geophysics (eds J. Milsom and A. Eriksen). <https://doi.org/10.1002/9780470972311.ch10>

- MOHO, 2020, Tromino Blu Portable ultra-light acquisition system for seismic noise and vibrations, International patents: Pub. No. WO2006011021 (A1), Pri. No. IT2004BO00449 20040719, USPTO 7.800.981, USER'S MANUAL, 144 p.
- Nakamura, Y., 1989. A method for dynamic characteristics estimation of subsurface using microtremor on the ground surface. Quarterly Report of Railway Technical Research Institute 30, 25–33. [http://refhub.elsevier.com/S0926-9851\(17\)30242-2/rtf0125](http://refhub.elsevier.com/S0926-9851(17)30242-2/rtf0125)
- Nakamura, Y., 2000. Clear identification of fundamental idea of Nakamura's technique and its applications. Proceedings of the 12<sup>th</sup> World Conference on Earthquake Engineering (8 pp., New Zealand). [http://refhub.elsevier.com/S0926-9851\(17\)30242-2/rtf0130](http://refhub.elsevier.com/S0926-9851(17)30242-2/rtf0130)
- Jeeban Panthi, Carole D. Johnson, Soni M. Pradhanang, Brian Savage, Mamoon Y. Ismail, Thomas B. Boving, 2023, Delineating bedrock topography with geophysical techniques: An implication for groundwater mapping, CATENA, Volume 230, 107258, ISSN 0341-8162, <https://doi.org/10.1016/j.catena.2023.107258>.
- R Core Team, 2023, R: A language and environment for statistical computing. R Foundation for Statistical Computing, Vienna, Austria. URL <https://www.R-project.org/>.
- U.S. Department of Transportation, Federal Highway Administration, 2020, Advanced Geotechnical Methods in Exploration (A-GaME), Center for Accelerating Innovation web page, accessed 03/31/2021, [https://www.fhwa.dot.gov/innovation/everydaycounts/edc\\_5/geotech\\_methods.cfm](https://www.fhwa.dot.gov/innovation/everydaycounts/edc_5/geotech_methods.cfm)
- SESAME WP04, 2004. Guidelines for the implementation of the H/V spectral ratio technique on ambient vibrations measurements, processing and interpretation.
- Welch, S.M., Degnan, J.R., and Terry, N.C., 2023, Electromagnetic induction and ground-penetrating radar surveys at transportation infrastructure sites in New Hampshire, 2022: U.S Geological Survey data release.
- Wickham, H., 2016, ggplot2: Elegant Graphics for Data Analysis. Springer-Verlag New York, ISBN 978-3-319-24277-4, <https://ggplot2.tidyverse.org>.
- Yuengling, K. R., 2022, Test Boring Report, Lee, 41322, State of New Hampshire Department of Transportation Materials & Research Bureau - Geotechnical Section, 8 pages
- Zohdy, A.A.R., Eaton, G.P., and Mabey, D.R., 1974, Application of surface geophysics to ground-water investigations: U.S. Geological Survey Techniques of Water-Resources Investigations, book 2, chap. D1, 86 p., <http://pubs.usgs.gov/twri/twri2-d1/>

**Non-destructive Surface Wave Geophysics Characterizes Salt Dissolution  
140m Under US Highway 50 at Brandy Lake, Reno County, Kansas**

**S. Johari Pannalal**

WSP USA

4600 E. Washington St., Suite 600

Phoenix, AZ 85034

(480)-318-6332

johari.pannalal@wsp.com

**Jeffrey R Keaton & Michael Rucker**

WSP USA

4600 E. Washington St., Suite 600

Phoenix, AZ 85034

jeff.keaton@wsp.com    michael.rucker@wsp.com

Prepared for the 72<sup>nd</sup> Highway Geology Symposium, August, 2023

### **Acknowledgements**

The authors would like to thank the Kansas Department of Transportation for providing technical information during project execution, facilitating access to master's theses that were funded by the Department, and authorizing our work products to be used for this paper.

### **Disclaimer**

Statements and views presented in this paper are strictly those of the author(s), and do not necessarily reflect positions held by their affiliations, the Highway Geology Symposium (HGS), or others acknowledged above. The mention of trade names for commercial products does not imply the approval or endorsement by HGS.

### **Copyright Notice**

Copyright © 2023 Highway Geology Symposium (HGS)

All Rights Reserved. Printed in the United States of America. No part of this publication may be reproduced or copied in any form or by any means – graphic, electronic, or mechanical, including photocopying, taping, or information storage and retrieval systems – without prior written permission of the HGS. This excludes the original authors.

## ABSTRACT

US Highway 50 in Reno County, Kansas, crosses Brandy Lake where ongoing dissolution of a salt bed 134m deep is causing local subsidence. High lake levels, happening more frequently and for longer periods, inundate low spots on the busy two-lane highway. Kansas Department of Transportation (KDOT) designed the road in 1963 and resurveyed it in April 2021. KDOT-funded University of Kansas Master's theses produced terrestrial laser scanning in 2009 and seismic reflection surveys in 2015. Interferometric Synthetic Aperture Radar (InSAR), proven for subsidence detection, was tested, but agricultural conditions proved unsuitable for interpretable interferograms. Seismic refraction microtremor (ReMi) measurements, a geophysical method utilizing surface (Rayleigh) wave dispersion physics to produce vertical 1-dimensional shear-wave subsurface profiles, were collected along highway shoulders without stopping traffic. Six stratigraphic profiles interpreted from ReMi line pairs (175.3m and 36.6m long with 7.6 and 3m geophone spacings) indicated five layers corresponding to two surficial units (aeolian and alluvial) overlying three sedimentary beds of the Permian Sumner Group (Ninnescah Shale, Wellington Shale, and Hutchinson Salt). ReMi profiles revealed shear-wave velocities consistent with interpreted MS thesis reflection seismic profiles. The shallowest subsurface horizon had lower shear-wave velocities within the active subsidence zone than beyond it. The MS thesis reflection seismic profile interpreted near-vertical faults within the Permian rocks above the salt within the active subsidence zone, but not beyond it. The ReMi interpretation supplemented the KDOT conventional survey and the MS thesis laser survey to quantify subsidence over an 11.4yr period, which allowed 30-year projection of continuing subsidence.

## INTRODUCTION

This paper presents the results of the study phase of a geotechnical transportation engineering project to develop designs for improvements to US Highway 50, east of Brandy Lake Road, Kansas, where the highway approaches Brandy Lake, approximately 15 miles east of Hutchinson, Kansas. The study area limits extend from the Brandy Lake Road intersection to the west to the South Buhler/Haven Road intersection to the east (Figure 1). The main project objective is to restore uniform grade and elevate the highway above the local inundation level when Brandy Lake is high; the existing bridge elevation serves as a maximum inundation level. To this extent, existing data review (both published and current survey results), field investigation and site characterization were conducted for the Brandy Lake section of US Highway 50 (Figure 1). The field investigation included performing Refraction Microtremor (ReMi) surveys to improve understanding of the subsurface geologic profile to the Hutchinson Salt Formation relevant to assessing the subsidence conditions at Brandy Lake.

Based on the site investigation results, the likely cause of localized subsidence, and limits and rates of subsidence, were identified. A companion paper by Keaton et al. (2023) identifies and describes the alternative mitigation measures for the highway and recommendations for design of roadway improvements.

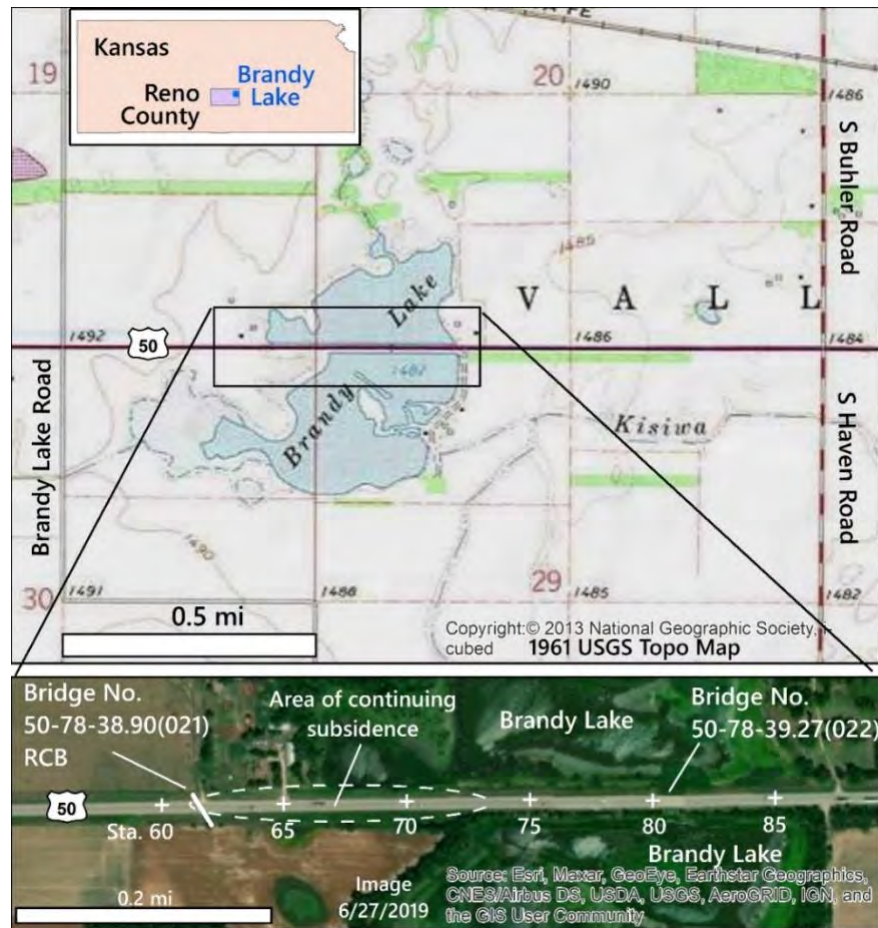


**Figure 1:** US Highway 50 across Brandy Lake, Reno County Kansas.

## **SITE GEOLOGY**

The geologic profile in the study area consists of late Pleistocene terrace deposits overlying Permian bedrock formations (Bayne, 1956). The Permian bedrock formations in the study area consist of bedded shale and evaporite deposits of the Ninnescah Shale and Wellington Formation of the Sumner Group that dip relatively gently toward the west (West et al., 2010; Walters, 1978; Keaton et al., 2023). The Hutchinson Salt Member is a subunit of the Wellington Formation at a depth of approximately 425 feet (Judy, 2015). The Brandy Lake area is within a naturally occurring zone of dissolution of the Hutchinson Salt. The surface expression of salt dissolution at depth is irregular subsidence depressions. The shallow aquifer in Pleistocene terrace deposits produces ponds and lakes where subsidence intersects the groundwater table.

Brandy Lake fills a likely subsidence feature that developed in recent geologic time as natural seepage of fresh groundwater into Permian age bedrock formations resulted in halite dissolution within the underlying Hutchinson Salt Formation. That Brandy Lake is noted on historic mapping back to the 19th Century is confirmation that it is a natural geological feature and not of anthropogenic origin, yet evident subsidence along the current US Highway 50 at the lake's western edge indicates that localized subsidence is a continuing phenomenon. The highway centerline elevation at the Brandy Lake Bridge (Sta. 81+00) was reported to be 1490 feet (KDOT, 1986) in 1986, and remains at 1490 feet in the 2021 Kansas Department of Transportation (KDOT) survey.

## **PREVIOUS STUDIES**

### **2021 KDOT Survey**

KDOT performed a thorough survey of US Highway 50 between Brandy Lake Road on the west and South Buhler Road/South Haven Road on the east in April 2021 (Figure 2). The intersection of US Highway 50 and Brandy Lake Road corresponds to US Highway 50 Sta. 45+00; the intersection of US Highway 50 and S Buhler/Haven Rd corresponds to US Highway 50 Sta. 125+00. KDOT's survey captured elevation at numerous cross section locations along the highway, as well as points away from the highway; the centerline profile (Figure 2) shows a reach between Sta. 61+00 and Sta. 73+00 with a low point at approximately Sta. 69+60 that has a somewhat Irregular profile. The area around this low point has been prone to flooding when the water level in Brandy Lake is high. KDOT used the point elevations to construct topographic contours along the highway, which were provided to WSP USA Environment & Infrastructure Inc. (WSP) for use on this project.

### **2015 Reflection Seismic Profiles (Judy, 2015)**

The master's thesis 'High resolution seismic reflection to characterize small scale mechanisms of large-scale natural dissolution in the Hutchinson Salt Member' (Judy, 2015) provided a geologic background summary for dissolution in the Hutchinson Salt Member, interpretation of the geologic profile underlying the Brandy Lake subsidence feature and vicinity, and relevant seismic parameters to help constrain seismic interpretations for this current project. Based on reflection seismic results, an interpreted bedrock profile (Judy, 2015, p 51) below

alluvium places the top of the Ninnescah Shale at a depth of approximately 40 meters (about 130 feet) depth, the top of the Wellington Formation at approximately 85 meters (about 280 feet) depth, and the top of the Hutchinson Salt Member at approximately 130 meters (about 430 feet) depth. Generalized modeled and smoothed compression wave (p-wave) velocities used in the reflection seismic analysis are also provided (Judy, 2015, p 46).

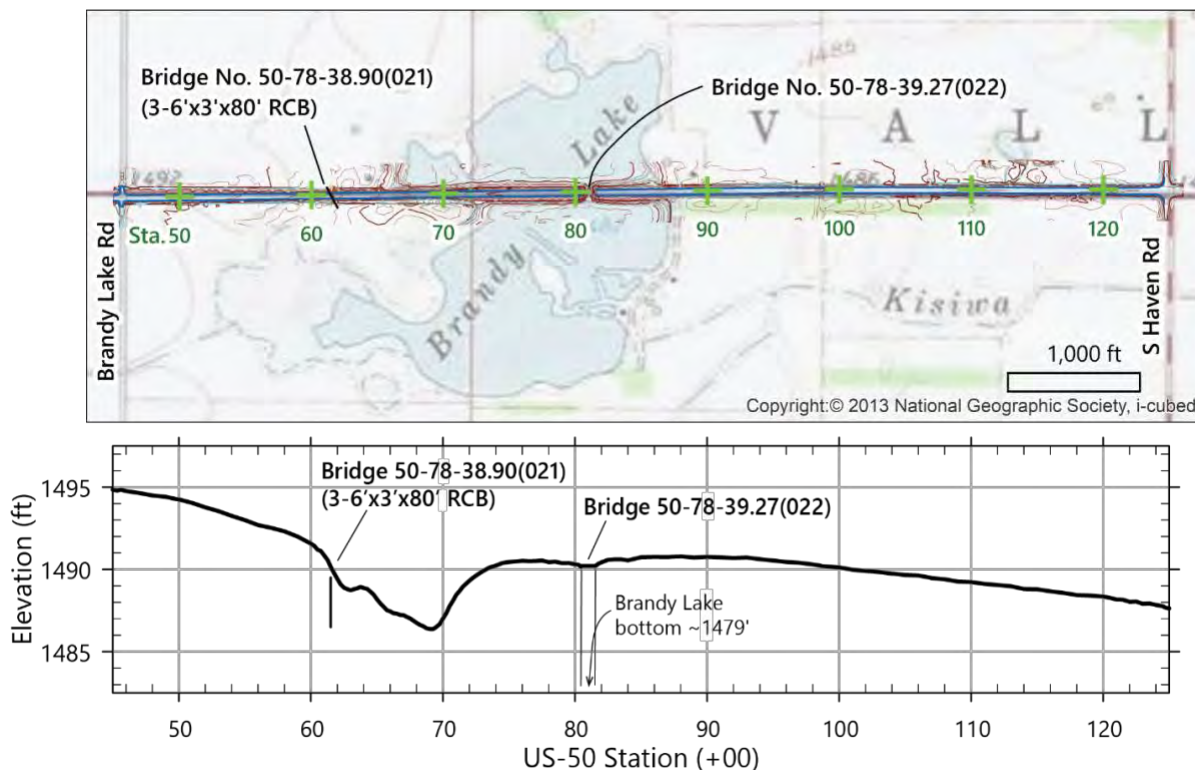


**Figure 2:** Location of KDOT survey data along US Highway 50 in the Brandy Lake study area.

### 2009 LiDAR Profiles (Herrs, 2010)

The master's thesis 'Quantifying Surface Subsidence along US Highway 50, Reno County, KS, using Terrestrial LiDAR' (Herrs, 2010) provides a detailed profile of the Brandy Lake subsidence feature dated to 2009. Three LiDAR surveys were performed in February 2009, May 2009, and November 2009, in an attempt to document a continuing subsidence rate, but no change in the subsidence profile was measured during that time. The measured length of the local subsidence feature was 358 meters, and the maximum apparent subsidence was 1.15 meters (3.77 ft) relative to extrapolation from the far-field highway grade. The reported RMS error in the LiDAR point cloud during the November 2009 survey was <1mm. Comparative profiles of the KDOT (2021) April 2021 centerline elevation and the Herrs (2010) November 2009 laser scan results (Figure 3) show subsidence between approximately Sta. 61+00 and Sta. 73+50. It should be noted that the 2009 profile was taken from Figure 29 in Herrs (2010) thesis, which was a plot of all laser strikes on the highway surface that captured the driving lanes including the centerline. The KDOT (2021) centerline survey was a physical survey with point measurements spaced at 50 or 25 ft directly on the centerline.

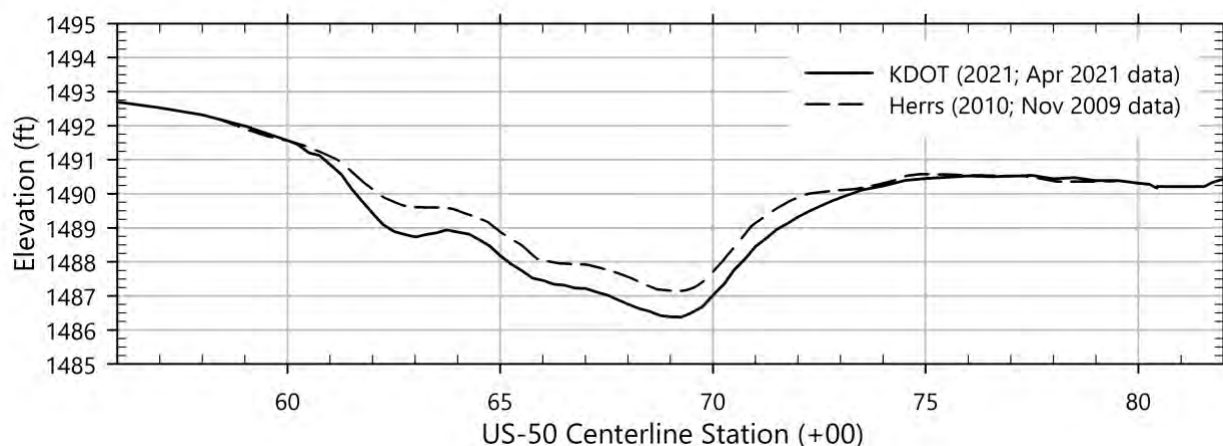


**Figure 3:** US Highway 50 centerline profiles from 2009 (Herrs, 2010) and 2021 (KDOT, 2021)

## FIELD INVESTIGATIONS

### Field Data Collection

The investigation was restricted to KDOT right of way along US Highway 50 and consisted of six ReMi surveys at between Sta. 50, east of Brandy Lake Road, and Sta. 93, east of Brandy Lake (Figure 4), encompassing the lake-forming subsidence area locally called a “sinkhole” (Herrs, 2010). The bridge at Sta. 81 on the highway spans two embankment sections which is the hydraulic connection between the southern and northern parts of Brandy Lake. The water level in the lake was a few feet lower than the pavement at the time of WSP’s field observations. Power lines supported on tall poles are located along the north side of the highway (Figure 5A). Thick vegetation encompasses the shorelines of the Brandy Lake, with grass up to a few feet tall, covering the entire area from the edge of the pavement to thicker vegetation along the lake margin (Figure 5B).

Shallow dips in the highway (Figure 6) were observed along ReMi Line 6 (Figure 4) in the area along US Highway 50 west of Brandy Lake where subsidence is documented in Figures 2 and 3. The crest of the westernmost dip in the highway (Figure 6A) terminates near the culvert (labeled as a RCB bridge in Figures 2 and 4) close to the private property on the northern side of the pavement (Figure 6B). A constant, relatively high volume of vehicles (e.g., cars, pickups, and trucks) was observed traveling on this major east-trending transcontinental highway during the field data collection.



**Figure 4:** Locations of the six-line ReMi survey along US Highway 50 at Brandy Lake.



**Figure 5:** Field photos during ReMi survey along US Highway 50 at Brandy Lake.  
**A.** View west along highway from west end of Line 2; power lines on north side of road; yellow box is Geometrics Geode 24-channel seismograph. **B.** View north from Line 2 at vegetation along road shoulder and Brandy Lake.



**Figure 6:** Field photos during ReMi survey along US Highway 50 at Brandy Lake. **A.** Enlargement of part of a photo looking west from Line 3; paint stripe on south side of road enhances the dips. **B.** View west from Line 5; guard rail adjacent to westbound vehicle is at residence driveway across from Line 6 (visible in Figure 4).

### Refraction Microtremor (ReMi) Subsurface Evaluation

Surface seismic Refraction Microtremor (ReMi) lines were completed at six locations (Figure 4) across and adjacent to the Brandy Lake subsidence area to complement Judy's (2015) reflection seismic characterization of the geologic profile down to the Hutchinson Salt Member in the Brandy Lake area. Results of the ReMi evaluation are a series of soil, alluvium and bedrock layers with interpreted thicknesses and seismic Rayleigh-wave velocities down to the Hutchinson Salt Member. Rayleigh wave velocities are a proxy for shear wave (s-wave) velocities, where the Rayleigh wave velocity propagating through a material is typically 0.9 to 0.95 times the corresponding s-wave velocity. S-wave velocity through a material is mathematically related to the material modulus; if and where the strength of a subsurface layer significantly changes across the project site, that change is likely identifiable from a change in s-wave velocity. That s-wave velocity change, in turn, likely indicates presence or absence and locations of softened upper stratigraphy overlying areas of dissolution in the underlying Hutchinson Salt Member.

### ReMi Field Procedures and Results

All six ReMi surveys were completed on September 29, 2021, adjacent to the pavement and shoulder of US Highway 50 at and near Brandy Lake (Figure 4). At each section, one 24-geophone (575-foot-long) array, consisting of two 12-geophone cables with 25-foot geophone spacings, and a 12-geophone (120 foot) array with 10-foot geophone spacing, were deployed. Data collection was performed using a Geometrics Geode 24-channel signal enhancement seismograph positioned at the center of the 575-foot 24-geophone array. The 24-geophone array at 25-foot geophone spacing provides a greater depth of investigation at a lower detail and resolution, whereas the 12-geophone array at 10-foot geophone spacing provides better detail and resolution at shallower depths.

All seismic lines were oriented parallel to the US Highway 50 alignment. Placements of the seismic lines were decided based on sampling both the areas close to the subsidence feature

and further from it. Seismic Line 1 was placed to the east of the Brandy Lake bridge, away from the known area of recent and current subsidence where the salt bed dissolution front may have already passed (see Keaton et al., 2023, Figure 6). The intent was to sample background s-wave velocities of the subsurface geological units east of the subsidence zone. Seismic Lines 2 and 3 were placed (in sequence adjacent to each other) on the north (westbound) side of US Highway 50 in the subsidence zone; Line 3 extended across the lowest point of ground surface deformation (Sta. 69, Figure 3). Seismic Lines 5 and 6 were placed on the south (eastbound) side of US Highway 50. Lines 3 and 5 were directly across the highway from each other. Seismic Line 6 was placed further west and adjacent to Line 5. The Seismic Line 4 was placed on the northern side of the US Highway 50 near the west end of the study area, close to the intersection of Brandy Lake Road, with the intention of sampling s-wave velocities of undisturbed subsurface geological units west of the subsidence feature and the subsurface dissolution front (see Keaton et al., 2023, Figure 6). Interpreted results for ReMi Lines 4 and 6 are displayed in Figure 7.

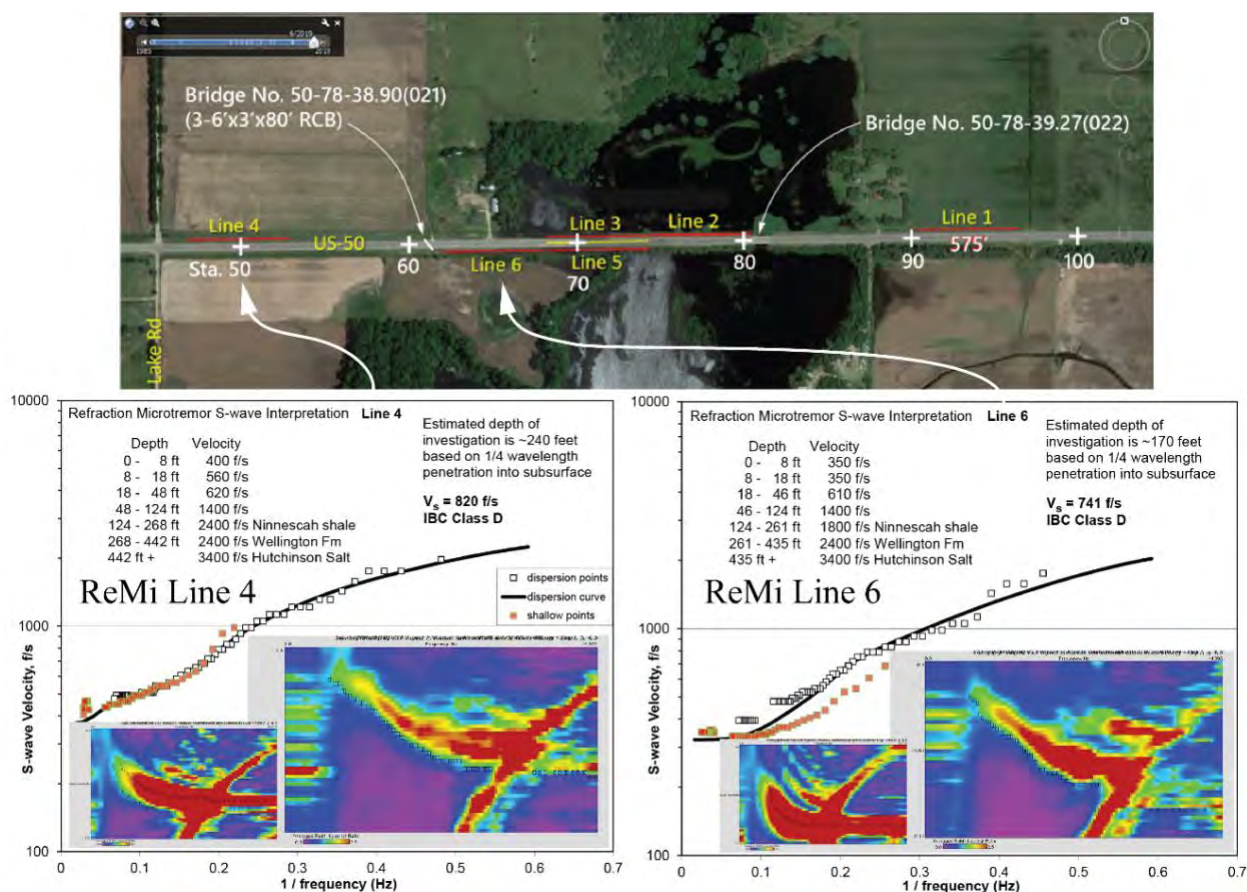


**Figure 2:** Examples of interpreted ReMi lines.

Data collection consisted of sampling the ambient or generated surface waves in a series of sampling events at each of the geophone array. For the 575-foot-long, 24-geophone array sampling event, 12 second sampling time at 1 millisecond sampling interval and 24 second sampling time at 2 millisecond sampling intervals were used. For the 120-foot-long, 12-geophone array, a 12 second sampling time at 1 millisecond sampling interval was used. A

minimum of at least 8 such sampling events were recorded at each seismic line setup. The vehicular traffic on the highway and the personnel jumping at the center (for 24-geophone array) and beyond the end (for 12-geophone array) of the seismic lines, were utilized as ambient surface (Rayleigh) wave energy. The jumps by the personnel were carried out when no vehicular traffic was on the adjacent highway. However, once the jumps were complete, the ambient traffic noise supplemented in sampling the Rayleigh waves during the 12- and 24-seconds sampling time. Both the traffic noise and the field personnel jumping were used as surface wave energy for refraction microtremor analysis for selected one-dimensional vertical surface wave (s-wave) profiles at each seismic line. Examples of interpreted seismic surveys are presented in Figure 7. Findings based on the ReMi interpretations are discussed in the following sections of this paper.

## DISCUSSION

### Comparison of 2021 KDOT Survey and 2009 LiDAR Profiling

The two topographic surveys of the subsiding portion of the US Highway 50 (Figure 3) indicated that less than one foot of subsidence occurred over the 11.4-year period of time between the two surveys. The main subsidence is limited to the reach between Sta. 61 and Sta. 74. The subsidence history along US Highway 50 at Brandy Lake is described in a companion paper by Keaton et al. (2023) that focuses on alternative mitigation strategies. The annualized subsidence rate exceeds 0.02 ft/yr between Sta. 62+00 and Sta. 72+00. The mean and standard deviation annualized subsidence rates are  $0.061 \pm 0.007$  ft/yr. The projected future subsidence amounts after 10, 20, and 30 years were calculated based on the measured 2009-2021 subsidence amount.

### Geologic Profile at Site per Reflection Seismic and ReMi Results

Refraction Microtremor software *SeisOpt ReMi* Version 3.0 from Optim Software was used to analyze ambient surface wave energy collected by the seismograph system. Resulting one-dimensional (vertical) surface Rayleigh wave velocity profiles closely approximate shear wave (s-wave) velocity profiles at the center of the ReMi geophone spread. Due to the nature of the geophysical techniques utilized, all depths, locations and velocities presented on the interpretations are approximate. The ReMi results described in this paper benefitted from the previous reflection seismic interpretations by Judy (2015) and from the relative simplicity of the stratified sedimentary bedrock geology of the region, which is well documented because of petroleum and mineral resources.

Lateral subsurface profile variability under a ReMi geophone array is weighted to the lower strength portion of the profile resulting in a lower average vertical s-wave velocity. Conservative estimations of ReMi s-wave depths of investigation, based on one-quarter wavelength of the lowest frequency signal that is consistent with the s-wave velocity and depth model, are included in the interpretations and ranged from about 120 to about 270 feet below ground surface; these depths reach to or incorporate the Ninescah Shale at the top of Permian age bedrock. The s-wave velocity profile interpretations were significantly influenced by deeper s-wave velocity horizons, and s-wave velocity horizons were interpreted to depths incorporating the Hutchinson Salt Member. Seismic velocity reversals, where softer, lower-velocity materials

could underlie moderate- to higher-velocity materials, might be detected in the vertical s-wave profiles obtained using the ReMi technique. In the geologic setting of the Brandy Lake area, velocity reversals could be indicative of weaker zones in the geologic profile; zones of significantly lower s-wave velocity may be indicative of subsurface zones of underlying current or past salt dissolution activity undermining the shallower geologic profile. However, ReMi interpretations are not unique. Approximate bedrock profiles interpreted from the previous seismic reflection surveys (Judy, 2015) were utilized as an initial model to constrain the ReMi interpretations. Discrete zones of material could have slower or faster velocities, and therefore, be weaker or stronger than indicated by the average velocities interpreted from the seismic data.

Due to the anticipated presence of shallow ground saturation from Brandy Lake, seismic refraction compression wave (p-wave) data were not collected for this project. P-wave velocities in saturated soils typically reflect the speed of sound in water (about 5,000 feet per second [f/s]) such that a water table can profoundly influence seismic refraction results. Where p-wave velocities were not otherwise measured and interpreted, s-wave results can be used to estimate corresponding p-wave velocities. Given a typical soil Poisson's ratio of 0.33, a p-wave velocity in unsaturated geologic media above the groundwater table can be estimated by doubling the corresponding s-wave velocity. In saturated ground conditions, the Poisson's ratio is typically higher and may approach 0.5 in loose saturated soils. In more competent geologic materials and rock, the potential influence of saturation typically becomes less pronounced as the strength of the material, and its corresponding s-wave velocity, increases. The combined average shear-wave velocity ( $V_s$ ) value for the upper 100 feet of the subsurface for seismic site characterization was calculated as part of the interpretations and is included in the ReMi results (e.g., Figure 7).

The shallower seismic velocity profile for the geologic subsurface consisting of surficial soils and alluvium overlying bedrock was interpreted as four layers (Table 1). The s-wave interpretations utilized surface wave information from both the short (10-foot spacing) and the long (25-foot spacing) geophone arrays to characterize the shallow portion of the subsurface geotechnical profile to depths to about 100 feet. Geotechnical parameters used to characterize seismic Site Classes 'D' and 'C' (IBC, 2009) provide a means to correlate some s-wave velocities to Standard Penetration Test (SPT) and undrained shear strength results where undrained shear strength is assumed to be equivalent to one half of the unconfined compressive strength (Figure 8). S wave velocities shallower than about 50 feet in depth are generally analogous to SPT values of 15 or less, and s-wave velocities deeper than about 50 feet are analogous to SPT values of 50 or more.

The deeper seismic velocity profile for the geologic bedrock subsurface profile was interpreted as three layers (Table 2). The s-wave interpretations utilized surface wave information from the long (25-foot spacings) geophone arrays to characterize the deeper portion of the subsurface geologic profile into the Hutchinson Salt Member beginning at interpreted depths of about 430 to 450 feet in the project area.

Table 1 – Summary of Shallow (Soils and Alluvium) Subsurface S-wave Profiles								
Seismic Line (E to W)	Horizon 1		Horizon 2		Horizon 3		Horizon 4	
	Depth (ft)	S-Wave Velocity (ft/s)						
Line 1	0 – 8	400	8 – 18	880	18 – 45	520	45 – 110	1,200
Line 2	0 – 8	400	8 – 18	500	18 – 48	520	48 – 124	1,300
Line 3	0 – 8	400	8 – 18	510	18 – 48	580	48 – 124	1,300
Line 5	0 – 8	490	8 – 18	490	18 – 51	560	51 – 129	1,400
Line 6	0 – 8	350	8 – 18	350	18 – 46	610	46 – 124	1,400
Line 4	0 – 8	400	8 – 18	560	18 – 48	620	48 – 124	1,400

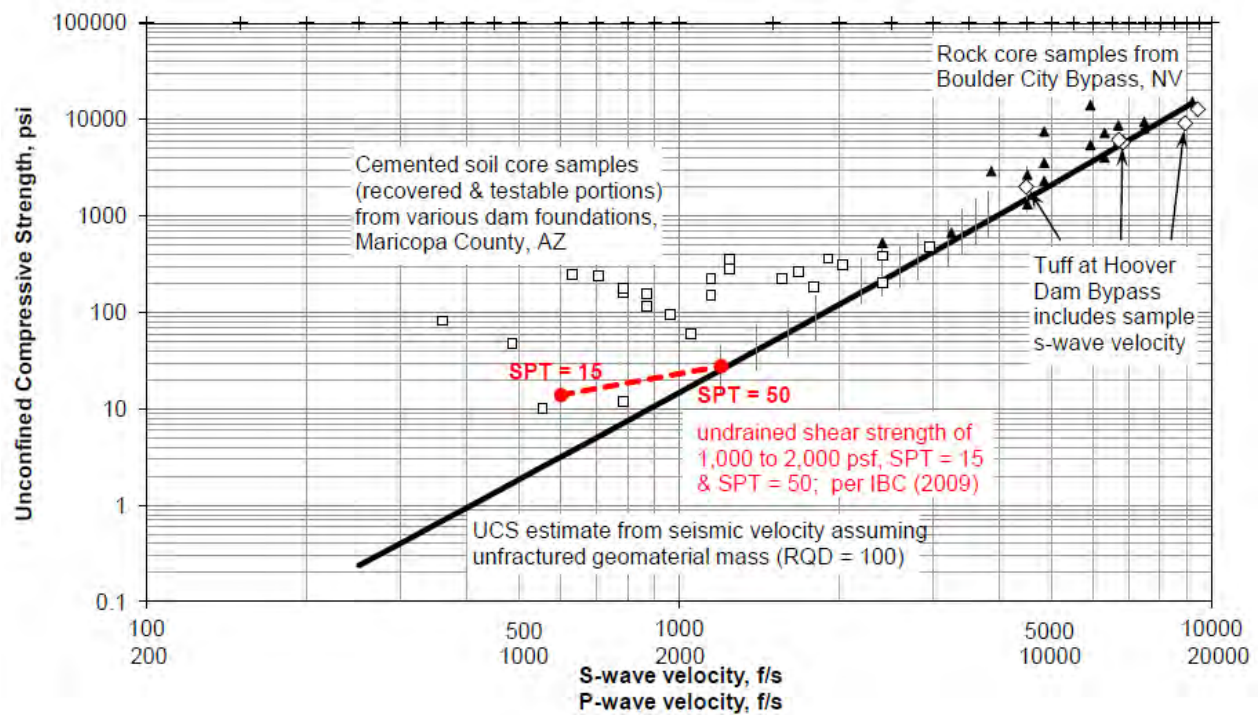


**Figure 8: Correlations of s-wave velocity with estimated typical geotechnical strength parameters based on empirical correlations and various site seismic velocity parameters (Rucker, 2008; IBC, 2009).**

Seismic Line	Ninnescah Shale		Wellington Fm		Hutchinson Salt	
	Depth (ft)	S-Wave Velocity (ft/s)	Depth (ft)	S-Wave Velocity (ft/s)	Depth (ft)	S-Wave Velocity (ft/s)
Line 1	110 – 284	1,900	284 – 433	2,400	433+	3,400
Line 2	124 – 268	1,900	268 – 442	2,400	442+	3,400
Line 3	124 – 268	1,900	268 – 442	2,400	442+	3,400
Line 5	129 – 274	1,800	274 – 448	2,400	448+	3,400
Line 6	124 – 261	1,800	261 – 435	2,400	435+	3,400
Line 4	124 – 268	2,400	268 – 442	2,400	442+	3,400
Reflection P-Wave Velocity Range (Judy, 2015)	~1,400 – 1,800 m/s ~4,600 – 5,900 f/s		~1,800 – 2,100 m/s ~5,900 – 6,900 f/s		~2,100 – 2,200 m/s ~6,900 – 7,200 f/s	

The interpreted s-wave velocity in the Ninnescah Shale above the Hutchinson Salt Member at ReMi Line 4 west of the subsidence zone was higher than the s-wave velocities at ReMi Lines 2, 3, 5 and 6 in the subsidence zone and Line 1 to the east of the subsidence zone. This distribution of s-wave velocities in the bedrock horizon is consistent with salt dissolution at the Hutchinson Salt Member inducing or enhancing fracturing in overlying bedrock, and thus reducing the velocities of seismic s-waves that propagate through that bedrock. ReMi Line 4 was positioned over undisturbed salt, which is consistent with the higher s-wave velocity and the uniform reflection seismic profile west of the subsidence zone. The remaining ReMi lines were likely located underlain by the dissolution front in the Hutchinson Salt Member (see Figure 6 in Keaton et al., 2023).

The lowest s-wave velocities in the shallow subsurface soil horizons were interpreted at ReMi Line 6. Line 6 was deployed entirely within the recent subsidence zone; the very low s-wave velocity soil profile likely reflects distress in and reduction of strength of the soil fabric resulting from subsidence-induced soil mass movement.

### **InSAR Evaluation and Interpretation of Current Subsidence Conditions**

Satellite-based Interferometry by Synthetic Aperture Radar (InSAR) provides a potential to remotely characterize subsidence across the project, and across the region, for recent to current time periods when survey data is not available. Beginning in 2002, WSP has been applying InSAR technology as an important tool to characterize active land subsidence and other ground movements over large expanses of land. InSAR analyses involve comparing two or more synthetic aperture radar (SAR) images of the same area over a sufficient time period (normally months to years) to permit measurement of relative elevation changes of the ground surface. A review of available technical literature indicated that InSAR was not being used to monitor land

subsidence in the area; pervasive agricultural land use activities and ground vegetation cover through the region are typically unfavorable for the application of InSAR technology to subsidence monitoring. KDOT engineers were interested in a limited effort to evaluate the effectiveness of SAR technology to detect subsidence of the scale at the Brandy Lake location. Only a brief description of the effort is warranted in this paper because the InSAR analysis suggested greater subsidence over a shorter period of time than actually occurred based on the 2009 laser scan and 2021 conventional survey measurements over a longer period of time.

The applicability of InSAR technology for subsidence characterization at the project site and along the US Highway 50 alignment was tested with Sentinel 2 Synthetic Aperture Radar (SAR) data obtained from the European Space Agency (ESA) website. Unwrapping (processing) of the SAR data was performed on the interferograms, in WSP's offices, and relative ground displacement profiles were developed along 8 km of the US Highway 50 alignment. Nine months of probable differential elevation change profiles were processed and developed. These profiles were centered at the maximum known subsidence at Brandy Lake within the project site and consisted of processed apparent differential elevations at point intervals of 20 meters extending for 4 km to the east and west of that subsidence zone. The resulting profiles cover a very short period of time in which to characterize this geologically active land subsidence in the area. Given the extensive agricultural activity adjacent to the highway profile and throughout the area covered by the interferograms, considerable 'noise' was anticipated to be present in the processed profile results. Given the short interferogram time periods, large apparent differential ground displacements between adjacent profile elevation points greater than  $\frac{1}{2}$  wavelength (28 mm) were considered to have resulted from ground surface disruption from interference due to nearby agricultural activity or radar signal noise. It is apparent that recent short-term subsidence rates and magnitudes as interpreted from the processed InSAR results are larger than the much longer-term subsidence inferred from LiDAR and survey profiles. Among the possibilities for this discrepancy are variabilities in localized subsidence rates over time and potential noise and/or errors in the InSAR data and processed results. However, comparison of InSAR results across two known active subsidence features on US Highway 50, Brandy Lake and nearby Victory Road, have geometries consistent with the previously measured subsidence features.

## CONCLUSIONS

WSP's analysis of information from a variety of sources supports a conclusion that subsidence along US Highway 50 in the study area between Brandy Lake Road and S Buhler/Haven Road is limited to a distance of approximately 1400 ft that appears to coincide with a series of high-angle normal and reverse faults in bedrock formations above the Hutchinson Salt Member interpreted from a reflection seismic survey (Judy, 2015). A comparison of the 2009 LiDAR survey with the April 2021 US Highway 50 centerline survey indicates a zone of active land subsidence that extends from about Sta. 60+00 to 74+00. From November 2009 to April 2021, a maximum of about 0.8 feet of subsidence has been documented along the highway between about Sta. 62+00 to 70+00. Comparing a 1986 plan sheet (KDOT, 1986) and the April 2021 KDOT survey indicates elevation stability at the bridge at Sta. 81+00 and essentially no discernable subsidence to the east of about Sta. 74+00.

Previously published interpretations of reflection seismic collected along US Highway 50 (Judy, 2015) are consistent with the survey comparison results. A zone of faults or fault-like features corresponding to underlying salt dissolution-induced distress to bedrock above the Hutchinson Salt Member were interpreted within the zone of active land subsidence, while the reflection seismic results to the west of the subsidence zone were consistent with no deformation interpreted as no salt dissolution. S-wave velocities in the Ninescah Shale above the Hutchinson Salt interpreted from the ReMi seismic survey results were higher to the west of the active subsidence zone and lower in and to the east of the subsidence zone, which is consistent with underlying salt dissolution impacting overlying bedrock units. The active subsidence zone is adjacent to the west edge of Brandy Lake, which results in local inundation of the driving lanes when the lake level is high. Systematic consideration of alternative mitigation approaches produced several approaches that have extremely high cost (ground improvement, spanning the subsidence zone with a bridge, and rerouting the highway), or are unlikely to be allowable, or do not meet highway standards (controlling the level of Brandy Lake, restrict use of the highway in general or when lanes are inundated). These alternative mitigation approaches are discussed in a companion paper by Keaton et al. (2023).

The faults or fault-like features underlying the subsidence zone likely constrain the lateral extent of near-term future subsidence. Thus, restoration of the highway grade may reasonably be confined to the current subsidence zone. Since Brandy Lake was originally a natural lake feature as documented by historic topographic maps, general subsidence at the lake area began as a natural geologic phenomenon rather than an anthropogenic phenomenon. Construction of a dam along the southeast margin of Brandy Lake, resulting in raised lake water levels, may have accelerated dissolution activity so that continuing future subsidence activity can be anticipated. Given the apparent chaotic nature of dissolution phenomena and severe constraints on characterizing relevant deep ground conditions, a reasonable best estimate for future subsidence may be based on the recent average rate of  $\sim 0.7$  feet in 11.4 years, or about  $0.061 \pm 0.007$  feet/year.

**REFERENCES:**

- Bayne, C. K. *Geology and ground-water resources of Reno County, Kansas*. Kansas Geological Survey, Bulletin 120, 1956, 130 p.
- Herrs, A.J. Quantifying Surface Subsidence along US Highway 50, Reno County, KS, using *Terrestrial LiDAR*: Master of Science thesis, University of Kansas, Lawrence, 2010.
- International Code Council (IBC), 2009, International Building Code. Table 1615.5.2. p 341.
- Judy, B.E. *High resolution seismic reflection to characterize small scale mechanisms of large-scale natural dissolution in the Hutchinson Salt Member*. Master of Science thesis, University of Kansas, Lawrence, 2015.
- Kansas Department of Transportation. *Construction Layout U.S.-50 over Brandy Lake Bridge No. 50-78-39.27(022) Sta. 81+00*. KDOT Project 50-78-K-2370-01, Reno County, Sheet No. 38 of 122, 1986.
- Keaton, J.R., and D.W. Eckhoff. Value engineering approach to geologic hazard risk management. *Transportation Research Record* No. 1288, 1990, pp. 168-174.
- Keaton, J.R., S.J. Pannalal, and M.L. Rucker. Mitigation Alternatives for Salt Dissolution Subsidence Impacting US Highway 50 at Brandy Lake, Reno County, Kansas. *Proceedings, 72nd Highway Geology Symposium*, Tacoma, WA, 2023 (this proceedings volume).
- Rucker, M.L. Estimating in-situ geo-material mass density, modulus and unconfined compressive strength from field seismic velocity measurements. *Highway Geophysics-Nondestructive Evaluation Conference*. Charlotte, NC, Dec. 1-4, 2008.
- Walters, R.F. *Land Subsidence in Central Kansas Related to Salt Dissolution*. Kansas Geological Survey Bulletin 214, 1978.
- West, R., K. B. Miller and W. L. Watney. *The Permian System in Kansas*. Kansas Geological Survey Bulletin 257, 2010.

**Mitigation Alternatives for Salt Dissolution Subsidence Impacting  
US Highway 50 at Brandy Lake, Reno County, Kansas**

**Jeffrey R Keaton**

WSP USA

4600 E. Washington St., Suite 600

Phoenix, AZ 85034

(323)-203-6958

jeff.keaton@wsp.com

**S Johari Pannalal & Michael L Rucker**

WSP USA

4600 E. Washington St., Suite 600

Phoenix, AZ 85034

johari.pannalal@wsp.com    michael.rucker@wsp.com

Prepared for the 72<sup>nd</sup> Highway Geology Symposium, August, 2023

### **Acknowledgements**

The authors would like to thank the Kansas Department of Transportation for providing technical information during project execution, facilitating access to master's theses that were funded by the Department, and authorizing our work products to be used for this paper.

### **Disclaimer**

Statements and views presented in this paper are strictly those of the authors, and do not necessarily reflect positions held by their affiliations, the Highway Geology Symposium (HGS), or others acknowledged above. The mention of trade names for commercial products does not imply the approval or endorsement by HGS.

### **Copyright Notice**

Copyright © 2023 Highway Geology Symposium (HGS)

All Rights Reserved. Printed in the United States of America. No part of this publication may be reproduced or copied in any form or by any means – graphic, electronic, or mechanical, including photocopying, taping, or information storage and retrieval systems – without prior written permission of the HGS. This excludes the original authors.

## ABSTRACT

US Highway 50 bisects Brandy Lake on an embankment with a short, pile-supported bridge near the lake's east side. Ongoing dissolution of bedded salt 134m deep is causing local subsidence with increasing problems for this busy two-lane highway designed in 1963 by Kansas Department of Transportation (KDOT). A low spot on the west side of the lake ponds water more frequently and for longer periods as subsidence progresses. KDOT funded a University of Kansas master's thesis that produced a terrestrial laser scan in November 2009 and self-performed conventional centerline survey in April 2021. Centerline elevation differences between the two surveys 11.4 years apart revealed a 457m-long zone of subsidence with 366m having more pronounced subsidence. WSP estimated subsidence and projected the highway centerline profile in 2031, 2041, and 2051. High water in Brandy Lake by 2051 could inundate the road by 1.8m.

Nine alternative mitigation strategies comprising five general approaches were described in terms of merits, drawbacks, and relative costs using a value-engineering approach to geologic hazard risk management. General approaches were A) Continue current practices, B) Modify the hazard, C) Modify what is at risk, D) Modify operation or procedure, and E) Avoid the hazard. Alternative strategies were: 1) Signage and occasional pavement overlays, 2) Deep ground improvement, 3) Control lake level, 4) Dikes along right-of-way, 5) Restrict highway use or limit speed/type of vehicle, 6) Raise highway profile with embankment, 7) Raise highway profile with bridge, 8) Close the highway when inundated, and 9) Reroute the highway.

## INTRODUCTION

This paper describes the second part of a geotechnical transportation engineering project focused on US Highway 50 at Brandy Lake, Reno County, Kansas (Figures 1 and 2). The objectives of this project were to design improvements to the two-lane highway to restore uniform grade across an area of gradual subsidence and elevate the road above local inundation when the level of Brandy Lake is high. High water for this project was taken as elevation 1490 feet (mean sea level datum), which is the elevation of the base of a pile-supported bridge connecting the highway across an approximately 120-foot-wide gap between compacted earth embankments across Brandy Lake (Figure 3).

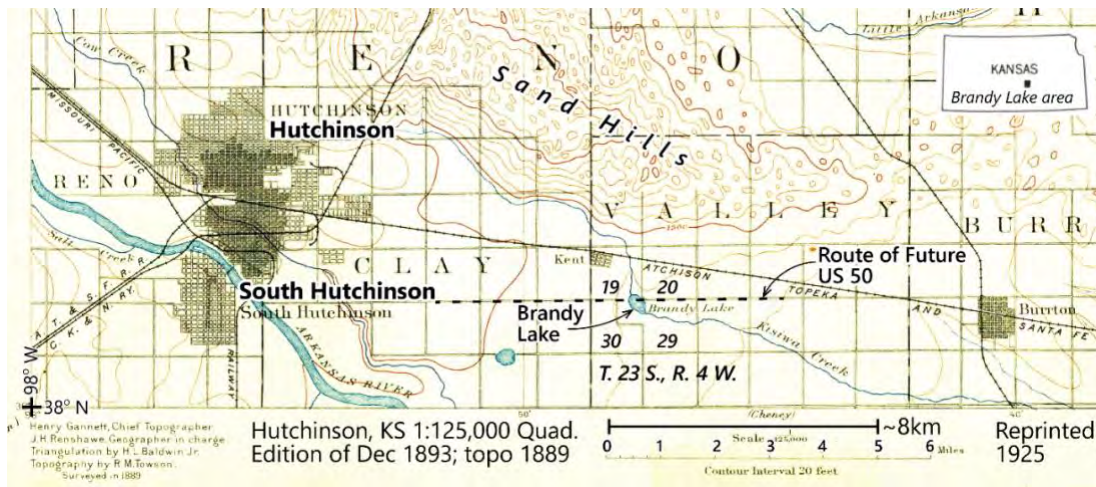


Figure 1. Brandy Lake location on an 1893 topographic map.

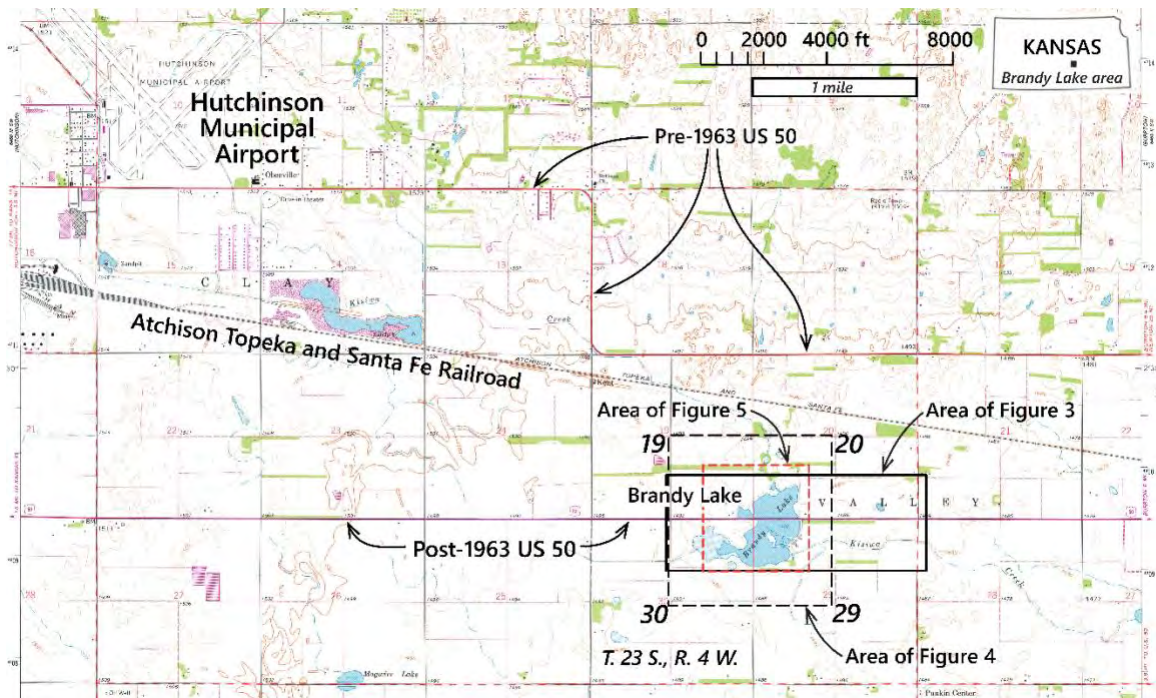
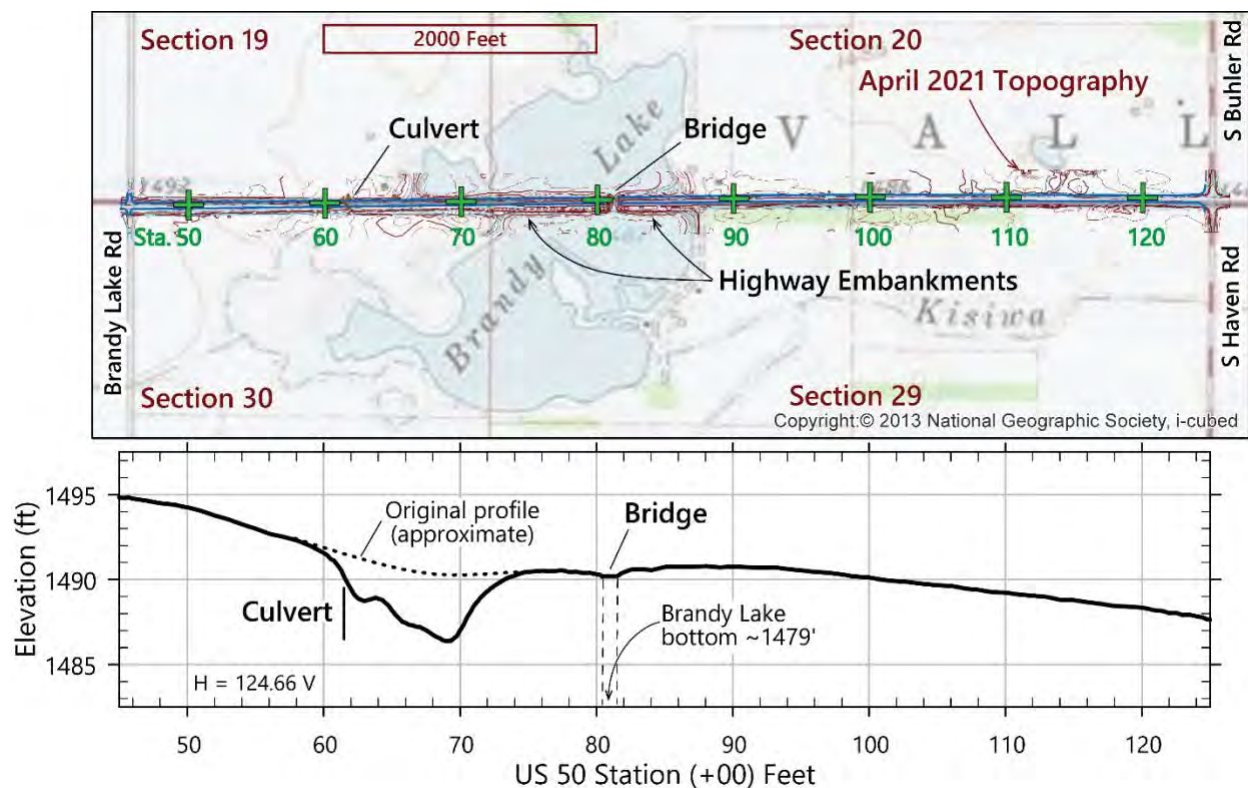


Figure 2. Brandy Lake location on Hutchinson SE 7.5-minute topographic quadrangle map (1961; photo revised 1978).



**Figure 3. US Highway 50 across Brandy Lake showing station numbers and locations of bridges on a 1961 topographic map (photo revised 1978) supplemented with April 2021 topography (upper diagram). Centerline 2021 topographic profile showing locations of the bridge, the culvert, and the area of major subsidence (lower diagram).**

Presumably Brandy Lake depicted in the 1893 topographic map (Figure 1) was unmodified from its natural condition. However, by 1961 (Figures 2 and 3), the southeast margin of the lake had been modified with embankments. The earliest aerial photograph available in the US Geological Survey online collection (<https://earthexplorer.usgs.gov/>) is from November 1954 (Figure 4, left image), approximately nine years before US Highway 50 was constructed across Brandy Lake in 1963. A second pre-1963 photograph available in the US Geological Survey online collection is from September 1959 (Figure 4, right image). The 1954 photograph shows low lake level, whereas the 1959 image shows higher lake level.

The most recent photograph of the Brandy Lake area in the US Geological Survey online collection depicts low water conditions in June 2012 (Figure 5, right image). A photograph from July 2008 (Figure 5, left image) shows Brandy Lake with high water conditions. The locations of the bridge (Sta. 81+00) and the culvert (Sta. 61+40) are labeled. Also labeled are three low areas in the 2012 photo that appear to be ponds in the 2008 photo.

The companion paper by Pannalal et al. (2023) describes the field investigation and site characterization of the Brandy Lake section of US Highway 50. Those findings served as the basis for defining the likely cause of the localized subsidence and limits and rates of subsidence, as well as identifying alternative mitigation measures for the highway. The remaining sections of this paper describe the geologic setting and alternative improvements for the highway.

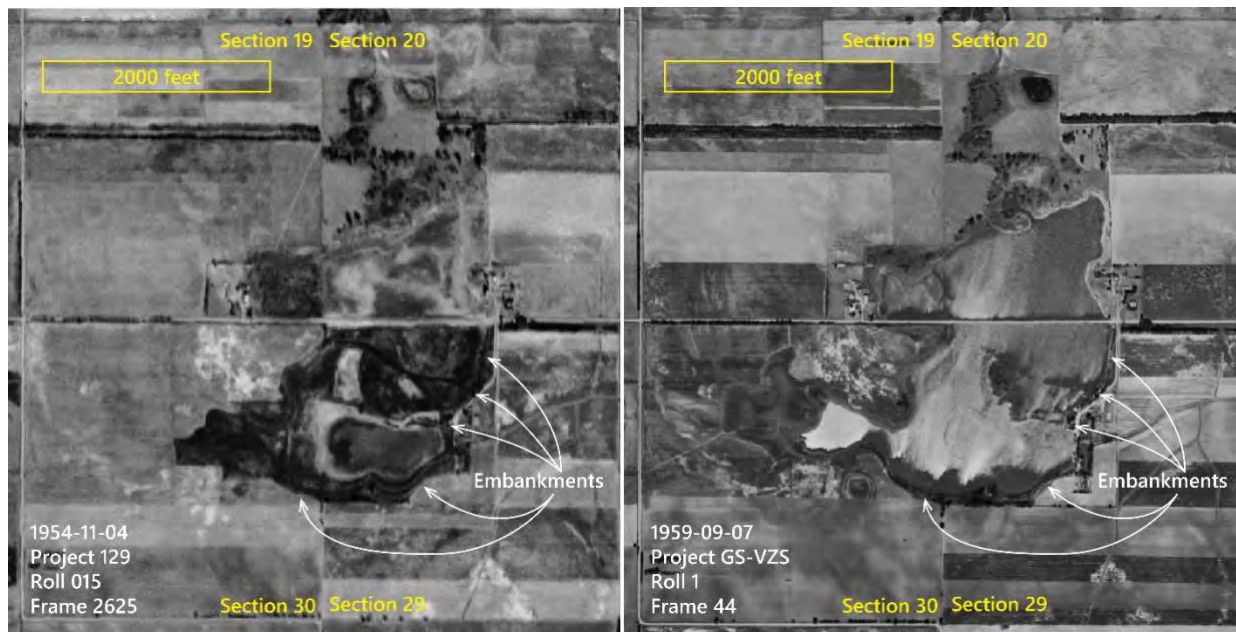


**Figure 4. Location of the future US Highway 50 across Brandy Lake in 1954 (left) and 1959 (right). The 1954 image shows low lake level, whereas the 1959 image shows high lake level.**

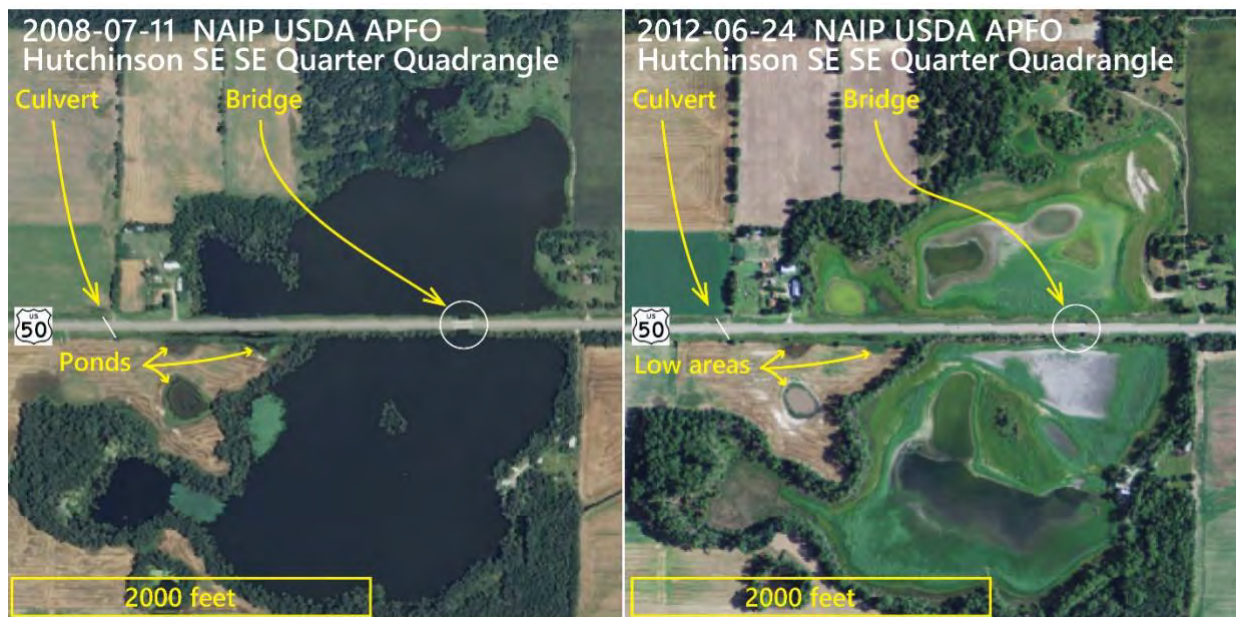


**Figure 5. Location of US Highway 50 across Brandy Lake in 2008 (left) and 2012 (right). The 2008 image shows high lake level, whereas the 2012 image shows low lake level.**

## GEOLOGIC SETTING

Oil was first discovered in Kansas in 1860, but the first well to produce commercial quantities of oil was drilled in 1892 (<https://geokansas.ku.edu/oil-and-gas-production-kansas>). Salt was discovered in South Hutchinson in 1887 in an oil exploration well drilled approximately 8 miles west of Brandy Lake (<https://www.renogov.org/267/Reno-County-History>). The oil

resource development results in the geology of the region being well known. The geologic profile in the Brandy Lake area consists of late Pleistocene terrace deposits overlying Permian bedrock (Bayne, 1956). The Permian bedrock formations in the study area consist of bedded shale and evaporite deposits of the Ninnescah Shale and Wellington Formation of the Sumner Group that dip relatively gently toward the west (Figure 6; Walters, 1978; West et al., 2010). The Hutchinson Salt Member is a subunit of the Wellington Formation at a depth of approximately 425 feet at Brandy Lake (Judy, 2015). The Brandy Lake area is within a naturally occurring zone of dissolution of the Hutchinson Salt located approximately 20 miles west of the where the salt bed would be exposed if it had not dissolved during late Cenozoic time. The surface expression of salt dissolution at depth is irregular subsidence-induced depressions in terrace deposits. The shallow aquifer in Pleistocene terrace deposits produces ponds and lakes, such as Brandy Lake, where subsidence intersects the groundwater table.

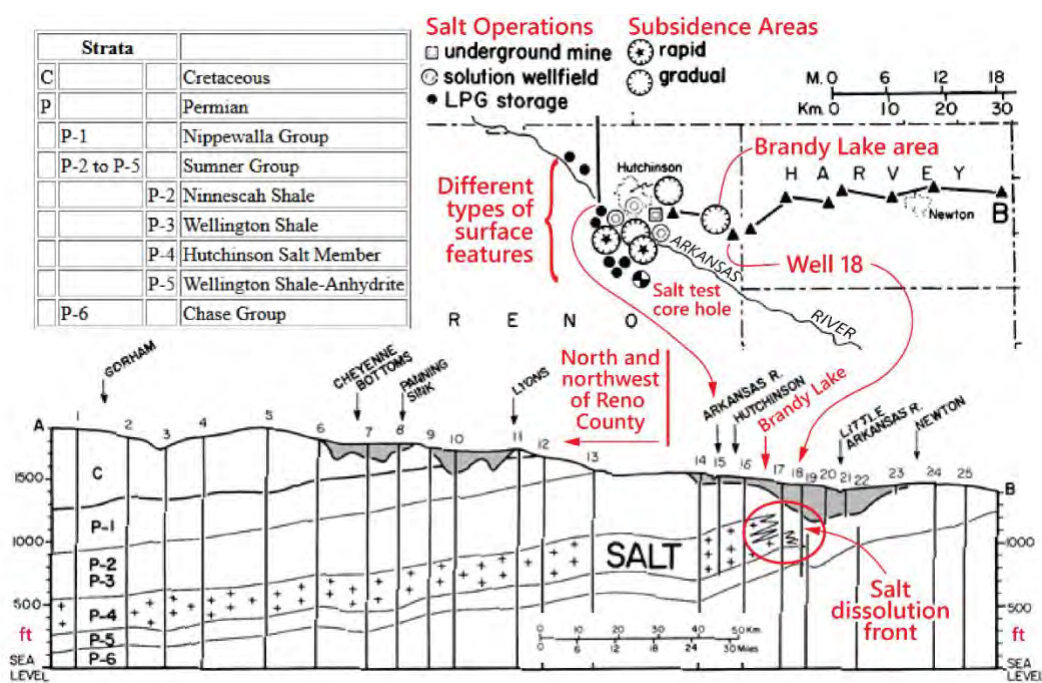


**Figure 6. Stratigraphy sketch in the Brandy Lake vicinity. Shaded areas in section are unconsolidated water-bearing beds. Modified from Walters (1978).**

Brandy Lake occupies a likely subsidence feature that developed in recent geologic time as natural seepage of fresh groundwater into Permian age bedrock formations resulted in halite dissolution within the underlying Hutchinson Salt Formation. That Brandy Lake is shown and named on the historic 1893 topographic map (Figure 1) is effective confirmation that it is a natural geological feature. The ongoing subsidence along the current US Highway 50 at the lake's western edge (Figure 3) indicates that localized subsidence is a continuing phenomenon. The US Highway 50 centerline elevation at the Brandy Lake Bridge (Sta 81+00) was reported to be 1490 feet (KDOT, 1986) in 1986, and remained at 1490 feet in the 2021 KDOT survey.

A Master of Science thesis entitled 'High resolution seismic reflection to characterize small scale mechanisms of large-scale natural dissolution in the Hutchinson Salt Member' (Judy, 2015) provides a geologic background summary for dissolution in the Hutchinson Salt Member,

interpretation of the geologic profile underlying the Brandy Lake subsidence feature and vicinity, and relevant seismic parameters to help constrain seismic interpretations for this current project. Based on reflection seismic results, an interpreted bedrock profile (Judy, 2015, p 51) below alluvium places the top of the Ninnescah Shale at a depth of approximately 130 feet, the top of the Wellington Formation at approximately 280 feet deep, and the top of the Hutchinson Salt Member at approximately 430 feet deep. Generalized modeled and smoothed compression wave (p-wave) velocities used in the reflection seismic analysis are also provided (Judy, 2015, p 46). An important interpretation in Judy's (2015) thesis was a 1200-foot-long zone of steeply dipping normal and reverse faults in the Wellington Formation and Ninnescah Shale above the Hutchinson Salt Member in the subsidence area along the west side of Brandy Lake. Similar fault traces were not interpreted elsewhere along the seismic reflection line.

## SUBSIDENCE HISTORY

The complete history of subsidence along the Brandy Lake segment of US Highway 50 in Reno County, KS, is unknown or at least undocumented in detail. A 2010 Master of Science thesis entitled "Quantifying surface subsidence along US Highway 50, Reno County KS, using terrestrial lidar" (Herrs, 2010) suggests that subsidence at Brandy Lake was becoming a nuisance by the early 2000's. Herrs (2010) performed three lidar surveys in 2009 (February, May, and November) in an attempt to document short-term subsidence rate, but no detectable change was documented among the three surveys. A stable benchmark distant from the subsidence area was used as the elevation reference. The November 2009 survey was used in the present analysis and compared to the April 2021 survey by Kansas Department of Transportation, an approximately 11.4-year time difference (Figure 7).

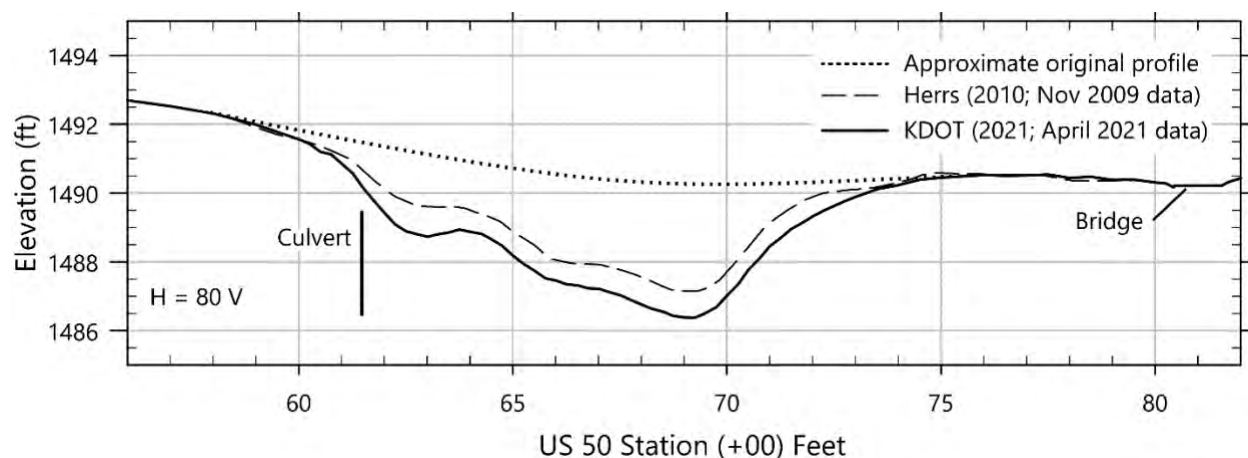


**Figure 7. Comparison of US Highway 50 centerline elevation profile from November 2009 and April 2021. Modified from Herrs (2010) and plotted from KDOT (2021).**

## SUBSIDENCE RATE AND FORECAST

The two topographic surveys of the subsiding portion of the US-50 highway (Figure 7) indicated that less than one foot of subsidence occurred over the approximately 11.4-year period of time between the two surveys (Figure 8). The main subsidence is limited to the reach between US-50 Sta. 60+00 and Sta. 74+00. The elevation profiles by Herrs (2010) from November 2009

and by KDOT (2021) from April 2021 are plotted at an enhanced vertical scale in Figure 8. The elevation difference between the two profiles is plotted on the supplemental y-axis as the amount of subsidence that occurred during the approximately 11.4-year period of time. That annualized rate exceeds 0.02 ft/yr between Sta. 62+00 and Sta. 72+00. The mean and standard deviation annualized subsidence rates are 0.061 ft/yr and 0.007 ft/yr. The projected future subsidence amounts after 10, 20, and 30 years were calculated based on the measured 2009-2021 subsidence amount. The mean and 84th percentile projected subsidence amounts are summarized in Table 1.

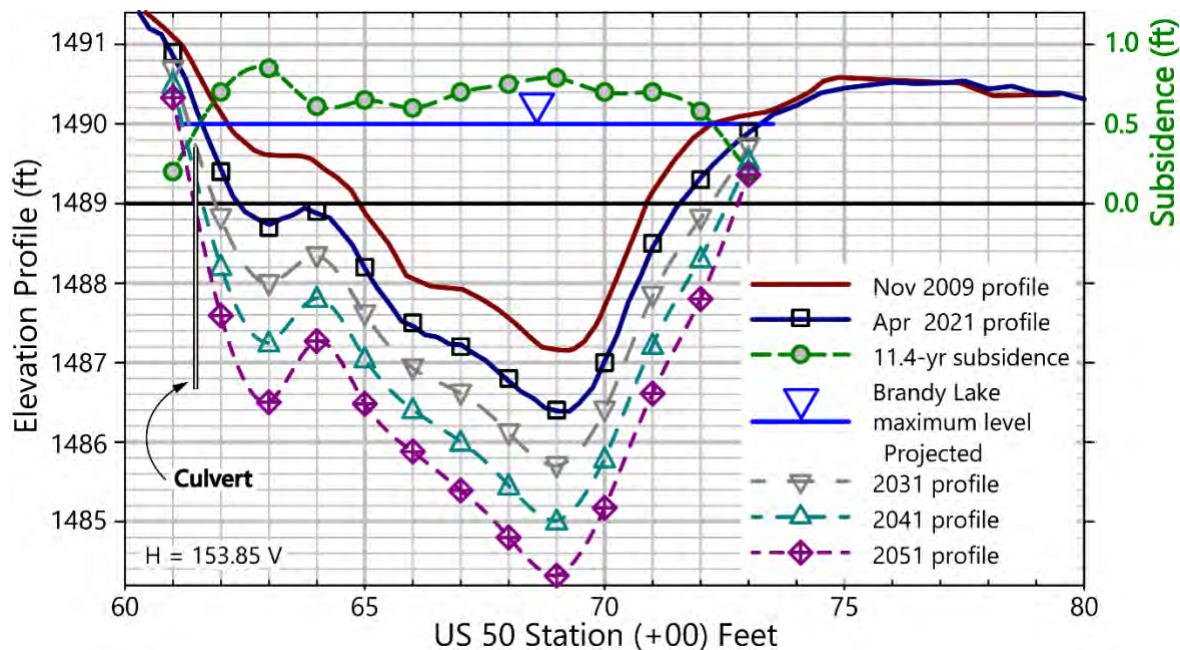


**Figure 8. Comparison of US Highway 50 centerline elevation profile from November 2009 and April 2021 (11.4 years). Modified from Herrs (2010) and plotted from KDOT (2021).**

<b>Table 1 – Calculated Subsidence Rate and Projected Subsidence</b> (Top row is subsidence rate; other rows are projected subsidence)		
Time Period (years)	Mean	Mean+1 Standard Deviation
11.4	0.061 feet/year	0.068 feet/year
10	0.61 feet	0.68 feet
20	1.21 feet	1.36 feet
30	1.82 feet	2.04 feet

## POTENTIAL ALTERNATIVE MITIGATION APPROACHES

Consideration was given to alternative approaches to mitigate the condition on US Highway 50 that results in inundation of driving lanes during periods that the water level in Brandy Lake is high. A systematic procedure for analyzing alternative responses to geologic hazards (Keaton and Eckhoff, 1990) has five types of approaches that are sequentially compared to an acceptable level of risk (Figure 9). Risk in this context is intended to be the product of the probability of a hazard occurring at damaging intensities and the cost of the damage or disruption that could be realized by such an occurrence of the hazard. The subsidence deformation and

subsequent inundation of US Highway 50 can be considered in a conceptual simple risk assessment without needing to have quantitative estimates of future inundation depths.

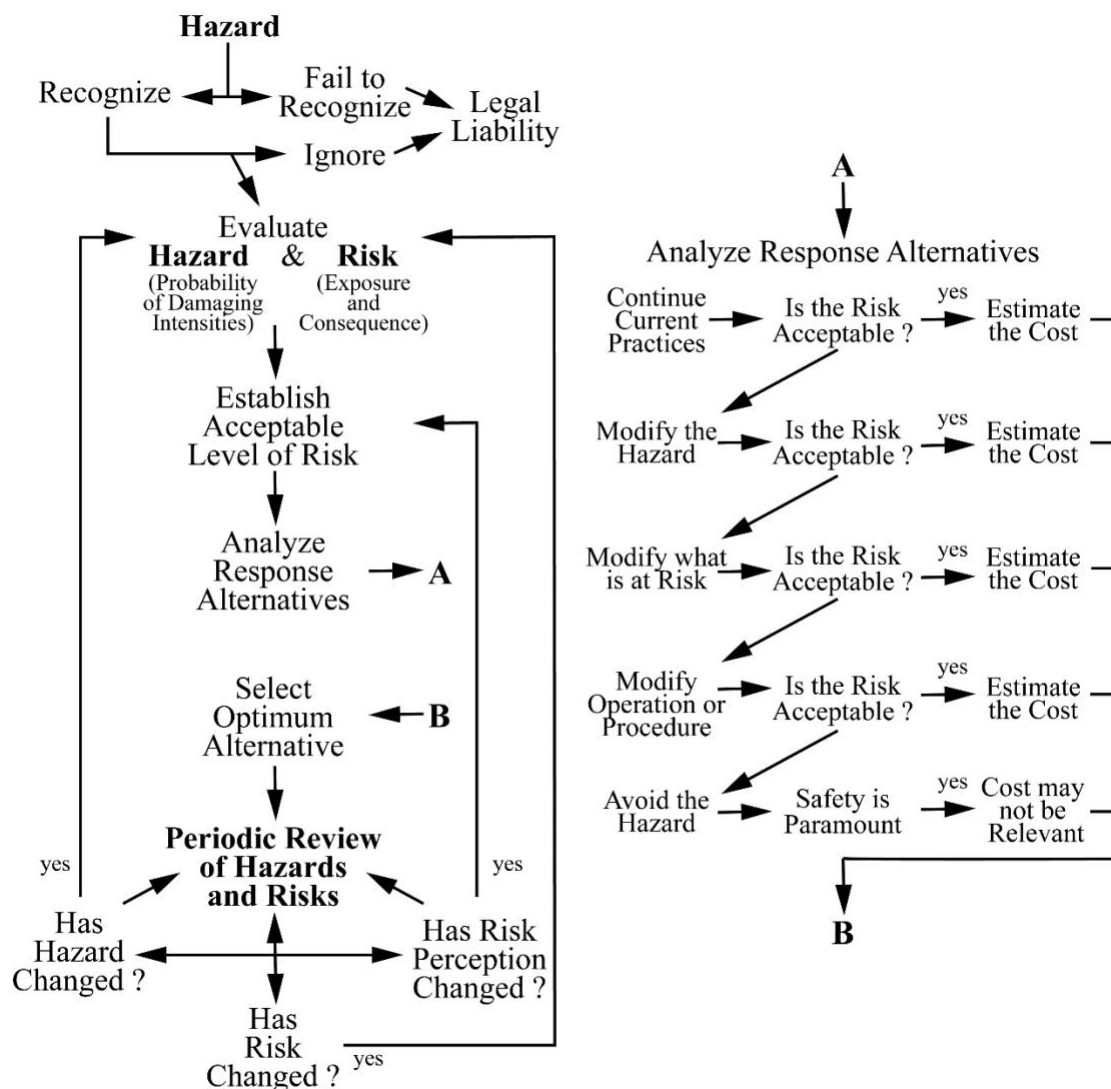


**Figure 9. A model for geologic hazard risk management. Modified from Keaton and Eckhoff (1990).**

The annualized subsidence rate is an index of the hazard ( $0.061 \pm 0.007$  ft/yr; Table 1), which is approximately 0.5 ft in 7.4 to 9.3 years. The two most rapidly subsiding areas during the ~11.4-yr period between surveys (Figure 8) suggest that 0.5 ft of subsidence could occur in ~6.72 yr at Sta. 63 and in ~7.23 yr at Sta. 69. The subsidence mechanism seems to be related to salt dissolution at depth with strain allowing the area of subsidence to continue to subside. Repeated centerline surveys every 2 to 4 years would advance understanding of the rate of continuing subsidence within incremental subsidence amounts of approximately 0.1 to 0.25 ft. Currently, two surveys ~11.4 years apart are the only data points on which the projected subsidence rate is based. The extent along the highway of continuing subsidence is taken to be fixed, but confirmation of the subsidence limits would be desirable.

The five types of approaches in the hazard-response model (Figure 9) are:

- 1) continue current practices,
- 2) modify the hazard,
- 3) modify what is at risk,
- 4) modify operation or procedure, and
- 5) avoid the hazard.

The assessment of approaches to the subsidence hazard adversely affecting US Highway 50 are listed in Table 2. The current practices for a subsidence area that intermittently becomes inundated typically consist of placing warning signs advising of the “road flooded ahead” condition when the road becomes inundated and placing an asphalt concrete overlay in the most severe of the inundation locations every approximately 5 years. These practices essentially are partly modifying operation or procedure of the traveling public and partly modifying what is at risk of inundation caused by continuing subsidence and high lake level.

The hazard has two aspects; subsidence of the highway and inundation of driving lanes. Modification of the subsidence hazard would require some sort of ground improvement that would have to extend to the depths at which it is occurring, presumably the Hutchinson Salt Member at a depth of over 400 feet. Ground improvement to such depths is intuitively impractical to consider for a segment of two-lane highway that is 1400 feet long.

Modification of the inundation hazard could be approached by controlling the maximum water level in Brandy Lake or by protecting the driving lanes from inundation. Controlling the maximum level of Brandy Lake could not be accomplished with efforts that are restricted to the US Highway 50 right-of-way. Water rights issues and lake usage protocols were not evaluated as part of the project, and neither have discharge permit requirements. Excavation within the lakebed in some geologic environments could increase the storage volume while maintaining the maximum water level. The upper soils at Brandy Lake are sandy and serve as the local aquifer. Therefore, the water level in Brandy Lake would likely be controlled by the piezometric surface in the sandy aquifer regardless of excavation into the bed of the lake.

Protecting the driving lanes from inundation could be attempted by constructing dike-like berms along the shoulders of the highway. Upward seepage from sandy aquifer deposits under the roadbed or the constructed dikes would likely result in the ultimate water level within the dikes reaching the level of the lake. Given the relatively small area of the highway width and length of the inundation zone, a pump system discharging into Brandy Lake adjacent to the constructed dikes might be able to keep the water level below the driving lanes. Stormwater captured by the dikes would need to be pumped into the lake regardless of the lake level. Discharge permits probably would be required. Flood control dikes would interfere with driveway access along the subsiding reach of US Highway 50. Icing of the driving lanes would be an additional hazard in the winter months.

<b>Table 2 - Summary of Potential Alternative Mitigation Approaches</b>				
<b>Approach</b>	<b>Description</b>	<b>Merits</b>	<b>Drawbacks</b>	<b>Relative Cost</b>
Continue current practices	Temporary signs; occasional overlays	Respond to actual conditions	Continued maintenance; will get worse with time; does not meet highway standards	Low
Modify hazard - subsidence	Ground improvement	Possibly stop or slow subsidence	Massive effort; may not be successful	Extremely high
Modify hazard – road inundation	Control lake level	Keep water off highway	Outside ROW; may not be acceptable to lake users; discharge permit needed	Moderate
Modify hazard – road inundation	Dikes along ROW	Keep water off highway	Seepage and stormwater pumping; discharge permit; driveway access interrupted during construction	Moderate
Modify what is at risk – motorist exposure	Restrict highway use /speed or limit type of vehicle	Reduce public exposure to harm	Limits public access; inconvenience to traveling public; does not meet highway standards	Low
Modify what is at risk – highway	Raise profile with embankment	Highway inundation eliminated; uniform highway profile; routine construction; construct in stages with one-lane traffic	Subsidence continues; driveway access interrupted during construction; occasional maintenance needed	High
Modify what is at risk – highway	Raise profile with bridge	Highway inundation eliminated; uniform highway profile; span subsidence zone	Infeasible without intermediate supports; traffic rerouted during construction	Extremely high
Modify operation or procedure	Signage warning of inundation, reduced speed	Essentially equivalent to current practice	Continued maintenance; will get worse with time; does not meet highway standards	Low
Avoid the hazard	Reroute highway	Known subsidence zone is avoided; highway open during construction	New ROW acquisition required; unknown hazards may require future mitigation	Extremely high

The elements at risk of damage or injury also have two aspects; the highway itself and motorists driving vehicles on the highway. Since US Highway 50 is a public access highway, requiring modification of the vehicles or restricting use of the highway to vehicles with certain characteristics is an untenable approach. An obvious approach that could be implemented within the KDOT right-of-way would be to raise the profile of the highway across the subsidence area or across the reach of the subsidence area that is subject to inundation using either a compacted fill embankment or a structural bridge. Accommodations probably would be needed to maintain access to driveways during construction. Raising the profile of the highway would not isolate the road from continuing subsidence; however, a grade could be designed that would have many years of service before inundation of driving lanes would become problematic again. An embankment could be designed with an elevated shape that would gradually subside to a target grade. A bridge structure might be designed with adjustable supports to maintain a grade while subsidence continues. A major bridge structure would be required to effectively span the current zone of subsidence while founding abutments on adjacent (currently) stable ground.

Modification of operation or procedure already is being done on the subsiding part of US Highway 50: permanent signs reading “No Driving on Shoulder” were present in 2009 during the time Herrs was conducting thesis research. Additional signage could be posted for inundation conditions that advises drivers to proceed at reduced speeds. Freezing temperatures in winter months could result in icing conditions of the inundated area, as well as above the inundation area from repeated splash-and-drip by successive passing vehicles.

The final alternative mitigation approach is to avoid the hazard. This would require relocating the highway around the active subsidence zone, which effectively would be around Brandy Lake. The potential for encountering other hazard zones that might require mitigation along a rerouted alignment is unknown. Substantial amounts of new right-of-way would have to be acquired for the “avoid the hazard” approach.

## CONCLUSIONS

Information from a variety of sources supported a conclusion that subsidence along US Highway 50 in the area around Brandy Lake is limited to a distance of approximately 1400 feet that appears to coincide with a series of high-angle normal and reverse faults in bedrock formations above the Hutchinson Salt Member interpreted from a reflection seismic survey (Judy, 2015). The subsidence zone is adjacent to the west margin of Brandy Lake which results in local inundation of both driving lanes when the lake level is high. Systematic consideration of alternative mitigation approaches (Table 2) identified several approaches that have extremely high cost (ground improvement, spanning the subsidence zone with a bridge, and rerouting the highway), or are unlikely to be allowable or do not meet highway standards (controlling the level of Brandy Lake, restrict use of the highway in general or when lanes are inundated).

Two of the alternative mitigation approaches have options that could be implemented within the existing right-of-way with the use of walls and allow continued use of the highway during construction. These alternatives could be implemented with additional right of way which would also allow the use of embankments in lieu of walls.

**Approach 1)** Protect the highway from lake inundation with flood control walls or compacted earth dikes on the highway shoulders and install automated pumps to remove seepage and storm water as it accumulates in the area protected by the walls or dikes. The wall- or dike-and-pump scheme would require vigilance, monitoring, and redundancy to ensure that pumps are continuously in working order and the walls or dikes are stable. A flood control permit might be required for this scheme. Guardrail would be required because the flood control walls or dikes would be a roadside hazard. Also, culvert would have to be extended. A cost estimate has not been prepared for this option, but the high initial cost of walls or dikes, plus the ongoing maintenance costs of the pumps, make this option unfavorable.

**Approach 2)** Raise the grade of the highway on a compacted earth embankment. The compacted embankment approach is conventional highway engineering and requires no extraordinary monitoring or maintenance. It was recommended as the solution to the subsidence-and-inundation condition. The initial construction of this option was estimated at \$2.3 million based on a 30% design assuming construction in 2024 and excluding right-of-way and engineering costs. The compacted earth embankment could be constructed within the existing right-of-way if retaining walls are used. Walls would be more expensive than right-of-way acquisition and require guard rail and maintenance. The existing culvert would have to be extended with the earth embankment option. The retaining wall option could be constructed without requiring the culvert to be extended.

Kansas Department of Transportation has adopted the recommended grade raise on the existing highway. Design plans have been completed and are ready to be issued for bid as of late June 2023. One lane of traffic will be maintained during construction, alternating sides as the grade is raised. The final grade will be overbuilt to accommodate continued subsidence over the next 30 years assuming that subsidence continues as it did between November 2009 and April 2021.

**REFERENCES:**

Bayne, C. K. *Geology and ground-water resources of Reno County, Kansas*. Kansas Geological Survey, Bulletin 120, 1956, 130 p.

Herrs, A. J. Quantifying Surface Subsidence along US Highway 50, Reno County, KS, using *Terrestrial LiDAR*: Master of Science thesis, University of Kansas, Lawrence, 2010.

Judy, B. E. *High resolution seismic reflection to characterize small scale mechanisms of large-scale natural dissolution in the Hutchinson Salt Member*. Master of Science thesis, University of Kansas, Lawrence, 2015.

KDOT. *Construction Layout U.S.-50 over Brandy Lake Bridge No. 50-78-39.27(022) Sta. 81+00*. Kansas Department of Transportation Project 50-78-K-2370-01, Reno County, Sheet No. 38 of 122, 1986.

Keaton, J. R., and D. W. Eckhoff. Value engineering approach to geologic hazard risk management. *Transportation Research Record* No. 1288, 1990, pp. 168-174.

Pannalal, S. J., J. R. Keaton and M. L. Rucker. Non-destructive Surface Wave Geophysics Characterizes Salt Dissolution 140m Under US Highway 50 at Brandy Lake, Reno County, Kansas. *Proceedings, 72nd Highway Geology Symposium*, Tacoma, WA, 2023 (this proceedings volume).

Walters, R. F. *Land Subsidence in Central Kansas Related to Salt Dissolution*. Kansas Geological Survey Bulletin 214, 1978.

West, R., K. B. Miller and W. L. Watney. *The Permian System in Kansas*. Kansas Geological Survey Bulletin 257, 2010.

## **Using State-of-the-Art Technologies and Tools for Geotechnical Investigation and Design**

Brian Collins  
BGC Engineering  
Suite 300 – 600 12<sup>th</sup> Street  
Golden, CO 80401  
360-597-8211  
bcollins@bgcengineering.ca

Cole Christiansen  
BGC Engineering  
Suite 300 – 600 12<sup>th</sup> Street  
Golden, CO 80401  
720-617-1848  
cchristiansen@bgcengineering.ca

Scott Anderson  
BGC Engineering  
Suite 300 – 600 12<sup>th</sup> Street  
Golden, CO 80401  
720-617-1873  
scanderson@bgcengineering.ca

Heather Brooks  
BGC Engineering  
Suite 500 – 1000 Centre Street NE  
Calgary, AB T2E 7W6  
587-323-5541  
hbrooks@bgcengineering.ca

Denny Capps  
Denali National Park & Preserve  
P.O. Box 9  
Denali Park, AK 99755  
907-683-9598  
denny\_capps@nps.gov

Evan Garich  
Western Federal Lands Highway Division  
610 East Fifth Street  
Vancouver, WA, 98660  
360-619-7824  
evan.garich@dot.gov

## **Disclaimer**

Statements and views presented in this paper are strictly those of the author(s), and do not necessarily reflect positions held by their affiliations, the Highway Geology Symposium (HGS), or others acknowledged above. The mention of trade names for commercial products does not imply the approval or endorsement by HGS.

Copyright © 2023 Highway Geology Symposium (HGS)

All Rights Reserved. Printed in the United States of America. No part of this publication may be reproduced or copied in any form or by any means – graphic, electronic, or mechanical, including photocopying, taping, or information storage and retrieval systems – without prior written permission of the HGS. This excludes the original author(s).

## **ABSTRACT**

A variety of innovative site investigation and subsurface modeling tools were implemented for the site investigation and design of a 475-foot single span bridge over the Pretty Rocks Landslide in Denali National Park. Remote sensing at the site included terrestrial and airborne lidar, InSAR, photogrammetry, and timelapse cameras. Site investigations included structural geologic mapping, helicopter-access drilling investigations, surface and downhole geophysical surveys, a weather station, and installation of remote monitoring units to transmit near-real-time weather, photo, and borehole instrumentation data. The site investigation data was loaded into an interactive GIS software platform with a live link to active instrumentation. These tools were used to inform decisions on bridge design, location, and alignment. For the design phase, a 3D geological model was developed to inform bridge foundation analysis and design. In addition, a 3D model of the proposed project was built that included the road alignment, cut and fill slopes, retaining walls, bridge superstructure and foundation, and geotechnical subsurface elements including thermosiphons, soil nails, micropiles, ground anchors, and rock dowels. The 3D model was available to the design team through a mobile App, a desktop App, and through a mixed reality headset. This tool was used to communicate the features of the design to the design team, the owner, the contractor, and other project stakeholders.

## INTRODUCTION

A variety of innovative and new site investigation and subsurface modeling tools were implemented for the site investigation and design of a 475-foot, single-span bridge over the Pretty Rocks Landslide in Denali National Park and Preserve (DNA), Alaska. Many of the tools implemented were part of the Federal Highway Administration (FHWA) Every Day Counts (EDC) No. 5 Advanced Geotechnical Methods of Exploration (A-GaME) initiative to deploy proven, yet underutilized technologies. These tools can be implemented on many projects to improve the understanding of the site and subsurface conditions. The project team includes consultants, the Federal Highway Administration (FHWA), the National Park Service (NPS), and a contractor. We used these tools to communicate complex site conditions and design concepts to both technical and non-technical professionals on the team as well as other project stakeholders.

## PROJECT BACKGROUND

The Denali Park Road is a 92.5 mile long dead-end road that heads west from the park entrance near Healy, Alaska to remote Kantishna, an outpost within in the heart of DNA. The first 15 miles of the Park Road is paved and open to public traffic. Past Mile 15, visitors are transported on buses to limit the number of vehicles traveling the Park Road. This project site is located at the Pretty Rocks Landslide at milepost 45.4. While the road is currently closed near the midpoint by the Pretty Rocks Landslide, the first half remains fully accessible to visitors and staff. A composite photograph of the landslide is shown in Figure 1 (1).

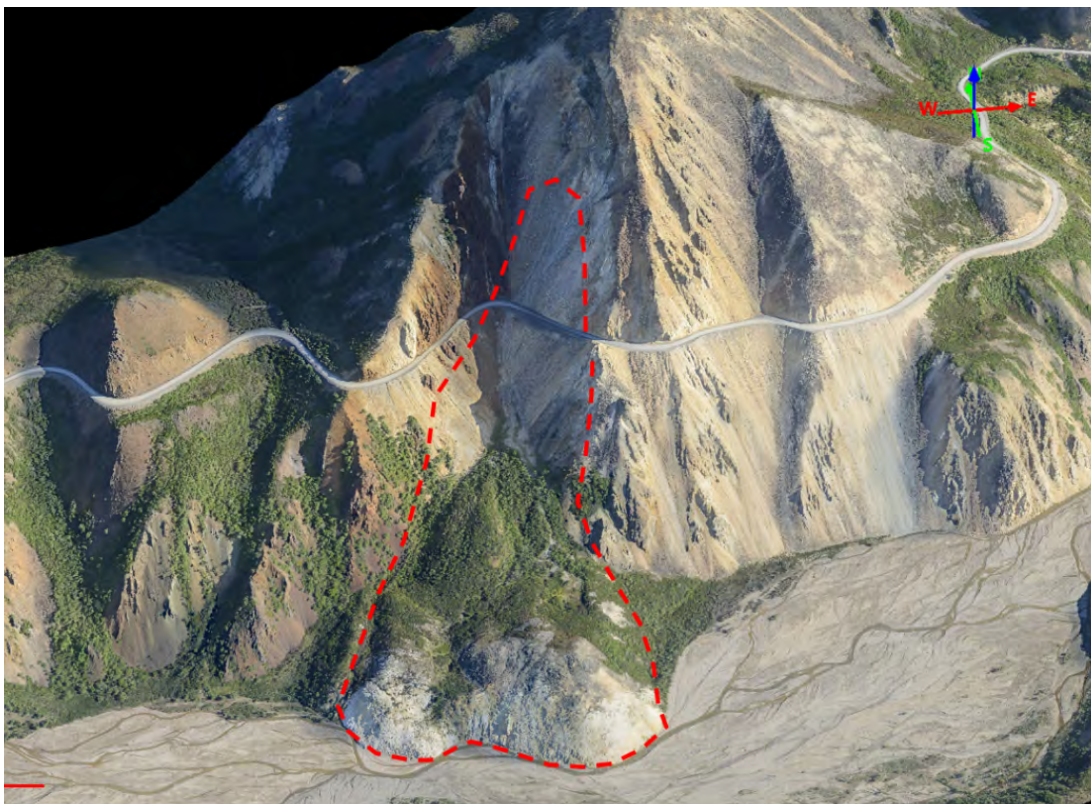


**Figure 1 - Composite photo of the Pretty Rocks Landslide from 2015 with approximate landslide outline indicated by red dashed line (1).**

The Denali Park Road was constructed across the Pretty Rocks Landslide in an area known as Polychrome Pass during the 1930s. It is unknown whether it was recognized as a landslide at the time, but by the 1980s, efforts were being made to maintain the serviceability of the road with maintenance every two to three years (2). In 2004, it was estimated that the annual vertical movement was between 1 and 3 inches per month. An increased rate of movement was noted by maintenance personnel in 2014; and in 2016 and 2017 the movement rate was estimated to be several inches per month through the summer. Between September 2018 and March 2019, the movement averaged approximately 12 inches per month. Between August of 2019 and January of 2020, the road was dropping an average of approximately 5 feet per month. At this time landslide movement was measured to be greatest in the summer and fall, decreasing in the winter and spring. Significant efforts were required to repair the road for spring road opening in 2021, and daily grading operations continued throughout the summer of 2021 to keep the road open. In August of 2021, maintenance efforts were no longer able to keep up with the slide movement and the National Park Service (NPS) decided it was no longer safe to keep the road open, so the road was closed at the Pretty Rocks Landslide. Based on a field laser rangefinder survey, the total vertical movement of the roadway was more than 60 feet between September 2021 and April 2023. NPS and Western Federal Lands Highway Division (WFLHD) studied design options for bypassing or repairing the slide completely. A bridge over the landslide was the preferred alternative selected by WFLHD and NPS.

The scope of work for the consultant design team on the project includes designing the 475-foot span bridge and the approach cut slopes and retaining walls. Thermosiphons were also part of the design due to a layer of ice encountered below the proposed Abutment No. 1. A conceptual image of the proposed bridge and other major project elements, which is a screenshot of a fully three dimensional (3D) mixed reality model used by the team, is shown in Figure 2.

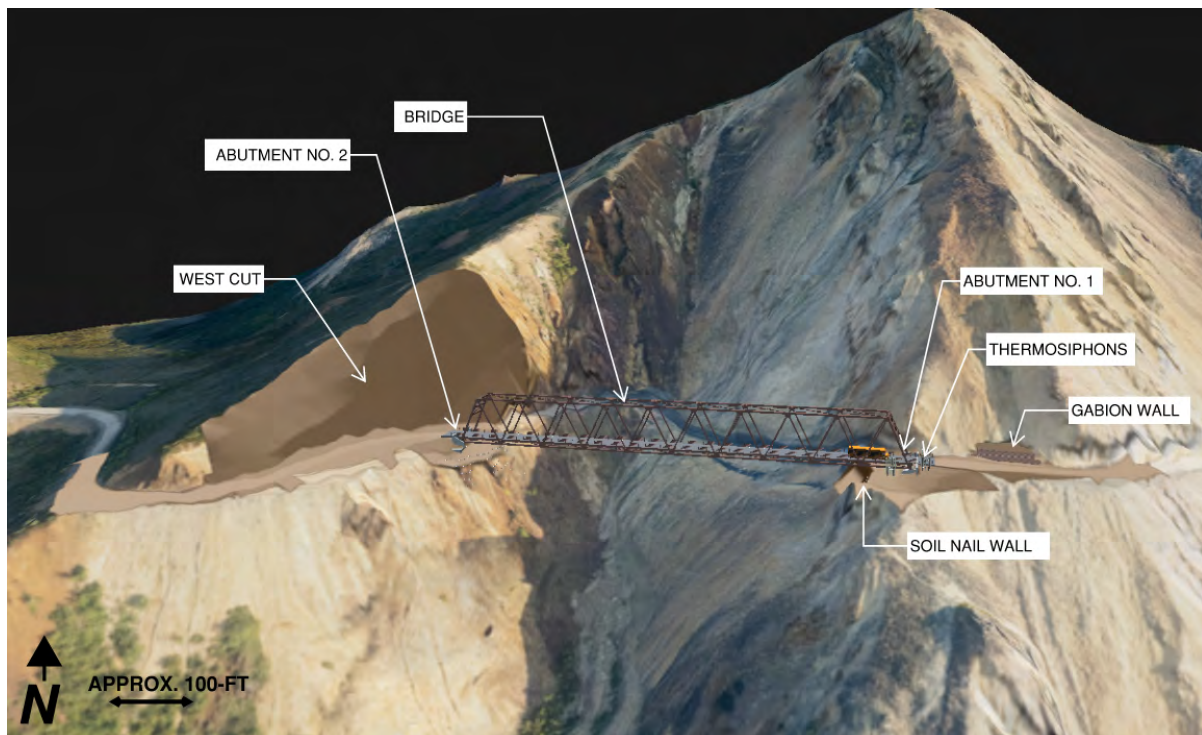


**Figure 2 - Proposed Bridge and Related Project Features.**

## REMOTE SENSING

A variety of remote sensing techniques were used to understand the movement within the landslide mass over time. Remote sensing at the site included InSAR, terrestrial and airborne lidar, and photogrammetry.

The airborne lidar, photogrammetry, and terrestrial lidar surfaces collected at the site are summarized in Table 1. These data are all hosted in the Cambio<sup>TM, 1</sup> web-based platform for easy visualization of these different data sources in a single view. An example of a lidar change detection plot in Cambio is shown in Figure 3.

**Table 1 - Airborne lidar, photogrammetry, and terrestrial lidar surfaces collected at Pretty Rocks Landslide.**

Data Type	Date	Provider	Vendor
Airborne Lidar	07/30/2018	Western Federal Lands Highway Division	Kodiak Mapping Inc.
	08/24/2022	DENA	The National Center for Airborne Laser Mapping
Photogrammetry /Fodar	06/15/2015	DENA	Fairbanks Fodar
	05/11/2017	DENA	Fairbanks Fodar
	08/20/2019	DENA	Fairbanks Fodar
	09/01/2021	DENA	Fairbanks Fodar
	04/07/2023	DENA	DENA
Terrestrial Lidar	05/26/2021	DENA	NPS Regional Office
	06/10/2021	DENA	DENA
	07/08/2021	DENA	DENA
	07/29/2021	DENA	DENA
	08/18/2021	DENA	NPS Regional Office, DENA
	09/14/2021	DENA	DENA

---

<sup>1</sup> Cambio<sup>TM</sup> is proprietary software developed and hosted by BGC to store site investigation data, historical studies or actions at the sites (e.g., surveys, geotechnical investigation logs, as-built reports, inspections, etc.), and recommendations, and to maintain an audit trail for the site.

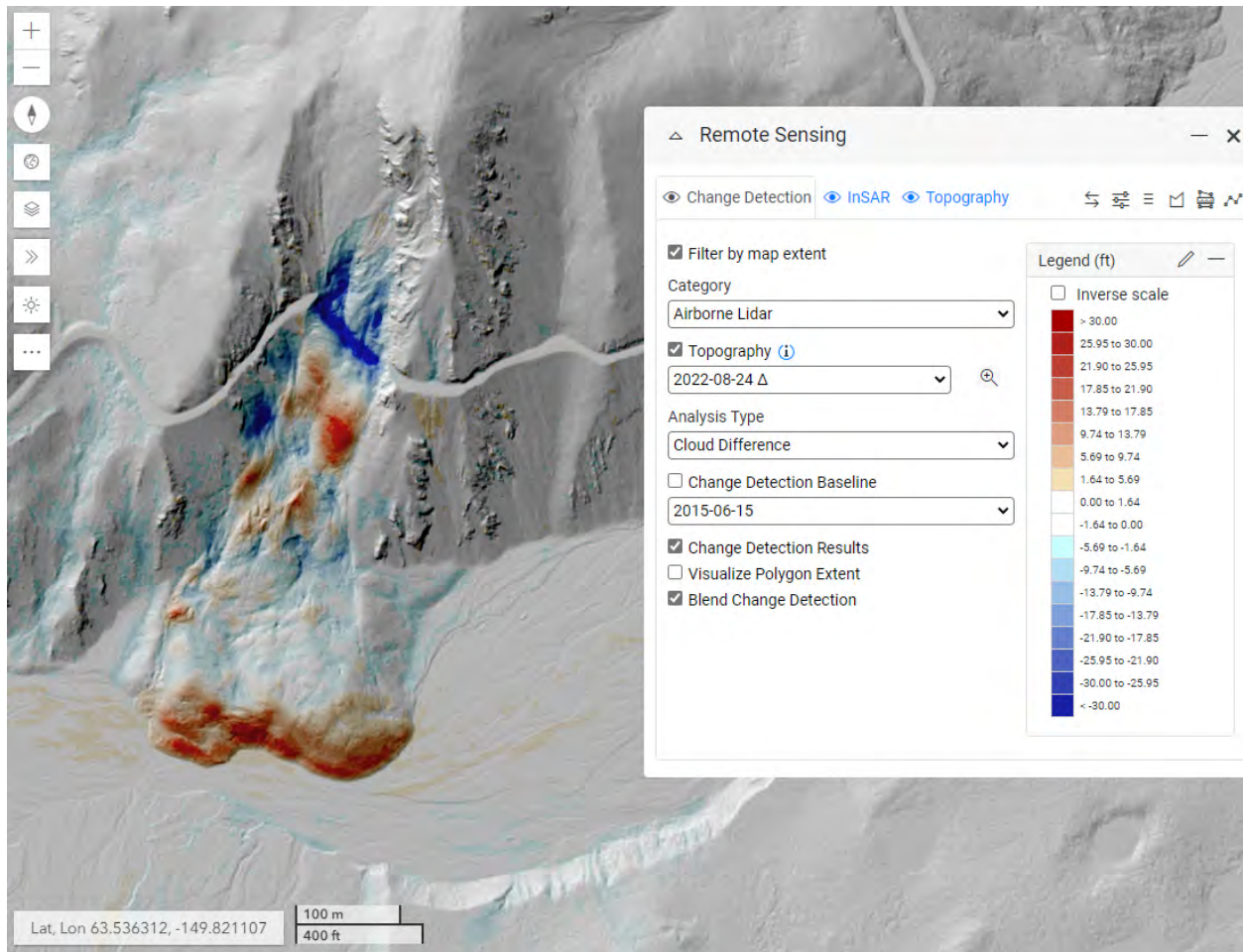


**Figure 3 - Lidar Change Detection between 6/15/2015 to 8/24/2022, viewed in Cambio.**

Change detection is measured from different data sources (airborne lidar, photogrammetry, terrestrial lidar) and in some cases, different lidar returns, each with different limitations, such as look angles, vegetation, snow cover and other considerations. The lidar datasets were analyzed for topographical change using a custom software developed by BGC. BGC used the M3C2 algorithm and an iterative closest point method of comparison and alignment of point cloud data to minimize the potential error and the limit of detection for meaningful movement (3). These values are a function of the original data quality and alignment, and some limitations and anomalies are inherent given the different sources (Table 1). The data here are of sufficient quality they can be used to assess movement trends and conditions across the site. The data and change detection results are presented in Cambio so that they can be viewed two-dimensionally (2D) in plan and profile, in 3D, compared spatially with other observations, and so that direct measurements of change can be made. In Cambio and in Figure 3, positive change is shown in a warm color and negative change is shown in a cool color, according to the dynamic change detection scale chosen and the legends presented. Positive change can be interpreted as material accumulation or bulging of the surface, and negative change can be interpreted as a settlement or loss of material. No color is shown where the change is less than the set limit of detection. This limit can be varied by the user, but the default level of  $\pm 1.64$  ft is set to minimize noise or error in the data and only present real changes due to ground move



boreholes were drilled to evaluate feasibility and constructability of a bridging and earthwork option at the Pretty Rocks Landslide. Between 2021 and 2022, 18 boreholes were completed to investigate proposed bridge foundation locations and proposed road alignments.

## **Geophysics**

Geophysical investigations of several sections of the Denali Park Road were completed in August 2016 (4). The purpose of these investigations was to determine the presence and extent of subsurface features and anomalies impacting road infrastructure. Geophysical techniques such as capacitive-couple resistivity (CCR), ground-penetrating radar (GPR) and electrical resistivity tomography (ERT) were utilized to survey the subsurface and the Pretty Rocks Landslide on Polychrome Pass (MP 44-46) was one of the locations surveyed.

During the 2021 and 2022 field investigation, BGC collected electrical resistivity tomography (ERT), seismic refraction tomography (SRT), and multi-channel analysis of surface waves (MASW) data along four surface profiles at the site. In addition to surface geophysics, vertical seismic profiling (VSP) data were also collected every 1.64 ft starting from the bottom of the borehole in three of the 2021 boreholes. The VSP data were used to develop shear wave velocity profiles that were used in the site-specific probabilistic seismic hazard analysis.

## **In Situ Testing**

The boreholes were advanced with hollow-stem auger, casing advancer, and HQ3 coring techniques. Standard Penetration Tests (SPTs) were completed to characterize the relative density and collect samples of the overburden. Downhole televiewer surveys were completed along uncased sections of boreholes in bedrock to characterize the discontinuities in the geologic units across the site. Downhole acoustic televiewer (ATV) surveys were completed in boreholes where groundwater was present and optical televiewer (OTV) surveys were completed in boreholes where groundwater was absent. The ATV survey produces a subsurface velocity profile that can delineate geological structure within the borehole wall. OTV survey methods use a downhole camera to record a photo of the borehole wall. Depth, dip, dip direction and aperture of discontinuities were determined from both the ATV and OTV surveys. An example OTV survey is shown in Figure 5 along with the core box photograph from the same interval (5). Figure 5 illustrates the benefit of the televiewer; layers of soil-filled discontinuities that are difficult to accurately describe because they are usually washed out of core can be clearly seen in the televiewer image log.

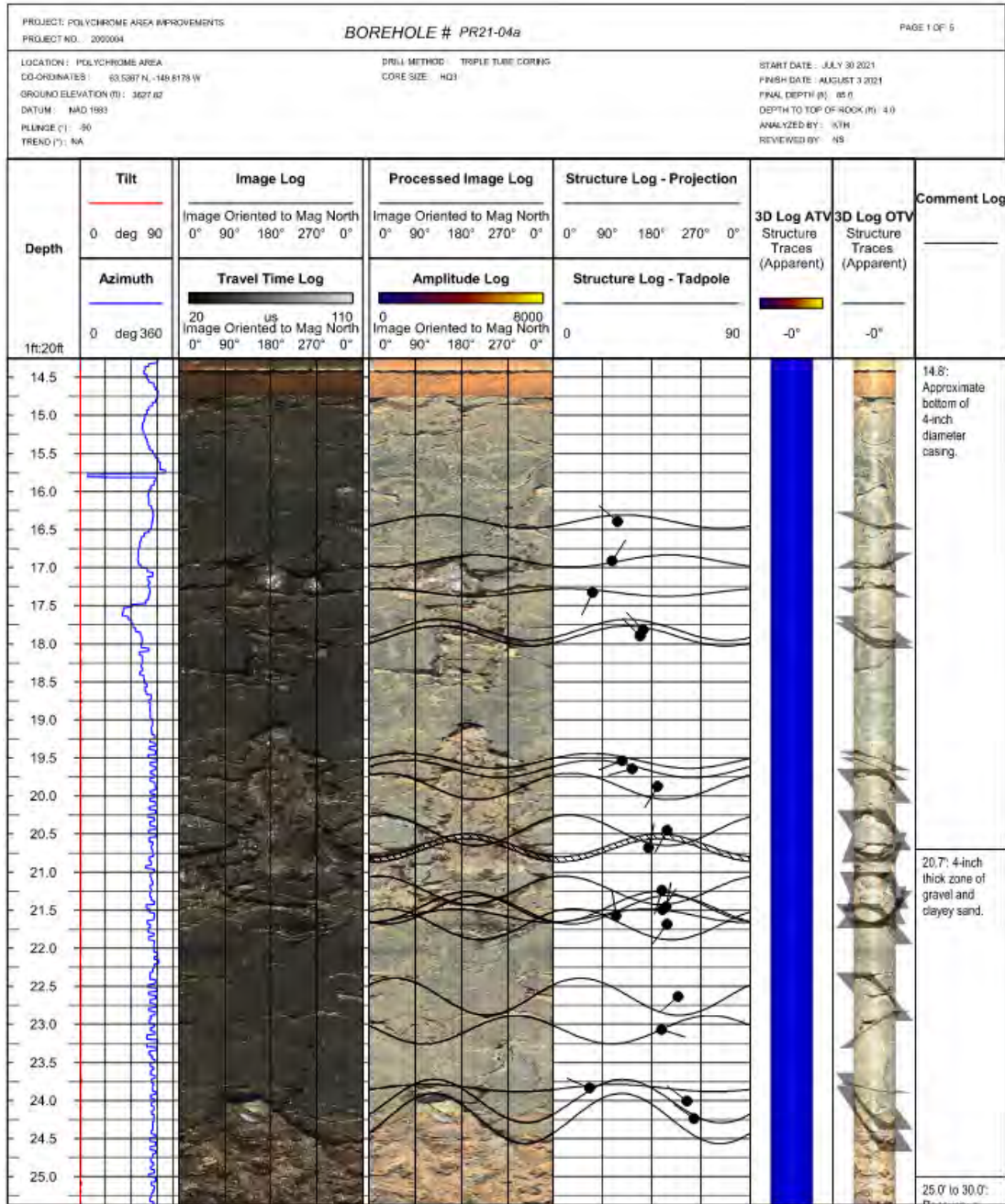


Figure 5 - Example Optical Televier Survey Report and Core Box from Same Interval.

The discontinuity data from the OTV and ATV surveys was combined with data collected from surface mapping and imported into BGC software to plot stereonet and interpretive kinematic plots that were used for slope stability analysis and cut slope design.

## **Instrumentation**

Geotechnical instrumentation was installed in boreholes to record in situ measurements and detect changes in the subsurface conditions over time. The instrumentation included vibrating wire piezometers, inclinometer casings, ShapeAccelArrays (SAA), thermistor strings, and temperature sensors.

### *Vibrating Wire Piezometers*

Vibrating wire piezometers (VWPs) were installed in most of the boreholes across the site to record pore water pressures. Typically, groundwater measurements with VWPs are some of the most useful data collected as part of a site investigation; however, at this site, the VWP data from the boreholes outside of the limits of the Pretty Rocks Landslide showed either: 1) dry conditions (i.e., the sensor did not observe a water table), or 2) frozen conditions (i.e., the sensor is located in a zone with an average ground temperature below freezing).

### *Slope Inclinometer Casing*

Slope inclinometer casing was installed in select 2018 and 2019 boreholes to record subsurface ground movement. Slope inclinometer casing requires a technician to manually complete readings using a slope inclinometer probe. Although typically it may take weeks or months to record subsurface landslide movement in an inclinometer casing, the rate of movement of the casings in boreholes within the Pretty Rocks Landslide was such that within days following installation the depth of the failure plane was recorded. The casings were typically displaced to the point where the probe could no longer pass within two weeks.

### *ShapeAccelArrays*

ShapeAccelArrays (SAAs) were installed in selected boreholes to record subsurface ground movement. SAAs consist of a series of micro-electro-mechanical systems accelerometers at selected intervals along a cable that is installed into casing inside the borehole and used to measure subsurface ground displacement. Although the SAAs serve a similar function as inclinometer casing, they can generally measure greater magnitudes of ground deformation before instrument failure when compared to slope inclinometer casing. The SAAs remain in the casing and record ground movement over time. The collected data is viewed through an online interface, Vista Data Vision.

Three SAAs were installed in boreholes within the limits of the Pretty Rocks Landslide as part of the 2018 subsurface investigation. These SAAs were eventually abandoned in place due to the magnitude of displacement. These SAAs recorded displacements as great as 68 inches over a 175-day monitoring period between August 2018 and February 2019 before shearing and termination of sensor function.

Five SAAs were installed in boreholes along the flanks of the Pretty Rocks Landslide during the 2021 and 2022 subsurface investigations to monitor for ground movement at potential bridge foundation locations. These SAAs are connected to an automated data acquisition system that collects the data and transmits it via satellite uplink in near real-time to a database. The collected data are viewed through an online interface, Vista Data Vision.

### *Thermistor Strings*

Thermistor strings were installed in one of the 2003 boreholes, five 2018 boreholes, three 2019 boreholes, and two of the 2021 boreholes. The two thermistor strings installed in 2021 are connected to the automated data acquisition system. Thermistor strings consist of a cable with thermistors located at selected intervals (typically two- or five-foot) installed into casing in the borehole and used to measure subsurface temperatures. Eight of the ten thermistor strings indicated the presence of permafrost, and the data indicates that the upper layer of the permafrost has temperatures between 0 and -1°C. It is interpreted that warming of the permafrost at the site is a likely contributor to the observed accelerated landslide movement.

### *Temperature Sensors*

Temperature sensors consist of a single temperature sensor and data logger and are placed at various depths within a borehole. Temperature sensors were placed in one of the 2021 boreholes.

### *Timelapse Camera*

A timelapse camera installed on the west side of the Pretty Rocks Landslide with a view of the road crossing over the landslide was installed by the DENA geology team. Videos made from the timelapse photographs can be viewed on the DENA website (6) at <https://www.nps.gov/dena/learn/nature/pretty-rocks.htm>. This tool was useful for communicating the landslide rate of movement to both technical and non-technical project stakeholders.

## **Geologic Field Mapping**

Geologic field mapping was completed by two geologists in 2022. The field work included mapping the stratigraphic and structural geologic relationships of the Teklanika Volcanics exposed at the proposed abutments and surrounding vicinity, the structural rock mass joint orientations, annotating field photos, and obtaining 3D lidar scans of the west abutment outcrop along the Denali Park Road. Geologic surface mapping was instrumental in connecting subsurface data in the 3D geological model. The results of this field investigation and borehole and instrumentation program were used to provide site-specific geological information and empirical inputs into subsequent kinematic slope analyses.

## **3D MODELS**

For the design phase, a 3D geological model was developed to inform the project geotechnical analysis and design. In addition, a 3D model of the proposed project was built to

communicate the features of the design to the design team, the owner, the contractor, and other project stakeholders.

### **Leapfrog Model**

Because of the site's complex geologic structure, a geologic model consisting of 3D triangular mesh surfaces was created using Leapfrog Works (7) for the east and west sides of the Pretty Rocks Landslide. The surfaces represent geotechnical unit boundaries that were used for thermal modeling and stability analyses, and were created using the following data:

- Drillhole logs (unit contacts)
- Televiwer surveys (unit contact orientations)
- Structural mapping (unit contact orientations and regional trends)
- Geologic mapping (unit contacts)
- Geophysics (frozen colluvium/bedrock contact).

Surfaces were fit through the contact points identified in the drillhole logs and geologic mapping and given orientations based on the televiwer and structural mapping data. In areas where the location or orientation of the contacts was poorly constrained, a regional orientation determined from structural mapping was applied to the surface. The base of the frozen colluvium surface along the west ridge was also defined using electrical resistivity geophysical data (5).

In addition, the major design elements were added to the Leapfrog model:

- Proposed bridge,
- Proposed footing,
- Proposed foundation ground anchors and micropiles,
- Proposed soil nail wall and soil nails,
- Proposed thermosiphons,
- Proposed gabion wall, and
- Proposed west cut slope.

Screenshots of the 3D geologic model are shown in Figure 6 and Figure 7. The top image in Figure 6 has all the geologic contacts projected onto the surface of the digital elevation model (DEM) with orthophotos overlaid onto it. The lower image has the DEM/orthophoto opacity set to 20 percent, which reveals the geologic contacts (shown as planes) with the design elements. The geologic units encountered in the boreholes are color-coded and the boreholes are over-sized for viewing clarity. Figure 7 illustrates the inclusion of the geophysical survey (ERT) results in the model combined with a 3D surface of the proposed west cut.

This model was the primary communication tool between engineering geologists and geotechnical engineers and used to create geotechnical design models for foundation analysis, wall analysis, and slope stability analysis. The software allowed the geotechnical design team to directly cut 2D cross-sections for model input and import the model coordinates directly into other software. The 3D geologic model was directly used in the setup of the 3D thermal model of the east side of the project (8). The 3D geologic model was used to review for possible conflicts of the subsurface geotechnical elements, including ground anchors, micropiles, soil nails, rock dowels, and thermosiphons.

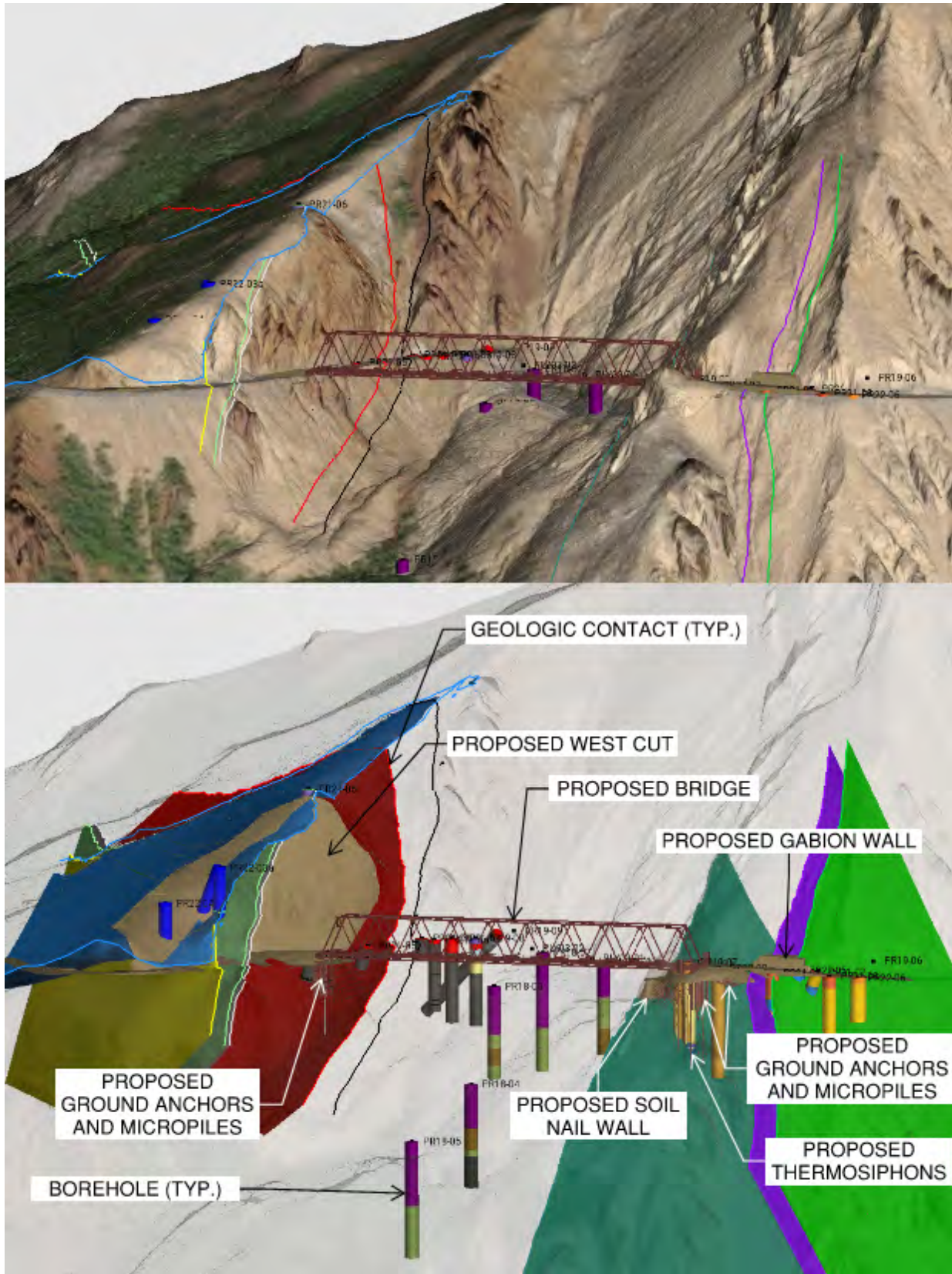


**Figure 6 - Screenshots of 3D Geologic Model, with DEM on (Top) and with DEM/orthophoto at 20% Opacity (Bottom).**

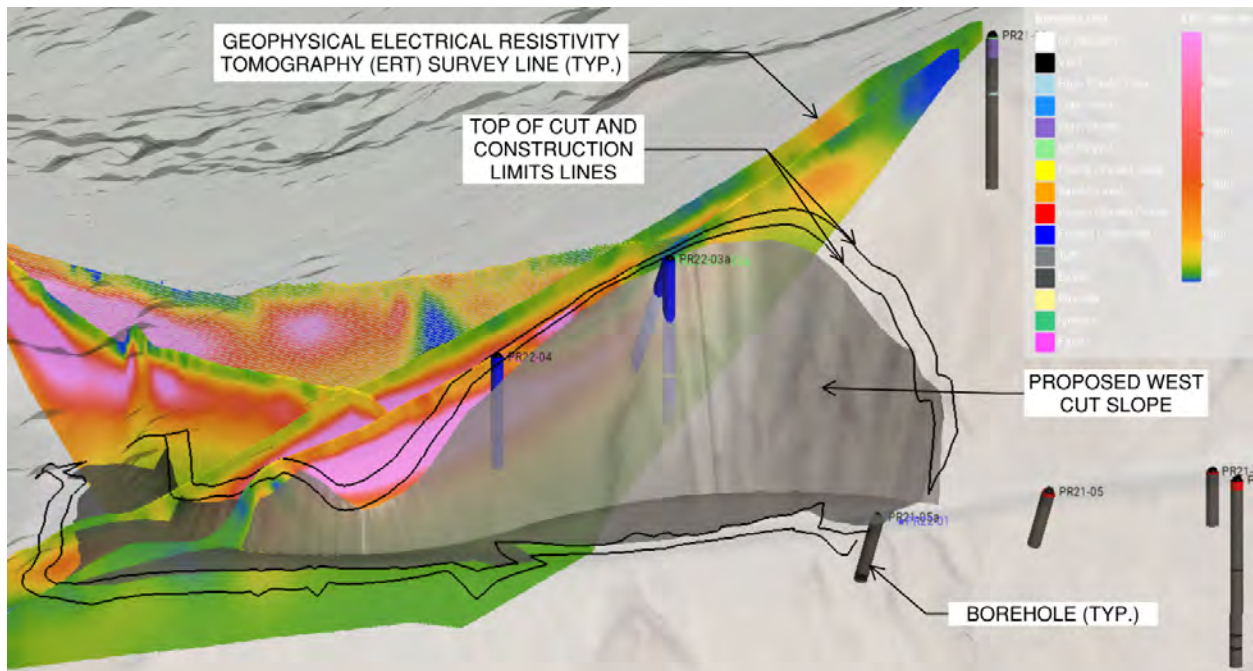


**Figure 7 - 3D Geologic Model of West Cut with Electrical Resistivity Tomography Survey Lines Shown and DEM/orthophoto at 20% Opacity.**

### Clirio Model

A 3D model of the proposed project was built in collaboration with Clirio that included the road alignment, cut and fill slopes, retaining walls, bridge superstructure and foundation, and geotechnical subsurface elements including thermosiphons, soil nails, micropiles, ground anchors, and rock dowels. The 3D model was available to the design team through a mobile App, a desktop App, and through a mixed-reality headset. This tool was used to communicate the features of the design to the design team, the owner, the contractor, and other stakeholders. An example ‘screenshot’ of the Clirio model is shown in Figure 8, though the term ‘screenshot’ is not very accurate because the mixed reality model exists in space and only through user choice is it projected to a screen. The major design features that can be seen in Figure 8 include the west cut, the bridge, a soil nail wall, a gabion wall, and thermosiphons. The upper image is a view of the project from the west approach road and the lower image is an underground view looking up at the foundation and soil nail wall elements at Abutment No. 1 (east abutment), including soil nails, ground anchors, micropiles, and thermosiphons.

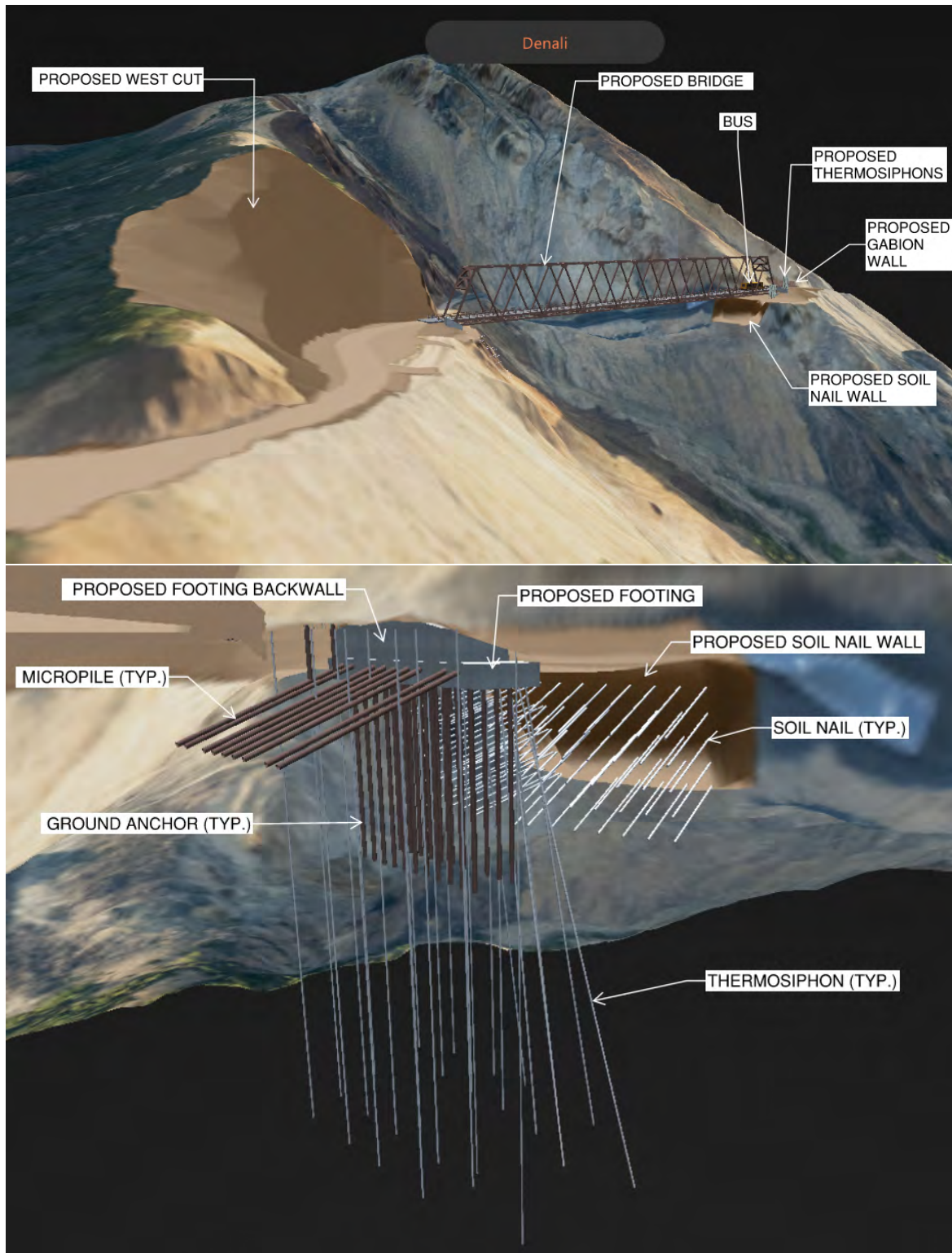


**Figure 8 – Clirio Screenshots of Proposed Construction. Upper Image is from West Approach Road. Lower Image is Below Ground View Looking Southwest towards Abutment No. 1 and the Soil Nail Wall.**

## SUMMARY AND CONCLUSIONS

A variety of new site investigation and subsurface modeling tools were implemented for the site investigation and design of a 475-foot single span bridge over the Pretty Rocks Landslide in DENA. The tools include several methods of remote sensing and photogrammetry, surface and downhole geophysical surveys, televiwer surveys, and remote monitoring of geotechnical instrumentation. Many of the tools implemented were part of the FHWA EDC-5 A-GaME initiative to deploy proven, yet underutilized technologies. These tools, combined with more conventional geotechnical investigation methods, were used to create a 3D geological model of the site that was used to support the design of the bridge, retaining walls, and cut slopes on the project. The tools were also used to support development of a 3D model of the project that was used to communicate the features of the design to the design team, the owner, the contractor, and other stakeholders. These tools can be implemented on many projects to improve the understanding of the site and subsurface conditions.

## REFERENCES

1. National Park Service. *Composite photo of the Pretty Rocks Landslide area from 2015*. <https://www.nps.gov/dena/learn/nature/pretty-rocks.htm>. Accessed April 4, 2023.
2. Western Federal Lands Highway Division (WFLHD). (2020). *Geotechnical Report No. 11-20, Pretty Rocks Landslide 2018-2019 Geotechnical Investigation and Conceptual Design Alternatives Report*.
3. Lato, M., van Veen, M., Ferrier, A., Weidner, L., and Graham, A. (2022) *Predicting the future by mapping the past: revolutionary innovations in Lidar change detection analysis are enabling regional scale mapping and identification of threats from geohazards*. Proceedings of the ASME 2022 13th International Pipeline Conference.
4. Bjella, K., Saari, S., Balsler, A., and Staples, A. (2017) *Denali National Park Roadway – Geophysical Investigations*, US Army Engineer Research and Development Center, Cold Regions Research and Engineering Laboratory, 89p.
5. BGC Engineering USA Inc. (2022, February 25). *Geotechnical Report 01-22, AK NPS DENA 10(49), Polychrome Area Improvements – Geotechnical Data Report*. Prepared for Western Federal Lands Highway Division, Federal Highway Administration, FHWA.
6. National Park Service Geology Team. *Time lapse of the Pretty Rocks Slump from July 21 to August 25, 2021*. <https://www.nps.gov/dena/learn/nature/pretty-rocks.htm>. Accessed June 30, 2023.
7. Seequent Limited. (2022). Leapfrog Works Software v.2021.2.4. Bentley Systems.
8. BGC Engineering USA Inc. (2022, March 29). *Geotechnical Report 06-22, Polychrome Area Improvements – Geotechnical Modeling Report*. Prepared for Western Federal Lands Highway Division, Federal Highway Administration, FHWA.

### **DISCLAIMER**

Statements and views presented in this paper are strictly those of the author(s), and do not necessarily reflect positions held by their affiliations, the Highway Geology Symposium (HGS), or others acknowledged above. The mention of trade names for commercial products does not imply the approval or endorsement by HGS.

### **COPYRIGHT NOTICE**

Copyright © 2023 Highway Geology Symposium (HGS)

All Rights Reserved. Printed in the United States of America. No part of this publication may be reproduced or copied in any form or by any means – graphic, electronic, or mechanical, including photocopying, taping, or information storage and retrieval systems – without prior written permission of the HGS. This excludes the original author(s).

**The Development and Utilization of a Cloud-Based Database and  
Visualization App for Pile Results and Design: PileTrac**

**Kyle Halverson**

Kansas Department of Transportation  
700 SW Harrison St  
Topeka, KS 66603  
(785) 291-3860  
Email: [kyle.halverson@ks.gov](mailto:kyle.halverson@ks.gov)

**William C Jones, P.E., P.G.**

Foundation Testing & Consulting LLC  
16500 Lucille St.  
Overland Park, KS 66062  
913-626-8499  
Email: [FTandC.com](mailto:FTandC.com)

Prepared for the 72<sup>nd</sup> Highway Geology Symposium, August, 2023

### **Acknowledgements**

Recognition is given to the following individuals for their assistance in facilitating and compiling current and historic data that has allowed Kansas DOT to progress forward with the development and utilization of PileTrac:

Casey Jones, P.E., P.G.: Foundation Testing and Consulting LLC  
Ronan Jones: Foundation Testing and Consulting LLC  
Ed Lewis: Kansas Department of Transportation  
Bob Henthorne, P.G.: Professional Engineering Consultants

### **Disclaimer**

Statements and views presented in this paper are strictly those of the author(s), and do not necessarily reflect positions held by their affiliations, the Highway Geology Symposium (HGS), or others acknowledged above. The mention of trade names for commercial products does not imply the approval or endorsement by HGS.

### **Copyright Notice**

Copyright © 2023 Highway Geology Symposium (HGS)

All Rights Reserved. Printed in the United States of America. No part of this publication may be reproduced or copied in any form or by any means – graphic, electronic, or mechanical, including photocopying, taping, or information storage and retrieval systems – without prior written permission of the HGS. This excludes the original author(s).

## ABSTRACT

The Kansas Department of Transportation (KDOT) with the assistance of Foundation Testing and Consulting (FTC) is utilizing a cloud-based database and visualization application called PileTrac for providing results of high-strain dynamic pile tests. This is done by using the PDA to provide a resource for the design and installation of pile supported bridges.

FTC developed the PileTrac application initially using data obtained from 58 bridge projects across the state of Kansas (50 FTC projects and 8 KDOT). The initial data sets in Piletrac showed KDOT an opportunity to make data driven decisions as it pertains to pile foundation design.

PileTrac allows KDOT, or other users, to identify common factors when piling has been driven much shallower or greater than plan, typical pile capacities for various pile section types and sizes, typical pile penetration depths in specific soil and bedrock profiles, as well as a variety of other pile and subsurface related values that help better guide pile design decisions and installation expectations

As FTC continues to add new data sets into PileTrac, it is expected that KDOT will be able to refine recommendations to pile supported bridges and better predict outcomes for pile design and installation on future projects.

## INTRODUCTION

In June 2020, the Kansas State Legislature passed the IKE Transportation Program. This program is the fourth comprehensive transportation program for the Kansas Department of Transportation (KDOT). Unlike previous programs, this program came right at the beginning of a global pandemic with historic work and material shortages. As many industries slowed or shut down, KDOT continued to march forward with designing and constructing new projects. These obstacles showed KDOT that it needed to be more accurate and efficient when making recommendations for foundations, in particular pile foundations. In an attempt to become more efficient, KDOT met with local geotechnical consultant Foundation Testing and Consultants (FTC), to discuss refining pile recommendations to help offset the material shortages and supply chain demands. FTC presented KDOT with the idea of creating cloud-based database and visualization application that could analyze historic pile data that could compare current projects to make data driven recommendations. This initial idea grew to what is now PileTrac.

## PILETRAC BACKGROUND AND DEVELOPMENT

FTC developed the PileTrac application initially using data obtained from 58 bridge projects across the state of Kansas (50 FTC projects and 8 KDOT). FTC has pile installation records associated with several hundred PDA tests for projects in Kansas and neighboring states. The initial data sets in Piletrac showed KDOT an opportunity to make data driven decisions as it pertains to pile foundation design. PileTrac allows KDOT or other users to identify common factors when piling has been driven much shallower or greater than plan, typical pile capacities for various pile section types and sizes, typical pile penetration depths in specific soil and bedrock profiles, as well as a variety of other pile and subsurface related values. These common factors help guide pile design decisions and installation expectations.

PileTrac additionally continues to expand to encompass more of the KDOT’s historical pile installation records. Currently, KDOT has installation data for over 150 driven piles entered

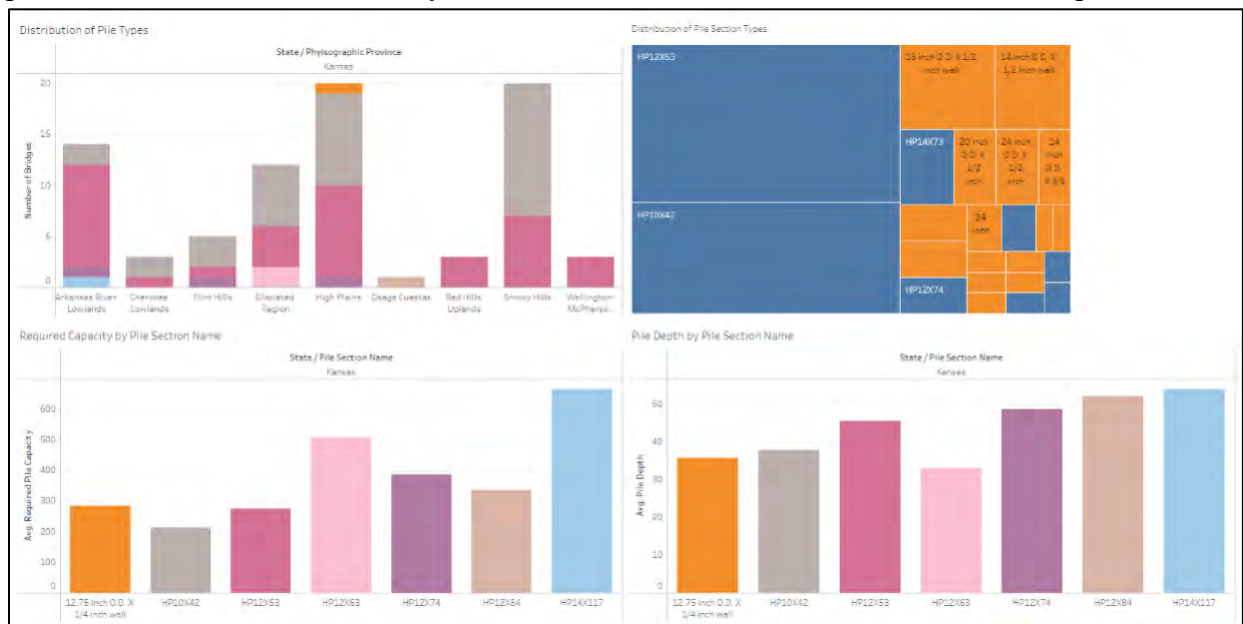


Figure 1: PileTrac Dashboard- Distribution of Pile Types

into PileTrac, and as more records are keyed into PileTrac, KDOT's ability to look at more projects in various locations across the state with similar site conditions increases. In Figure 1, above, is a visual representation of pile type distribution along with the geologic setting is displayed.

## KANSAS GEOLOGY AND FOUNDATION TYPE

The KDOT's most common foundation type is an H-Pile footing. Geologically, Kansas is separated into eleven (11) different physiographic regions as seen in Figure 2. These regions play a significant role in determining which foundations will be utilized on a specific KDOT structure. In the High Plains, the Arkansas River Lowlands, and the Wellington-McPherson Lowlands, end-bearing H-Pile are exclusively used due to the relatively shallow depth to bedrock. In the Smoky Hills and the Glaciated Region of Kansas, H-Pile are predominately used but not exclusively. All the other physiographic regions utilize H-Pile but other foundation types such as drilled shafts and spread footing are generally considered more cost effective. Furthermore, generally speaking, the depth of bedrock significantly increases from east to west across the state. Where this is not always the case, an adequate geotechnical investigation can help refine foundation recommendations.

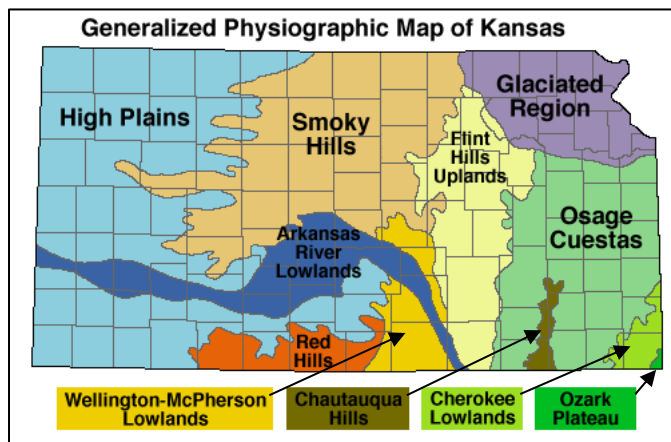


Figure 2: Generalized Physiographic Map of Kansas with arrows indicating smaller regions within the state

The recommendations for a specific foundation type are looked at in various scenarios; depth to bedrock, subsurface conditions, and scour potential to name a few. In Southeast Kansas where bedrock is Pennsylvanian to Mississippian aged with thicker limestone and shale sequences and near the surface, drill shafts and spread footings are a better recommendation. Conversely in Northwest Kansas, where Quaternary aged alluvium deposited from the erosion of the Rocky Mountains covers western Kansas the depth to bedrock can exceed 120 feet below surface. At these locations H-Pile recommendations (based on side friction design) are more suitable.

## KDOT BRIDGE FOUNDATION RECOMMENDATION

Bridge Foundation Geology Reports (BFGR) are produced for every bridge size structure on KDOT's system. These reports date back to the early 1950s when KDOT was the Kansas Department of Roads. Over the years these reports have changed along with standards, guidance, and specifications. As a result, KDOT has a significant amount of historical data. However, a lot of this historical data, while helpful in the initial stages of the bridge foundation investigation, does not provide much assistance when making recommendations for today's standards.

A BFGR will include sections describing the underlying geology and its characteristics, foundations recommendations, hydrology, site specific seismic site classification, lateral load analysis, investigation procedures, and boring logs. Commonly, foundation recommendations will provide bridge designers with options from piling to drilled shafts and spread footings that suit the subsurface conditions. Additionally, these recommendations will indicate the anticipated maximum depth of the recommended foundation type along with nominal and factored geotechnical resistances. The Figure 3 below is an example of how KDOT Geology summarizes piling recommendations within a BFGR.

**Ramp L over UPRR**  
**Br. No. 96 -87-25.89 (864)**  
**Centerline Elevation information for H-pile**

Location	Station	Top of Bedrock Elevation	HP-10x42 Tip Elevation	HP-12x53 Tip Elevation	HP-12x74 Tip Elevation	HP-14x89 Tip Elevation
Abut. 1	1051+24.39	1283.5	1263.0	1263.0	1263.0	1263.0
Pier 1	1052+04.39	1283.7	1263.0	1263.0	1263.0	1263.0
Pier 2	1053+23.39	1284.3	1263.0	1263.0	1263.0	1263.0
Abut. 2	1054+05.04	1286.1	1263.0	1263.0	1263.0	1263.0

**LRFD Design**  
**Resistance and Phi Factor Information**

	HP-10x42	HP-12x53	HP-12x74	HP-14x89
$R_n$ (kips)	310	388	545	653
$R_r$ (kips)	186	233	327	392
Phi	0.60	0.60	0.60	0.60

Figure 3: KDOT Geology H-Pile Recommendation and LRFD Design Information

As seen above in Figure 3, the H-Piles are recommended to penetrate the underlying bedrock an anticipated 19 feet to 23 feet. This recommendation was based on the quality of the bedrock observed with borings, utilization of DrivenPiles software, and geologic experience installing H-Pile in similar conditions. However, what was not utilized were historical field tests, and “as-built” information. This is due to the lack of confidence that H-Pile would terminate at a similar elevation as the existing structure due to the increased load per pile. KDOT, prior to LRFD Standards, relied heavily on a field test method which locally was called the “air hammer”. This field method utilized an old pneumatic pile hammer to drive A-Rods into the subsurface at a timed penetration rate. KDOT Geologists would set a timer and log the rate at which the rods advanced 1 foot. Figure 4, is a typical drive log sheet representing the penetration rate from the surface to a depth of 110 feet. It was calculated that if it took longer than 120 seconds to advance 0.1 feet, that would be the expected pile tip elevation with a capacity of 55 tons per pile. However, in the early 2000’s when LRFD replaced ASD standards, the

**Kansas Department of Transportation**  
 Geology Section

Project No. KA-0387-01 Date 8/28/2008  
 Bridge No. Operator JN  
 County Clark Weather Sunny  
 Elevation 1787.66 Station 361+58.50 16ft SDG No. AH1

DEPTH	0.0-1.0	1.0-2.0	2.0-3.0	3.0-4.0	4.0-5.0					
0-5	8	8	4	12	6	18	5	23	13	36
5-10	18	18	13	31	9	40	7	47	5	52
10-15	6	6	3	9	3	12	5	17	10	27
15-20	11	11	8	19	4	23	5	28	7	35
20-25	6	6	6	12	5	17	5	22	6	28
25-30	6	6	4	10	4	14	6	20	8	28
30-35	5	5	5	10	7	17	7	24	11	35
35-40	11	11	7	18	14	32	11	43	12	55
40-45	13	13	19	32	17	49	24	73	26	99
45-50	19	19	16	35	25	60	19	79	18	97
50-55	20	20	27	47	28	75	21	96	16	112
55-60	14	14	14	28	21	49	30	79	40	119
60-65	36	36	52	88	69	157	62	219	54	273
65-70	40	40	36	76	57	133	52	185	55	240
70-75	55	55	68	123	117	240	124	364	110	474
75-80	108	108	90	198	124	322	89	411	119	530
80-85	113	113	91	204	115	319	114	433	141	574
85-90	182	182	140	322	168	490	109	599	148	747
90-95	183	183	154	337	212	549	299	848	352	1200
95-100	359	359	295	654	277	931	157	1088	191	1279
100-105	230	230	231	461	326	787	279	1066	276	1342
105-110	393	393	348	741	397	1138	395	1533	719	2252
110-115										
115-120										

Refusal is 120 seconds per 0.1 feet.  
 No. 2 McC&T air hammer timed at seconds per 1 foot.  
 Remarks: Refusal = 110.00  
 WIL = 10.2

Figure 4: KDOT typical Air Hammer Log with penetration rates to 110 ft.

“air hammer” became an ineffective way to predict pile tip elevations making “as-built” information less reliable. As a result, KDOT invested in CPT and DrivePoint to help refine pile recommendations.

## **PILETRAC APPLICATION AND UTILIZATION**

The Piletrac database application consists of 2 major components: (1) a relational database and (2) a cloud-based set of dashboards. The underlying database contains information for a given bridge such as location, size, number, type of piling and subsurface profile information obtained from the project plans. Also included are required pile capacity and required pile lengths and planned installation depths and associated results from PDA testing. The PDA test results include overall capacity during initial drive and associated restrrike tests, pile set values, hammer ram stroke, hammer type and size and pile installation depths. The process for populating the database involves curating the data by transcribing key values onto written summary data entry sheets and reviewing it for accuracy and completeness by a senior level project engineer or geologist. This data is then entered into the database using electronic forms and uploaded to the online database that forms the basis for the online dashboards and data visualizations. The written summary forms are maintained in an archive for reference for the source data used in the applications. These forms are also attached to copies of the relevant bridge drawings and the PDA test reports.

The database is then linked by FTC to the PileTrac online application. The cloud-based set of dashboards that were developed for the application are used for selecting and presenting the information obtained from the underlying database to illustrate results and trends. The user of the Piletrac application can review, filter and add selection criteria to the data visualizations for various pile related scenarios. For example, the user could examine the average total pile penetration depth into a weathered shale bedrock for an entire county. The user could then filter the data to look at penetration depths for a given pile section or a range in required or actual pile capacity or for various pile driving hammers. In this way, certain relationships become apparent, even ones which can be rather unexpected. This permits identification of underlying causes (root cause analysis) and even the ability to predict trends and likely future outcomes. FTC is able to modify these plots or create new plots or new combinations of plots to provide alternative methods for data analysis and visualizations. Furthermore, interfacing with the data in such an interactive way is far more intuitive than running conventional database queries. As a result, the amount of training for a user of the PileTrac application is minimal compared to what would be associated with traditional database applications.

The underlying PileTrac database is currently large enough such that many meaningful relationships have become apparent. Such relationships include the ability to obtain a very good estimation of what the ending pile set, and hammer ram stroke would be for a given pile section type and size for a specific required capacity and hammer size and type before pile installation is performed. Utilizing such historical data in this way can be more accurate than the results that may have been indicated by performing a pre-construction wave equation analysis. However, even when used in general terms, it is possible to assess whether a given pile hammer would be suitable for use given the particular set of pile installation and capacity requirements.

It is also helpful to have access to a summary of historical pile installation data for the designer of a new project to reference what typical pile types, installation depths and capacity results have been obtained. Such a system can augment the institutional knowledge that exists at an organization relative to likely pile design and pile installation requirements.

## UTILIZING PILETRAC TO ASSIST IN PILE RECOMMENDATIONS

KDOT has utilized several methods to help determine pile lengths and penetration. These methods have proven to be effective and accurate but not always precise, which has led to some projects having significant overruns and/or underruns on pile. Furthermore, with the inconsistency of pile lengths and coupled with supply chain issues, KDOT recognized that a need to be both more accurate and precise was necessary.

With the addition of PileTrac, KDOT now has an additional tool in our toolbox to help refine recommendations which is expediting construction and allowing for more accurate and precise pile length prediction. KDOT is applying borings from the foundation investigation, historical high strain dynamic testing in similar subsurface conditions and inputting the information into PileTrac to help improve pile recommendations. As a result, KDOT has taken PileTrac and implemented it into our standard process of running analysis for pile length recommendations. Additionally, PileTrac has numerous other valuable functions that are displayed in Figure 5.

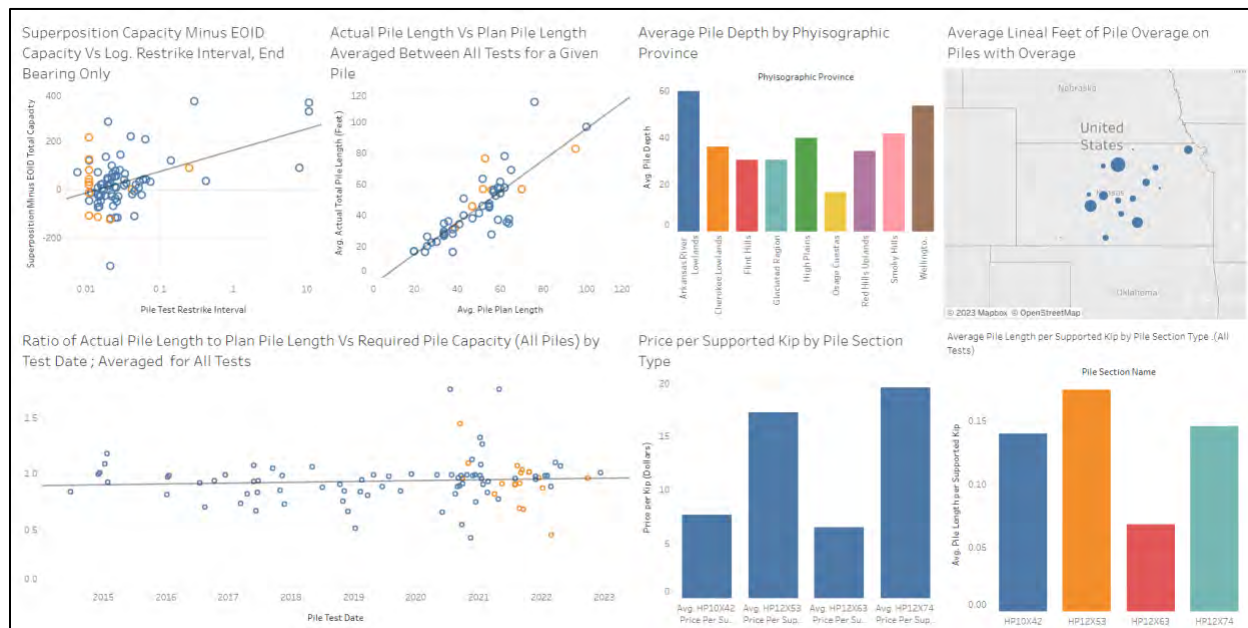


**Figure 5: PileTrac Master Dashboard-Pile Depth by Physiographic Province, Actual Pile Length vs Plan Pile Length, EOID vs Restrike, Average Lineal Feet of Pile on Pile with Overages**

For KDOT, utilizing historical data with visual representation has been significantly beneficial. These graphical displays or “dashboards” allow KDOT geologists to look not only at site specific boring logs, and “as-built” information, but also compare those results with other projects that may have similar site conditions. For example, in south central Kansas the Permian age Wellington Shale Formation is highly variable in the degree of weathering variation of

engineering properties. By utilizing the various dashboards within PileTrac, KDOT geologists can look at the average pile penetration into that rock (Figure 6), average pile capacity per pile section (Figure 7), pile depth vs bedrock depth (Figure 8), and numerous others.

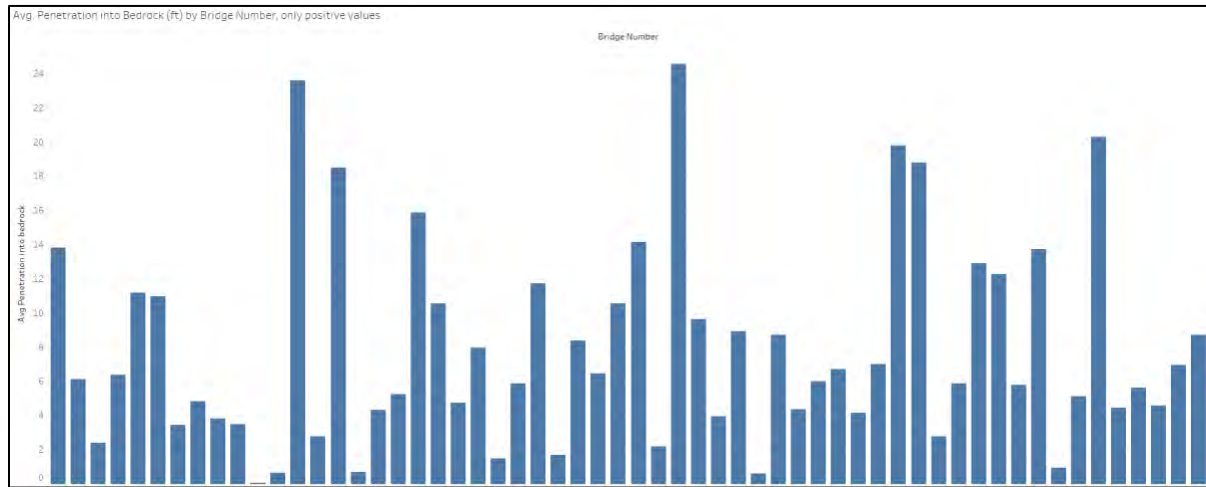


Figure 6: PileTrac Dashboard- Average Penetration into Bedrock

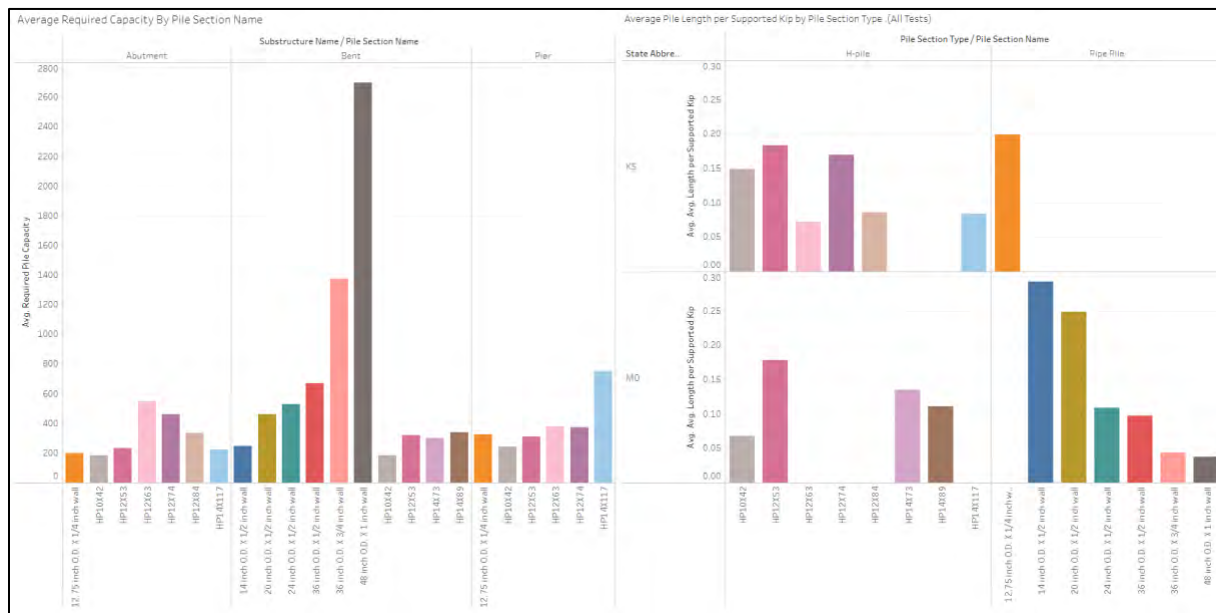


Figure 7: PileTrac Dashboard- Average Required Capacity by Pile Section, Average Pile Length per Supported Kip by Pile Section Type

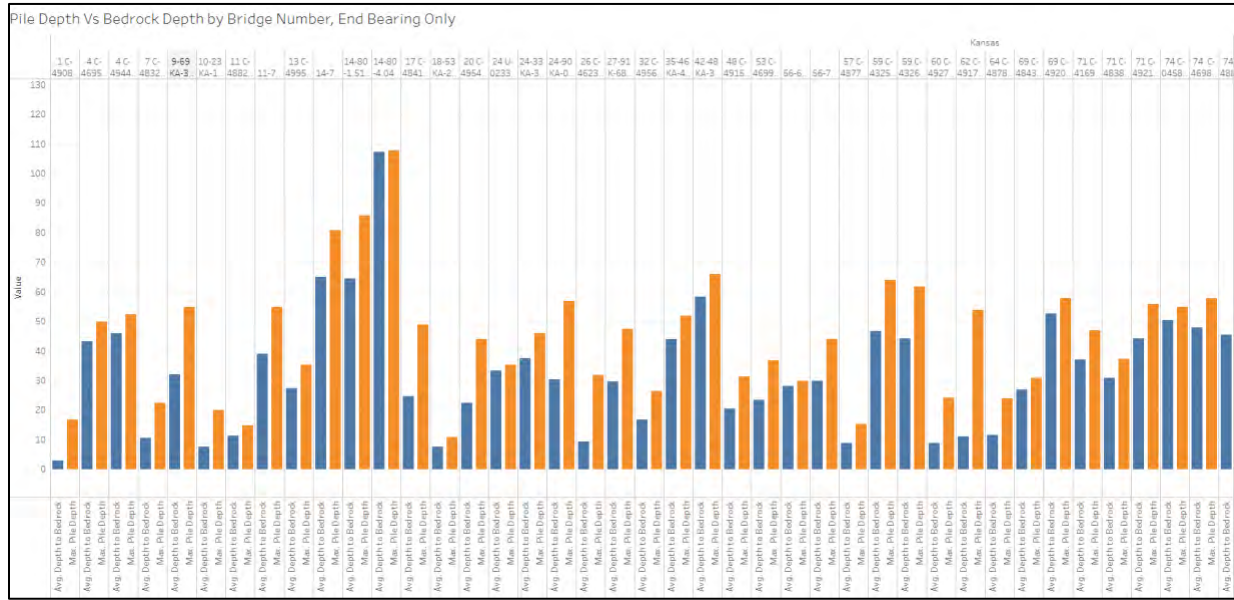


Figure 6: PileTrac Dashboard- Pile Depth vs Bedrock Depth by Bridge Number, End Capacity Only

KDOT, with these additional tools, has another level of confidence when making recommendations. The comparison of historic and current data will allow for more data driven decisions with the expectations that projects will have less change orders and delays.

**FUTURE KDOT USES OF PILETRAC**

As more projects come in, KDOT Geologists will continue to assess and utilize the necessary tools to better predict pile tip elevation. Current methods with the utilization of PileTrac have provided KDOT additional confidence that pile recommendations are both more accurate and precise. The current projects KDOT is running comparisons on using PileTrac have yet to be built, but the initial indication from FTC’s projects is that pile recommendations are better and closer to design recommendations.

Furthermore, what KDOT is beginning to look at is how PileTrac can be used during construction. There are several dashboards within PileTrac that can help construction inspectors verify hammer size suitability. These visual representations can provide inspectors with a set and stroke for a given hammer size to look for, and a capacity versus depth for a specific hammer as well. As a cloud-based application, PileTrac can be used in the field as a real-time confirmation of pile capacity and hammer verification. That

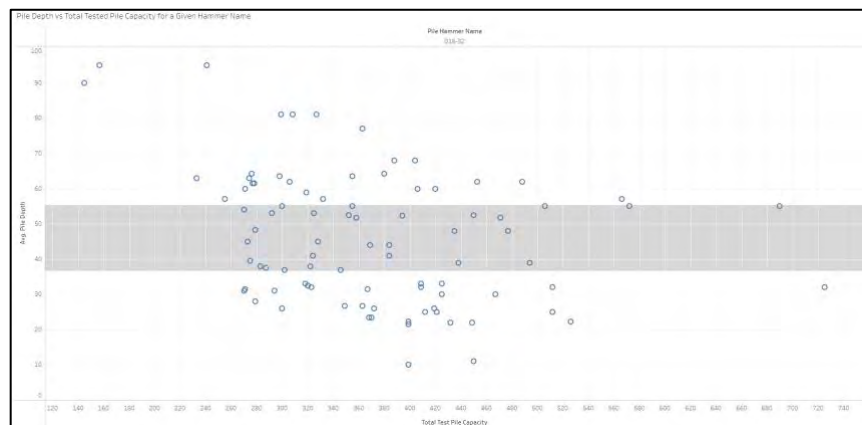


Figure 7: PileTrac Dashboard- Pile Depth vs Total Tested Pile Capacity for given Hammer Name; D16-32

said, PileTrac will not govern the inspector's approval, but be used to assist the inspectors. The Pile Driving Analyzer will provide the site-specific penetrations, set, stroke, and capacity.

## **CONCLUSION**

KDOT's existing method of predicting pile tip elevation became less accurate when LRFD standards were implemented. The field investigation tests that historically were very reliable were no longer consistent and KDOT needed to change, therefore KDOT looked at ways to supplement the field investigation and traditional driven pile software when making pile recommendations. As a result, KDOT looked outside and collaborated with FTC to refine pile recommendations.

FTC's development of the cloud-based application, PileTrac has demonstrated to KDOT that it can be a useful tool when predicting pile tip elevations. PileTrac has allowed KDOT to reference historical information, in a graphical display to look at projects with similar site conditions and make data driven decisions. This visualization aspect of PileTrac has multiple levels of data that KDOT Geologists can now reference. The database, which PileTrac pulls information from, provides KDOT with information that historically has been difficult to reference, and puts it into a dashboard that can be customized to what the geologist wants to see. Consequently, KDOT is now able to use multiple different methods to make better, more accurate pile recommendations.

KDOT will continue to look to refine pile recommendations using traditional field methods along with driven pile software and now PileTrac. The goal of becoming more precise and accurate will always be the challenge, but with more tools this goal becomes a little more achievable.

## **REFERENCES**

1. Website: Kansas Geological Survey. Physiographic Map of Kansas.  
<http://www.kgs.ku.edu/Physio/physio.html>. Accessed April, 2023.
2. Foundation Testing Consultant (2023). PileTrac Database (2.0). [Computer Software].

## **Pavement at Bridge End Bump Elimination**

### **Jeremiah Kokes**

Tennessee Department of Transportation  
Materials and Tests Division/Geotechnical Engineering Section  
Building A, 1<sup>st</sup> Floor, 7345 Region Ln.  
Knoxville, TN 37914  
(865) 594-2705  
jeremiah.kokes@tn.gov

### **Robert Jowers**

Tennessee Department of Transportation  
Materials and Tests Division/Geotechnical Engineering Section  
Building A, 1<sup>st</sup> Floor, 6601 Centennial Blvd.  
Nashville, TN 37243  
(615) 350-4133  
robert.jowers@tn.gov

Prepared for the 72<sup>nd</sup> Highway Geology Symposium, August, 2023

### **Acknowledgements**

The authors would like to thank the individuals/entities for their contributions in the work described:

Ted Kniazewycz – TDOT  
Ulises Martinez - TDOT  
Ginger Bennett – USACE

### **Disclaimer**

Statements and views presented in this paper are strictly those of the author(s), and do not necessarily reflect positions held by their affiliations, the Highway Geology Symposium (HGS), or others acknowledged above. The mention of trade names for commercial products does not imply the approval or endorsement by HGS.

### **Copyright Notice**

Copyright © 2023 Highway Geology Symposium (HGS)

All Rights Reserved. Printed in the United States of America. No part of this publication may be reproduced or copied in any form or by any means – graphic, electronic, or mechanical, including photocopying, taping, or information storage and retrieval systems – without prior written permission of the HGS. This excludes the original author(s).

### **ABSTRACT**

The “bump at the bridge end” has long been a concern in many states. Issues such as settlement, drainage, and poor sub-base have been identified as contributors to the problem. In addition, the transition from rigid pavement to flexible pavement may cause the “bump”. Concrete is unyielding. However, soil is not, and its compaction may vary. Quality construction is imperative to reducing the impact of the “bump”. Fill material should be placed and compacted as per TDOT specifications, but the results are not always satisfactory. TDOT Structures issued a new standard drawing STD-10-2 in 2020. This new standard drawing is supported by FHWA guidance from FHWA-HRT-17-080 “Design and Construction Guidelines for Geosynthetic Reinforced Soil Abutments and Integrated Bridge Systems”, June 2018. Current TDOT sponsored research focuses on embankment settlement and enhanced soil reinforcing in an effort to reduce or potentially eliminating the “bump”. There are numerous examples hazards to the travelling public due to the “bump” throughout the state of Tennessee, especially on interstates. One such example is the I-840 corridor in Williamson County, Tennessee. The TDOT Materials and Tests Division Roadway Profiler performed rideability tests indicating bridge issues on I-840 centered between MM 10.00 to 23.70 eastbound, and MM 17.12 to 23.93 westbound in 2018. Additional geotechnical site characterization was performed in 2018 and 2021 to identify the primary issues leading to settlement development. The net result was resurfacing projects that included bridge end remediation efforts begun in 2021. These rideability tests were again performed in 2023 for comparison, which the results are currently being compiled.

## INTRODUCTION

The “bump at the bridge end” has long been a concern for many transportation departments, including the Tennessee Department of Transportation (TDOT). Also known as the “bridge bump” or “bump” is a phenomenon where a noticeable vertical transition occurs between the end of the bridge deck and the approach slab and asphalt of the abutment or Pavement at Bridge Ends (PABE) in TDOT terminology. Issues such as settlement, drainage, and poor subgrade have been identified as contributors to the problem. In addition, the transition from flexible pavement to the bridge approach slab may cause the “bump”. The concrete of the approach slab is unyielding, however, soil under it is not. Settlement issues of the slabs can result in a variety of problems, including differential settlement, abutment fill erosion, pavement cracking, damage to bridge structural elements and poor ride quality (Figure 1). This issue creates an uncomfortable driving experience, cargo damage, increased freight costs, public complaints, decreased vehicle handling and grip, and increased operational costs due to frequent repairs and manhours where the “bump” has developed. This paper presents TDOT’s recent experience with investigating and repairing the “bump”.

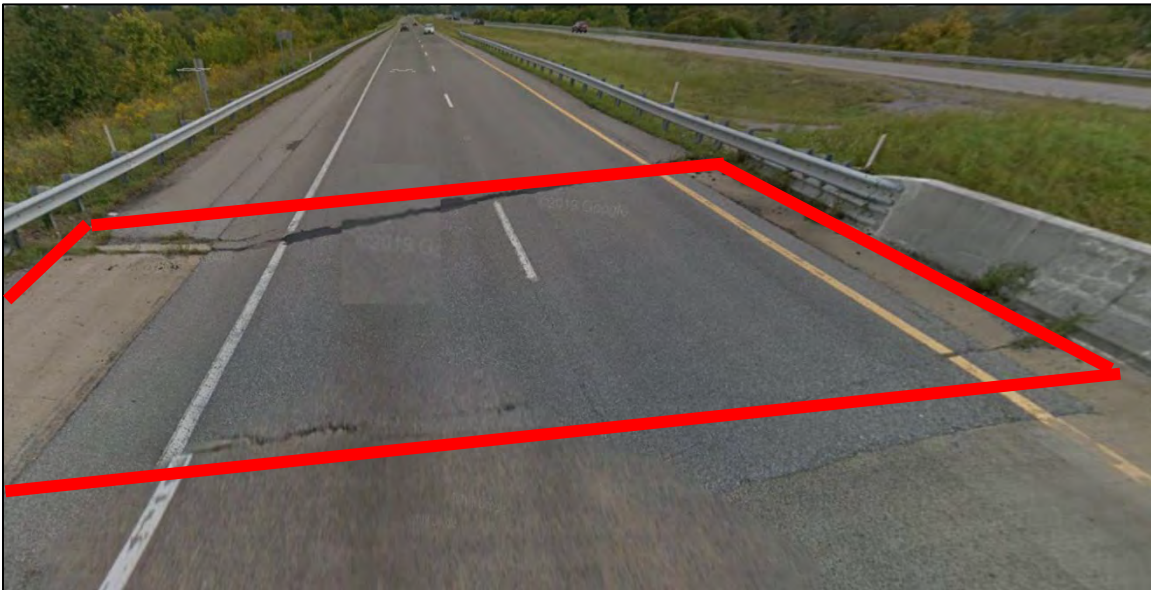


**Figure 1 – Typical PABE with approach slab related “bump” on I-840 in Williamson County, Tennessee. The approach slab is within the red lines (image source Google Earth, 2019).**

## BRIDGE BUMP CAUSES

### NCHRP Synthesis 234

In the National Cooperative Highway Research Project (NCHRP) Synthesis of Highway Practice 234 “Settlement of Bridge Approaches (The Bump at the End of the Bridge)”, 1997 identified from a literature review the primary factors that lead to the “bump” and categorized

them (Table 1). Synthesis 234 emphasized that the “bump” develops at the interface of the geotechnical engineer’s or engineering geologist’s design of the embankment and the structural engineer’s design of the bridge. The formation of silos between different disciplines and the compartmentalization of information and data within transportation departments directly leads to this physical representation of a lack of teamwork and open-mindedness. The Synthesis noted that a proper foundation and embankment design must be informed by a thorough geotechnical soils and geology report.

**Table 1 - Causes of Bridge Approach Problems Categorized (from Synthesis 234, 1997)**

<p><i>Differential Settlements</i> Compress of natural soils Compression of embankment soils Local compression at bridge/pavement interface (PABE)</p>	<p>Primary consolidation, secondary compression, and creep Volume changes and distortional movement/creep of embankment soils Inadequate compaction at the bridge/pavement interface, drainage and erosion problems, rutting/distortion of pavement section, traffic loading, and thermal bridge movements</p>
<p><i>Movement of Abutments</i> Vertical movement  Horizontal movement</p>	<p>Settlement of soil beneath, down drag, erosion of soil beneath and around the abutment  Excessive lateral pressures, thermal movements, swelling pressure from expansive soils, and lateral deformation of embankment and natural soils</p>
<p><i>Design/Construction Problems</i> Engineer-related Contractor-related  Inspector-related/Poor quality control Design-related</p>	<p>Improper materials, lift thickness, and compaction requirements Improper equipment, over excavation for abutment construction, and survey/grade errors Lack of inspection personnel and improper inspection personnel training No provision for bridge expansion/contraction spill-through design resulting in the migration of fill material from behind the abutment</p>

### **NCHRP Scan Team Report 19-01, 2020**

TDOT was a participating agency, along with 11 other state transportation agencies, in the National Cooperative Highway Research Project (NCHRP) 20-68D Domestic Scan 19-01 “Leading Practices for Detailing Bridge Ends and Approach Pavements to Limit Distress and Deterioration” (Figure 2). Ted Kniazewycz, of TDOT, served as a Scan 19-01 team member. Both TDOT and Mr. Kniazewycz were selected due to TDOT’s long history with integral piers and jointless bridges. A report with the best practices and current research of the participating transportation agencies was released in October 2020.

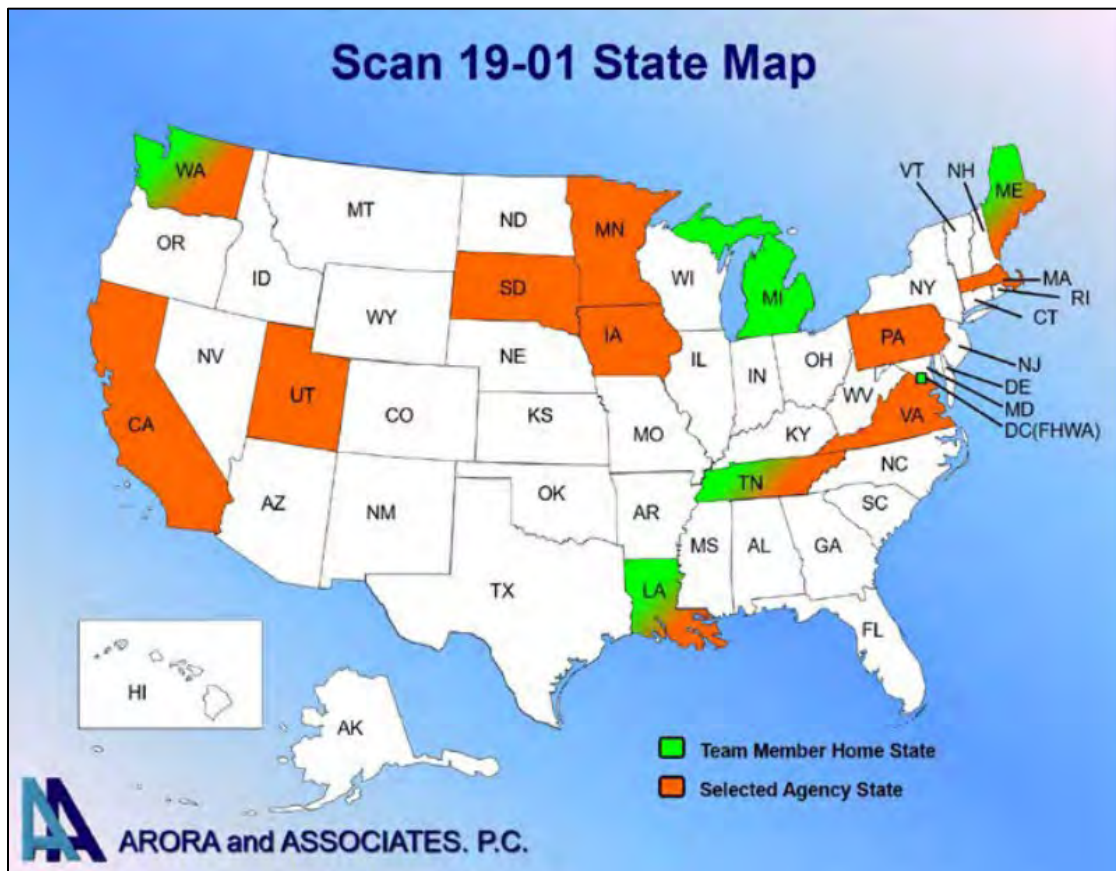


**Figure 2 - Map of participating transportation agencies and location of Scan team members (from Scan Team Report 19-01, 2020).**

The approach slab settling was identified as a major problem. Controlling drainage was identified as a requirement to controlling the settlement. Integral abutments and improved sub-base were identified as benefits to further reducing approach slab settlement and reducing the “bump”. TDOT’s preference for jointless bridges means that integral abutments have already been implemented on TDOT’s bridge assets. At the PABE, a combination of poor compaction and drainage behind the endwall/abutment was identified as an issue contributing to the approach slab subsidence along with the transition from the flexible pavement to the rigid approach slab (Figure 3).

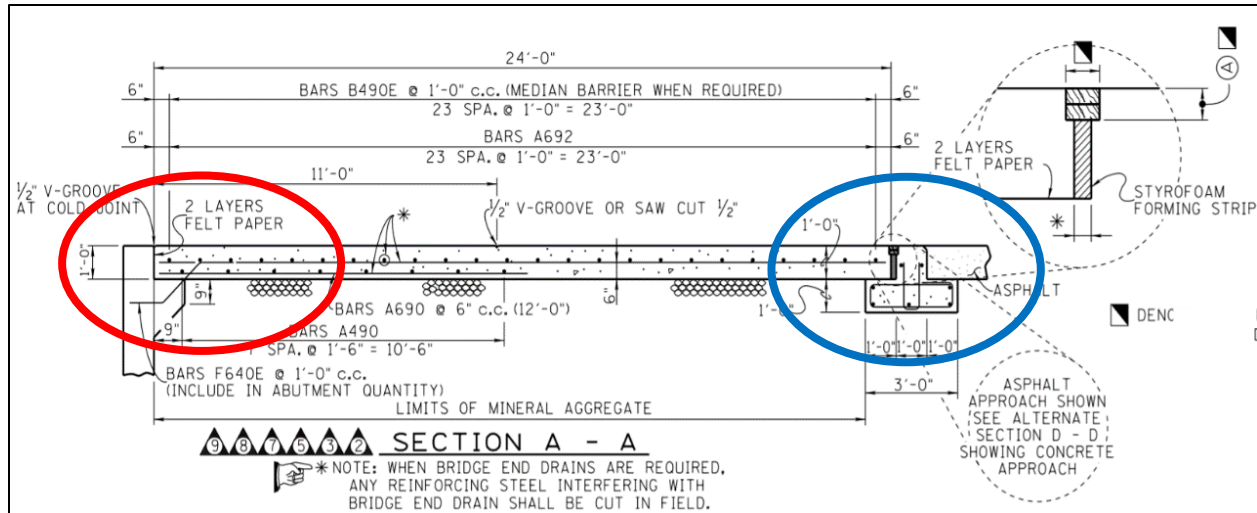


**Figure 3 - The locations that lead to the "bump" in a typical PABE diagram. The area within the red oval is the fill behind the endwall/abutment subject to settlement if not compacted or drained adequately. The area within the blue oval is subject to differential settlement due to the transition from flexible pavement to the rigid approach slab (from Kniazewycz, 2020).**

*TDOT Standard Drawing STD-10-2*

The ultimate result of Scan 19-01 was the creation of a new TDOT Structures standard design, TDOT Structures STD-10-2 “Miscellaneous Abutment and Pavement at Bridge Ends Backfill Details”, that was supervised by Mr. Kniazewycz (Figure 4). The new standard drawing creates a free draining, geosynthetic reinforced, mineral aggregate backfill that increase the bearing capacity and reduces the differential settlement of the flexible pavement and rigid approach slab. The design was tested during the 2015 I40 Fast Fix 8, the 2018 I-840/I-24 Ramp, and the 2019 I-240 Memfix 4 prior to its adoption (Kniazewycz, 2020). The new standard drawing is also supported by FHWA guidance from FHWA-HRT-17-080 “Design and Construction Guidelines for Geosynthetic Reinforced Soil Abutments and Integrated Bridge Systems”, June 2018.

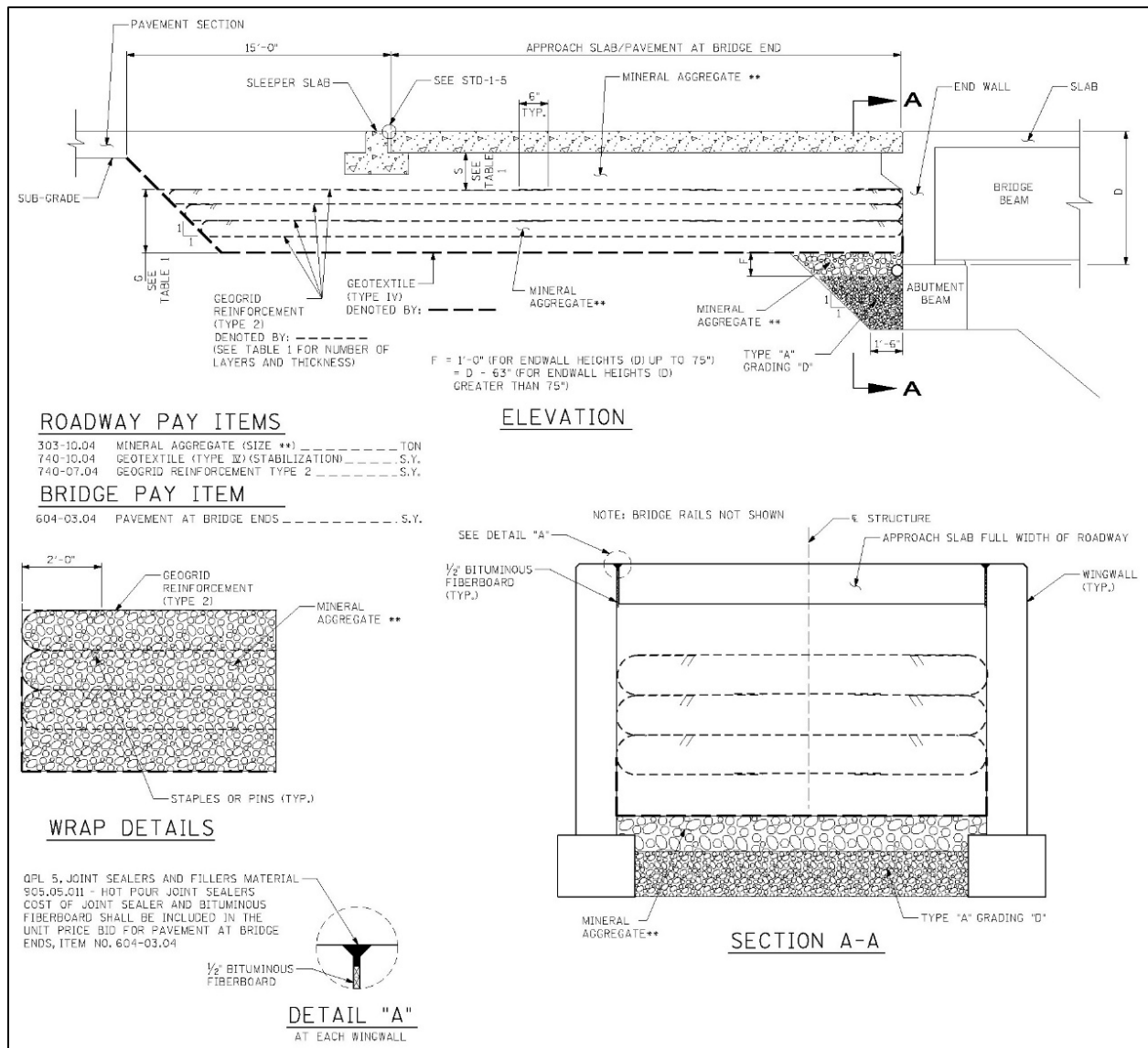


**Figure 4 – Select portions of TDOT Structures STD-10-2 2020 “Miscellaneous Abutment and Pavement at Bridge Ends Backfill Details” showing the elements of the reinforced backfill.**

The standard design extends mineral aggregate backfill from the abutment/endwall to fifteen (15) feet past the end of the approach slab. A layer of geotextile, meeting American Association of State Highway and Transportation Officials (AASHTO) M 288 Stabilization Class 1, is placed along the base of the fill to separate the soil embankment fill and the mineral aggregate fill. A layer or multiple layers of mineral aggregate backfill are placed in varying thickness based on the minimum endwall/wingwall height (Table 2). Each layer is wrapped by geogrid with long term tensile strength greater than or equal to 2400 pounds per foot. A drainage layer of mineral aggregate 12 inches in thickness for endwall heights of 36 to 75 inches, or a drainage layer thickness of endwall height minus 63 inches where the endwall is greater than 75 inches in height. The drainage layer conducts water towards the drainage pipe. Base stone is

placed behind the abutment beam and below the drainage layer and drainage pipe due to its low permeability. For additional specification see the complete standard design drawing at:

[https://www.tn.gov/content/dam/tn/tdot/roadway-design/documents/standard\\_drawings/structure\\_standard\\_drawings/current/new-structures/STD-10-2.pdf](https://www.tn.gov/content/dam/tn/tdot/roadway-design/documents/standard_drawings/structure_standard_drawings/current/new-structures/STD-10-2.pdf)

**Table 2 – Geogrid-Encapsulated Mineral Aggregate Backfill Specifications  
(from TDOT STD-10-2)**

Layer Description	D = Minimum Endwall/Wingwall Height (inches) (Does not include the height of the abutment beam or wing beam)							
	D < 36"	36" ≤ D ≤ 40"	41" ≤ D ≤ 49"	49" ≤ D ≤ 55"	56" ≤ D ≤ 62"	63" ≤ D ≤ 68"	69" ≤ D ≤ 75"	D ≥ 76"
Mineral Aggregate Layer "S"	14"	S=D-22"	S=D-27"	S=D-34"	S=D-40.5"	S=D-48"	S=D-54"	S=21"
Geogrid-Encapsulated Layer "G"	1 layer @ 4' = 4"	1 layer @ 4' = 4"	2 layers @ 4.5" = 9"	2 layers @ 8" = 16"	3 layers @ 7.5" = 22.5"	4 layers @ 7.5" = 30"	4 layers @ 9" = 36"	4 layers @ 9" = 36"

## CASE STUDY IN "BRIDGE BUMP" REPAIR: WILLIAMSON COUNTY I-840

### Background

The Middle Tennessee I-840 corridor is a half-ellipse shaped interstate that bypasses Nashville to the south that began as State Route (SR) 840 (Figure 5). The route was constructed between 1992 and 2012. In 2015 the FHWA redesignated it as I-840. The route is 77.28 miles long divided into eastbound and westbound lanes through Dickson, Hickman, Williamson, Rutherford, and Wilson Counties. It serves the cities of Lebanon, Murfreesboro, Franklin, and Dickson. The annual average daily traffic (AADT) on I-840 in Williamson County ranged between 15,221 to 46,810 in 2022.

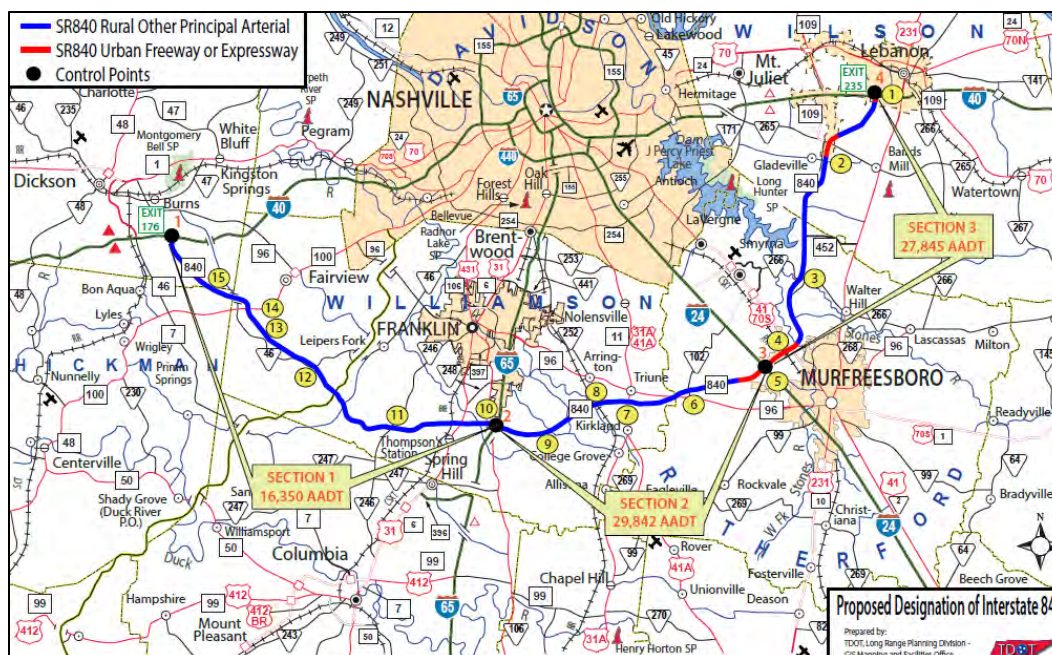


**Figure 5 - The Tennessee I-840 Corridor (image TDOT).**

Since the roadway was opened in Williamson County, approximately twelve (12) years ago, significant subsidence had developed including many “bridge bumps”. TDOT Materials and Tests Division Roadway Profiler was deployed by the Geotechnical Engineering Section (GES) to perform rideability tests in 2018. The Profiler determined the dips, including “bridge bumps”, were centered between mile post (MP) 10.00 to 23.70 eastbound, and MM 17.12 to 23.93 westbound (Bennett and Smith, 2018). The ride quality was reported in International Roughness Index (IRI).

The IRI is the statistic used to measure how smooth or rough a pavement surface is. The lower the calculated IRI, the smoother the pavement will ride. The higher the IRI, the rougher the pavement will ride. According to the FHWA IRI Categories for roadways, anything greater than 170 is “unacceptable”. The TDOT specification for bridge deck and approaches is an IRI of 190 or 250 for roadways with speed limits below 40 miles per hour. The TDOT specification for Mean Roughness for the full length of the deck plus approaches of a IRI of 130. The results of the Profiler are shown in Figures 6 through 11. Multiple bridge approaches along the Williamson County I-840 corridor had IRIs over 170 (Bennett and Smith, 2018).

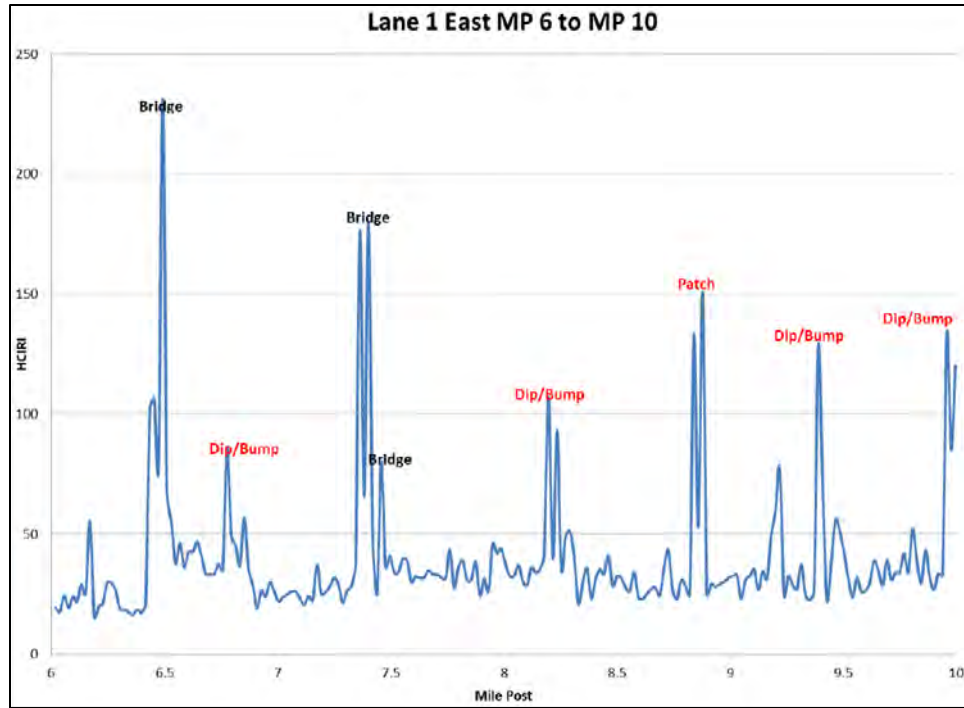


Figure 6 – Results of the Roadway Profiler along eastbound I-840 between MP 6 to 10 (source TDOT Materials & Tests).

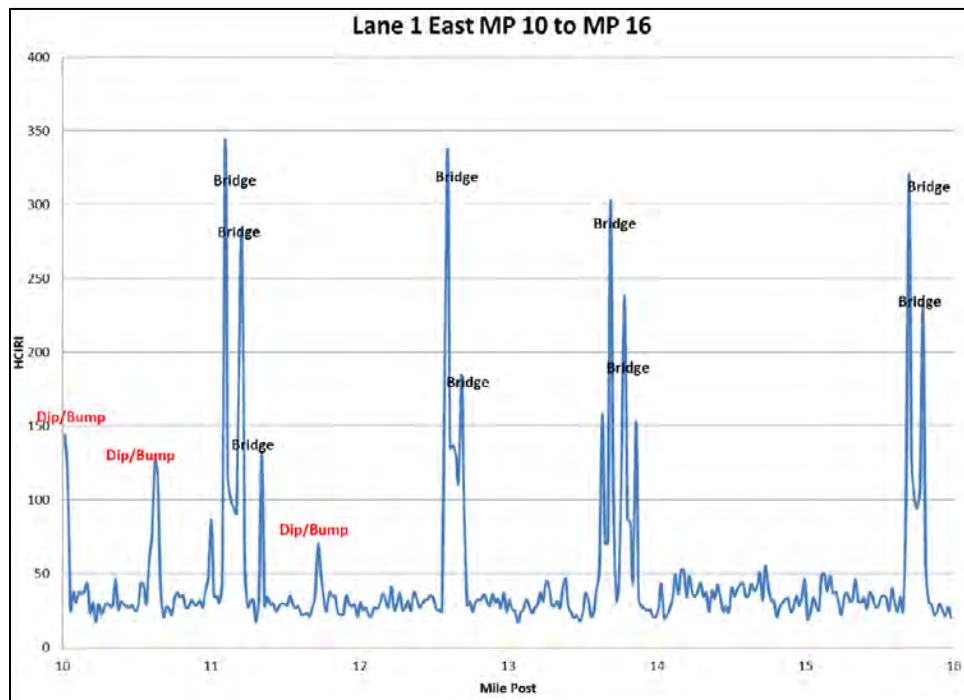
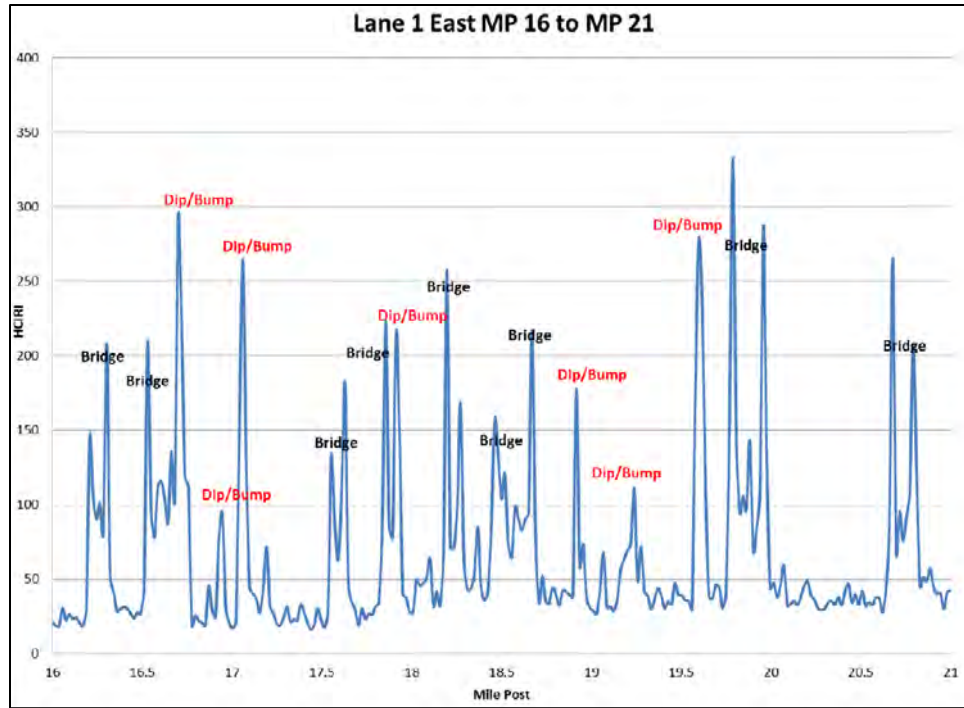
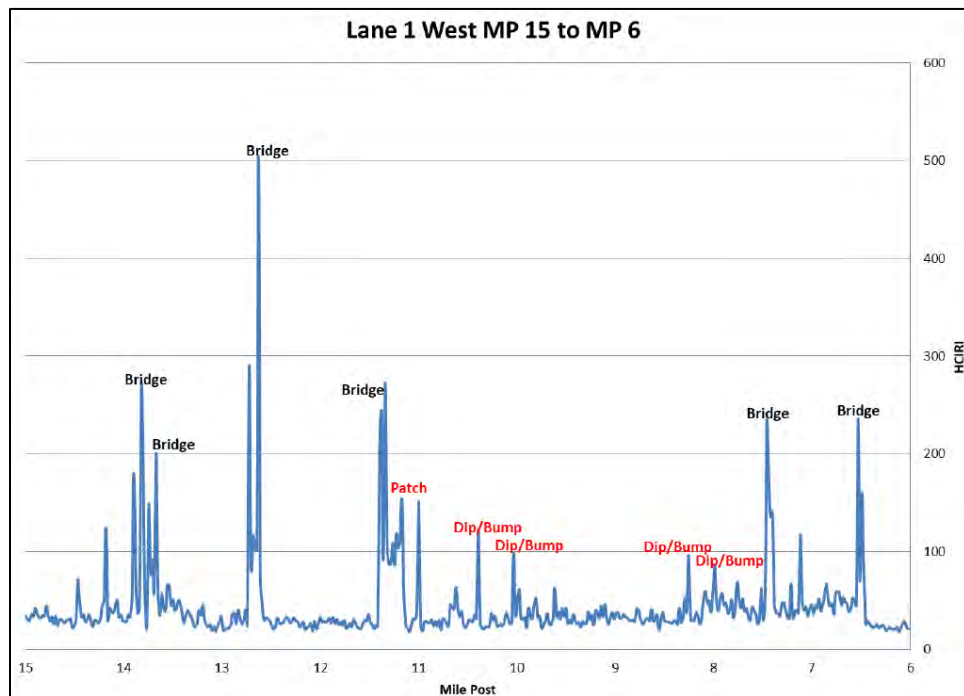


Figure 7 – Results of the Roadway Profiler along eastbound I-840 between MP 10 to 16 (source TDOT Materials & Tests).



**Figure 8 – Results of the Roadway Profiler along eastbound I-840 between MP 16 to 21 (source TDOT Materials & Tests).**



**Figure 9 – Results of the Roadway Profiler along westbound I-840 between MP 6 to 15 (source TDOT Materials & Tests).**

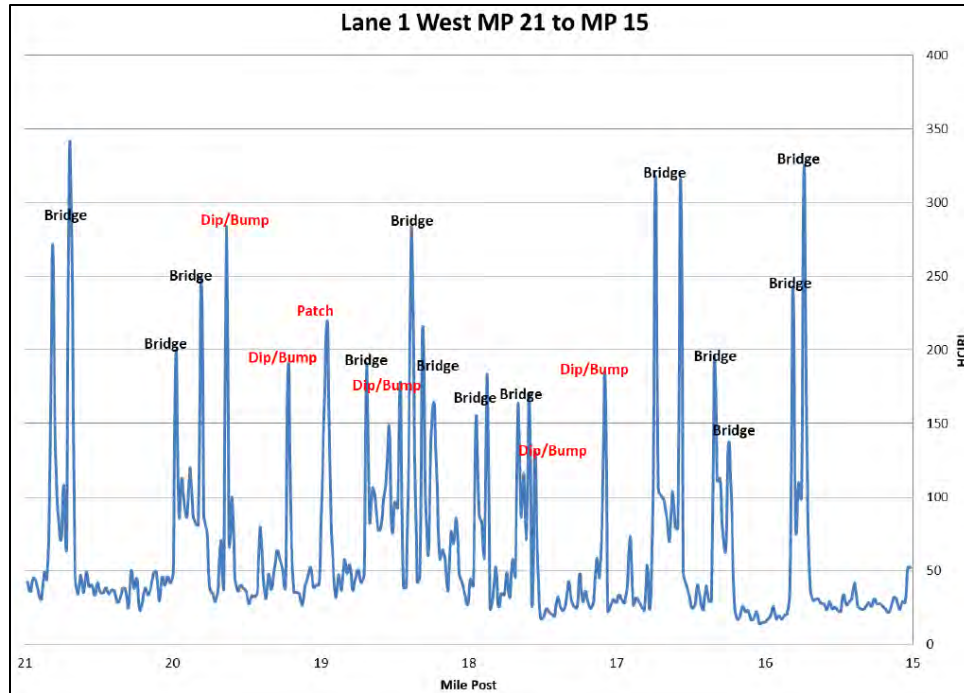


**Figure 10 – Results of the Roadway Profiler along westbound I-840 between MP 15 to 21 (source TDOT Materials & Tests).**

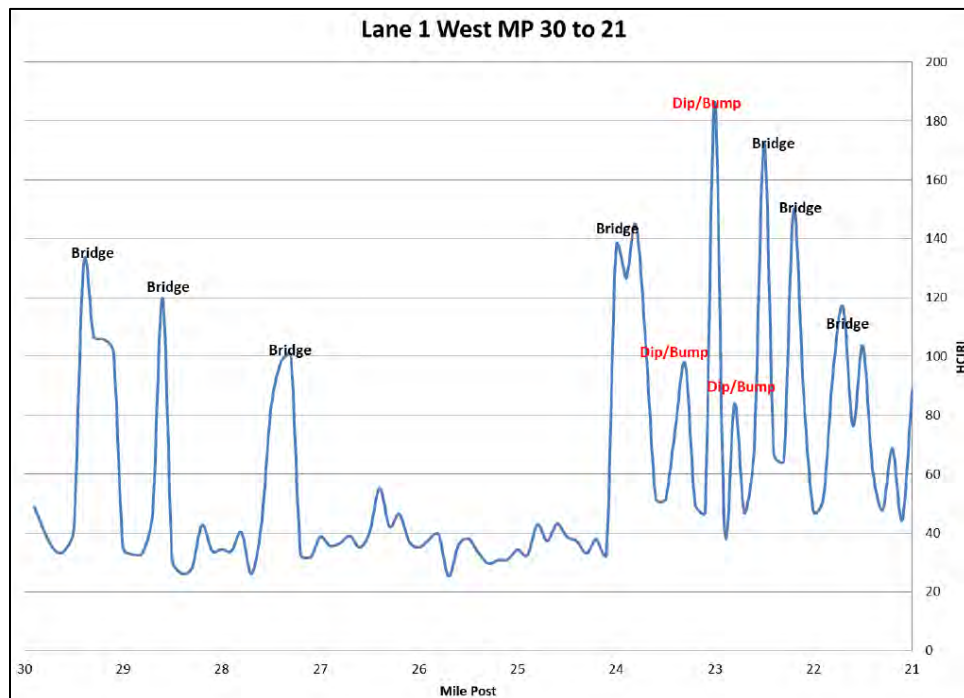


**Figure 11 – Results of the Roadway Profiler along westbound I-840 between MP 21 to 30 (source TDOT Materials & Tests).**

## Geology, Soils, and Site Conditions

As the roadway segment of I-840 traverses Williamson County, the physiographic province transitions from the Western Highland Rim and into the outer portions of the Central Basin of Tennessee (Figure 12).

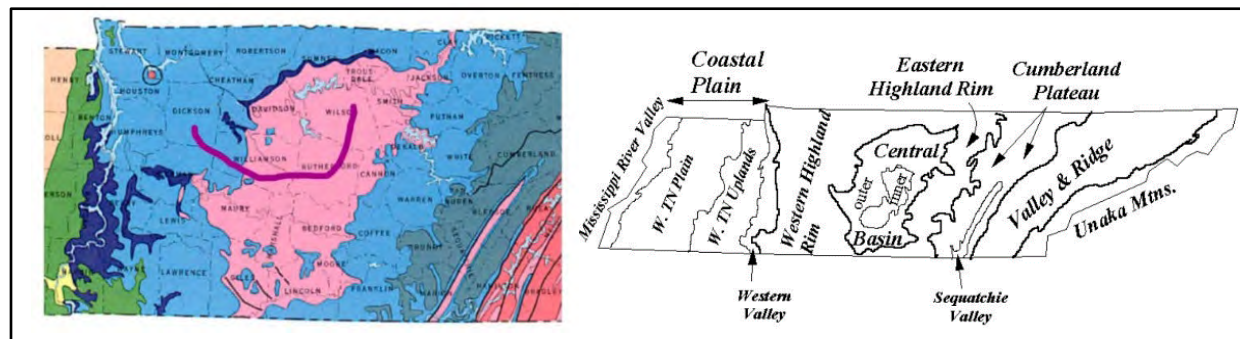


**Figure 12 – An excerpt of the Generalized Tennessee Geologic map and Tennessee Physiographic Province map. The pink shade corresponds to the Ordovician aged formations of the Central Basin. The dark and light blue corresponds to the Devonian-Silurian (dark blue) and Mississippian (light blue) aged formations of the Highland Rim. The magenta line is the approximate location of the I-840 corridor (from Burns and Jowers, 2021).**

The Western Highland Rim is characterized by steep hills and valleys. The surficial overburden material consists of weathered soil residuum of interbedded limestone and shale of the Warsaw, Ft. Payne, Leipers, and Catheys Formations. This soil material is typically classified as silty clay with varying amounts of chert. The soil overburden deposits are generally thicker throughout the Western Highland Rim than the overburden deposits found in the Central Basin. Karst development is present in the Highland Rim; however, it is not as highly developed as that found in the Central Basin. Numerous springs, seeps and sinkholes are present in the general area, and it is reasonable to think that springs and seeps are present below the valley fill sections of the constructed roadway.

The Central Basin landform is characterized as rolling hills to nearly flat. Sections of the I-840 alignment built within the Central Basin are generally underlain by limestone of the Ridley, Lebanon, and to a lesser extent the Carters Formations with well-developed karst topography. The well-developed karst drainage along this section is a major component of the overall drainage for this area and tends to drain surface and subsurface water.

In 2018, GES was tasked with characterizing the various subsidence dips, including bridge approaches. A total of 20 borings were advanced in both the eastbound and westbound lanes. The subsurface exploration program revealed soft to firm, moist to saturated embankment fills overlying a soft to firm, moist to saturated natural ground. Results of the stabilization plan recommended drilling horizontal drains into the base of the embankment to provide drainage, but logistics prevented this from being accomplished (Bennett and Smith, 2018). A further 12 borings with 9 piezometers inserted in the borings were conducted to characterize the corridor's embankments in 2021. The piezometer readings indicate that the fill embankments are still in an

“undrained” state in the ten- or twelve-years following construction (Burns and Jowers, 2021). This condition has led to continuous settlement and erosion of the backfill in the abutments (Figure 13) (Jowers, 2023).



*Figure 13 - Erosion of abutment backfill due to settlement (Photo Rivers 08/19/2021).*

### **Williamson County I-840 Resurfacing Project**

Following the 2021 Geotech investigation, TDOT began resurfacing programs for the Williamson County I-840 Corridor between MP 8 to 24. The existing PABEs with high IRI were removed and replaced with PABEs that are in compliance with STD-10-2 (Figures 14 through 17) (Jowers, 2023). The results have been promising. TDOT Materials and Tests Division Roadway Profiler was deployed in 2023 to reevaluate the I-840 riding surface. The results final report is due to be released soon.



***Figure 14 - Williamson I-840 removal of the existing approach slab during the PABE replacement (image Region 3 TDOT).***



*Figure 15 - Williamson I-840 mineral aggregate backfill being compacted. Note the geogrid in the foreground (image Region 3 TDOT).*



**Figure 16 - Williamson I-840 approach slab replacement (image Region 3 TDOT)**



**Figure 17- Williamson I-840 finalizing the resurfacing of the PABE (image Region 3 TDOT).**

## **CONCLUSION**

The new TDOT standard drawing STD-10-2 appears to be effective at reducing the “bump at the end of the bridge” problem for existing bridges. TDOT will continue to replace failing PABEs with backfill in compliance with STD-10-2 and new construction will incorporate the design. GES waits for the results of the 2023 rideability test results. Recent research was performed by the University of Memphis, under the sponsorship of TDOT and FHWA. They performed 3D subsurface measurements and imaging utilizing ground penetrating radar (GPR) and multi-channel analysis of surface waves (MASW) to delineate soil layers in Shelby County, Tennessee. These measurements were used to create finite element (FE) models to evaluate different mitigation and repair strategies (Camp, et.al, 2021). Hopefully this research will aid TDOT and other transportation agencies in determining if a full PABE replacement is warranted.

**REFERENCES:**

- Conference Presentations
  1. Kniazewycz, T. A. Smoothing the Bump at the End of the Bridge. At *Section Virtual Conference*, ASCE Tennessee, 2020.
  2. Jowers, R. Fixing the Bump at the End of the Bridge. At *TDOT Operations Symposium*, TDOT, 2023.
- Federal Government Reports
  1. Briaud, J. L., James, R. W, and Hoffman, S.B. *Settlement of Bridge Approaches (The Bump at the End of the Bridge)*. Synthesis of Highway Practice 234, NCHRP, Transportation Research Board, 1997.
  2. DeRuyver, J, Eaton, D. Garcia, R. R., Khaleghi, B., Kniazewycz, T. A., Lancaster, A, and Walsh, J. *Leading Practices for Detailing Bridge Ends and Approach Pavements to Limit Distress and Deterioration*, NCHRP Project 20-68D, Scan 19-01, NCHRP, 2020.
  3. FHWA, *Design and Construction Guidelines for Geosynthetic Reinforced Soil Abutments and Integrated Bridge Systems*, FHWA-HRT-17-080, U.S. Department of Transportation, 2018.
- Tennessee State Reports
  1. TDOT Structures, *Miscellaneous Abutment and Pavement at Bridge Ends Backfill Details*, TDOT STD-10-2, 2020.
  2. Bennett, G. and Smith, T, *I-840 Pavement Settlement Issues (MM 7 – MM 22) Williamson County*, Geotechnical Project Memo, TDOT GES, 2018.
  3. Burns, T and Jowers, R, *Subsidence Dips Along I-840 Between the SR-100 and SR-6 Interchanges Williamson County*, Soils and Geology Report, TDOT GES, 2022.
  4. Camp, C. V., Pezeshk, S, Kashani, A, and Dangkoa, D, *Bump at the End of the Bridge: Enhanced Remediation Decision Making via 3D Measurement and Advanced 3D Dynamic Analysis*, RES2019-21, University of Memphis and TDOT, 2021.

**Mitigation of Bridge Foundations, US 460 Bridges over Marrowbone Creek  
and KY 195, Pond Creek, and CSX RR, KY 80 and Russell Fork River**

**Tony Beckham P.G.**  
Kentucky Transportation Cabinet  
Division of Structural Design  
Geotechnical Services Branch  
1236 Wilkinson Blvd,  
Frankfort, KY 40601  
502 782-3821  
tony.beckham@ky.gov

Prepared for the 72<sup>nd</sup> Highway Geology Symposium, August 2023

### **Disclaimer**

Statements and views presented in this paper are strictly those of the author(s), and do not necessarily reflect positions held by their affiliations, the Highway Geology Symposium (HGS), or others acknowledged above. The mention of trade names for commercial products does not imply the approval or endorsement by HGS.

### **Copyright Notice**

Copyright © 2023 Highway Geology Symposium (HGS)

All Rights Reserved. Printed in the United States of America. No part of this publication may be reproduced or copied in any form or by any means – graphic, electronic, or mechanical, including photocopying, taping, or information storage and retrieval systems – without prior written permission of the HGS. This excludes the original author(s).

## ABSTRACT

Design and construction of relocated US 460 in Pike County has been done in phases for several years. The new route will replace current US 460, a narrow congested two-lane roadway in the eastern Kentucky mountains, with an alignment along many segments adjacent to the Russell Fork River. Proximity to the river causes numerous landslides. Rock falls also occur frequently.

Poor quality bedrock, not encountered during initial design borings, was discovered during construction of three large bridges on relocated US Route 460. During construction of benches needed for slope stability and bridge foundations, clastic dikes, weathered and cracked bedrock were discovered leading to numerous mitigation methods that were required to provide adequate bearing and minimum distances to top of adjacent benches for spread footing foundations. Most of the bedrock quality issues were contributed to highly weathered shale and nearly vertical clastic dike type joints with non-uniform, irregular spacing. Most of the joints were filled with highly weathered non-durable shale in vertical bedding planes. Removal of bedrock when constructing the benches contributed to loss of confinement causing the joints to relax and open, creating large crevices near pier and abutment foundations.

Construction of the three bridges was staggered using three separate contracts. Total distance between the bridges is approximately four miles. Due to bedrock issues encountered at Marrowbone and Pond Creek bridges an angle rock core drilling was performed before foundation and bench construction at the Russell Fork bridge. Although the angle drilling was performed after the contract was awarded, information obtained allowed modifications to the foundations design and construction to proceed quickly.

Successful mitigation measures consisted of lowering footings into durable bedrock, construction of drilled shaft/spread footing combinations, Portland cement and shotcrete walls with rock anchors (post tensioned cable strands and solid bars).

## INTRODUCTION

Poor quality bedrock not encountered during initial design borings was discovered during construction of three bridges on relocated US Route 460 located in the mountainous region of eastern Kentucky (Figure 1). Several of the borings performed for design could not be done within the foundation footprint. During construction of benches and spread footing foundations at all three bridges, bedrock issues were discovered leading to different mitigation methods that were required to provide adequate bearing and minimum distances to top of adjacent benches. Most of the bedrock quality issues were contributed to highly weathered shale and nearly vertical clastic dike type joints with non-uniform, irregular spacing. Vertical bedding in the joints (clastic dikes) consisted of highly weathered non-durable shale. The vertically bedded joints were not encountered during the original design borings. Removal of bedrock when constructing the benches contributed to loss of confinement causing the joints to relax and open creating large crevices near pier and foundations.

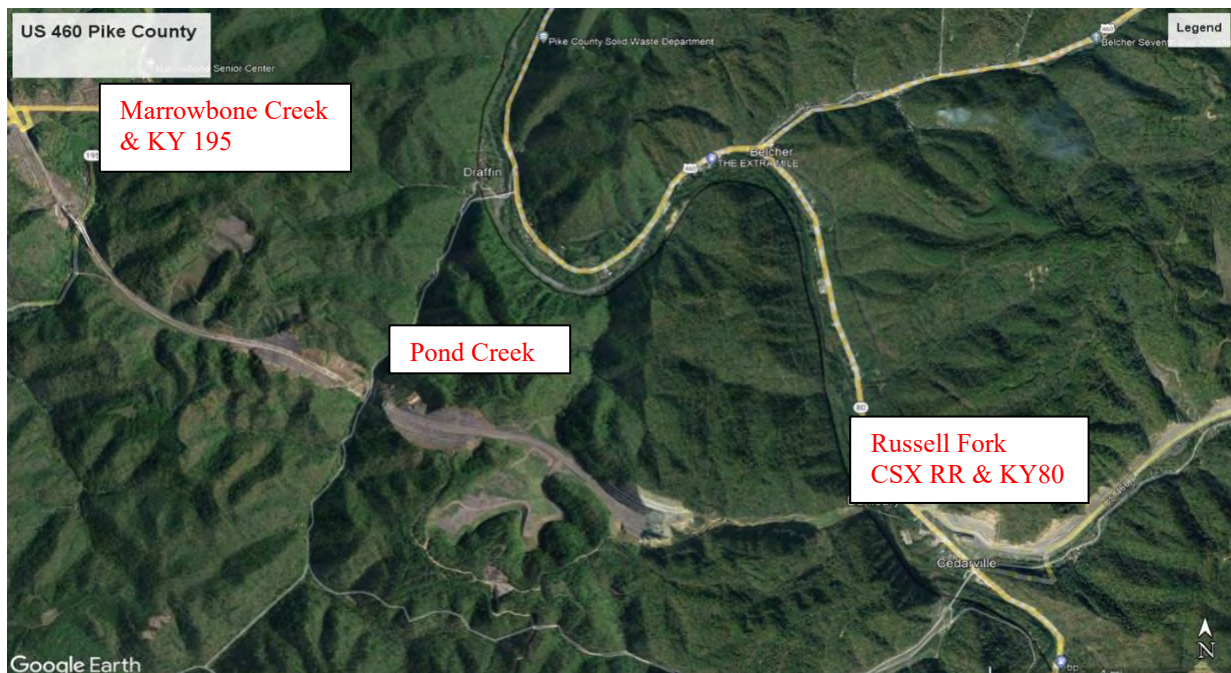


Figure 1 Aerial View of bridges, future US 460. Distance is about 4.2 miles between Marrowbone and Russell Fork bridges.

### US 460 over Marrowbone Creek and KY Route 195

Geotechnical design recommendations for the two structures (EB and WB) were completed in 2003 (1). A contract was awarded for construction of the two 9 span bridges in 2008. Numerous bedrock issues, mainly at both abutments and Piers 1, 2 and 7. Contractual issues created major delays and termination of the contract before final construction was completed. A new contract was awarded in 2016 for completion of the bridge with updated foundation design recommendations (2 and 3). Construction of both bridges was completed in mid-2020. Other bedrock issues, weathered shale, clevises, and clastic dikes were discovered during the final inspection of the bridges in October 2020 (4).

### Initial Mitigation Measures During Construction

Several mitigation measures were designed and completed during initial construction of the original contract. Both abutments and Piers 1 and 2 were demolished and relocated into the cut. Westbound abutment No. 1 was relocated about 46 feet into the existing cut and the Bottom of Footing (BOF) lowered approximately 12 feet. The east bound abutment No. 1 was relocated about 77 feet and with BOF lowered 15 feet. West bound span No. 1 length was increased from 100 to 115 feet, Span No. 2 was increased from 85 to 135 feet. Span No. 3 was increased from 135 to 165 feet. Drilled shafts were also included in a redesign to replace spread footings at Piers 2 and 7 foundations. Additional excavation and mass concrete was required to achieve adequate bearing capacity at foundations for both (EB and WB) Pier Nos. 5 and WB Pier 6 foundations. Drilled shafts were also constructed at one critical corner of each of the east end No.2 abutments due to the minimum distance from edge of footing to face of the underlying bench not achieved due to weathering of shale and relaxation of clastic dikes. Photos of some of the piers and foundations prior to demolishing and relocating are shown in Figures 2 through 8. Plan and elevation views of original design in 2008 and modified design, 2016, are shown in Appendix A.

<b>Table 1. Changes Both Abutments and Piers Nos. 1, 2 and 7 Prior to 20: Marrowbone</b>				
	Original Location	Location after Redesign	Original BOF Elevation	BOF/BOS Elevations after Redesign
WB Abut. No. 1	530+21	529+74.66	953.0	938.0
EB Abut. No. 1	530+85	530+07.75	950.0	938.0
Pier 1 WB	531+21	530+89.66	904.5	887.0
Pier 1 EB	531+70	531+22.75	915.0	887.0
Pier 2 WB	532+21	531+89.66	849.0	857.0/830.0
Pier 2 EB	532+25	532+22.75	860.0	857.0/830.0
Pier 7 WB	538+75	538+73.74	785.0	808.0/760.0*
Pier 7 EB	539+30	539+29	785.0	808.0/780.0*
WB Abut. No. 2	541+25	541+23.74	918.82	913.0/896.0**
EB. Abut. No. 2	541+90	541+89	918.62	913.0/896.0**
*Approximate drilled shaft tips (bottom of rock socket), 2 at Pier 2, 3 at Pier 7				
**One drilled shaft per each abutment at critical corner				

## Mitigation measures after 2020

The clastic dikes and fissures at Piers 8 and No. 2 abutments were not discovered until a 2020 field investigation was performed.



Figure 2. Abutment No. 1 foundation west bound before relocating into cut.

During the final inspection in October 2020 a large fissure was observed adjacent to the Pier 8 west bound bridge spread footing foundation. The crevice had apparently grown larger due to stress relief caused by removal of bedrock to construct benches below the footing. Vertical, clastic dikes with highly weathered thin bedding planes dikes were observed in the crevice. Several other crevices with weathered, vertical bedding planes were also located during field investigations. The fissures (clastic dikes) generally trended parallel to the crevice adjacent to bench face at Pier 8 WB with one trending directly under the foundation of WB Pier 8 toward Pier 8. EB Other crevices were observed near both No. 2 abutments. Vertical clastic dikes in highly weathered shale were also observed at the abutments No. 2 during subsequent field investigations. See Figures 9 through 12.

A contract was awarded to a consultant in December 2020 to design mitigation measures to prevent future widening of the crevices and potential failure of the foundations (4). Angle drilling was performed to supplement existing borings obtained during design to determine location of the vertical features. An additional clastic dike was observed in the bench cut and confirmed to be extending under both Pier 8 (WB and EB) foundations. A cast in place PCC wall with post tensioned stranded rock anchors was designed to prevent expansion of crevices at the WB Pier 8 foundation. A shotcrete wall with post tensioned strand anchors was designed for the EB pier 8 (Figures 13-15). Shotcrete walls with post tensioned solid bar nails were designed for No 2 abutments (east end). Construction of mitigation units at both Piers 8 and Abutment Nos. 2 was completed in May 2023.



Figure 3. Pier 1 EB prior to relocating.

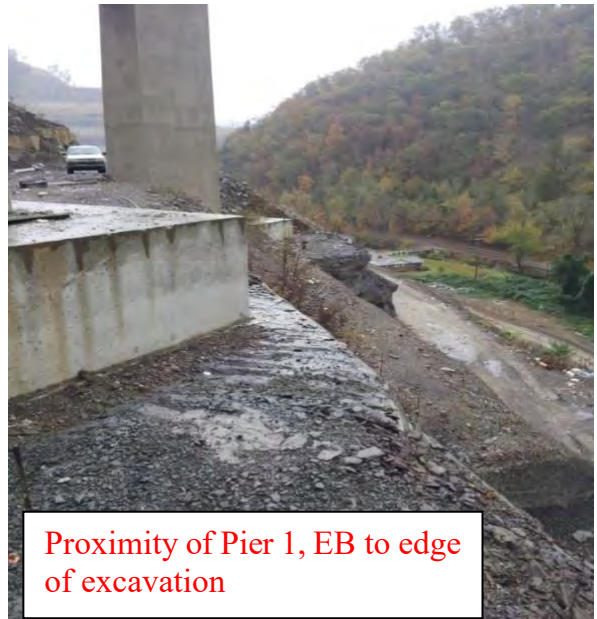


Figure 4. Pier 1 EB prior to relocating.



Figure 5. Pier 1 WB initial construction.

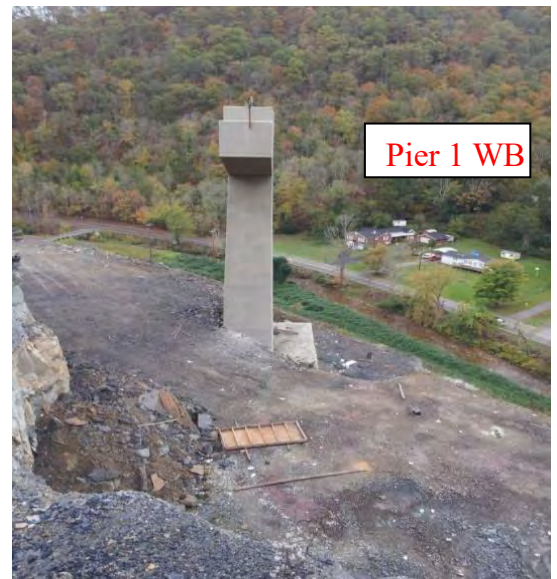


Figure 6. Pier 1 WB before replacing.



Figure 7. Clastic dike and coal seam at Pier 2 WB.

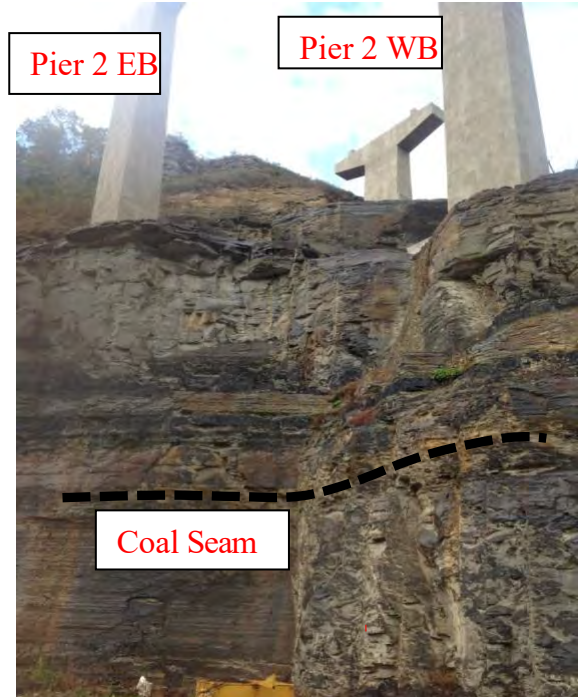


Figure 8. Weathered bedrock and coal seam.



Figure 9 Fissure at Pier 8 WB.



Figure 10. Fissure at Pier 8 WB, October 2020, orange pin is at corner of footing.



Figure 11. Clastic dike at Abutment 2 eastbound.



Figure 12. Clastic dike at Abutment 2 eastbound.



Figure 13. Pier 8 WB post tensioned PCC wall and EB Post tensioned anchor sleeves.



Figure 14. Completed post tensioned concrete wall, Pier 8 WB.



Figure 15. Completed shotcrete anchored Abut. 2 EB.



Figure 16. Aerial view of Marrowbone Bridge in 2020 Abutment No.1 is on right. Notice color of Piers 1 and 2 showing newer construction.

## US 460 over Pond Creek Road

Construction of the two five span bridges (EB and WB) begin in 2017. Geotechnical foundation recommendations were completed in 2012 (5). Weathered bedrock combined with joints were discovered during construction at Pier 4 EB in December 2019 and Pier 1 EB in



Figure 17. Excavation for Pond Creek Bridge Pier 4 EB foundation.



Figure 18. Anchored Concrete wall on cut face, Pier 4 EB, Pond Creek.



Figure 19 Anchored Wall, Pier 4 EB, Pond Creek.

December 2020. Footings at both abutments No. 1 (EB and WB) abutments were lowered six to ten feet and replaced with mass concrete due to poor quality bedrock encountered during foundation excavation. During a field investigation in December 2019 the bench for footings at Pier 4 eastbound was at or near proposed grade. Construction of the spread footing foundation had not begun. The proposed location for the Pier 4 EB footing right of centerline falls with the front right corner extending beyond the underlying top of the lower bench face. Additionally, the bedrock visible at the right edge of the excavation and at the top of the lower bench face is weathered sandstone grading into durable to nondurable siltstone/shale. Quality of the rock underlying, at the front right corner of the proposed footing was not considered competent to support for the presumptive factored bearing resistance (Figure17). An additional shallow excavation near the centerline and back edge of the same footing indicated weathered sandstone as well but with slightly less weathering to a depth of  $\pm 2'$ . An additional investigation, including

borings, was performed and a stepped concrete retaining wall with rock anchors was designed and constructed to provide additional support and prevent further degradation of the bench face below the Pier 4 EB foundation (Figures 18 and 19).

The proposed Pier 4 WB footing location appeared to be located over durable sandstone considered competent support for the presumptive factored resistance. Additionally, the footing corners appeared to meet the setback criteria minimum, 15 feet of sound rock, 10 feet thickness, between footing edge and top of lower bench face.

A recommendation was made to contact the Geotechnical Branch for all piers and abutments yet to be constructed to stress the need to comply with footings reaching 2 feet of embedment into sound rock with poured concrete contacting the edges of the prepared excavations (7).

The required setback criteria (15 feet) into competent bedrock from the bench face was not achieved when the Pier 1 WB footing was excavated in December 2020 to plan elevation (Figure 20). A clastic dike and joints were also present. The bottom of footing elevation was lowered approximately four feet into competent sandstone to meet plan requirements.



Figure 20. Joints and clastic dike at Pier 1 WB footing, Pond Creek.

## US 460 over Russell Fork River, CSX RR and KY Route 80

The contract for construction of the two 12-span bridges was awarded in November 2021. Due to bedrock issues encountered at the bridges over Marrowbone and Pond Creeks an angle drilling program was initiated in February 2021 to determine locations of any clastic dike joints or other bedrock issues located at or near bridge foundations (Figure 21). Drilling results indicated clastic dikes and weathered bedrock at Pier 1 EB and both Piers 2 would require



Figure 21. Angle drilling Pier 1 EB Russell Fork.



Figure 22 Clastic dike below Pier 1 EB foundation.



Figure 23. H piles placed in mass concrete to support Pier 1 EB foundation, Russell Fork.

mitigation to provide adequate bearing for the spread footing foundations and obtain minimum setback distances (10 feet) from foundations to top of benches.

A large clastic dike with highly weathered vertical bedding planes was encountered during the angled exploratory core drilling at Pier 1 EB (Figure 22). The footing was lowered approximately ten feet to competent bedrock to provide adequate bearing capacity and to meet the minimum setback distance from the bench face. Mass concrete was then placed in the excavation to

plan bottom of footing elevation. Steel H- piles (Figure 23) placed in the mass concrete to extend into the concrete for the footing to provide support between the mass concrete and footing (10).

Pier 2 EB foundation was lowered 17 feet into competent bedrock to avoid a coal seam encountered eleven feet below plan BOF and be constructed at an elevation below a highly weathered clastic dike (Figures 24 to 26). The coal seam and a clastic dike were documented

during in angle drilling borings. Due to the large elevation change a pier redesign was performed by the project structural engineering consultant (10).



Figure 24. Pier 2 EB location, Russell Fork.



Figure 25. Pier 2 EB location, Russell Fork.



Figure 26. Clastic dike in bench face below proposed Pier 2 EB elevation, Russell Fork.

Mass concrete (Figure 27) was placed at abutment No. 2 west bound due poor-quality bedrock not meeting the minimum offset distance from foundation to top of the lower bench face (11).



Figure 27. Additional mass concrete (left side) at Abutment No.2 WB looking east



Figure 28. View from Abutment 2 looking east May 2023, Russell Fork.

## Summary

Weathered bedrock combined with unfavorable joints and clastic dike orientations led to several types of mitigation efforts to provide adequate bearing and minimum clear distances from cut faces at three bridges for the future US 460 corridor. Most of the bedrock features were not identified during design due to difficulties obtaining cores at the foundation locations. Clastic dikes infilled with highly weathered shale and vertical joints documented during initial coring.

Based on issues at Marrowbone and Pond Creek bridges, angle drilling was performed to document bedrock concerns prior to construction

### **Lessons Learned**

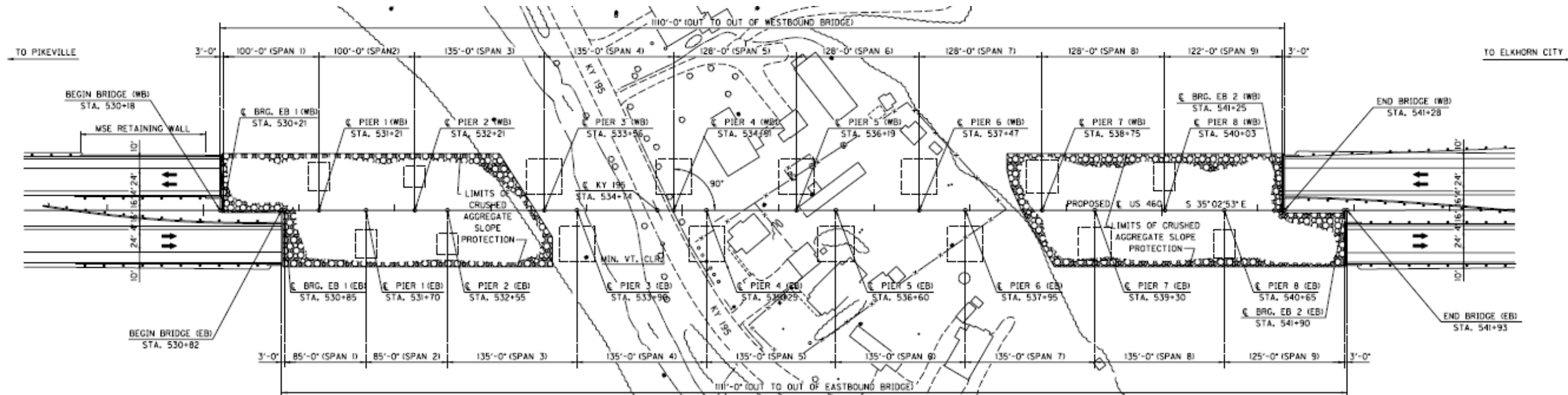
Knowing the features depths and orientation of the undesirable features assisted in designing mitigation measures. Any future bridge designs in this region should require borings at structure foundations including angle structures are located on mountains. Numerous design and construction changes were needed to construct pier and abutment foundations to obtain specified bearing recommendations and minimum setback distances from vertical bench faces

### **REFERENCES:**

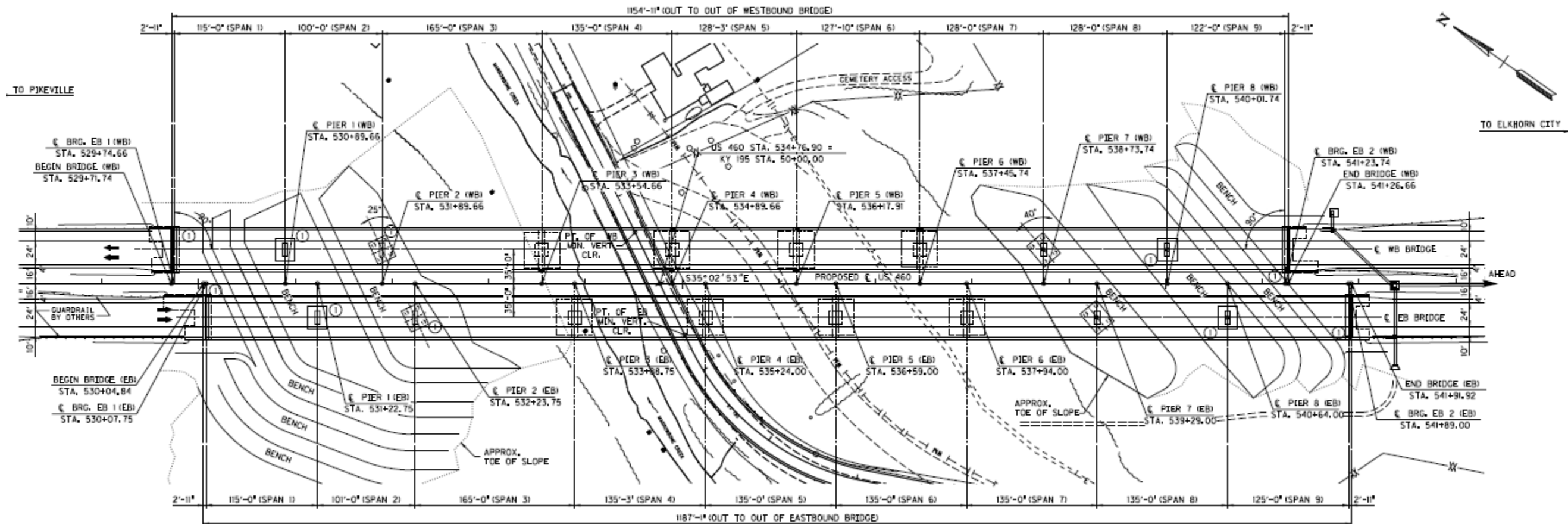
#### KYTC Reports

1. Molen, D. KYTC Geotechnical Report S-067 -2003, Bridge over KY 195 and Marrowbone Creek, May 2003
2. Greer, D., Asher, B., and Blevins, M. KYTC Internal communication KYTC October 2013
3. Greer, D. KYTC Geotechnical Report C-002-2014, Bridge over KY 195 and Marrowbone Creek, Abutments 1 and 2, Piers 1, 2, 7 8 July 2015
4. Stantec Consulting Engineers KYTC Geotechnical Report SA 011-2000, US 460 over Marrowbone Creek, Evaluation of Eastbound and Westbound Pier 8 & Abutment 2, January 2022
5. Greer, D. KYTC Geotechnical Report SA-016 -2012, Bridge over Pond Creek, August 2012
6. Greer, D. KYTC Geotechnical Report SA-016 -2015, Bridge over Pond Creek, May 2015
7. Ross, A. KYTC Geotechnical Report C-007-2019 US 460 over Pond Creek Pier 4, January 2020
8. Beckham, T. KYTC Geotechnical Report, C-002-2021 US 460 over Pond Creek, Pier 1 WBL Foundation, January 2021
9. Greer, D. KYTC Geotechnical Report S-018 -2010, Bridge over Russell Fork, May 2010
10. Beckham, T. KYTC Geotechnical Report, C-003-2021 US 460 over CSX RR, Russell Fork, and KY 80 Pier1 EBL, Pier 2 EBL and Pier 2 WBL Spread Footings, May 2021
11. Beckham, T. KYTC Geotechnical Report, C-005-2021US 460 over CSX R.R., Russell Fork, and KY 80 WB Abutment 2, April 2021

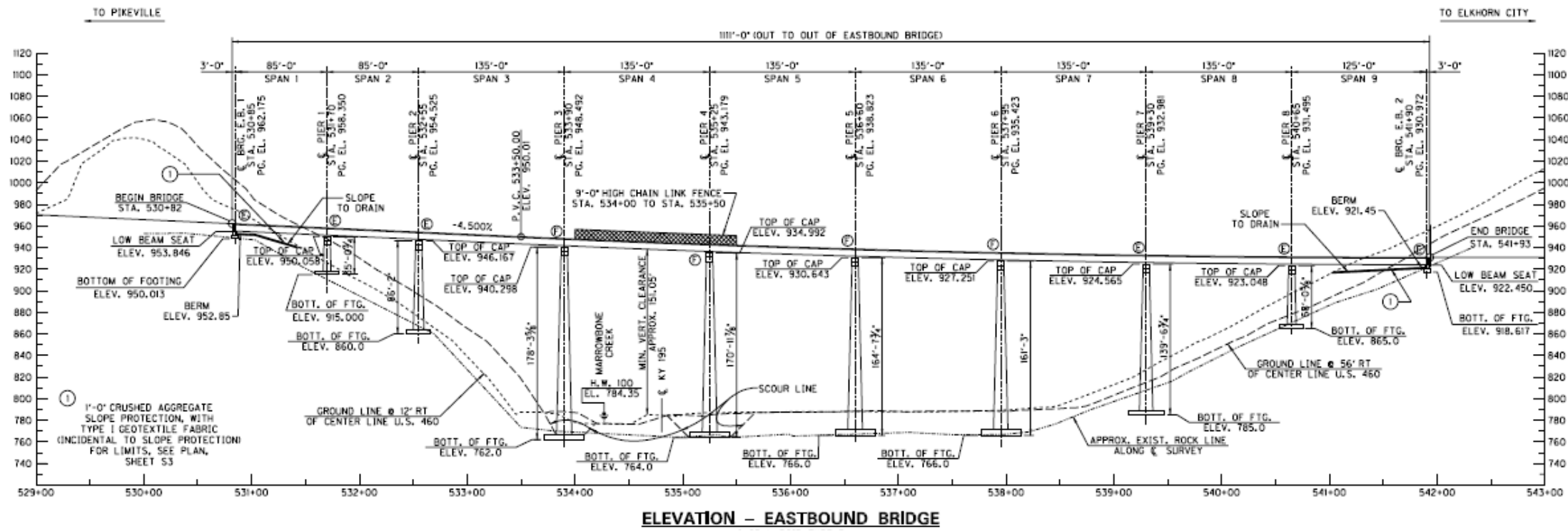
Appendix A  
Plan Views  
Elevation Views  
Original Design 2018  
Modifications 2016



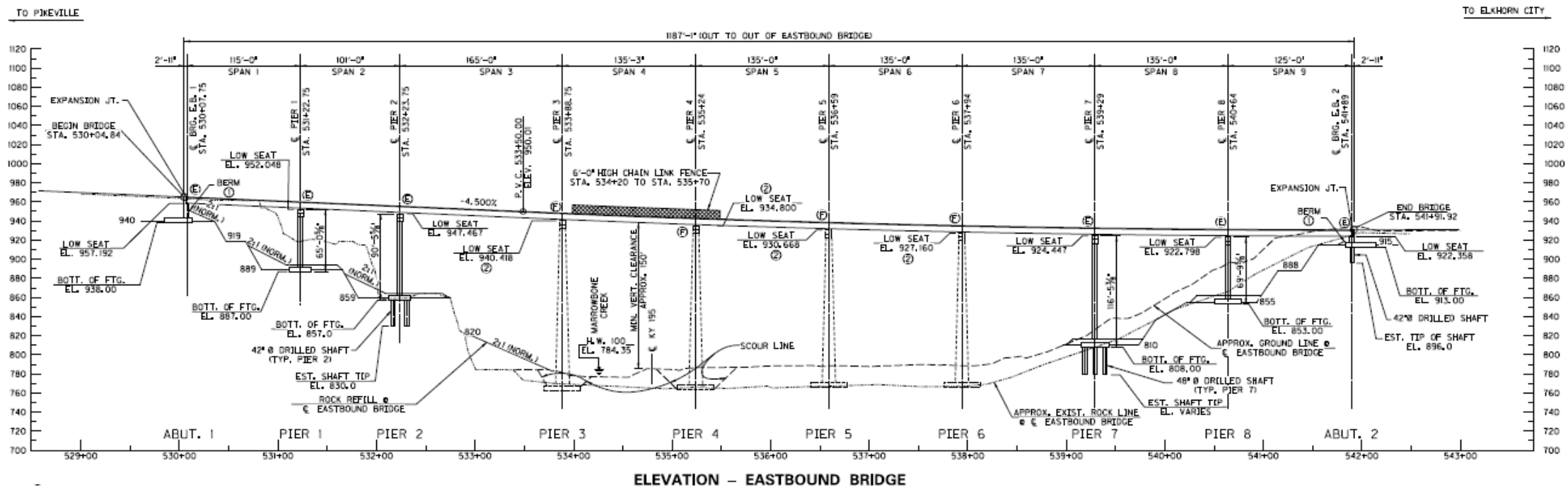
Original 2008 Plan View.



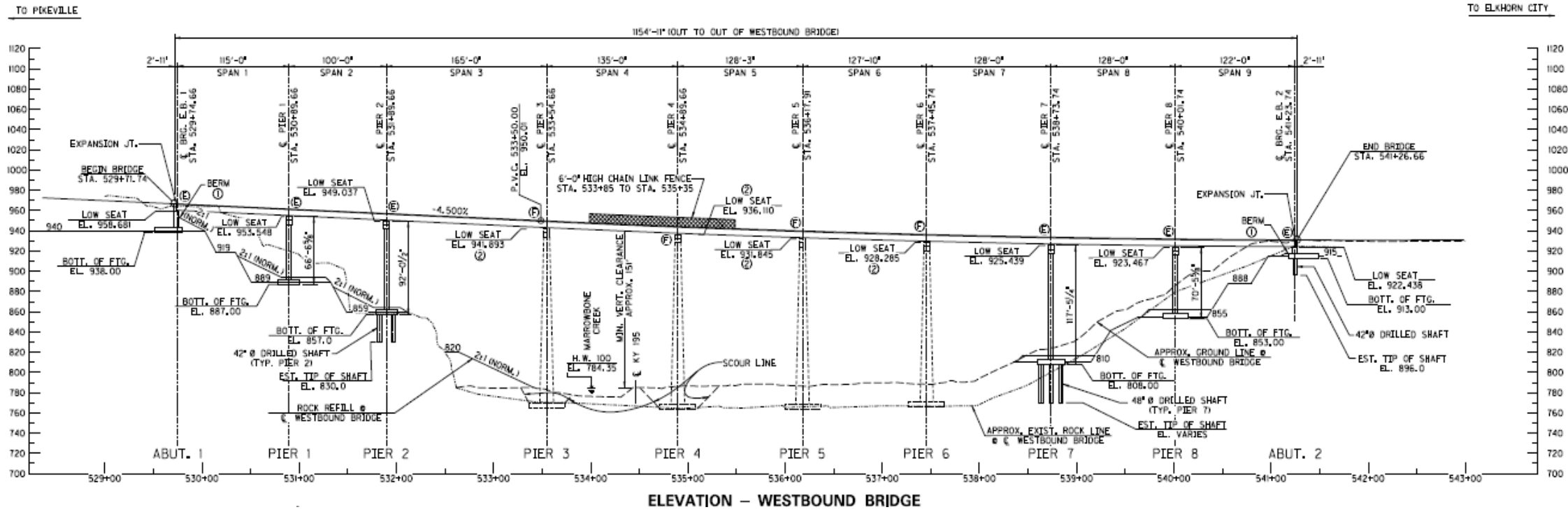
Plan View after Modifications 2016.



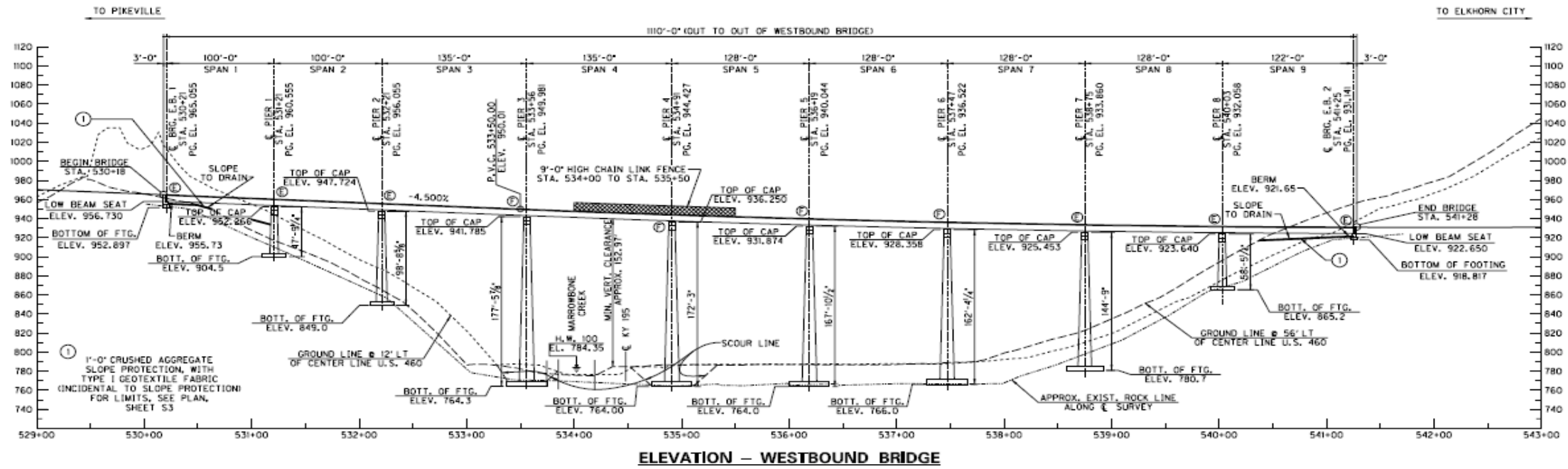
Original Elevation EB Bridge 2008



Elevation EB Bridge After Modifications 2016



Original Elevation WB Bridge 2008



Elevation WB Bridge after Modifications 2016

**Latest Developments to Increase the Quality Of  
Flexible Rockfall Protection Barriers**

**Tim Shevlin, PG**  
Geobrugg NA, LLC  
Algodones, NM 87001  
503-423-7258  
Tim.shevlin@geobrugg.com

**Armin Roduner**  
Geobrugg,  
Romanshorn, Switzerland  
Armin.roduner@geobrugg.com

**Helene Lanter**  
Geobrugg,  
Romanshorn, Switzerland  
Helen.lanter@geobrugg.com

### **Acknowledgements**

We like to thank the SLF-WSL Institute for Snow and Avalanche Research as well as Innosuisse for the collaboration on the research project Innonet researching on rockfall barrier service loads for rock impacts with spin.

### **Disclaimer**

Statements and views presented in this paper are strictly those of the author(s), and do not necessarily reflect positions held by their affiliations, the Highway Geology Symposium (HGS), or others acknowledged above. The mention of trade names for commercial products does not imply the approval or endorsement by HGS.

### **Copyright Notice**

Copyright © 2023 Highway Geology Symposium (HGS)

All Rights Reserved. Printed in the United States of America. No part of this publication may be reproduced or copied in any form or by any means – graphic, electronic, or mechanical, including photocopying, taping, or information storage and retrieval systems – without prior written permission of the HGS. This excludes the original author(s).

## ABSTRACT

In the last 30 years, flexible rockfall barriers made of steel wire nets have become established worldwide as a protective solution. To ensure that these barriers can effectively stop the dynamic impact of rockfall, several guidelines have been introduced worldwide since 2001. Even with guidelines there is low awareness that the capacity of a rockfall barriers is dependent on the net impact location, and how to evaluate the rockfall barrier capacity in load cases outside the requirements of the approval tests differs worldwide. In 2019 an Innosuisse-sponsored 3-year research project was granted to the WSL Institute for Snow and Avalanche Research SLF, together with the industry partner Geobruigg, for testing fully instrumented rockfall barriers to investigate rockfall impact position variability into flexible barriers systems. The results justify additional tests to the existing European certification procedure allowing a better quantification of the energy capacity of the protective surface of rockfall barriers.

Keywords: Rockfall, 1:1 field tests, Flexible protection barrier, Multiple Loading.

## ROCKFALL CERTIFICATION PROCEDURES AND GUIDELINES WORLDWIDE

To ensure that flexible rockfall barriers can effectively stop the dynamic impact of rockfall, several guidelines have been introduced worldwide since 2001. They include proof of functional suitability through 1:1 field tests, as well as proof of serviceability. In 2001, the first guideline for approval of rockfall protection kits was published in Switzerland (Gerber 2001), followed in 2008, by a European approval and conformity verification procedure for rockfall protection nets, called ETAG 027 (EOTA 2008). In 2018, ETAG 027 was transformed into a European Assessment Document EAD 340059-00-0106 (EOTA 2018). The EAD specifies standardised and reproducible load cases and is the most commonly used guideline worldwide by designers (Peila & Ronco 2009, Volkwein et al. 2019, MBIE 2016, TRB 2016).

However, long-term experience shows that other, natural, load cases happen which are not covered by the "laboratory-like" tests prescribed in the EAD. The EAD lacks any statements on practical applications in the field. Additionally, the energy uptake of rockfall barriers has developed exponentially. In 1980, energies ranged around 200kJ with low velocities ( $10 \text{ m.s}^{-1}$ ) (Baumann & Gerber 2018). Today, flexible barriers are solutions against rockfalls with broad protection capabilities ranging from 50 kJ to 11'000 kJ (EOTA 2023) and certification velocities of a minimum  $25 \text{ m.s}^{-1}$  (EOTA 2018). Therefore, some countries have additional requirements that add to the European standards.

Here, the Swiss, European, Austrian, French, Italian and New Zealand guidelines are roughly summarised in the paper *Rockfall Barrier Service Loads for Rock Impacts with Spin* (Caviezel et al. 2022). Some examples of protection kit failures are described in section 2.1 highlighting the missing practical field applications of the guidelines. The methodology of further field testing and "laboratory" testing is then described in section 2.2 to assess further realistic load case scenarios. The following scenarios are then treated by means of 1:1 tests to increase the quality of rockfall protection systems and to offer more safety through additional test procedures.

### 1.1 European Certification Guideline

Following the original Swiss guideline, in 2008, the ETAG 027 (EOTA 2008) was the first European testing standard that made it possible to compare different rockfall barriers based on their energy level in for European countries. The test procedure is based on tests at two different energy levels: Service Energy Level (SEL) and Maximum Energy Level (MEL) (EOTA 2018). The SEL test consists of two consecutive impacts with a third of the maximum energy level without maintenance to the kit in contrast to the single Swiss 50% SEL impact. The SEL Launch 1 is passed if there are no ruptures to any kit components. SEL 2 is passed if the block is stopped by the kit and the block has not touched the ground until the kit has reached maximum elongation during the test. The MEL launch is passed if the block is retained by the kit. A detailed description of damages after a MEL impact has to be provided and included in the ETA. The impact location is set for all three launches in the middle of the central functional module (Figure 1), representing the most favourable impact location for the barrier.

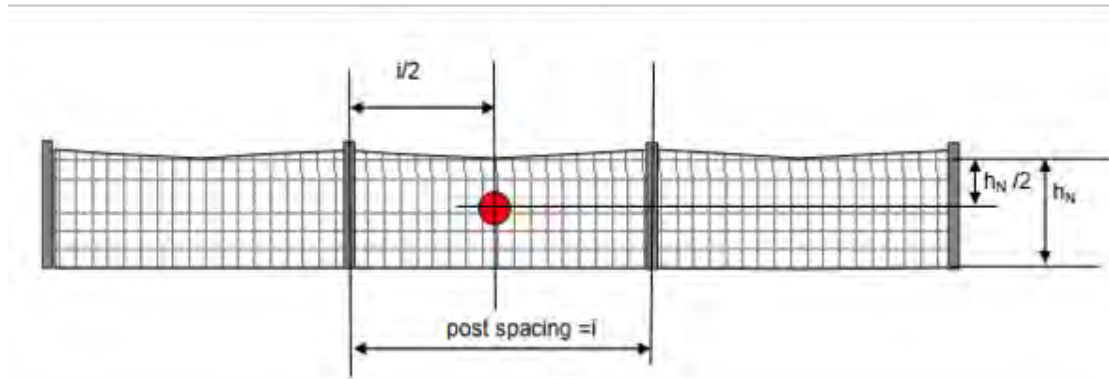


**Figure 1. Impact Location of the SEL and MEL Launches during certification tests (EOTA 2018).**

## 1.2 Additional guidelines superseding European Certification

The above-mentioned guidelines are presented shortly here, a more extensive summary can be found in Caviezel et al. (2022). Broadly speaking, they act as a complement to the European Certification to address the limitations of said certification (symmetrically force distribution, no consideration of block shape, block rotation etc.) and cover aspects such as foundations, anchor loads etc that are not mentioned in the EAD.

In Switzerland the uncertainties when testing barriers are accounted for by introducing a safety factor: The forces measured in the approval include not only the more stringent conditions of the vertical drop but also the compensating effects of the central position in which the test bodies impact the net. Eccentric strains nearer the posts or nearer the bearing ropes will subject individual ropes to additional forces which are not yet known.

In Austria, ONR 24810 was published in 2013 and amended in 2021. Partial safety factors are introduced, to mitigate the favourable centric impacts in the middle field during the approval tests, and the optimal symmetrical distribution of forces at the anchors. Higher forces at the anchorage points are also expected here for decentralised impacts.

In France, the CEREMA published the "National Regulation for Flexible Rockfall Barriers" (Bost, 2014) which complements the EAD in the following: Focus on work and not on the product: the product must adapt to the location and not the other way around.

In the case of Italy, project recommendations are added that are detailed in UNI 11211 (2018), which are not directly related to the requirements of the rockfall protection kit, it only proposes the use of SEL instead of MEL as design criteria. Concerning the safety factors, the standard approach follows the basic rules of Eurocodes, amplifying the actions and reducing the reactions.

The New Zealand guideline discusses both approaches of the UNI and ONR with the use of partial safety factors, mainly for the design approaches, and applying a reduction factor on the barrier energy rating (MBIE 2016).

### 1.3 Rockfall Barrier Capacity

The specification, however, of realistic service loads for flexible rockfall barriers is an ongoing concern in rockfall engineering. The question inevitably arises as to whether vertical drop tests, in the middle of the middle field of a three-field system, which do not consider block rotations, are representative of loads encountered by barriers in real terrain.

Further, the awareness that the capacity of a rockfall barrier is different depending on the impact location, and how to deal with the so-called remaining capacity of rockfall barriers, in load cases outside the approval tests, differ worldwide. By exaggerating the problem, one can illustrate the problem with Figure 2 and 3. Technically, according to (EOTA, 2018), a barrier is fulfilling its retaining capacity over a certain area, in this case the middle of the middle field of the test system (Figure 2).



**Figure 2. Symbolic illustration of the energy capacity (in % of MEL) distribution in the barrier system based on current testing method.**

Any other kind of possible impact is not considered. Adversely, what is commonly expected of a rockfall barrier's protection surface? A fully covered area such as represented in Figure 3. In some countries, specialized designers are aware of this fact and solve the problem by over-dimensioning the rockfall barriers to ensure the availability of residual capacity outside of the middle field. In other countries, however, authorities and/or designers assume that a rockfall system absorbs certain energy, even in marginal areas or in case of an eccentric hit. Protective solutions are consequently not necessarily designed properly.



**Figure 3. Symbolic illustration of the energy capacity (in % of MEL) distribution in the barrier system assumed by anybody not familiar with the topic.**

## NEW ROCKFALL TESTING IN THE FIELD AND IN THE “LAB”

### 2.1 Failures in the field over the years

Many examples can be found in Caviezel et al. & Mastrojannis (2022, 2022) where certified barriers failed to stop the rock. The main problems relate to force concentration in the post head area due to eccentric impacts, impacts in the lateral, untested, fields as well direct damages to posts and base plates. The impact source also differs from the standardized test scenario with differently shaped rocks and rock's rotational component.

Bichler & Stelzer (2022) reviewed the performance of a 1000 kJ rockfall barrier over approximately ten years. This example showcases nicely what a barrier must go through during its service life and how far these scenarios are from the standardized certification impacts.

### 2.2 Research in the field

The current state of research in Europe is well summarised in Caviezel et al. (2022). In short, the work of Heiss (2017) shows that analytical calculation or numerical simulation are not a suitable alternative to 1:1 field testing, mainly because of the complexity of the dynamic processes. According to his research results, asymmetrical hits are absolutely necessary for the evaluation of protective systems. The national research project C2ROP was launched in France in 2016 in which the behaviour of rockfall barriers under natural load cases is also investigated more closely, with 1:1 field tests with lateral impacts as well as multiple loading scenarios.

In 2019 a research project was started, funded by Innosuisse, led by the Snow and Avalanche Research Institute (SLF) of the Federal Forest and Landscape Research Institute (WSL), with a flexible rockfall protection fence manufacturer, Geobrugg, as the industry partner. The aim was to investigate random natural load cases hits into a fully instrumented barrier (Figure 4) and propose some additional testing scenarios for the standardised testing facility, Walenstadt, in Switzerland. The random hits were meant to show the most important force concentrations in the barrier and the tests led in Walenstadt, allowed to get as close as possible to the same peak loadings while ensuring repeatability. A summary of the testing campaigns is found in Sanchez et al (2019) as well as in Caviezel et al. (2022).



**Figure 4. Left: A test block, released by helicopter bounces, rolls and slides down the slope. Right: Fully instrumented flexible rockfall protection barrier experiencing a random rock impact.**

## 2.3 Translation to tests in the “lab”

The test facility "Lochezen" in Walenstadt, Switzerland began operating in 2001. The test site was to certify net barrier systems, as well as conduct research on the mechanical behavior of barrier components (nets, brake elements, ropes). Over the last two decades, several hundred tests of rockfall barriers have been carried out at this facility, and systems from various manufacturers have been tested and certified. The barriers are installed at a height of 15 m on an almost vertical block face. Normally three fields are installed with 10 m post spacing. Using a derrick crane, the test blocks can be positioned above the barrier and dropped. Sensors capture forces in the barrier components, primarily ropes; high-speed video recordings are used to capture the deformations of the barrier system over time.

## RESULTS

One of the findings from the full-scale experiments is that it is possible to structure the additional tests for approval in a similar way to what authorities have been demanding since the 1990s. These tests can be carried out in addition to the tests required by the EAD in order to give design engineers and the ultimate owners of the rockfall barriers more certainty about the capacity of the entire protective surface. The proposed additional tests in Caviezel et al. (2022) are on one hand an impact in a single field of a barrier, instead of a three-field system which is equivalent to a border field impact. On the other hand, an eccentric impact is proposed in the middle field of a three-field system, as this impact translates best to the random impacts in the net as well as the rotation of the blocks. These proposed scenarios were taken over by Geobruagg, additionally to the CE certification, and implemented during the development of a new rockfall barrier line (Figure 5, TSUS Report 2021a). Further tests were deemed of interest to push knowledge further in terms of the uptake capacity of a barrier as well as the proof of constructional adaptations in the field. These test results are described in further detail in the following subsections.

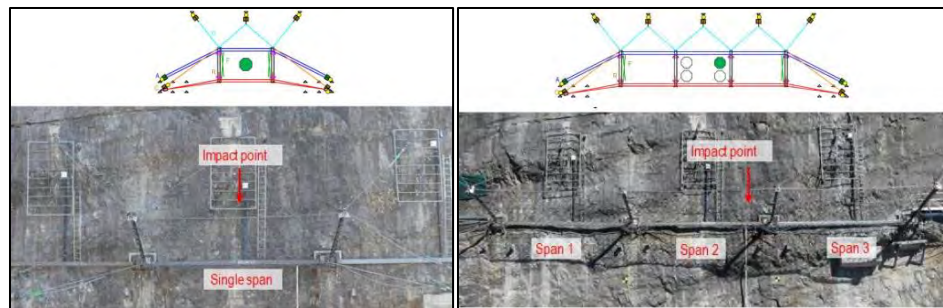


**Figure 5. Left: Single span impact at Maximum Energy Level, corresponding to a border field impact. Right: Eccentric impact at Maximum Energy Level, in the top corner, near the post head of the middle field of a three-field system. Example of a 1'000 kJ rockfall barrier (TSUS, 2021a)**

### 3.1 Support Rope Separation

Depending on the site where a barrier is installed, constructional adaptations need to be made to ensure the full functionality of the barrier. When a barrier exceeds a certain length, a

separation of the support ropes of the barrier is necessary, to ensure that the forces acting upon the barrier arrive at a timely interval to the anchors on either side, so that the energy-dissipating elements can be activated. In Switzerland, it is customary to do so after a length of 60m. But this setup has never been tested before. A support rope separation was successfully tested in 2021, during the development of the new barrier line, by means of two consecutive maximum energy level tests on either side of the support rope separation (Figure 6, TSUS 2021b).

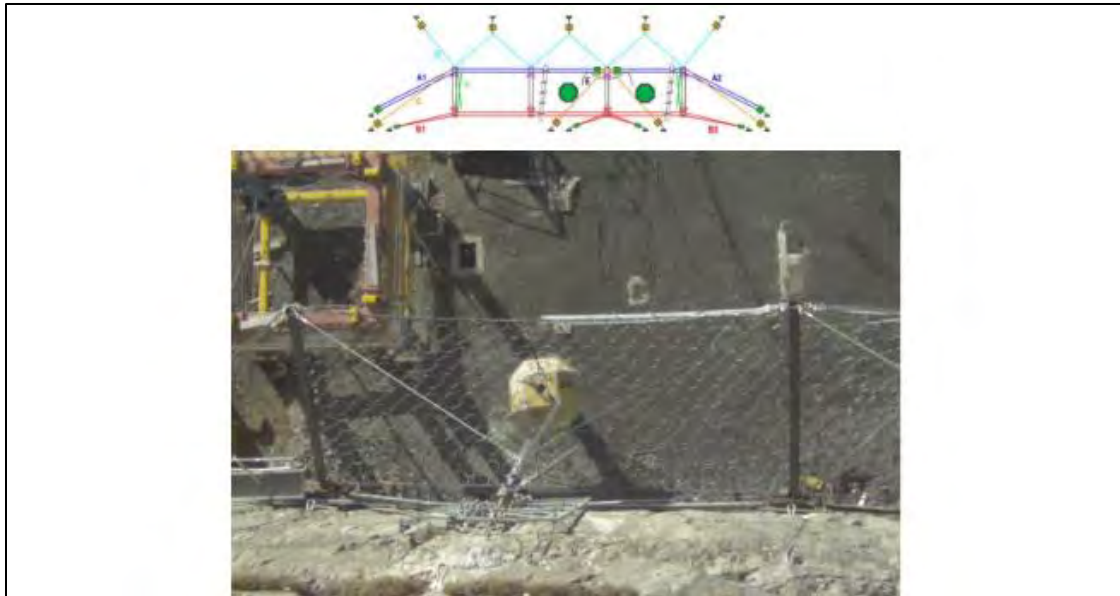


**Figure 6. Support Rope Separation Test on a 2'000 kJ rockfall barrier (TSUS, 2021b). The bottom support ropes are led to two anchors on the ground while the top support ropes are separated and connected at the post head instead of being also led to anchors in the ground. This ensures that no support rope gets hit during an impact.**

### 3.2 Multiple Impacts

Finally, an always-arising interrogation lay in the question of how much rest capacity a barrier has when dimensioned in order to receive Service Energy Level impacts (SEL). Therefore, after certifying a 3'000 kJ barrier with a MEL and two consecutive SEL hits, further SEL hits were launched in various locations, trying to replicate impacts observed in the field over the years as well as during the research project with the SLF. It was decided, after the two SELs in the middle field, to impact twice a lateral field, then a post and a final impact in the middle field again (Figure 7). The barrier successfully managed to retain all six SELs load cases (TSUS, 2021c).

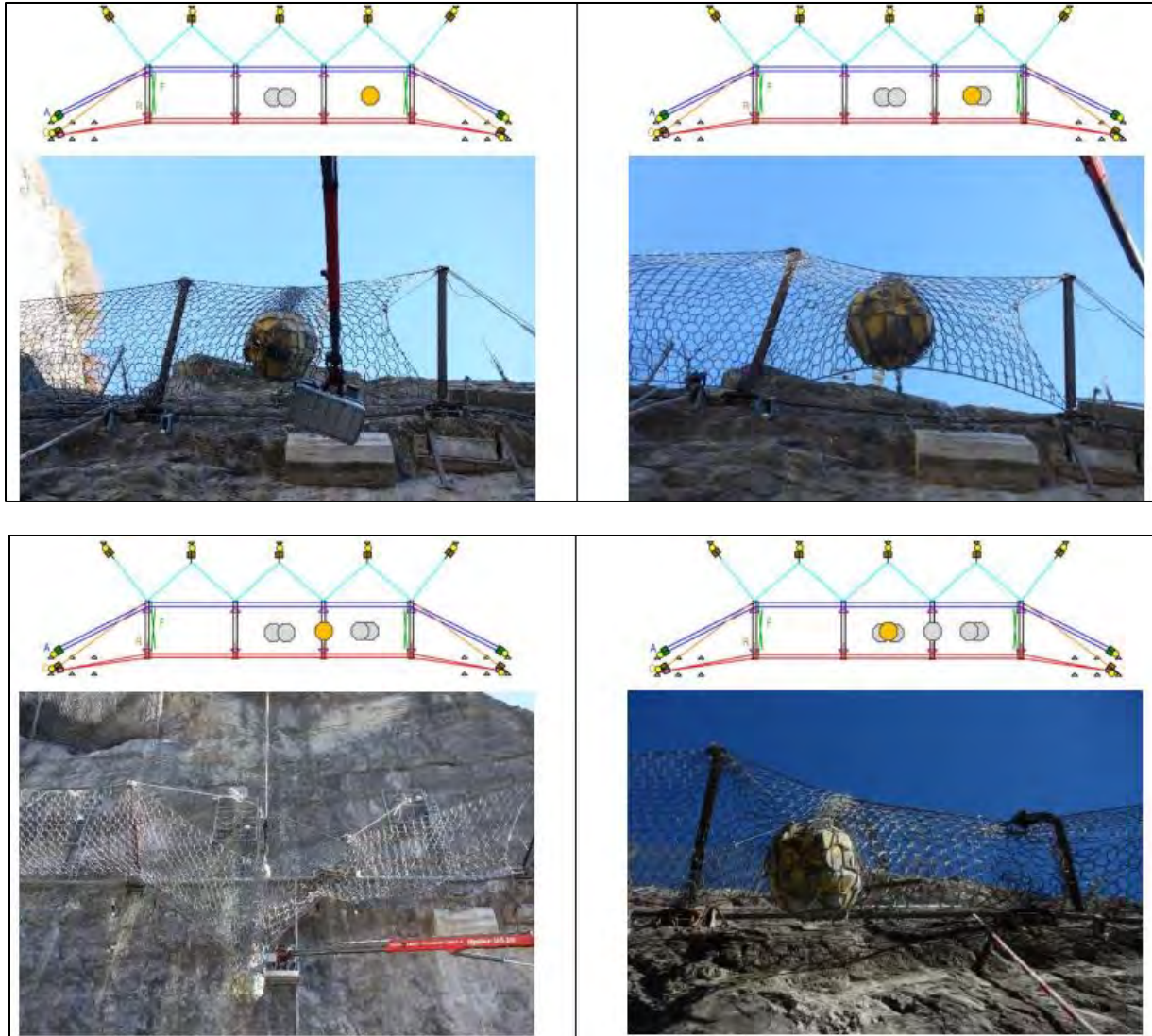


**Figure 7. Succession of several SEL impacts in the same barrier without repairs between tests (TSUS, 2021c).**

### 3.3 Additional Loads

Some of the results of this research project, include that if disc-shaped bodies are to be expected and the topography allows an increase in rotational speed, a reinforcement of the net for point loads arising from rock rotations should be considered (Caviezel et al., 2022). Indeed, falling bodies hitting a rockfall barrier with high rotational energies lead to higher loads than would be expected from testing and certification, according to the European Assessment Document (EAD). The length of the system needs to be adapted, as well as the lateral spreading is much higher with wheel-shaped blocks, and the probability of impacting border fields rises (Caviezel et al., 2022). The main danger is that the increased forces on the protective surface cannot absorb the higher tangential forces and fails.

Two substitute loads that guarantee the best possible coverage along the entire length of the barrier line were, therefore, determined to reproduce the tangential forces caused by the rotation and consider border field hits. These additional tests lead to a new assessment of the energy capacity absorption of the protection surface of a rockfall barrier. The results of these tests are highlighted in Figure 8.

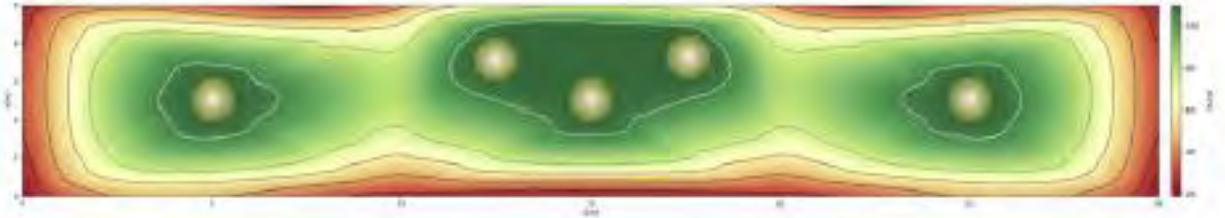


**Figure 8. Schematic illustration of the theoretical energy distribution (in % of MEL) on the barrier surface considering the full-scale test in the natural environment and the additional vertical tests on critical points of the protective surface.**

## CONCLUSION

Over the last 15 years, falling block protection kits have become established as an efficient protective measure, and the solution is recognized worldwide. The energy absorption capacity has increased by a factor of 6 from a maximum of 1'500 kJ to 11'000 kJ. The higher performance of the systems, the new markets and the worldwide established EAD test (EOTA 2018) has created a competition that exists in many markets. Flexible barriers have evolved from being a specialized solution for specific/narrow energy level locations to cost-efficient systems widely used. But the described testing avoids real conditions and thus, the performance issues lead to failures. Therefore, it is difficult for the planner to determine the most cost-optimized solution for an adequate protection measure. The research project on rockfall barrier service loads by the SLF-WSL and even further testing can answer some of these questions.

To conclude, there are weaknesses in the existing certification tests for rockfall barriers. The tests at the Flüela Pass confirmed that the load cases with rotating blocks and eccentric impacts, as well as border field impacts, generate different forces in the rockfall system compared to the standardised test procedure according to EAD 340059-00-0106. This fact demonstrates the problems of defining barrier length in practical problems. In the case of uniform fall bodies and an uneven morphology, the height of the barrier is also not to be neglected. Adding some expert knowledge leads to rockfall protection kits with a maximum achievable proofed protection surface.

## REFERENCES

- Austrian Standards International. ONR 24810 - Technischer Steinschlagschutz. Ausgabe 2021-05-01.
- Baumann, R. and Gerber, W. 2018. Grundlagen zur Qualitätsbeurteilung von Steinschlagschutznetzen und deren Fundation. Anleitung für die Praxis. Tech. rep. Federal Office for the Environment (FOEN).\
- Bichler A., Stelzer G., 2022. Long term performance of a rockfall fence. Proceedings of RocExs, 2022, Japan.
- Bost M., 2014. Écrans de filet pare-bloc dynamiques : Recommendations pour leurs spécifications. Jan. 2014.
- Caviezel A., Munch J., Bartelt P., Lanter, A. 2022. Rockfall Barrier Service Loads for Rock Impacts with Spin. Theory and Experiments. WSL Ber. 125.81 p.
- EOTA 2008. ETAG 027 Guideline for European Technical Approval of Falling Rock Protection Kits. Tech. rep. Belgium: EOTA.
- EOTA 2018. EAD-340059-00-0106-2018 Falling Rock Protection Kits. En. Tech. rep. Belgium: EOTA.
- EOTA, ETA Database 2023. <https://www.eota.eu/etassessments>, (accessed 10.02.2023).
- Gerber, W. 2001. Richtlinie über die Typenprüfung von Schutznetzen gegen Steinschlag. Tech. Rep. Swiss Agency for the Environment, Forests and Landscape (SAEFL), Swiss Federal Research Institute WSL.
- Heiss, C., 2017. Überlegungen zur Sicherung von Personen und Infrastrukturbauwerken gegen Steinschlag im alpinen Bereichen unter besonderer Berücksichtigung von flexiblen Steinschlagschutzsystemen. PhD thesis, Montanuniversität Leoben, Austria.
- Mastrojannis, E., 2022. Occurrences, causes and probability of rockfall protection fences failures in D-A-CH region and suggestions for optimizing rockfall protection fences test procedures based on analysis of fall body impact positions. MSc Thesis Technical University of Munich (TUM), unpublished.
- Ministry of Business, Innovation and Employment (MBIE) 2016. Rockfall: Design considerations for passive protection structures. en-NZ. Guidance. Wellington, New Zealand.
- Peila, D. and Ronco, C. 2009. Design of rockfall net fences and the new ETAG 027 European Guideline. Technical Note in Natural Hazards and Earth System Science vol.9, no.4, pp. 1291-1298.
- Sanchez, M., Caviezel, A., 2019. Full-scale testing of Rockfall Nets in Real Terrain. WSL Report, en. issue, Birmensdorf.
- Transportation Research Board (TRB). 2016. Guidelines for Certification and Management of Flexible Rockfall Protection Systems. Ed. By Ben Arndt et al., Washington DC: The National Academies Press.

TSUS, 2021a. Technical report No. 70210080/01: Summary of evaluation and assessment of eccentric and single span impact tests on ROCCO-1000. Building testing and research institute, Slovak Republic.

TSUS, 2021b. Technical report No.70210080/04: Summary of evaluation and assessment of eccentric and single field maximum energy impact tests and subsequent service energy impact tests on ROCCO-3000.

TSUS, 2021c. Technical report No.70210080/02: Summary of evaluation and assessment of eccentric, single span and support rope separation impact tests on ROCCO-2000.

UNI 11211-4, U. Opere Di Difesa Dalla Cadutta Massi – Parte 4: Progetto Ed Esecutivo. 2018.

Volkwein A., Gerber, W., Klette, J., Spescha, G., 2019. Review of Approval of Flexible Rockfall Protection Systems According to ETAG 027. Technical Note, Geosciences 2019, 9, 49.

**An Innovative Early Warning System  
for Rockfall Protection Systems and Events**

**Michael Koutsourais, PE**  
Maccaferri, Inc.  
10303 Governor Lane Blvd.  
Williamsport, MD 21795  
301-641-8072  
m.koutsourais@maccaferri.com

**Luca Gobbin and Alberto Grimod**  
Officine Maccaferri Spa  
Via Kennedy 10  
Zola Predosa (BO), Italy  
l.gobbin@maccaferri.com

**Sage Evans, PG**  
Maccaferri, Inc.  
10303 Governor Lane Blvd.  
Williamsport, MD 21795  
385-243-4175  
s.evans@maccaferri.com

Prepared for the 72<sup>nd</sup> Highway Geology Symposium, August 2023

### **Disclaimer**

Statements and views presented in this paper are strictly those of the author(s), and do not necessarily reflect positions held by their affiliations, the Highway Geology Symposium (HGS), or others acknowledged above. The mention of trade names for commercial products does not imply the approval or endorsement by HGS.

### **Copyright © 2023 Highway Geology Symposium (HGS)**

All Rights Reserved. Printed in the United States of America. No part of this publication may be reproduced or copied in any form or by any means – graphic, electronic, or mechanical, including photocopying, taping, or information storage and retrieval systems – without prior written permission of the HGS. This excludes the original authors.

### **ABSTRACT**

The paper describes an innovative alert system developed to verify if a rockfall or debris flow protection system is impacted, or if an event, such as a landslide or rockfall, might happen.

This new alert system, HELLOMAC, is installed directly on the rockfall/debris flow protection structure or on the landslide or unstable rock surface, and an acquisition unit (Hubir) is used to collect the data of up to 100 devices in a radius of 5 km and transmit an alerting message by satellite and/or GPRS.

The paper describes the alert system in detail and its different applications, and it presents a very interesting installation along SS 34, a major road in northern Italy running alongside Lake Maggiore and connecting the city of Verbania with the Swiss border.

## INTRODUCTION

As communities and infrastructure expand into more remote regions of the world, geohazard protection systems are often employed for protection against rockfall, debris flow and shallow landslides. As a result, the need for these protection systems is ever-growing, and the knowledge of where a protection system has been employed, or should be employed, and when an event has occurred is important as resources are applied.

Rockfall protection systems are often installed in remote areas, very difficult to access, where the use of a helicopter is commonly required. It is, therefore, possible to lose track of, or forget about where these systems are installed, and it can also be difficult to know when a barrier has been impacted, or when and where material has accumulated within a drapery system. This information is very important to understand if maintenance, or the complete replacement of the system is required and when these operations are needed. Otherwise, frequent visual checks are needed to ensure the safety of the public and to guarantee the integrity of the geohazard protection system.

## ALERT SYSTEM FOR ROCKFALL PROTECTION

One of the main aspects of rockfall protection systems is its maintenance to ensure the serviceability and functionality of the system. In consideration of international standards moving towards specifying and requiring monitoring and alert systems to be installed on rockfall protection systems, after years of research and development, and in line with the recommendation of UNI 11211-5 (May 2019) and the UNI 11211-2 (June 2007) norms, an innovative early warning and impact alert system, HELLOMAC, has been developed by Maccaferri to monitor the in-field conditions of existing rockfall protection systems.

HELLOMAC is an alloy disk with thin tie rods or “arms” that extend out from the disk as shown in Figure 1. The arms connect the disk to the different positions on the rockfall protection system. An antenna, located on the top of the device, sends the alarm signal when an event has occurred. The main structure of the HELLOMAC unit is made of a highly resistant and durable argal aluminum alloy.



**Figure 1: The HELLOMAC Device**

## FIELDS OF APPLICATION

Calibrated and tested by the Polytechnic of Milan, HELLOMAC can be used to monitor rockfall and debris flow protection systems for impact, or to determine the need for mitigation in a certain location. Often installed in remote areas, this new device is compact and robust and can be applied to simple and secured draperies, rockfall barriers and attenuators, and debris flow barriers as shown in Figure 2. HELLOMAC provides real-time information about the occurrence of an impact event and can be installed on any type of rockfall system or calibrated and retrofitted to an existing system.

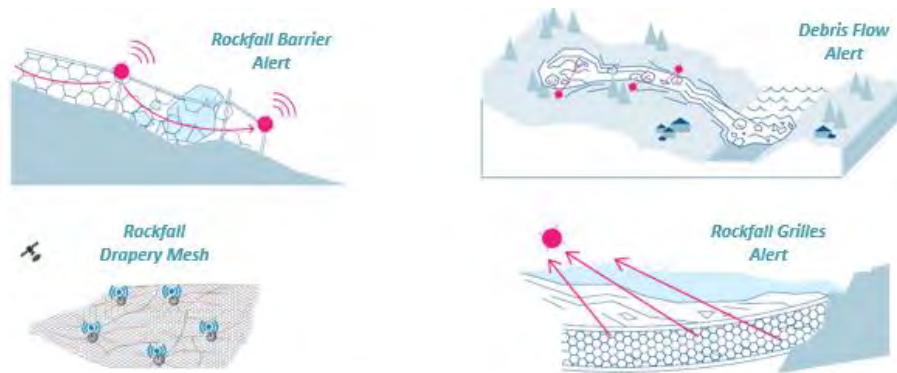


**Figure 2: Fields of Application**

HELLOMAC sends a notification in real-time when a rockfall or debris flow event occurs. The alarm is immediately sent to email, text, or via smartphone app and can be used to activate local sirens and signals. It will communicate with the user on a daily basis to inform about the conditions of the protection system. This also gives assurance to the user that the device is still working. HELLOMAC is designed to be used as an event alert system, however, it is also suited to monitor specific locations where natural events might occur, thus enabling decision makers to investigate and decide if and where a protection system should be installed. For example, it can be installed on a site with a high risk of an event to record all the history of the events to help determine whether a protection system is necessary. In this case, it could be useful to connect HELLOMAC to sirens and signals to alert people in case of an event, even when no protection system has yet been installed.

## BENEFITS AND ADVANTAGES

The HELLOMAC device is installed directly on rockfall mitigation systems and can be calibrated according to the type of structure and the specific needs of the project and client. It works by detecting the calibrated deformations of the net, mesh or barriers once they are impacted. The device is designed to operate in an environment with high energy impacts and aggressive climatic conditions, without any electric connection wires or wiring activities.

Compared to other monitoring systems, the HELLOMAC offers the following advantages:

- Lightweight and Easy to Install – the HELLOMAC device is small, lightweight and compact, 12 inches (30 cm) in diameter, weighs 18 lbs (8 kg), and installed without the need for skilled workers;
- Low Maintenance - the device does not need any maintenance unless the protection system has been severely impacted. In that case, the device just needs to be reset after replacing or fixing the barrier or drapery;
- Functionality and Reliability - after several years of research and testing in the field and the final check performed in cooperation with the Polytechnic of Milan, it is guaranteed to be 100% functional for different energy levels.

HELLOMAC daily transmits the location and the status of the monitored structure. In this way, the user can quickly check on a computer, tablet or smart phone the location of the system (GPS coordinates) and if it has been impacted. There is not a big amount of data transmitted, and its simplicity avoids data transmission issues.

HELLOMAC is tested against impacts up to 16 g (157 m/s<sup>2</sup>; 515 ft/s<sup>2</sup>) of acceleration and is designed to operate in aggressive climates such as rain, snow, wind and intense sun. It can also withstand temperatures between -40° F (-40° C) and 140° F (60° C). Moreover, even though only one (1) battery is needed to operate, HELLOMAC has seven (7) internal lithium polymer batteries, for safety reasons, with an estimated lifespan of at least five (5) years, and the battery level is communicated daily to the user.

## INSTALLATION

The HELLOMAC device can be calibrated to be installed on tested rockfall protection kits (ETAG 027 / EAD 340059-00-0106 / EAD 340089-00-0106). By knowing the main deformation characteristics recorded during the full-scale tests (MEL and/or SEL), users can choose to have an alert if the installed rockfall barrier is impacted with a serviceability energy level (SEL) or the maximum energy level (MEL). The system can be installed on all types of barriers, no matter the energy absorption, the height or the producer.

The transmitting tool of the HELLOMAC device is usually installed at the top of the rockfall barrier post as shown in Figure 3. The device can be installed either upslope or downslope on the barrier post, but it is recommended to be installed downslope to prevent impact.

The transmitting tool is connected to eight (8) tie rods attached to control points that are fixed to the interception structure, four (4) extending from each side of the post and connected to two spans of the barrier as shown in Figure 4. The tie rods are properly calibrated according to the deformation parameters measured from the full-scale tests and are positioned to monitor different vertical and horizontal locations of each interception panel, thereby informing about the exact location of impact. The length of each tie rod is specific to the barrier being monitored and

can be retrofit to an existing barrier. One device can control several different points spread approx. 65 to 90 ft. (20 to 28 m) along the barrier.



**Figure 3: Installation of the HELLOMAC Device on the Barrier Post**

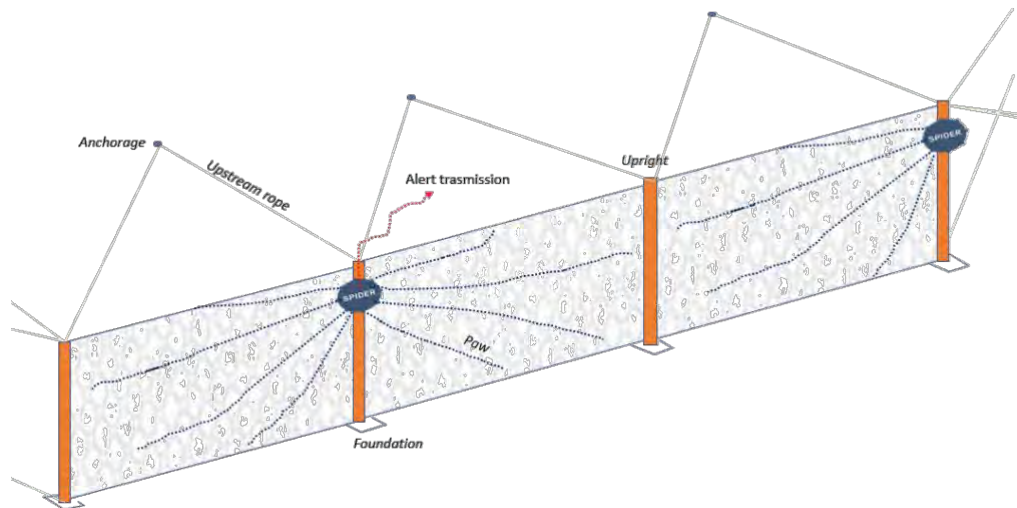


**Figure 4: Tie Rods Connect the Transmitting Device to the Adjacent Interception Panels**

The HELLOMAC is calibrated for each specific rockfall barrier based on the barrier's deformation response to impact. Note that if a barrier is impacted, but the energy does not reach the calibrated deformation response, nothing happens. If the energy level is high enough to reach the calibrated deformation response, the alarm is sent.

Figure 5 shows the calibrated tie-rod dimensions and positions for a specific barrier and how they would be installed on the interception panel. The length of each tie-rod is associated with a specific location to be installed on the interception panel.

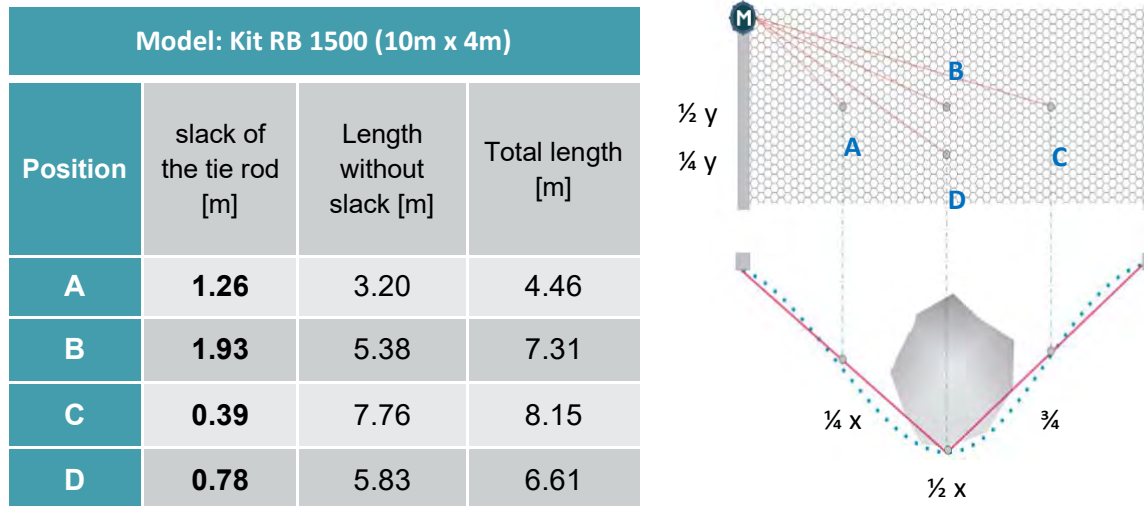


**Figure 5: Example of Tie-Rod Dimensions Calibrated to a Rockfall Barrier**

## DATA TRANSMISSION

The alarm signal provides notification using either a Satellite or GSM network, ensuring full coverage all around the world, even in remote areas. It is also possible to connect traffic lights, signals, sirens and gates which can be automatically activated by the alert signal. Information is collected and sent to a computer or phone via satellite (recommended) or 4G to a central software by region, and then forwarded via SMS, email or APP or simply through login to the same software. By using the dedicated app, it is possible to keep the protection system monitored at all times and to have all the information available including geolocation, alert signals, notifications and all other pertinent data.

## CASE HISTORY

Over the summer of 2022, Maccaferri was involved in a comprehensive rockfall protection intervention along SS 34, a major road in northern Italy that runs alongside Lake Maggiore, connecting the city of Verbania with the Swiss border, where HELLOMAC, a smart sensor technology, was integrated to ensure the local community's safety. Despite the beauty of driving alongside the lakeshore, this road had some hidden risks. Surveys were made and according to the findings, the slopes and ridges above the road were causing a serious risk of rockfall. Should this road be blocked, major circulation disruptions would lead to economic damage to local businesses and cause potential isolation of local communities. Unfortunately, a fatal accident also occurred, proving how this slope instability was endangering the safety of people travelling on the road. The situation required a prompt response by the local authorities.

Public authorities, private clients, and the general public are becoming more sensitive to the concept of risk and more focused and committed to the reduction of it to guarantee a higher level of safety. For this reason, the City of Verbania contacted Maccaferri and asked for a major rockfall mitigation plan, which was to include protective measures to mitigate the risk of rockfall, as well as an impact warning system. The impact warning system is not usually part of traditional rockfall protection systems, but the authorities requested this feature to alert the public that an event has occurred so security measures may be taken. The total value of the project was over \$10 million and spanned approximately 19 miles (30 km) of the national highway.

After careful examination of the area, Maccaferri recommended both active and passive rockfall protection systems. The active interventions were designed and implemented where the rocky ridges were close to the roadway: a double twist drapery mesh was used to cover the rock face and contain the falling debris.

At the design stage, it was estimated that, if detachment occurred, the potentially unstable rock blocks would roll down the slope and reach the road with an energy of 500-600 kJ. Therefore, in addition to the active drapery system, conventional dynamic rockfall barriers were designed at the Service Energy Level (SEL) of 500-600 kJ in order to reduce the maintenance interventions in case of repeated impacts over time.

Figure 6 shows the installed rockfall barriers, Maccaferri RB1500 and RB2000, chosen to provide a Maximum Energy Level (MEL) rating of 3 times the SEL, or 1500 kJ and 2000 kJ, respectively. Twelve alignments of RB2000 barriers and two alignments of RB1500 barriers were installed, all with an interception height of 13 ft (4 m), allowing nearly 2 miles (3 km) of linear protection.



**Figure 6: Installed Rockfall Barriers Above SS 34 in Verbania, Italy**

The rockfall barrier systems were integrated with the HELLOMAC monitoring device. The rockfall barriers were equipped with over 40 HELLOMAC devices, which were all connected to the same transceiver device, Hubir. The transceiver was installed in a safe area, where it can easily be checked following an impact. Figures 7 and 8 show the HELLOMAC transmitter device attached to the barrier post and the tie-rods connected to the interception panel of the barrier.



**Figure 7: HELLOMAC Installed on Barrier Post**



**Figure 8: Tie-Rods of HELLOMAC System Connected to the Interception Panel**

## CONCLUSION

A new reliable device to monitor impacts against rockfall and debris flow protection systems is introduced. HELLOMAC is a cutting-edge solution that leverages IoT and sensor technology to detect events such as impacts, slope and installed rockfall or debris flow barrier detachments and deformations. HELLOMAC is an alert system that detects any impact on the entire barrier panel or deformation to a rockfall protection system, assuming the energy exceeds the calibrated deformation threshold. HELLOMAC has arms, or ‘tie rods’, that are calibrated to detect a change in deformation within the barrier panel.

All information is collected via satellite or 4G and each device uses its own frequency. The internal 4G allows the system to identify the event location(s), also mapping the alarmed areas (land registry), even in remote areas.

The HELLOMAC app provides daily monitoring of the system's status, and if an impact occurs, an alert is immediately sent, ensuring real-time and accurate monitoring. Without requiring skilled or trained workers, the HELLOMAC is extremely simple to install, does not need any configuration and calibration on site, and can be installed on existing structures without affecting the system's certification. Maintenance and replacement are very quick and easy as well. Moreover, a sophisticated electronic solution inside the device guarantees early warning detection for several years with an internal battery only, without the need for an auxiliary power supply.

**An Overview of Rope Work Accidents  
for the Geohazard Profession**

**Todd Hansen, PE, SPRAT L3, PCIA L2**  
FHWA WFLHD  
610 E 5<sup>th</sup> St  
Vancouver WA, 98661  
(360) 619-7903  
todd.hansen@dot.gov

Prepared for the 72<sup>nd</sup> Highway Geology Symposium, August, 2023

### **Acknowledgements**

The author would like to thank the individuals/entities for their contributions in the work described:

Rock Scalers who made this effort worthwhile and necessary.  
My FHWA colleagues who helped me present this topic.  
Mike Marshall, GRI for providing recreational accident data.

### **Disclaimer**

Statements and views presented in this paper are strictly those of the author(s), and do not necessarily reflect positions held by their affiliations, the Highway Geology Symposium (HGS), or others acknowledged above. The mention of trade names for commercial products does not imply the approval or endorsement by HGS.

### **Notice**

This document is prepared by a technical representative of the U.S. Department of Transportation (USDOT) in the interest of information exchange. The U.S. Government assumes no liability for the use of the information contained in this document. The U.S. Government does not endorse products or manufacturers. Trademarks, manufacturers' or trade association's names appear in this report only because they are considered essential to the objective of the document.

### **Copyright Notice**

Copyright © 2023 Highway Geology Symposium (HGS)

All Rights Reserved. Printed in the United States of America. No part of this publication may be reproduced or copied in any form or by any means – graphic, electronic, or mechanical, including photocopying, taping, or information storage and retrieval systems – without prior written permission of the HGS. This excludes the original author(s).

### **ABSTRACT**

Major accidents have occurred in every rope access certifying organization, suggesting current standards and techniques reduce but do not eliminate the hazards associated with rope access. Previous studies of recreational climbing and industrial rope access accidents have established baseline statistics that can be referenced against the few geohazard related accidents that have occurred. Ideally a rope training program would universally incorporate accident history to improve training methods and contingency planning for rescues, but knowledge of accidents and standards is not centrally shared.

For geohazard professionals, the review and enforcement of on-rope work is inconsistently applied by different jurisdictions and regulatory agencies. Differing standards of practice are reported by standardization councils, creating confusion and inconsistent performance evaluations based on the regulator's knowledge. Few standard operating procedures exist that are specific to geohazard specialists. Continued development of geohazard rope methods will enhance the entire industry and improve credibility when dealing with regulatory agencies or industrial rope access groups.

The Federal Highway Administration does not explicitly endorse any particular rope use method and cannot be expected to develop practicing methods for the rope work industry. Where FHWA does take a leading role is ensuring that all contracted rope practitioners follow the selected standard of practice stated in their submittal for projects under Federal jurisdiction. This approach led to the development of a new "Slope Scaling" specification to ensure geohazard mitigation work is performed using a documented and transparent program. The application of this new specification combined with continued monitoring of reported rope accidents will hopefully identify common factors leading up to those accidents, thereby doing what can be done to improve site safety on all Federal projects using geohazard rope professionals.

## INTRODUCTION

For decades several agencies and companies have safely worked on slopes with rope, with over one million on-slope man-hours recorded without accidents. That did not stop outside groups from attempting to apply far-reaching industrial rope access standards with the clear desire to extend influence into the geohazard professions.

Without their own unified standard of practice or enforceable specifications, the default judgement tended to be against the geohazard profession. A typical practice of Geohazard professionals is to either maintain existing robust rope work standards of practice or to seek certification through an industrial rope access trade group. While both options are acceptable, and still performed, a dangerous complacency developed in the early 2010's for thousands of rope access practitioners who would be told that the numerous system redundancies equated to zero fatalities and few reported injuries. Within the decade, this statement was proven wrong many times leading to higher scrutiny for rope practitioners.

While individual agencies and corporations have independently endured the increasing chatter from industrial rope methods encroaching onto geohazard slopes, no unified code or universal standard has been developed or adopted which creates an opening for interpretation of what constitutes proper gear (Figure 1). Because of this recognized gap of an unregulated work practice, the FP-24 standard specification manual for Federal Highway Administration (FHWA) will include a new standard for all projects administered on or by Federal contracts.



**Figure 1 – Incorrect use of a fall harness and mixed equipment for rope access (Source: FHWA, Todd Hansen).**

### **Limitations on Methodology and Collection of Accident Data**

Tracking industrial accidents on rope is only a priority to those who regularly use rope for work access, which includes rope access technicians (RAT) and geohazard professionals. This paper represents several years of searching through official sources and unverifiable forums, with the goal of capturing the context for any mention of accidents related to industrial rope access methods. The hazard of following online forums is the bias and ignorance associated with personal opinions. But in the nascent rope access industry forum chats were sometimes the only place to mention an accident. Some forum reports were later corroborated by official news outlets or inquest findings, yet many others remained the only reliable source of information for the RATs themselves.

There are two codified groups responsible for certifying the majority of RAT in the world, the Industrial Rope Access Training Association (IRATA) and the Society for Professional Rope Access Technicians (SPRAT). The UK based IRATA predates the USA based SPRAT, and both are credible, well-operated groups dedicated to advancing the rope access profession. Unfortunately, there is a regionalism to the certifications, with IRATA slowly encroaching world-wide, while SPRAT remains solely a certification for the USA and Canada.

Another main difference is that IRATA represents the companies who hire RATs while SPRAT represents the individual technician. These minor differences do not detract from the overarching goal to ensure good practice and proper training, but they do lead to contrary approaches when representing respective members.

Since beginning the search for accident data online and continuing to today, there was no unified database of rope accidents. IRATA and SPRAT websites have details on notable incidents, ranging from initial “Safety Bulletins” to reports which have taken years to be published. For example, in 2013 obscure posts on an IRATA forum reported a fatality described a “fall from height on a drill ship in South Korea.” An official statement from IRATA website indicated that further details would be provided, but in the following years no further information has been shared. Other accidents, some causing serious injury, have been investigated and published as official findings in IRATA Safety Bulletins, many of which are later adopted into training protocols. But informational voids are also created when no follow-up information is provided, and rope accidents go unacknowledged.

In contrast the US Mine Safety and Health Administration (MSHA) will publish a “Fatality Alert” immediately following a serious accident and focus on a detailed final report at a later time. The intent with this method is to raise awareness of the basic events leading to the accident, because some information is better than nothing. Then later, a detailed final report is produced by MSHA and incorporates the original release with additional findings, as needed.

For accident information on rope, there are difficulties with the limited data sources, parsing fact from hyperbole on social media posts and the rope access groups vying for dominance. Therefore, the accidents presented in this paper are not meant to be all encompassing or capture all critical details. Instead, noted accidents are provided for the geohazard community on rope and follow the same theme as the MSHA alert; some information is better than nothing.

## **The Original Problem**

Rope supported slope access work is a calculated-risk activity undertaken by experienced professionals, ranging from rock specialists with decades of experience to registered geologists or professional engineers. So, when one of those few highly credentialed individuals have an accident, it is alarming . Within the last decade a handful of geohazard specialists using ropes for slope access, and even more rope access technicians (RAT), have had serious accidents performing standard work on rope. The geohazard specialist victims were veteran professionals with many years of experience and not who would be expected to be a casualty. For those with similar experiences or working knowledge these accidents raise the inevitable question of what happened, how did it happen and what can be done to prevent a repeat.

## **Recreational Related Accidents**

Rope access technicians and slope access technicians use similar means and methods first developed by the alpine mountaineering and traditional rock-climbing communities. In some regards the techniques used by geohazard professionals working steep unstable slopes predate the practices and methods used by industrial RATs. Yet to establish a baseline comparison for

RAT and geohazard rope users, accident data collected by the American Alpine Club (AAC) between 2014-2017 was reviewed. Typical accidents common to both recreational and industrial rope access activities were selected and accident data on whether the event occurred on rock or snow was excluded.

Another baseline comparison for recreational climbing accident rates is the 2012 Wilderness and Environmental Medicine Journal (WEMJ) paper “Rock Climbing Rescues: Causes, Injuries and Trends in Boulder County, CO”. Most notably the WEMJ paper cited accidents were caused as a result of inexperience, inadequate use of equipment, or improper technique.

Recreational climbing accident data indicated that more falls occur in ascent, which is to be expected for sport lead-climbing. Of all the causes noted in the AAC reports, errors on a descending rappel was the most common factor of cataloged accidents, leading to uncontrolled descent or failure of the system. Possibly, the most surprising factor was that the highest number of accidents occurred amongst the most experienced climbers. Compared to other experienced climbers who have accident rates 3 times more than climbers with 1-3 years’ experience and 7 times more than a novice climber. Statistically this means the riskiest recreational climbers are those with the most experience. Yet while the average recreational accident rate would generally remain the same, the worldwide rate of industrial rope access serious and fatal accidents increased from 2008 to the present day.

### **What Happened at the Brent Charlie Platform?**

On June 16, 2011, an industrial rope access technician was killed after falling from the BP Brent Charlie oil platform in the North Sea. This accident was the first real fatality to capture everyone’s attention in the RAT community, because the industry promoted backup system failed. Prior to this accident both IRATA and SPRAT had endorsed their rope access programs as the best, safest methods to do work on rope, because of a dual rope system redundancy required for all work. This system redundancy did not save the worker that day, and what is more chilling is that for 4 years, no official account was given by any group or agency. This person was a Level 1 RAT certified by IRATA who was working with two other Level 3 RAT Supervisors. Following a UK Health & Safety Inquest plus serious criticisms from the UK Oil & Gas Unions regarding delays, the IRATA finally published the August 28, 2015 “Fall from height” report. The IRATA report summarized the worksite organization and events leading to the fatal accident of a rope access technician working on a North Sea platform.

Official findings determined that the worker had rappelled through an access hole in the base of the platform, which had required directing ropes over sharp metal edges. As the worker climbed up to exit the work area, the rope protection was shifted exposing the sharp metal beams which cut the main rope (Figure 2). The report states the backup device was being held by the worker to reposition it on the rope when the rope was cut. The backup device appears to have not been engaged until after the worker fell over 30 feet, generating enough energy to snap the backup rope when it finally caught. The IRATA reporting body specifically noted that RAT users must never grab the body of a backup device or place hands above a device, and that rope and edge protection training must be emphasized. IRATA’s report also determined that the job

hazard analysis (JHA) did not identify this risk, which “could be a result of the prevailing site conditions, which may have hidden or masked the hazard.”



**Figure 2 – Failed main and backup ropes on the Brent Charlie Platform (IRATA “Fall From Height” report, 2015)**

While the IRATA findings focused on equipment and RAT skills, the report left out important details on how a JHA missed the worksite hazards. The casualty was an entry-level RAT who was accompanied by two RAT supervisors, and both missed the hazard that led to the accident. We can therefore assume that neither of the senior level RATs entered the work area to inspect and check prior to beginning work.

### **More Rope Access Accidents**

Between 2008 and 2019 there would be an estimated 20 industrial rope access fatalities worldwide. Fourteen of those were caused by falls, rope failure, or working at height. In comparison this is a lower incident rate than the approximate 30 recreational climbing fatalities every year in North America.

*IRATA Work and Safety Analysis (WASA) 2014* states that the total number of accident/incident reports submitted for 2014 was 74, fewer accidents when compared to 2013 when there were 109

reported accidents and 164 in 2012. This decrease in numbers is attributed to problems encountered with the reporting procedure. According to their data, the rate of serious injury (defined as more than 7 days off work) in 2014 was 68.4 injuries per 100,000 workforce, however that is after analysis of the data was converted to an equivalent workforce. In 2014 the IRATA trained workforce totaled 12,519 technicians and logged 16.81 million hours in aggregate. Only 34 injuries (fatality, major injury, >7-day, <7-day and ill health) were reported to the organization. However, the report acknowledges that a 2013 fatality as well as an aggravated hernia were omitted from the analysis. Injuries were primarily caused by being struck by falling objects, working with industrial tools, and operator error of rope equipment.

Several of the incidents described in the 2014 WASA were described as ‘omissions’ and included failure to rig rescue equipment and unintentional detachment leading to a fall. There were seven instances of damaged or severed ropes reported by members. These included a rope cut by an elevator, wind damage from ropes left overnight, two separate instances of ropes untying leading to a fall and a rope ‘snapping’ under strain. Of the six notable falls on or from rope, three were a result of uncontrolled rope descent attributable to poor technique, two occurred during training and the last was an unsupervised rappel attempt that resulted in a 5-story fall. One of the training falls was a result of detaching accidentally from all ropes and the second fell onto his connection lanyard during aid climbing.

In comparison to 2014, the 2013 WASA data shows the IRATA trained workforce totaled 12,039 technicians and logged 15.94 million hours in aggregate for an accident rate of 64 per 100,000 workers. Only 32 injuries were reported to the organization. Twenty of the reported incidents were attributed to unsafe acts, omissions, or incorrect rope techniques. The single fatality was attributed to an elevator cutting the technician’s primary lanyard anchor resulting in a fall of 112-ft down an elevator enclosure. While no official report has been released detailing this specific accident, this may be the “fall from height” on the South Korean drill ship. An unfortunate outcome of this incident is the withholding of details and the length of time it is taking for an official report to emerge to the public. No follow up report on the 2013 accident has been made publicly available and an internet search only brings up the March 6, 2014, IRATA Safety Notice.

The 2018 WASA notes 148 reported instances, of which were 62 serious incidents and 3 were deaths for the 2017 working year with 15,530 technicians. Two of the fatalities were a result of falling off rope and one fatality resulted from being struck by a rockfall. IRATA notes the concerning trend in the WASA, stating the “fatalities contributed to an increase in the 5-year fatality rate to well above the range of most other related data.” For injuries alone, the accident rate became 110 per 100,000 workers, a 62% increase between 2014 and 2017. Also, the fatality rate rose dramatically to 33 per 100,000 equivalents, a rate that is more than 4 times that of the rate for “agriculture, forestry and fisheries” which has long held the highest accident rates for fatalities among industrial categories. Comparing the 2018 accident rate to the 2014 rate, the number of rope accidents doubled in four years while the number of technicians only rose 29% since the 2014 report.

Worldwide, other rope groups are found to nationally represent rope access technicians. Within Europe are the smaller national organizations SOFT (Norway), FISAT (Germany) and

SFETH (France). The South Pacific contains the ARAA (Australia), IRAANZ (New Zealand) and nominally SRAA (Singapore). Surprisingly some of the fatalities and major accidents were first, if not only, reported by representative national groups by local media.

The Norwegian *SOFT Safety Report* for 2015 focuses on 37 reported near misses, incidents and accidents that occurred during that year, over 272,575 hours (241,048 working and 34,527 training). Previously in 2014, the number of incidents and accidents also numbered 37 over 336,628 hours, which the study inferred as a rate increase. While the accident rate appeared to decrease, the *SOFT Safety Report* implied a possible correlation between the improved overall safety with a decrease in working hours, possibly due to the global oil market crash. The report from Norway does not attempt to tie the increase in accidents to the lackluster energy sector, but it is an interesting observation made by the SOFT authors. The SOFT study also found that rope clamps (ascenders) and ropes each had 4 attributable incidents reported, and both types of equipment are identified as being problems in past studies.

The 2017 *SOFT Safety Report* notes a reduction in accidents but raises concerns regarding the rope access industry in Norway, overall. While the number of hours on rope rose 6.3% from the previous year the number of accidents dropped from 15 to 11 published accidents. SOFT refers to these incidents as “published accidents” because only certified companies self-reported any accidents. As stated in the *Safety Report*, “*This means that less than 1/5 of our members finds it worth sharing this type of (accident) information. This is discouraging and worrying.*” The report goes on to note that many experienced rope access professionals are leaving the industry because of increased competition driving down billable rates and difficulty meeting construction schedules. There is also an increasing trend of employees leaving rope access companies only to return as self-employed contractors. The *2017 Safety Report* summarized the result of these trends best, stating that, “*(rope access) development is definitely going the wrong way. Economics rules and good culture within (rope access) companies disintegrates. (sic)*”

### **IRATA Identified Accident Factors**

The events or actions leading up to rope accidents can be generally split into three categories. These categories are well-known, common-sense factors for any industrial or recreational application; what is different in the geohazard industry is the increase in professional applications of rope work. As increased Federal funding and State DOTs focus on widening highways in steep slopes, the number of projects requiring slope access rope work seem to keep growing.

The top three reasons for documented accidents in IRATA’s 2018 WASA also correlate to AAC and WEMJ identified factors, and are listed in **Error! Reference source not found.**

<b>Table 1 – Common Factors Related to All Documented Rope Accidents</b>		
<b>Baseline Accident Factor</b>	<b>2018 WASA Identified Factor</b>	<b>Possible Reasons</b>
Human Element	“Human Factor” “Falling (Dropped) Objects”	<ul style="list-style-type: none"> <li>• Experience</li> <li>• Attitude</li> <li>• Attention level</li> <li>• Outside influence</li> </ul>
Equipment	“Equipment Problem”	<ul style="list-style-type: none"> <li>• Improper application</li> <li>• Overloaded system</li> <li>• Service life</li> </ul>
Site Conditions	“Fail to Identify Hazard”	<ul style="list-style-type: none"> <li>• Not evaluated</li> <li>• Dynamically changing site</li> <li>• Hidden, undetectable hazards</li> </ul>

Accident statistics can be categorized in many ways, but the factors listed in the table above can generally be applied to most if not all situations. Note that “failure to identify hazards” continues to be a leading factor for rope access accidents.

### **Geohazard Professional Slope Access Accident**

Since the inception of Caltrans’ rope program there have been few accidents on rope with over one million aggregate hours of on-rope experience. Following years of no serious accidents, in 2013 there were two fatalities and one serious injury all resulting from a single rockslide event. The accident was a result of rockfall debris striking the victims and unrelated to any failure of the rope access methodology, nor did the technicians make any errors on rope that could have changed the outcome of the events. Official CalOSHA findings determined that the Caltrans rope program was correctly trained and applied, but the slope was not assessed for geologic hazards as part of the standard job hazard analysis. This assessment coincides with the 2018 WASA report that identified site protection and hazard identification as areas in need of improvement within the IRATA framework. Caltrans Scalers now perform a Slope Scaling Assessment which requires evaluation by a Geotechnical specialist if hazardous criteria are identified in the first site assessment.

### **Aggregate Rope Worker Accidents and Deaths**

The data presented in Table 1 **Error! Reference source not found.** is a compilation of official media releases from organizations as well as rumors gleaned from rope technician online forums. Fatalities listed in the 2018 WASA report are not listed in the table because no pertinent details of the accidents could be found at the time of this writing. The purpose of this table is to present known serious accidents with the intent of learning from others’ mistakes and misfortune.

**Table 1 - Accidents on rope utilizing industrial access and slope access techniques.**

<b>Date</b>	<b>Location</b>	<b>Age</b>	<b>Casualty</b>	<b>Accident Description</b>	<b>Industry</b>
June 24, 2008	Queensland, Australia	34	Broken ribs, strains	9-storey fall from collected excess rope.	Window washer
Feb 22, 2009	BC Canada	24	Death	Negligent rockfall	Scaler
August 1, 2009	Kazakhstan	4x victims	Death	High winds blew workers into high rise windows, blunt trauma.	Window washer
Dec 2, 2010	Vancouver, BC	30	Death	Not anchored, fell through access hole.	Canopy maintenance
June 3, 2011	Dubai, UAE	25	Death	Fatal fall off Citadel Tower.	Window washer
June 16, 2011	North Sea, UK	37	Death	Ropes cut on sharp metal edge.	Offshore oil rig
June 30, 2011	Wellington, NZ	20s to 30s	Dislocated toe	Both ropes failed, fell on parked car.	Window washer
January 25, 2012	North Sea, Germany	31	Death	Victim attached to ladder, ladder detached from turbine and sank.	Wind turbine
February 10, 2012	Auckland, NZ	18	Critical Condition	Anchor failure resulted in 15m fall to sidewalk.	Window washer
April 24, 2013	Siskiyou County, CA	3x victims	Death (2), Injury (1)	Workers struck by rockfall.	Scaler
July 9, 2013	Aschaffenburg, Germany	33	Death	120m fall from tower.	Telecom
July 15, 2013	Wesseling, Germany	39	Death	170m fall from chimney, corroded anchors failed.	Telecom
September 27, 2013	Edinburgh, Scotland	25	Wrists and back broken	Both ropes failed, 40ft fall.	Window washer
October 13, 2013	South Korea	Unknown	Death	Both ropes cut by elevator, 112ft fall.	Offshore oil rig
Nov 26, 2013	Mannheim, Germany	41	Serious injury	Rope cut by 3rd party, 10m fall.	Window washer
May 19, 2014	Singapore? Australia?	27	Death	Suffocated inside tube, on rope.	Offshore oil rig

Sept 4, 2014	North Sea, UK	43	Death	Not anchored, fell through open hole in floor grating.	Offshore oil rig
<b>Table 2 - Accidents on rope continued.</b>					
<b>Date</b>	<b>Location</b>	<b>Age</b>	<b>Casualty</b>	<b>Accident Description</b>	<b>Industry</b>
August 5, 2015	Sydney, Australia	40s	Head and spine broken	3-storey fall, headfirst through glass bus shelter.	Window washer
October 12, 2015	Sydney, Australia	Unknown	Leg injuries	4-storey fall onto balcony.	Window washer
Jan 2016	Western Australia	Unknown	Head, leg injuries	Rockfall hit open pit mine scaler	Scaler
July 3, 2016	Pratt County, Kansas	41	Serious injury	126ft fall into soft mud, landed on back.	Wind turbine
July 7, 2016	San Fran, CA	Unknown	Broken back	60ft fall when detached from rope.	Scaler
July 21, 2016	Huxley, Iowa	31	Death	60ft fall inside turbine, victim left suspended 30ft prior to rescue.	Wind turbine
Jan 2017	Khalifa Stadium, Qatar	40	Death	Fell 40m at “dangerous” workplace only supplying “lethal equipment”	Vertical Construct
March 2017	Tasmania	Unknown	Death	Rockfall hit open pit mine scaler	Scaler
March 20, 2018	Golden, CO	40	Death	70ft fall when stepped out of crane basket onto slope.	Scaler
July 4 2019	Wolfe Co., KY	40s	Broken vertebrae, fingers	Uncontrolled free fall descent using incorrect rigging, dynamic rope	Rescue
Jan 2020	Western Australia	Unknown	Foot injury	Rockfall hit open pit mine scaler	Scaler
June 5, 2020	Inglewood CA	37	Death	Fell 120ft after tripping and falling through unsecured ceiling panel	Vertical Construct
Nov 11, 2021	Wellington NZ	Unknown	Serious injury	Fell 5-storeys, possibly working under duress then	Window washer
Dec 2021		Multiple	Intimidation	CEO hits, pushed workers down stairs after company fired for flagrant violations	Window Washers

June 2, 2023	Western Australia	Unknown	Death	Fall from height (assumed) no other details available	Offshore oil rig
--------------	-------------------	---------	-------	---	------------------

### More Specialty Certifications Are Not The Answer

Geohazard mitigation projects constantly deal with the inherent dangers associated with rockfall and unstable slopes, with the added risk multiplier from the work being performed at height. A 2013 *Comparison Study between ISO 22846 and IRATA Code of Practice* reviewed differences in the two documents with the intent of identifying omissions and major differences. ISO recommends worksite supervision be managed by workers with experience reflecting the complexity or degree of risk. ISO 22846-2: 2012 required that the work to be performed dictates the level of expertise the supervisor and technicians should have. With this assertion ISO acknowledges that not all specialty work is the same, and assigned supervisors need to have practical knowledge and not just meet a training criterion. This is especially true for geotechnical professionals responding to emergency geohazard events with the overall expectation of getting the situation under control and the road open as soon as feasibly possible with properly trained personnel (Figure 3).



**Figure 3 - Incorrectly rigged anchors are an indication of unsupervised or untrained rope workers (Source: FHWA, Todd Hansen)**

In comparison, only IRATA Level 3 technicians are permitted to be difficult access supervisors on projects requiring rope access. However, there is no certification that these Level 3s have the experience and training of how to identify the site-specific hazards at an unstable rock slope before they are given such a role. Industrial rope access technical skills alone are no assurance that a Level 3 is competent to supervise evaluation and construction of a geohazard mitigation site. IRATA Rope Supervisors do lead workers on challenging industrial projects but that does not directly correlate to understanding natural geohazards and rock cut construction. IRATA has suggested that some form of continued training in supervision with a final assessment is recommended to develop leadership roles. This would result in an additional level of training and certification beyond what is required for industrial RATs, just to supervise rockfall scalers. Considering that there is documented proof that more experienced recreational climbers are at higher risk of accidents, there is a risk of a similar correlation for experienced rope access technicians.

### **Specification 262 Slope Scaling**

To prevent the possibility of industrial rope access operations occurring outside of skillset, another approach should be considered that will prevent overconfident technicians from working beyond their skillset. This can be done using performance-based guidance that FHWA is updating in the Standard Specifications for Construction of Roads and Bridges on Federal Highway Projects (FP-24) which will contain “*Section 262 Slope Scaling*”. The new Section 262 replaces the previous use of “Section 623 General Labor” to capture scaling hours and requirements. For too long there has been an unmet need to create a nationwide standard for performing rock scaling work on slopes. Therefore, the intent of this new section is to create performance-based specifications that require the rockfall contractor to have standards of practice for their rope program. This simple approach allows us to undertake a thorough review of a rockfall contractor’s credentials with the ability to identify deficiencies or learn new ideas from their training and standard program. The benefit of this approach is that it allows a contractor to follow existing rope protocol from certified trainers or develop their own internal, robust rope program.

The new Section 262 Slope Scaling encourages continued development of rockfall specific rope programs by incorporating existing programs from PCIA and industrial rope access while also allowing an “equivalent internal training certification program” (262.03(b)). This allowance is critical because it allows regularly practicing scalers to improve the industry faster than if we relied upon updated standards to be codified by committee. Section 262 includes language in anticipation of the argument that an internal training program is liable to encourage deceptive submittals. The submittal documents require proof that the nearest rescue team or first responders have been contacted and consulted. This is required because not every fire response district has a technical rescue and paramedic response capability. Capable first responders will also want to review the rope methods being used and develop a rescue plan that can be rapidly implemented if the need arises. Also included in the new Section 262 and enforceable based on the Federal Acquisition Regulation clause 52.236 pertaining to workmanship, is a statement that allows FHWA to “remove any slope scaler working or directing others to work in an incompetent, careless or unsafe manner.” Where previously only apprentice scalers could be removed for unsafe actions, this updated version holds all workers accountable regardless of skill

level. Considering that expert recreation climbers are 3 to 7 times as likely to be seriously injured as other climbers, it is critical that any rope worker can be dismissed from a project. If the CEO of a New Zealand window washing company is willing to risk one worker falling and physically attack the remaining employees who stand up for their own rights, then Section 262 is written for those rare cases of intimidation being used to push workers beyond safe working practice of using an incorrect rope for example (Figure 4).



**Figure 4 – Sample of rope used for rappelling on a FHWA project (Source: FHWA, Todd Hansen)**

The goal to conduct geohazard work as safely as possible can be achieved by encouraging robust company rope programs and by not relying on the industry to self-regulate. By simply asking a rockfall contractor how they plan to perform the work and then evaluate them based on how well they can follow their own prepared plan, the new Section 262 gives accountability and freedom. While a company has the freedom to improve and develop its own rope supported slope access programs, the requirements within Section 262 hold everyone accountable for following that program. Rock scaling companies and individuals will use that freedom responsibly or be required to stop or delay work while addressing concerns.

**REFERENCES:**

- American Alpine Club. *Accidents in North American Climbing 2017*. American Alpine Club, place of publication not identified, 2017.
- Industrial Rope Access Trade Association International. *WASA Report 2013*. IRATA, place of publication not identified, 2013.
- Industrial Rope Access Trade Association International. *IRATA - Fall From Height*. IRATA, Kent, UK, 2015.
- Lack D.A., Sheets A.L., Entin J.M., Christenson D.C.. *Rock climbing rescues: causes, injuries, and trends in Boulder County, Colorado*. *Wilderness Environ Med*. 2012 Sep;23(3):223-30. doi: 10.1016/j.wem.2012.04.002. Epub 2012 Jun 22. PMID: 22727678.
- The heightec Group Ltd. *Comparison Study between ISO 22846 and IRATA Code of Practice*, place of publication not identified, 2014.
- Samarbeidsorganet for tilkomstteknikk (SOFT). *2017 SOFT Report*. Stavanger, Norway, 2017.

**Rock Stabilization at Pompeys Pillar National Monument: The Use of  
Numerical Modeling to Analyze Risk of Failure**

**Anya Brose**

Itasca Consulting Group  
111 Third Avenue S  
Minneapolis, MN 55401  
(612)677-2448  
abrose@itascacg.com

**Ryan Peterson**

Itasca Consulting Group  
111 Third Avenue S  
Minneapolis, MN 55401  
(612) 677-2450  
rpeterson@itascacg.com

**Lee Petersen**

Itasca Consulting Group  
111 Third Avenue S  
Minneapolis, MN 55401  
(612)371-4711  
lpetersen@itascacg.com

Prepared for the 72<sup>nd</sup> Highway Geology Symposium, August 2023

### **Acknowledgements**

The authors would like to thank the individuals for their contributions in the work described:

John A. Reffit – Pompeys Pillar National Monument

Joshua Helm– Pompeys Pillar National Monument

Joel Swenson – Barr Engineering

Eric Leagjeld – Bolton & Menk

### **Disclaimer**

Statements and views presented in this paper are strictly those of the author(s), and do not necessarily reflect positions held by their affiliations, the Highway Geology Symposium (HGS), or others acknowledged above. The mention of trade names for commercial products does not imply the approval or endorsement by HGS.

### **Copyright**

Copyright © 2023 Highway Geology Symposium (HGS)

All Rights Reserved. Printed in the United States of America. No part of this publication may be reproduced or copied in any form or by any means – graphic, electronic, or mechanical, including photocopying, taping, or information storage and retrieval systems – without prior written permission of the HGS. This excludes the original author(s).

## ABSTRACT

Pompeys Pillar National Monument (PPNM) is a 200-foot-high sandstone outcrop containing hundreds of prehistoric and historic features, including William Clark's signature, scribed into the sandstone rock in 1806. Located 30 miles east of Billings, Montana, Pompeys Pillar is a heavily visited attraction with 30,000 visitors each year. The Bureau of Land Management (BLM), which manages the site, has identified that the sandstone and shale outcrop, which contains William Clark's signature (herein referred to as the Signature Block), is vulnerable to erosion. Itasca was retained by the BLM to assess the stability of the Signature Block and to evaluate remedial measures.

A sequence of mixed shales and siltstones with interbedded sandstone layers lie underneath the sandstone unit containing William Clark's signature. The condition and higher weathering rate of the shale and siltstone layers could impact the support to the overlying sandstone blocks.

A site investigation and laboratory testing provided valuable insight into the jointing and bedding, siltstone condition, and rock strength. High-resolution scans, drone-based videography, and photogrammetry of the pillar were previously collected to establish the model geometry. During the site investigation, preliminary instrumentation was installed. Next, a 3D geometry model of the critical areas was developed for a stability assessment. This assessment was performed using Itasca's *3DEC* discrete element software. To assess shale erosion in the simulations, increasing amounts of shale and siltstone were removed from the model and block stability was assessed at each stage. Based on the modeling results, along with BLM feedback, remediation recommendations were provided by Itasca.

## INTRODUCTION AND BACKGROUND

Itasca Consulting Group (Itasca) was retained by the Bureau of Land Management (BLM) to investigate rock stability at Pompeys Pillar National Monument (PPNM). Background information about the project was provided in the request for proposal (BLM, 2020):

*The Department of Interior (DOI), Bureau of Land Management (BLM) manages the Pompeys Pillar National Monument (PPNM), located 30 miles east of Billings, Montana. Due to the historic significance of PPNM there is also joint interest in the site by the National Park Service (NPS) National Historic Trails Program, Lewis and Clark Trail Heritage Foundation, and Lewis and Clark Trust to name a few. This national historical site contains William Clark's signature, scribed into the sandstone rock in the year 1806. After William Clark left his mark on the rock, various other travelers from fur trappers to homesteaders left their own inscriptions. The monument attracts 30,000 visitors each year, many of whom traverse a wooden boardwalk and stairs that ascend the high rock outcropping which contains the historic signature.*

The rock stability issues were described as follows (ibid):

*PPNM is a sandstone outcrop that sits on a 51-acre parcel and stands 200 feet tall adjacent to the Yellowstone river, that has been carved into by populations over hundreds or even thousands of years. The Monument is vulnerable to weather induced erosion, which has been demonstrated by the loss of prehistoric petroglyphs since the BLM took over management of the Pillar.*

Itasca formed a team with two other firms, including Bolton and Menk, Inc. (BMI) for scanning and photogrammetry services, and Barr Engineering (Barr) for instrumentation.

This paper describes the work, findings, and recommendations resulting from the investigation.

## GEOLOGIC SETTING

### Geology

Pompeys Pillar is a part of the Lance Formation, which consists of alternating beds of sandstones and shales. The Lance Formation is 700–1,500 feet thick and is underlain by the Bear Paw Shale (Hancock, 1919). Thirty percent of the Lance Formation consists of channel sandstones at least 20 feet thick, and 70% is composed of thinner sandstone and finer-grained interfluvial sedimentary rocks (Connor, 1917). The geometry of the outcrop is largely formed by the meandering of the adjacent Yellowstone River. The Lance Formation is inclined downward toward the east at a rate of about 12 feet to the mile (Hancock, 1919).

## Local Stratigraphy

There are four major rock layers exposed on the east, south, and west side of the Pillar. Working up from the flat at the base of the pillar, these layers are: a lower sequence of shales and siltstones with interbedded sandstone layers; the lower sandstone; an upper sequence of mixed shales and siltstones with interbedded sandstone layers; and the upper sandstone (see Figure 1). Above the upper sandstone, there is a poorly exposed sandstone with many thin shale interbeds. The north side of the pillar does not have high vertical cliffs, but rather slopes more gradually in steps down to the base elevation.

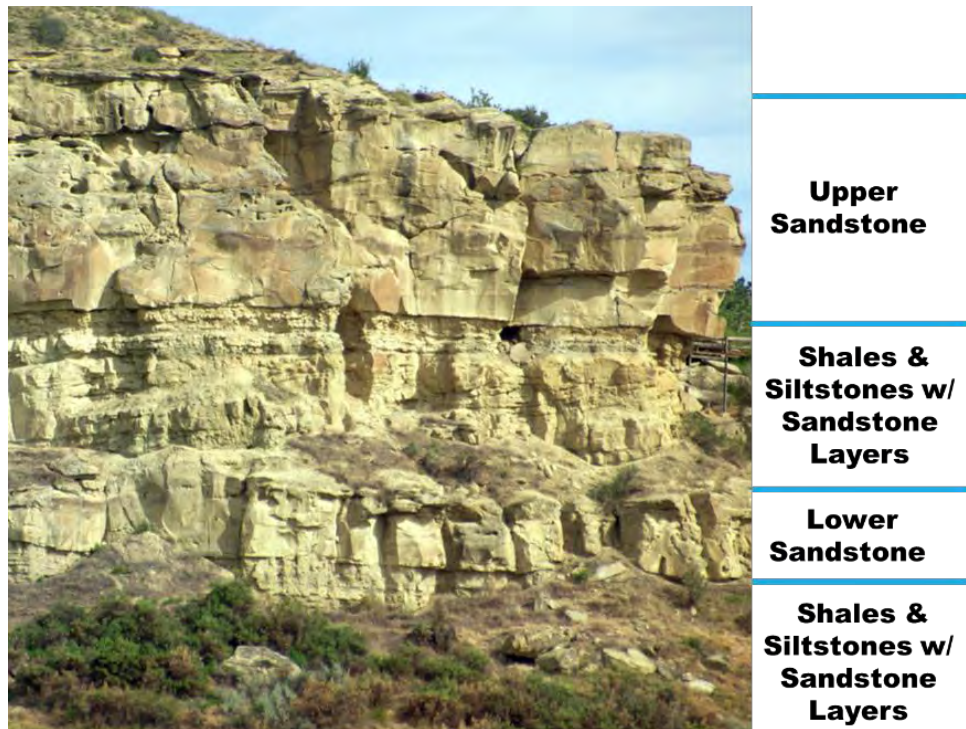


**Figure 1** Local Stratigraphy

## SITE INVESTIGATION AND LABORATORY TESTING

Itasca staff visited Pompeys Pillar National Monument occurred in July 2020 and during the first week of March 2021. The second site visit concentrated on the characterization of the Signature Block area on the east side of the outcrop and the Turtle Rock area on the west side of the outcrop. The work conducted during the visit included:

- Rock mass characterization, especially the weak shale and siltstone at the face.
- Collecting cores for laboratory testing.
- Observations of joint condition.

Much of this work was done from rental cranes, as shown in Figure 2.



**Figure 2 Cranes Used for Close-up Site Investigation Activities**

The siltstone, shale, and sandstone layers under the Signature Block were characterized by close-up observations, sounding, and a Schmidt hammer (see Figure 3). The weakest, most friable layers were found immediately under the sandstone and from 27 inches to 47 inches below the sandstone.

Sandstone cores were collected from a previous rockfall block, as shown in Figure 4. Five cores were collected for three UCS tests and 20 Brazilian tests.

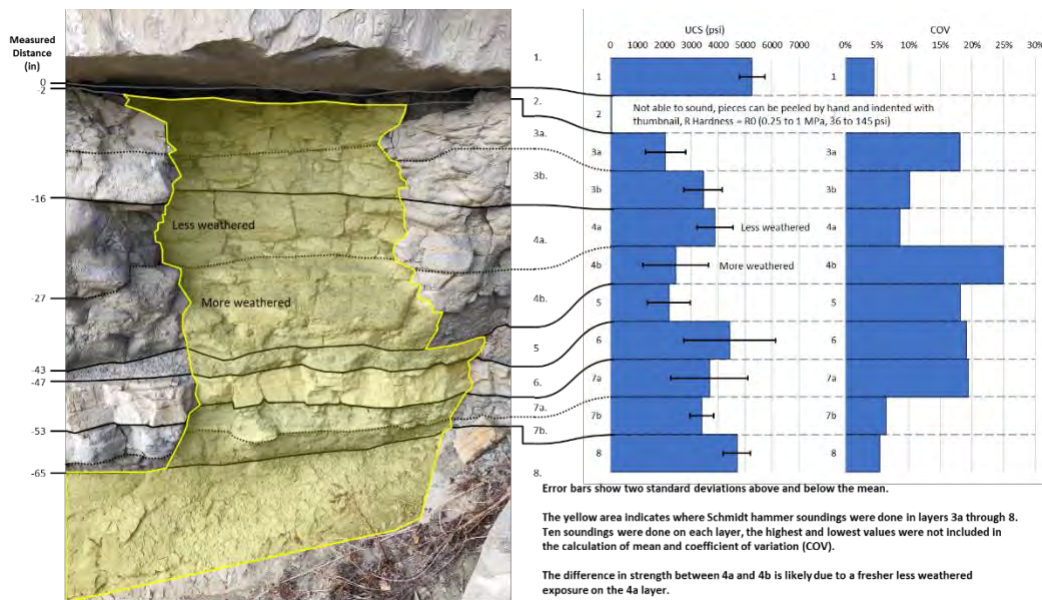


**Figure 3 Siltstone, Shale, and Sandstone Characterization Findings**



**Figure 4 Sandstone Core Collection**

The findings from the closeup observations of the Signature Block and Turtle Rock areas were eventually incorporated in the *3DEC* models. Figure 5 shows a subset of the features used in the Signature Block model, where the figure background is the point cloud developed from photogrammetry previously collected by BMI.



**Figure 5 Subset of the Signature Block's Joint and Bedding Plane**

## ROCK BLOCK MONITORING SYSTEM

A design phase instrumentation and monitoring program was developed by Barr and Itasca, to collect a block and joint deformation baseline. Itasca, in consultation with BLM archeology staff, identified sensor locations. Barr installed the sensors, dataloggers, and telemetry.

As of June 2021, the latest rock block monitoring system has been installed with ten crackmeters (CM), three reflectorless electronic distance meters (DM), and four tiltmeters (TM). Figure 6 shows an image of the crack gauges installed near the Signature Block. Figure 7 and Figure 8 **Error! Reference source not found.** illustrate the names and locations of the instruments at: Signature blocks east and north face, Signature blocks top, respectively. Trigger limits were established from baseline measurements.

The instrument data is automatically uploaded to a cloud-based host that is accessible via a web interface. This allows for periodic review by BLM staff and their consultants. This also allows for automatic notifications when measurements exceed the established trigger limits.



**Figure 6** Crack Gauge Locations Near the Signature

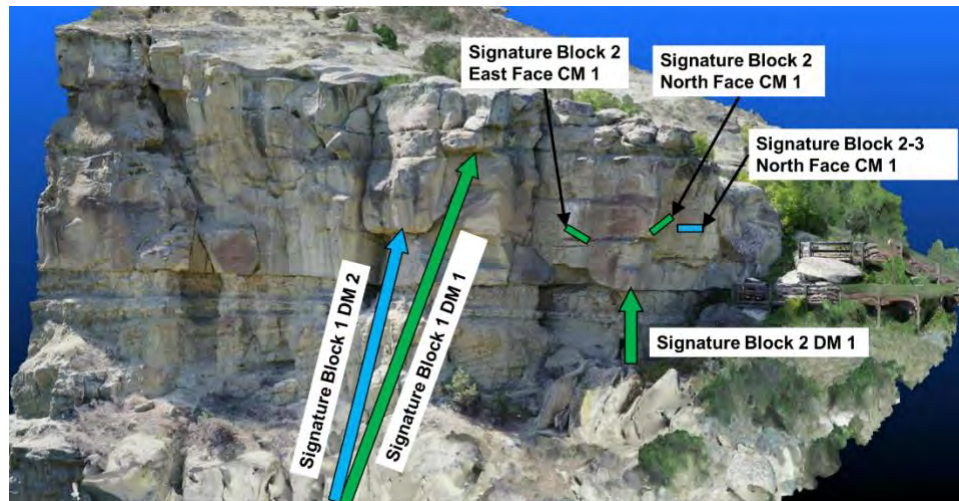


**Figure 7** Signature Blocks East and North Face Instrumentation

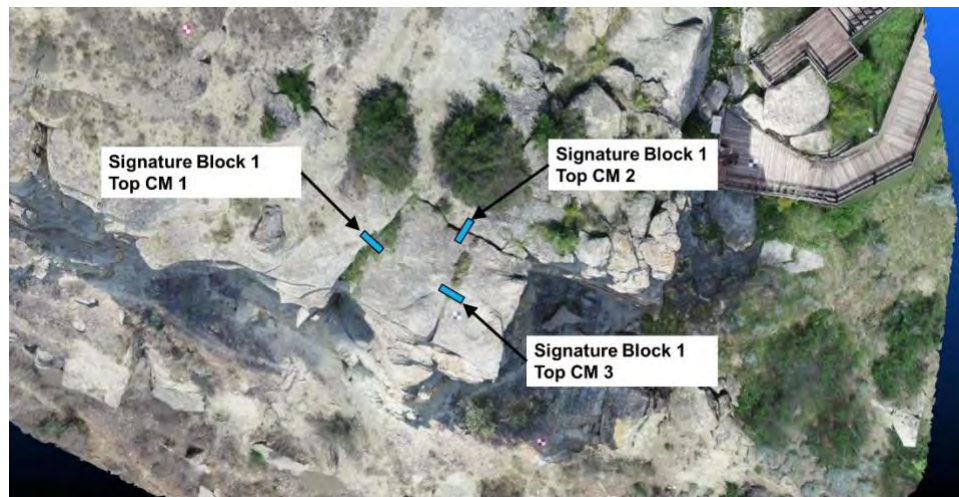


**Figure 8** Signature Blocks Top Instrumentation

### ***3DEC* MODELING**

Rock block stability was assessed using the Itasca software *3DEC*. *3DEC* is a three-dimensional numerical modeling code for advanced geotechnical analysis of soil, rock, groundwater, structural support, and masonry (Itasca Consulting Group, 2016). *3DEC* simulates the response of discontinuous media (such as jointed rock or masonry bricks) that is subject to either static or dynamic loading. The numerical formulation is based on the distinct element method (DEM) for discontinuum modeling.

The discontinuous material is represented as an assemblage of discrete blocks. The discontinuities are treated as boundary conditions between blocks; large displacements along discontinuities and rotations of blocks are allowed. Individual blocks behave (based on constitutive and joint models) as either rigid or deformable (i.e., meshed into finite difference zones) material. Continuous and

discontinuous joint patterns can be generated on a statistical basis. A joint structure can be built into the model directly from the geologic mapping. For this project, joints and bedding planes were added explicitly to the model.

### Signature Block Area 3DEC Analysis

The rock blocks at the Signature Area were numbered to facilitate coordination, as seen in Figure 9. The Signature Block area modeled using 3DEC is illustrated in Figure 10. The modeling area covered approximately 90 feet in length and 50 feet in height. Figure 11 shows the rock blocks in the Signature Block area formed by joints and bedding planes. The geometry was created using the mesh obtained from photogrammetry and then imported into 3DEC.

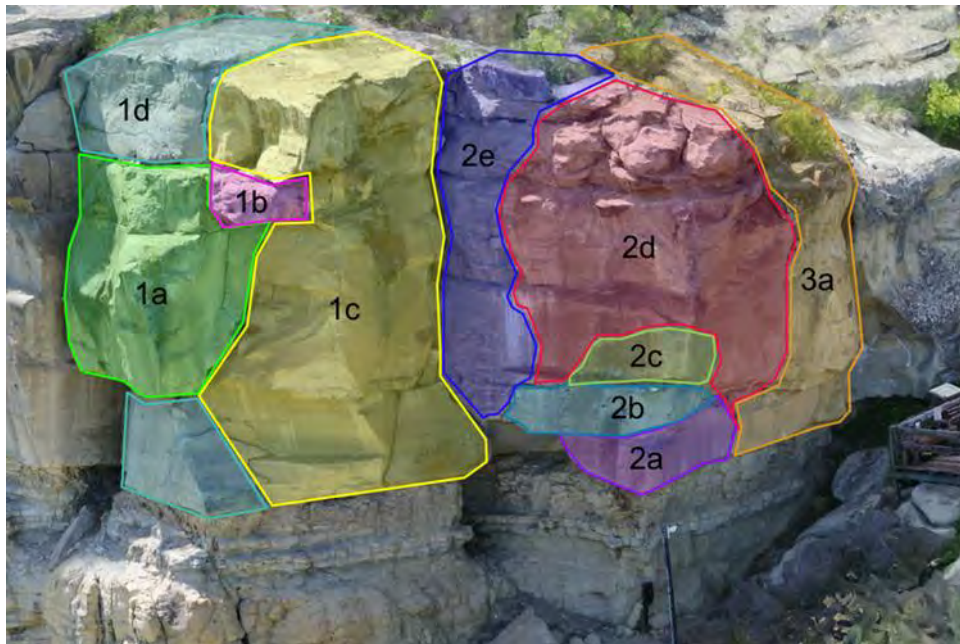


**Figure 9** Numbered Sub-blocks in the Signature Block Area



**Figure 10** 3D Mesh for the Signature Block Area Obtained from Photogrammetry

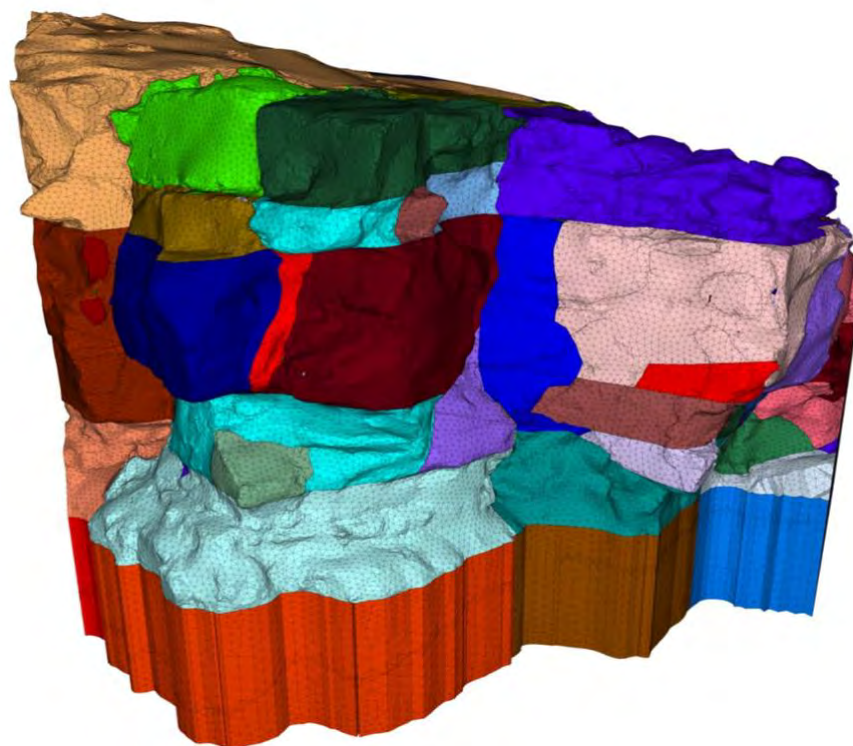


**Figure 11** Signature Block Model mesh in 3DEC

The sandstone blocks that form the Signature Block are underlain by an approximately 10-foot-thick layer of shale and siltstone. This layer is weathered near the surface and has undercut the overlying sandstone, creating a risk for instability.

To examine the stability of the undercut sandstone, the following *3DEC* modeling procedure was developed:

- The model was brought to equilibrium using elastic properties.
- Plastic properties (Mohr-Coulomb Constitutive Model) were assigned and the model was brought to equilibrium again.
- Displacement histories and velocity thresholds were used to assess model stability.
- Stability was assessed using two methods:
  - Siltstone was incrementally removed from the model:
    - The existing maximum extent of the weathered shale layer (the shale limit) was traced around the Signature Block area (Figure 12).
    - Up to 6 feet of siltstone was removed in 0.5-foot increments.
  - A strength reduction analysis was performed on all materials and all joints/bedding. (The strength reduction factor (SRF) was applied to cohesion, friction, and tension in the sandstone and siltstone volumes as well as all joints and bedding planes).

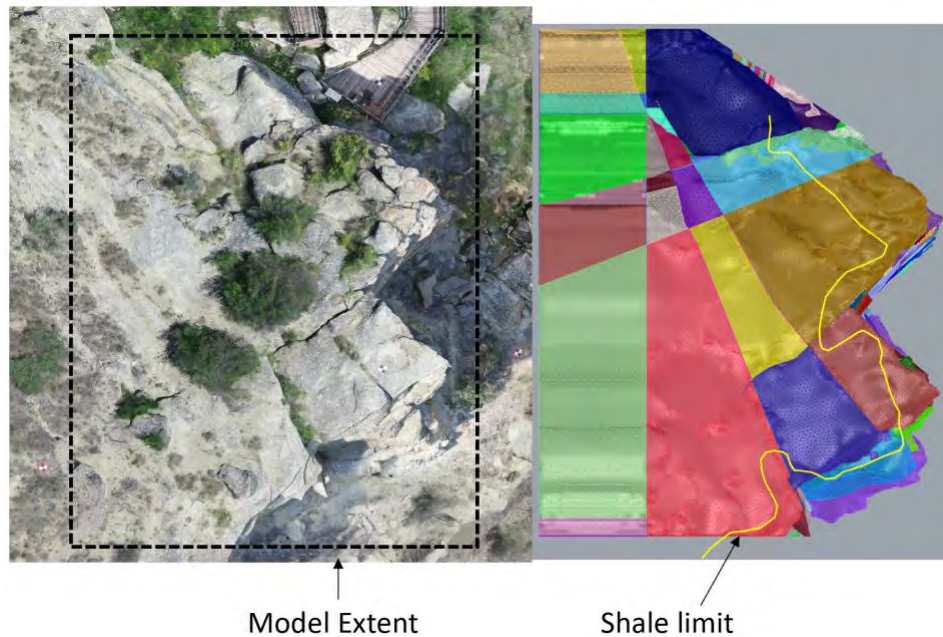


**Figure 12 Signature Block Plan View Illustrating Model Extent and Shale Limit**

Velocity contours across the Signature Block area, as well as displacement histories at various locations along the Signature Blocks, were used to estimate block stability.

For the incremental siltstone removal method, the displacement histories are shown in Figure 13. (Note that the model includes all the blocks and subblocks shown in Figure 11, although Figure 13 shows history results for only 16 locations: two on Block 1a, one on Block 1b, eight on Block 1c, four on Block 2, and one of Block 3.) The dashed vertical line represents the model step when each siltstone cut was removed (each cut represents 0.5 feet of siltstone removal). The cut after which the block is unstable is highlighted in red. The displacement histories show that Block 2 becomes unstable after 2.5 feet of shale is removed (Cut 5) and Blocks 1 and 3 become unstable after 3 feet of shale is removed (Cut 6).

Velocity contours with magnitudes above 0.003ft/sec represent unstable volumes. Figure 14 shows the velocity contours after 2.5 feet of siltstone is removed (Cut 5 shown on left) and after 3 feet of siltstone is removed (Cut 6 shown on right). After 2.5 feet of siltstone is removed, Block 2 has velocities are more than 0.003ft/sec, indicating instability. Once increased to 3 feet of siltstone removal, all blocks in the Signature Block area are unstable.

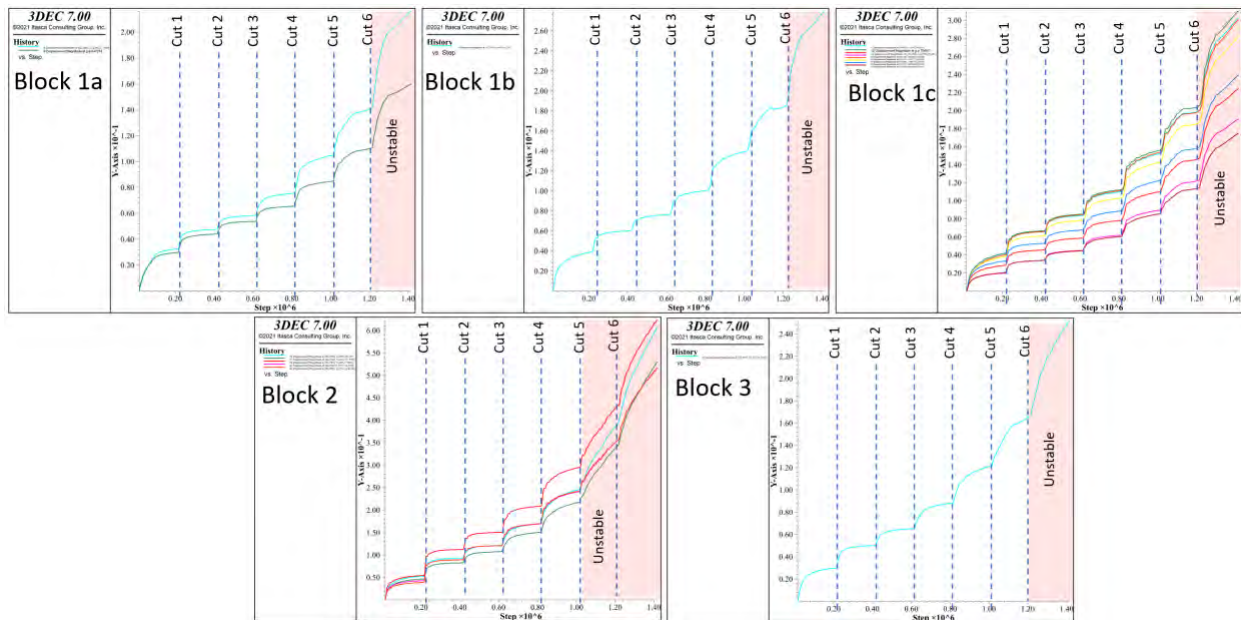


**Figure 13 Signature Block Displacement Histories for Incremental Siltstone Removal**

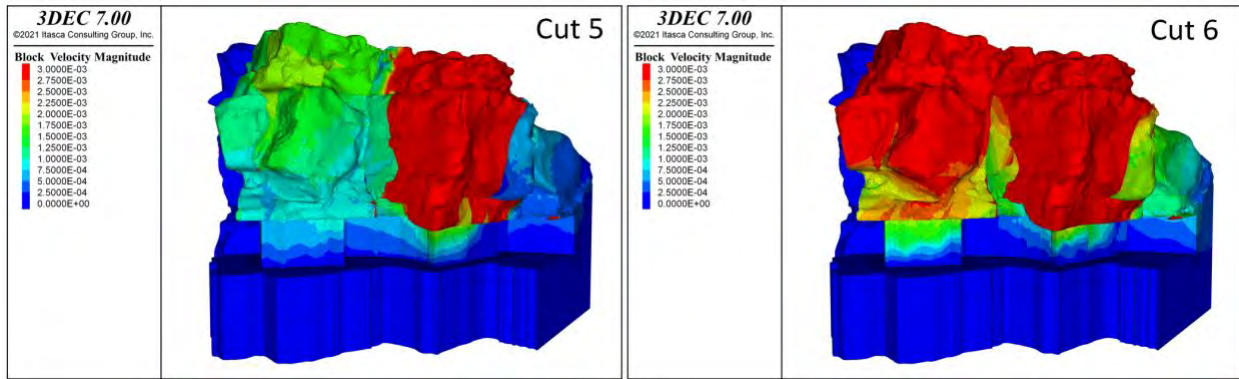


**Figure 14 Signature Block Velocity Contours for Cuts 5 and 6**

The displacement histories for the global strength reduction method are shown in Figure 15. The dashed vertical line represents the model step when each strength reduction occurred. The stage at which the block became unstable is highlighted in red. The displacement histories show that Block 2 becomes unstable with after an SRF of 1.3 and Blocks 1 and 3 become unstable after an SRF of 1.6.

Velocity contours with magnitudes above 0.003ft/sec represent the extent of unstable volumes. Figure 16 shows the velocity contours after an SRF of 1.3 (shown on left) and 1.6 (shown on right). After an SRF of 1.3, Block 2 is showing continued movement, indicating instability. Once increased to an SRF of 1.6, all blocks in the Signature Block area show continued movement.

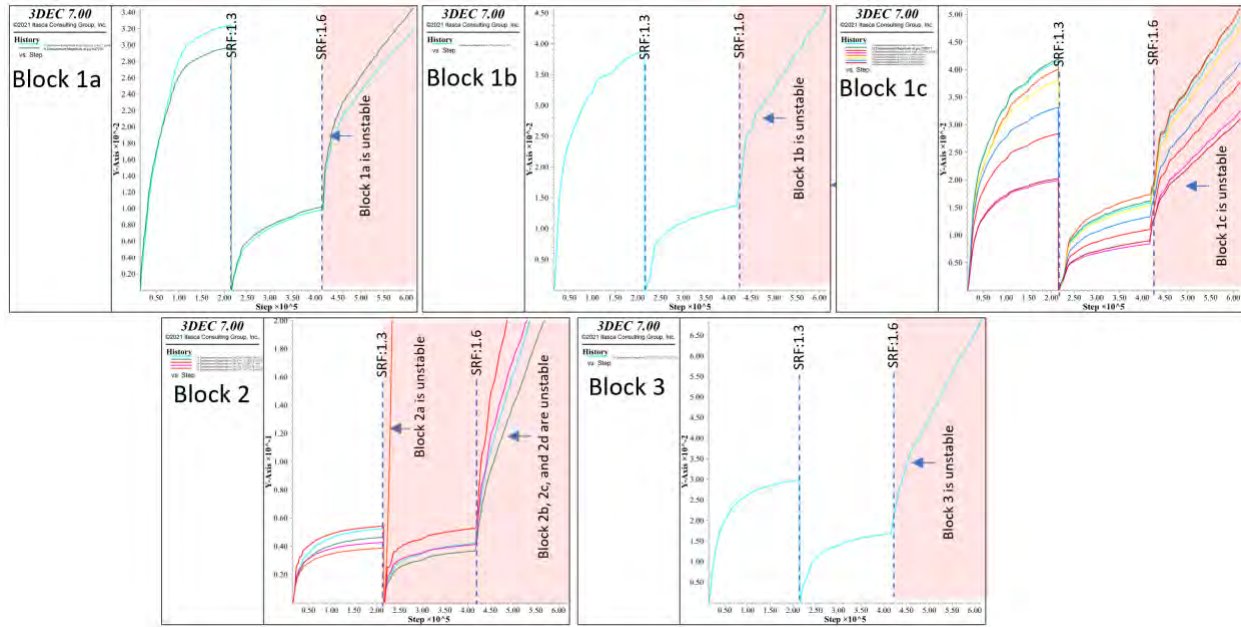


**Figure 15 Signature Block Displacement Histories for Global Strength Reduction**

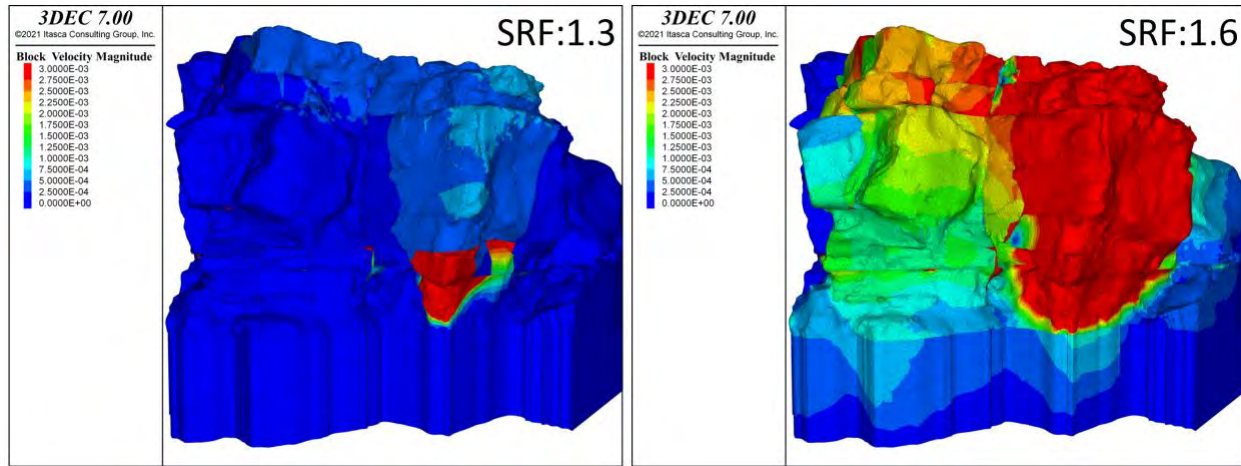


**Figure 16 Signature Block Velocity Contours for Global Strength Reduction**

A summary of the siltstone removal model is shown in Figure 17. The measurements listed on each rock block indicates how much siltstone was removed prior to instability. A summary of the global strength reduction model is shown in Figure 18. Each rock block is labeled with the SRF at which the block became unstable.

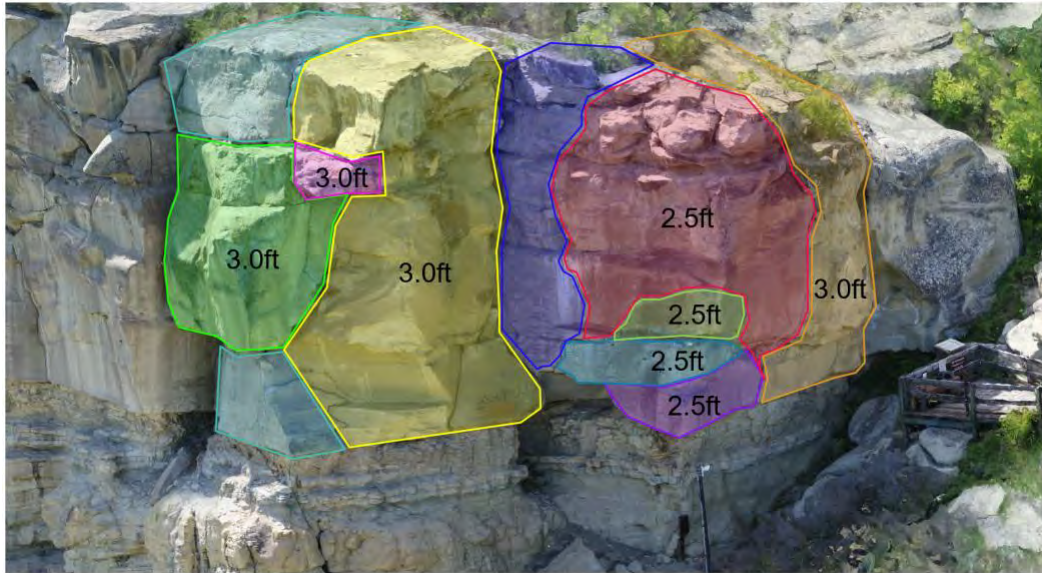


**Figure 17** Amount of Siltstone Removal to Cause Instability

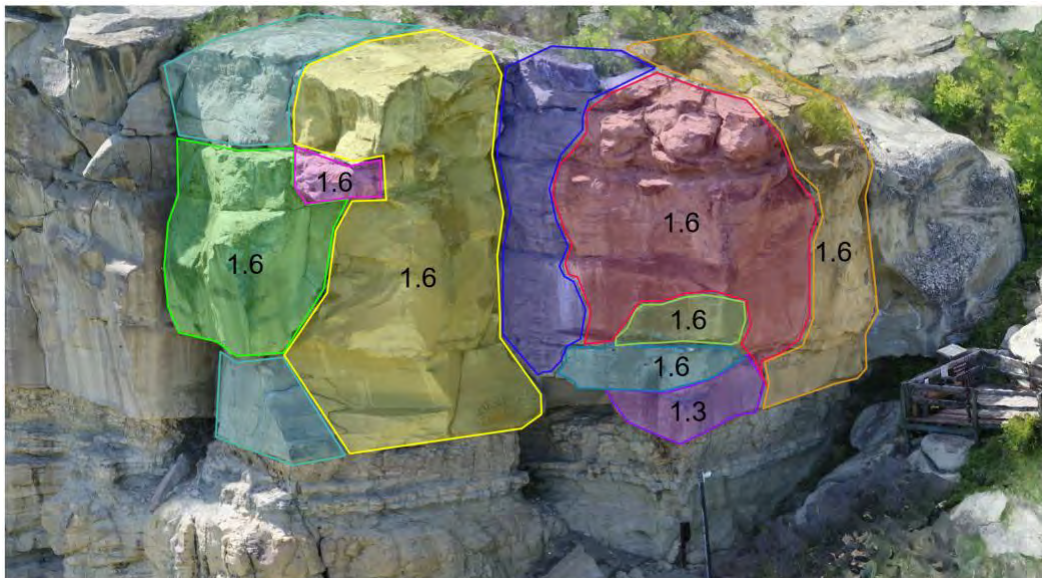


**Figure 18** Global SRF Stability

### SHALE AND SILTSTONE STABILIZATION ANALYSIS

*3DEC* was used to assess the effectiveness of shale and siltstone stabilization. This remedial measure was represented by 0.5 feet of shotcrete applied to the outer layer of the siltstone in the global strength reduction model to determine the efficacy of shotcrete in stabilizing the blocks. Figure 19 shows the displacement histories after 0.5 feet of shotcrete has been applied to the siltstone. The strength reduction at which instability occurs increases to greater than 2.5 in all blocks except for Block 2a, which is marginally stable after an SRF of 2.2. (For reference, the

values without shotcrete were 1.6 except for Block 2a at 1.3, see Figure 18.) This is also reflected in the velocity contours shown in Figure 20.

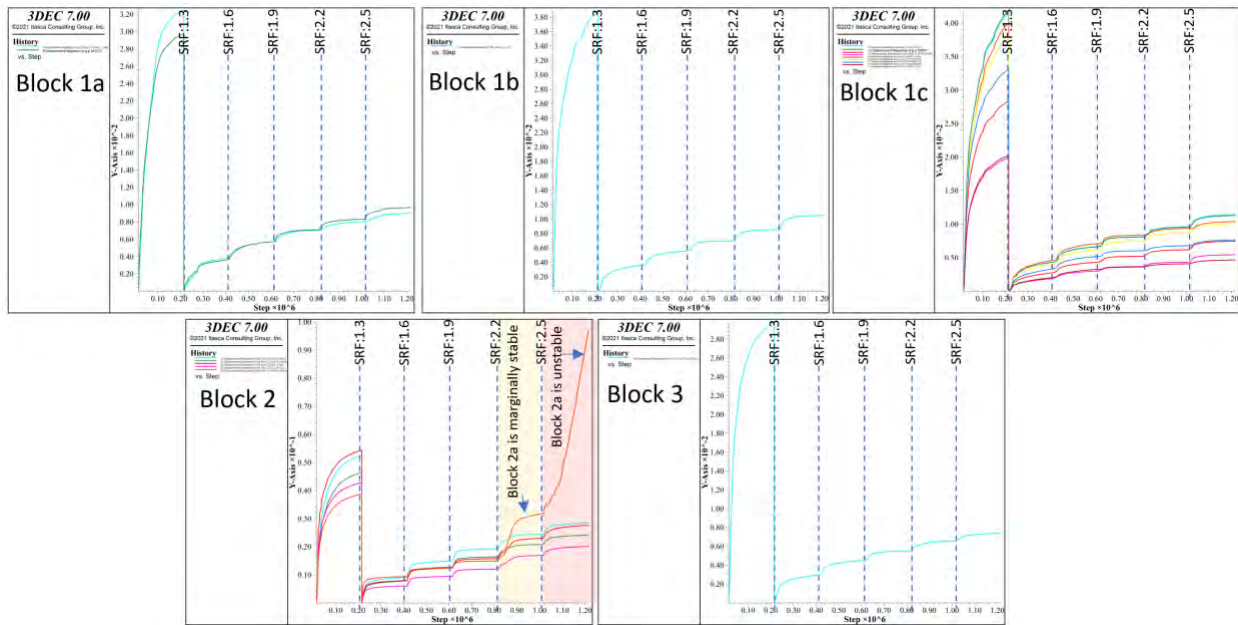


**Figure 19 Signature Block Displacement Histories for Global SR with 0.5 feet of Shotcrete**

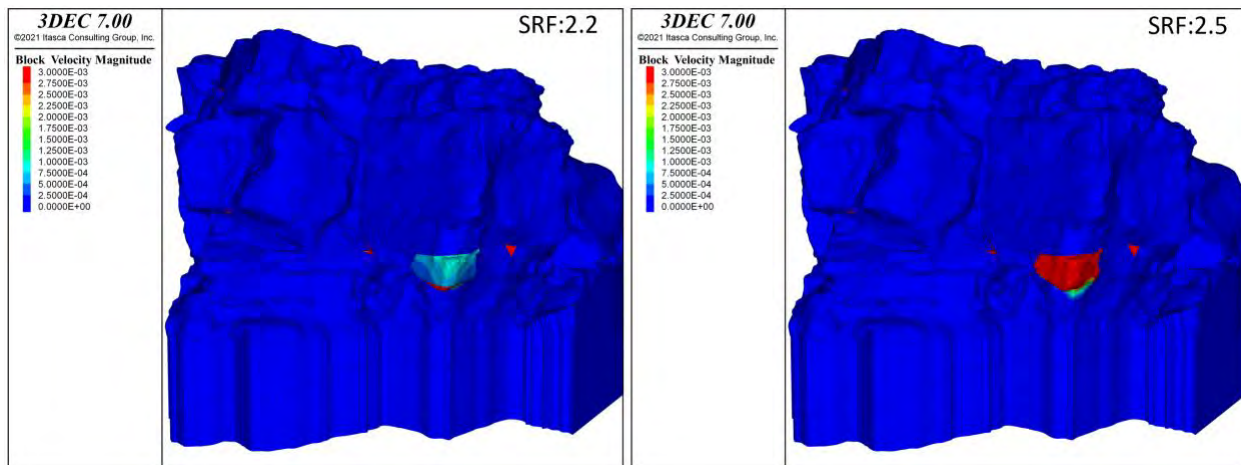


**Figure 20 Signature Block Velocity Contours for Global SR with 0.5 feet of Shotcrete**

Figure 21 summarizes the shotcrete modeling results. Each rock block is labeled with the SRF at which the block becomes unstable.

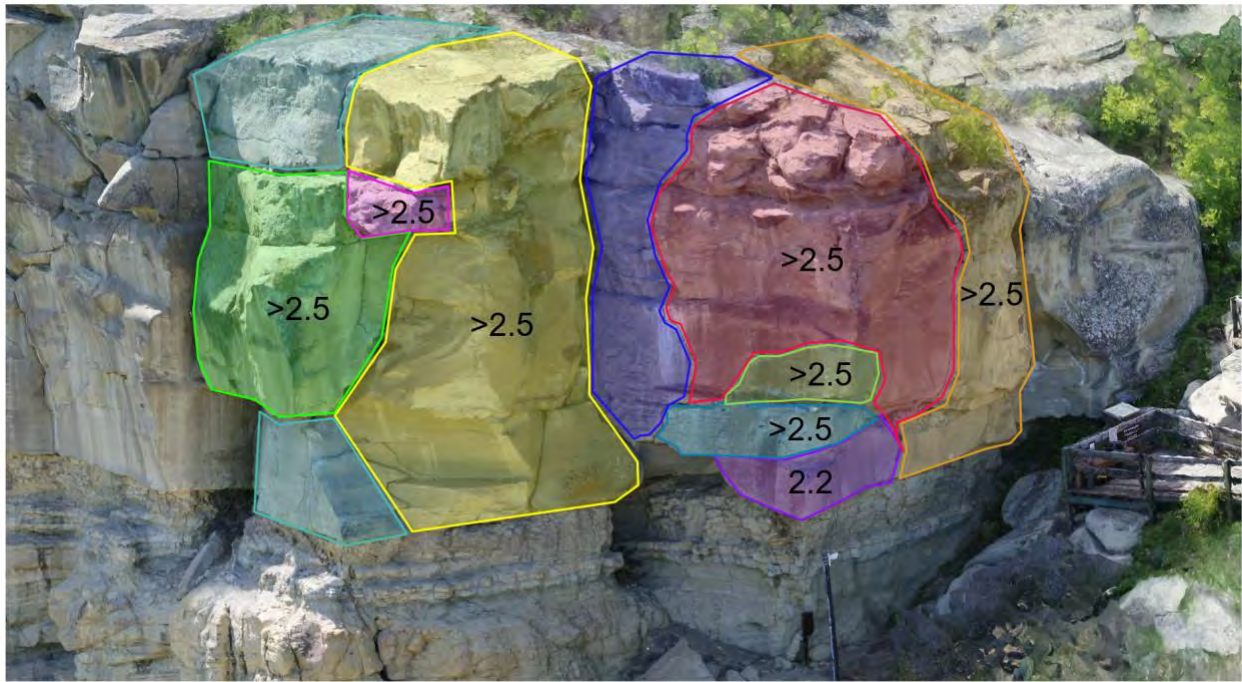


**Figure 21 Global SRF Stability with 0.5 feet Shotcrete**

## CONCLUSIONS

Itasca was hired by the BLM to assess the stability of the Signature Block area of Pompeys Pillar National Monument. A site investigation was conducted to develop accurate geometry and reasonable material parameters. A *3DEC* model was built to analyze the stability and potential stabilization measures of the undercut sandstone at the Signature Block. Stability of the rock blocks were assessed using two methods: by incrementally removing siltstone from the face of the outcrop, and by performing a strength reduction. This provided an estimate of siltstone weathering that would cause instability, as well as an overall stability assessment with the current geometry. Lastly, siltstone stabilization was modeled. Shotcrete applied to the shale and siltstone added confinement to these layers and resulting in an increase of the stability of sandstone blocks in the Signature Block area.

**REFERENCES:**

- Federal Government Reports
  1. Bureau of Land Management. (2020) “Scope of Services, Pompey’s Pillar National Monument Rock Stabilization.”
  2. Connor, C. (1917) “The Lance Formation Petrography and Stratigraphy, Powder River Basin and Nearby Basins, Wyoming and Montana,” U.S. Geological Survey Bulletin 1917-4.
- Journal
  1. Hancock, E. T. (1919) “Geology and Oil and Gas Prospects of the Huntley Field, Montana.,” *Contributions to Economic Geology, 1919, Part II, Mineral Fuels*, pp. 105–148.
- Software Manual
  1. Itasca Consulting Group, Inc. (2016) *3DEC — Three-Dimensional Distinct Element Code (Version 5.2)*. Minneapolis: Itasca.

**Padden Creek I-5 Stream Crossing  
Tiered Hybrid Retaining Wall**

**Mark Rose, PE**

Senior Geotechnical Engineer, GeoEngineers Inc.  
1101 Fawcett Ave, Suite 200  
Tacoma, WA 98402  
(360) 922-5106  
mrose@geoengineers.com

**Sean Cool, PE**

Associate Geotechnical Engineer, GeoEngineers Inc.  
554 West Bakerview Road  
Bellingham, Washington 98226  
(360) 922-5094  
scool@geoengineers.com

Prepared for the 72<sup>nd</sup> Highway Geology Symposium, August 2023, for the *Retaining Structures*  
or *Geological and Geotechnical Innovations* categories.

### **Acknowledgments**

The authors would like to thank the entire Padden Creek Project Team for their contributions and collaboration:

Washington State Department of Transportation  
KPFK Consulting Engineers  
Granite Construction

### **Disclaimer**

Statements and views presented in this paper are strictly those of the authors, and do not necessarily reflect positions held by their affiliations, the Highway Geology Symposium (HGS), or others acknowledged above. The mention of trade names for commercial products does not imply approval or endorsement by HGS.

### **Copyright Notice**

Copyright © 2023 Highway Geology Symposium (HGS)

All Rights Reserved. Printed in the United States of America. No part of this publication may be reproduced or copied in any form or by any means – graphic, electronic, or mechanical, including photocopying, taping, or information storage and retrieval systems – without prior written permission of the HGS. This excludes the original authors.

## ABSTRACT

To comply with a federal injunction requiring corrected fish barriers, the Washington State Department of Transportation (WSDOT) had to replace the undersized Padden Creek crossing at Interstate 5 (I-5) near Bellingham, Washington. With a new stream alignment 30 to 40 feet below the interstate grade, the project would require significant disruptive excavation—and an estimated 400 traffic impact days for I-5.

GeoEngineers designed an innovative two-tiered wall system to enable accelerated top-down construction, ultimately decreasing the total number of traffic impact days on I-5 to 225 and allowing the entire southbound bridge to be built in just 37 days. The wall system consisted of a Geosynthetic Reinforced Soil Integrated Bridge Structure (GRS-IBS) to support the bridge itself and a lower soldier pile and ground anchor wall to support excavation to stream grade. This approach accelerated construction significantly and allowed project contractor Granite Construction to use a top-down construction methodology instead of more traditional bottom-up sequencing.

With this approach, the permanent lower soldier pile and ground anchor wall could be constructed as excavation progressed down while providing lateral support for the upper GRS-IBS system. Thanks to this clever strategy, contractors could wait to excavate the bulk of the new stream channel (more than 30,000 cubic yards of material) until after the new bridges were already built and I-5 traffic was in its permanent alignment.

## INTRODUCTION

The Washington State Department of Transportation (WSDOT) is in the middle of a long-term effort to correct stream crossings across the state so that critical fish species can access upstream habitat. The Padden Creek crossing of I-5 near Bellingham, Washington did not meet fish passage requirements, so WSDOT needed to replace the undersized concrete box culvert (5-foot by 5-foot and 425-foot-long) with two full-span bridges for north and southbound I-5 and a 53-foot-wide buried arch at an adjacent city street. This complex project would require significant excavation and traffic disruption—as many as 400 traffic impact days for I-5.

As a KPFF/Granite Construction design-build team member, GeoEngineers developed an innovative two-tiered wall system that allowed top-down construction sequencing and reduced traffic impact days by nearly 50 percent. The wall system consisted of a Geosynthetic Reinforced Soil Integrated Bridge Structure (GRS-IBS) to support the bridge itself and a lower soldier pile and ground anchor wall to support excavation to stream grade. Thanks to this design strategy, contractor Granite Construction could wait to excavate the bulk of the new stream channel (more than 30,000 cubic yards of material) until after the new bridges were built and I-5 traffic was in its permanent alignment.

This paper provides a case study of the two-tiered wall system used for the Padden Creek I-5 crossing, and a discussion of how this geotechnical and construction strategy may be applicable to other highway engineering projects, where it could help transportation agencies reduce road closures and traffic impacts.

### **Fish Barriers: An Environmental and Economic Issue**

Fishing is an important industry in Washington State, both now and historically. However, a combination of infrastructure and environmental factors are harming this critical natural and economic resource. Dams, culverts, bridges, and other man-made infrastructure are blocking fish species like salmon from swimming upstream from the ocean to critical spawning and rearing habitat. The number of Chinook salmon has been steadily decreasing since 1984 (*1*) and is not expected to recover without human intervention.

For decades, Washington Tribes and environmentalists have advocated for corrections to the infrastructure and artificial channels that are preventing fish from accessing traditional spawning and rearing habitat in the state. In 2013, a U.S. District Court ruling finally clarified the issue. A federal injunction required Washington State to accelerate efforts to improve fish passage for salmon and steelhead across a large area west of the Cascade Mountains and north of the Willapa and Columbia River drainage basins. As of 2022, WSDOT has corrected more than 100 fish barriers and restored access to at least 474 miles of salmon and steelhead habitat with fish-friendly culverts and bridges like those at the I-5 Padden Creek crossing.

## SITE CHALLENGES

### Regional Topography

Padden Creek crossed I-5 from east to west via a 425-foot-long, 5-foot by 5-foot concrete box culvert that ran beneath the north and southbound lanes at a 2.5 to 3.5 percent gradient. To meet fish passage standards, the project would replace the antiquated culvert with two 45-foot-long full-span bridges that would provide room for a carefully designed—and much wider—stream habitat beneath. With a stream alignment 30 to 40 feet below the I-5 grade, this meant as much as 30,000 cubic yards of material had to be excavated during construction.



**Figure 1 – Pre-construction concrete box culvert under I-5.**

The project site is underlain by Tertiary period rocks (Chuckanut Formation) that have experienced several glaciation depositional events in the Pleistocene epoch. The surficial geology of the site was mapped as Pleistocene undifferentiated glacial deposits (Qgd), with Tertiary sedimentary rock ( $E_{cp}$ ) of the Chuckanut Formation – Padden Member mapped closely to the south of the site (2). Undifferentiated glacial deposits consist of glacially deposited sand, gravel, silt, and clay of variable density due to the range of depositional and glacial consolidation conditions. Undifferentiated glacial deposits at this site predominantly consisted of silty and clayey sand and gravel of medium dense to dense condition indicating partial glacial consolidation effect. During the geotechnical investigation, the team encountered sandstone bedrock of the Chuckanut Formation under the undifferentiated unit. Figure 2 shows the project location in relation to mapped surface geology.

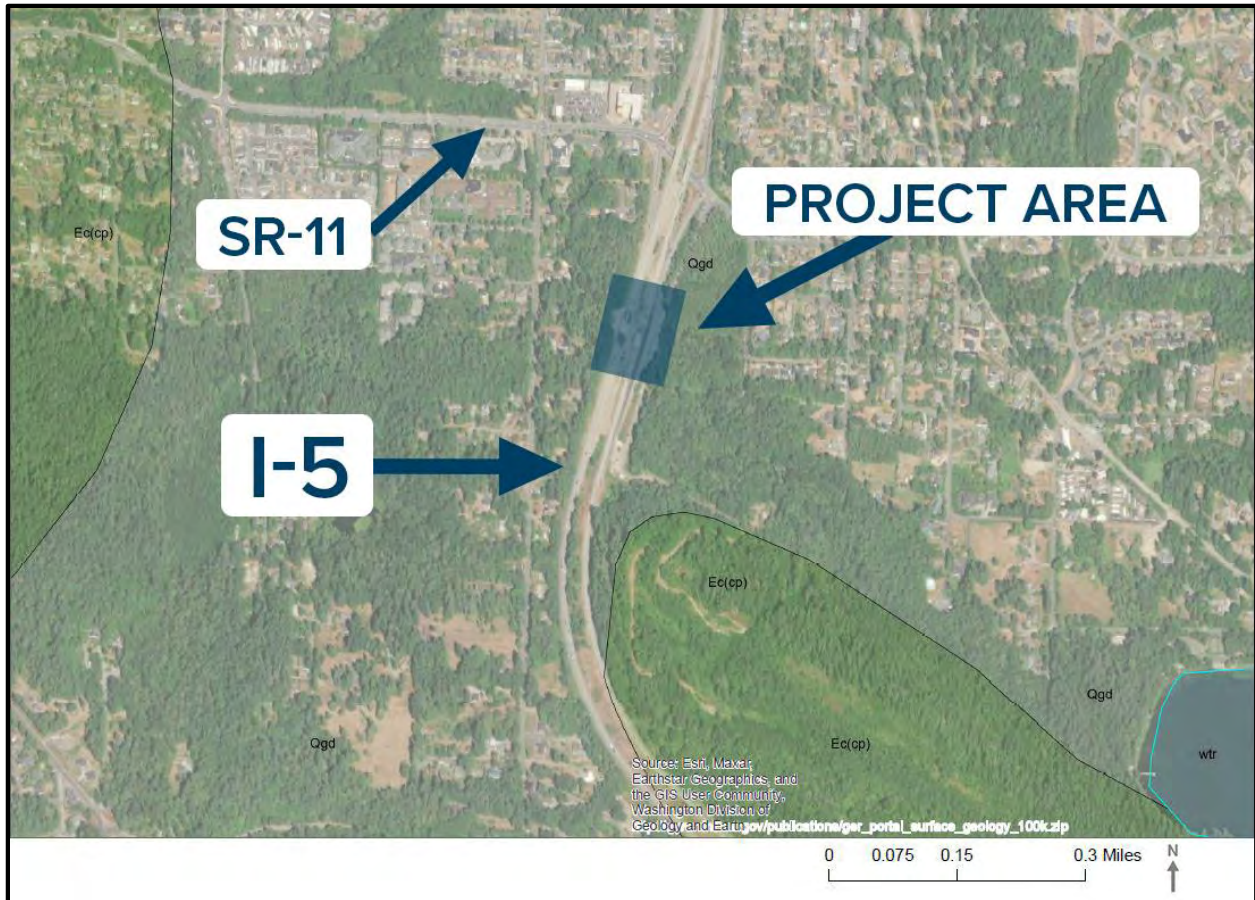


**Figure 2 – Project vicinity map with geologic contacts mapping. From the Washington State Department of Natural Resources (2, 3).**

Thanks to a wealth of local project experience, GeoEngineers knew the bedrock contact elevation in this region was highly variable, especially where glacial deposits and bedrock are mapped near one another—and sandstone rock was observed in the stream channel just 200 feet upstream of the northbound bridge site. The team also noted fill embankments at the site that were used to support the highway grade. The fill material was locally derived and included soils of glacial origin and sandstone fill of various size particles, including boulder-sized material.

Based on site-specific geotechnical investigations completed first by WSDOT and subsequently by GeoEngineers, the team confirmed site soils consisted of embankment fill overlying undifferentiated glacial deposits, overlying sandstone bedrock. A cross-sectional profile of site geology is shown in Figure 3. Explorations at the site consisted of drilled boreholes, and GeoEngineers’ geotechnical team also performed a supplementary geophysical investigation in the vicinity of the crossing using a microtremor array surface wave (MASW) procedure.

The MASW investigation had the two-fold advantage of investigating the bedrock contact surface (for sharp changes in contact elevation and anomalies) and providing shear wave velocity values for seismic design. The MASW investigation was preferred over alternative

exploration methods due to its minimal traffic disruption and lower cost of completion. The resultant shear wave velocity data was correlated with discrete boring data to aid in interpreting bedrock contact, as shown for one transect in Figure 4. Sedimentary bedrock was interpreted to occur where the soil profile had a shear wave velocity of 1,500 to 1,900 feet per second.

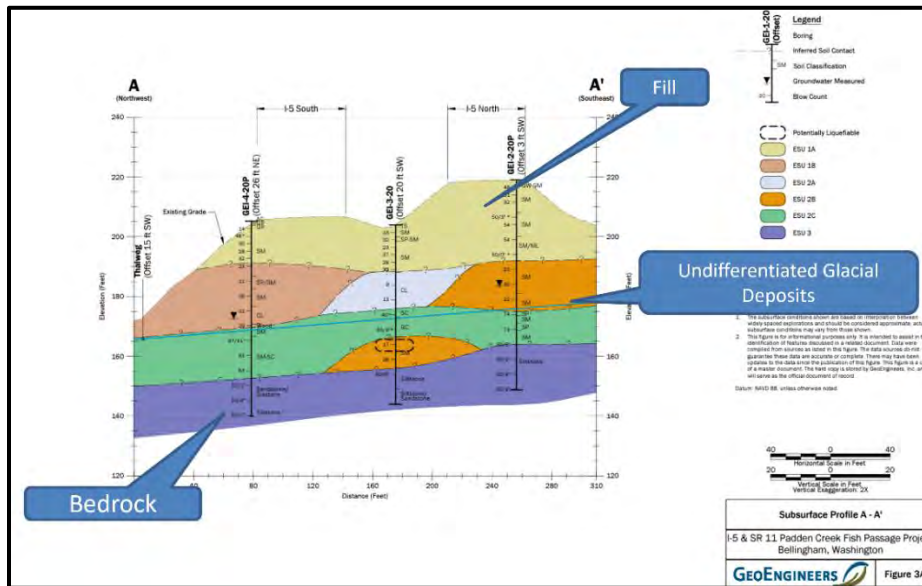


Figure 3 – Subsurface geology of the site.

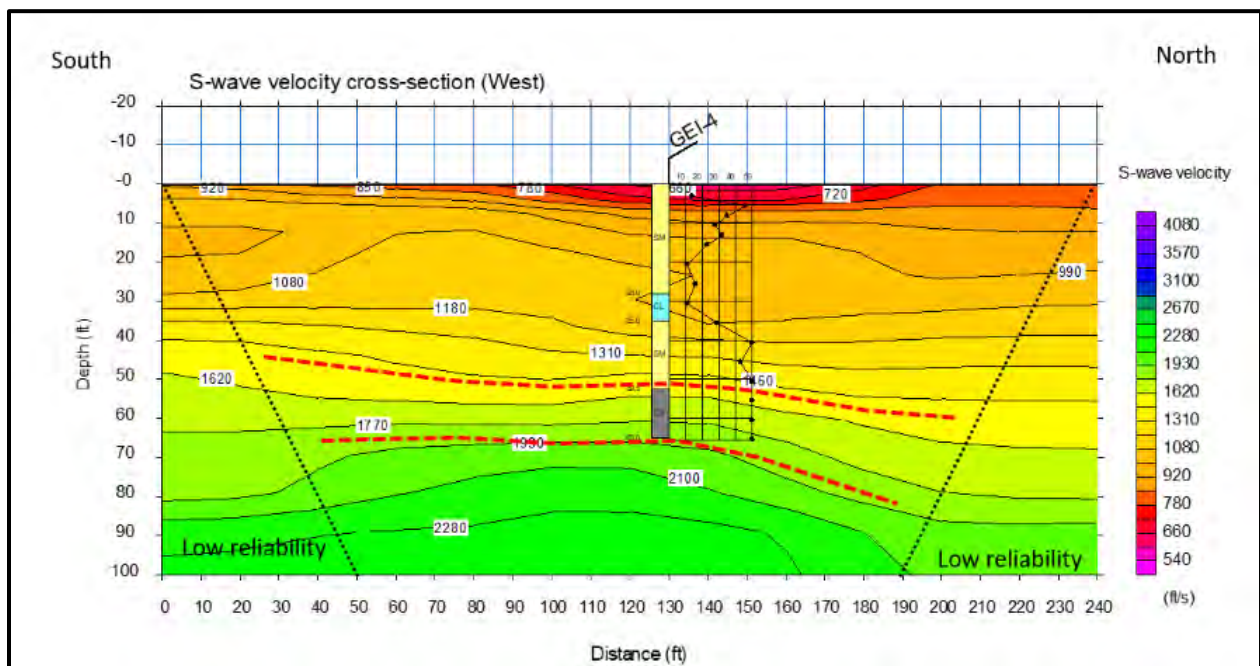


Figure 4 – MASW shear wave velocity profile for the west highway shoulder (4).

## **Potential Traffic Impacts**

I-5 is the primary north-south artery through Western Washington, and significant lane closures were not acceptable to WSDOT. A major WSDOT project goal was to reduce, minimize or eliminate impacts to the traveling public and local community by developing and implementing construction strategies that reduced or eliminated road and/or lane closure on the freeway and local streets.

Early on, the project team estimated that construction would require more than a year's worth of I-5 traffic impact days because of the scale of excavation required. Preliminary WSDOT plans called for traditional bridges that were 155 to 170 feet long, including concrete approach slabs. The project contract assumed a combined 400 days (200 for each bridge) of impacts for northbound and southbound lanes. Daytime and long-term lane closures were not permitted.

## **Environmental Considerations During Construction**

Environmental stewardship was another important project goal for WSDOT. Granite needed to bypass Padden Creek during bridge construction, and environmental regulations limited any stream bypass to a short summer construction window between July 1 and September 30. Planned construction below the creek's ordinary high-water elevation could only occur during this time period.

## **A TWO-TIERED GEOTECHNICAL SOLUTION**

### **Supporting a Top-Down Approach**

The design-build team eventually settled on a unique combination of creative construction sequencing and innovative engineering to drastically reduce traffic impacts. Traditionally, bridges and similar structures are built using a bottom-up sequence, where contractors begin with excavation and then build the structure upward from the foundation. Although this method is usually easier to design, it would have caused massive traffic impacts on I-5 if used for the Padden Creek crossing and required much larger temporary shoring walls to support the temporary bypasses. Instead, the design-build team suggested a top-down approach that allowed the I-5 bridges to be built first—ultimately reducing traffic impact days by nearly 50 percent compared to initial estimates.

In top-down construction sequencing, permanent internal structures are built as excavation progresses down, providing lateral support for the retaining walls along the way. By completing the upper bridge superstructure first, most of the excavation could wait until after I-5 traffic was in its permanent alignment. See Figure 5 below for a detailed breakdown of the top-down construction sequence.

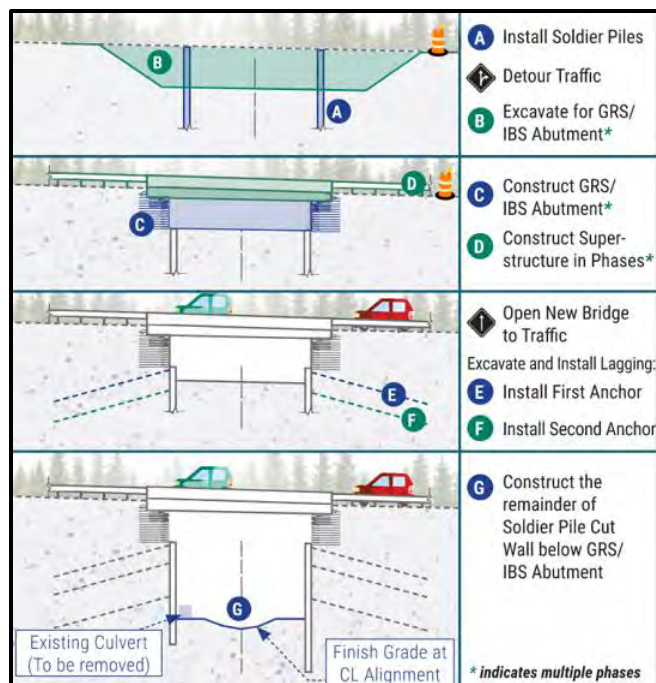


**Figure 5 – Top-down construction sequence**

To be a viable approach, the team needed a shoring system capable of supporting the bridge during excavation. They settled on a unique, two-tiered wall system consisting of a Geosynthetic Reinforced Soil Integrated Bridge Structure (GRS-IBS) to support the bridge itself and a lower soldier pile and ground anchor wall to support excavation to stream grade.

### Upper Tier: GRS-IBS Wall

GeoEngineers provided geotechnical design recommendations for 12-foot-tall GRS-IBS abutments to support the north and southbound I-5 bridges, taking advantage of this cost-effective and increasingly popular geotechnical bridge support solution. GRS-IBS is a construction technique that combines geosynthetic materials with compacted soil—much like mechanically stabilized earth (MSE) walls—to create a stable and durable bridge foundation.

GRS-IBS abutments contain three key elements: a reinforced soil foundation, the abutment structure, and the integrated approach. The bridge is supported by layers of compacted granular fill alternated with layers of geosynthetic reinforcement. These closely integrated layers create an efficient and stable composite structure with exceptional load-bearing capacity, surpassing their intended design limits while maintaining predictable and dependable performance.

The GRS-IBS was first developed by the Federal Highway Association (FHWA) in the 1990s and benefits and applications of the system have been documented in FHWA-HRT-17-080 (4). A GRS-IBS can be built quicker and at a lower cost with equal or improved performance compared to traditional shallow or pile-supported bridges, under appropriate design (and geologic) conditions. The bridge superstructure is placed directly on the GRS-IBS substructure,



## Lower Tier: Soldier Pile and Ground Anchor Wall

Although GRS-IBS walls would provide efficient support for the I-5 bridges, excavation was still problematic. The depth from roadway grade to stream channel grade would normally mean a wall height greater than 30 feet, and designers were considering extending the abutment walls even farther, below the design stream scour elevation. Full excavation and construction of a single large GRS-IBS would require significant earthwork and more traffic bypass time, and the timing of wall construction would need to be very precise to make sure the base of the wall would be built in the summer during the in-stream work window.

This unique combination of structural requirements, environmental requirements, and temporary traffic impacts inspired the team to design an unconventional solution: a lower tier of soldier pile and permanent ground anchor shoring walls to complement the upper GRS-IBS wall and protect it from potential scour and channel migration.

The final I-5 crossing design included two continuous parallel soldier pile walls below the GRS-IBS bridge abutments to support excavation to stream grade, as shown in Figure 7. The 25 to 30-foot walls extended the full length of the crossing on either side of Padden Creek and were designed to include bridge and traffic surcharge under the I-5 lanes.

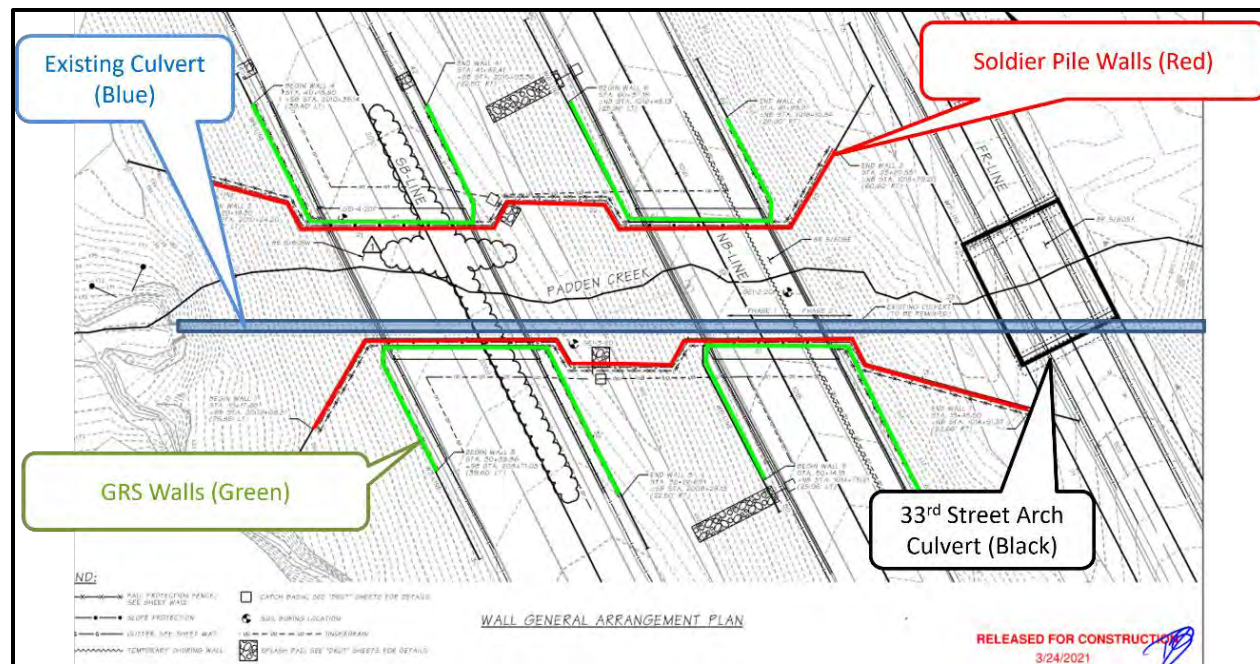


Figure 7 – Padden Creek Crossing wall arrangement plan.

## Design Considerations

Because of the complexity of the wall system and the design-build nature of the project, the design components of the two-tiered wall systems were coordinated by specialists from the design-build team. Design roles specific to the two-tiered wall design were as follows:

- Stream Engineer: dictated required channel migration width and therefore bridge span length.
- Geotechnical Engineer: GRS bearing resistance parameters, sliding coefficient, lateral earth pressure development (including surcharge and seismic pressure), Permanent Ground Anchor (PGA) bond stress parameters, settlement estimates, system global stability.
- Structural Engineer: Bridge girder design, soldier pile design, PGA design loading, wall transition detailing.
- GRS Wall Designer: GRS geosynthetic and geogrid reinforcement detailing.
- Shoring Subcontractor: PGA sizing and detailing to meet loading criteria.

The GRS abutment design is similar to a typical mechanically stabilized earth wall, with the added consideration of bridge loading. Failure checks for internal and external stability and bearing capacity were performed. Since the GRS wall was set immediately above and slightly behind the soldier pile wall, only the global stability of the combined two-tiered wall system was evaluated rather than performing this analysis for the walls individually. The GRS has the special requirement of design for girder and deck loads.

The lower soldier pile wall required design considerations for GRS-IBS surcharge loading and sliding force in addition to typical loading for active earth pressure, hydrostatic pressure below the groundwater table, traffic surcharge, and seismic pressure for extreme event limit state.

### **Advantages of the Two-Tiered Shoring Wall**

The hybrid wall system for the Padden Creek crossing provided a number of advantages when compared to more traditional bridge support structures. As noted previously, GRS-IBS walls are quicker and easier to construct thanks to their lightweight and easy-to-handle materials, eliminating the need for specialized heavy machinery. They also eliminated the need for approach slabs, according to WSDOT and FHWA recommendations, and made additional concrete pours unnecessary. More typical bridge foundations would require a concrete foundation, pile cap, and abutment concrete—all of which can take days to pour and let cure.

This flexible two-tiered system also allowed the geotechnical design team to use active earth pressure rather than higher at-rest pressure in design calculations. Traditional concrete abutments are often fixed from deflection by bridge superstructure elements and require calculations using at-rest soil pressure, which is typically at least 50 percent greater than active pressure conditions. This is particularly significant for seismic design where earth pressures under the at-rest earth pressure condition may be at least double active pressure conditions. The GRS-IBS and permanent ground anchor walls are both flexible, so the use of active earth pressures in the design was appropriate and resulted in a more efficient structure.



**Figure 8 – Bridge and two-tiered wall system construction in progress prior to permanent concrete fascia construction.**

The geotechnical team also wanted to minimize construction delays and risks associated with the site's variable bedrock conditions. A bridge supported on deep foundations would have meant bearing into the underlying bedrock unit. Although the MASW investigation showed no sharp anomalies in the bedrock surface, dips in bedrock elevation were possible. If unexpected changes in bedrock were encountered, it would have required a pile or drilled shaft reinforcement cage on site, or design alterations to allow for lower soil strength parameters.

Most significantly, the two-tiered wall design allowed project contractor Granite Construction to use a top-down construction approach. This meant most of the required excavation (more than 30,000 cubic yards of material) could be delayed until after the new bridge decks were built and I-5 traffic was in its permanent alignment, and the in-water work required for the lower wall could be precisely scheduled during the required work window.

Granite also collaborated with WSDOT during practical design to reduce temporary lane and shoulder widths by several feet, eliminating an entire phase of construction detour on mainline I-5. Coupled with the top-down approach, this allowed the team to construct the southbound I-5 bridge and re-open it to traffic in the permanent alignment in just 37 days. Although some temporary bypass lanes, traffic shifts, and overnight lane closures were still required, the team finished construction without a single complete closure of I-5.

Together, the top-down sequencing, hybrid retaining wall, and other design and construction efficiencies decreased the total number of traffic impact days on I-5 from 400 to just 225 days, a reduction of nearly 50 percent.

## **CONSTRUCTION CHALLENGES**

### **Importance of Construction Phasing**

The construction sequencing was key and critical to the success of the Padden Creek project. The team carefully analyzed and ordered each step. For instance, the soldier piles could not be installed after the GRS-IBS because of the low overhead clearance of the bridge girders. The final construction phasing plan for the wall system included 1) soldier pile installation, 2) GRS-IBS bridge construction, 3) soldier pile excavation and PGA installation, and 4) the permanent wall facing.

Construction phasing and sequencing were not without challenges. Because of space limitations, the I-5 northbound lanes had to be built in two separate stages to complete the full width of the road. Coupled with a skew of the GRS wall face, a portion of the reinforcing grid for the second phase would have intersected with the temporary facing for the first phase, rendering the grid too short. These steps were split into two construction phases, as shown in Figure 9A and Figure 9B on page 15. The team added additional geogrid parallel to the road direction to accommodate this condition.

### **Overcoming Obstructions**

As is typical in geotechnical construction in fill and glacial soils, obstructions were encountered during the drilling of soldier piles and PGAs. Even though the MASW results indicated bedrock was not likely to be an issue, there was some concern that specific cantilever soldier piles located near the ends of the soldier pile walls would encounter bedrock, so the team had design contingencies ready if drilling refusal conditions were encountered using standard drilling (as opposed to specialty rock drilling equipment). Overall, the construction team did not encounter unusually high bedrock during drilling activities which resulted in drilling refusal.

### **Limiting PGA Bond Lengths**

The permanent ground anchors (PGA) for the soldier pile wall had to support significant design loads up to 300 kips, but long PGA bond lengths are discouraged or prohibited by WSDOT guidelines. Bond lengths over 40 feet are closely scrutinized and bond lengths over 50 feet are not permitted at all. To achieve the required design loads with shorter PGAs, the contractor was able to install larger diameter test anchors and prove a 3.5 kip per square foot design bond stress, keeping the installed PGA bond lengths under 40 feet.

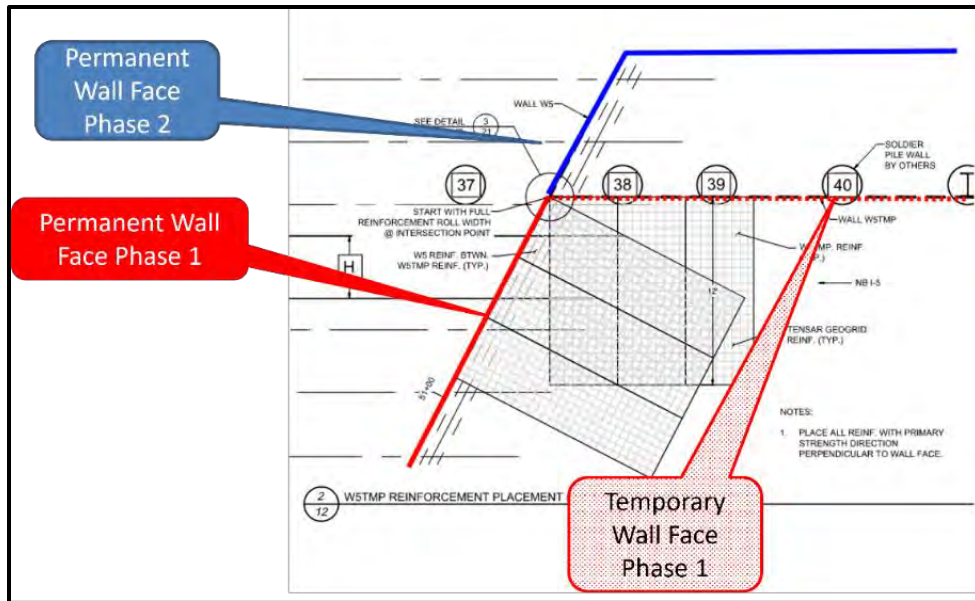


Figure 9A – GRS Construction Phase 1

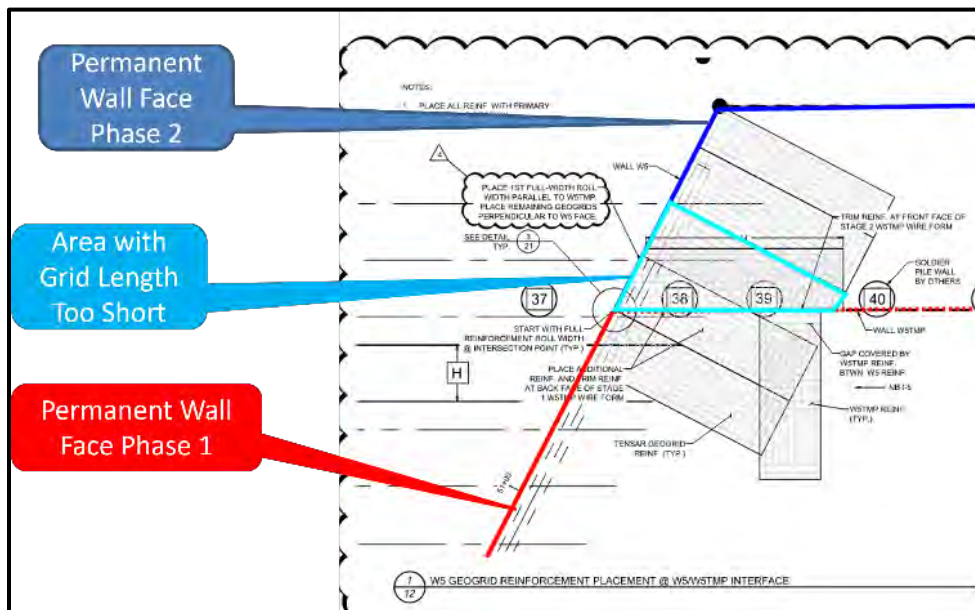


Figure 9B – GRS Construction Phase 2

## CONSTRUCTION MONITORING

WSDOT requirements for a geotechnical instrumentation plan (GIP), and general good practice, called for a monitoring program of the two-tiered wall system to measure performance during and after construction. The monitoring program included:

- Optical survey monitoring of the road surface, GRS-IBS wall, and soldier pile wall to measure horizontal and vertical movement. Performed daily to monthly depending on the construction activity.
- Remote inclinometers on the soldier pile walls to measure horizontal movement continuously.
- In-place inclinometers on soldier pile walls to measure horizontal movement at discrete time intervals (weekly to monthly).

We typically observed limited horizontal movement of survey markers and inclinometers for both the GRS and soldier pile walls (typically less than 0.75 inches). Vertical movements were typically observed in the range of 0.5 to 1.5 total inches for GRS abutment survey locations, as shown in Figure 10A and Figure 10B. Little to no vertical settlement was observed in the soldier piles, which was expected as the pile tips were constructed in undifferentiated glacial deposits or bedrock.

Typically, inclinometer casing is installed with the soldier pile along the center of the pile flange opposite the excavation. One of the challenges of the two-tiered wall system, as designed, was that it required the inclinometers to be installed adjacent to the front flange of the soldier pile. This meant that temporary timber lagging had to be set immediately behind the casing to abut the pile flange.

The inclinometer's location led to several instances of errant readings caused by construction activities, as there was no good way to protect the casings aside from careful construction practices. Accurate readings required careful discernment between casing movement caused by construction interference and actual wall movement due to increased earth pressure as excavation progressed. The authors recommend considering alternative monitoring methods, such as remote optical surveys, in lieu of inclinometer monitoring in future cases.

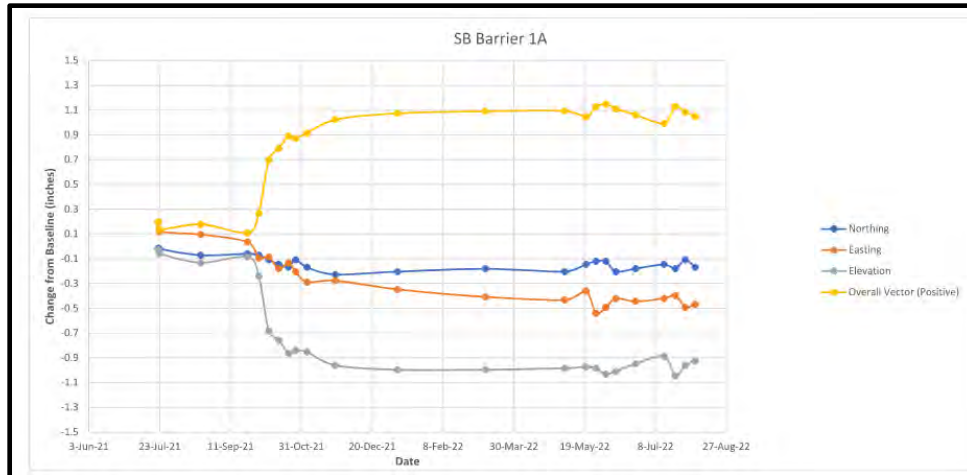


**Figure 10A – Optical survey measurements for GRS Wall 4 at roadway surface marker location.**



**Figure 10B – Wall face marker locations corresponding with optical survey results in Figure 10A.**

## LESSONS LEARNED

### Wider Applicability of Design and Approach

The two-tiered wall system proved to be an effective approach to this challenging stream-crossing project that required both rapid bridge construction and relatively deep excavation. The construction of the GRS-IBS bridge allowed for rapid construction of the permanent roadway alignment and supporting superstructure, and the excavation and construction of the lower shoring wall to required stream scour elevations could progress with minimal disturbance to the permanent travel lanes.

Application of this two-tiered wall system (GRS-IBS bridge abutments above a soldier pile wall) has numerous potential applications in highway engineering projects where grade

separation is required, and the separation elevation is high enough that the GRS-IBS system alone may not be feasible. Potential applications include:

- Fish passage/culvert replacement projects like the Padden Creek crossing.
- New or widened underpasses for roadway, rail, or trail crossings.
- Constructing lids over urban freeways.
- Utility crossing construction, if tunneling methods are deemed infeasible.

Every project and site is unique, but the authors believe a similar two-tiered wall system can provide significant advantages when conditions are suitable. The GRS-IBS wall was appropriate for the Padden Creek site's topology—moderate strength fill and undifferentiated glacial deposits that could support the strength, service, and extreme limit foundation loads for the size of the GRS-IBS system. The medium bridge span lengths of 45 feet also met WSDOT and FHWA recommendations.

Certain topographic conditions and design factors may limit the feasibility of GRS-IBS in other highway projects, including:

- Greater span lengths (60+ feet per current WSDOT requirements)
- Strength and service limit load requirements that exceed design limitations.
- Very soft to medium stiff compressible clays and silts, which may experience excessive settlement and fail to meet the service limit condition.
- Liquefiable soils, which may settle or experience strength loss in an extreme event condition.

The use of longer spans or higher loads than currently recommended may be feasible based on advanced analysis techniques, but verification would require very close collaboration with the design team members. GRS-IBS could potentially be implemented on soft ground or liquefiable sites with the right ground improvement techniques, but due to potentially higher costs, it should be compared to traditional deep foundation-supported bridge systems and analyzed on a case-by-case basis.

## CONCLUSION

In this paper, we have seen how the Padden Creek design-build team designed and constructed a sustainable fish habitat beneath an active interstate—and did it with minimal traffic disruptions. The team used an innovative two-tiered shoring wall and top-down construction to decrease the total number of traffic impact days on I-5 from 400 to just 225 and build the entire southbound bridge in just 37 days.

The project's fish passage and habitat goals were successful, fulfilling WSDOT's requirements under the 2013 federal injunction. The team replaced the old 5-foot by 5-foot box culvert with two full-span bridges for north and southbound I-5 that restored fish passage to more than five miles of upstream rearing and spawning habitat. The project included approximately 1,000 feet of newly designed stream channel and more than 100 habitat features like root wads and off-channel habitat that will shelter young fish and evolve with the stream

system over time. Within two weeks of finishing construction, salmon, steelhead, and other fish were observed swimming and spawning throughout the restored Padden Creek reach, demonstrating the immediate success of the stream crossing and environmental features.

The project's success depended on close collaboration and trust between teaming partners and WSDOT. The design of the GRS-IBS system also required strong coordination between design engineers (geotechnical, structural, and GRS), general and subcontractors, and WSDOT.

The authors see strong potential for similar GRS-IBS and soldier pile wall hybrid systems in other highway engineering projects where significant grade separation is required and construction must be completed on a short timetable. Other WSDOT consultants are already considering this unique approach to bridge construction and excavation support that can put cars back on the highway, and fish in the stream, even more efficiently.



**Figure 12 – Completed Padden Creek Crossing of I-5.**

**REFERENCES:**

1. Environmental Protection Agency. *Health of the Salish Sea Ecosystem Report: Chinook Salmon*. <https://www.epa.gov/salish-sea/chinook-salmon> Accessed June 1, 2023.
2. Lapen, T.J. *Geologic Map of the Bellingham 1:1000,00 Quadrangle, Washington*. Open File Report 2000-5. Washington State Department of Natural Resources, 2000.
3. Washington State Department of Natural Resources. *Washington Geologic Information Portal*. <https://geologyportal.dnr.wa.gov/> Accessed June 1, 2023.
4. Bull, K. and K. Hayashi. *Report on the Geophysical Method for Padden Creek Crossing, Bellingham, Washington*. OYO Corporation, Pacific, 2020.
5. Adams, A. and J. Nicks. *Design and Construction Guidelines for Geosynthetic Reinforced Soil Abutments and Integrated Bridge Systems*. Report FHWA-HRT-17-080. Federal Highway Administration, U.S. Department of Transportation, 2018.
6. *Bridge Design Manual LRFD*. Manual M 23-50.19. Washington State Department of Transportation, July 2019.
7. *Geotechnical Design Manual*. Manual M 46-03.12. Washington State Department of Transportation, July 2019.
8. *LRFD Bridge Design Specifications, 8th Edition*. ISBN 9781560516545. American Association of State Highway and Transportation Officials (AASHTO), 2017.

## The Erodibility Index in Washington State's Intermediate Geomaterials: The need for a practical tool.

**Robert Humphries, LEG**

WSDOT State Hydraulics Office  
310 Maple Park Ave. SE  
Olympia, WA 98504-7331  
360-628-1102  
[robert.humphries@wsdot.wa.gov](mailto:robert.humphries@wsdot.wa.gov)

**Gabriel Taylor, LEG**

WSDOT State Geotechnical Office  
310 Maple Park Ave. SE  
Olympia, WA 98504-7331  
[gabe.taylor@wsdot.wa.gov](mailto:gabe.taylor@wsdot.wa.gov)  
360-709-5586

**Casey Kramer, PE**

Natural Waters, LLC  
310 Maple Park Ave. SE  
Olympia, WA 98504-7331  
[ckramer@naturalwaters.design](mailto:ckramer@naturalwaters.design)  
360-519-7251

**Luke Assink, PE**

WSDOT State Hydraulics Office  
310 Maple Park Ave. SE  
Olympia, WA 98504-7331  
[luke.assink@wsdot.wa.gov](mailto:luke.assink@wsdot.wa.gov)  
360-705-7269

**Andrew Fiske, PE**

WSDOT State Geotechnical Office  
310 Maple Park Ave. SE  
Olympia, WA 98504-7331  
[andrew.fiske@wsdot.wa.gov](mailto:andrew.fiske@wsdot.wa.gov)  
360-709-5456

**Julie Heilman, PE**

WSDOT State Hydraulics Office  
310 Maple Park Ave. SE  
Olympia, WA 98504-7331  
[julie.heilman@wsdot.wa.gov](mailto:julie.heilman@wsdot.wa.gov)  
360-705-7262

### **Acknowledgements**

The authors would like to thank the following individuals for their contributions to this work:

Dr. George W. Annandale – GWA, Inc.

Dr. Paul Schlotfeldt – WSP

Mr. Richard W. Humphries - WSP

### **Disclaimer**

Statements and views presented in this paper are strictly those of the authors, and do not necessarily reflect positions held by their affiliations, the Highway Geology Symposium (HGS), or others acknowledged above. The mention of trade names for commercial products does not imply the approval or endorsement by HGS.

### **Copyright Notice**

Copyright © 2023 Highway Geology Symposium (HGS)

All Rights Reserved. Printed in the United States of America. No part of this publication may be reproduced or copied in any form or by any means – graphic, electronic, or mechanical, including photocopying, taping, or information storage and retrieval systems – without prior written permission of the HGS. This excludes the original authors.

## ABSTRACT

WSDOT's Fish Passage project is replacing hundreds of culverts that are barriers to fish migration. However, most of these crossings also impeded the flow of sediment and water, as well as fish. The associated disruption in geomorphic processes typically results in upstream sediment deposition and a downstream scour pool, causing the crossing to serve as a sediment trap and a grade control structure. The design of the replacement structures must account for future conditions that aim to reestablish geomorphic continuity. This often requires wider structures with open bottoms and deeper foundations to accommodate potential vertical scour. Because many of these crossings occur in the Puget Sound lowlands, they are often underlain by and/or founded on glacial sediments. Many of the available methods utilized to determine scour for the design of water crossings do not adequately address the erosion-resistant properties of common geomaterials found in Washington State, like weathered bedrock or glacial till. Termed Intermediate Geomaterials (IGMs), these materials can be more resistant to erosion than granular sediment. Without methods to assess the erosion resistant properties of these materials, designs are often forced to make conservative assumptions resulting in deeper foundations and increased project costs. The Erodibility Index Method (EI) is applied around the world for similar purposes. The EI is a geomechanical index method used to assess the likelihood of scour of any earth material by flowing water. This paper presents several WSDOT Fish Passage projects in the context of the Erodibility Index threshold and suggests potential future applications.

## INTRODUCTION

In response to the Fish Passage Injunction issued by the US District Court in 2013, the Washington State Department of Transportation (WSDOT) is replacing hundreds of culverts that have historically been barriers to fish migration. Many of these historical culverts are under-sized compared to the river, or stream, they historically conveyed. To meet modern design requirements and decrease the size discrepancy between the river's historic channel migration zone and the crossing dimensions, the replacement structures are often larger and open-bottomed, requiring deeper foundations.

WSDOT requires that these larger structures undergo a rigorous design process including a scour assessment that applies the methods described in HEC 18, HEC 20, and HEC 23 (FHWA 2012, 2012, and 2001). Although these documents enable an assessment of the scour potential of a wide variety of scour processes in varied materials, their treatment of weak rock and Intermediate Geomaterials (IGMs) can force some assumptions within the methods that often result in an overestimate of scour dimensions.

Given our active tectonic setting and our recent glacial past, Washington State has an abundance of IGMs in the Puget Lowlands. Because of this, IGMs frequently compose the foundation material for these crossing replacement structures in WSDOT Fish Passage Projects. Consequently, their susceptibility to scour becomes an important and expensive design variable. In this paper we propose a modification to the application of the Erodibility Index Method (EIM) regarding the assessment of IGMs.

### Problem Statement

Scour of earth materials occurs as a complex process, or interconnected series of processes, resulting in landscape change. Theoretical and process-based understandings of scour provide considerable insight into these processes, but the application of these techniques for design purposes is often impractical solely based on the incompatibility between the data requirements of the methods and the data available (Van Rijn, 2008; Frizell, 2008, Lamb et al., 2015; Shan et al., 2015).

The standard guidance documents enable the calculation of scour of a range of earth materials via multiple processes, including non-cohesive sediment transport, block removal of bedrock at pier foundations, and even cohesive sediment. In fact, the Erodibility Index Method for rock scour is presented in section 4.7.2 of HEC 18 (FHWA, 2012). However, the recommended method for assessing cohesive sediment uses an empirical correlation to the rate of erosion above a critical shear stress. This approach requires a time-series of the flow record. In the absence of nearby hydrometric data, this approach often requires the creation of a synthetic discharge time series, introducing another source of uncertainty and computational complexity.

The traditional approaches to scour divide earth materials into three types; cohesive, non-cohesive, and rock. Given the lack of information available to apply the more complex scour methods, particularly in the initial stages of a project and when our crossings are founded on IGM, WSDOT needs a practical tool to assess the potential for scour. In this assessment we

propose the application of a fourth earth material type to represent the erosion-resistant properties of IGMs.

### **Intermediate GeoMaterials (IGMs)**

Washington is a mountainous state with active tectonics and a recent glacial history. This geologic setting has resulted in the widespread presence of IGMs, which are earth materials with engineering properties that fall somewhere between rock and soil. Examples of IGMs in Washington State include glacial tills and weathered sedimentary bedrock. Both of these IGM materials are commonly found at the ground surface in Washington State, especially in the Northwest and Olympic Regions.

Glacial till is a deposit that was directly emplaced by ice and then overridden and overconsolidated by glacial loading. The result is a concrete-like material that is commonly referred to as 'hardpan.' Glacial till is heterogenous (varying in composition) but typically consists of a bimodal grain size distribution with a matrix of hard clay, silt and sand, and gravel and cobble clasts unevenly distributed within the matrix. Glacial till deposited by the Vashon continental ice sheet mantles much of the lowland areas of the Puget Sound region. Alpine glacial tills are common in the glacially carved valleys of the Cascade and Olympic Mountain Ranges. Till lacks bedding, jointing, and other common characteristics of rock. However, it exhibits cohesion and cementation, and has been observed to be more resistant to scour than the constituent sediments alone.

Deeply weathered sedimentary rock is common in Washington State, especially in the Willapa Hills of the Olympic Region. This IGM exhibits relict bedding and other bedrock structure but has often weathered to a residual soil and has lost most of the strength characteristic of the underlying fresh bedrock. This material is often mistaken for soil during geotechnical drilling, as the recovered samples are disturbed by the time they are observed by a drill crew inspector or geologist. In-situ, weathered bedrock exhibits more resistance to scour than the constituent sediments, due to relict cohesion and cementation, but cannot be characterized well using the tools typically used for bedrock.

In addition to the challenges associated with characterizing engineering properties of IGMs, these materials are difficult to sample with geotechnical drilling and difficult to test in geotechnical labs. Standard geotechnical sampling methods for soil include the Standard Penetrometer (SPT), Shelby Tubes, and Piston Samplers. These methods will not typically be capable of penetrating into very dense glacial till and may disrupt weathered bedrock in such a way that it is no longer recognizable as rock once the sample is retrieved from the borehole. Rock coring methods often wash away fine-grained portions of IGMs, resulting in little to no recovery. With careful and skillful drilling, we have been successful in recovering some samples of IGMs with rock core barrel methods. We have found that careful drilling and sample preservation techniques are required to recover samples and transport them to the lab without disturbance or desiccation. However, IGM samples are often delicate. If they are allowed to dry, they typically fracture and are no longer suitable for laboratory testing. Even if successfully transported to the lab, IGM samples are difficult to handle and cut into suitable specimens for specialized geotechnical laboratory test, such as triaxial testing.

## Limits of This Assessment

- As presented in this paper, the EIM assesses the potential for the occurrence of scour and not the magnitude of scour.
  - Scour magnitude can be assessed with the EIM if the rate of stream power decay on the bed during scour hole development is known. See Annandale 2006 for more information.
- The case studies assessed in this report are in various stages of construction.
  - This report was conducted externally to WSDOT's design processes.
  - The results of this assessment have not been incorporated into the designs of these structures.
  - No scour monitoring has been conducted to confirm or refute the scour assessments presented in this report.
- The bimodal grain size distribution that is characteristic of dimictic glacial till can result in the coarse particles acting as an armoring layer when a till unit experiences scour. The armoring effect is correlated to a suite of complex, interconnect processes and characteristics (Pike et al., 2018). Unfortunately, one of these characteristics is the randomly heterogeneous distribution of coarse particles within any given till unit. The local concentrations of coarse particles cannot be reliably predicted and are therefore unsuitable for design purposes and are excluded from this assessment.
- Scour by abrasion is not included in the EIM (see Sklar and Dietrich, 2001).
- The presence of weaker material at depth increases the likelihood of significant scour. If such a condition exists, caution is advised.
- Scour assessment methods and data must match the scale of the scour processes. Mapping scale and unit delineation are just a few examples of data types that can obscure scour processes.

## METHODS

### The Erodibility Index Method (EIM): The Threshold Version

The ability of flowing, turbulent water to erode earth materials can be quantified by comparing the portion of the fluid's energy applied to the boundary of the channel, to the ability of the earth material that composes the channel boundary to resist erosion using the Erodibility Index Method. The Erodibility Index Method (EIM) is a geomechanical index that uses the data collected during a standard, subsurface, geotechnical investigation to assess the ability of any earth material to resist erosion by flowing water.

An application of the EIM is conducted by placing the conditions of a project site within a phase diagram defined by the Erodibility Index (EI) on the x-axis and the Applied Stream Power of the site conditions on the y-axis and comparing the site results to a threshold of scour (Annandale, 1995 & 2006). WSDOT presents this phase diagram without data in Figure 1. The diagonal line that divides the plot is the threshold of scour. Project conditions that plot above the line are likely to result in scour, while those that plot below the line are likely to resist scour. The black, double-ended arrows relate only to the x-axis and represent the typical EI values for earth materials, or the relative effort needed to excavate the material.

Similar to the familiar Shields' diagram, which depicts the threshold of incipient motion (Shields, 1936), the dashed line in Figure 1 also identifies a threshold of motion or scour, and not a rate of transport or scour. This is an important distinction from scour methods that integrate with respect to time, as this version of the EIM can answer the question 'can scour occur,' but not the often more important question 'how much scour is likely to occur?' The EIM can predict scour magnitudes, but only if the change in hydraulic conditions on the bed as scour progresses are known. Interestingly, when plotted on the dimensional axes of grain size and shear stress, Shields' threshold of motion is approximately congruent with Annandale's definition of the Erodibility Index threshold of scour for non-cohesive particles of sand size and larger.

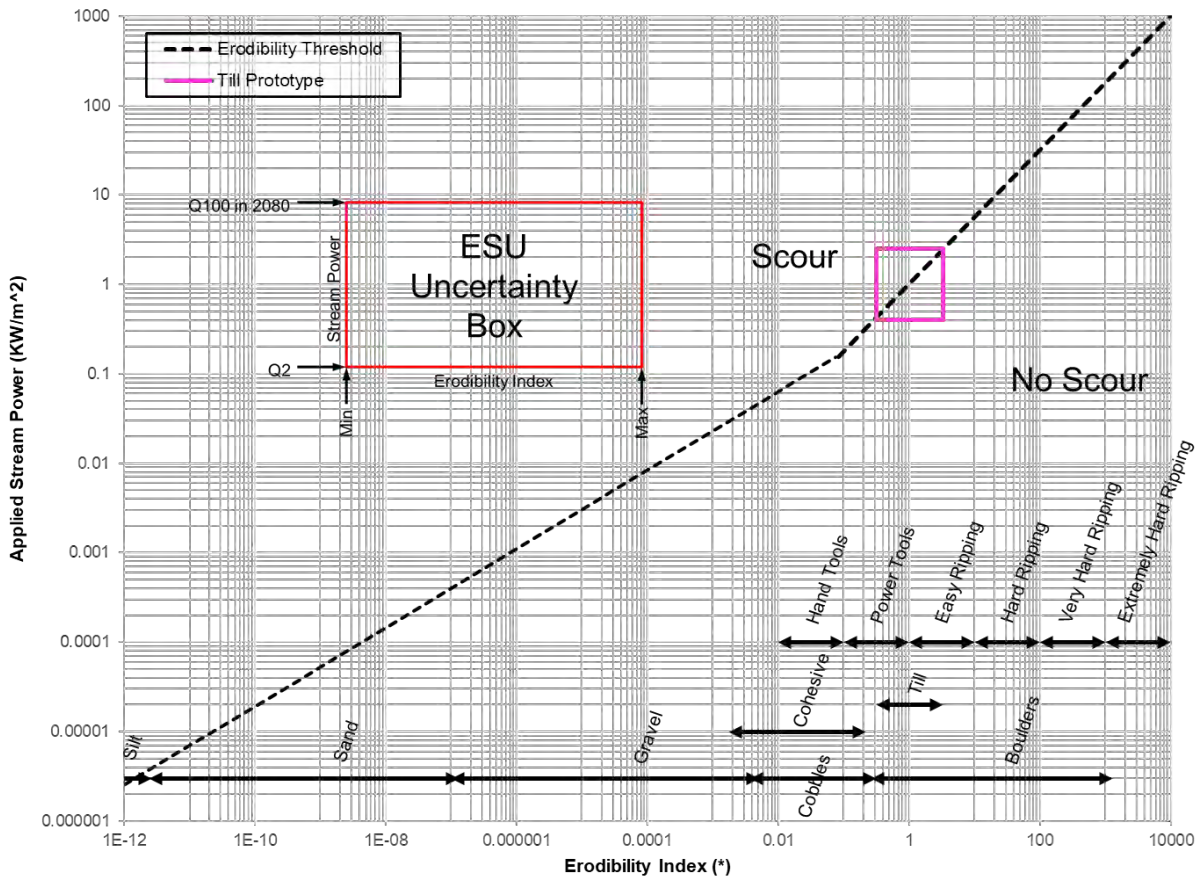


**Figure 1 –The Erodibility Index Method Scour Threshold Plot**

### *Depicting Uncertainty*

Unfortunately, the uncertainty in an EIM assessment can be large and come from multiple, indistinguishable sources. These sources can include methodological uncertainty, statistical uncertainty, measurement uncertainty, and the spatial and temporal integration of data, or absence thereof, based on hydraulic/geologic/geotechnical interpretations. And these are just the known unknowns. Fortunately, the known, cumulative uncertainty can be depicted within the EIM. In this assessment we have applied a minimum and maximum value for each input parameter that goes into the EI. On the EI axis (x-axis in Figure 1), the depicted min-max values

come from data sets with multiple samples from a single ESU, or from qualitative index category ranges as defined in the tables of the EIM for each ESU (Annandale, 2006; NRCS, 2001).

The ability to quantify uncertainty within a scour assessment is a highlight of the EIM. In the discussion section below, WSDOT discusses the multiple sources of uncertainty and variability in assessing scour. In this assessment, WSDOT calculates a range of values for both axes of the EIM plot. The EI axis range is defined by the product of the minimum or the product maximum values for each input variable for each Engineering Stratigraphic Unit (ESU) assessed. The y-axis of the EIM is defined by the hydraulic conditions and the design criteria of any project. In this assessment, WSDOT applied the 2-year return interval flood discharge and the 100-year in 2080 predicted flood discharge. In this assessment, WSDOT has calculated a minimum and maximum EI value for 20 ESUs, and a range of stream power values, for each of our 9 case study sites. For each ESU and project, these ranges are represented by a red box, labeled the 'ESU Uncertainty Box' in Figure 1. The results of this assessment are presented in the Case Studies section, and the topic of uncertainty is continued in the Discussion section.

## Hydraulics

The ability of flowing water to scour of earth materials is controlled by turbulence generated near, or within, the sub-viscous boundary layer, which in rivers is located on, or near the bed of the channel. Turbulence can be assessed by measuring fluctuations in velocity and pressure near the bed (McLean and Nikora, 2006). The scour capabilities of turbulent water can be estimated by taking the standard deviation of a high-frequency time-series of pressure or velocity data. Using pressure data, the results of such a calculation represent the magnitude of the average fluctuation away from the mean, which Annandale (2006) correlates to all scour processes.

Although the above approach supplies a conceptual basis for these calculations, in practice this approach is rarely applied except in physical modeling laboratories where instrumentation and experimental conditions can be controlled. In practice, because collecting real world data during peak discharge conditions is dangerous, expensive, and holds substantial uncertainty, WSDOT is assessing the use of Annandale's (2006) empirical approach using Applied Stream Power from Boundary Shear Stress.

### *Stream Power*

Total Stream Power ( $\Omega$ ) is the available power supply per unit length of stream and can be expressed as:

$$\Omega = \rho_w g Q S$$

In which,  $\rho_w$  is the density of water in units of  $\text{kg/m}^3$ ,  $g$  is acceleration due to gravity at earth's surface ( $9.807 \text{ m/s}^2$ ),  $Q$  is the specific discharge of concern in cubic meters per second ( $\text{m}^3/\text{s}$ ), and  $S$  is the dimensionless hydraulic gradient (\*) (Bagnold, 1966).

Total Stream Power is often incorrectly assumed to completely dissipate on an area of the bed. In plunge pools downstream of dams this area can be the energy dissipation pad, or the footprint of the impact jet. For rivers, Bagnold (1966) rephrased the Total Stream Power equation to Available Stream Power ( $\omega$ ) in a column of fluid over a unit area of bed as:

$$\omega = \frac{\rho_w g Q S}{w} = \rho_w g \bar{d} S \bar{u} = \tau_b \bar{u}$$

Where  $\bar{d}$  is the average depth across the main channel in units of meters (m), S is the reach averaged slope of the water or bed surface along the channel thalweg,  $\tau_b$  is Boundary Shear Stress is in units of Pascals, and  $\bar{u}$  is average velocity of the water (m/s). This calculation results in Available Stream Power ( $\omega$ ) expressed in units of W/m<sup>2</sup>. Available Stream Power can be applied in the EIM for preliminary calculations and planning purposes, but doing so biases the Stream Power values upwards.

To decrease the uncertainty associated with the inaccurate assumption that all energy within the fluid is applied to the boundary, as described above, Annandale developed an equation to calculate Applied Stream Power ( $P_a$ ) and calibrated the EIM to it. Applied Stream Power is the part of the Available Stream Power that is applied to the bed and can be calculated directly from Boundary Shear Stress using Annandale's (2006) equation:

$$P_a = 1000 \times 7.853 \left( \frac{(\tau_b^{3/2})}{\sqrt{\rho_w}} \right)$$

Where  $\tau_b$  is Boundary Shear Stress is in units of Pascals. The one thousand coefficient converts the resulting units of Applied Stream Power to Kilowatts per square meter (KW/m<sup>2</sup>), the typical units of the y-axis in an EIM plot.

### *Shear Stress*

In our case studies, WSDOT has sourced Boundary Shear Stress values from two methods; the depth-slope product method as described below and the hydraulic modeling results from the Preliminary and Final Hydraulic Design (PHD) reports associated with the Fish Passage projects. In PHD reports, these shear stress values are provided in pounds per square foot (psf) and need to be converted to Pascals before use in the above equation.

The depth-slope product method of calculating Boundary Shear Stress estimates the vector component of the weight of the water in the direction of flow and can be expressed as:

$$\tau_b = \rho_w g \bar{d} S$$

Where  $\rho_w$  is the density of water in units of kg/m<sup>3</sup>, g is acceleration due to gravity at earth's surface (9.807 m/s<sup>2</sup>),  $\bar{d}$  is the average depth across the main channel in units of meters (m), and S is the reach averaged slope of the water or bed surface along the channel thalweg.

The above phrasing of the Boundary Shear Stress equation is only valid in channels with a width-to-depth ratio less than 20 and gradients less than 2%. Steeper, narrower channels should use the following form of the equation instead:

$$\tau_b = \rho_w g R \sin \alpha$$

Where R is the hydraulic radius and equal to the cross-sectional area of the flow (in square meters) divided by the wetted perimeter of channel (in meters) and  $\alpha$  is the angle between the channel bed and horizontal in degrees. The resulting units of a depth-slope product Boundary Shear Stress calculation are Pascals (Pa or N/m<sup>2</sup>).

The other source of Boundary Shear Stress values applied in this investigation are from PHD, or FHD, reports completed for each Fish Passage project. Within the F/PHD reports, WSDOT requires that the main channel, cross-sectionally average Boundary Shear Stress values for multiple cross sections, distributed over several hundred feet both up and downstream of, and at the crossing, be reported in a table typically titled ‘Average Main Channel Hydraulic Results for Proposed Conditions.’ In this assessment, WSDOT has applied the maximum shear stress value from all cross sections for the 2-year and Projected 2080 100-year conditions from these tables. WSDOT reports shear stress values in pounds per square foot (lb/ft<sup>2</sup>) and must be converted into Pascals before being applied in the equation above.

Above, WSDOT presents two methods for calculating shear stress: the depth-slope product (or the hydraulics radius-hydraulic gradient product) and the hydraulic modeling results from the PHD reports. It is important to note that the methods and input parameters applied in both of these methods can bias the results. The depth-slope product is based on a cross-sectional-averaged depth and a reach-averaged slope. The multiple averages in this calculation cause the results to potentially be skewed towards smaller values because of the regression to the mean. Conversely, WSDOT applies the maximum value from a population of main-channel-only cross-sectionally-averaged shear stress values from multiple cross sections up- and downstream of the crossing in the proposed condition from the hydraulic modeling results in the PHD reports. Although the maximum value from this population can be at the crossing in the proposed condition, that pattern is not consistent at all sites and has the potential to skew the result towards larger values.

### **The Erodibility Index (EI)**

The product of the four primary parameters (Mass Strength, Block Size, Intergranular Friction, and Ground Structure Numbers) ( $M_s$ ,  $K_b$ ,  $K_d$ ,  $J_s$ ) results in an EI value and can be expressed as:

$$EI = M_s * K_b * K_d * J_s$$

Each of these four primary parameters represents a fundamental component of an earth material’s ability to resist erosion and each can be correlated to several empirical correlations, proxy variables, and qualitative indices. All of the relations within the erodibility index are based on empirical correlations. The proper equation, input value and source, level of uncertainty, and

assumptions change depending not just on the types of materials and scour processes, but also on the project goals at all stages and a project's appetite for/tolerance of uncertainty and risk.

For each of the three material types, rock, non-cohesive, and cohesive, the EI can apply several methods, enabling it to assess all naturally occurring earth material. The EIM is an adaptable platform. It can be applied at a range of spatial scales, and for a range of project stages from preliminary assessments at the scoping level of a project to detailed comparisons of project-scale geologic/geotechnical data and three-dimensional hydraulic modeling of multiple stages scour progression. The index table for each parameter are presented in several documents, but are collected in the easiest usable format in NRCS (2001).

### *Mass Strength Number (Ms)*

The Mass Strength (Ms) number represents the influence of interparticle bonding on the ability of an earth material to resist erosion. Ms broadly captures the shear strength of an earth material related to cohesive forces. These cohesive forces can take multiple forms and originate from multiple processes, including covalent or ionic electromagnetic interparticle bonding (such as iron oxide cementation and van de Waals forces), cohesion due to moisture (depending on conditions and assumptions), and the influence of processes such as over consolidation under glacial loading.

Shear Strength is the primary input parameter for Ms and is proportional to the units of force per unit area, typically expressed in the EIM in MegaPascals (MPa). Ms can be assessed using a range of methods depending on the material properties. In the case of rock scour the UCS is multiplied by the dimensionless coefficient of relative density (Cr). Cr is defined as the density of the project rock ( $\rho_{\text{sample}}$ ) relative to a reference density ( $\rho_{\text{reference}}$ ), which Annandale (2006) defines as 2,700 kg/m<sup>3</sup>.

$$M_s = C_r * UCS \quad \text{when } UCS > 10 \text{ MPa, or}$$

$$M_s = C_r * 0.78 * USC^{1.05} \quad \text{when } UCS \leq 10 \text{ MPa}$$

$$C_r = \frac{\rho_{\text{sample}}}{\rho_{\text{reference}}}$$

Annadale (2006) says that non-cohesive particles at the surface should have a default Ms value of 0.02, but for subsurface cohesive and non-cohesive materials, Ms can empirically correlated to the n-value from a standard penetration test (SPT). Figure 2 present the relation between n-values and Ms, which can also be found in Tables 52-2 and 52-3 (NRCS 2001).

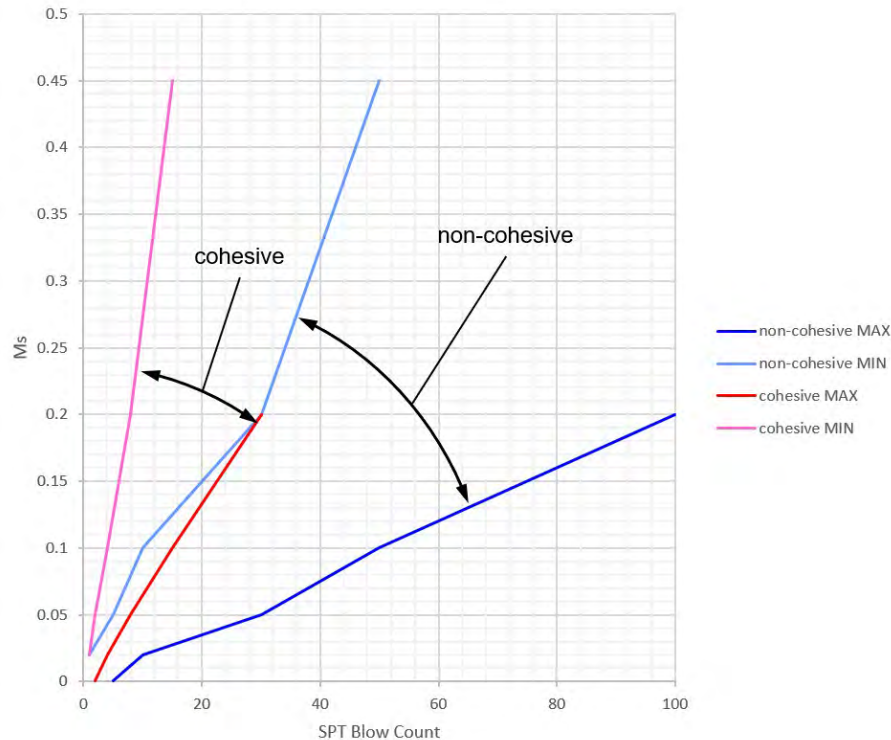


**Figure 2 – n-values vs. Ms number for cohesive and non-cohesive materials.**

In addition to being correlated with UCS and n-values, the Ms parameter has also been correlated to Tensile Strength, Vane Shear Strength (VSS), Undrained Shear Strength (UDSS), Drained Shear Strength (DSS), and the In-situ Deformation Modulus (IDM)(NRCS, 2001; Annandale, 2006).

#### *Block Size Number (Kb)*

The Block Size Number (Kb) represents the weight of a characteristic particle or block size on the ability of an earth material to resist erosion. Consequently, the equations that define Kb relates to the size of the particle of block. In rock, Kb can be calculated using the following equation:

$$K_b = \frac{RQD}{J_n}$$

Where RQD is Rock Quality Designation which signifies the degree of jointing or fracturing in a rock mass measured as a percentage. The percentage is calculated as the ratio between the sum of the length of sound, individual pieces of rock core greater than 100mm relative to the total length of the core run. Jn is the Joint Set Number as defined in Kristen (1982).

Annandale (2006) defines Kb as equal to 1 for cohesive material, but for non-cohesive material Kb is defined as:

$$K_b = 1000d_{50}^3$$

$d_{50}$  is the diameter of the median particle of the armored layer of the bed material in meters (m). The units of  $K_b$  for non-cohesive material are volume, and the coefficient of one thousand is unitless.

*Discontinuity Bond Shear Strength or Intergranular Friction Number (Kd)*

The Discontinuity Bond Shear Strength Number, also known as the Intergranular Friction Number ( $K_d$ ), captures the role of interparticle and inter-block friction on the ability of an earth material to resist erosion.

In rock,  $K_d$  is correlated to the ratio of Joint Roughness ( $J_r$ ) to Joint Alteration ( $J_a$ ). This can be expressed as:

$$K_d = \frac{J_r}{J_a}$$

$J_r$  is defined by an index table that relates the joint aperture and roughness pattern to a Joint Roughness Number (Kirsten, 1982) (Table 52-8 NRCS 2001).  $J_r$  is unitless and ranges from 0.5 to 4.0. Similarly,  $J_a$  is defined by an index table (Table 52-9 NRCS 2001) and correlated to the aperture of the joint and the geomechanical properties of the material within the joint.  $J_a$  ranges from a high value of 0.75 and a low value of 18. The ratio of joint roughness to joint alteration empirically captures the residual inter-block friction that contributes to the ability of a rock block to resist mobilization.

Similarly,  $K_d$  in cohesive and non-cohesive material is defined as the tangent of intergranular friction, also called the angle of internal friction, and can be expressed as:

$$K_d = \tan(\phi)$$

It is important to note that in materials where the angle of peak friction is greater than the angle of residual friction, it is the residual friction angle that should be applied in the calculation of  $K_d$ . By relying on residual friction,  $K_d$  empirically incorporates only the contribution of friction between particles on an earth material's ability to resist erosion, and purposefully excludes the interparticle bonds and interlocking particles that can result in a larger peak friction value.  $K_d$  is conceptually similar to the residual strength of a soil.

In non-cohesive material, when laboratory data is not available,  $\phi$  can be estimated from a variety of index methods that modify a base value relative to particle angularity, median particle diameter, sorting (or grading) of the sample, and the relative density of the sample material.

In cohesive material,  $\phi$  is correlated to the liquid limit (LL) and the clay percentage of a sample via the following equations:

$$\text{For } \leq 20\% \text{ clay: } \phi'_r = 169.58 (LL)^{-0.4925}$$

$$\text{For } 25 - 45\% \text{ clay: } \phi'_r = 329.56 (LL)^{-0.7100}$$

$$\text{For } \geq 50\% \text{ clay: } \phi'_r = 234.73 (LL)^{-0.6655}$$

These relations were developed by Stark and Eid (1994) and are also presented as equations 52-7, 52-8, and 52-9 in NRCS (2001). It is important to note that although the LL is generally correlated with cohesion, for calculations of Kd, the LL is inversely correlated to the phi value and intergranular friction. The forces of cohesion are not captured in the Kd parameter as the negative exponents in the equations above highlight. Cohesive properties should be captured in the Ms number. This topic is addressed further in the discussion section below.

A Kd value calculated from rock represents a ratio of two index values, consequently the units are dimensionless and, for rock, the values range from 0.03 to 5.3. Similarly, Kd calculated from a phi value is also a dimensionless ratio. The phi values of most sediment ranges from 10° to 45°, resulting in Kd for sediment values that range from 0.17 to 1.0.

### *Relative Ground Structure Number (Js)*

The Relative Ground Structure number (Js) represents the interaction between the orientation of rock joints and the flow vectors in plunging flow or jets. In rock, Js is an index value that relates the effective dip of the least favorable joint set and block dimensions (Table 4.25 HEC18 (2012), Table 52-12 NRCS 2001). The effective dip is the angle between apparent dip of the least favorable discontinuity in a vertical plane, parallel to flow, and the orientation of the dominant flow vector. In rock, the applied values of Js range between 0.37 and 1.50. When assessing scour in cohesive and non-cohesive sediment, Annandale (2006) recommends setting Js equal to 1 in most fluvial conditions with subcritical flow. Js is a dimensionless parameter.

### **Characteristic Materials**

The traditional approaches to scour calculations categorize earth materials into 3 general types; cohesive, non-cohesive, and rock. In this assessment we propose the application of a fourth category representing IGMs, such as glacial till. WSDOT presents the characteristic EI values for each earth material in Table 1. The values for cohesive and non-cohesive material originate from typical results and are applied as described in Annandale (2006), but the values applied to Glacial Till are applied based on the professional judgement of the authors and their familiarity with IGMs. Unlike non-cohesive material, where the values are set to a default at the ground surface (where scour takes place), and unlike cohesive material, where mass strength (Ms) is set to the full range of values for cohesive materials listed in Table 52-3 (NRCS 2001), the Ms values for Till are sourced from Annandale (2006)(and Table 4.22 HEC 18 (2012)). Specifically, WSDOT applies the Ms values from the low end of Very Soft Rock to the low end of Soft Rock, ranging from 0.87 to 3.95. This range makes Ms (and cohesion) the dominant force in determining the ability of a Till to resist erosion. WSDOT uses a wide range of phi values to capture the variability of the Till, from 20 to 40 degrees. This results in Kd values ranging from

0.36 to 0.84. WSDOT assigns Till a  $K_b$  of 1, in remove the influence of particle size, and a  $J_s$  value of 1, which is the default for fluvial systems.

**Table 1 – EI values for characteristic earth materials.**

Unit	Ms: Mass Strength		Kb: Block Size				Kd: Interparticle Friction				Js: Discontinuity		EI	
			D90	D50	Kb		phi		Kd		Max	Min		
	Max	Min	mm	mm	Max	Min	Max	Min	Max	Min	Max	Min	Max	Min
Boulders	0.02	0.02	4,000	250	64,000	15.625	45	40	1	0.84	1	1	1,280	0.26
Cobbles	0.02	0.02	250	64	15.625	0.26	45	35	1	0.70	1	1	0.31	3.7E-03
Gravel	0.02	0.02	64	2	0.26	8.0E-06	45	32	1	0.62	1	1	5.2E-03	1E-07
Sand	0.02	0.02	2	0.063	8.0E-06	2.5E-10	40	26	0.84	0.49	1	1	1.3E-07	2.4E-12
Silt	0.02	0.02	0.063	0.004	2.5E-10	6.4E-14	27.6	15	0.52	0.27	1	1	2.6E-12	3.4E-16
Cohesion	0.41	0.02	na	na	1	1	28	5	0.53	0.09	1	1	0.22	1.7E-03
Glacial Till	3.95	0.87	na	na	1	1	40	20	0.84	0.36	1	1	3.31	0.32

## CASE STUDIES

The following sub-sections provide a brief summary of the site conditions and the subsurface data for the 9 sites included in this assessment. These sites are in various stages of design and construction. Consequently, WSDOT has not made any design decisions based on the results of this work, nor has sufficient time elapsed for measurable scour to occur at the already constructed projects. The hydraulic and geotechnical data that are applied in the EIM for each of the pertinent ESUs at each of the nine sites, for a total of twenty individual ESUs, are presented in Table 3. The units within these ESUs include cohesive, non-cohesive, rock, and IGMs.

### SR 92 @ Lundeen Creek

Lundeen Creek originates near Lake Cassidy and flows about 1.7 miles southeast to the project site where it will be conveyed under SR 92 via the project culvert. The prominent topographic features and surficial deposits in the project vicinity represent complex and fluctuating environments that include glacial advance, occupation, retreat, post-glacial fluvial and lake deposition, and modern development.

*The ESUs that may scour at this project can be described as:*

- ESU 2 – Alluvium deposits (Qyal): ESU 2 represents alluvial sediments deposited by Lundeen Creek. ESU 2 consists of very loose gravel with organics.
- ESU 3 – Vashon glacial Till (Qvt): ESU 3 represents sediments deposited at the base of the Vashon glacier as it was advancing. ESU 3 was subdivided as follows:
  - ESU 3a – Vashon glacial till (Qvt): ESU 3a primarily consists of very dense silty sand.
  - ESU 3b – Vashon glacial till – gravel (Qvt-gravel): ESU 3b consists of a very dense silty gravel bed within ESU 3a.

### *Results at Lundeen Creek*

The results of the EIM assessment at Lundeen Creek (Figure 3) show that the alluvial deposits (ESU 2) are likely to scour during the modeled discharges, but that both the Till units (ESU 3a and 3b) are likely to resist scour.

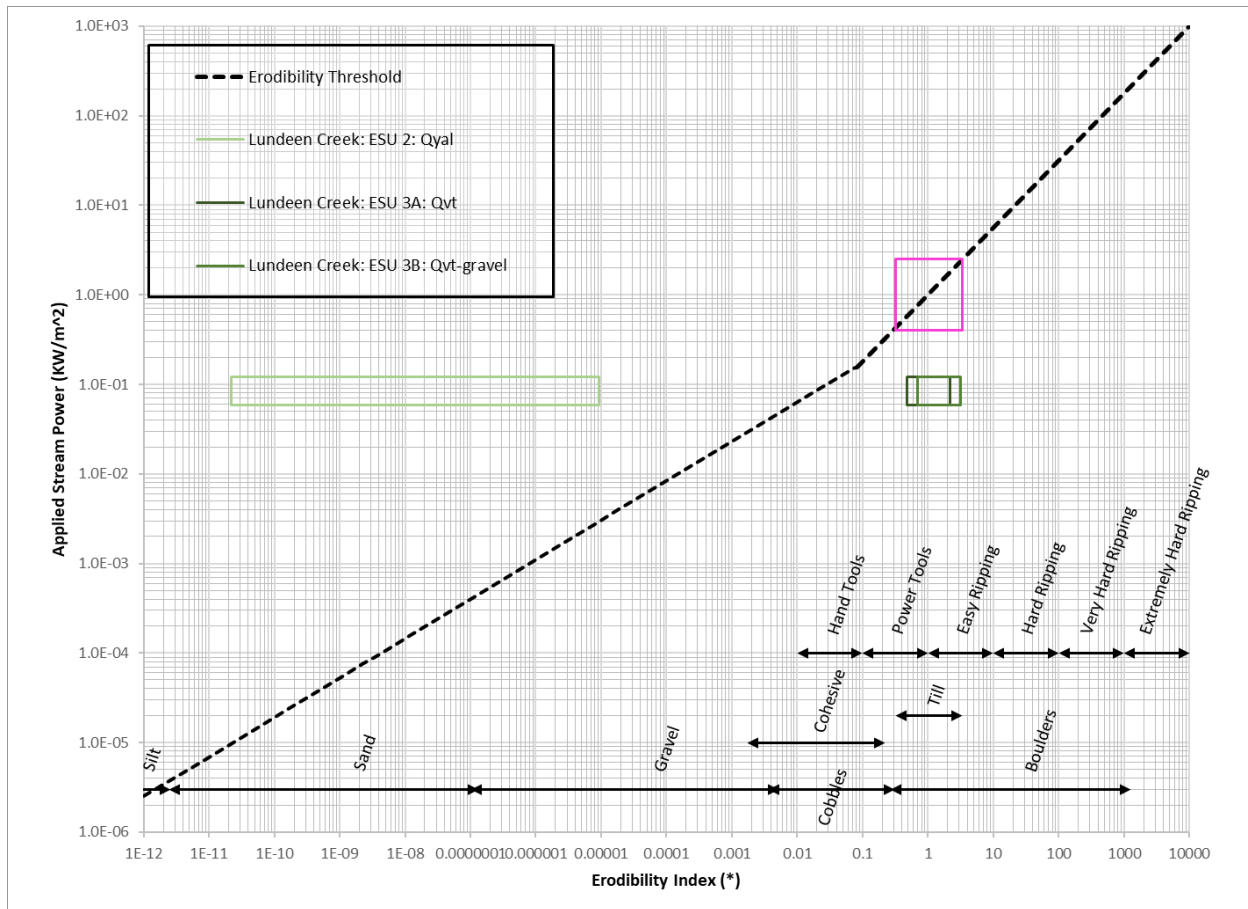


**Figure 3 – EIM results for Lundeen Creek crossing.**

### SR 528 @ Munson Creek

In the project vicinity, SR 528 is aligned east-west, climbing the western margin of the Getchell Plateau. The Getchell Plateau is a gently undulating, low-relief glacial upland dissected by multiple, northwest-aligned ravines including that of Munson Creek. Munson Creek drains a wetland system on the Getchell Plateau and flows northwestward where it is conveyed underneath SR 528 via the project culvert. Munson Creek confluences with Allen Creek ~2.3 miles downstream of the project site. Allen Creek flows into Ebey Slough 1.7 miles downstream of the confluence.

*The ESUs that may scour at this project can be described as:*

- ESU 2 – Vashon recessional ablation till (Qvat): ESU 2 represents glacial melt out till and fluvial sediments that were deposited as glacial ice was receding and wasting. ESU 2 primarily consists of medium dense to dense, silty sand with gravel. ESU 2 is a poorly indurated diamict and is not considered glacially overconsolidated. ESU 2 may contain cobbles and boulders, such as the approximately 5-foot-diameter boulder observed upstream of the culvert inlet.

- ESU 3 – Vashon glacial till (Qvt): ESU 3 represents sediments deposited at the base of the Vashon glacier as it was advancing. ESU 3 is primarily dense to very dense, silty sand with gravel. The less dense upper 5 feet of ESU 3 likely represents a weathered zone.
- ESU 4 – Vashon glaciolacustrine deposits (Qvgl): ESU 4 consists of primarily fine-grained sediments deposited in proglacial lakes as the Vashon glacier advanced. ESU 4 consists of very stiff to hard clay with sandy silt beds that are approximately 5 feet thick. ESU 4 is assumed to be overconsolidated and includes local slickensides.

### Results at Munson Creek

The results of the EIM assessment at Munson Creek (Figure 4) show that ESU 2, the ablation Till is unlikely to scour, as is glacial till of ESU 3, but glaciolacustrine sediment of ESU 4 is likely scour. Because the uncertainty range of ESU 2 and 3 is close to the threshold of scour, and because ESU 4 represents a more easily erodible unit at depth, further assessment is warranted (Figure 4).

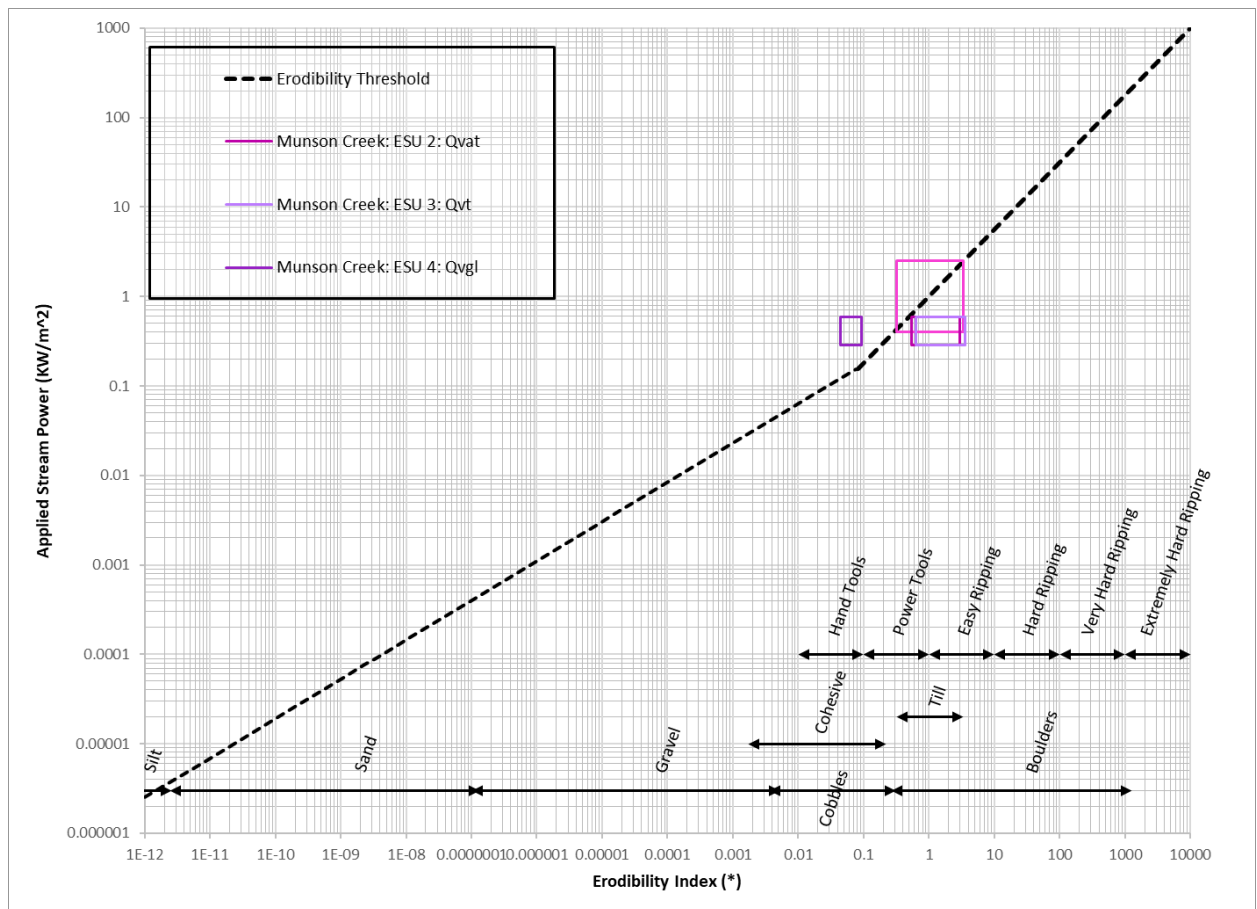


**Figure 4 – EIM results for Munson Creek crossing.**

## SR 119 @ UNT to Lake Cushman

The project site is situated on SR 119 in Lake Cushman Park. At this location, the unnamed tributary flows generally west through a wooded area, under SR 119, and into Lake Cushman, approximately 600 ft. west of the culvert outlet.

*The ESU that may scour at this project can be described as:*

- ESU 2 (Vashon-age ice contact deposits): ESU 2 represents Vashon-age ice contact deposits (Q<sub>gic</sub>). These are sediments deposited by glacial meltwater or ice or both. These deposits have been overconsolidated by glacial ice. Sediments deposited include cobble, gravel, sand, and minor silt and clay deposited as ablation till, flow till, or lodgment till. ESU 2 is generally characterized as loose sandy silt with gravel and very dense silty gravel with sand, well graded gravel with silt and sand, silty sand with gravel, and silty clayey sand with gravel.

### *Results at UNT to Lake Cushman*

The results of the EIM assessment at the UNT to Lake Cushman show that the uncertainty range of the unit lies within the characteristic range for till material and across the threshold of scour (Figure 6). The photograph in Figure 5 shows the vertical riverbank of the channel where scour process has cut into the Till unit. The scoured bank qualitatively confirms the result of the EIM.



**Figure 5 – Photograph of Till unit at UNT to Lake Cushman.**

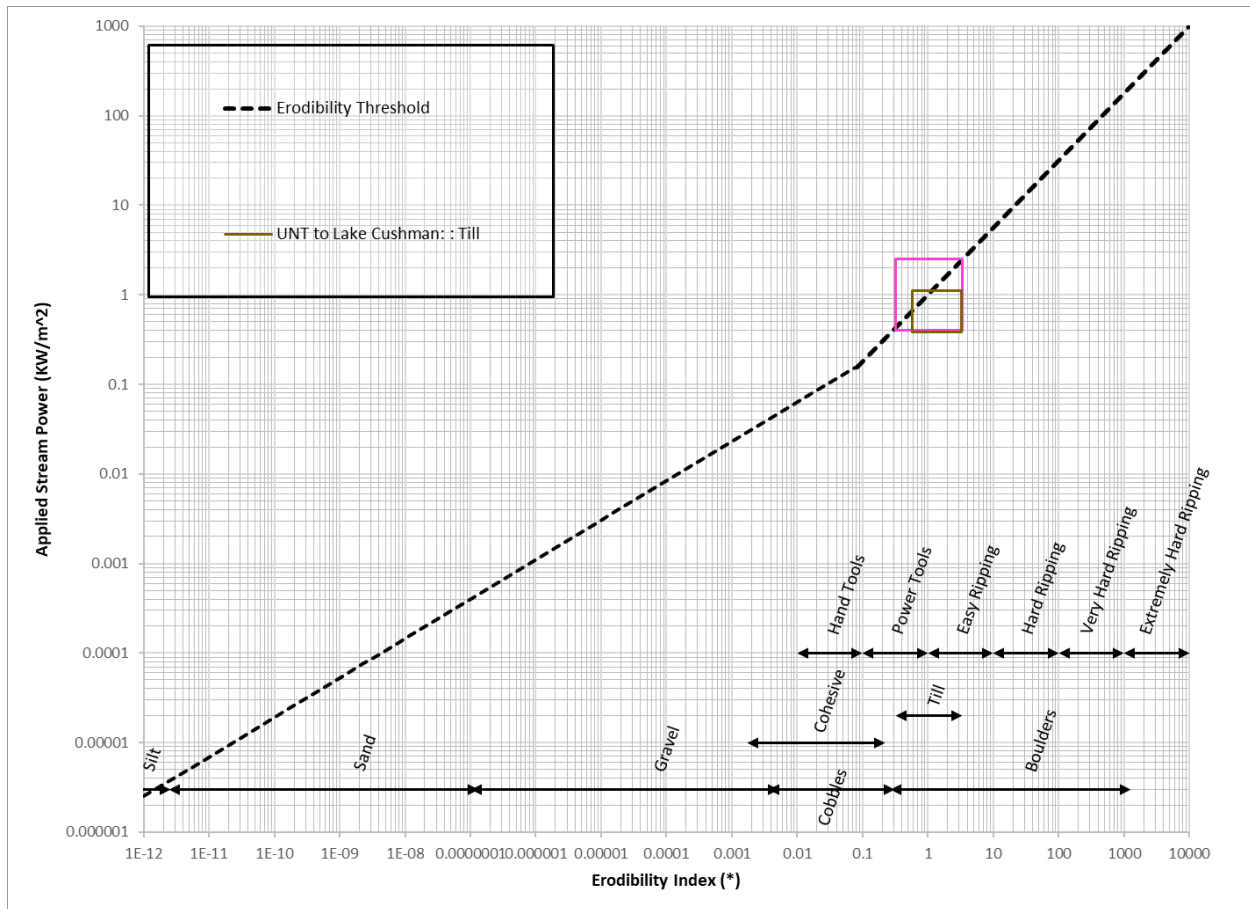


**Figure 6 – EIM results for UNT to Lake Cushman crossing.**

### **SR 542 @ UNT to the NF Nooksack River**

The Project site is located at MP 31.57 along SR 542, in the North Fork of the Nooksack River valley, approximately 1,350 ft. east of the intersection of SR 542 and Winter Creek Road in unincorporated Whatcom County. The unnamed tributary to North Fork Nooksack River flows under SR 542 from south to north.

*The ESUs that may scour at this project can be described as:*

- ESU 2 (Landslide deposits): ESU 2 represents landslide deposits. We divide ESU 2 into two subunits:
  - ESU 2a – characterized as medium dense to very dense, moist to wet, brown to gray, subangular to angular, poorly graded gravel with silt and sand, and silty sand with gravel.
  - ESU 2b – characterized as medium dense to very dense, brown to gray, moist, subangular to angular cobbles, boulders, and gravelly rubble in a matrix of silty sand with gravel, exhibiting diamict texture.

### Results at UNT to the Nooksack River

The results of the EIM assessment for the UNT to Lake Cushman (Figure 7) show that both units ESU 2a and 2b both have the potential to scour under the proposed conditions.

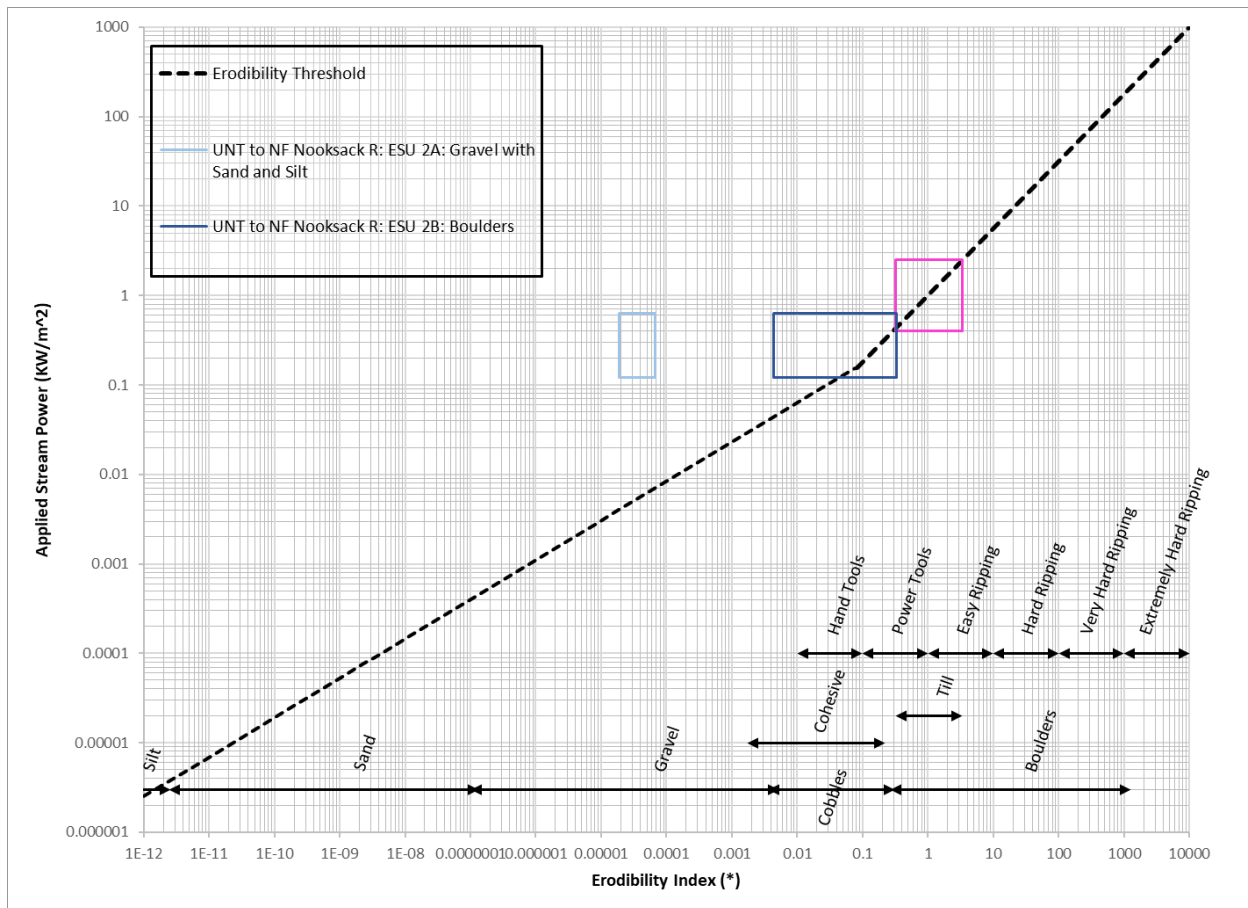


**Figure 7 – EIM results for the NF of the Nooksack River crossing.**

### SR 204 @ UNT to Ebey Slough

The project culvert is located on SR 204, about 3,000 ft. north of the SR 2 / SR 204 interchange and about 800 feet southwest of the intersection of Everett Road and SR 204. The culvert conveys the UNT to Ebey Slough under SR 204 from southeast to northwest through an about 4 ft. diameter round culvert. Near the project site, SR 204 is generally aligned southwest to northeast, traversing the western margin of the Getchell Plateau as it climbs to its junction with SR 9 near Lake Stevens.

The Getchell Plateau is a gently undulating, low-relief glacial upland dissected by multiple, northwest-aligned ravines, including that of UNT to Ebey Slough. UNT to Ebey Slough drains a wetland system on the Getchell Plateau and flows northwest to the Project site where it curves westward to descend to the Snohomish River estuary. UNT to Ebey Slough is ditched for about 1,800 ft. through the low-relief estuary before it empties into Ebey Slough about 2,500 ft. west of the Project site. Ebey Slough is part of a network of tidal channels that form the Snohomish River estuary.

The stream channel is inset into the relatively flat bottom of the ravine, with ravine side slopes inclined at about 1.5H:1V. The southern ravine crest is locally oversteepened with evidence of landslide activity including headscarps and debris lobes. About 15 ft. upstream of the inlet, woody debris is trapped behind a fallen log in the channel and about 2 ft. of loose sand is piled behind the blockage.

*The ESUs that may scour at this project can be described as:*

- ESU 3 – Alluvium deposits (Qyal) that represent fluvial sediments deposited by the UNT to Ebey Slough. ESU 3 consists of dense gravel with organics. Fines may have been washed out from gravel-rich samples during drilling.
- ESU 4 – pre-Vashon nonglacial deposits (Qpn): ESU 4 consists of interbedded clays, silts, sand, and peat that were deposited in the fluctuating lacustrine and fluvial environments of the nonglacial Olympia Interval that preceded the Vashon glacial stage. These deposits are grouped together into a unit that includes both nonglacial deposits and the earliest glacial deposits (likely Vashon advance glaciolacustrine deposits). We infer that the sediments encountered in project borings include only pre-Vashon nonglacial deposits given the organic content, peat beds, and presence of mica sand. ESU 4 is typically brown in color and include fine organics and varying amounts of peat.
  - ESU 4a – pre-Vashon nonglacial cohesive silt and clay (Qpnl - cohesive): ESU 4a consists of dense to very dense silt and very stiff to hard clay with varying amounts of fine mica sand and organics. The silts and clays are relatively low plasticity (PI < 16).
  - ESU 4b – pre-Vashon nonglacial non-cohesive lacustrine and fluvial deposits—sand (Qpnl/Qpnf – non-cohesive): ESU 4b consists of dense to very dense, non-plastic silt with fine mica sand and fine to medium silty sand. ESU 4b typically includes organics and fine peat lenses. The sand beds are typically about 5 to 10 feet thick.

#### *Results at UNT to Ebey Slough*

The results of the EIM at UNT to Ebey Slough show that all the assessed ESUs are likely to scour at the proposed conditions (Figure 8).

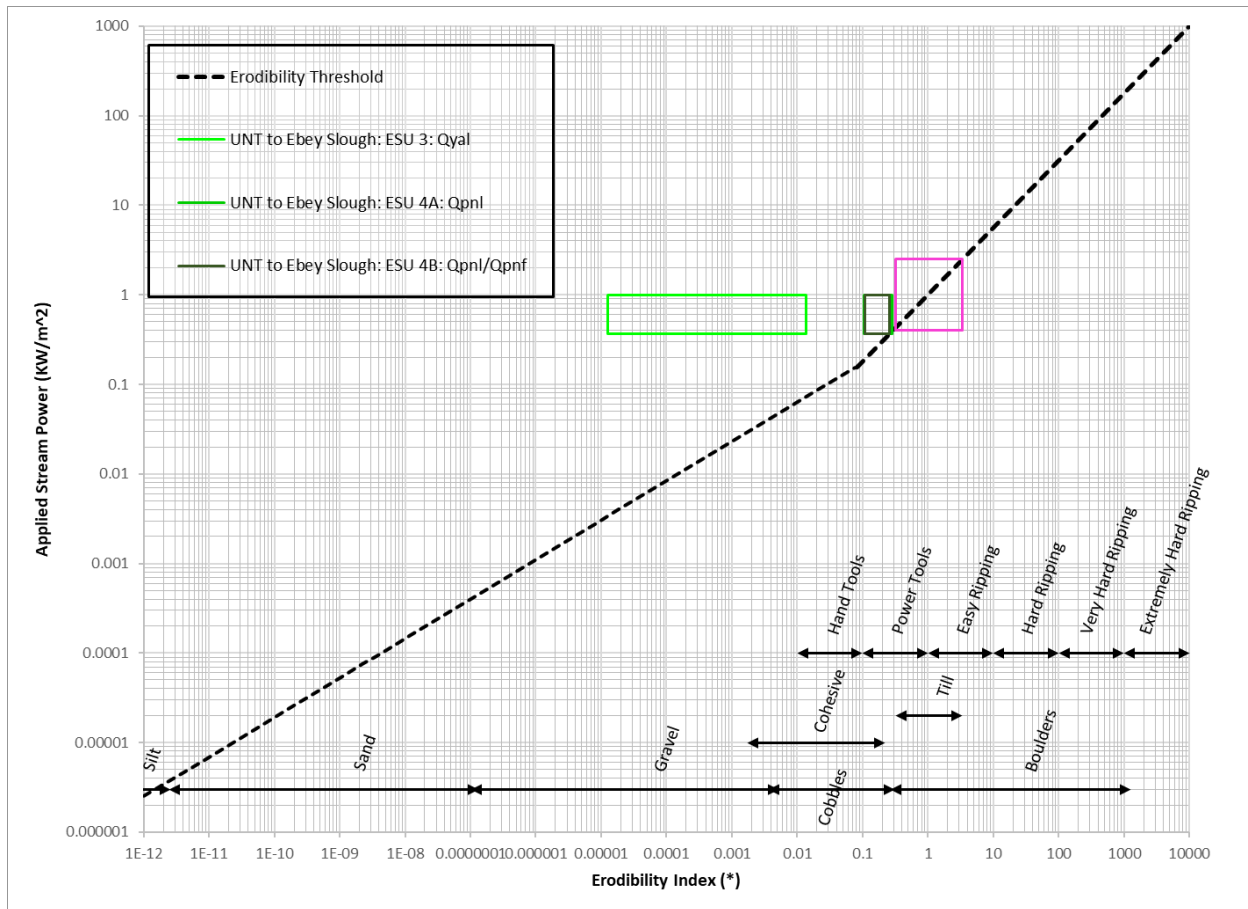


**Figure 8 – EIM results for UNT to Ebey Slough crossing.**

### SR 112 @ Butler Creek

The Butler Creek crossing on SR 112 is underlain by the Upper Member of the Twin River Formation, a.k.a. the Pysht Formation, a marine siltstone. Based on the geologic mapping, the site is situated on the north dipping side of a structural anticline, with the E-W trending hinge located nearby to the south. Bedding of the siltstone at the site is assumed to be dipping approximately downstream at  $\sim 25^\circ$ . This siltstone has been observed in the stream channel, under a thin layer of alluvial gravel.

*The ESUs that may scour at this project can be described as:*

- ESU 2 was originally a siltstone from the Pysht River Formation, but it has weathered completely to a material described as a Fat Clay (see photo in Figure 9).
- ESU 3 is a Siltstone from the Pysht Formation. The material is assumed to have closely spaced fractures and bedding planes. Based on site reconnaissance, the bedrock is intact at the ground surface, but moderately weak and highly weathered.

*Results at Butler Creek*

The results of the EIM assessment at Butler Creek show that ESU 2 is likely to scour, and that ESU 3 is likely to resist scour (Figure 10).



**Figure 9 –Siltstone rock core on left and profile on right.**

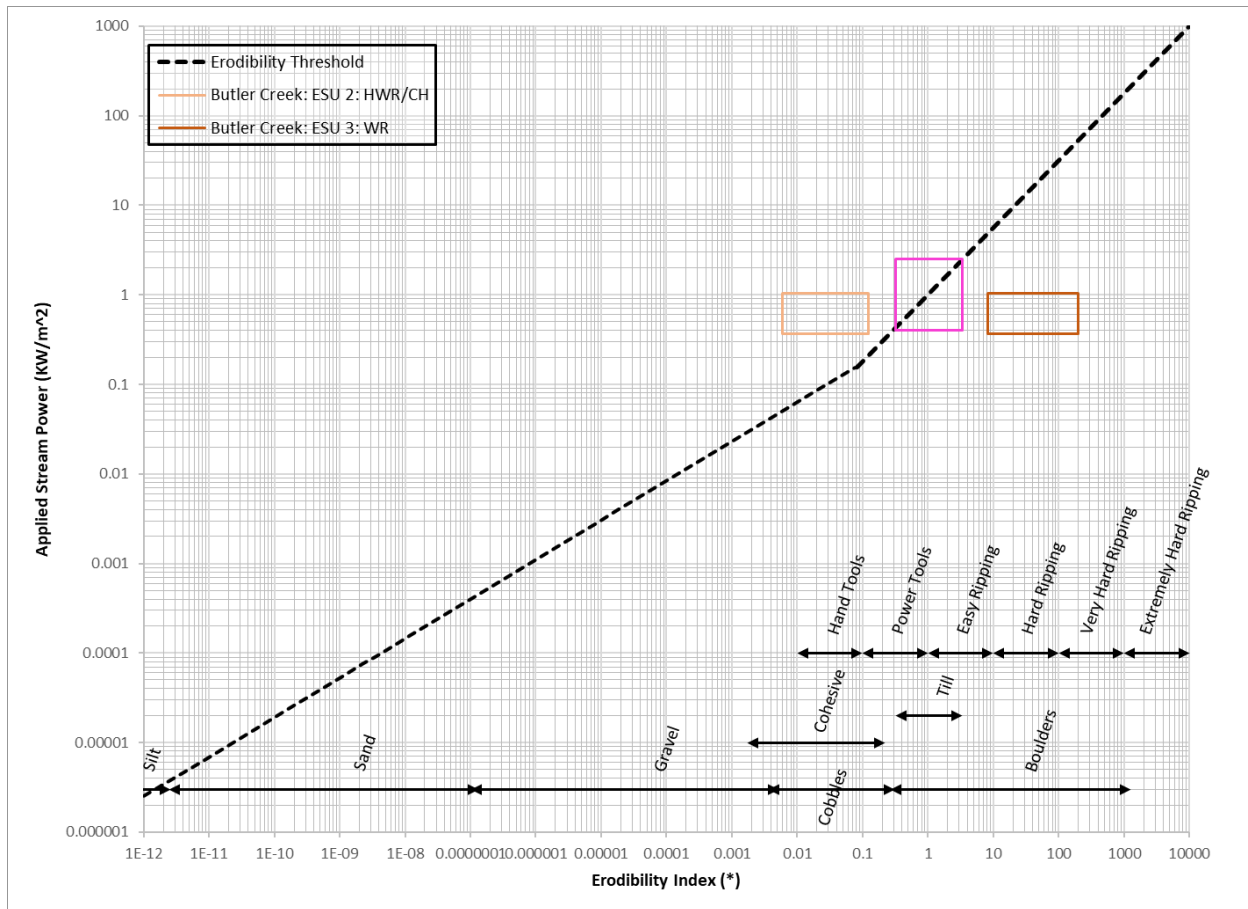


**Figure 10 – EIM results for Butler Creek crossing.**

### SR 112 @ UNT to Hoko River

Upstream of the culvert, the stream flows through a wetland area with no defined single channel. The wetland extends between 500 and 600 feet upstream. Above this point the stream flows through the ravine of an upland forested area, with potential wetland areas along some of the margins of the stream. At the outlet, the culvert is elevated above the stream where a scour hole has developed. The stream channel is well defined as it flows approximately 300 feet before branching through a wetland area.

The presence of the wetland upstream of the culvert reduces stream flow velocities and causes sediment deposition at the inlet. The reduced flow and lack of a single well-defined channel in the wetland area also limits the stream's ability to convey woody material. As a result of limited sediment transport from the upper watershed, the UNT downstream of the culvert is incising to balance out the stream energy with the sediment load.

*The ESUs that may scour at this project can be described as:*

- ESU 2 – Glacial Drift: Lacustrine Deposits
  - Very soft to dense, elastic silt, lean to fat clay, and clayey gravel. D50 0.10mm

- HEC 18 erodibility class Medium (III)
- ESU 3 – Siltstone Bedrock

### Results at UNT to Hoko River

The results of the EIM at UNT to Hoko River show that ESU 2, the glacial drift and lacustrine deposit, is likely to scour, but that ESU 3 the Siltstone bedrock is unlikely to scour (Figure 11).

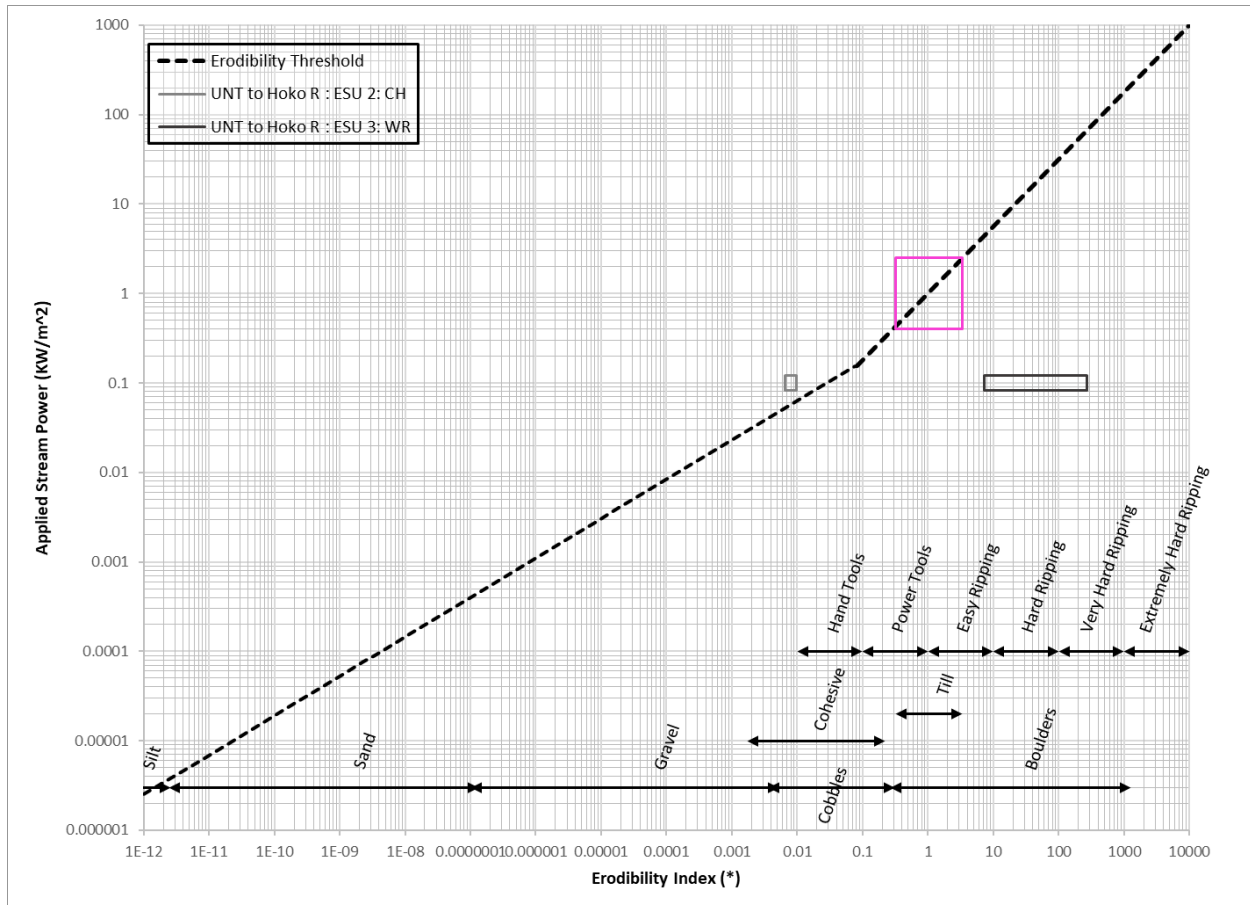


**Figure 11 – EIM results for UNT to Hoko River crossing.**

### SR 202 @ Evans Creek

Evans Creek crosses under SR 202 between Redmond and Fall City, Washington, in a locally forested and agrarian area with residential and light commercial infrastructure nearby. At the crossing, Evans Creek is a coarse bedded stream with steep, heavily vegetated banks and large woody material present throughout. A concrete fish ladder parallels the crossing. Scour at the crossing could interact with ESUs 2b and 3.

*The ESUs that may scour at this project can be described as:*

- ESU 2b: Alluvium and Unconsolidated Glacial Deposits. Consists primarily of loose to medium dense, silty sand and silty gravel.

- ESU 3: Glacially overconsolidated deposits: Consists of dense to very dense, silt, silty sand, and gravel.

### Results at Evans Creek

The results of the EIM at UNT to Evans Creek show that scour of the alluvial and glacial clastic material (ESU 2) is likely and that scour of the Till (ESU 3) is less likely, but still possible and that further investigation is called for (Figure 12).

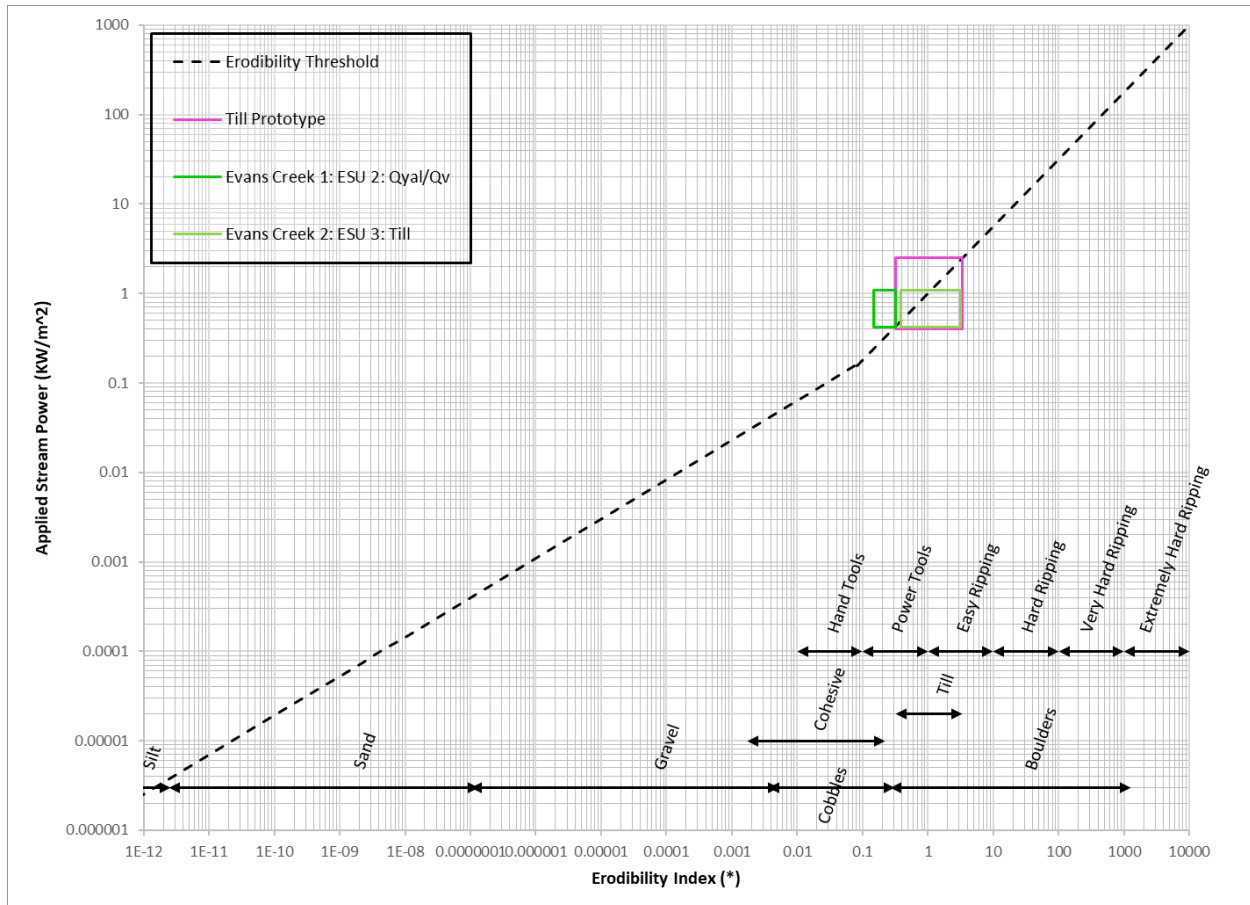


**Figure 12 – EIM results for Evans Creek crossing.**

### US 101 @ Grader Creek

The sinuosity of the stream decreases downstream of the crossing as the stream encounters bedrock. This straightening of the channel is a result of the increased resistance to erosion provided by the rock. The downstream bedrock limits the lateral migration of the stream. The departure from centerline for the outside bank is much smaller on the downstream side than on the upstream side.

*The ESUs that may scour at this project can be described as:*

- Marine Sedimentary Rock (OEm) is present at the Grader Creek site below the alluvium and alpine glacial outwash.

- Weathered Rock: In the upper part of the unit, it can be described as a weather, medium to very dense, well graded sedimentary unit with particles varying in size from cobbles to clays.
- Rocks: In the lower, the unweathered part of the unit consists of sandstone and siltstone (Figure 13).

*Results at Grader Creek*

The results of the EIM at Grader Creek show that the weather rock is likely to erode, but that the un-weathered rock is not likely to scour under the project conditions (Figure 14).



**Figure 13 –Siltstone rock core.**

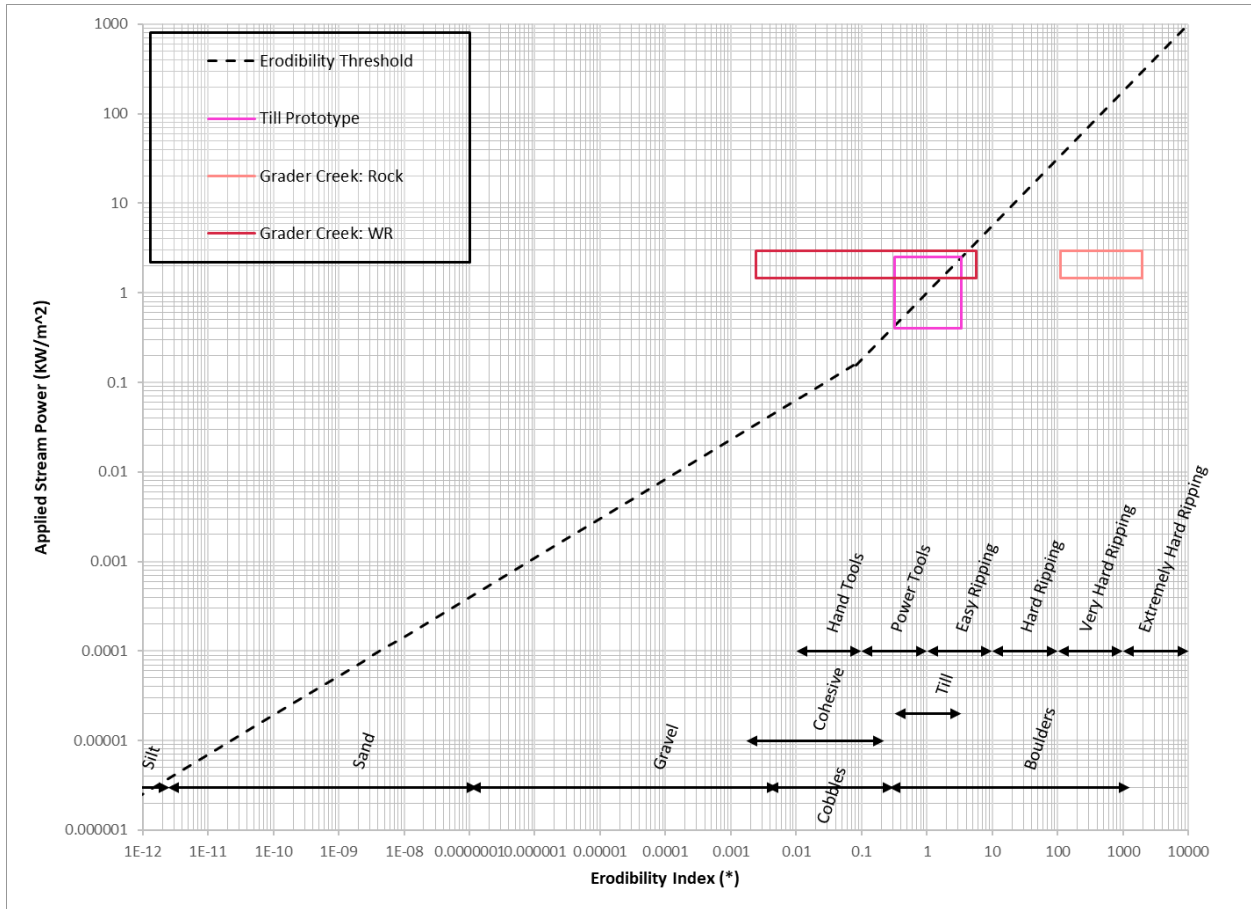


**Figure 14 – EIM results for Grader Creek crossing.**

**Summary of Case Studies**

In Table 2 and Figure 15, WSDOT presents the hydraulic and geotechnical input data needed for, and the results of the EIM assessment for the 20 ESUs in the nine case study sites presented above. In Figure 15, the 4 material types have been color coded to illustrate their range of susceptibility to erosion.



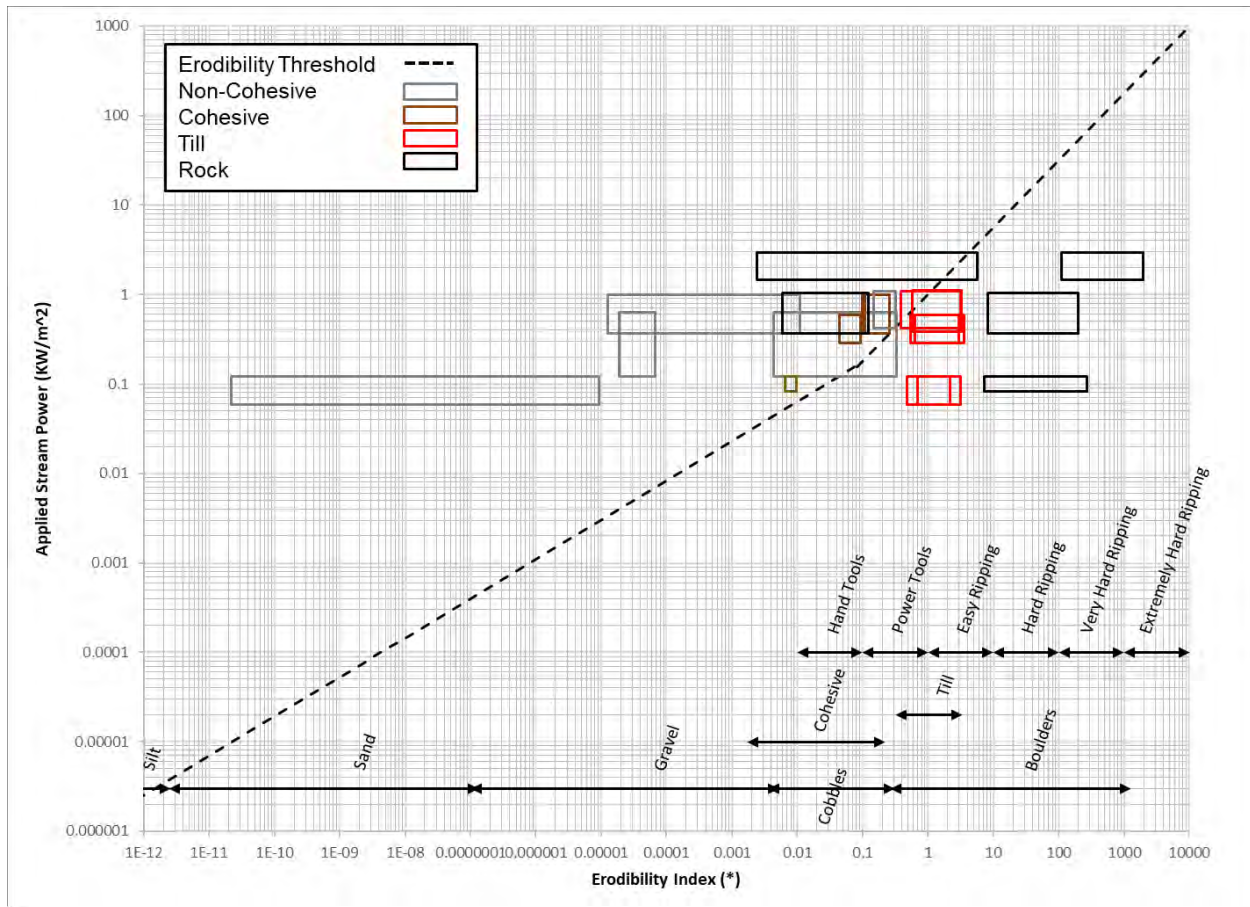


Figure 15 – EIM results for Grader Creek crossing.

## DISCUSSION OF METHODS

The EIM is a modern, scour focused version of an older index method that was originally developed as guidelines for tunnel reinforcement design for tunnels in rock by Barton (et al., 1974), called the Q-system. The method was further developed by Kirsten (1982, 1988), who turned it into the Excavatability Index (also known as the Rippability Index) which compares the ability of an earth material to resist excavation to the horsepower and manufactures model of the machine needed to excavate it (Rucker, 2006). In his (1995) paper and (2006) book, Annandale built on these concepts to develop the EIM, enabling the assessment of any earth material's ability to resist erosion. The EIM added the Js parameter and expanded the method beyond the limits of competent rock, into the realm of non-cohesive sediment, cohesive material, weak and/or weather rock, and weakly cemented sediments.

### Ms: Discussion

Using n-values as a proxy for the Ms number results in a data gap created between earth materials that refuse an SPT sampler and earth materials that are sufficiently coherent for a core

sample to be collected and a Shear Strength test to be conducted. Although the empirical and index correlations cover this gap, in practice obtaining an undisturbed sample from depth, which is required to conduct a Shear Strength test, is difficult, largely due to drilling and sampling methods. An SPT sampler often reaches refusal, for a variety of reasons, before competent bedrock is reached, and rock coring methods introduce water and are not designed to sample material weaker than competent bedrock. This gap in sampling method creates a gap in data for IGMs.

The NRCS (2001) tables that relate the Ms number to non-cohesive and cohesive soil (Tables 52-2 and 52-3 respectively) show a maximum number of blow counts (n-value) as 50 for non-cohesive and 30 for cohesive material. In application, using the n-value correlation tables limits the maximum Ms value for all non-rock earth materials is 0.6 MPa.

In this assessment WSDOT has applied the range of shear strength values for very soft and the low end of soft rock from two sources; HEC 18 (FHWA 2012) and WSDOT's familiarity with Till. WSDOT's range for Ms for Till ranges from 0.87 to 3.95. The low end of this range comes from HEC 18 (FHWA, 2012) shear strength values for weak rock with range from 100 to 200 psi (0.7 to 1.4 MPa). The high end of this range, where Ms = 3.95, comes from WSDOT's familiarity with Till using the qualitative index descriptions for 'soft rock' that can be scraped with a knife, but be only slightly dented with firm blows from a geologic hammer (Table 52-2 and 52-3 NRCS 2001).

Importantly, analyses for the shear strength of Till needs to be conducted on intact samples, meaning that both sample structure and sample moisture must be maintained between sampling and testing. The loss of material strength after drying out, is a well document property of Till (Pike et al., 2018, Keaton and Mishra, 2010). WSDOT believes that testing under in-situ conditions is proper as Till that is experiencing vertical scour by flowing water is likely to be wet.

## **Kb: Discussion**

Kb is comparable to the vertical axis of the GSI (Brown and Hoek, 1980; Schlotfeldt and Carter, 2018), but site-specific calibration is recommended. However, the conversion between the GSI and the scour of competent rock has been robustly accomplished by Pells (2016, 2017). The Pij system, introduced by Dershowitz & Herda (1992), is also represented on the vertical axis of the GSI. The Pij presents a comprehensive framework for accurately defining fracture intensity within a rock mass. The subscript *i* describes the dimensions of the collected data (boring, face, volume) and the subscript *j* describes the type of fracture data (count, length, area, volume). Schlotfeldt and Carter (2018) have developed an updated version, termed the vGSI, that enables the conversion of a P<sub>30</sub> value (fracture count to block volume expressed in units of 1/m<sup>3</sup>) to a value of P<sub>32</sub> (fracture area per block volume expressed in units of 1/m). Intuitively, because P<sub>30</sub> (VFC Rating and Volumetric Fracture Density) and P<sub>32</sub> (Volumetric Fracture Intensity) can be depicted on the x-axis of the GSI along with Kb, it stands to reason that P<sub>33</sub> (Volumetric Fracture Porosity) should also be able to be correlated alongside them. P<sub>33</sub> is measured as fracture volume over block volume making it dimensionless. Interestingly, sediment porosity can

be expressed in similar terms, although a correlation with erodibility is not established in the literature.

### **Kd: Discussion**

Discontinuity Bond Shear Strength or Intergranular Friction (Kd) It is important to note that although the LL is generally correlated with cohesion, for calculation of Kd, the LL is inversely correlated to the phi value and intergranular friction. The forces of cohesion are not captured in the Kd parameter as the negative exponents in the equations relating LL to phi highlight. Cohesive properties should be captured in the Ms number as discussed above.

### **EIM: Uncertainty and Variability**

Using ranges to capture the uncertainty, material, and process variability in space can result in the uncertainty boxes that straddle the threshold of scour. It is tempting to interpret this result as meaning that only the weaker portions of the material will scour during the higher magnitude discharge conditions, but because the various types of uncertainty cannot be distinguished from one another, any result in which a portion of the box is above the threshold of scour warrants additional assessment.

The uncertainty of the EIM scour threshold can be presented within upper and lower confidence intervals paralleling the threshold (Wibowo et al., 2005). As the uncertainty within each ESU is greater than the uncertainty bounded by these confidence limits, WSDOT has not included the uncertainty of the threshold in this assessment. Similarly, Pells (2016) has provided scour magnitude ranges for zones above the threshold of scour. These regions are oriented parallel to Annandale's (1995) threshold and relate broadly to the order of magnitude of anticipated scour. Unfortunately, Pells method (2016, 2017) termed the eGSI, is intended for scour assessments in scour resistant rock downstream of large dams for single, high-magnitude, discharge events like dam overtopping flows. As a result, the eGSI method specifically excludes the role of cohesion by eliminating the Ms parameter and coupling their method to the Kb (block size) and Kd (interparticle friction) parameters. Interestingly, Kb and Kd are the vertical and horizontal axis of the Geologic Strength Index (GSI) (Brown and Hoek, 1980; Schlotfeldt and Carter, 2018). Consequently, similar zones depicting approximate scour magnitude cannot be extended outside of conditions where block dynamics dominate scour, yet. However, although no values of the magnitude of scour can be estimate for cohesive materials on the EIM plot, it can be stated that distance above the Annandale (1995) threshold and scour magnitude are likely to be correlated.

In the GSI, Kd is represented on the horizontal axis, which is also scaled to J-cond, which is short for joint condition, a parameter that also represents inter-block friction based on the properties of the discontinuities (Hoek and Brown, 1980; Schlotfeldt and Carter, 2018). Consequently, in both rock and non-cohesive material, the Kb and Kd parameters are block or particle size and interparticle friction. Both the vGSI, the eGSI and the EIM correlate these parameters and then modify them with additional parameters for customized purposes. Pell (2017) has taken this correlation a step further for conditions with highly scour resistant bedrock, but because of the specific conditions being assessed, Ms is (appropriately) excluded from the method. Additionally, the discharge condition being assessed in Pells work (also appropriately)

represents the stream power of the peak discharge of a high magnitude event. The exclusion of cohesion and time dependent scour processes is logical when the scour resistance is controlled by block dynamics. However, when interparticle bonding is the dominant EIM parameter resisting erosion the influence of the block size parameter ( $K_b$ ) is removed by being set to 1, and the intergranular friction parameter varies from 0.2 to 1.0.

Interestingly, the work of Pells (2016; 2017), which also builds on the GSI and EIM but focuses only on bedrock scour downstream from dams, explicitly excludes the  $M_s$  parameter, as it plays almost no role in block stability when scour is controlled by block dynamics (Pells, 2016). Conversely, when considering scour by abrasion from particle impact, Sklar and Detrich (2001) indicate that tensile strength of the material is the most strongly correlated parameter to scour as it relates to long term channel profile change.

## **SUMMARY**

In this preliminary assessment of scour potential at 9 WSDOT Fish Passage Stream Crossings, we propose the addition of a new material type for Intermediate Geomaterials within the Erodibility Index Method framework. We propose an adaptation to the Erodibility Index Method to assess the ability of Intermediate Geomaterials to resist scour. Our approach involves using the material strength of soft rock to capture the potential variability of the  $M_s$  parameter. As we continue this work, we will assess the ability of a range of geotechnical and geophysical tests, as well as qualitative observations, and other data to refine our ability to assess IGMs. WSDOT intends to continue our assessment the applicability of the EIM to project planning, risk assessments, and infrastructure design. If we are able to consistently rely on IGMs, like Till, to resist erosion under certain conditions, there is the potential for substantial cost savings.

## ACRONYMS

UNT = Unnamed Tributary  
 EIM = Erodibility Index Method  
 EI = Erodibility Index  
 ESU = Engineering Stratigraphic Unit  
 GSI = Geologic Strength Index  
 HEC = Hydraulic Engineering Circular  
 IDM = In-situ Deformation Modulus  
 IGM = Intermediate Geomaterials  
 Js = Discontinuity Orientation number  
 Kb = Block Size number  
 Kd = Intergranular Friction number  
 Ms = Mass Strength  
 n = blow counts from an SPT test  
 PHD, FHD = Preliminary or Final Hydraulic Design Report  
 PSF = pounds per square foot  
 UCS = Unconfined/Uniaxial Compressive Strength  
 UDSS = Undrained Shear Strength  
 US = United States of America  
 WSDOT = Washington State Department of Transportation  
 VSS = Vane Shear Strength

## REFERENCE

Annandale, G. W. "Erodibility." *Journal of hydraulic research* 33, no. 4 (1995): 471-494.

Annandale, G. W. *Scour Technology: Mechanics and Engineering Practice*. New York: McGraw-Hill Education, (2006).

Bagnold, Ralph Alger. *An approach to the sediment transport problem from general physics*. US government printing office, 1966.

Barton, Nicholas, Reidar Lien, and J. J. R. M. Lunde. "Engineering classification of rock masses for the design of tunnel support." *Rock mechanics* 6 (1974): 189-236.

Brown, E. T., and E. Hoek. *Underground excavations in rock*. CRC Press, 1980.

Dershowitz, William S., and Hans H. Herda. "Interpretation of fracture spacing and intensity." In *The 33rd US Symposium on Rock Mechanics (USRMS)*. OnePetro, 1992.

FHWA 2023. *Highways in the River Environment: Roads, Rivers, and Floodplains-Second Edition*, Hydraulic Engineering Circular 16, Publication No. FHWA-NHI-23-004, Federal Highway Administration, Washington, DC.

FHWA 2009. *Bridge Scour and Stream Instability Countermeasures: Experience, Selection, and Design Guidance*-Third Edition, Vol. 1, Hydraulic Engineering Circular 23, Publication No. FHWA-NHI-09-111, Federal Highway Administration, Washington, DC.

FHWA 2012. *Stream Stability at Highway Structures*, Fourth Edition, Hydraulic Engineering Circular No. 20 (HEC-20), Publication No. FHWA-HIF-12-004, Federal Highway Administration, Springfield, VA.

FHWA 2012. *Evaluating Scour at Bridges*, Hydraulic Engineering Circular 18, FHWA-HIF-12-003, National Highway Institute, Federal Highway Administration, Arlington, VA.

Frizell, K. Warren. *Uplift and crack flow resulting from high velocity discharges over open offset joints: laboratory studies*. US Department of the Interior, Bureau of Reclamation, Technical Service Center, 2008.

Keaton, Jeffrey R., and Su K. Mishra. "Modified slake durability test for erodible rock material." In *Scour and Erosion*, pp. 743-748. 2010.

Kirsten, H.A.D., 1982, A classification system for excavation in natural materials: *Civil Engineer in South Africa*, 24(7), 293-308.

-----1988, Case histories of groundmass characterization for excavatability, in Kirkaldie, L, *Rock Classification Systems for Engineering Purposes*, ASTM STP 984: American Society for Testing and Materials, Philadelphia, Pennsylvania, 102-120.

Lamb, Michael P., Noah J. Finnegan, Joel S. Scheingross, and Leonard S. Sklar. New insights into the mechanics of fluvial bedrock erosion through flume experiments and theory. *Geomorphology* 244 (2015): 33-55.

McLean, S. R., and V. I. Nikora. "Characteristics of turbulent unidirectional flow over rough beds: Double-averaging perspective with particular focus on sand dunes and gravel beds." *Water resources research* 42, no. 10 (2006).

NRCS, 2001, Field procedures guide for the headcut erodability index, Chapter 52, Part 628, National Engineering Handbook: U.S. Department of Agriculture Natural Resources Conservation Service, 210-VINEH, rev. 1, March.

Pells, S. E. "Assessment and surveillance of erosion risk in unlined spillways." In *Proceeding of International symposium on Appropriate technology to ensure proper development, operation and maintenance of dams in developing countries*, Johannesburg, South Africa, pp. 269-78. 2016.

Pells, Steven E., Kurt Douglas, Philip JN Pells, Robin Fell, and William L. Peirson. "Rock mass erodibility." *Journal of Hydraulic Engineering* 143, no. 5 (2017): 06016031.

Pike, Leila, Susan Gaskin, and Peter Ashmore. "Flume tests on fluvial erosion mechanisms in till-bed channels." *Earth Surface Processes and Landforms* 43, no. 1 (2018): 259-270.

Rucker, M. "Surface geophysics as a tool for characterization existing bridge foundation and scour conditions." In *Proceedings of the conference on applied geophysics, Missouri, USA*. 2006.

Rucker, Michael L. "A rippability index approach for characterizing weathered granites." In *Vail Rocks 1999, The 37th US Symposium on Rock Mechanics (USRMS)*. OnePetro, 1999.

Rucker, Michael L. "Seismic refraction interpretation with velocity gradient and depth of investigation." In *Proceedings of the Geophysics 2002 conference*, April, pp. 15-19. 2002.

Schlotfeldt, P., and T. G. Carter. "A new and unified approach to improved scalability and volumetric fracture intensity quantification for GSI and rockmass strength and deformability estimation." *International Journal of Rock Mechanics and Mining Sciences* 110 (2018): 48-67.

Shan, Haoyin, Jerry Shen, Roger Kilgore, and Kornel Kerenyi. *Scour in cohesive soils*. No. FHWA-HRT-15-033. United States. Federal Highway Administration. Office of Infrastructure Research and Development, 2015.

Shields, A. "Anwendung der Ähnlichkeitsmechanik unter turbulenzforschung auf die geschiebebewegung." Technische Hochschule, Berlin, (1936).

Stark, Timothy D., and Hisham T. Eid. "Drained residual strength of cohesive soils." *Journal of Geotechnical Engineering* 120, no. 5 (1994): 856-871.

Sklar, Leonard S., and William E. Dietrich. "Sediment and rock strength controls on river incision into bedrock." *Geology* 29, no. 12 (2001): 1087-1090.

Van Rijn, Leo C. *Principles of sediment transport in rivers, estuaries, coastal seas and oceans*. 2008.

Wibowo, J. L., D. E. Yule, E. V. E. L. Y. N. Villanueva, and D. M. Temple. "Earth and rock surface spillway erosion risk assessment." In *Alaska Rocks 2005, The 40th US Symposium on Rock Mechanics (USRMS)*. OnePetro, 2005.

## **Accelerating the transition to digital deliverables**

**Katie Aguilar, PE.**

Seequent

3827 Lafayette Street,

Denver, CO 80205

M +678.234.1311

Katie.Aguilar@seequent.com

**Phil Child**

Seequent

Systems House, Burnt Meadow Rd. Moons Moat North Industrial Estate,

Redditch, UK, B98 9PA

T +44 1527 68888 D +44 121 7966 894

Phil.Child@seequent.com

**Jesse Greenwald**

Seequent

3827 Lafayette Street,

Denver, CO 80205

T 858-410-6877

Jesse.Greenwald@seequent.com

Prepared for the 72<sup>nd</sup> Highway Geology Symposium, August 2023



### **Acknowledgements**

The authors would like to thank the following individuals for their contributions to the paper:

Carl Grice, Sequent  
Oliver Carnaby, Seequent  
Matt Gamlin, Arcadis

### **Disclaimer**

Statements and views presented in this paper are strictly those of the author(s), and do not necessarily reflect positions held by their affiliations, the Highway Geology Symposium (HGS), or others acknowledged above. The mention of trade names for commercial products does not imply the approval or endorsement by HGS.

### **Copyright**

Copyright © 2022 Highway Geology Symposium (HGS)

All Rights Reserved. Printed in the United States of America. No part of this publication may be reproduced or copied in any form or by any means – graphic, electronic, or mechanical, including photocopying, taping, or information storage and retrieval systems – without prior written permission of the HGS. This excludes the original author(s).

## ABSTRACT

No one denies the digital age is here. Data is being generated and transferred faster than many of us are prepared to speak. In fact, some estimate that 3.5 quintillion bytes of digital data is created every day.

Within the Civil Industry, the scale of projects in infrastructure are getting larger. Organizations are being required to do more with less. Going digital seems to be the only way an organization can keep up with bigger projects, more projects, and shorter project timelines. The benefits of BIM and digital delivery to help with these industry shifts are well documented and understood.

The transportation industry National organization such as Federal Highways Administration (FHWA), American Associations of State Highways and Transportation Officials (AASHTO) and the Transportation Research Board (TRB) are providing resources to help DOTs and other organizations adopt digital delivery.

Several DOTs are piloting digital delivery programs. There is a huge opportunity to embrace cloud connected technology to ensure subsurface data is an integral part of digital delivery initiatives. Software used needs to take in to account the unique needs and requirements of the subsurface investigation, evaluation of a site, design of structures, and maintenance of those structures.

This paper will review previous, current, and emerging technologies that are driving organizations to adopt digital delivery. It will also examine issues that are keeping subsurface data from being fully integrated into the digital delivery models, and how these issues are being addressed within the industry now.

## **STATE OF THE PRACTICE FOR ENGINEERED STRUCTURES**

Transportation agencies are shifting to digital delivery. This is not PDFs or electronic paper, but a radical change to 3D engineered models. It is a step away from 2D plans and in to model based delivery. In an article published by Mitchell et al, nine states are piloting projects using a Model as the Legal Document (MALD), while eighteen states have bridge and roadway pilot projects using Model-based deliveries.

The Transportation Research Board (TRB) provides documentation to help States take a stepwise approach to shifting to digital delivery with the document Guidebook for Data and Information Systems for Transportation Asset Management. No shift is instant. And states must take a plotted, well planned course. From Mitchell et al:

*The FHWA has invested more than \$35 million on BIM-related studies and deployment through research and Every Day Counts initiatives. And the FHWA, AASHTO, and others are moving toward a national open data standard that will be seamless across digital applications from software providers, collaborating closely with building SMART International and the Open Geospatial Consortium.*

Federal and state agencies are investing in the process. And yet, a review of these initiatives clearly demonstrates a focus on the visible infrastructure such as bridges and retaining walls, and even the subsurface infrastructures such as foundations.

The shift to digital delivery is driven in part based upon researching confirming the benefits including fewer change orders (Mitchell et al, 2023). In a survey of DOTs and federal agencies performed in 2016, it was identified that the annual cost of change orders from subsurface conditions was as much as \$10 million per agency, and the cost approached 1% of the agencies' total budget for new construction (Boeckmann and Loehr, 2016). With the known effects of change orders and cost overruns being led by geotechnical causes, and the proven research showing benefits of digital delivery, it would be in agencies' interests to not only standardize subsurface investigation, but to integrate a subsurface model based upon subsurface data into the digital data deliveries. And yet this is slow to progress.

Issues keeping the subsurface from being integrated into a digital delivery model are complex. But the incentive to change is present. The need is there, as is the technology.

## **ISSUES DRIVING THE ADOPTION FOR DIGITAL DELIVERY IN THE GEOTECHNICAL INDUSTRY**

The issues driving digital data delivery for construction in the infrastructure are the same for the surface world and subsurface which supports those structures. These include volumes of data, variety of data, and shorter project turnaround times.

In the geotechnical sphere, the standard penetration test is still the norm and standard by which all other tests are judged. But projects are getting bigger resulting in 100's to 1000's of boreholes in a single project with several rigs across a single site.

Add in the different types of data from field tests that can now be collected and are often required on large infrastructure projects during a site investigation. This includes Environmental Site Assessment (ESA) data such as PID and FID test results, Cone Penetrometer Testing (CPT), Measurements while Drilling (MWD), and field strength testing. Add in standard activities including sampling, sample tracking, and lab tests, and results can quickly bring a single borehole to having hundreds of data records associated with it.

As technologies and construction methods evolve, they become more efficient. And the turnaround time for projects is getting shorter. This means geotechnical information must be available for designing engineers earlier in the project process to begin a design. Manual and bespoke processes are no longer fit for purpose.

## **ISSUES PREVENTING INTEGRATION OF DIGITAL DELIVERY**

With all these drivers for change, things are still holding the geotechnical industry back. Historically security and access have been issues, but with cloud computing being generally accepted, those concerns are less.

The geotechnical world is about uncertainty. The only facts we have are from our borehole, samples we pull and test, and perhaps some geophysical testing. Our discomfort for change is holding our industry back. Geotechnical engineering has a method that is “good enough.” There are many organizations nursing a decades old PC in a lab to host outdated software because of a lack of initiative to invest in new technology to help analyze and understand an organization’s biggest, most valuable asset: geotechnical data. The geotechnical industry accepts “good enough” here because the process and limitations are known. Professionals are comfortable with ‘good enough.’

Often, by manually entering data time and time again, geo professionals get a feel for the conditions on a site. In this site process geo professionals learn the soil and rock classifications, understand the lab results better, and correlate results to descriptions. Descriptions, in turn, are refined, honed, and grouped for design. All of this is summarized in tables and charts on an engineer’s desktop, and bespoke to the project. With each step in the process, with each manual data entry, manipulation, and review the engineer becomes more familiar and confident in site conditions, and confident in simplifications, estimates, and recommendations.

But as projects get bigger and bigger, with hundreds of data points per location, such manual, hands on approaches are not feasible. New methods to QA, review, and understand a site must be created.

Legal challenges associated with MALD also cause hesitancy. Industry professionals understand a model is an interpretation of subsurface conditions based upon our understanding of the site learned and refined through working with data. But do others who may view and want to use the data understand this? Where does the legal liability for using an interpretation lie?

The standard of logs and 2D cross sections allows for disclosures, protecting geo professionals from unintended, factual use of interpretations. They reflect an understanding of a

site at discrete intervals. They also require others to create their own models and interpretations. And others do so assume their own risk.

## **ENTER THE CLOUD**

By now most of us are familiar with “The Cloud,” vernacular for cloud computing. From Microsoft the cloud is “... a vast network of remote servers around the globe ... Instead of accessing files and data from a local or personal computer, you are accessing them online from any Internet-capable device...” Anyone who has used social media, Gmail, or Microsoft Teams has used The Cloud. Most people in countries with accessible internet know the collaborative power of the Cloud. Cloud computing is known for being centralized, allowing a user with internet access to access information anytime, anywhere. It is the single source of truth. If a user downloads something, they know it is a snapshot of a few pieces of data. Anyone with rights can access data, information, and reports quickly and easily. Large amounts of data can be manipulated and evaluated. These same concepts apply to a Geotechnical Information Management (GIM) system based on the cloud: access by anyone, anywhere, if permissions are granted.

When working with a cloud application for GIMs it must have standard tools geared towards our industry. But it must also allow for development and innovation by users to meet specific requirements. It must allow for innovation and evolution.

The data in the database is in distinct, small points, and the only source of truth. Every project places professional and corporate integrity on the line. And yet, as an industry, accepting risk with data management is the norm: security, current data, correct data, etc. On the flip side, our industry does not accept risk with models as a deliverable. And yet both a geotechnical log and a model have a level of interpretation.

## **CONNECTED WORKFLOWS**

The current state of practice with a desktop application requires data import/export to work with other applications. Geo professionals are entering and then re-entering it repeatedly throughout the data life cycle. Figure 1 represents six distinct workflows. For each workflow chances are pretty good a geo professional will touch the data at least once to enter or manipulate the data manually using a bespoke process. All the entry and manual work opens the door for mistakes. Any QA done previously is null and the process must be repeated. Equations used in calculations must be checked. Even data import/export is taking away from a single source of truth. Once a user exports data from a database, the data is dated.

With a single source of truth, a connected data environment, evaluation tools are always reaching into the single source of truth and extracting the most current data from a site. Standard equations are used. Standard variables can be selected.

Tools available to geo professionals have been desktop applications which, although powerful, are limited in data sharing and connecting to other applications. Desktop applications

are capable for bespoke tasks, but not scalable for projects, accessible for collaboration, nor secure.

Access to the cloud is secure. Organizations utilizing the Cloud need to know their data will not be used or seen by external agents unless authorized.

The cloud is also scalable. What works for an office of two people can work for an office of 200, or a team of 2000+ scattered around the globe.

With access from anywhere, working with the cloud allows for collaboration on a global scale without the issues of working over a server.

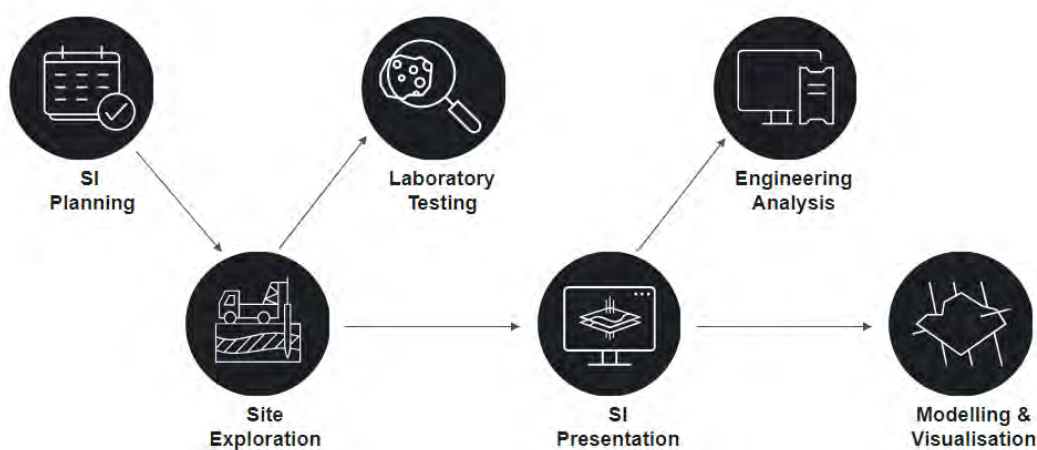


**Figure 1: Disconnected geotechnical workflow**

However, with the Cloud and its power comes a necessary change. With a cloud based GIMs system, applications are reaching into the single source of truth and pulling data. Cross sections can be built in CAD. Graphs and summary tables are built with Power BI and/or Excel features that access the database. This is a great efficiency and adds reliability to data. However, no longer are geo professionals getting a feel for what is there as they build bespoke analysis graphs for data, CADD cross sections, and summary tables and graphs for reports. In fact, with the right tools, the GIMs system eliminates all need for data re-entry or manual data manipulation.

The figure below shows a single database for six primary workflows in a connected data environment. Data is not being imported or exported. Rather, tools external to the database call

the data and the geo professional can work with, evaluate, and understand the data using standard tools for design, modeling, and evaluation.



**Figure 2: Connected Workflow with a common data environment**

This begs the question “how is a geo professional supposed to gain an understanding of the site without re-entering data?” Any GIM system must be fit for purpose and produce not just the proof of work done (aka issue geotechnical logs) and store data but also provide tools for geo professionals to re-imagine and enhance site analysis methods. These must include tools commonly used and accessible to all users. This can be as simple as filters and grouping mechanisms in the database.

It must also include geospatial capabilities to visualize projects in relation to each other, as well as borehole locations within a project. Advanced filters tied into the geospatial capabilities allow geo professionals to view project phases, group borehole locations based upon material or other database qualities such as lab results or depth to water.

There must also be capabilities for large, complex organizations to add functionality that enhances tools commonly used by geo professionals such as Excel, Power BI, and other, more advanced graphing tools. In other words, a modern tool must be extensible and programmable. An Open API allows organizations to create custom tools that enable advanced workflows for their personnel across all workflows.

## EVALUATION TOOLS IN ACTION

In a webinar presented by Ground Engineering and Seequent featuring Arcadis in May 2023, professionals from Arcadis present how they overcame challenges of huge datasets, QA, collaborative work (by distance and working with external organizations), and creating different tools for site evaluation of large amounts of data for a collaborative project.

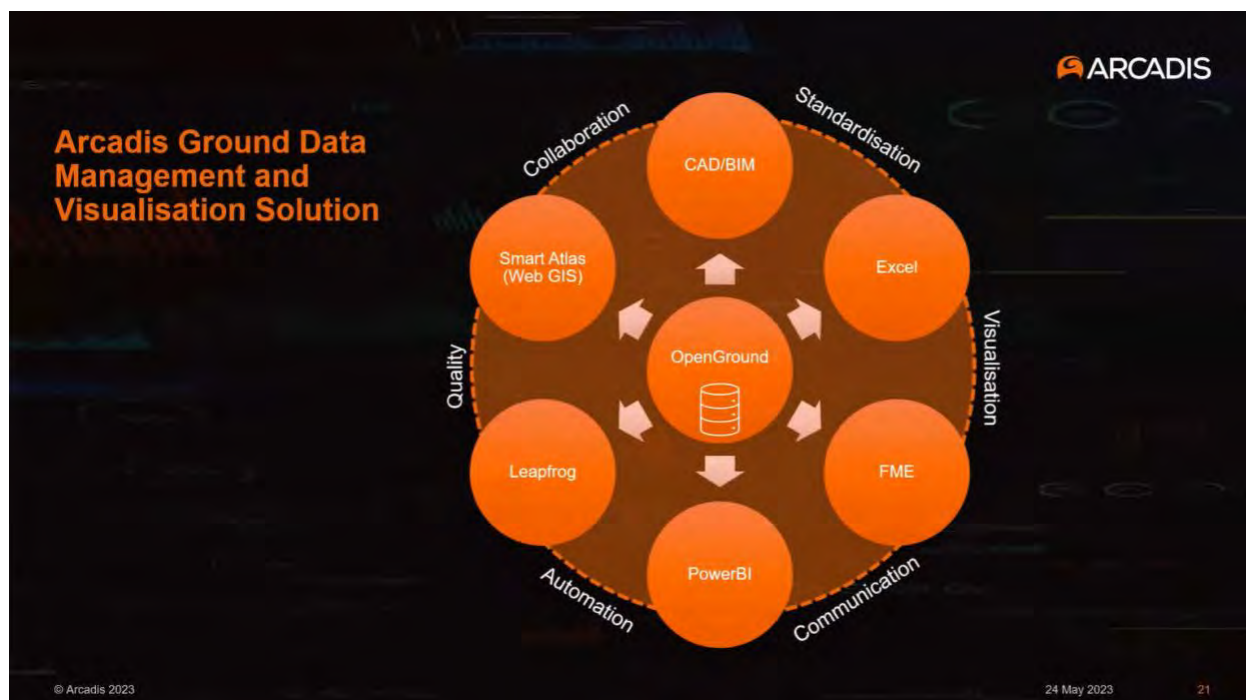


**Figure 3: Arcadis Ground Data Management Visualization Solution**

OpenGround, a cloud based geotechnical information management system, was their backbone and standard database. Arcadis utilized standard tools with built in access to the data in OpenGround to visualize data including Excel and Leapfrog. However, Arcadis also used Open Ground's Application Programming Interface (API) to connect the OpenGround database to other applications for advanced QA (FME) and analysis (Smart Atlas and Power BI). Note that OpenGround now does have a standard connection for Power BI.

Standardization enabled collaboration, visualization, communication across groups on a large-scale project with personnel external to Arcadis, as well as internally. Standardization enabled automation of complicated processes across large data sets including QA, evaluation, and modeling. In the diagram above, the standardization allowed the use of standard OpenGround tools and bespoke processes to create connected data workflows. By centralizing to a single, standard database Arcadis was able to efficiently turn around thousands of data points from site investigations from many contractors to contractors and engineers waiting on data to take the next steps in design and construction. Arcadis is confident in the quality of the data presented to others for use in the project thanks to the automation of QA. Internally they could use the data from OpenGround with other applications. The image below shows a model which combines data from OpenGround (boreholes), a Leapfrog geological model that used geotechnical information from OpenGround, and the Building Information Model (BIM).

Without a standardized database with API capabilities a model such as shown would prove an enormous undertaking: from QA of data entered manually, time to enter data, and even time to create the model in a single system vs using tools fit for purpose and integrating results. Using the standard database being accessed via the API makes it a matter of a few clicks. It is work to program and build the program using the API, but once built it is a simple, repeatable, scalable by project process for end users.

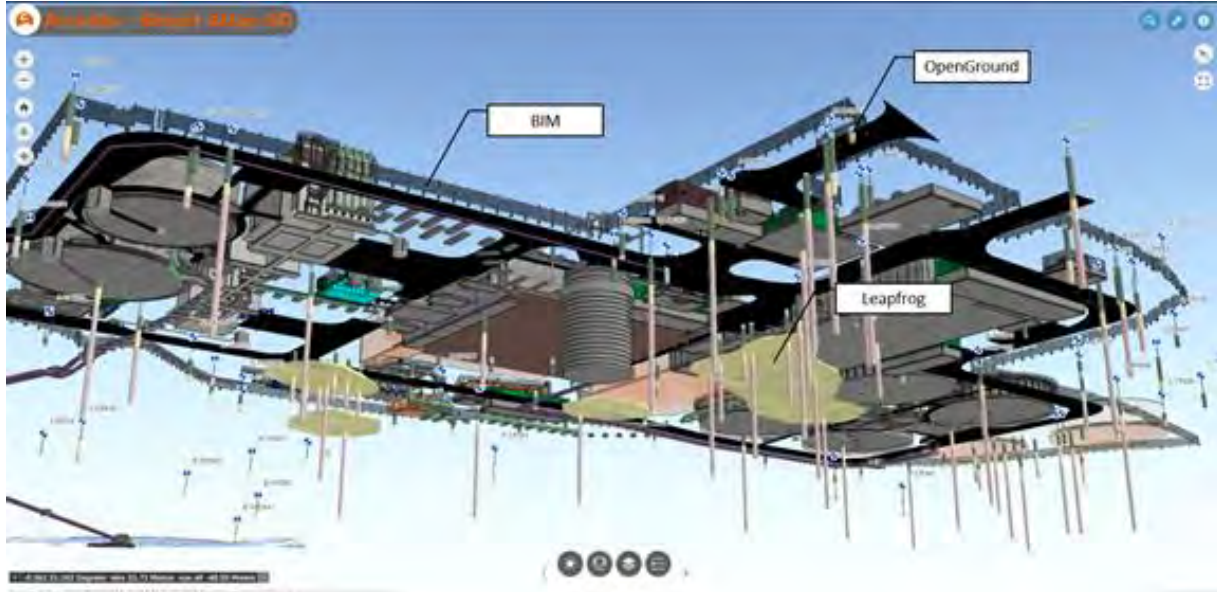


**Figure 4: A comprehensive model with as built and geotechnical data**

Dashboards built by Arcadis in Power BI enabled advanced review and analysis of materials across sites. Arcadis engineers and geologists could be reasonably comfortable with materials present and making recommendations for design. The image below is two Power BI dashboard Arcadis used to evaluate materials across a site. In a project with large amounts of data, a manual evaluation for the data would take days. The Power BI dashboard, once built, is a

scalable, repeatable process for end users to better evaluate any site, and can allow an evaluation in hours as the tool is standardized.

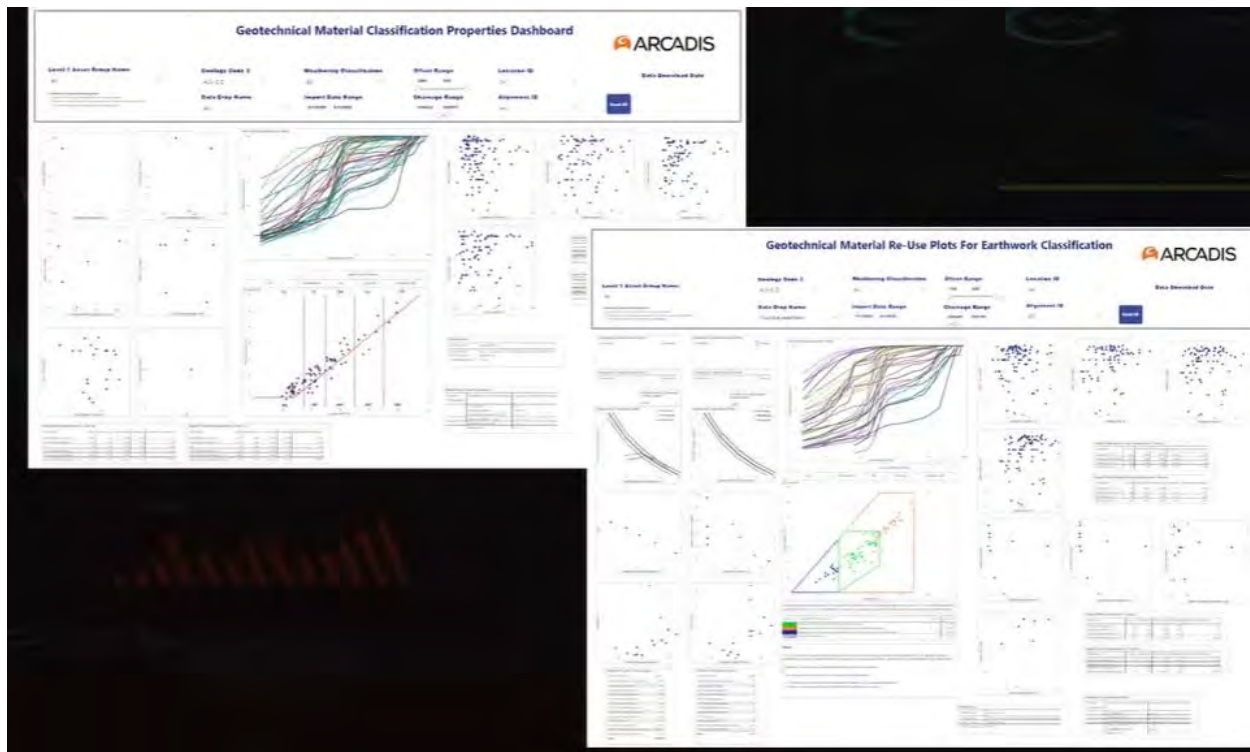


**Figure 5: A dashboard using Power BI to evaluate geotechnical materials.**

## IMPLEMENTATION

Automation cannot happen without support from management to change, as well as an understanding of end objectives, current processes. For the processes an understanding of limitations to current tools and processes and key objectives for the new technology are critical to adopting new systems, as well as building useful, fit for purpose, scalable tools to enable site evaluation and analysis by geo professionals. The tools are not built nor implemented in a day. It does take time, planning, and work. Once a workflow (and not the entire system) is ready for roll out. A plan to help users change to the new technology must be utilized. Motivation to overcome the status quo must be clearly stated starting with corporate objectives and how a new technology will achieve corporate objectives, as well as how the new workflows are a work in progress and will overcome existing pains experienced by users. This work must be started well before rollout so managers and end users know what to expect and can plan accordingly.

## SUMMARY

Digital data delivery can help alleviate costs associated with change orders in the civil industry. Given the cost and effects of change orders due to encountered subsurface conditions to projects, integration of subsurface models into existing design projects can alleviate costs of geotechnically related change orders as well.

Technology will not solve all issues. Especially as demands to evaluate more data with fewer resources grow. However, bespoke, manual processes are no longer fit for purpose. With a planned approach the geotechnical industry can move beyond bespoke spreadsheets and manual evaluation of data.

Geotechnical Information Management is not new. But the concept of cloud computing in Geotechnical Information Management is. The general benefits of working in the cloud (collaboration, scalability, and security, to name three), with tools fit for purpose to geotechnical requirements can help propel an organization forward to adopt new, fit for purpose, tools for site evaluation and design.

Well planned adoption plans with success examples will help reluctant users adopt new technology. Many steps are well written and documented in the Guidebook for Data and Information Systems for Transportation Asset Management.

**REFERENCES:**

Boeckmann, A.Z and Loehr, J.E, *Influence of Geotechnical Investigation and Subsurface Conditions on Claims, Change Orders, and Overruns*, Transportation Research Board, Washington DC, 2016.

Mitchell, Alexa, P.E., Steen, Jennifer P.E., PMP, ENV SP, and Sharp, Will P.E., PTOE Transportation agencies shift toward digital delivery. *American Society of Engineers*, ASCE, (2023), accessed June 2023, <https://www.asce.org/publications-and-news/civil-engineering-source/civil-engineering-magazine/issues/magazine-issue/article/2023/03/transportation-agencies-shift-toward-digital-delivery>.

*Guidebook for Data and Information Systems for Transportation Asset Management NCHRP Research Report 956.*, Transportation Research Board website, 2021, Transportation Research Board, accessed June 2023, <http://nap.nationalacademies.org/26126>.

Microsoft, *What is the Cloud* Microsoft website, Microsoft, 2023, accessed June, 2023 <https://azure.microsoft.com/en-us/resources/cloud-computing-dictionary/what-is-the-cloud>.  
*Webinar: Connecting data and geotechnical teams*, Ground Engineering website, Ground Engineering, 2023, accessed June 2023, <https://www.geplus.co.uk/news/webinar-connecting-data-and-geotechnical-teams-29-03-2023/>.

Multi-Scale Multi-Season Land-based Erosion Modeling and Monitoring for Infrastructure  
Management

New England Transportation Consortium Research Project 19-2

Bin Wang  
GZA GeoEnvironmental, Inc.  
249 Vanderbilt Ave.  
Norwood, MA 02062  
(781) 278-5809  
Bin.Wang@gza.com

Daniel Stapleton  
GZA GeoEnvironmental, Inc.  
249 Vanderbilt Ave.  
Norwood, MA 02062  
(781) 278-5809  
Daniel.Stapleton@gza.com

Christopher Snow  
GZA GeoEnvironmental, Inc.  
707 Sable Oaks Drive, Suite 150  
South Portland, ME 04106  
Christopher.Snow@gza.com

Aimee Mountain  
GZA GeoEnvironmental, Inc.  
707 Sable Oaks Drive, Suite 150  
South Portland, ME 04106  
Aimee.Mountain@gza.com

### Acknowledgements

The authors would like to thank the individuals/entities for their contributions in the work described:

Neil Olson, New Hampshire Department of Environmental Services (Technical Committee Chair)  
Sara Ghatee, Connecticut Department of Transportation  
Kate Maguire, Maine Department of Transportation  
Pete Connors, Massachusetts Department of Transportation  
Colin Franco, Rhode Island Department of Transportation  
Callie Ewald, Vermont Agency of Transportation  
Ann Scholz, New Hampshire Department of Transportation (Advisory Committee Liaison)

### Disclaimer

Statements and views presented in this paper are strictly those of the author(s), and do not necessarily reflect positions held by their affiliations, the Highway Geology Symposium (HGS), or others acknowledged above. The mention of trade names for commercial products does not imply the approval or endorsement by HGS.

### Copyright Notice

Copyright © 2023 Highway Geology Symposium (HGS)

All Rights Reserved. Printed in the United States of America. No part of this publication may be reproduced or copied in any form or by any means – graphic, electronic, or mechanical, including photocopying, taping, or information storage and retrieval systems – without prior written permission of the HGS. This excludes the original authors.

## ABSTRACT

Soil erosion and slope instability issues are a major concern for New England state Departments of Transportation (DOT), roadway planners, and designers, impacting the cost to maintain transportation networks and other critical infrastructure. Effective screening tools used for modeling, monitoring, and forecasting erosion can aid in assessing erosion and slope failure susceptibility, which is critical for regional operations and planning.

GZA developed a screening-level tool to identify roadways vulnerability to erosion and slope failures based on a number of factors, using the latest GIS Enterprise technology. The work is being performed in collaboration with the New England Transportation Consortium (NETC). The project objective was to develop a multi-scale, multi-season land-based erosion and landslide modeling and monitoring toolkit for infrastructure management for all the New England states (including Maine, New Hampshire, Vermont, Massachusetts, Rhode Island, and Connecticut).

The prototype Esri ArcGIS toolkit was developed for the MaineDOT based on Maine's state-wide GIS data such as topography, land use, surficial geology, and roadway system inventory. Various environmental parameters were considered as risk factors for roadways, including proximity to surface water body, proximity to the 100-year floodplain, and slope geometric information.

A large set of slope stability simulations were assembled to capture key geotechnical parameters including soil type, material strength, and groundwater depth. This set formed the basis of a "Response Function" that was used to interpolate to all the grid cells in the study area. The end deliverables of this project, i.e., the Esri GIS web viewer, included multiple risk analysis data layers for users to interact with and identify high, medium, and low hazard areas, for screening, analysis, and planning purposes for the Maine DOT.

The innovative approach developed for this project is applicable to other states or even regions and adaptable for future improvements such as inclusion of climate change considerations.

## INTRODUCTION

Soil erosion and landslides are a major concern for Departments of Transportation (DOTs), roadway planners, and designers, impacting the cost to maintain transportation networks and other critical infrastructure. With limited operational resources and funding available for maintenance and repairs, effective screening tools can aid in assessing erosion and landslide susceptibility, improving the decision-making ability for transportation operations and planning.

The main objective of the study was to develop a systematic approach and framework to evaluate and screen potential for erosion and slope instability along roadway corridors where instability could impact roadways. The work was performed in collaboration with the New England Transportation Consortium (NETC). The project objective was to develop a multi-scale, multi-season land-based erosion and landslide modeling and monitoring toolkit for infrastructure management for all the New England states.

## LITERATURE REVIEW AND USER SURVEY

The first step in the development of the model and toolkit was a literature review to collect and compile available information regarding: 1) slope instability susceptibility; and 2) modeling capabilities suitable for the New England region, including means and methods used by others.

Previous studies from New England and other parts of the country were identified, summarized, and cataloged. We also identified information and causative factors that appear to be relevant for this project (e.g., MGS-a and MGS-b). GZA focused on studies that appeared to have application to the New England states (i.e., studies done in areas with similar geography, landscapes and climate), and that were conducted by government agencies such as state departments of transportation (DOT) (e.g., Clift and Springton, Mabee and Duncan, Spigel), the US Geologic Survey (USGS) (e.g., USGS landslide inventory) and U.S. Army Corps of Engineers (USACE).

We also identified studies that used a Geographic Information System (GIS) based approach for spatial hazard analysis for slope stability (landslide and/or erosion) (e.g., Ramandathan, et al.) We also researched publicly available datasets that could be used for the toolkit development.

The user survey provided insights of different background and varying experience levels with GIS from potential toolkit users. Figure 1 provides the example output from the survey. Respondents of this survey cover a wide range of technical backgrounds, including geology, geotechnical, hydrology, CAD, GIS, and management. Approximately 80% are engineers, scientists and geologists. Majority of the participants indicate that their work requires the use of GIS and they are familiar with online applications and/or desktop GIS. There is a strong preference for using GIS-based technology within the New England state DOTs and ESRI (ArcGIS and ArcMap) appears to be the predominant software package used by the state government agencies.

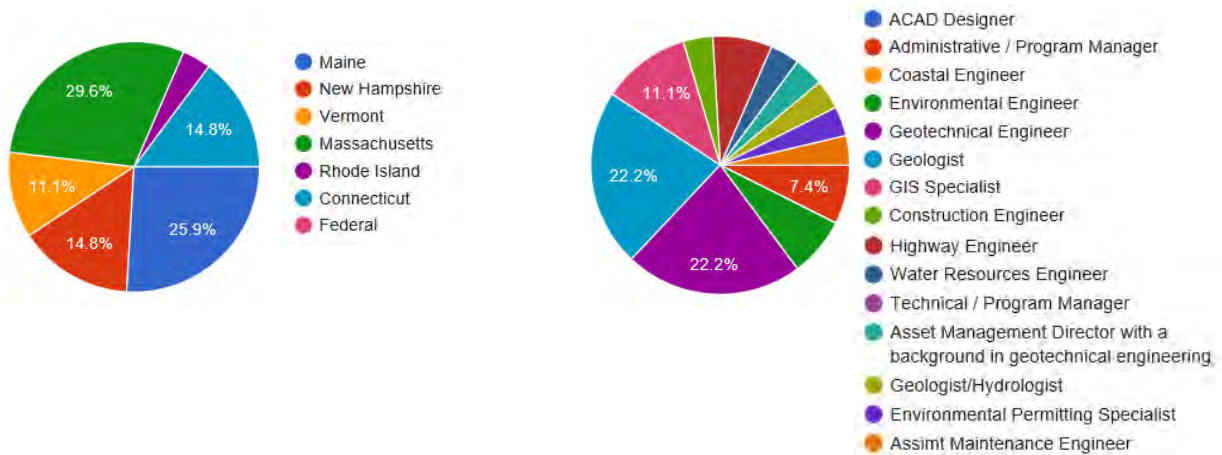


**Figure 1 – Distributions by State and Professions of Survey Respondents**

The results of both the literature review and project survey indicated that a web-based viewer and a heuristic/deterministic model for slope stability and erosion has been the dominant approach used by others (e.g., research publications and projects). The models developed by others predominantly analyzed topography as the primary variable, with additional variables of surface cover, geology and precipitation-driven change to soil moisture.

### ANALYSIS AND MODELING

Following a comprehensive review of existing literature, available source data, and analytical methods, GZA started to develop our own approach to identify critical parameters, perform analyses, and generate model outputs of soil slope stability and potential erosion areas.

GZA developed model applications to evaluate and screen for erosion and slope stability zones along roadway corridors that have the potential to impact roadways. We understand the predominant characteristics that impact roadway failure include, but are not limited to:

- Surficial geology (i.e., geologic formation and soil material/geotechnical properties);
- Topography (including several geometric parameters such as elevation, slope, and aspect); and
- Flood/water-related failure mechanisms such as surface erosion (e.g., overtopping and wave impact), internal erosion (e.g., underseepage and piping); material softening by saturation; pavement failure (seepage and wave loads and flotation); and culvert failure or overtopping.

Figure 2 presents a simple schematic of the road-side slopes for this study. We grouped slopes into two main categories: source slopes and support slopes, which are defined by their relative elevation to the nearest roadway segment. GZA adopted an analytical concept “analogous” to the Response Surface method widely adopted by USACE and FEMA for their coastal storm surge flood studies (e.g., Resio et al., and USACE 2015).

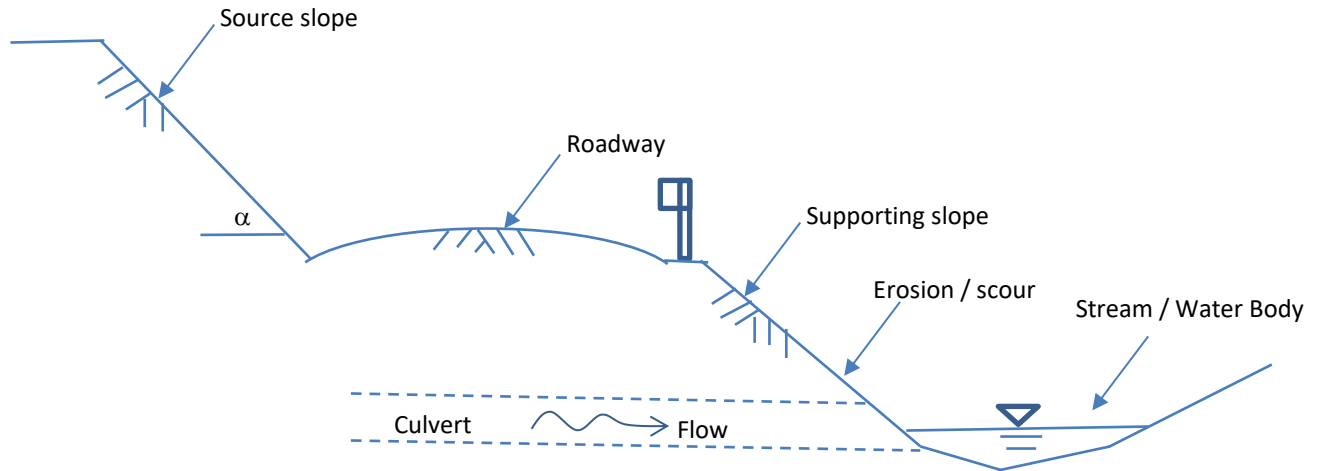


**Figure 2 – Simplified Schematic of Slope Model**

GZA’s workflow included the following steps, as summarized in the graphic below:

- Select key input parameters that affect slope stability (Step 1);
- Discretize parameter space per surficial geological information (Step 2);
- Assemble a base parameter combination set for numerical simulations (Step 3);
- Perform numerical slope stability analysis using simplified geotechnical material properties (Step 3);
- Include varying groundwater conditions (Step 3); and
- Establish an interpolation and extrapolation scheme for scenarios that are not directly modeled (Steps 4 and 5).

Complex geometry such as slope length, slope surface curvature and toe undercutting were considered as additional hazard contributing factors and were simulated as part of the sensitivity analysis. External loading, such as surcharge from traffic, was not included in the final toolkit as part of this project but could be considered and incorporated in future development.

SLOPE/W (submodule of GeoStudio v.2018), a widely used commercial slope stability software program for analyzing soil slopes, was used. SLOPE/W can effectively analyze both simple and complex problems for a variety of slip surface shapes, pore-water pressure conditions, soil properties, and loading conditions. Figure 2 presents a simple schematic of the geometry modeled in SLOPE/W. GZA used the Morgenstern-Price (M-P) method with half-Sine side function (SLOPE/W default).

Different surficial geological datasets available from MGS/USGS were examined and the 250k (scale) unified state-wide layer was selected as input. The material geological descriptions are presented in Table 1. For simplicity, GZA classified the soils into three main categories:

- granular soils with frictional angle ( $\theta$ ) as the soil strength parameter;
- cohesive soils with undrained shear strength ( $s_u$ ) as the soil strength parameter;
- rock – weathered or intact bedrock (not modeled at this stage).

**Table 1 - GZA Classification for 1:250,000-Scale Surficial Geology Maps**

Symbol	Geologic Unit	Materials	Origin	Material Classification
a	Stream alluvium (includes Holocene flood plain, stream terrace, and alluvial fan deposits)	Sand, gravel, and silt.	Deposited on flood plains and stream beds by postglacial streams.	G1
s	Swamp, marsh, and bog deposits (includes both fresh-water and salt-water marshes)	Peat, muck, clay, silt, and sand.	Formed by accumulation of sediments and organic material in depressions and other poorly drained areas.	C1
b	Beach deposits	Sand and gravel.	Includes beach sediments formed by wave and current action, and sand dunes derived from these deposits.	G2
eb	Emerged beach deposits	Sand and gravel.	Formed by wave erosion of till or other materials during the late-glacial marine submergence of parts of southern Maine.	G2
e	Eolian deposits	Sand.	Windblown sand. Derived from wind erosion of glacial sediments and deposited in late-glacial to postglacial time.	G2
L	Lake-bottom deposits	Silt, clay, and sand. Commonly well stratified, and may be rhythmically bedded.	Composed of sediments that washed out of late Wisconsinan glacial ice and accumulated on the floors of glacial lakes.	C2
m	Glaciomarine deposits (fine-grained facies)	Silt, clay, sand, and minor amounts of gravel.	Composed of glacial sediments that accumulated on the ocean floor. Formed during the late-glacial marine submergence of lowland areas in southern Maine.	C1
ms	Glaciomarine deposits (coarse-grained facies)	Sand, gravel, and minor amounts of silt.	Deposited where glacial meltwater streams and currents entered the sea.	G2
go	Glacial outwash deposits	Sand and gravel.	Deposited by meltwater streams in front of the receding late Wisconsinan ice margin.	G2
g	Ice-contact glaciofluvial deposits (exclusive of eskers)	Sand, gravel, and silt.	Deposited by meltwater streams adjacent to stagnant glacial ice.	G2
ge	Eskers	Gravel and sand.	Chiefly deposited by meltwater streams flowing in tunnels within or beneath the late Wisconsinan ice sheet.	G3

Symbol	Geologic Unit	Materials	Origin	Material Classification
sm	Stagnation moraine	Mostly till, but also includes variable percentages of undifferentiated sand and gravel.	Deposited during the dissipation of stagnant glacial ice.	G3
em	End moraines	Till or sand and gravel. May be very bouldery. Commonly interbedded with or overlain by glaciomarine sediments in areas that experienced late-glacial marine submergence.	Deposited in the marginal zone of the late Wisconsinan ice sheet, by glacial ice and/or meltwater flowing out of the ice.	G3
rm	Ribbed moraine	Till is the principal constituent, but stratified sediments are present in some of the deposits.	Origin uncertain. Deposited either at the margin of or beneath the late Wisconsinan ice sheet.	G3
t	Till	Heterogeneous mixture of sand, silt, clay, and stones.	Deposited directly by glacial ice.	G3
n/a	Thin drift	Area of many bedrock outcrops and/or thin surficial deposits (generally less than 3 m thick).	Commonly the result of non-deposition of glacial sediments, but the surficial materials in some coastal areas have been largely removed by marine erosion in late-glacial time.	G3
n/a	Thin drift, undifferentiated	Area of many bedrock outcrops and/or near-surface bedrock where the surficial materials have not been mapped.	Same as other thin-drift areas.	G2
rk	Bedrock	Area of extensive bedrock outcrop, or where the bedrock has only a thin cover of soil and vegetation.	Same as the thin-drift areas.	R

## Notes:

1. Source table downloaded from <https://www.maine.gov/dacf/mgs/pubs/mapuse/series/surf-250/surf-exp.htm>.
2. G denotes granular soil; C denotes cohesive soil; and R denotes rock.
3. Numeric values 1 through 3 denote increasing density and/or shear strength.

For each soil type (granular or cohesive), GZA divided them into three subgroups, with simplified, representative soil strength properties based on engineering judgment and local knowledge, as presented in Table 2. For example, G1, a granular soil with the lowest frictional angle, represents silty sandy materials with relatively low density, whereas G3, with the highest frictional angle, represents gravelly materials or dense sandy soils, such as glacial till. Fine-

grained glaciomarine deposits were largely classified as C1, a cohesive soil with very low shear strength (or cohesion value).

Two groundwater conditions were assumed to represent:

- relatively dry condition with a groundwater table approximately 10 feet below ground surface; and
- relatively wet condition with a groundwater table approximately 3 feet at crest of the slope and exiting the ground surface at the slope toe.

**Table 2: Summary of Material Properties for SLOPE/W Simulations**

Parameter	Granular Soil			Cohesive Soil			Rock
	G1	G2	G3	C1	C2	C3	R
Material Code in GIS *	101	102	103	201	202	203	300
Unit Weight (pcf)	118	125	135	120	120	120	150 - 170
Friction Angle (°)	28	32	38	0	0	0	--
Undrained Shear Strength (psf)	0	0	0	350	750	1,250	--

Note: \* code (integer) assigned for identification purposes during computations in this study. No computation performed for rock at this stage. “pcf” denotes pounds per cubic foot; “psf” denotes pounds per square foot.

**Dry and wet groundwater conditions can be a result of various factors such as precipitation, material types, slope aspect and curvature, local hydrologic setting and seasonal variations.**

presents an example SLOPE/W geometry used for this study. GZA selected a slope size of 100 feet in horizontal distance from crest to toe. Simulated SLOPE/W results are summarized in Table 3. Critical Factor of Safety (FoS) values from the critical slip surface are presented in the table, which are the slip surface that produce the minimum FoS value of all the slip surfaces analyzed by the program in each simulation.

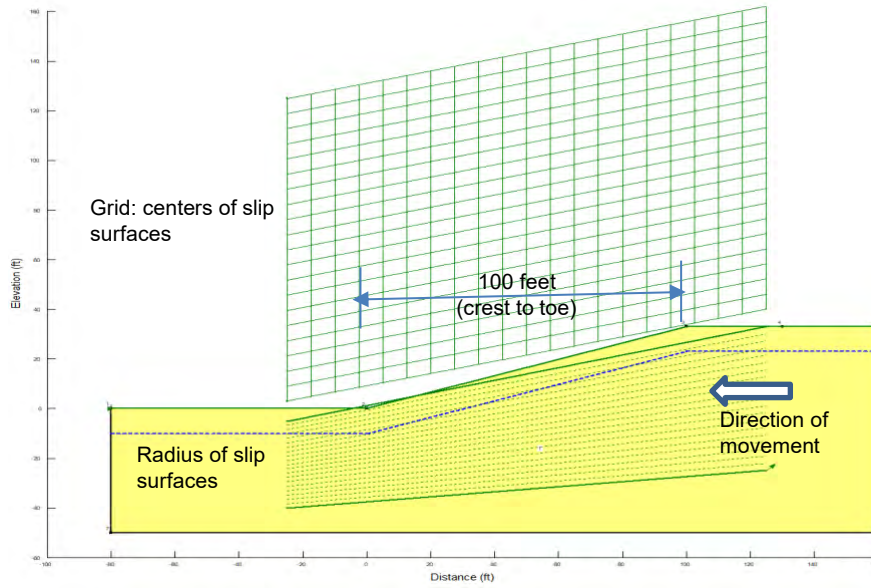
In general, a shallower groundwater table tends to lower the FoS in granular soil slopes, whereas the difference is less noticeable in cohesive soils. FoS values are positively correlated with increasing soil strength parameters. Figure 4 presents the SLOPE/W simulation results for the granular and cohesive soils. These curves can be viewed as discrete slices from a 4-dimensional (response) surface, with the response being the factor of safety and the variables being the slope angle, material type and groundwater conditions. Based on the SLOPE/W modeling results, FoS values for all slope angles (from 0 to 120%) can be determined using 1-dimensional spline interpolation and the interpolated FoS dataset (Figure 5) was used for calculations in GIS.

Natural soil slopes, regardless of material types or geometry, becomes inherently unstable when the slope exceeds 100% (i.e., 1-to-1 slope), consistent with our modeling results and general knowledge. Additional material types and/or parameters can be incorporated in the model when needed, under the modular structure of the overall approach. Note that multi-layered geometry is beyond the scope of this screening level analysis. Stratigraphy should be considered for site-specific slope stability studies and engineering design.

**Table 3: Summary of SLOPE/W-calculated Factors of Safety**

Row ID	Soil Type	Key Parameter	Slope (H:V)	Slope (%)	FoS (wet)	FoS (dry)
1	G1	$\phi = 28^\circ$	6:1	17%	1.85	3.07
2			4:1	25%	1.23	2.05
3			3:1	33%	0.90	1.53
4			2:1	50%	0.53	0.96
5			1.5:1	67%	0.33	0.66
6			1:1	100%	0.10	0.34
7	G2	$\phi = 32^\circ$	6:1	17%	2.28	3.69
8			4:1	25%	1.52	2.48
9			3:1	33%	1.11	1.85
10			2:1	50%	0.66	1.16
11			1.5:1	67%	0.42	0.80
12			1:1	100%	0.12	0.43
13	G3	$\phi = 38^\circ$	6:1	17%	3.00	4.60
14			4:1	25%	2.00	3.13
15			3:1	33%	1.48	2.33
16			2:1	50%	0.89	1.47
17			1.5:1	67%	0.58	1.02
18			1:1	100%	0.21	0.55
19	C1	Su = 350 psf	6:1	17%	1.09	1.09
20			4:1	25%	0.72	0.72
21			3:1	33%	0.53	0.53

Row ID	Soil Type	Key Parameter	Slope (H:V)	Slope (%)	FoS (wet)	FoS (dry)
22			2:1	50%	0.34	0.34
23			1.5:1	67%	0.22	0.22
24			1:1	100%	0.10	0.14
25	C2	Su = 750 psf	6:1	17%	2.34	2.33
26			4:1	25%	1.64	1.64
27			3:1	33%	1.15	1.15
28			2:1	50%	0.72	0.72
29			1.5:1	67%	0.48	0.49
30			1:1	100%	0.13	0.23
31	C3	Su = 1,250 psf	6:1	17%	3.89	3.89
32			4:1	25%	2.58	2.57
33			3:1	33%	1.92	1.91
34			2:1	50%	1.21	1.20
35			1.5:1	67%	0.83	0.82
36			1:1	100%	0.49	0.49
37	R	Rock	----- Not modeled -----			



Note: Example shows a 3H:1V slope with one uniform material. Grid and radius method used for Grid and radius for circular slip surfaces.

**Figure 3 – SLOPE/W Model – Example**

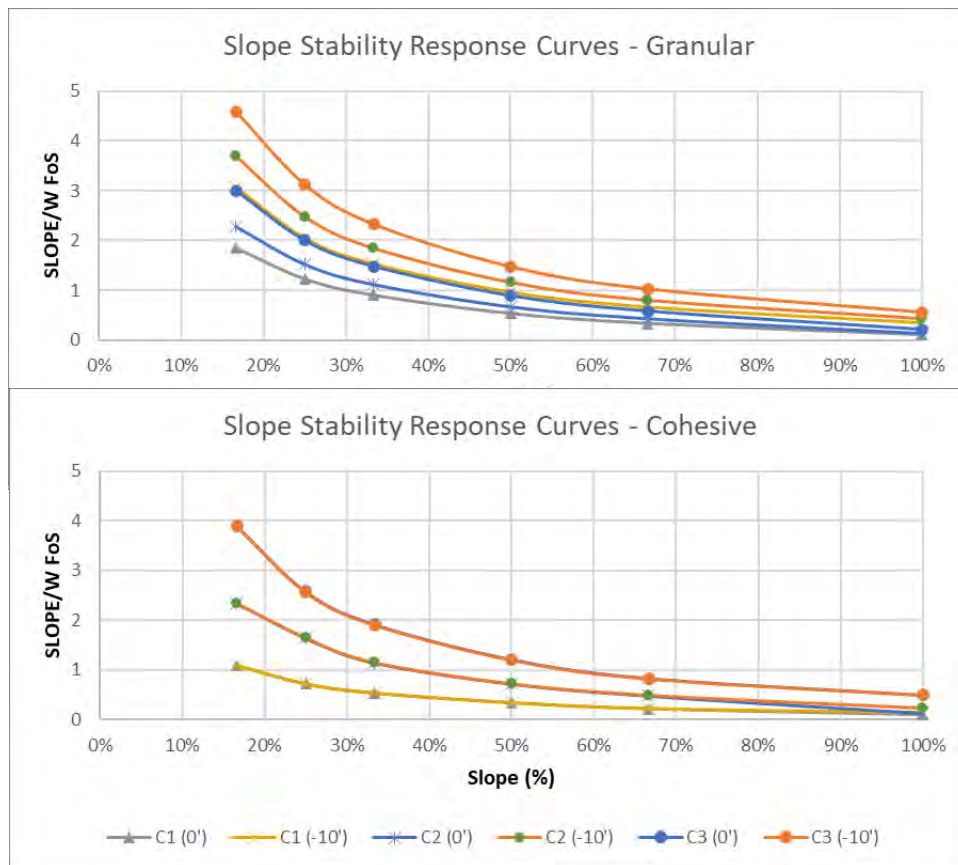


**Figure 4: SLOPE/W-calculated Factors of Safety**

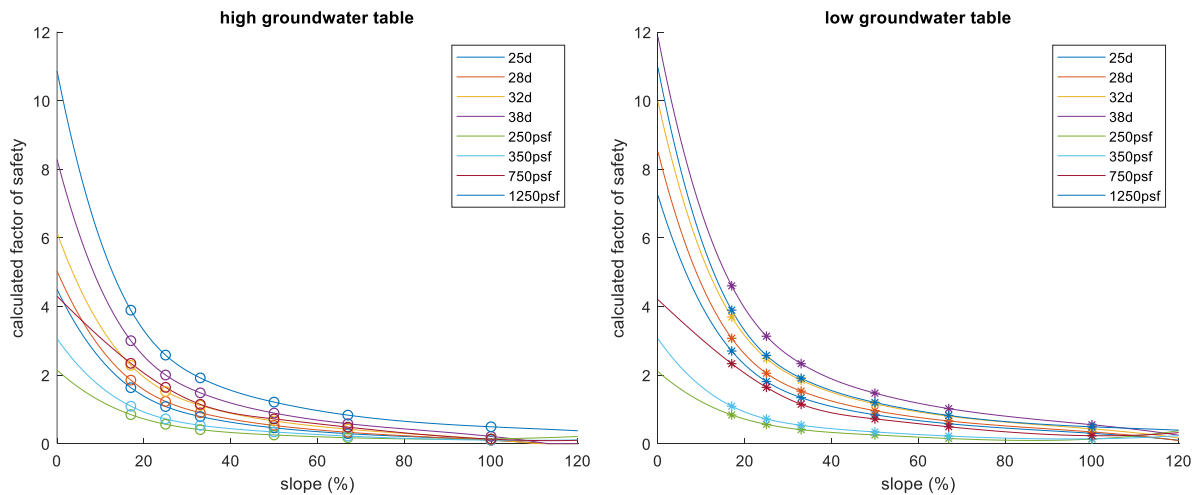


**Figure 5: Interpolated Factors of Safety**

Upon completion of the numerical slope stability analysis, the following list of fields was assembled to determine the hazard indices for roadway-impacting slopes for each grid cell with a size of 10 feet by 10 feet for the entire State of Maine:

- Easting (X) and Northing (Y) in universal transverse mercator (UTM) zone 19 north (19N) coordinate system;
- Grid cell elevation, slope, aspect and curvature;
- MGS 250k surficial material type;
- NRCS land cover type;
- Roadway surface elevation and roadway segment aspect;
- Distances from grid cell to the nearest roadway segment, hydrographic feature and culvert; and
- FEMA special flood hazard area designations (flood zones and base flood elevation (BFE), if available);

Computations were performed using Python scripts and Model Builder in ArcGIS. Output results were included in the NETC 19-2 Project Viewer (ESRI ArcGIS web mapping application) developed by GZA and could be displayed as various map layers/attributes.

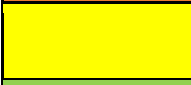
## GROUND TRUTHING AND MONITORING

For this “Ground Truthing” task, field data and engineering experience from past GZA projects were applied at selected “test sites” to verify and validate the modeled slope stability results. In addition, landslide susceptibility maps produced by MGS were compared to our modeled results as part of the verification and validation process. GZA selected a number of “test sites” based on the following criteria:

- Known past slope failure or stability issues;
- Proximity to water bodies (river or ocean);
- Availability of site-specific subsurface exploration geotechnical information;
- Past project experience combined with local knowledge; and

- Coverage of both soil types, cohesive and granular.

**Table 4: Color Scale for Slope Hazard Mapping at Test Sites**

Map Color <sup>1</sup> Code	Predicted Stability Zone	Relative Hazard Index Ranking	Estimated Factor of Safety (FoS)	Probability of Instability	Possible Influence of Stabilizing or Destabilizing Factors
	Unstable	Very High (5)	<0.9	90%	Stabilizing factors required to achieve/maintain stability
	Threshold of instability	High (4)	0.9 – 1.1	>50%	
	Nominally stable	Moderate (3)	1.1 – 1.3	10%	Minor destabilizing factors needed to cause failure
	Moderately stable	Low (2)	1.3 – 1.5	--	Moderate destabilizing factors needed to cause failure
	Stable	Very Low (1)	>1.5	--	Significant destabilizing factors needed to cause failure

### Test Site 1 – Lake Auburn

The City of Auburn was selected due to its proximity to Lake Auburn and Androscoggin River with varying terrain and land cover types. The surficial material type in Auburn is locally referred to as the Presumpscot Deposit. It consists largely of soft clay, classified by GZA as “C1”<sup>2</sup> characterized as having undrained shear strength of 350 pounds per square foot (psf), with lesser layers of marine deltaic sands and silts. The Presumpscot Deposit is also the source of many if not most Maine landslides. GZA was involved with a previous roadside embankment slope project along Route 136 in 2010. Some natural failures had occurred due to oversteepening of the riverbank adjacent to the roadway. However, the major failure was triggered by installation of steel sheet piles during proposed reconfiguration of the slope. Figure 6 presents the predicted slope failure hazard indices along Route 136, adjacent to Androscoggin River. The calculation was based on a Light Detection and Ranging (LiDAR) dataset dated 2009, prior to the major failure incident in Summer 2010. It is clear that the modeled results were able to capture the low factor of safety values at the toe of the slope, which led to predicted high hazard level (red dots). Figure 7 presents two representative photographs from the site, post-failure and post-construction.

<sup>1</sup> Very Low = Dark Green in Auburn; Blue in Kennebunk

<sup>2</sup> Refer to Table 3 for soil classifications.



Note: Aerial image more recent than 2010; topography LiDAR from 2009. Failure occurred in Summer 2010.

**Figure 6: Slope Failure Site at Route 136**



Note: Top image after failure incident in September 2010; bottom image after construction/remediation completed in December 2010.

**Figure 7: Project Photographs for Route 136 Slope Failure**

### Test Site 2 – Coastal Kennebunk

The modeled results also identified areas where coastal erosion is apparent based on existing topography and slopes such as near the Kennebunk River mouth area (at the confluence with the Atlantic Ocean), as shown in **Figure 8**. The orange/red pixels highlight drainage channels that are actively eroding and forming the gullied terrain previously described. The area known as Great Hill at the oceanfront of the river mouth is highlighted due to the steep slopes adjacent to the water, even though the area is mapped as dense sand/grave/silt glacial till deposits. By observation, this area has been stabilized repeatedly with a combination of riprap and stone-filled

gabion mattresses and continues to actively erode and experience surficial sloughing failures. Note that the hazard index model does not directly consider flood effects such as elevated water levels, waves and resultant erosion. FEMA flood hazard zones will be included in the toolkit as a reference layer.

### Comparison with MGS Landslide Susceptibility Map – Kennebunk, ME

According to Maine Geological Survey (MGS-c), “landslides are one of the most common geologic hazards in Maine, causing damage in both rural and urban areas of the state.” What many of the documented landslide incidents had in common was that they occurred in areas underlain by a glaciomarine clay and stratified sand deposit called the Presumpscot Formation, and usually occurred in areas with steep slopes. Rainfall is one of the common triggering factors, in combination with poor drainage. The Presumpscot Formation is a widespread blanket of glaciomarine silt, clay, and sand that covers much of coastal Maine and inland lowlands and has proven to be highly susceptible to slope failure. The MGS produced a series of Landslide Susceptibility Maps for areas in Maine. The maps focused on areas underlain by glaciomarine deposits, and in particular, the marine clay of the Presumpscot Formation.

MGS use the following two categories of risk factors in the study, including:

- Geomorphic Risk Factors (such as slope, curvature, aspect, and slope height); and
- Soil properties (such as surficial geologic materials).

GZA converted the MGS map (MGS-b) titled “Landslide Sites and Areas of Landslide Susceptibility, Town of Kennebunk, Maine” in PDF format to a jpeg file and used features such as roads and town lines to georeference the map in GIS so it could be compared to model results.

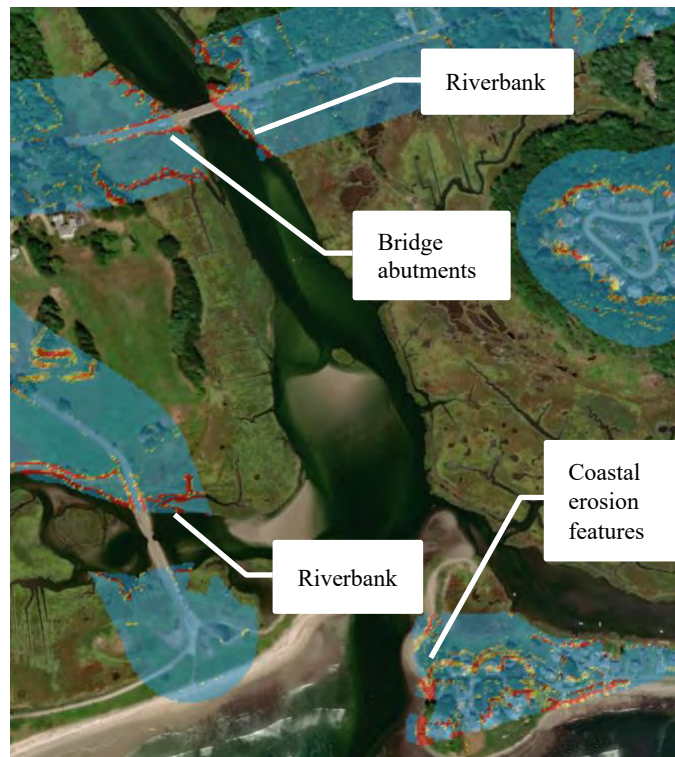
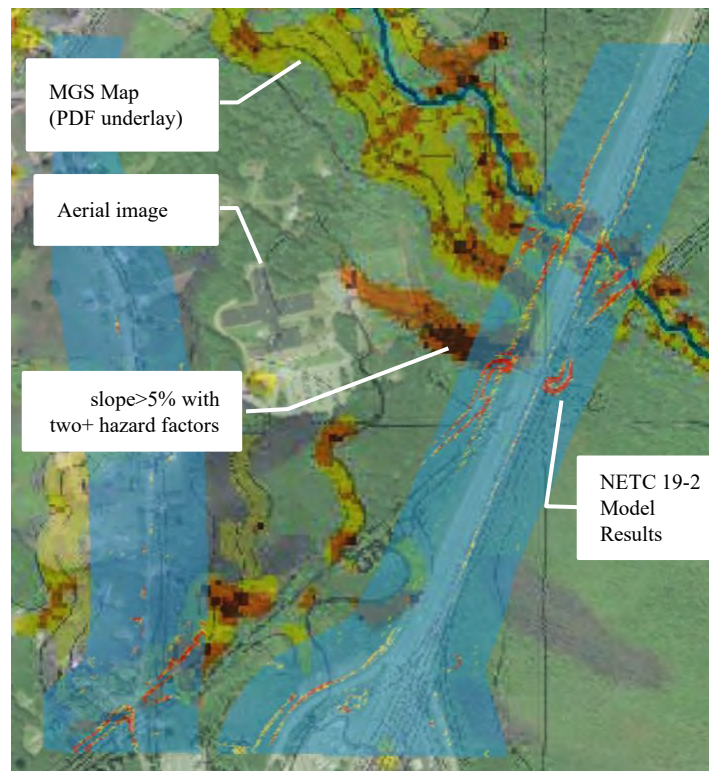


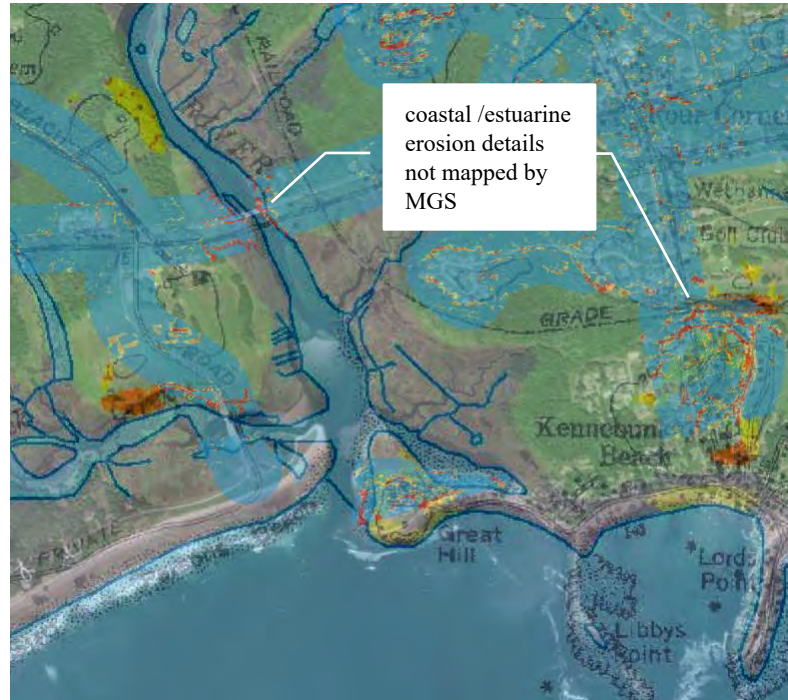
**Figure 8: Coastal Erosion and Instability, Kennebunk, Maine**

**Figure 9** presents an image where MGS mapping results and NETC 19-2 modeling results are overlaid on top of each other for comparison. Our study results have a focus on existing roadways, whereas MGS results cover the entire land area. There is, overall, agreement between the MGS predictions and NETC 19-2 modeling results, in terms of where high hazard areas are located (darker/warmer colors). It is apparent that the NETC 19-2 modeling results are significantly higher in resolution (green to red scale), compared to the MGS mapped color blocks (yellow to dark brown color scale; refer to MGS map legend). The MGS results appear to have predicted more “high hazard” areas than this study. GZA’s results seems to match the underlying terrain and manmade features more accurately than MGS land-based mapping results, mostly because of the fine resolution (3-meter by 3-meter) and the use of generalized rotational stability analyses as the basis for the current model. **Figure 10** indicates that the NETC 19-2 modeling results are more capable of detecting more detailed potential failure features in general, even if the terrain is generally very gently sloping in the coastal areas.



Note: Aerial image and MGS landslide susceptibility map overlaid with NETC 19-2 computed slope stability hazard index.

**Figure 9: Comparison of NETC 19-2 Results and Landslide Susceptibility Map – I-95**



Note: Aerial image and MGS landslide susceptibility map overlaid with GZA computed slope stability hazard index.

**Figure 10: Comparison of NETC 19-2 Results and Landslide Susceptibility Map – Coast**

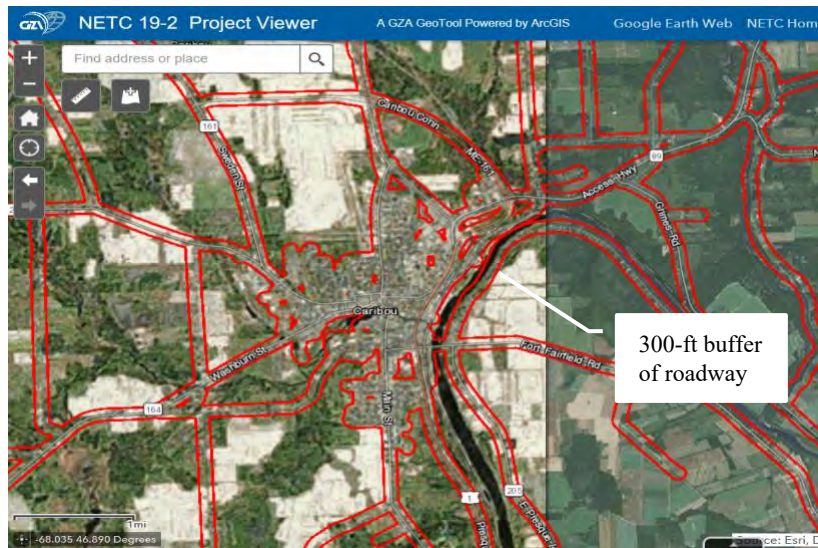
## TOOLKIT DEVELOPMENT

### Toolkit Development Process

In general, GZA downloaded and processed data layers from various publicly available sources such as U.S. Geologic Survey (USGS) and Maine Department of Transportation (MaineDOT). Using ESRI ArcMap, data was then clipped to separate sets based on Maine county boundaries for easier data management and processing. GZA developed tools using ESRI ModelBuilder for spatial data analysis/processing.

A total of nine (9) results layers for the toolkit / data viewer were produced, including: 1) Proximity to Surface Water; 2) Proximity to Culvert; 3) Proximity to FEMA's Special Flood Hazard Areas Results; 4) Slope Types; 5) Relative Aspect; 6) Geotechnical Material Types; 7) Factor of Safety; 8) Slope Hazard Index; and 9) Culvert Hazard Index.

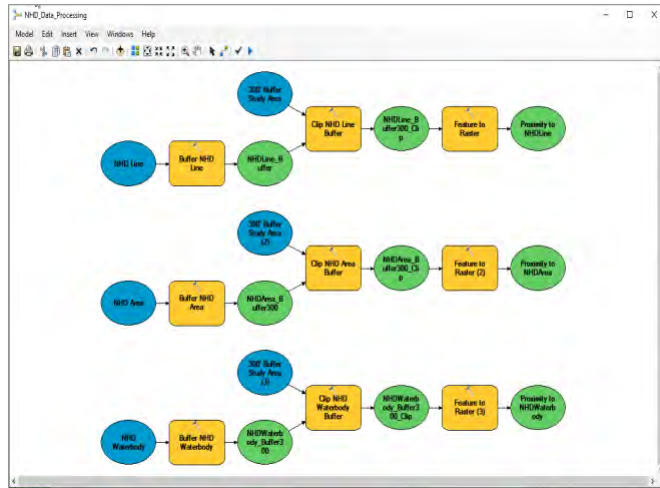
Data were processed and saved in raster format. The base geospatial data is the 300-foot buffer zone from the road features contained in the MaineDOT public roads centerline feature class, as shown in Figure 11, based on the assumption that slope instability or erosion beyond 300 feet from the roads has a less significant impact on roadway traffic and safety. Interim layers (also included and presented in the toolkit) served as the necessary input for others. Layers below are presented in the order of our overall workflow.



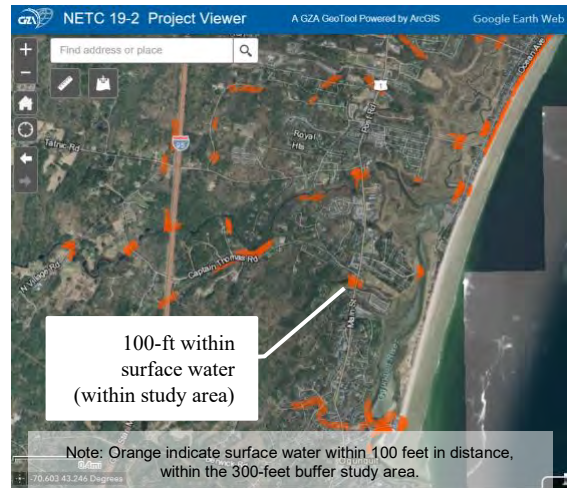
Note: Red outlines represent the study area.

**Figure 11: NETC 19-2 Study Area – 300 feet Buffer along Public Roadways**

An example ModelBuilder is shown in Figure 12(a), which presents the ArcMap ModelBuilder Flow Chart, which highlights the key steps of the geoprocessing model. One-hundred-feet was selected as the screening criteria. As a result, the proximity to surface water layer represents areas that are within 100 feet from water sources (such as perennial streams, ponds, and lakes), as shown in the example image in **Error! Reference source not found.2(b)**.



(a)



(b)

**Figure 12: (a) Model for Processing NHD Data; and (b) Proximity to Surface Water**

**Figure 13** presents the results layer in the NETC 19-2 Project Viewer for the final slope stability hazard index layer. Warmer colors indicate a greater likelihood for slope failure (including landslide).

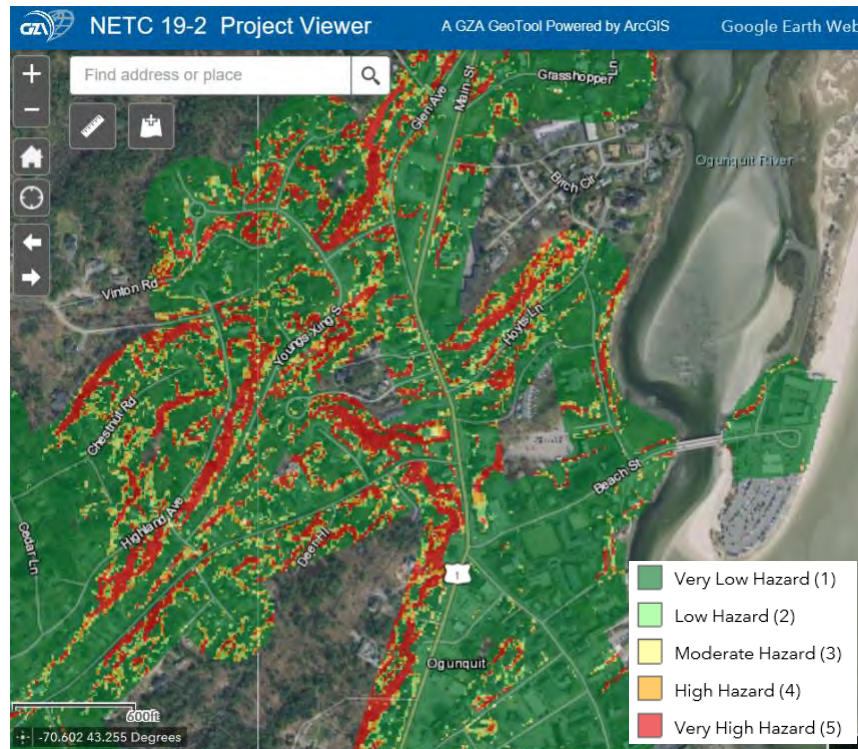


**Figure 13: Example View of Hazard Index**

## SUMMARY

This erosion and slope stability modeling toolkit is intended to serve as a screening tool for MaineDOT for operation and planning purposes. The high resolution of the source data and results layers made it possible for roadway segment-level assessment. Key take-aways of the study include:

- This screening tool allows easy navigation of a large area and screening for slope/erosion issues without performing complex numerical modeling or calculations.
- The toolkit highlights high hazard areas spatially in a GIS mapping platform so that areas require additional site-specific analysis can be easily identified. Similarly, the toolkit can be used for maintenance or repair planning.
- For erosion-prone areas, screening level assessment can be performed by turning on various results layers such as proximity to water, culverts, and FEMA Special Flood Hazard Areas.
- Certain man-made structures such as steep bridge abutments or roadway embankments were captured as high hazard features. They can be screened out if the DOT has site- or project-specific information to support such a decision.
- The screening toolkit captures certain man-made structures such as bridge abutments and steep roadway embankments as high hazard features. For the Maine database, they can be screened out using the surficial geologic type “Artificial fill” where that layer is included on the MGS 1:24,000 surficial geology maps.
- A high hazard index presented in the toolkit result layer does not mean this location is going to have a slope failure right away. It simply points out that this area has a relatively high

potential of experiencing some kind of slope instability or erosion issue, compared with the surrounding areas.

- The prototype toolkit has a user-friendly ESRI GIS interface that allows users to conservatively assess vulnerabilities in the roadway systems in the State of Maine. The model can be readily expanded to other states and regions due to the plug and play architecture of the framework.

## **PROPOSED FUTURE IMPROVEMENTS AND IMPLEMENTATION**

The toolkit was developed by design as a modular geospatial software system utilizing Esri ArcGIS Enterprise and is highly adaptable to incorporate future modification. Opportunities for future modification include:

- Compilation of the base data and development of the screening stability calculation for other states. This would require identification of the available state-wide base data sets, geotechnical material type categorizing of the surficial material types, and inputting the required data and parameters into the data processing model. The model relies heavily on the geotechnical interpretation of the surficial geology and must be catered to each state's surficial geology mapping. The modular nature of the toolkit allows for integration with the mapping data available in each state.
- Incorporation of an Esri ArcGIS Dashboard for information access and management could be used for roadway maintenance and planning.
- Incorporation of additional, layer modules for other natural hazard data (e.g., seismic, flood).
- Incorporation of real time monitoring and sensor data (such as slope displacement sensors).
- Incorporation of widgets for added functionality (e.g., printing and data export) and analysis capability.

This article is an adapted version of the original full-length NETC 19-2 report, which is available for viewing and downloading from the following URL:

<https://www.newenglandtransportationconsortium.org/completed-research-project-reports/>.

## REFERENCES:

Clift, A. E. and Springton, G. Vermont Geological Survey - *Protocol for Identification of Areas Sensitive to Landslide Hazards in Vermont*, University of Norwich, 2012.

MGS-a. Landslide Sites and Areas of Landslide Susceptibility, Town of Kennebunk, Maine, by Maine Geological Survey, Open File No. 09-28, 2009.

MGS-b. Landslide Sites and Areas of Landslide Susceptibility, Town of Kittery, Maine, by Maine Geological Survey, Open File No. 09-30, 2009.

MGS-c, Landslide Susceptibility Mapping in Maine, (available at the Maine Geological Survey Publications site [https://digitalmaine.com/mgs\\_publications/453/](https://digitalmaine.com/mgs_publications/453/)), 2010

Mabee, S. B. and Duncan, C. *Slope Stability Map of Massachusetts*, by UMass Geosciences, 2013.

Ramandatha R., Aydilek, A. H., and Tanyu, B.F. *Development of a GIS-based failure investigation system for highway soil slopes*, *Frontiers of Earth Science*, 9, 165-178, 2015.

Resio, D.T., J. Irish, and M. Cialone, “A surge response function approach to coastal hazard assessment – part 1: basic concepts“, *Natural Hazards*, 2009. 51:163–182. DOI 10.1007/s11069-009-9379-y

Spigel, L.J. *Maine Landslide Guide*, Open File No. 20-9, Maine Geological Survey, 2020.

USGS, *U.S. Landslide Inventory*, <https://www.usgs.gov/tools/us-landslide-inventory>, accessed 2023.

USACE, *North Atlantic Coast Comprehensive Study (NACCS) Coastal Storm Hazards from Virginia to Maine*, ERDC/CHL TR-15-5, November 2015.

## **Integrating Field Data with Physics Engine Simulations of Fragmental Rockfalls**

### **Ruairidh MacPhail**

Queen's University  
36 Union Street, Kingston,  
Ontario, Canada, K7L 3N6  
(613)-539-0384  
ruairidh.macphail@queensu.ca

### **Kyle Laporte**

Queen's University  
36 Union Street, Kingston,  
Ontario, Canada, K7L 3N6  
kyle.laporte@queensu.ca

### **Jean Hutchinson**

Queen's University  
36 Union Street, Kingston,  
Ontario, Canada, K7L 3N6  
hutchinj@queensu.ca

### **Rob Harrap**

Queen's University  
36 Union Street, Kingston,  
Ontario, Canada, K7L 3N6  
harrap@queensu.ca

Prepared for the 72<sup>nd</sup> Highway Geology Symposium, August, 2023

### **Acknowledgements**

The authors would like to thank and acknowledge the Departments of Transportation from Washington, Colorado, Tennessee and California, as well as the Ministry of Transportation and Infrastructure from British Columbia for providing the videos analyzed to make the database used in this paper.

### **Disclaimer**

Statements and views presented in this paper are strictly those of the author(s), and do not necessarily reflect positions held by their affiliations, the Highway Geology Symposium (HGS), or others acknowledged above. The mention of trade names for commercial products does not imply the approval or endorsement by HGS.

### **Copyright Notice**

Copyright © 2023 Highway Geology Symposium (HGS)

All Rights Reserved. Printed in the United States of America. No part of this publication may be reproduced or copied in any form or by any means – graphic, electronic, or mechanical, including photocopying, taping, or information storage and retrieval systems – without prior written permission of the HGS. This excludes the original author(s).

## ABSTRACT

Rockfall numerical models are used to evaluate and plan highway scaling and slope protection projects. The simulation tools have been upgraded in recent years to include simulation of fragment shape, the protection provided by forests, and to consider three-dimensional geometry of slopes. The work reported in this paper is focused on the ultimate goal of developing fragmental rockfalls using physics engines.

To facilitate this objective, 193 videos of rockfall events initiated during slope maintenance were analyzed to create a database. This video data provides critical information on fragmentation, if it occurs, by capturing shape data and the full trajectory of the rockfall and any fragments produced. The variables considered cover slope and rockfall geology, shape and size are tracked alongside vegetation, and the occurrence of fragmentation. This has enabled analysis on the potential effects of geology and shape on the occurrence of fragmentation and the shape of fragments subsequently produced.

Based on initial analysis of the data, several trends are apparent. Rock type and slope material both appear to affect whether fragmentation occurs or not while a rockfall is moving down slope. Rockfalls with a compact initial shape fragment less often compared to differently shaped rockfalls. The initial rockfall shapes also have an effect on the shape of fragments produced. The three major rock types each have preferred rockfall and fragment shapes.

In the future, we will be using this database to identify events for rockfall trajectory calibration and fragmentation model development. The scope of this model will also be expanded as more varied data is added to the database, which may change or reinforce existing trends. We intend to share the database with the research community once we obtain a more broadly representative sample size of usable data.

## INTRODUCTION

Rockfall presents a constant hazard to linear infrastructure with the capacity to cause damage to property, temporary closures, and potentially injury or loss of life. Understanding how these events occur and how the rock blocks behave while moving down slope and where they come to rest is important to developing appropriate mitigation strategies. Fragmentation specifically is important to consider, as the individual fragments can have significant variation in trajectory from an intact block (1, 2). This is poorly considered using most current modeling practices, as the phenomenon of rockfall fragmentation is not well understood (1, 2).

Traditionally, rockfalls have been analyzed through tests in highly controlled areas (3, 4, 5, 6) or sporadic monitoring of a slope (7, 8). This monitoring is often done through the repeated collection of 3-Dimensional (3D) models of the slope using LiDAR or Structure From Motion (SFM) photogrammetry. Each model represents a replica of the slope at the time it was captured. Change detection, where two 3D representations of a slope are compared at two different points in time (9), provides a measure of the changes.

Change detection results cannot identify multiple rockfall events occurring at different times between scans, or a fragmental rockfall, as fragmentation occurs between the two timesteps being analyzed. Additional data such as video footage is needed alongside the change detection to assess fragmentation, as it can fill in the information gap with evidence of what actually occurred.

Video data of rockfall is limited in both number of events, and quality of the video, because rockfall events are challenging to predict and capture on camera (10). Rockfall drop tests yield high quality video data of the events, however, they are rarely performed due to the high cost. The majority of these tests are performed in quarries with limited slope geometry and geological variability. Data covering a range of different geological settings and slopes are required to better understand the factors influencing the occurrence of fragmentation and the process as a whole.

To support an investigation into these factors we have created a database of rockfall video footage, with the aim of collecting data from a wider range of geological settings across North America. We requested videos of both fragmental and non-fragmental rockfall events to provide evidence for why some events fragment and others do not. As of July 25th, 2023, we have received 193 videos from four U.S. state Departments of Transportation (DOT), and one Canadian Provincial Ministry of Transportation.

In this paper we present the state of our database to date. We will discuss how the footage was obtained, best practices for gathering videos, and report on initial analysis results regarding fragmentation. We also present an application of the database in calibrating an in-development

rockfall fragmentation simulation, and conclude with a discussion of how this work will continue moving forward.

## COLLECTION OF DATA

As noted above, the objective of data collection to support model calibration and development, is to understand the trajectory(s) and any fragmentation that occurs during the rockfall. Change detection is an effective tool to aid in the tracking, cataloguing and recreating of rockfall on slopes where continuous monitoring is not necessary or possible. Slope geometry data can also be strategically captured directly after a known event, in an attempt to focus on the change caused by one event in particular. However, critical information about fragmentation and exact trajectories are missing from an analysis done using only change detection. In some rare cases, if change was induced by the impact of rockfall fragments, it may be possible to interpolate some of the trajectories. A video of the rockfall can be used to track and understand the trajectory or solve for the number of fragments, if any, that are created during the rockfall event.

Rockfall drop tests enable control of the environment and data collection process. In these environments the slope is surveyed or otherwise captured in 3D with locations on site plotted in a coordinate system. This coordinate system allows the calculation of exact distances from the 3D model or between the surveyed points. Several papers have shown that velocity, trajectory, bounce locations and height, kinetic energy and shape characteristics can be extracted from optimally set up videos of rockfall drop tests (3, 4, 6, 11). Despite this, it is uncertain how much information can be extracted from video based data alone, or what forms of supplemental information are needed as a minimum to accurately gather trajectory, velocity and shape data.

A major limitation of video data is that it is 2-Dimensional (2D) and lacks information about detailed depth in the video plane. A minimum of 2 orthogonal viewpoint are required for video footage to simulate 3D. Impact locations can be tracked from videos and located on a 3D slope model. Ideally, a 3D model of the site can be acquired initially and after each significant rockfall event, to permit change detection analysis. This will provide unique information, when it is known that only one rockfall occurred between data acquisitions.

The video footage can also be used to analyze fragmentation events, if they occur, and to track the full trajectory of the rockfall object and any fragments produced. A video can capture the rockfall impact over several frames, allowing for visual detection of fragmentation occurring in real time. Throughout the frames of a video with a fragmental event, a rock will impact and energy will dissipate through the creation of cracks, which will then propagate until the rock is fragmented (5). More videos of the fragmentation event are required to visualize how cracks initiate and propagate in different rockfall shapes and geologies to determine the key factors affecting fragmentation.

Data was initially planned to be collected directly by the researchers, however, due to limitations placed on research travel as part of the COVID-19 lockdown, this became impossible. As such,

data for this project was collected by requesting any available videos of rockfall from all associated DOTs. Requests for data were also made at research update meetings when other parties were present, including the British Columbia Ministry of Transportation and Infrastructure. The videos gathered cover at least 57 different instances of slope maintenance with across at minimum of 33 different roads. Some roads were covered twice, however, there were no repeat instances of the same slope captured at different dates of scaling. The videos span dates between 2004 and 2022, most videos were captured between 2020-2022.

Videos used in this analysis are captured during slope maintenance campaigns as these are ideal sources of data. Rockfall are guaranteed to occur at the planned date and time in a controlled environment. Equipment set up can be planned out in advance so that videos can capture rockfall in real time and provide information about the slope and rockmass from one dataset. This must be done in a minimally invasive manner as the normal operation of the maintenance project can't be interrupted by the data collection process, and those collecting the data must be located away from any potential impact by the falling rocks. The rockfalls produced from maintenance campaigns do have an artificial initial velocity as they are being initiated manually. This could affect the total energy of the rockfall as well as the runout distance. For the purposes of investigating how and why fragmentation occurs, it currently can not be discerned whether this will have a significant effect.

Data was collected in this way to maximize the amount of video footage acquired at a low cost under the existing research constraints. Videos of rockfall can be captured on a phone camera at the lowest level of data quality, up to a stabilized DSLR or UAV images at higher levels of quality. All rockfall videos were accepted regardless of video quality, however, higher quality videos or videos with additional site specific information yielded more information and information of a higher quality. Additional data, including scale, site geology, geomechanical information, and slope morphology, is crucial to enable the quantification of several variables from video data. Minimal additional data was provided for the rockfall videos supplied by the various sources. As a result, it was not possible to accurately quantify size, trajectory and speed information from the videos for this research.

## **DEVELOPMENT OF DATA COLLECTION BEST PRACTICES**

The sporadic nature of data collection allowed for feedback on the quality of videos gathered and investigation into how to improve data quality at several stages. Best practices were developed by the authors to provide practical information regarding the capture of higher quality data. This process was iterative and refined every time more data was collected. Initially the best practice document synthesized rockfall drop test and automated shape finding research, as well as the authors' knowledge of equipment, into a user friendly manual. This focused on camera movement, focus and field of view. Rockfall drop tests generally provide ideal videos because the environment can be controlled, however, this is not possible during a maintenance campaign as it would significantly slow the work down. Instead, our research focussed on rockfalls generated from the slope by various maintenance methods. Different equipment also influences

the data collection best practices. All available video capturing equipment could not be accounted for, instead three different pieces of equipment were focused on, cell phone and DSLR cameras, and UAVs.

Data collection best practices fall into four different categories of data with different collection methods. These are photographic, video, 3D model and equipment specific data. It is assumed that specific equipment, such as LiDAR or Survey equipment, is being operated by a competent individual, so the best practices detail only when to capture this data. Several best practice recommendations involve the repeated capture of data on the slope, rockfall and road conditions. The term significant rockfall event is used to inform when data collection should be repeated. It is described for the purposes of this work as a rockfall causing change large enough to be observed on the slope. A singular video angle set up to capture all events across a whole slope will not be focused enough on any singular event to be of significant use.

Photographic data is generally supplementary information that helps understanding of the slope and road conditions. Site overview photos cover the whole slope and show the area surrounding the predicted rockfall location, the road and the ditch, if present. These photos can be used to assess ditch capacity, and slope scale structures. It is important that the photos are focused and adjusted properly as colour information can be useful to inform estimations of slope structure and geology.

In maintenance scaling campaigns there are areas on the slope where it is known rockfall will occur. This information can be used to capture photos focusing on the predicted source zone before rockfall. Enough photos for an overlap of 66% between photos in a strip and 33% between strips should be obtained for the creation of a SFM model. The same data collection process should be followed after the rockfall event has occurred. Comparison of time sequential 3D models of the source zone can enable change detection and the creation of a 3-D hull of the rockfall (12). These photos should be taken initially before any work is done and after each significant rockfall event as the slope changes.

The debris zone is another crucial area that is often not fully captured by video data. Photos highlighting the full spread of debris from a singular rockfall event can supplement videos. The spreading effects of fragmentation are important to analyze as this is another key element of understanding and managing rockfall hazards (3, 8).

Videos of the rockfall event are the most important data for this research. Videos should capture the complete rockfall path, including the source zone and initiation to the final resting location of all fragments. These videos allow analysis of rockfall in real time and capture fragmental behaviour, in addition to the effects on rockfall trajectory. In order to do so, the rockfall object must be clear and large enough in view to see the fragmentation process. In some instances, dust

generated by the rockfall event will obscure the view sufficiently to prevent this data from being collected.

Ideally the slope is captured in full before the scaling campaign begins and at the end of the campaign. In doing so, the videos can be linked to a 3D representation of the slope. Best practices were outlined for SFM slope capturing for this project but will not be discussed here. Please contact the authors for any questions or to obtain a copy of the data collection guidance documents.

## DATABASE OVERVIEW

To facilitate an investigation into fragmentation across the different slopes and geological settings, a database was created that records 66 different variables from 193 videos. All videos received before July 25<sup>th</sup>, 2022 have been analyzed and included within the database for this paper. Some of these variables were estimated from a visual analysis of the available video data. The road name or number was often given and used along with a general knowledge of geology and the source state or province geology to make estimates. Slope and rockfall rock type data were provided for 14 of the 193 videos and estimated for the remaining 179. There is limited lithological data in the database, as this is more challenging to estimate from video data and was not provided by those working on site.

There are a roughly even number of igneous and sedimentary rockfall events in the database (70 and 68 videos respectively) and fewer metamorphic rockfall events (50 videos). The database does capture a broad range of videos across the three rock types, however, each rock type has one dominant lithology that is represented. As such the videos are not representative of the whole rock type. Igneous rockfall videos are mainly represented by andesite rockfall events with 60 of the 70 videos being from andesite, three videos are of columnar basalt. Sandstone is by far the most represented sedimentary rock with 50 of the 68 videos being of sandstone rockfall events. The lithology of metamorphic slopes were challenging to identify, 14 videos are of migmatite and four videos are on metasedimentary slope complexes. In total 61 of the 193 videos do not have an accurately discernable lithology.

There is a minimum threshold for video quality beyond which the video can not be analyzed by itself. All videos can be added to the database for analysis, however, only some are sufficiently high quality videos to enable higher level analysis. As a result, a video rating system was developed. All videos received were rated using a four-tiered video rating system, ranging from category A to D, based on the amount of data that could be extracted. The system was created as a means of integrating the database research with work being done to investigate rockfall modeling inside a video game engine as a continuation of work performed by Ondercin in 2016 (13) and Sala in 2019 (14). Only Category A and B videos are usable to enable back analysis, however, the Category C videos can still yield valuable information within a database.

The Categories are defined as follows;

- Category A videos are high quality videos showing the complete path of rockfall and all fragments with minimal camera movement and can be stabilized.
- Category B videos are decent quality videos showing the complete trajectory of rockfall and all fragments. However, these videos are potentially missing individual frames of data, could have significant camera movement or may have frames partially obscured by dust.
- Category C videos are poor quality videos, missing some data (more than just a few frames), yet still show the fragmentation event or enough rockfall movement to be potentially useful. In some cases, the missing information may be remedied with extra data.
- Category D videos are any videos that do not show rockfall or have no apparent use because they are too blurry or low quality. These videos could be useful to gather information about the slope or rockmass if the video covers the same slope/slope area as a higher quality (Category A or B) video.

Category A and B are separated by the quality of the video and amount of camera movement or stability. A Category B video may not be stabilized or they may pan while zoomed to follow the rockfall or fragments. Lack of stability or significant camera movement can introduce errors in tracking the rockfall or a fragment path. Category B videos may not capture the rockfall in a large enough in frame to accurately understand shape information, even though the trajectory can still be followed. There are a limited number of videos that fully capture the fragmental event in real time and are of a quality to enable a detailed analysis with no missing information. It is through having many videos from various slopes in an array of geological settings, that investigations into the effects of geology on the occurrence of fragmentation as well as the effects of fragmentation on rockfall trajectory and rockfall hazard can be performed.

## **DATABASE ANALYSIS**

A wide array of different information is collected and housed within the database. The variables consider slope geology, geometry, location, vegetation, as well as rockfall geology, geometry, trajectory, fragmentation and fragment shape. Several video specific variables, such as resolution, frame rate, and equipment, are tracked to enable investigation into the minimum required data quality. Information about the method of initiation is also collected for future investigation into the potential affects of the initiation method (pry bar, air bag, human throw or machine scaling) on rockfall trajectory and fragmentation.

A frequency magnitude curve is often used to approximate the occurrence of rockfall of various sizes (15, 16). These curves are slope specific and tend to exhibit a power law trend for the frequency of rockfall, where more small rockfall events occur with a decreasing amount of larger

rockfall events. The fragmental rockfall video database does not follow the expected frequency magnitude power law curve that most slopes exhibit, however. The data was collected across many different slopes, with each individual rockfall being generated by maintenance activities. As such, this database lacks the temporal element of a traditional frequency magnitude curve, and is limited to the block sizes that are large enough to be identified for scaling campaigns, but which are small enough to be generated using these methods.

The estimated size of the primary rockfall events assessed is plotted in Figure 1. A traditional data pattern would result in the fewer numbers of each group of rockfalls, as the volume increases. This pattern is not observed in this data. It is hypothesised that two factors are influencing this deviation. There are a large number of rockfall events that occur during a scaling campaign, leading to selective capturing of rockfall events, especially in an informal data collection scenario. It is therefore hypothesized that the number of rockfall videos is not an accurate reflection of the true number and size distribution of rockfalls initiated during a scaling project. Videos taken appear to focus on medium sized rockfalls, resulting in fewer videos of small rockfall events. The under sampling of small rockfalls is also because when there are multiple rockfalls in one video, the rockfall that is best seen or has the most data is tracked by the videographer. Small rockfalls are often more challenging to see, as a result, these events are often not analyzed and added to the database.

Secondly, it is hypothesised that the increase in medium (0.05 to 0.4 m<sup>3</sup>) sized rockfalls in the database is due to the focus of the slope maintenance work. Scaling specifically targets rocks that are identified as a potential hazard, and that can be liberated by scaling methods. Larger blocks are sometimes removed by controlled blasting. To the knowledge of the authors, there is no specific research explaining the effect of slope maintenance on the frequency magnitude curve of a slope, because longer duration maintenance records have not been made available as data sources.

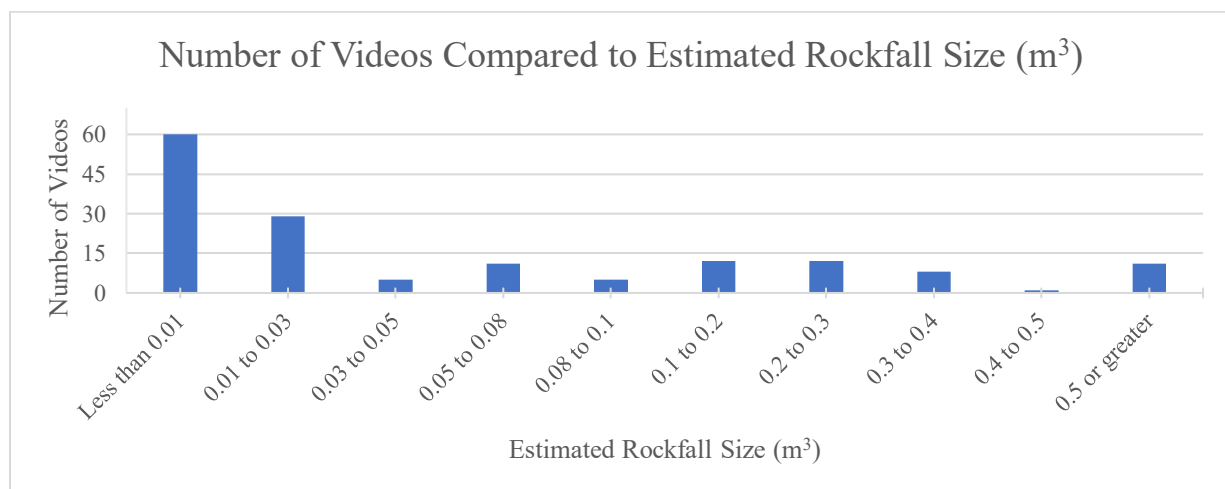


**Figure 1: Number of Videos Compared to Estimated Rockfall Size (m<sup>3</sup>)**

## TRENDS IN OCCURRENCE OF FRAGMENTATION

Research suggests that a fragmental rockfall will likely affect a longer section of linear infrastructure and take a significantly different trajectory compared to a non-fragmental rockfall (1, 8). Fragmentation not only changes the trajectory, but also affects the size and shape of the rockfall. The reduced size and different shape of fragments will yield different kinetic and rotational energies as the weight and moment of inertia of the rockfall changes (1, 11). As a result, prediction of fragmentation should be included in hazard analysis of linear infrastructure and rockfall modelling.

Fragmentation can occur either along existing structure within the rock block or due to impact induced fracturing of the intact rock. Research into factors with a potential effect on fragmentation of a rockfall have show that structure is a critical factor, as fragmentation often occurs along existing structure (17). The kinetic energy at time of impact also plays a role, where higher kinetic energies at impact increase the intensity of fragmentation (5, 18). Despite the knowledge that these factors influence fragmentation, the extent of their effects is not well understood (4, 17).

As shown in Figure 2 the analysis of the database at present has yielded an interesting trend on the potential effect of geology on fragmentation. Considering videos where it was possible to determine events with fragmentation and non fragmentation, Igneous rocks fragment more often (72%), followed by Sedimentary (62%) and Metamorphic rocks (57%).

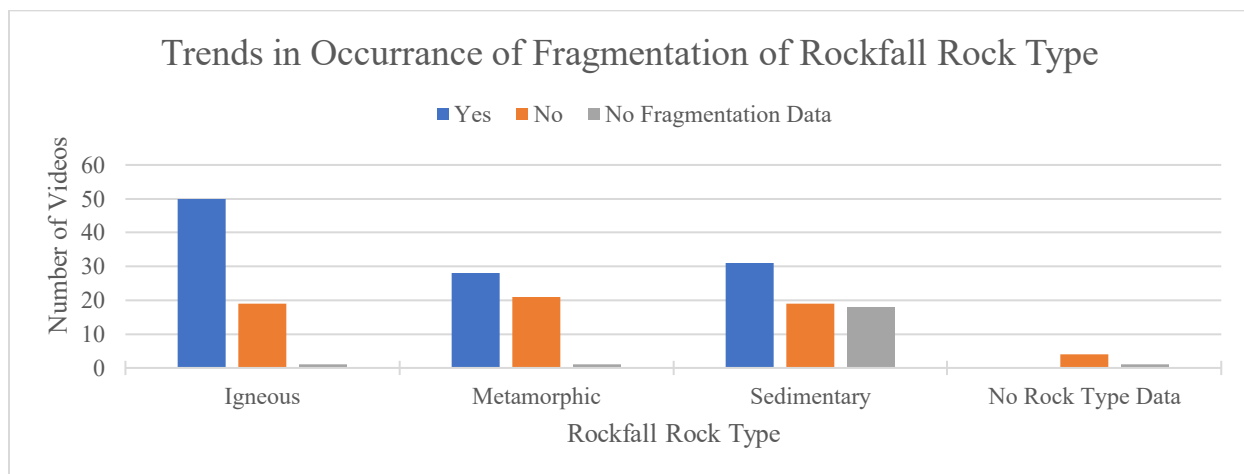


**Figure 2: Trends in Occurrence of Fragmentation of Rockfall Rock Type**

The Coefficients Of Restitution (COR) are used in rockfall modeling to calculate the change in rotational and kinetic energy at each impact of the rockfall object on the slope (19). The slope material at the impact location determines the amount of energy absorbed upon each impact as the COR is material dependant (4, 19, 20). Fragmentation occurs when there is enough force applied to either existing structure within the rockfall object or intact rock to initiate crack

propagation resulting in the separation of one section of the rockfall from another (5). Loose material, such as soil and talus, absorbs more energy on impact than bedrock and decreases the amount of energy within the rockfall (19, 21). The likelihood of fragmentation appears to be decreased for rockfall on soil or talus (5). The first impact material is defined as the slope material at the rockfall object's first impact. It can be seen in Figure 3 that most rockfall with a first impact on rock go on to fragment at some point during their fall, and that most fragmental rockfall have a first impact on rock. A total of 80% of videos showing fragmentation have a first impact on rock, with 12% and 3% of fragmental videos having a first impact on soil and talus respectively. Most non-fragmental rockfall have a first impact on soil with 48% of videos, while 26% of non fragmental videos have a first impact on talus and rock each.

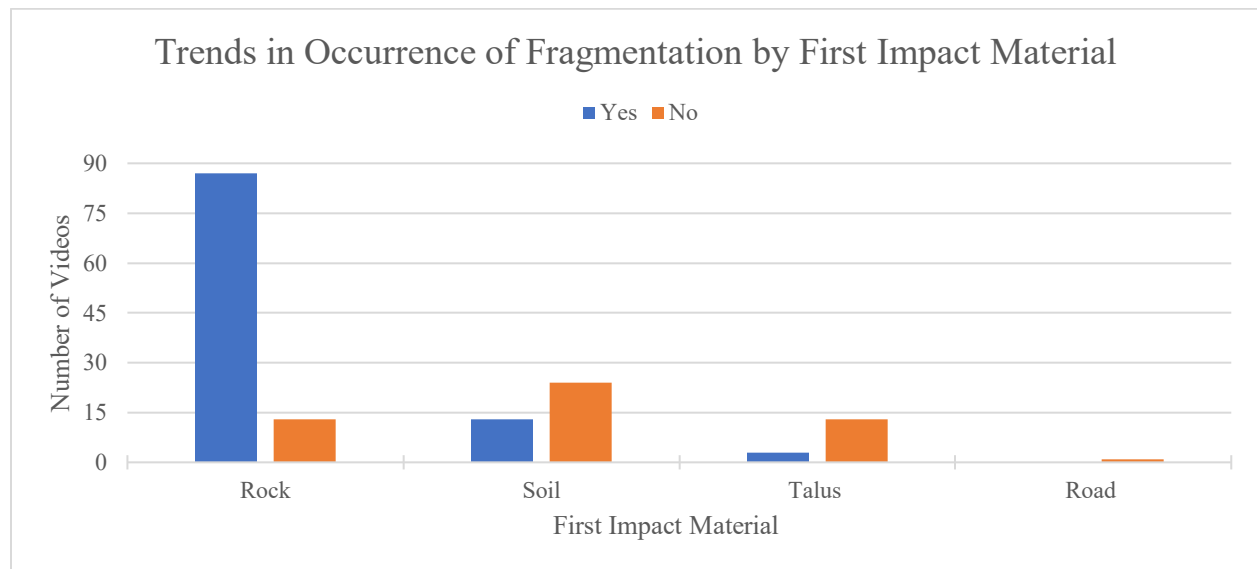


**Figure 3: Trends in Occurrence of Fragmentation by First Impact Material**

This trend is also observable when only videos that fragment on first impact are included. There are 109 videos with fragmentation, wherein 72 of these rockfalls fragmented on the first impact. The majority of these videos (61 of 72) that fragment on the first impact landed on a rock surface, with nine videos fragmenting on soil. These nine videos fall into one of two categories either, disaggregating along pre-existing structure or experienced a prolonged freefall before the first impact on soil.

The shape of the rockfall object is linked to the occurrence of fragmentation in the videos reviewed to date. As seen in Figure 4, bladed rockfalls have the highest rate of fragmentation (74). Compact rockfall fragmented the least (53%). Platy and elongated have a fragmentation rate between bladed and compact shapes, at 70%. Rockfall shape can often be predicted based on the slope structure and resulting block geometry.

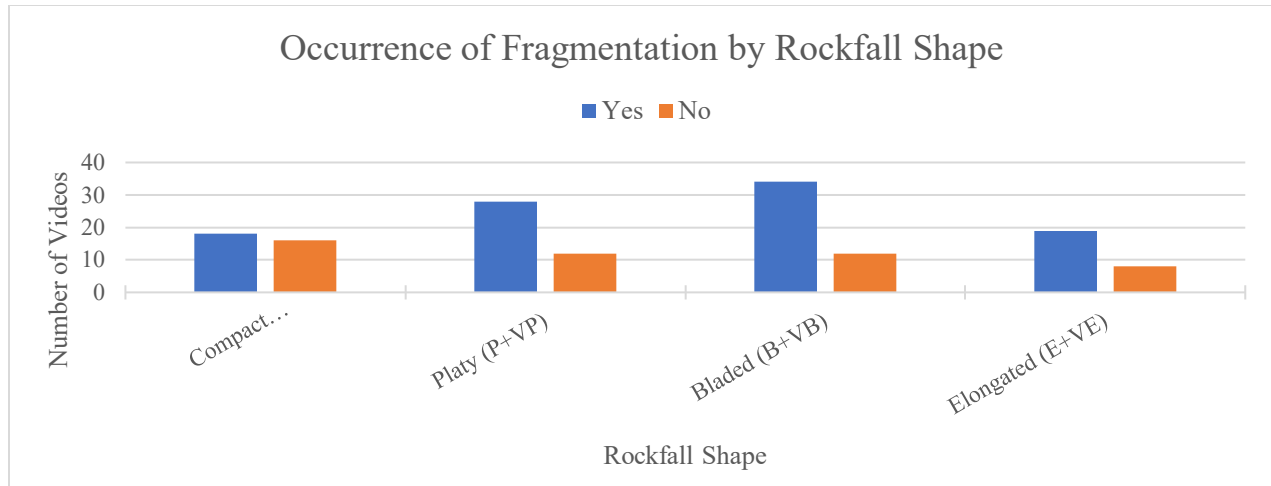


**Figure 4: Occurrence of Fragmentation by Rockfall Shape.**

### TRENDS IN ROCKFALL AND FRAGMENT SHAPE

Rockfall shape can affect the trajectory, speed and impact parameters of rockfalls and any fragments produced (11). It is important to understand trends in the shape of rockfall or fragments as they can affect variables that factor into a hazard analysis and the outcomes of a rockfall model, such as speed, trajectory and size (11). In this research, rockfall shape is classified using aspect ratios in the same way as Bonneau et al. in 2019 (22). Aspect ratios are estimated based on visual analysis of the videos and are used because they are a relative measurement that can be made without knowing specific dimensions within a video.

The three different rock types produce different rockfall and fragment shape trends, as seen in Figures 5, 6 and 7. Table 1 shows that igneous rockfalls occur more often in platy and bladed shapes with very few videos from the other shape categories. Videos of metamorphic rockfall are more commonly bladed in shape. Sedimentary rock has a less clear trend with respect to rockfall shape, however, have a greater variety of rockfall shapes compared to the other rock types.

Rock Type	Rockfall Shape									
	C	CP	CB	CE	P	B	E	VP	VB	VE
Igneous	10	2	1	0	18	18	11	2	1	0
Metamorphic	8	1	0	0	5	14	3	2	1	1
Sedimentary	8	0	1	0	11	5	12	8	7	3

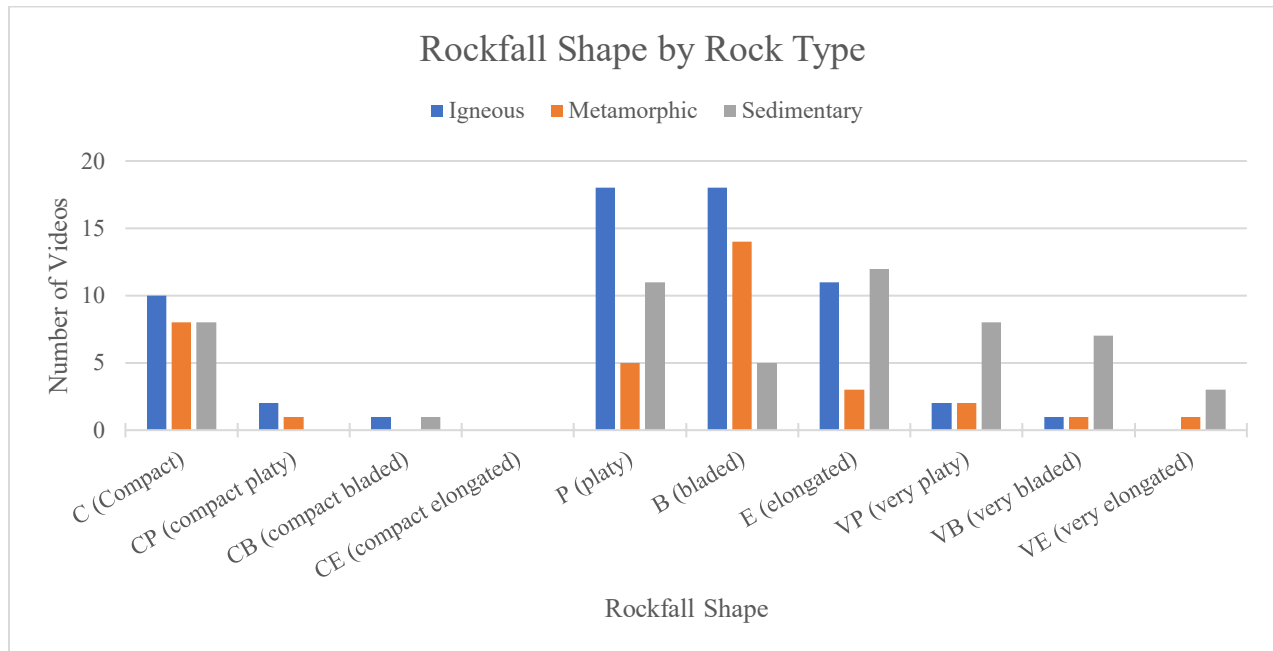


**Figure 5: Rockfall Shape by Rock Type**

Fragment shape is separated into primary and secondary to more accurately represent all fragments produced. The primary fragment shape is the most common shape, based on axis ratios and the previously defined shape classes. Secondary fragment shape is the second most common shape. If there is only one prevalent fragment shape, then there will be no secondary fragment shape. The aspect ratios are extracted from the videos by assessing the rockfall as it rotates. In order to do so, the three main axis of the rockfall must be visible in at least one frame from each video.

The different rockfall rock types have preferred primary fragment shapes as seen in Figure 6. Igneous rockfall produce bladed primary fragments in 21 of the 70 videos of fragmental igneous rockfall. When not fragmenting into bladed primary fragments, igneous rockfall produced platy, compact and elongated primary fragment shapes in 10, 8 and 6 videos respectively with very little representation of any other shape class. Sedimentary and metamorphic rock types have more variety in the primary fragment shapes produced. Metamorphic rockfall most commonly produce compact primary fragment shapes, at 9 videos. Platy, bladed or elongated primary fragment shapes were produced roughly equally where 4 videos have platy primary fragments and 5 videos have bladed and elongated primary fragments for fragmental metamorphic videos. Sedimentary rockfall display a wider array of primary fragment shapes. There is not a single clearly preferred primary fragment shape for sedimentary rockfall within the database and sedimentary rockfall have the most videos with a lack of fragment shape data at 18 of the 49 videos of fragmental sedimentary rockfall. This is because dust clouds obscured the fragment shapes in these videos. The remaining 31 videos that fragment are most commonly bladed with 7

videos, followed by 5 platy and very bladed, 4 compact and very platy, then 2 elongated and very elongated.

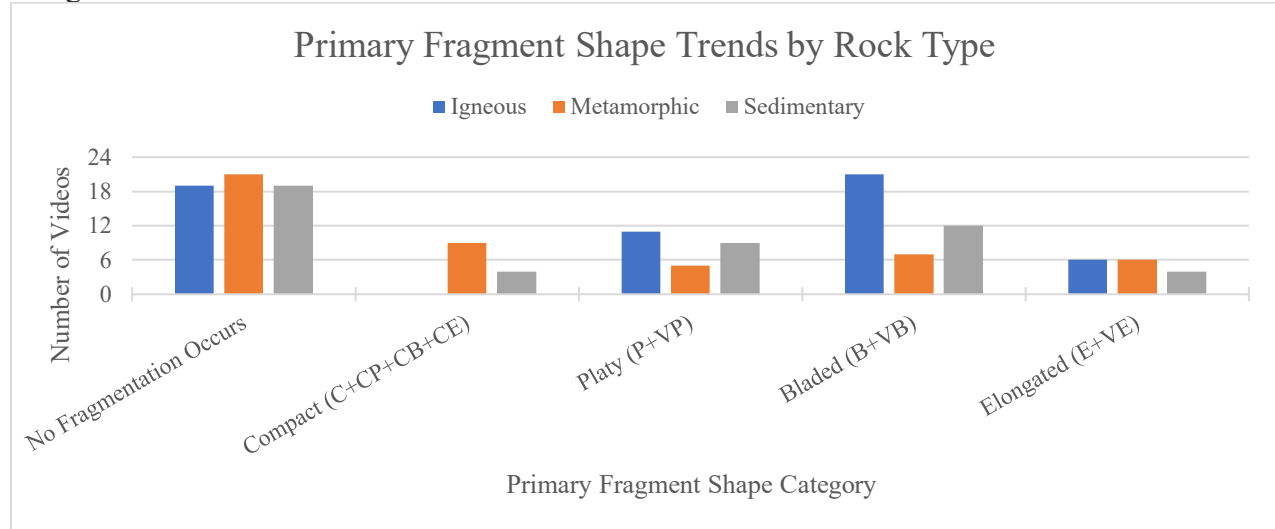


**Figure 6: Primary Fragment Shape Trends by Rock Type.**

Both primary and secondary fragment trends are important to analyze individually and as a whole to understand the shapes that are being created during fragmentation. As shown in Figure 7, only 18 videos displayed no secondary fragment shape despite fragmentation occurring and a primary fragment shape being discernable. This indicates that in 86 of the fragmental videos with a primary fragment shape, the fragments are represented by more than a single fragment shape. There is an increase in the presence of compact fragment shapes in the secondary category. Sedimentary rockfalls tend to produce the most compact secondary fragments, with 12, more than any other fragment shapes. Igneous rockfalls produced an equal amount of compact and bladed secondary fragments, at 16, and 9 platy fragments. Bladed secondary fragments are the most common from metamorphic rockfall at 9 videos with 8 videos having compact secondary fragments.

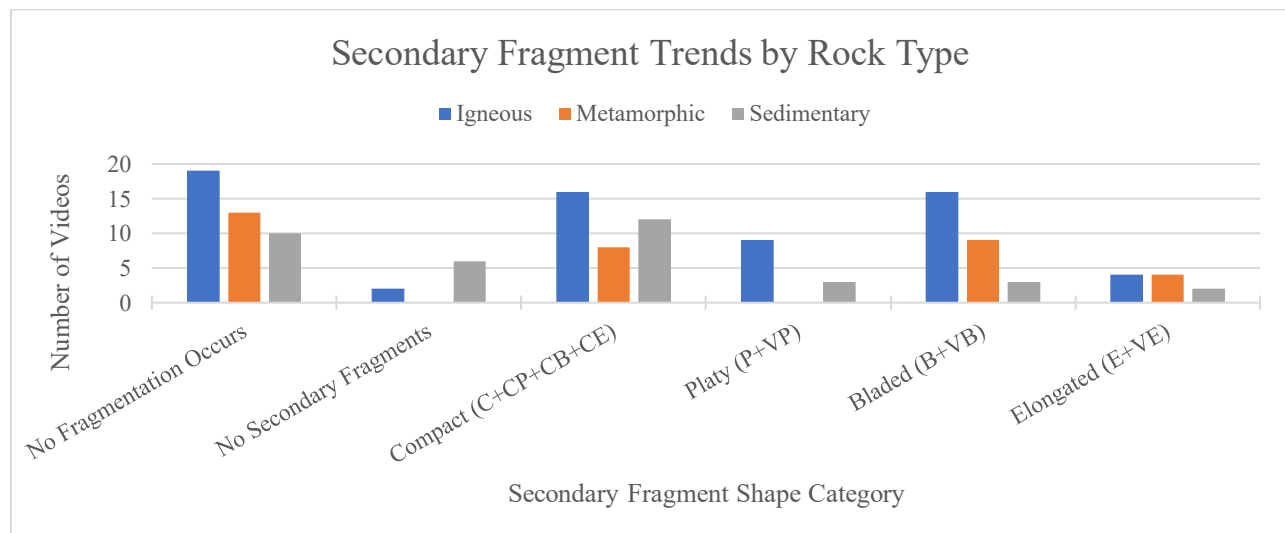


**Figure 7: Secondary Fragment Shape Trends by Rock Type.**

All shape classes will not be used for all analysis, instead, the categories will be combined into only four categories, each composed of several previous categories. This results in only compact, platy, bladed and elongated categories. The compact category includes compact platy, compact bladed and compact elongated. The platy, bladed and elongated categories then include the extreme ends of each category.

Bladed is by far the most common fragment shape from either primary or secondary fragment shapes combined with a total of 65 videos capturing bladed fragment shapes. Instances where the primary fragment shape is not bladed have a secondary fragment shape of bladed in 25 of the 64 videos without a bladed primary fragment shape. Compact is the second most common fragment shape with 59 videos having compact primary or secondary fragment shapes. Compact is the secondary fragment shape in 36 of the 81 rockfall with a different primary fragment shape. Platy and elongated shaped fragments occur less frequently but at a roughly even rate with 34 and 35 videos having either fragment shape in the primary or secondary category.

Rockfall shape seems to affect the shape of both primary and secondary fragments created during fragmentation. Compact rockfall evenly produce compact, bladed and elongated primary fragments as well as compact and bladed secondary fragments. Platy rockfall tend to produce platy and bladed primary fragments with only four instances of other primary fragment shapes. Secondary fragments tend to be either bladed or compact with a second tier of platy and elongated. Rockfall with a bladed shape most often produce bladed shaped primary fragments. Compact, platy and elongated primary fragments are still produced at roughly even, though lesser, rates of occurrence for bladed rockfall. Secondary fragment shapes of bladed rockfall are mainly compact with the remaining shapes all represented to a smaller degree. Elongated rockfall produced the most bladed and elongated primary fragments, as well as, compact secondary fragments.

## **DEVELOPING A FRAGMENTAL ROCKFALL MODEL**

One application for the rockfall database is to identify events for rockfall trajectory calibration and fragmentation model development. The mechanics of rockfall fragmentation are difficult to quantify and implement in a model due to the complexity of the impact and fragmentation process, its dependence on several site-specific variables, and a lack of holistic case studies that can be used for reference.

Following work done by Ondercin in 2016 (13) and Sala in 2019 (14), we are developing a rockfall fragmentation simulation using the Unity game engine. This affords us several benefits such as tools to support realistic environment models, interface design, and perspective controls, but most importantly supports customizable dynamic physics behavior through its physics engine.

While Ondercin's work laid the foundation for building a rockfall simulation in this manner and Sala's work extended this approach to include several rock slope event case studies and developed a basic approach to fragmentation modeling, our current focus is on a more comprehensive fragmentation model that behaves more realistically and can be tuned to consider different input scenarios. Since a deterministic model of the physics of interacting blocks in a rockfall, and more importantly the details of the fragmentation process are not available, tuning an approximate model against field cases is the best available approach.

Currently, the rockfall simulation features fragmentation options before or during runtime, pseudorandom variations in fragmentation pattern, fragmentation of fragments, arbitrarily set damage thresholds, and a rudimentary implementation of planar joint fragmentation. These features are all modifying the Voronoi fragmentation process commonly found in 3D modeling software such as Blender. This method works by placing a set number of points at different positions through a 3D object and subdividing the object into fragments based on those points (23). While Voronoi fragmentation is functional for a proof of concept and simulation testing, we are working towards developing a more realistic approach to modeling fragmentation.

This event database is vital to the development of such a fragmentation model as it provides real examples of how a block of a particular material in a particular setting behaved and fragmented in a rockfall scenario. While video alone is insufficient data for capturing the totality of a rockfall event, it is still helpful in several ways. Along with providing a visual reference to compare our simulation outputs with, good video footage allows us to interpret further information such as number of fragments, size of fragments, size distribution of fragments, number of bounces, bounce heights, area of impact, spatial distribution of fragments at the toe of the slope and more.

Several of these quantities are approximations at best, when the only data provided for an event is a video recording. Combining the video data with images and LiDAR scans of the site before and after the event took place, photos of the fragment distribution, and field notes such as rock type, composition, and joint orientations allows us to construct a more complete picture of the event as it occurred. The more complete this picture becomes, the better we can calibrate our rockfall fragmentation behavior to match it.

## **CONCLUSIONS AND FUTURE WORK**

In summary, we created a database to capture the results of analysis of a video footage from a variety of geological settings and slopes. This footage is useful for understanding how rockfall events occur and is crucial for understanding fragmentation specifically. Our initial analysis of the data shows that rock type and slope material both appear to affect whether or not a rockfall will fragment while moving down slope. Rockfalls with a compact initial rockfall shape also fragment less often than rockfalls with a different initial shape. The three rock types discussed also have preferred initial rockfall shapes and fragment shapes as shown in Table 2, and each initial rockfall shape has a preferred fragment shape as shown in Table 3. The spreading effect of

fragmentation on the trajectory of the rockfall was observed throughout the videos, where after fragmentation the fragments would disperse from the gravity parallel line. The slope geometry, number of fragments produced, and the amount of talus or soil on slope were also analyzed for their effects on fragmentation, however, these trends were less evident. These trends could be refined through the addition of more videos to the database.

**Table 2 - Relationships Between Rock Types and Preferred Rockfall and Fragment Shapes**

<b>Rock Type</b>	<b>Initial Block Shape</b>	<b>Most Common Fragment Shape(s)</b>
Igneous	Bladed and Platy	Compact and Bladed
Metamorphic	Bladed	Compact
Sedimentary	Elongated and Platy	Compact and Bladed

**Table 3 - Relationship Between Initial Rockfall Shape and Fragment Shape**

<b>Initial Rock Block Shape</b>	<b>Most Common Fragment Shape(s)</b>
Compact	Compact and Bladed
Platy	Compact, Platy and Bladed
Bladed	Compact and Bladed
Elongated	Compact and Bladed

Moving forward, our immediate goals are to develop the rockfall fragmentation simulation to a testable state and to use the database as described to calibrate the fragmentation model in various case studies. Based on that calibration dataset we can perform a sensitivity analysis on the simulation inputs, improve the fragmentation model, and focus on implementing features to extract output data as applicable.

With respect to the database our aim is to continue expanding it with new content as it becomes available, and actively encourage our research partners to contribute where they are able. As more varied data is added, current trends may change or be reinforced. Once the database reaches a more broadly representative sample size of higher quality data, we intend to share it with the research community to facilitate different research goals across a wider array of applications.

**REFERENCES:**

1. Giacomini et al. Experimental studies on fragmentation of rock falls on impact with rock surfaces. *International Journal of Rock Mechanics and Mining Sciences* vol. 46(4), 2009, pp. 708-715.
2. Crosta et al. Key Issues in Rock Fall Modeling, Hazard and Risk Assessment for Rockfall Protection. *Engineering Geology for Society and Territory* vol. 2, 2015, pp. 43-58.
3. Matas et al. Simulation of Full-Scale Rockfall Tests with a Fragmentation Model. *Geosciences* vol. 10(5), 2020, 168.
4. Gili et al. Rockfalls: analysis of the block fragmentation through field experiments. *Landslides* vol. vol. 19, 2022, pp. 1009-1029.
5. Guccione et al. An Experimental Setup to Study the Fragmentation of Rocks Upon Impact. *Rock Mechanics and Rock Engineering* vol. 54, 2021, pp. 4201-4233.
6. Noel et al. Rockfall trajectory reconstruction : A flexible method utilizing video footage and high resolution terrain models. *Earth Surface Dynamics* vol. 10(6), 2022, pp.1141-1164.
7. Kromer et al. Managing rockfall risk through baseline monitoring of precursors using a terrestrial laser scanner. *Canadian Geotechnical journal* vol. 54(7), 2017, pp. 953-967.
8. Corominas et al. Quantitative analysis of risk from fragmental rockfalls. *Landslides* vol. 16, 2019, pp. 5-21.
9. Kromer et al. A 4D Filtering and Calibration Technique for Small-Scale Point Cloud Change Detection with a Terrestrial Laser Scanner. *Remote Sensing* vol. 7(10), 2015, 13029-13052.
10. Hantz et al. Definitions and Concepts for Quantitative Rockfall Hazard and Risk Analysis. *Geosciences* vol. 11(4), 2021, 158.
11. Caviezel et al. The relevance of rock shape over mass – implications for rockfall hazard assessments. *Nature Communications* vol.12, 2021, 5546.
12. Bonneau, D. DiFrancesco, P-M. and Hutchinson, J. Surface Reconstruction for Three-Dimensional Rockfall Volumetric Analysis. *International Society for Photogrammetry and Remote Sensing International Journal of Geo-Information* vol. 8, 2019, 12.
13. Ondercine, M. An Exploration of Rockfall Modelling through Game Engines. M.A.Sc., Queen's University, Kingston, Ontario, 2016.
14. Sala, Z. GAME-ENGINE BASED ROCKFALL MODELLING; TESTING AND APPLICATION OF A NEW ROCKFALL SIMULATION TOOL. M.A.Sc., Queen's University, Kingston, Ontario, 2018.
15. Guerin et al. Quantifying 40 years of rockfall activity in Yosemite Valley with historical Structure-from-Motion photogrammetry and terrestrial laser scanning. *Geomorphology* vol. 356, 2020, 107069.
16. Graber, A. and Santi, P. Power law models for rockfall frequency-magnitude distributions: review and identification of factors that influence the scaling exponent. *Geomorphology* vol. 418, 2022, 108463.
17. Ruiz-Carulla, R. and Corominas, J. Analysis of Rockfalls by Means of a Fractal Fragmentation Model. *Rock Mechanics and Rock Engineering* vol. 53, 2019, pp. 1433-1455.
18. Zhao et al. Investigation of rock fragmentation during rockfalls and rock avalanches via 3-D discrete element analyses. *Journal of Geophysical Research: Earth Surface* vol. 122(3), 2017, pp. 678-695.
19. Bi et al. Investigating the Effect of Preimpact Energy Dissipation on Coefficient of Restitution regarding the Slope-Boulder Interaction. *Advances in Civil Engineering* vol. 2021, 2021, 9929119

20. Bourrier et al. Bayesian stochastic modeling of a spherical rock bouncing. *Natural hazards and Earth System Sciences* vol. 9(3), 2009, pp. 831-846.
21. Pichler, B., Hellmich, Ch. and Mang, H.A. Impact of rocks onto gravel Design and evaluation of experiments. *International Journal of Impact Engineering* vol. 31, 2005, pp. 559-578.
22. Bonneau et al. Three-dimensional rockfall shape back analysis: methods and implications. *Natural Hazards and Earth System Sciences* vol. 19(12), 2019, pp. 2745-2765.
23. Rayfire Studios. *Rayfire for Unity*. Rayfire Studios.  
<https://assetstore.unity.com/packages/tools/game-toolkits/rayfire-for-unity-148690> Accessed June 14, 2023.

## **Emergency Response and Cures for Karst on Chemical Road**

**Sarah McInnes, PE**

PennDOT Engineering District 6-0  
7000 Geerdes Boulevard, King of Prussia, PA 19406  
610-205-6544  
[smcinnnes@pa.gov](mailto:smcinnnes@pa.gov)

**Timothy Homan, PE**

PennDOT Engineering District 6-0  
7000 Geerdes Boulevard, King of Prussia, PA 19406  
610-585-8254  
[tihoman@pa.gov](mailto:tihoman@pa.gov)

**Jeremy J. Brown, PE**

Schnabel Engineering  
3 Dickinson Drive, Suite 200, Chadds Ford, PA 19317  
610-696-6066  
[jbrown@schnabel-eng.com](mailto:jbrown@schnabel-eng.com)

Prepared for the 72<sup>nd</sup> Highway Geology Symposium, August 2023

### **Acknowledgements**

The authors would like to thank the following individuals/entities for their contributions in the work described:

Pennsylvania Department of Transportation, Engineering District 6-0  
Schnabel Engineering  
Temple University  
Traffic Planning and Design, Inc.  
Susquehanna Civil, Inc.  
Road-Con, Inc.  
Keller North America

### **Disclaimer**

Statements and views presented in this paper are strictly those of the author(s), and do not necessarily reflect positions held by their affiliations, the Highway Geology Symposium (HGS), or others acknowledged above. The mention of trade names for commercial products does not imply the approval or endorsement by HGS.

### **Copyright Notice**

Copyright © 2023 Highway Geology Symposium (HGS)

All Rights Reserved. Printed in the United States of America. No part of this publication may be reproduced or copied in any form or by any means – graphic, electronic, or mechanical, including photocopying, taping, or information storage and retrieval systems – without prior written permission of the HGS. This excludes the original author(s).

## ABSTRACT

A section of Chemical Road in Plymouth Township, Pennsylvania, had been experiencing subsidence due to karst geology since August 2020. On February 28, 2021, a sinkhole in the roadway closed the I-476 northbound off-ramp lane onto eastbound Chemical Road. Additional sinkholes were observed in the creek adjacent to the embankment slope supporting the road, and ongoing subsidence created a hazardous condition. Due to safety concerns from the progressive sinkhole activity, PennDOT closed the road and initiated an emergency project. Working closely together, the project team developed an expedited design that included grouting and sinkhole plugging treatment to reduce the risk of future subsidence. The design and construction of the repair had to be completed by the end of 2021 to reopen the road and restore public safety and mobility in the Plymouth Meeting area.

The design team performed geophysical and test boring explorations and produced bid documents for PennDOT review within one month of closing the roadway. Subsequently, the project was advertised a month later. Due to the schedule and complex nature of karst, collaboration during construction was critical. The project also involved several challenges with right-of-way, environmental, utilities, and hydrology/hydraulics issues. The team worked together to reopen the roadway in mid-December 2021. This schedule would not have been possible without effective and consistent communication among the team members. This paper describes the challenges presented by the project and how they were addressed by the team to meet the goal of restoring the roadway as quickly as possible.

## INTRODUCTION

A section of SR 3015 (Chemical Road) and the adjacent streambed of Plymouth Creek in Plymouth Township, Montgomery County, Pennsylvania, experienced subsidence and sinkhole activity after a tropical storm event. The site is mapped as being underlain by carbonate bedrock, and several karst-related events were observed at the site from August 2020 to March 2021 that affected multiple lanes of Chemical Road. After a February 28, 2021, sinkhole event, PennDOT initiated a geotechnical/geophysical investigation and settlement monitoring. Due to further sinkhole/subsidence activity across all five lanes, PennDOT closed Chemical Road for safety on March 25, 2021, and initiated an emergency project. PennDOT Engineering District 6-0 retained Schnabel Engineering (Schnabel) to lead the evaluation and design of the project. Schnabel was supported by subconsultants Traffic Planning and Design (TPD) and Susquehanna Civil Inc. (SCI). All four entities are referred to as the “design team.”

The project area is about 1,000 ft long, generally runs in the east-west direction, and is located between I-476 and West Germantown Pike. The technical direction of the lanes traveling to the west and east are southbound and northbound, respectively. At this location, the roadway is five lanes wide, with two southbound lanes (vehicle movement toward the west at the project site) and three northbound lanes (vehicle movement toward the east at the project site); the outside northbound lane is a dedicated off-ramp from NB I-476. The Average Daily Traffic (ADT) at this segment of road is nearly 27,000 vehicles. The southbound lanes of Chemical Road are supported by a 15 to 20 ft tall embankment with a slope that varies from approximately 1.5H:1V to 2H:1V within the project area. At the base of the embankment is Plymouth Creek, which is typically dry until after significant precipitation. There are a considerable number of subsurface and overhead utilities running along Chemical Road. The Plymouth Meeting area is a generally congested traffic area located just outside Philadelphia and includes the junction of I-276 (Pennsylvania Turnpike) and I-476 (Blue Route) along with several critical arterials that also serve as access to I-76 (Schuylkill Expressway). Chemical Road serves as a critical link between Ridge Pike and Germantown Pike and provides access to and from I-476 as shown on Figure 1.

To restore mobility in the congested Plymouth Meeting area, the emergency construction needed to be completed and Chemical Road reopened by the end of 2021. The site constraints posed several challenges and required effective and consistent communication among all team members to meet this goal. The site constraints discussed in this paper include complex karst geology, presence of Plymouth Creek with respect to a source of water for sinkholes, flooding of the creek during rain events, environmental permitting considerations for working in the creek, right-of-way (ROW) and access, dense system of underground utilities, overhead utilities, and the steep embankment slope adjacent to the roadway. These site features and the accelerated schedule resulted in a complex project that had to be designed and constructed in a short amount of time to reopen the road by the desired deadline.

This paper discusses the collaboration required to execute the project, including the “Cures” for karst, which cannot technically be “Cured” but was treated in order to reduce the risk of future sinkholes and subsidence.

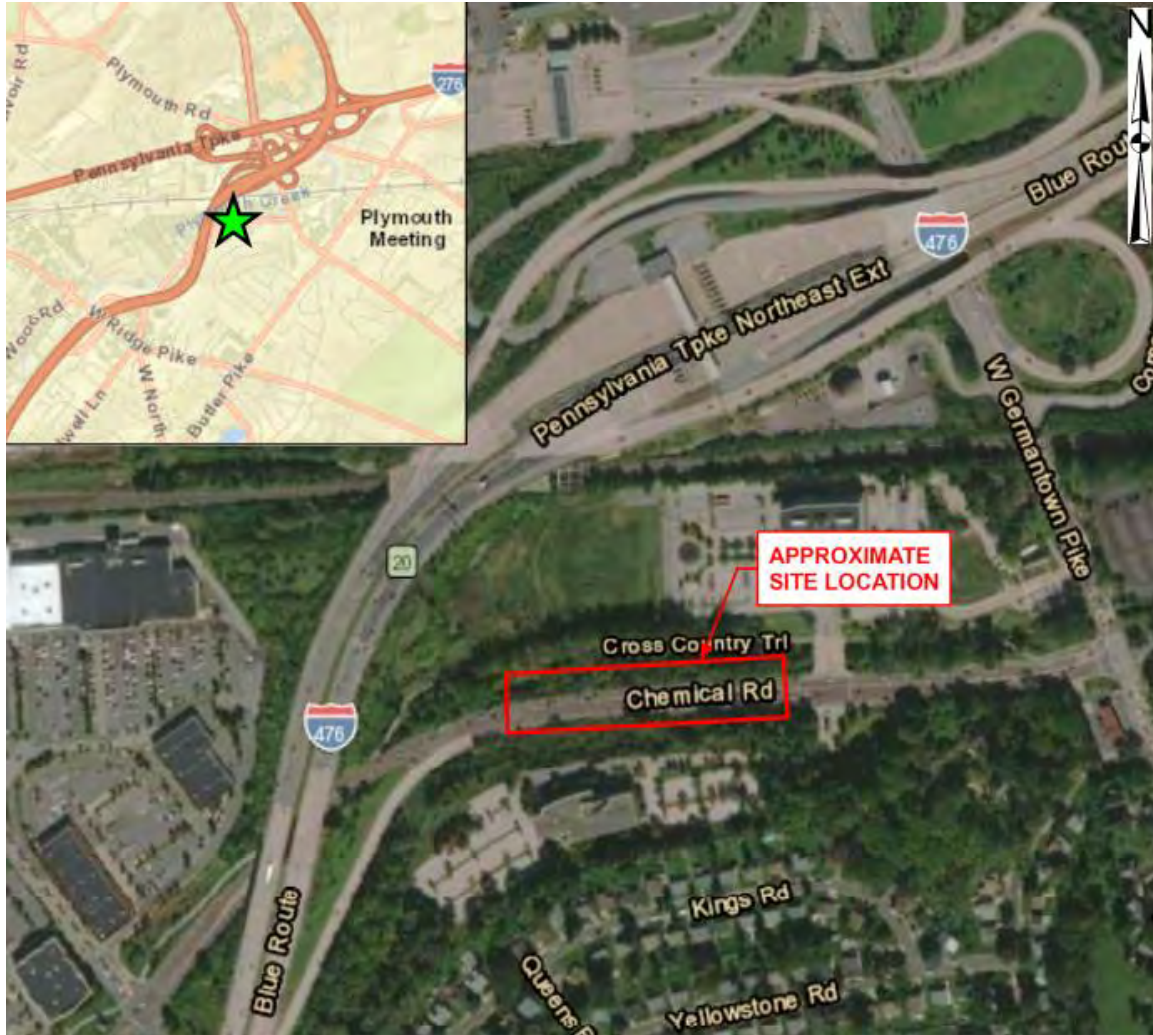
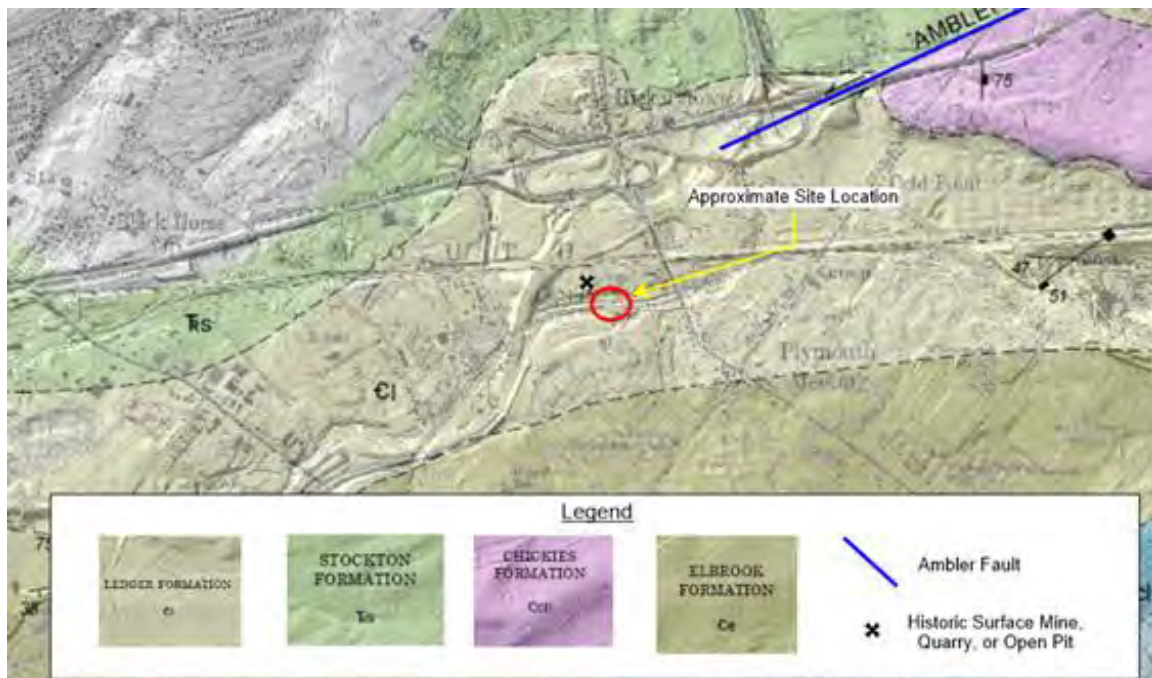


Figure 1 – Location Map

### REGIONAL GEOLOGY (1, 2, 3)

The site is located within the Piedmont Lowland Section of the Piedmont Physiographic Province and is underlain by the Cambrian Age rock of the Ledger Formation (C1) (Kochanov 2016). In the surrounding area, the Chickies (Cch), Stockton (C<sup>rs</sup>), and Elbrook (Ce) Formations are mapped and consist of mudstone and siltstone, crystalline quartzite, and dolomite, respectively. Figure 2 includes the approximate site location overlain on a bedrock geologic map.



**Figure 2 – Geologic Map Of The Project Area**

The Ledger Formation consists of dolomite, which is a carbonate rock and is commonly susceptible to chemical weathering and karst feature development such as deeply weathered fracture zones, pinnacled bedrock surface, soft soil adjacent to the bedrock, and sinkholes. According to Karst Features in Pennsylvania, provided by the Pennsylvania Department of Conservation and Natural Resources (PADCNR), approximately 160 karst features (surface depressions and sinkholes) are mapped within about a 1.5-mile radius in this formation.

### TIMELINE OF EVENTS

In August 2020, Tropical Storm Isaias caused widespread flooding in the Philadelphia area and dropped up to 9 inches of rain in Montgomery County. Subsidence occurred in the outermost southbound lane of Chemical Road immediately following the tropical storm. Repairs were made by PennDOT Maintenance due to the subsidence of the roadway, curb, and guide rail. Following this treatment, subsidence continued for several months, and the outside southbound lane was eventually closed.

During a site visit on December 3, 2020, Schnabel and PennDOT personnel observed a sinkhole within Plymouth Creek at the toe of the embankment. A geosynthetic liner in the creek was damaged and undermined in the observed sinkhole. The recently repaired section of asphalt and concrete curb showed signs of additional subsidence with cracking observed over a wide area of roadway surrounding the repaired pavement. Additionally, two overhead utility poles spaced about 300 ft apart appeared to have tilted toward Plymouth Creek, causing their guywires to become loose.

On February 28, 2021, a new sinkhole event in the outside northbound lane (across the roadway from the subsided area in the southbound lane) caused the NB I-476 off-ramp lane to be closed as shown on Figure 3. Due to continued observed subsidence on the roadway, PennDOT initiated the closure of Chemical Road on March 25, 2021, and classified the project as an “emergency” project. PennDOT initiated an emergency geotechnical and geophysical investigation to be conducted, led by Schnabel, to develop sinkhole treatment recommendations.



**Figure 3 – Sinkhole Repair on I-476 Off-ramp with Chemical Road  
Southbound Lane Closed Prior to Closure of Chemical Road**

During the first week of March 2021, notice of intent to enter and legislator letters were sent out in advance of survey and geophysical field work. Schnabel began the geophysical investigation on March 8, 2021, and in early April 2021 a test boring program was undertaken based on the data from the geophysical investigation.

Numerous critical design activities were performed between March and May 2021 to advertise the project in time to complete construction by the end of 2021. Activities included site visits, surveying, test borings, geophysical investigations, lab testing, hydrology and hydraulics (H&H) evaluation, utility coordination, constructability reviews, ROW evaluation, permitting, and preparation of a construction bid package.

After the geotechnical and geophysical investigation, a Limited Mobility Grout (LMG) plan was developed. Bid documents were developed and the project was advertised, awarded, and the general contractor received Notice-to-Proceed on July 6, 2021. The contractor proceeded with performing sinkhole treatment and roadway reconstruction. Schnabel then conducted a post-grouting geophysical investigation between December 12 and 15, 2021, before the roadway officially reopened to the public on December 21, 2021.

## **PROJECT CHALLENGES AND DESIGN TEAM APPROACH (4)**

Due to the complex site constraints, the design team had to act quickly to advance bid package development and advertisement. Once the roadway was closed in late March, expediting design and permitting was even more critical. At that time, weekly coordination meetings were held between PennDOT, Schnabel, TPD, and SCI personnel to coordinate necessary resources and expedite submissions, approvals, and permits. During the meetings, follow-up or side meetings were identified and held, as necessary. These meetings were invaluable to the team and fostered collaboration that continued throughout the duration of the project to navigate and overcome the various site challenges and constraints that are discussed below.

The project received emergency funding from the Federal Highway Administration (FHWA). The funding stipulated that the length of roadway to be repaired was approximately 300 ft. The design considered this stipulation when evaluating the site and developing the bid documents.

### **Subsurface Conditions and Investigation**

The local bedrock (dolomite) is a carbonate rock and, therefore, susceptible to weathering and karst feature development such as deeply weathered fracture zones, pinnacled bedrock surface, soft soil adjacent to the bedrock, subsidence, and sinkholes. This complex geology required a thorough subsurface investigation to evaluate and delineate the extent of the area that needed to be treated.

To delineate the lateral and vertical extent of the roadway requiring remediation, the team initiated a subsurface investigation. Three geophysical methods were used: Ground Penetrating Radar to evaluate shallow subsidence features, and Electrical Resistivity Imaging and Multichannel Analysis of Surface Waves for assessing deeper karst features. Test boring locations were selected based on the geophysical results. As a result, continuous geophysical cross-sections (see Figure 4) with test boring data superimposed on them were created to interpret the site conditions and delineate the extent of sinkhole treatment.

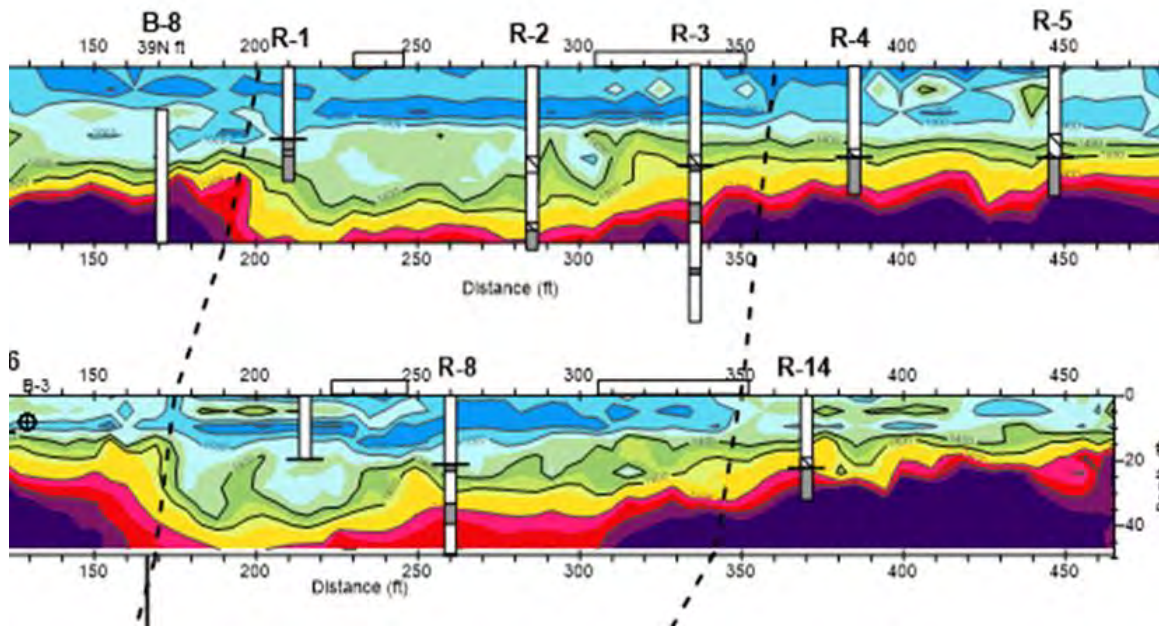


**Figure 4 – Example of Test Borings Plotted on Geophysical Cross-Sections**

Based on the investigation results, the team recommended implementing an LMG within the roadway. The LMG program was intended to improve the sinkhole-prone soil/rock conditions underlying the roadway and stabilize the roadway embankment to reduce the risk of future sinkhole activity and subsidence. The LMG method allowed for remediation between the dense utilities, and the grouting provisions had requirements for lowering grout pressures adjacent to utilities. Battered grout holes were specified to stabilize the roadway embankment slope and were used to thread between and underneath utilities. Sinkholes in the creek and soft zones in the roadway were recommended to be repaired by removing loose material and plugging with flowable fill and rock, as necessary.

### Utilities

Numerous subsurface utilities are present at the site. Critical subsurface utilities include a 20-inch gas line, a 10-inch sewer line, an electric duct bank, active and abandoned water lines, a communication line duct bank, and drainage pipes. Overhead power lines are located behind the existing guide rail at the top of the embankment slope. Lastly, two parallel gas transmission lines cross Chemical Road diagonally near the intersection of the I-476 off-ramp. Utility coordination was critical to notify utility owners of the situation and maintain communications during design and through construction.

There was a risk of impacting utilities during grouting operations and inducing movement from the pressure. During design, the team employed geophysical methods to designate (Level B) the number, depth, and types of utilities in the project area. Due to the numerous utilities at the site, it was critical to locate (with soft dig) and monitor utilities before grouting the nearly 400 grout holes. A unique special provision was developed that set minimum requirements and procedures for locating utilities, installing monitoring points, and monitoring utilities. The utility

monitoring was specified to be automated; therefore, real-time movements were monitored to detect movements early and reduce the risk of service disruptions and the need for additional utility work that could cause delays to reopening the road.

### **Right-of-Way (ROW) and Site Access**

The sinkholes in Plymouth Creek were outside PennDOT's ROW, and their presence could have caused a loss of embankment material or grout to enter the creek during repairs. The Cross County Trail runs parallel to the roadway on the opposite side of Plymouth Creek and could not be impacted; therefore, a temporary construction easement in the adjacent private property was required. PennDOT personnel communicated closely with the property owner, who was also impacted by the roadway closure, to obtain a waiver to access the property. This was a critical step in the project because ROW negotiations can typically elongate overall project schedules. Access to the Cross County Trail was maintained during construction by accessing the creek from Chemical Road.

### **Plymouth Creek**

Based on observations at the site, the Plymouth Creek streambed is typically dry between storm events (known as a losing stream). The 100-year storm level is at the top of the roadway embankment. During storm events, water was observed flowing from the creek into sinkholes located in the creek bed. Groundwater is likely flowing along the regional trend, and fluctuations in groundwater levels can cause bedrock solutioning and soil voids that can contribute to the development of sinkholes below and adjacent to the stream.

For the work in Plymouth Creek, PADEP determined that a Small Projects Permit was required. While the Small Project Permit was in progress, the team obtained an emergency permit to allow access for construction vehicles in the event of slope failure during design. To complete the work in the creek, the team assessed access alternatives to minimize the impacts on nearby property owners and the Cross County Trail. The selected alternative involved an access road being constructed into the steep embankment from Chemical Road. An H&H evaluation resulted in two 60-inch diameter pipes being installed so the access road could accommodate high flows in the creek from storm events during construction (the remnants of Hurricane Ida impacted the site during construction).

### **Stream Restoration Alternatives Analysis**

PennDOT and Schnabel discussed streambed restoration alternatives to repair sinkholes in the channel of Plymouth Creek adjacent to the roadway embankment. It was determined that the scope of work within Plymouth Creek would be limited to spot sinkhole plug repairs. This alternative minimizes the disturbance to the existing streambed and, in conjunction with LMG, focuses on the goal to stabilize the roadway and embankment supporting the roadway.

Other alternatives discussed included more extensive treatments to reduce water infiltration within this stretch of creek, including installation of a low-permeability liner with riprap stabilization or injecting LMG along Plymouth Creek and shotcrete with wire mesh

reinforcement along the embankment. Due to the karst conditions within the creek and observed deterioration of the liner that was previously installed as an attempt to reduce water infiltration, it is likely that the creek bed will experience additional sinkholes at this location in the future even with extensive treatments. Therefore, the extensive repairs within the creek would likely be a short-term solution for sinkhole remediation. Furthermore, installation of a low-permeability liner could induce a large hydraulic gradient adjacent to the end of the liner that could result in a higher risk of inducing sinkholes just outside of the treated area.

### **Schedule and Construction Sequence**

The use of design-build delivery for traffic control, E&S plans, and ROW was considered, but due to the accelerated schedule it became necessary to obtain final approvals prior to bidding to avoid expected delays associated with these activities during construction. A construction sequence was developed to achieve the technical goals for the project and accommodate the accelerated schedule. The sequence dictated that grouting begin on the south side (opposite Plymouth Creek), while sinkhole plugging in the creek would be performed concurrently to seal off major openings and reduce the risk of grout entering the creek during grouting of the northern portion of the roadway. Once the sinkhole plugs in the creek were completed, grouting the northern portion of the road could be performed to achieve cut-off of the north side. This sequencing provided time for a temporary access road to be constructed to enter the creek for sinkhole plugging before grouting the northern portion of the roadway.

### **Post-Grouting Evaluation**

The team performed post-grouting activities to evaluate the grouting program. This included confirmation coring of grouted zones that indicated the grout injected improved the subgrade. Additionally, post-grouting geophysics was performed to compare with the pre-grouting data. The results of this evaluation are discussed below.

## **CONSTRUCTION CONSIDERATIONS**

PennDOT personnel served as the construction manager and inspector-in-charge of construction activities and were supported by Pennoni Associates Inc. staff who provided construction inspection services. Schnabel provided full-time construction observation and consultation services for the specialty geotechnical work. Road-Con served as the general contractor and constructed the access road into Plymouth Creek, and performed sinkhole plugging, subgrade preparation, paving, and other general construction work. The LMG work was subcontracted to Keller. Effective communication facilitated by the design team continued into construction, where periodic but frequent coordination meetings were held either via teleconference or on-site meetings. Several notable aspects of the project during construction are discussed below.

### **Bidding Requirements**

PennDOT bidding rules require the prime contractor to perform at least 51% of the dollar amount of the total contract value. PennDOT utilizes low-bid procurement, and the majority of

work and associated cost of construction for this project were related to the LMG operations. As a result, only one contractor would have had all necessary prequalifications to bid on the project. Coordination with PennDOT Central Office was required to waive the 51% requirement to allow for a competitive bid while allowing more drilling and grouting specialists to pursue this project. This also allowed contractors who regularly perform PennDOT work and are familiar with the requirements of PennDOT contracts to partner with specialized drilling and grouting subcontractors to submit bids.

### **Environmental Permit Approval**

An emergency environmental permit was issued for this project by the Pennsylvania Department of Environmental Protection (PADEP) to begin work with an understanding that a Small Projects Permit would be requested and approved before any of the in-stream work took place to stabilize and repair the sinkholes in Plymouth Creek. Due to the accelerated design, bid, and construction schedules, the contract was awarded prior to the issuance of the Small Projects Permit. Through communication and cooperation with the PennDOT District 6-0 Environmental Unit and PADEP, the Emergency Permit was extended by 60 days to allow for the work in the roadway to continue while the Small Projects Permit was approved. Road-Con was able to work with project staff and adjust their construction schedule and order of work to prioritize work outside of Plymouth Creek until the PADEP and Army Corps of Engineers' permits were finalized on August 13, 2021, and work in Plymouth Creek could begin.

### **Paving Schedule**

Asphalt paving was scheduled to take place in December 2021 and be completed prior to the end of the year. While it is not rare for asphalt paving to take place in December in this part of the state, this required a stricter quality control plan and close monitoring of weather conditions and temperature to complete the work. Meeting these paving goals was also important, as many plants close in January and February to perform yearly maintenance and getting material becomes more difficult in the winter months.

### **SINKHOLE TREATMENT (5)**

Sinkhole treatment at the site consisted of sinkhole plugging and LMG. In order to monitor impacts to utilities during grouting, utility monitoring points (UMPs) were installed. These activities are described in more detail below.

## Sinkhole Plugging

### *Plymouth Creek Sinkhole Plugging*

The scope of work within Plymouth Creek adjacent to the roadway embankment involved excavating loose material from within known/observed sinkholes and backfilling with flowable fill using the detail presented in Figure 5. This process is referred to as “plugging.” The excavated areas encountered rock pinnacles with areas of mixed soil/rock conditions. The visual observation of pinnacles confirmed the geophysical and geotechnical investigations and is typical of high-density sinkhole occurrences in shallow karst. Figure 6 shows the sinkhole plugging in Plymouth Creek.

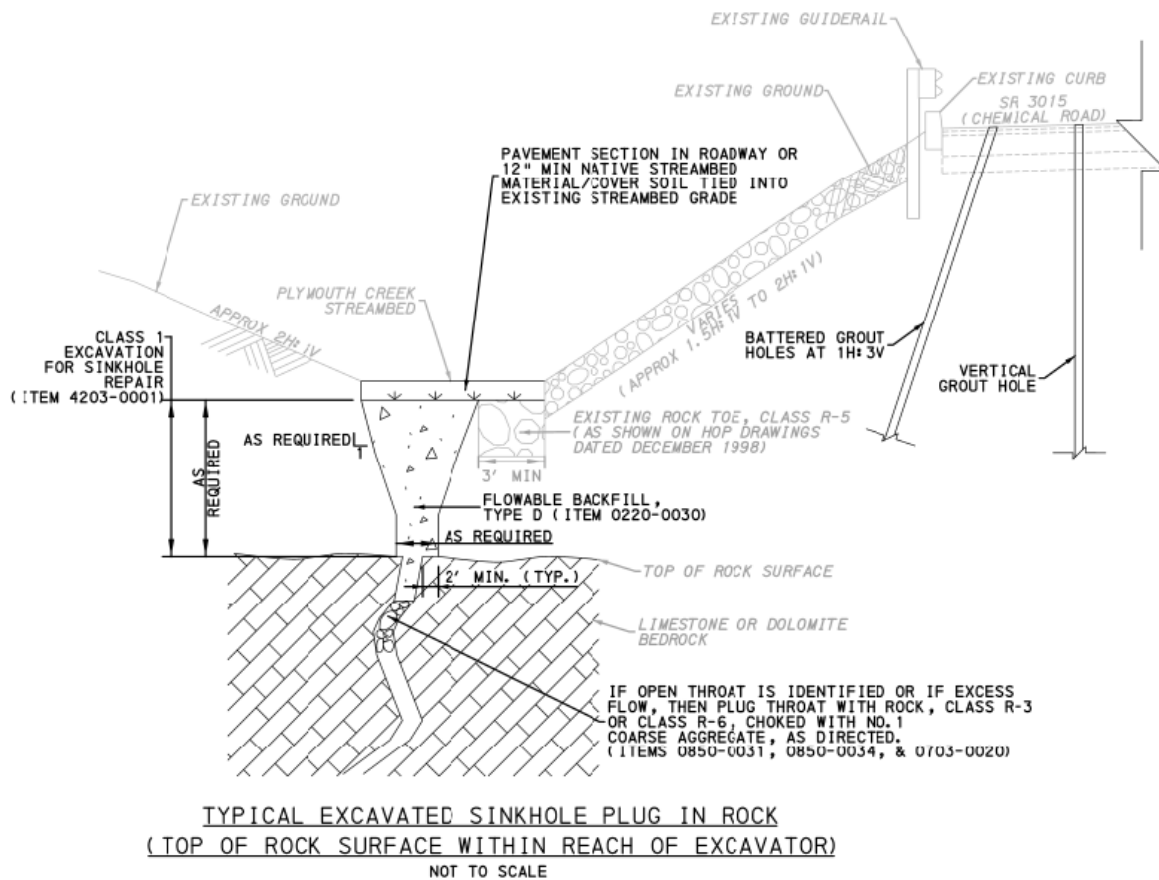


**Figure 5 – Sinkhole Plug Detail**



**Figure 6 – Sinkhole Plugging in Plymouth Creek**

### *Undercuts and Sinkhole Plugging in Roadway*

After the existing pavement and subbase were stripped, representatives from Schnabel, Pennoni, and PennDOT observed proof-rolling operations with a loaded triaxle dump truck and with a handheld geoprobe to evaluate the subgrade conditions. Four areas were identified that needed an undercut below proposed bottom of subbase. These areas were identified based on a combination of observing soil heaving around the tires during the proof-rolling operation, GPR data from the geophysical investigation, instrumentation data, and grouting operations. Upon completion of the undercuts, the areas were backfilled with dense-graded aggregate, compacted using a jumping jack, and roller compacted to meet the existing subgrade.

### **Utility Locating and Monitoring Points**

Road-Con performed test holes and a utility monitoring program as required by the Utility Locating and Monitoring special provision. Test holes were performed at roughly a 50-ft spacing along each utility to assist with laying out LMG drill holes. The UMP consisted of a reflective mini-prism attached to a riser pipe within a PVC sleeve. The prisms were sighted by an automated motorized total station (AMTS) for hourly readings during construction. A total of 48 monitoring points were installed: eight points per utility, spaced at roughly 50 ft through the LMG area.

Periodic deformation monitoring reports were provided and reported UMP deformation (i.e., movement) data, specific instruments that exceeded a movement limit, and a brief summary of construction activities over the course of the monitoring period. The deformation data were illustrated with plots showing the monitoring point movement over time. The project alert limit was  $\pm 0.24$  inch, and the threshold limit was  $\pm 0.48$  inch. Based on the overall data, eight and seven UMPs exceeded the alert and threshold limits, respectively. The trend in monitoring data generally indicated the deformation stabilized in most of these UMPs; three UMPs indicated a continued relatively slow deformation rate up until the UMPs were abandoned. The reports also included specific grout holes that were drilled or pressure grouted and their location with respect to adjacent UMPs in an attempt to correlate the construction activities to deformations. However, in general, the majority of the UMPs experiencing deformation did not occur at the time of adjacent drilling or grouting operations. Notably, most of the UMPs that exhibited signs of deformation were within the area of recent karst activity (sinkholes/subsidence) and higher grout takes.

Upon completion of LMG operations and surficial sinkhole repairs, the UMPs were removed, and the standpipes were left in place and gravity filled with grout.

### **Limited Mobility Grouting (LMG) Program**

Keller performed the LMG work from August 6 to November 8, 2021. The grouting program consisted of 273 primary grout holes, 83 secondary grout holes, and 42 tertiary grout holes. Generally, the primary grout holes were situated in a grid pattern with an approximate 10-ft spacing. The spacing was modified to fit the road curvature, and LMG hole locations were adjusted to provide adequate clearance from utilities.

Keller used a Gill Beetle rig for drilling operations. A 4-inch diameter down-hole hammer was used to advance the holes to depths ranging from 10 to 127 ft below grade. The holes were drilled “open-hole,” then cased at the time of grouting. Where the top of rock was less than 50 ft, the holes were terminated at least 5 ft into rock; where the top of rock was greater than 50 ft, the holes terminated in 2 ft of rock. After terminating one hole at a depth of 127 ft when encountering rock at 126 ft, Schnabel and PennDOT decided to limit the maximum drilling depth to 100 ft because greater depths were not deemed necessary to stabilize the roadbed. Generally, the grout holes encountered a large area of shallow, competent rock where lower grout takes were observed in the southeast portion of the site. In the northern and western areas of the site, where typically thin and shallow layers of rock underlain by soil were encountered and higher grout takes were observed, deeper grout holes were drilled.

Keller used a Maxim Link-Belt LS-138H II crane, Comacchio MC 28 rig, and Klemm Bohrtechnik KR 801-3GS rig for the grouting operations. The MC 28 drilled battered holes as shown on Figure 7.



**Figure 7 – Battered Grout Hole Drilling at Embankment Slope Adjacent to Overhead Wires**

At the beginning of the project, Ready-mix grout was provided by JDM Materials Co. of Huntingdon Valley, Pennsylvania. However, due to pumpability issues with the JDM mix, Keller changed the grout supplier to GFP Mobile Mix Supply, LLC of Wilmington, Delaware (GFP Mobile), who batched the grout on site in their mobile-mix concrete truck. The mobile-mix concrete truck (shown in Figure 8) had the ability to mix the grout with specified proportions of cement, aggregate, and water as specified by on-site personnel. The grout was pumped through hoses and risers connected to the crane or rigs and down a 3.38-inch inner diameter flush-joint threaded casing for the two drill rigs, and a 3.5-inch inner diameter for the crane stinger.



**Figure 8 – Limited Mobility Grouting With Crane Mounted Stinger and Mobile Grout Mix Batch Truck**

The LMG operation consisted of the following:

- Grout was injected under pressure as the casing was extracted in 2-ft stages. The grout injection rates were limited to 2 cubic feet per minute (cfm). Each 2-ft stage was terminated based on the grout volumes, pressures, and/or grout and heaving observed as outlined in the *Limited Mobility Grouting* specification.
- Secondary and tertiary holes were added, with generally lower pressures, in areas where the primary holes experienced relatively higher grout volumes per stage.
- Battered grout holes with batters of 1H:3V were generally used to perform LMG within portions of the embankment slope. Battered holes with a 1H:4V batter were also used behind the embankment crest to perform LMG within the embankment and to target areas below the existing sewer and gas utilities that were not accessible with vertical holes.
- Two grout mixes were reviewed and approved by the Department and both grout mix designs met the slump and strength criteria in the specifications. Road-Con and Schnabel generally performed slump testing at least once per truck on material batched from the GFP mobile-mix truck. Road-Con prepared the grout cylinders and tested their 28-day unconfined

compressive strength and provided the results to PennDOT. Based on the cylinder break results of tested samples provided between August 11 and September 9, 2021, the results exceeded the minimum required 28-day unconfined compressive strengths of 1,000 psi. Cylinder breaks after 7 days also exceed 1,000 psi for cylinders cast up to September 30, 2021.

- Pump calibration tests were performed when new pumps were used on site to determine the quantity of grout injected per stroke. In addition, daily calibration factors were calculated based on the number of daily strokes and grout batched by the GFP's metered concrete truck, deducting estimated losses in the hoses, risers, pump, and casing removal, and clogs if they occurred. The daily calibrations were calculated as a back-check for quantities and to verify the consistency of the equipment.
- Keller utilized 3 pumps throughout the project. The Putzmeister TK-50 pump was used for the majority of the project; the Reed C70s and Putzmeister TK-20 were used when the TK-50 was undergoing service repairs.
- Per the *Limited Mobility Grouting* specification, LMG was temporarily halted at holes where 2 consecutive grout takes greater than 25 cf occurred. At these locations, the tooling was removed and the grout injection was halted for at least 12 hours to allow the grout to set. The holes were then redrilled and grouted to completion.
- Grouting under pressure was generally terminated within 10 ft of the ground surface due to grout daylighting out of the hole and, in some areas, when surface heave was observed. These holes were then backfilled with grout under gravity pressure. Where LMG holes were located within 6 ft radially of utilities, the LMG holes were gravity filled with grout.

Schnabel provided on-site construction observation for the majority of the drilling and full-time for grouting operations to establish necessary drilling depths; verify casing installation; test the slump of the grout; and observe the grout pressures, volumes, and surface movement to assess when a 2-ft stage was completed. At times, Pennoni and Schnabel's subconsultant, SCI, provided support for observation of drilling and grouting operations.

Grout volumes per hole varied substantially across the site, ranging from 4.0 to 758.5 cf. The site contained areas of shallow rock where lower grout takes per hole were observed. Other areas contained deeper rock and suspected karst features based on drilling observations (rock pinnacles, open voids, soil-filled voids, etc.) where much higher grout takes per hole were recorded. Figure 9 shows a plan view representation of the grout volumes. The top image shows the total grout volume of each hole as a color contour, and the bottom shows the average grout volume per foot for each hole as a color contour. A summary of the average grout volumes per linear foot of drilling depth (cf/ft) is presented in Table 1.

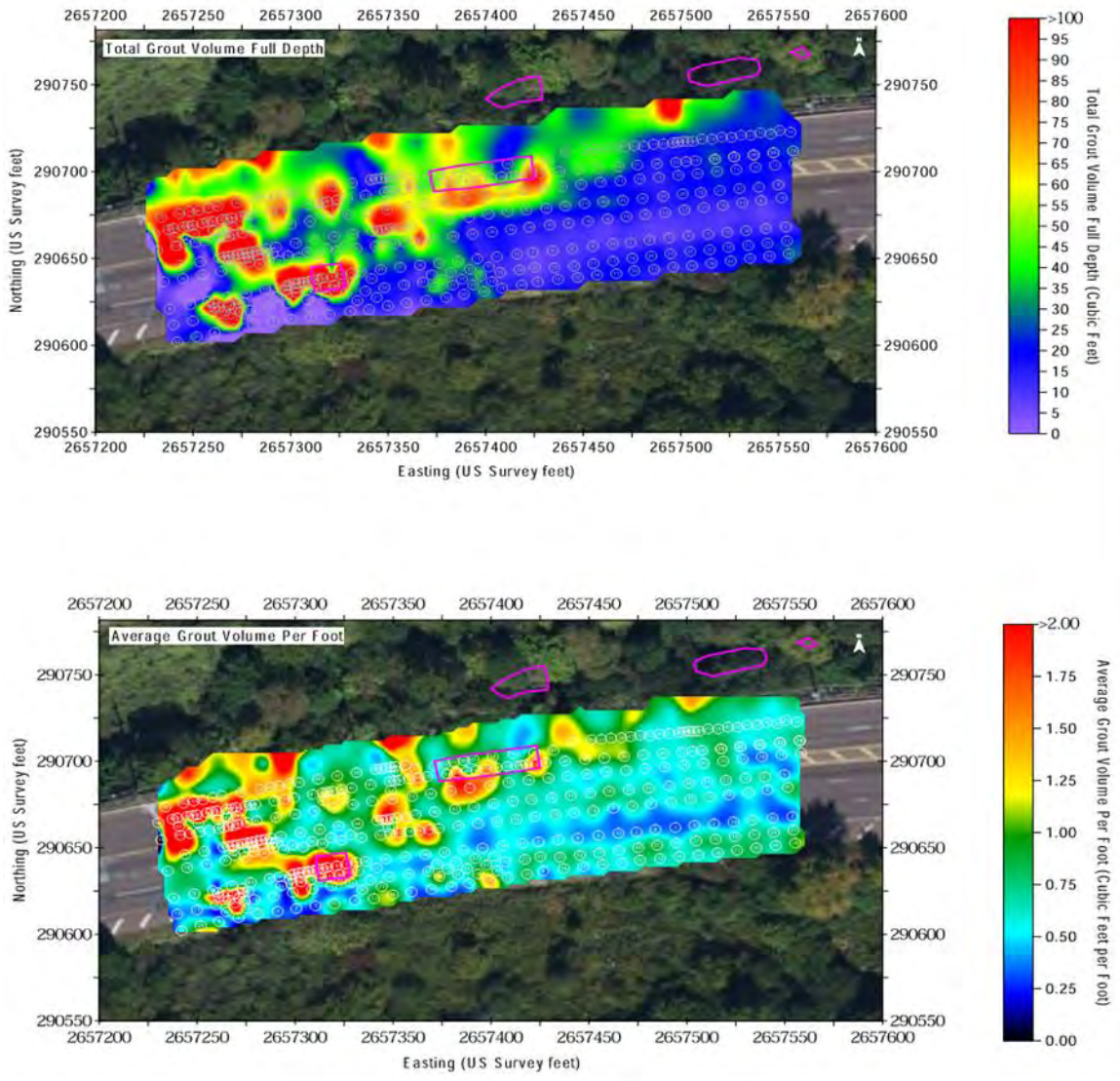


**Figure 9 – Total Grout Volume Full Depth (Top) and Average Grout Volume per Foot Depth (Bottom)**

<b>Table 1 – Grout Takes per Grout Hole Type</b>			
LMG Hole Type	Average Grout Volumes (cubic feet) per Linear Foot of Drilled Depth (# of holes)		
	<1 cf/ft	1 – 3 cf/ft	>3 cf/ft
Primary	219	43	11
Secondary	37	35	11
Tertiary	27	14	2
Total	282	92	24

## **GROUTING VERIFICATION (6)**

To assess the placement of LMG and subsurface improvement from the sinkhole plugging and grouting operations, several verification methods were performed. These methods included the comparison of primary, secondary, and tertiary hole grout takes and associated pressures; verification test borings, post-grouting geophysics; and proof rolling of the final subgrade.

### **Analysis of Primary, Secondary, and Tertiary Hole Grout Takes**

Grout takes were continuously monitored during the LMG program to evaluate the subsurface conditions and to determine if secondary and/or tertiary holes were required. The relative improvement of the soil and rock conditions was verified by monitoring the grout takes and injection pressures at the secondary and tertiary hole locations relative to those at adjacent primary/secondary holes.

Secondary holes were added between select primary holes (typically spaced 5 ft on center from adjacent primary holes), and tertiary holes were added between select secondary and primary holes (typically spaced 2.5 ft on center from adjacent primary/secondary holes). The overall trend of the secondary holes showed the grout takes per stage were generally reduced with higher injection pressures observed, compared to the values recorded at the adjacent primary hole locations. Higher grout takes per stage and/or low grouting pressures were observed in some secondary grout holes; in those cases, tertiary holes were added.

### **Verification Test Borings**

The verification test boring program included four borings drilled between October 27 and November 3, 2021. Continuous Standard Penetration Testing (SPT) and split-barrel wireline rock coring were performed at all test borings in accordance with PennDOT Publication 222. SCI provided full-time inspection of the verification test borings. The test borings were located in areas adjacent to LMG holes with higher grout volumes. The objective of the verification test borings was to evaluate the subsurface conditions and to identify lateral migration of the grout, particularly at depths with high grout takes. The verification borings encountered some zones of soft soils and/or low-recovery rock, and soil below the top of rock. The grout logs in adjacent LMG holes often indicated areas of higher grout takes corresponding to the depths of those conditions encountered in the verification borings. The low recovery rock may be the result of weathered rock or soil washed away during the coring operations. Notably, the verification test borings encountered cured grout in several areas indicating the lateral migration of grout as a result of the LMG operation.

### **Post-Grouting Geophysical Investigation**

A geophysical investigation was conducted before and after the LMG grouting program. A “Pre-Grout Geophysical Investigation” was conducted to define the extent of karst zones to help guide the grouting program, and the “Post-Grout Geophysical Investigation” was performed to evaluate the results of the grouting program.

Schnabel conducted the Pre-Grout Geophysical Investigation from March 8 to 22, 2021. In summary, it included three non-invasive methods: electrical resistivity imaging (ERI), multi-channel analysis of surface waves (MASW), and ground-penetrating radar (GPR). ERI data was collected in the adjacent creek bed north of the road, in the right SB lane, and in the NB shoulder of the off-ramp from I-476. MASW data was collected in the right NB lane and in the SB lanes. GPR data was collected in the NB and SB lanes.

Following the grouting, Schnabel collected MASW data for the Post-Grout Geophysical Investigation from December 9 to 16, 2021. MASW was the only method conducted post-grout by Schnabel. Additional geophysical data was collected by Temple University personnel for research purposes.

Below is a description of the MASW comparisons and results of the pre- and post-grouting investigations.

### **Geophysical Comparisons and Results**

MASW was used to evaluate the results of the LMG grouting plan by comparing the pre- and post-velocity models generated from MASW with the volume of grout that was injected at various locations. The construction schedule allowed the grout to cure for about 30 days while subgrade preparation and paving operations were performed prior to conducting the post-grout MASW, which gave the grout sufficient time to achieve its design strength. It was expected that the cured grout made the bulk of the subsurface soils stiffer, thereby allowing shear waves to travel faster in the grouted areas compared to the pre-grout velocities.

#### *Pre-Grout Velocity Compared to Grout Volume*

Following grouting, one of the first steps was to compare the pre-grout shear wave velocity to total grout volumes. Figure 10 shows this contoured in plan view, trimmed to include only the areal extent that was grouted. The top image shows the average shear wave velocity among all depths, and the bottom image shows the total grout volume among the full grout hole depth. The total grout volume contours assume the grout injected stayed within the grout hole location, either in vertical holes or battered holes. In reality, it is possible that the grout migrated away from the grout hole in areas with weaker rock and looser, softer soils.

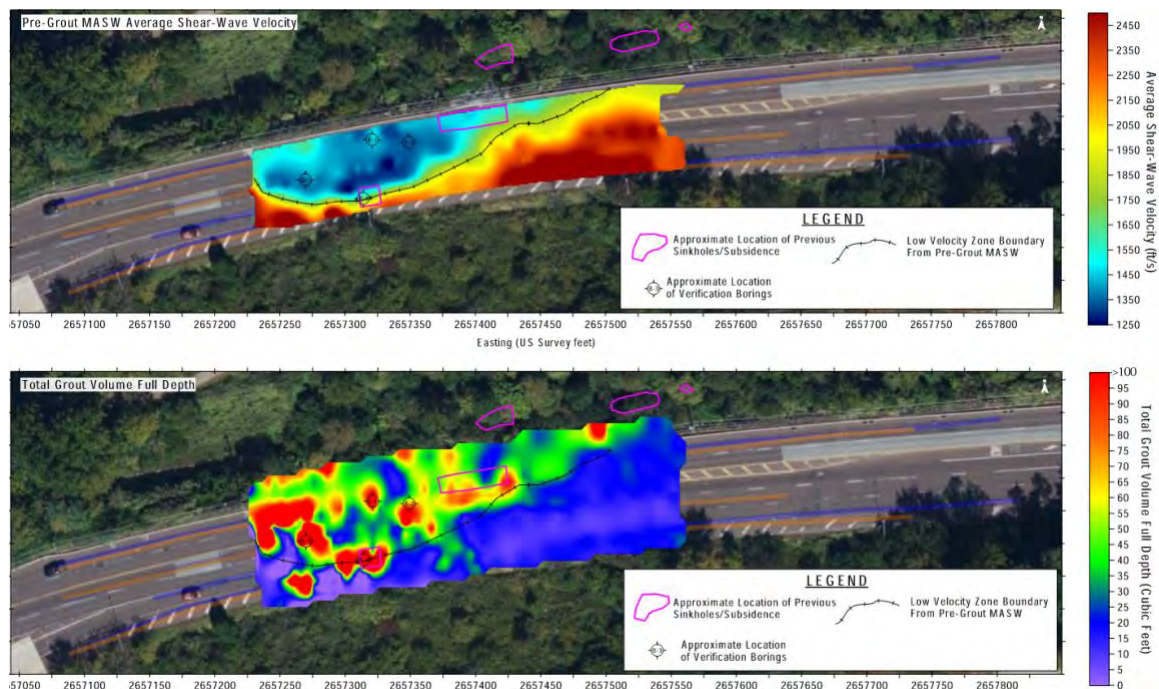


**Figure 10 – Average Shear Wave Velocity Full Depth (Top) and Total Grout Volume Full Depth (Bottom)**

Comparing the two plots on Figure 10, the most notable feature is the correlation between the low velocity zone and the area with higher grout takes. This area is outlined and labeled the “low velocity zone boundary from pre-grout MASW” on the top image of Figure 10 and is based on the MASW results. Without MASW results north of the road, we cannot constrain the shape of this low velocity zone north of the road.

The same outline from the MASW is overlain on the total grout volume plan on the bottom image of Figure 10, and there is good correlation between the low velocity zone boundary in most places. There are some zones of higher grout takes extending farther south than the low velocity zone boundary in the southwest portion of the grouted area. It was interpreted that zones of higher grout takes outside the low velocity zone boundary may show areas where the grout migrated away from the vertical, and possibly in a northern direction, to fill in soft soil zones north of the grout holes. In general, it was expected that the grout filled more open space and compressed looser soils where the velocity was initially lower, thereby resulting in a correlation of higher grout take to initial lower velocity. Outside this low velocity zone boundary area, the pre-grout average velocity is typically higher and the corresponding grout volumes are lower; this was interpreted to mean that less grout was injected due to relatively higher initial strengths in the soil and rock. These results correspond with the pre-grout test borings and depth to rock noted while drilling the grout holes that indicated the deepest top of rock was located in this lower velocity zone.

### Pre-Grout Velocity Compared to Post-Grout Velocity

In general, within the entire grouted area, the average velocity increased from 1,972 ft/sec to 2,042 ft/sec: a change of 70 ft/sec, or a 4% increase. Most of the areas with similar pre-and post-grout velocities correspond with the injection of shallow- and gravity-fed grout and are generally to the south and east sides of the grouted area. This area represents approximately 50% of the overall grouted area. In these areas, where the velocities are similar, the average velocity is about 2,179 ft/sec, and there was a negligible change.

All the MASW lines show an increase in velocity in the area referred to as the “low velocity zone boundary from pre-grout MASW” as shown in Figure 11. These areas also correspond with the greatest amount of grout volumes that were injected; this was interpreted to mean that the grout has increased the velocity, meaning the areas that were grouted were densified compared to before the grouting program.

Figure 11 displays the pre- and post-grout shear wave average velocity in plan view; the top image is the same as that on Figure 10, but the bottom image shows the post-grout MASW average shear wave velocity. Within the low velocity zone from pre-grout MASW, the average shear wave velocity generally increased from about 1,479 ft/sec before grouting to about 1,634 ft/sec after grout injection: a 155 ft/sec change. This increase of about 10% is an indication that the grouting program densified and stiffened the low velocity soil zone that was observed in the pre-grout MASW.

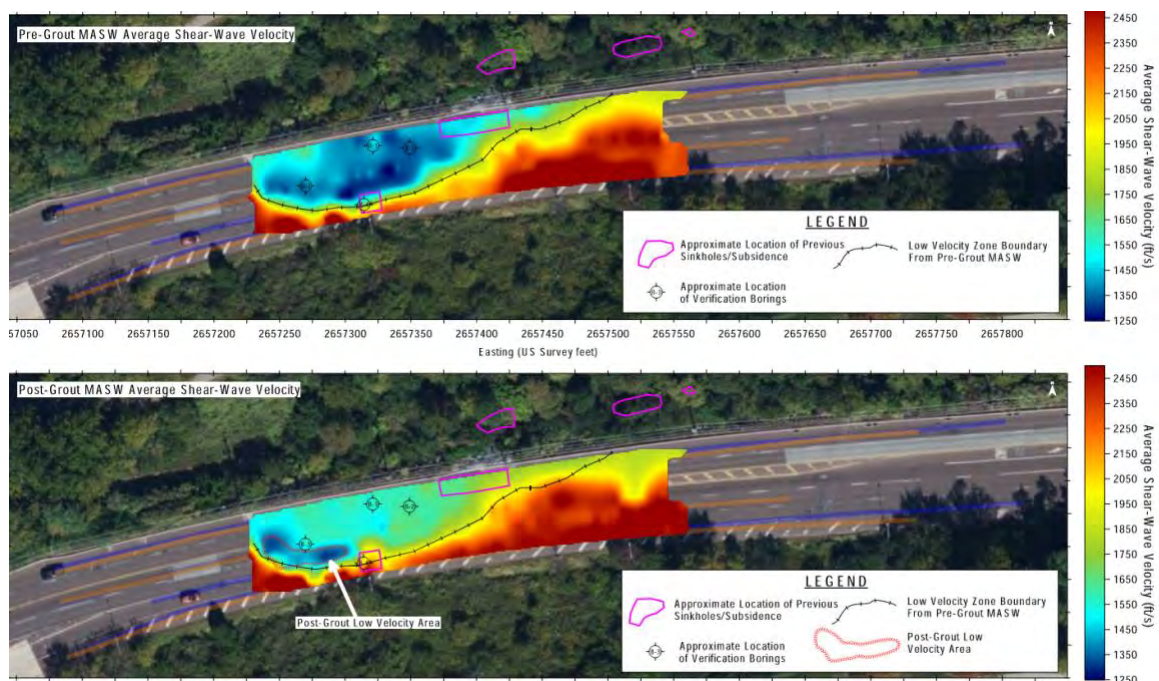


**Figure 11 – Average Shear Wave Velocity Before Grouting (Top) and Shear Wave Velocity After Grouting (Bottom)**

Comparing the pre- and post-grout velocities in the grouted regions only (i.e., removing the effect on shear wave velocity of the materials deeper than the bottom of the grout holes) shows the average shear wave velocity increased from about 1,263 ft/sec before grouting to about 1,455 ft/sec after grout injection: a 192 ft/sec change. This is an increase of about 15%, which represents the increase in shear wave velocity within the grouted zone.

#### *Post-Grout Low Velocity Area*

A location to note is in the southwest corner of the low velocity zone, where there is an area where the velocity did not increase after grouting. This area is called out on Figure 11 as the “post-grout low velocity area.” It was observed that this is an area mostly observed on Lines 2 and 3 at a depth of about 25 to 40 ft, and it is a zone where the velocity appears to have not increased in velocity post grout. In these areas, the average velocity is about 1,409 ft/sec, and there was a negligible change. Verification Boring B-3 is located just to the outside of the “Post-Grout Low Velocity Area.” The log of B-3 shows highly variable materials including intermittent soft soils and zones of no recovery, weight-of-hammer (WOH) materials, and thin dolomite layers. The location and specific depths from B-3 do not line up exactly with the post-grout low velocity zone. This is expected because of variations in resolution between test borings and MASW, and the offset of B-3 from the low velocity zone in highly variable subsurface conditions. In this general area, grout drill holes encountered rock at depths of approximately 9 to 16 ft below ground surface. These grout holes were generally terminated 5 ft into rock in accordance with the grouting plan. Based on the grout drill hole data, the “Post-Grout Low Velocity Area” may be situated below a rock ledge; therefore, this low velocity area was likely not grouted because the drilling refusal criteria was achieved prior to encountering it.

#### *Geophysics Summary*

There are some other small and isolated or localized areas where velocity values decrease; this is likely due to poor data quality and high dispersion curve attenuation due to possible interference from underground utilities. One further thing to note: it was expected that there was not a precise match between grouted volumes and velocities because the grout does not remain in a cylinder directly where the casing was installed, and it likely migrated laterally where soft soil zones and voids exist. Therefore, specific areal correlation may not show the exact location of the grout. Additionally, MASW resolution is not as fine as the grout take measurements.

In summary, there was a sound correlation between the pre-grout MASW and the areas with high grout takes. This indicates the MASW was an effective tool for identifying the required extent of the grouting program in the planning phase, and that the high grout takes were located in the low velocity zones. The areas with high grout takes correlated well with the pre-grout MASW models. This is also confirmed by the post-grout MASW models because an increase of about 4% overall was observed within the grouted area. Within the low velocity zone that was most improved by grouting, there was a 10% velocity increase.

**SUMMARY**

The success of this difficult and expedited project was a direct result of the cooperation and dedication of the entire team. Determining the detailed and comprehensive approach at the outset, coupled with the extraordinary commitment of every team member, from project manager and designer to consultant and contractor, led to the successful remediation and opening of Chemical Road in a nearly record amount of time.

**REFERENCES**

1. Jones, W. K. Physical Structure of the Epikarst. *Acta Carsologica*, Vol. 42 (2-3), 2013.
2. Kochanov, W.E. *Geology of part of the Chester Valley area, Chester, Delaware, Montgomery, and Philadelphia Counties, Pennsylvania*. Pennsylvania Geological Survey, 4<sup>th</sup> ser., Open File Report OFGA 16-01.0, 2016.
3. Kochanov, W.E., Lichtinger, J.F., and Becker, M. *Sinkholes and karst-related features of Montgomery County, Pennsylvania*. Pennsylvania Geological Survey, 4<sup>th</sup> ser., Open File Report 93-02, 1993.
4. Schnabel Engineering, LLC. *Sinkhole/Subsidence Investigation and Treatment Design Report, S.R. 3015 (Chemical Road), Section SNK*, 2021.
5. Schnabel Engineering, LLC. *Sinkhole Treatment Summary Report, S.R. 3015 (Chemical Road), Section SNK*, 2022.
6. Mayer, Christopher M. et al. Using Geophysics to Evaluate the Results of a Grouting Program in Karstic Geology. *71<sup>st</sup> Highway Geology Symposium*, Asheville, North Carolina, May 2022.

**A Comprehensive Approach to Rock Slope Design Solutions along NC-88 in  
Ashe County, North Carolina**

**Brooklyne Goode, GIT**  
HDR Engineering, Inc.  
555 Fayetteville Street, Suite 900  
Raleigh, NC 27601  
(919) 518-3501  
brooklyne.goode@hdrinc.com

**Bret Watkins, PG**  
HDR Engineering, Inc.  
4645 Village Square Drive, Suite F  
Paducah, KY 42001  
(270) 538-1530  
bret.watkins@hdrinc.com

Prepared for the 72<sup>nd</sup> Highway Geology Symposium, August, 2023

### **Acknowledgements**

D. Clayton Elliott, PG, NCDOT Geotechnical Engineering Unit  
D. Matthew Mullen, PE, NCDOT Geotechnical Engineering Unit  
Malcolm F. Schaeffer, LG, HDR Consultant

### **Disclaimer**

Statements and views presented in this paper are strictly those of the author(s), and do not necessarily reflect positions held by their affiliations, the Highway Geology Symposium (HGS), or others acknowledged above. The mention of trade names for commercial products does not imply the approval or endorsement by HGS.

### **Copyright Notice**

Copyright © 2023 Highway Geology Symposium (HGS)

All Rights Reserved. Printed in the United States of America. No part of this publication may be reproduced or copied in any form or by any means – graphic, electronic, or mechanical, including photocopying, taping, or information storage and retrieval systems – without prior written permission of the HGS. This excludes the original author(s).

## ABSTRACT

In early 2023, HDR performed detailed surveys of multiple rock slopes along 3 miles of NC-88 in support of realignment efforts of a critical highway corridor between Warrentonville and Smethport in Ashe County, North Carolina. The project alignment is physiographically situated in North Carolina's Eastern Blue Ridge Province. The local lithology generally consists of amphibolite, biotite gneiss, and mica schist of the Ashe Metamorphic Suite / Tallulah Falls Formation (Neoproterozoic). The proposed project involves multiple rock cuts to support widening and realigning NC-88, with some cuts exceeding 200 feet in height. Design complexities include difficult terrain, limited sight distances, increased traffic, rockfall hazards, and limited right-of-way access.

HDR executed a comprehensive approach to rock slope design, which included inspecting and geohazard scoring of existing rock cuts using the Unstable Slope Management Program (USMP) method and detailed geologic mapping of over 1,100 discontinuities on existing rock cuts. At a critical section of the project, seismic refraction and MASW surveys were performed, and an angled bore was advanced to 132.5 feet in depth to collect rock core and inspect subsurface discontinuities with optical/acoustic televiewing.

Collected data was used to inform global and subglobal (rockfall) stability analyses for each proposed cut, which revealed a high likelihood of planar and wedge failures at some of the most significant cuts. Preliminary design solutions, estimated quantities, long-term maintenance considerations, and right-of-way impacts customized for each proposed cut were then presented to NCDOT.

## INTRODUCTION

In February 2022, HDR and the North Carolina Department of Transportation Geotechnical Engineering Unit (NCDOT GEU) performed a site visit to a 3.8-mile long corridor of NC-88 generally spanning north to south from Warrensville to Smethport in Ashe County, North Carolina. The general location of the site is shown in Figure 1.

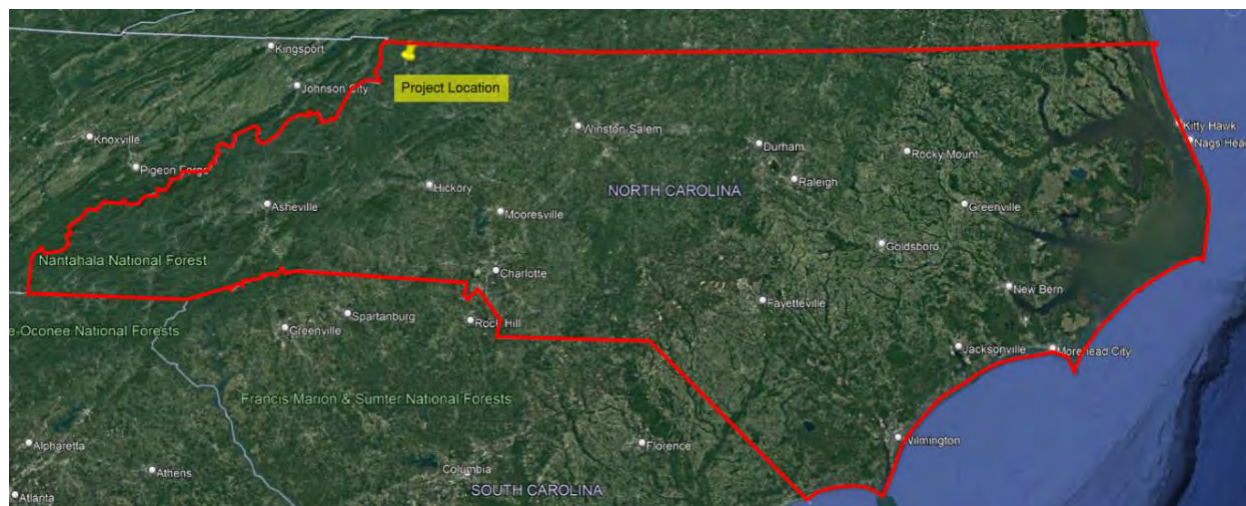


**Figure 1 – Project Location Map**

The goal of the site visit was to inspect the corridor to develop a project scope suitable for assessing the subsurface and geologic conditions of the realignment and widening project, which aims to alleviate traffic issues and hazards regarding the current roadway. Hazards and constraints included rugged difficult terrain, limited right-of-way access, limited sight distances, elevated traffic, and the potential for rockfall. The proposed project, while largely concerned with the realignment and widening of NC-88, also involves the design of two new bridges and 17 retaining walls. From the site visit and subsequent review of published data and roadway cross sections, 12 separate rock cuts were identified. To properly assess the proposed cut areas, HDR proposed a comprehensive geologic investigation scope that included the following:

- Perform rockfall hazard ratings of the 12 existing road cuts.
- Geologic field mapping of existing roadway cuts cataloguing major discontinuity sets.
- Assess discontinuity conditions of exposed rock faces.
- For the large mountain cut, advance rock soundings and one angle boring with optical/acoustic televiewer. Perform seismic refraction and MASW surveys to estimate rockline and overburden thicknesses.
- Perform global and subglobal stability analyses of proposed rock cuts.
- Develop design options and related quantities and ROM costs for NCDOT Roadway Design.

This scope is detailed in the following sections and discuss our project findings to-date.

## **GEOLOGIC SETTING**

The project alignment is situated in the Blue Ridge Physiographic Province where topographic relief is moderate to high, with massive resistant rocks producing mountain and ridge tops, with subsequent valleys tending to follow weaker rock deposits. The dominant lithology of the slopes is equigranular amphibolite but muscovite-biotite gneiss and schist are also present, all of which belong to the Ashe Metamorphic Suite and Tallulah Falls Formation of the late Proterozoic eon (NCGS, 1985). Figure 2 provides a regional geologic map of the project corridor with associated slope rock cut segments.

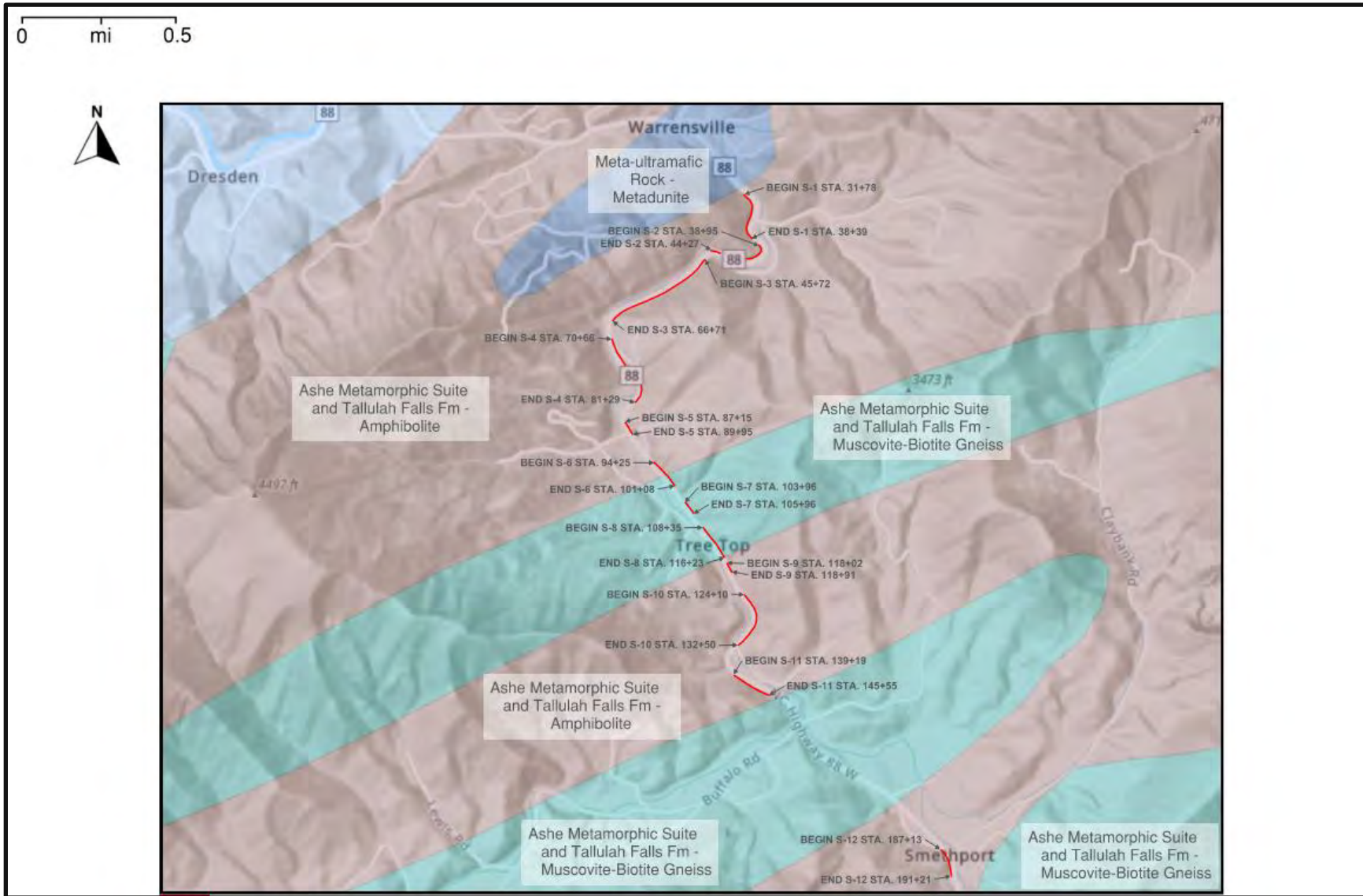


Figure 2 – Geologic Map & Slope Segments along NC-88 Project Corridor

## FIELDWORK

The field effort for this geologic investigation was conducted in January through May 2023 and is further discussed below.

### Rockfall Hazard Potential

HDR contacted NCDOT Division personnel regarding rockfall history along the corridor. According to these personnel, to-date only minor activity has been recorded; however, observations of the existing cuts revealed loose overhanging wedge blocks associated with widely-spaced joint and foliation surfaces (Photo 1).



**Photo 1 – Loose Block (Toppling Hazard)**

Preliminary and detailed rockfall hazard ratings for each of the twelve existing rock cuts were performed in January through February 2023 to gauge existing rockfall potential and risk to motoring public utilizing the FHWA’s “*Unstable Slope Management Program (USMP) For Federal Land Management Agencies*” (Publication No. FHWA FLH-19-002) (Beckstrand, et. al., 2019). The USMP rating process provides an assessment of baseline slope conditions and factors from which to compare to future slope design criteria and attempts to quantify rockfall or

landslide risk based on qualitative observations. Five criteria are assessed for the preliminary rating (ditch effectiveness, rockfall history, block size/volume event, usage impact, and traffic) with 12 additional criteria scored to develop the detailed slope and risk rating scores, including drainage, precipitation, geometry, maintenance, geologic conditions, exposure, sight distance, right-of-way, and environmental/cultural impacts. The USMP rating process produces three scores related to rockfall risk: a preliminary rockfall rating, a detailed rockfall slope hazard rating, and a detailed risk rating. The sum of the detailed slope hazard and risk rating scores are used to obtain a total USMP score of good, fair, or poor for each slope. Total scores for each of the twelve existing slopes included ten “poor” ratings and two “fair” ratings. Based on this information, a high likelihood of future and more frequent rockfall exists if the current roadway is left unattended.

## Slope Evaluations

From January through February 2023, HDR performed geologic evaluations at each of the 12 existing road cuts. Prior to performing field inspections, the location, positioning, and general geometries of exposed rock cuts along NC-88 were estimated by comparing scaled layout sheets, published maps, and cross-sections. The road-level field evaluation was conducted by HDR’s engineering geologists from January 23<sup>rd</sup> to February 14<sup>th</sup>, 2023. Weather ranged from snow flurries to sunny, with temperatures ranging from mid-20s to mid-50s. Field personnel donned appropriate high-visibility personal protective equipment (PPE) prior to performing inspections. Temporary single-lane closures were initiated by traffic control personnel with the use of a flagging crew, pilot car, and appropriate signage. Slope-specific baseline stationing was established along the shoulder edge at 50-ft intervals using a measuring wheel referenced to roadway features and latitude-longitude coordinates for slope beginning and ending points for each significant exposed rock cut along NC-88. Photomosaic sheets for each slope were prepared by field personnel and were used to document on-slope roadway-level observations (Figure 3).

In general, three rock types were observed:

- Amphibolite: Observed at all slope locations except slope S-6:
  - Moderately hard to very hard, slightly to heavily weathered, fine to coarse hornblende crystal textures.
  - Fine- to coarse-grained garnet and epidote veins were observed at several localities.
- Gneiss: Observed at all slope locations except slopes S-1, S-10, and S-12:
  - Thinly foliated, medium hard to very hard, slightly to heavily weathered, fine to coarse biotite and plagioclase feldspar crystal textures with minor potassium feldspar crystal textures.
- Schist: Observed at all slope locations except slope S-12:
  - Thinly laminated, very soft to medium hard, slightly to heavily weathered, fine to medium muscovite crystal textures.
  - Localized fine-grained garnets were observed at intermittent locations within the schist.
  - Often poorly exposed and decomposed to residuum, thinly interfingering with amphibolite and gneiss.

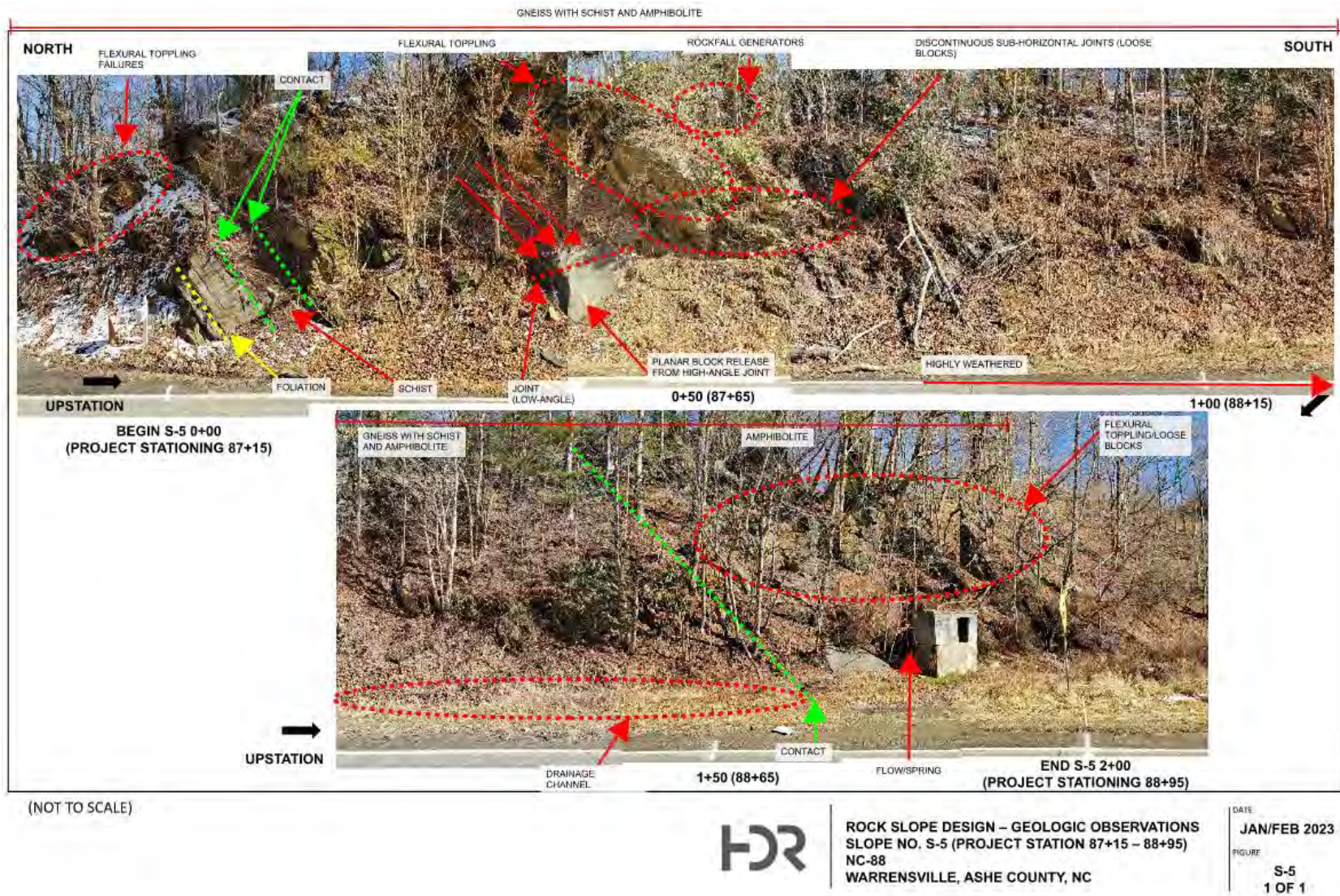


Figure 3 – Photomosaic Sheet for Slope S-5

## Geologic Structure Mapping

Measurements of discontinuity conditions and orientations were recorded on field data sheets, including approximate station, plane and rock type, dip / dip direction, length / separation / amplitude. Over 1,100 discontinuity measurements were taken on foliations and joint sets along the slopes (Photo 2).



**Photo 2 – Geologic Structure Mapping at slope S-2**

Initially the discontinuity orientations were separated by slope; however, foliation and joint trends at each slope appeared to be relatively similar to each other and were thus combined (Figure 4).

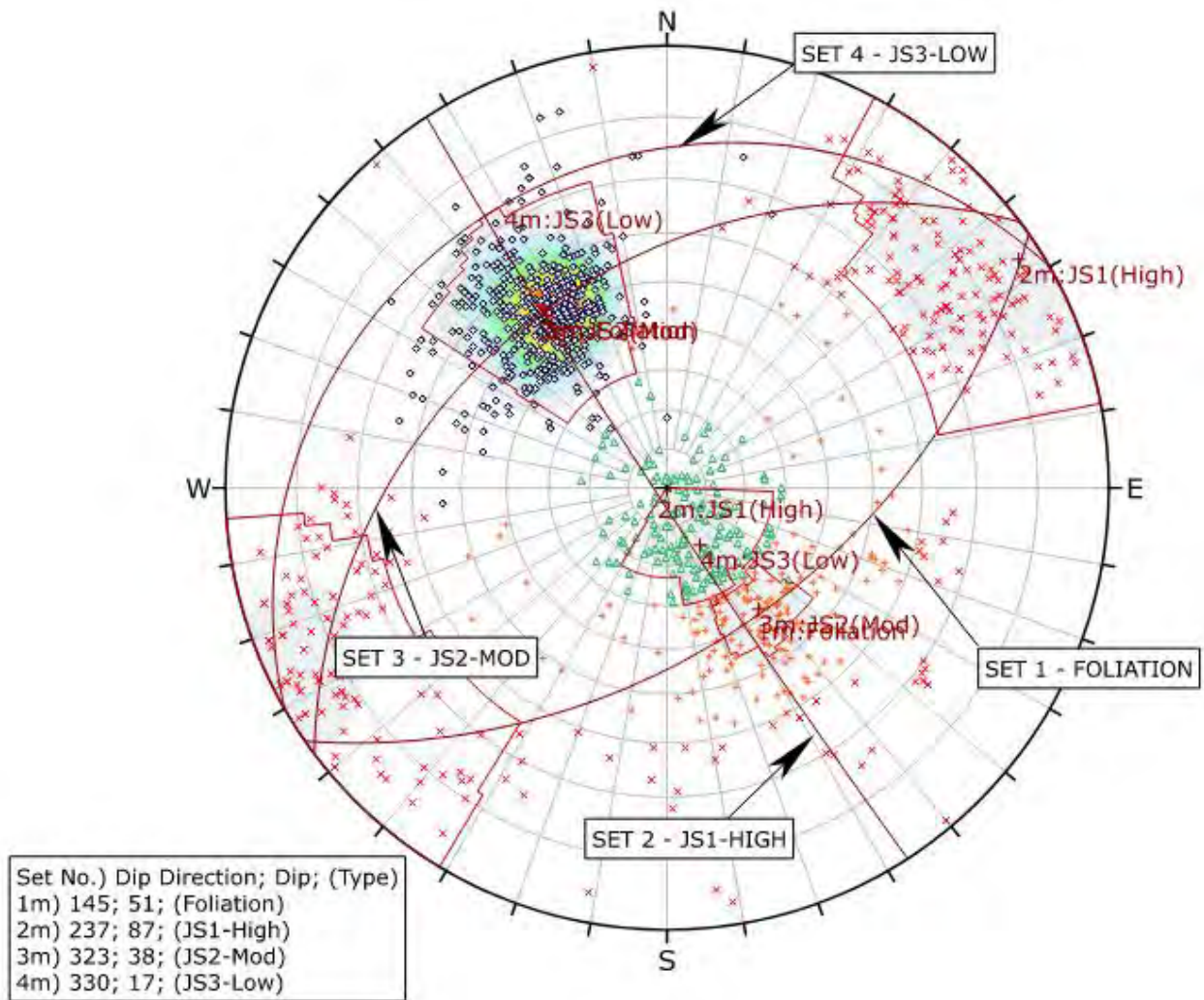


Figure 4 – Stereographic Pole-Plot Projection – All Discontinuities Combined

### Joint Compressive Strength

“R-value” strength readings were collected off exposed joint and foliation rock surfaces using a calibrated Type L Schmidt rebound hammer. Using the method and graphs employed by Deere (1966), R-value measurements can be roughly correlated to estimated uniaxial compressive strength of rock surfaces (UCS).

The Schmidt hammer test (ISRM 1978), a quantitative method for determining the compressive strength of a discontinuity, was employed on joint and foliation planes along various outcrops across the project alignment for amphibolite, gneiss, and schist rock types. Each discontinuity surface is tested 10 times, with the five lowest readings of each test group being discarded, and the mean rebound value was calculated from the five highest values from each test. The angle and direction of each test was recorded in the field and appropriate correction was

made in accordance with ISRM 1978. The uniaxial compressive strength was estimated for each foliation / joint plane for each subsequent rock type using the mean rebound number (r) and the applicable rock density value ( $\gamma$  in pounds per cubic feet (pcf)) to estimate the uniaxial compressive strength (UCS) using the following equation (Deere and Miller 1966):

$$(EQ10) \log_{10}(\sigma_c) = 0.00014 * \gamma * r + 3.16$$

Where:  $\sigma_c$  is the uniaxial compressive strength in pounds per square inch (psi)

Rock density values were obtained from referenced material and prior experience working with similar lithologies. Density values of 181, 168, and 179 pcf were used for amphibolite, gneiss, and schist, respectively. The Schmidt hammer results are presented in Table 1. The average  $\sigma_c$  is 12,359 psi for all Schmidt hammer measurements (158 measurements), 14,062 psi for Schmidt hammer measurements on joint surfaces (94 measurements), and 10,657 psi for Schmidt hammer measurements on foliation surfaces (64 measurements).

	Amphibolite Foliation	Amphibolite Joint	Gneiss Foliation	Gneiss Joint	Schist Foliation	Schist Joint
<b>Count (N) =</b>	45	78	14	13	5	3
<b>Mean =</b>	18,318	21,141	7,758	10,606	5,894	10,438
<b>Median =</b>	16,184	19,621	7,593	9,752	3,681	11,058
<b>SD =</b>	11,060	10,569	3,846	5,946	3,702	3,462
<b>+1 SD =</b>	29,378	31,710	11,604	16,553	9,596	13,900
<b>-1 SD =</b>	7,258	10,572	3,912	4,660	2,193	6,976
<b>Minimum =</b>	5,097	3,122	3,016	2,594	2,973	6,708
<b>Maximum =</b>	58,079	54,788	16,181	23,639	11,673	13,548
1. Uniaxial Compressive Strength Estimate (pounds per square inch). (Deere and Miller, 1966)						

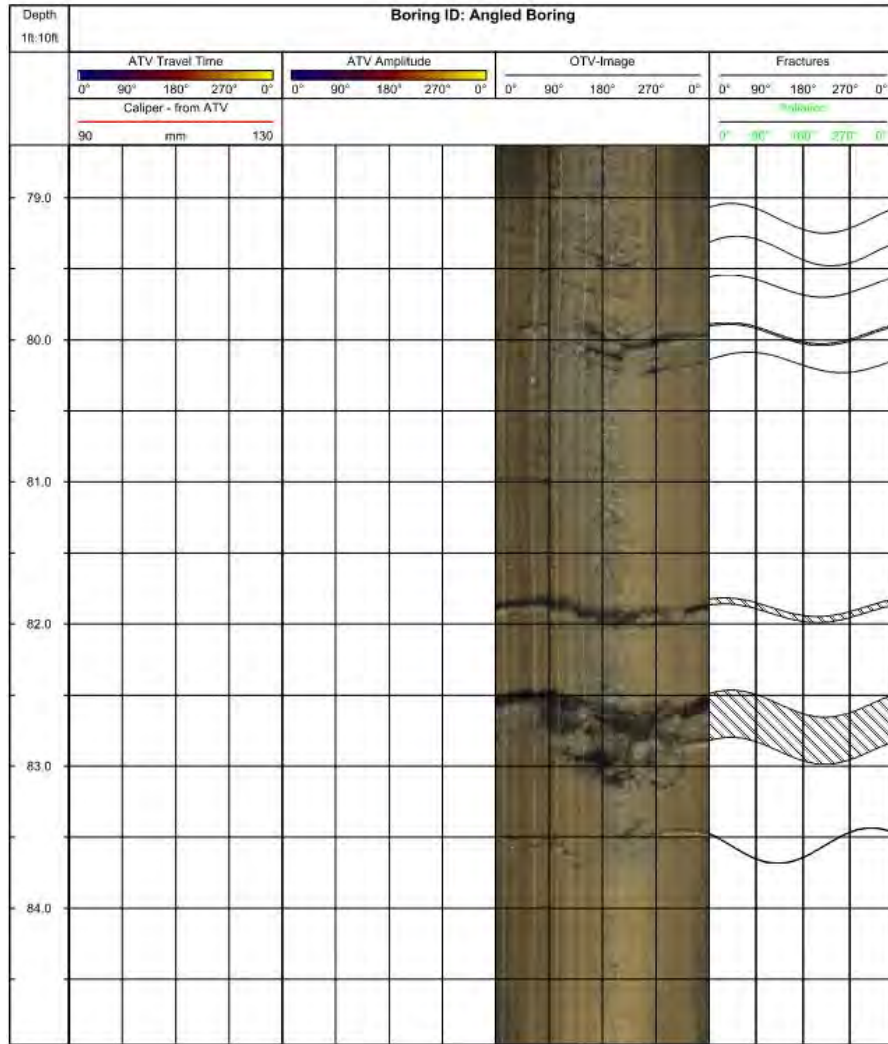
**Table 1 – Schmidt Hammer Results**

## Subsurface Investigation

Due to the rugged terrain, thick vegetation, and complexities regarding right-of-way access, subsurface drilling was limited in scope. In total, 129 borings were advanced along the project corridor, 51 of which involved rock coring.

The site subsurface investigation was conducted from January to May 2023. Borings in the vicinity of the 12 rock slopes included 13 Standard Penetration Test (SPT) borings, one rock

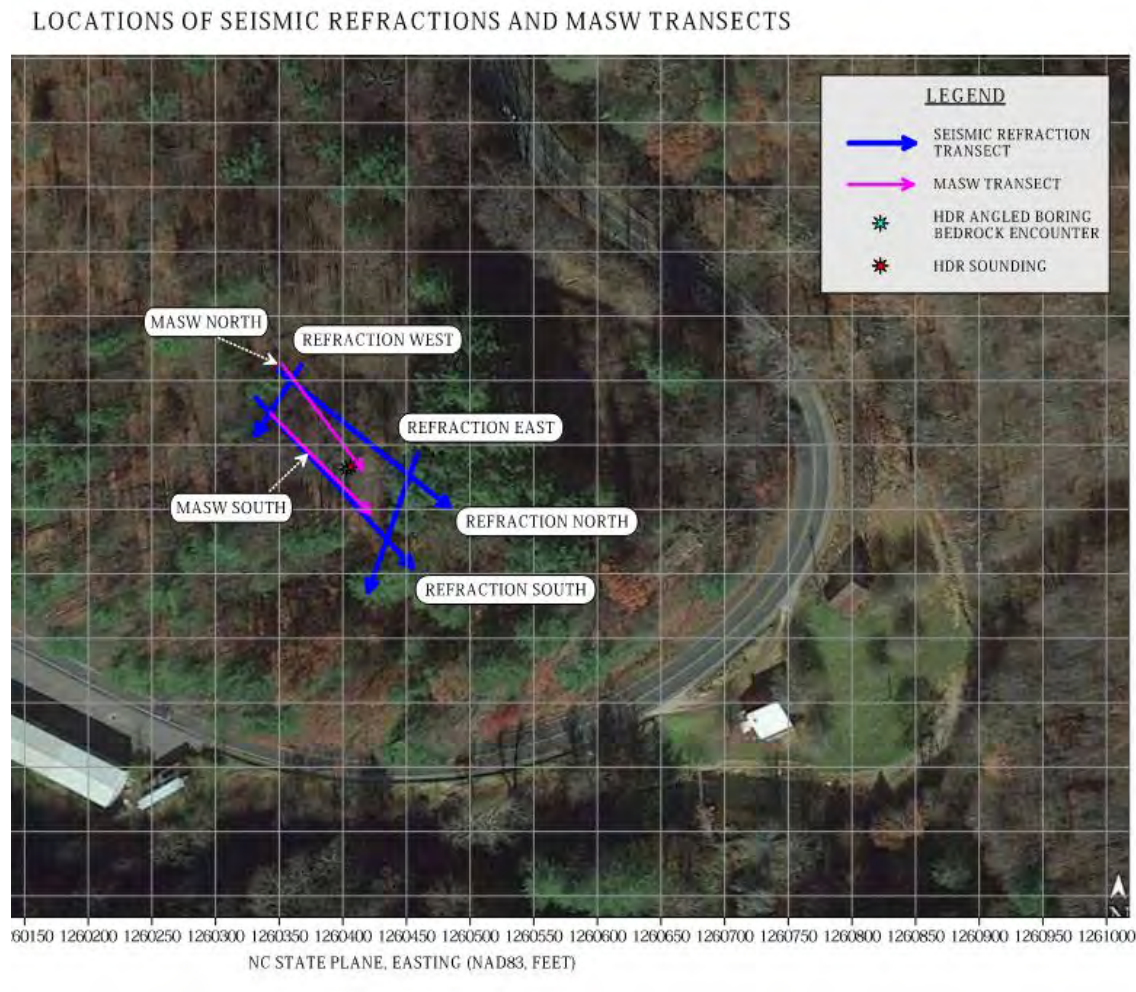




**Photo 4 – Optical Televiewer in Angled Boring**

### Geophysical Investigation

To estimate overburden thicknesses and rockline trends at the proposed mountain cut, four seismic refraction transit lines and two Multi-channel Analysis of Surface Waves (MASW) transit lines were oriented as depicted in Figure 5.

**Figure 5 – Seismic Refraction & MASW Transit Lines**

P- and S-wave velocities were mapped at each transit cross section and compared against the Caterpillar Performance Handbook (Edition 48) to correlate seismic wave velocities against rippable (crystalline rock) or non-rippable (residual soil / saprolite).

Results show a significantly thicker level of overburden (greater than 20-ft) than initially anticipated due to the presence of crystalline rock outcrops at the slope crest. Figure 6 presents an example of the southern seismic refraction slope transect.

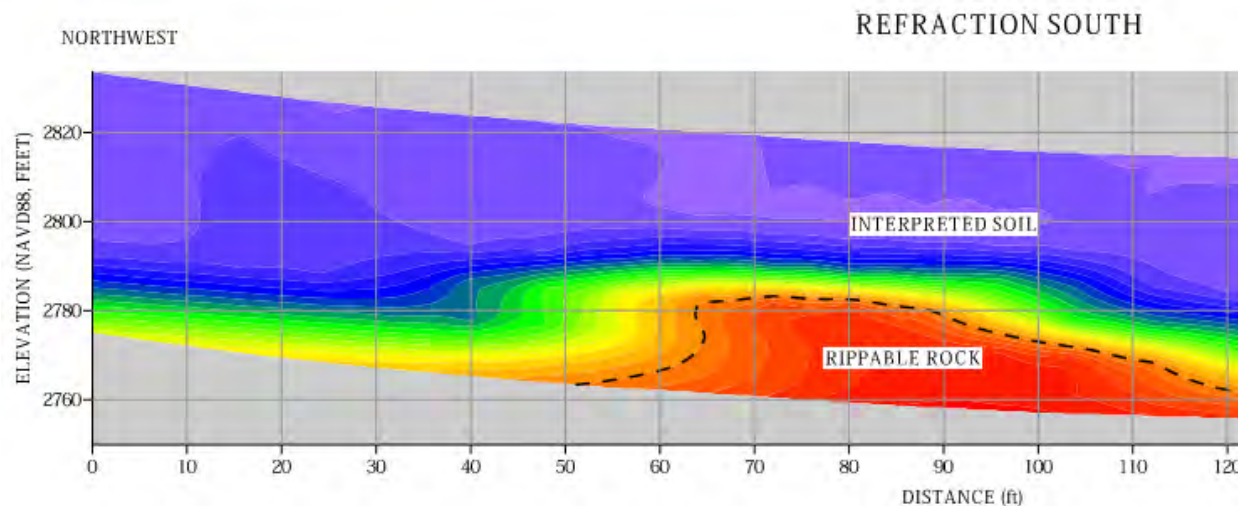


**Figure 6 – Example of Seismic Refraction South Transect**

## ASSESSING GLOBAL STABILITY

### Kinematic Analyses

As shown in Figure 4, four discontinuity trends were statistically derived through cluster analyses using the Rocscience program DIPS® from the 1,101 total measurements:

- Foliation – average strike of 055°, dip of 145°, and dip direction of 51°
- Low-Angle Joint – average strike of 240°, dip of 17°, and dip direction of 330°
- Moderate-Angle Joint – average strike of 233°, dip of 38°, and dip direction of 323°
- High-Angle Joint – average strike of 147°, dip of 87°, and dip direction of 237°

These aggregate trends were used for Kinematic analyses, which assess the potential / likelihood for global rock instabilities caused by bedrock discontinuity orientations relative to an existing or proposed rock cut. Global slope failure conditions are categorized into planar sliding, wedge sliding, and flexural / direct toppling. Thirty-two (32) cut orientations were estimated across the proposed alignment and compared against the aggregate joint and foliation trends with 45° (1:1) and 63° (0.5:1) cuts. Results indicate most rock cuts oriented with a 1:1 cut show a low likelihood of failure. However, a 0.5:1 cut angle results in potential daylighting of the predominant foliation discontinuity, which indicates a moderate to high likelihood of planar and wedge sliding failures for cut slopes dipping to the southeast, coinciding with sections of the corridor mountain cut (Figure 7).

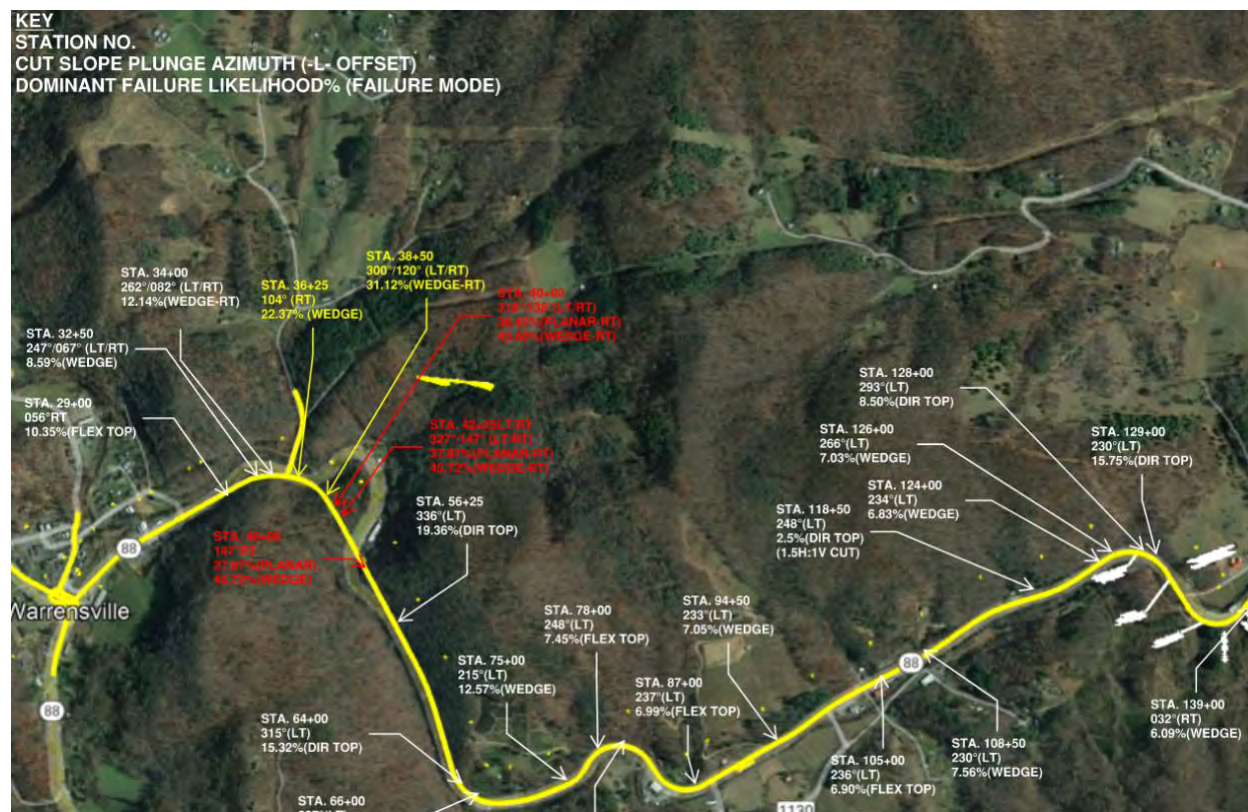


Figure 7 – Example of Kinematic Analysis Summary for 0.5:1 Rock Cuts

## Planar / Wedge Stability

Planar and wedge stability analyses were performed to evaluate the feasibility of rock slope reinforcement options with a 0.5:1 rock slope along the mountain cut corridor. The Rocscience program RocPlane® was used to estimate the external forces required to maintain planar and wedge features on the slope. Inputs to the program included the following:

- 1) GEOMETRY
  - a. Slope Height,  $h = 80$  ft. (benched).
  - b. Slope Angle =  $63^\circ$  (0.5:1).
  - c. Failure Plane Angle =  $51^\circ$ .
  - d. Upper Face Angle =  $0^\circ$ . (bench surface with 20 ft width).
- 2) BARTON-BANDIS SHEAR STRENGTH INPUTS (failure on foliation plane in amphibolite with thin interlayers of mica schist and biotite gneiss; assume mean of mica schist UCS estimates).
  - a. Joint Roughness Coefficient (JRC) = 2.7 (based on in situ joint amplitude/lengths)
  - b. Joint Compressive Strength (JCS) =  $850 \text{ kips/ft}^2 / 2.5 = 340 \text{ kips/ft}^2$
  - c. Base (Residual Friction) Angle,  $\phi_{\text{res}} = 23^\circ$  (referenced for mica schist)
  - d. Rock Unit Weight =  $0.172 \text{ kips/ft}^3$
- 3) PLANE WATER PRESSURE
  - a. 40% of slope height filled with Toe Distribution Model.

#### 4) EXTERNAL FORCES

- a. Force applied to the slope surface to estimate required anchor force (kips/ft – force per foot of width of potential planar block) to provide a factor of safety (FS)  $\geq 1.5$ .
- b. Using these inputs without rock anchor/external force, the FS is 0.29.

Figure 8 presents the critical section used for stability analyses. A FS  $\geq 1.5$  requires an external force of 128 kips/ft installed perpendicular to the rock cut face (27° down from horizontal) as shown on the 2-D perspective (Figure 9).

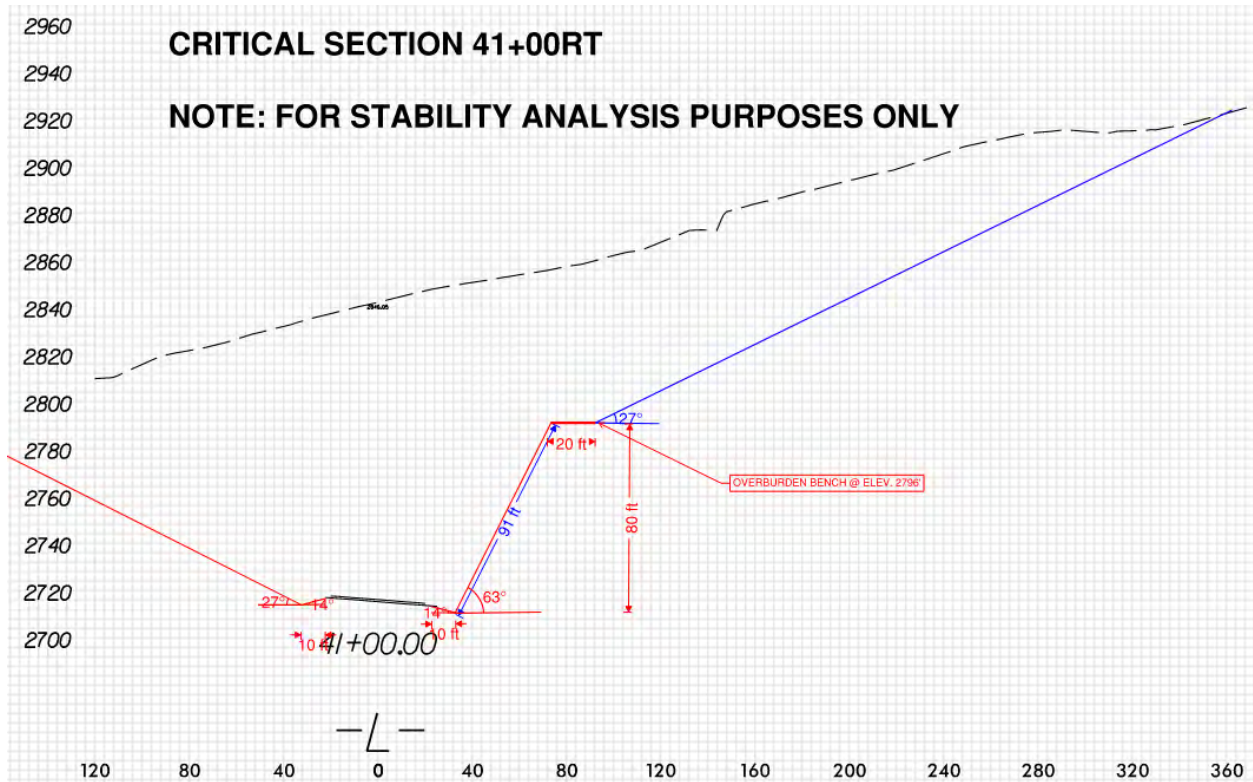
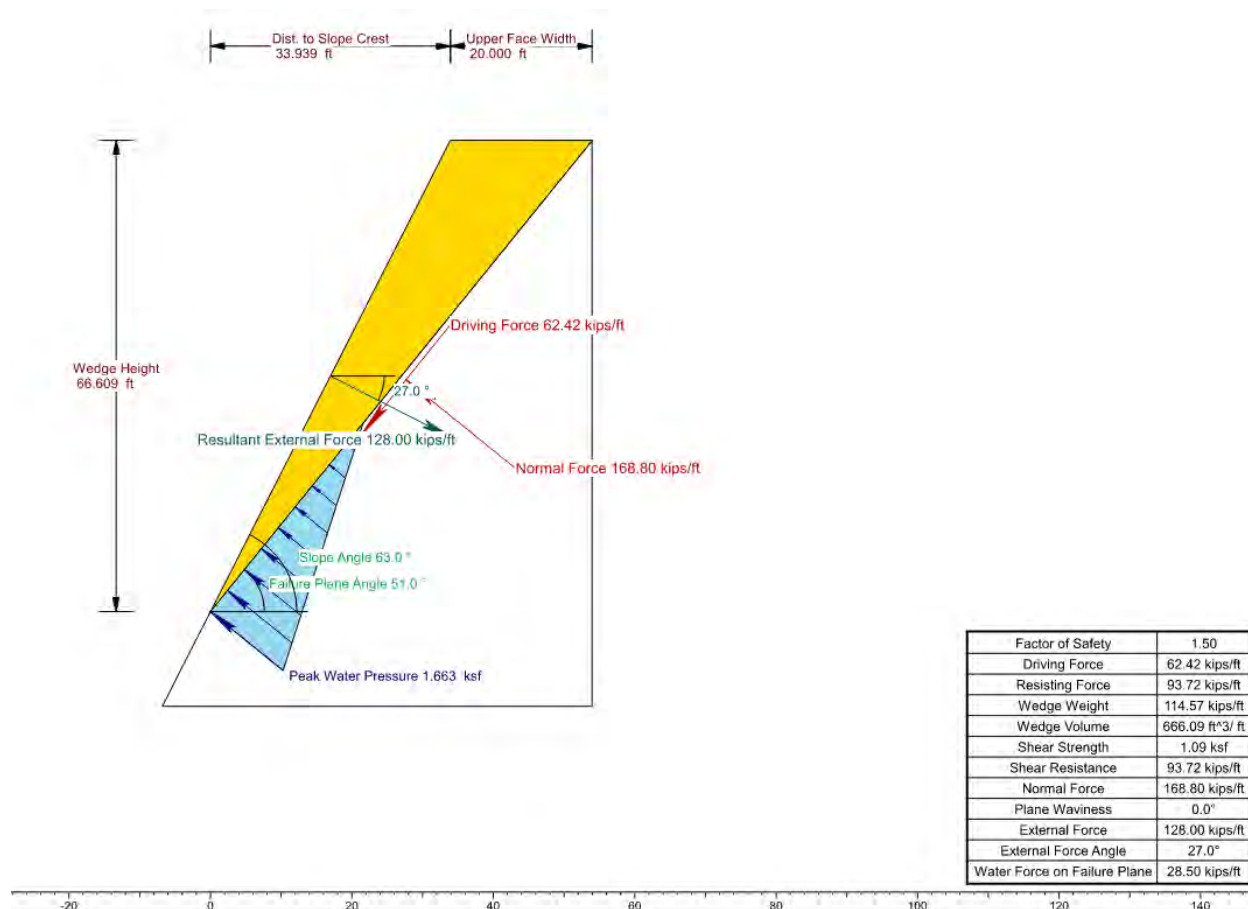


Figure 8 – Critical Section used for Planar Stability Analysis



**Figure 9 – 2-D Perspective of Planar Feature from Stability Analysis**

By dividing the required external forces over the planar representational surface area, the optimal slope reinforcement scenario included the following elements:

- Anchor Type: No. 8 (1”) 150KSI Bars
- Anchor Spacing: 7-ft offset pattern spacing.
- Anchor Length: 25-ft (10-ft minimum bonded lengths with 3” bond diameter)

Wedge stability analyses were also attempted using the Rocscience SWedge® program; however the resulting external forces were less conservative, therefore the RocPlane® outputs were used for design purposes.

### ASSESSING SUBGLOBAL (ROCKFALL) STABILITY

2-D probabilistic rockfall simulations were conducted at critical sections for each of the twelve slope segments using the Rocscience 2D RocFall® software program. A 90% design rockfall retention in catchment was used. After consultation with NCDOT, the following slope design constraints were also enacted:

- Presplitting will be required on all slopes steeper than 1:1.
- No benching of the proposed rock cuts, aside from a lithologic bench at the weathered rock / competent rock hinge point, regardless of cut heights.
- The minimum proposed catchment width is 10 feet, with a 4:1 geometry presented in all rockfall scenarios.

In total, future rockfall potential of proposed 1:1 and 0.5:1 cuts was modeled at fourteen discrete locations across the alignment. This limited set included four rockfall scenarios to estimate the effectiveness of proposed rock cut geometries of 0.5:1 and 1:1 rock cuts. For each of these two proposed rock cut angles, catchment geometry was modeled based on two scenarios: a limited catchment with the use of a barrier and an expanded catchment that provides a 90% design retention without the use of a barrier. The 90% rockfall design retention is required based on NCDOT Geotechnical Investigation and Recommendations Manual guidelines (Section 4.5.2).

Observations and vertical extents of each material unit on the slope were estimated and given a representative name that correlated to a range of values for surface roughness, the normal coefficient (Rn) and tangential coefficient (Rt). Surface roughness is defined as the perpendicular variation of the slope within the slope distance equal to the radius of a potential falling rock. Rn is a measure of the degree of elasticity in a collision normal to the slope, and Rt is a measure of frictional resistance to movement parallel to the slope. Model input values for each slope material type simulated are provided on Table 1 below.

**Table 2: Slope Input Parameter Values**

Slope Material Properties	Slope Roughness (ft)		Tangential Coefficient (Rt)	Normal Coefficient (Rn)
	Spacing	Amplitude		
Rock cut face	1.5	1.5	0.71	0.32
Rock cut bench	--	--	0.71	0.32
Catchment floor	1.0	1.5	0.85	0.32
Pavement (asphalt)	--	--	0.90	0.40

\* Parameters selected based on HDR experience with similar slope conditions.  
 \*\* 3x normalized standard deviation of most parameters was used.

For analysis purposes, rockfall generator (seeder) elevations were defined and characterized based on observable outcrops / exposures, subsurface investigation data (where available), and slope cross-section features. Amphibolite and schistose gneiss with density values of 180 and 175 pcf (respectively) and block sizes of 1'x1', 1'x2', 2'x3', 5'x6', and 6'x6' were simulated as rock seeder projectiles. Horizontal and vertical starting velocities for each seeder of 1 ft/sec were used and 100 rockfall events were modeled for each rock seeder type at each seeder elevation (1,000 total rockfalls per seeder). An example output cross section of a 1:1 cut is provided in Figure 10.

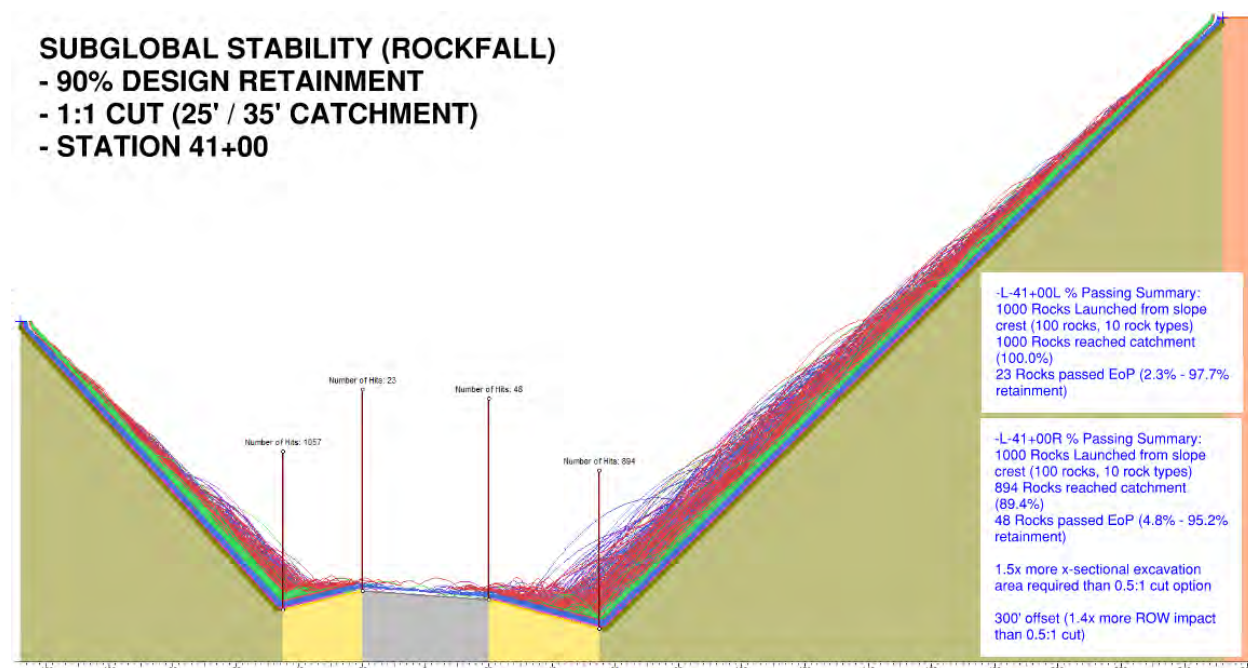


**Figure 10 – 2-D RocFall Output (1:1 Cut, expanded rockfall catchment, Sta. 41+00)**

The rockfall analysis results regarding percentage of modeled rocks reaching the catchment and passing over the edge of pavement were summarized and tabulated for NCDOT. Outputs also included average and maximum bounce heights and total kinetic energies, which were used to develop rockfall protection systems, where needed.

## SUMMARY & LESSONS LEARNED

The comprehensive approach to assessing and evaluating the 12 proposed rock cuts in support of the NC-88 realignment and widening project were distilled down to produce four sets of mitigation options:

- 0.5:1 Crystalline rock cut with reduced (10-ft) catchment and rockfall barrier system.
- 0.5:1 Crystalline rock cut with expanded catchment (no rockfall barrier system required).
- 1:1 Crystalline rock cut with reduced (10-ft) catchment and rockfall barrier / drape system.
- 1:1 Crystalline rock cut with expanded catchment (no rockfall barrier system required).

Some of the developed options were not suited for all of the proposed cuts based on existing conditions and were discarded. In general, the options were presented with approximate quantities and considerations for construction and long-term maintenance in an easily summarized qualitative format (Figure 11).

As one can imagine, the quantities and costs associated with rock excavation through a mountain cut are significant. These items were previously unforeseen due to the timing of geotechnical and geological professional engagement. Due to the delayed input, the proposed

roadway alignment has been revised to minimize the mountain cut section. An in-person “brainstorming” session earlier in the design process could have produced additional value and possibly avoided the redesign efforts.

In general, the amount of data collected for this project was ample, given the project constraints (e.g., limited access and heavy foliage). Despite this, data gaps occurred. Some of these probably could have been mitigated with a combination of aerial mapping and specially trained rope-access technicians to better evaluate the upper portions of the rock slopes during the initial field investigation. Due to the redesign, additional investigation efforts will be performed and attempts will be made to fill in these data gaps.

GEOHAZARD MITIGATION / ROCK SLOPE DESIGN PRELIMINARY EVALUATION OF OPTIONS				DESCRIPTION OF FAILURE MODES (FM)								
SLOPE ID: NC-88_S-12				FM1 - FAILURE OF SOIL/COLLUVIUM/PWR ABOVE CRYSTALLINE ROCK MASS								
SLOPE LOCATION: STATION 187+25 - 191+25 RT				FM2 - SUB-GLOBAL FAILURE (RAVELING/DISLODGING OF SMALLER ROCK FRAGMENTS LESS THAN 6-FT IN SIZE)								
PROJECT: NCDOT R-5832 ASHE CO				FM3 - GLOBAL SLOPE FAILURE ALONG PLANAR/WEDGE/TOPPLE FEATURES								
DATE: 4/27/2023 CHECKED BY: BW				EFFECTIVENESS/COST CRITERIA								
EFFECTIVENESS				INITIAL COST	ROW IMPACT	MAINTENANCE IMPACT	DESIGN LIFE (YRS)	COMPLEXITY	HIGH (H)	MEDIUM (M)	LOW (L)	
MITIGATION OPTIONS									FM1	FM2	FM3	SPECIAL CONSIDERATIONS
OPTION 1a - 0.5:1 CUT W/ WIDE CATCHMENT				M	M	M	L	H	M	25	M	Less traffic impact; Less ROW impact; Mod. maintenance; Less excavation quantities
OPTION 2a - 1:1 CUT W/ WIDE CATCHMENT				M	H	H	M	M	M	25	L	High traffic impact; High ROW impact; Low complexity; Most excavation quantities
OPTION 2b - 1:1 CUT W/ REDUCED CATCHMENT				M	M	H	H	L	H	50	M	Less traffic impact; Less ROW impact; Higher complexity; Least excavation quantities
<b>SUMMARY OF OPTIONS</b>												
OPTION 1a - 0.5:1 Cut in crystalline rock mass; 15-ft overburden bench; 2:1 cut slope in PWR / soil; increased catchment to retain 90% of rockfall based on modeling of critical sections without the use of a barrier or drape. Requires presplit blasting.												
OPTION 1b - 0.5:1 Cut in crystalline rock mass; 15-ft overburden bench; 2:1 cut slope in PWR / soil; reduced catchment to 10 feet to reduce ROW impact and excavation quantities. Requires presplit blasting. NOT EVALUATED - Minimum 25-ft catchment required to remove existing benches.												
OPTION 2a - 1:1 Cut in crystalline rock mass; 10-ft overburden bench; 2:1 cut slope in PWR / soil; increased catchment to retain 90% of rockfall based on modeling of critical sections without the use of a barrier or drape.												
OPTION 2b - 1:1 Cut in crystalline rock mass; 10-ft overburden bench; 2:1 cut slope in PWR / soil; reduced catchment to 10 feet to reduce ROW impact and excavation quantities. Based on rockfall modeling of critical section, a 6-ft barrier (min. 300kj energy rating) will be required along the edge of roadway.												
<small>NOTE: ANY CONCEPTUAL QUANTITIES PRESENTED ARE APPROXIMATE AND ARE NOT INFLATION-ADJUSTED.                      PROPOSED OPTIONS WILL REQUIRE THE USE OF A SPECIALTY SLOPE CONTRACTOR WITH RELEVANT EXPERIENCE.                      NOTE: THIS EVALUATION IS PRELIMINARY AND CONCEPTUAL IN NATURE WITH THE INTENT OF PROVIDING THE USER A RELATIVE COMPARISON OF POSSIBLE DESIGN STRATEGIES AND ASSOCIATED IMPLICATIONS. FURTHER ANALYSIS IS NECESSARY TO FULLY EVALUATE THE EFFECTIVENESS OF THE DESIGN OPTIONS PRESENTED HEREIN.</small>												

**Figure 11 - Example of Preliminary Evaluation Summary of Rock Slope Design Options**

**REFERENCES:**

Caterpillar. *Caterpillar Performance Handbook*. 48<sup>th</sup> Edition. Peoria, Illinois, June 2018.

Beckstrand, D., et al. 2019. "Unstable Slope Management Program for Federal Land Management Agencies". Federal Highway Administration. Report No. FHWA-FLH-19-002. January 2019.

Deere, D. U., and R. P. Miller. 1966. Engineering classification and index properties of intact rock: Air Force Weapons Laboratory Technical Report AFWL-TR-65-116, 277p.

International Society for Rock Mechanics (ISRM). 1978. Suggested methods for the quantitative description of discontinuities in rock masses. *International Journal of Rock Mechanics, Mining Sciences & Geomechanical Abstracts*, 15, p. 319-368.

NCGS. 1985. Geologic Map of North Carolina. North Carolina Geological Survey, scale 1:500,000.

# **A Hybrid Design Approach for Surface Stabilization of Soil Slopes Using Steel Wire Mesh: Towards a Deformation Based Design**

**Luca Gobbin and Alberto Grimod**

Officine Maccaferri Spa  
Via Kennedy 10  
Zola Predosa (BO), Italy  
l.gobbin@maccaferri.com  
a.grimod@maccaferri.com

**Michael Koutsourais, PE**

Maccaferri, Inc.  
10303 Governor Lane Blvd.  
Williamsport, MD 21795  
301-641-8072  
m.koutsourais@maccaferri.com

**Lucas Martins**

Maccaferri, Inc.  
10303 Governor Lane Blvd.  
Williamsport, MD 21795  
240-707-0633  
l.martins@maccaferri.com

Prepared for the 72<sup>nd</sup> Highway Geology Symposium, August 2023

### **Disclaimer**

Statements and views presented in this paper are strictly those of the author(s), and do not necessarily reflect positions held by their affiliations, the Highway Geology Symposium (HGS), or others acknowledged above. The mention of trade names for commercial products does not imply the approval or endorsement by HGS.

### **Copyright © 2023 Highway Geology Symposium (HGS)**

All Rights Reserved. Printed in the United States of America. No part of this publication may be reproduced or copied in any form or by any means – graphic, electronic, or mechanical, including photocopying, taping, or information storage and retrieval systems – without prior written permission of the HGS. This excludes the original authors.

### **ABSTRACT**

Anchored (or pinned) wire mesh, commonly employed as passive stabilizing systems for potentially unstable slopes in granular soil or highly fragmented weak rock, are composite structures consisting of wire mesh, steel plates and reinforcing bars/ties. Their stabilizing action is determined by the complex interaction of such elements with the underlying unstable layer, depending on the geometry of the slope, the stabilizing intervention, mechanical properties of the soil and mesh, and the intensity and time variability of applied loads (especially environmental loads, e.g. seasonal water table variations). Standard design approaches are often based on an Ultimate Limit State hypothesis (ULS), assuming the full mobilization of both the ultimate soil resistance and the ultimate tensile force in the wire mesh. Such hypothesis can potentially lead to an unsafe design, especially when passive stabilizing systems are considered, since the stabilizing action is mobilized only upon the activation of soil displacement.

In the present paper, based on recent advances in design methods for slope stabilizing systems, an advanced “hybrid” method is presented combining an ULS analysis of the unstable slope with a Serviceability Limit State analysis (SLS) for the wire mesh. This hybrid method allows the designer to easily and consistently estimate the affect of soil displacement on the factor of safety of the slope, thus proving the efficacy of the wire mesh to reduce soil displacement and allow the influence of both its strength and stiffness to be determined.

## INTRODUCTION

The aim of soil nailing is to improve the soil slope stability when there are unfavorable stability conditions. The stability is achieved by inserting reinforcement bars in the soil. These anchors mobilize friction forces along the entire length and contribute to improve stability conditions when displacement in the soil occurs (Schlosser F. et al., 2002; Soulas R., 1991; BS 8006-2; Byrne, R.J et al., 1998). The stabilizing friction forces are passively generated when the soil rupture begins. The protection of the exposed surface of the soil reinforced slope is obtained with a facing (flexible, as a steel wire mesh, or rigid, as shotcrete) able to contain the soil between the nails, prevent erosion of the surface and assume an aesthetic function (Giacchetti et al., 2011).

Design approaches and dimensioning criteria for slope stabilization measures have been investigated since the beginning of the last century by means of empirical, theoretical and numerical research. It is now recognized that there are different factors mainly influencing the design process, such as (i) slope geometry, (ii) geotechnical properties of the slope, (iii) type and position of the stabilizing elements (i.e. nails), (iv) shape and amplitude of the unstable soil displacement profile, (v) water table, and (vi) amplitude and time evolution of the destabilizing loads (especially when environmental loads are considered). This is particularly true in the case of anchored wired mesh installed on unstable slopes (soil nailing) composed of inclined layers of slightly cemented soil or highly fragmented rocks. For this type of intervention, composed of a steel wire mesh anchored to the ground by means of plates and reinforcing bars (anchors) full grouted along their entire length, the stabilizing action is governed by the complex interaction between all the components. The stabilizing reaction is mobilized only if a displacement occurs; and for this reason, the system must be considered as a passive intervention: the mesh, defined as a structural flexible facing (BS 8006-2), starts to stabilize the soil only if the soil starts to move between a pattern of anchors. Consequently, a rational design procedure would require a displacement-based approach in order to provide a safe and consistent estimation of the stabilizing action.



**Figure 1: Large Punch Displacement of Flexible Structural Facing Loaded by the Soil as the Cables Reduce Mesh Displacement**

Standard design procedures are instead usually force-based approaches, often assuming oversimplified hypotheses either regarding the geometry or mechanical behavior of the system. They are generally not able to properly consider all the abovementioned factors; they are more suited to preliminary design, rather than final design. Moreover, they assume the full mobilization of the stabilizing action regardless of the relative movements between the slope and the wire mesh. In other words, they disregard the deformation characteristics of the retaining system and focus on its Ultimate Limit State (ULS) condition only. This obviously implies that no reference at all can be made to the performance of the stabilizing intervention in terms of limiting the slope displacement, which is often the actual variable of interest.

On the other hand, accurate numerical approaches, for instance, based on advanced 3D modelling of the slope together with the stabilizing system, are available, but excessively demanding both in terms of theoretical know-how and computational time and can hardly be considered an easy approach to the issue. The number of parameters, which generally require an extensive geotechnical survey and laboratory testing, are not always easy to define, and the influence of the single parameter is often difficult to understand.

Moreover, the implementation of accurate models and their calibration needs time and experience. These aspects regarding numerical modeling often make their use hard when dealing with the design of stabilization of small landslides, when the resources, both time and money, are limited. When considering nails and steel mesh, moreover, the correct modelling of the mesh and of its interaction with soil is itself a hard task, owing to the, unfortunately common, lack of soil mechanical characterization, and to the difficult characterization of the mesh properties since standard testing procedures are available only for a limited type of mesh, requiring large displacement computational schemes.

For the abovementioned reasons, the need for simplified methods capable of explicitly considering soil and mesh deformation properties is evident, and it would positively contribute to the improvement of safe design procedures. A recent study on sustainable slope stabilizing methods (PRIN, 2011) provides a reference framework for the design of stabilizing measures, defining three different approaches with the following increasing order of complexity: (a) Limit State Methods, (b) Hybrid Methods, and (c) Displacement Methods.

The Limit State Methods introduce perfectly-rigid plastic constitutive relationships for both the soil constituting the slope and the stabilization structure. These methods estimate the maximum load the structure can transfer to the slope with the underlying assumption that the load transferred from the retaining structure to the slope is independent from the relative displacement between the unstable soil mass and the structure. ULS methods belong to this category. Alternatively, Hybrid Methods explicitly introduce a soil-structure interaction model describing the evolution of the stabilizing force with respect to the relative soil-mesh displacement. The resulting function, often called “Characteristic Function” or “Characteristic Curve”, is then used within the framework of the standard Limit Equilibrium analyses for assessing the stability of a slope. The Hybrid Methods combine an Ultimate Limit State for the stability assessment of the unstable soil mass with a Serviceability Limit State approach for the retaining structure. The fundamental finding is that the resulting slope stability analysis, usually summarized by a global Safety Factor of the system, is directly dependent on the displacement of

the slope, thus providing an explicit, objective and consistent measurement of the performance of the stabilizing intervention.

Displacement Methods also use the concept of the “Characteristic Function”, but they explicitly provide a time integration of the motion equation of the unstable soil mass, thus allowing the evaluation of the long-term behavior of the studied system. This paper will be uniquely focused on “Hybrid Methods” introducing the fundamental concept of the characteristic curve too.

## FLEXIBLE STRUCTURAL FACING

As per the British Standard 8006-2, Flexible Structural Facing, for soil nailing application, may be used to provide long-term stability of the face by supporting the soil between nail locations and transmitting the load from the soil to the soil nails via the nail heads. Flexible facing may be used to provide support through the mobilization of tensile forces within them, and therefore some deformation is required for a component of these forces to act normal to the face. Flexible facings are not normally recommended for permanent slopes in excess of 60° to 70°.

Based on the BS 8006-2, punch tests are fundamental for modelling the mesh applied to soil nail slopes. In order to standardize a procedure to carry out laboratory punch tests, the Italian National Unification (UNI) has published in 2012 the UNI 11437. This norm has been transposed to the ISO 17745 and ISO 17746, thus, manufacturers can easily define the punch resistance of their mesh.

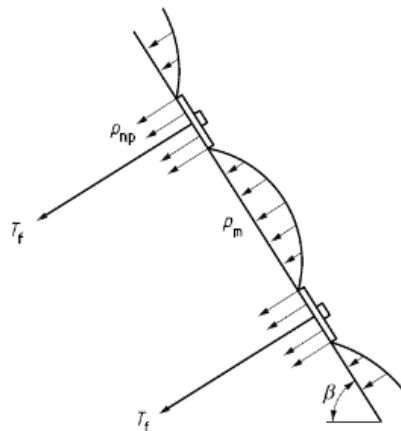


**Figure 2: Flexible Structural Facing (BS 8006-2)**

## DESIGN APPROACH

In the following section, attention will be uniquely focused on the case of homogeneous unstable layers of thickness  $s$  on a slope with inclination  $\alpha$  and total height  $H$ .

With reference to the simplified two-dimensional model for the reinforcement of the surficial unstable layer of a soil slope shown in Figure 3, a sub-structuring approach is used to study the stability of the surficial soil mass separately from other structural components.

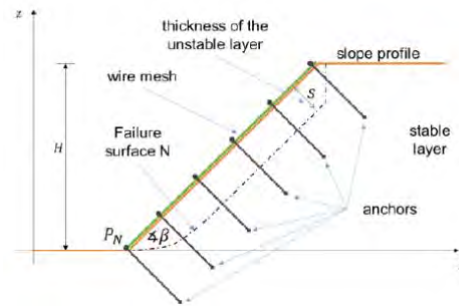


**Figure 3: Model of An Unstable Soil Slope Reinforced with a Passive Anchored Wire Mesh**

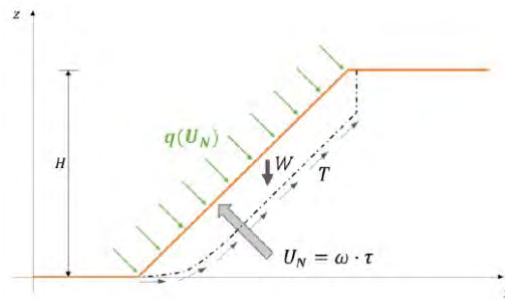


**Figure 4: Forces Involved in the Model of An Unstable Soil Slope Reinforced with a Passive Anchored Wire Mesh**

The soil mass is subject to the self-weight,  $W$ , to the shear force,  $T$ , mobilized along its failure surface, and to the stabilizing contact pressure,  $q$ , arising between the mesh and the slope profile (Figure 4). In general, no initial pre-stressing action is imposed to the anchors, as passive intervention systems are only considered, and the contact pressure,  $q$ , is only mobilized upon the activation of a local normal displacement,  $U_N$ , of the soil. As a result, a relationship,  $q = q(U_N)$ , is introduced. From a structural point of view, the anchored steel wire mesh is then subjected to a displacement-controlled loading process governed by the normal component,  $U_N$ , of the underlying soil displacement profile.

In this work, for the sake of simplicity, the axial deformability of the anchors will be disregarded with respect to soil and mesh deformability, and the mesh anchoring points will then be considered as fixed.

A key role in the present innovative design method is represented by the explicit definition of the relationship,  $q = q(U_N)$ , named hereafter as the “characteristic curve” of the system. The fundamental importance of the characteristic curve is that it represents a “generalized” constitutive law for each span of the mesh and for the underlying soil (i.e. at the

“macro” scale of the structure), reproducing the behavior of the system from its working condition until its incipient failure. The characteristic curve strictly depends on both the deformation and the strength of the involved materials, namely the soil and the wire mesh. Indeed, only a proper description of this interaction allows an accurate quantitative evaluation of the stabilizing action, and, thus, the definition of safe design solutions. This is particularly important when deformable structures are considered, as it is for steel mesh. In this case, in fact, the peak value of the characteristic curve, representing the maximum stabilizing pressure,  $q$ , that can be supported by a span of the mesh, is also strictly dependent on the relative stiffness between the mesh and the soil deformation of the two involved materials. Therefore, the failure of the system is largely affected by the deformation values too. The usual design methods often adopted in practice are generally based on simplified Ultimate Limit State approaches and they disregard the soil/mesh relative stiffness.

### LEM and Hybrid Methods

Standard Limit Equilibrium Methods (LEM) usually study the stability of a soil mass along a failure surface,  $F$ , by adopting the following equation:

$$E_k = R_k / FS + A_{k,lim} \quad (1)$$

expressing the equilibrium among the driving action ( $E$ , generally given by the weight of the unstable soil mass), the mobilized soil strength ( $R$ ) and the limit value of the stabilizing action ( $A$ ) provided by the stabilizing intervention. In Equation 1, all the three terms are computed with reference to a specific failure mechanism, and by adopting the characteristic values of the mechanical parameters (subscript  $k$ ) and a safety factor  $FS$  is also introduced as a soil strength reduction factor. Alternatively, the same equation could also be written with reference to the design values of the cited quantities, once partial safety factors are introduced depending on the adopted design standards. The following inequality is hence written:

$$E_d < R_d + A_{d,lim} \quad (2)$$

In both cases, the contribution of the stabilizing structure is only considered at its limit condition, coinciding with the peak value, without explicitly modelling the soil-mesh interaction. No direct relationship can be then built between the safety level of the slope, the working condition of the mesh and the soil displacement.

The proposed method, on the contrary, is based on an innovative “hybrid” approach (Galli et al., 2017). The key concept is that the equilibrium of the soil mass is still analyzed by means of usual LEM, but the stabilizing action provided by the passive structural elements is expressed as a function of the relative soil-structure displacement. In other words, hybrid methods combine an Ultimate Limit State approach (ULS) with respect to soil strength to analyze the stability of the slope, with a Serviceability Limit State approach (SLS) with respect to the soil-structure interaction. This approach is consistent with the idea of dealing with prevention interventions, i.e. to design structures aimed at preventing the triggering of a failure mechanism within the slope, but allowing small pre-failure soil displacements, sufficient to activate the soil-mesh interaction.

From a computational point of view, the equilibrium of the potentially unstable soil mass is studied with reference to a small-displacement scheme, i.e. by neglecting slope movements and writing the global equilibrium equations for the soil mass with respect to its initial undeformed state. The local soil-mesh interaction giving rise to the  $q = q(U_N)$  curve, is on the contrary necessarily studied by adopting a large-displacement scheme, in order to correctly capture the membrane behavior of the mesh, as it will be discussed. The formal governing equation can then be simply written in the general form as follows:

$$E_k = R_k / F_S + A_k(\mathbf{U}) \quad (3)$$

extending the validity of Equation (1) to hybrid methods, through the definition of a “characteristic” function of the system,  $A = A(\mathbf{U})$ , expressing the evolution of the global stabilizing action,  $A$  (in this case, the integral of the mobilized contact pressures,  $q$ , between the slope profile and the mesh) with the displacement field  $\mathbf{U}$  of the slope. The key concepts deriving from the introduction of such characteristic function are that:

- (a) the influence of the soil-mesh relative stiffness on the stabilizing force (affecting also its peak strength value) can be explicitly captured,
- (b) the safety level of the surficial soil layer of the slope in presence of the stabilizing system becomes a function of the soil displacement pattern, and
- (c) the working condition of the mesh for the desired safety level of the surficial unstable layer can be explicitly evaluated.

Equation (3), in fact, conceptually introduces a relationship between the safety level (generally expressed as  $FS$ ) and the soil displacement field, as sketched in Figure 5. Starting from the initial pre-intervention value of the safety factor,  $FS = 0$ , the designer can explicitly relate the chosen design value,  $FS_{d}$ , of the safety factor to the corresponding soil displacement amplitude, and to the working condition of the mesh.

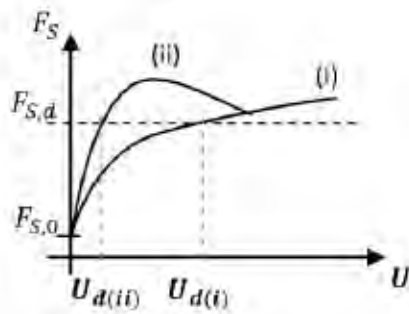


**Figure 5: Relationship Between the Slope Safety Factor,  $FS$ , and the Soil Displacement for: (i) Ductile and (ii) Fragile Stabilizing Systems**

Hybrid methods cannot, however, be used to foresee the long-term behavior of the system (e.g. the expected on site displacement after the installation of the mesh), since they do not consider any time-evolution law of the system. Furthermore, it should be observed that,

theoretically, a slide is triggered whenever  $F_{S,0} < 1$ , and the soil, as it is in all passive prevention systems, would continuously slide only until a new stable equilibrium condition is reached (i.e.  $FS = 1$ ).

All the design conditions characterized by  $F_{S,d} > 1$  cannot then ideally be reached in practice, and the displacement values,  $U_d$ , computed by hybrid methods are therefore only meant as a measure of the performance of the system for a fixed safety level of the slope.

Finally, Hybrid Methods are suitable for the design of prevention measures, conceptually referred to as a pre-failure condition of the investigated instability. This is a fundamental difference with respect to protection measures, which are on the contrary aimed at controlling the evolution of the phenomenon after the onset of a global failure mechanism. In this case, completely different computational tools would in fact be required, based on large displacement approaches and capable of accounting relevant changes in the slope geometry, as it is, for example, for debris flow protection interventions.

## SLOPE ANALYSIS

The hybrid method described has been implemented in the proprietary software named Mac S-Design developed by Officine Maccaferri Spa in collaboration with the department of Civil and Environmental engineering of Politecnico di Milano. Mac S-Design is a design tool which can support engineers to design soil nailing systems with steel mesh (structural flexible facing) for surficial slope instabilities. The main assumptions and the geometry adopted for the stability analyses of the surficial unstable soil layer implemented in the software are hereby presented.

A sketch of the adopted slope profile is presented in Figure 6. In particular, a slope of total height,  $H$ , constituted by a homogeneous layer of granular material with uniform thickness,  $s$ , and slope angle inclination,  $\beta$ , along a stable deep layer, is considered. A water table at a uniform depth along the slope is present, and, depending on the mechanical properties of the unstable layer, tension cracks at the top of the slope may be considered.

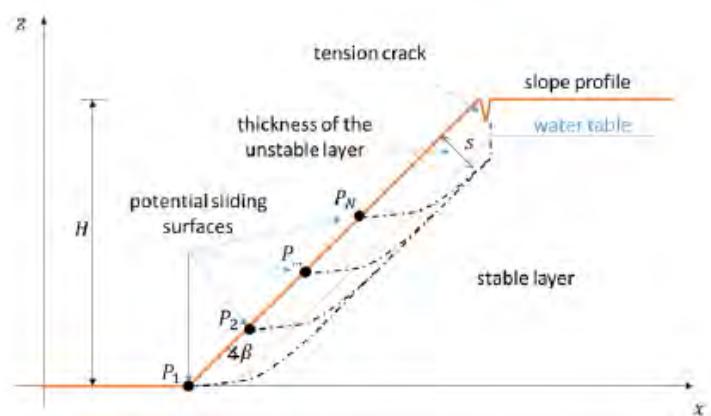


**Figure 6: Slope Cross Section Model**

It is interesting to underline that this tool is quite unique, because it takes into consideration the failure mechanism along the entire slope; while other mesh-design software are based on the behavior of the mesh only between a pattern of nails, considering an undefined slope. Field investigations have shown that this innovative assumption is fundamental for the design of the steel wire mesh and nails, as shown in Figure 7.



**Figure 7: Example of a Soil Nail Slope Where the Soil Has Slid Underneath the Mesh, and the Foundation of the Nail Drastically Reduced**

Only translational failure mechanisms of the unstable layer, starting from the crest of the slope and extending until their emerging points,  $P$ , along the slope, are considered. In general,  $N$  unique failure surfaces are defined.

Two different approaches have been implemented in the design tool; the first one is more suitable to steep slopes, and the second to gentle slopes. Both approaches are simultaneously run in the code, and the solutions, consistently with usual LEM approaches, are derived by comparing all the considered failure mechanisms, and showing a suitable envelope of the obtained results.

It is worth noting that both the approaches are based on Limit Equilibrium assumptions, and that the difference between the two is actually limited to a different procedure for the evaluation of the toe stabilizing action provided to the unstable layer.

The stabilizing effect provided by the anchors to the surficial unstable layer, modelled as a simple additional resisting force parallel to the sliding plane, would actually require the definition of specific characteristic curves. The objective of this paper, however, for the sake of simplicity and owing to the minor contribution of this term to the overall stability of the slope, their effect is independently estimated by adopting a simplified analytical procedure, proposed by Di Laora et al. (2017) for slope stabilizing piles and based on an ULS approach. The contribution of nails to the global stability of the whole slope is then not considered through this approach.

In the considered method, the total resisting force provided by each single anchor against soil displacement is computed by considering the different possible failure mechanisms that can

be triggered at the local level of the soil-anchor interaction. Six different failure mechanisms are considered possible, depending on the geometry of the problem (thickness of the unstable layer, length and diameter of the anchor) and on the strength parameters of both the soil and the anchor.

All six solutions are summarized in the non-dimensional abacus of Figure 8 (Di Laora et al.; 2017), where the dimensionless value,  $t_d$ , of the stabilizing action is plotted for increasing values of the dimensionless length,  $\lambda$ , of the anchor.

The dimensionless value,  $t_d$ , corresponds to a force,  $T$ , provided by an anchor of diameter,  $d$ , grouted in a hole of diameter,  $D$  (generally coinciding with the ideal diameter of the grouted section), in a soil layer of unit weight,  $\gamma$ , and thickness,  $s$ . The,  $\lambda$ , parameter expresses the ratio between the anchor length,  $l_2$ , beyond the sliding plane and the thickness of the unstable layer,  $l_1=s$ ).

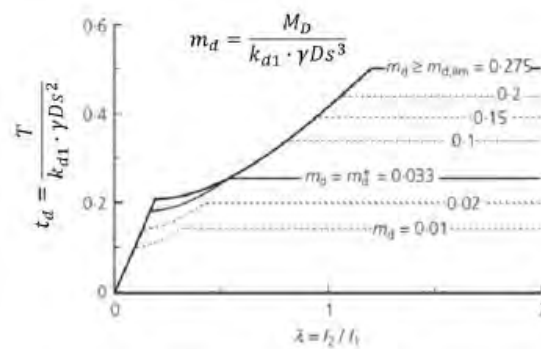


**Figure 8: Values of the Dimensionless Stabilizing Action,  $t_d$ , Provided by One Single Anchor (Di Laora et al., 2017)**

The values of,  $t_d$ , are strictly influenced by the activation of the plastic hinges in the anchor, and, consequently, different curves are plotted in the abacus, depending on the value of the dimensionless bending strength,  $m_d$  (function of the yielding bending moment,  $M_d$ , of the anchor section). It is worth noting that the value,  $M_d$ , does not necessarily correspond with the ultimate strength,  $M_y$ , of the anchor in pure bending test, but, through the well-known  $M-N$  interaction domain for the anchor section (usually, a steel rod), it depends on the value,  $N_d$ , of the tensile action,  $N$ , as shown in Figure 9, where  $N_y$  represents the ultimate strength in pure tensile tests mobilized in the anchor by the pressure,  $q$ , developed over each single span of the mesh at the soil-mesh interface.

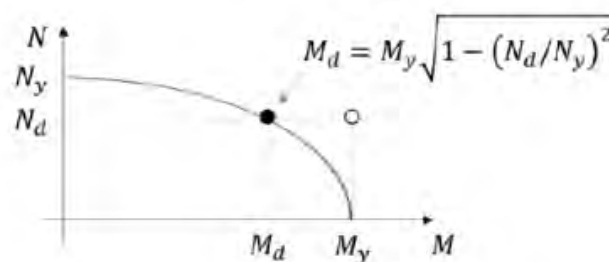


**Figure 9: M-N Interaction Diagram for an Anchor Steel Section**

Consequently, the actual stabilizing action,  $T$ , provided by each anchor along the sliding plane can be evaluated only by means of a coupled analysis, accounting for both the bending and the tensile response of the anchor. In other words, the working condition of the mesh also influences the anchor resistance against transverse soil sliding. At each run, the code solves this coupled problem by numerically determining the couple of values  $(M_d, N_d)$  laying on the boundary of the  $M-N$  interaction domain. Such condition also represents the safety check for the anchor, at least for the section where a plastic hinge is activated, since a maximum value in the bending moment diagram is expected with a nil value of the shear force.

The obtained value of the stabilizing action,  $T$ , under the hypothesis that no significant interaction arises between neighboring anchors (i.e. each anchor is independent from the others), is then simply introduced in the slope stability analysis as an additional equivalent cohesive strength acting along the sliding plane of the unstable layer, and uniformly distributed over the area of influence of each anchor.

As far as seismic analyses are considered, a pseudo-static approach has been implemented. Seismic actions are modelled as equivalent static forces along the vertical and horizontal directions and expressed as a fraction of the total soil weight through the pseudo-static coefficients,  $k_v$  and  $k_h$ , respectively.

This conceptual framework of analysis is adopted in Mac S-Design to study the stability of a slope. The procedure is applied to assess the Factor of Safety both in the actual state, namely the “pre-intervention” phase, as well as to design the intervention, namely a stability analysis suitable to verify the applied system.

### The Characteristic Curve

Following the definition of Equation (2), for each considered failure mechanism, the characteristic function represents the relationship between the “far field” soil displacement,  $\mathbf{U}$  (i.e., the soil displacement for the considered failure mechanism), and the mobilized stabilizing action at the soil-structure interface:

$$A = A(\mathbf{U}) \quad (4)$$

In general cases, the displacement,  $\mathbf{U}$ , is represented by an entire soil profile, so that Equation (4) is of vectorial nature.

In the specific case of anchored wire mesh and sliding failure mechanisms, however, the stabilizing action is represented by the distributed pressure,  $q$ , while the far field displacement corresponds with the normal component,  $U_N$ , (with respect to the slope profile) of the total displacement,  $U_T$ , of the active block,  $P'-P''-Q$ , so that a scalar function:

$$q = q(U_N) \quad (5)$$

called “characteristic curve”, can be adopted to describe the entire interaction problem.

In Figure 10, the ideal case of an active block,  $P'-P''-Q$ , interacting with a single span of an anchored wire mesh is sketched, with the underlying hypothesis that the active length,  $L_a$ , of the failure mechanism coincides with the longitudinal spacing,  $i_L$ , of the anchored spike plates along the slope (a specific reduction factor is then introduced on the characteristic curve for the case  $L_a < i_L$ ).

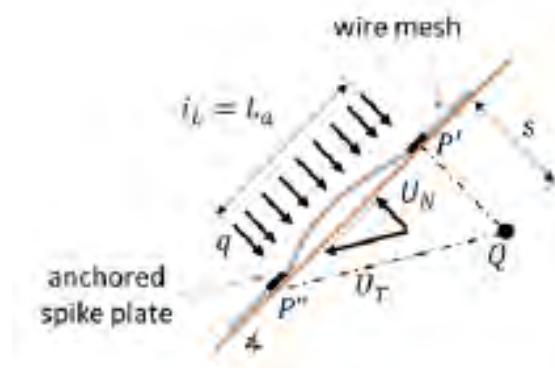


**Figure 10: Qualitative Deformation of a Span of an Anchored Wire Mesh Subjected to a Soil Displacement,  $U_N$ , and Developing an Average Stabilizing Pressure,  $q$ , Over Its Active Length,  $L_a$**

The characteristic curve conceptually represents the relationship between the average value of the contact pressure,  $q$ , mobilized between the soil and the mesh over a span of the mesh and the corresponding normal displacement of the backfill soil material.

The mobilized tensile action in each anchor can be evaluated by simply integrating the pressure,  $q$ , over the area of influence of the anchor. The characteristic curve is fundamentally dependent on the mechanical characteristics of both the soil and the mesh used to retain the unstable backfill soil in the case of a real application. A slope reinforced with a cortical mesh can be then schematized as a series of nails loaded by the pressure,  $q$ , transferred through the relevant influence area of the mesh.

### Approach 1

In this approach the stability analysis is run by approximating the sliding surfaces sketched in Figure 6 by means of a two-block failure mechanism along the slope, as shown in Figure 11. Each failure mechanism is composed by a layer of thickness,  $s$ , and length,  $L$ , sliding along the inclined plane according to a translational displacement field,  $U$ . The toe of the failure mechanism is instead composed of a rigid triangular block (points  $P'-P''-Q$ ), sliding along its base failure plane of a quantity,  $U_T$ , corresponding to a normal displacement component,  $U_N$ , with respect to the slope over a length,  $L_a$  (between points  $P'$  and  $P''$ ). In presence of the wire mesh, this length,  $L_a$ , represents the “active” length of the stabilizing system, i.e. the zone of the slope where the stabilizing contact pressure,  $q$ , is mobilized between the mesh and the slope.



condition before moving to the second phase. In the pre-analysis phase, the stabilizing pressure,  $q$ , provided by the mesh, is assumed to be null, being the mesh system is not yet installed. This procedure allows the minimum pre-analysis Factor of Safety ( $FS_0$ ) to be evaluated for the surficial instable layer of the slope.

In this stage of pre-analysis, the user can run parametric analyses both to investigate the sensitivity of the input parameters and to assess their critical combination related to a factor of safety,  $FS_0$ . The pre-analysis is important in order to assess the potential instability of the surficial soil layer as an initial step of the subsequent stability analyses. Having a preliminary assessment of the stability could also lead the user to the selection of the more appropriate product and system for the intervention.

## Results

The results of the stability analyses for a prescribed  $FS$  value is generally expressed as an envelope of the values of the mobilized pressure,  $q$ , along the active length,  $L_a$ , for each considered failure mechanism in the surficial layer and for the two adopted stability analyses. If the values of  $q$  are plotted against the elevation,  $z$ , of each mechanism, the resulting red curve in Figure 13 represents the profile of the computed pressure distribution for a fixed value of safety factor  $FS$ . It is worth noting that the curve in Figure 11 does not represent the expected pressure distribution in service conditions for the stabilizing system, but only the envelope of the possible pressure values corresponding with the imposed  $FS$  value.

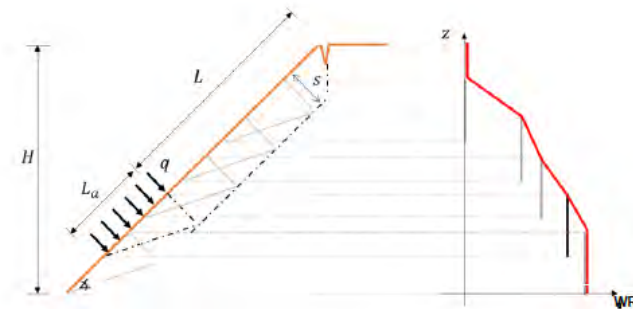


**Figure 13: Envelope of the Required Contact Pressure Distribution Along the Slope**

The code output also provides the values of the tensile forces developed in the anchors, corresponding with the computed distribution of the pressure,  $q$ , having already checked, as a result of the coupled analysis, the working condition ( $M_d, N_d$ ) in the  $M-N$  interaction domain for the sections where plastic hinges are activated. This pressure,  $q$ , allows then a meaningful working ratio parameter to be introduced in order to easily check the behavior of the mesh. Such output parameter is expressed as a percent (%) and this indicates the maximum ratio under which the mesh performs compared to its capacity. The verification on the mesh is satisfied when the working ratio does not exceed 100%.

## CONCLUSIONS

This paper presents an innovative method which is deemed suitable to design steel mesh systems used in combination with passive soil nails for surficial soil slope stability (i.e. soil nailing with flexible structural facing as defined by the BS 8006-2). The innovative aspect of the proposed method is that, as opposed to traditional LEM for slope stability, the “hybrid” approach combines the LEM for the equilibrium of the soil mass, and expresses the stabilizing action provided by the passive structural elements (i.e. the steel mesh) as a function of the relative soil-mesh displacement. This is possible through the introduction of a “characteristic curve” which represents the relationship between the average value of the contact pressure,  $q$ , mobilized between the soil and the mesh over a span of the mesh and the corresponding normal displacement of the slope soil material. Hybrid methods combine an Ultimate Limit State approach (ULS) with respect to soil strength to analyze the stability of the slope, with a Serviceability Limit State approach (SLS) with respect to the soil-structure interaction. This approach is consistent with the idea of dealing with prevention interventions, which translates into allowing small pre-failure soil displacements, sufficient to activate the soil-mesh interaction. The method described has been implemented in the proprietary software named Mac S-Design. The Mac S-Design code allows the user to run a pre-analysis (i.e. without any stabilizing mesh or nails), and then allows the designer to conduct a verification of the system components (i.e. mesh strength, nail capacity) for a prescribed target factor-of-safety. According to the authors, this innovative method is a more realistic representation of the steel mesh behavior when used in combination of nails for surficial soil slope stability problems as compared to traditional LEM approaches where the mesh is modelled as a rigid boundary developing resisting forces independently of the deformation field involved. Actual installations show that a mesh can withstand considerable deformation, and that the provided stabilizing force is highly dependent on the soil-mesh interaction and on the displacement field.

## REFERENCES:

1. Bertolo P., Oggeri C., Peila D. (2009). “Full scale testing of draped nets for rock fall protection” Canadian Geotechnical Journal, No. 46 pp. 306-317.
2. Bonati A., e Galimberti V. (2004). “Valutazione sperimentale di sistemi di difesa attiva dalla caduta massi” in atti “Bonifica dei versanti rocciosi per la difesa del territorio” - Trento 2004, Peila D. Editor.
3. Butterfield R. 1980. A simple analysis of the load capacity of rigid footings on granular materials. Journée de Géotechnique, ENTPE, Lyon, France, 128–137.
4. BS 8006-2, 2011. Code of practice for Strengthened/ reinforced soils and other fills – Part 2: Soil Nailing design.
5. Byrne R.J, Cotton D., Porterfield J., Wolshlag C., e Ueblacker G.,(1998). “Manual for design & construction monitoring of soil nail walls” U.S. Department of transportation – Federal Highway Administration. FHWA A-SA-96-06R – Washington D.C
6. Cazzuffi D, Cardile G, Gioffrè D (2014). Geosynthetic engineering and vegetation growth in soil reinforcement applications. Transp Infrastruct Geotechnol 1:262–300.
7. Cola S. and Sanvitale N., 2011. Interazione tra rivestimento, barre e terreno nelle pareti sostenute con soil nailing”. XXIV CNG-Innovazione tecnologica nell’ingegneria geotecnica. Napoli, 22-24 june 2011. Vol.1, pp 217-230. ISBN 978-88-97517-02-3. Invited paper.

8. Di Laora, R., Maiorano, R.M.S., Aversa, S. (2017). Ultimate lateral load of slope-stabilising piles. *Géotechnique Letters* 7, 237–244.
9. EN 10223-3 (2013). Steel wire and wire products for fencing and netting - Part 3: Hexagonal steel wire mesh products for civil engineering purposes
10. Flumm D., Ruegger R. (2001). “Slope stabilization with high performance steel wire meshes with nails and anchors – International Symposium Earth reinforcement, Fukuoka, Japan.
11. Fredlund, D.G., Rahardjo, H. (1993). *Soil Mechanics for Unsaturated Soils*. ISBN:9780471850083 |Online ISBN:9780470172759 |DOI:10.1002/9780470172759. Copyright © 1993 John Wiley & Sons, Inc.
12. Galli, A., Maiorano, R.M.S., di Prisco, C., Aversa, S. (2017). Design of slope-stabilizing piles: From Ultimate Limit State approaches to displacement-based methods. *Rivista Italiana di Geotecnica*, 51(3), pp. 77-93.
13. Giacchetti G., Grimod A., Cheer D. (2011). Soil Nailing with flexible structural facing: design and experience. *World Landslide Forum, Rome 2011*.
14. Grimod A., Giacchetti G., Peirone B. (2013). Design of flexible structural facing in soil nailing. *Geo Montreal 2013*.
15. Hoffman, P. (2016). Contributions of Janbu and Lade as applied to Reinforced Soil. *Proceedings of the 17th Nordic Geotechnical Meeting, 25th - 28th of May, Reykjavik*.
16. Janbu, N. (1963). Soil Compressibility as Determined by Oedometer and Triaxial Tests, *European Conference on Soil Mechanics and Foundation Engineering, Wiesbaden, Germany, Vol. 1*, pp. 19-25.
17. ISO 17745 (2016). Steel wire ring net panels — Definitions and specifications
18. ISO 17746 (2016). Steel wire rope net panels and rolls — Definitions and specifications
19. Lade, P.V., and Nelson, R.B. (1987). Modelling the Elastic Behavior of Granular Materials, *International Journal for Numerical and Analytical Methods in Geomechanics*, 11, 521-542
20. Lancellotta R. (2012). *Geotecnica*. Ed. Zanichelli.
21. Muhunthan B., Shu S., Sasiharan N., Hattamleh O.A., Badger T.C., Lowell S.M., Duffy J.D. (2005). “Analysis and design of wire mesh/cable net slope protection - Final Research Report WA-RD 612.1” Washington State Transportation Commission Department of Transportation/U.S. Department of Transportation Federal Highway Administration.
22. PRIN 2011. La mitigazione del rischio da frana mediante interventi sostenibili. Coord.naz.: prof. L.Cascini.
23. Schlosser F., (Chairman) (2002). “Additif 2002 aux recommandations clouterre 1991 pour la conception, le calcul, l’exécution et le controle des soustènements realises par cluage des soil”, Presses Ponts et chaussées.
24. Soulas R., (Chairman) (1991). “Recommandations clouterre 1991 pour la conception, le calcul, l’exécution et le controle des soustènements realises par cluage des soil”, Presses Ponts et chaussées.
25. UNI 11437 (2012). Opere di difesa dalla caduta massi. Prove su reti per rivestimento di versanti.



THANK YOU FOR ATTENDING THE 72<sup>ND</sup> ANNUAL  
HIGHWAY GEOLOGY SYMPOSIUM

